CAVE INCEPTION AND DEVELOPMENT IN CALEDONIDE METACARBONATE ROCKS

By

Trevor Laurence Faulkner

Limestone Research Group
University of Huddersfield
Queensgate, Huddersfield, HD1 3DH, UK

A thesis submitted to the University of Huddersfield in partial requirements for the Degree of Doctor of Philosophy

To adapt a maxim from a previous career: "If you can't measure it, you can't understand it"

"There is an extensive vocabulary of special terms to describe karst landforms which can be confusing to the uninitiated, and even to the expert" (Summerfield, 1991, p149)

"It is a new ground you are walking on, you do not know the way" (John Steinbeck, The Pearl)

Abstract

This is the first comprehensive study of cave inception and development in metacarbonate rocks. The main study area is a 40000km^2 region in central Scandinavia that contains over 1000 individual metacarbonate outcrops, and has nearly 1000 recorded karst caves (with passage lengths up to 5.6km). The area, which was repeatedly glaciated in the late Cenozoic, comprises a suite of nappes in the Cambro–Silurian Caledonides, a paleic range of mountains with terranes presently occurring on both sides of the northern Atlantic. Information about the stripe karst and non-stripe karst outcrops and their contained caves was assembled into computer-based databases, enabling relationships between the internal attributes of the caves and their external geological and geomorphological environments to be analysed. A rather consistent pattern emerged. For example, karst hydrological system distances are invariably shorter than 3.5km, and cave passages are positioned randomly in a vertical dimension, whilst commonly remaining within 50m of the overlying surface. This consistency is suggestive that the relevant cave inception, development and removal processes operated at a regional scale, and over long timescales. A consequence of the *epigean* association of caves with the landscape is that cave development can only be understood in the context of the geomorphological evolution of the host region. A review of the latest knowledge of the inception and development of caves in sedimentary limestones concluded that the speleogenesis of the central Scandinavian caves cannot be explained by these ideas. Five new inter-related conceptual models are constructed to explain cave development in metacarbonate rocks in the various Caledonide terranes. These are:

1. The *tectonic inception model* - this shows that it is only open fracture routes, primarily created by the seismic shocks that accompany deglaciation, which can provide the opportunity for dissolution of metalimestone rocks that have negligible primary porosity.

2. The *external model of cave development* - this black-box approach reveals how the formation, development and destruction of the karst caves are related to the evolution of their local landscape. During the Pleistocene, these processes were dominated by the cycle of glaciation, leading to *cyclic speleogenesis*, and the development of ever-longer and deeper systems, where the maximum distance to the surface commonly remains within one-eighth of the extent of change in local relief.

3. The *hydrogeological model* - this demonstrates that the caves developed to their mapped dimensions in timescales compatible with the first two models, within the constraints imposed by the physics and chemistry of calcite dissolution and erosion, primarily in almost pure water. *Relict* caves were predominantly formed in phreatic conditions beneath active deglacial ice-dammed lakes, with asymmetric distributions on east- and west-facing slopes. *Mainly vadose* caves developed during the present interglacial, primarily vadose, conditions, with maximum dimensions determined by catchment area. *Combination* caves developed during both deglacial and interglacial stages. The cross-sections of phreatic passages obey a non-fractal distribution, because they enlarged at maximum rates in similar timescales. Phreatic cave entrances could be enlarged at high altitudes by freeze / thaw processes at the surface of ice-dammed lakes, and at low altitudes by marine activity during isostatic uplift.

4. The *internal static and dynamic model of cave development* - this white-box approach demonstrates that many caves have 'upside-down' morphology, with relict phreatic passages overlying a single, primarily vadose, streamway. Both types of passage are guided along inception surfaces that follow the structural geology and fractures of the carbonate outcrops. Dynamically, the caves developed in a 'Top-Down, Middle-Outwards' (TDMO) sequence that may have extended over several glacial cycles, and passages in the older *multi-cycle* caves were removed downwards and inwards by glacial erosion.

5. The *Caledonide model* - this shows that the same processes (with some refinements) applied to cave development in most of the other (non-central Scandinavian) Caledonide areas. The prime influences on cave dimensions were the thicknesses of the successive northern Atlantic glacial icesheets and the positions of the caves relative to deglacial ice-dammed lakes and to local topography. Other influences included contact metamorphism, proximity to major thrusts, and marine incursions. With knowledge of these influences for each area, mean cave dimensions can be predicted.

The thesis provides the opportunity for the five models to be extended, so that cave development in other glaciated metamorphic and *sedimentary* limestones can be better understood, and to be inverted, so that landscape evolution can be derived from cave data.

Preface

The idea of studying cave development in Caledonide metacarbonate rocks was proposed by the author in an application to register for a part-time research degree at the Limestone Research Group, University of Huddersfield (Faulkner, 1997). The proposal identified two phases of work. Part A would examine the geology, geomorphology and hydrology of the caves in south Nordland, Norway. Part B would develop a conceptual model for cave development in that area and test the applicability of the model in other parts of the world with similar geological environments.

The knowledge gained during Part A (Faulkner, 1999a and 2001) and the work required to complete Part B were summarised and discussed by Faulkner (1999b). That report expanded the area of study to embrace more completely the full range of the Caledonide nappes in the whole of *central* Scandinavia, and proposed that the cave development model required both internal and external frameworks. The internal framework would show how cave morphologies are guided by the geological attributes of the carbonate outcrops. The external framework would show how the formation, development and destruction of karst caves are related to the geomorphological development of the host region.

The origin of the marble caves of Scandinavia has remained enigmatic for over a century, with many conflicting views being presented, sometimes by the same author. The reason became apparent as the proposed models grew in number and complexity. Because of the intimate association of the caves with their local landscape, it became necessary to study the geomorphological evolution of the whole study area itself, so as to understand the processes involved in the development of the karst caves. This required a multidisciplinary development of concepts in many subjects that are beyond the normal province of karst geomorphology. Consequently, the research journey was longer than anticipated and the text of this thesis is longer than originally planned.

In undertaking this unfunded, curiosity-driven research, the author drew on his experience of exploring caves in Scandinavia, having led or participated in 13 expeditions there since 1972, and having visited over 500 caves, most of which were previously unrecorded. Field trips in 1997, 1998 and 2000, each of 7–9 weeks duration, provided more targeted information about the caves and karsts. Additionally, in order to make comparisons with caves in metacarbonate outcrops in other Caledonide terranes, the author made one-week field trips to northern America (1996, 2002), Scotland (1997, 1999), Shetland (1999) and Ireland (1996, 1997, 1998).

The thesis resembles a detective story, in which the basic problem is simply stated (How did the caves form?), but the answer is rather complicated, and yet is capable of explanation by a simple concept that has not been proposed previously. This basic concept (realised after the 2000 field trip to Elgfjell) led to further questions, which were also capable of resolution as levels of understanding grew deeper. A most satisfactory outcome (for the author) is that the answers to these more detailed questions were nearly always found from within the scope of the basic concept itself, creating a robust thesis.

Trevor Faulkner

June 2005

Acknowledgements

I wish particularly to thank my two supervisors, Professor John Gunn (University of Huddersfield) and Dr. David Lowe (British Geological Survey), for their patience in continuing to support and assist what has become a long project. Invaluable advice and encouragement were also provided by many staff in the Geography Department at Huddersfield. In Norway, I have benefited from discussions with Professor Stein-Erik Lauritzen, Arne Grønlie, and Ulf Holbye. The people at the Norges Geologiske Undersøkelse in Trondheim were always a great help when I visited the library there, as were the staff in the offices of many Norwegian Kommunes, where I was often provided with local large-scale maps. Rod Gayer generously invited me to attend his lectures on Caledonian–Appalachian Tectonics at the University of Cardiff, and a field trip with Colin Davenport and his students at the University of East Anglia to study neotectonics in the Scottish Caledonides was extremely beneficial. The knowledge-base of the caves in the south Nordland area could not have been acquired without the friendship of the many people who took part in the various expeditions from 1972 to 1996. Of special significance were the field trips in 1997, 1998 and 2000, when I was variously accompanied by David St.Pierre, and by Edgar Johnsen and Odd Johansen from Norway. I thank them all for their companionship in the field, and David St.Pierre for drawing my attention to Grønlie (1975). In Sweden, I was similarly helped at the library of the Sveriges Geologiska Undersökning, and by members of the Sveriges Speleolog-Förbund, particularly Rune Magnusson, who provided me with a copy of the Swedish cave database. Torbjörn Doj provided me with information about caves east of the E6 in southern Nordland. On the academic side, this thesis could not have come to many of its conclusions without the written works of many authors in many disciplines who remain unknown to me, but are thanked nevertheless. I am especially grateful for conversations and emails with Professor Art Palmer (State University of New York) and Professor Wolfgang Dreybrodt (University of Bremen) who helped me approach the problem of aqueous calcite dissolution at low temperature without carbonic acid. Edgar Johnsen translated the abstract into Norwegian.

Keywords

allochthon, aquiclude, breakthrough, Caledonide, cave location, chemical inception, combination cave, cyclic speleogenesis, dedolomitization, deglacial speleogenesis, deglaciation, englacial, epigean, foliation, glacial situation, Holocene, hydraulic ratio, hydrogeological, ice-dammed lake, ice margin, inception fracture, inception surface, interglacial speleogenesis, isobase, isostasy, jökulhlaup, mainly vadose cave, marble, marine limit, metacarbonate, Mid Pleistocene Revolution, nappe, near surface aquifer, neotectonics, nunatak, Nye channel, one-eighth relationship, paleic surface, relict cave, Röthlisberger channel, sea level, seismicity, skarn, subglacial lake, subglacial reservoir, subglacial waterway, subsurface cave distance, tectonic inception, tidewater glacier, Top-Down, Middle-Outwards (TDMO) model, upside-down morphology, Vertical and Angled Stripe Karst, Weichselian.

CONTENTS

APPENDICES

LIST OF FIGURES

LIST OF TABLES

LIST OF PHOTOGRAPHS

Photo	D1.1	Swanlake Cave	D1
	D1.2	Klausmark Sink entrance	D1
	D1.3	Hornet Pot, Bulandsdal	D1
	D1.4	Twin Ducks Passage, Sirijordgrotta	D5
	D1.5	Eccles Gallery, Sirijordgrotta	D5
	D1.6	Arctic Passage, Sirijordgrotta	D5
	D1.7	Upstream waterfall, Sirijordgrotta	D5
	D1.8	Kidney Lake Cave	D5
	D1.9	Chamber in Gåsvasstindhola	D5
	D1.10	Godvassdalgrotta	D6
	D1.11	Shaft in Elgfjellhola	D6
	D1.12	Scallop in Elgfjellhola	D6
	D1.13	Secret Stream Cave, Elgfjell	D6
	D1.14	Slickensides in Paradox Cave	D7
	D1.15	Sarvejaellagrotta, Elgfjell	D7
	D1.16	Brown Stains Cave, Elgfjell	D7
	D1.17	Above Brown Stains Cave	D7
	D1.18	Diverging flow	D7
	D1.19	Injection Cave, Elgfjell	D7
	D1.20	Horizontal tectonic movement on Elgfjell	D8
	D1.21	Slot Chamber, Jegerhullet	D8
	D1.22	Cliff Cave entrances	D8
	D1.23	Cliff Cave entrance from inside	D8
	D1.24	Vatnhullet entrance	D9
	D1.25	Shattered marble	D9
	D1.26	Bjørkåsgrotta	D9
	D1.27	Geitklauvgrotta streamway	D9
	D1.28	Megachamber, Geitklauvgrotta	D9
	D1.29	Split arch in Geitklauvgrotta	D9
	D1.30	Neotectonism in streambed	D10
	D1.31	Cascade Pot	D10
	D1.32	Kammelv Sink	D10
	D1.33	Luktindgrotta	D10
	D1.34	Almdalselv cliffs	D10
	D1.35	Almdalselv gorge	D10
	D1.36	The Blockpile, Kvannlihola 2	D11
	D1.37	The Big Finger, Kvannlihola 2	D11
	D1.38	Grønndalsgrotta	D11
	D1.39	Bekkehølet, Grønndal	D11
	D1.40	Landbrua resurgence	D11
	D1.41	Sjliengojukke waterfall	D11
	D3.1	Nedre Jordbruvatn and Tverrfjell, from Jordhulefjell	D29
	D3.2	Durmålstind dry canyon	D31
	D3.3	Durmålstind canyon blockfield	D31
	D3.4	Dry canyon beside Toerfjellhola plateau	D31
	D3.5	Toerfjellhola resurgence	D31
	D4.1	Dry Passage in Bulandsdalgrotta	D48
	D4.2	Mollusc borings	D50
	D5.1	Sand bank in Invasjonsgrotta	D58
	D6.1	Tectonic movement in Poll Seomar	D76
	D6.2	Speleothems in Poll Seomar	D76
	D6.3	Stripe karst in Shetland	D80

Photographs are by the author, except where indicated.

ABBREVIATIONS AND NOTATIONS

NGF	Norsk Grotteforbund	BCRA	British Cave Research Association
SSF	Sveriges Speleolog-Förbund	UTM	Universal Transverse Mercator
NGU	Norges Geologiske Undersøkelse	GPS	Global Positioning System
SGU	Sveriges Geologiska Undersökning	NSW	New South Wales

Z	Zone		
HNC	Helgeland Nappe Complex	Z7	Åkervik to Fiplingdal
Z1	Coastal Area	Z8	Eastern Area
Z2	Fjord Area	Z9	Nesna Shear Zone
Z3	Central Granite Area	RNC	Rödingsfjäll Nappe Complex
Z4	Eiterådal and Jordbruelv	ZA	Bleikvassli Area
Z5	Mosjøen to Fjellryggen	ZB	Bjerka and Stor Akersvatn
Z6	Hemnes to Dunnfjell	ZC	Southern and Border Area
KU	Køli Nappes - Upper Nappes: Fauske, Gasak, Akfjell, Hattfjelldal, Jofjell, Krutvatnet Nappes		
KG	Køli Nappes - Middle Nappes: Gjersvik Nappe		
KL	Køli Nappes - Middle Nappes: Leipikvattnet / Orklump Nappe		
KS	Køli Nappes - Middle Nappes: Stikke / Virvass Nappe + Remdalen Repetition		
KB	Køli Nappes - Lower Nappes: Bjørkvatn / Joesjø Nappe		
SU	Seve Units	SB	Seve Belts (Western, Central and Eastern)
ML	Middle and Lower Allochthons		

A	Aragonite	CD	Calcian Dolomite
LMC	Low Magnesian Calcite	MD	Magnesian Dolomite
HMC	High Magnesian Calcite	SD	Stoichiometric Dolomite
DL	Dolomitic Limestone	CCD	Calcite Compensation Depth

OIS	Oxygen Isotope Stage	MSW	Main Scandinavian Watershed
DO	Dansgaard-Oeschger cycle	L	Litre
LGM	Last Glacial Maximum	atm.	Atmospheres
YD	Younger Dryas	cal. a	Calendar years
IRD	Ice-Rafted Detritus	^{14}Ca BP	Radiocarbon years Before Present (AD1950)

KT	Karst Type	R	Contact metamorphism
V/VSK	Vertical Stripe Karst	T	Proximity to a major thrust
A/ASK	Angled Stripe Karst	CT	Cave Type – see section 5.2.5 for each type
L/LAK	Low Angle Karst	CL	Cave Location – see section 5.3.4 for each location
C/CFK	Complexly Folded Karst	GS	Glacial Situation – see section 5.3.5 for each situation

CA	Catchment Area	RC	Relict Cave
XS	Cross-section	MV	Mainly Vadose cave
VR	Vertical range	CC	Combination Cave
SE	Sink Entrance	Sh	Shaft
RE	Resurgence Entrance	BC	Boulder Choke
DE	Relict Entrance	RV	Relict Vadose
CS	Cave Stream	DC	Chemical Deposits
SP	Sump Pool	FS	Fluvial Sediments
Ch	Chamber	HG	Hydraulic Gradient (Head / Path Length)
		HR	Hydraulic Ratio (Head / Path Length^2)
DML	Deglaciation Marine Limit	SGL	Subglacial Lake
GML	Glaciation Marine Limit	SGR	Subglacial Reservoir
IDL	Ice-Dammed Lake	hp-SGR	High pressure SGR
PBL	Plastic Behaviour Limit	lp-SGR	Low pressure SGR
N	Nye channel	ap-SGR	Air pressure SGR
R	Röthlisberger channel	SGW	Subglacial Waterway
IHH	Inception Horizon Hypothesis	TDMO	Top - Down, Middle – Outwards

Utdrag

Dette er den første omfattende studie av grotters begynnelse og utvikling i metakalksoner. Hovedstudiet omfatter en 40000km^2 stor region i midtre Skandinavia som inneholder over 1000 forskjellige kalksteinsområder, og har nermere 1000 dokumenterte karst huler (med lengder opp til 5,6km) Området, som ble gjentatte ganger nediset i sen Cenozoisk tid, omfatter en rekke skyvedekker i Cambro-Silurisk Kaledonider, en paleisk fjellrekke med terreng som nå finnes på begge sider av Nord-Atlanteren. Informasjonen om stripe karst og andre kalksteinshøyder og deres innhold av grotter ble samlet i en computerbasert database, som gjorde det mulig å analysere slektskapet mellom indre egenskaper i grottene og deres ytre geologiske og geomorfologiske omgivelser. Et heller overensstemmende mønster viste seg. For eksempel, lengdene på karsthydrologiske systemer er ufravikelig kortere enn 3,5 km, og hulegangene er sjelden i en vertikal posisjon, mens vanlig finnes de innen 50 m av den overliggende overflaten. Denne entydigheten peker på at den relevante begynnelsen av hulene, utvikling og fjernings prosesser virket i en regional skala, og over lange tidsrom. En konsekvens av den nære assosiasjoen av grotter med landskapet er at grotteutvikling kan bare bli forstått i sammenheng med den geomorfologiske utviklingen av vertsregionen. En gjennomgang av den nyeste kjennskap til begynnelsen og utviklingen av grotter i sedimentære kalkberg konkluderte med at huleutviklingen i midtre Skandinavia ikke kan forklares med disse ideene. Fem ny innbyrdes beslektede modeller er konstruert for å forklare grotteutvikling i metakalkfjell i de forskjellige Kaledonske områder. Disse er:

1. Den tektoniske begynnelses modell - denne viser at det bare er åpnede sprekkeruter, opprinnelig skapt av de seismiske rystelser som følger med avisingen, som kan gi anledning for oppløsning av metakalkstein som har ubetydelig porøsitet.

2. Den ytre modell av huleutvikling - denne "svart-box" tilnærmingen avslører at dannelsen, utviklingen og nedbrytingen av karstgrotter er beslektet med utviklingen av det landskap de befinner seg i. Under Pleistocene, var disse prosessene dominert av perioder med nedising, som førte til periodisk grottetilblivelse, og utvikling av stadig lengre og dypere systemer, hvor maksimal distanse til overflaten vanligvis gjenstår innenfor en åttendedel av forandringen i det lokale relieff.

3. Den hydrogeologiske modell - denne beviser at grottene utviklet seg til deres kartlagte dimensjoner på tidsrom overensstemmende med de to første modellene, innenfor den tvang pålagt av fysikken og kalsitt-oppløsningskjemi og erosjon, hovedsakelig i rent vatn. Relikte grotter ble overveiende utviklet under hel vannfylling nede i aktive bredemte sjøer i avisingstiden,med asymmetrisk avrenning på øst og vestvendte skråninger. For det meste vadose grotter ble utviklet hovedsakelig under nåværende interglasial, som bekkeløp, med maksimum dimensjoner bestemt av nedbørfeltet.Kombinasjonsgrotter utviklet seg under både avisings og mellomistidsforhold. Tverrsnittet av freatiske passasjer adlyder en non-fraktal fordeling, fordi de utviklet seg med maksimal hastighet i samme tidsrom. Freatiske huleåpninger høgt til fjells kunne bli forstørret av frost / tine prosesser ved overflaten av bredemte sjøer, og ved havnivået ev marin aktivitet under isostatisk landhevning.

4. Den indre statiske og dynamiske modell - denne "kvit-box" tilnærmingen viser at mange grotter har "ovenfra-ned" morfologi, med relikte freatiske ganger over en enkel, først og fremst vados bekkeprofil. Begge typer av ganger er ledet langs begynnelser som følger geologiens struktur og sprekker i kalkfjellet. Dynamiske, grottene utviklet i en "Top-Down, Middle-Outwards" sekvens (TDMO) som kan ha strukket seg over flere glasiale perioder, og passasjer i de eldre "mange-sykllers" grotter ble fjernet innover og nedover av glasial erosjon.

5.Den Kaledonske modell - denne viser at de samme prosesser (med noen raffinementer) kan anvendes på grotteutvikling i de fleste andre Kaledonske områder. Den største innflytelsen på grottedimensjoner var tykkelsene på de nordatlantiske nedisingene og hulenes posisjoner i forhold til avisingenes bredemte sjøer og til lokal topografi. Andre innflytelser inkluderte kontakt metamorfose, nærhet til større trykksoner, og marine framstøt. Med kjennskap til disse påvirkningene for hvert område, kan middels grotte-dimensjoner forutsies.

Avhandlingen gir anledning til å utvide de fem modellene, slik at grotteutvikling i andre nedisede metamorfe og sedimentære kalkfjell kan bli bedre forstått, og omvendt, slik at landskapsutvikling kan utledes fra grottedata.

Frontispiece 1 **The Jordbruelv Waterfall (Z4)**
Gorge created where the Jordbruelv meets the limestone. Neotectonic horizontal joints in vertical stripe karst provide a focus for tectonic inception

Frontispiece 2 **Entrance to Eiterådal Resurgence Cave (Z4)**
The epigean nature of this cave is typical of many caves in the study area.

CHAPTER 1 INTRODUCTION

The main aim of this thesis is *to develop a conceptual model for cave development in metacarbonate rocks in central Scandinavia, and to test the applicability of the model in similar geological environments in other parts of the world.* The background to the research project is described in the Preface.

1.1 Research objectives

It was a project aim to derive the speleogenetic processes for the caves and karsts of metacarbonate rocks from first principles, and to provide *system information*, to meet challenges set by Ford and Williams (1989, 248–249) and Quinif (1998, p1). However, the author's approach is, of necessity, conditioned by a previous level of understanding of speleogenesis in sedimentary, rather than in metamorphic, limestones. Rather than study a small number of caves in detail, the available evidence from published sources and from the author's field work was reviewed for *all* the known caves and carbonate outcrops across the whole of central Scandinavia.

This thesis does not seek to replace the existing theories of cave development, which primarily apply to sedimentary karsts. However, it does introduce a new paradigm to explain the development of caves in Caledonide metamorphic limestones, and elements of this paradigm may also be applicable in other karst situations. It became appropriate to expand the originally-conceived *internal* model into static and dynamic models of internal cave morphologies, and to add the *tectonic inception*, *hydrogeological* and *Caledonide* models to the originally-conceived *external* model. Together, these five models comprise the paradigm that is necessary to gain a deeper insight into the evolution of the caves in Caledonide metalimestones.

The objectives of this thesis are therefore to use the derived data and the five models collectively to address the key questions concerning Caledonide speleogenesis:

1. Is there any systematic variation of karstification across the main study area, and how does this compare with the karstification of the other Caledonide terranes?
2. What are the processes involved in the evolution of the caves?
3. Is there is a *prima facie* case that similar processes and timescales operate across the whole study area, and in the other parts of the Caledonides?
4. What are the timescales over which the caves evolved, and how do these relate to local geomorphological events?
5. What are the key parameters that have dominant roles in karst evolution across all the Caledonides?

1.2 Methodology

The following activities were performed within this project, many being discussed in later Chapters. They are listed in order of initiation, but were commonly pursued iteratively and in parallel. With hindsight, this methodology follows the *global analysis conceptual approach* used by Tognini (2001).

1.2.1 Literature search

The references list over 600 papers that contributed to the project. Several are very recent, showing that many conclusions in this thesis could not have been reached if the project had been tackled earlier. Literature was studied in five main areas:

- General geology, metamorphic geology, geomorphology and karst geomorphology
- Geological research into the development of the Scandinavian (and other) Caledonides, with particular emphasis on the study area and its metacarbonate outcrops
- Cave exploration in the study area, and other related areas
- Cave science in Norway and Sweden
- Related subjects: Quaternary glaciations, glaciology, the Holocene, seismology and tectonics, isostasy and sea level, the physics and chemistry of limestone dissolution, and the hydrogeology of crystalline rocks.

1.2.2 Course and conference attendance

Knowledge of many of the above topics was also gained from attending courses held at the Universities of Huddersfield and Cardiff, together with attending other conferences and seminars.

1.2.3 Use of topographical and geological maps

Karst outcrops and features were recorded on published maps.

1.2.4 Field work

Information about the location of caves and the characteristics of their local karst outcrops were recorded in the field together with underground studies and surveys.

1.3.5 Computer databases

Databases were generated for all the karst outcrops and caves in central Scandinavia and cave databases were generated for many of the other Caledonide terranes. Factual deductions about cave attributes were then derived from computer analyses of these databases.

1.2.6 Synthesis

The knowledge gained from the above activities was synthesised to prepare the five conceptual models of cave development, using the thesis as a working document. A comprehensive four-cycle revision process then maximised internal feedback, whilst maintaining consistency.

1.3 Thesis structure

Following this Introduction, the thesis comprises three main parts. The contemporary knowledge of both the geological history of central Scandinavia and the speleogenesis of sedimentary and glaciated carbonates is reviewed in Chapters 2 and 3, supported by data in Appendix A. In the second part, Chapters 4 and 5 with Appendices B and C discuss the author's studies of the karsts and caves of central Scandinavia. Conclusions are presented at the end of Chapter 5. In the third part of the thesis, Chapters 6–10 with Appendices C and D present the conceptual models that propose the way the caves have developed, from five different, but complementary, frameworks. These models were derived from the knowledge and evidence presented in the first two parts, and they extend from a consideration of the caves in the study area itself, to some of the metacarbonate karsts of the other Caledonide terranes. Information about the caves of central Scandinavia was assembled and analysed by considering the *external* and *internal* attributes of each of the caves and its environment. This external-internal theme is also used to structure the order in which sections and sub-sections are presented. Ages discussed in this thesis later than 50ka BP refer commonly to radiocarbon years (^{14}Ca BP, i.e. before AD1950). Karst terminology follows the definitions of Lowe and Waltham (1995), except where specified in the text and in the Appendices. New terms are summarised under Abbreviations and Notations.

1.4 The study area (Figures 1.1 and 1.2)

The study area extends from the Atlantic Ocean, with many coastal islands off the western coast of Norway, across the international border into Sweden to the east. The western third of the area comprises the totality of the Helgeland Nappe Complex (HNC; section 2.1 discusses the geological terms used). This is bordered to the north at Ranafjord in the county of Nordland at 66°20', where the HNC overlies the Rødingsfjell Nappe Complex (RNC). The border to the south is the Grong–Olden Culmination at 64°30', where stratigraphically lower rocks come to the surface. Grong is in the county of Nord Trøndelag, some 60km south of the border with Nordland, and some 160km north of Trondheim. In defining the eastern limit, the north–south extent of the HNC is continued eastward, across the Norwegian / Swedish border, and generally across the lower nappes as far as the Caledonide thrust front. However, the incomplete publication to date of modern geological maps in the Swedish part of the area led to the northern section of the eastern border being defined along the edges of some of the available geological maps, and along internal structures. This rather arbitrary eastern edge to the study area is of no great significance. No known carbonate caves exist there, and from the evidence farther south, there are likely to be only a few small carbonate outcrops.

The Norwegian part of the study area lies in the counties of Nordland and Nord Trøndelag. It is within the region of Helgeland, which also extends north of Ranafjord. This part is called 'north central Norway' in this thesis, a term used in some geological papers. The Swedish part of the study area lies within the counties of Västerbottensland and Jämtland, called the 'central Swedish Caledonides' in this thesis. The whole area measures about 200km by 200km, i.e. 40000km^2, which is roughly the size of

Switzerland. Figure 1.1 locates important towns, fjords, rivers and catchment areas. Figure 1.2 is a diagrammatic map that delimits the study area and identifies the topographical and geological maps used.

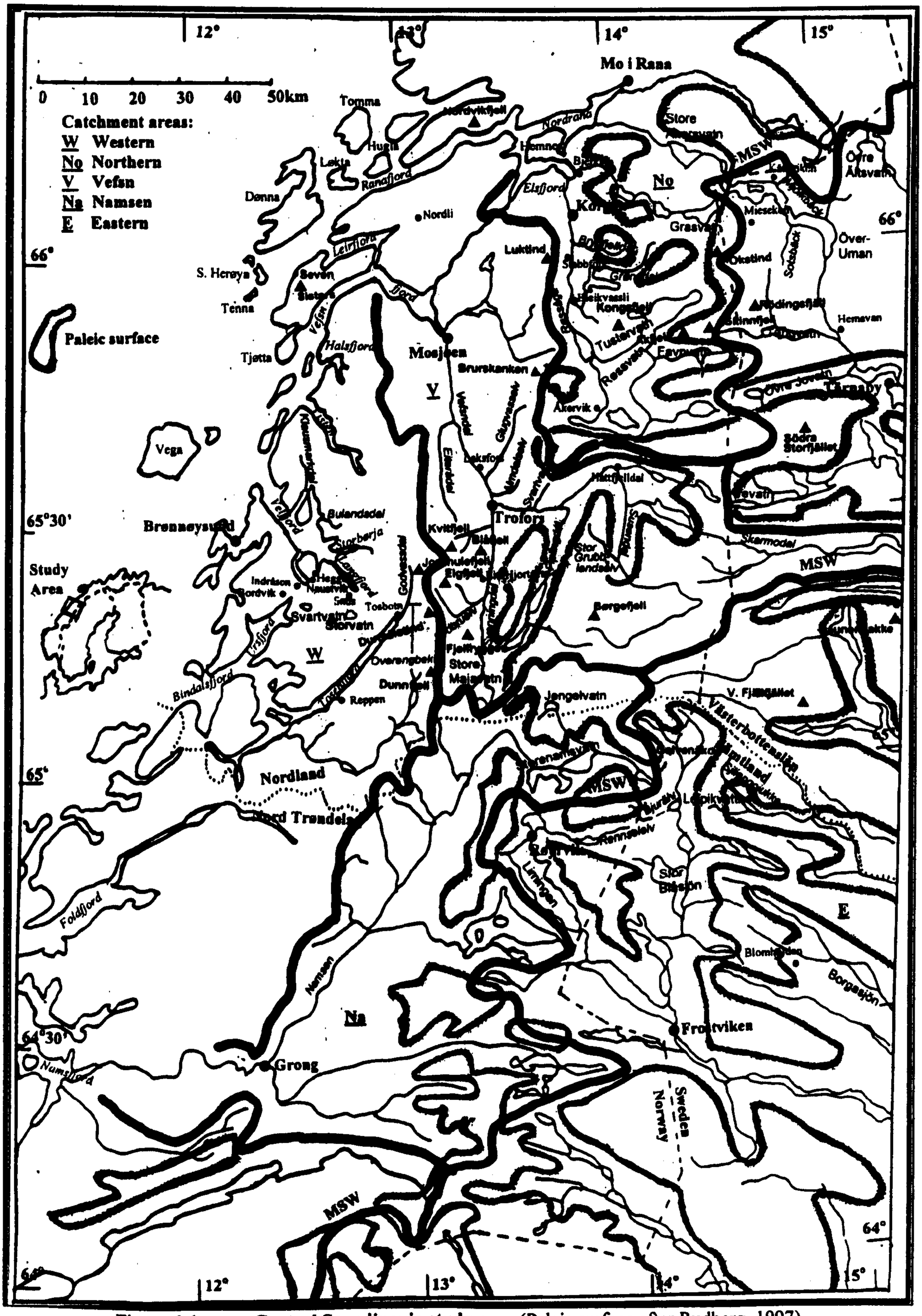

Figure 1.1 **Central Scandinavia study area** (Paleic surface after Rudberg, 1997)

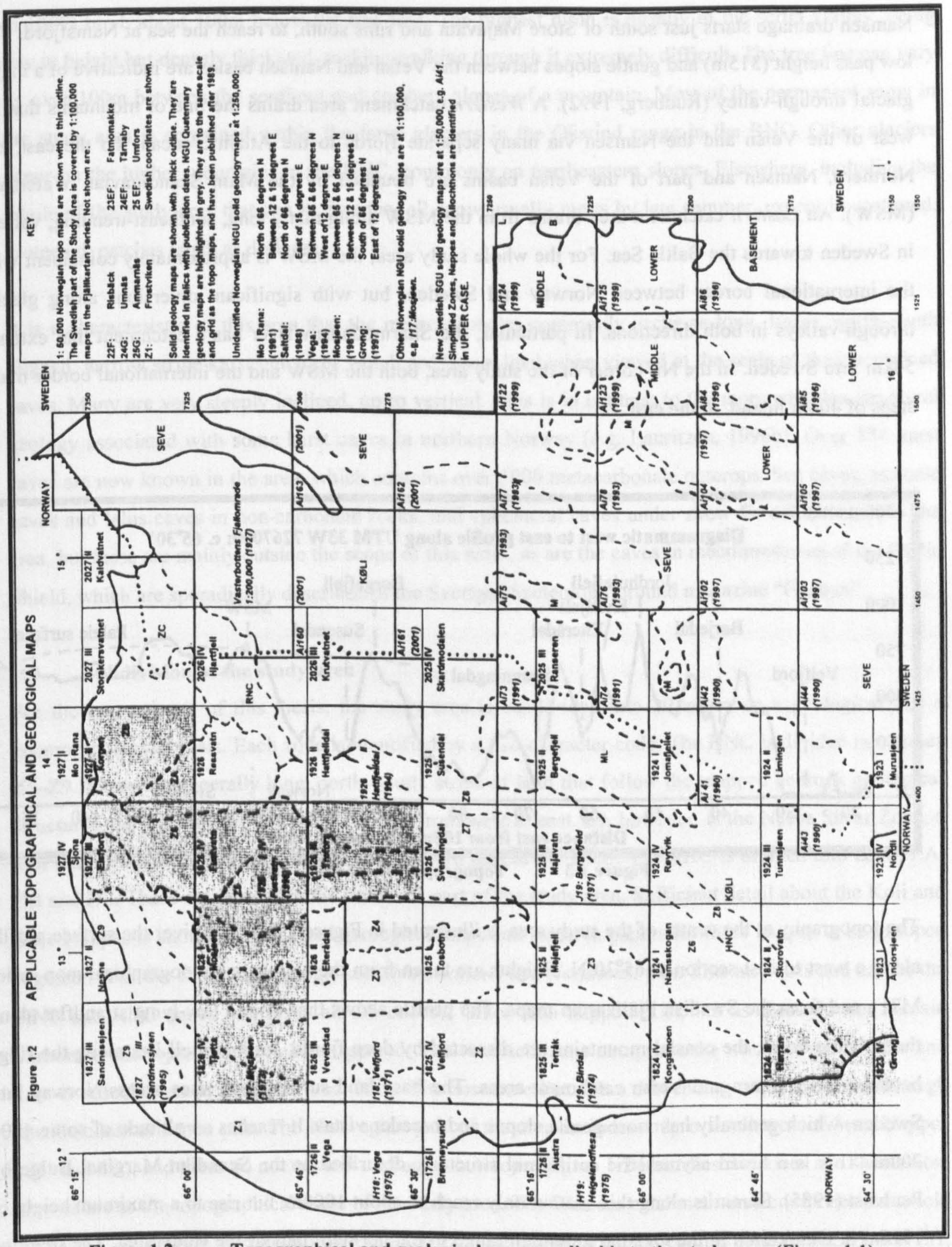

Figure 1.2 Topographical and geological maps applicable to the study area (Figure 1.1)

In the centre of the study area are three large drainage basins that are referred to here as the *Northern*, the *Vefsn*, and the *Namsen* catchment areas. The Northern catchment area includes the lakes Store Akersvatn, Grasvatnet and Røssvatnet, which are near the Swedish border, and which eventually discharge into the sea at Ranafjord. The Vefsn basin drains northward from Store Majavatn, initially along Svenningdal, to Vefsnfjord at Mosjøen. It collects drainage at Trofors from the Susna and from the Skarmodalselv. The

Namsen drainage starts just south of Store Majavatn and runs south, to reach the sea at Namsfjord. The low pass height (315m) and gentle slopes between the Vefsn and Namsen basins are indicative of a major glacial through-valley (Rudberg, 1992). A *Western* catchment area drains the line of mountains that lie west of the Vefsn and the Namsen via many separate fjords to the Atlantic ocean. To the east, the Northern, Namsen and part of the Vefsn basins are bounded by the Main Scandinavian Watershed (MSW). An *Eastern* catchment area drains from the MSW along many long, southeast-trending, valleys in Sweden towards the Baltic Sea. For the whole study area, the MSW is approximately coincident with the international border between Norway and Sweden, but with significant diversions along glacial through-valleys in both directions. In particular, the Skarmodalselv river has a catchment that extends 54km into Sweden. In the NE corner of the study area, both the MSW and the international border make steps of 40km inland, to the east.

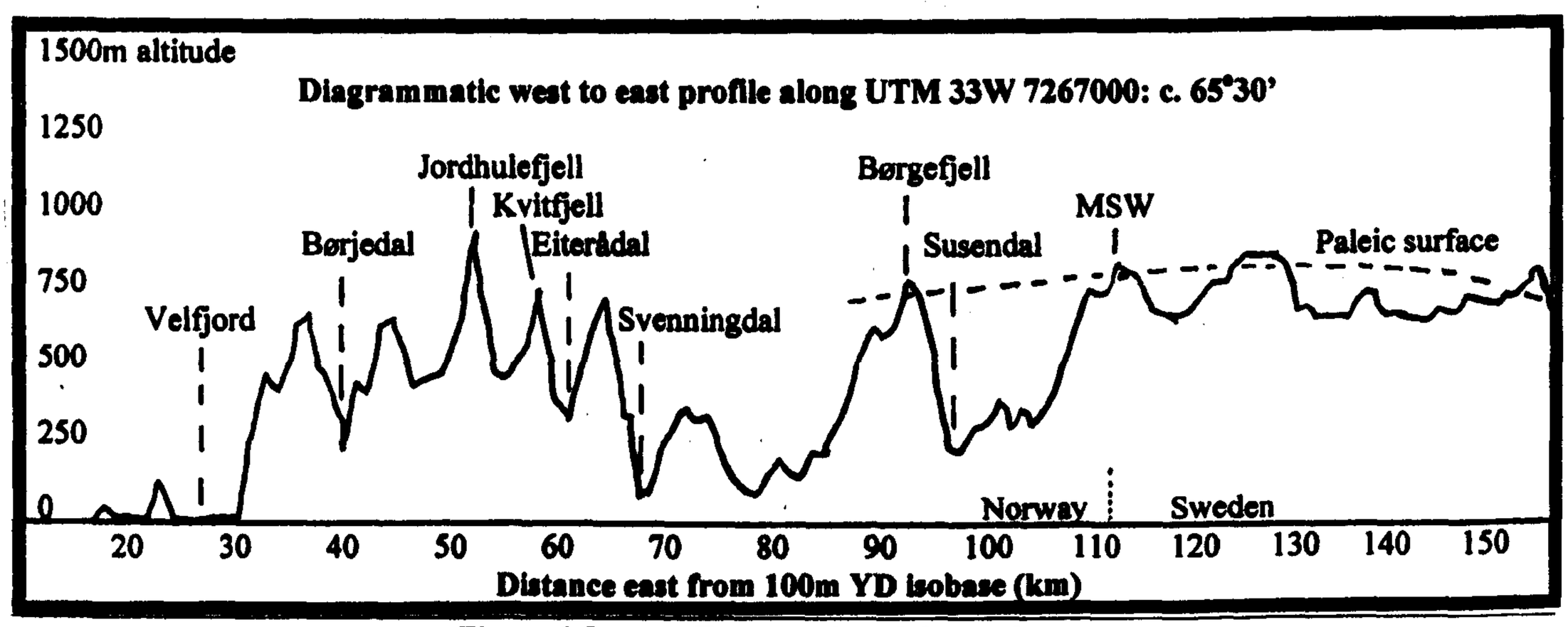

Figure 1.3 Topography of the study area

The topography at the centre of the study area is illustrated in Figure 1.3, which gives the surface profile along a west to east section at 65°30'N. Heights are taken from the Norwegian topographical map series M711 and from the Swedish Fjällkartan maps. The profile shows that from a low-lying strandflat along the Atlantic coast, the coastal mountains are dissected by deep fjords. Jordhulefjell lies along the ridge between the Western and Vefsn catchment areas. The base land surface then rises across Norway into Sweden, which generally has more gentle slopes and broader vistas. It reaches an altitude of some 400–700m. This is a broad asymmetric antiformal structure, described as the Scandian Marginal Bulge by Peulvast (1985). Summits along this section only reach to about 1000m, but rise to a maximum height of 1916m at Oksskolten in the Okstind mountain range in the northern part of the study area. The tree line gently ascends towards the east, starting at a height of about 400m on the coast and reaching a fairly constant elevation of 800m some 80km inland. Hence, in Sweden, most of the land surface is below the tree line along this section, making progress on foot quite difficult if not following a good path. Some 50km north, the mountains are much higher and the tree line is also some 50m lower, so that the higher slopes are grassy or consist of bare rock, even in Sweden. Some 50km south, the tree line is about 50m higher. The forest consists generally of mixed silver birch, pine and spruce at lower altitudes, giving way

to 100% birch about 100m below the tree line. The highest birch is usually of the scrub variety, being low in height but densely thicketed, making walking through it extremely difficult. The tree line can vary by over 100m between the southern and northern slopes of a mountain. Most of the permanent snow in the study area is contained within the large glaciers in the Okstind range in the RNC. Other glaciers occur on the higher mountains in the HNC, commonly on northeastern slopes. Elsewhere, including the whole of the study area that lies in Sweden, all snow usually melts by late summer, except in scattered, protected, patches (such as dolines).

It is a characteristic of this area that the metacarbonates commonly occur as long, linear, north–south aligned, narrow stripe karst outcrops, which are homoclinal when viewed at the scale of their contained caves. Many are very steeply inclined, up to vertical. This is in contrast to the more complex structural geology associated with some karst caves in northern Norway (e.g. Lauritzen, 1996b). Over 884 karst caves are now known in the area, which contains over 1000 metacarbonate outcrops. Sea caves, tectonic caves and talus caves in non-carbonate rocks, and ephemeral caves under snow fields also exist in the area, but these are mainly outside the scope of this work, as are the caves in metalimestones of the Baltic Shield, which are sporadically described in the Sveriges Speleolog-Forbund magazine "Grottan".

1.5 Subdivision of the study area

For the convenience of this thesis, the study area is subdivided into 20 zones on a geological and a geomorphological basis. Each zone is identified by a two-character code. The HNC is divided into zones Z1–Z9. These are generally long, north–south, strips of land that follow the mapped bedrock geological structures and watersheds, and are numbered from west to east. Z9, however, is the Nesna Shear Zone, a unit that forms the lower boundary of the northern part of the HNC. The RNC is divided into zones ZA, ZB and ZC. These are located in the northeast part of the study area. Sufficient detail about the Køli and Seve Nappes is shown on published geological maps and research papers for these nappes to be grouped together. (For the chosen groupings, see *Abbreviations and Notations,* pxx. This also lists and names the HNC and RNC zones and gives all the codes). Other Køli nappes exist, but as these do not contain carbonate outcrops, they have been ignored. The twentieth zone comprises the whole of the Middle and Lower Allochthons in the study area (ML). The zones are listed in a descending sequence down through the Caledonian nappe pile. The Norwegian part of the area includes only a small area of Seve Nappes (SU and SB), and these do not contain carbonate outcrops. Figure 1.2 identifies the zones and shows how they relate to the topographical maps of the study area. The Western catchment area comprises the whole of Z1, Z2, Z3 and Z9, and the northern part of Z6. The Northern catchment has parts of Z6, Z7, Z8, ZA, ZB, ZC and the Køli nappes. The Vefsn catchment area comprises the whole of Z4 and Z5, and parts of Z6, Z7, Z8, ZA, the Køli nappes and ML. The Namsen catchment area contains parts of Z6, Z7, Z8, Køli and Seve nappes, and ML. The Eastern catchment area comprises parts of ZB, ZC, Køli and Seve nappes, and ML.

1.6 Cave exploration in central Scandinavia

Knowledge of the karst caves is dependent on the work of many people. The resulting total picture of known cave locations and characteristics is necessarily biased by the methods and motivations of each of them. Thus, in order to gain a better understanding of the true speleogenetic nature of the region, the revelation and recording of cave sites, firstly of littoral caves by seafaring travellers, then by geologists, and finally by sporting cavers, requires some analysis. This last group has developed working techniques such that, at present, 'new' caves can be found and explored almost at will.

The places investigated for caves are inevitably conditioned by the methods of access. Before the 1960s, road access to northern Norway was along the narrow E6, via Grong and Mosjøen. Its gravel surface made journey times very long. There were few side roads. Since then, every year saw an improvement to the road network, and gravel roads were extended into many side valleys. However, even now, some potential karst areas are still too remote to encourage access during short visits.

1.6.1 Cave exploration in Norway

Large coastal caves were reported in Norway by at least the 12th Century (St.Pierre D, 1988). The formal reporting and exploration of caves in inland limestones from about 1870 led to a continuous increase in the number of recorded caves. Most of these limestone caves are in the county of Nordland, and many caves up to several kilometres in length have now been explored north of the study area. Up till July 2000, the longest was the **Okshola-Kristihola** system at about 11km, with a depth of 185m. The deepest is **Rågge Javre-Raige** at about 580m. From 1870 to the Second World War, the discoveries were mainly made by Norwegian geologists during field mapping. An important work (Helland, 1907) gave many locations of holes and streams that go underground. Large caves were reported by Oxaal (1914). One of these, **Grønligrotta**, was opened to the public as a showcave. Horn (1937) described some of the caves in the Rana–Svartisen district, and Horn (1947) gave lengths for 19 caves in the county. Prior to the advent of the systematic reporting of caves, many were known and used by local people. There are accounts of small-scale human habitation, and, more rarely, signs of use of dry entrance areas for storage and shelter by the Sami people, whilst tending reindeer in remote locations.

For a period after 1945, new Norwegian caves were almost entirely discovered by expeditions that visited the country from abroad. The bottom of **Larshullet** in Rana was reached in 1951, at a depth of 326m, by a combined French, British and Norwegian team. From the mid-1950s, most expeditions came from Britain. From 1964 to 1979, typically four or five groups from English caving clubs visited Norway each year. This activity reached a peak in 1977, when nine such groups went to Norway.

The 1980s saw a reversal in the roles of English and Norwegian groups. Between one and four English clubs still visited each year. However, it is clear from reading the Norwegian caving journal *Norsk Grotteblad*, that local clubs and members of the Norsk Grotteforbund (NGF, founded in 1977) were making up to eight discovery caving trips per year. These were sometimes in joint Anglo / Norwegian

expeditions. Whereas significant new caves were still being found, exploration was also becoming more technical. Some of the longer caves were 'pushed' farther into more difficult parts, by climbing or by diving. For example, another 300m-deep system, **Greftkjelen**, was extended and attempts were made to connect it to **Greftsprekka**, which has an entrance nearby. Cave divers completed a 500m-long dive through the **Glomvatn Underground Outlet** and started the exploration of a submerged system deep below Plurdal.

Local cave exploration was maintained at the same level into the 1990s, whereas the number of English expeditions reduced to only about one per year. Undoubtedly, cave explorers have now visited the majority of the easier, open, 'stream cave possible' sites that appear on both the old 1:100000 and the new 1:50000 series maps. Nevertheless, a recent reward is **Tjoarvekrajgge**, in northern Nordland. This system, which is now c. 17km long (the longest in Scandinavia) and 502m deep, is still being extended by a joint Swedish-Norwegian team. An important karst area lies in the kommune of Rana, just to the north of the main study area (St.Pierre and St.Pierre, 1969 and 1971).

Karst caves are also known south of the study area, although not in great numbers. Significant caves have been explored east of Steinkjer, at Molde near the coast, in the Jotunheimen mountains of southern Norway, and near Oslo. The most recent account of the contemporary state of cave exploration in Norway was by St.Pierre, D (1988). St.Pierre (2003) listed Norway's longest and deepest caves.

1.6.2 Cave exploration in north central Norway

Cave exploration in north central Norway also started during geological mapping early in the 20th century. Hoel (1906) reported caves in Z2, and Oxaal (1910) discussed two of the few caves in the area to become minor tourist attractions: **Jordbrua** and **Marmorgrotta** in Rennselelvdal (KL). Helland (1907 and 1909) referred to many caves and underground streams. The report of one of the visits of Professor Jean Corbel from Lyons to Scandinavia covered the Rennselelvdal karst (Corbel, 1952a). Corbel (1957) discussed many other karst sites in north central Norway. Corbel's observations caused British caving expeditions to visit Norway, but during the 1960s and 1970s these concentrated most of their effort north of Mo i Rana. Despite having many (narrow) limestone outcrops, the southern part of Nordland seemed to be less promising for cave discovery. There were very few caves recorded south of Mo. The underground streams that were marked on maps did not extend across a large vertical range. The steeply-banded limestones were also of an uncertain vertical extent. Accordingly, the first purely caving visits to the area were not until those of David Heap's team in 1967 and 1968. Since then, several British caving teams made repeat visits. These include 'South Nordland Expeditions', most of which were led or participated in by the author, and which usually occurred every two years in the 1980s and 1990s. Although no very long or very deep caves were found, most of these three-week expeditions reported about 40 'new' caves, with 3–5km of total new passage length. Some more distant karst areas were accessed by backpacking all the equipment needed up to a mountain camp, which was then occupied for

up to two weeks. No areas have yet been visited that would require more than one day's walk from the nearest road.

A Swedish team has also recorded previously unknown caves in the area in recent years, especially in Z5, Z6, Z7, ZA and ZC. The field trips by the author in 1997, 1998 and 2000 revealed the existence of over 65 more caves, with total passage length of over 5km. Some of these remain incompletely explored and no details have been published to date. From about 1997, cave explorers living at Brønnøysund and Mosjøen started to find and explore caves in their vicinity. Local enterprise has also attempted a small trade in adventure caving for tourists at several sites.

At present, over 700 adequately-reported caves are known in south Nordland, with a total passage length of 58km. Additionally, 100 unexplored or incompletely-reported caves exist. The longest known caves are two stream caves, **Toerfjellhola** (Z3) and **Stor Grubblandsgrotta** (KU), which are both nearly 2km long. The deepest cave is **Ytterlihullet** (ZA), which is 180m deep. Cave cross-sections vary from under $1m^2$ (commonly) up to $100m^2$ (rarely). The caves occur at altitudes from over 900m down to sea level, and the longer ones typically contain active stream passages with several sumps in spring and summer, below higher-level abandoned passages. Speleothems are rare in general, but some individual caves and passages are well decorated. A more complete summary of cave exploration in Helgeland was described by Faulkner (2000c).

Throughout the area, the larger and more easily-accessible caves are regularly visited by local people, leading to some graffiti and the removal of speleothems. However, most caves known to the author in south Nordland have not been revisited after their first exploration. It was standard practice to make cave surveys without marking survey stations permanently, and it was never necessary to insert bolts to facilitate the descent of shafts. The overwhelming majority of these caves therefore remain in a near-pristine condition, and are ideal objects for scientific study.

1.6.3 Cave exploration in Sweden

Sweden has many tectonic and talus caves formed in the Proterozoic rocks of the Baltic Shield, east of the study area. Many of these have been known for a long period of time, but they remain out of scope for this study because of their location and the non-carbonate nature of the rock. These old rocks also contain some metacarbonate outcrops, with perhaps some 20 karst caves up to 20m in length, but they have been little investigated and are also out of scope.

The karst caves of Sweden, commonly referred to as "mountain caves" (fjällgrottorna), occur within 60km of the Norwegian border, in the Swedish part of the Caledonides. As in Norway, the early reporting of caves in metacarbonates fell to geologists in the course of mapping. The first such cave, **Svenoniusgrottan**, in the Bjurälv valley (KL) was recorded in 1879 (Svenonius, 1880 and 1910). The Svenonius account discussed the karst landscape in this valley, which has many deep conical dolines

formed in alluvium. It has since become one of the most visited educational karst sites in Sweden. The next recorded karst location appears to be at **Tjårrogrottorna** (KU), which was located in 1927 (Beskow, 1929), and this is also within the study area. It is mentioned in local tourist literature (Wilhelmsson, 1997) and was also described by Faulkner (2000a).

The impetus for a more systematic search for karst caves in Sweden undoubtedly came from the work of Corbel. His visits to Scandinavia during the early 1950s included the Bjurälv area and the Björkliden area at Tornetrask, which is east of Narvik in northern Norway (Corbel, 1952a and 1957). **Lullihatjårrogrottan** at Björkliden has become one of the longer caves of Sweden at 1300m. Early visits to this cave were by Swedish academics from Lund University, and then from Chalmers Technical High School in 1964.

A large increase in cave discovery and exploration all over Sweden resulted from the formation of the Sveriges Speleolog-Förbund (SSF) on 28 May 1966. Subsequent discoveries were reported meticulously in its organ *Grottan*, which has been published four times per year in an almost unbroken sequence since 1966. The first issues were edited by the pioneer speleologist Leander Tell. Hence, in complete contrast to Norway, the record of cave discovery in Sweden can be ascertained by reading just one source. Furthermore, all karst caves were explored by Swedish-led expeditions, with only occasional assistance from visiting foreign cavers. The momentum is maintained by an SSF mountain camp of one to two weeks each summer, which rotates around all the major karst areas. In another contrast with Norway, several review publications brought the contemporary state of knowledge of Swedish caves to the attention of all Swedish cavers and, indeed, to a wider public. These included works by Tell (1955 and 1974), Engh and Sjöberg (1981, from which much of the above information has been derived) and Åström (1986). Useful overview articles published in *Grottan* include Westerdahl (1974) and Sjöberg (1986, 1996e and 1997). A computer-based database of all known caves in Sweden, including tectonic caves, is maintained by the SSF (R. Magnusson, Sveriges Speleolog-Förbund, pers. comm., 1998).

Westerdahl and Linden (Westerdahl, 1974) divided the Swedish Caledonide carbonate outcrops in the counties of Norbotten and Västerbotten among eight areas, to which Engh and Sjöberg (1981) added a ninth in the northern part of the county of Jämtland. Areas I to VI lie to the north of the study area, and areas VII, VIII and IX lie within the study area. Not included in this scheme are the scattered karsts in the various nappes south of area IX and the study area, which might loosely be called the Östersund area. Area II (Tornetrask) and area IV (Padjelanta–Virihaure) are each subdivided into three major karst regions. These six regions have been visited many times since the 1960s, yielding six caves over 500m long, the longest being **Övre Kåppasjokkgrottan** in area II at over 2.1km. The second deepest cave in Sweden is **Vuoitaskallogrottan** in area II, at 140m depth.

Apart from the many major caves found in the study area (section 1.6.4), a long cave formed in *sedimentary* Silurian limestones has been repeatedly extended since the 1960s. This is

Lummelundagrottan, on the island of Gotland in the Baltic Sea. Now about 5km in length, it vies with **Korallgrottan** (KL) in area IX to be the longest cave in Sweden, as each cave leapfrogs ahead of the other when new passages are added to the surveys.

1.6.4 Cave exploration in the central Swedish Caledonides

There are 156 adequately-reported caves in the central Swedish Caledonides, with a total passage length of 16km, plus some 50 smaller, incompletely-reported, caves. Swedish cave exploration in the study area started at its NE corner in the mid-1960s in area VII, near the lake Över-Uman and east of the Okstind mountains. Engh and Sjöberg (1981) divided area VII into four regions: Övre Ältsvattnet (A); Kåtaviken–Mjölkbäcken (B); Mieseken (which contains **Labyrintgrottan**) –Arttjårro (C); and Sotsbäcken–SW Artfjäll (D). Regions B and C lie in RNC ZC. Regions A and D lie in the Köli (Upper) KU zone. Two major Swedish caves, **Sotsbäcksgrottan** (KU) and **Labyrintgrottan** (ZC), were explored in 1966. They were since extended during fairly regular visits to reach c. 1850m and c. 2500m in length. Over 100 shorter caves (up to 320m length) were explored by the Övre Altsvatten Expedition in 1970 (Oldham and Oldham, 1971; Sjöberg *et al.*, 1971; Sjöberg, 1980). The Kåtaviken area has been visited sporadically by cavers since 1966 and was also publicised locally as a "Grottstig" (cave path) by Wilhelmsson (1997). The path provides a 4km-long walk to caves and karst features that people are invited to explore as far as they wish. The longest cave here is **Östra Jordbäcksgrottan** (ZC). This is 460m long, with a relatively large descending stream passage, and is 45m deep. The SW Artfjäll area includes Rödingsfjäll, where a stream descends along a narrow limestone outcrop. **Glimåkragrottorna** (ZC) and other short caves were explored there in 1978, although the area was visited briefly in 1970 and 1972 (Lindh, 1978a). Further finds were made in 1986 (Norberg, 1987) and the area was visited by the annual SSF mountain meeting in 1987 (Sjöberg, 1987c; Lundberg, 1987). Area VIII (Södra Storfjället) is encircled by KU carbonate outcrops, but has hardly been investigated by cavers since the discovery of **Tjårrogrottorna** on its north side (Beskow, 1929). The south side of the mountain has also been visited, when the clean-washed cave **Rajagrottan** was explored (Sjöberg, 1972).

Despite the lack of long caves along its 2km-long underground stream course, the "spectacular" Bjurälv karst valley in area IX (KL) has continued to attract sporadic caving visits. In the very dry conditions of summer 1978 it was possible to enter a cave at the main sink, and **Övre Bjurälvsgrottan** was found to be 200m long and 15m deep (Lindh, 1978b). The cave could not be re-entered until August, 2002. However, this area has compensated in another way, through the discovery of the extensive and complex **Korallgrottan** (KL; Doj, 1985). Its subsequent exploration over the next decade revealed a magnificent cave, with many interesting features, which is now nearly 6km long and is 144m deep. The cave exists at several levels above an active series, and has several entrances. The longest traverse through the cave provides one of the best non-vertical sporting caving trips in Scandinavia.

1.7 Cave and karst science in Scandinavia

The sections below present a brief historical review of the development of cave science in Scandinavia. Section 3.3 provides a fuller treatment of ideas relevant to this thesis.

1.7.1 Cave and karst science in Norway

In parallel with reporting caves found during mapping, the early Norwegian geologists also made studies inside the caves and developed ideas about how the caves formed. A review of their opinions on speleogenesis is presented in sections 3.3.1–3.3.3. Vogt (1897) presented information about the occurrence of metacarbonates across the whole country, including north central Norway (*ibid.*, pp 240–265). Hoel (1906) reported marine shells inside caves at altitudes above 100m in Z2. Rekstad (1914) gave chemical analyses of various limestones, including some from the study area. Rekstad (1917) mentioned caves and potholes, also in Z2. Horn (1937) introduced the term "strip (or stripe) karst" to describe the predominantly narrow bands of metalimestones in which many of the karst caves of Norway are located, and the term "green karst" to illustrate the forested nature of many karst environments. His later work (Horn, 1947, published posthumously) discussed the botany of cave entrances and the faunal remains found in some caves, including bones of brown bear, *Ursos arctos.*

Corbel (1952a) discussed the Rennselelvdal karst in KL in Norway with its continuation over the watershed into Bjurälvdal in Sweden. Corbel (1957) examined the role of climate in limestone erosion with material taken from all over Scandinavia (north central Norway: *ibid.*, pp 211–218), Spitsbergen, Greenland, Britain, Ireland and Canada. Railton (1954) discussed a visit to the caves of northern Nordland made with Corbel in 1951, and gave his own observations about the paucity of speleothems. Jenkins (1959) discussed geological guidance in the shape and direction of caves passages, cave sediments, faunal remains, speleothems and cave development for three caves in the Svartisen area. A review of the then state of scientific knowledge of Norwegian caves was published by St.Pierre, S (1967). There are no known scientific references dating from the 1970s. St.Pierre, S (1980 and 1988) discussed her studies in **Grønligrotta**.

The more technical approach to cave exploration of the 1980s was accompanied by a more rigorously-scientific treatment of the Norwegian caves. Caves were visited not just for exploration or survey, but also to study their morphology, and their internal deposits of stalagmite, clastic sediments, and possible archaeological artefacts. A field trip to the karst areas was organised as part of a symposium on Arctic and Alpine karst held at Oslo, and the importance of protecting caves as vulnerable sources of scientific information about earlier climate and geological history was recognised. The papers or abstracts from this symposium were published in a theme issue of *Norsk Geografisk Tidsskrift* (Lauritzen, 1984a). The number of scientific papers about Norwegian caves expanded considerably in recent years, with particular attention being paid to the dating of stalagmites. A theme issue of *Cave Science* brought together 11 scientific and review papers (Faulkner and St.Pierre, 1988). A second karst conference, on the theme of the karst record and climatic change, was held at the University of Bergen in August 1996.

Eight papers drew on evidence from Norwegian caves (Lauritzen, 1996a; Yonge, 1997). Field trips were also made to karst areas in southern and northern Norway.

Most of the Norwegian scientific studies since the early 1980s derive from work in caves in *northern* Norway. Very little scientific work has been undertaken within the north central Norway study area. The one cave to receive in-depth study is **Sirijordgrotta** (Z4) in Eiterådal. A hydrological and hydrochemical description of the karst aquifer was presented in a 204-page thesis (Øvstedal, 1991). Lauritzen and St.Pierre (1982) dated a stalagmite from the cave, and an account of its sedimentation was provided in a 261-page thesis (Valen, 1991; summarised in Valen *et al.*, 1997). Publication of the results of the study of around 10000 bone fragments from the pitfall Elk Shaft is awaited.

At the periphery of karst science, papers have also been published on caves in non-carbonate rocks (e.g. Schrøder, 1989), coastal caves (e.g. Sjöberg, 1988) and glacial processes (e.g. Smart, 1984; Theakstone, 1988). Østbye *et al.* (1987) described invertebrates from several Norwegian caves, including **Sirijordgrotta** (Z4). Dolmen and Arnekleiv (1990) and Arnekleiv and Dolmen (1992) provided information about freshwater insects and aquatic invertebrates in caves in Rana and at eight cave locations along the river Jordbruelv (Z4).

1.7.2 Cave and karst science in Sweden

As in Norway, the first assessments of Swedish karst were also made by the geologists who were working in those areas. A report on the limestone and dolostone outcrops in northern Sweden, including all the study area, was presented by Shaikh *et al.* (1989). Corbel (1952a) studied the Bjurälv karst (KL). Becker (1980), Nordell (1952), Sjöberg and Engh (1979) and Wellander (1981) wrote papers with similar titles about the Bjurälvdal karst landscape. Deposition during glacials and interglacials at **Korallgrottan** (KL) was discussed by Isacsson (1989, 1994 and 1999).

The Kåtaviken (ZC) karst was discussed by Berg (1979) and Nisell (1986). Norberg *et al.* (1988) studied the Kåtaviken and Rödingsfjäll (KU) karst areas, both within this study area. The most comprehensive study of one large cave and its karst area in the central Swedish Caledonides was at **Sotsbäcksgrottan** (KU; Helldén 1973, 1974a, 1974b and 1975). Jasinski (1978) compared corrosion rates at Mieseken (ZC) with those at **Lummelundagrottan** on Gotland.

Engh (1977) briefly discussed the surface morphology of karst areas above the timber line in the Swedish Caledonides, and Engh (1980) considered Scandinavian speleochronology with information from area IIA at Tornetrask. Swedish workers also studied non-carbonate caves. For example, Bergsten (1976) wrote about the genesis of caves in Swedish Precambrian rock. Sjöberg (1987a and 1987b) studied caves as indicators of neotectonics, and completed a PhD thesis on this subject (Sjöberg, 1994, with an English abstract in Sjöberg, 1996a).

CHAPTER 2 GEOLOGY AND GEOMORPHOLOGY OF CENTRAL SCANDINAVIA

The purpose of this Chapter is to provide the geological and geomorphological context in which the karst caves developed, starting with a description of the structure of the Caledonides. This primarily derives from the Caledonian Orogeny, which is discussed in more detail in Appendix A1. The complex history of the Scandinavian carbonates and their properties are assessed in Appendix A2. The Chapter continues with a review of the geomorphological evolution of the study area during the Cenozoic, and concludes by considering the influences of the major glaciations of the Late Tertiary and the Pleistocene.

2.1 Structure

Much of the information in this section and Appendix A1 was derived from a comprehensive analysis of the Caledonian orogeny in Scandinavia and related areas by Gee and Sturt (1985). Contemporary geological research indicates that the rocks along the western coastal belt of Scandinavia derive their composition and structure from a highly-complex system of mountain building associated with the plate tectonic opening and closing of the Iapetus Ocean, from Late Precambrian to Mid Palaeozoic times: the Caledonian Orogeny (Gee and Sturt, 1985; Gayer, 1985; Soper *et al.*, 1992; Van Staal *et al.*, 1998). Thus, the region is part of the Caledonian–Appalachian fold and thrust mountain belt that once formed a continuous linear chain extending some 10000km from what is now Spitsbergen to the modern Gulf of Mexico, with an average width of about 1000km (Gayer, 1985: Editorial).

During its formation, the mountain belt was subjected to the effects of strike-slip movements, as it gradually moved northward from its original southern latitudes. Subsequent orogenies, and the opening and spreading of the Atlantic Ocean, caused it to be broken up into many geographically-dispersed and geological-varying terranes, of which 20 have been identified, and which now reside on both sides of the Atlantic (Barker and Gayer, 1985).

Of interest in this thesis is the fact that the former Caledonian–Appalachian mountain chain dispersed into terranes that at the present day are known to contain metamorphic carbonate rocks that either contain, or may contain, karst caves. These occur in Spitsbergen, Shetland, Scotland, Ireland, eastern Greenland, and in some of the New England states of the USA, as well as in Scandinavia, as compared in Chapter 10.

2.1.1 Scandinavia and the Caledonides

In Scandinavia, the remnant rocks of the Caledonian Orogeny occur along an 1800km-long belt with a width that varies between 200 and 400km. This belt forms the Scandian mountain chain. Most of the rocks were originally formed at the western edge of the Baltic craton, on the eastern side of the Iapetus Ocean, although the westernmost probably derive from the Laurentian craton. The closure of Iapetus produced a complex series of thrust sheets and nappes as the rocks of the Caledonides were transported southeastwards on to the older rocks of the Baltic craton. The Baltic shield foreland remained generally

undeformed during this process, although some of it, and its crystalline cover rock, also got caught up into the over-riding nappe pile, especially to the west. The rocks of the thrust sheets are composed of both metasedimentary and igneous assemblages of Late Proterozoic to Silurian, or even, Devonian ages that previously extended beyond the present thrust front (Hossack and Cooper, 1986).

The tectono-stratigraphic structure of Scandinavia comprises four major allochthons: the Uppermost, the Upper, the Middle and the Lower (Figure 2.1). These are separated everywhere from the Precambrian basement by a thin sedimentary rock layer. The unmoved combination of basement and cover is commonly termed the Autochthon, although Hossack and Cooper (1986, p289) suggested that even most of this unit is allochthonous. The basement and cover rocks that did get pushed a short distance are described as the "Lowermost" Allochthon or as the Parautochthon (e.g. Roberts and Gee, 1985). In northern Norway, the Uppermost Allochthon, which probably originated to the east of rocks that now form eastern Greenland (Roberts *et al.*, 2002), comprises the Tromsø Nappe, the Beiarn Nappe and the Rødingsfjell Nappe Complex (RNC). In the north central Norwegian part of the study area it comprises the Helgeland Nappe Complex (HNC) and the RNC. The Uppermost Allochthon does not occur south of the HNC, and in Sweden its only occurrence is in a part of the RNC that overlaps the border. This is in ZC, within the study area. Various individual nappes make up the Upper Allochthon. In central Scandinavia, it comprises two groups of Nappes referred to as the Køli Nappes and the Seve Nappes. South of here, the Køli Nappes are replaced by a group of nappes that comprise the Trondheim Nappe Complex, and the two major nappe groupings continue south to Sognefjord in southern Norway. The Middle, Lower and Lowermost allochthons contain nappes that occur along the whole length of the Scandes, from the northernmost coast of Norway to the south at Stavanger, with a spur also continuing to Oslofjord. In general, lower nappes are encountered when travelling west to east from the Atlantic coast. A characteristic of the Scandinavian Caledonides is the presence of two lines of 'windows' within the upper nappes, in which rocks from the Middle and Lower Allochthons, or the basement, crop out. These lines of windows occur along the coast and some 80km inland. The nappes beneath the Uppermost Allochthon wedge out backwards and into 'branch lines' towards the west. The Caledonide nappes are separated from each other tectonically, and do not prograde upwards, although lithostratigraphical affinities can be traced upwards from the Autochthon, perhaps as far as the Seve Nappes (Stephens *et al.*, 1985, p155). The contact at the base of the Uppermost Allochthon is characterised by a zone of brittle fracture, as it contains imbricate tectonic wedges and lenses (Stephens *et al.*, 1985). Figure 2.2 is a schematic profile through the study area to show the tectonic structure.

Some authors (e.g. Hossack and Cooper, 1986) use an alternative terminology for the tectono-stratigraphical structure of the Scandinavian Caledonides. Thus, the Uppermost, Upper, Middle and Lower Allochthons are replaced non-equivalently by the "Exotic Nappe Complex", the "Oceanic Sheets", the "Crystalline Sheets" and the "Baltic Cover Sheets". Whereas these terms may be more descriptive of the origins of the nappes, the previous terminology is retained throughout this thesis, because nearly all the available geological maps use the earlier terms.

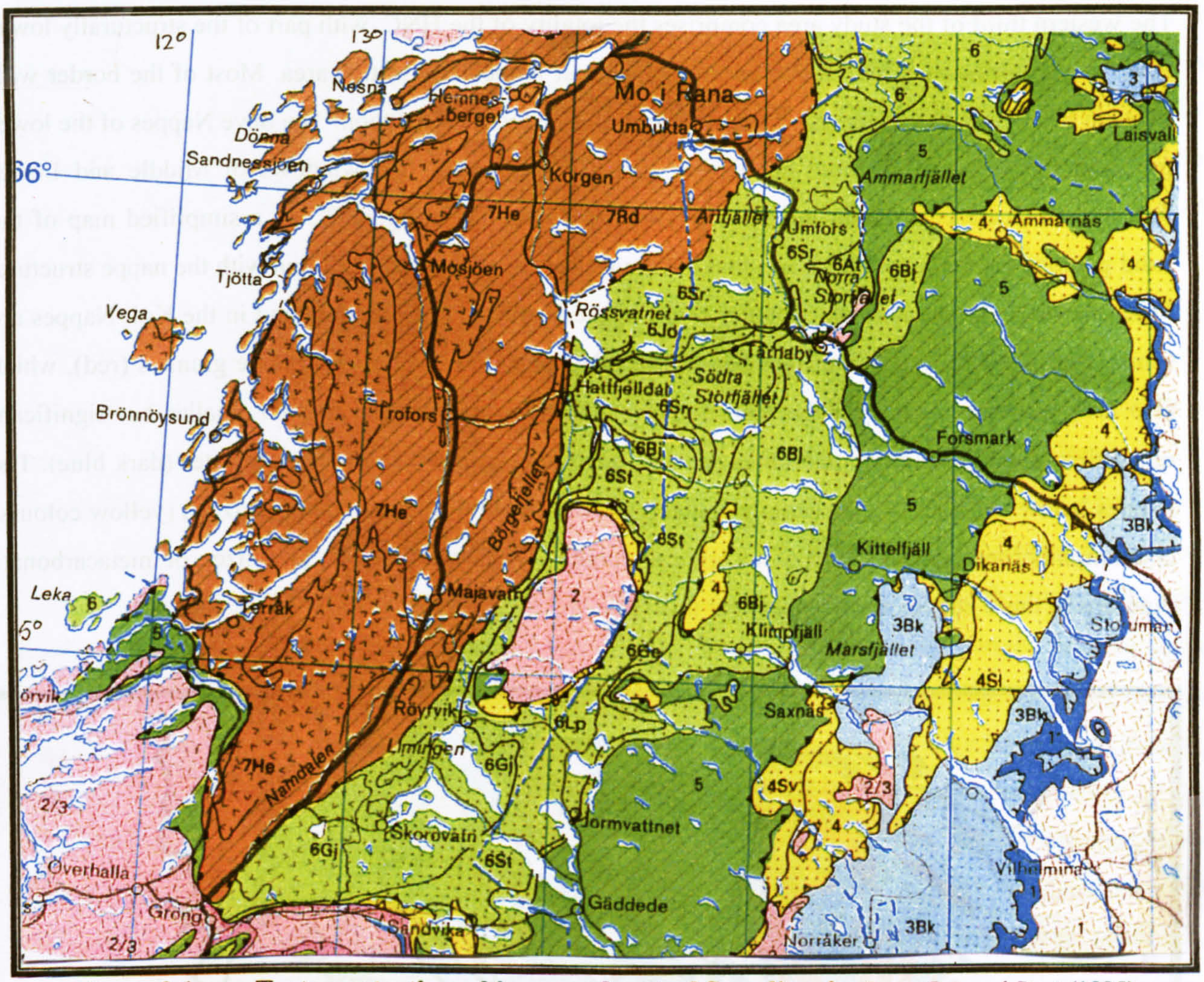

Figure 2.1 **Tectono-stratigraphic map of central Scandinavia.** From Gee and Sturt (1985)

Figure 2.2 **Schematic profile through study area at 65°30' to 64° 30'.**
From Stephens *et al.* (1985, Fig. 2)

Key to Figures 2.1 and 2.2:

1 Autochthon: Precambrian basement and sedimentary rock cover
2 Parautochthon: Precambrian crystalline rocks and sedimentary rock cover
3 Lower Allochthon: Precambrian crystalline rocks and sedimentary rock cover
4 Middle Allochthon
5 Upper Allochthon: Seve Nappes
6 Upper Allochthon: Køli Nappes
7 Uppermost Allochthon: Helgeland Nappe Complex and Rödingsfjäll Nappe Complex

2.1.2 Central Scandinavia

The western third of the study area comprises the totality of the HNC, with part of the structurally lower RNC in the northeast. These make up the Uppermost Allochthon in this area. Most of the border with Sweden lies within the upper (Køli Nappes) part of the Upper Allochthon. The Seve Nappes of the lower part and the lower allochthons lie farther east. To the south, two windows of Middle and Lower Allochthons coalesce to form the "Grong–Olden Culmination". Figure 2.3 is a simplified map of the solid geology for the area that shows that the facies lineaments commonly align with the nappe structure. From the map, the predominant country rocks in the Uppermost Allochthon and in the Køli Nappes are schists and phyllites (coloured light blue). The HNC and RNC contain extensive granites (red), which also crop out sporadically in the Køli Nappes. All these nappes also contain smaller but significant quantities of gabbros and amphibolites (green), quartzites (yellow) and metacarbonates (dark blue). The nappes below the Køli Nappes mainly comprise schists, phyllites, gneiss and quartzites (yellow colours) and amphibolites (green), with some granite (pink). The small number and sizes of metacarbonate outcrops in these nappes are not shown at this scale.

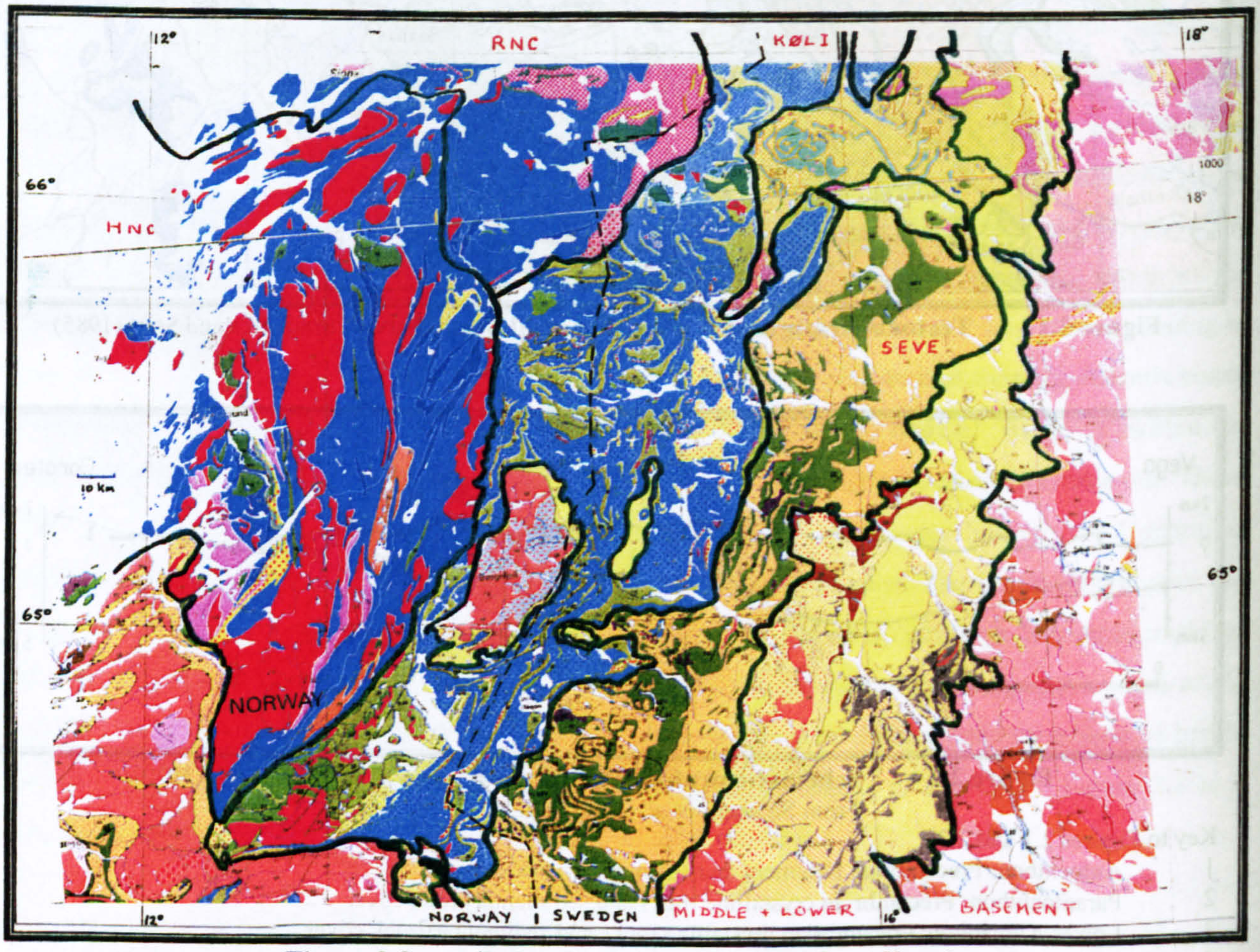

Figure 2.3 Bedrock geology of central Scandinavia

From Geological Maps: Northern and Central Fennoscandia. 1:1000000. 1985 and 1996. Refer to text for simplified explanation and guide to colours.

2.2 Cenozoic geomorphology

The Caledonides started to drift northwards in the Precambrian, almost reaching present latitudes by the start of the Cenozoic (Appendix A1.3.2). In common with Britain and Greenland, Norway's migration continued throughout the Tertiary, but now may be more stable. The approximate north central Norway latitudes were: Palaeocene (60Ma): 60°N; Eocene (40Ma): 62°N; Late Oligocene (25Ma): 64°N; Middle Miocene (15Ma): 66°N; Late Miocene (6Ma): c. 66°N; Pliocene (3Ma): 65°N; Present: 65°N (Torsvik *et al.*, 2002).

2.2.1 The paleic surface

Gjessing (1967) described the development of Norway's *Paleic Surface,* which he attributed to a probable combination of uplift and climate change dating from the Tertiary or the Mesozoic. He distinguished between two types of present landforms. Paleic forms are recognised by their 'old' appearance and even, rounded, character. Young forms developed subsequently by fluvial and glacial processes, including the present actively-eroding rivers, where frost weathering is dominant. The two types are most easily distinguished where geological (structural) control is less important. In many parts of Norway, the paleic forms are locally grouped at similar altitudes. In general, they consist of convex summits above relatively steep (>10°) hill-slopes to a sharp knick at the level of a basin floor. Basins, depressions and broad paleic valleys seemed to have formed all over Norway, independently of the surrounding country and the distance from, and the height above, local base level, and did not necessarily drain to the sea. Gjessing surmised that this paleic land surface resulted from intense deep chemical weathering in warm, arid or semi-arid, conditions with removal of material by subaerial slope processes, such as are found in the southwestern USA today. The Mesozoic (Mid Jurassic) and Tertiary deeply-weathered parts of the bedrock were mainly removed by subsequent glaciations, although some are still preserved below Mesozoic deposits in southern Sweden.

Riis (1996) observed that the paleic surface is composed of at least three distinct preglacial erosion surfaces: a sub-Cambrian peneplain that envelopes the summits of Precambrian rocks; a Mesozoic peneplain at a smooth-domed envelope of the highest summits of resistant quartzites and gabbros; and a Tertiary plain with isolated hills. Studies in the Døvre–Rondana area of southern Norway showed that three main paleic surfaces occur in steps, and that these are equivalent to summit profiles (Bonow *et al.*, 2000). The broad surfaces align with the present main glacial and fluvial valleys and cut across different bedrocks. The oldest (highest) paleic surface represents a sub-Cretaceous envelope that can be extended from the present basement rocks of Sweden into the sky over Norway. The glacial impact on the paleic surfaces is pronounced only in the major valleys.

Stuevold and Eldholm (1996) stated that the pre-uplift paleic surface had an altitudinal range from 0–500m. In the Swedish part of the study area, which better maintains the paleic SE fluvial drainage, it forms the whole surface, except along major valley floors. The paleic landscape on the Norwegian side of the border has been largely replaced by a steep relief and a SE migration of the water divide caused by

greater westward erosion. This has resulted from increased precipitation and the formation of U-shaped glacial valleys. Rudberg (1997) produced interpretative, and somewhat subjective, maps of the paleic surface (which he defined as a *"surface not too much changed by glacial erosion"*). According to an interpolation by this author on to Figure 1.1, the paleic surface does not extend farther west in the study area than HNC Z4. The karst significance of the paleic surface is addressed in section 5.3.4.

2.2.2 Cenozoic uplifts

Following a limited, local, Late Jurassic, uplift (Riis, 1996, p346) and the Cretaceous peneplanation, Scandinavia was uplifted in two phases, in the Palaeogene and in the Neogene (Solheim *et al.*, 1996; Riis, 1996). An important epeirogenic uplift of the Scandes probably began in the Palaeocene, when the Norwegian Sea started to form along a flexural hinge line parallel to the coast. These movements were reinforced by warm, humid-climate erosion to the west, allowing more continental uplift, clastic deposition, subsidence offshore as sea level fell again, and local peneplanation of softer cover rocks down to the basement. By Oligocene times, the shape of the present topography was well established: a narrow low-lying fringe between the mountains and the sea, broad shallow valleys within the Caledonide nappes, and large plains across the Baltic Shield. The effects were most marked in the Miocene and Pliocene, when, despite cooler semi-arid climates, offshore subsidence at rifted basins increased sharply, coupled with the landscape rising to a much higher level, but now with lower basins and deeper valleys (particularly those along the less resistant metasediments). It has been suggested that the rapid and sustained elevation of the Scandinavian land surface contributed to the onset of the subsequent glaciations (Cloetingh *et al.*, 1992; Doré, 1992).

Doré (1992) modelled the Tertiary uplift of the *"Base Tertiary Surface"* (i.e. the paleic surface) that remained after the Cretaceous in south Norway as a gently rising sinusoid, which continues as a depression into the North Sea. The total vertical amplitude is over 4km, and the half wave length is about 300km. He postulated that this bulge continued into northern Norway, perhaps assisted by tectonic movements that may not need to be invoked for southern Norway.

Riis (1996) discussed the uplifts from the Mesozoic to the Pleistocene, by correlation with offshore data. In the study area, Riis mapped the Late Cretaceous / Palaeogene uplift as 600m at the coast, rising to a maximum of 1200m near Tärnaby. His map for Plio-Pleistocene net uplift shows further coastal and maximum uplifts of c. 600m and 800m. At the same time, Plio-Pleistocene erosion removed some 500–700m of bedrock. Apparently, Pleistocene uplift continues today in southern Norway, but from the evidence of its wide strandflat, and dated karst materials, there has been no significant (non-isostatic) uplift in mid-Norway in the last 0.5Ma, in contrast to the observations of Mörner (1979 and 1980). Riis (1992 and 1996) considered the various components of uplift during the Tertiary and Quaternary and concluded that the uplifts cannot be fully explained by calculations based on glacial and erosional unloading, so that they require tectonic mechanisms. He also noted that deposits dated to 300ka in *caves* that are themselves situated more than 1000m below local mountain summits show that there was a

considerable relief in north central Norway way back into the Quaternary. Rudberg (1997, p200) observed that glacial erosional uplift was greater west of the residual paleic surface, because the thickness of lost rock is some 10 times higher there.

In contrast to Riis (1996), Stuevold and Eldholm (1996) suggested that a flexural uplift mechanism involving both the mainland and part of the shelf in the Late Oligocene to Miocene is sufficient to explain the local uplift. This uplift event is well separated in time from the regional syn-rift uplift associated with the opening of the northern Atlantic at the Palaeocene–Eocene transition. In their explanation, the Palaeogene uplift was confined to a narrow region offshore from north central Norway, but with a visible expression in the Lofoten Islands in northern Norway. They cited authors who noted that uplifted peneplains never survive 40Ma, and that complete Scandinavian peneplanation was not achieved until the Late Oligocene. A major Late Oligocene uplift is related to a major lowstand in eustatic and local relative sea level. This caused an observed unconformity in offshore sedimentation that may be equivalent to the onshore paleic surface. Sea levels recovered in the Early Miocene. With global cooling, long-term eustatic and local sea levels fell again until an even greater fall near the Miocene–Pliocene transition at 5.5Ma. This created a regional Early Pliocene depositional unconformity above Early Miocene offshore sedimentary wedges, which was interpreted as the start of a predominant tectonic uplift. This uplift caused greater fluvial, and increasingly glacial, erosion and sediment supply (rather than the previous mainly chemical weathering) to 'old' Pliocene wedges on the main continental shelf. The process itself further accentuated offshore subsidence and onshore uplift. The dramatic increase in ice-rafted debris at ~2.6Ma is marked by a seismic reflector (PL3) at the base of 'younger' Pliocene wedges that are restricted to the slope and outermost shelf. This flexural uplift model implies a hinge line some 150km offshore, and a westward advancing coastline as uplift proceeded. In the study area, the palaeo coastline varied from about 20–30km east of its present position at the start of the Miocene. Stuevold and Eldholm (1996) calculated that the *average* Neogene erosion west of the water divide was ~1.1km, with the deepest and maximum erosion of 1.0–1.8km along a narrow zone near the present coastline. From an estimate that 10m of erosion produces 7m of uplift, the area of maximum tectonic uplift, 0.9–1.0km, corresponds to the coastal region of maximum erosion. These authors also suggested that uplift started earlier, and became greater, going from south to north across the study area, as evidenced by a change from old, only slightly rejuvenated, landforms in Trøndelag to more alpine mountains farther north.

Henriksen and Vorren (1996) studied the late Cenozoic sedimentation and uplift history at the Vøring Plateau on the mid-Norwegian continental shelf (Figure 2.5). The shelf contains six main seismic units above a Cretaceous base. These are Palaeocene and Eocene sediments overlain by younger mega sequences described as Units A–D. The thin Unit A was deposited throughout most of the Miocene in a deep, open, shelf environment. Unit B is a thick sedimentary wedge of deltaic appearance of *either* Oligocene *or* Early Pliocene age. Twelve sequences of clay, sand, silt and diamicton are recognised in Unit C. It is tentatively dated to between 3.0 and 0.8Ma. Unit D blankets the shelf area with an inferred

age younger than 0.8Ma. Whereas Unit B exhibits a sedimentation rate of $8x10^{-3}cma^{-1}$ (if of Pliocene age), Units C and D together show a rate of $42x10^{-3}cma^{-1}$ and indicate a dramatic increase in sedimentary input. A major fall in sea level, and corresponding mainland uplift, is inferred from Unit A in the Late Miocene, at a time of local cooling. An Early Pliocene age for the deltaic Unit B would imply a major Neogene transgression at 5.0Ma, caused by a tectonic subsidence of the northern Atlantic, and uplift and erosion of the basin flank. The lithology of Unit C points to a glacigenic origin from the front of a grounded icesheet at the palaeo shelf edge. Its sequence boundaries represent low sedimentation during interstadials. The shelf edge has prograded 100km westward since 3.0Ma. Thus, these authors' study supports a view of major uplift in the Late Miocene / Early Pliocene, followed by major glaciations and erosion after about 3.0Ma, with a changed style of glaciation after about 0.8Ma.

In summary, the uplift of the Baltic Shield in the Mesozoic, Scandian uplift during the Cenozoic and then differential erosion combined to recreate the Scandes to the form that exists today, in an 1800km-long alignment. This is, in general, roughly coincident with the original Caledonides, and makes a good fit in the study area, which is practically devoid of post Caledonian sediments, apart from Quaternary glacial deposits. The locations of mountains and the highest summits are controlled by the distribution of the most resistant rock types (usually igneous or meta-igneous), and by the original Caledonide structures.

2.3 Tertiary / Quaternary glaciations

The Quaternary history of Scandinavia was discussed comprehensively by Donner (1995), and compared with the similar history in northern America by Andersen and Borns (1997). The impacts of late Cenozoic glaciations on basin evolution off the west and north coasts of Norway were described at a workshop held in 1994, as summarised by Solheim *et al.* (1996).

2.3.1 Glacial evolution

The mean annual temperature of central Europe remained above 20°C during the Palaeocene and the Eocene. It then started to decline until it reached about 14°C at the end of the Miocene, no doubt in response to the drift northwards of the European landmass (section 2.2). Subsequently (post 3.8Ma: Mangerud *et al.*, 1996, p19), temperatures fell further and fluctuated wildly as the earth was subjected to large-scale glaciations, especially after about 2.8Ma in the Pliocene. During the Pleistocene, the maximum mean annual central Europe temperature reached 10°C during interglacials, but fell below 0°C at the height of each glaciation. In southern Scandinavia, the mean annual temperature fell below -10°C and the mean July temperature fell below 0°C during glaciations. The glaciations in the study area were thus probably somewhat more severe than *present* conditions at Spitsbergen, which has a mean annual temperature of -8°C (Horn, 1947).

The number of glaciations and the geographical extent of each one are not known precisely, but there may have been more than 30 full glacial-interglacial cycles, including nine major glacials after 0.9Ma

(Mangerud *et al.*, 1996, p21). For the last 2.5Ma, oxygen isotope $^{18}O/^{16}O$ ($\delta^{18}O$) records from deep sea cores that measure the *global ice volume* can be used to infer the magnitude of each Scandinavian glaciation, and the ice-rafted detritus (IRD) content in deep sea sediments correlates closely with the extent of the icesheets (Mangerud *et al.*, 1996, pp22–23). These records indicate periodicities that can be explained by the glacial events being triggered by earth-orbit cycles of solar insolation, with strong covariation of CO_2 and temperature (Cuffey and Vimeux, 2001). The existence of Miocene terrestrial glacial deposits in Germany (Ehlers, 1996, p249) and IRD in the Norwegian Sea dated from 5.5Ma onwards by Jansen and Sjøholm (1991) suggest that small-scale glaciations started in the Late Miocene. Mangerud *et al.* (1996, p22) noted that small, but significant, IRD pulses dated to 11Ma (10.2Ma: Stuevold and Eldholm, 1996), indicating that Nordic Sea icesheets existed *early* in the Late Miocene. The volume of this detritus increased by one or two orders of magnitude after 2.75Ma and there were extensive glaciations in northern Europe after 2.57Ma. From 5.5–2.57Ma, the smaller IRD fluxes may have arisen from just valley and fjord glaciers in Scandinavia, or alternatively from drifting icebergs calving from Greenland and Spitsbergen.

Maslin *et al.* (1995) reviewed recent evidence for the sequence of Tertiary / Quaternary glaciations, and discussed theories that they were initiated by the long term cooling of the northern hemisphere by the elevation of the Himalayas, supplemented by the submergence of the Bering Strait at 3.2Ma and the closure of the Pacific–Caribbean gateway by the emergence of the Panama Isthmus at 2Ma. They concluded that icesheets first reached continental margins in Eurasia at 2.74Ma, in Alaska at 2.70Ma, and in northern America at 2.54Ma. The amplitude of high-latitude summer insolation cycles varies with a period of c. 400ka, so that orbital forcing triggered the intensification of northern hemisphere glaciation between 2.74 and 2.54Ma. Interglacials comprise less than 10% of the climate record during the past 2.5Ma (Adkins *et al.*, 1997).

Two main phases of Pliocene–Pleistocene continental-scale glaciations are recognised. From 2.8–0.9Ma, large ice volumes accumulated during each glaciation in 41ka *obliquity* cycles. They represent intermediate-sized Scandinavian mountain-centred icesheets, during a period with cool interglacials. Thus, there was a 1.5 / 2.0Ma period of rather moderately-varying glacial conditions, with large erosion of the Scandinavian mainland (Mangerud *et al.*, 1996, p22). The glaciations since 0.9Ma (the *Mid Pleistocene Revolution*) were more extensive, with icesheet centres moving eastwards from the coastal mountains as far as the Baltic coast, as each glaciation proceeded. These glaciations were triggered predominantly in 100ka *orbital eccentricity* cycles (Solheim *et al.*, 1996). Petit *et al.* (1999) suggested that, during terminations, the climatic forcings are related to the Milankovich orbital frequencies, especially the 100ka eccentricity cycle, and that these effects are amplified by CO_2 and CH_4 greenhouse gas increases and by the ice albedo feedback as icesheets melt. The interglacials also became warmer and longer after 0.9Ma (Jansen and Sjöberg, 1991; Mangerud *et al.*, 1996, p22). From the re-deposition of continental shelf material it is clear that these icesheets grew large enough to cover and erode sizeable proportions of the Norwegian shelf (Jansen and Sjöberg, 1991). Mangerud *et al.* (1996, p23) also

concluded that the stadial–interstadial fluctuations of the Scandinavian icesheet followed the *precession* cycles of the earth's orbit of around 23ka. Farther north, at Svalbard and the Barents Sea, the fewer glacial advances apparently follow the 41ka cycles of the tilt of the earth's rotational axis: at higher latitudes the earth's tilt is more important for summer insolation than the precession that dominates in Scandinavia. Thus, the icesheets were probably centred farther north from 2.8–0.9Ma, when compared to the icesheets that followed the Mid Pleistocene Revolution. The Barents Sea area was consequently probably eroded below sea level during the earlier period.

Rutherford and D'Hondt (2000) concluded that the transition from 41ka to 100ka glacial cycles actually occurred over a period from 1.5–0.6Ma, the 100ka cycles being sustained by increased heat flows northward across the Equator that strengthened a *semi-precession* cycle of 11.5ka period in the northern hemisphere. Riis (1996, p355) noted that the shelf Pleistocene sediments of c. 0.8Ma age rest unconformably on tilted Tertiary sediments. As this is also near the age of the change in glaciation cyclicity, he also (c.f. Henriksen and Vorren, 1996; section 2.2.2) postulated a change in sedimentation pattern as the longer, larger, glaciations transported material right out beyond the shelf margin. This change in load distribution could also have initiated increased crustal uplift on land. Raymo (1998) suggested that rapid deglaciation only occurred after the switch to 100ka cycles, which permitted the build-up of large and unstable icesheets. Denton (2000) considered that each 100ka glacial cycle begins when salinity in the Nordic areas is diluted by deep water from a collapsing west Antarctic icesheet, and ends after gravitational collapse of maximal northern icesheets reduces the supply of icebergs, increasing the salinity.

Pointing out that icesheets grow at the slow rate of snowfall, but shrink at the faster rate of surface melting or the even faster rate of icesheet surging, Clark *et al.* (1999) also noted that there is a strong connection between ice flow and the underlying geology. If the icesheet base is at the pressure melting point, as well as movement by internal ice deformation, basal water facilitates both basal sliding of the ice and deformation of any unconsolidated sediments. They argued that, at the inception of northern hemisphere glaciation, northern America and Fennoscandia were covered by a thick, deeply weathered, regolith that had accumulated during the Tertiary (c.f. Gjessing, 1967; section 2.2.1). This widespread soft bed allowed fast ice flows that maintained relatively thin (~2km), low-volume icesheets, which responded *linearly* to the 23 and 41ka obliquity and precessional orbital forcings. However, after sufficient glacial erosion of the regolith [creating the Tertiary shelf deposits noted by Riis, 1996, and called Unit C by Henriksen and Vorren, 1996], exposure of crystalline bedrocks in core areas caused icesheets formed after the Mid Pleistocene Revolution (set at 1.2Ma therein) to thicken (~3km) and enlarge enough to achieve a *non-linear* response to the 100ka eccentricity cycle, so that these later icesheets actually drove the global climate cycle rather than being driven by it. This change in the thickness and style of glaciations is of direct relevance to the evolution of endokarst within the Caledonides, as discussed in Chapters 6–10. The Clark *et al.* (1999) theory also explained the rapid deglaciation of the later, more widespread, icesheets. Late in the 100ka cycle, these icesheets advanced

onto marginal low-relief and low-friction soft-bed zones on continental shelves. Subsequent thawing of permafrost by geothermal heating then allowed fast ice discharge into the Atlantic, supplemented by fast soft-bed ice flows across the inner areas of Hudson Bay and the Baltic Sea, which triggered rapid deglaciation.

It appears likely that the first extensive glaciation was the Eburonian, dated from 1.8–1.4Ma, from the evidence of Fennoscandian rocks in the Netherlands and of till on the Norwegian shelf. This probably reached the Norwegian shelf edge, as did the Menapian, dated at 1.1Ma (Mangerud *et al*, 1996, Fig. 3). These authors concluded that the Scandinavian icesheet extended to or beyond the west coast of Norway during 1Ma of the last 2.6Ma, including for about 400ka during the Eburonian. For 90% of this time, Scandinavia was partly covered by intermediate-sized icesheets. The ice front probably reached the shelf edge five to seven times during the last 780ka (*Ibid.*, p23). Sejrup *et al.* (2000) concluded from a study of sediments in the Norwegian Channel (a route for glacial ice streams flowing from the Baltic area), that after Oxygen Isotope Stage 13 (OIS13) at 0.5Ma, most likely all glacial stages experienced such maxima.

The most recent review of Fennoscandian glaciations was by Fredin (2002). He suggested that small glaciations may have started as early as Mid Miocene (14Ma), medium-sized icesheets from about 7Ma, major glaciations from 2.8–2.5Ma, and full-scale continental glaciations from 0.9Ma. He showed that *"mountain glaciations"* (i.e. cirque glaciers, valley glaciers, and local to regional icesheets) occurred in Scandinavia throughout much of the Late Pliocene and Pleistocene. From Fredin (2002, Fig. 7b), glaciations probably reached across the continental shelf on some eight occasions since the Mid Pleistocene Revolution (at OIS22, 18?, 16, 12, 10, 8, 6 and 2), but there were perhaps only five major interglacials in the same interval (at OIS11, 9, 7, 5e and 1). Before this, there were many mountain glaciations and deglaciations, but without a major interglacial, except that a full-scale continental glaciation probably occurred at c. 1.85Ma (OIS62), and a major interglacial at c. 1.75Ma (OIS59). This scheme omits a Menapian glaciation at around 1.1Ma. According to Mangerud *et al.* (1996, p23), there were about 15 interglacials in the last 2.6Ma that were as warm as, or nearly as warm as, the Holocene and that lasted 10–15ka. This approximately agrees with the number of interglacials that were too warm for mountain glaciation to survive (Fredin, 2002, Fig. 7b).

2.3.2 Later Quaternary glaciations

Traditionally, four major glaciations with three interglacials were recognised in northern Europe during a Pleistocene age thought to have lasted about 1Ma, as shown with other correlations in Table 2.1. Later research showed that there were many stadials and interstadials that confuse this simple pattern, and the ages of these events are still being clarified by correlation to deep-sea Oxygen Isotope Stages. As the Cromerian I deposits are older than the magnetostratigraphic Matuyama to Brunhes boundary at 780ka, it is clear that the originally-described Menapian glaciation is much more ancient than the other three glaciations. All glaciations in northern Europe were centred on Fennoscandian icesheets, and the moraine

limits of the last three 'traditional' glacials on the mainland are well-studied. Thus, glacially transported erratic boulders from Norway and Sweden are found in Denmark and Germany.

Of the last three glaciations, the oldest two, the Elsterian and the Saalian, were the most extensive, with moraines some 500km south of the Baltic Sea coast. The final glaciation, the Weichselian, reached only about 200km south of the coast. Rudberg (1992) provided some evidence of multiple glaciations in Scandinavia by studying topographical morphology. Because global sea level started to fall prior to the growth of Scandinavian icesheets, the onset of at least the Weichselian glaciation started elsewhere, i.e. in northern America and / or Antarctica (Mangerud *et al.*, 1979). Indeed, the Scandinavian glacial cycles tend to lag those of northern America, and the rapid cooling and warming at the beginning and end of each Scandinavian glaciation is attributable to the 'switching' off and on of the Atlantic Current into the Norwegian Sea by the amount of ice in the northern Atlantic.

Table 2.1 Traditional glaciations (From Andersen and Borns, 1997, and other sources)

Northern Europe	British Isles	The Alps	Northern America	OIS
Glacial **Interglacial**	**Glacial** **Interglacial**	**Glacial** **Interglacial**	**Glacial** **Interglacial**	**Glacial** **Interglacial**
Holocene	Flandrian	Holocene	Holocene	OIS1
Weichsel	Devensian	Würm	Wisconsin	OIS2–OIS5d
Eemian	Ipswichian	R–W	Sangamon	OIS5e
Saale	Wolstonian	Riss	Illinolan	OIS6
Holstein	Hoxnian	M–R	Yarmouth	OIS7
Elster	Anglian	Mindel	Kansan	OIS8
Cromer	Cromerian	G–M	Aftonian	OIS9
Menap	Beestonan	Gunz	Nebraskan	

Petit *et al.* (1999) described in detail the climate and atmospheric history of the past 420ka based on evidence from the Vostok ice core, east Antarctica (Figure 2.4). The Vostok station is at an elevation of 3488m and has a mean temperature of -55°C. (See Appendix A3.3 for a discussion about subglacial lakes below the Antarctic icesheet). The ice core record extends through four major climate cycles, with ice slightly older than 400ka at a depth of 3310m. Figure 2.4 shows that the successions of changes through each climate cycle and glacial termination were similar, and that the atmospheric and climatic properties oscillated between stable bounds. Each cycle experienced an irregular saw-tooth decline in global atmospheric temperature down to c. -8°C as stadials and interstadials succeeded each other, and a very rapid rise to c. 2°C at each termination. The Younger Dryas stadial at the end of the Weichselian (Termination I) had no counterpart in Terminations II, III and IV. The10ka stable warm period of the Holocene is longer than the 4ka periods above 1°C at the ends of Terminations II and IV, and longer also than the very peaky warm period at the end of Termination III. The east Antarctic climate record was recently extended to 740ka (covering eight glacial cycles) with an ice core from Dome C whose upper part matches the Vostok data (EPICA community members, 2004). The record showed that Termination V preceded a 28ka-long interglacial at OIS11 (the *Mid Brunhes Event*) that delimited two different patterns of climate. Between the Mid Pleistocene Revolution at c. 900ka and this event at c. 430ka, Antarctic glacial maxima were commonly somewhat less cold than prior to later terminations, but the

interglacials were significantly less warm than subsequently, and did not reach the Holocene temperature.

Winograd *et al.* (1997) deduced that the Vostok record is effectively synchronised to a $\delta^{18}O$ record from 565–60ka in vein calcite from Devil's Hole, Nevada. They assigned the last four interglacials to OIS5e, 7e, 9c and 11c, arguing that they each had a duration in the range 20–26ka. By studying planktonic foraminifera deposited in the Red Sea over the last 500ka, Rohling *et al.* (1998) estimated a sea level lowstand of 120±5m at the Weichselian maximum at 20ka. Lowstands in other glacial cycles have been up to 20m below this level. Interglacial highstands have been up to 20m above the Holocene level, equivalent to the volume of present Greenland and west Antarctic icesheets.

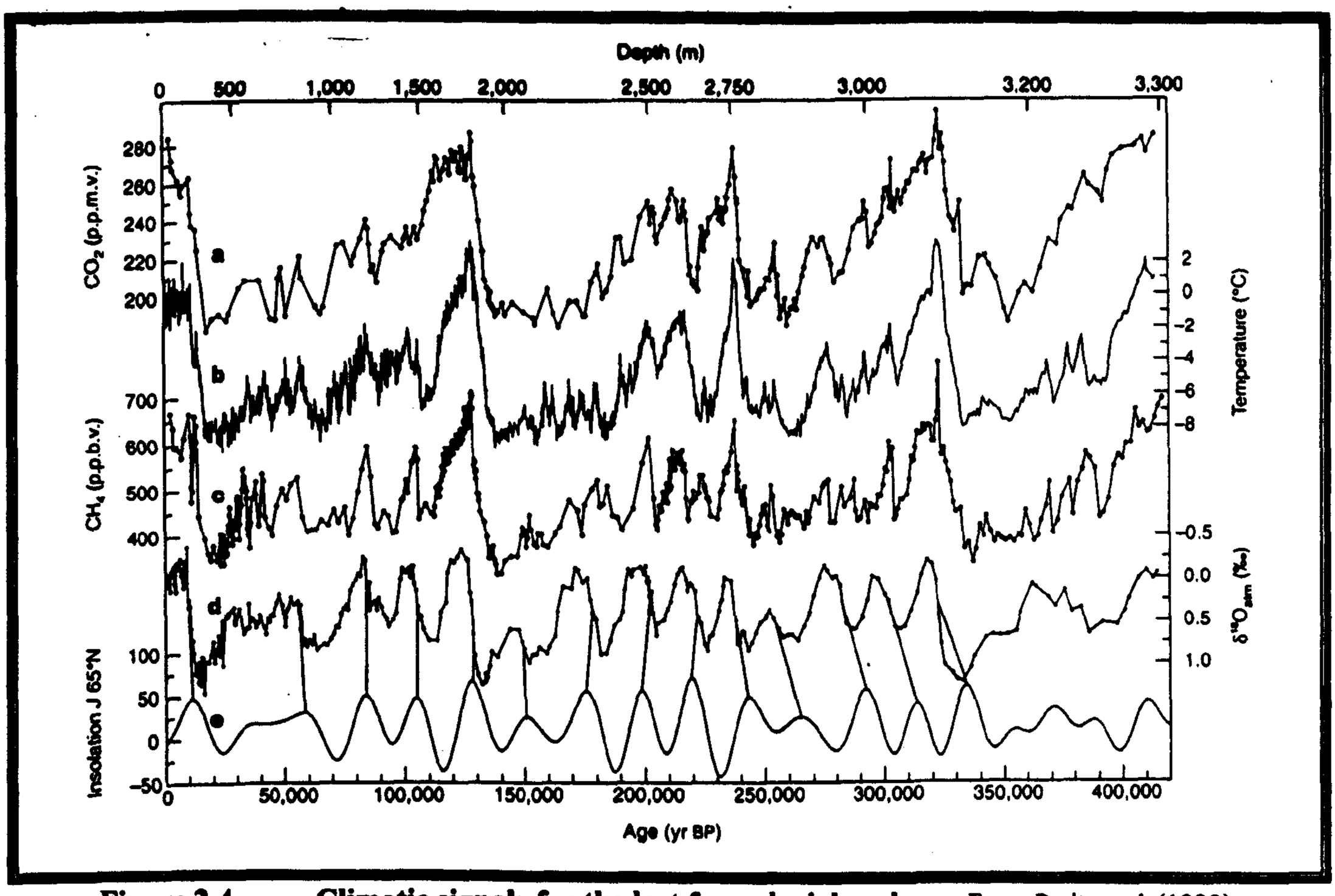

Figure 2.4 Climatic signals for the last four glacial cycles From Petit *et al.* (1999).

The last two interglacials, the Holsteinian and the Eemian, probably experienced mid-latitude mean summer temperatures which were 2°C warmer than today. Fennoscandia was a large island during the Eemian at 125ka (OIS5e), because of a globally-raised sea level and an incomplete isostatic rebound (Mangerud *et al.*, 1979; Dansgaard and Duplessey, 1981). There was little, if any, remnant ice, the mountain summits supported alpine vegetation, the lower slopes were covered by birch, pine and spruce, and there were broadleaf forests in southern Sweden. According to Kukla *et al.* (1997), the Eemian in Europe lasted from 130–107ka, although high-latitude ice started to grow again after 117ka. Sea level rise in the Early Eemian was so rapid that it overtook isostatic rebound along the whole northern Russian lowland coast, possibly peaking between 132 and 130ka (Funder, 2000). This also supports the earlier evidence that the Saalian Glaciation was much more extensive than the Weichselian. Andersen and Mangerud (1989) showed that the glacial fluctuations for the Eemian–Weichselian in Fennoscandia

corresponded roughly with climate fluctuations in France, Germany and Holland. Lototskaya and Ganssen (1999) described the structure of Termination II and that of the Eemian, which they suggested reached its highest sea-surface temperature at 122ka, when the eustatic sea level reached a maximum that was 6m higher than at present, probably caused by the melting of much of the Greenland icesheet (Huybrechts, 2002, p220). According to Adkins *et al.* (1997), Eemian climate instability in the northern Atlantic lasted from 129–118ka, when a transition to glacial oceanic conditions occurred within 400a.

2.3.3 Weichselian glaciation in Scandinavia

Traditionally, the Weichselian period was divided into three stadials or glacial peaks (Early, Middle and Late), and into two interstadials, when temperatures could rise to the level seen during interglacials. Mangerud (1991) presented a 'state of the art' review of knowledge of the last Ice Age at a symposium in Uppsala in 1990. He produced schematic glaciation curves for the west and east sides of the Scandinavian mountains that show the rather short-lived, mountain-based, Herning and Rederstall stadials, which correlate to OIS5d and 5b (117–105 and 93–85ka). The only Weichselian interstadials that were really forested in northern Germany were the Brørup and the Odderade, during which the Scandinavian icesheet almost entirely melted. These correlate to stages 5c and 5a (105–93 and 85–74ka). The Scandinavian mountains then remained glaciated throughout the major stadial OIS4, until after the Last Glacial Maximum (LGM) at OIS2, with only the coast becoming free of ice during the Bø and Ålesund interstadials at the beginning and end of OIS3. Donner (1996) also discussed the Early and Middle Weichselian interstadials in central Scandinavia. However, previous reconstructions were severely challenged by Forsström and Punkari (1997). They argued that all absolute dating methods are unreliable, and that sediments previously regarded as *in situ* Brørup and Odderade interstadial deposits were mixed and redeposited from Eemian interglacial sediments during glaciation. In their reconstruction, the minimum size of the Weichselian icesheet, since its formation at OIS5d, equalled its Younger Dryas extent, with larger extensions occurring at each stadial.

The Weichselian glaciation was modelled by Holmlund and Fastook (1995) and by Klemen *et al.* (1997; Figure 2.5) with good similarities. According to Holmlund and Fastook it lasted from about 112ka until 10ka, the start of the Holocene. Their model shows that the early stadials (OIS5d and 5b) reached a maximum at 90ka, but the icesheet only covered the mountains and the Kola Peninsular. Thereafter, a considerable recession reduced the icesheet to the mountain area by 82ka. The middle stadial (OIS4) began at 78ka and came to a maximum stillstand at 61ka (74–60ka: Arnold *et al.*, 2002), when the icesheet reached parts of southern Sweden. A slow recession initiated the second interstadial (OIS3) until 53ka, when the icesheet generally grew by further advances and smaller recessions. The Late stadial began with a major advance at 37ka, and reached the German coast at 30ka.

The Holmlund and Fastook (1995) model indicates that the mountains of the study area were probably glaciated to varying thicknesses continuously from 112–10ka. Close to the Atlantic coast, however, the sizes of valley glaciers waxed and waned during the stadials and interstadials. Neither the Early nor the

Middle stadial icesheets extended very far from the Atlantic coast line, which was probably ice-free during the interstadials. According to Mangerud *et al.* (1996, p13), the Weichselian glacial front passed the coastline at least four times: once each during the Early and Late Weichselian and twice during the Middle Weichselian, suggesting that the middle period actually experienced two stadials and two interstadials. Evidence from France, Germany and Fennoscandia suggests that the last stadial, which was the most extensive and long lasting, can be subdivided into several smaller glacial oscillations, with the oscillations becoming more subdued to the north.

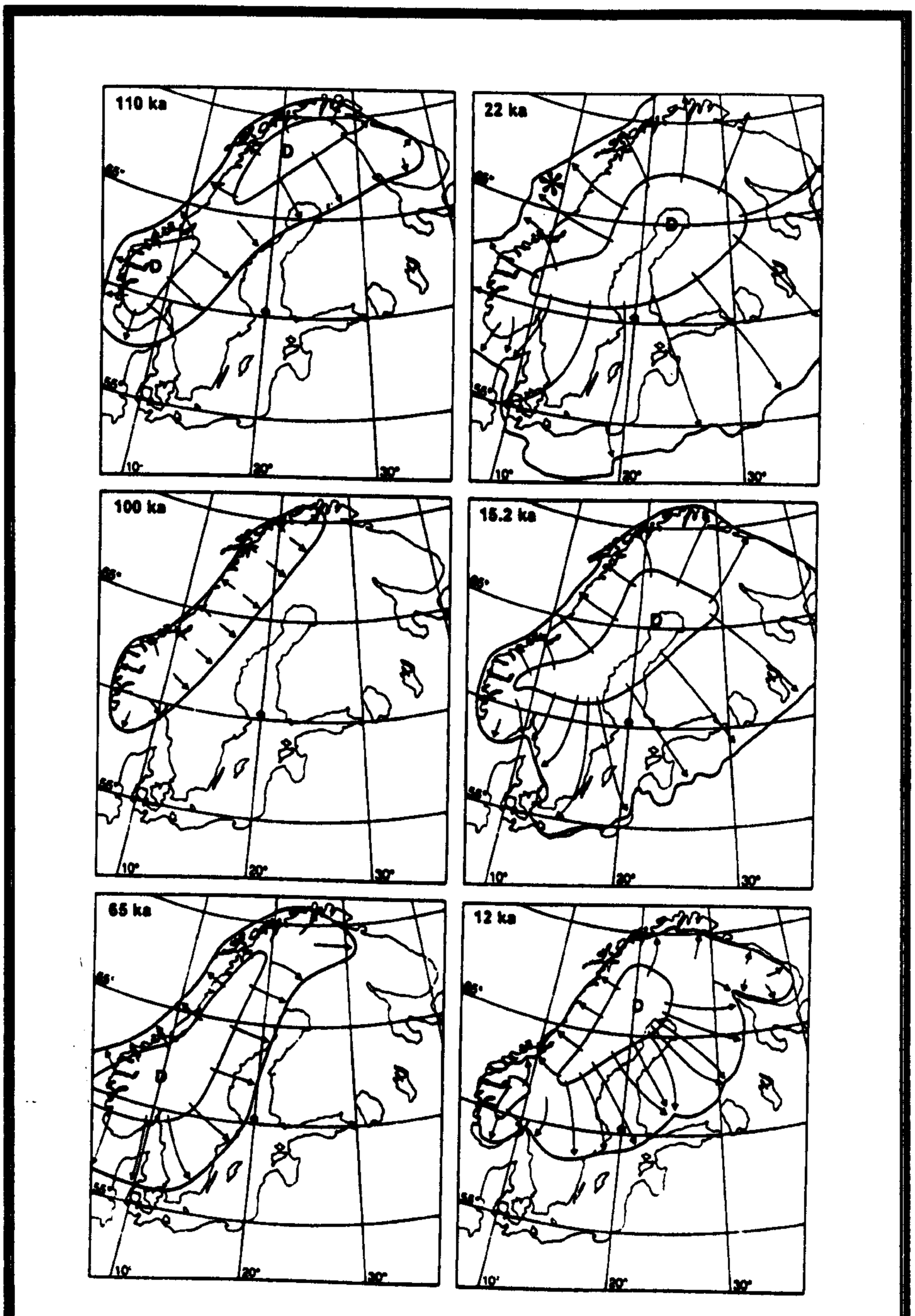

Figure 2.5 **Weichselian icesheet dimensions**
* Vøring Plateau. From Klemen *et al.* (1997, Fig. 11)

North central Norway rises to lower elevations than the domes to north and south and thus provided a lower barrier to the late Cenozoic east to west ice movements. This is seen in the Klemen *et al.* (1997)

glacial model that commonly shows a major bend in the ice divides, caused by outflow to the NW (Figure 2.5). Hence, the saddle-like feature of central Scandinavia was a focus for ice flow, and thus experienced sufficient glacial erosion to remove much of its paleic surface, despite its icesheet being less thick. Stuevold and Eldholm (1996) noted that the sedimented Norwegian continental shelf is widest at the Vøring Plateau, adjacent to this lower central region (Figure 2.5). The many long and deep fjords that penetrate far inland are indicators of the large volumes of ice that flowed westwards. The erosive power of these westerly icesheet movements is demonstrated by the maximum depths of the fjords in the study area. These are, from north to south (Figure 1.1): Nordrana 540m, Elsfjord 208m, Ranafjord 440m, Leirfjord 340m, Vefsnfjord 450m, Halsfjord 245m, Visten 220m, Velfjord 400m, Ursfjord 535m, Tosenfjord 552m, Bindalsfjord 720m (one of the deepest fjords in Norway) and Foldfjord 200m.

The general instability of the past climate (apart from during the Holocene) is also recorded in the 250ka GRIP ice core record from Greenland (Dansgaard *et al.*, 1993). During the Weichselian glaciation, the northern Atlantic region experienced two related oscillations of abrupt climate change (Alley, 1998). In the Dansgaard-Oeschger (DO) cycle (e.g. Broecker, 1994; Bond and Lotti, 1995; Stauffer *et al.*, 1998), significant and very rapid jumps of temperature (~7°C) and other climatic variables occurred at roughly 1500a intervals, perhaps linked to variations in solar radiation (Bond *et al.*, 2001). A slow and progressive saw-tooth cooling (~14°C) through several DO cycles comprise the lower-frequency, but irregular, "*Bond*" cycles (e.g. Bond *et al.*, 1992), which are marked by thick "*Heinrich*" IRD layers in sea-floor sediments at their coldest parts, matching Heinrich events to cold stadials (Bond *et al.*, 1993; Broecker, 1994). This enhanced ice-rafting occurred roughly twice during each precessional cycle throughout the Weichselian, with a mean period of 11000±1000a (Heinrich, 1988). The thicker parts of the layers lie near Hudson Bay, so that the events are assumed to be associated with large discharges of meltwater and armadas of icebergs, perhaps triggered by jökulhlaups (Johnson and Lauritzen, 1995). There were some six major Heinrich events (H6 to H1) of commonly increasing severity in the last glacial cycle, plus possibly the Younger Dryas event (H0), and the end of the Saalian (H7, Broecker, 1994). Each was followed by a rapid warming at the start of the next Bond cycle (or interstadial, Johnsen *et al.*, 1992).

Bond *et al.* (1997) showed, from small-scale IRD events, that mini-DO cycles continued into the Holocene at the same interval of 1470±500a. The coolings did not exceed 20% of the glacial–interglacial temperature change, but caused well-known cool events at 8200 cal. a BP and at the Little Ice Age. The authors concluded that DO cycles operate independently of the glacial–interglacial climate, but are amplified during glaciation. According to Oppo *et al.* (1998) and McManus *et al.* (1999), DO cycles and Heinrich events persisted throughout the glacial cycles of the past 0.5Ma. Dowdeswell *et al.* (1999) reported little correlation between Heinrich events and Nordic seas IRD, suggesting different behaviours for the Laurentide and Fennoscandian icesheets. Lambeck *et al.* (2002) and Rahmstorf (2002) presented reviews of links between climate, sea levels, and rapid switches in ocean circulation patterns during the Plio–Pleistocene. According to Rial (2004), the saw-tooth decline in temperature and the DO cycles are

explained by the global climate system, which transforms the amplitude modulation of global temperature by astronomical effects into frequency modulation of global ice extent.

2.3.4 Late Weichselian glaciation and the study area

Controversial insights to the Middle and Late Weichselian were provided briefly by Olsen (1997) and more comprehensively by Olsen *et al.* (2001a; 2001b). These authors used new information from terrestrial moraines, deep-sea sediments and ice cores to proxy the climate. They suggested that the Middle stadial lasted from 42–39ka, with the maximum extent of the ice about half way across the continental shelf. A "Hattfjelldal interstadial I" then lasted until 30ka, and for some of this time a very high-level, ice-free, temperate Atlantic sea water inundated adjacent inland areas and reached to 67°N, so that much of coastal Norway was occasionally free of ice. Dwarf birch and fern grew in Hattfjelldal (KU). The icesheet shrank to the Norway / Sweden border region and to the Jotunheimen range of southern Norway. Thereafter, Olsen *et al.* (2001b) showed stadials and interstadials at approximately 3000a intervals: an advance from 30–28ka, similar to the Middle stadial; a "Hattfjelldal interstadial II" from 28–24ka; and the largest Weichselian stadial (the Last Glacial Maximum, LGM1) from 24–21ka, when the icesheet reached the edge of the continental shelf, some 250km west of the north central Norway coastline. [For the first 2000a it may have connected across the North Sea to the icesheet that covered the northern parts of Britain and Ireland]. A "Trofors interstadial" followed from 21–17ka, with the sea completely clear of ice at 19ka. This was succeeded by a second large stadial, LGM2, from 17–13.5ka. The icesheet extended some 150km offshore at 15ka, a time when Fjeldskaar (1994) modelled the sea level at 125m below the present level. LGM2 was terminated by abrupt warming at the start of the Bølling interstadial. According to Lambeck *et al.* (2002), eustatic sea level lowering was c. 50m at 60ka. Global ice volumes approached maximum values at 30ka, and then remained nearly constant until 19ka. Arnold *et al.* (2002, Fig. 4) modelled a possible minimum icesheet that only lay above the 500m contour in the study area, together with valley glaciers, for the period 60–36 / 30ka.

The ice retreats and high sea levels were also very significant for the Hattfjelldal II and Trofors interstadials (although not quite as great as in Hattfjelldal interstadial I), when the climate was cold and dry. These results partly depend on radiocarbon-dated sediments from 5m- and 10m-thick inland stratigraphies. Hattfjelldal and Trofors are in KU and Z6, in the heart of the study area. Recent finds of pre-Late Weichselian marine influence at coastal and inland sites in Norway, elevated *above* early Holocene levels, were reviewed by Olsen and Grøsfjeld (1999) and by Olsen *et al.* (2001a; 2001b). The last paper inferred that several study area sites well above Holocene marine limits were reached by the sea during the interval 35–18ka. (See further discussion in sections 8.1.3 and 8.8.3). Olsen and Grøsfjeld (1999) concluded that the c. 6000a cyclicity of glacier variation is matched by a 6300a ice-growth and glacio-isostatic rebound period during the interval 45–15ka, assuming an *average* depression of at least 50m [presumably below the early Holocene sea level].

According to this new "yo-yo" glaciation model of Olsen *et al.* (2001b), the Weichselian icesheet was essentially unstable, with rapid ice advance quickly followed by rapid retreat, or moderate advance followed by moderate decay. Their model better fits a "thin ice" model of the LGM icesheet (section 2.3.5), and they also postulated that rapid changes in relative sea level in response to changes in glacial isostatic loading contributed to the instability. They explained a lack of calcareous marine mollusc shells with ages in the interval 27–13.4ka along the Norwegian coast by a combination of perennial sea ice cover and dissolution in cold acidic water from high meltwater discharges and / or CO_2-rich water formed under sea ice. Their paper also proposed a simple cave sediment stratigraphy model with diamicton (sporadically with bones and speleothems) overlying fine-grained sediments to indicate an ice-free to ice cover (interstadial–stadial) cycle. The criticisms of Forsström and Punkari (1997, section 2.3.3) are assumed by this author not to apply to their work.

The Olsen (1997) scheme challenged the concept of a continuously retreating icesheet from c. 20ka, as shown on a glacial chronology map by Andersen and Karlsen (1986). Their map is not disputed after 14.5ka, being similar in the study area to a map by Lundqvist (1986, Fig. 3) in his review of the Late Weichselian glaciation in Scandinavia. Thus, the marine shoreline was estimated to have reached Vega at 13, Brønnøysund at 12, Velfjord at 11, and Tosenfjord at 10ka. The maps show that, at the uncertain age of 9ka, the ice margin reached the lakes Røssvatn and Store Namsvattnet, along a line only 25km west of the MSW.

The ice retreats accelerated from 13–11ka during the Bølling / Allerød interstadial (interrupted by a short Older Dryas cold period at 12ka), but then a much cooler period of about 1000a, the Younger Dryas (YD) stadial, caused a small re-advance of the peripheral valley glaciers and the icesheet in the west, whilst, at the same time, the icesheet continued to reduce in thickness in the east. Andersen *et al.* (1981; 1982; 1995a; 1995b) identified marginal moraines that represent five glacial events in the study area: A (12300±200), B (11000–10300), C (10100±200), D (9550±200) and E (9300±200). The A (Vega) moraines coincide with the Older Dryas. The B (Tjøtta) glacial event in north central Norway suggests a cooling incursion of arctic water (with appropriate fauna) with the YD glacial advance at 11000. The glaciers retreated again after 10500, but re-advanced slightly at 10100, as recorded in moraines at the C (Nordli) event, which is also in the study area. Fastook and Holmlund (1994) and Holmlund and Fastook (1995) agreed, by modelling, that the YD cold climate signal barely exceeded 500 years, but was followed by a lagging 500 year stillstand in eastern Scandinavia. Other authors, including Svendsen and Mangerud (1987), regarded the "Main Line" of the extensive belt of YD Ra-moraines along the Norwegian coast as being dated at 10300, after which the Holocene melting of the icesheet was very rapid. A glacial geological map (Sollid and Torp, 1984) shows the main moraines and ice flow directions for the whole of Norway. 1:50000 Quaternary maps are being published by Norges Geologiske Undersøkelse, which show dated moraines for several parts of the study area.

Lehman and Keigwin (1992) showed that sudden changes in the flow of warm Atlantic surface waters into the Norwegian Sea occurred frequently during the last deglaciation, as the extent of sea ice changed. Broecker *et al.* (1998) and Clark *et al.* (2001) suggested that the various pre-YD oscillations occurred when the southern margin of the Laurentide Icesheet was located at the Great Lakes. Melting of the lakes allowed glacial water to flow to the northern Atlantic via the Hudson and St. Lawrence rivers, initiating a return to a cool period. When the lakes froze again, water was diverted to the Mississippi, to start a warm period, and to repeat the cycle. The later (YD) cooling was also supplemented by icebergs released from Hudson Bay, and by the rapid drainage of the Baltic Ice Lake.

2.3.5 Extent of glaciation

The direction of ice movement at the height of each stadial was generally radial from the thickest part of the icesheet. For the rather narrow Early Weichselian stadial, the ice divide was west of the highest mountains, so that the major ice flows were to the southeast, across northern Sweden. At the LGM, the thickest ice, and therefore the divide, was over the northern end of the Gulf of Bothnia, so that ice flowed to the west or to the northwest across all the Scandian mountains. The main movement at the surface and in the body of the icesheet was roughly westward across the study area. At its base, and particularly as the icesheets waned, movement was more oriented along valleys. This explains two distinct U-shaped valley profiles observed by the author in the NW-facing Bryggfjelldal (ZA): a valley glacier profile incised below a broader profile that extends up to the surrounding plateau level. Grønlie (1975, p448) noted that in the Durmålstind area (Z3 / Z4, on the watershed between the Western and Vefsn catchment areas), glacial scouring was very intense, with a plastic character. The general absence of heavily weathered summits, rock pinnacles and autochthonous blockfields (Sollid and Sørbel, 1979) demonstrates that most of the study area was covered by the icesheet, as these features are diagnostic of the intense frost-weathering of nunatak areas. Grønlie (1975) also pointed out that ice in side valleys is impeded by ice in main valleys, so that side valleys are over-deepened in their upper part, but near the junction they are eroded less and are left hanging (*ibid.*, p451), as at the V-shaped lower part of Eiterådal (Z4, *ibid.*, p453). The greatest glacial sculpting formed the most 'peaky' mountains along the coast, with alpine 'horn' summits occurring, for example, on the islands of Dønna and Løkta (Z1 / Z9).

Nesje *et al.* (1987) discussed the formula $H = 3.4L^{1/2}$, where H (m) is the height of the LGM ice at a distance L (m) inland from the edge of the icesheet at the continental shelf, for the coast some 400km south of the study area. Ignoring the reduced thickness of the icesheet in central Scandinavia (section 2.3.3), application of the same formula would indicate that the LGM icesheet was some 1700m thick at the coast (c. 250km east of the continental shelf) and nearly 2000m thick at the Okstind mountains (ignoring isostatic effects). Thus, the whole of the study area was *potentially* covered by the icesheet at the Weichselian LGM.

Nesje and Dahl (1992) modelled a "thin ice" 3D reconstruction of the Late Weichselian icesheet at its maximum. Their diagrams indicate that the ice thickness varied considerably, creating a multi-domed and

asymmetrical surface rising to altitude maxima of 2000m and thickness maxima of some 1600m, so that nunataks would have projected through the ice, including, perhaps, the highest Okstind peaks in the study area. This contrasts with the "thick ice" models of other authors, which suggest an entirely ice-covered landmass. (Mörner, 1980, gave a maximum thickness of 3050m at the Swedish Baltic coast; Donner, 1995, p96 showed a more uniform icesheet with a maximum thickness of >2500m; Fjeldskaar, 1994, showed a maximum thickness of 3200m). Fjeldskaar (2000) argued that the "thin ice" model would give significant deviations from the observed tilting of palaeo shorelines. Unconvinced by the Mörner (1980) tectonic component of postglacial uplift, he preferred his own 1994 model, for which all uplift was essentially glacio-isostatic (in agreement with Olsen and Grøsfjeld, 1999). The physical observations of Klemen and Hättestrand (1999), suggestive of a frozen-bed core, and a high-domed and stable icesheet, also argue against the "thin ice" model, as do the glacial erratics up to 1700m altitude seen by Grønlie (1975, p446) on the summits of mountains near Hattfjelldal in the study area. However, one 1559m peak projected 50m above the ice level, and the higher erratics could date from an earlier, thicker, icesheet such as the Saalian or Elsterian. Moreover, Boulton *et al.* (2001) reconstructed the flows within the Weichselian icesheet from satellite images of large-scale lineations of eskers, moraines and drumlins. Their evidence for relatively narrow, faster-flowing, ice streams within the retreating icesheet again argued for the "thin ice" model.

Two optional reconstructions of global ice margins and sea levels at the LGM were presented by the CLIMAP project in 1981, summarised by Clark and Mix (2002). The "minimum" model restricted ice margins to near-continental margins and accounted for 127m of ice-equivalent sea level lowering. The "maximum" model included marine-based icesheets and accounted for 163m of sea level lowering. The EPILOG program is revisiting the CLIMAP study. It has found that although LGM icesheet margins were close to the CLIMAP maximum model, their ice thicknesses differed, suggesting that the range of eustatic sea level lowering was from 120 to only 135m (Clark and Mix, 2002). This discussion therefore leans towards an assumption that some peaks stood out as nunataks at the LGM in the study area.

This concludes an initial review of glacial events relevant to the study area, prior to the arguments presented in Chapters 6–10. The various processes that applied during glaciations are described in Appendix A3.

2.4 Holocene

The Holocene interglacial period in Scandinavia was described by Andersen (1980), Donner (1995), and Andersen and Borns (1997). Lauritzen (1996c) presented a Holocene mean annual temperature curve for Mo i Rana (just north of the study area), based on speleothem stable isotopes. The Holocene is usually subdivided into five chronozones on the basis of radiocarbon dating of organic deposits. However, radiocarbon dating suffers from many problems, including the 'radiocarbon plateaux', when atmospheric ^{14}C decreased, perhaps due to lower solar radiation. Since about 1993, dendrochronology has enabled

Holocene radiocarbon dates to be calibrated to calendar years. The Younger Dryas / Holocene transition at 10000^{14}Ca BP, identified in a lake sediment in western Norway, was thus matched to give a calendar date of 11530+40/-60 cal. a BP (Gulliksen *et al.*, 1998). In this section, dates refer to radiocarbon years before AD1950 or to historical dates.

2.4.1 Preboreal 10000–9000

The period following the Younger Dryas (YD) cold signal after 10500 was one of gradual, then rapid, warming, but still with glacial fluctuations, perhaps caused by high precipitation (Lundqvist, 1986). A temperature rise of c. 7°C in 50 years at Greenland was cited by Gulliksen *et al.* (1998). Alley *et al.* (1993) reported, from studies of the GISP2 ice core, that snow accumulation doubled in Greenland at the end of the YD, with most of the change occurring in *just one year* (as had also happened at the start of the Bølling interstadial). The northern Atlantic became ice-free soon after 10000, and the Scandinavian icesheet retreated eastwards, up the fjords. End moraines clustered at 9900, 9600 and 9300 in the study area and elsewhere indicate small advances and retreats. Dead-ice areas and lakes dammed by ice and moraines formed on each side of the cols as they were exposed, because the ice melted first on the summits and the higher ridges (Lundqvist, 1972). The water initially flowed westwards, commonly via high 'up-valley' outlets (section 8.4.8).

The western, ice-free, parts of the land supported park tundra, with birch in the south. Much of Norway was deglaciated by 9000, the sea level rose (opposing a considerable isostatic uplift), but a remnant, stagnant, icecap remained over Sweden. This re-emphasises that the ice divides lay to the east of the underlying water divides. The climate became much warmer, with birch, pine and spruce repopulating central Norway.

2.4.2 Boreal 9000–8000

The icesheet had gone by 8500, finally disappearing from an area approximately coincident with the eastern edge of the Caledonide nappes (Lundqvist, 1986, Fig. 3). From the evidence of elm growing at altitudes of 700m in southern Norway, the snow line there was 400m higher than now. Thus, it is likely that, from 8500–8000, most of Scandinavia was also free of mountain glaciers (Ehlers, 1996, p311).

Kame terraces and dead-ice topography are dominant in much of central Scandinavia. The lower valleys of the Nordland mountain ridge display thick glaciofluvial accumulations that were later cut by rivers to form terraces. This is in some contrast to Sweden and Finland, where the deglaciation commonly formed sinuous eskers, and almost-annually-varying stream channels. The easternmost part of the study area in Sweden exhibits very long SE-directed river valleys and lakes in plateau areas of rather low relief, which are remarkable for the extent of the till deposits and the size and number of erratic boulders on the surface. The deglaciation of the whole study area and its effect on karst and caves is deduced in more detail in Chapter 8.

2.4.3 Atlantic 8000–5000

Except for a glacial advance from 7600–7100 and a short advance at c. 6600 (Karlén and Kuylenstierna, 1996), the Atlantic chronozone was relatively moist and warm in northern Europe, with the Holocene Climatic Optimum at 5000 supporting broad-leaf and oak forests in southern Scandinavia. The mean annual temperature there rose to 10°C, with the mean July temperature being 20°C. Paradoxically, the moist weather also assisted a regeneration of the glaciers in the mountains at 6300 and 5600 (Karlén, 1988), and a corresponding drop in the tree line.

2.4.4 Subboreal 5000–2500

Pollen records indicate that 5300–4900 and 3500–2800 were drier than the Atlantic chronozone. These warm and dry periods favoured the expansion of trees in both north and south Norway. The period 4800–3800 was characterised by high-frequency glacial fluctuations in southern Norway (Dahl and Nesje, 1994). Climatic deterioration started again at 2800 and the valley glaciers advanced in consequence, some remaining continuously until the present.

2.4.5 Subatlantic 2500–present

By 2500, a cool, moist, climate had replaced the warm, moist, climate of the Atlantic chronozone, with temperatures and glacial extents rather like those of today throughout the period, but with small fluctuations. Modern mean annual and mean July southern Scandinavia temperatures are 7° and 16°C. The broad-leaf forests have generally retreated back to spruce, pine and birch, whereas the glaciers have *generally* advanced. Griffey and Worsley (1978) studied Neoglacial glacier variations in the Okstind mountains, and concluded that there were three major Neoglacial advances at 3000–2500, at 1250–1000, and at the "Little Ice Age", which reached its maximum in the eighteenth century (except for a few small glaciers that attained maxima early in the twentieth century). Each of these expansion episodes reached nearly-identical terminal positions, when the glaciers occupied an area that was some 30% greater than the 53.5km^2 covered at present, and the valley glaciers were up to 1km longer. However, the highest peaks still protruded as nunataks. The evidence showed that there had been no other glacial advances of this extent since the Boreal. (A basal peat from just outside this area of Neoglacial advance was dated to 8083±160). Historical records in Norway commonly show strong glacier advances down valleys from AD1700 to AD1750, and from AD1925–1930. Glacial retreats are recorded in the 'Roman Period' around AD200, and at the present time from AD1930–1960 (e.g. Theakstone, 1964), and perhaps until AD2004, but with local exceptions.

The pine tree limit followed a general trend down to its present modern level from altitudes up to 300m higher at 9000–8500. Fluctuations may correlate with variations of solar irradiation with a lag of 150 years (Karlén and Kuylenstierna, 1996). Since 5000, almost half of this lowering resulted from glacio-isostatic recovery, and just over half was caused by "orbital forcing" climatic factors. The various environmental conditions that apply at present are summarised in Appendix A4.

2.4.6 Isostatic rebound

The Holocene cooling may have resulted from the Fennoscandian uplift relative to sea level that, since the start of the Holocene, has reached 125m (north central Norway coast), 225m (central Swedish Caledonide thrust front), and 295m at the central point of the previous icesheet at the Swedish coast on the northern Baltic (various sources). The last elevation was proved by the discovery of marine features at this altitude. The contemporary (1992) rates of uplift at these three places are 3, 6 and 9mma^{-1}. Grønlie (1975, p453) remarked that isostatic depression reaches nearly one third of the ice thickness. Although difficult to determine accurately, the maximum *absolute* Fennoscandian uplift since 13000, following the LGM, was shown by Mörner (1979, Fig. 26 and 1980) to be 830m at the icesheet centre, and 300m at the north central Norway coast. The maximum subsidence in the North Sea Basin was 170m. The absolute uplift at the icesheet centre was 570m since the Younger Dryas. The NW Europe "regional eustatic" sea level rise was some 90m since the LGM, and some 40m from the start of the Holocene until 6ka, after which it has been almost static (Mörner, 1979, Fig. 16; Pirazzoli, 1996, p90). These compare to a *global* eustatic sea level rise in the range 120–135m since the LGM (section 2.3.5). However, Mörner (1980, p263) suggested that the *local* sea level reached as low as -245m at the LGM, i.e. far below the eustatic depth. Mörner (1979 and 1980) presented evidence that the Holocene uplift had exponential and linear factors that were caused by two different mechanisms, supported by Nesje and Dahl (1992), who argued that postglacial uplift is not just dependent on icesheet loading.

Dehls *et al.* (2000) published a neotectonic map for Norway and adjacent areas based on the latest levelling information and techniques. Their plotting of present uplift curves revealed a structure far more complex than the long straight lines of earlier authors, including Sørensen *et al.* (1987). In the Velfjord area, their isolines are quite curved, although remaining fairly parallel, and follow more easterly trends than previous representations. It seems likely that this structure differs from the previous YD isobase representation because the original strong vertical isostatic uplift has decayed into a more complex tectonic movement with both vertical and horizontal components. The influence that isostasy and varying sea levels have on cave development is addressed in Chapter 8.

This Chapter and Appendices A1–A4 have now provided the geological and geomorphological context within which the Caledonide metacarbonates were formed, and with a working assumption that many of these processes were complete prior to the onset of the karstification that is presently visible. After a review of the current knowledge of speleogenesis and glaciated karst in Chapter 3, Chapter 4 presents a detailed study of the carbonate outcrops of the study area, building on some of the concepts discussed in Appendix A2.

CHAPTER 3 CURRENT KNOWLEDGE OF SPELEOGENESIS AND GLACIATED KARST

The aims of this Chapter are a) to introduce the development of ideas about the ways caves form in sedimentary carbonates, b) to review current knowledge of the geomorphological and karstic impacts of glaciation, and then c) to discuss the current knowledge about the formation of caves in the Scandinavian Caledonide metalimestones against these backgrounds. From this set of views and information, and the data presented in Chapters 4 and 5, models for cave development in the study area itself can then be proposed.

Historically, the speleogenesis and development of caves in metacarbonate rocks has received very little attention, despite metalimestones and metadolostones accounting for a large proportion of global carbonate outcrops. For example, the word *marble* was only mentioned on six pages by Ford and Williams (1989). Klimchouk *et al.* (2000) gave examples of caves formed in metalimestones, but drew no conclusions about their genesis. Thus, there has been no attempt to provide a general model for cave development in metalimestones, nor even a discussion about whether such a general model exists. Nearly all the work on generic cave development to date has assumed a setting of a sedimentary limestone outcrop. Furthermore, this setting has commonly been regarded as rather extensive, and not very confined, so that many early models of cave genesis were described on the basis of horizontal or sub-horizontal limestones, perhaps lying between strata of other sedimentary, but insoluble, rocks. The modern approach has extended to encompass dipping limestones, but, interestingly in the context of this study, it was not until Osborne (1999) that there was an analytical consideration of caves occurring in vertical, or near vertical, sedimentary limestone beds.

3.1 Caves and karsts in sedimentary carbonate rocks

The scientific study of caves and karst has now been in progress for over 100 years, initially from a qualitative rather than a quantitative analysis. The historical development of this knowledge, up to about 1990, was reviewed by Lowe (1992b; 2000a), Ford (1998), and White (2000a). The most comprehensive reviews of speleogenesis were those by Ford and Williams (1989) and by Klimchouk *et al.* (2000). It would be inappropriate to repeat here the work undertaken by these authors in their analyses of the early literature. Instead, various speleological topics are introduced briefly, without necessarily citing the original references, where it is anticipated that these topics may be important in understanding the speleogenesis of endokarst in glaciated metacarbonates. Information from more contemporary papers is discussed in more detail, as appropriate.

3.1.1 Zones and watertables v. open independent passages

The most important early speleological observation was the distinction between vadose and phreatic passage profiles, with the deduction that such profiles were developed by streams with an air-surface that flowed under the direct influence of gravity and by streams that completely flooded the passage and

flowed under the prime influence of hydrostatic pressure. Because vadose flow is commonly at a higher elevation than phreatic flow, three "hydrographical zones" of vadose, shallow (or epi-) phreatic and deep phreatic water came to be recognised. Thus, the basic (but now resolved) conflicts in Speleology, which were present from the beginning of the scientific investigation, were to determine which of these three zones provides the major focus for cave formation, and to decide whether the concept of a watertable, as applied to other sedimentary strata, had any relevance in karst.

The American geomorphologist WM Davis developed a two-cycle theory of landform development, in which fluvial erosion eventually reduces a mountainous landscape to a flat peneplain. Rapid uplift then creates a high plateau, so that the process can be repeated. The theory was extended to cover the karst situation, so that conditions external to the underground limestone could be used to explain speleogenesis within the limestone. In the first cycle, Davis postulated a deep, phreatic, slow dissolution, which lasts for millions of years as meteoric water replaces formational water in the limestone. Uplift and downcutting of valleys lowers the watertable and causes subsequent shallow phreatic dissolution in shorter timescales, which begins to form cave passages. In the second cycle, further uplift causes downcutting of valleys, to promote vadose enlargement above the watertable. The cycles are repeated, with possible links between mineralization and cave formation.

A commonly-ignored stream piracy theory of cave formation (Woodward, 1961) associated the cave-forming process with the history of the adjacent surface drainage system. Woodward postulated that relatively sudden events, such as a fall in sea level, deglaciation, major climatic change, relocation of a surface steam, or the breakthrough of an impervious barrier, can trigger the initiation of cave development via the piracy of an existing surface or underground stream by a new drainage route. Some of his ideas seem to anticipate the Palmer / Dreybrodt model (section 3.1.13) and concepts developed in Chapters 8 and 9 of this thesis.

Methods to model the length distributions of caves in a region were proposed by Curl (1958; 1960; 1966; 1986), the last paper using a fractal approach. Laverty (1987) also suggested that individual cave lengths behave as fractals. Ford and Williams (1989, p245) used log rank / log size correlation (Zipf) plots to demonstrate linear relationships for cave length and depth at a world scale. Badino (2001a) plotted the logarithm of the number of caves longer than a particular length against the logarithm of length, and found a linear law. He concluded that the processes that influence the existence and the explored length of karst caves in sedimentary limestones appear to be scale invariant and related by hidden fractal behaviour. However, Badino found that cave *depths* are not scale invariant: on a global view, cave depth has a 'scale' of 270m, and is probably connected with a mountain or limestone-thickness scale. (Section 6.5.2 proposes instead that the subsurface cave distance is a more useful parameter in metalimestones). Howard (1971) proposed measures of topological complexity of cave networks, and considered their utility as indices of their mode of origin.

3.1.2 Chemical and hydrological models

After the 1930s, the study of karst became more analytical. For example, WE Davies (1960) postulated a four-stage sequence of shallow phreatic development in folded limestone, starting with *random* dissolution at depth along bedding planes linked via joints with the *most prominent zone of dissolution being at the junction of two limestone lithologies.* However, some observations about cave passages in the folded sedimentary limestones of the Appalachians conflict with passage morphologies in the dipping metamorphic limestones of the study area, especially his remark that *"many caves in folded limestone show very little relationship between the bedding of the rock and the development of passages"* (*Ibid.*, p8). Nevertheless, he did state that "*where the dip of the beds is greater than 80°, the major development of passages almost always follows the bedding planes*" (*Ibid.*, p8) and he did discuss fracturing caused by stress conditions in the rock, both being observations with resonance in the study area.

The *"exceptionally complicated"* (White, 1977, p505) dissolutional chemistry of limestone is still being studied. Much groundwork was undertaken by the 'Bristol School' of academic speleologists on the basis of practical experiments in the 1960s and 1970s in the Mendip Hills in the UK, and in County Clare in Ireland. Their outputs included Atkinson (1968), Picknett (1976), Picknett and Stenner (1978), and Trudgill (1985). Atkinson (1977) showed that groundwater flow in Mendip occurs as both turbulent flow in conduits and as diffuse Darcian flow in fine fractures.

The discovery of mixing corrosion (e.g. Bögli, 1964) showed that the mixing of two saturated solutions with varying CO_2 concentrations always produces an unsaturated, aggressive, solution. The large-scale dissolutional enlargement of water-filled passages seemed to be explained: even if calculations showed that the main flow became saturated beyond a particular point, a subsidiary input could always make the water aggressive again. However, dissolution along micro-conduits could still not be explained at this stage, as Weyl (1958) showed that slow-moving water in joints of 0.2mm width (for example) would become saturated and non-aggressive within the first 10mm: the *penetration distance*. Faced with this apparent impossibility of speleogenesis by carbonic acid, Howard (1964) proposed the *in situ* generation of strong acid to initiate and enlarge long micro-conduits and offered various mathematical treatments. SN Davis (1966) suggested that there would be no movement through the very low primary porosity of limestone, not even in joints with widths up to 10microns. By using a wire probe, he found that fresh limestone outcrops had fractures up to 20microns wide, and invoked groundwater pumping through earth tides, earthquakes and other processes to achieve a dissolutional flow. Diurnal tidal pumping would tend to prevent re-cementation within the fracture.

Sippel and Glover (1964) found experimentally that a slight increase in solubility with depth is negligible compared with the effects of temperature and P_{CO2}, up to a rise in hydrostatic pressure of 200 atmospheres. Palmer (1991, p6) also stated that pressures up to 25 atmospheres (~260m of water depth)

have little effect on (carbonate) equilibria. No results have been published of any pressure effect on activity coefficients (e.g. by Dreybrodt, 1988). It is therefore assumed herein that this is also negligible.

The transition from *laminar* to *turbulent* flow was shown to occur commonly at a conduit diameter of 5–10mm (White and Longyear, 1962; Atkinson, 1968; Wigley, 1975; but see section 8.5.2). Thrailkill (1968) reported the laboratory analysis of flows through pipe networks. He concluded that, under common limestone aquifer conditions, the flow pattern is the same under Darcy, laminar, turbulent or mixed flow, and that flow in shallow conduits should not be significantly greater than flow in deep conduits. Curl (1971) stated that short karst conduits with laminar or turbulent flows that remain unsaturated enlarge to diameters and volumetric flow rates proportional to the inverse of their length raised to a power between one-third and two-thirds. Thrailkill (1968) also considered the problems of vadose seepage and the enhanced dissolution possible when waters lose temperature (e.g. on meeting a watertable), mix, or change flow rate (as in a flood). Smart and Whitaker (1988) discussed the transition of primary, *porosity*, flow to secondary, *permeability*, flow. By the time of White (1988, p148) *"The modelling of equilibrium processes in carbonate waters has reached a mature stage of development, but kinetic modelling is in its beginnings"*. Understanding carbonate dissolution kinetics is important for studies of cavern enlargement, because waters flowing through well-developed karst systems rarely have the time needed (c. 10 days) to reach equilibrium (White, 1984, p227; White, 1988, p213). Recent summaries of calcite equilibrium chemistry include those by Dreybrodt (2000) and Gabrovsek (2000, pp18–22). Aspects of the dissolutional chemistry of dolostones and other carbonates are considered in section 3.1.15 and Appendix A2.

3.1.3 Kinetic trigger

The micro-conduit saturation problem was resolved by White (1977) in his discussion of laboratory tests of the dissolution of pure synthetic calcite in sea water conducted by Berner and Morse (1974). They had found that the rate of calcite dissolution varies by nearly five orders of magnitude, depending on the degree of under-saturation, and proposed that the graph of calcite dissolution rate passes through three regions as the solution becomes more saturated. Similar conclusions were reached by Plummer and Wigley (1976) and by Plummer, Wigley and Parkhurst (1978). These authors studied the dissolution of pure calcite in CO_2 / pure water systems over ranges of temperature and CO_2 pressures. The former paper concluded that the rate of dissolution of calcite in natural environments may be influenced by both transport processes (especially in low pH solutions) and surface-reaction processes (especially in higher pH solutions near to equilibrium). The latter paper showed that three different physico-chemico kinetic mechanisms participate in calcite dissolution: chemical reactions at the calcite surface; transport of various species in the aqueous solution; and the slow conversion of H_2O and CO_2 into H^+ and HCO_3^- ions. Each of the three mechanisms can become overall rate-limiting in suitable conditions, as the ratio of solutional volume to calcite surface area, and other variables, are changed (section 3.1.13). Nevertheless, equilibrium should be reached within a few years at most. Aquifers that take much longer times to reach

calcite saturation point to the significance of the inhibition of dissolution rate by other metal and oxidate ions in natural waters, including micromolar concentrations of PO_4^{3-}, which cause *"higher-order kinetics"*, as equilibrium is approached (section 3.1.14). The latter paper also derived what is now called the *PWP equation*, to give the *pure calcite* dissolution rate at fixed P_{CO2} and temperature. In practice, the rates calculated are commonly too high by about an order of magnitude for *natural* limestones. Sjöberg (1978) confirmed the inhibiting effects of Mg^{2+}, PO_4^{3-}, SO_4^{2-} and sea water on the dissolution of synthetic calcite powder, and found that dissolved organics had no measurable effect. Sjöberg and Rickard (1984) studied calcite dissolution rates in aqueous KCl solutions, far from equilibrium. Their summary diagram showed a 3x3 matrix of mechanisms and regimes for varying temperature and pH

White (1977) introduced the idea of a "*kinetic trigger*", by postulating that saturation by calcium carbonate is never fully achieved. This means that there is still some aggressiveness left to cause gradual carbonate dissolution along the full length of the flow. The first path to allow water to leave the aquifer under-saturated and below a critical level becomes the *victor route*, with a subsequent more rapid enlargement. He also noted that if mixing of two waters led to an under-saturation great enough to shift the system into a different kinetics regime, then dissolution could accelerate beyond that expected purely by the mixing corrosion effect, a conclusion quantified by Romanov *et al.* (2003). White thought that the transition from a *fracture aquifer* to a *conduit aquifer* occurs at diameters from 1– 10mm, to coincide with the size range for the transition from laminar to turbulent flow. Another coincidence reported by White (1979) is that the critical velocity above which clastic sediments are prevented from clogging fracture permeability occurs at a similar fracture width.

Despite the many papers that explore the dissolution chemistry of calcium carbonate, and to a lesser extent that of dolomite (Appendix A2.8), no references are known that fully differentiate the varying equilibrium and kinetic chemical behaviours between the Aragonite, Low Magnesian Calcite, High Magnesian Calcite (and other) forms of calcium carbonate (Appendix A2.4). Some of this information may be deduced from Rauch and White (1977, Fig. 6), who studied dissolution rates under closed, turbulent, flow conditions. Svensson and Dreybrodt (1992) provided more details, whilst admitting that a large programme of work was required to gain more insight into the *inhibition* of calcite dissolution. The way in which the kinetic trigger idea and the resolution of many aspects of the kinetic behaviour of natural calcite in carbonic acid led to a comprehensive physico-chemico model for the development of conduits and caves is discussed in sections 3.1.13–3.1.15.

3.1.4 Geological rationalisations

Although discussions about individual cave and karst sites involved an appreciation of the local geological setting, the generic models of cave development produced from the scientific treatments prior to about the 1980s still tended to regard the limestone bedrock and aquifer as a homogeneous fabric, within which caves developed from an, as yet unknown, *inception* process. The importance of geological

guidance became increasingly recognised after the observation of preferential 'carrier beds' and downward limits at shale aquicludes. For example, in the caves of the Yorkshire Dales, UK, Waltham (1970) demonstrated: a) the guidance by "shale" layers along major bedding partings; b) the initial phreatic phase above vadose passage sections; and c) the lack of a regional watertable. Waltham (1971; 1974) revealed a basic geological and stratigraphical guidance on cave development, whilst suggesting the evolution and chronology of the Lost John's System in Yorkshire.

Rauch (1972) undertook a laboratory analysis of carbonic acid flows through limestone lithologies of varying purity and crystal size, and found that sulphuric acid from pyrite could increase carbonate dissolution, and produce vugs in dolostones and limestones. Palmer (1991) also showed that sulphuric acid could be produced from the oxidation of pyrite in limestone sequences, and showed that, in horizontal maze caves, two dimensions are controlled by joints and the third dimension by stratigraphy.

The major achievement of this period was a rationalisation of the watertable / no watertable debate in the papers of firstly DC Ford (1965a, 1968, 1971b), which studied cavern development in the Mendip Hills, UK, and secondly of Ford and Ewers (1978), as presented again in Ford and Williams (1989, p26). This work showed convincingly that caves can develop in all three hydrographical zones (section 3.1.1), and proposed that the actual cave networks produced are guided by fissure frequency and geological structure. The Ford and Ewers *Four-state Model* of cave development in both flat-lying and homoclinal sedimentary limestones postulated that deep, phreatic-loop, caves form in State 1, with a low fissure density. At an increased fissure density, State 2 caves form where the tops of the phreatic loops intersect the piezometric surface. Gradational passages with a free air-space can bypass the loop tops. State 3 caves have a mixture of smaller-amplitude phreatic loops and watertable-levelled components. At a high level of fissure frequency, State 4 caves form long horizontal river passages along the watertable. In all cases, new passage elements commonly propagate headwards from the outlet spring. Ford and Ewers (1978) suggested that fissure frequency in a limestone aquifer decreases with depth, but increases with time, and (*Ibid.*, p1794) noted that the fissure frequency is generally high in tight folding. Palmer (1990, p199) stated that the frequency and width of available fractures increase with relief. These observations commonly apply in the study area (Chapter 6). Ford (1998; 2000) introduced States 0 and 5, to cover the extremes of zero fractures (without caves) and dense fractures, where flow is too diffuse to form passable conduits, to specify the *amplified four-state model.*

Although the universality of the Four-state Model has been questioned, its common applicability has also been confirmed from physical and chemical principles (Gabrovsek, 2000, pp113–133; Gabrovsek and Dreybrodt, 2001; Kaufmann, 2002). Difficulties may arise in defining the scale of the fracture openings and their frequency, and in considering the *primary* porosity of the limestone, which in some lithologies (e.g. Pleistocene limestones) may be a major factor. (Porosity is highly variable between lithologies, whilst probably remaining almost constant with depth, if not with geological time). Bitterli and Jeannin

(1997) considered that the Four-state Model may not apply generally to Alpine karst, where the "high" fracture density should lead to shallow phreatic caves, rather than caves with phreatic loops many hundreds of metres in amplitude, as in the Sieben Hengste cave. Their analysis of vadose–phreatic transition points and related palaeo spring levels showed that this system evolved downwards via eight successive discrete phreatic levels, perhaps starting in the Pliocene. In the context of this study, the genesis of each flow system appears to be fast compared to the evolution of the landscape (otherwise the discrete phases would not be recognisable), suggesting that there is a relationship between the lowering of spring levels and valley entrenchment by major glaciations (Chapters 7–9). Bitterli and Jeannin (1997) concluded that the recent numerical models of karst dissolution (i.e. the Palmer / Dreybrodt model: section 3.1.13) explain many features of the Sieben Hengste system, and that spring positions and hydraulic gradients appear to play an even more important role in explaining the geometry of conduit networks than the fracture setting. In a discussion at the end of Jeannin *et al.* (2000), DC Ford confirmed that the illustrations for the Four-state model are for the simple case where the drainage and stratal dip share the same direction, and the debate was continued by Worthington (2001; section 3.1.12), Ford (2002) and Worthington (2002).

In contrast to the evidence of *geological* guidance of passage development, Palmer (1984a; 1984b; 1987) showed that, in stable areas with shallow dip, as at Mammoth Cave, Kentucky, cave levels can be correlated with *geomorphological* base-levels, and thus be used to interpret the evolution of landscape. The third paper explained how, in favourable situations, long-lasting external base-levels can be determined by finding elevations of former vadose–phreatic transition points, whilst carefully interpreting perched phreatic loops in the vadose zone. However, the method is difficult to apply in mountainous areas with steep hydraulic gradients (section 3.2.2). Palmer (1990, p195) remarked that, whereas phreatic conduits exhibit a long-term stability, vadose channels are continuously susceptible to route diversion. Brahana *et al.* (1988, p342) mentioned three possible major base-level controls: sea level, perennial streams, and impervious rock formations. In the study area, lakes and tarns that occupy glacially-scoured basins can also act as base-levels.

3.1.5 Strong acids and thermal waters

The potential role of locally-generated strong acids in promoting early conduit initiation was also considered by, *inter alia*, TD Ford (1963), Morehouse (1968), Egemeier (1987) and, in passing, by Palmer (1991, p18). Hill (1981; 1995) suggested that the formation of the extensive Carlsbad Caverns and Lechugilla Cave in New Mexico relied on the *in situ* generation of sulphuric acid by oxidation of H_2S from solutions rising from deep hydrocarbon-rich deposits. This *sulphuric acid karst* gave a practical example of the strong acid ideas of previous authors. Jakucs (1977) discussed the non-karstic corrosion of limestone by humic acid from soils, and by sulphuric and nitric acids from oxidation reactions. The presence of sulphate reducing bacteria within the sub-permafrost aquifer at south Spitsbergen was reported by Lauritzen and Bottrell (1994). Osborne (2001b) observed that palaeokarst deposits and less

soluble units in caves in eastern Australia are commonly altered by emplacement of pyrite and dolomite, thought to be derived from ascending thermal waters.

Worthington and Ford (1995) examined a possible relationship between an epigene / hypogene cave distinction (Palmer, 1991; section 3.1.16) and non-thermal / thermal spring waters, by studying the chemistry and temperature of risings in the Sierra Madre Oriental (Mexico), the Rocky Mountains Front Range (Canada) and the Peak District (England). In these three areas, the lower altitude, regionally-derived, thermal water flows always have higher sulphate concentrations than the higher altitude, locally-derived, non-thermal water flows, especially at times of low flow. Reduced temperature and sulphate concentration in thermal springs at high stage could be explained by mixing with locally derived groundwaters. The emergence of sulphate ions from springs as a waste product is indicative of a dissolution chemistry involving sulphuric acid in conduit enlargement. They concluded that the morphological distinction between epigene and hypogene caves cannot be extended to classify carbonate aquifers into two types, as the initial enlargement of epigene conduits may also have been influenced by deep waters with sulphur chemistries. Thus, it appeared that many, *or possibly most* [!], epigene caves were initiated by hypogene, sulphate producing, processes.

Sustersic (1997) hinted and Pezdic *et al.* (1998) proposed that speleo-inception is promoted at dolostone / limestone contacts, because silica-rich solutions can decompose dolomite at low temperatures (2–16°C) to produce clay minerals and abundant CO_2. Lauritzen (1981, p14) noted that sulphide minerals are common in contact metamorphic limestones in Norway and Lauritzen and Lundberg (1999, p665) mentioned in passing the possibility of oxidation of sulphide grains (from mica schist and iron oxide ores adjacent to the marble) to sulphuric acid at **Søylegrotta** near Mo i Rana, in northern Norway. These mechanisms could apply potentially in the study area.

Bottrell *et al.* (2000a; 2000b) reviewed the literature on strong acids. Whereas other workers regarded examples of strong acid dissolution as *special* cases, these authors regarded them as *extreme* cases of speleogenesis, perhaps by ubiquitous processes not based exclusively on carbonic acid. A variety of chemical deposits within carbonate successions can produce sulphuric acid in many situations. These include *sulphides*, especially iron pyrites, which oxidise in the presence of dissolved oxygen, perhaps with suitable bacteria, and *sulphates*, which can be reduced by microbial activity to H_2S, which, in turn, can then be oxidised to H_2SO_4. It appears that almost any iron salts, and many sulphates, can lead to sulphuric acid production. Whenever H_2SO_4 is released, reaction with carbonate increases porosity and generates CO_2, which, in its turn, makes the solution more aggressive, causing *double solvency*. Because the strong acid is generated locally, perhaps along the whole length of a fracture or aquifer, large quantities of carbonate may be consumed quickly, without relying on *"kinetic triggers"* and high-order kinetics for conduit breakthrough (section 3.1.14).

3.1.6 Palaeokarst

The importance of palaeokarst is increasingly recognised as proving that processes of karstification have existed on earth over long periods of geological time. TD Ford (1984 and 1989) reviewed the widespread evidence of palaeokarst in, particularly, the Carboniferous limestone areas of Britain. Most of these originated as a covered karst, i.e. developed under soil or other superficial deposits, and became buried karsts after being buried beneath deposits of younger strata. In the Peak District, the Dinantian limestone sedimentation was cyclic, with marine transgressions and regressions and intermittent vulcanicity. Exokarst features were developed during maximum regressions, when the lime sediment was exposed at the surface, as can be seen today where volcanic tuff horizons are removed from limestone exposures. Post Dinantian uplift was followed by Namurian sediments filling deep grykes and caves. The mineral deposits of Derbyshire are thought to have originated from hydrothermal solutions penetrating into fissures that resulted from Late Carboniferous tectonic movements, and into pre-existing cavities, to create *hydrothermal palaeokarst*.

Osborne (1986) provided evidence for "multiple karstification", starting at the latest in the Tertiary in some places in New South Wales, Australia, and starting in the Cretaceous in Timor Caves, NSW. Lithified Tertiary sediments of sandstone and conglomerate turbidites in the Wellington Caves indicate that sub-aqueous mass flows can totally infill pre-existing passages. Smart *et al.* (1988) reviewed the existence of Neptunian dykes and related features. The books edited by James and Choquette (1988) and Bosak *et al.* (1989) reported the evidence for palaeokarst from many sites around the world, the oldest being in early Proterozoic carbonate rocks in Canada. Palaeokarsts that accumulate petroleum were found by drilling wells in NW China. They occur in late Precambrian and Ordovician sedimentary limestones and dolomites (undefined) at depths up to 5400m (Cao *et al.*, 1999). Osborne (2000) discussed the need to redefine the term "palaeokarst", and the need to distinguish between "palaeo" and modern sediments in caves that can be entered today and which display multiple karstification phases.

Bassett (1985, p287) remarked that Silurian quartz sands "*finally covered Caradoc* (Mid Ordovician) *karstic surfaces in the north*" (of Norway). "*At least one period of karstification*" is identifiable in a shallow carbonate – dolomite – evaporite sequence in Silurian beds (*Ibid.*, p289). These statements take the time of possible early cave formation and burial in the Scandinavian Caledonides back to the Ordovician / Silurian, pre-dating the completion of the Caledonian Orogeny. Similar evidence is also available from Scotland, as Palmer *et al.* (1980) reported palaeokarstic fissures up to 150m deep in Early Cambrian Durness Group carbonates. The fissures are filled with breccias derived from overlying Ordovician dolostones, suggesting a Mid to Late Cambrian orogenic phase, during which karstification, or possibly the tectonic opening of rifts, occurred. Clearly, all the above examples avoided subsequent high-grade metamorphism.

Lauritzen (1988a; 1989c) discussed the Scandinavian evidence in more detail. No more-recent palaeokarsts are known, but Lauritzen surmised that fragments of Tertiary palaeokarst, formed during up to 60Ma of deep weathering, *should* exist, even if not yet recognised, and some of the few very large relict caves at high altitudes that are known in northern Norway *may* be examples of Tertiary karst. There are no reported examples of palaeokarst from Sweden and none from the study area. Sections 10.4 and 10.6.7 conclude that they do not exist in the non-Arctic *metamorphic* carbonates of the Caledonides.

3.1.7 Palaeohydraulics

Scallop and sediment grain sizes are used in Chapter 8 to estimate flow rates in study area caves. The properties of scallops and flutes were described in mathematical treatments by Curl (1966a and 1974). From Curl (1966a, Fig. 1), the product of scallop length in centimetres and flow velocity in cms^{-1} is roughly $400cm^2s^{-1}$, at 0°C. The steeper face of the scallop points downstream. Stable flute patterns only occur in fully turbulent flow, with a channel Reynolds number in the range 200000–2000000 (*Ibid.*, p132). The uniform dissolution of a patterned surface increases the sharpness of cusps (*Ibid.*, p145), but eventually removes the pattern (*Ibid.*, p154), and scallops do not form when their size would equal the passage diameter (*Ibid.*, p153), as occurs with low-velocity ponded flow (e.g. below an icecap). Lauritzen (1981d) presented a methodology for determining flow direction from a statistical analysis of scallop asymmetry, although this method may not always be practical in metalimestone with schistosity (Kirkland, 1958). Lauritzen *et al.* (1983; 1985) deduced that scallops represent the highest stages of flow, not the mean rates. Urushibara-Yoshino *et al.* (1996; 1997) studied the formation, by abrasion, of floor scallops in Irimizu Cave in Japan, which has formed in well-crystallized *marble* with a grain size of 3–4mm. However, Murphy *et al.* (2000) reported examples of contrasting scallop size populations between the floor and roof of the same, wholly-phreatically-formed, passages, indicating potential difficulties in determining appropriate flow rates. Floor-level channel karren-like abrasion features in flood conduits were described by Murphy and Cordingley (1999).

Gale (1981) discussed the inferences about the palaeohydraulics of cave streams from studies of cave sediments. Gale (1984) considered the very complex hydraulics of conduit flow in carbonate aquifers from the evidence of scallops, transported sediments, friction and roughness. Phreatic and vadose flows are commonly turbulent (Reynolds Number > 2000) and subcritical (tranquil), with Froude Number <0.5. He deduced that flows at $1.45ms^{-1}$, at the upper end of the known velocity range, are competent to entrain "particles" of ~0.59–2.9m (metres) diameter. However, with the number of unknown variables involved, it is clear that no *simple* relationship can be stated between cave sediment particle size and flow rate. An abstract by Bosch (1998) made the important point that, in cave systems, there is a self-regulation of clastic deposition to maintain most efficient water flow. (If a passage becomes choked by sediment, water will flow to higher levels until the pressure rises sufficiently to flush the sediment downstream). He also defined *young karst* as having ephemeral underground streams in low flow, but surface flow in

flood, and *mature karst* as exhibiting an absence of surface streams. (See also comparable work by Smart, 1988 in section 3.1.10). A quantitative theory for sediment transport was also mentioned.

Lauritzen (1986c) calculated the present mean conduit radial increase in the **Glomdal Underground Outlet** (formed in marble) in northern Norway (section 3.3.3) to be $0.8mma^{-1}$, from the increase in hardness between the inlet and the outlet. A study of scallops in the same system showed that the dominant discharge that guides scallop morphometry is the highest discharge of 2–15% duration, when corrosion rates are also highest. This *scallop dominant discharge* also appeared to be proportional to the contemporary catchment area (Lauritzen *et al.*, 1983 and 1985; Lauritzen, 1989d).

3.1.8 Epikarst and subcutaneous zones

The significance of the epikarst began to be appreciated from the mid 1970s (Ford and Williams, 1989, p206). It is sometimes defined as both the soil layer and the subcutaneous zone, which is a zone of highly weathered rock lying above the relatively unweathered rockmass of a karst aquifer (Lowe and Waltham, 1995). Other definitions equate the epikarst zone just with the subcutaneous zone. Palmer (1991, p12) noted that surface openings result from epigenic dissolution at its most aggressive. Gunn (1981a; 1983) discussed the hydrological processes in karst depressions at Waitomo, New Zealand, showing that there are six main flow components. It is now known that the great majority (although the 98% reported by Worthington, 1991 is atypical) of autogenic corrosion occurs in the subcutaneous zone, which may only penetrate some 10–20m below the surface, and which is sub-parallel to the topographical slope (Ford and Williams, 1989, pp404, 532). Kosa (1989) considered a vertical cave as a deep karren feature, and an important paper by Sweet (1989) considered subcutaneous drainage and cave development in short caves in a glaciated karst in Canada, which are all within 25m of the surface. In various papers, Brahana *et al.* (1988, p342), Klimchouk (1995; 1997b) and Klimchouk *et al.* (1996) discussed the fissuring of the epikarst due to the mechanical processes of stress relief, temperature cycling, earth tides, hydraulic loading, frost wedging, tectonic activity, chemical weathering, uplift, denudation, and inherited karst porosity. The properties of the epikarst as an aquifer were described by Klimchouk (1995; 1997b) in terms of vertical percolation, water storage, and flow concentration at the base of the epikarst zone. Hidden shaft tops at the base of the epikarst were revealed via epikarst passages, or by later glacial scouring, when a shaft descends from within a karren field without a surrounding doline (for which there are examples in the study area). He proposed that epikarst processes start again at an early stage after deglaciation, and that much of the corrosion in the epikarst arises from *condensation processes* (section 3.1.9). Tyc (1997) discussed epikarstic features in zones affected by periglacial processes, and Puech and Jeannin (1997) considered the hydraulic behaviour of epikarst. In a field trip after the twelfth International Speleological Congress in Switzerland, 1997, they demonstrated, from rapidly-draining boreholes, that conduits in the epikarst may be apparently unconnected, even if situated within 5m of each other. Klimchouk (2000a) pointed out that the increased frequency and widths of fissures in the epikarst means that the low-order dissolution kinetics and breakthrough concepts need

not apply, i.e. *vertical (tectonic) leakage paths above open passages do not need speleogenic initiation.* These ideas are explored in Chapters 6–9, and study area caves are regarded as occurring in a special type of epikarst (section 10.6.2).

3.1.9 Condensation corrosion

Ford and Williams (1989, p309) discussed condensation corrosion in the context of hydrothermal caves. Palmer (1990, p187; 1991, p18) remarked that trickles of water from fissures absorb CO_2 to become aggressive and condensation water formed in the CO_2-rich air of a cave is very aggressive. Exposed surfaces exhibit high porosity and a friable (or stable) weathering rind, with etching, small pits, "box work" or bellholes. The condensation water commonly seeps back to floor level to deposit speleothems, disintegrated carbonate rock, and other deposits. Lauritzen (1990b) suggested that condensation corrosion caused wall retreat in a relict cave passage in **Hammernesgrotta** in northern Norway (section 3.3.3). Simms (1999) used the condensation corrosion concept to explain the development of "weird karst" in the west of Ireland (or "tube karren": Simms, 2002) and Tarhule-Lips and Ford (1998) used it to explain the formation of bellholes. They estimated a mean corrosion rate of $0.024 mm a^{-1}$. The role of condensation underground received a fuller treatment by Dublyansky and Dublyansky (2000). They suggested that condensation may explain the residual flow of springs during prolonged dry periods. Clearly, the weathering of cave walls (e.g. Zupan Hajna, 2001) is a complex process, with potential relevance to the study area. It depends on external climate and internal microclimate, as flowstone may also be deposited, or the walls may remain dry and unweathered.

3.1.10 Exokarst

Smart (1988) proposed a method to relate the evolution of a karst landscape to the size of underlying karst conduits and the frequency of overflow across the surface. He suggested that karst evolves from *fluvial* landscapes (initially without exokarst, and with most flow being surficial above conduits less than c. 0.5m in diameter) to *fluviokarst* (with karst landforms, such as dry valleys, above conduits up to 1m in diameter) to *holokarst* (with dolines and poljes, above larger conduits that carry most of the flow). He deduced that the evolution rate is primarily dependent on the lack of saturation of the recharge, although his model was generated before the knowledge of higher-order kinetics (section 3.1.14).

Sustersic (1996) considered the theoretical model of a landscape that developed solely upon carbonate rock that extends well below surface level and that is not influenced by other rocks types. He proposed that eight conditions need to be met to enable the development of *Pure Karst* and his model demonstrated that the exokarst surface is then a uniform system of centrically-organised depressions and elevations, as realised in tropical tower karst, where natural circumstances are closest to ideal conditions. The model of Ahnert and Williams (1997) produced similar results. According to the Sustersic model, *merokarsts* are imperfect karst landscapes in which at least one of the eight conditions is not met. *Stripe karst* appears to be an extreme example of merokarst in which three conditions are not met, partly explaining why

polygonal tower or cone karsts are completely absent from the metacarbonates of the Caledonides. Gams (1994) discussed various types of contact karst (apparently in horizontally-bedded limestones). These included narrow bands of limestone between impermeable sediments that may receive concentrated flows of allogenic water. He stated that *"corrosion is particularly intensive when allogenic water comes from an area of silicate rocks"* (*Ibid.*, p39), which is the case in the study area.

3.1.11 Cave destruction

Perhaps the latest topic to receive academic attention is the way in which caves become removed from an eroding landscape. Whereas this topic was discussed briefly in theoretical terms by Lowe (1992a) and by Lowe and Gunn (1997), Sustersic (1998) gave examples of *Unroofed (or Roofless or Surface) Caves* in Slovenia. Internal deposits from caves that no longer have roofs are now exposed there to direct meteoric erosion. Further examples were described by Mihevc (1999) and by Knez and Slabe (2001; 2002). Natural arches are diagnostic of unroofed caves, and cliffs above sinks and resurgences indicate truncation of previously longer passages. In Australia, Osborne (2001a) commented that roofless caves are more common in areas of low relief. Sustersic (1999) defined a *speleothanatic* zone at the epikarstic top of a vertical speleogenetic space through which caves seem to move upward, where the corrosional attack of all rock surfaces leads to complete annihilation. The relevance of the general concept in the study area is discussed in Chapter 7.

3.1.12 Inception and timescales of speleogenesis

The problem of the actual initiation of the very first proto-conduits was at first commonly ignored, regarded as inexplicable (section 3.1.4), or dismissed as in some way 'tectonic'. However, in the 1980s, that is after Ford and Ewers (1978) gave an explanation for cave genesis at the macro scale, and with the benefit of the discovery of ancient palaeokarsts in many parts of the world, it became possible to re-examine the initiation problem from a geological and hydrological perspective, as well as from a growing chemical understanding.

Kastning (1984) proposed that a structural framework determines initial groundwater circulation routes. By studying three separate sub-horizontally-bedded karst areas in the USA, Kastning showed that fault zones and joint sets can commonly be related and dated to distinct episodes of regional and local tectonism. These fractures can guide the development of karst landforms (e.g. lines of dolines and cave passage configurations), although, in some situations, dip and strike guidance can be more important. He noted that joints associated with folds and faults are locally abundant. Small joints also probably formed during expansion of bedrock in response to removal of overburden by fluvial or glacial erosion, or to subsidence and spalling along escarpments. These ideas are considered in Chapter 6. Kastning explained the preference of cave passages in one locality to follow one fracture set rather than another, more dominant, fracture set by attributing an *initial openness* to fractures formed by *extension* rather then the more *closed* character of fractures formed by *compression.* Palmer (1972; 1975) noted that geological

structure partly controls collapse of passage ceilings, a process that may block active conduits and lead to back-flooding, diversion routes, and maze passages. Mylroie and Carew (1986; 1987) suggested that inception could date back towards the formation of the host rock, but noted that passages in both the Bahamas and in glaciated areas could form 1m diameter tubes in 10ka (but see section 8.5.2 for even faster estimates), so that caves related to the modern landscape probably develop in a modern episode, e.g. a postglacial timeframe.

The role of cave inception in and adjacent to karst aquifers was addressed in two PhD theses, published almost contemporaneously (Worthington, 1991; Lowe, 1992a). Worthington studied karst hydrogeology in the Canadian Rocky Mountains, and found from observations at the karst springs at the Crowsnest Pass that there is a vertical hierarchy in the aquifer. He described these as: thermal springs, with long deep paths; underflow springs; full flow springs; and overflow springs, with local shallow paths. He also found that there is a high sulphate concentration in the deep (inception) waters.

Worthington (1994) discussed *Triple Porosity* limestone aquifers (White, 1977): primary porosity within the crystal structure; secondary porosity along fractures; and tertiary porosity along dissolutional conduits. Thus, groundwater may take years to traverse the first tens of metres of fractures to reach a conduit, and then travel several kilometres to reach the spring in just a few hours. Worthington and Ford (1997) proposed seven test methods for aquifer channels and suggested that permeability and porosity are explained by compaction i.e. burial depth. Worthington *et al.* (2000a and b) studied porosity and permeability in four contrasting, unconfined, sedimentary carbonate aquifers and found that dissolutional channels add little to porosity, but enhance the permeability of fractured rock by up to three orders of magnitude. Worthington (1999) reported the similarity between the proportions of matrix, fracture and channel flow and storage in these contrasting aquifers. Worthington (2001) noted a relationship between flow depth and flow path / stratal dip, doubting the Ford and Ewers (1978) Four-state Model (section 3.1.4). However, his explanation was based on viscosity reduction, and therefore increased flow rate, caused by geothermal heating at depth. This seems to be an uncertain argument, because it ignores the reduction in geothermal gradient caused by downward-flowing water, as discussed by Sippel and Glover (1964) and especially by Luetscher and Jeannin (2004).

Lowe (1992a) proposed an Inception Horizon Hypothesis (IHH) for the origin of limestone caverns in which the first initiation of proto-conduits occurs as a syngenetic cave formational process during diagenesis, which may be accompanied by strong acid dissolution. This long, slow, non-karstic, inception phase is driven by capillarity, earth tides (Davis and Moore, 1965; Davis, 1966), or ionic diffusion at great depth and over great distances, all within stratigraphical partings or within adjacent porous or fractured *clastic* rocks. These Inception Horizons can function as aquifuges, aquicludes, aquitards or aquifers at different stages, relative to the adjacent limestone. Susceptible beds may be removed totally by dissolution at several levels, as the dissolutional flow moves into the more soluble limestone via an

anastomising network of micro-tubes. Within this network, victor tubes grow, whilst still taking laminar flow during the "gestation" phase. When diameters of 5–10mm are reached, turbulent flow increases the growth rate. Lowe suggested that inception and other enlarged features can survive folding and tectonism and influence subsequent speleogenesis, as drainage routes are intercepted by surface lowering. Resurgences form at progressively lower inception horizons, until vadose incision occurs with headward erosion back towards the various inputs. The hypothesis includes the possible re-invasion of abandoned levels, if outlets become blocked, and also new sink inlets can modify existing higher tiers. The whole cycle can be repeated through several geomorphological events, because persistent open voids in some palaeokarsts can act as the focus for renewed cave formation. Similarly, buried palaeo (exo) karstic horizons can act as new Inception Horizons, after subsequent uplift and the onset of erosion. Thus, palaeokarst, whilst demonstrating the long timescale over which karst processes have acted on the earth, can also promote a new generation of cave development.

Whereas Lowe's Hypothesis relied on (near) vertical, tectonically-derived, joints and faults to provide linking pathways for inception flows between Horizons, he did not discuss the actual size of these fractured pathways. Although terms such as "open" and "relatively open" were used, the whole concept considered them to be rather closed tectonic discontinuities, which only allow fluid movement by the same processes of capillarity, earth tides, and ionic diffusion. Thus, he did not consider the possibility that, in some situations, tectonic movement might produce 3D networks of interconnected joint, fault and bedding-orientated fractures of sufficient size that his inception, and, indeed, gestation phases could be bypassed by relatively fast-flowing aggressive meteoric water, especially on hillsides with high hydraulic gradients, as implied by Kastning (1984, p374). See also Faulkner (1998) and Chapters 6–9. Ford (1965a, pp113, 117, 120, 121, 125) suggested or implied that open fractures contributed to the early development of the major caves in the Mendip Hills, UK.

A short paper by Lowe (1998) showed that inception can represent the transition between diagenesis and speleogenesis in *sedimentary* limestones. He suggested that inception must follow a) tectonic discontinuities; b) stratigraphical discontinuities; c) pre-existing weaknesses (e.g. palaeokarst); or a combination of all three. Lowe (1999) re-appraised the work of Waltham (1970; 1971a; 1974) and gave an explanation of cave development in the Yorkshire Dales, UK, based on pre-tectonic inception along Inception Horizons and on the intersection of flow routes by glacial down-cutting. Lowe (2000) further developed the IHH and discussed the idea of continuous voids resulting from movement across bedding planes (see also Faulkner, 1998). However, Palmer (1999a, p194) threw some doubt on the importance of deep-seated dissolution along inception horizons, from structural evidence.

After the publication of the two theses about karst hydrogeology and inception, further evidence of ancient, and deep-seated, inception became available. Thus, Ford (1995) and others discussed the development of hydrothermal caves and Klimchouk (1997a, and especially 2000b) reviewed deep-seated

hypogenic and artesian speleogenesis. Klimchouk's second paper stressed the importance of cross-formational hydraulic communication in the development of artesian (confined) speleogenesis, demonstrating that this commonly forms maze caves, supplementing the conditions described by Palmer (1991; section 3.1.16).

Sustersic (1997) described Inception Horizons in Slovenia, including some at dolomite boundaries. Osborne (1999; 2001b; 2001c) reported the existence of inception "horizons" in vertical to steeply-dipping sedimentary limestones in NSW, Australia. He noted that such inception horizons are likely to be discontinuous and lensoid in shape. Some of his examples seem relevant to the morphology of caves and karst in vertical and angled stripe karst in the study area, including the presence of sheer limestone cliffs, gorges, dry valleys, natural bridges, tiered cave passages, the effect of dip and surface slope relationships, and clastic sediment blockages causing paragenesis. However, his other observations probably have no counterpart in Caledonide metalimestones, such as marginal valley development, blind passage terminations (which Osborne, 2001b considered were formed by rising hydrothermal waters; Klimchouk, 2000b, p252), and the production and later exposure of palaeokarst. TD Ford (2000) discussed vertically-orientated inception routes along vein cavities subjected to tectonic movement, at depths that only reach down to 200m below the top of the (sedimentary) limestone.

3.1.13 The Palmer / Dreybrodt model

The basic principles that govern the physico-chemico processes of the inception, gestation and enlargement phases of phreatic cave development were resolved in what this thesis refers to as the Palmer / Dreybrodt model. This built on the Weyl (1958) concept of penetration length, quantified the White (1977) kinetic trigger and incorporated mixing corrosion where appropriate.

Palmer (1981; 1984a; 1984b; 1991; 1999a; 2000b) discussed the hydrochemical factors in the origin of limestone caves. Closed conduit *laminar* flow is governed by the Darcy and Hagen-Poiseuille equations, and closed conduit or open channel (vadose) *turbulent* flow by the Darcy-Weisbach equation. These may be compared to Ohm's Law for phreatic flow, so that the flow rate is equal to the head loss divided by a resistance. The resistance is related to aperture size, and is commonly proportional to the length of the fracture. Hence, the flow along an inclined straight tube is proportional to the sine of the slope angle. This value equates to the hydraulic gradient (HG), which in these calculations is always measured as the head loss divided by the full path length along a conduit (not the projected plan length of the path, as used for soils and porous rocks), and so reaches a value of unity for a waterfall. It can exceed unity if the water input to the conduit is already under pressure, as at the base of an overlying lake or reservoir.

Palmer (1991) showed that in phreatic passages: 1) The wall retreat rate levels off at a maximum of c. $1 mma^{-1}$; 2) Passages grow large if active for a long period of time, roughly independent of discharge rate; 3) A constant wall retreat rate depends on an increasing discharge rate (to maintain phreatic conditions,

as commonly occurs due to progressive captures); 4) Beyond about 90% saturation, the reaction rate drops sharply by one to two orders of magnitude (citing White, 1977, in his review of Berner and Morse, 1974); 5) The maximum dissolution rate is quickly reached if the hydraulic gradient is steep, as can occur during floods. These effects were represented graphically in plots of Passage Radius v. Wall Retreat Rate v. Degree of Saturation.

In various publications, Dreybrodt and co-workers also reported the mathematical and chemical modelling of the early and later stages of karst evolution. Dreybrodt (1981a) calculated calcite dissolution rates in systems both open and closed to CO_2, and with mixing corrosion. At large volume: surface area ratios, the surface reactions limit dissolution rate; at low ratios, the hydration of CO_2 is rate limiting. Dreybrodt (1981b) concluded that mixing corrosion at fracture intersections is *alone* sufficient to explain phreatic passage formation within tens of thousands of years, although White (1984, p231) argued that his own observed experimental *reduction* in calcite dissolution rate compared to that predicted by the PWP model (section 3.1.3) may explain the *initial* enlargement of fractures to proto-conduits without the need for mixing corrosion. Buhmann and Dreybrodt (1985a; 1985b) and Dreybrodt (1987; 1988, pp140–176) gave theoretical models and experimental results to predict pure calcite dissolution rates in the extreme open and closed conditions of CO_2 availability for both laminar and turbulent flow along films and fractures of various widths and volume / area ratios. Turbulent flow was thought to give dissolution rates higher than those for laminar flow in both conditions by a factor of ten: Dreybrodt (1987, Fig. 12) showed a wall-retreat rate of $3.8 mma^{-1}$ in a turbulent closed system at 10°C (with the high initial P_{CO2} of $5x10^{-2}$ atm.).

The high dissolution rates in turbulent motion may, however, be illusory, because they must be reduced by the presence of a laminar flow *diffusion boundary layer* adjacent to the dissolving surface whose thickness is partly determined by the roughness of the wall (Dreybrodt and Buhmann, 1991). In practice, the maximum dissolution rate in large phreatic conduits appears to be c. $1x10^{-7} mmolcm^{-2}s^{-1}$, equating to the maximum wall retreat rate of c. $1 mma^{-1}$ found by Palmer (1981). Dreybrodt *et al.* (1996) further studied the rate-limiting effect caused by the slow conversion of CO_2 in closed, narrow, apertures with laminar flow, which they found applied to solutions that were more than 20% saturated. Liu and Dreybrodt (1997) studied this effect in turbulent flow with a diffusion boundary layer. They found significant effects when $P_{CO2} < 0.01$ atm. for boundary layer thickness < 0.1mm and when $P_{CO2} > 0.01$ atm. for boundary layer thickness > 0.01mm, which were confirmed because there were no changes in dissolution rate between pure and natural calcite under the same conditions. The Palmer / Dreybrodt model is utilised in Chapter 8 to explain cave development in the metalimestones of the glaciated Caledonides.

3.1.14 Higher-order kinetics and breakthrough times

Dreybrodt (1988) presented the knowledge of physical and chemical karst processes up to that time. He considered that mixing corrosion is widespread (*Ibid.*, p5), and that *surface karst development can be closely related to the state of underground karstification* (see also Palmer, 1984a, pp203–206; Palmer, 1991, p11). However, Dreybrodt (1989) remarked that the theory of higher-order kinetics shows that mixing corrosion only plays a supporting role in the *initiation* of karst systems.

Dreybrodt (1989b and 1990) gave both a review of the historical development of ideas about calcite dissolution and a model for the dissolutional widening of primary fractures across a wide range of geological and chemical parameters. Despite his laboratory finding (section 3.1.15) that the dissolution rate for *pure synthetic calcite* varies in direct proportion to the difference between the actual concentration and the equilibrium (saturation) concentration and follows the PWP Model predictions (section 3.1.3), Dreybrodt modelled the results of other workers who showed that *natural* calcite (presumably LMC) exhibits second- and fourth-order kinetics above saturation values of 70–90% (i.e. the rate is proportional to the square or the fourth power of the difference). Dreybrodt (1988, pp229–248) calculated the first-, second- and fourth-kinetic order penetration lengths and aperture sizes of initial karst channels under various hydrogeological conditions, close to saturation.

Initially, fast first-order kinetics apply along the penetration length of a small-aperture fracture, and slow fourth-order kinetics apply from there to the outlet, but with the positive feedback effect of a widening path that raises the flow rate, reduces the concentration, and increases the dissolution rate. The first-order regime slowly advances until *breakthrough* occurs at the outlet, approximately coincident with the onset of turbulent flow. Thereafter, faster first-order dissolution applies at an even rate along the whole length of the fracture. Prior to breakthrough, almost all enlargement takes place in the upstream 10% of the fissure, so that the entrance area develops as a funnel shape from the karst surface (Palmer, 1991, p10). At its maximum, the pre-breakthrough enlargement rate is proportional to the cube of the fissure width (Palmer, 1991, p16), because the laminar flow rate varies as width cubed. Because first-order kinetics and penetration lengths are an order of magnitude higher for turbulent flow, the new widening rate is about $1 mm a^{-1}$ along the whole channel, so that large phreatic passages develop relatively quickly after breakthrough, from exit apertures that commonly vary from 1–10cm in width (dependent on conduit length and hydraulic gradient). Graphs presented by Dreybrodt (1990) include: the variation in fracture width along its length with time; increasing flow-rate with time; and breakthrough times for various apertures, hydraulic gradients and fracture lengths.

Dreybrodt (1990) regarded the breakthrough time as the *karstification time*. In shallow systems, this may be several 10ka for fractures 1km in length, and several Ma for fractures several 10km in length. Timescales are reduced if the hydraulic gradient is increased to several percent, or if the initial aperture is wider than c. 0.15mm. Applying the model to practical settings showed that once breakthrough is

achieved, the hydraulic head can be reduced, leading to the development of the next headward fracture, so that a system of channels can integrate backward into the rock, and so that bypassing across the top of a phreatic loop of length 20m is feasible in several 10ka.

Because breakthrough time is not very sensitive to the first- and fourth-order reaction constants, caves can form in a wide variety of limestone lithologies (Dreybrodt, 1992). However, even small-scale karstification (below 100m fracture length, as applies to many karst systems in the study area) is critically dependent on the *equilibrium* concentration at a low HG, and therefore on high initial CO_2 partial pressures from vegetation. Conduits as short as 20m, with HG=10%, still require 30000 years for breakthrough if situated below bare rocks, in which case only an atmospheric level of P_{CO2} is available (0.034%), when calcite saturates at 0.7mmolL^{-1} (or 70mgL^{-1}). [Sauter *et al.* (1997), Liedl and Sauter (1998) and Sauter and Liedl (2000) discussed catchment-scale modelling approaches for karst aquifer genesis. The first paper stated that a rise in temperature from 5 to 15°C can reduce karstification time from 50ka to 10ka, mainly due to increased production of CO_2]. At the other extreme, dissolutional dolines are systems with short fracture lengths, but steep hydraulic gradients, which can develop in very short periods of time, from 200 years down to as low as 4 years. Indeed, short fractures that are less than four times the penetration length achieve breakthrough to turbulent flow within a short time without utilising higher-order kinetics. The evidence from Gunn and Gagen (1987) of newly-formed dolines in abandoned limestone quarries supports this theory of rapid channel enlargement for vertical fractures, as does the problem of leakage below reservoirs (Palmer, 1988; Dreybrodt, 1989, 1990, 1992, 1996).

Groves and Howard (1994) modelled a cylindrical conduit in closed conditions of laminar flow, to determine the dissolution of initial apertures by carbonic acid, with user-selectable options for the dissolution rate expressions used by earlier researchers. Their models claimed to show that there are minimum hydrochemical conditions in which caves can develop. Thus, their Fig. 7 indicated that even if the hydraulic gradient is increased to 1.0 (vertical), then a minimum initial aperture size of 0.025mm applies, for all values of P_{CO2}, below which conduits cannot enlarge, even in millions of years. However, Dreybrodt (1996) showed that no such threshold widths actually exist in the karstification of narrow, broad, fractures, and they are also invalid for circular conduits. This clarification is important, as without it, there may be no physico-chemico justification for the concept of the long-timescale evolution of karst conduits along deeply-buried inception horizons (Lowe, 1992a; section 3.1.12).

For a broad fracture under higher-order kinetics, breakthrough time varies as a_0^{-2} and equals the ratio of a_0 to the initial widening rate at the exit, where a_0 is the initial aperture (Dreybrodt, 1996). Also, breakthrough takes ten times longer for a square or circular conduit than for a broad fracture with the same aperture. Thus, initial karstification proceeds mainly along bedding planes and joints, rather than along intersections between such fractures, and does *not* need to rely on the mixing corrosion possibility discussed by Dreybrodt (1981b). However, citing Tsang and Tsang (1989), who studied flow-channelling

in fractures with varying apertures, Dreybrodt also suggested that channelling within an uneven broad fracture may also *increase* breakthrough time (although Hanna and Rajaram, 1998, reported that aperture variability accelerates conduit growth). Also, because the viscosity of water is temperature dependent, reducing the temperature from 20 to 0°C tends to double breakthrough times (ignoring the increase in calcite equilibrium solubility). Dreybrodt (1998) stated that breakthrough is achieved quickly after the initial width of the exit is doubled, and in systems with a high hydraulic ratio.

Dreybrodt (1996 and 1998) noted that breakthrough time is almost independent of the degree of saturation of the input water, being governed instead by the initial width of the fracture, by the slow dissolution rate at the exit, and by the *hydraulic ratio* (HR), which he defined as the ratio of the hydraulic gradient to the path-length (i.e. Head/Path length^2). After breakthrough, passage enlargement is greater for low concentration, low hardness, allogenic, water than for higher concentration, higher hardness, autogenic, water. These arguments are developed in section 8.5 to derive breakthrough times and subsequent enlargement rates in karst inundated by glacial meltwaters.

Gabrovsek (2000, pp72–84) and Gabrovsek and Dreybrodt (2000) discussed the role of mixing corrosion in calcite-aggressive H_2O / CO_2 / $CaCO_3$ solutions in early limestone aquifer evolution. By combining the effects of mixing corrosion and higher order kinetics, they came to the surprising conclusion *"that mixing corrosion is only active (if present) in the early stage of karstification before breakthrough. At breakthrough, the concentration at the confluence drops drastically, such that the undersaturation resulting from the dissolution kinetics becomes far larger than that caused by mixing. Therefore mixing corrosion is practically absent in mature karst conduits"* (*Ibid.*, p1187). The apparently-conflicting conclusions about the importance of mixing corrosion were resolved by Romanov *et al.* (2003), who modelled 2D networks with two inputs of varying degrees of saturation. For (assumed allogenic) inputs well away from saturation, *"breakthrough behaviour"* dominates, where differing input chemistries are unimportant. For (assumed autogenic) inputs of differing but more than 99% saturation, *"mixing corrosion behaviour"* and higher-order kinetics cause very slow channel enlargements that can eventually reach metre-scale diameters without passing through a breakthrough stage. Chapter 8 shows that "breakthrough behaviour" is more important in the study area than "mixing corrosion behaviour", which applies to long and deep-seated inception horizons (section 3.1.12).

Dreybrodt and Gabrovsek (2000a) concluded that if the inflow to an aperture is already greater than 99% saturated, then "breakthrough" does not occur, and the conduit widens uniformly along its entire length, at a rate of only 10^{-9}cma^{-1}. Thus, sub-micron-wide fracture systems several kilometres in length take up to 10Ma to achieve widths of 0.1mm. *This provided for the first time a physical / chemical / mathematical underpinning to the Inception Horizon Hypothesis* (section 3.1.12). Dreybrodt and Gabrovsek (2000a) and Gabrovsek (2000, pp38–42) also analysed the case of first-order kinetics when the inflow is completely *unsaturated* and the hydraulic ratio is high. For initial apertures in the range 1–4x10^{-2}cm,

breakthrough times are almost instantaneous in geological timescales for either linear or non-linear kinetics (around 20 years, using the Dreybrodt measured parameters) for hydraulic ratios greater than the range 10–0.1. This showed that some dams constructed in karst landscapes may fail quickly under first-order kinetics alone or under higher-order kinetics at lower hydraulic ratios. See also Dreybrodt (1996; 1998). However, for each aperture size, *reducing* the appropriate hydraulic ratio causes a rapid increase in breakthrough times, eventually to beyond a reasonable geological timescale (10^9 years) for the continued existence of the host bedrock.

Bauer *et al.* (1999) modelled the reservoir leakage problem to show that 0.4mm diameter conduits beneath a dam could achieve breakthrough to turbulent flows, with dissolution along parallel paths, 15 years after the construction of a 40m deep reservoir, *if water transfer occurred between the conduits and the original fractures*. In the general case, such exchange flow could accelerate breakthrough time by a factor of 100 (Bauer *et al.* 2003). Dreybrodt *et al.* (2001) modelled rapid leakage below a dam on karst rock containing fractures with a log-normal distribution of initial aperture widths. If a cave passage already existed below the dam, a vertical pathway of dissolutional widening could achieve breakthrough at the cave in 11 years. This explains the formation of sinkholes on the floors of reservoirs in karst areas. The literature on the reservoir problem is important because of possible analogies with breakthrough and enlargement in various glacial settings (sections 8.5 and 8.6).

3.1.15 Limestone lithology and foreign ions

Buhmann and Dreybrodt (1987), Dreybrodt (1988, pp30–34 and 176–179) and Dreybrodt (2000, pp133–135) explored LMC dissolution in dilute aqueous solutions in the presence of other ions found in karst waters, such as Mg^{2+}, Na^{+}, Cl^{-} and SO_4^{2-}, noting that experimental results reported previously were often contradictory, especially for Mg^{2+} (Appendix A2.8). Their theoretical and experimental treatment dealt primarily with open systems and turbulent flow in unsaturated layers of water 1cm thick. Three mechanisms were considered: ionic strength effect (by addition of ions other than Ca^{2+} and CO_3^{2-}), common-ion effect (by addition of Ca^{2+} and CO_3^{2-} ions), and the ion-pair effect (by the addition of SO_4^{2-} ions to form $CaSO_4$). They found that, for geological applications (not under inception conditions), there is commonly no significant change in rate constants in the presence of foreign ions. However, $MgCO_3$ did reduce calcite solubility, by the common ion effect, and tests on samples of (presumably) HMC gave dissolution rates half those of LMC.

Svensson and Dreybrodt (1992) measured dissolution rates close to equilibrium for 16 natural marble LMC samples, 19 natural limestone LMC samples, pure calcite, and calcareous mud. They found that dissolution kinetics in the system H_2O / CO_2 / $CaCO_3$ are *linear* up to saturation for *pure synthetic calcite*. However, all *natural* LMC samples showed a drastic reduction of rate close to equilibrium in comparison. Tests with synthetic HMC samples gave similar results, with slightly different values. All

natural limestones (including A and HMC) exhibit higher-order dissolution kinetics near saturation, and have breakthrough times similar to those of natural calcite (W. Dreybrodt, pers. comm., 2002).

Section 3.1.3 noted the possibility that low concentrations of foreign ions may cause the inhibition of calcite dissolution and the trigger to higher-order kinetics close to equilibrium. This was further discussed by Dreybrodt (1988, pp136–139) and tested by Svensson and Dreybrodt (1992), who investigated the dissolution of synthetic calcite in an H_2O / CO_2 solution containing added PO_4^{3-} ions. The result was that the calcite showed a drastic reduction in dissolution rate close to equilibrium that was of the same form as that of the natural LMC samples. Furthermore, when the *natural* samples were tested with added PO_4^{3-} ions, there was only a small extra reduction in rates. The authors speculated that the inhibition of synthetic calcite originated from the adsorption of Ca^{2+} ions to the crystal surface close to sites already "poisoned" by PO_4^{3-} ions. In the case of natural calcite samples, such sites are already "poisoned" by other inhibitors, so that the scope for further inhibition by PO_4^{3-} ions is reduced.

Eisenlohr *et al.* (1997; 1999), also reported by Dreybrodt (1997) and Dreybrodt and Eisenlohr (2000), studied further the changes in dissolution kinetics of limestone by intrinsic impurities. They noted that earlier research had reported a general *increase* in the reaction rate *order* (and hence a reduction in reaction *rate*) when the ratio of solution volume to surface area increases above 0.1cm, in contrast to the slow CO_2 conversion effect which reduces reaction rates below a ratio of 0.1cm. They found by experiment that the various kinetic parameters depend on the thickness of calcite removed by dissolution (which is proportional to the volume/area ratio) up to a typical thickness of 5×10^{-4}cm, after which the parameters remain constant. The most pure sample showed the smallest variation, and they concluded that the effect was caused by an irreversible adsorption of inhibitors (which must have originated from the limestone sample) on to the reaction surface. Surface analysis of an LMC sample revealed a significant quantity of aluminosilicates, presumably acting as inhibitors, which the authors suspected derive from the dissolutional disintegration of small clay particles incorporated within the limestone matrix. Hence, it was proposed that this inhibition effect explains the wealth of conflicting experimental data, *because dissolution rates obtained from freshly-broken samples are not realistic of natural processes.* Instead, it is necessary to dissolve samples first in carbonic acid to remove 0.01mm of thickness and allow the adsorption of the inhibitors before measuring dissolution rates. The geological consequence of this finding is that aluminosilicates (which occur in the study area) and possibly other metal and phosphate ions accumulate as inhibitors on the surface of a limestone fracture, so that the kinetic regime progresses up to an *eleventh* order as thickness is removed during early conduit evolution. The effect is that water remains more aggressive farther along the fracture and breakthrough times previously modelled on fourth-order kinetics are *reduced by an order of magnitude* for initial apertures of 0.05mm (and hardly reduced at all for initial apertures of 0.3mm at a hydraulic gradient above 0.5). Thus, the gestation process is speeded up and the evolution of karst aquifers over several kilometres in fractures of 0.05mm now becomes feasible in less than 1Ma.

Dreybrodt and Eisenlohr (2000) summarised the present knowledge of the dissolution of natural limestones. The PWP equation is only fully applicable in turbulent flow, far from equilibrium, when the volume to surface area ratio is >0.1cm, as only then are surface reactions rate controlling. Even in turbulent flow, a laminar diffusion boundary layer may reduce the reaction rate. Otherwise, when CO_2 conversion or diffusion is rate limiting, reaction rates are reduced. Close to equilibrium, rates are predominantly controlled by surface reactions, and linear kinetics only applies for pure calcite without intrinsic impurities. With the presence of foreign ions, calcite reaction rates may be reduced by the common-ion effect and by non-linear kinetics caused by the adsorption of inhibitors to the calcite surface. The paradox is that the slower is the reaction rate, then the shorter is the breakthrough time, because the solution remains less saturated farther along the conduit.

3.1.16 Cave morphology

Independently of Dreybrodt, Palmer (1984a; 1991) made a similar analysis of calcite dissolution with similar results, and showed how various hydrogeological conditions enable the development of particular cave morphologies and patterns. Passages influenced by bedding plane partings are sinuous and curvilinear. Those along dissolutionally enlarged joints and high-angle faults are straight and fissure-like, with angular intersections. Palmer distinguished between *epigenic* caves with recharge at sink points, along sinking streams or into porous soluble rock, which develop synchronously with their landscape and so rarely survive more than a few million years, and *hypogenic* caves, which are formed by acids of deep-seated origin or by cooling of thermal water, with no relation to recharge through the overlying surface. Another major distinction was between phreatic *branchwork caves* (dendritic), formed by waters with higher hydraulic heads converging towards large flow, low head, phreatic passages (as also described by Dreybrodt, 1990), and phreatic *maze caves*. These can form in situations with steep hydraulic gradients and short flow paths, where dissolution quickly reaches a maximum uniform rate along many alternate paths of varying size. Alternatively, mazes can form if several fissures receive similar recharge, as may occur from bank storage along entrenched rivers, or from diffuse recharge through a permeable cap rock, or beneath isolated hills of limestone (Palmer, 1975). Branchwork caves are well-adjusted to the geomorphic history of the valleys to which they drain. Vadose passages commonly follow down-dip, gravitational, independent, perhaps parallel, steepest possible, routes from allogenic inputs with no *inherent* (non-geological) tendency for convergence. Their hydraulic gradients equate to passage slope. Canyon passage widths are proportional to their slope, but enlarge further if water forms a spray, as occurs down shafts. Vertical shaft walls dissolve at up to $1.2mma^{-1}$, according to White (1990, p170). Floods can cause hydraulic gradients to steepen and phreatic conditions to return, but with high flow rates and very aggressive water. Thus, all available fissures can enlarge at maximum rates to produce a maze of interconnecting passages and diversion conduits above the level of the existing branchwork, or even above vadose passages, especially over constrictions and blockages (a form of *paragenesis*, first proposed by Palmer, 1972). This *flood-water injection* can also enlarge *dead-end* fissures and cause

bedding plane anastomoses, a study area example of which is described in Appendix B1.4. Both types of feature diminish in size away from the source passage. Thus, anastomosis may *not* be diagnostic of early speleogenesis (Palmer, 1972; 1984, pp174, 195, 196).

Palmer (1990, p198) discussed various cave types and features. Palmer (1991) included a summary chart of cave patterns and their relationship to both dominant "porosity" (fractures / bedding partings / primary porosity) and type of recharge (dolines / stream sinks / diffuse recharge / hypogenic recharge). Section 5.7.1 considers the applicability of this chart (Figure 5.7) to the study area caves. His main conclusions were also summarised by Palmer (1997; 2000a; 2001). The middle reference introduced the idea that convex topography is less favourable to cave development, as runoff is less concentrated.

A major deduction by Dreybrodt (1998) was that breakthrough time depends critically on the fracture length (for fourth-order kinetics, doubling the length increases the time by a factor of six). Thus, areas of comparable hydraulic head where the geological setting allows short percolating pathways permit intensive karstification with many small caves and a more intensive conduit network with multiple and branched pathways to form quickly in several 10ka. In contrast, where the fracture lengths are long, a few long caves form with simple, mainly linear, passages that take many Ma for breakthrough. This suggests that deep inception horizons provide long, but simple, flow paths and short, shallow, systems can be more complex, as for many systems in the study area (Chapter 9). He also noted that in highly fractured geological settings (i.e. in State 5, DC Ford, 2000), karstification may be intense, but major caves systems are missing. A surprising result from Dreybrodt and Siemers (2000) is that if *any* parameter is varied so as to *decrease* the breakthrough time, then the cave pattern always becomes more complex. Hence, the pattern of cave evolution is not only determined by the original geology, but may also depend on the equilibrium concentration of the recharge, which could be influenced by the climate and vegetation.

Kaufmann and Braun (1999) modelled karst aquifer evolution in fractured, non-porous, rocks (in phreatic conditions only), by using the three concepts of calcite dissolution (with nth order kinetics prior to breakthrough), flow in a pipe with an enlarging radius (where they noted that the onset of turbulence limits the flow rate, as the turbulent flow rate is smaller than the laminar flow rate in the same conduit), and flow in an inclined 2D network of fractures. They chose to discretize this aquifer into an *unstructured* mesh, which they claimed was more realistic than the rectangular geometry used by previous authors. By defining a *maze index*, M, such that if all conduits are similarly enlarged, $M = 1$ (maze caves) and if only a few conduits are enlarged, $M << 1$ (dendritic caves), they were able to show how the resulting cave patterns were determined by varying hydraulic gradient and initial diameter. The larger the head and the larger the initial diameter, then the greater is the maze index, agreeing with Dreybrodt and Siemers (2000) because the breakthrough time would reduce.

3.1.17 Tectonics and Karst

The importance of both slow moving and seismic tectonic action on the inception of caves and the roles that caves can play in recording the tectonic history of an area were discussed at the International Symposium of Karst and Tectonics that was held at Han-sur-Lesse in Belgium in March 1998, as reviewed by Faulkner (1998). Any large scale compression or extension force can locally cause smaller scale compressional *and* extensional movements, creating open fractures, because the movement boundary is usually irregular rather than planar. If the fractures connect, water circulation is possible and karstification is promoted. Secondary permeability is zero in unfractured rocks and increases to provide braided channels as fracturing increases. Evidence accumulated by the 1990s also suggests that the recording of tectonic events in caves is a common phenomenon. Some studies of fallen speleothems and cracked flowstones conclude that they must have broken by seismic activity. Rock movements were deduced in cave walls from observations of dislocated calcite veins and stylolites.

Many presentations during the Symposium showed photographs of displaced karst shapes on opposite sides of passages and bedding plane slips revealed in passage cross sections. Very large underground chambers may have a mainly tectonic origin, formed by slow moving extension, and fallen slabs from walls and ceiling may provide supporting evidence. Postglacial, slow, gravitational slope movements and tensional release may be the mechanisms for the apparent and continuing tectonic extension of joints into straight walled shafts that cut down to pre-existing cave systems located under crests and ridges close to the steep slopes of deeply embedded valleys. The evidence leading to *tectonic speleogenesis* is both spatial and temporal. Many speakers showed examples of correspondences between karst locations and tectonic regions. These arise from the frequent association of carbonate rocks with active plate boundaries and associated deformation zones. It also appears that karstification does not just follow pre-arranged passive geological structures: there is an increasing body of evidence from palaeokarst that karstification and major tectonic activity occur together. To summarise, the evidence from the Symposium was that tectonic activity is all around us, with tiny but continuous bedding and fault movements interrupted by large seismic events at infrequent intervals. These movements create voids from which cave inception can start and be repeated. Cave development is an integral part of the geological history of the host region. After endokarstic enlargement, the caves created can themselves record the later tectonic history of the area.

Whereas Choppy (1997) regarded tectonics as playing a limited part in karst development, Bitterli (1997) described the gravitational downslope sliding of large carbonate masses in Switzerland to create "tectonic" limestone caves. Marrett *et al.* (1999) found that *natural fractures in a Texas limestone show strong linear trends for log-log plots of cumulative frequency versus kinematic aperture of more than three orders of magnitude*: >0.01mm apertures occurred at $100m^{-1}$; >1mm apertures occurred at $1m^{-1}$; >10mm apertures occurred at $0.1m^{-1}$.

Salomon (1999) discussed the time factor in karstification, and noted (without referring to the Palmer / Dreybrodt model) that in high mountains, with high hydraulic gradients, karstification is rapid. He suggested that periods of tectonic stability commonly favour the development of horizontal karst levels, but that karst has an exceptional capacity to adapt to external tectonic modification. Without referring to the IHH, he gave examples where the lowering of base levels by faulting causes the development of passages leading to lower springs, and conversely, the elevation of base levels, or their obstruction by clastic sediments, produces new passages leading to elevated outlets. Urbani (2001) discussed the palaeoseismic record in Venezuela, where fallen marble fragments were dated by co-located bat bones at 9300a, i.e. early in the Holocene, when the earth experienced rapid climatic change. An area of Caracas has 81 tectonic caves showing rotated blocks and ruptured speleothems. The relevance of tectonism to the caves in Caledonide metacarbonates is addressed in Chapter 6.

3.1.18 The hydrogeology of fractured rocks

Section 3.1 has so far reviewed speleogenesis in sedimentary limestones from both a geomorphological and a physico-chemico perspective. However, the aim of this thesis is to understand speleogenesis in crystalline *metacarbonate* rocks. In order to gain such an understanding, the hydrogeology of such rocks is henceforth considered as a 'halfway house' between that of sedimentary limestones and that of crystalline (igneous and metamorphic) *non-carbonate* rocks. Hence, a study of the hydrogeology of these, so called, "hard rocks" should be a beneficial exercise, although this subject is only briefly discussed in standard hydrology and groundwater text books (e.g. Freeze and Cherry, 1979; Ward and Robinson, 1990; Price, 1996).

Crystalline rocks have negligible matrix porosity and permeability, commonly giving a low storage. However, appreciable *fracture* permeability generally occurs within tens of metres of the ground surface for these lithologies. Fracture apertures up to 1mm are common, with a general trend of permeability decrease with depth, although active water-flows into mines at depths of 1km indicate the great depth to which fracture permeability can exist. Skjeseth (1957) noted that in Norwegian Cambro-Silurian (crystalline) formations, the locations of springs are clearly determined by the stratigraphy and tectonics: springs commonly occur along abandoned stream channels, following fractures and joints.

Discharges from fractures in wells and boreholes in igneous and metamorphic rocks provide drinking water all over the world: Paillet *et al.* (1987, Mirror Lake, New Hampshire and near Oracle, Arizona); Randall *et al.* (1988, NE Appalachians, USA); Howard *et al.* (1992, Uganda); Sekhar *et al.* (1994) and Maréchal *et al.* (2004): India; Boulton *et al.* (1996, crystalline basement rocks of the Scandinavian shield); Mabee (1999, *glaciated* metamorphic rocks on Georgetown Island, Maine); Shapiro (2001, Mirror Lake, New Hampshire); Drew *et al.* (2001, Pinardville Quadrangle, New Hampshire). Well-yields are comparatively small, but are locally important as water sources for farms and homes. Banks *et al.* (1996) reported c. 100000 bedrock boreholes in Norway, with a further 4000 being drilled annually.

Henriksen (1995) studied 760 domestic wells drilled to depths from 14–155m in "hard rocks" in the mountains of southern Norway, which had flow rates up to a maximum of c. 330Lmin^{-1}. She found a general decrease in well-yield with depth (measured as specific discharge in Lh^{-1} per metre of borehole length), and well-performance seemed to be independent of lithology (which consisted mainly of gneisses, granites, gabbros and phyllites, but did not include carbonates or amphibolites). Histograms of well-yields showed a log-normal distribution.

Gustafson and Krasny (1994) reviewed crystalline "hard rock" aquifers from around the world, but principally exposed in the Precambrian shield areas and in the cores of major mountain ranges that altogether comprise some 20% of the land surface. They noted that hydraulic conductivity normally varies by several orders of magnitude within the same rock unit, and commonly within short distances. In these rocks, groundwater is transmitted via fractures, fissures and zones of crushed rock. Large conductive zones, formed during a brittle stage of the rock's history after formation, may extend for several tens of kilometres and across different units. As classical definitions of aquifers are ill-suited to describe flow and storage of groundwater in fractured crystalline rock, they proposed that the term *aquifer* should be here replaced by the term *hydraulic conductor*.

Tests of the hydrogeological properties of hard rocks commonly show that *no average hydraulic conductivity exists that is independent of scale.* Rather, plots of cumulative percent are usually log-normally distributed, leading to the "*conclusion that the fracture set is a continuous sample of conductive features of different magnitudes*" (Gustafson and Krasny, 1994, p66), and that the fracture system has a *fractal dimension*. Hydraulic conductivities show a decreasing trend with depth, both for the rock in general and for penetrated conductive fracture zones, but with a large scatter around the regression curves. The hydraulic conductivity may vary from 10^{-11}ms^{-1} at ~700m depth to 10^{-7}ms^{-1} at ~50m depth (and to 10^{-5}ms^{-1} at ~10m depth: Banks *et al.*, 1996), although Boulton *et al.* (1996) noted from pumping tests that the crystalline basement rocks of the Scandinavian shield show hydraulic conductivities in the range 10^{-12}–10^{-6}ms^{-1} (at 100m depth).

Gustafson and Krasny (1994) also noted that a composite aquifer, conformable to the land surface, usually consists of a weathered regolith underlain by the fissured zone of bedrock. This "*near surface aquifer*" (*Ibid.*, p69) reaches up to a few tens of metres in thickness and, despite *local* heterogeneity, can commonly be regarded as *regionally* approximately uniform, usually characterised by a regionally-valid mean transmissivity. Such hard rock aquifers have low groundwater storage, with limited retention, especially in sloping areas. Thus, groundwater resources of hard rock aquifers strongly depend on present recharge, and this commonly increases with altitude, because of increased snowmelt and reduced evapotranspiration. Additionally, despite low transmissivity, a higher hydraulic gradient enables the transmission of larger fluxes of groundwater.

Krasny (2002) found that a regionally-prevailing transmissivity of 0.1–100m^2day^{-1} (or well-yield or specific capacity of c. $1x10^{-3}$–$1x10^{0}Ls^{-1}m^{-1}$) applies to hard rock environments throughout the world. He divided such rocks into three zones: upper weathered, middle fractured and lower massive. Because the permeability of non-carbonate rocks typically decreases through geological time, young fractures are the most important. Using a log scale, Krasny defined six classes of transmissivity *magnitude* (with fluvial deposits ranging up to c. $10^4m^2day^{-1}$) and six classes of transmissivity *variation* (using standard deviations: hard rocks vary from "fairly" to "considerably" heterogeneous). He noted that *crystalline limestones (marbles) commonly have transmissivities 5–10 times higher than other crystalline rocks.* The groundwater runoff from hard rock mountains can approach 50% of the *infiltration* (i.e. precipitation remaining after evapotranspiration: up to $15Ls^{-1}km^{-2}$).

Moving away from strictly crystalline rocks, probably the best example of a non-karstic groundwater flow path in carbonates is Devils Hole, Nevada (Riggs *et al.*, 1994). This flooded planar fissure is some 130m deep, with an opening width of some 2m. It has apparently formed by continuous extension in arid conditions without karst dissolution (but with calcite deposition) in Palaeozoic sedimentary limestones and dolostones over a period of more than 500ka in response to regional tectonism, whilst being supplied from a karstic recharge area. Meigs and Beauheim (2001), Haggerty *et al.* (2001) and McKenna *et al.* (2001) described tracer tests in fractured, sedimentary, microcrystalline and silty "Culebra" dolomites located about 230m below the surface in New Mexico. The effects of dolomite dissolution were not considered to be important. Palmer (1990, p205) noted that the fracture pattern followed by a floodwater maze in Blue Spring Cave, Indiana, USA differs from that in the rest of the cave. The pattern was apparently formed by stresses related to the local breakdown that causes the floods.

The literature on the non-endokarstic hydrogeology of *metamorphic* carbonates is sparse. Ford (1967) discussed a blue dolomitized limestone marble of unstated metamorphic grade in a stripe karst setting at Mt. Tupper, British Columbia, Canada. A $0.7m^3s^{-1}$ stream flowed underground for 53 minutes to a rising that is 480m below, and 2km from, the main sink, but this is obviously via an unexplored karst conduit. There is an extensive literature on the endokarst cave systems in the high to low grade metamorphic limestones of Scandinavia (e.g. Lauritzen, 1996; Sjöberg, 1997; Faulkner, 2000; this thesis), but little on the hydraulic properties of wells drilled into marbles. Andreo *et al.* (1997) discussed metacarbonate aquifers and karstification in the Sierra Blanca and Sierra Mijas of southern Spain

In summary, since about the late-1980s, the study of the hydrogeology of crystalline rocks has shown that such rocks can also act as aquifers for storage and flow. Crystalline rock fractures have a fractal dimension and decrease in size with depth, providing an effective *'near surface aquifer'* of commonly tens of metres thickness. Their discharges may supply natural springs and household wells and boreholes, flood mines, and put at risk the underground containment of hazardous wastes. Fractures are utilised within the crystalline rocks (which have negligible primary porosity, and which do not develop

dissolutional conduits). However, *flow rates are extremely variable and difficult to predict in the field, and there is good evidence of flow channelling at many scales*. The language of this *parallel literature* is already familiar to *karst* hydrologists, because, in this respect, the behaviour of hard rock aquifers is similar to that of karst aquifers in sedimentary limestones, but with much smaller maximal hydraulic conductivities.

From the evidence provided by the cited authors, flow rates in fractured crystalline rocks can exceed the breakthrough point that, in limestones, would mark the transition from laminar to turbulent conditions, and fast dissolution. Similar processes should also apply to metamorphic limestones, and, indeed, to sedimentary limestones, as shown by Palmer (1975), who discussed the possible effects of mechanical fracture enlargement, and by Ford and Worley (1977b), who illustrated how fault movement can generate voids available for phreatic dissolution in Derbyshire, England. In these cases, the slow inception and gestation phases of *chemical* inception may be *bypassed*, because some karst passages may develop under phreatic conditions, at high wall-retreat rates, immediately after the inundation of fractures formed *tectonically*. Further, the considerable knowledge of fracture geometries and modelling techniques, as developed for these "hard rock" lithologies, becomes available for use by karst hydrologists, when studying speleological inception and early conduit enlargement. The concept that our knowledge of permeability development in karst aquifers can generally be strengthened by the lessons from crystalline rocks was reported briefly by Faulkner (2003). The idea that *tectonic inception* provides the mechanism for the initiation of caves in the metalimestones of the Caledonides is developed further in Chapter 6 *et seq*. of this thesis.

3.2 Caves and karsts in glacial environments

The development of the Scandinavian metalimestone caves must be considered alongside an appreciation of all the possible effects of the multiple Mio-Plio-Pleistocene glaciations. These effects may act both directly on the caves themselves, and indirectly by substantially modifying the local landscape. Thus, the intimate nature of the glacial environment provides a second differentiation from some of the classical studies of karst geomorphology in sedimentary limestones. Many questions arise about glacial conditions and some of the views expressed appear to be contradictory. This section considers the extent to which glacial karstic environments have been addressed in published geomorphological and speleological texts.

3.2.1 Early glaciation ideas by karst researchers

Glennie (1952) reported evidence of frozen bodies of water in chalk that can open rifts and cause the folding of bedding planes. He suggested that open joints, fractures, and collapses in Ogof Fynnon Ddu in south Wales could have been caused by deep freezing. The relationships between karst and glaciers, periglacial conditions and temporarily frozen ground were discussed by Corbel (1957, pp439–458). He stated that arctic snow takes several years to be transformed into ice, because there are few freeze-thaw

alterations, the interior of the ice being consistently well below freezing. The snow coats the ice with a thick heavy layer that remains at 0°C, whatever the latitude, and imparts a pressure that causes some Greenland ice streams to advance more than 40m per day. He contrasted arctic glaciers with less cold alpine glaciers. Streams flow under alpine glaciers, which can erode the underlying rock, something which he said is *practically unknown in the Arctic.* [His use of the term "Arctic" presumably applied to permafrosted Greenland and Svalbard and not to northern Norway]. Warwick (1971) cited Corbel (1957) as suggesting that the youthful nature of the karstification in NW Scotland (as known at that time!) was caused by older traces being removed by glacial erosion, as considered in Chapter 7. On the other hand, Davis and Krinsley (1960; Appendix D6.4.2) described a cave in the periglacial conditions of NE Greenland that has clearly survived glaciation, as orange and red silt deposits (indicative of a palaeo mild climatic regime) are still preserved under a flowstone cap.

Warwick (1971, p126) made the interesting assertion that ice confined within a valley must exert considerable pressure on the floor and sides: "*Many glacial troughs in Norway have a system of joints roughly parallel to the valley sides, which are considered to be due to pressure release….they could guide water downwards and develop into caves*". Ford and Ewers (1978, p1793) also noted a common increase in fissure frequency within 20–100m of valley walls (Photo 3.1). Warwick (1971) additionally suggested that glacial pressures exerted through the rock might result in spalling from the sides of caves in the valley walls, especially if they were parallel to the valley axis. By studying passages and the Big Chamber in Ogof Fynnon Ddu 2, he also noted that, if close to the surface, steady pressure from an overlying icesheet could cause massive block falls, especially along the walls, where the fallen blocks retain their original stratigraphic relationships. These ideas are considered further in Chapters 6 and 7.

Photo 3.1 Entrance to Johngrotta (Z2), Tosenfjord
Tectonic openings caused by pressure relief at side of fjord.
Caving lamp for scale, at entrance to 15m-long fissure.

Regarding the infill of shafts with glacial till and fluvio-glacial deposits, Warwick (1971) suggested that the base of the icesheet could stretch across the mouth of a shaft, perhaps starting as a snow bridge (for which there are many contemporary examples). The till was deposited when stagnant ice melted above. Also, glacial till could penetrate shallow caves in a slurry-like solifluction stream, and if the passage

became choked, water could back up and act as a settling pond for much finer material. His opinion was that, in general, the deposits associated with icesheets tended to block up old cave systems. He also thought that little surface water could reach caves beneath the ice, and any that did would *not* be aggressive, due to lack of bacterially-derived CO_2. Thus, he suggested that an ice covering would severely reduce the development of caves. At the ice front, there would be a seasonal regime of winter quiescence, and small-scale summer activity. Where the ice front coincided with a hillside, the circulation of water in (any) vadose zone might be maintained. Warwick considered that periglacial conditions and postglacial annual freeze-thaw regimes mainly affect cave entrances. Spalling, jagged rock faces, scree and frost breccia result, whereas some distance inside, in a more even temperature regime, the walls are much smoother.

Horizontal *proglacial* caves in Poland were described by Glazek *et al.* (1977). Mietusia, the longest cave in Poland, was thought to have developed during the late Würm, in a manner similar to Castleguard Cave, Canada, and in conditions similar to those at Castleguard today. Nearby is Sniezna Cave, the deepest shaft system in Poland, which is formed along steeply-dipping bedding planes with little observable corrosion. The bedding planes were thus interpreted to be tectonic fissures that were widened by stress relaxation and slope creep, as the local glacier melted.

Glover (1977) proposed a conceptual model of cave development in a glaciated region, dividing the glacial cycle into four main stages. Ford (1977a) stated that one of three conditions prevails in the presence of glacier ice: (i) the ice base is "polar" [i.e. frozen] and karst water circulation ceases; (ii) the ice base has water present and the ice thickness is much greater than the karst terrain relief. The caves flood and there is slow CO_2-depleted circulation, speleothem dissolution and deposition of varved silts and calcitic clays; (iii) the ice base has water present, but the karst terrain relief is similar to, or exceeds, the ice thickness. In the third case, increased hydraulic gradients lead to accelerated karst erosion. This condition can apply during glacial advance, and especially during glacial decay, for brief periods up to centuries.

Ideas developed by Ford (1965b) may be extended to diagnose the glacial history of stream passages. He proposed that streambed potholes and hanging potholes in St. Cuthbert's Swallet and in Swildon's Hole, Mendip Hills, England developed during long periods of high discharge, as a result of *"climatic fluctuations of the (Pleistocene) glaciation"* (*Ibid.*, p32). Thus, counting the number of levels of hanging potholes in the walls of the more complex caves in the study area could reveal the number of glacial discharge events that the passage has experienced. (However, none are known: Appendix B2.7). Ford and Williams (1989, p301) stated that stream potholes are most common and display the most regular form in hard limestones, in dolomites and (pre-eminently) in marbles, because dissolution in the swirling water reinforces the grinding, and may replace it entirely.

3.2.2 More recent glacial karst research

Smart (1984a) discussed glacier hydrology and the potential for subglacial karstification. He noted that proglacial streams can carry heavy sediment loads that may limit karst circulation. Subglacial streams can form a dendritic network leading to the glacier snout, which can create stable Nye (N) channels in the underlying bedrock. Such Nye channels are more likely to develop karst because of their fixed position and association with bedrock discontinuities. A subglacial karst drainage system could then provide the ultimate Nye channel (as at **Kvithola**, northern Norway: Lauritzen, 1986a). Unstable Röthlisberger (R) channels develop within the ice, and migrate with the glacier, but close up in winter. Fountain *et al.* (2005) showed that much of the hydrological system in 'temperate' glaciers can be dominated by connected fractures that convey water at slow speeds, and Hodgkins (1997) demonstrated the existence of hydrological storage and drainage even within some 'polar' glaciers.

Subglacial activity is very high in summer below the extremity of the Columbia ice field, as shown by active speleothem deposition and high water levels in parts of Castleguard Cave, Canada. It was inferred that surface meltwater passes directly through the ice into vertical karstic shafts. Conduit evolution at Castleguard could have taken from 100ka to several Ma, citing the Palmer (1981) method. Smart (1984a) thought that the limited depth to which crevasses can penetrate a glacier limits karst to zones of rather thin ice that experience extensive flow. Thus, he suggested that the best situation for subglacial karst is at a relatively high elevation, near the firn line of a relatively small-scale glacier. Basal regelation films (Appendix A3.3) could link to a widely-distributed percolation flow system in the karst. Smart (1983) suggested that *high pressure regelation water* could *initiate* subglacial karst. A freely-draining karst may reduce basal glacier pressures and thereby reduce glacial erosion rates, explaining the apparent "resistance" of carbonate rocks to glacial erosion. Conditions beneath polar, cold-based, glaciers or icesheets are quite different. Ford (1987) and Ford and Williams (1989, pp472–496) noted that cold, dry-based, glaciers are frozen to the bedrock and may wrench blocks away as the ice creeps past. Glacitectonic cavities can be created, especially in carbonate rocks, due to earlier dissolutional weaknesses in bedding planes and joints, as described by Rea and Whalley (1994).

Ford and Williams (1989) differentiated between two types of alpine karst: *Pyrenean*, where glaciers are confined to the highest ground, so that meltwater can discharge into karst inputs, but karst outputs are not glaciated; and *Canadian*, where the glacier ice occupies all the valleys and extends beyond the output springs so that opportunities for karst development are more restricted. These two types also appear to represent conditions at the onset and at the decay of a Scandinavian glaciation (Chapter 8). Ford and Williams also discussed the types of karst landforms in glaciated terrains. Many dolines form at low points prepared by glacial scour. Kotlic dolines (or schacht dolinen or schneedolinen) have steep-to-vertical sides on scoured fractures, which trap and conserve snow, becoming sites of accelerated corrosion. There are many examples of these within the stripe karsts of the study area. Similarly, dolines and shafts, created beneath the ice, may occupy what are now anomalous hydrological positions, as can

be seen throughout central Scandinavia. They suggested that they were created below crevasses in the ice [which form above an irregular bedrock surface]. Most *large* karst depressions in glaciated terrains are *polygenetic*, i.e. they formed during repeated glacial and karst episodes. However, these are rare in the study area (section 4.4.3). Noting that the *cirque* is the basic alpine glacial landform, in carbonate rocks these may be over-deepened by glacial scour to form closed depressions, which may now function karstically. These are also rare in stripe karst settings. The apparent cirque at Elgfjell (Z4, Appendix B1.4), which lies across many bands of limestone, has few among more than 100 cave entrances in such a situation. Ford (1983) stated that, in the Canadian karst, springs commonly issue in a hanging position in the valley walls, without lithological perching control. Such hanging positions are also common in the study area, but usually occur at least at a minor lithological barrier (section 4.4.2).

In considering the effects of glacier action on existing karst systems, Ford (1983) and Ford and Williams (1989, p483) listed nine different effects in destructive, inhibitive, preservative and stimulative conditions; the destructive and stimulative conditions are especially relevant in the study area (Chapters 6–9). They concluded that the development of karst landforms and systems is particularly complex in formerly glaciated terrains, and analysis is complicated by the inheritance of previous glacial effects.

Ford (1986) noted that probably the fastest rates of cave genesis in the world could occur at *ice margins*, during mountain glacier advance and retreat. Ford and Williams (1989) also described *nival karst*, where there is heavy snowfall and a large annual snowmelt, as occurs in the study area. However, the effects of snow patch deepening are subordinate to the effects of glaciation. They indicated that permafrosted zones based on latitude may be continuous, or regionally or temporally discontinuous. The freezing process is weak because of the release of latent heat. Thus, little energy is required to keep karst conduits open: a flow of $5Ls^{-1}$ may be sufficient. Also, the freezing point of water decreases if it contains dissolved solids, again constraining the extent of freezing. They took the Nahanni karst in Canada as the model for alpine permafrost with a deep thermoactive layer. It has a mean annual temperature of c. -7°C, a temperature range of -50 to +35°C, and exhibits unimpeded conduit drainage. A spectacular surface karst developed in these discontinuous permafrost conditions *after* the region was last glaciated, which was before 350ka. Ford (1977a) explained how these surficial landforms developed in a size hierarchy by the same processes, but at greatly varying scales. These processes may be similar to those reported by Warwick (1971) in citing Ciry (1959), who suggested that in Burgundy (France) there had been a deep zone of permafrost, and that a shallow karstic system developed in the active layer above, which melted out each year, producing *cutaneous caves*. Farther north in Canada, the mean annual temperature is lower, and the summer temperature is cooler than 5°C. Here the thermoactive layer may be less than one metre deep. Whereas it might be anticipated that groundwater circulation down to the base of the active layer would favour development of a subcutaneous karst, in practice the surface is usually reduced to a felsenmeer.

Lauritzen (1998) reviewed karst morphogenesis in the Arctic, with examples from Spitsbergen. He discussed the continuity of hydrology from a warm-based glacier to a seasonal supra-permafrost aquifer (thereby providing increased hydraulic gradient and flow), and the abundant evidence of perennial *sub-permafrost aquifer flow*. He deduced that smaller exokarst forms tend to become erased by glacier action, whereas large forms may be preserved and infilled with glacial drift. Phreatic caves formed in seemingly 'impossible' positions arise from *"subglacial speleogenesis"*.

Audra (1994) studied speleogenesis in three Alpine karst settings. He concluded that high-altitude surface remnants and palaeokarsts derive from intensive Palaeocene karst formation. During the Miocene, cone karst formed above large, horizontal, phreatic, underground networks fed from very large drainage basins. Strong Alpine uplift in the Pliocene added vertical networks to the existing systems, and reduced the sizes of catchment areas. Pleistocene glaciations lowered the surface and both extended the networks and deposited sedimentary sequences and varves. Interglacials contributed flowstone-floors, especially beneath wooded areas. Audra (1994, pp218, 252) concluded that most enlargement of tubular Alpine galleries occurs in the temporarily-phreatic (*epiphreatic*) zone, resulting from the fluctuating discharges of varying glacial conditions. Bini *et al.* (1998) discussed the relationships between karst and Alpine valley glaciers. The new paradigm of Alpine cave development, in which most speleogenesis occurred under conditions completely unlike those of today, and in which Quaternary glaciations had only a modifying role (especially at low altitudes), was also discussed by Audra (2001), Bini (2001) and Tognini (2001). Apparently, longitudinal Alpine valleys were formed structurally, and not initiated by river or glacier entrenchment. Horizontal passages result from low and stable topographic gradients, and vertical elements arise from abrupt changes in base level. Falling levels entrench valleys and form endokarst shafts; rising levels flood cave systems and create Vauclusian risings.

Häuselmann (2002) and Häuselmann *et al.* (2003) developed the idea of successive passage development related to Alpine valley floor and spring outlet lowering by glacial erosion (Bitterli and Jeannin, 1997; section 3.1.4). They agreed with Audra (1994) that most phreatic enlargement takes place during corrosive flood conditions in the epiphreatic zone, where this dominates over low stage vadose erosion. According to Häuselmann, when flooding occurs, the system functions by upstream loops filling and overflowing to the next loop downstream. Thus, the water level within a complex cave varies from nearly horizontal in lower passages at low stage to become more steeply-sloping towards the outlet spring in higher epiphreatic passages at high stage. When the flood subsides, water drains from the higher passages to the lower passages via phreatic "soutirage" conduits that are commonly too small to explore and that only occur at the upstream end of a system. This thesis linked the Ford and Ewers (1978) Four-state model to the Audra (1994) paradigm, and relocated upstream vadose – phreatic transition points (section 3.1.4) to the top of the epiphreatic zone.

3.2.3 The role of carbon dioxide

Corbel (1954, as cited by Jakucs, 1977, p104) presented data to show that limestone erosion rates are higher by a factor of ten in cold zones than in warm zones, for each range of annual precipitation. However, Jakucs pointed out that this information cannot be used to infer that karstification is ten times as intense in arctic and alpine situations as in tropical karst, because Corbel had ignored the effects of evapotranspiration, production of CO_2 from inorganic and biogenic origins, and the dissolutional effects of inorganic and organic acids. Ford (1971a, p605) reported that equilibrium solute concentrations fall off sharply above the tree line in the Rocky Mountains. Helldén (1973, p195) pointed out that the much higher concentration of CO_2 found beneath vegetation and soil cover does not occur in glacial conditions, nor above a contemporary tree line, as confirmed in cave measurements by Ek and Gewelt (1985). Jakucs (1977, p109) presented unsourced data to show that, in high mountains and periglacial climatic zones, atmospheric CO_2 accounted for 45% of karst corrosion, but in temperate zones this reduced to just 7%, with biogenic CO_2 accounting for 54%. He also stated that the intensity of karst corrosion was twelve times higher in tropical climates than in high-mountain situations, contradicting Corbel (1954).

From the above, the role of carbon dioxide clearly varies in different climatic environments. High concentrations of carbonic acid can be attained in cold regions because the equilibrium solubility of CO_2 in water doubles from 0.52–1.01mgL^{-1}, when the temperature is reduced from 20–0°C (Ford and Williams, 1989, p54). Higher CO_2 concentrations can therefore be expected in both cold rain and snowfall. Drizzle is also more aggressive than heavy rain, as small raindrops absorb more CO_2 per volume than large drops (FD Miotke, University of Hannover, pers. comm., 1997). However, Miotke (pers. comm., 1997) remarked that snowmelt is less aggressive than rain, as air CO_2 does not so easily reach equilibrium with meltwater under a snow field. Accompanying the increased CO_2 solubility, Dreybrodt (1998, p36) pointed out that the *viscosity* of water is doubled, and therefore the flow rate through a system of fractures is halved, when temperature is reduced from 25–0°C.

There is conflicting information about conditions under snow and ice. Cogley and McCann (1971) suggested that, as snow ages, its aggressiveness towards calcite decreases. Helldén (1973, p195) cited Williams (1949) as saying that CO_2 concentration in air under a snowfield can be twice that of atmospheric air at normal pressure. Smart (1981) noted that during the freezing part of a regelation cycle beneath a glacier (Appendix A3.3), solutes (including calcite) can be excluded from the ice as precipitates, and CO_2 forms bubbles because it is less soluble in ice than in water. Thus, from the high partial pressure below a thick icesheet, the possibility arises of a high concentration of CO_2 in melting regelation waters. Lauritzen (1986b) reviewed previous studies of the CO_2 content of glacier ice and showed that, in fact, basal ice and ablation areas are depleted, when compared to snow and accumulation areas, by up to two orders of magnitude. Deep subglacial water may have a solvent capacity of only 13mgL^{-1} $CaCO_3$, at a P_{CO2} of ~10^{-6}atm. (Lauritzen, 1986a and b). Ford (1971a) was also strongly suggestive of depleted CO_2 beneath thick glacial ice, away from the snout. According to Siegert *et al.* (2001), the HCO_3^- concentration in water sampled from subglacial environments and in accreted ice from near-surface water in subglacial

Lake Vostok (Appendix A3.3) is only 0.3meqL^{-1} (18ppm). This is much less than recorded for Norwegian cave waters, as shown in Table A2.4. Lauritzen (1986b) used a theoretical modelling approach to show that with depleted waters under closed subglacial conditions speleogenesis from tight fractures would be negligibly slow, but that subglacial modification of existing conduits could be effective to produce significant cave volumes if there is a sufficiently high flow rate, despite the low solvent capacity. These ideas are pursued further in section 8.5.

Warwick (1956, p150) noted that where percolation water enters a cold cave, especially near to an entrance, CO_2 would be given off on freezing and $CaCO_3$ would be precipitated rapidly in fine crystals, probably forming moonmilk. Such moonmilk occurs in the entrance passages at **Møllebekkgrotta 3** (Z5) and **Øyåskjeleren** (Z4; Photo 3.2), for example. The concept was supported by Smart (1983), who described extensive subglacial precipitates on the benches around Mount Castleguard, Canada; by Hubbard and Hubbard (1998), who discussed the precipitation of carbonate deposits beneath a glacier in Switzerland; and by Killawee *et al.* (1998), who froze dilute solutions in the laboratory. Smart (1983) noted, from the small stalactite forms on vertical bedrock faces, that water had also passed through tiny fissures in the carbonate bedrock. Ford *et al.* (1970) reported fragile precipitates of calcite and dolomite at the soles of temperate glaciers, perhaps caused by supersaturation after reduction of hydrostatic pressure. Mulvaney *et al.* (1988) discussed sulphuric acid at grain boundaries in Antarctic ice (although sulphur was undetectable in the bulk of the ice).

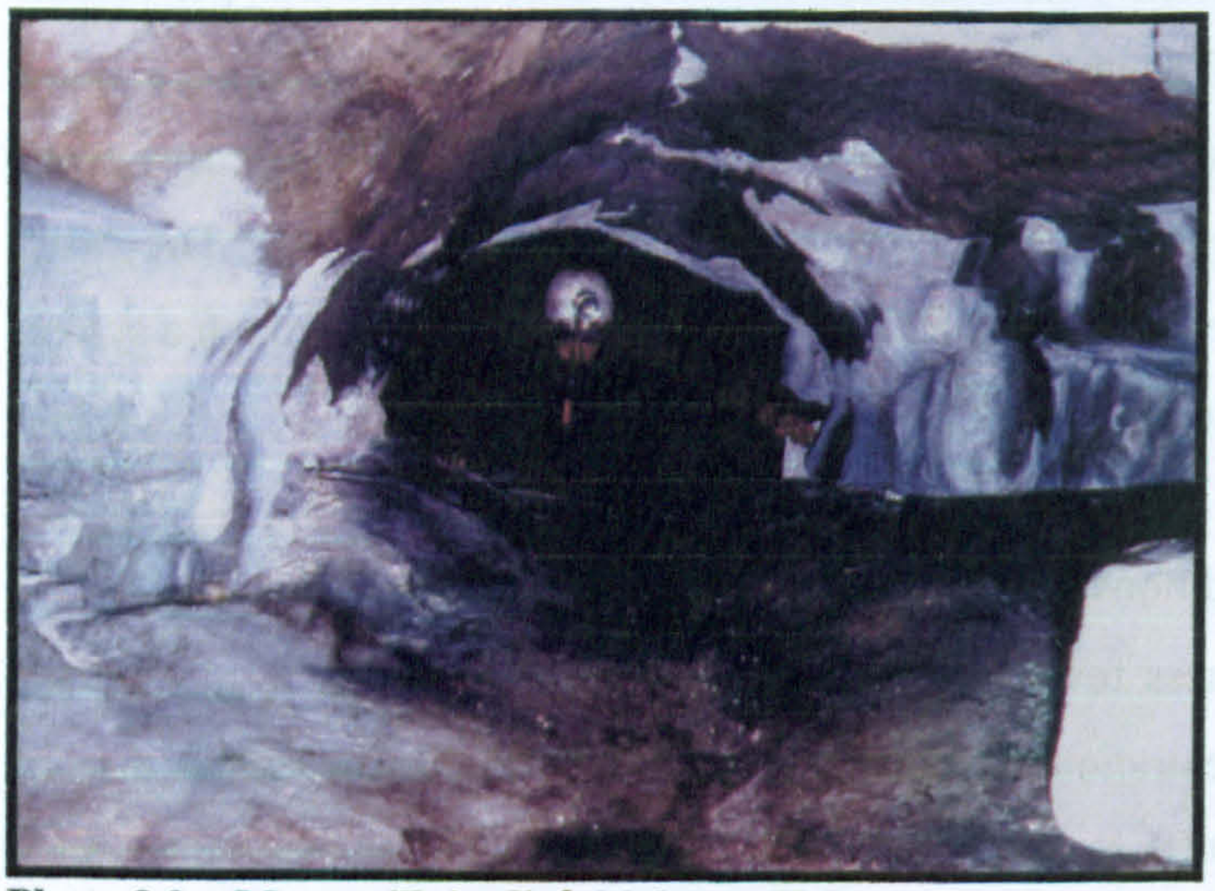

Photo 3.2 Moonmilk in Øyåskjeleren (Z4)
Moonmilk deposits commonly occur in entrance passages. This phreatic passage leads from the enlarged main entrance (Photo 8.2). Photo by A. Marshall.

Smart (1984b) considered the counter-intuitive possibility of speleothem deposition during glacial periods, and sedimentation during interglacials, from his study of Castleguard Cave, which he compared to **Øyfjellgrotta** (Z5). See also Appendix B1.5 and a different interpretation in section 8.8.3. Lauritzen (1993, p27) presented a diagram to show the effect on speleothem growth in Norway of interglacial, periglacial and full glacial conditions.

3.2.4 Glacier caves

Davies (1961) visited two types of glacier caves formed on bedrock in Svartisen, northern Norway. Pulina (1984) described caves in glaciers in Spitsbergen. These are large valley glaciers, which, because of intense recession, have large amounts of liquid water circulation even in the polar winter. Such glaciers can themselves exhibit exokarst and endokarst forms that resemble many features of limestone karst. There are two types of drainage systems: N channel marginal passages located within medial moraines or between the glacier margin and the unglaciated valley slope, commonly founded on solid bedrock, and R channel central conduits located wholly within the ice mass at depths up to 40m.

Theakstone (1988) discussed glacier caves and subglacial water in Nordland, Norway. Many subglacial channels are dry in winter, but discharge and water pressure increase rapidly with snow melt. Caves form within the glacier ice where streams flowing down adjacent valley sides continue beneath the ice, and may be explorable until the overlying ice is 50m thick. Others form where the moving ice loses contact with an irregular surface. Workers in the USA and Canada have found that 20–30% of a *retreating* glacier base is not in contact with the bed, but is separated by connected water-filled cavities. Although the meltwater from glacier ice is very pure, subglacial water can be rich in sediments and dissolved load.

Badino (2001b) discussed the improvement in exploration techniques of the last two decades that enabled a general model of glacial karst phenomenology to be described. Commonly, swallow-holes and crevasses form at the same places on glacial surfaces each year, despite the movement of the ice (c.f. whirlpools in a river bed). However, their formation conditions need to be considered separately, because cave conduits do not form where water is absorbed uniformly by crevasses. Most speleological research is limited to large, level, temperate, glaciers, where subglacial rivers flow for up to 1200m within the ice itself, at depths up to 20m, except for the last few tens of metres where they may emerge to daylight below a thin snout from a single conduit, as either a single torrent or as a delta. In larger glaciers, a deeper network can form in summer. These cavities commonly start with a waterfall shaft 40–60m deep, and may lead to short horizontal canyons and shallow waterfalls. A diminishing canyon may then lead to a terminal pool of water at a *subglacial reservoir* that is less than 100m below the overlying surface. There is no unique watertable in glaciers, but many interconnected storage systems. An epidermic and a deeper drainage system are common, which may meet near the glacial front.

The ice behaves like a rock at low pressures and at temperatures below freezing near the surface and caves and crevasses can survive for more than one season, becoming dry and moving down-slope with the glacier. At greater depths and higher pressures, the ice is deformed by plastic flow and behaves like a fluid, so that, at 70–80m depth, a cavity has an average life span of only one season. Below the *plastic behaviour limit* (PBL), collapse times are shorter, caves readily disappear into a fluid mass of ice, and deep relict tunnels cannot exist. If a deep conduit is full of water, collapse is delayed because the pressure of the denser water rises faster than the ice pressure. (The specific gravity of water is

1.000gmcc^{-1}, compared with 0.917gmcc^{-1} for ice). From borehole measurements inside cold-surface glaciers in Svalbard (Hodgkins, 1997, Fig.2) it appears that the PBL of warm-based icesheets may coincide with the depth at which the temperature rises to equal the pressure melting point.

Streams can form in summer on the glacier surface, commonly flowing into depressions at places where glacier tongues converge. At high stage, a glacial whirlpool can occur above a shaft that may enlarge and deepen to 60m or more throughout the season. Each such *moulin* is assumed to be an input to a deep dendritic drainage system with turbulent phreatic flows that commonly feed just one single channel. Most of this system lies above the bedrock and above the PBL. Because the freezing point of water reduces by 7.5x10^{-3}°C for each increase in pressure of one atmosphere, descending water tends to melt the local ice, whereas ascending water tends to freeze. (The pressure melting point beneath 2km of ice is -1.3°C). Hence, the rising limbs of deep U-shaped structures tend to close up, and very deep internal Vauclusian risings cannot form. When the deeper parts of the system become more constricted by freezing, the glacial whirlpool on the surface can become a lake, and the system can continue to exist as a static reservoir that descends downwards with the glacier, even in the absence of drainage. At high stage, water on a passage floor tends to excavate a channel, whereas water droplets on the ceiling tend to freeze. Thus, deep conduits gradually move downward through the ice (at about one metre per week), the network tends to settle as low as possible, and bypasses also tend to be eliminated. The Badino (2001b) model showed that with a flow of 1m^{3}s^{-1}, tunnels at a depth of 100m have a stable diameter of c. 90cm and water speeds of 1.5ms^{-1}. If the flow is reduced to 0.1m^{3}s^{-1}, the equilibrium diameter is 35cm and the speed is 1ms^{-1}. At the start of winter, water flows and pressures reduce and conduits begin to cave in, filling cavities vertically at a rate of perhaps two metres per week. Each year, the deep network is dragged down with the glacier and crushed, whilst new and deep systems form below new glacial whirlpools. Thus, the overall picture is that the deep network moves up-slope at the same speed as the glacier moves downhill.

The hydrology of icesheets and glaciers and their relationships to karst during study area deglaciation is analysed in greater detail in Chapter 8 and Appendices D2–D5.

3.3 Karst geomorphology in Scandinavia

As discussed in section 3.1, most present hypotheses and generic models of karst cave inception and development concern broadly holokarstic, non-metamorphic, sedimentary, limestones. The early classical studies were primarily about the *processes* involved within karst aquifers. Increasingly it became possible to discuss the *chronology* of events, and then to propose some minimum dates for the enlargement of individual cave passages on the basis of the dating of various cave deposits. How relevant is all this information about process and timescale to the caves of the central Scandinavian Caledonides? Here, the caves are commonly formed in merokarsts in metalimestones of various metamorphic grades. The foliation is commonly steeply dipping (at least within the study area, which may be an extreme

example within the Caledonides) and the aquifers are usually very confined. The whole area has been repeatedly and extensively glaciated. Hence, it is not immediately certain that much of the world-wide knowledge gained about sedimentary karst is applicable in this rather exotic situation.

Within Scandinavia, most discussion about cave geomorphology used to focus on the chronology of events in relation to glaciation. Thus, the early hypotheses sought to justify a primarily 'preglacial', 'subglacial' or 'postglacial' origin for the caves studied, most of which had a primarily relict phreatic morphology. These works were written from early in the 20th Century, when only four major Pleistocene glaciations were known. Subsequently, there was a much greater use of quantifiable erosion rates and valley entrenchment rates, coupled with the dating of internal sediments, to determine possible timescales within the much more complex picture of multiple Mio-Plio-Pleistocene glacials and interglacials that has emerged (section 2.3). This section summarises the knowledge and views presented by previous workers, in a roughly historical sequence. Some of this work was done in the study area, but most of it was undertaken in northern Norway. However, little work has been done to parallel the studies of Worthington (1991) and Lowe (1992a), i.e. to model the detailed behaviour of the karst aquifers and to consider how the first proto-conduits formed in solid marble.

3.3.1 Postglacial and proglacial views

The postglacial view of speleogenesis is that caves started to form at the end of the final Weichselian glaciation, when the valleys were still occupied by temperate glaciers. Hoel (1906) studied the special cases of **Aunhattenhule** and **Langskjellighattengrottene** near Velfjord (Z2), which were near the shore line prior to the postglacial isostatic uplift. He considered three possible formation mechanisms for the caves: erosion by fresh water streams, erosion by the sea, and "dislocations", and decided that all these caves were formed by sea erosion. Based on arguments about altitudes and strandlines, Hoel concluded that the caves were formed at a late glacial stage, except the higher cave at Langskjellighatten, which must therefore be interglacial. However, St.Pierre and St.Pierre (1980, p73) cited Rekstad (1917), who dismissed the possibility of the formation of any of the caves at Langskjellighatten by marine erosion, because of their elevation. Section 8.8.2 deduces that these caves were formed early during the Weichselian deglaciation, and some entrances were then enlarged by the sea.

In the opinion of Oxaal (1914), as cited by Horn (1947), **Grønligrotta** and other caves in Rana, northern Norway, had a *proglacial* origin, being formed at a glacial margin. Oxaal did however accept the possibility that the first "plan" of the caves could have had its beginning during "the interglacial". Oxaal (1916) showed that **Grønligrotta**, and caves at Naustvik (Z2, **Hallaran**?), could *not* be *postglacial,* because they contain large foreign rocks brought in by ice. The postglacial view was shared by Corbel (1957), a reversal of the subglacial opinion of Corbel (1952b). His 1957 conclusion was that the present size of the caves could be explained by proglacial and postglacial developments, caused by very high precipitation immediately after the deglaciation, with high CO_2 concentrations in a cold climate. Corbel

(1952a) related karstification at the lower level of Rennselelven (KL) to the level of a glacial lake at an altitude of 500m and noted that the nearby Bjurälv karst valley was also occupied by an extended glacial lake (Appendix D2.6). See section 3.2.3 for further consideration of Corbel's views. Jakucs (1977, p121) discussed the karstification processes in glacial and periglacial conditions, and supported the view (attributed incorrectly to Horn) that Scandinavian caves developed in periglacial conditions in not more than 8000 to 10000 years.

3.3.2 Subglacial views

The first exponent of the subglacial view of endokarst formation was the Norwegian geologist Gunnar Horn, as published by Horn (1937) and posthumously by Horn (1947). He noted that the majority of caves are now quite dry (and situated within a well-wooded "Green Karst" of long, narrow, limestone outcrops, which he called "Stripe Karst"). Hence, he argued, they could not have a postglacial origin, although he thought that some small, active, caves with sumps probably had a short formation time. On the other hand, the cave altitudes are some 500m below the presumed watertable level of the pre-Ice Age [paleic] ground surface at the level of the present mountain peaks. He argued that cave formation at 500m depth seemed unlikely because, if so formed, the caves should be larger than they are, in comparison with large European caves, because of the long elapsed time involved in their formation. Hence, he thought the caves could not be preglacial or even interglacial. Thus, Horn deduced that the caves had a subglacial origin. He cited Werenskiold (1922, p9) and Sverdup (1935) who worked in Spitsbergen. They found that, whereas the permafrost there generally occurs down to 200–250m in rock not covered by snow or ice, there is no permafrost directly under an active glacier that is more than 400m wide (see also Horn, 1935, and compare with evidence of warm-based glaciation, Appendix A3.3). Such a glacier has a base just above freezing, so that meltwater can pass into fissures in any underlying limestone outcrop and form subglacial karst. He also noted that cave entrances occur in arbitrary, commonly "impossible", positions relative to the present topography. Thus, Horn postulated that a slow movement of water first circulated in joints and other channels and then formed dissolutional phreatic pressure tubes that enlarged over a long period of time to the size of the present caves. He argued that the water moved slowly, because he thought there was little mechanical erosion in the caves: if the water was fast flowing, there would be fewer projections. Hence, the mainly-phreatic passages were all drained when the ice melted, leaving the dry caves that can be explored today. Additionally, Horn thought that the paucity of dripstone formations in the caves is because the caves are relatively young. The *"dissolutional phreatic pressure tube"* concept is supported in this thesis, although the mode and timescale of inception and enlargement differ significantly (Chapter 8).

Kirkland (1958, p84) concluded that the subglacial hypothesis satisfactorily explained the development of all caves in the south Svartisen area of northern Norway. These are primarily relict, with phreatically-formed cross-sections. He thought the caves *originated* in the Tertiary, below a watertable, but *developed* mainly in pseudo-phreatic conditions below icesheets, during the last glaciation. Some caves also

experienced limited Holocene vadose modifications by misfit streams. He also argued that phreatic passages with fragile projecting schist blades must have developed from chemical erosion by slow-moving water. He found no evidence that phreatic developments were related to falls of watertable levels (*Ibid.*, p72), and hence deduced that tiered phreatic passages could only develop simultaneously. Observing the lack of any former surface drainage pattern associated with karst "sink holes" [i.e. dolines], he concluded additionally that the *exokarst* was "fossil" [i.e. relict], and therefore also of glacial origin (*Ibid.*, p61). Wolfe (1967) deduced that the upper, phreatic, part of **Jordbrugrotta** in Plurdal (12km north of the study area) formed during the last glaciation or during the most recent interglacial period, whereas the lower, vadose, part of the cave developed post-glacially. In his papers about **Sotsbäcksgrottan** (KU), Helldén (1973, 1974a and 1975) argued that glaciofluvial accumulations indicate a partially-subglacial genesis. Moreover, because evidence of an ice-dammed lake at Över-Uman (Appendix D2.6) was only 20m above the present level, he considered this was far too low to have influenced the development of this cave.

Lauritzen (1981c and 1984b) discussed the evidence for subglacial karstification in Glomdal, northern Norway, whilst suggesting from the work of previous authors that, generally, Norwegian caves have *polygenetic* origins. He deduced from their morphology that the caves in Glomdal had experienced seven phases of development. In some passages, he observed paragenetic features (Lauritzen and Lauritsen, 1995) superimposed on vadose features, which suggested that a reversed flow had occurred after a stage of base-level lowering. The diagram he presented shows a total flow reversal from the normal downhill flow that prevails during interglacials, to an uphill flow that occurs when a lower outlet is blocked by ice and the cave is in a subglacial situation. However, he noted the problem of the depleted aggressiveness in subglacial waters, so that it was not proven that entire cave passages with radii of 1–2m could form in subglacial conditions. He therefore suggested that the (present) powerful allogenic water is important for passage enlargement in the narrow carbonate outcrops in which many Norwegian caves are found. From principles embodied in the PWP Equation (section 3.1.3), Lauritzen (1986b) concluded that subglacial inception was unlikely, but that under high flow rates, conduits could enlarge to 2m diameter in 1000a. Lauritzen (1981c) also proposed a classification for phreatic caves in glacial landforms: paleic surface caves; valley shoulder caves; and active valley floor caves. Lauritzen (1990b) added a fourth class: hanging valley wall cave. Section 5.3.4 of this thesis introduces three more *cave location* classes.

Kvithola, at Fauske in northern Norway, was presented as an example of ice contact speleogenesis by Lauritzen (1986a). Its very steep, but phreatic, 130m-long passage formed in a fracture zone that is less than 10m from the wall of the local valley, so that the cave post-dates the creation of the valley. Mean scallop lengths of about 8cm showed that the flow rate was c. $1m^3s^{-1}$, at a velocity of c. $50cms^{-1}$ (section 3.1.7), giving a water residence time of only 4 minutes within the cave. If wall retreat rates lay between $0.1–1mma^{-1}$, the conduit could form within 7500–750a. Lauritzen concluded that **Kvithola** formed at the margin of, and well below the surface of, a local valley glacier to which it supplied a subglacial stream.

3.3.3 Interglacial and preglacial views

With our present knowledge of the Weichselian glaciation (section 2.3.4), the previous opinions about interglacial speleogenesis should perhaps be interpreted to mean an origin prior to the Weichselian LGM. Railton (1954) studied caves in Rana, just north of the study area. Undoubtedly familiar with the contemporary theories about cave formation in sedimentary limestone, he ascribed a deep phreatic, and at least interglacial, origin to them. Thus, he described **Grønligrotta**, **Setergrotta**, **Hammernesgrotta** and **Opsalgrotta** as network caves with impervious overburdens, which had been formed by very slow moving water when the watertable was some 300m higher than now. He suggested that **Larshullet**, **Olavsgrotta** and **Lapphullet** perhaps formed by water flow from (lake) Reingardslivatnet, with a maximum hydrostatic head of 330m. Initially phreatic, development in **Larshullet** then alternated seasonally between vadose and "pseudo" [i.e. epi] phreatic, as the recharge rate caused water to back up well above the sedimented outlet. A lower lake level then cut the water supply and drained the caves. Railton explained the general lack of speleothems by the small depth of limestone above them, or because of the impervious cover rock.

Jenkins (1959) reported on the Svartisen area of northern Norway. He suggested that **Pikhauggrotta** possibly originated as an early Tertiary small-scale phreatic system, because its glacially-truncated entrances indicate that the main cave development preceded the last glacial phase. The main development was by fast-flowing (epi) phreatic water during subglacial drainage, and then by drainage from a proglacial lake followed by vadose modification in the Holocene. (Jenkins also gave a possible alternative origin as starting at the proglacial stage). He thought that **Fosshullet** had a similar history, together with an early postglacial phreatic modification phase. Theakstone (1964) also thought it likely that **Pikhauggrotta** and other local caves originated in the Tertiary, but were enlarged principally by subglacial meltwater. However, Renwick (1962) estimated that the active phreatic **Glomdal Underground Outlet** (also in the Svartisen area) developed in only 30ka, by measuring flow rates and assuming dissolution rates (although his treatment was criticized by Aub, 1963, as being simplified and unreliable). Lauritzen (1980) reported micro-erosion meter readings on marble that indicate local denudation rates (Appendix A2.6). From this data, he calculated that the **Glomdal Underground Outlet** is older than 40ka, suggesting that this significant flooded conduit has at least an interstadial origin, but may not be interglacial.

Engh (1980, summarized in English by Lagerström, 1980) reported the discovery of **Vuoitaskallogrottan** in the Vadve valley in northern Sweden. Its apparent vertical range of 155m includes a vertical shaft of 58m. This and other nearby caves are in topographically high positions, 100–200m above the present valley floor in an almost vertical wall. Engh argued that these are "hanging caves", i.e. fragments of bigger systems that existed before the U-shaped valley was cut out, and so cannot have formed, or even have developed, in the Holocene. Believing that these caves are interglacial or preglacial, he claimed that they could not be subglacial, because a lack of speleothems indicated a lack

of water circulation, as he thought would apply underneath an ice cover. He also cited Warwick (1956; 1971; section 3.2.1) who said that caves do not grow in subglacial conditions.

In another study of **Pikhauggrottene**, Lauritzen (1982) discussed the palaeocurrents and cave morphology. He noted that subglacial flow under temperate glaciers can show uphill segments and paragenesis, with large amounts of water available. However, subglacial flow under full (polar) glaciations was neither confirmed nor rejected. He cited Ford (1977a), who said that in these conditions groundwater circulation ceases, with a large-scale silting of cave passages. **Pikhauggrottene** consist predominantly of phreatic passages. Vadose elements account for only c. 4% of passage length, and paragenetic roof modifications account for c. 10%. The scallop directions suggested a uniform network flow to the south, and there was evidence for subsequent sediment fill and paragenetic incision. Lauritzen thought that the local 'watertable' lowered from 610 to 575m, when a high discharge occurred. Then it lowered to the present watertable at <560m. Lauritzen deduced that if the main shift in watertable was caused by bedrock erosion, then probably this occurred at 220ka. Two alternative origins were presented: preglacial, in a paleic valley system; or subglacial, and then during deglaciation, when the paragenetic changes occurred. The Jenkins (1959) alternative possibility of proglacial genesis was rejected. From the evidence of **Kvithola** (section 3.3.2), Lauritzen (1986b) thought it likely that the relict caves situated several hundred metres above valley floors represent glacially truncated fragments of caves developed in early interglacials or in the Tertiary, agreeing with Engh (1980).

Sirijordgrotta (Z4; Appendix B1.4) is the only cave in the Norwegian part of the study area whose morphology and sediments were the subject of detailed analysis. St.Pierre and St.Pierre (1980) revealed that the cave had experienced a complex history, as they observed unsorted sediments in Birch Passage, graded sediments in River Gallery, and fining up sequences to very fine particles at the top of sediment banks. These deposits indicate flood events, fluctuating flows, and ponding during peak flow conditions. They suggested that these deposits could be explained by subglacial formation, inundation by melting ice and subsequent draining. This would explain the lack of a dry valley below the Main Entrance, although such a dry valley could have been removed by glacial truncation. The lower vadose series was formed after the sudden removal of ice, and the lowering of the outlet level. A more detailed study of the sediments described four main depositional environments (Valen and Lauritzen, 1989; Valen, 1991; Valen *et al.*, 1997; Appendix B2.10). In sections sampled for palaeomagnetism (Table A5.1), only the laminated clay sequence in Arctic Passage was presumed to have been deposited subglacially over a long time span. This was tentatively correlated to the Lake Mungo palaeomagnetic excursion at c. 28ka, during full ice cover and glacial damming. Three deglacial flushing sediments were probably deposited about 10.4ka. This is some 700a before the final local deglaciation at 9.7^{14}Cka, from a moraine north of Mosjøen (Valen *et al.*, 1997; Appendix D3.7). The oldest flowstone was dated to 128ka (Table A5.1), perhaps following a high energy deglaciation of the Saalian, or earlier, icesheet, thus confirming an interglacial age, at least for the main development of **Sirijordgrotta**.

Holbye (1983a; 1983b; 1983c) and Holbye and Lauritzen (1983) discussed the geomorphological development of the deep **Greftkjelen** in northern Norway. The cave has developed within a highly complex folded metacarbonate structure, with shear joints. It displays eight phases of trunk conduit development, each defined by a series of phreatic loops showing vadose downcutting from loop tops. The later phases show interactions between the cave and the landscape development during both glacials and interglacials. From stalagmite dating (Table A5.1), the cave was considered to have an origin at least at 500ka. This author's deductions are presented in Appendix D6.1.1.

The speleogenesis of **Hammernesgrotta** received further attention after the work of Railton (1954). Lauritzen (1981a) offered two possibilities. If the caves formed below a watertable (with an altitude near the present entrances), then he suggested an inter- or pre-glacial speleogenesis. If there was no definite watertable, then he suggested subglacial speleogenesis by large paraphreatic fluctuations in an englacial watertable. Haugane and Grønlie (1988) attributed a Miocene age of formation, in discussing the problems of explaining large phreatic passages in Nordland that are today remote from any major drainage systems. They argued that **Hammernesgrotta** must have been formed from a large water supply, which must have been from the area of the main valley catchment. This is presently focused on the lake Langvatn, which is now 163–173m below the caves, whose origin must therefore pre-date the late Quaternary. They thought that the large passage enlargement required water with a high CO_2 concentration and a high (biogenic) acidity. These could be provided in a temperate and humid climate, rather than in a glacial environment inhibited by permafrost and depletion of CO_2 in deep subglacial ice. Prior to the Tertiary uplift, Scandinavia had been reduced to a peneplain, so they contended that Mid to Late Tertiary would be the favoured time for cave development, after sufficient uplift, and prior to climate deterioration at 4.5Ma. They argued that Quaternary karstification was mainly during the warm interstadials, which is when the main speleothem growth is recorded, and that subglacial caves can only rarely form relatively quickly. In support of this argument, they noted that the limited denudation of speleothems is consistent with a limited dissolution capacity of glacial meltwater. Assuming no cave development below sea level, the uplift curves at **Hammernesgrotta** indicated that its earliest time of formation was the early Miocene (25Ma), at 300m below the contemporary watertable. These authors further suggested that *all* the major caves originally formed during the Miocene.

Lauritzen (1990b) provided more information and deductions about **Hammernesgrotta**. Stalagmites from the cave *are* bulk corroded and their bases were apparently dated between 350ka and 1250ka (Table A5.1). This age was constrained to 500ka by Lauritzen *et al.* (1994) on the basis of amino acid dating. Lauritzen (1990b) noted, from scallop orientations, that some chimneys acted as bypass loops of glacially-blocked conduits, so that the cave system may have developed by headward linking of phreatic loops (as discussed by Ford and Williams, 1989). Also, rather than form phreatic loops in the deepest possible position in the aquifer, the cave position seems peculiarly high. This suggested to Lauritzen that

the flow was perched by an aquiclude downstream of the cave, which was therefore formed by a shallow phreatic development or by repetitive englacial flooding. The final active phase could have been with modest flows upheld by ice damming just above the level of the present entrances. By referring to various published figures, and by following a concept proposed in Ford *et al.* (1981), Lauritzen assumed an average valley to have an entrenchment rate between 150–550mm ka^{-1} for full glacial / interglacial cycles, and modelled the cave development using estimated discharge and wall retreat rates. His result was that cave initiation was likely to have started at 1.1Ma–320ka, which does not conflict with the stalagmite dates. He also argued that the cave was unlikely to have formed in the Miocene, on the basis that the relict passages would be much larger than observed today, because "*the wall retreat rate from condensation* (section 3.1.9) *and winnowing is at least 0.2mm* ka^{-1} (during interglacials, *Ibid.*, p35)". For water-filled caves, Lauritzen commented that *"as soon as a cave becomes an active part of a phreatic system, the growth is almost instantaneous when seen from the Cenozoic timescale of millions of years"* (*Ibid.*, p35). The paper presented a diagram to show the hypothetical relationship between the age of a cave, its diameter, and its altitude. For a cave to have initiated earlier than 1.6Ma (the strict Plio-Pleistocene boundary), it must have a diameter greater than 3m and an altitude over "base level" of at least 240m. Lauritzen could find only four caves in Norway that meet these criteria. [On this hypothesis, **Gåsvasstindhola** (Z4) would be the oldest cave in the study area. It has a maximum diameter of 10m and a base level elevation of 200m, and so would still fit inside a Pleistocene genesis].

This author considers that, in fact, **Hammernesgrotta** and all relict phreatic caves in the Caledonides formed beneath many deglacial ice-dammed lakes, in the manner described in Chapter 8. Formation beneath deep water is supported by the work of Auler (1995, Fig. 3), who described the speleogenesis of caves beneath lakes in Brazil. His survey of discrete network cave systems along a cliff edge is similar to the survey of **Hammernesgrotta** by Haugane and Grønlie (1988, Fig. 3).

Sjöberg (1991a) used the Lauritzen (1990b) model to suggest that, in the whole of Sweden, only **Vuoitaskallogrottan** in the Vadve valley could have originated in Tertiary times. Also in Sweden, Norberg *et al.* (1988) studied the two karst areas of Kåtaviken (ZC) and Rödingsfjället (KU). Using methods described in Lauritzen (1982), they measured scallops to determine maximum flow rates. Combining these data with estimated denudation rates, they calculated an age range of 9–60ka for the caves in Rödingsfjället. Isacsson (1989; 1994; 1999) discussed the cave deposits in **Korallgrottan** (KL), but radiometric dating is awaited. The depositional sequence consists of four sediment types. Type A is coarse-grained calcified sand and gravel that probably filled three quarters of the cave's volume, but has since been washed out during (he presumed) glaciations and interglacials. According to Isacsson (1999), the cave reached its present dimensions at the end of the Pliocene, before glaciation scoured the present U-shaped valley.

According to Lauritsen and Lauritzen (1996), the 800m-long **Storsteinhola** has the largest paragenetic canyon in Norway. This is c. 5m wide and c. 10m high. It rises towards **Norcemgrotta**. A maze of epiphreatic tubes beneath the paragenetic canyon represents two subsequent rejuvenation phases. A deglaciation phase of vadose entrenchment had a maximum flow rate of 2–5m^3s^{-1}, from scallop morphometry. However, the present catchment area is 4km^2, which would only provide 0.25m^3s^{-1}, from an infiltration rate of 2ma^{-1}. [Hence, if this example is representative, the deglaciation phase can increase annual run off through caves by a factor at least in the range 8–20: see Chapter 8]. The paragenesis was thought to have operated over a long timescale (10–100ka), as it shows 10m of vertical corrasion against a stable base level, which cannot be seen in the present topographical situation. Lauritsen and Lauritzen (1996) thought it unlikely that ice-damming or a sea level could have provided a stable base level for this long period, and deduced, therefore, that the base level for the paragenesis was controlled by a more resistant bedrock lithology. Study of the Tertiary paleic surface and Tertiary uplift suggested that the Kjøpsvik caves are much younger than the paleic landscape, but much older than the Weichselian glaciation.

The justifications for speleogenesis prior to the LGM rely increasingly on U-series dating of speleothem, and undoubtedly all the relict caves mentioned in this section have pre-Weichselian origins. Three main dating methods have been employed in Scandinavia: radio-carbon dating of organic material, palaeomagnetic dating of fine clastic sediments and U-series techniques for various calcitic deposits. The results of these datings and the conclusions drawn from them are summarised in Appendix A5. Scandinavian karst water chemistry is summarised in Appendix A2.5 and various erosion rate determinations are considered in Appendices A2.6 and A3.5.

This section completes the introductory part of this thesis, which has now discussed the geological evolution of the study area and our knowledge of speleogenesis and its relationship to glaciation, prior to the work undertaken for this project. So far, little new work by this author has been described, although this review from the perspective of glaciated metamorphic karst is itself original. Chapters 4 and 5 describe in detail the factual results obtained from the author's analysis of the assembled knowledge of the karst outcrops and caves in the study area.

CHAPTER 4 THE KARSTS OF CENTRAL SCANDINAVIA

The preceding Chapters introduced this thesis and discussed the present ranges of knowledge about the geological history of the Scandinavian Caledonides, about speleogenesis in general, and about speleogenesis in glaciated karst terrains. This led to the review in section 3.3 of the work already done to understand speleogenesis in Scandinavia. The purpose of *this* chapter is to report this author's analysis of the various metacarbonate outcrops that occur within the central Scandinavian study area.

4.1 Information about limestone and dolostone outcrops

Information about carbonate outcrops in the study area was assembled into a database from various sources, so that tectono-stratigraphic trends could be identified for various geological attributes and so that these could be compared with variations of karst attributes across the study area.

4.1.1 NGU and SGU mapping

Figure 1.2 identified the geological maps utilised in this study. The bedrock geology of the whole study area has been mapped to a scale of at least 1:250000 by Norges Geologiske Undersøkelse (NGU) and by Sveriges Geologiska Undersökning (SGU). In Norway, the bulk of the area is covered by the Mosjøen sheet at that scale. This dates from 1981 (Gustavson, 1988). The remaining small-scale maps for the Norwegian part of the area were published by the NGU after this, with the solid-geology map for Grong (1997) completing the series. The western part of the Mosjøen sheet had previously been mapped at 1:100000, in a map series published in the 1970s. These geological maps were based on the older 1:100000 series topographical maps that date from about 1900. From the mid-1980s, bedrock maps were published at 1:50000, on sheets that correspond to the new topographical maps that are based on aerial photography. In the study area, about twenty such maps were published in black and white, but these are not easy to interpret and were not consulted. Three applicable coloured maps have been published in this series since 1992, and these have all been utilised in this study. Additionally, NGU has recently published eight Quaternary Geology maps that also coincide with the 1:50000 topographical maps. These show karst features with a special symbol. A study by the author in 1998 revealed that *not one* of these symbols coincided with a known karst cave. During the 1998 field trip, it was found that, in general, the karst symbol did indicate *exokarst* features: usually dolines, and, in one case, a previously unrecorded, small, cave. It was confirmed by discussion with the NGU in Trondheim that individual geologists decide on the criteria for showing the karst symbol. Because of the varying ages and scales of the bedrock maps, the recording of nappe structures and identification of rock types has also varied, with sporadic areas of conflict between maps. Experience has shown that, in Norway, those carbonate outcrops with widths less than 100m (or 50m on the newer maps) are rarely represented.

In Sweden, the northern part of the study area in Västerbotten was mapped at 1:200000 (1927), and at 1:400000 (1955). The later map shows more carbonate outcrops than the earlier one, but neither has a

modern understanding of the nappe structure. Presumably, these maps did not attempt to represent every narrow carbonate outcrop. Part of the area south of 65°45' is now well-covered by 25 bedrock maps at a scale of 1:50000. This map series also covers land well to the east of all the known karst caves. The Køli and Seve nappes are represented in great detail, and the uncertainties of their exact structure are being resolved as new maps are published. Field experience in 1998 showed that the Swedish maps tend to *exaggerate* the extents of carbonate outcrops. Additionally, the SGU maps use the same colour to represent marble and calc-silicate rocks in the Seve Nappes. During the 1998 field trip, many mapped, small, lens-shaped outcrops in the Seve Nappes and in the Lower Allochthon could not readily be located or identified as being calcitic or dolomitic. This was perhaps because they were masked under the cover of forest and till, or perhaps because they are, in reality, calc-silicate outcrops. Other, longer, "stripe karst" outcrops in the lower Køli Nappes were found to have widths of only c. 5m, despite being represented on 1:50000 maps.

4.1.2 The Central Scandinavian Carbonate Rock Outcrops Database

The author assembled information about the carbonate outcrops in the study area by taking information from all the above sources, coupled with personal experience and other published reports of karst caves that exist along *unmapped* limestone outcrops. This information was placed into a computer-based database constructed using Microsoft Excel with Windows XP: *The Central Scandinavian Caledonide Carbonate Rock Outcrops Database* (Appendix C1). Where there are conflicts, information from later maps at larger scales is preferred. If a piece of information about an unmapped outcrop is not known (e.g. length or width) then, rather than leave a blank field in the database that could derogate later statistics, an estimate of the value is included, but shown in italics. (The number of known, but unmapped, outcrops is only c. 30). Outcrops are recorded down to c. 0.01km^2 in size, typically 200m long and 50m wide.

The database is organised according to the tectono-stratigraphical structure of the area (section 2.1) and the division of the area into zones (section 1.5). Each identified separate outcrop occupies one row in the database tables, and information about it is held in 30 fields organised into columns. Outcrops in each zone are grouped together under each applicable topographical map, and listed in a generally west to east and north to south order. The database holds details of just over 1000 carbonate outcrops. Its capacity is thus about 30000 pieces of information, plus summary information for each map and then each zone.

Each carbonate outcrop was marked up by hand on the appropriate topographical map (usually the Norwegian 1:50000 series M711). Because this transfer of information was commonly from a 1:250000, or other scale, bedrock geological map, the outcrop positions and outlines are not particularly accurate. However, experience has shown that the use of such marked-up topographical maps usually enables the outcrops to be located in the field, and related to mapped or observed karst features. Until more of the coloured 1:50000 geological maps become available, a more accurate representation is probably not

achievable, because most of the available coloured geological maps are still based on the old, rather inaccurate, 1:100000 topographical maps.

A convenient, fairly central, 2 alpha + 6 figure UTM grid reference is held in the database to identify each outcrop, or, where a Swedish co-ordinate has to be used, this is based on the Swedish 10 digit RN co-ordinate system. The maximum altitude for each outcrop, together with its maximum vertical ranges along its length and across its width, were recorded by studying contours on the topographical map. The total length of each outcrop (including lengths of multiple limbs, if applicable) was determined by measuring with a ruler on the geological map. The visited lengths of those outcrops examined by cavers looking for caves are estimated from the author's records.

A figure for an estimated, or measured, mean width is also recorded, and used to provide an estimate of the area of the outcrop (and dolomite area, if applicable) in square kilometres. This is probably accurate to within 20% of the geological map representation. A note about the shape of the outcrop helps speed up later checks between the maps and the database. Data about strike, dip and mineralogy are taken from the geological maps, or from personal observation. Simple 1 or 0 fields indicate if the outcrop is at, or close to, an adjacent igneous pluton (and therefore probably subjected to a repeated, contact, metamorphism); is at, or close to, a major thrust boundary; has been visited by cavers; or is mapped as dolomite.

A late addition to the database shows whether each outcrop lies mainly east or west of a major ridge. The numbers of mapped karst features and bodies of water on limestone, as derived from topographical maps, are also recorded. By reference to two Cave Databases (section 5.1), the database also shows the total number of recorded caves and the total passage lengths in each outcrop, together with other notes, including the number of features noted as Quaternary karst by geologists.

4.2 Attributes of metacarbonate outcrops

This section analyses the various attributes of the metacarbonate outcrops, whose variations and trends as the allochthons are descended eastwards are shown in Table 4.1. The HNC and RNC of the Uppermost Allochthon are sometimes better considered together, as the rather small area of the RNC in the chosen study area may not be representative of its larger extent farther north.

4.2.1 The distribution of metalimestone and metadolostone outcrops

The total number of recorded carbonate outcrops is 1006. These have a total surface area of about 860km^2, which represents less than 3% of the whole study area. However, the areal proportion of carbonates in each nappe group shows a consistent decline when passing downwards stratigraphically. For the HNC and RNC it is about 6%; for the Køli Nappes it is about 2%; for the Seve 0.2% (and much of this may be calc-silicate rock); and for the Middle and Lower Allochthons taken together only 0.1%. (There are actually no carbonate outcrops in the Middle Allochthon). The numbers of outcrops, their

total length, and their total *visited* length, show a similar general decline. Because of the narrow widths of most stripe karst carbonate outcrops, the simplest measure of carbonate extent is *length*, and the total carbonate outcrop length is some 3200km. The mean width is 159m. The mean length and mean area per outcrop also show *general* reductions down through the nappes, although they both peak in the RNC. The study area means are 3.2km and 0.9 km^2. (The large figures for the Lower Allochthon that reverse the trend are caused by one large dolostone outcrop that contains nearly half the ML total carbonate area). About 20% of both calcitic and dolomitic outcrops have been visited by cave explorers, who have walked along some 14% of the total outcrop length (c. 450km). However, only small distances have been covered along the smaller carbonate outcrops in the Seve Nappes and in the Lower Allochthon.

Table 4.1 Variations of metacarbonate attributes with tectono-stratigraphic structure

Nappe complex	HNC	RNC	KØLI	SEVE	ML	ALL	Units	E. TREND
Total area	9950	1762	9336	4443	6276	31767	km^2	No trend
Main country rock	Schist	Schist	Various	Various	Various			
Main metamorphic grade[1]	Am	Am	Am/Gr	Am	SubGr			Decreasing[2]
No. of carbonate outcrops	536	74	252	123	21	1006	No.	Decreasing
Total carbonate area	560	126	163	7	5	861	km^2	Decreasing
% carbonate area	5.6%	7.1%	1.8%	0.15%	0.08%	2.7%	%	Decreasing
Mean outcrop area	1.05	1.70	0.65	0.05	0.24	0.86	km^2	Decreasing
Total outcrop length	1911	472	680	99	31	3193	km	Decreasing
Mean length per outcrop	3.6	6.4	2.7	0.8	1.5	3.2	km	Decreasing
No. of visited outcrops	125	31	30	5	4	195	No.	Decreasing
Total visited length	252	101	94	0.4	0.3	447	km	Decreasing
No. of dolostone outcrops	16	12	21	0	15	64	No.	No trend
% dolostone outcrops	3%	16%	8%	0%	71%	6%	%	Increasing[2,3]
Total dolostone area	10.8	12.6	26.3	0.0	4.9	54.6	km^2	Increasing[4]
Mean dolostone area	0.67	1.05	1.25	–	0.33	0.85	km^2	Increasing[4]
Dolostone to carb. area ratio	2%	10%	16%	0%	96%	6%	%	Increasing[3]
Maximum dip	90	90	90	80	45	90	Deg.	Decreasing
Mean dip	63	42	42	30	33	52	Deg.	Decreasing
Minimum dip	10	0	10	5	10	0	Deg.	No trend
Mean outcrop widths	190	225	127	57	110	159	m	Decreasing[4]
Mean length / mean width	19	28	21	14	14	20		Decreasing
% contact metamorphism	48%	1%	2%	0%	0%	26%	%	Decreasing
% outcrops near thrusts	6%	7%	27%	11%	57%	13%	%	Increasing[2]
% outcrops east of major ridge	46%	35%	70%	87%	100%	57%	%	Increasing
No. of mapped karst features	196	123	72	0	0	391	No.	Decreasing
No. of features per outcrop	0.37	1.66	0.29	0	0	0.39		No trend
No. features per 10km outcrop	1.0	2.6	1.1	0	0	1.2		No trend
No. water bodies on limestone	141	38	59	6	1	245	No.	Decreasing
No. water bodies per outcrop	0.26	0.51	0.23	0.05	0.05	0.24		Decreasing
No. water bodies per 10km	0.74	0.81	0.87	0.61	0.32	0.76		No trend

[1] Amphibolite–Greenschist–Sub Greenschist facies
[2] Except Seve
[3] Dolostone values tend to increase with reducing metamorphic grade
[4] Except ML

Of the 1006 recorded outcrops, only 64 are mapped as dolostones: some 6%. They have the same mean area per outcrop of 0.9km^2, but the proportion of dolostone area to total carbonate area *generally increases* as the nappes are descended, except that no dolostones occur in the Seve nappes. This apparent relationship between metamorphic grade and dominance of calcitic limestone over dolomite is discussed in Appendix A2.10. The records for the Seve nappes may be confused (section 4.1.1) because the 123 recorded Seve outcrops are identified on the SGU 1:50000 maps as "*marble, generally calcitic, calc-*

silicate rocks". Thus, it is unclear if some of these outcrops are calcitic metacarbonates, whereas others are calc-silicates, or whether a proportion of the outcrops contain rocks of both types.

Another complication is that not all Swedish geological maps differentiate between limestones and dolostones. Thus, a rather deep blue colour may be annotated as "*limestone or dolomite*", "*calcitic and dolomitic marble*" or as "*marble*". These outcrops are recorded as calcitic in the database, except where the word "dolomite" is used first. Field experience in 1998 highlighted the difficulty facing the mapping geologists: the two rock types are commonly intermingled within the same outcrop. Thus, slivers of mainly dolomite probably occur in many of the metalimestones of the whole study area, and within outcrops that appear to be completely dolomitized, larger parts can be found that are very calcitic. Dallmann (1987, p45) observed that carbonates in the Hattfjelldal Nappe (KU) have rhythmic calcite-dolomite laminations. He cited Gebelein and Hoffmann (1973), who described such features as dolomitic laminae at former algal layers, and calcitic laminae for the sediment in between. Because most of the geological mapping was undertaken prior to the Tucker and Wright (1990) classification of carbonate types (Appendix A2.4), a more accurate description of bedrock carbonate types cannot be gained from published geological maps, and the use of the word "dolomite" may cover all carbonates that are not clearly LMC, including those of a yellow / brown colour that are probably HMC or DL.

4.2.2 Altitudinal range

The maximum, mean and minimum altitudes of carbonate outcrops commonly increase eastwards across the zones, as far as the Køli nappes, and then decrease again because of the Scandian Marginal Bulge (section 1.4), as observed in the database details. In each zone, maximum altitudes of the mapped carbonate outcrops commonly occur in each of the 25m altitude ranges from about 60% of the maximum altitude of the highest outcrop down to the maximum altitude of the lowest outcrop. (The highest 30–40% of the carbonate altitude range is commonly populated less densely with carbonate outcrops, because of reduced land area). Only RNC zones ZA and ZB, the Upper Køli Nappes (KU), and the Middle and Lower Allochthons (ML) have sparser carbonate distributions that do not occur at least at 25m intervals. It is therefore assumed that the vertical distribution of carbonate outcrops across the whole study area is essentially random. This is understandable, because the present distribution of most carbonate outcrops derives from intense metamorphism, folding and thrusting during the formation of the Caledonian mountain chain. These processes caused originally-sedimentary limestones to descend to depths up to 50km, where they were thinned, broken and redistributed, before they returned towards the surface by uplift and erosion. At the scale involved, where each outcrop is very small compared to the size of the zone, a random vertical distribution arises, conditioned by the topography.

There is a wide spread in vertical ranges of the carbonate outcrops, from a few metres, up to 956m for an (unvisited) outcrop in ZC. Typically, a long outcrop crosses and passes through several valleys along its mapped length. Hence, because of the large vertical ranges of many carbonate outcrops, carbonate exposures commonly occur at a wide range of altitudes in each zone, from a regional base level up to the

highest point of the highest outcrop. For all HNC and RNC zones, except Z4, Z7, ZA and ZC, the regional base level is sea level. For nappes that are completely inland, the regional base level is commonly a large 'inland sea', down to which many carbonate outcrops descend. The mean vertical range for the carbonate outcrops in each zone commonly reduces eastwards, but with a peak in the RNC, following the trend for mean outcrop length.

4.2.3 Foliation

Although the recorded angles of dip of the surface outcrops vary considerably within most zones, a general trend of less-tightly-packed folding is observed as the nappes are descended eastwards. Throughout nearly all the HNC, outcrops can be found with dips clustered towards the vertical. Average recorded dips in each HNC zone range from 54–73°. In the RNC, the average ranges from 37–58°. In the Køli Nappes, some near-vertical Leipikvattnet Nappe (KL) outcrops cause a slight trend reversal, so that the whole Køli averages range from 32–69°. The reducing trend is resumed in the Seve Nappes and in the Lower Allochthon, where the recorded dip averages vary from 28–33°. Figure 4.1 illustrates the maximum, mean and minimum angles of dip for each zone and Table 4.1 gives the corresponding values for each nappe complex. In all zones, large proportions (19–75%) of the mapped outcrops have dips that are recorded on geological maps, or were noted by personal observation. Most of these samples are probably representative of the whole set of outcrops. However, in Z8, ZC and KS, there are longitudinal or latitudinal gaps in the records so that their samples may not be fully representative.

Within each surface outcrop the angle of dip may vary, but the metacarbonate outcrops are commonly relatively homoclinal at the scale of the explored caves, presenting essentially planar foliations. Thus, each recorded angle of dip is commonly typical of the whole outcrop. Exceptions include the complex folding at Kvitfjell (Z4; Photo C2.4), at **Nedre Helveteshullet** (Z7, which has formed at the top of an anticline), and at **Labyrintgrottan** (ZC, where the metalimestone is folded parallel to the strike, with a wavelength of only tens of metres). Outcrop dips tend to reduce near to nappe boundaries, where outcrop strikes are commonly aligned parallel to thrust zones.

The HNC Zones Z1–Z8 are characterised by many long, linear, strike-aligned, carbonate outcrops that roughly follow north to south directions. Hence, east and west dip directions predominate over north and south in the HNC. In Z1–Z3, which are adjacent to the coast, easterly dips predominate over westerly. Farther east, and especially close to the HNC basement thrust at Z8, Caledonide over-thrusting caused the outcrops to dip overwhelmingly to the west. HNC Z9, which comprises a lower nappe thrusting over that part of the RNC that lies to the north of the study area, differs completely: 76% of its measured outcrops dip to the south, and none to the east or west. Within that part of the RNC that lies within the study area, ZA passes underneath Z8 along a north–south thrust zone (Photo 4.1), and has all its recorded outcrops dipping to the west, mirroring the situation in Z8. Farther east, dip directions in ZB and ZC have no dominant trend: north, south, east and west directions, and vertical and horizontal foliation, all occur. Three sub-horizontal outcrops in ZC are the only such known in the whole study area. Below the

Uppermost Allochthon, carbonate outcrops predominantly dip to the north, with some significant proportions to the south and to the west. Very few dip to the east. In the Hattfjelldal Nappe (KU) and in the Gjersvik Nappe (KG), both of which pass beneath Z8 along the north–south thrust zone south of ZA, the north-dipping trend is commonly replaced by a westerly one.

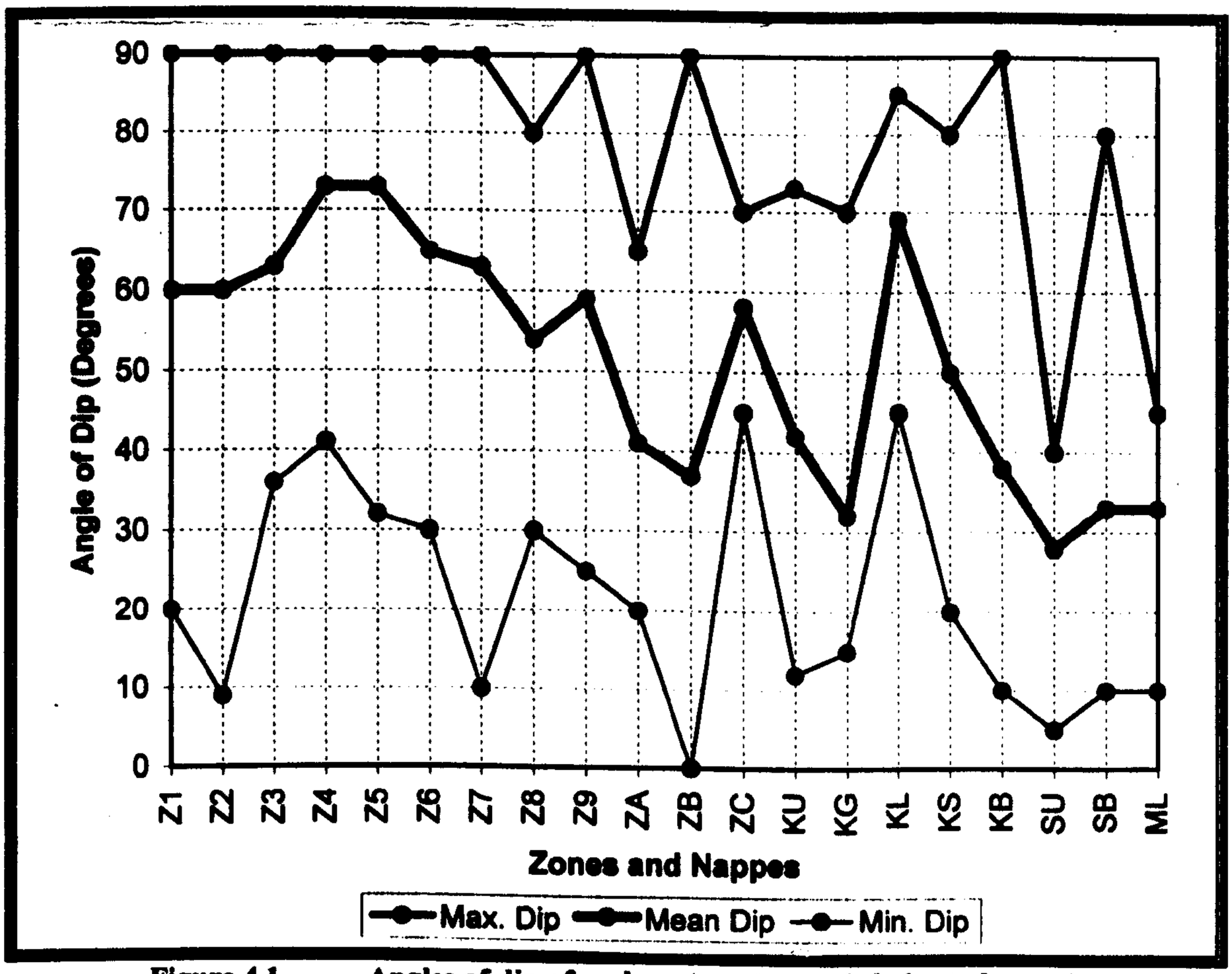

Figure 4.1 Angles of dip of carbonate outcrops (whole study area)

As a very general rule, wide outcrops have less-steep foliation. The width of the widest outcrop with vertical foliation is c. 800m (Almdalselv, Z7). Table 4.1 shows that the mean outcrop widths have the same declining trend as mean lengths and mean areas (section 4.2.1). The carbonate outcrops generally retain their "stripe karst" character, with lengths much greater than widths, throughout the whole tectono-stratigraphic structure. However, the ratio of mean outcrop length to mean width does decline eastwards, showing that as outcrop sizes and dip angles decrease, the outcrops themselves become less linear.

The structural differences between the HNC and RNC were discussed by Stephens *et al.* (1985, p153), who argued that there were two major deformation phases in the Uppermost Allochthon. The first affected the basement gneisses, with amphibolite facies metamorphism and deformation aligned north–south in the HNC, but with east–west "cross-folding" in parts of the RNC. After deposition of the sedimentary carbonates, iron ores and shales onto the folded metabasement, the whole assembly was deformed again by a second phase of amphibolite metamorphism with folding aligned north–south that left the cover rocks in tightly pinched synclines and over-printed the first phase. Whereas the contact between the HNC and the RNC pre-dates the last phase, there is also evidence of multiple movements along the contact zone (Table D1.1: item 48; section 6.3.3; Photo 4.1).

Photo 4.1 The HNC / RNC thrust zone
Metacarbonate exposures with tectonic openings at a road cut beside the E6 road, south of Korgen.

Photo 4.2 The HNC / Køli thrust zone
The Grubblandselv flows over a cliff at the base of the HNC onto dark Køli metalimestone. The stepped appearance of the overthrust is seen to the north.

The processes of metamorphism and thrusting caused a random vertical distribution of carbonate outcrops (section 4.2.2). However, the areal distributions are clearly not random, as they were driven by plate tectonic forces that caused overthrusting of the nappe pile from west to east. This is especially well seen in the study area at the thrust zone aligned north–south where the HNC overrides the RNC in the north (Photo 4.1) and overrides the Køli Nappes farther south (Photo 4.2). The consequence is the squeezing of the carbonate sequences, generally into north–south aligned linear outcrops. Whereas it is to be expected that the higher the maximum altitude of an outcrop then the more likely it is to persist for a longer distance, this effect is commonly only observed in that part of the study area that is east of Z4. The reason for this may be that it is from about Z5 eastwards that the maximum and average dips of the carbonate outcrops start to reduce (Figure 4.1). Hence, in Z1–Z4, folding and thrusting were more intense, producing near vertical imbricate structures where minor thrusts are more likely to sever the outcrop into discontinuous segments. In addition, and perhaps more importantly, large igneous intrusions are prevalent internally within Z1–Z4, Z8 and in the Hattfjelldal Nappe (KU), but are commonly non-existent in the other parts of the study area. These also disrupted the previously-existing linear carbonate outcrops during their formation. It has also been proposed that during continental collision, the deeper part of a subducting slab can break off and drift down into the mantle (Davies and von Blanckenburg, 1998). This loss of weight causes rapid uplift immediately above, which can break up the continental plate and allow buoyant slivers and "pips" to rise to the surface.

4.2.4 Contact metamorphism

A proportion of the carbonate outcrops experienced high temperature, low pressure, contact metamorphism from intrusive gabbros or granites, particularly in the HNC. This typically removed organic material, so that the carbonate rock was refoliated with less prominent bands (Gustavson, 1988, p12), or so that it became a predominantly massive white colour, perhaps with intruded darker dykes and sills (Appendices A2.2 and A2.3). The occurrence of outcrops altered by contact metamorphism sharply declines as the nappes are descended (Table 4.1). None occur below the stratigraphical level of the Køli nappes. The only one in Sweden is at Övre Ältsvattnet (KU, Appendix B1.13). The field experience is that only caves lying within a 250m-wide *effective* aureole around a pluton exhibit limestone altered by contact metamorphism. Sections 5.3.2 and 5.7.4 discuss the influence that contact metamorphism has on cave development.

4.2.5 Proximity of carbonate outcrops to major thrust zones

The Carbonate Rock Outcrops Database records whether each outcrop occurs adjoining, or near to, one of the mapped thrusts. These are commonly the major thrusts between the various nappes, but include more minor, internal, thrusts. In the whole study area, 132 carbonate outcrops are recorded as occurring near a thrust (13%). The percentage of outcrops lying near thrusts commonly *increases* as the nappes are descended (Table 4.1). The preference for marble to flow more readily than quartzitic rocks was discussed by Brodie and Rutter (2000), who concluded that calcite rock flow is predominantly grain-size-sensitive, whereas the natural flow of quartzite is an intercrystalline plastic process. Olesen (1988) also noted that amphibolites are more ductile than quartzites, so that a fault through quartzites may disappear where it traverses amphibolite rocks. Section 5.3.3 discusses karst caves that occur near major thrusts.

4.2.6 Outcrop situations relative to major ridges

Large differences in cave distributions and dimensions were noted on each side of major ridges aligned north–south (section 5.3.5). Hence, it became important to know if these differences are influenced by the relative situations of the carbonate outcrops. A new field was therefore included in the Outcrops Database to assign all outcrops as being either east or west of a local major ridge. Where this distinction was difficult to draw, for example with east–west aligned outcrops and in low-lying or plateau areas, altitudes and / or moraine alignments were also considered, to achieve consistency with the definitions of *glacial situation*, as applied to caves (section 5.3.5). Table 4.1 shows that some 57% of study area outcrops lie to the east of a major ridge (and 43% lie to the west). If only those zones that contain caves are considered (i.e. ignoring KG, KS, SU, SB and ML: section 5.2), the east / west distribution of outcrops becomes 50% / 50%. As expected, there is a general trend for the easterly percentages to increase in the direction west to east, as the nappes are descended, because coastal outcrops all lie west of the mountains and many Swedish outcrops lie east of the Main Scandinavian Watershed (MSW). This increasing trend is commonly maintained within the HNC, RNC and Køli zones, except for Z8 and ZB, which lie west of the MSW, and for ZC, which straddles the MSW. See also section 5.3.5.

4.2.7 Mapped karst features

All instances of possible mapped karst features taken from published topographical maps of the entire area were recorded in the Outcrops Database against each coincident carbonate outcrop. These features are predominantly the sinks or risings of surface streams, but they may also include small lakes and tarns along carbonate outcrops without outlets, and individual caves. The Norwegian M711 series maps cover Norway and the Swedish border region at a scale of 1:50000. 'Disappearing streams', where a continuous blue line is replaced by a pecked blue line for some distance, indicate where surface flow is not visible on aerial photographs. They were mapped independently of knowledge of the geological outcrops. Whereas some of these features mark stream flows under boulder piles, the field experience is that the great majority do indicate allogenic inputs or subterranean outputs at carbonate outcrops, some of which are not shown on the geological maps. Caves have been found at many of these sites. The remaining sites almost invariably confirmed the karst feature indicated, even if entry to an underground passage could not be achieved. 'Disappearing streams' are recorded as two features in the database: a sink and a rising. For some places, black and white Norwegian "economic" maps at scales of 1:5000 and 1:10000 were also consulted. These provide larger-scale information, typically up to altitudes of 500m, and commonly show many other small streams as pecked black lines. Although some of these are coincident with carbonate outcrops, field experience is that, whereas they may correspond to small sinks and risings, they rarely reveal previously-unknown cave entrances: these flow paths have not yet created conduit systems that are large enough to enter. Consequently, features that are only shown on economic maps are not included in the Outcrops Database. However, the economic maps were very useful in providing topographical details for karst area surveys.

Unfortunately, some of the larger streams that are mapped as being continuous on the M711 series maps actually sink underground at carbonate outcrops, and may enter explorable cave systems. Thus, the M711 map information, whilst being the best topographical guide to endokarstic activity, also needs to be treated with caution. The Swedish 1:100000 Fjällkartan map series was used for those parts of the study area not covered by Norwegian maps. These are not as detailed as the 1:50000 maps, and probably under-represent the numbers of possible karst features in their areas, because few are shown.

Table 4.1 shows that the total number of mapped karst features decreases as the allochthons are descended, although the RNC has a disproportionately high number per outcrop. The mean for the whole area is 1.2 mapped karst features per 10km of outcrop, showing that karst and underground drainage are relatively common phenomena. This value seems roughly constant in the HNC and the Køli nappes, although, again, the RNC value is much higher. The carbonates in the Seve nappes and Lower Allochthon have no mapped karst features, perhaps because these all lie in Swedish areas mapped only at smaller scales.

4.2.8 Water bodies on limestone

In contrast to the mapped karst features, which are suggestive of speleogenetic processes, the topographical maps also show many streams that flow directly on the surface and along, or across, carbonate outcrops in most zones. Similarly, the maps also show permanent bodies of water that lie along carbonate outcrops. These phenomena may be regarded as non-karstic features, suggestive of a lack of speleogenesis. If any result from karst conduits of various sizes being permanently inundated, it would be expected that the phreatic water would rise to the surface lower down the outcrop. The only place where this is known to occur is at the 'vanishing lake' of Engjavatn, which has an outlet at the cave **Aunholet** (Z2). Anecdotal reports indicate that, on rare occasions, this lake drains completely, sometimes after prolonged dry weather. The number of occurrences of these water bodies on limestone per 10km of carbonate outcrop is remarkably constant across the study area, lying in the range 0.76±0.15 for all allochthons except the Lower Allochthon (Table 4.1).

Across the study area, about 40 metalimestone outcrops display at least one mapped karst feature and at least one body of water. Thus, a single outcrop can exhibit both speleogenetic processes, and a resistance to such processes. As most basins and lakes in Scandinavia were formed by glacial scouring, reinforced during every stadial, it seems that conduits that could drain such water bodies have not in all cases had the opportunity to develop since the end of the last glaciation.

4.2.9 Field appearance of metacarbonates

Calcitic metalimestones in Norway were said by Horn (1937) to form "stripe karst". The field appearance of the clean-washed rock is commonly also very striped, particularly in the HNC. A black, grey, blue, brown, yellow (and at several outcrops in KU, red) colour can alternate with cream or white to create attractive stripes, with bands at the millimetre to centimetre scale. The colourings are commonly caused by thin layers of mica and / or graphite, which were derived from adjacent clays and / or organic material during metamorphism. These *foliation* layers commonly lie parallel to the line of the outcrop. Such rocks, while often considered too 'impure' to quarry, are always highly calcitic, giving very vigorous reactions with dilute HCl (Table A2.2). In general, lower-grade calcites are darker in colour, because they retain more organic material (Gustavson, 1988, p12). In contrast to limestones, massive outcrops of dolostones commonly display no striped appearance at all, with little visible layering (Photo 4.3). They are usually pure white or weathered cream or faint pink in appearance when observed in quarries and road cuts. Tremolite is a common associated mineral. Dolostones commonly show no visual reaction when tested with dilute HCl, but a faintly-audible fizz may be heard when the rock is placed near to the ear, probably from the reaction of calcite grains within the matrix. Outcrops with a yellow / brown appearance may contain HMC or DL, with additional Fe^{2+} from siderite, rather than consisting of dolomite (Appendix A2.4). They commonly react very vigorously with dilute HCl (Table A2.2).

Photo 4.3 White dolostone
The Grubblandselv flowing over metadolostone upstream of **Stor Grubblandsgrotta** (KU). Caves are rarely formed in this lithology.

The field appearance of exposed carbonate rock also depends on the extent of weathering. It can vary from the rather white, rounded, form, which is similar to that of many weathered sedimentary limestones at the surface, to the striped, sculpted, form seen in stream beds, at waterfalls, and inside cave stream passages. Carbonate bedrock is commonly stained, or covered by clay washings, in dry parts of cave passages. It is also not uncommon to observe such bedrock with a hard, black, veneer on its outer surfaces. This may resemble an amphibolite, but such a rock can reveal a white calcitic interior when freshly-broken. Section 4.4 discusses the *exokarstic* properties of carbonate rocks.

4.2.10 Outcrop conclusions

The carbonate outcrops, whose key attributes are summarised in Table 4.1, provide a geological template against which the karst caves of the study area developed and can be considered further. Chapter 5 attempts to reveal if and how the various attributes of the caves vary with the attributes of their confining carbonate outcrops. A key question is whether, and to what extent, the various cave characteristics follow the general eastward trends that can be assigned to the local geology. From this information it may be possible to make deductions about any common or varying cave inception and development processes, and determine possible timescales for cave formation and destruction across the whole area.

4.3 Non-carbonate rocks

In contrast to many global karst areas, the karst caves of central Scandinavia occur within larger landforms not formed by karst processes, because the carbonate outcrops account for <3% of the study area (section 4.2.1) and where they do occur they are commonly relatively narrow. The caves occur in both stripe karst and non-stripe karst settings, commonly at the contacts between the metalimestones and the non-carbonate rocks. Hence, it is necessary to appreciate what the other country rocks are, because it is from these rocks that allogenic streams run into the caves and because the non-carbonate rocks are also encountered within the caves themselves (section 5.7.4).

4.3.1 Skarns

The metasomatic reactions leading to the production of various calc-silicate skarns are discussed in Appendix A2.2. The NGU and SGU maps refer to calc-silicate rocks, without identifying individual minerals. As skarns are produced from carbonates, they can occur alongside the limestones, or as total replacements, and hence they also display a striped appearance, both regionally and when observed in hand-specimen. From the geological maps, skarn rocks appear proximal to carbonates in all the zones of the Uppermost Allochthon except for Z5, Z8 and Z9. There are no mapped skarns in the Køli Nappes, as expected from the discussion in Appendix A2.10 about the lower metamorphic grade of the Køli preserving a higher proportion of dolomite. As mentioned in section 4.2.1, the SGU maps do not distinguish between marbles and skarns in the Seve Nappes. Here, the relatively high metamorphic grade probably facilitated dedolomitization with calc-silicate rocks produced as by-products. Calc-silicate impurities are also noted as occurring in some dolomites of the Lower Allochthon.

4.3.2 Mica schist

Mica schists of various types form the bulk of the country rocks of the whole study area. They occur extensively in every zone. In the Uppermost Allochthon and in the Seve Nappes, mica schist, calcitic mica schist, mica gneiss, calc phyllites and quartzites accompany carbonate outcrops. Garnet mica schist, biotite and muscovite mica schist and mica gneiss were all identified from internal cave bedrock samples after the 1997 and 1998 field study trips. In the lower grade Køli Nappes, greenstones and greenschists, grey, quartz and graphitic phyllites, tuffite and greywackes predominate as contact rocks to carbonates. Several schists were identified from internal cave bedrock samples in the Køli Nappes, but they are much rarer than in the HNC and RNC. The impression gained from a more limited field experience in the caves of the Køli Nappes is that internal aquicludes are also much less common. In the Lower Allochthon, the carbonate contact rocks are commonly shales, arkoses and quartzites.

4.3.3 Granitic intrusions and plutons

Plutonic intrusions, commonly with accompanying dyke swarms, occur in all the zones of the Uppermost Allochthon and at Övre Ältsvattnet (KU), but not at all as carbonate contact rocks in the lower nappes, although some carbonate outcrops in KU also adjoin HNC granites. The largest granitic pluton is in Z3.

Its surface extent measures some 125x20km. Many other large outcrops exist, especially in Z2, Z6 and Z8. The metamorphic effect of these intrusions on the carbonates has not been studied in detail, but the high-T, low-P, contact metamorphism conditions are expected to facilitate dedolomitization with the production of calc-silicates as discussed in Appendix A2.10. Certainly, the extensive, non-linear, metalimestones near Storvatn (Z2) appear different from the normal striped variety, as they are very white and not banded (Faulkner and Newton, 1995, p4; section 4.2.4) and dykes and sills are observed in local cave passages (section 5.7.4). The lithology of the various plutons varies from granite to diorite and trondhjemite. One internal cave sample was provisionally identified as tonalite.

4.3.4 Amphibolites and gabbros

Dark-coloured mafic rocks of amphibolite and gabbro are found proximal to carbonates in all zones of the Uppermost Allochthon. They are also mapped in KB, SU and SB, but not in the other Køli Nappes nor in ML. In SU, the carbonate or calc-silicate outcrops nearly all occur within enclosing outcrops of amphibolite. Two types of amphibolite are possible: ortho and para. In the former, a previously-igneous rock (commonly an intrusive dyke or sill) is metamorphosed. In para-amphibolites, an originally-argillaceous sedimentary rock is metamorphosed. The geological maps rarely distinguish between the two, and in the very steeply-dipping bands of metacarbonates in the HNC it is difficult to make the distinction in the field. Several samples of amphibolite were identified from internal cave bedrock in the HNC. The amphibolites there are not necessarily as extensive as enclosing carbonates: a massive vertical lens of unknown height of presumably ortho-amphibolite occurs in **Anastomosegrotta** (Z4). It is some 30m long, has rounded 2–2.5m-wide ends, and narrows to a width of 0.5m along much of its length.

4.4 Karst geomorphology (exokarst)

In comparison with the literature reviewed in sections 3.1.8 and 3.1.10, the Scandinavian reports of surface karst are comparatively sparse. Engh (1977) studied the 14 known *holokarst* areas of Sweden. They are mainly above the present treeline, but within 200m of it. Hence, they are all situated below the ancient treeline of the warm Boreal period. They can exhibit >900km^{-2} "joint dolines" (enlarged kluftkarren) if there is little soil cover, and contain three caves longer than 1.5km. Dye tests showed that there is not normally a homogeneous karst water surface, as only two areas had more springs than swallow holes. In contrast, the *merokarst* areas contain impure limestones, with an almost vertical dip and with few karren features. Their swallow holes connect to only one spring, and the caves are small, narrow, active and only up to 150m in length.

The most thorough qualitative and morphometric study of exokarst was that by Helldén (1973; 1975; and especially 1974) above the **Sotsbäcksgrottan** system (KU), until a statistical treatment of the Glomfjell karst area in northern Norway by Finnesand (2003). Onac (1991) discussed exokarst at two areas near Narvik in northern Norway, and noted the limited depth of endokarst. He explained the existence of lakes lying on karstifiable bedrock as resulting from the karst immaturity (see also section 4.2.8). Lauritzen

(1991b) provided the only brief, qualitative, overview of the occurrence of exokarst features in Norway. Several authors have described the dolines with >10m diameters in till above the metacarbonate aquifer along the Bjurälv karst area (KL, sections 1.6.3, 1.7.2 and Appendix B1.15). The works by Corbel preceded these reports and included many sketches of karst areas both in plan and in section. For example, Corbel (1952a, 209–210, 217; 1952b, p266; 1953, p341) included diagrams to show the relationships between dolines and epikarst drainage routes, although this term was not then in use.

Moe and Johannessen (1980) described cavities in calcareous rocks in the littoral zone of northern Norway, with widths up to 3cm, which they assumed were formed by the feeding of *Littorina* snails on algae. Holbye (1989) introduced the term *bowl karren*, which he distinguished from *kamenitzas*, to describe littoral karst in northern Norway. The "bowls" vary in size groups from a few centimetres to 4m in diameter (c.f. Appendix B1.1). Holbye thought that they were probably formed by the turbulence of aggressive sea water, and then developed further during uplift.

In the experience of this author, the central Scandinavian karst geomorphology exhibits the various karst processes and landforms described by Ford and Williams (1989) in many situations. However, these occur only at small and medium scales, being commonly constrained by narrow linear carbonate outcrops. Underground drainage routes longer than a few kilometres are unknown. Below the treeline the subcutaneous zone of highly-weathered limestone lies beneath a soil and till cover that may be several metres thick, whereas above the treeline it commonly forms the outcrop surface. The following sections summarise some of the more obvious landform features seen in the karst areas.

4.4.1 Ridge and gully structures

The topography of the study area remains strongly guided by rock type and tectonic structure (section 2.2.2). Much of the country rock is foliated mica schist. Hence, the carbonate outcrops commonly meet, and / or are intermingled with, linear N–S strike-aligned schist outcrops, along which run major and minor valleys. Below the tree line it can be difficult to determine the local lithology, because exposures are hidden by vegetation and soils. There is no simple topographical rule for placing the limestones, because long ridges and gullies commonly follow both the limestones and the schists along the strike. A gully may coincide with a limestone outcrop that is wedged between walls of non-carbonate rock on each side. Equally common is a (perhaps anticlinal) limestone ridge that overlooks schists on each side. In this case, dry cave entrances, shafts and dolines may be found along the limestone ridge tops. The *edges* of gullies and valleys in limestone commonly provide a locus for dolines and allogenic stream sinks. Kirkland (1958) noted the presence of similar conformable furrows along-strike at south Svartisen, some 30km north of the study area. Horn (1947) reported that crystalline limestone can provide a greater resistance to glacial erosion than adjacent schists, suggesting that the furrows arise from glacial scouring.

Strong guiding features are the foliation dips of both the carbonates and the adjoining non-karstic rocks. The dip in the HNC is commonly nearly vertical (section 4.2.3), so that there are commonly no 'cover' rocks above the carbonates. Consequently, for example, the concept of the erosion of a cover rock, which causes previous sinks to be abandoned as new ones form at the latest contact, is not well displayed in the west of the study area. Farther east, the local dips tend to flatten out (section 4.2.3), and some of the karst geomorphology becomes more 'classical' in appearance. Indeed, longer drainage systems occur in ZC, KU and KL, all in the eastern part of the area. Hence, the whole region may be regarded as a natural laboratory for studying the effect of outcrop dip on surface (and underground) karst geomorphology, within stripe karst and other karstic environments.

4.4.2 Cave entrance positions

Sink entrances occur in three main topographical positions. Where a significant allogenic stream sinks into the limestone, this may occur along the bed or lower wall of an active valley with steep sides that continues forward as a dry valley with little change of thalweg. The extent of vegetation on the following dry boulder floor gives an indication of the maturity of the sink and its potential for overflowing at high stage. Commonly, the preceding valley is along the strike of a narrow limestone outcrop between walls of non-carbonates, showing that water does not always flow underground at the first contact with limestone. Another typical sink location is at the end of a blind valley, below a steep cliff and rarely >10m high. In this case, it is common to find a shallower vegetated dry valley continuing along the strike. In following this upper dry valley towards a probable rising it may become even shallower as it merges into a complex pattern of ridges and hollows that mask the lithological contacts, so that in the wider limestone outcrops no single dry valley may lead directly to the resurgence. Blind valley ends (and dolines) can also occur very close to the top edges of steep cliffs above deeper orthogonal valleys, i.e. just before an abrupt change of slope at a valley shoulder that is called a "sva" in parts of Norway. Karst sinks are also found in gently sloping parts of the landscape and on the paleic surface.

Resurgence entrances also occur at three main topographical positions: (1) at the heads of 'conventional' pocket valleys, as in sedimentary limestones; (2) at any part of the profile of the continuing along-strike dry valley, i.e. from an enterable conduit at the base of the valley, up to a hanging opening above the valley floor from which the stream descends as a waterfall; (3) at the head of a waterfall, or series of cascades, in the steep cliffs, or sides, of a deep valley that is orthogonal or angled to the strike, where the sinking stream commonly enters the cave above near the valley shoulder.

In the case of a continuing, higher-level, dry valley, the stream may resurge again on one side of the base of a collapse doline, and sink again on the other, in a manner described by Palmer (1990, p198). The landform of an intermittently-sinking and -rising stream that follows a narrow limestone outcrop down a hillside is extremely common, and may be repeated several times as altitude is lost. The Norwegian topographical maps (at both the old scale of 1:100000 and the modern scale of 1:50000) commonly show

such underground streams as a pecked black or blue line. The length of this pecked line is an unreliable indicator of the potential length of a single karst system because of the intermittent nature of much of the karst drainage. The final resurgence may be at an area of much lower relief, where the stream joins a larger one or flows into a lake, but there are also many examples of such resurgences from one of the three main positions described above. The overall effect of the karst drainage is commonly to provide a bypass route for a mountain stream, and this can occur even on steep hillsides, where dry waterfalls up to 10m high can be left in the bed of the abandoned valley.

In addition to all the above allogenic recharge and discharge positions, some water-worn *relict* entrances lie along the summits or walls of strike-aligned ridges of limestone, in 'impossible' positions. In this case, for the entrance to have previously functioned actively, it is necessary to postulate that the limestone was more resistant to subsequent erosion (perhaps glacial) than the adjoining lithologies, or that the entrance was active at a time of raised water levels such as could occur beneath a valley glacier, icecap, icesheet or at the margins of an ice-dammed lake.

One of only two known Swedish poljes lies at the north end of Mieseken (ZC, R. Sjöberg, University of Stockholm, pers. comm., 1998). A (perhaps unique to Scandinavia) 'vanishing lake' occurs at Engjavatn (Z2, section 4.2.8). No estavelles are reported in the study area, but, at times of spring melt, strong resurgences and immediate sinks can form at fast-flowing pools in small and normally-dry dolines, informally termed *'risinks'* by the author. Examples occur at Litl Hjortskar (Z5), where, also at spring melt, a small rising was observed as a fountain that gushed up to a height of 30cm from the ground, which here is a metre above an adjacent hollow (Photo 7.2).

Cave passages commonly follow the direction of surface slope downstream and there are no known examples of caves in the study area that run deep into a valley side to emerge into another major valley that is separate from the first. Similarly there are no known underground drainage routes that link two major valleys in this way. There are, however, examples of caves and streams that start on one side of a relatively small-scale limestone ridge, to emerge on the other side of the same ridge. Thus, the thickness of rock above each cave is generally modest, measuring only up to several tens of metres, as seen from cave survey sections (Appendix B1) and as discussed in sections 5.3.7, 6.1.4 and 6.5.2.

4.4.3 Dolines

Above the assumed line of the underground drainage it is common to find both solution and collapse dolines. These rarely exceed 15m in diameter or 10m in depth, and most are therefore *not* polygenetic (section 3.2.2). They may be blocked at the base, or may provide entrances to the karst drainage. In seeking entrances to caves that are not enterable at either a sink or resurgence, it is not uncommon to find that an entrance occurs along the strike within a few metres of the sink or resurgence. This entrance may be at a doline leading to a large passage above or along the stream, or may be via a small, and usually

short, shaft. Thus, small dolines may be used to indicate the strike of the limestone, because they commonly occur in linear arrangements above the karst outcrop, perhaps being concentrated mainly near the sink and resurgence extremities of an underground system to which they act as 'windows'. Towards the end of the spring melt, the last remaining snow still fills the dolines and dry valleys. Invariably, this drains away underground during June and July, except at high altitudes.

4.4.4 Pavements and karren

Below the tree line, the carbonate outcrops are rarely exposed away from road cuts, cliffs or mountain streams, and so limestone pavements are not seen. Kirkland (1958) noted the presence of clints at Svartisen, but pavements were usually absent beneath vegetation. Above the tree line and birch scrub, the limestones form easily-visible outcrops that show glacial scouring and smoothing, where clints and grykes can also be found. Some of the latter are large enough to enter, and may form shafts into underlying cave passages. Although not studied in any detail, various types of karren are known, for example on Elgfjell (Z4) and on Kongsfell (ZB). It is generally accepted that these landform types were formed subglacially and during postglacial erosion (Lowe and Waltham, 1995, p23).

4.4.5 Dolostone karst

Mapped dolostone outcrops commonly include calcitic metalimestones (section 4.2.1), and hence in studying the surface landforms above such outcrops it is difficult to know from superficial observations if any karst features are truly representative of say, calcian dolomite (CD), or are examples of LMC, HMC or DL calcitic exokarst, or if they occur at contacts between calcitic and dolomitic carbonates. The question is further compounded by the appearance of dry ridges and gullies on mica schist outcrops (section 4.4.1). Several mapped dolostone outcrops were visited during the 1998 field study, and small karst landforms *were* commonly found on the mapped dolostones. These included small sinks and risings, grykes, dolines, and small fissures in outcrops. In some cases, when the adjacent bedrock was tested with dilute HCl, a vigorous reaction resulted indicating the presence of calcite. Otherwise, the reaction was only audible and not visible, indicating a more dolomitic lithology.

Despite considerable searching by the author, only one small cave has been found in presumed metadolostone bedrock (**Tjuvhelleren**, ZB, in a dolostone cliff). It is 4m long, 2m wide and 3m high and has been utilised as a shelter. An eyehole just above the entrance confirms a karst origin. The bedrock gave only an audible reaction with dilute HCl and appears to contain tremolite. However, even this lithology contains too little $MgCO_3$ to be a complete dolomite (Appendix A2.4). Hence, there appear to be no known karst caves in a true metadolomite in the study area, although **Dolstadgrotta** (Z5, near Mosjøen) appears to be in a mapped dolostone outcrop. This cave has reportedly been blocked for safety reasons. As dolostones account for some 6% of the carbonate outcrops, and 6% of the carbonate area, some 60 caves might be expected to have formed in this variety of metacarbonate, if similar processes have applied. It is thus concluded that *karst caves are not formed in true metadolostones (if they*

themselves exist). The observed lack of karst caves in the mapped dolostones of the study area, and in Scandinavia generally (Appendix A2.7), fits well with the low dissolution rates of all dolostones, and in particular with the very low dissolution rates of metamorphic dolostones at low temperatures, as discussed in Appendix A2.8.

4.4.6 Karst on high magnesian calcite and dolomitic limestone

The conclusion in section 4.4.5 certainly does not preclude the ability of caves to form in HMC or DL *metalimestones*. Such highly calcitic bedrocks, inferred from a weathered colour of yellow or brown, have only been recorded in the Uppermost Allochthon in the study area, and the cave databases record nearly 30 caves that may have formed in them. Appendix A2.7 discusses caves formed at the junction of various limestone lithologies in northern Norway. Probably the best example of a junction between the grey-banded metalimestone and the yellow / brown striped variety in the RNC in the study area is at Mieseken (ZC, in Sweden). Here, the long cave **Labyrintgrottan** (Appendix B1.12) appears to have formed entirely within the folded grey limestone. However, several adjacent very short caves are also found in a brown limestone.

The only places in the HNC where the yellow type is known to occur are at Kvitfjell and at Elgfjell (Photos 4.4 and 4.5). These are both in Z4, and may have originally formed one long carbonate structure before it was split by complex folding on the southern slope of Kvitfjell (Photo C2.4). This folding is itself unusual for the HNC, which has mainly homoclinal outcrops. The yellow limestone abuts the grey limestone at both Kvitfjell and Elgfjell (Appendix B1.4), and cave entrances are found along the junction at both places. On Elgfjell at least, caves are found in both types (Faulkner and Newton, 1990).

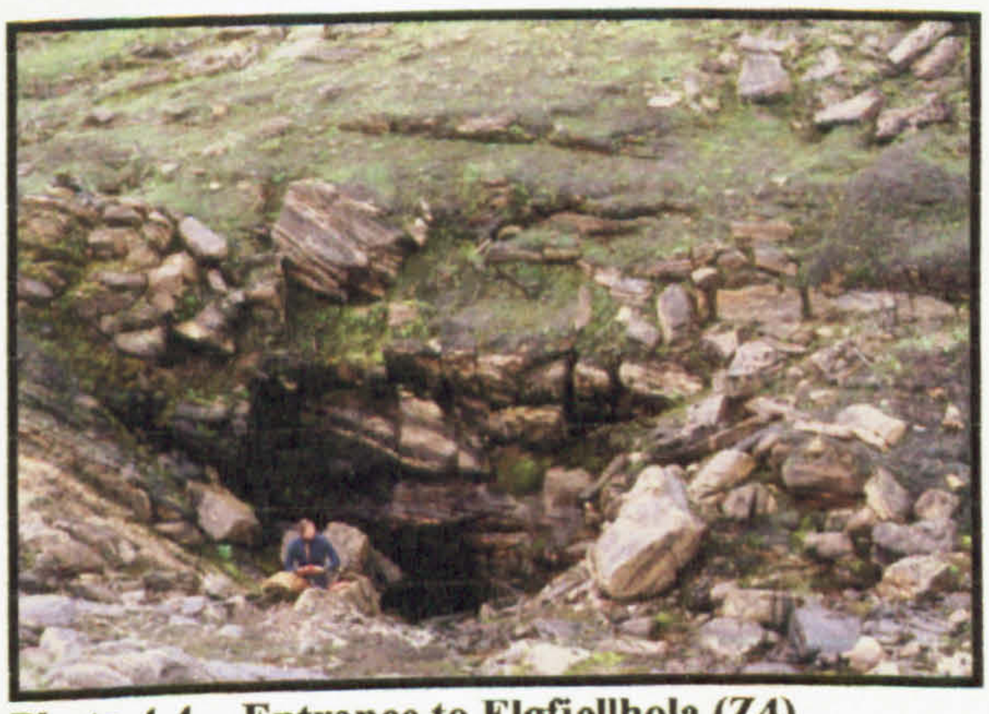

Photo 4.4 Entrance to Elgfjellhola (Z4)
At junction of yellow / brown striped marble (probably HMC) and grey marble. Figure for scale.

Photo 4.5 Near Sarvenvårtoehullet, Elgfjell
Angled stripe karst at junction of yellow / brown striped and grey marbles.

The rarity of both the HMC / DL yellow striped metacarbonates and complexly folded karst (CFK: section 5.3.1) that displays recumbent folds in the horizontal plane (e.g. Photos C2.2 and C2.4) and their coincidence at Kvitfjell and Elgfjell suggests a possible common origin. Thus, the repeated cycle of prograde and retrograde metamorphism that apparently caused dedolomitization (Appendix A2.10) may have terminated in these locations with pressure–temperature–fluid conditions that facilitated complex

ductile folding contemporaneously with crystallisations into pairs of commonly-adjoining HMC and LMC metacalcites. The absence in the databases of HMC / DL and CFK in carbonates subjected to contact metamorphism suggests that high temperature – low pressure conditions did not favour the production of HMC /DL and / or replaced these minerals with LMC or dolostone, of which 157 and 5 such outcrops are recorded with R=1.

This Chapter has discussed the central Scandinavian karsts in general terms. Prior to this thesis, there have been no studies of topographical situations that might be potentially favourable for cave formation and development within a wider view of the landscape than just the immediate karst area. Chapter 5 considers the caves and their external and internal attributes within these karst and topographical environments. The presumed effects of glacial environments and processes on cave development in Scandinavia were discussed in Chapter 3, and are reconsidered in the third part of this thesis.

CHAPTER 5 THE CAVES OF CENTRAL SCANDINAVIA

There is insufficient space in this thesis to give a full account of the geological structures and geomorphology of each zone and all its reported karst caves. Instead, the longer caves in each zone are presented in Appendix B1, together with a brief discussion about their character and situation, to illustrate the varying morphologies of the caves in the study area. This Chapter describes the databases constructed to record standard attributes for *all* the caves, and draws together qualitative and quantitative conclusions about the caves in relationship to the carbonate outcrops and local topography.

5.1 Cave databases

Data about the caves in the Norwegian and Swedish parts of the study area are held in separate computer-based databases that are constructed using Microsoft Excel with Windows XP and that follow a similar organisation to that of the Carbonate Rock Outcrops Database (section 4.1.2). Each recorded cave occupies one row in the database tables, and information about it is held in 44 fields organised into columns. Caves are grouped by carbonate outcrop, in the order in which outcrops are held in the Outcrops Database. The fields are divided into two main headings: External Cave Attributes and Internal Cave Attributes, which are defined in Appendix C2 together with notes about derivation and accuracy.

5.1.1 North Central Norway Cave Database

Information about the caves in north central Norway was collected from all the published references, and from data assembled during an expedition in 1996 and the field study trips of 1997, 1998 and 2000. The database (Appendix C3) holds details of 728 adequately-reported caves, and thus has a capacity of about 32000 pieces of information, plus map and zone summaries. Only the cave name is recorded (if known) if a cave is poorly described (e.g. location or length is missing) and the record is not included in any subsequent analysis, including the total number of caves for each area. The approximate number of these poorly-reported caves is an additional 80. Many of these are short, but some are unexplored.

5.1.2 Central Swedish Caledonides Cave Database

Information about the caves in the Swedish part of the study area was collected from all the published references, from a database that is maintained by the SSF, and from data assembled during the field study trips of 1997, 1998 and 2000. The database (Appendix C4) holds details of 156 adequately-reported caves, and thus has a capacity of over 6000 pieces of information, plus map and zone summaries. The number of poorly-reported caves not included in totals is c. 30.

5.2 Cave dimensions

This section shows how the cave dimensions recorded in the cave databases vary across the zones and nappes and with the dimensions of the carbonate outcrops. Tables and commentary present data assembled from a combined Excel database constructed from the two cave databases (Appendix C5), and

from further pivot table analysis. The observations deduced in succeeding sections should be regarded as descriptive, because discussion is commonly based on changes in mean values, although coefficients of variation of cave dimensions lie in the range 100–400%. For example, the mean length of all caves is 85m, whereas the median length is only 23m. A rigorous statistical treatment is beyond the scope of this thesis, but a preliminary analysis showed that the distributions of L, VR, XS and volume for the full set of caves have large positive skews in the range 3.6–12.4 (or Pearson's gamma of 0.7–1.1) and high peaks in the kurtosis range 18–218, whereas these functions would all equal zero for a normal distribution. Only minimum HG approximates to a normal distribution: coefficient of variation 92%; skew 1.65; Pearson's gamma 0.93 and kurtosis 2.05. The distributions of the logarithms of all these dimensions approximate much more closely to a normal curve: coefficient of variation 30–96%; skew -0.03–+0.56; Pearson's gamma -0.13–+0.63 and kurtosis -0.31–+0.09, so that tests of significance could be undertaken usefully on logarithmic data.

5.2.1 The distribution and dimensions of karst caves

The approximate percentage occurrences of the caves and of their total lengths in the five main catchment areas (section 1.4) are: Western: 23% and 19%; Northern: 10% and 13%; Vefsn: 45% and 43%; Namsen: 3% and 2%; and Eastern: 19% and 23%. The Namsen catchment area comprises 20 caves at Dunnfjell in Z6 plus 8 caves in Z8. The Eastern area contains all the Swedish caves, plus 8 Norwegian caves that lie in KL. The similarities in the percentages show that mean cave length is roughly constant in each main catchment area, suggesting that geological, glacial and geomorphological differences among the catchment areas did not exert major influences on the development of those caves that presently exist.

Section 4.2.1 and Table 4.1 discussed the variations in the metacarbonate outcrops across the nappe complexes. This section continues this analysis into the variations of the main cave dimensions, with relevant data presented in Table 5.1. The reducing trend eastwards between the Uppermost Allochthon and the Køli nappes for the carbonate outcrop dimensions is also apparent for the total number of caves, their total lengths and their total volumes. However, because the mean lengths, cross-sections and volumes of caves in the smaller RNC area (which contains three of the largest caves) are higher than those in the HNC, the total lengths and volumes per unit nappe area peak in the RNC.

Table 5.1 shows that most mean cave dimensions, when expressed in various ways for each nappe complex, vary within a factor of two of the whole area mean, and that within these variations, increasing, decreasing and null trends all occur as the nappe complexes are descended. Caves appear to be somewhat longer and to have larger mean volumes farther east, although this could be an artefact of exploration and recording bias. Smaller caves may be more neglected and / or more covered by glacial till in Sweden. It is difficult to decide this issue, because the number of caves, their mean lengths and mean volumes are higher in the Køli nappes than in the HNC for each visited carbonate outcrop, but remarkably similar when expressed as values *per kilometre* of visited outcrop.

Table 5.1 Variations of cave dimensions with tectono-stratigraphic structure

Nappe complex	HNC	RNC	KØLI	SEVE	ML	ALL	Units	E. TREND
Total area	9950	1762	9336	4443	6276	31767	**km^2**	No trend
No. carbonate outcrops	536	74	252	123	21	1006	**No.**	Decreasing
Total carbonate area	560	126	163	7	5	861	**km^2**	Decreasing
Total carbonate area	5.6	7.1	1.8	0.2	0.1	2.7	**%**	Decreasing
Mean outcrop area	1.05	1.70	0.65	0.05	0.24	0.86	**km^2**	Decreasing
Total outcrop length	1911	472	680	99	31	3193	**km**	Decreasing
Mean length per outcrop	3.6	6.4	2.7	0.8	1.5	3.2	**km**	Decreasing
No. visited outcrops	125	31	30	5	4	195	**No.**	Decreasing
Total visited length	252	101	94	0.4	0.3	447	**km**	Decreasing
No. of caves	626	102	156	0	0	884	**No.**	Decreasing
% of caves	70.8%	11.5%	17.6%			100%	**%**	Decreasing
No. caves/100 km^2 nappe area	6.29	5.79	1.67			2.78	**10^2No. km^{-2}**	Decreasing
Total cave length	47276	11173	16432			74881	**m**	Decreasing
% of total cave length	63.1%	14.9%	21.9%			100%	**%**	Decreasing
Tot.length/100km^2nappe area	475	634	176			236	**10^2m km^{-2}**	Decreasing
Total cave volume	251	67	101			419	**10^3m^3**	Decreasing
Total vol./100 km^2 nappe area	2524	3779	1085			1319	**$10^2m^3km^{-2}$**	Decreasing
Mean cave length	76	110	105			85	**m**	Increasing
Mean cave VR	8.5	11.6	8.4			8.8	**m**	RNC max.
Mean cave min. HG	28%	27%	26%			27%	**%**	Small decr.
Mean cave XS	3.4	4.3	3.6			3.5	**m^2**	RNC max.
Mean cave volume	401	653	649			474	**m^3**	Increasing
Mean cave CA	2.8	3.9	9.2			4.1	**km^2**	Increasing
Mean cave XS/CA	18.2	2.7	2.3			11.9	**m^2km^{-2}**	Decreasing
No. of caves per outcrop	1.17	1.38	0.62			0.88	**No.**	Decreasing
No. caves per visited outcrop	5.01	3.28	5.20			4.53	**No.**	RNC min.
No. caves per km^2 outcrop	1.12	0.81	0.96			1.03	**No.km^{-2}**	No trend
No. of caves per km outcrop	0.33	0.22	0.23			0.28	**No.km^{-1}**	Decreasing
No. caves / km visited outcrop	2.5	1.0	1.7			2.0	**No.km^{-1}**	Decreasing
Mean cave length per outcrop	88	151	65			74	**m**	RNC max.
Mean length / visited outcrop	378	359	548			384	**m**	Increasing
Mean length / km^2 outcrop	84	89	101			87	**m km^{-2}**	Increasing
Mean cave length/km outcrop	25	24	24			23	**m km^{-1}**	No trend
Mean length/km visited outcr.	188	111	175			167	**m km^{-1}**	RNC min.
Mean cave volume / outcrop	470	900	402			417	**m^3**	RNC max.
Mean volume / visited outcrop	2009	2141	3376			2148	**m3**	Increasing
Mean volume / km^2 outcrop	448	530	621			487	**m^3km^{-2}**	Increasing
Mean volume per km outcrop	131	142	149			131	**m^3km^{-1}**	Small incr.
Mean vol. /km visited outcrop	998	659	1076			937	**m^3km^{-1}**	RNC min.
Outcrop contact metam.	48%	1.4%	1.6%	0%	0%	26%	**%**	Decreasing
Caves contact metamorphism	28%	2.0%	17%			23%	**%**	No trend
Cave length with contact met.	25%	0.5%	7%			17%	**%**	Low propn
Outcrops near thrusts	6%	7%	27%	11%	57%	13%	**%**	Increasing
Caves near thrusts	1.4%	2.9%	56%			11%	**%**	Increasing
Cave length near thrusts	2.0%	15%	84%			20%	**%**	High propn
Outcrops east of major ridge	46%	35%	70%	87%	100%	57%	**%**	Increasing
Caves east of a major ridge *	77%	57%	88%			77%	**%**	High propn
Cave length east of a ridge *	79%	48%	94%			78%	**%**	High propn

* Excludes all caves in the coastal location (section 5.3.4)

Whereas the mean vertical range also peaks in the RNC (which contains **Ytterlihullet**, ZA, Appendix B1.10, the deepest cave in the area), the means for the HNC and the Køli nappes are almost identical. An overall summary, therefore, is that, within the declining eastward trends in total carbonate outcrop and total cave dimensions, there is a greater consistency in the mean dimensions of the individual caves.

However, one external attribute, the mean cave catchment area, shows a strongly *increasing* trend to the east, but this has certainly not resulted in any *proportionate* increase in mean cave dimensions.

The final nine rows of Table 5.1 compare the percentages of carbonate outcrops, caves and total cave lengths for each of three external attributes. The percentage of caves in limestone altered by contact metamorphism (R=1) is less than expected from the proportion of such outcrops in the HNC, but more than expected in the Køli nappes. In all cases, contact metamorphism inhibits mean cave lengths. The opposite trend appears for caves near thrusts (T=1), where this always increases mean length. Caves occur disproportionately on the east side of major ridges compared with the proportion of carbonate outcrops (E=1), although *overall* mean cave lengths are very similar on each side of a ridge. These conclusions are analysed further in section 5.3.

In order to see if the main dimensional trends are visible *within* each nappe (especially in the HNC), the *zonal* variations of the mean cave dimensions are presented in Table 5.2. (No caves are known in zones KG, KS, SU, SB and ML). This also shows a degree of consistency between the *proportion* of caves lying in each zone and the *proportion* of total cave passage length that these caves represent, as shown by the rather small spread in mean cave length across the zones: for zones with more than 4% of the total population (35 caves, i.e. those not shaded in Table 5.2), the mean cave length varies, probably non-systematically, from 55–106m. The mean cave VR, the mean minimum HG, the mean cross-section, and the mean cave volume also seem to vary non-systematically across the HNC zones. The studied caves have minimum HGs that range from 0.8% for the 2600m-long **Labyrintgrottan** (ZA), up to 100% (vertical shafts), for which there are examples in most zones. Thus, cave dimensions are probably less dependent on their zone than on the properties of the individual carbonate outcrops and local geomorphology. Where zones appear to influence cave dimensions, they probably act as proxies for other external cave attributes (section 5.3).

Table 5.2 Zonal variations of cave dimensions (Shaded zones have <35 caves)

Zone	No. of caves	Total cave length (km)	% of all caves	% of total cave length	Mean cave length (m)	Mean cave VR (m)	Mean cave min. HG (%)	Mean cave XS (m^2)	Mean cave volume (m^3)	Mean cave CA (km^2)	Mean cave XS/CA (m^2km^{-2})
Z9	1	0.03	0.1	0.0	25	5.0	20	10.0	250	0.2	50.0
Z1	4	0.03	0.5	0.0	8	2.3	34	5.5	49	0.1	55.0
Z2	165	10.87	18.7	14.5	66	7.7	22	3.8	308	2.0	10.2
Z3	36	3.32	4.1	4.4	92	10.3	36	2.2	451	2.1	4.7
Z4	182	14.49	20.6	19.4	80	9.2	33	2.9	419	2.0	37.8
Z5	79	7.69	8.9	10.3	97	9.8	26	3.1	514	1.8	3.2
Z6	64	5.20	7.2	6.9	81	9.0	23	3.6	413	5.4	4.1
Z7	87	4.81	9.8	6.4	55	6.4	30	4.2	418	5.7	3.8
Z8	8	0.83	0.9	1.1	103	9.0	17	2.3	486	0.2	9.2
ZA	37	3.92	4.2	5.2	106	13.3	24	5.6	864	5.5	2.8
ZB	7	1.41	0.8	1.9	201	10.9	24	7.4	1047	4.4	5.7
ZC	58	5.84	6.6	7.8	101	10.6	29	3.1	470	2.8	2.2
KU	125	9.65	14.1	12.9	77	8.4	26	3.5	529	6.4	2.4
KL	29	6.71	3.3	9.0	231	8.8	26	3.9	1204	20.4	0.3
KB	2	0.07	0.2	0.1	35	7.0	19	2.1	71	0.3	12.1
ALL	884	74.88	100.0	100.0	85	8.8	27	3.5	474	4.0	11.9

5.2.2 Cave catchment areas (CA)

The largest cave catchment area is c. 1700 km^2 in extent. It includes the whole catchment for the artificially dammed 'Inland Sea' of Røssvatn (ZA), and has a mean annual flow-rate of c. 57m^3s^{-1} (Appendix A4.4). Because it is so exceptional, it is excluded from the analysis of catchment area in Table 5.2. Several caves in the study area have a CA of c. 40km^2, but the great majority have catchments of <6km^2. There are also many examples of significant caves at high altitudes that have very small contemporary catchments. The mean CA for caves in the Norwegian part of the area is 3.6km^2 (excluding the Røssvatn catchments). In the Swedish part it is 6.1km^2, giving a mean CA for all the caves of 4.0km^2. The zonal means tend to increase eastwards, as the land-surface rises, and as the scenery becomes more subdued. However, because of the very wide distribution of cave catchments, averages may not be helpful. The large peak in KL is caused by the small number of caves in two main valleys.

There is a considerable, but non-systematic, variation of cave dimension to CA ratios across the zones. Indeed, the mean XS/CA ratio at each cave is very variable, as shown in the final column of Table 5.2. Because individual catchment areas vary by three orders of magnitude (from ~0.01–40km^2), there is commonly little correspondence between mean cave XS/CA ratios and ratios of mean zone XS / mean zone CA. The very high mean XS/CA value in Z4 is caused by the relatively large passages on the plateau of Elgfjell, which are situated near ridge-tops at altitudes of c. 600m. Hence, it is difficult to observe any consistent relationships between the cave catchment areas and cave length, cross-sectional area or volume for the total set of caves, leading to the initial conclusion that *cave dimensions appear to be independent of catchment area* (but sections 5.4 and 5.5 give a more detailed analysis).

5.2.3 Total cave length and volume for the whole study area

Because karst conduits are natural features of the landscape, their dimensions can range in size from the kilometre-scale down to at least the centimetre-scale. A roughly continuous distribution of decreasing size against increasing frequency might be expected. Thus, in theoretical terms, discussions based on mean numbers, mean lengths, mean volumes etc. might be considered to be without meaning. A rigorous treatment, which is beyond the scope of this thesis, would use rank/size correlation plots (Ford and Williams, 1989, p245) and a fractal calculus, as proposed by Curl (1986). In practical terms, however, it is found in the study area that such mean values are of some utility, when applied to distributions of explored caves with lengths of 5m or more. Thus, a set of 40 newly-explored caves would invariably have a mean surveyed length between 70 and 100m. This applies even when the set consists of caves from several different zones, as well as, commonly, from the same zone (Table 5.2). This rather constant mean cave length also applies when caves are grouped by individual external attributes (sections 5.3.1–5.3.5). The reasons for the validity of natural mean dimensions are examined further in Chapter 8. Hence, there are some characteristics of the naturally-formed caves and the behaviour and motivation of cave explorers and surveyors that combine together to create a simple model of cave existence, which can be used as a predictive tool. Estimates of the unexplored but explorable cave potential of the study area can

be made by assuming no difference in cave frequency distributions for caves of 5m length or more between the total visited length of carbonate outcrops (447km) and the total mapped length (3193km). Taking data from Table 5.1, such a calculation leads to the estimates in Table 5.3.

Table 5.3 Estimated cave potential

Dimension	Units	Known cave totals	Frequency per visited km	Estimated totals for 3193km
Number of caves	No.	884	2.0	6386
Total passage length	km	75	0.17	543
Total cave volume	10^3m^3	419	0.94	3027
Mean cave length	m	85		85
Mean passage cross-section	m^2	3.5		3.5
Mean cave volume	m^3	474		474

The calculation assumes that the visited outcrops are representative of the whole set of outcrops in each zone, and that the visited length of each of these outcrops is also representative. A study of individual zones showed that the visited outcrops commonly do represent most of the geographic and altitudinal spread of the full set of outcrops. The size of the visited outcrop sample is probably significant, because some 20% (195) of all recorded outcrops have now been visited by cavers searching for caves: 25% (163) in Norway) and 9% (32) in Sweden. However, cave exploration has been very much biased towards visiting those sites that are identified as possible karst features, either on the 1:50,000 Norwegian topographical maps, or from local reports, and searches of other carbonate outcrops have been biased towards the larger outcrops and the western zones. Thus, future explorations may reveal proportionately fewer, and smaller, caves, so that the estimates in Table 5.3 probably represent the greatest possible figures. The estimates may not be excessively high, because 66% (129) of all visited outcrops have yielded at least one cave. These figures split into 69% (112) (Norway) and 54% (17) (Sweden). If outcrops below the Köli Nappes are ignored, then the Swedish figure rises to 79% (17 out of 23 visited outcrops). A complication is that some caves occur in carbonate outcrops not recorded on geological maps. For these, the likely dimensions of the outcrops were estimated from personal observation or experience. As these unmapped outcrops only number about 32 (all in Norway) out of the 195 visited outcrops (16%), this should not cause a significant perturbation to the above figures. On the one hand, the number of outcrops that are still unknown and unmapped is unpredictable, but a proportion will contain additional caves. On the other hand, many of the unmapped outcrops containing significant caves may now have been visited, as the main karst features drawn on topographical maps have undoubtedly been investigated by now.

5.2.4 Cave altitudes and vertical ranges (VR)

The Carbonate Rock Outcrops Database records the maximum altitude reached for each outcrop in the study area, together with the vertical range measured along the total length of each outcrop. The two Caves Databases record the altitude of the highest entrance and the vertical range for each cave. Table 5.4 is constructed from zonal summaries of this data.

Table 5.4 Carbonate outcrop and cave altitudes and vertical ranges (m)

Zone	Max. max. carb. alt.	Max. cave alt.	Mean max. carb. alt.	Mean max. cave alt.	Min. max. carb. alt.	Min. cave alt.	Max. carb. VR	Max. cave VR	Mean carb. VR	Mean cave VR
Z9	600	113	116	113	10	113	225	5	95	5.0
Z1	100	25	27	24	5	20	100	3	26	2.8
Z2	849	580	176	182	5	3	560	53	129	7.7
Z3	1000	680	421	387	40	5	690	101	220	10.3
Z4	1000	940	584	570	140	100	687	90	224	9.2
Z5	980	880	342	450	40	55	730	105	177	9.8
Z6	900	515	393	331	70	40	630	80	190	9.0
Z7	1200	770	606	526	310	175	780	30	219	6.4
Z8	1220	735	786	684	460	660	750	45	230	9.0
ZA	980	817	595	437	240	93	738	180	213	13.3
ZB	1220	620	634	530	200	402	740	28	235	10.9
ZC	1340	900	734	680	390	550	956	60	248	10.6
KU	1392	926	740	718	370	423	842	110	163	8.4
KG	840		667		510		201		109	
KL	740	620	561	502	475	460	280	144	89	8.8
KS	1080		761		480		330		82	
KB	1280	920	732	860	440	800	480	11	84	7.0
SU	1097		740		540		200		49	
SB	1110		720		460		320		64	
ML	728		510		360		228		54	
ALL	1392	940	*542	475	5	3	956	180	*145	8.8

* Average of above figures. Shaded zones have <35 caves.

The following observations from Table 5.4 apply to the nine unshaded zones with more than 35 caves (section 5.2.1): (a) columns 2 and 3 show that the maximum cave altitude is always more than 50% of the maximum outcrop altitude, but is rarely within 10% of it; (b) from columns 4 and 5, the mean cave altitude is always within 30% of the mean maximum outcrop altitude, and column 7 shows that minimum cave altitudes can vary almost down to sea-level. The present and early Holocene altitudes of the treelines do not appear to influence the mean zonal entrance altitude (not shown in Table 5.4); (c) from columns 8 and 9, the maximum cave vertical range is always less than 15% of the maximum outcrop vertical range, except for **Ytterlihullet** (ZA, Appendix B1.10) at 24%, or 29% of its own outcrop VR. The **Korallgrottan** (KL, Appendix B1.15) VR is 51% of the VR of its outcrop, which is the KL outcrop with the largest VR; (d) columns 10 and 11 show that the mean cave vertical range is never more than 6% of the mean outcrop vertical range. (The small sample in KL is at 10%. The mean outcrop vertical range for HNC, RNC and Køli taken together is 153m); (e) the distribution of mean cave vertical ranges in column 11 also shows a remarkably low variation, lying within the range 6.4–13.3m. The means exhibit a shallow peak in the RNC zones, as ZA, ZB and ZC occupy the top three rankings in the table.

Section 4.2.2 concluded that the vertical distribution of carbonate outcrops is essentially random, and that surface exposures are common in all zones at all altitudes, from a regional base level up to the highest outcrop. Observations a) and b) above suggest that cave entrances can be found in any limestone outcrop and that the vertical distribution of their entrance altitudes is also probably random, except that they have rarely been recorded close to the maximum altitude of the highest outcrop. This exception

probably does not arise from exploration being biased towards lower altitudes, because section 5.3.5 also shows that caves rarely occur near summits, although many occur along minor ridges.

For most zones of the study area, scatter diagrams were plotted to show the distribution of cave entrance altitudes eastwards. In all zones, the cave entrance altitudes are well-scattered vertically, with no obvious concentrations, although in KL the cave entrances have similar altitudes because they all occur in essentially the same long carbonate outcrop, as discussed in Appendix B1.15. The scatter diagrams differentiate between active caves and relict caves (as defined in section 5.4), and show that the relict cave entrance altitudes are well-scattered both vertically and horizontally amongst the distribution of all cave entrances. Hence, this zone by zone analysis supports the above conclusion that cave entrance altitudes are scattered randomly below summit areas, within the overall constraints of the local topography and the carbonate outcrops.

Observations c) and d) above indicate that rarely, if ever, do the depths of the cave systems approach the potential of the vertical exposure of their containing limestone outcrops. Only five caves are known to exceed 100m in depth (section 5.3.6), and the overall mean depth is only 8.8m. **Korallgrottan**, and to a lesser extent **Ytterlihullet,** are quite exceptional in both their depths (144m and 180m) and the vertical proportions of their limestone outcrops that they exploit. Their karst types (section 5.3.1) may be significant, because **Ytterlihullet** is in low angle karst and **Korallgrottan** is in angled stripe karst, but most of its length is along the strike. There is also no single cave system in the study area that exploits the full range of glaciated valley topographical situations from sink to resurgence.

Scatter diagrams were also plotted for most zones of the study area to show the distribution of cave lengths and vertical ranges against cave entrance altitudes, for both active and relict caves. There is commonly a good spread of lengths and depths at all applicable altitudes, although within individual zones the longest and deepest caves may peak about one or two altitude values. Taking the study area as a whole, there is no obvious relationship between active or relict cave lengths or vertical ranges and their entrance altitudes. This result may be considered alongside the comment by Helldén (1975, p25) that in **Sotsbäcksgrottan** (KU, Appendix B1.13) *"It has been impossible to relate the levels of the passage systems to fluctuations in the erosion base level"*. This cave has a sink entrance at the paleic surface, and an undived resurgence sump that is 80m above the lake Över-Uman, the local base-level.

For each zone, a scatter diagram was plotted to show the relationship between the length and vertical range for every cave in the zone. These diagrams show that there is little, if any, relationship between the length and the vertical range of cave systems anywhere in the study area. There are few deep shafts in these caves. The deepest is a 30m-deep, steeply-sloping, underground shaft in **JOBshullet** (Z2). In **Djupdalshullet** (KU), there are 15m and 13m vertical pitches within the same deeper shaft.

5.2.5 Cave types (CT)

The cave databases record the *type of cave* for each entry, from a classification scheme devised by the author that is based on his experience of applicable cave passage relationships in the study area. These are defined in Appendix C2.2 and cave types S and a–h are illustrated in Figure 5.1.

CT	Morphology	Plan	Projected elevation
S	Shaft		
a	Linear	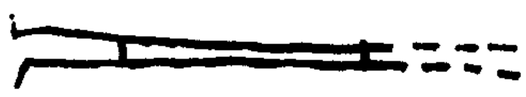	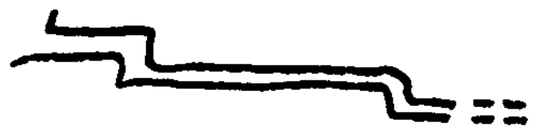
b	Meander		
c	Rectilinear	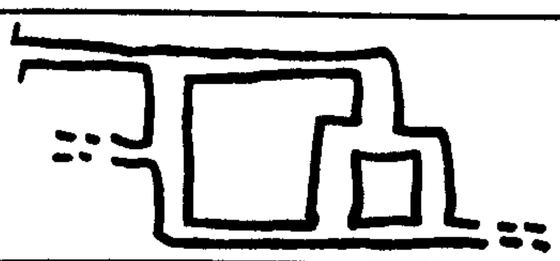	
d	Dendritic	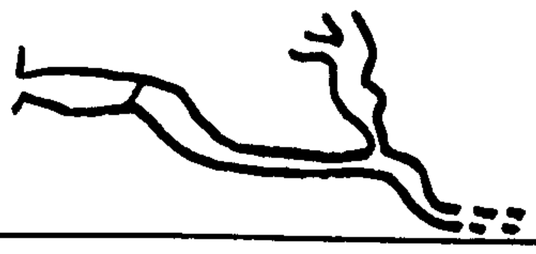	
e	Tiered linear	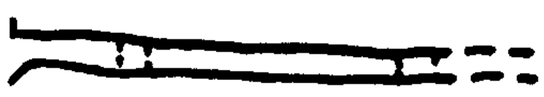	
f	Tiered rectilinear	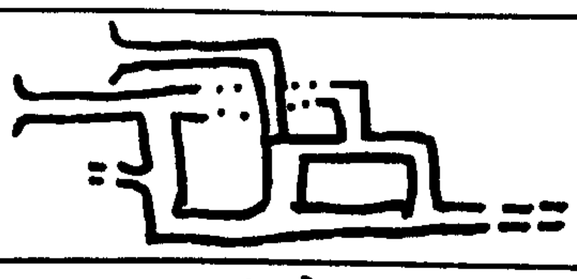	
g	Tiered dendritic		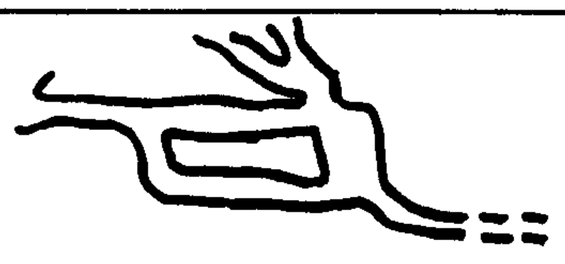
h	Complex	f + g + sloping phreatic passages	

Figure 5.1 Cave Types

Cave dimensions for each cave type are shown in Table 5.5. This information was assembled from the combined cave database and from derived pivot table analyses, which are not presented in full, to economise on space. Single shafts account for c. 10% of the recorded cave population, and the 'process' types account for another 3%. For the bulk of the caves, 'simple' caves are the most numerous, because >60% of all the reported caves are single linear or meandering passages (types a and b). These may be of phreatic or vadose development or both.

Table 5.5 Variations of cave dimensions with cave type

Cave Type	No. of caves	Total cave length (km)	% of caves	% of total cave length	Mean cave length (m)	Mean cave VR (m)	Mean cave min. HG (%)	Mean cave XS (m^2)	Mean cave volume (m^3)	Mean cave CA (km^2)	Mean cave XS/CA (m^2km^{-2})
S	90	0.93	10.2	1.2	10	7.3	81	3.1	39	2.1	10.4
a	315	7.05	35.6	9.4	22	4.2	28	3.1	128	3.8	7.0
b	230	11.60	26.0	15.5	50	7.7	18	3.4	273	4.6	14.5
c	57	6.40	6.4	8.5	112	7.8	14	3.7	488	6.5	7.2
d	59	7.76	6.7	10.4	132	12.2	13	3.8	856	5.1	19.8
e	17	2.20	1.9	2.9	130	14.7	20	3.7	699	3.5	2.6
f	23	3.41	2.6	4.6	148	15.4	15	2.8	469	4.2	7.2
g	28	7.03	3.2	9.4	251	20.6	18	4.6	1657	3.0	40.5
h	39	27.42	4.4	36.6	703	38.6	11	4.6	3964	2.7	10.7
Hy	12	0.61	1.4	0.8	50	8.8	21	10.1	544	2.9	24.2
I	3	0.28	0.3	0.4	92	11.0	33	3.7	602	7.0	0.5
J	0	0									
L	7	0.08	0.8	0.1	12	3.1	36	7.1	91	2.7	36.8
R	0	0									
T	4	0.11	0.5	0.2	29	9.5	31	6.5	335	7.1	42.1
ALL	884	74.88	100.0	100.0	85	8.8	27	3.5	474	4.0	11.9

The numbers of caves of each type tend to *reduce* with the complexity of the type (a–h), whereas the mean cave length, the mean cave vertical range, and the mean cave volume all *increase* fairly smoothly with complexity. These are as expected, because the longer a cave is, then the more degrees of freedom it has to display a complex morphology, and the definitions of the more complex cave types include references to levels and shafts, which are related to the vertical range. These observations commonly apply to caves in all 'inner' zones (i.e. all cave zones, excluding Z1, Z9 and KB), and in all main karst types, cave locations, glacial situations, combinations of contact metamorphism and proximity to thrusts (as defined in section 5.3) and for all cave hydrological classes where appropriate (section 5.4). The total length of caves in each cave type shows no systematic trend, although the 39 caves of the most complex type (h) account for a disproportionately large length (27422m of the total cave passage length of 74881m).

Mean cave XS, CA and XS/CA ratios show little relationship to cave type (a–h). The 12 hybrid caves (Hy) have a very large mean XS of $10.1m^2$, a large mean XS/CA ratio, and relatively large volumes for their short lengths, as expected for caves modified by marine action. The 7 purely littoral caves (L) have twice the average mean XS and a very large mean XS/CA ratio, again, as expected, if they have formed by marine action rather than by meteoric dissolution. The mean minimum hydraulic gradient has a commonly reducing trend with cave type, because cave lengths vary much more than cave depths.

To summarise, the typical cave consists of a single passage that is less than 100m long and less than 10m deep. However, caves over a kilometre in length and over 100m in depth also occur in the area, and these can display extremely complex arrangements of inter-linked passages at several levels, which do not appear to be strongly controlled by the external attributes.

5.3 External cave attributes

This section reviews how the various external attributes recorded in the two cave databases vary across the zones and nappes of the study area, and discusses what influences they may have on cave dimensions.

5.3.1 Karst types (KT) and foliation

The declining, across-zone, trend in the stratal dip of the mapped carbonates was discussed in section 4.2.3 and Figure 4.1. A similar, but less clear, trend is also found in the angles of dip of the foliation measured inside the caves themselves, as shown for each zone on Figure 5.2. The overall mean 'cave measured' dip angles are: HNC 70°; RNC 45°; and Køli 39°. The discussion on individual caves in Appendix B1 highlighted the importance of the dip of the containing limestone and Chapter 9 also records that the geological properties of the carbonate bedrock play an important role in influencing cave morphology, as seen in the shapes of passages and in the relationships between them. Kirkland (1958) observed that, in the Svartisen area of northern Norway, caves are commonly conformable to the bedding and to major joint sets. In the study area, cave passages are commonly conformable to the strike, to the dip of the foliation and to joint sets.

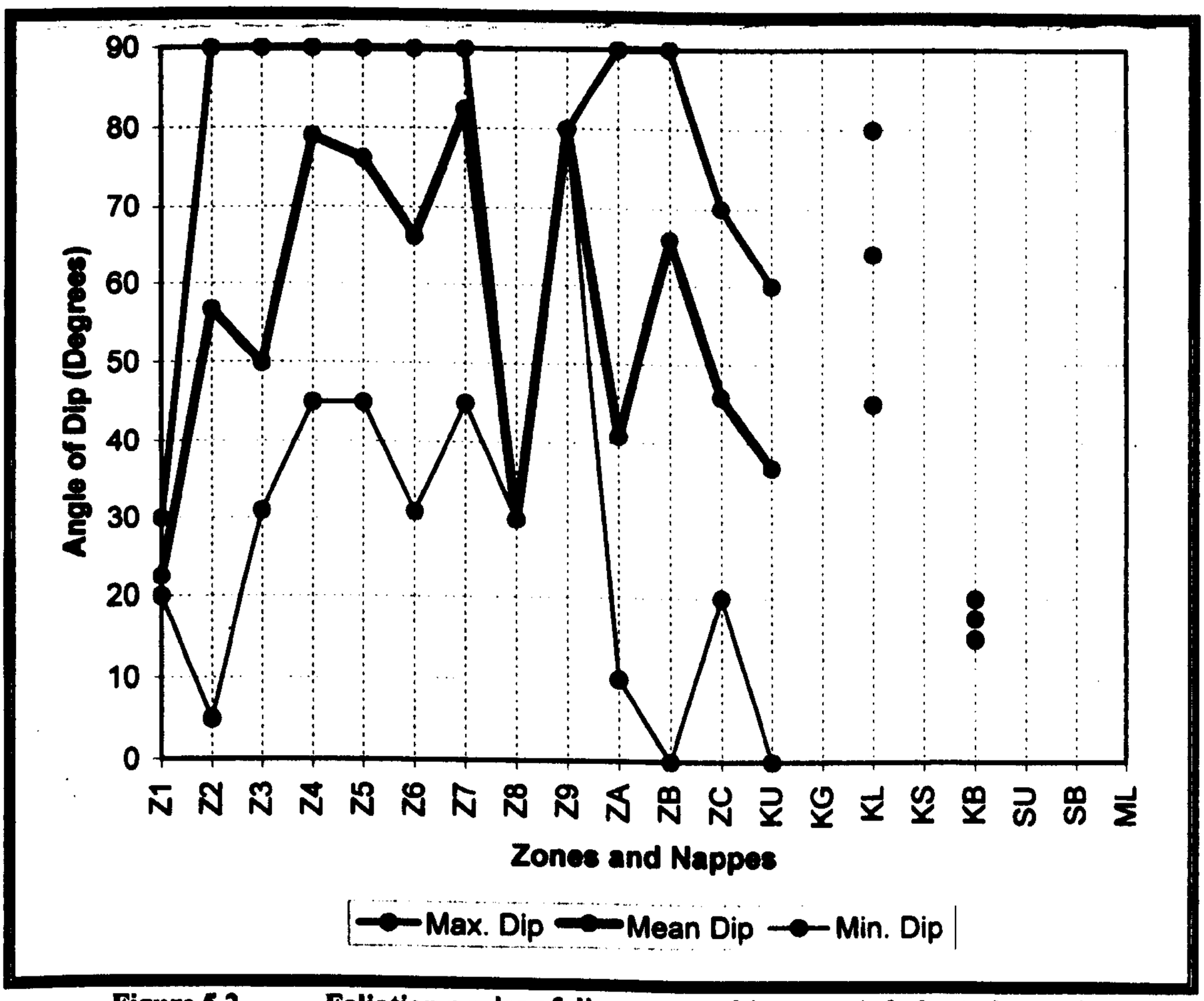

Figure 5.2 Foliation angles of dip measured in caves (whole study area)

In order to simplify analysis, the containing karst at each fully-reported cave in the study area is classified as one of a number of *karst types* in the cave databases, as defined in Appendix C2.1 and as illustrated in Figure 5.3. Cave dimensions for each karst type are shown in Table 5.6.

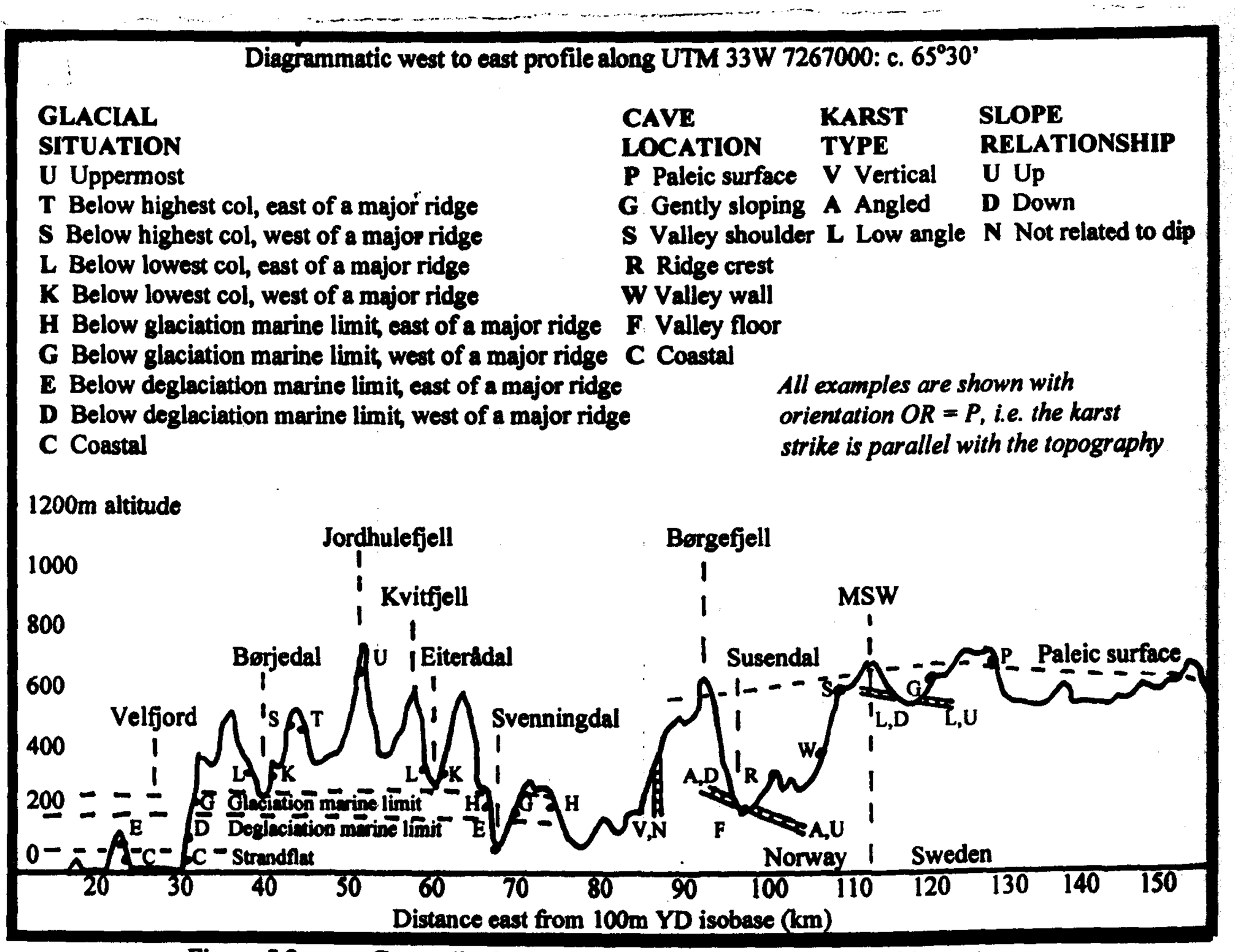

Figure 5.3 **Generalised cave locations, glacial situations and karst types**

Table 5.6 **Cave dimensions and karst type**

Karst Type	Units	V	A	L	C	X	ALL
No. of caves	No.	235	480	127	3	39	884
Total cave length	km	20.25	37.79	12.64	2.91	1.30	74.88
% of caves	%	26.6	54.3	14.4	0.3	4.4	100
% of total cave length	%	27.0	50.5	16.9	3.9	1.7	100
Mean cave length	m	86	79	100	968	33	85
Mean cave VR	m	8.6	9.0	9.5	17.3	5.5	8.8
Mean cave min. HG	%	33	25	25	7	29	27
Mean cave XS	m^2	3.0	3.8	3.8	3.2	3.1	3.5
Mean cave volume	m^3	460	428	703	3738	127	474
Mean cave CA	km^2	3.3	4.0	6.1	1.9	1.5	4.0
Mean cave XS/CA	m^2km^{-2}	8.7	16.0	4.8	1.7	5.0	11.9

Caves occur in approximate V:A:L ratios of 2:4:1. Caves in type V are only recorded in HNC and RNC, plus **Landbrua** in KL. They do not occur in the Swedish part of the study area. Caves in type A are scattered across most zones and nappes. Caves in type L only occur in Z1, Z2 and Z8 of the HNC, and in most of the lower nappes. Thus, the karst types agree with the eastward decreasing trend in dip angles. The table also shows that there is little difference in the mean cave lengths from the overall study area mean of 85m for the two main karst types, with an indication that caves in low angle karsts are somewhat longer, and have larger volumes. The mean cave vertical range and the mean minimum hydraulic gradient appear to be little dependent on the karst type, with a slight *increase* in mean VR as the karst dip angle

decreases, but a *decrease* in mean minimum HG if the foliation is not vertical. Caves in vertical karsts have somewhat smaller passage cross-sections than caves in angled and low angle karsts, perhaps because of exploration bias towards the west. The catchment area appears to increase as the karst angle of dip decreases, but in this case the karst type is acting as a proxy for a progression eastwards, as discussed in section 5.2.2. The mean XS/CA ratios show wide variations, with no trend.

By comparing Tables 5.6 and 5.7, it is apparent that the most complex cave type, h, occurs less frequently than expected from the full cave populations if KT=V, and more frequently if KT=A or L. The reason for the low frequency of cave type h in vertical stripe karst is probably the criterion of 'steeply sloping (phreatic) passages' in its definition: only five such caves are known in VSK: **Toerfjellhola** (Z3), **Sirijordgrotta** (Z4), **Etasjegrotta** (Z4), **Geitklauvgrotta** (Z5) and **Blåfjellgrotta** (Z5). These caves therefore demonstrate that angled, along-strike, phreatically-formed, ramp passages can occur in vertically foliated metalimestones, as well as in angled stripe karst and low angle karst. The small number of type h caves with KT=V contrasts with their longer mean lengths. Indeed, Table 5.7 shows that the mean major cave dimensions (length, VR and volume) of type h caves all reduce with foliation dip (V:A:L), in contrast to differing rankings for the total set of caves. The larger cross-sections and smaller catchment areas of type h caves suggest that these caves in particular were developed primarily before present hydrologies became established, for all karst types. The two caves of type h in complexly folded karst with steeply sloping ramps are **Kvitfjellhola** (Z4) and **Labyrintgrottan** (ZA).

Table 5.7 Cave type h dimensions and karst type

Karst Type	Units	V	A	L	C	X	ALL h
No. of type h caves	No.	5	23	9	2	0	39
% of type h caves	%	12.8	59.0	23.1	5.1		100.0
Mean cave length	m	1232	641	414	1403		703
Mean cave VR	m	53.6	39.8	31.1	21.0		38.6
Mean cave min. HG	%	4	11	14	6		11
Mean cave XS	m^2	6.3	4.2	4.9	3.3		4.6
Mean cave volume	m^3	8191	3231	3156	5456		3964
Mean cave CA	km^2	2.2	2.4	4.1	1.9		2.7
Mean cave XS/CA	m^2km^{-2}	3.2	14.9	6.1	1.8		10.7

Unlike the mean outcrop widths determined from the carbonate rock outcrops database, which seem to decrease eastward across the nappe complexes (section 4.2.3), the mean outcrop widths recorded at the caves themselves *increase* as the nappes are descended: HNC 355m; RNC 527m; and Køli 1363m. The HNC and RNC mean widths are roughly twice as wide as the mean widths of all their carbonate outcrops, and the Køli mean width at caves is wider by an order of magnitude than the total mean Køli width. This may indicate a preference for caves to form in wider outcrops, but the exploratory bias is also to visit the larger outcrops first. Additionally, there are examples of caves formed in outcrops down to 3m wide (and less), and internal aquiclude layers also commonly reduce the effective width of the carbonate outcrop at the cave. This finding was tested at the zonal level. The mean widths of the carbonate outcrops vary non-systematically through the HNC, RNC and Køli Nappes from 432m in Z1 to

53m in KS. They remain narrow in the nappes below the Køli, where the outcrops are commonly much shorter. Plots of the number of caves and total passage length against visited outcrop width were made for most zones. They show no relationship, so that endokarst density seems to be independent of outcrop width. This result suggests that caves may form along the edges of carbonate outcrops, or along aquiclude contacts, or occupy the full width of narrow outcrops.

5.3.2 Contact metamorphism (R)

Section 4.2.4 discussed the sharp eastward decline of carbonate outcrops subjected to contact metamorphism (R=1) across the study area nappes. A similar trend is seen at the outcrops in which the explored caves are found: HNC 178 caves; RNC 2 caves; and Køli 27 caves. The 27 caves in the Køli nappes all lie in the large metacarbonate outcrop near Övre Ältsvattnet (KU, Appendix B1.13), in which small-scale Swedish geological maps indicate several granitic intrusions. Half the caves recorded in this area lie within 250m of an intrusive rock. In these caves, the foliation is generally removed, so that the dip is more difficult to determine, and the metalimestone karst is predominantly white, sporadically with intrusive aquiclude rocks.

Table 5.8 shows that mean cave lengths, vertical ranges, minimum hydraulic gradients, cross-sections and volumes are all smaller if the host carbonate was affected by contact metamorphism (R=1), for both T=0 and T=1 (section 5.3.3). However, the mean logarithms of each of these dimensions (and their standard deviations) are commonly similar for each R and T combination. This shows that the restrictions caused by contact metamorphism apply disproportionately to the caves with the greatest dimensions, because of the positive skew in the dimension distributions (section 5.2). The small number of caves adjacent to both intrusions and thrusts follows from the tendency for igneous plutons to 'stick' nappes together, restricting thrusting.

Table 5.8 Cave dimensions, contact metamorphism and proximity to major thrusts

Contact metamorphism and thrusts	Units	R=0 T=0	R=1 T=0	R=0 T=1	R=1 T=1	ALL
No. of caves	No.	587	198	90	9	884
Total cave length	km	48.11	11.99	13.84	0.95	74.88
% of caves	%	66	22	10	1	100
% of total cave length	%	64	16	18	1	100
Mean cave length	m	82	61	154	105	85
Mean cave VR	m	8.9	7.5	11.3	9.7	8.8
Mean cave min. HG	%	28	24	30	17	27
Mean cave XS	m^2	3.6	3.0	4.4	3.1	3.5
Mean cave volume	m^3	467	256	989	565	474
Mean cave CA	km^2	3.6	3.1	9.4	0.5	4.0
Mean cave XS/CA	m^2km^{-2}	15.2	6.4	3.1	8.5	11.9

5.3.3 Proximity to major thrusts (T)

Section 4.2.5 discussed the generally increasing trend of carbonate outcrops to lie near major and internal thrusts as the nappes are descended. Only 12 caves occur in outcrops that are near thrusts in the HNC and

RNC. Most of these are quite short: the longest, **Nedre Jengelgrotta** (Z8), is only 460m long. However, 87 caves are near thrust boundaries in the Køli Nappes. These include: a) the caves at Rödingsfjäll and Sotsbäck, including **Sotsbäcksgrottan** (1850m), which all lie at the top of KU beneath the RNC sole thrust (Appendix B1.13); and b) the caves in KL, including the Bjurälv karst and **Korallgrottan** (5600m long), which all occur in one dismembered outcrop that lies near to, and in places on the base of, the Leipikvattnet Nappe (Appendix B1.15). Thus, the evidence from the caves is in agreement with the general trend from the carbonates database, and the occurrence of two of the three longest Swedish caves in the study area at thrust zones may not be coincidental. The possibility that the presence of a thrust zone could cause fractures and fissures in the limestone that promote cave development was not addressed by Helldén (1975). No records have been kept of the occurrence of large faults (with displacements of several metres) within the carbonate outcrops, and none have been reported from inside any of the caves of the area. However, it is noted in passing, that **Åkervikgrotta** (Z7) is close to a large normal fault, and **Nordlysgrotta** (Z2), which contains a linear rift some 220m long, is probably fault-aligned, as is the nearby **Marimyntgrotta**.

Table 5.8 shows that mean cave lengths, vertical ranges, cross-sections and volumes are all greater if the host carbonate was affected by thrusting (T=1), for both R=0 and R=1. As argued in section 5.3.2, these larger sizes appear to apply disproportionately to the caves with the greatest dimensions. The mean minimum hydraulic gradient for caves near thrusts (29%) remains close to the study area average (27%). The larger mean catchment area for caves with R=0 and T=1 (9.4km^2) arises because there are more thrusts and less intrusions in the eastern part of the study area, where catchment areas increase in size. **Gårdsfjellgrotta** (Z6) and a group of eight low angle karst caves at Jengelvatn (Z8) are distinctive, because they all lie along the sole of the HNC thrust and are assigned both T=1 and R=1.

By comparing Tables 5.8 and 5.9, it can be seen that the frequencies of the most complex caves, type h, in each R, T combination do not vary greatly from those in the full cave population. Their mean cave dimensions are also reduced with contact metamorphism, and increased with thrusting. These findings that *contact* metamorphism restricts cave development compared with purely *regional* metamorphism, whereas thrusting commonly enhances cave development, are discussed further in section 6.5.1.

Table 5.9 Cave type h dimensions, contact metamorphism and thrusts

Contact metamorphism and thrusts	Units	R=0 T=0	R=1 T=0	R=0 T=1	R=1 T=1	ALL h
No. of type h caves	No.	22	11	6	0	39
% of type h caves	%	56	28	15		100
Mean cave length	m	646	303	1645		703
Mean cave VR	m	39.0	24.6	62.7		38.6
Mean cave min. HG	%	10	13	9		11
Mean cave XS	m^2	4.4	4.3	5.8		4.6
Mean cave volume	m^3	3561	1374	10187		3964
Mean cave CA	km^2	2.2	1.1	7.9		2.7
Mean cave XS/CA	m^2km^{-2}	14.1	8.6	1.9		10.7

5.3.4 Cave locations (CL)

Homoclinal stripe karsts occur in various geometrical relationships to the surface topography at the location of each cave. From the experience with sedimentary limestones, these relationships are expected to influence the presence of caves, the positions of cave entrances, and internal cave morphology and hydrology. In an attempt to determine if there are such relationships for the study area caves, further external cave attributes are defined in Appendix C2.1 and quantified in the two cave databases. These are *Cave Location* (CL), *Slope Relationship* (SR) and *Orientation* (OR).

Section 2.2.1 discussed the apparent extent of the *paleic surface* in the study area (CL=P), according to Rudberg (1997). By plotting assumed surfaces on to the topographical maps of the area, it was found in this study that they commonly, but not universally, occur at altitudes over 700m, rising to 900m over mountain ranges, and are typically characterised by even, parallel, contours. They lie above the tree line in Norway, where they commonly correspond to the more resistant, higher, mountains of igneous emplacements. There are no carbonate outcrops at the paleic surface west of Z4. Paleic surfaces that expose proportions of carbonate outcrops occur in Z7, Z8 and all lower nappes, and increase eastwards. In the Norwegian part of the study area, *caves* only lie fully on the paleic surface in Z7. In the Swedish part, most carbonate outcrops, and 67% of the karst caves, are located on the paleic surface. Some of the longer caves of the study area are thus located beneath the assumed paleic surface, including **Labyrintgrottan** (ZC) and **Sotsbäcksgrottan** (KU). **Ytterlihullet** (ZA), although close to the paleic surface, is assigned to the S location.

The relationships between cave dimensions and cave locations are listed in Table 5.10. These figures reveal some notable variations amongst the different cave locations. Thus, paleic surfaces favour caves that are slightly shorter, less deep and have smaller cross-sections and volumes than the total average, despite having larger-than-average catchment areas. Valley shoulder and ridge locations favour longer and deeper caves, with larger volumes, and yet, because of their high locations within their local landscapes, they have very small catchment areas. Caves located on valley walls are somewhat deeper than average, but are shorter and smaller. These findings may indicate the ease with which new fractures can form in narrow ridges and at angular valley shoulders, and may suggest a slightly more tectonically-stable condition along the walls of glacial valleys (Chapter 6). Caves in valley floors are less deep, and have catchment areas that are around twice the average (as expected), but they are only *slightly* longer and larger than the average. These observations clearly demonstrate that cave dimensions are *commonly* not related to present catchment areas, as also shown by the large variations in mean XS/CA ratios. The mean minimum HG shows little variation, although a higher value occurs for caves in location S, because of their larger mean VR. Coastal caves are commonly very short and shallow. Whereas deep coastal caves would be submerged and difficult to explore, there are no reports of submarine resurgences along the coast of the study area. However, **Langfjordgrotta** (Z2) is at an altitude of only 10m. Its resurgence entrance leads to a sump deeper than 10m, which heads towards a sinking lake at an altitude of 43m,

some 1500m away. Thus, this long system acted as a submarine resurgence prior to its emergence by isostatic uplift some 1500 years ago (Figure 8.1b). The cave type h dimensions for each cave location are given in Table 5.11, which shows some variations in rank order compared with the full set. In particular, three type h caves with CL=S reverse the full set trend, with restricted mean lengths and volumes.

Table 5.10 Cave dimensions and cave location

Cave Location	Units	C	F	W	R	S	G	P	ALL
No. of caves	No.	15	246	197	62	57	197	110	884
Total cave length	km	0.23	23.30	13.01	7.83	5.90	15.74	8.87	74.88
% of caves	%	1.7	27.8	22.3	7.0	6.4	22.3	12.4	100
% of total length	%	0.3	31.1	17.4	10.5	7.9	21.0	11.8	100
Mean cave length	m	15	95	66	126	104	80	81	85
Mean cave VR	m	2.9	7.4	10.0	11.8	14.2	8.4	7.2	8.8
Mean cave min. HG	%	31	22	30	28	39	28	26	27
Mean cave XS	m^2	4.0	4.2	3.1	4.0	3.1	3.9	2.2	3.5
Mean cave volume	m^3	70	523	321	614	663	549	382	474
Mean cave CA	km^2	8.6	8.2	1.6	0.8	0.9	2.2	5.1	4.0
Mean cave XS/CA	m^2km^{-2}	17.3	4.9	25.5	31.0	11.1	6.5	1.9	11.9

Table 5.11 Cave type h dimensions and cave location

Cave Location	Units	C	F	W	R	S	G	P	ALL h
No. of type h caves	No.	0	8	9	5	3	5	9	39
Total h cave length	km	0	10.25	3.23	3.99	1.14	3.06	5.76	27.42
% of type h caves	%		21	23	13	8	13	23	100
% of total cave length	%		37	12	15	4	11	21	100
Mean cave length	m		1281	359	798	381	611	639	703
Mean cave VR	m		43.4	39.6	43.2	29.0	38.8	34.0	38.6
Mean cave min. HG	%		6	14	6	16	10	12	11
Mean cave XS	m^2		5.1	4.4	4.2	4.2	6.8	3.3	4.6
Mean cave volume	m^3		6422	2223	3561	2021	5532	3519	3964
Mean cave CA	km^2		6.9	1.6	1.2	0.8	1.7	2.3	2.7
Mean cave XS/CA	m^2km^{-2}		4.1	30.6	5.7	10.5	5.5	2.2	10.7

Because stripe karsts are commonly aligned with valleys and ridges, it is appropriate to consider the *slope relationship* to the dip of the foliation at each cave, as discussed by Osborne (1999, Fig. 12). Table 5.12 shows that over 70% of the caves are situated where there is no relationship between the surface slope and the dip of the foliation, because many caves are in vertical stripe karst or in cave location F. The mean cave length and vertical range for caves in slope relation U are somewhat more restricted than those of caves in slope relation D. This is *Heap's Hypothesis: "...limestone which dips very steeply back into the hill....usually limits cave development in Norway"* (Heap, 1975, p5), also supported by Osborne (1999, Fig. 12), which appears to be confirmed for vertical range, and more weakly confirmed for cave length. The mean minimum HG and cross-section show little variation.

Regarding *orientation*, Table 5.13 shows that nearly 80% of the caves are indeed situated where the outcrop strike is aligned with the local topography. It appears that caves may be longer and deeper (but smaller) where the strike is angled to the topography, and shorter (giving a high minimum HG) where it is orthogonal, but these are much smaller samples. Where there is a parallel relationship or no relationship, the mean cave dimensions are very close to the overall means.

Table 5.12 Cave dimensions and slope relationship

Slope relationship	Units	D	N	U	X	ALL
No. of caves	No.	85	636	141	22	884
Total cave length	km	6.91	57.53	9.69	0.75	74.88
% of caves	%	9.6	71.9	16.0	2.5	100
% of total cave length	%	9.2	76.8	12.9	1.0	100
Mean cave length	m	81	90	69	34	85
Mean cave VR	m	12.4	8.3	9.5	6.6	8.8
Mean cave min. HG	%	30	26	30	24	27
Mean cave XS	m^2	3.8	3.5	3.5	3.1	3.5

Table 5.13 Cave dimensions and orientation

Orientation	Units	P	A	O	N	X	ALL
No. of caves	No.	694	35	32	109	14	884
Total cave length	km	57.87	5.33	2.21	9.08	0.40	74.88
% of caves	%	78.5	4.0	3.6	12.3	1.6	100
% of total cave length	%	77.3	7.0	3.0	12.1	0.5	100
Mean cave length	m	83	152	69	83	28	85
Mean cave VR	m	8.6	15.3	8.7	8.9	4.9	8.8
Mean cave min. HG	%	27	33	44	23	26	27
Mean cave XS	m^2	3.6	2.5	3.2	3.6	2.3	3.5

5.3.5 Glacial Situations (GS)

It is hypothesised herein that the hydrogeological development of the karst caves is influenced by their settings relative to the various situations that occurred during the Quaternary glaciations, where the elevation of the *glacial situation* of each cave is defined in Appendix C2.1 and illustrated in Figure 5.3. The significance of glacial situations is clarified in section 8.1.5. In summary, they are primarily altitude and isobase dependent, descending from near a high peak down towards sea-level, and are not strongly linked to the surface topography at the cave. Caves occur commonly in each of the main glacial situations T to D in all cave locations (apart from the coastal and paleic surface extremes), suggesting that the main cave location and glacial situation attributes are independently variable. However, large percentages (39% and 34%) of caves with GS=S and T have CL=P, in the higher (paleic) parts of the landscape, primarily in Sweden.

Table 5.14 summarises the relationships between cave dimensions and the paired west and east glacial situations. Nearly half the caves are in situation L, only two cave fragments (in Z4) are in the uppermost situation, U, only 1.7% are coastal, C, and only 2.0% are in situation S. Situation C only occurs in Z1, Z2 and Z3, and D, E, G and H only occur in ZA and zones to the west, agreeing with their proximity to the sea. Situations K and L occur in all *inner* zones (section 5.2.5), except that K does not occur in Z8 and KL, and L does not occur in ZB. Situations S and T occur more sparsely.

Only 214 of the 884 caves (24%) lie west of major ridges, despite the occurrence there of 50% of the carbonate outcrops in those zones that have known caves (section 4.2.6). This under-representation is evident for all GS=D, G, K and S, and in most zones. Mean cave lengths, vertical ranges and volumes are

higher for caves *east* of major ridges but below marine limits (GS=E and H), and higher for caves *west* of major ridges but above marine limits (GS=K and S). The differences in mean length and volume between GS=K and L would be greater if **Korallgrottan** (KL, length 5600m), whose VR straddles the lowest local col elevation, was assigned GS=T instead of L. The very high mean VR for GS=S (22.1m) is partly accounted for by the presence of **Ytterlihullet** (ZA, 180m deep, GS=S), which also straddles its lowest col. However, even without the inclusion of **Ytterlihullet**, the other 17 caves still have a large mean VR of 12.8m. Mean minimum HGs do not vary much between east and west counterparts.

Table 5.14 Cave dimensions and glacial situation

Glacial situation	C	D	E	G	H	K	L	S	T	U	ALL
No. of caves	15	23	67	30	64	128	419	18	118	2	884
Total cave length	0.23	1.19	6.07	1.82	7.86	11.85	37.91	2.02	5.91	0.01	74.88
% of caves	1.7	2.6	7.6	3.4	7.2	14.5	47.4	2.0	13.3	0.2	100
% of length	0.3	1.6	8.1	2.4	10.5	15.8	50.6	2.7	7.9	0.02	100
Mean length	15	52	91	61	123	93	90	112	50	7	85
Mean cave VR	2.9	5.8	8.3	6.2	10.9	9.7	9.1	22.1	6.2	2.0	8.8
Mean min. HG	31	21	18	17	22	27	30	27	30	29	27
Mean cave XS	4.0	5.9	4.6	3.9	3.8	3.9	3.2	4.8	2.7	2.0	3.5
Mean volume	70	302	514	282	965	561	479	636	190	14	474
Mean cave CA	8.6	2.7	1.7	2.5	4.0	7.3	4.0	1.7	2.2	0.5	4.0
Mean XS/CA	17.3	20.3	11.4	5.0	7.1	2.9	18.0	3.8	3.7	4.0	11.9

Units as Table 5.8. Glacial situations east of a major ridge are shaded.

Mean cave cross-sections are consistently higher west of major ridges, and consistently reduce for both east and west situations at higher altitudes (except for the large value for the small sample with GS=S, and despite the existence of some large passages at high altitude). However, there are no similar trends in mean CA, which suggests that many caves did not develop under present conditions.

The values in Table 5.14 show that mean cave dimensions vary as much with glacial situation as with cave location (section 5.3.4). The increases in cross-section for caves below marine limits (especially west-facing), and in volume for GS=E and H, may arise from enlargement of entrance areas by wave action during glaciation and deglaciation (section 8.8), and as may be supported by the large values of mean XS/CA occurring in the three lowest glacial situations (C, D and E). The relatively larger XS/CA ratios for caves above the deglaciation marine limit but below the lowest col that presently drain eastwards suggests that caves with GS=H and L enlarged less under present conditions than caves that drain westwards (GS=G and K). No similar conclusion can be drawn for caves above the lowest col (GS=S or T). Any caves previously existing in the very high U situation may have been preferentially weathered away by glacial erosion. These relationships are analysed in more detail in section 5.5, where caves are divided into *hydrological* classes.

Table 5.15 provides similar information for just type h caves, which occur even more predominantly on the east side of major ridges. There are none below marine limits and on western sides, but otherwise, the

rank orders for GS occurrences are fairly similar to those for the full set. Mean vertical ranges are higher on the western sides above the glaciation marine limit, but mean cave lengths and volumes are variable.

Table 5.15 Cave type h dimensions and glacial situation

Glacial situation	C	D	E	G	H	K	L	S	T	U	ALL h
No. of caves	0	0	5	0	6	3	19	1	5	0	39
Total cave length	0	0	1.21	0	4.40	2.49	17.05	0.32	1.96	0	27.42
% of caves			13		15	8	49	3	13		100
% of length			4		16	9	62	1	7		100
Mean length			241		734	830	897	316	391		703
Mean cave VR			16.8		51.7	55.7	40.4	50.0	25.6		38.6
Mean min. HG			12		12	10	10	16	8		11
Mean cave XS			4.4		8.2	5.0	4.1	2.5	2.4		4.6
Mean volume			1070		7254	4587	4533	790	1007		3964
Mean cave CA			1.1		1.7	1.1	3.8	1.5	2.7		2.7
Mean XS/CA			10.2		8.0	5.0	15.5	1.7	1.3		10.7

Units as Table 5.8. Glacial situations east of a major ridge are shaded

5.3.6 The longest and deepest caves in the study area

The 12 longest and 12 deepest caves in central Scandinavia are shown in Tables 5.16 and 5.17, which also record their external attributes and cave types. The first ranking cave in each table is exceptional within the study area. Thus, **Korallgrottan** (KL) has a length of 5600m, which is more than twice the length of the second ranking cave, and **Ytterlihullet** (ZA) has a depth of 180m, which is 25% more than that of the second ranking cave.

Most zones and nappes are represented in each table, showing no zonal trend, except that there are no representatives from the 'outer' cave zones Z1, Z9 and KB, i.e. the extreme north, west and east zones of the HNC / RNC / Køli sequence. The longest and deepest caves formed in a contact metamorphism karst are ranked eleventh and sixth, whereas three of the five longest caves and two of the three deepest caves are formed near thrust boundaries, again illustrating the restrictive and enhancing effects of igneous intrusions and thrust zones. The longest and deepest caves are concentrated in glacial situations H, K and L, with only the exceptional **Ytterlihullet** (assigned GS=S) and **Korallgrottan** (assigned GS=L) having their highest and lowest points above and below the level of the lowest local pass. Thus, very long and deep caves are commonly absent at the altitudinal extremes. Additionally, glacial situation G is noticeably absent. As with the whole set of caves (section 5.3.5), the number of *longest* caves is higher on the *eastern* side of adjacent mountain ranges and ridges, as only **Toerfjellhola**, **Grønndalsgrotta** and **Akersvanngrotta** (with GS=K) lie west of major watersheds. The mean length of these eastern caves is 1903m, which is greater than the 1399m mean length of the western caves, in contrast to the finding in section 5.3.5 that total *mean* cave dimensions above the glaciation marine limit are higher *west* of major ridges. The numbers (12 and 6) with east- and west-draining systems in the deepest 18 systems (Table 5.18) also seem significant, and in this case their mean VRs (71m and 87m) follow the previous rule.

Table 5.16 Longest caves

LONGEST CAVES	L (m)	Z	C	R	T	GS	CL	KT	SR	OR	CA (km^2)	CT	Min. HG %	XS/CA (m^2km^{-2})
Korallgrottan	5600	KL	S	0	1	L	F	A	N	P	3.5	h	2.6	1.4
Labyrintgrottan	2600	ZC	S	0	0	L	P	C	N	P	2.5	h	0.8	1.6
Toerfjellhola	1896	Z3	N	0	0	K	R	V	N	A	1.1	h	5.3	5.5
Stor Grubblandsgrotta	1890	KU	N	0	1	L	F	A	N	N	19.0	h	2.6	0.3
Sotsbäcksgrottan	1850	KU	S	0	1	L	P	L	N	A	2.5	h	5.9	4.0
Sirijordgrotta	1411	Z4	N	0	0	H	G	V	N	P	2.0	h	5.5	6.0
Grønndalsgrotta	1400	ZA	N	0	0	K	S	L	U	P	5.0	h	5.0	2.0
Etasjegrotta	1055	Z4	N	0	0	L	F	V	N	P	3.0	h	4.0	1.0
Geitklauvgrotta	935	Z5	N	0	0	H	G	V	N	P	3.5	h	1.7	2.4
Akersvanngrotta	900	ZB	N	0	0	K	G	L	N	N	1.0	c	2.2	2.0
Svartdalgrotta	899	Z2	N	1	0	H	S	L	D	P	0.3	h	5.9	24.0
Kvannlihola	889	Z7	N	0	0	L	G	V	N	P	2.0	d	2.1	7.5

Table 5.17 Deepest caves

DEEPEST CAVES	VR (m)	Z	C	R	T	GS	CL	KT	SR	OR	CA (km^2)	CT	Min. HG %	XS/CA (m^2km^{-2})
Ytterlihullet	180	ZA	N	0	0	S	S	L	D	N	0.4	d	25.7	20.0
Korallgrottan	144	KL	S	0	1	L	F	A	N	P	3.5	h	2.6	1.4
Sotsbäcksgrottan	110	KU	S	0	1	L	P	L	N	A	2.5	h	5.9	4.0
Øyfjelligrotta	105	Z5	N	0	0	H	W	A	D	P	2.0	h	13.1	7.5
Toerfjellhola	101	Z3	N	0	0	K	R	V	N	A	1.1	h	5.3	5.5
Luktindgrotta	80	Z6	N	1	0	L	R	A	N	P	5.0	b	13.3	1.2
Sirijordgrotta	78	Z4	N	0	0	H	G	V	N	P	2.0	h	5.5	6.0
Grønndalsgrotta	70	ZA	N	0	0	K	S	L	U	P	5.0	h	5.0	2.0
Klofthølet	60	ZC	N	0	0	K	G	A	N	N	10.2	b	28.6	2.9
Cold Wind Cave	58	Z3	N	0	0	K	W	V	N	A	0.7	g	15.6	8.6
Djupdalshullet	55	KU	N	0	1	L	W	A	U	P	0.8	a	22.9	18.8
Svartdalgrotta	53	Z2	N	1	0	H	S	L	D	P	0.3	h	5.9	24.0

Z: Zone C: Country N: Norway S: Sweden

All main karst types and all cave locations except the coastal are well-represented in Tables 5.16 and 5.17, although the longest caves do not occur at CL=W. Hence, long and deep caves can indeed occur in most geological and local topographical conditions. The long caves seem to favour conditions where there is no relationship between the angle of dip of the karst and the surface slope, and no long or deep caves occur where the karst strike is orthogonal to the glacial topography. However, there are only 32 caves with this condition, which may be too small a sample to draw firm conclusions. The catchment areas for these caves vary from 0.3–24km^2, with no discernible trend. As expected (section 5.2.5), most long caves are of the most complex type, h, but deep caves exhibit a greater range of cave types. The longest and deepest caves thus occur in a slightly restricted set of the various external attributes. The shorter and less deep caves can be expected to occupy the various conditions more completely, so that, overall, there should be few direct relationships between cave types and the external variables, supporting the observation made at the end of section 5.2.5.

The 12 longest caves have minimum HGs from 0.8–5.9%, in the lowest part of the possible range (Table 5.5), again suggestive that HG varies as the inverse of the cave length. The 12 deepest caves have HGs

from 2.6–28.6%, still in the lower part of the possible range, which seems to be counter-intuitive, but this is again explained by the mainly inverse relationship between HG and cave length. Furthermore, there seems to be little relationship between the minimum HG and the cave type for either the 12 longest or the 12 deepest systems. The lack of any obvious relationship between length and catchment area, and the small catchment areas for many of the deepest caves, strongly suggests that these caves could not have formed primarily by dissolution in the present climatic environment. However, all but three of the longest and deepest caves have individual XS/CA ratios that are much lower than the study area mean of 11.9m^2km^{-2}. This suggests that a considerable proportion of these caves did enlarge under present interglacial conditions. Thus, the longest and deepest caves commonly exhibit enlargement under both earlier and interglacial climatic environments.

5.3.7 Distance from surface

Because the mean vertical ranges for the caves in the study area are small (sections 5.2.1 and 5.2.4), it is surmised that VR is not the most important geomorphological measurement for caves situated in steeply sloping locations. Accordingly, Table 5.18 records the maximum *subsurface cave distance* from the centres of passages (section 6.5.2: Figure 6.3) in the 18 deepest systems, taking the information from the surveyed sectional profiles of the caves and from local maps.

Table 5.18 Maximum subsurface cave distance

DEEPEST CAVES	VR (m)	Zone	Country	R	T	GS	CL	KT	SR	OR	Max. subsurface cave distance (m)
Ytterlihullet	180	ZA	Norway	0	0	S	S	L	D	N	c. 93
Korallgrottan	144	KL	Sweden	0	1	L	F	A	N	P	50?
Sotsbäcksgrottan	110	KU	Sweden	0	1	L	P	L	N	A	50
Øyfjellgrotta	105	Z5	Norway	0	0	H	W	A	D	P	40
Toerfjellhola	101	Z3	Norway	0	0	K	R	V	N	A	47
Luktindgrotta	80	Z6	Norway	1	0	L	R	A	N	P	15
Sirijordgrotta	78	Z4	Norway	0	0	H	G	V	N	P	45
Grønndalsgrotta	70	ZA	Norway	0	0	K	S	L	U	P	40
Klofthølet	60	ZC	Norway	0	0	K	G	A	N	N	50
Cold Wind Cave	58	Z3	Norway	0	0	K	W	V	N	A	c. 50
Djupdalshullet	55	KU	Norway	0	1	L	W	A	U	P	50
Svartdalgrotta	53	Z2	Norway	1	0	H	S	L	D	P	50, to cliff
Stor Grubblandsgrotta	50	KU	Norway	0	1	L	F	A	N	N	50
Baaagrotta	50	ZC	Norway	0	0	S	G	A	N	P	40
JOBshullet	46	Z2	Norway	1	0	H	R	A	N	P	25, to ridge walls
Östra Jordbäcksgrottan	45	ZC	Sweden	0	0	T	W	A	U	P	27
Nedre Jengelgrotta	45	Z8	Norway	1	1	L	G	L	N	P	10?
Etasjegrotta	42	Z4	Norway	0	0	L	F	V	N	P	40

? These are uncertain, as cave survey elevations have not been published.

The data reveal that the maximum rock thicknesses for each cave are commonly much less than the cave vertical ranges, especially for the deeper systems. The greatest rock thickness above any cave formed in vertical or angled stripe karst is about 50m. Only **Ytterlihullet** (ZA, in LAK) has a greater rock thickness

(c. 93m) above the lowest parts of its streamway. Hence, many caves in the study area gain depth below a gently descending surface slope, to which they keep within a relatively close range. This suggests that caves in vertical and angled stripe karst have formed entirely within an upper zone of fractured rock that has a maximum thickness of ~50m. This zone might, perhaps, be compared to the epikarst or subcutaneous zone of sedimentary limestone, but in the case of metamorphic stripe karst, there is no lower 'percolation' zone and probably no cave development below the level of fracture porosity.

5.4 Hydrological cave classes

The 'cave type' classification (section 5.2.5) was devised to represent the internal structure of the caves in a manner that is primarily neutral to their mode and timescale of formation. Another approach is to consider the relationship of the caves to their present climatic and hydrological environment. A clear distinction can be made between the large number of caves that exist independently of present drainage *('relict caves')*, and those that are integrated within their local meteoric fluvial systems (*'active caves'*). A second distinction within the active caves is between those that contain relict passages and / or levels above active streamways, and those that only consist of active streamways. It is shown in section 5.6.7 that the relict caves, and the relict passages within active caves, were predominantly developed *phreatically*. Caves that only consist of explorable active streamways are regarded as '*mainly vadose caves*' in their mode of development, although their early formation would usually have been phreatic and they may contain (commonly short) active phreatic sections. Thus, the total set of caves may also be divided into (phreatic) relict caves, mainly vadose caves, and *'combination caves'*, which consist of both relict phreatic passages and / or levels, and active, mainly vadose, streamways. This section introduces the properties of these three classes of cave, by further pivot table analyses of the combined cave database, and section 5.5 compares the influences that the external attributes have had on them.

5.4.1 Relict caves (RC)

Those caves with zero cave streams (CS=0; Appendix B2.2) are regarded as relict caves. The dimensions of these caves in each zone are presented in Table 5.19. Some 279 (32%) of the recorded caves are relict, varying non-systematically from 17–54% across the inner zones. However, they account for only 13% (about 9km) of the total length of cave passage, this percentage varying non-systematically from 2–79% across the same zones. The high percentage in ZB arises from the presence of the 900m-long **Akersvanngrotta**. Relict caves have a mean length of only 34m, and this has some consistency across the unshaded zones with larger sample sizes. The zonal volumes and VRs are similarly restricted, only averaging 131m^3 and 5.9m in total, and, together with the mean minimum HGs, do not show a systematic variation. The mean cross-sections (Photo 5.1) and catchment areas of relict caves are variable zone by zone and the mean XS/CA ratio for all relict caves has the high value of 20.3m^2km^{-2}, suggesting that a large proportion of cave development occurred in relict caves before the establishment of present hydrological conditions.

Table 5.19 Zonal variations of relict cave dimensions

Zone	No. of relict caves	Relict % per zone	Relict cave length % per zone	Mean relict cave length (m)	Mean relict cave VR (m)	Mean relict cave min. HG (%)	Mean relict cave XS (m^2)	Mean relict cave volume (m^3)	Mean relict cave CA (km^2)	Mean relict cave XS/CA (m^2km^{-2})
Z9	1	100	100	25	5.0	20	10.0	250	0.2	50.0
Z1	4	100	100	8	2.3	34	5.5	49	0.1	55.0
Z2	45	27	16	38	6.4	26	4.5	168	1.7	16.8
Z3	15	42	12	28	5.2	37	1.9	57	2.6	2.8
Z4	99	54	21	31	6.8	41	2.5	83	1.0	42.8
Z5	15	19	5	28	4.5	29	3.2	202	2.0	2.6
Z6	16	25	7	24	5.0	39	2.6	106	3.2	2.1
Z7	19	22	8	19	5.8	37	5.9	255	3.8	8.3
Z8	2	25	2	7	2.0	29	2.0	14	0.3	6.7
ZA	11	30	22	80	6.6	30	3.5	306	3.5	3.6
ZB	3	43	79	371	11.0	27	4.0	1163	3.2	7.6
ZC	22	38	6	16	4.3	29	2.1	42	2.3	2.1
KU	22	18	5	23	5.6	23	1.6	57	7.0	0.6
KL	5	17	2	24	4.4	33	4.7	170	20.8	0.3
KB	0									
ALL RELICT	279	32	13	34	5.9	34	3.1	131	2.6	20.3
ALL CAVES	884	100	100	85	8.8	27	3.5	474	4.0	11.9

Shaded zones have <35 caves. Relict caves have CS=0

Photo 5.1 Oxbow Passage, Jegerhullet (Z4)
A relict phreatic passage, with cross-sectional area somewhat larger than the mean for all relict caves.
Photo by Pete Hann

Table 5.20 lists relict caves that are ≥100m long or ≥40m deep. This shows that the longer relict caves are biased towards the western zones (especially Z4), as none occur stratigraphically lower than ZB, and, therefore, there are none in Sweden. They also occur in most external attribute classes, but not with T=1 (because of the western bias), and only one is below the deglacial marine limit. Three are in 're-metamorphosed' karst (R=1), a representative proportion. The maximum length is 900m, but the maximum VR is only 40m. The trend for west-facing relict caves to be longer is confirmed, because 44% of this group lie to the west compared with only 21% for all relict caves. Only eight relict caves have lengths ≥200m. The short mean length of relict caves may be explained by an increased probability of allogenic streams to enter caves that are longer, thereby forming combination caves. Their restricted mean vertical range arises from the absence of a vadose entrenchment phase.

Table 5.20 Longest and deepest relict caves

RELICT CAVES	L (m)	VR (m)	SD	Z	C	R	T	GS	CL	KT	SR	OR	CA (km^2)	CT	Min. HG %	XS/CA (m^2km^{-2})
Akersvanngrotta	900	20	15?	ZB	N	0	0	K	G	L	N	N	1.0	c	2	2.0
Sarvejaellagrotta	411	31	24	Z4	N	0	0	L	W	A	U	P	0.1	h	8	15.0
Two Bridges Cave	395	36	30	Z2	N	1	0	K	W	A	D	P	1.5	h	9	2.0
Øyåskjeleren	300	15	15	Z4	N	0	0	H	S	V	N	P	0.1	f	5	10.0
Revhølet	268	15?	20?	ZA	N	0	0	K	G	L	U	P	5.0	g	6	0.8
200m Grotta	250	15?	20?	ZA	N	0	0	K	G	L	U	P	5.0	d	6	0.8
Leirskarelvgrotta	210	10?	10?	ZB	N	0	0	K	F	A	N	P	8.5	l	5	0.9
Dripsteinhola	200	30	30	Z6	N	1	0	K	G	A	D	P	0.8	h	15	7.5
Balcony Cave	175	18	14	Z3	N	0	0	H	W	A	D	P	25.0	f	10	0.1
Kalkdalgrotta	165	16	16	Z2	N	0	0	D	G	A	N	P	1.8	b	10	1.2
Saeterbekkgrotta	153	9	9	Z5	N	0	0	L	F	A	N	P	4.0	a	6	1.2
Musk Cave	150	30?	30?	Z4	N	0	0	L	W	A	U	P	0.01	b	20	400.0
Ridge Pot	140	13	13	Z4	N	0	0	L	G	A	N	P	0.1	g	9	10.0
Fault cave	119	16	16	Z4	N	0	0	T	R	V	N	P	0.7	d	13	8.6
Kidney Lake Cave	114	16	16	Z4	N	0	0	T	R	V	N	P	0.8	b	14	7.5
Grotte Aug. 82	60	40	40	Z2	N	1	0	L	F	A	N	P	0.5	e	67	6.0

SD: Max. Subsurface Cave Distance (m) Z: Zone C: Country N: Norway S: Sweden

Many cave types are represented in Table 5.20 and catchment areas and minimum HGs are very variable, showing that this group of caves seems to have even more 'random' attributes than the total set. The individual XS/CA ratios show a large range (0.1–400 m^2km^{-2}). Several small relict caves in the study area have even smaller ratios (min: 0.03m^2km^{-2}), whereas **Shelter Cave** (Z4) has a ratio of 800m^2km^{-2}, the greatest in the whole study area, giving a spread of four orders of magnitude. Because of their phreatic nature, those relict caves with small ratios cannot be considered to have developed in present conditions, as can be assumed for active caves with small XS/CA ratios. Rather, there is just *no relationship* between present catchment area and the dimensions of relict caves.

The only relict type h cave additional to the three listed in Table 5.20 is the short **Draugenshullet** (Z2), which is in LAK, unlike the other relict type h caves that are in ASK. All but **Sarvejaellagrotta** are in 're-metamorphosed' limestone, and all have CL=W, except **Dripsteinhola**, which has CL=G.

5.4.2 Mainly vadose caves (MV)

A large proportion of the caves appear to be 'immature' in their development, identified in the cave databases as mainly vadose (MV=1). All these caves are active, with one or more cave streams (CS>0), and they seem to have developed primarily under vadose conditions. They may include active phreatic sections (sumps) along their streamways, but they do not contain separate relict phreatic passages or significant phreatic upper levels above the stream passages. Some of the caves include relict vadose passages (RV), but as these caves are all active, this probably represents rather recent stream capture within the same cave. Most of this class comprises active shafts (CT=S) and cave types a–d, in accordance with their definitions. For convenience, this class also includes a few short caves that are mainly submerged, including sumped resurgences. One such cave is a hybrid, **Aunholet** (Z2), and another, **Nedre Laksfors Rising** (Z5), is assigned cave type f, because it consists of a flooded resurgence dived to the top of a shaft.

It seems likely that these caves evolved to their present morphology and dimensions under climatic conditions similar to those of the present, and they may therefore differ fundamentally from caves with significant relict phreatic development. The occurrence of mainly vadose caves in each zone is shown in Table 5.21. From these data, 245 of the total 884 caves (28%) are mainly vadose, although this proportion varies considerably and non-systematically across the zones. Mainly vadose caves account for only 9% of total passage length. They have a mean length of only 26m and the means of XS, volume and VR are similarly restricted. However, zonal mean catchment areas are commonly large, and the mean XS/CA ratios are commonly small, showing that MV cave development is, indeed, closely related to present hydrology. The mean dimensions of MV caves in zones ZC, KU and KL are commonly smaller than the total MV means, suggesting that vadose development is driven by the present hydraulic gradient, which reduces in the softer scenery in Sweden. Although a full statistical treatment is needed for this subject, these preliminary findings provide evidence to support *Lauritzen's Conjecture* that the caves in Norway fall into two sets: those whose dimensions are related to present catchment areas, and those that are not (S-E Lauritzen, pers. comm., 1998).

Table 5.22 lists the 13 mainly vadose caves that are ≥100m long. As with the longer relict caves (section 5.4.1), these longer MV caves are biased towards the western zones, with none east of ZB, and, therefore, none in Sweden. This explains why none have T=1, nor KT= L. Two caves have R=1, which is quite representative. The cave locations are biased towards valley floors and walls, as may be expected. Their glacial situations are almost all above marine limits, with GS=K, L and T each having four representatives, showing no east to west bias between GS=L and K. The maximum length is only 208m, and the maximum vertical range is only 22m. Minimum HGs are restricted to the range 3–19%, with possibly an inverse relationship with cave length. The short MV mean cave length is explained by the extremely epigean nature of MV cave development, as all MV caves lie within 20m of the surface, and truncation is therefore more likely. The MV restricted vertical ranges arise from the absence of a significant phreatic development phase.

Table 5.21 Zonal variations of mainly vadose cave dimensions

Zone	No. of MV caves	MV % per zone	MV cave length % per zone	Mean MV cave length (m)	Mean MV cave VR (m)	Mean MV cave min. HG (%)	Mean MV cave XS (m^2)	Mean MV cave volume (m^3)	Mean MV cave CA (km^2)	Mean MV cave XS/CA (m^2km^{-2})
Z9	0									
Z1	0									
Z2	62	38	15	27	4.0	24	2.3	65	2.5	3.9
Z3	13	36	7	17	4.2	44	1.6	38	0.6	5.6
Z4	16	9	1	13	2.7	32	1.4	22	3.9	5.4
Z5	33	42	18	43	6.5	29	1.9	86	1.8	1.9
Z6	14	22	6	21	3.6	23	1.9	49	3.0	1.4
Z7	41	47	26	30	4.1	34	2.6	90	7.0	1.9
Z8	3	38	9	24	2.7	17	1.0	24	0.2	5.0
ZA	8	22	4	21	2.9	16	2.5	58	5.9	1.3
ZB	2	29	12	85	4.0	9	2.0	235	8.5	0.2
ZC	4	7	1	12	3.5	34	1.6	35	0.8	2.8
KU	40	32	8	19	2.3	22	2.0	37	7.3	1.4
KL	7	24	2	19	1.5	11	2.1	45	26.7	0.4
KB	2	100	100	35	7.0	19	2.1	71	0.3	12.1
ALL MV	245	28	9	26	3.9	27	2.1	62	4.7	2.8
ALL CAVES	884	100	100	85	8.8	27	3.5	474	4.0	11.9

Table 5.22 Longest mainly vadose caves

MAINLY VADOSE CAVES	L (m)	VR (m)	SD	Z	C	R	T	GS	CL	KT	SR	OR	CA (km^2)	CT	Min. HG %	XS/CA (m^2km^{-2})
Col Cave	208	15	10	Z5	N	0	0	T	W	V	N	P	1.2	a	7	0.8
Doorway Cave	182	5	5	Z7	N	0	0	L	G	V	N	P	0.5	b	3	4.0
Saeterfjellhullet	180	20	20	Z2	N	1	0	L	W	A	U	A	0.2	d	11	7.5
Drowning Cave	174	9	9	Z5	N	0	0	L	W	A	N	P	3.0	b	5	0.3
Rainbow Cave	160	22	5	Z5	N	0	0	T	W	V	N	P	1.2	b	14	3.3
Tøimskar Stream Cave	160	12	12	Z7	N	0	0	L	G	V	N	P	0.7	a	8	2.9
Gully Sinks	150	5?	5?	ZB	N	0	0	K	F	A	N	P	8.5	d	3	0.4
Cascade Pot	144	11	10	Z5	N	0	0	T	F	V	N	P	1.5	b	8	1.3
Memorial Cave	126	5	5	Z7	N	0	0	K	F	A	N	P	15.0	c	4	0.3
Cairn Pot	113	15	10	Z5	N	0	0	T	W	V	N	P	1.3	b	13	1.5
Whirlpool Cave	107	6	6	Z7	N	0	0	K	F	A	N	P	15.0	d	6	0.3
Trap Cave	105	20	4	Z2	N	1	0	H	R	V	N	P	0.7	b	19	2.9
Dåaranjueniehola	100	15	15	Z3	N	0	0	K	F	A	N	A	0.5	a	15	6.0

SD: Max. Subsurface Cave Distance (m) Z: Zone C: Country N: Norway S: Sweden

The catchment areas of the caves in Table 5.22 are quite variable, without an apparent relationship with cave length, but their XS/CA ratios have a fairly tight spread, because the highest, **Saeterfjellhullet** (Z2, $7.5m^2km^{-2}$) has a value that is well inside the study area mean of $11.9m^2km^{-2}$. The mean XS/CA ratio for these caves is $2.4m^2km^{-2}$, which is even lower than that for all MV caves of $2.8m^2km^{-2}$ (Table 5.21). The full range of XS/CA ratios for all MV caves is from 0.01–$25m^2km^{-2}$ (**Blade Crawl**, Z7 to **Cave 2N2**, Elgfjell, Z4). Thus, it could be estimated initially that any cave with an XS/CA ratio above about $25m^2km^{-2}$ (or perhaps a lower limit) cannot have enlarged solely under present conditions. The reason for the extremely variable catchment areas and XS/CA ratios even for MV caves could be that, from the

method of estimation (Appendix C2.1), the CA values in the cave databases do not represent accurately the annual recharge at each cave, because, depending on topography, much of the precipitation could bypass the caves and / or overflow them at high stage. Figure 5.4 shows how cave cross-section varies with estimated catchment area for each of the MV caves and that there appears to be a relationship between the *maximum* cave cross-section and the logarithm of its catchment area (ignoring the special case of the **Svartås Doline**, Z2):

Maximum MV cave XS ≈ c. 3(2+logCA) m^2, where CA is expressed in km^2.

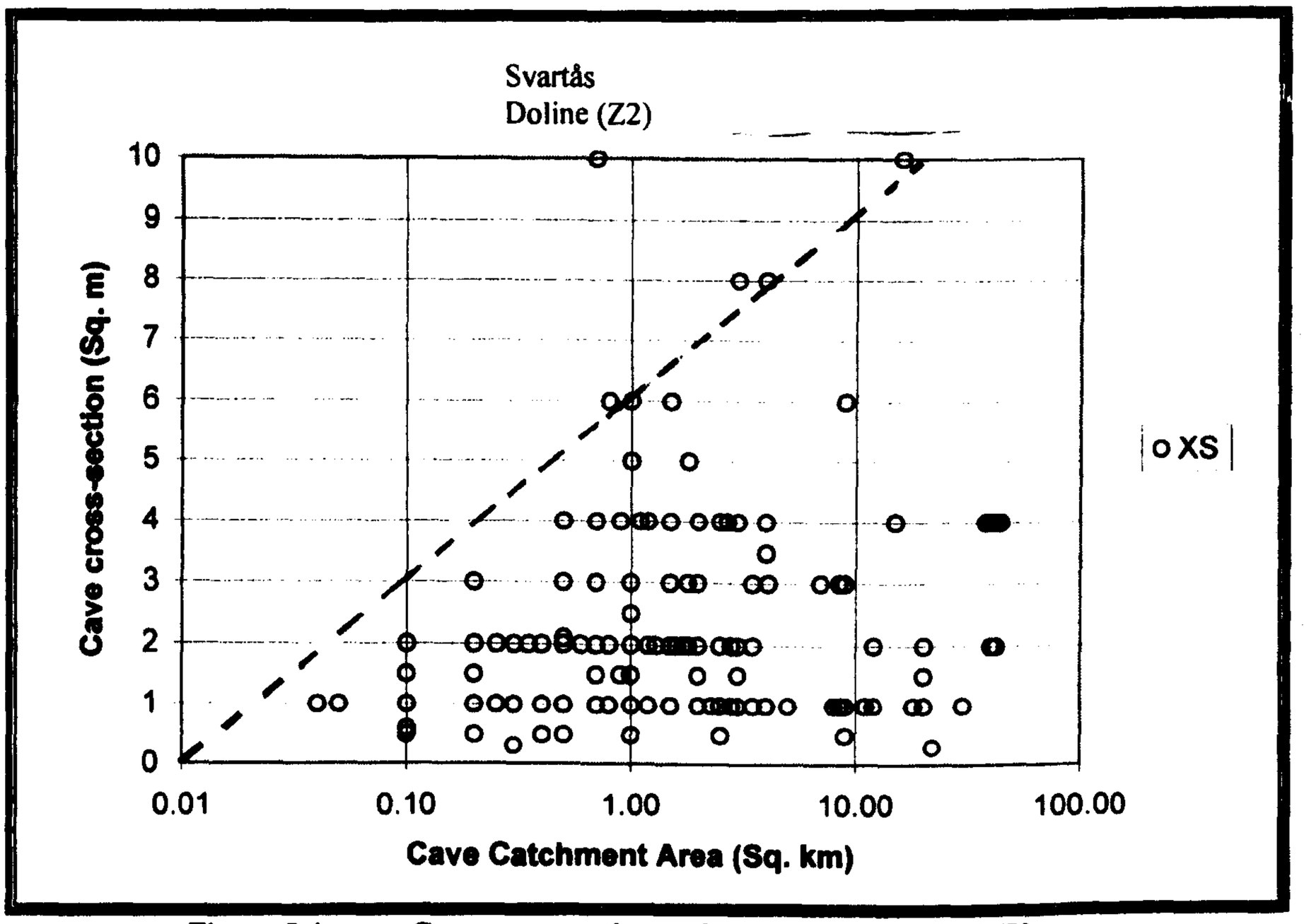

Figure 5.4 Cave cross-section and catchment area for MV caves

Figures 5.5 and 5.6 also illustrate possible relationships between maximum cave length and volume and the logarithm of catchment area:

Maximum MV cave length ≈ c. 60(2+logCA) m

Maximum MV cave volume ≈ c. 150(2+logCA) m^3

The constant values in these equations were determined from plots of MV caves at valley floors (CL=F), which are more likely to capture the full flows from their catchment areas (not shown separately). The three equations are not mathematically consistent when taken together, because they do not represent any one cave, but the maximum envelope obeyed by all MV caves. It is rare for a cave to approach the maximum for more than one of these dimensions. No such simple relationships exist for non-MV caves (the great majority), because they can have large dimensions with very small catchment areas.

Whereas a consistent relationship between cross-section and catchment area can be visualised conceptually, one between cave length and catchment area is not so obvious. However, caves are only explorable above a cross-sectional size related to the human body, and the internal variations in cross-

section, whether caused by changes in passage size or changes in sediment thicknesses, means that exploration length, and therefore also the recorded volume, is a function of cross-section, at least for smaller caves, such as these MV caves.

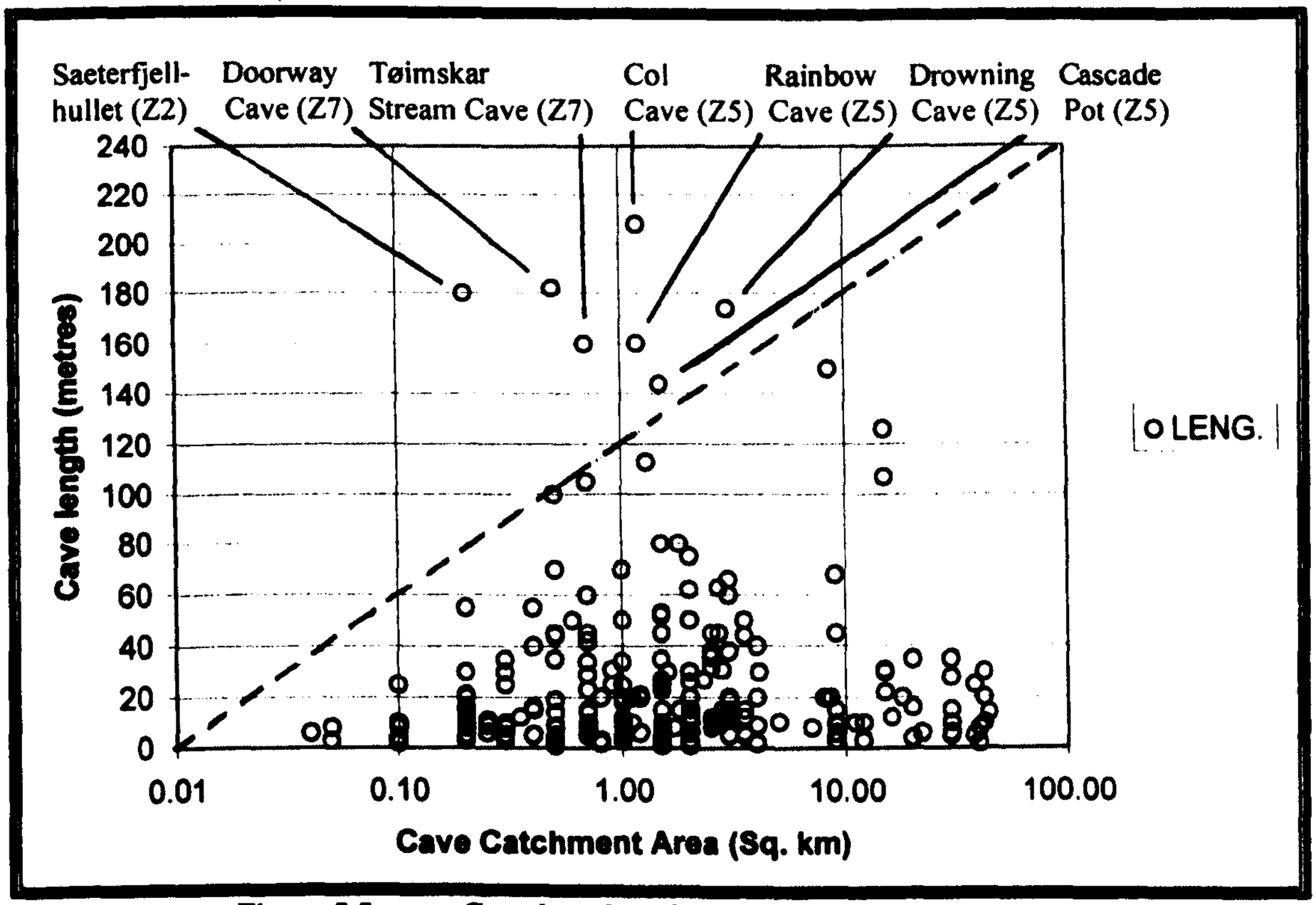

Figure 5.5 Cave length and catchment area for MV caves

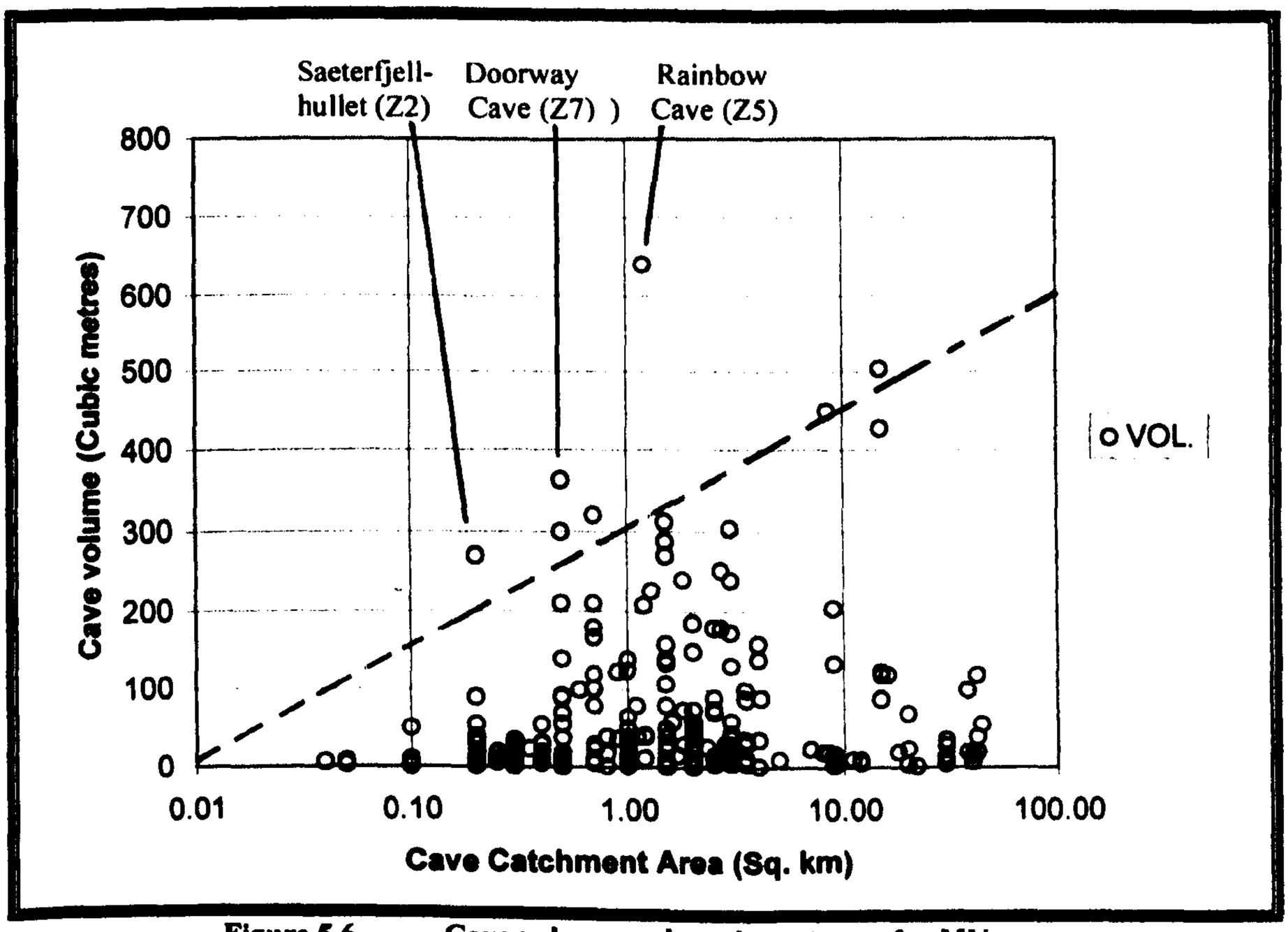

Figure 5.6 Cave volume and catchment area for MV caves

Figure 5.5 suggests (for example) that it is only possible to explore truly vadose caves that are longer than 120m if they have a catchment area $\geq 1 km^2$, which is equivalent to a mean continuous flow rate c. $32 Ls^{-1}$ throughout the Holocene, assuming a mean Holocene infiltration rate of $1 ma^{-1}$.

Those few caves shown above the 'maximum' lines in Figures 5.5 and 5.6 probably illustrate some difficulty in distinguishing between border-line MV caves and combination caves, when the study is restricted to cave surveys. Indeed, it may now be possible to invert this discussion, and conclude that those caves cannot really have formed entirely by vadose processes, because they fall above the 'maximum' lines. On this basis, at least the top six caves in Table 5.22 may be too long to have developed wholly within the Holocene, although their cross-sections do lie within the limits of Figure 5.4. Furthermore, although the three formulae appear to apply for CA≤10km^2, some of the few caves plotted with XS≥6m^2 on Figure 5.4 (at a CA ≥1km^2) have short, presumably phreatic, oxbows, and others are primarily short passages to sumps at sinks and resurgences, whilst still fulfilling the criteria for the MV class. Thus, caves assigned to the MV class with XS>c. 6m^2 may be transitional between fully vadose caves and combination caves, or else they may represent those few active caves that have developed primarily by phreatic processes during the Holocene.

There are probably no examples of MV caves with a vadose entrenchment greater than 3m (except, perhaps, at shafts), which implies a maximum Holocene floor-lowering rate of c. 0.3mma^{-1} from the effects of both chemical and mechanical erosion. **Skrømthølet** (KU) is the (water-filled) MV cave with the largest cross-section (10m^2). A Holocene enlargement to this size would require a dissolutional wall retreat rate of c. 0.2mm a^{-1}, which is well below the maximum 1mma^{-1} allowed by the Palmer / Dreybrodt model (section 3.1.13). Therefore, all the above findings about MV caves are consistent with these caves enlarging to present sizes during the time of the Holocene. MV caves that plot well below the maximum lines may either not capture the full flow from their catchment areas, or else they did not start to enlarge until after the beginning of the Holocene period. Additionally, some lengths and volumes may be constrained by the dimensions of the containing metacarbonate outcrops.

The formula for maximum XS shows that the use of a simple XS/CA ratio to determine if a cave could have developed wholly from vadose processes (as initially estimated above) is incorrect. Instead, it is concluded that a cave could be entirely vadose only if XS ≤ 6m^2 and XS ≤ 3(2+logCA) m^2. To compare this with the previous estimate, for catchments from 0.03–1.00–10km^2, the maximum XS/CA ratio for caves to develop wholly by vadose processes within the Holocene varies from 50–6–0.9m^{2}km^{-2}.

5.4.3 Combination caves (CC)

The combination class of cave includes all those that are not counted as relict or mainly vadose, i.e. those caves that contain *both* relict phreatic passages or levels, and active streamways. It also includes the active caves (CS>0) of cave type S, Hy, I, L and T, although the morphologies of these caves have not been studied in detail. More caves that are mainly shafts (CT=S) could perhaps be assigned as mainly vadose (MV=1), although some may have developed nearly to their present sizes during deglacial outflows under both phreatic and vadose conditions.

Combination caves account for 360 (41%) of the recorded caves, the percentages varying non-systematically across the inner zones (Tables 5.23). Mean cave dimensions are consistently large, although the mean minimum HG and the mean XS/CA ratio are close to the study area averages. The longest and deepest caves in the study area (as listed in tables 5.16, 5.17 and 5.18) are almost invariably combination caves: the only significant exception is **Akersvanngrotta** (ZB), a relict cave of length 900m.

Table 5.23 Zonal variations of combination cave dimensions

Zone	No. of comb. caves	Comb. caves % per zone	Comb. cave length % per zone	Mean comb. cave length (m)	Mean comb cave VR (m)	Mean comb cave min. HG (%)	Mean comb cave XS (m^2)	Mean comb. cave volume (m^3)	Mean comb cave CA (km^2)	Mean comb. cave XS/CA (m^2km^{-2})
Z9	0									
Z1	0									
Z2	58	35	69	130	12.7	18	4.7	677	1.7	11.9
Z3	8	22	81	336	29.9	19	3.8	1863	3.7	6.5
Z4	67	37	77	167	14.4	21	3.8	1010	3.0	38.2
Z5	31	39	76	189	15.7	22	4.5	1121	1.7	4.8
Z6	34	53	87	133	13.2	15	4.7	707	7.4	6.2
Z7	27	31	67	119	10.3	21	5.5	1031	5.1	3.5
Z8	3	38	90	247	20.0	10	3.7	1263	0.2	15.0
ZA	18	49	73	160	21.9	24	8.2	1564	6.5	2.9
ZB	2	29	9	63	17.5	33	18.0	1686	2.2	8.2
ZC	32	55	93	170	9.0	28	4.2	820	3.4	2.1
KU	63	50	87	133	13.2	29	5.2	1007	5.1	3.6
KL	17	59	96	380	13.1	30	4.4	1986	17.7	0.4
KB	0									
ALL COMB.	360	41	79	164	14.5	23	4.8	1020	4.6	11.6
ALL CAVES	884	100	100	85	8.8	27	3.5	474	4.0	11.9

5.5 Cave classes compared

This section reviews how the three hydrological cave classes and their cave types compare amongst each other and how they are influenced by karst type, contact metamorphism and thrusting, cave location and glacial situation.

5.5.1 Occurrences and dimensions

The major cave dimensions for each of the three cave classes against cave types and the four main external attributes were derived from pivot tables, as listed in Tables 5.24–5.28 in the following sections. Their overall occurrences are: relict 32%, mainly vadose 28% and combination 41%. Because the mean lengths of relict caves and MV caves are only 34m and 26m, 79% (c. 59km) of total passage length (c. 75km) is contained in combination caves, which have a mean length of 164m. It is hypothesised here that most relict caves and the set of mainly vadose caves have each separately experienced only one phase of cave enlargement after inception, whereas the combination caves are more representative of the range of enlargement opportunities that were available to the caves during the local geomorphological evolution.

The total study area mean cave length, VR, XS and volume *all* increase in the order mainly vadose: relict: combination, with mean values always much greater for combination caves. This is expected for MV caves, because they mainly comprise cave types a–d. The order is consistently maintained for each classification for all cave types and for all four external cave attributes, except that the rank orders of MV and relict caves are sporadically reversed, commonly for small sample sizes that still give similar values. Overall mean minimum HGs are greatest for relict caves, and least for combination caves. They vary among the external attributes and their detailed classifications.

The overall mean catchment areas increase in the order relict: combination: mainly vadose caves, whereas XS/CA ratios decrease in the same order, so that combination caves appear to be transitional between the relict caves, whose dimensions are independent of CA (section 5.4.1), and the MV caves, whose *maximum* dimensions are related to CA by simple formulae (section 5.4.2). If this is the case, then a proportion of the mean XS of combination caves may be quantitatively attributable to the present vadose mechanical and chemical erosion, and the rest to development under different climatic conditions. Thus, the maximum dimensions of the lowest, presently-active, parts of combination caves should be governed by the same formulae as the MV caves, so that their minimum relict dimensions could be obtained by subtraction. This means that the higher the ratio of XS/CA for a study area cave, then the smaller is the proportion of vadose development experienced. Because it is deduced in section 5.5.6 that MV caves enlarged during the Holocene, it also follows that the smaller is the XS/CA ratio, then the 'younger' is the cave. The use of this method to illustrate development phases of individual caves is beyond the scope of this thesis. However, as an example, the large combination cave **Stor Grubblandsgrotta** (KU, Appendix B1.13) has CA=19km^2 and a mean XS=c. 6m^2, giving an XS/CA ratio of only 0.3m^{2}km^{-2}. From the relationships proposed at the end of section 5.4.2, all its explored passages could have developed under vadose conditions within the Holocene, if cave morphology is ignored.

From Tables 5.25–5.28, the cave class CA order is maintained for 5 of 20 major external attribute classifications, but in eight places combination caves have greater mean CAs than mainly vadose caves. Paradoxically, in three places (CL=P and GS=G and H) combination caves have smaller mean CAs than relict caves and in six places (CL=S and R (small samples), CL=W, GS=S, T and G (small samples)) mainly vadose caves have the smallest mean CAs of all classes, or they are all similar. The mean XS/CA ratio order is maintained for 13 of the 20 classifications, but combination caves have higher values than relict caves in four places. In three places (R=0 and T=1, CL=P and GS=S (small sample)) relict caves have the smallest mean XS/CA ratio of all classes. On no occasion does an MV cave have the highest XS/CA ratio.

A conclusion from this analysis is that the overall study area finding that vadose development is related to larger CAs and smaller XS/CA ratios and that phreatic development tends to obey the reverse rule is

maintained fairly well for most classifications of the external attributes. Mainly vadose caves are the most restricted in their dimensional development of the three hydrological cave classes, suggesting that they have experienced less efficient cave enlarging processes, perhaps over shorter periods of time, than the other two classes. The frequencies and mean dimensions of type h combination caves for each external attribute have values almost identical to those of the full set of type h caves (Tables 5.7, 5.9, 5.11 and 5.15), because combination caves account for 90% of all type h caves.

5.5.2 Cave classes and cave types

Table 5.24 shows how the attributes of the caves of each hydrological class vary with cave type. The numbers of relict caves, mainly vadose caves and combination caves of each cave type (a–h) tend to reduce with complexity (except that combination cave types f–h actually increase), whereas the mean cave length, mean vertical range and mean volume tend to increase, but more sporadically than for the total set of caves (Table 5.5). The means of these values for relict and mainly vadose caves for each of the cave types a–h are less or much less than the means for combination caves. Additionally, the means of these values for all the relict caves and for all the mainly vadose caves are also all much less than the means of the values for all combination caves. These consistently reduced dimensions provide some quantification to the hypothesis that both the relict caves and the mainly vadose caves have experienced less 'development', in terms of timescale and / or processes, than the combination caves.

The mean minimum hydraulic gradients show a reducing trend with cave type for all cave classes, as found with the total set of caves, with relict cave values being commonly greater than combination cave values and similar to MV cave values for cave types a–d. This suggests that minimum hydraulic gradient is little influenced by a cave being relict or active, being mainly influenced by cave length.

Mean cross-sections of relict and MV caves are less than for the combination caves for all cave types. Mean catchment areas of relict caves are commonly lower than those of MV caves and combination caves, which might explain why these caves are, indeed, relict. The MV shafts (CT=S) appear to have greater mean XS and XS/CA values than the other MV caves, suggesting that they either enlarged faster than the vadose passages (section 3.1.16), or that some of this sample is incorrectly assigned.

Mean XS and mean CA show little relationship with cave type a–h for relict and combination caves, strongly suggesting that these caves did not develop primarily under present hydrological conditions. However, MV caves appear to have increasing trends for both values for cave types a–d (which increase in mean length), as expected from the discussion in section 5.4.2. Additionally, the mean XS/CA ratios are small and close together for MV caves type a–d and the rank order of decreasing XS/CA ratios for relict: combination: MV caves is maintained for most cave types. This supports the concept that the maximum dimensions of MV caves are controlled by their present catchment areas, which also control the maximum vadose passage dimensions of the intermediate combination caves.

5.5.3 Cave classes and karst types

Karst type trends (Table 5.25) display interesting variations when considering the standard order V:A:L of decreasing foliation dip. Because these karst types all occur in the approximate ratios of 2:4:1 for MV, relict and combination caves, the cave hydrological classes appear to be distributed fairly randomly amongst each other. The karst types themselves exert little influence on the *existence* of caves in each hydrological class, because their occurrence frequencies are remarkably consistent for KT=V, A and L. Mean length and volume commonly decrease in the standard order for mainly vadose caves, but increase for relict caves, and are at a minimum for the large population with KT=A for the intermediate combination caves. Mean VR and mean minimum HG decrease for both MV and relict caves, but commonly increase for combination caves. These particular trends *do* seem to be direct functions of foliation dip, as they are not apparent in an east or west direction across the zones (Tables 5.19, 5.21 and 5.23). Mean XS increases for combination caves, but relict and MV caves show no trend. On the other hand, mean CA increases for MV caves and relict caves (probably just following the eastern trend of more subdued scenery into Sweden), but show no trend for combination caves. The mean XS/CA ratios peak for KT=A for relict and combination caves, but decrease in sympathy with the CA increase for MV caves.

Table 5.25 Cave dimensions, cave hydrological classes and karst types

Cave hydrological class	Dim. — KT	No. of caves	% of class	Mean cave length (m)	Mean cave VR (m)	Mean cave min. HG (%)	Mean cave XS (m^2)	Mean cave volume (m^3)	Mean cave CA (km^2)	Mean cave XS/CA (m^2km^{-2})
Mainly vadose	V	78	31.8	29	4.8	34	1.8	63	2.1	3.0
Mainly vadose	A	119	48.6	28	3.8	22	2.3	71	5.9	2.7
Mainly vadose	L	35	14.3	18	2.9	23	1.8	35	8.1	2.5
Mainly vadose	C									
Mainly vadose	X	13	5.3	16	2.3	26	2.3	41	1.3	3.3
MV	ALL	245	27.7*	26	3.9	27	2.1	62	4.7	2.8
Relict	V	75	26.9	25	6.5	45	3.1	76	1.6	17.2
Relict	A	153	54.8	34	6.2	31	3.4	155	2.7	25.9
Relict	L	38	13.6	57	4.5	22	2.6	171	4.9	8.4
Relict	C									
Relict	X	13	4.7	19	3.8	36	2.5	53	0.7	7.0
RELICT	ALL	279	31.6*	34	5.9	34	3.1	131	2.6	20.3
Combination	V	82	22.8	196	14.1	20	4.1	1187	6.1	6.4
Combination	A	208	57.8	141	14.1	23	4.9	833	3.9	16.3
Combination	L	54	15.0	182	17.4	27	5.9	1511	5.6	3.7
Combination	C	3	0.8	968	17.3	7	3.2	3738	1.9	1.7
Combination	X	13	3.6	65	10.5	24	4.5	288	2.6	4.7
COMB.	ALL	360	40.7*	164	14.5	23	4.8	1020	4.6	11.6
All	V	235	26.6	86	8.6	33	3.0	460	3.3	8.7
All	A	480	54.3	79	9.0	25	3.8	428	4.0	16.0
All	L	127	14.4	100	9.5	25	3.8	703	6.1	4.8
All	C	3	0.3	968	17.3	7	3.2	3738	1.9	1.7
All	X	39	4.4	33	5.5	29	3.1	127	1.5	5.0
ALL	ALL	884	100.0	85	8.8	27	3.5	474	4.0	11.9

* % of all caves

Table 5.24 Cave dimensions, cave hydrological classes and cave types

Cave hydrological class	Dim. — CT	No. of caves	% of class	Mean cave length (m)	Mean cave VR (m)	Mean cave min. HG (%)	Mean cave XS (m^2)	Mean cave volume (m^3)	Mean cave CA (km^2)	Mean cave XS/CA (m^2km^{-2})
Mainly vadose	S	20	8.2	8	4.9	71	2.7	21	2.8	**5.6**
Mainly vadose	a	114	46.5	18	2.9	29	1.7	37	4.2	**2.4**
Mainly vadose	b	78	31.8	36	4.7	16	2.3	85	5.8	**2.6**
Mainly vadose	c	13	5.3	37	4.5	19	2.2	99	3.4	**2.1**
Mainly vadose	d	18	7.3	53	5.1	12	2.6	135	6.8	**3.3**
Mainly vadose	f	1	0.4	15	6.0	40	2.0	30	3.0	**0.7**
Mainly vadose	Hy	1	0.4	27	4.0	15	4.0	108	1.5	**2.7**
MV	ALL	245	27.7*	26	3.9	27	2.1	62	4.7	**2.8**
TOT. SUBSET	S, a-d	751	85.0*	46	6.6	29	3.4	257	4.1	**11.1**
Relict	S	47	16.8	11	8.0	85	3.2	44	1.3	**14.5**
Relict	a	112	40.1	17	4.0	28	3.2	103	3.0	**11.2**
Relict	b	64	22.9	31	5.4	19	2.0	80	1.9	**32.5**
Relict	c	14	5.0	108	6.6	18	3.9	333	6.4	**9.4**
Relict	d	10	3.6	69	7.1	16	3.2	301	2.1	**87.1**
Relict	e	3	1.1	34	14.7	35	1.7	74	3.3	**2.3**
Relict	f	6	2.2	111	11.3	15	2.0	186	5.1	**7.7**
Relict	g	3	1.1	149	12.7	13	2.3	431	1.8	**6.9**
Relict	h	4	1.4	264	27.5	14	3.6	800	0.7	**9.5**
Relict	Hy	6	2.2	30	4.8	20	9.4	340	1.0	**44.6**
Relict	I	1	0.4	210	10.0	5	8.0	1680	8.5	**0.9**
Relict	L	6	2.2	10	3.0	39	7.3	85	0.8	**42.8**
Relict	T	3	1.1	14	3.0	28	3.3	63	9.4	**2.9**
RELICT	ALL	279	31.6*	34	5.9	34	3.1	131	2.6	**20.3**
Combination	S	23	6.4	12	8.1	80	3.3	46	3.1	**6.2**
Combination	a	89	24.7	35	6.4	27	4.8	276	4.2	**7.4**
Combination	b	88	24.4	77	11.9	20	5.4	581	5.4	**12.0**
Combination	c	30	8.3	147	9.9	9	4.3	729	7.8	**8.4**
Combination	d	31	8.6	197	18.0	13	4.8	1453	5.1	**7.7**
Combination	e	14	3.9	150	14.7	16	4.2	832	3.5	**2.6**
Combination	f	16	4.4	171	17.5	14	3.2	602	3.9	**7.4**
Combination	g	25	6.9	263	21.6	18	4.9	1805	3.1	**44.6**
Combination	h	35	9.7	753	39.9	10	4.7	4325	3.0	**10.8**
Combination	Hy	5	1.4	80	14.4	23	12.2	875	5.4	**4.1**
Combination	I	2	0.6	33	11.5	47	1.5	63	6.3	**0.3**
Combination	L	1	0.3	21	4.0	19	6.0	126	14.0	**0.4**
Combination	T	1	0.3	72	29.0	40	16.0	1152	0.1	**160.0**
COMB.	ALL	360	40.7*	164	14.5	23	4.8	1020	4.6	**11.6**
All	S	90	10.2	10	7.3	81	3.1	39	2.1	**10.4**
All	a	315	35.6	22	4.2	28	3.1	128	3.8	**7.0**
All	b	230	26.0	50	7.7	18	3.4	273	4.6	**14.5**
All	c	57	6.4	112	7.8	14	3.7	488	6.5	**7.2**
All	d	59	6.7	132	12.2	13	3.8	856	5.1	**19.8**
All	e	17	1.9	130	14.7	20	3.7	699	3.5	**2.6**
All	f	23	2.6	148	15.4	15	2.8	469	4.2	**7.2**
All	g	28	3.2	251	20.6	18	4.6	1657	3.0	**40.5**
All	h	39	4.4	703	38.6	11	4.6	3964	2.7	**10.7**
All	Hy	12	1.4	50	8.8	21	10.1	544	2.9	**24.2**
All	I	3	0.3	92	11.0	33	3.7	602	7.0	**0.5**
All	L	7	0.8	12	3.1	36	7.1	91	2.7	**36.8**
All	T	4	0.5	29	9.5	31	6.5	335	7.1	**42.1**
ALL	ALL	**884**	100.0	**85**	**8.8**	**27**	**3.5**	**474**	**4.0**	**11.9**

* % of all caves

From these results, it is inferred that steep foliations favour longer vadose caves but shorter phreatic caves, and low angle foliations favour the reverse. Vertical range is paradoxical, because steep foliations seem to favour deeper vadose *and* relict phreatic caves, perhaps up to a particular depth, but low angle karst favours deeper caves with combinations of vadose and relict phreatic passages. The larger cross-sections in low angle karst for combination caves may be explained by this karst favouring *vadose* passage entrenchment, as well as the opening of deeper fractures. The smaller mean cross-sections of MV caves and relict caves with KT=L may be artefacts of smaller sample sizes. Additionally, foliation dip may have a neutral effect on the chemical dissolution of phreatic passages in relict caves and combination caves.

5.5.4 Cave classes, contact metamorphism and thrusts

The occurrence percentages of caves in the four contact metamorphism (R=0 or 1) and thrusting (T=0 or 1) combinations are shown in Table 5.26 for each cave hydrological class. 66% of all caves have R=0 and T=0, and this combination has the highest population in all cave classes. The combination R=1 and T=1 only occurs in 1% of the caves, and this small sample is not considered further. The other two combinations display considerable variations in the percentages of the cave classes. Thus, the existence of mainly vadose caves is favoured over both relict caves and combination caves if R=1, and combination caves are strongly favoured over both MV and relict caves if T=1. The latter result may be partly explained, because it is shown below that thrusting seems to favour vadose enlargement. Thus, vadose flows in caves that would otherwise remain relict created more combination caves where T=1.

In contrast to the smaller mean dimensions of combination caves affected by contact metamorphism (R=1), MV cave mean dimensions are similar, most relict cave mean dimensions are only slightly smaller and the relict cave mean VR is actually *larger*. Mean dimensions are greater for combination caves in proximity to a thrust (T=1), except that mean VR is slightly less. However, MV cave mean dimensions are *smaller* if T=1, except that mean cross-section is larger, perhaps following the eastward increase in mean catchment area. Relict cave mean length, cross-section and volume are similar, and only mean VR is much larger. Combination caves have larger mean catchment areas and smaller mean XS/CA ratios for both R=1 and T=1, suggesting a closer relationship to present hydrology and therefore a higher proportion of vadose development in each case. Mainly vadose caves have a larger mean CA for T=1, but each mean XS/CA value remains close to the low overall MV cave mean of $2.8m^2km^{-2}$. This suggests that 'vadose favouring' effects have little impact on vadose caves themselves. Relict caves that do not have R=0 and T=0 demonstrate a proportion of hidden vadose development, because their mean XS/CA ratios are much less for both R=1 and T=1 (when mean CAs are also larger). The trend of eastwardly-increasing catchment area is shown by the smaller total mean CA for R=1 and the larger total mean CA for T=1.

Table 5.26 Cave dimensions, cave classes, contact metamorphism and thrusting

Cave hydro-logical class	Dimension R, T	No. of caves	% of class	Mean cave length (m)	Mean cave VR (m)	Mean cave min. HG (%)	Mean cave XS (m^2)	Mean cave volume (m^3)	Mean cave CA (km^2)	Mean cave XS/CA (m^2km^{-2})
MV	R=0 T=0	142	58.0	28	4.1	29	2.0	64	5.0	2.8
MV	R=1 T=0	82	33.5	26	3.9	24	2.1	63	3.0	2.9
MV	R=0 T=1	18	7.3	20	2.2	19	2.3	46	11.1	2.5
MV	R=1 T=1	3	1.2	24	2.7	17	1.0	24	0.2	5.0
MV	ALL	245	27.7*	26	3.9	27	2.1	62	4.7	2.8
Relict	R=0 T=0	218	78.1	34	5.7	34	3.2	134	2.4	24.0
Relict	R=1 T=0	45	16.1	33	6.6	31	2.7	119	1.7	8.3
Relict	R=0 T=1	14	5.0	31	8.4	38	3.4	139	8.9	1.8
Relict	R=1 T=1	2	0.7	7	2.0	29	2.0	14	0.3	6.7
RELICT	ALL	279	31.6*	34	5.9	34	3.1	131	2.6	20.3
Comb.	R=0 T=0	227	63.1	162	15.1	22	4.9	1039	3.7	14.4
Comb.	R=1 T=0	71	19.7	118	12.1	19	4.2	566	4.1	9.2
Comb.	R=0 T=1	58	16.1	225	14.8	24	5.4	1487	8.9	3.6
Comb.	R=1 T=1	4	1.1	215	18.8	19	5.3	1247	0.9	12.1
COMB.	ALL	360	40.7*	164	14.5	23	4.8	1020	4.6	11.6
All	R=0 T=0	587	66.4	82	8.9	28	3.6	467	3.6	15.2
All	R=1 T=0	198	22.4	61	7.5	24	3.0	256	3.1	6.4
All	R=0 T=1	90	10.2	154	11.3	30	4.4	989	9.4	3.1
All	R=1 T=1	9	1.0	105	9.7	17	3.1	565	0.5	8.5
ALL	ALL	884	100.0	85	8.8	27	3.5	474	4.0	11.9

* % of all caves

The above discussion shows that the earlier simple observations that contact metamorphism and proximity to a thrust act in opposing directions to restrict and to enhance cave development (sections 5.3.2 and 5.3.3) commonly remain valid for combination caves but commonly are not valid for MV and relict caves. The reason is probably that R and T disproportionately influence longer fractures (section 5.3.2), and therefore have a greater effect on the combination caves that are commonly much longer than the relict and MV caves. Additionally, thrusting may only affect combination caves, because they have experienced more than one phase of enlargement after inception. The commonly-smaller mean length of MV caves at T=1 is inexplicable at present, as are the various anomalies concerning the variations in vertical range.

5.5.5 Cave classes and cave locations

Table 5.27 shows that mainly vadose caves and combination caves have cave location occurrences in almost identical rank orders, although the order for relict caves is different. However, there are large variations in the percentage of each cave hydrological class occurring at each cave location. Thus, relict caves disproportionately account for 42%, 63% and 40% of all caves in shoulder, ridge and wall locations (CL=S, R and W), reducing MV occurrences to only 9%, 8% and 21%. (These figures are not shown explicitly in Table 5.27). In the other direction, MV caves account for 37% at valley floors (CL=F), reducing relict caves to 19% there. The small samples at coastal locations (CL=C) have only 13% of combination caves, and are not considered further. Combination caves comprise the largest class

at all other cave locations, except CL=R (29%). Hence, shoulder, ridge and (less importantly) wall locations appear to favour phreatic development over vadose, and floor locations appear to favour the reverse, when compared with the more 'standard' occurrence distributions at the less steep paleic and gently sloping locations (CL=P and G). The MV and combination caves with the largest mean vertical ranges also occur at shoulder, ridge and wall locations, but relict cave mean VRs show little variation about their overall mean of 5.9m, except for low values at CL=P and C. Some active caves at CL=S have lower resurgence entrances at a knick point above a surface waterfall, and so are not at all graded to local topography. This indicates immature vadose development, probably entirely within the Holocene (e.g. **Kvitfjellgrotta**, Z4, Photo C2.4 and the unexplored **Naeverskardhullet**, ZA, Photo C2.6).

Table 5.27 Cave dimensions, cave hydrological classes and cave locations

Cave hydrological class	Dim. — CL	No. of caves	% of class	Mean cave length (m)	Mean cave VR (m)	Mean cave min. HG (%)	Mean cave XS (m^2)	Mean cave volume (m^3)	Mean cave CA (km^2)	Mean cave XS/CA (m^2km^{-2})
MV	P	35	14.3	19	2.3	21	1.7	33	7.7	2.0
MV	G	64	26.1	25	3.8	31	2.2	60	1.6	2.8
MV	S	5	2.0	10	5.6	57	1.4	15	0.2	8.5
MV	R	5	2.0	25	5.6	46	2.0	52	0.9	3.3
MV	W	41	16.7	38	6.1	29	1.8	78	1.0	3.0
MV	F	91	37.1	27	3.4	21	2.3	71	7.2	2.6
MV	C	4	1.6	13	2.8	47	2.4	27	20.7	4.0
MV	ALL	245	27.7*	26	3.9	27	2.1	62	4.7	2.8
Relict	P	26	9.3	17	3.5	24	1.6	44	5.6	1.3
Relict	G	58	20.8	52	6.6	32	2.9	157	1.4	7.2
Relict	S	24	8.6	28	6.5	53	2.2	68	0.7	11.6
Relict	R	39	14.0	32	6.0	32	4.0	160	0.8	25.5
Relict	W	78	28.0	32	6.4	38	2.9	126	1.8	45.8
Relict	F	45	16.1	32	5.9	28	4.2	182	6.3	2.9
Relict	C	9	3.2	10	2.2	28	4.2	47	3.4	26.7
RELICT	ALL	279	31.6*	34	5.9	34	3.1	131	2.6	20.3
Combination	P	49	13.6	159	12.7	31	3.0	810	2.9	2.2
Combination	G	75	20.8	149	13.6	22	6.0	1268	3.2	9.0
Combination	S	28	7.8	185	22.3	23	4.2	1289	1.2	11.2
Combination	R	18	5.0	358	25.9	14	4.6	1754	0.9	50.5
Combination	W	78	21.7	115	15.6	23	3.9	644	1.7	16.9
Combination	F	110	30.6	176	11.3	21	5.7	1036	9.8	7.7
Combination	C	2	0.6	43	6.5	16	6.0	258	8.0	1.7
COMB.	ALL	360	40.7*	164	14.5	23	4.8	1020	4.6	11.6
All	P	110	12.4	81	7.2	26	2.2	382	5.1	1.9
All	G	197	22.3	80	8.4	28	3.9	549	2.2	6.5
All	S	57	6.4	104	14.2	39	3.1	663	0.9	11.1
All	R	62	7.0	126	11.8	28	4.0	614	0.8	31.0
All	W	197	22.3	66	10.0	30	3.1	321	1.6	25.5
All	F	246	27.8	95	7.4	22	4.2	523	8.2	4.9
All	C	15	1.7	15	2.9	31	4.0	70	8.6	17.3
ALL	ALL	884	100.0	85	8.8	27	3.5	474	4.0	11.9

* % of all caves Paired locations are shown by alternate shading

It is convenient to pair cave locations in the commonly 'upward' order CL=F/W: R/S: G/P, although CL=G is not necessarily at a relatively high level. Within these pairings, all internal mean cave dimensions except vertical range commonly decrease upwards for all cave classes. However, there is much less consistency in CAs decreasing upwards (and XS/CA ratios increasing upwards) than for the internal cave dimensions. Apart from VR, mean MV cave dimensions tend to decrease for cave location pairs in the order F/W: G/P: R/S, again showing the lower vadose development in shoulder and ridge locations. The reason may be that vadose water soon drained out of fractures in these locations, reducing the timescale for their enlargement. Relict cave mean lengths hardly vary between the lower two pairings, whereas cross-sections and volumes decrease upwards. Combination caves have the largest mean lengths and volumes at CL=R/S, with CL=F/W and G/P having smaller but similar values. Their paired cross-sections decrease upwards slightly and also decrease upwards within pairings.

For all cave hydrological classes, the smallest mean catchment areas and the largest mean XS/CA ratios commonly occur at CL=R/S, although relict caves have a large mean XS/CA ratio at CL=W. The largest mean CAs commonly occur at CL=F/W, although MV caves have a slightly higher value at the CL=G/P pair. The smallest mean XS/CA ratios always occur at CL=G/P. The MV cave locations have relatively high mean CAs (except CL=S) and their mean XS/CA values (except for CL=S) are concentrated close to the overall MV cave mean value, suggesting again a relationship between XS and CA, so that vadose chemical and mechanical erosion is closely related to present catchment area, for most MV cave locations.

To summarise the above results, the vadose development of vertical range (in both MV and combination caves) is favoured most strongly at shoulder, ridge and wall locations where MV cave minimum hydraulic gradients are greatest, but vadose development of length is probably least favoured at shoulder and ridge locations. Phreatic vertical development appears to be independent of cave location, but phreatic length development appears to be particularly favoured at shoulders and ridges, from the evidence of the rather small samples of combination caves there. For all cave classes, the largest mean cross-sections occur along valley floors, where catchment areas are greatest. Because caves of all three hydrological classes are commonly distributed across all cave locations (and most glacial situations: section 5.5.6), cave entrance altitudes are well-scattered vertically, despite the preponderance of relict caves and the rarity of mainly vadose caves at CL=R and S.

5.5.6 Cave classes and glacial situations

The mean dimensions of caves in each hydrological class at each glacial situation are presented in Table 5.28, in a format that allows cave class trends and the differences for each west and east counterpart to be observed directly. Two small caves at GS=U are omitted. The small sample of caves at GS=C is also omitted, but the same set of caves is included at CL=C in Table 5.27.

Table 5.28 Cave dimensions, cave hydrological classes and glacial situations

Highest elevation and dimension	Relict caves West	Comb. caves West	MV caves West	All caves West	Relict caves East	Comb. caves East	MV caves East	All caves East
Highest col	**GS=S**	**GS=S**	**GS=S**	**GS=S**	**GS=T**	**GS=T**	**GS=T**	**GS=T**
No. of caves	*1*	*14*	*3*	*18*	49	41	28	118
% of class	*0.4*	*3.9*	*1.2*	*2.0**	17.6	11.4	11.4	13.3*
Mean length	*8*	*141*	*13*	*112*	21	93	38	50
Mean VR	*1.0*	*27.7*	*3.0*	*22.1*	5.1	8.6	4.6	6.2
Mean min. HG	*13*	*28*	*27*	*27*	33	30	24	30
Mean XS	*1.0*	*5.3*	*4.0*	*4.8*	2.9	3.0	1.9	2.7
Mean volume	*8*	*806*	*53*	*636*	76	400	80	190
Mean CA	*1.6*	*1.8*	*1.1*	*1.7*	2.1	2.9	1.6	2.2
Mean XS/CA	*0.6*	*4.1*	*3.6*	*3.8*	4.7	3.5	2.4	3.7
Lowest col	**GS=K**	**GS=K**	**GS=K**	**GS=K**	**GS=L**	**GS=L**	**GS=L**	**GS=L**
No. of caves	31	50	47	128	131	179	109	419
% of class	11.0	13.9	19.3	14.5*	46.9	49.7	44.5	47.4*
Mean length	89	156	27	93	26	178	24	90
Mean VR	8.3	16.3	3.8	9.7	6.2	14.4	3.9	9.1
Mean min. HG	41	20	26	27	37	24	30	30
Mean XS	3.3	6.0	2.0	3.9	2.7	4.5	1.8	3.2
Mean volume	343	1150	79	561	103	1018	45	479
Mean CA	3.8	10.4	6.3	7.3	2.9	4.5	4.6	4.0
Mean XS/CA	4.5	2.4	2.3	2.9	32.4	16.8	2.7	18.0
GML	**GS=G**	**GS=G**	**GS=G**	**GS=G**	**GS=H**	**GS=H**	**GS=H**	**GS=H**
No. of caves	*8*	*7*	15	30	19	28	17	64
% of class	*2.9*	*1.9*	6.1	3.4*	6.8	7.8	6.9	7.2*
Mean length	*42*	*147*	30	61	40	237	27	123
Mean VR	*7.9*	*10.4*	3.3	6.2	5.4	18.5	4.7	10.9
Mean min. HG	*22*	*8*	19	17	29	17	23	22
Mean XS	*4.4*	*4.7*	3.2	3.9	2.3	5.5	2.5	3.8
Mean volume	*201*	*785*	91	282	87	2107	65	965
Mean CA	*3.0*	*2.6*	2.2	2.5	2.5	1.5	9.9	4.0
Mean XS/CA	*12.3*	*1.8*	2.6	5.0	8.1	8.2	4.0	7.1
DML	**GS=D**	**GS=D**	**GS=D**	**GS=D**	**GS=E**	**GS=E**	**GS=E**	**GS=E**
No. of caves	*9*	*5*	*9*	23	20	34	13	67
% of class	*3.2*	*1.4*	*3.7*	2.6*	7.2	9.4	5.3	7.6*
Mean length	*47*	*125*	*16*	52	25	154	27	91
Mean VR	*7.3*	*8.6*	*2.7*	5.8	3.9	12.5	3.8	8.3
Mean min. HG	*25*	*17*	*19*	21	22	15	17	18
Mean XS	*8.4*	*8.2*	*2.1*	5.9	4.1	5.5	2.9	4.6
Mean volume	*327*	*731*	*39*	302	100	918	91	514
Mean CA	*0.9*	*6.9*	*2.2*	2.7	1.1	2.2	1.1	1.7
Mean XS/CA	*39.4*	*14.8*	*4.4*	20.3	9.9	15.3	3.2	11.4
ALL	**SKGD**	**SKGD**	**SKGD**	**SKGD**	**TLHE**	**TLHE**	**TLHE**	**TLHE**
No. of caves	49	76	74	199	219	282	167	668
% of class	18.3	21.2	30.7	23.0*	81.7	78.8	69.3	77.0*
Mean length	72	150	26	85	26	169	27	86
Mean VR	7.9	17.4	3.5	9.9	5.7	13.4	4.1	8.5
Mean min. HG	34	20	24	25	34	23	27	28
Mean XS	4.4	5.9	2.3	4.2	2.8	4.5	2.0	3.3
Mean volume	310	1025	76	496	95	1024	56	478
Mean CA	3.1	7.9	4.8	5.5	2.5	3.7	4.4	3.5
Mean XS/CA	12.1	3.5	2.7	5.3	22.0	13.8	2.8	13.8

Units as Tables 5.25–5.27 *Small samples are shown in italics (<4% of cave class)*

GML Glaciation marine limit DML Deglaciation marine limit

Shaded values are much larger than their east or west counterpart * % of all caves

The percentages of relict, combination and MV caves in each glacial situation are fairly similar to each other. Nearly half of all caves in each class are at GS=L, and very few are at GS=S. Each class is under-represented in all west-draining situations. However, the westward representation differences *below the glaciation marine limit* (GS=D and G) are much less for the small number of MV caves there than for relict and combination caves. Ignoring the one 8m-long relict cave at GS=S, i.e. **Gömstället grotta** (KU), which has a doubtful relict nature, the relict cave mean length, VR, XS and volume in each glacial situation on the west of major ridges are consistently larger than those on the east, both above and below marine limits. Additionally, relict caves situated below both marine limits commonly have marine-enlarged cross-sections (sections 5.3.5 and 8.8) that are larger than the total relict cave mean of 3.1m^2 (Table 5.27).

Relict cave mean minimum HGs and XS/CA ratios are commonly larger and catchment areas are commonly smaller than those of mainly vadose caves and of combination caves. The XS and CA relationships confirm that relict caves developed less under present interglacial conditions than the caves of other classes, as expected. The mean CAs of the relict caves do not vary much between east and west counterparts, remaining consistently smaller than the study area mean of 4.0km^2 (Table 5.27). Consequently, these caves had less opportunity to collect allogenic drainage, partly explaining why they remain relict. Above the glaciation marine limit, the mean relict XS/CA ratios are larger for eastward-draining valleys, whereas below this limit, they are larger for westward-draining valleys. This suggests that 'higher' relict caves east of major ridges are even less related to the present hydrology than those on the western sides and that marine enlargement was greater for 'lower' relict caves facing west than for those facing east, in agreement with the differences in mean cross-sections.

In complete contrast to relict caves, which commonly have larger dimensions for western glacial situations, the mean length, VR, minimum HG and XS for MV caves with GS=L are *all* within 15% of those with GS=K. Thus, for MV caves, there is little difference in mean dimensions for caves that are above the glaciation marine limit but below the lowest local col, whether they lie east or west of major ridges. There is also variety in the western or eastern ranking of these MV cave mean dimensions for lower glacial situations. This provides further evidence that, uniquely amongst the three hydrological cave classes, MV caves commonly developed under present conditions at all glacial situations. The mean XS/CA ratios of MV caves also commonly reduce upwards, following the reduction of vegetation and soil cover with altitude and the consequent reduction of biogenic CO_2 and humic acids. MV caves also show less increase in mean cross-sections in the deglacial marine situations C, D and E compared with other hydrological classes, suggesting that they did not exist to be enlarged by wave action when their carbonate outcrops emerged from below sea level at the start of the Holocene (section 8.8.2).

MV cave mean catchment areas are commonly larger than those of relict caves, but in most glacial situations they are smaller than for combination caves. This suggests that the vadose development (and

therefore the mean vadose XS) of combination caves is commonly greater than that of MV caves. The MV cave mean XS/CA ratios are much smaller than those of relict and combination caves in most glacial situations, remaining close to their MV overall mean of $2.8m^2km^{-2}$ (Table 5.27), again confirming that MV caves are much more closely related to present hydrology than the other two cave classes. As a set of caves, MV caves are rather smaller than relict caves, because most of their dimensions are smaller in most glacial situations. This suggests that across the whole of the study area, those conditions that favour enlargement of phreatic passages are somewhat more important than those that favour vadose entrenchment, and this principle should also apply to combination caves.

Combination caves have mean internal dimensions that are much larger than those of relict and MV caves in nearly all glacial situations. The conclusions about glacial situation and total cave occurrences and dimensions (section 5.3.5) also commonly apply to combination caves. Thus, their mean lengths, VRs, XSs and volumes commonly remain greater *west* of major ridges but above glaciation marine limits and commonly greater *east* of major ridges but below marine limits. The greater mean length at GS=L compared with GS=K is accounted for by the long length of **Korallgrottan** (KU). If this cave was assigned GS=T instead of GS=L (section 5.3.5), the mean length at GS=L would become 151m, i.e. less than the 156m at GS=K. Combination cave mean XS also tends to increase with lowering altitude, and mean minimum HGs do not vary much between east and west counterparts (except for GS=G and H). The relatively large volume for GS=H, XS for GS=C, D and E and XS/CA ratio for GS=D and E are again suggestive of enlargement of such combination caves by marine action.

The west to east differences are less marked for combination caves than for relict caves, illustrating the intermediate position of combination caves between relict caves and MV caves in this respect and the 'competition' between phreatic and vadose processes. The differences remain large enough to confirm that, in combination caves, those conditions that favour enlargement of phreatic passages are more important than those that favour vadose entrenchment, as suggested above.

Because the trends for combination caves and for all caves (section 5.3.5) are so similar, it seems possible that combination caves could merely represent relict caves that enlarged in a single phreatic phase before experiencing vadose entrenchment. If this is the case, then the overall mean combination cave XS ($4.8m^2$: Table 5.27) should equal the sum of the mean relict cave XS ($3.1\ m^2$) and the mean MV cave XS ($2.1\ m^2$). Thus, if the mean vadose cross-sections in combination and MV caves are similar, the mean relict cave XS appears to be too large by $0.4\ m^2$ (13%). However, for most glacial situations below the marine limits (GS=C, D, E and G), the relict cave mean cross-sections are disproportionately large, so that the enlargement of entrance areas by marine activity may distort the total mean figures. For higher situations (GS=H to S, but excluding T), the mean combination cave XSs are commonly greater than the sums of the mean XS for relict and MV caves. This suggests that, in these cases, some combination caves started their phreatic development before the relict caves (in perhaps an earlier phase) and / or they

started their vadose entrenchment before the MV caves and / or they have a mean vadose XS that is larger than for MV caves because of their larger mean catchment areas in most higher glacial situations.

The variations in mean cave dimensions for each cave hydrological class at each glacial situation are subtle and complex. At this stage, there seem to be few obvious explanations, and yet there are sufficient internal consistencies to suggest that the variations arise from local geomorphological processes, rather than just being derived stochastically. Succeeding chapters, especially Chapter 8 and its section 8.1.10, address this issue further and derive models that demonstrate the importance of glacial situation in the karst evolution of the study area.

5.6 Internal cave attribute trends

The various internal attributes recorded in the cave databases and the influences that the external attributes and cave classes have on them are discussed in Appendix B2 and summarised in this section.

5.6.1. Cave class influences

Because relict caves contain no SE, RE, CS or SP and have few RV, comparisons of these hydrological attributes among the cave classes have little value. However, the frequencies of all the other internal attributes increase in the order mainly vadose: relict: combination and this trend is commonly observed within each karst type, in agreement with the same trends in the major cave dimensions (section 5.5.3).

5.6.2. Cave type influences

Appendix B2 shows that cave type, and therefore cave length, is a major determinant of all internal attribute frequencies, except SE and RE. This relationship is also commonly maintained within all cave classes (where appropriate), all karst types, all (most for RV and FS) cave locations and most glacial situations. The increases of BC with cave type are more erratic for each attribute, and are more rarely observed in each glacial situation. The cave type increase in DC is only observed in those cave locations and glacial situations where DC is well represented.

5.6.3 Vadose and phreatic favouring

The concept of 'vadose favouring' of cave occurrences and dimensions was introduced in section 5.5.3, where it was proposed that some external attributes favour vadose over phreatic passage development, and vice versa. Thus, broadly speaking, the development of long vadose passages is favoured by large CAs and small XS/CA ratios, whereas phreatic passages are independent of CA (section 5.4.1). Vertical stripe karst (VSK) favours longer MV caves, but low angle karst (LAK) favours longer phreatic caves (section 5.5.3). The existence of MV caves is favoured if R=1 (although their mean length reduces) and vadose cross-sections increase if T=1 (section 5.5.4). Cave locations R, S and W favour phreatic caves, and location F favours vadose caves (section 5.5.5). The large differences in occurrence and dimensions for phreatic passages in west and east glacial situations are not observed in MV caves (section 5.5.6).

Vadose or phreatic favouring by external attributes is also observable for the internal, non-dimensional, cave attributes. These influences can be understood by noting that a) the hydrological internal cave attributes of sink and resurgence entrances, cave streams and sump pools appear to be all *diagnostic of vadose development*, and b) relict entrances, chambers, shafts, boulder chokes, chemical deposits and fluvial sediments appear to be commonly *diagnostic of phreatic development,* because they occur least frequently in MV caves. Thus, although LAK increases the mean SE and RE of active caves, it reduces the number of their DE, and increases the DE of relict caves. Hence, reducing the foliation angle is commonly 'phreatic favouring'. This 'phreatic favouring' of reducing foliation angle is supported by the increase in Ch, BC, DC and FS as dip reduces. Only the shaft frequency decreases, because of the relative ease with which shafts form in VSK. Contact metamorphism (R=1) and thrusting (T=1) both tend to favour vadose development, because SE, RE, CS and SP commonly increase, whereas DE and Sh decrease. Cave locations R and S are especially 'phreatic favouring', because SE, RE and CS decrease, whereas DE, Sh and FS all increase. The eastern glacial situations are also 'phreatic favouring' because DE, Sh (commonly) and DC are greater there, but SE and RE are greater to the west. RV is also greater to the east, which suggests that even relict vadose passages had significant phreatic origins. This finding agrees with the greater occurrences of relict and combination caves on the eastern sides of ridges, but contrasts with their commonly larger dimensions (including cross-section) on the west (section 5.5.6).

To summarise, in contrast to the general zonal trends recognised for the carbonate outcrop and external cave attributes, the internal cave attributes commonly display fewer, and weaker, trends. They have less-strong relationships with the external attributes, so that their mean values tend to remain more constant, as partly shown in Table B2.1. However, there is considerable consistency in the phreatic or vadose influences of the various external attributes when considering cave occurrences, dimensions and internal attributes. The reasons for these influences are deduced in chapters 6–9.

With the large amounts of data now available, and the finding that they display a considerable measure of consistency, a full statistical treatment would be a large but worthwhile task, but one that is beyond the scope of this thesis. Thus, the suspicion that cave internal attributes commonly follow Poisson, normal and lognormal distributions that are statistically significant remains untested.

5.7 Cave morphology in the study area

Many descriptions of the metamorphic karst caves in Scandinavia refer, in general terms, to the guidance of cave passage morphometry by structural geological features, such as folding, faulting and the presence of inter-layered aquicludes. Cave surveys commonly show the angle of dip and direction of strike, where these are straightforward, together with guiding mica schist layers. Probably the most comprehensive study of geological guidance is that by Holbye (1983a, b, c), who analysed the highly-complex refolded geometry of the host rock and the passage development at the **Greftkjelen / Greftsprekka** system in northern Norway. A block diagram to explain their relationships was reproduced by Ford and Williams

(1989, p40). Sjöberg (1979) explained that **Trollhullet** and **Vest Trollhullet** (KU) formed near the hinge of a long, narrow, anticlinal, outcrop that runs parallel to the valley. The first cave developed along-strike in the northern limb, which dips into the valley side. The second cave formed along-strike in the southern limb, which dips parallel to the valley slope. Bottrell (1988) discussed the geological controls on speleogenesis at Glomdal, northern Norway, as discussed in Appendix A2.7. However, despite these isolated examples, the relationships between local geology and cave geomorphology have rarely been studied in detail, neither at the scope of individual caves, nor in a wider scope to embrace caves across a region. Sections 5.2–5.6 discussed the various elements that together comprise a cave system in the study area. This section takes a broader view, to discuss the passage morphologies that are observed in the caves and to consider the main influences on internal cave morphology.

5.7.1 Cave plans

The cave type classification defined in Figure 5.1 may be compared with the 15 cave patterns and their relationship to types of recharge and porosity given by Palmer (1991; Figure 5.7).

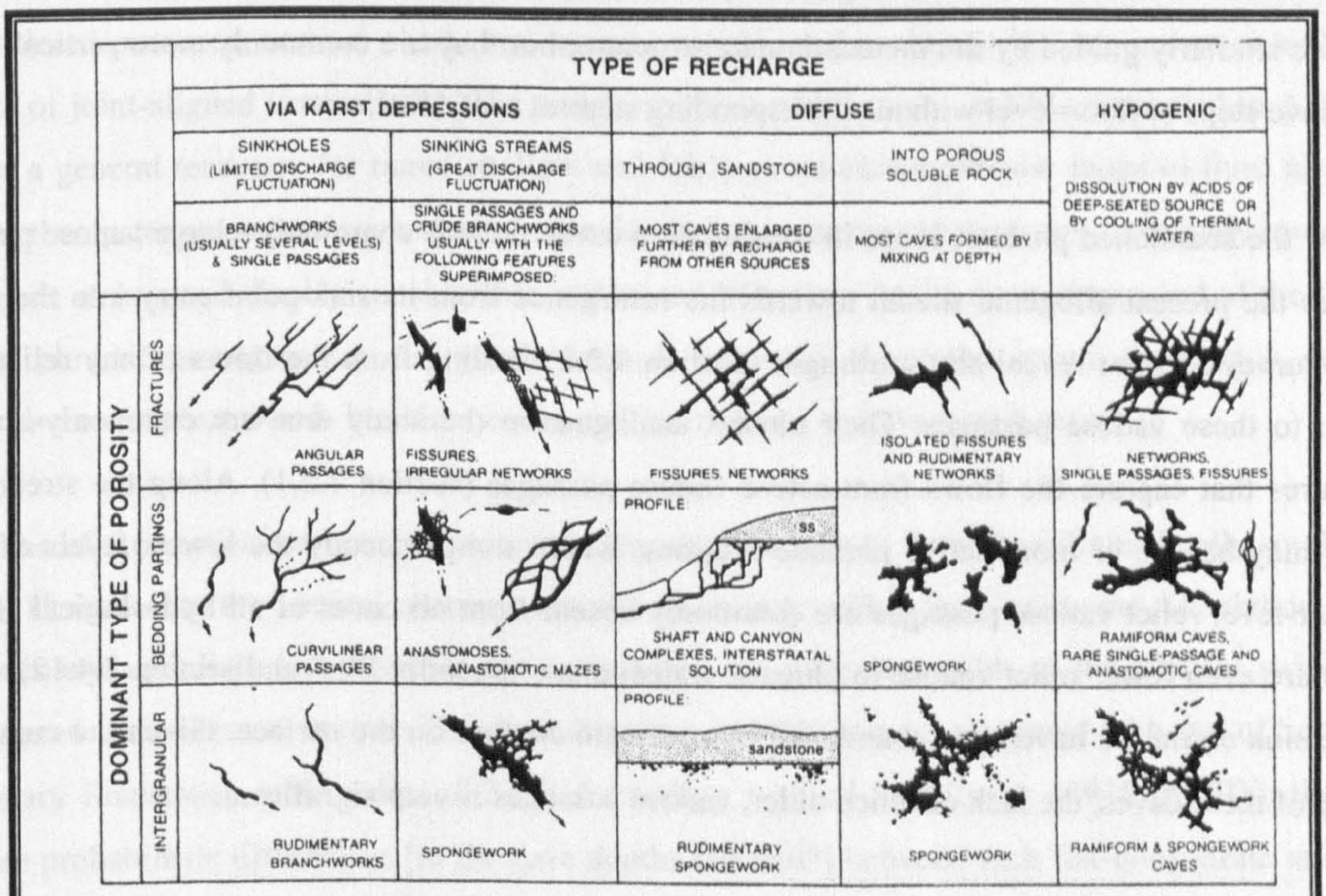

Figure 25. Summary of cave patterns and their relationship to types of recharge and porosity. Maps are plan views unless otherwise noted and are generalized to represent typical caves in each category. Many exhibit rudimentary forms, multiple stages of development, or combinations of more than one type. Individual passages differ in specific layout according to the local physical setting.

Figure 5.7 Karst cave patterns (Palmer, 1991, Fig. 25)

Palmer's scheme was designed to illustrate typical passage morphologies for intergranular, bedding parting and fracture porosities for each of various types of recharge in sedimentary limestones in non-glacial situations (section 3.1.16). In this thesis, cave types a, b, d and e lead to the more complex g (tiered dendritic). They are similar to the Palmer patterns for sinkhole recharge into bedding partings with dominant porosity (giving sinuous, curvilinear passages) and into fractures (giving angular, fissure-like, passages). Types c and f (rectilinear and tiered rectilinear) approximate to Palmer's networks and

mazes formed along sinking streams or by diffuse recharge through sandstone into fractures. The most complex, type h, resembles Palmer's shaft and canyon complexes, formed by interstratal dissolution by recharge through sandstone into bedding partings. Caves comparable to Palmer's "spongework" and "ramiform" patterns are totally absent from the study area. Because these patterns are diagnostic of intergranular porosity, of diffuse recharge into porous rock, and of hypogean recharge, these mechanisms can be disregarded in central Scandinavia.

5.7.2 Passage profiles

The cave survey sections presented in Appendix B1 show that most of the longer, more complex, caves display upper-level passages that have a single shallow, phreatic loop (or part loop), long profile and that have phreatic cross-sections. Individual phreatic passages almost never comprise multiple loops. As well as passages with roughly circular and elliptical profiles, many phreatic passages have profile shapes that are determined by the angle of dip and the impurities within the metalimestone. Thus, cross-sections are commonly square or rectangular in vertical stripe karst, with one, or even both, wall(s) comprising an aquiclude rock. Cross-sections in angled stripe karst are commonly rhomboid-shaped. Vadose passages may be similarly guided by the metacarbonate structure, but they are commonly more vertical in profile, and have steps at floor-level without corresponding steps at roof-level.

Below the abandoned phreatic loops in combination caves there is commonly a large vadose passage that carries the present allogenic stream towards the resurgence from its sink-point entry into the cave. The cave surveys do not reveal any soutirages (section 3.2.2) leading from the floors of any relict passages down to these vadose passages. Their closest analogues in the study area are commonly-inaccessible fractures that capture the flows from active vadose passages (section 7.2.1). Along the stream passage there may be one or more active phreatic sections, where sumps occupy the lowest levels of the cave. Higher-level relict vadose passages are commonly absent from all caves of all hydrological classes and there are even fewer relict vadose to phreatic transitions (Appendix B2.7 and section 8.4.12). However, some sink entrances have been abandoned by upstream capture on the surface. Given the complexity of many of these caves, the lack of relict, older, vadose passages is very significant.

The vadose, shallow phreatic and deep phreatic illustrations of cave development theories provided by Ford and Ewers (1978, Fig. 3) all show many vadose inlets reaching down to phreatic passages nearer to resurgence level, as indeed does the Four-state Model of Ford and Williams (1989, Fig. 7.14). These are 'snapshot' profiles that are intended to illustrate the active routes through a cave system at any point in time. They are only representative of the mainly vadose caves of the study area. However, from the above discussion, the combination caves appear commonly to possess an *'upside-down'* profile when compared to these profiles, because phreatic passages lie *above* vadose passages. The combination caves appear instead to be somewhat similar to, but less complex than, the multiphase example from the Mendip Hills (UK; Ford and Williams, 1989, Fig. 7.16f), where relict multiple phreatic loops lie above an active

streamway that is vadose, at least in its upstream parts. The relict caves are remarkable in having predominantly developed phreatically, without significant vadose captures or entrenchments.

5.7.3 Influence of karst type

Etasjegrotta (Z4; cave type h; Appendix B1.4: Figure B1.8) is proposed as the ultimate example of a combination cave formed in monoclinal vertical stripe karst (VSK), because it displays the most vertically-tiered phreatic passages in vertical stripe karst in the study area, and perhaps in the world. Vertically-tiered passages that may be connected directly by tall or short *vertical* shafts mainly occur in VSK. Observations inside such caves reveal that the vertically-foliated limestone supports three main orthogonal joint systems. One system is a set of horizontal joint planes that are normal to the vertical plane of the outcrop and could be confused with the bedding planes of classical sedimentary limestones. The other two sets of joint planes are vertical. One set is strike-aligned and parallel to the banding, impurities and aquicludes within the limestone; the other set is normal to the vertical plane of the outcrop. Thus, VSK can support cave morphologies that are very similar to those in horizontally-bedded limestones, within the confines of the narrow outcrop. They include such features as anastomoses, phreatic tiered passages, vertical shafts and avens, vertical meandering vadose streamways, and small networks of joint-aligned vertical rifts. The survey sections of the caves in VSK presented in Appendix B1 show a general tendency for tiered shallow and fairly symmetrical phreatic loops to form along the strike. At the upstream ends of such systems, the descending passage segments are commonly invaded by an allogenic stream and display considerable vadose modification. At the downstream end of the system, unaltered phreatic passages may rise gently towards entrances above the stream resurgence, or ramp upwards more steeply, towards boulder chokes and / or dolines, to form type h caves.

The widths of the vertical carbonate outcrops in the study area vary from the infinitesimally small up to c. 800m. However, as the vertical outcrops are almost entirely within the Uppermost Allochthon, which contains many aquiclude layers within the carbonates, the effective width of the vertical stripe karst rarely exceeds a few tens of metres. The distinctiveness of VSK may be compared with that of horizontal sedimentary limestones with a dip of 2–5°. According to Ford and Ewers (1978, p1793), there are important probabilistic differences [in the cave depths reached?] between such flat-lying strata and strata that dip more steeply. Palmer (1999b) showed statistically that the tendencies for vadose passages to follow the dip direction, and phreatic passages to the follow strike direction, are most applicable in prominently-bedded strata with very low dip and few fractures. Section 5.5.3 showed that the mean depth of combination caves increases as the metalimestone foliation *decreases*, whereas they reduce for relict and MV caves. Hence, there are also probabilistic differences for the dip of metalimestones, although the effects may vary from those of sedimentary limestones.

Gevirgrotta on Elgfjell (Z4; cave type h; Appendix B1.4: Figure B1.6) is proposed as a good example for combination caves formed in monoclinal angled stripe karst (ASK). In ASK, passages at different

levels are typically offset down dip, and have less directly-vertical linkages: shafts and avens are commonly steeply inclined. Phreatic loops are less symmetrical, and utilise aslant dip and joint directions. Joint systems in angled stripe karst commonly have the same relationship to the foliation as those in vertical stripe karst, and therefore form inclined planes, which guide passage cross-sectional shapes. These caves also show a general tendency for (offset) tiered shallow and fairly symmetrical phreatic loops to form along the strike. In caves formed in VSK or ASK, water flow is always either directly or generally along strike. It is suspected that phreatic passages tend to form along the hanging wall and vadose passages along the foot wall in ASK, but this was difficult to verify from cave surveys.

The low angle karsts (LAK) support a variety of passage forms and linkages, and therefore no one cave is a representative example. Some water flow may be generally down-dip, i.e. normal to the strike. Very few horizontal outcrops are known, but in **Akersvanngrotta** (ZB), a single-level rectilinear network relict cave has formed in sub-horizontal metacarbonates, below a mica schist caprock, as cave type c. Its plan morphology is probably guided by two sets of fairly widely-spaced vertical joints that are orthogonal to each other, as discussed further in Appendix B1.11.

The extent to which cave morphology is affected by lithological variations within the metalimestone is unknown. In the study area, the most important distinction is probably between the mainly grey calcitic limestones and the yellow / brown variety that is assumed to be HMC or DL (Appendix A2.4 and section 4.4.6). Although several cave entrances occur at or near the junctions of these two varieties (e.g. **Sarvenvårtoehullet**, Z4 and **Labyrintgrottan**, ZC), present surveys do not indicate the variety of limestone in individual passages, and so conclusions cannot be drawn. Any future underground studies would need to overcome the problem that many caves at such a junction are primarily relict, so that limestone surfaces are not clean-washed and the lithology is not immediately identifiable.

5.7.4 Influence of aquicludes

An important geological factor in determining cave morphology in central Scandinavia is the presence of aquicludes within, and adjoining, the carbonate bedrock. The common non-carbonate rocks that are associated with metalimestone outcrops were described in section 4.3, together with information about their occurrence in the various nappes of the study area, including their occurrence within the karst caves. The two cave databases record non-carbonate rock samples from several caves. Where aquicludes are present within caves, their influence on cave morphology is prominent.

An impression from field experience is that nearly all aquiclude rocks occur as internal layers within the carbonates, or as the adjacent country rock, and that they therefore share the same local strike and dip, over the whole range from vertical to horizontal foliation. Commonly, they do *not* occur as dykes or sills within the caves. It is mainly in some of the caves of Z2, where the carbonates were extensively altered and their foliation dips reduced by contact metamorphism from large intrusive plutons (R=1), that

intrusive dykes and sills can easily be recognised underground. For example, a folded dyke in **Mølnvatngrotta** that is orthogonal to the cave passage (in ASK) has formed a one-metre-high waterfall along the streamway (Photo 5.2).

The morphological effect of the aquicludes is most pronounced in the caves in VSK in the HNC. These are formed commonly as straight linear passages, or as vertically tiered passages, alongside a vertical wall of non-carbonate rock. The other wall of the passage may similarly be formed alongside another aquiclude, with the intermediate limestone being removed, to create a rectangular cross-section (section 5.7.2). As the aquiclude separation varies randomly, these passag s can be low and wide, square, or high and narrow. In **Kvitfjellhola** (Z4), a passage formed in Comp exly Folded Karst alongside just one aquiclude wall has a 'quarter tube' in the roof rather than th s more usual half tube, which is the diagnostic form for early phreatic development or for paragenesis. Where several parallel vertical aquicludes occur, it is common to see small, parallel, sub-horizontal passages at the same level. Vadose streamways are typically narrower, with just one wall against the aquiclude. Thin blades of the non-carbonate rock commonly protrude vertically, standing proud of the dissolved limestone. The largest size noted for these blades approaches a metre in **Røssågagrotta** (ZA; Appendix A4.4 and section 5.2.2). Peak flow in this system after heavy rain and during the early spring-melt must be much greater than the author-estimated 57m^3s^{-1} mean annual flow, all contributing to limestone dissolution adjacent to the aquiclude blade.

Non-carbonate layers typically act as complete aquicludes if they maintain a thickness greater than c. 30cm. They can be breached by karst waters and provide 'doors' or 'windows' that can be walked or crawled through into passages formed in the next vertical layer of limestone where they become narrower (Photo 5.3). Typically, all the waterfalls (Photos 5.2 and 5.4) and many sumps in the caves in VSK (Photo 5.5) occur at places where a mainly vadose stream has breached a non-carbonate aquiclude. It is only by breaching these layers that caves can enter a second plan dimension that is orthogonal to the plane of the carbonate outcrop and larger than the separation distance between the aquicludes.

The effects of the aquiclude rocks on cave morphology in ASK are less well understood. These layers should occur with similar frequencies and thicknesses across the strikes of the carbonate outcrops as in the vertical case. However, whether phreatic passages form preferentially above or below angled aquicludes, and whether vadose streamways cut down into the limestone below a sloping aquiclude wall, or erode into a sloping aquiclude itself, are questions that remain unaddressed (c.f. section 5.7.3). An impression from field experience is that as the angle of dip of the limestone reduces below c. 70°, then the frequency of breaches of the aquiclude layers also reduces.

In caves in LAK, aquiclude rocks commonly form roofs and / or floors of passages that are otherwise formed within marble. Again, they cause obstacles to exploration, such as waterfalls where they are

breached at floor level by a vadose stream, and sumps, where gently-dipping non-carbonate roofs form perched sumps, along a streamway. The farther the dip moves away from the vertical, then the more a non-carbonate rock should behave as an Inception Horizon (Lowe, 1992). These features are seen especially well in some of the caves of the RNC (e.g. **Ytterlihullet**, ZA), which are commonly formed in marbles that dip gently to the west towards the thrust zone beneath the HNC.

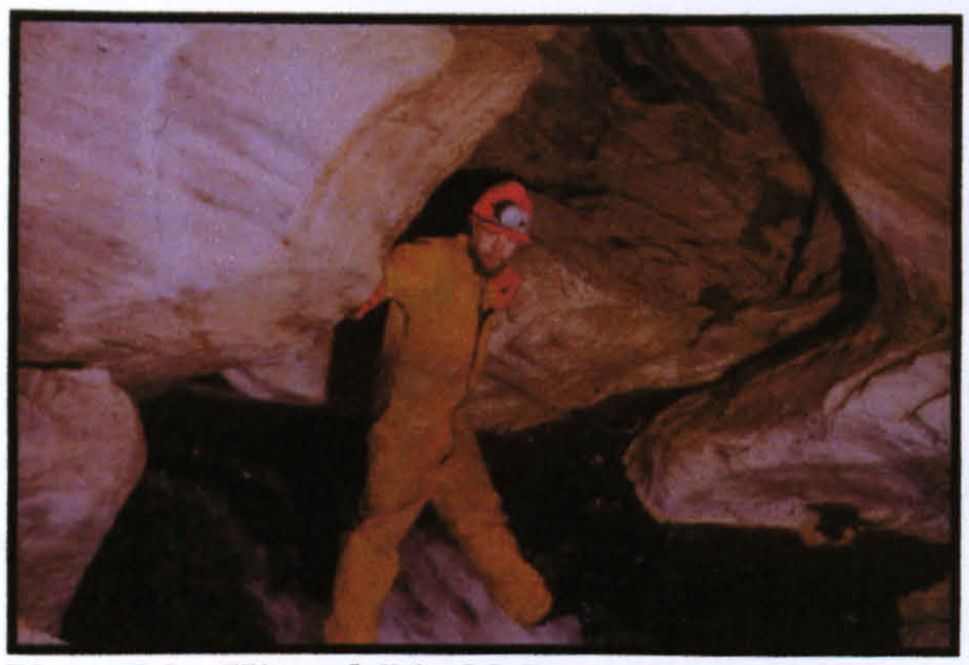

Photo 5.2 Waterfall in Mølnvatngrotta (Z2)
Formed at amphibolite barrier with white angled stripe karst marble, altered by contact metamorphism.

Photo 5.3 Bulandsdalgrotta (Z2)
Bright marble streamway, passing through left wall of amphibolite. Photo by M. Smith.

Photo 5.4 5m Cascade, Sirijordgrotta (Z4)
Formed where the active stream has breached schist impurities within the vertical stripe karst

Photo 5.5 Klausmarkgrotta (Z2)
Upstream sump in phreatic passage formed against a near-vertical wall of amphibolite

The relationship between the frequency and thickness of internal aquicludes and the lengths and depths of caves is unknown, but there is no evidence that aquicludes affect overall cave dimensions, except that passages may be constrained to lie within a metalimestone sandwich bounded by extensive sheets of non-metacarbonates. Caves form commonly at the junction between limestone and an aquiclude rock, such as mica schist, along one edge of the karst outcrop. Sporadically, an allogenic stream sinks at one edge of an outcrop to rise lower-down, along the strike, but from the other edge of the same limestone outcrop. A corollary to the lack of dissolution of *metadolostones* to form caves (section 4.4.5) is that these rocks may instead be regarded as aquicludes when observed underground, so that they should behave as other non-metalimestones in this respect.

5.8 Relationships between caves, carbonate outcrops and topography

This section draws together the major conclusions from Chapters 4 and 5 about the relationships between caves, carbonate outcrops and topography, to complete the factual review and analysis of study area caves and karst. From apparent haphazard arrangements of metacarbonate outcrops and karst caves, several consistent patterns have emerged that point the way towards a single, if complex, explanation of cave inception and development.

5.8.1 *Approximate dimensional consistency across the zones*

The data in sections 4.2.1 and 5.2.1 show that karst frequencies and total cave dimensions in the study area follow the declining eastward trend in the extent of carbonate outcrops. A simple normalising parameter that can be used to model and predict the numbers of mapped karst features, the total length and volume of caves and the frequencies of many internal attributes is the total length of carbonate outcrop in each zone. Karst caves have formed in clusters along these outcrops in all carbonate-bearing nappes down to the lower Køli Nappes, but there are no significant, explored, caves at the geographical extremities of the study area, i.e. at the coast in Z1 and Z9, and in the east in KB. None are known in the Seve Nappes, or in the Lower Allochthon, where there are only relatively few, small, carbonate outcrops.

5.8.2 *Dimensional independence from metalimestone lithology*

Each carbonate outcrop has undergone various complex and individually uncertain processes of diagenesis, dolomitization, prograde and retrograde contact and / or regional metamorphism, dedolomitization and partial conversion to calc-silicate skarns. Predominantly, the outcrops are of Low Magnesian Calcite (LMC) composition. Yellow / brown layers of a presumed (less stable) High Magnesian Calcite (HMC) or Dolomitic Limestone (DL) composition occur uniquely in HNC Z4 and RNC ZA, and contain cave passages. The declining frequency of interlayered aquicludes follows a similar pattern to the decreasing metamorphic grade down through the nappes. This pattern cannot be detected in the frequencies and dimensions of karst features and caves per kilometre of metalimestone outcrop in each zone. Hence, it is concluded that cave dimensions are independent of the lithological history and chemical purity of the limestones, except that high temperature contact metamorphism tends to restrict overall cave development, whereas proximity to major thrust zones considerably enhances it. Thus, the number, length and volume of karst caves and the frequency of underground drainage are governed primarily by the solubility of the metalimestone (both LMC and HMC / DL), however it has been derived, and are little influenced by, for example, crystal size or interlayered impurities. Quartz and mica from interlayered schists may also promote erosion by abrasion. This independence of limestone chemistry certainly does **not** extend to pure dolomite outcrops. Although exokarst features and one short cave have been found by the author in rocks appearing to be dolostones, no caves are found in true metadolostone rocks (i.e. those with more than 42% of $MgCO_3$).

5.8.3 *Apparent independence of altitude and catchment area*

Sections 4.2.2 and 5.2.4 demonstrated that the vertical distribution of the carbonate outcrops is essentially random, and that cave entrance altitudes are scattered randomly within the overall constraints of the local topography and carbonate outcrops. An exception is that there are no significant, explored, caves at the altitudinal extremities, i.e. at the strandflat, and at the uppermost glacial situation. Indeed, there are no known karst caves above 940m, although many carbonate outcrops lie above this altitude, up to a maximum of 1392m (in KU). This lack of caves at very high altitudes seems significant (Chapter 8). Furthermore, mean lengths, cross-sections, volumes and vertical ranges of the full set of caves are mainly independent of altitude (but vary with glacial situation), unrelated to the local tree line, and not related to the contemporary cave catchment area, except as discussed in section 5.8.9.

5.8.4 *The shallow, epigean, nature of most cave systems*

The vertical ranges of the carbonate outcrops (which can exceed 900m) do not appear to influence the depth of cave systems, which have a study area mean of only 8.8m, because many of the caves appear to occupy only the near-surface part of the limestone outcrop (Photo: Frontispiece 2). Cave vertical ranges, and the maximum depths of passages, or distances from the adjacent land surface, appear to be influenced by the dip of the foliation, with caves in low angle karst having deeper potentials. Section 5.3.7 showed that the maximum subsurface cave distance in VSK is 50m, whereas it is 93m in LAK.

5.8.5 *Influence of cave location and glacial situation*

There appears to be no *systematic* influence of zonal position and altitude on cave dimensions and internal attributes, as the mean values remain roughly constant in samples of sufficient size, although the means represent broad distributions, with large standard deviations of natural measurements. However, the various external cave attributes are more influential, and can vary the mean values by up to +100% to -50% (taking the extreme example of cave volume), especially if cave location and glacial situation are considered together. Of particular note is that caves in valley shoulder and ridge locations, which may be tectonically less stable (Chapter 6), tend to be longer and deeper, and contain more shafts, than the study area average. There are major frequency and dimensional differences between all the caves situated west of major ridges compared with all those on the eastern sides. Thus, the mean dimensions of all caves above the glacial marine limit are greater on the western sides of major ridges compared with the eastern sides, despite their smaller frequency, and despite the dominance of caves on the eastern sides within the 12 longest caves and 18 deepest caves (section 5.3.6).

5.8.6 *Importance of marine influences to entrance sizes*

Caves below the deglacial marine limit and, to a lesser extent, caves below the glacial marine limit, tend to have obviously-enlarged entrances compared with higher caves. This is also illustrated numerically by an increased mean cross-section for such caves and shows the effect that marine action and ice wedging can have on pre-existing cave passages during isostatic changes.

5.8.7 *Internal morphological guidance by limestone dip and by aquicludes*

Within the general west to east decline in the angles of dip of the limestone outcrops and of their foliation, the dips can vary markedly within each zone. The longer caves, as well as the deeper caves, seem to form in limestones with rather low angles of dip. The dip of the foliation is a major influence on internal cave passage shapes, orientations and relationships. Where aquicludes occur, they also have a very strong influence on internal passage shapes and alignments. Additionally, many cave entrances are situated at the along-strike junction of the limestone with an aquiclude country rock, and this contact is commonly observed to form a wall of the internal cave passages.

5.8.8 *Importance of glacial situation to internal deposits*

The frequencies with which the caves display internal chemical and clastic deposits reduce for higher glacial situations. Assuming that most of these deposits date from the Holocene, it is suggested that this trend follows the reduction in annual temperature with altitude, the corresponding reduction in vegetation and soil cover, the associated increase in extent and duration of winter snow cover, the reduced sediment load in higher deglacial outflows and the increased flushing power of streams flowing from larger catchment areas to the east.

5.8.9 *Importance of cave classes*

The caves of the study area have been grouped into three large hydrological cave classes: mainly vadose, relict and combination caves, which occur randomly intermingled amongst each other geographically and altitudinally. The mean cave class occurrences, dimensions and non-hydrological internal attributes consistently follow this same rank order.

Combination caves display the greatest variety of processes because they contain relict phreatic passages above active stream passages, which themselves combine vadose and phreatic elements. Most relict and mainly vadose caves experienced single (but different) development processes after inception, because all their mean cave dimensions are smaller than those of the combination caves, making them even more epigean in nature. The distinction between phreatic and vadose processes is confirmed, because the mean ratio of cave cross-section to present catchment area reduces markedly from relict to combination to mainly vadose caves. This suggests that only the mainly vadose caves and the active parts of combination caves have dimensions directly related to the flow-rates of present allogenic recharge, for which simple formulae for maximum dimensions were deduced (section 5.4.2).

The external cave attributes variously favour phreatic or vadose development. In particular, the occurrence and dimensional differences apparent on western and eastern sides of major ridges are primarily a phreatic effect, with mainly vadose caves exhibiting more uniform characteristics. Cave internal attributes are themselves diagnostic of the prime development process, because the hydrological attributes indicate vadose entrenchment and the non-hydrological attributes indicate phreatic

enlargement. Also, it is only the mainly vadose caves that do not have enlarged entrances below the deglaciation marine limit. This suggests that they developed after the start of the Holocene, whereas relict caves and at least the relict phreatic parts of combination caves were then already in existence. Chapters 8 and 9 discuss the probable development processes and timescales for each cave class.

5.8.10 *Consistent pattern of cave types and morphologies*

Sections 5.2.5 and 5.3 showed that the distribution of cave types is fairly consistent across all the zones, and that all cave types commonly occur in most karst types, in most cave locations, in most glacial situations, in all contact metamorphism / thrust combinations, and in both relict and combination cave classes. In all zones, two thirds of all caves appear to consist of a single linear or meandering passage, and these commonly represent the shorter caves. The longest cave in each zone commonly has the most complex type of passage arrangement. These commonly display interconnected, abandoned, shallow, phreatic-loop passages above a large, mainly vadose, streamway that may pass through several submerged sections. Present karst recharge is predominantly allogenic, and relatively few caves have more than one active stream. However, high-level static sumps are rare, as are relict vadose passages and the vadose entrenchment of relict phreatic passages, which is even more rarely found at the 'downstream but ascending' end of phreatic loops.

There is a high frequency of multiple entrances for the caves (the area mean is 1.5 entrances per cave), although many of these are relict, and even short caves can have many entrances. The frequencies and probabilities of the non-hydrological internal cave attributes commonly follow the increase in cave complexity, as identified by the cave type, and are therefore roughly related to cave length, for all three cave hydrological classes. There is a very low frequency of significant chambers, and these are concentrated in the more complex caves. There are also very few large boulder chokes in the caves, and only 34 restrict further exploration. Only 4.5% of the caves contain significant speleothems or other chemical deposits. These must therefore be regarded as consistently rare, although those that do exist can be very distinctive. Some 22% of the caves contain recorded clastic deposits. There is much evidence for the complete inundation of some caves during large modern flood events, and the consequent progressive movement and flushing of earlier deposits down, and eventually out of, the caves.

5.8.11 *Consistent karst development processes*

The above conclusions confirm that the major dimensions and much of the internal cave morphologies are independent of zonal geographical position and individual cave altitude. This suggests that similar cave inception, cave development and cave removal processes operate, and have operated, across all zones of the whole study area, for similar periods of time and with similar effectiveness.

This outcome is hardly surprising, because the zones of the study area share a common geological history after the Devonian, when thrusting caused by the final docking of the Laurentian plate with the Baltic

plate brought all the zones together in basically their present form. Thereafter, peneplanation in the Carboniferous was followed by uplift and subsequent erosion in both the Mesozoic and Cenozoic. The whole area has since suffered multiple glaciations during the Late Miocene, Pliocene and Pleistocene, when huge icesheets formed over the whole of Scandinavia. These glaciations have dominated the evolution to the present day landscape, which is still shaped by the geological structures. The climatic changes since the start of the Holocene have been fairly uniform across the whole study area, as discussed in section 2.4 and Appendix A4. Any moderating influence of varying tree line, mean annual temperature and mean annual precipitation on karst development (other than on internal deposits) across the study area is considered to be slight.

5.8.12 *Consistent palaeokarst processes*

As the whole area is almost devoid of post-Caledonian sediments, the timescale of possible karst development is very long. Carbon dioxide was available in rainwater from before the original formation of the Caledonides. Thus, the various processes of cave inception, development and removal may be normal components of landscape development since the Caledonian Orogeny. Within this continuum of processes, individual caves may develop relatively quickly or slowly, and persist in the landscape for short or long time periods, depending on geological constraints and topographical inheritance. Hence, the known caves may represent a range of examples from long persistence caves (perhaps represented by relict and combination caves), through to more-recently-developed caves (probably represented by the mainly vadose caves).

Many kilometres of bedrock were eroded from above the present surface after the Caledonian Orogeny, but due to the random nature of the vertical distribution of the present carbonate outcrops and their general alignment with tectonic structures, it seems likely that the distributions of such outcrops in previous landscapes were similar to those at present. That is, they would occupy about the same proportion of land area, and have a similar distribution of length, width and area. The outcrops would also be aligned generally N–S or NNE–SSW, and occupy all parts of the vertical range. The vertical range of each outcrop or group of outcrops would however depend on the degree of peneplanation and uplift applicable at the time. Additionally, the carbonate outcrops would comprise similar lithologies and contain about the same amount and types of non-karstic impurities. Thus, at the zonal scale, the geological distribution of surficial lithologies can be regarded as roughly a constant throughout the time since the Caledonide events. Hence, the conclusion that each present zone represents a continuum of processes of cave inception, development and removal, with a distribution of timescales being represented for each phase, may be extended to any time period back to the Early Devonian. For all this time, the whole area can be regarded as a single entity regarding climate and uplift, so that at each point in time, the same processes applied across the whole region (and indeed to other parts of the Scandinavian Caledonides). As arid periods would slow down all erosional and dissolutional processes, and very wet periods would speed them up, these climatic effects moderated the age distribution of the

caves. However, at any one point in time, the physical distribution of caves, their lengths and their volumes remained related roughly to the contemporary lengths of the carbonate outcrops, although they would not necessarily have mean dimensions similar to present values.

The effects of uplift, peneplanation and glaciation also moderated this general model, because erosional processes generated a set of deeper and longer caves during times of high uplift, and destruction or infilling of caves occurred during peneplanation, tectonic sinking or marine invasion. Internal cave morphologies across the whole study area also varied across geological time from the effects of the multiple glaciations. It is known that Scandinavian karst caves became flooded, and acted as component parts of glacial hydraulic regimes, during the onset, maturity and recession of the Scandinavian ice caps (e.g. Lauritzen, 1986). Thus, total cave dimensions, and the proportion of phreatic to vadose passage elements across the study area increased in a consistent fashion across the whole area during periods of glacial activity.

5.8.13 *Single series of cave development models*

Taking a broad view of the above conclusions, the study area, its carbonate outcrops, and its karst caves can be regarded as a rather consistent entity in which the sequences and timescales of cave development can be considered further. Thus, it should be possible to construct a single series of models to describe cave development processes that apply commonly across the whole area, to which variations determined by the external cave attributes of karst type, contact metamorphism, thrusting, cave location and glacial situation can be applied universally. Indeed, this Chapter 5 itself provides the first of these models: the *Static* Internal Model of Cave Development. This is a framework that describes the present snapshot view of internal cave morphologies and how they are influenced by their geological and geomorphological environments. To achieve this model it has been necessary to describe some 24 individual external attributes that apply to each of three major cave hydrological classes. The numerical data presented herein can be used within the framework to model and predict the character of the known, and the unknown, caves of the area as represented by the quantifiable internal cave attributes.

5.9 The inter-related five main hypothetical models

The static internal model answers the question 'what', when describing the physical properties of the caves. It is now necessary to address the questions 'why', 'how' and 'when' the caves came to exist in their present form and to propose the sequences of passage development within the caves themselves.

The main aim of this thesis is *to develop a conceptual model for cave development in metacarbonate rocks in central Scandinavia, and to test the applicability of the model in similar geological environments in other parts of the world* (section 1.1). It is now appropriate to introduce the five main hypotheses used to underpin the conceptual model. The conceptual model requires external and internal frameworks. The external framework (Chapters 6, 7, 8 and 10) shows how the formation, development and destruction of karst caves are related to the geomorphological evolution of the host region. The internal framework (Chapters 5 and 9) shows how cave morphologies are guided by the geological attributes of the carbonate aquifers, in both space and time. The external and internal frameworks are supported by the following hypothetical models:

1. The Tectonic Inception Model (Chapter 6). This shows that it is only open fracture routes, primarily created by the seismic shocks that accompany deglaciation, which provided the opportunity for dissolution of metalimestone rocks that have negligible primary porosity.

2. The External Model of Cave Development for central Scandinavia (Chapter 7). This black-box approach reveals how the formation, development and destruction of the karst caves were related to the evolution of their local landscape, for all time periods. In this approach, the cave is regarded as an unknown system between sink and resurgence.

3. The Hydrogeological Model (Chapter 8). This model demonstrates that the present caves developed to their mapped dimensions in timescales compatible with the first two models, within the constraints imposed by the physics and chemistry of calcite dissolution and erosion in almost pure water, in both deglacial phreatic and interglacial, primarily vadose, conditions.

4. The Internal Model of Cave Development (Chapter 9). This dynamic white-box approach demonstrates the sequence of evolution of karst aquifers and caves along inception surfaces and inception fractures that follow the structural geology of the carbonate outcrops, to reach the present static internal cave morphologies described in Chapter 5.

5. The Caledonide Model (Chapter 10). This model shows that the same processes commonly apply to cave development in most of the Caledonide terranes that exhibit metalimestone outcrops, and that the prime influences on present cave and karst occurrence and dimensions are the severity and frequency of northern Atlantic glaciations.

CHAPTER 6 TECTONIC INCEPTION

The factual review of the karsts and caves of the Caledonides of central Scandinavia, as presented in Chapters 4 and 5, revealed many fundamental differences between these caves and those formed in sedimentary limestones. The most obvious difference is the metamorphic grade of the karst bedrock, and its very low primary porosity. Allied to this is the fine-scale foliation and consequent lack of 'bedding-plane' partings. Indeed, for the western part of the study area in the HNC the foliation is commonly vertical, and any sub-horizontal openings must be along joints or other fractures. The vertical foliation and metamorphic history led to the occurrence of many completely separate 'stripe karsts', in which their contained caves are, by necessity, commonly short and completely unrelated to each other internally, even if proximate in the field. However, despite the large vertical ranges of some of the metalimestone outcrops, the deepest cave is only 180m deep, and only four others are more than 100m deep. Additionally, despite the long lengths of some of the karst outcrops, there are no regional scale caves, nor even regional hydrogeological drainage systems. Recharge to the karst is primarily allogenic, with autogenic recharge being relatively insignificant, and mainly occurring during the spring snowmelt. The caves are relatively short, and commonly extremely epigean: there is a total absence of long, hypogean, cave systems. Cave development has been predominantly phreatic, so that, commonly, just a single vadose streamway underlies upper-level relict passages that have, almost universally, developed phreatically with few vadose elements, creating an *upside-down* morphology. Thus, in many different ways, these caves have their own morphological style, recognisable right across the area, which differentiates them from caves formed in 'classical' karsts. Chapters 6–9 attempt to explain the various geomorphological and climatic processes that combined to create the caves in their present form. The first question to address is "Why do these caves exist at all?"

6.1 The inception problem

The Inception Horizon Hypothesis (IHH; section 3.1.12) proposed that the first initiation of proto-conduits occurs as a syngenetic cave formational process during diagenesis (which may be accompanied by strong acid dissolution). The long, slow, *non-karstic*, inception phase is driven by capillarity, earth tides or ionic diffusion at great depth and over great distances *within stratigraphical partings* or *adjacent porous or fractured rocks*. How does this hypothesis stand in relation to the karsts and caves of the study area?

6.1.1 Lack of primary porosity

From the discussion in Appendices A2.2 and A2.3 it is clear that most of the high-grade metalimestones of the study area can exhibit no memory of their original diagenesis, after their subduction and metamorphism to marble at elevated temperatures and pressures. Thus, any proto-conduits originally formed syngenetically during diagenesis were closed as the rock experienced chemical and physical changes in lithology. The recrystallisation to metacalcite produced a rock with a primary porosity that

can be regarded as negligible, even over the long timescales available for 'conventional' inception. The same applies to any mica schist, amphibolite, granite or gneiss lying adjacent to the marble: these rocks could not have sufficient primary porosity to act as aquifers carrying water to the limestone surface.

6.1.2 Lack of stratigraphical horizons

Taking the case of caves in vertical stripe karst (VSK), these commonly display morphologies similar to those in horizontally-bedded limestones (section 5.7.3). However, the inception horizons that guide the formation of horizontal passages along particular sedimentary bedding planes are completely absent in horizontal passages in VSK. The foliation is orthogonal to, not parallel to, such passages, and there are no consistent systems of horizontal sills or other intrusions to act as inception horizons.

6.1.3 Lack of regional-scale systems

The IHH suggests that inception takes place over extremely long timescales, at great depths and over great distances. There is no evidence that such a mechanism has taken place in the study area. Certainly, there are no explorable caves that meet these criteria, there are no known allogenic or autogenic sink-to-rising drainage systems more than 3.5km in length, and there is no evidence of very deep cavities or wells in the metacarbonates. Indeed, regional-scale inception is not possible in small, short, and possibly shallow, metalimestone outcrops. Yet caves do occur in such outcrops.

6.1.4 Existence of shallow systems

Most caves in the study area have vertical ranges of less than 10m, which rarely exceed 15% of the outcrop vertical range (section 5.2.4). It is self-evident when visiting such systems (e.g. a short shallow 'through cave' that carries a vadose stream from one entrance to another) that such passages have no relationship to any deeper, regional-scale, hydrogeology, even if it existed. Whereas it could perhaps be considered as a possibility that *all* such short caves are the lowest remnants of much longer systems formed deep below landscapes that have since been eroded away, this seems most unlikely as the carbonate outcrops would not have been consistently longer in the past than they are at present.

6.1.5 The implausibility of the IHH to explain inception in some metalimestones

From the four arguments presented above, it is clearly implausible to expect the IHH, as summarised simply in section 6.1, to account for the inception of the overwhelming majority of caves in the study area. However, elements of the Hypothesis may explain parts of the inception process in some caves, or groups of caves. For example, inception that is *guided* along sub-horizontal aquicludes within the foliation of marbles in low angle karst (LAK) seems very likely, as at **Ytterlihullet** (ZA). Similarly, inception along-strike at lithological boundaries within lower grade metacarbonates in angled stripe karst (ASK), as at **Korallgrottan** (KL) is also feasible. However, even in these examples, some other mechanism seems to be needed to explain an initial porosity.

6.2 The tectonic solution

Despite the difficulty in utilising the IHH in its pure form to explain the inception of any of the studied caves, these caves exist and must have origins that at least post-date the last phase of metamorphic activity. As discussed in sections 5.8.10–5.8.13, the consistent style of the caves across the whole area suggests that a consistent set of processes guided the inception, development and destruction of caves in all timescales since the formation of the Caledonides. Two major clues to the inception process were noted in analysing the morphology of the studied caves: externally, their epigean association with the landscape, and internally, the dominance of relict phreatic passages.

6.2.1 Association of caves with landscape

All cave passages in VSK and ASK lie within 50m of the overlying surface (section 5.3.7), as do caves at Glomdal in northern Norway (Lauritzen, 1988b). Even in **Ytterlihullet** (ZA, LAK), all parts of its streamway are <95m below the surface. Its stream resurges, flows along a short surface valley, and sinks again in the same limestone outcrop before finally resurging some 200m above the limestone base, which is c. 100m above the valley floor. Thus, this cave and most other active caves act in harmony with local hydrology and have an intimate, *epigean*, association with their local landscape. Hence, it seems safe to assume that these caves evolved in association with, and at a similar time to, their local topography. As observed in Appendix A3.5, the dominating process that governed the shaping of the visible landscape is the cycle of glaciation and deglaciation that was repeated many times since the late Tertiary.

6.2.2 Relict phreatic passages

All the relict caves of the area appear to have developed phreatic lly, as have nearly all the higher level abandoned passages in the active caves (Appendix B2.7). Howe er, in most cases, it is not possible to imagine present circumstances, even at times of high flow or flo d during spring melt, when these caves could be inundated with meteoric water to create phreatic con itions for their enlargement. It *may* be possible to envisage earlier landscapes where these passages were submerged under meteoric conditions, but a much simpler explanation is to consider that these passages enlarged subglacially or during deglaciation phases, when whole valleys could be inundated by glacial meltwater.

6.2.3 Tectonic inception model

The development (and destruction) of the present suite of karst caves can therefore be addressed by considering the way that glaciation has eroded the land surface, and perhaps provided sufficiently aggressive meltwaters to enlarge passages by dissolution. But these processes cannot explain the actual inception along proto-conduits. Without such openings, glacial meltwaters would not penetrate into high grade metalimestone, even under pressure.

The *Tectonic Inception Model* of this thesis hypothesises that, through several separate, but commonly related, mechanisms, the stress release arising from the isostatic rebound and surface erosion that accompanied the deglaciation of the study area at the end of each glacial cycle, plus longer-timescale

plate tectonics, caused the formation of tectonic fractures in the upper (epikarstic) part of the limestone (Photo 6.1). These fractures commonly follow planes of foliation and planes orthogonal to it. Thus, openings are created along *inception surfaces* between the limestone and adjacent aquicludes (which may include dolostones), and by *inception fractures* that are entirely within the limestone, but are commonly (though not universally) parallel to, or orthogonal to, the foliation. This model builds on the observations that "*the continuing seismic and tectonic activity* (in similar settings) *in Scotland may be best understood in terms of a 'partially detached' thin upper crustal layer*" (Davenport *et al.*, 1989, p191) and that near-surface limestones, and dolostones especially, are not very ductile and produce brittle fractures during folding, faulting and removal of overburden stress by erosion (e.g. Doré and Jensen, 1996, pp426–427). In this context, Appendix A3.4 assumed that the maximum thickness of permafrost during glaciation is c. 100m. Hence, rock above this level is subjected to more severe temperature cycling and freeze-thaw processes than rock below it, and is therefore more likely to form inception fractures when triggered by seismicity. The practical expression of these processes was provided by Boulton *et al.* (1996, p403), who noted from pumping tests that the crystalline basement rocks of the Scandinavian shield (primarily non-carbonates) have "*a surface horizon of fractured bedrock about 100m thick which has a hydraulic conductivity of* $10^{-6}ms^{-1}$". This provides a *near surface aquifer* that is commonly found in crystalline rocks worldwide (Gustafson and Krasny, 1994; section 3.1.18).

Photo 6.1 Marble epikarst at Indråsen (Z2)
Shattered nature of the epikarst in high-quality metalimestone altered by contact metamorphism at Indråsen quarry.

The idea of tectonic inception in karst rocks has a precedent, because Riggs *et al.* (1994; section 3.1.18) proposed the tectonic speleogenesis of Devils Hole, Nevada. The only known (and largely ignored) paper to discuss the importance of fracturing by stress release in the development of cave passages in sedimentary limestones was by Sasowsky and White (1994). These authors anticipated some of the independently-deduced processes described in this thesis, but for a non-glacial setting in Tennessee.

6.2.4 The glacial / tectonic cycle

Because the tectonically-induced inception fractures are commonly produced at the *end* of each glaciation, there may not always be sufficient time for phreatic passages to enlarge to explorable dimensions during the remaining time of that particular deglaciation. Hence, the cyclic processes of glaciation, deglaciation and tectonic opening combine together to develop cave passages: the tectonic inception at the end of one deglaciation provides voids and fractures that permit the circulation of aggressive waters, both during that deglaciation and during the next glacial and deglacial phases. As the cycle repeats itself, passages near the surface enlarge and become removed by glacial and fluvial erosion (as noted by Isacsson, 1994, at **Korallgrottan**, KL), and new passages form at geologically lower levels.

6.3 Formation of tectonic fractures

Tectonic inception (and indeed any *inception* hypothesis) is not easy to *prove*. Tectonic fractures are likely to be too narrow to observe visually. Any such fractures that lead to karstic dissolution and enlargement to explorable passages may no longer be in a recognisable form. Thus, the Tectonic Inception Hypothesis will be supported by an accumulation of circumstantial evidence. The following sections discuss general modes of fracture formation in the Scandinavian Caledonides, the evidence for tectonic activity in Scandinavia and in the study area itself, and what evidence there is for tectonic inception from the metalimestone caves of central Scandinavia. The *hydrogeology* of fractured rock was discussed in section 3.1.18, and that of fractured metalimestone is considered in Chapter 8.

6.3.1 Caledonide evidence for tectonic activity

Section 3.1.17 and Faulkner (1998) discussed the latest ideas on the importance of tectonic activity to cave development in sedimentary limestones. The idea that tectonism *sensu lato* has influenced karst cave development in at least the Caledonides has been suggested, or hinted at, by several authors. Thus, Hoel (1906, p8) raised the possibility (before dismissing it) that **Aunhattenhullet 1, 2 and 3** (Z2) and **Langskjellighattengrotta** (Z2) were formed by "dislocations". Horn (1947: McGrady translation, 1978, p135) noted that the Norwegian coastal area at the Arctic Circle is still unstable tectonically, which should favour joint formation, or the widening of old joints. Kirkland (1958) thought that collapsed blocks on the floors of chambers in the Svartisen area could have resulted from movements along faults and from seismic disturbances. Lauritzen (1989a, 1989b and 1991b, p122) suggested that cave passages in Norway are almost always guided by the line of intersection between two planes (but see section 6.4). His statistical analysis of several metalimestone caves revealed that commonly shear fractures (faults and shear joints) and less commonly tension fractures are utilised as primary guiding voids for speleogenesis. Attempts to predict cave passage trends were made by modelling the fractures, which gave acceptable results in some situations. Lauritzen did not consider the possibility that the fractures in metamorphic limestones remain sealed, but act to guide inception in the adjacent rock (as suggested for sedimentary strata by Lowe, 1992a), because he relied on the assertion that "*from the theory of speleogenesis it follows that cave conduits are formed from pre-existing fractures*" (Lauritzen, 1989b, p118). Onac

(1991) noted caves formed by gravitational mass movement near Narvik, and the influence of tectonic faults in guiding subterranean streams.

As noted in section 3.1.18, Randall *et al.* (1988) reported on the hydrogeological framework of the NE Appalachians, a region that has a comparable metamorphic Caledonide geology to the study area. They noted high hydraulic yields from fractured non-porous bedrock, especially from wells that intersect contacts between different lithologies. Earlier work was quoted that showed that fractures decrease in size and frequency some 50–75m below the surface. "*Zones of tension fracture and zones perpendicular to the bedrock fabric are more likely to be open and bear water than zones of shear fracture or zones parallel to the bedrock fabric*" (*Ibid.*, p179). The watertable configuration in uplands nearly replicates the topography throughout the region, so that inter-basin flow systems involving significant flux have not been shown to exist. *All these observations seem relevant to the study area.* Carlsten and Stråhle (2001) reported that open, and partly-open, fissures were found in a borehole at Bodagrottorna in non-carbonate rock on the Swedish Baltic coast at depths at least down to 150m, in an area that was very active seismically in the early Holocene.

Seismic and aseismic tectonic activities that lead to the creation of fractures can arise from several separate mechanisms. The evidence for considerable uplift, starting from a rapid rise at the start of the Holocene is well documented, and some of it was discussed in section 2.4.6. That part of the evidence for uplift that is associated with caves includes Sjöberg (1981a and b), who discussed 50 elevated caves in east Sweden formed by cobble abrasion at the coast of the Baltic sea or its predecessors, and Sjöberg (1988) who discussed elevated coastal caves in central Norway. That seismic tectonic activity accompanied the uplift was documented by: Husebye *et al.* (1978); Mörner (1980); Stephansson and Carlsson (1980), who discussed a Caledonian Zone of seismicity; Anderson (1980), who suggested that the maximum number of earthquakes (brittle shear failures) after deglaciation would occur just inland along the coast, especially in regions of large elevation differences perpendicular to the coastline; Sjöberg (1987a and 1987b), who classified Swedish neotectonic cave types as occurring a) in split roches moutonées, b) in collapsed mountain slopes, and c) in sub-horizontally displaced mountain tops, and who postulated that talus caves in Sweden were formed by earthquakes caused by the early and rapid (20–50cma^{-1}) Holocene uplift (although an alternative mode of formation for the Swedish talus caves in Precambrian rocks was proposed by Bergsten, 1976, who thought that they formed by the movement of rock masses caused by the pressure of over-riding glaciers); Sjöberg (1996b), who dated the formation of scree and talus caves by a huge tectonic event at 9400–9200a BP; Sjöberg (1996c) and Mörner (2003), who recorded that, for the first time, the Swedish nuclear industry has had to accept that Sweden suffered heavy earthquakes immediately after the Weichselian glaciation; Sjöberg (1996d), who listed Swedish Holocene earthquakes with magnitudes from 5–8 and showed how the formation of seismotectonic caves could be dated by studying soft sediment deformation in varved clay, as also discussed by Sjöberg (1999a; 1999b); Kejonen (1997), who described seismotectonic crevice caves in Finland that developed from 12–8ka BP; Laberg and Vorren (2000), who described Holocene megaslides in northern Norway;

and by Mörner (2003) who presented 15 papers to demonstrate that Scandinavia was an area of high seismic activity at the time of deglaciation.

Mörner *et al.* (2000) noted that palaeoseismic events occurred in the Stockholm area about every 20 *varve years* from ~10490 to ~10410a BP, and listed 15 events in Sweden with magnitudes between 6 and >8 from ~12500 to ~1000a BP, some being associated with tsunamis. As the records came from the whole of Sweden, no region could be considered aseismic during the deglaciation period. The formation of the Bodagrottor talus cave (close to the borehole discussed in a previous paragraph) by the 'blowing-up' of a roche moutonée occurred at 9663a BP, by the dating of a varve that arose from a synchronous earthquake-generated tsunami that swept across the Baltic sea 33 varve-years after local deglaciation. From the size of the individually moved blocks, this earthquake may have had a magnitude greater than 9–10. A map produced by Mörner *et al.* (2000, Fig. 1) shows that each seismic event occurred as the ice margin passed overhead. Thus, from all this evidence, it is sensible to suggest that some fractures in the metacarbonates of the Caledonides were caused by surface strain release, or by deeper seismic activity, associated with the fast, early Holocene, uplift, at a time coincident with the passing of the ice margin.

The uplift was not necessarily uniform, even at a local scale. Differential uplifts caused crevasses and other changes of slope, particularly along ridges. Braathen *et al.* (2004) described four types of failure of rock slopes that occur especially in valley shoulder locations (CL=S), where this thesis shows that cave dimensions are maximised (section 5.3.4). Additionally, Warwick (1971), Ford and Ewers (1978) and Lauritzen (1986a) suggested that pressure release at the sides of valleys could create fracture zones, including after melting of the local valley glacier (section 3.2.1; Photo 3.1).

Rohr-Torp (1994) confirmed that fractures in Scandinavian crystalline rocks are strongly related to isostatic uplift, rather than being a common phenomenon among all regions with crystalline rocks. He found excellent linear relationships (R^2>0.85) between the local present rate of uplift (which itself is positively correlated with the total Holocene uplift) and the mean and median of both borehole yield and the reducing depth required to achieve an adequate yield, at sites across southern Norway. Concluding that young tectonic events have rejuvenated old fractures, he proposed a simple rule to predict the typical yield of a randomly-placed drilled well in Precambrian rocks in Fennoscandia: the yield is 180Lh^{-1} at a place with 0mma^{-1} uplift from a well at 80–85m depth, increasing by 100Lh^{-1}, from a required depth of 6m less, for each extra mma^{-1} of uplift. Present study area uplift rates vary from 2.5–5.5mma^{-1} (at the coast to beyond the MSW). The fracture patterns and dimensions that may support this groundwater storage and flow in Norway were discussed by Banks *et al.* (1996) and by Gudmundsson *et al.* (2002). Ford (1983, p157) referred to this mechanism in Canada as *"isostatic groundwater pumping"*.

Thorson (2000) noted that, with the new recognition of the effects of glacial mass transfers, there is now a blurring between the study of basic tectonics, and the study of *glaciotectonics*, and further, that seemingly trivial changes in stress may be sufficient to nucleate earthquakes, especially if there is a

change in *crustal pore pressure*. Citing other authors, he reported that crustal permeability reduces systematically with depth in a simple log-log relationship spanning at least 10 orders of magnitude. Muir-Wood (2000) discussed a new generation of models of glacial unloading of the lithosphere that show that the horizontal strains developed may have a greater potential for seismotectonics than just the vertical component of rebound. Whereas changes in vertical stress instantaneously follow the ice load, the changes in horizontal stress are chiefly a function of the viscoelastic response of the underlying mantle. Thus, at deglaciation, tectonic strain energy that was accumulated during the whole period in which the icesheet had been in place "*can be liberated in a major seismic outburst*" (*Ibid.*, p1410). Modelled horizontal velocities along the Norwegian continental margin are ~2mma^{-1} away from the icesheet centre. Stewart *et al.* (2000) noted that horizontal plate motions normally drive crustal deformation, but with the onset of glaciation, this style is overprinted by the glacial stress, and new horizontal crustal motions increase outwards from the icesheet centre. Their Fig. 3a showed that subglacial water penetrates into the crust below enhanced icemelt in topographic hollows, increasing the pore-water pressure. Their model showed that large icesheets stabilise underlying crustal faults, whereas deglaciation destabilises the faults. Periods of cover by maximal Scandinavian icesheets represent times of seismic quiescence, due to the muffling effect of the weight of ice, as the land is gradually compressed and isostatically depressed (Johnston, 1987). Each glaciation tends to reverse the direction of tectonic movement of the previous deglaciation. The reverse movement occurs in smaller steps of lower seismic intensity, because ice sheets take longer to grow than to decay, and may be incomplete because of the prevailing stress from the mid-Atlantic ridge push. For small icesheets of radius c. 333km, ice loading increases stability only at shallow depths, and promotes instability at greater depths. Stability is decreased beyond the ice margin for all icesheets, and it is also decreased there during deglaciation, relative to the pre-glacial state. Thus, the effects of icesheets vary as they wax and wane and seismic activity can also occur during glaciations, prior to a 'pulse' of deglaciation seismotectonics.

Hunt and Malin (1998) suggested that the six major ice-rafting Heinrich events from 70–14.5^{14}Cka BP (section 2.3.3), known from layers of rock-fragments in Atlantic sediments from NE Canada, were triggered by ice-load-induced earthquakes around the perimeter of the Laurentide icesheet. In Fennoscandia, faulting is linked to zones with very steep ice gradients (which must occur early or late in the life of an icesheet), or to the final stages of recession, when the bulk of seismic activity probably occurs within a few hundred years. Following Johnston (1987), who noted that artificial reservoirs can trigger earthquakes by increasing hydrostatic pressure, it occurs to this author that local deglacial earthquakes may also be triggered by the formation of ice-dammed lakes (section 8.4). Fjeldskaar *et al.* (2000) suggested that stress-generating mechanisms can be grouped into three classes: first-order stresses across *Fennoscandia* that arise from the NW–SE compression normal to the mid-Atlantic ridge at the plate margin, which propagate stresses through an elastic lithosphere; second-order stresses that are limited to *Scandinavia*; and third-order stresses that relate to *local* features (e.g. topography) and rarely extend beyond ~100km.

Any of the above mechanisms may result in fractures that are open to the surface. Such fractures have the potential to fill with water in summer, so that any freezing during winter would subject the rock to increased stress. The magnitude of any widening is proportional to the sub-zero (°C) temperature at the surface (Matsuoka, 2001). Although most widening is reversed on thawing, there is a tendency for the fracture to be permanently enlarged, and then to admit a higher volume of water during the next freezing cycle. The temperature cycling of rocks of differing lithologies that have unequal coefficients of thermal expansion would also promote fracture enlargement along contact zones. Indeed, Gudmundsson *et al.* (2002, p64) stated that "*stresses tend to concentrate at the contact between dyke rock and the host rock and generate fractures that may conduct groundwater*". Thus, it is envisaged that tectonic inception commonly leads to a growth in the size of the near-surface fracture network, even without invoking karstic processes. If ice-dammed lakes completely froze in winter, then submerged fractures would also be subjected to further stress.

Another mechanism to increase fracturisation is *hydrofracturing* (e.g. Gudmundsson *et al.*, 2002). As discussed in Appendix A3.4, this process can force groundwater upwards through bedrock at gaps in permafrost, and this may possibly apply to metacarbonates during parts of the glacial cycle. A hydrofracturing technique to increase the well-yields of boreholes in crystalline rocks is to inject water under high pressure, to dilate existing fractures or to create new fractures. This can increase hydraulic conductivity by two orders of magnitude in the vicinity of the borehole (Howard *et al.*, 1992). At the base of a 500m-deep ice-dammed lake, the pressure would be 50 atm. Thus, water can be injected into fractures that may occur within any underlying metalimestones, and, according to Banks *et al.* (1996, p230), such pressures in a borehole may be sufficient to stimulate already fractured bedrock, and, possibly, to create new fractures. However, unlike at a pressurised borehole, the water pressures within fractures beneath deep lakes could be evenly distributed at each depth, so that the potential for hydrofracturing would appear to be more limited. Nevertheless, strain release, lubricated by the water, could still arise from local pressure differences between the rock and the water. Additionally, if the injected water froze during a period of local permafrost, fractures, and especially horizontal fractures, would be widened. A further mechanism suggested by Banks *et al.* (1996, p226) is that frictional stress at the base of a glacier, coupled with hydraulic fracturing (e.g. below a deep ice-dammed lake: Chapter 8), may develop permeability in underlying rock.

There is no reason to suppose that the concentrated seismic creation of fractures during Holocene deglaciation was unique: similar processes must have occurred during the approach of all previous Cenozoic interglacials (and perhaps interstadials), although the magnitude of the effects varied. From the speleothem chronozones proposed for Norway (Lauritzen, 1991a, Table 1), there are long intervals of several 10ka when speleothems did not grow, and full glacial coverage can be inferred. It therefore seems likely that large magnitude earthquakes only occurred once per 100ka glacial cycle. Similarly, the deglaciation of earlier icesheets, even going back to the Varanger Ice Age from ~620–580Ma during the formation of the Caledonides, can be expected to have caused earthquakes and near-surface fractures that

would promote tectonic inception in exposed limestones and metalimestones. However, along with the surface bedrocks, any caves formed therein are likely to have been eroded away well before now, or to have disappeared during metamorphism. Another mechanism for creating tectonic fractures was probably important during the slow, but large, Mesozoic and Cenozoic uplifts (Appendix A1.3.2 and section 2.2.2). Such uplifts of a large, rigid, crust were almost certainly accompanied by both seismic and slow tectonic movements, possibly creating in this case a deeper-seated set of fractures, but without ice wedging in the warmer climates. This tectonic activity was probably also supplemented by adjustments made during erosional unloading as the surface weathered.

6.3.2 Neotectonics

In addition to the postglacial uplift, there are two main sources of evidence of *neotectonics* in Scandinavia: the earthquake record, and the observation of movement along faults (e.g. Husebye *et al.*, 1978; Olesen, 1988; Bungum, 1989; Olesen *et al.*, 1992; Olesen *et al.*, 1995). The science of seismology has developed considerably since the early 1980s, with the use of local instrumentation that can record small earthquakes of magnitude 2. The results are summarised on a neotectonics map by Dehls *et al.* (2000a; Figure 6.1). The seismic events tend to follow N–S alignments at depths commonly focused above 15km at the Atlantic Ridge, along the Continental Shelf edge, along the Norwegian coast, rather randomly along the border and onto the Swedish shield, and along the Swedish Baltic coast.

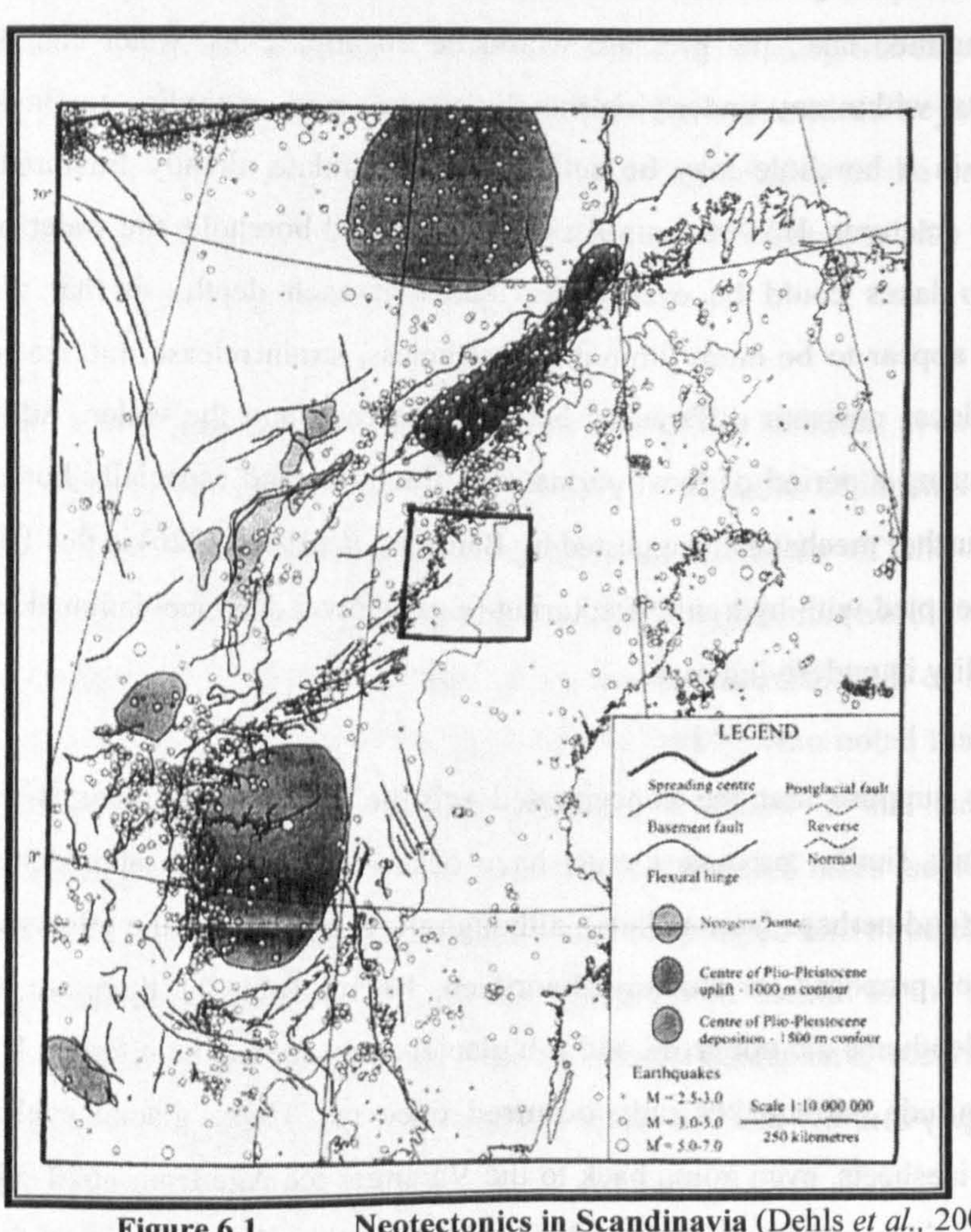

Figure 6.1 **Neotectonics in Scandinavia** (Dehls *et al.*, 2000a)
The study area is indicated

Many earthquakes have occurred in north Nordland and along the coast of southern Norway since 1750 AD, but lower frequencies and magnitudes coincide with the study area, which occupies part of the 'saddle' position between higher mountain ranges. Central Scandinavia probably acted as a focus for ice flow during late Cenozoic glaciations (section 2.3.3). With thinner icesheets, there was less stress relief and lower seismicity at each deglaciation. Additionally, increased ice flow increases glacial erosion, leading to less surface relief and less differential stress, and the increased sedimentation on the Vøring Plateau may have a dampening effect. The historical record of significant, but comparatively smaller and less frequent neotectonic earthquakes in the study area (Figure 6.2) *may* be representative of relative seismic activity during the whole Holocene, although, following the 'pulse' of deglaciation seismotectonics, the style of seismicity does change, as noted by Stewart *et al.* (2000, p1381): "*Whereas present-day seismicity is concentrated around the margins of the former icesheet, on deglaciation, earthquakes predominated at the centre of the rebound dome*". However, neotectonic earthquakes do follow the *Rana Fault Complex* south along the coast of the study area, and the largest recorded Northern European near-shore earthquake, of magnitude 5.8, occurred on 31 August 1819 AD in Rana, just north of the study area. Some 10000 micro earthquake shocks were recorded instrumentally at Meløy, 70km north of the study area, during 10 weeks in 1978 (Bungum *et al.*, 1979). These were up to magnitude 3.2, were heard and felt locally, and caused cracks in walls and chimneys.

The documented active postglacial faults are commonly NE–SW-trending reverse faults that lie within a 400km x 400km area in northern Fennoscandia (e.g. Arvidsson, 1996). Their lengths and maximum scarp heights vary from 3–150km and from 1–30m. Fault offsets range up to 13m (Dehls *et al.*, 2000b). A magnitude 4 earthquake occurred near one of these faults in 1996, and *large amounts of groundwater poured out of the escarpment*. The fault length to offset ratio indicates that the structure itself resulted from an earthquake with a magnitude above 7. The work of Olesen *et al.* (2004, p17) "*supports previous conclusions regarding a major seismic 'pulse' (with several magnitude 7–8 earthquakes) which followed immediately after the deglaciation of northern Fennoscandia*".

The earthquakes may not just be caused by isostatic rebound after the removal of ice. They may also indicate the opportunity for adjustment to glacial erosion after the 'muffling' effect of the ice cover has gone. The W–E Båsmoen Fault can be traced for 50km along Ranafjord (Figure 6.2). It has a maximum displacement of 10m, escarpments up to 80m, provides evidence of recent movements (30–40cm between 8780 and 3880a BP: Hicks *et al.*, 2000), and was associated with the 1819 earthquake. The 2km-wide fault zone is just north of the junction between the HNC and the RNC along the northern extremity of the study area for part of its length, and displays an anomalously *high* present uplift of 9.2mma^{-1} at Hemnes (Z6), and anomalously *low* uplifts for the islands of Hugla (Z9) and Tomma (Olesen *et al.*, 1995). The Rana area was the subject of an in-depth seismic study, NEONOR, from 1997–1999 (Hicks *et al.*, 2000). Some 267 local earthquakes were recorded, with magnitudes up to 2.8. The data showed a predominance of normal to strike-slip faulting with the tension axis normal to the coast, the same direction as the compression axis in other areas. "*The Rana area has a significant amount of the total seismic activity in*

onshore northern Norway" (*Ibid.*, p1431). However, none of this particular activity was directly connected to the Båsmoen Fault. The authors concluded that postglacial uplift is the most likely cause for this continuing high level of seismic activity.

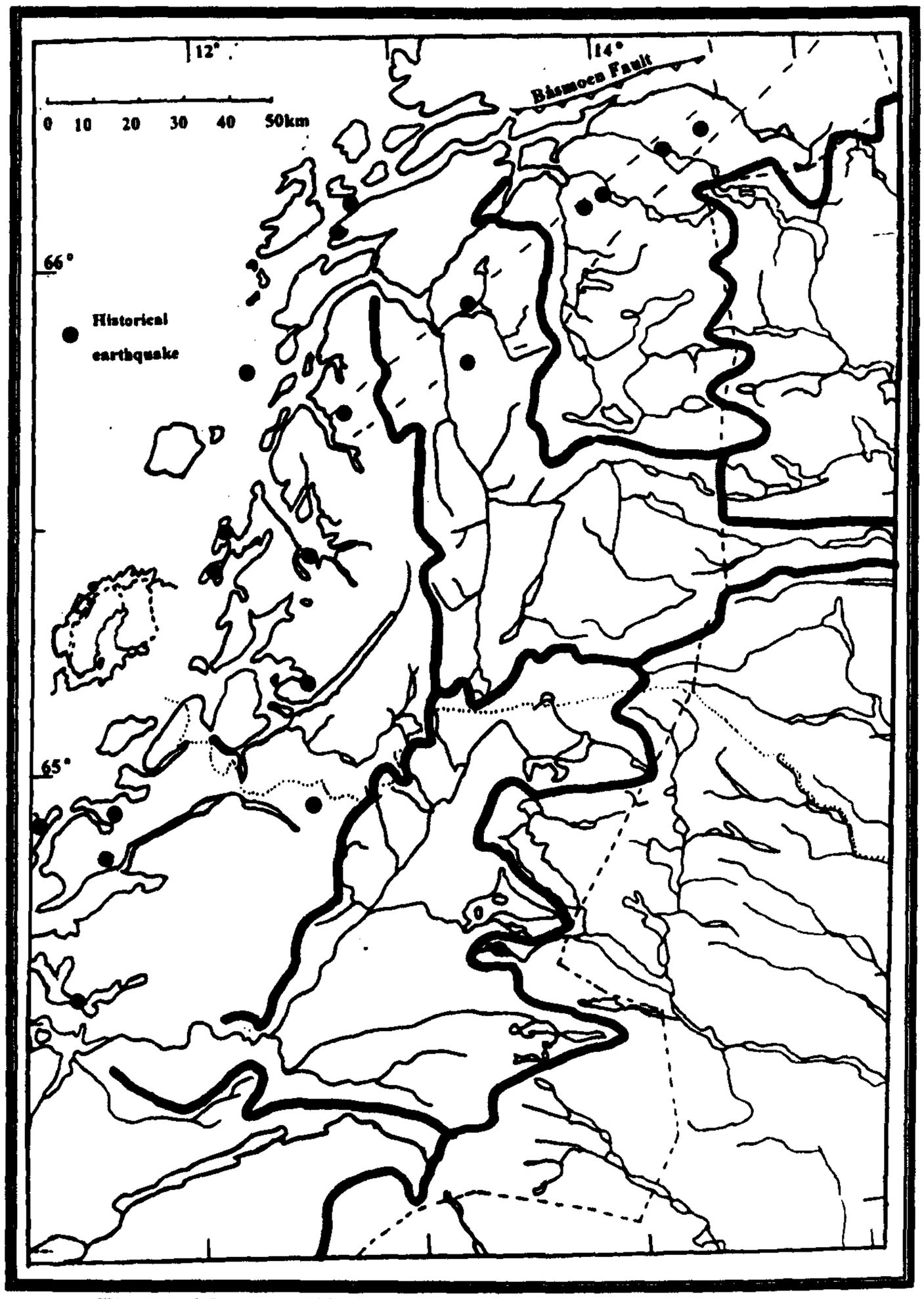

Figure 6.2 **Historical earthquakes in the study area**
(Various sources)

Muir-Wood (2000) suggested that the constructive or destructive interference between the postglacial and (plate) tectonic strain fields is strongly dependent on the 'original' tectonic regime, i.e. whether it is primarily extensional, compressional or strike-slip, and predicted that the present-day effects include alternating quadrants of enhanced seismicity and aseismicity around both rebound domes and former peripheral forebulges. His model showed a highly *seismic* forebulge offshore along the Norwegian coastal area, in front of an *aseismic* quadrant over northern Scandinavia with an apex at the centre of the previous icesheet, and a *seismic* quadrant over southern Norway and Sweden. The model is reasonably consistent with the seismic record from 1880 to 1990. Thus, the long postglacial faults (above) that arose from large earthquakes soon after the Holocene deglaciation in northern Scandinavia now lie in a region of reduced seismicity, as do, for example, Ireland and NE Scotland. This model was offered as an

explanation for the contrasts in seismicity between regions that in other respects have similar geological histories. Muir-Wood (2000) also discussed postglacial very shallow stress-relief phenomena, known as 'pop-ups', which are prevalent along the margins of the Laurentian icesheet, but relatively unknown in Scandinavia. However, Roberts (2000) reported offset structures in boreholes at road-cuts that are regarded as stress-relief features initiated by blasting. Fjeldskaar *et al.* (2000) supported the finding of Muir-Wood (2000) that stresses in western Scandinavia arise from the constructive interaction of postglacial uplift and ridge push, and noted that deep earthquakes occur mainly *offshore*, whereas shallow earthquakes occur predominantly *onshore*. Normal faulting (extensional regime) is dominant, with horizontal tension perpendicular to the coast. They explained the high seismic activity offshore from mid-Norway as being caused by the high bending stress in the transition zone between uplift and subsidence, which, as Hicks *et al.* (2000) remarked, is the zone with highest postglacial uplift gradients.

Olesen *et al.* (2004, Appendix A) included 54 classified claims of neotectonic movements from onshore mainland Norway. This was prior to new evidence discussed in section 6.3.3. The earthquakes and fault movements are commonly parallel manifestations of neotectonic activity that arise from both glacial isostatic uplift and longer-term plate tectonic ridge-push forces caused by oceanic spreading from the Atlantic Ridge. Thus, the bedrocks of the area are subjected to a mainly horizontal compressional stress-field (of >20Mpa at depths of 200–800m in the Ranafjord area: Olesen *et al.*, 1995), commonly orthogonal to their strike, which may be relieved in various ways. Within road tunnels there is anecdotal evidence that civil engineers report the sounds of rock moving, and 'rock bursts' occur when rocks fall from the roof, after blasting is complete. At the surface, crushed rocks and slipped blocks and notches on skylines may indicate postglacial movements along faults and nappe boundaries. Olesen *et al.* (1992) reported that as well as Holocene movement along one major fault in Finnmark (the northernmost county in Norway), the earliest detectable displacement is of *Proterozoic* age, indicating an extremely long-lived fault zone. Such fault zones lie parallel to the strike of the foliation, and give low resistivity readings *due to ingress of water into fractures*. Accommodation faults can lie sub-parallel to the main fault, a short distance away. Whereas the plate tectonic processes constitute the most important fault-generating mechanism in Finnmark, stress relief could still have been *triggered* during the deglaciation period.

There are no known *extensive* faults wholly within the study area, which, as noted above, is less seismically active, although Olesen *et al.* (1995) showed an earthquake zone that extends NE across the north of the study area, passing through Mosjøen and Korgen (Figure 6.2). Even with the publication of all recent Norwegian seismic events above magnitude 2 on the World Wide Web, there is insufficient data to correlate these events with the geological structure of the study area. Because the Weichselian icesheet had melted by 8500^{14}Ca BP, the present pattern of neotectonic seismic activity corresponds more to the *horizontal* stress field. As well as being concentrated at the centre of the rebound dome, the earthquake pattern from 10000–8500^{14}Ca BP was probably aligned along the mountain ranges, and represented the *vertical* isostatic rebound. During the similar deglaciation of Scotland, local movements

were caused by differential glacial load flexure stresses (Davenport *et al.*, 1989; Ringrose *et al.*, 1991), at places with the steepest ice gradients (Stewart *et al.*, 2000).

Heki (2001) showed that the interseismic stress build-up in NE Japan is modulated by the weight of winter snowfall, which reaches depths up to 3m in the backbone mountain range. GPS readings show that the mountains subside in winter, with vertical amplitudes of ~2cm peak-to-peak. At the same time, horizontal deformation up to 5mm occurs, with the land shortening beneath the load, and extending outside of it. A winter atmospheric pressure increase of ~1kPa acts as the equivalent of an additional snow depth of 25cm, enhancing the annual signature by ~10%. There is the *possibility* of earthquakes being triggered by these stress changes. It seems very probable that similar processes act in central Scandinavia to supplement other neotectonic activity, and to contribute to the continual enlargement of near-surface fractures within the metalimestones.

A conclusion from this review of neotectonic activity is that the seismic and aseismic creation and enlargement of near-surface fractures continued throughout each interglacial, to supplement the more intense fracture sets produced at each deglaciation. These processes probably combine to create a spectrum of fracture widths, lengths, frequencies and interconnectivities within the metalimestones. Such fracture systems may include subsystems that vary from being too small to transmit water, to those that are great enough to permit turbulent flow (without requiring karstic dissolution) over path lengths that in the study area reach up to 3.5km, as at Vallerdal (KL).

6.3.3 Evidence for tectonic activity from the study area

None of the 54 claimed examples of Norwegian neotectonic movement (section 6.3.2) lie within the study area. The lithologies of affected or adjacent rocks are rarely given, but there is no indication that any are in carbonate rocks. Thus, the list of 56 possible examples of tectonic movements presented in Appendix D1 may be the first recorded for the study area, and the first observed in both exokarstic and endokarstic situations. These uncorroborated observations were made by the author after the importance of tectonic activity to speleogenesis had become apparent, primarily during field trips in 1998 and 2000 and by the study of previous photographs. Altitudes range from near sea level to 770m. Elgfjell (Z4) provides many good examples. Most underground examples are intended to provide direct evidence of movement, after formation of the observing passage, rather than direct evidence of tectonic inception.

Only one observation concerns fallen, broken or curved stalactites and stalagmites, which are good diagnostics of earthquakes and relative roof movement. A few more unrecorded examples probably do exist, but speleothems are rare in the study area anyway (Appendix B2.9), and most of those that do exist are small and probably grew in the Holocene, *after* the large earthquakes occurred. Speleothems that grew in earlier interglacial periods have commonly been removed by subsequent deglaciations. The few chambers with roof spans greater than c. 6m commonly contain fallen blocks, which almost universally comprise limestones with clean, sharp, angular surfaces. This is suggestive that they fell after deglacial

deposition, and are situated high enough above streamways to have been little-eroded by Holocene flood waters. Only two of the chambers are lit by daylight from nearby entrances, so that only these two may experience severe, seasonal, frost action. The others (as noted) are not in entrance areas, and disturbance by seismic shock seems the best explanation for the occurrence of fallen limestone blocks. However, all the large chambers are within 30m of the overlying surface, and most within 15m, so that a second possible process is downward flexing of the roof by the weight of an over-riding icesheet (providing the cave was not filled by ice or water), as proposed by Warwick (1971; section 3.2.1), and upward flexing when the ice melted. A third explanation based on the freezing to a total ice fill during glacial conditions also cannot be ruled out.

It is the author's opinion, made after the 1998, 2000 and 2002 field trips to central Scandinavia and to northern America, that evidence of recent small neotectonic movement (e.g. bedrock movement that displays sharp edges or slickensides, without subsequent calcite dissolution or deposition) can probably be found in all relict and combination caves in metalimestones in the Caledonides. The rarity of observations from caves in the Køli nappes is probably not significant, because the author has looked for tectonic movements less often there.

On the basis of the available data, there appear to have been many movements in limestone in VSK and steep ASK. Those in VSK seem to occur in either vertical or horizontal slabs that are typically 1–3m thick, with the other dimensions of unknown extent. The movements, presumably caused by compressive stress from west to east, are commonly horizontal, normal to the strike, and with typical moved distances of only a few centimetres (and, rarely, several tens of centimetres), as expressed at the surface and within cave passages. The horizontal movement of vertical slabs of limestone 1–3m thick is compatible with the survey leg length of many caves in the study area, suggesting that joint systems (in, e.g., VSK) may be accounted for by this process (Photos D1.12, D1.14 and D1.38). Longer straight passage elements, and very wide, but low, passages, may arise from the horizontal movement of horizontal slabs of limestone (Photos D1.1, D1.6, D1.8, D1.20, D1.23, D1.27 and D1.37). These observations agree with those of Olesen *et al.* (2004, p13): *"the Norwegian bedrock consists of individual blocks that, to some degree, move independently of each other"*. According to Mörner (2003, p72), a passing seismic wave can cause bedrock to lift up and then sink back, whilst the ground is being severely shaken. This probably happened at **Cliff Cave** (Z4; Photos D1.22 and D1.23). Exfoliation fractures subparallel to the surface may also form by rapid erosional and deglacial unloading, perhaps supplemented by hydrofracturing (Gudmundsson *et al.*, 2002).With most tectonic movements being only a few centimetres, explorable cave passages are unlikely to be truncated along faults, and no such blind passages are known in the area.

A possible alternative explanation is that there has not been any movement, but that differential erosion or corrosion has given the appearance of movement. This could arise particularly if the apparent movement is aligned with the foliation. However, the visual and photographic evidence for tectonic movements at observations 18, 19, 22, 24, 29, 37 and 38 (Table D1.1) is compelling. The evidence

provided at **Elgfjellhola** (Z4; observation 18) is particularly convincing, because the movements are *across* the foliation. The evidence of protruding fault gouge wafers at surface sites (observations 22 and 39) that appear to cross-cut karren and stream channels suggests that these movements occurred in the Holocene, after the transport of ice across the area. This type of observation assumes that the wafers were extruded beyond the faces of the limestone blocks by seismic movement. An alternative explanation is that there was no extrusion, the movement occurred in an indeterminately-earlier timescale, and Holocene chemical dissolution of the surface has left the more resistant wafers exposed to a height that indicates the maximum extent of local surface lowering, or wall retreat in a cave. The wafers are calcitic, with polished surfaces and unknown dissolutional characteristics.

Whereas the movements along fractures in caves primarily formed by karstic dissolution are commonly small (the c. 1m movement in **Cliff Cave**, Z4, Photo D1.23 is exceptional), the movements at the purely *tectonic* caves are much greater, with *minimum* movements of around one metre. The observed tectonic movements in karst caves commonly follow the plane of the supposed inception fracture. Additionally, all caves probably display a high concentration of joints and fractures (c.f. the epikarst in sedimentary limestones) that lie parallel or normal to the plane of foliation, and in some cases at other angles. These openings may not show lateral movement, but the variable degree of sharpness or smoothing by dissolutional water indicates that they probably represent a general settling upwards of large superficial carbonate blocks after seismic shocks. The sporadic lines of speleothems beneath roof joints indicate 'failed' vertical inception fractures, which transmit water more readily in vadose rather than phreatic conditions, and in which precipitation is not possible without degassing of CO_2.

6.4 Evidence for tectonic inception

It is self-evident that if tectonic caves can form in non-carbonate rocks, such as the entrance to **Secret Stream Cave** (Elgfjell, Z4) in mica schist (Photo D1.13), then, despite metalimestone perhaps being slightly more ductile than some other local lithologies, there almost certainly exist natural conditions that promote the creation of tectonic caves in marbles. Indeed, Table D1.1 lists several apparently-tectonic caves in limestone. Such caves may be recognised by their angular or triangular passage profiles, especially at roof level (sediments, clastic materials and fallen rock may still provide a flatter, sub-horizontal, floor). It is also self-evident that if a limestone tectonic cave later became part of a drainage route, under vadose or phreatic conditions, then normal karstic chemical and mechanical erosion processes would apply, and, over time, the passage would enlarge. If the drainage was phreatic, then eventually the evidence of its tectonic inception could dissolve away. Even in vadose conditions, the signs of an original tectonic movement may be destroyed in all but the highest, perhaps inaccessible, levels. The only known examples in the study area of caves in metalimestone that possibly enlarged tectonically to explorable dimensions and later enlarged significantly by karstic processes are **Nordlysgrotta** and **Marimyntgrotta** (Z2). However, whenever a karst passage has been studied by the author, it has *always* been found to follow either the contact between metalimestone and another, non-carbonate, rock, *or* a narrow (commonly horizontal in VSK) fracture plane in the limestone. Because

there are likely to be rheological differences between rocks of differing lithologies, tectonic fractures are particularly likely to form at lithological contacts, under all conditions of seismic and aseismic tectonic movement. It is not necessary to have *intersecting* fractures for tectonic inception: apertures are uneven, and channel flow follows the widest part of the opening (Hanna and Rajaram, 1998). Nor is movement along the plane of the fracture necessary: a separating aperture adjacent to, or within, the limestone is sufficient. Such local rock splitting, especially vertical, may arise near the surface from deglacial and erosional unloading, without necessarily being triggered by seismic or aseismic processes.

On the basis of the accepted facts of seismic and slow tectonic activity in Norway (section 6.3), it is argued here that *all* the *karst* caves of the study area were subject to tectonic *inception*. Tectonic activity creates fractures, as shown in section 6.3.3, and some of these fractures must be open, as shown by the extreme cases of explorable tectonic caves. For the vertical stripe karsts in the Helgeland Nappe Complex (at least), it seems probable that horizontal movements produce sub-linear sections of horizontal fractures with apertures that match the mm- and cm-scale banding of the foliation. The availability of aggressive waters during meteoric and glacial conditions that can pass easily through connected fissures that lie close to the surface, and that commonly have high hydraulic gradients (Photo 7.2) promotes karstic enlargement. Indeed, just as it seems impossible for karst caves to exist in the metalimestones of the study area without tectonic inception (section 6.1), it also seems impossible for them *not* to exist, given the tectonic history and the availability and flow regimes of aggressive waters. Hence, *all the karst caves are hybrids*. After tectonic inception, conduits enlarged by dissolutional karstic processes, some with marine modification, and some with observable tectonic modification subsequent to inception. Photo 6.2 is an example of an enlarged proto-conduit on Elgfjell (Z4) that developed phreatically from a horizontal inception fracture. *Monogenetic* cave types in carbonate rocks include wholly tectonic caves, wholly sea caves (formed by wave action), and *jettegryter* (rock-mills, formed by mechanical action during deglaciation).

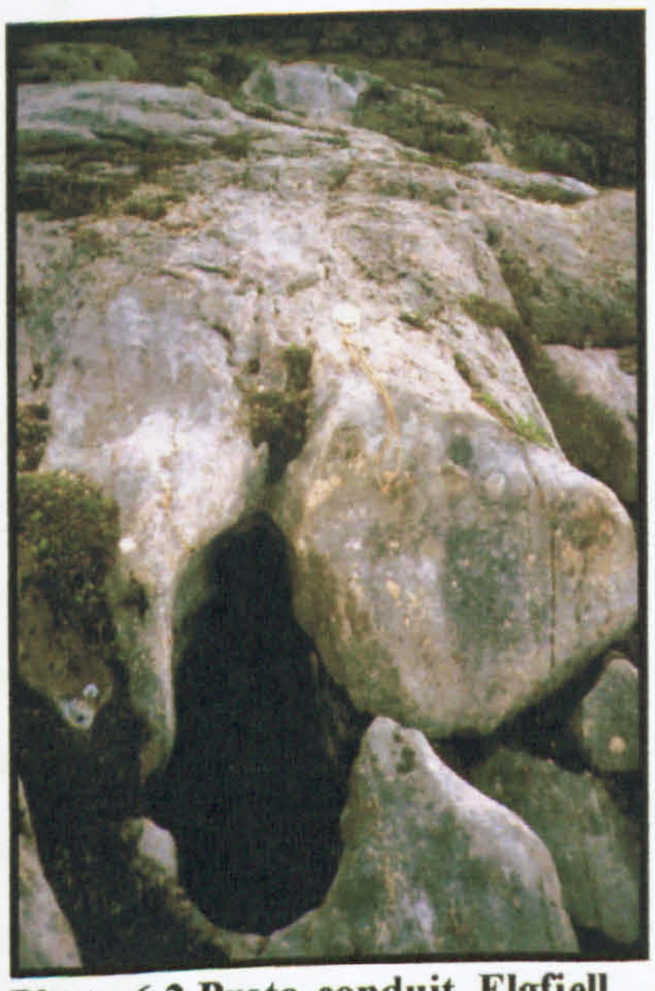

Photo 6.2 Proto-conduit, Elgfjell
Enlarged from horizontal inception fracture. Compass for scale.

6.5 Relationship between seismicity and extent of cave development

The neotectonics map (Figure 6.1) seems to suggest a rough relationship between the frequency and magnitude of earthquakes, and the lengths and depths of karst caves in a region. This linkage is considered further in this section.

6.5.1 Neotectonics and caves

The areas of Norway that are seismically the most active at present are the south Norway coast area, which has virtually no carbonate outcrops, and that part of the county of Nordland that is north of the study area. The area of northern Norway from Mo i Rana to Narvik has caves up to 17km in length and up to 580m in vertical range (Appendix D6.1.1). In contrast, the study area *may* have a comparable density of karst caves, but with lengths and VRs only up to 5.6km and 180m. It is therefore hypothesised that the depth of inception fractures below the surface, and hence the total lengths of potential proto-conduits, are related to the magnitude, and perhaps to the frequency, of local deglacial earthquakes. As this seismicity is probably related to the scale of isostatic uplift and to the differential pressure change that occurs along valley walls as the icesheet recedes (Davenport *et al.*, 1989; Ringrose *et al.*, 1991), it follows that cave depth and length = function (fracture depth and extent) = function (strength of tectonic activity) = function (change of ice thickness during deglaciation).

From the above conclusion, it can be anticipated that the caves with the greatest dimensions lie along the Swedish border area, because the icesheet was thickest there during each glacial and this should cause the largest earthquakes at the end of each deglaciation, and therefore the most extensive and deepest set of fractures. This may account, at least in part, for the presence near the border of four of the five longest caves of the study area (Table 5.16): **Korallgrottan** (KL), **Labyrintgrottan** (ZC), **Stor Grubblandsgrotta** (KU) and **Sotsbäcksgrottan** (KU). The three deepest caves (Table 5.17) also lie in this region: **Ytterlihullet** (ZA), **Korallgrottan** (KL) and **Sotsbäcksgrottan** (KU).

The relationship between seismicity and cave development is supported by the evidence summarised in section 5.8.2, that those caves in close proximity to a major thrust zone have larger-than-average mean dimensions, whereas those in close proximity to a major igneous pluton tend to be smaller. If the enhancing relationships are, in fact, directly controlled by the thrust attribute (rather than this just acting as a proxy for some other controlling variable), then this implies that the reactivation of old thrusts by deglacial seismic shocks promotes fracturing in adjacent metacarbonate outcrops, creating longer and deeper voids for cave inception. To be effective at the deepest parts of each cave, these movements must have been more recent than the time it would take for the bedrock above to be removed by the erosional lowering of the surface. Two mechanisms are possible to explain the restricting case. Firstly, the previous high-temperature contact metamorphism of metalimestone may reduce its fracturing ability, by making the rock more homogeneous. Secondly, the presence of a large igneous pluton may, of itself, reduce the magnitude of local earthquakes, and, therefore, their ability to create long and deep fractures. Of the five

caves mentioned above, three occur disproportionately near a major thrust zone (T=1), and none lie in an outcrop subjected to contact metamorphism, again lending support to the relationship hypothesis.

6.5.2 Subsurface cave distance

Sections 5.3.7 and 6.1.4 discussed the shallow nature of most cave systems, suggesting that caves in stripe karsts have formed entirely within an upper zone of fractured rock. In section 6.5.1, it was hypothesised that there is some relationship between cave depth and the local change of ice thickness during deglaciation. A more direct relationship is likely to be with the maximum distance of cave passages from the overlying surface. This *subsurface cave distance* is taken to be the length along a line orthogonal to the surface and the centre of any intersected passage (Figure 6.3). For short caves and vertical caves, it approximates to the cave vertical range, which is the vertical difference between the highest and lowest explored points of a cave.

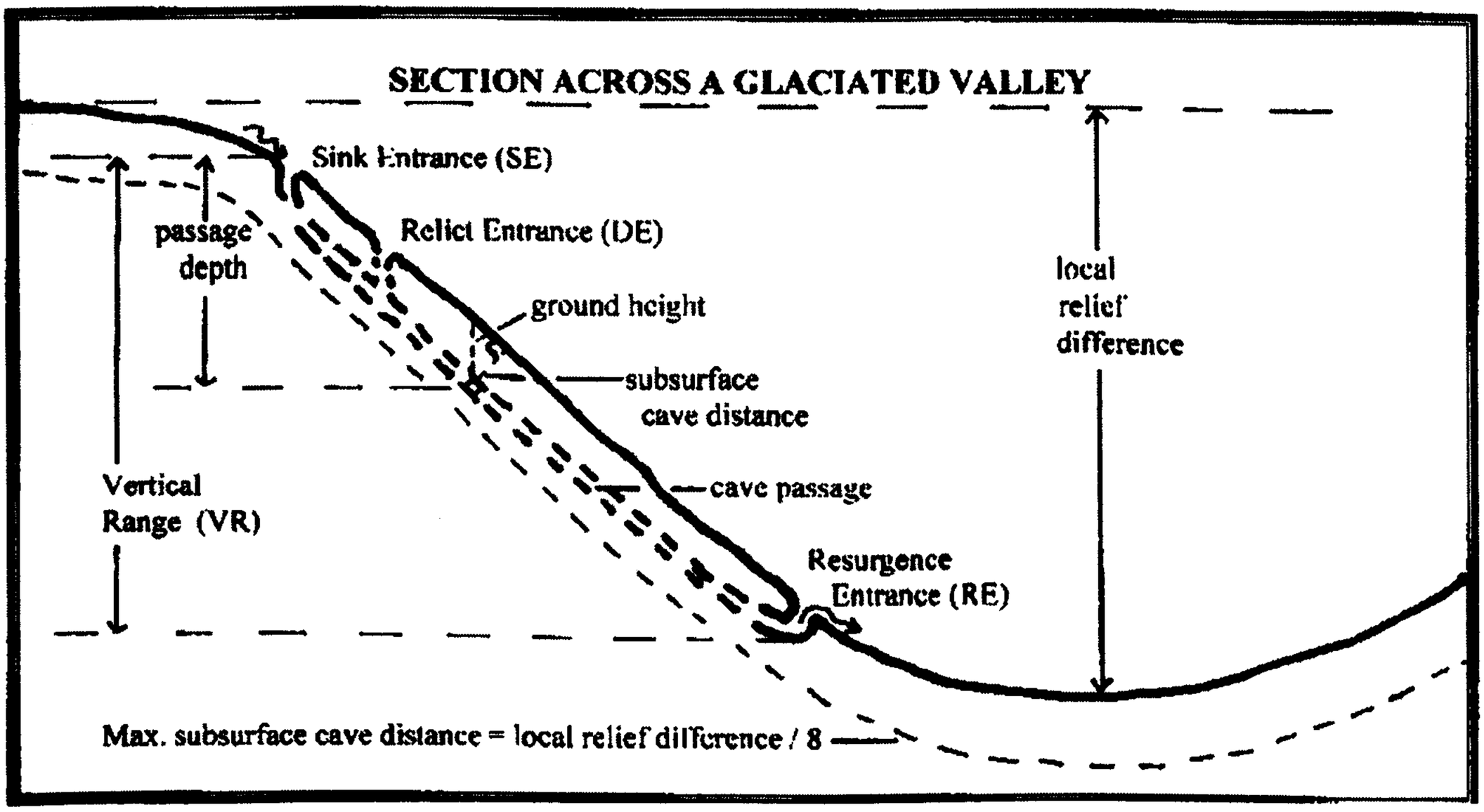

Figure 6.3 Subsurface cave distance and other terms

In order to test the distance and relief relationship, the maximum subsurface cave distances of 39 of the deeper caves of the study area (obtained from cave survey sections) were plotted against the local relief differences (Figure 6.4). The local relief differences were taken from the 1:50000 topographical maps by measuring the height of the local ridge-shoulder above the base of the valley, where the slope profile was consistently steep. The caves occur at any altitude along this profile, and the total lengths of the profiles were always less than a few kilometres. There are few caves in areas of local relief difference of less than 100m, and none of these have VR>10m. Figure 6.4 shows that the maximum distance of cave passages (and therefore of dissolutionally enlarged inception fractures) from the surface is commonly one-eighth, or less, of the extent of the change of local relief. The *maximum* envelope for the relationship of subsurface cave distance to local relief difference appears to be approximately linear, at least for a local change in relief of up to 400m, and perhaps up to 800m. Most of the inner zones of the study area are

represented by the caves shown in Figure 6.4, which shows that the one-eighth relationship probably applies across the whole area. Four of the 39 caves in Figure 6.4 are relict caves, 35 are combination caves and 15 (38%) are type h, the most complex caves.

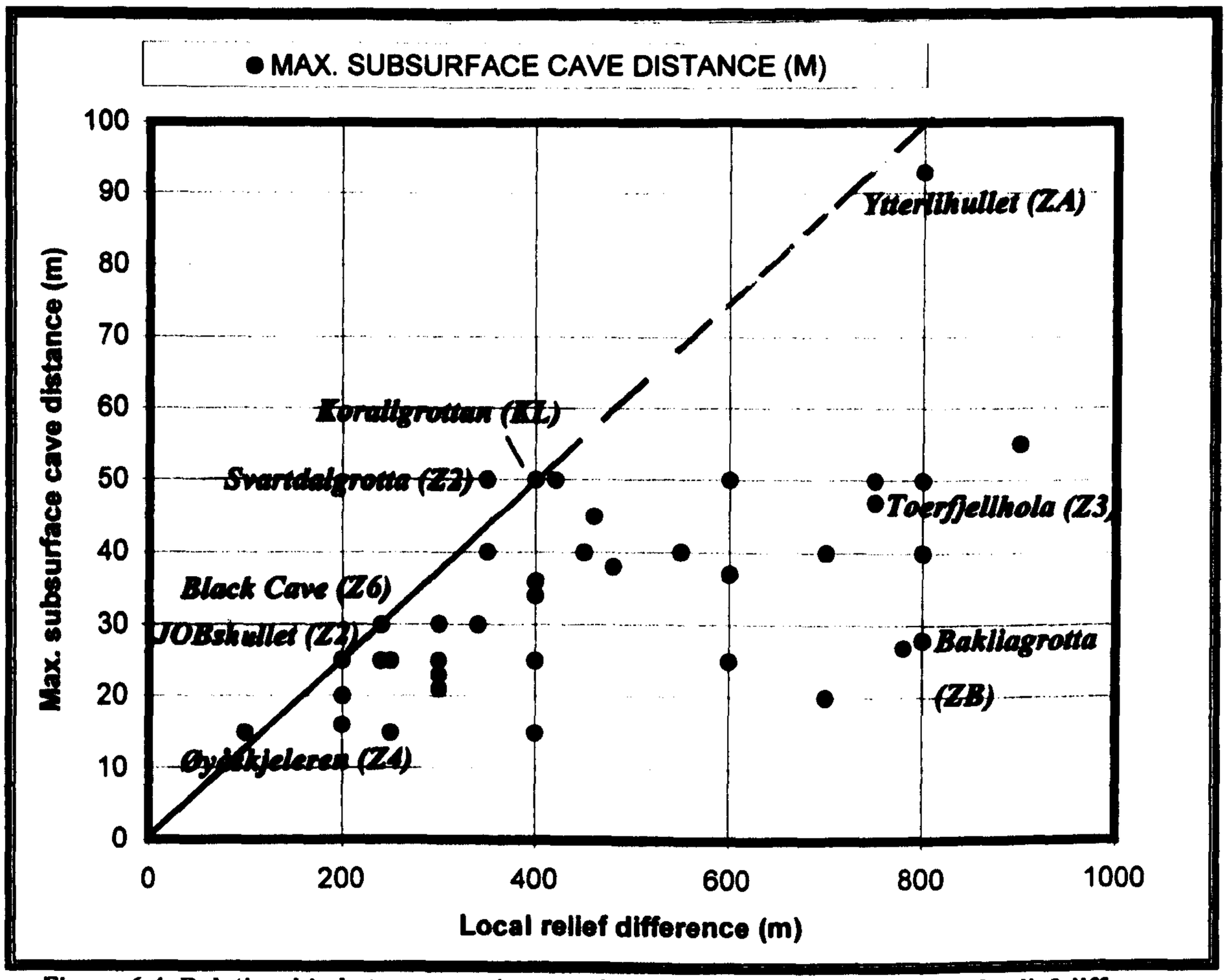

Figure 6.4 Relationship between maximum subsurface cave distance and local relief difference

6.5.3 The influence of external attributes on inception fractures

The relationship between seismicity and the extent of cave development is explored further in Table 6.1. Information about how the various external cave attributes influence mean cave vertical ranges, lengths and volumes was taken from Tables 5.6–5.14. From Table 6.1, the contact metamorphism, thrust proximity, cave location and glacial situation attributes have the most consistent effect on the main cave dimensions. Karst type, slope relationship and orientation have much less consistent influences. The influences on cross-section are examined in Chapter 8.

The percentages of the 39 caves in Figure 6.4 with each value of each of the influencing external attributes were compared with the same percentages in the total set of caves. This exercise showed that the individual attributes that promote caves towards the one-eighth limit of the distance / relief relationship are the same as the VR key influences in Table 6.1. Thus, R=1 only occurs in 18% of the 39 caves compared with 23% overall and T=1 occurs rather more often (13%, compared with 11%). Cave locations CL=F and P are under-represented, CL=G and W are similarly represented, and CL=R and S have two to three times the representation. The glacial situation is slightly more complex, because GS=E,

L and T are under-represented and GS=D and G are similarly represented. However, GS=H, K and S are over-represented. The rank order representations of karst type, slope relationship and orientation attributes for the 39 caves do not vary from those of the full set of caves.

Table 6.1 External attribute influences on mean cave vertical range

External attribute	Mean VR <8.8m	Mean VR ~ c. 8.8m	Mean VR >8.8m	Notes
Karst Type	V	A	L	Other cave dimensions vary
Contact metamorphism	R=1	R=0		Similar for all cave dimensions
Thrust proximity		T=0	T=1	Similar for all cave dimensions
Cave Location	F and **P**	**G** and W	**R** and **S**	Locations in **bold** have similar influences for mean length and mean volume
Slope Relationship	N		D and U	Other cave dimensions vary
Orientation	P	N and O	A	Other cave dimensions vary
Glacial Situation	D, **E**, G and **T**	**L**	**H**, K and S	Similar for mean length and volume. Eastern situations are shown in **bold**

Refer to section 5.3 for individual attribute definitions Excludes attributes with populations <2%

These results confirm that the seismic production of deep inception fractures is *enhanced* near major thrusts, in ridge and shoulder cave locations, and above westward-draining valleys that are above the glaciation marine limit. Inception fracture depths are *restricted* near igneous intrusions, at coastal, valley floor and paleic cave locations, and both below the deglacial marine limit and in the large population above eastward-draining valleys that are above the highest local col. Karst type, slope relationship and orientation do not have much influence on the distance / relief relationship. The differing properties of caves east and west of major ridges are discussed further in Chapter 8.

The proximity of the caves in Figure 6.4 to the one-eighth 'limit' can be discussed in terms of the competition between their various external attributes. Only **Øyåskjeleren** (Z4) and **Svartdalgrotta** (Z2) exceed the normal relationship, with subsurface cave distances that reach about one-seventh the local relief difference. Not only are these two caves situated in the shoulder cave location (CL=S) at GS=H, they also both lie behind large vertical cliffs, suggesting that the effect of seismic shock is magnified even more by steep topography. In the case of **Svartdalgrotta**, this overcomes the restrictive effect of an adjacent, but small, intrusive outcrop. **Korallgrottan** (KL) is shown at the one-eighth limit, probably because of its proximity to a thrust, despite lying essentially in a valley floor location at GS=S. However, its maximum distance from the surface is only estimated approximately. **JOBshullet** (Z2) also lies on the one-eighth line, despite being surrounded by an enormous granite outcrop, probably because it is at GS=H and has its cave location in a narrow ridge, which is seismically very favourable. Fractures in R and S locations are also more likely to open farther by ice wedging and by gravitational mass movement, explaining why caves in these locations have the largest numbers of entrances per cave (Appendix B2.1), creating many *through caves*.

Previous discussions (Appendix B1.10 and sections 5.2.4, 5.3.4, 5.3.7, 5.8.4 and 6.1.5) suggested that part of **Ytterlihullet** (ZA) achieves its exceptional (for this study area) 93m subsurface cave distance because it occurs in a low angle karst with interlayered amphibolites that acted as inception horizons. This remains a valid factor, but the cave is also situated at GS=S and CL=S, on the eastern shoulder (i.e. facing west) of the largest and deepest glaciated valley in the study area. This is 5000m wide and 800m deep and lies below the Okstind mountain range that has the area's largest remnant glacier. The cave is thus ideally situated to take advantage of deep fractures produced by high-magnitude seismic events that shook the area after each of its deglaciations. From Figure 6.4, inception fractures formed along the observed amphibolite layers still lie within the limits of the one-eighth relationship.

From the evidence in Figure 6.4, fractures are created only rarely up to the one-eighth 'limit'. Additionally, their enlargement into cave passages at the depths reached must be constrained by the extent of the limestone outcrop in that area, and by the geological and topographical inheritance: passages can only develop in size (even under deglacial conditions) if there is a suitable hydraulic pathway. Deep fractures that have no route back to the surface can only fill with static water, and not enlarge. Thus, some caves with subsurface depths that are well inside the one-eighth line can be explained by a lack of suitable limestone extent (e.g. **Bakliagrotta**, ZB, and perhaps **Toerfjellhola**, Z3). At the extreme, areas that do *not* exhibit cave systems, or that contain unexpectedly shallow systems, despite containing extensive striped metalimestone outcrops, such as Stordal (Z2), may be areas of anomalously low seismicity. Indeed, the Stordal marble lies along the floor of a glacially-rounded valley that is surrounded by large plutons of quartz diorite and trondheimite, so that its lack of karstification can be ascribed to the contact metamorphism restriction and to its location. The many short and shallow caves at Övre Ältsvatn (KU) commonly lie in a low angle karst, 'remetamorphosed' in places by granitic intrusions, on a paleic surface plateau in glacial situations L and T. Thus, their small dimensions probably derive from both contact metamorphism and their location and situation. These all reduce local seismic activity and, additionally, CL=P restricts the opportunities for deep hydrogeological drainage.

A conclusion from the above commentary is that the largest positive influence on the production of inception fractures is the seismic magnification that can occur at cave locations R and S, especially if near a re-activated fault or thrust. Other locations and attributes are much less influential in enhancing or restricting cave development.

6.5.4 Fracture separations

The surveys of 34 of the more complex caves in the cave databases reveal (Table 6.2) that the mean vertical separation between sub-horizontal phreatic passage tiers varies from 2–13m (overall mean c. 5m) and the mean horizontal separation between near-vertical shafts and joints varies from 3–50m (overall mean c. 16m). The ratio of mean shaft separation to mean tier separation varies from 1–10 (overall mean c. 4.6). All these ranges appear to be independent of karst type. Because Marrett *et al.* (1999; section 3.1.17) provided evidence that fracture apertures in limestone follow a power-law scaling, it might be

assumed that, at any one time and place, fracture apertures commonly decrease with depth, so that the horizontal and vertical separations between tectonic fractures of a particular aperture size *increase* with depth, i.e. they become less frequent. However, from the survey sections of the two caves with the most passage tiers in the study area (8 in **Toerfjellhola**, Z3, and c. 20 in **Etasjegrotta**, Z4), there is little evidence of an increase in fracture separation with subsurface cave distance, which in these cases approaches 50m. It is assumed therefore that within the "*partially detached thin upper crustal layer*" of Davenport *et al.* (1989; section 6.2.3), fractures occur at essentially random intervals, but that the distance of this detachment from the contemporary surface equals the maximum subsurface cave distance. This random arrangement within an upper crustal layer contrasts with the finding of Milanovic (1981, p48) that the "*depth of karstification*" in sedimentary limestone obeys an exponential law.

Table 6.2 Separations between passage tiers and between shafts

Cave	Zone	KT	CT	Mean tier separation (m)	Mean shaft separation (m)	Ratio shaft/ tier
Klausmark System	Z2	A	h	3	3–30	1–10
Two Bridges Cave	Z2	A	h	4	20	5
Hornet Pot	Z2	A	g	6	30	5
Lislvatngrotta	Z2	A	g	3	25	8
Tourist Cave	Z2	A	g	4 - 8	22	3–5
Svartdalgrotta	Z2	L	h	10	10–20	1–2
Neptune's Cave	Z2	A	h	5 - 10	10–15	1–3
Balcony Cave	Z3	A	f	2	4	2
Toerfjellhola	Z3	V	h	5	12–22	2–4
Øyåskjeleren	Z4	V	f	5	8	2
Eiterådalgrotta	Z4	A	g	5	50	10
Sirijordgrotta	Z4	V	h	8	16	2
Håpgrotta	Z4	A	h	3	10	3
Green Valley Cave	Z4	V	e	2	5	2.5
Jordhulefjellhullet	Z4	V	f	4	20	5
Pustehola	Z4	A	h	6	12	2
Brown Stains Cave	Z4	A	g	4	10	2.5
Sarvenvårtoehullet	Z4	A	g	5	20	4
Gevirgrotta	Z4	A	h	5	15	3
Sarvejaellagrottene	Z4	A	h	8	12	1.5
Jegerhullet	Z4	A	h	3	10	3
Etasjegrotta	Z4	V	h	2	7	3.5
Invasjonsgrotta	Z4	V	f	13	40	3
Anastomosegrotta	Z4	V	e	3	8	3
Møllebekkgrottene	Z5	V	g	2	8	4
Geitklauvgrotta	Z5	V	h	3	6	2
Kompassgrotta	Z5	V	g	5	10	2
Blåfjellgrotta	Z5	V	h	4	10	2.5
Høgligrotta	Z6	A	f	4	10	2.5
Kvannlihola	Z7	V	d	5	50?	10
Grønndalsgrotta	ZA	L	g	8	16	2
Gielasvaratjgrottan	KU (Sw)	L	h	2	3	1.5
Sotsbäcksgrottan	KU (Sw)	L	h	10	20	2
Korallgrottan	KU (Sw)	A	h	4	18	4
SUMMARY		All	defgh	2 - 13	3–50	1–10
MEANS				5	16	4.6

6.6 Cenozoic seismicity

The tectonic inception concepts are explored further in Chapter 10, which makes comparisons between the caves of the study area and those in other parts of the Caledonides. If the existence of cave passages in metalimestones can indeed be used as a proxy for the formation of tectonic fractures, then the conclusions in this chapter are important in the field of seismology: they imply that fracture creation mainly arises from local earthquakes caused by adjustment to local-scale *differential* ice load, rather than from earthquakes or slow tectonic movements caused by Scandinavian-scale isostatic uplift or by mid-Atlantic ridge-push. Additionally, the presence and structure of the cave passages themselves may provide a method to deduce the strength and nature of the deglacial earthquakes.

From the evidence of water bodies on limestone (section 4.2.8), which suggests a lack of speleogenesis in parts of many limestone outcrops, it is assumed that tectonic activities and fractures occur in *clusters* along the various outcrops. As each successive glaciation deepened glacial valleys and fjords further, the ice thickness variation, and therefore the intensity of seismic shock in some earthquake zones, must have increased during the time of the Mio–Plio–Pleistocene glaciations, whilst remaining approximately concentrated on the same position. Hence, each successive deglaciation commonly re-activated previous fracture sets, and extended them farther along, and farther below, the contemporary surface than the previous one. Because the present maximum subsurface cave distance is commonly one-eighth the range of local relief, it seems likely that both the depth of the partially detached crustal layer and the subsurface distance of cave passages also increased at one-eighth the rate of glacial valley deepening. However, acting synchronously with this deepening, there is also the probability that previous palaeo caves were removed by glacial stripping. The competition between these two processes is explored in the following Chapter, to create a general external model of cave development.

CHAPTER 7 THE EXTERNAL MODEL

The aim of this chapter is to analyse how the study area caves developed in the context of the geomorphological evolution of their host region. Ideas discussed in Chapter 6 indicate that cave passages have the opportunity to enlarge from inception fractures that deepen after each glacial cycle. And yet, this deepening process is itself a consequence of the deepening of glacial valleys, which must also impact existing caves. An external model of cave development is derived in a black box approach by considering the caves as simple conduits at the competitive interface between the lowering surface and the deepening maximum subsurface cave distance.

7.1 Cyclic speleogenesis

As summarised in section 6.2.1, most *active* caves in the study area act in harmony with local hydrology and have an intimate epigean association with their local landscape. Because relict caves appear to differ from combination caves only by their chance lack of allogenic stream capture (section 5.5.6), it is hypothesised that the development of all study area caves is integrated with the local geomorphological evolution. In late Cenozoic times, the overall dominating process for exokarst, endokarst and non-karst geomorphology was the cycle of repeated glaciations and deglaciations. This was accompanied by the tectonic and mass movement activity necessary for the creation of inception fractures, which not only guide cave morphology, but provide the earliest pathways for aggressive waters (Chapter 6). The existence of palaeokarst caves from the Proterozoic to the mid Cenozoic, as Baltica moved north, is conjectural. It can be envisaged that caves developed slowly, in the more arid conditions, and only during floods. With less frequent and less strong tectonic events, caves reached smaller depths below the surface. However, with less dramatic processes acting over longer timescales, the largest passage sizes may still have been significant. Direct evidence of these passages is probably not observable now, firstly, because *all* caves would have enlarged in cross-section during the Mio–Plio–Pleistocene glaciations (Chapter 8), except perhaps for those that remain filled with palaeokarstic sediments (of which none are known in the study area), but, more importantly, because such caves would have been removed by surface lowering.

The Norwegian rate of valley lowering lies in the range 15–55m per 100ka glacial cycle (Tables A3.1 and A3.2). It also seems reasonable to assume that basal valley wall-retreat rates are in a similar range. **Sirijordgrotta** (Z4) has possible Holstein, Eemian and Holocene interglacial spring outlets at altitudes of 275m, 235m and 205m (Figure B1.5). These valley-floor lowerings of c. 40m and c. 30m during the Saalian and Weichselian glaciations may be typical for other local major N–S aligned glacial valleys. Because almost all cave passages in the study area occur within 50m of their overlying surface (Table 5.18), the removal and destruction of their higher and 'outer' levels by glacial erosion *must* be a significant component of the endokarst processes. Evidence for such 'unroofing' and 'dewalling' is presented in section 7.2. Cave destruction in sedimentary limestones was discussed in section 3.1.11. The

Sustersic (1999) concept of a *speleothanatic* 'death' zone below the surface, towards which caves appear to move, is one that is readily applicable to the study area caves. However, Sustersic did not discuss the idea that cave formation and cave destruction can proceed together, so that caves can also seem to move simultaneously *downward* through the carbonate lithology. The idea behind the *External Model of Cave Development* is that, viewed over several glacial cycles, individual caves develop downwards via tectonically-induced inception fractures, whilst, *at the same time,* appearing to move upwards, as their upper levels become destroyed near the lowering surface, to create *palaeo caves in the sky!* In the long term, any very old passage would actually slowly *ascend* relative to sea level before being destroyed, as isostatic adjustment compensates for weight lost by erosion. However, the mean elevation of caves within the whole landscape slowly *descends* relative to sea level, as the land erodes back to a peneplain. (Appendix A1.2.3 noted that up to 10km thickness of thrust sheets may have eroded away since the Devonian).

From the above logic, speleogenesis in the study area currently follows the glacial cycle. Caves may pass through one, or more, inception–enlargement–destruction sequences. It is suggested that caves systems ought commonly to be described in *four* dimensions, so that a cave, e.g. in vertical stripe karst (VSK), may be said to migrate vertically downwards over time, always exploiting and enlarging fractures below the level of its explorable passages at ever lower lithological levels, whilst the land surface follows behind it, removing the upper levels. Hence, in VSK, the *geographical coordinate* position of a cave may hardly change over long periods of time (or it may slowly migrate along the strike), whilst its detailed internal morphology evolves under the influence of the structural geology that it encounters during its total lifetime. The shortest *cave existence time* is less than one glaciation cycle, where the inherited situation is unable to provide tectonic fractures that go deeper than the thickness of carbonate bedrock removed by glacial and fluvial erosion per cycle. In this case, successions of independent (in four dimensions) *single-cycle* caves or conduits follow the lowering surface down through the lithology (Figure 7.1). The *longest* cave existence time occurs when, in the extreme, a single cave migrates all the way down from the upper karst surface formed during an orogeny, to the base of that carbonate outcrop as all the intermediate rock is removed. This *multi-cycle* cave development model is considered more fully in section 7.3.

It is envisaged that the phreatic enlargement of conduits primarily takes place under the surface of ice-dammed lakes (IDLs, Chapter 8). This enlargement occurs simultaneously with a corresponding dissolutional *lowering of the exokarstic surface*. With large quantities of very under-saturated water available at the limestone surface and in its underlying conduits, the rate of cave wall retreat commonly must equal the rate of surface lowering i.e. a passage radius increase of one metre would occur in the same time interval as a surface lowering of one metre. As passage radii rarely exceed a few metres, this constrains the total carbonate surface lowering by chemical dissolution to about one metre per glaciation, an amount that is not significant at the macro geomorphological scale, as represented on topographical maps, where the dominant processes are glacial scouring and fluvial erosion.

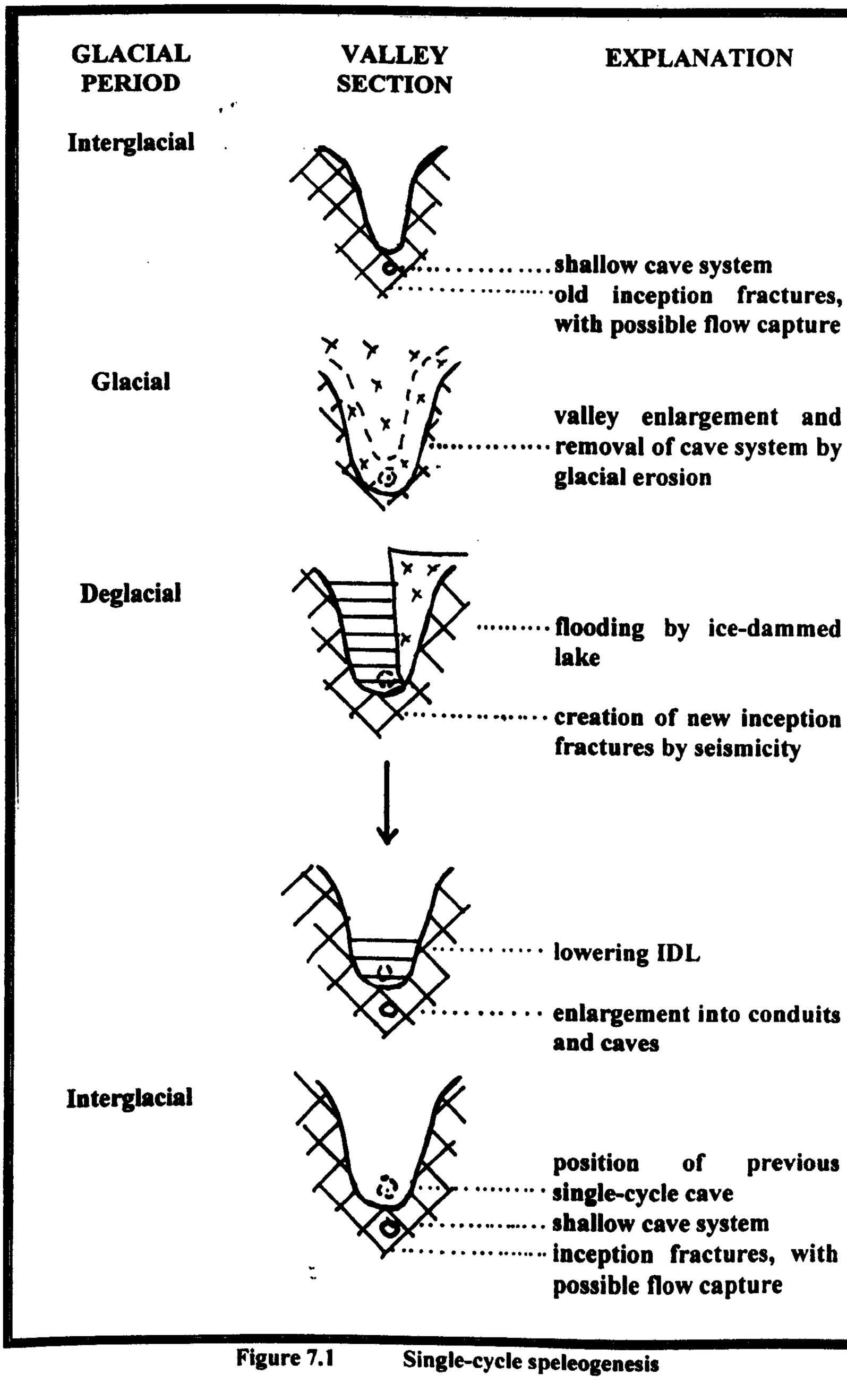

Figure 7.1 Single-cycle speleogenesis

7.2 Evidence for recent conduit formation and passage destruction

The interglacial vadose and phreatic enlargement processes are obviously visible at present in mainly vadose caves and in the streamways of combination caves. Less obviously, there is also observable evidence of both the first phase and the final phase of single-cycle cave development. Thus, the possible Holocene exploitation of inception fractures and the effects of glacial erosion on pre-existing caves were recorded during the various field trips.

7.2.1 Exploitation of recent fractures

Table 7.1 records 23 examples from many study area zones of present water flows along inaccessible fractures and conduits that lie below explorable cave passages or that appear as surface springs during the spring melt. *None* of these *underflow* routes is equivalent to a soutirage (sections 3.2.2 and 5.7.2), nor to the vadose entrenchment of a phreatic passage. Keyhole profiles are fairly common at the lowest level cave passages, but they do not require a new inception fracture for their vertical development: chemical and mechanical erosion of an existing passage floor are sufficient. Additional to the 23 inaccessible examples, the narrow vadose slot below a previous resurgence at Slot Chamber in **Jegerhullet** (Z4; no. 15; Photos D1.21 and 7.1) can be followed to the surface. These examples are *all* cases where the stream flow has migrated below the level of a continuing passage (or the surface) and has thus exploited an open fracture. It is hypothesised that such fractures were formed tectonically late in the Weichselian deglaciation. They commonly had insufficient time for dissolutional enlargement to reach explorable dimensions (Figure 7.1). If they had formed tectonically before a previous interglacial, they could have enlarged to form significant phreatic passages in the time available during phases of the last glaciation and deglaciation, as shown in Chapter 8. Such recent flow routes will be targets for enlargement during any future glacial / deglacial cycle.

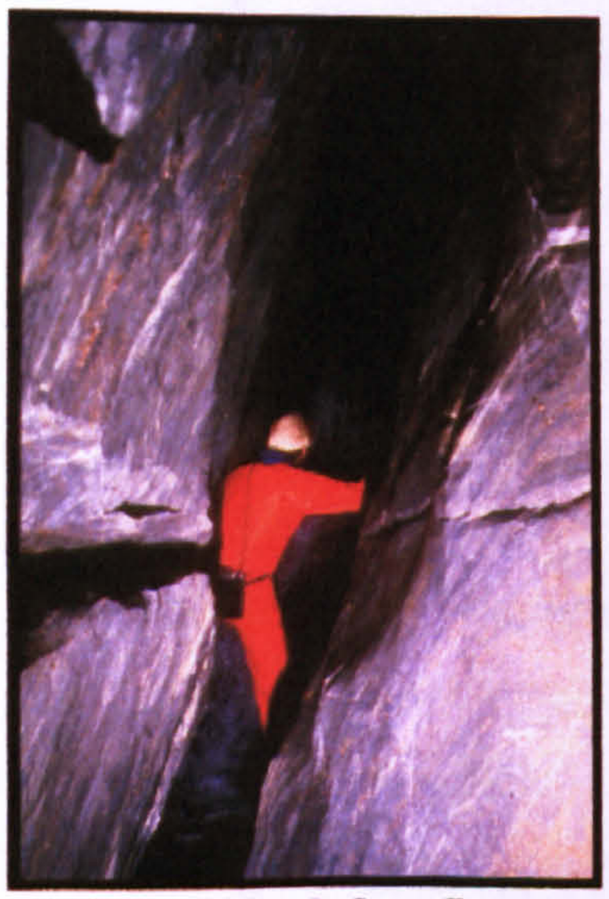

Photo 7.1 Slot below final chamber of Jegerhullet (Z4)
This Holocene vadose capture passage in VSK leads to the surface behind the camera, beyond a previous Vauclusian rising that is now blocked (Photo D1.21). Photo by P. Hann.

Photo 7.3 Spring on Hemnesøya (Z6)
Water emerges from metalimestone fractures at the HNC / RNC thrust zone

Photo 7.2 Fountain at Litl Hjortskar(Z5)
Spring at high stage from metalimestone fractures 1m above level of adjacent stream

Table 7.1 Examples of (probably Holocene) hydrological exploitation of lower fractures

No.	Location	Observation	Reference
1 Z2	Søvikgr. (Svarthullet?) UP84771285	Disappearance of water below waterfall	Ive (1980)
2 Z2	Bulandsdalgrotta UN90536700	Flow from Wet Passage into small fissures	Faulkner and Newton (1995, Fig. 7)
3 Z2	Nordlysgrotta UN81035251	Stream enters main rift from impenetrable passage	Author's unpublished cave sketch
4 Z2	Svartdalgrotta UN82074465	Inaccessible route from base of Wet Pitch to resurgence on surface	Figure B1.1
5 Z2	Skyttergravhola UN855423	Inaccessible stream route near end of cave	Faulkner and Newton (1995, Fig. 21)
6 Z2	Mølnvatngrotta UN85724155	Inaccessible stream route from Waterfall Chamber to resurgence on surface	Faulkner and Newton (1995, Fig. 22)
7 Z3	Toerfjellhola VN08424982	Several inaccessible stream routes	Figure B1.3
8 Z3	Cave of the Cold Wind VN08775007	Several inaccessible stream routes	Faulkner and Newton (1995, Fig. 17)
9 Z4	Sirijordgrotta VN15027065	Stream route from sump below 10m pitch to Elk Sump	Figure B1.5
10 Z4	Sfinxhullet, Kvitfjell VN15446270	Stream route from *above* Dry Pitch	Author's unpublished cave survey
11 Z4	Gåsvasstindhola VN15175400	Inaccessible stream routes	Faulkner and Newton (1990, Fig. 20)
12 Z4	Jordhulefjellhullet VN11875080	Inaccessible stream routes	Faulkner (1987, Fig. 10)
13 Z4	Elgfjellhola VN14525084	Stream route below pitch	Faulkner and Newton (1990, Fig. 9)
14 Z4	Buktgrotta VN15495142	Inaccessible stream routes	Faulkner and Newton (1990, Fig.18)
15 Z4	Jegerhullet VN15644702	Fissure passage below Slot Chamber, large enough to be entered	Faulkner (1987, Fig. 7) Photo 7.1
16 Z4	Invasjonsgrotta VN15924600	Stream route from Odd Chamber (*above* the flooded Whybro Passage)	Faulkner and Newton (1990, Fig. 7)
17 Z5	Møllebekkgrotta 2 & 3 VN21137835	Capture Passage below M3 entrance + stream route to resurgence on surface, at low flow	Author's unpublished cave survey
18 Z5	Trench Pot VN22276595	Stream route from The Pit	Author's unpublished cave survey
19 Z5	Kompassgrotta VN21675921	Three lower stream routes	Newton and Faulkner (1992, Fig. 11)
20 Z5	Litle Hjortskar VN223527	Karst area with very immature hydrology, with fountain rising during flood conditions	Photo 7.2
21 Z6	Gårdsfjellgrotta VP46054705	Stream lost under boulders to re-appear from small resurgence sump	Whitehouse (1969)
22 Z6	Høgligrotta VP22121260	Lowest stream route disappears along small fissures, to re-appear from resurgence sump	Author's unpublished cave survey
23 Z6	Hemnesøya VP44354215	Water springs from fracture in cliff beside road at the HNC / RNC thrust zone	Photo 7.3
24 KU	Renstängselgrottorna VP92672200	Inaccessible streamway	Sjöberg (1991b)

Co-ordinates are to UTM WGS84. HNC and RNC zones and Køli Nappes are listed in the 'No.' column.

7.2.2 The unroofing, dewalling and removal of cave passages

As with tectonic inception, the removal of cave passages by glacial erosion is difficult to *prove*. Little work has been undertaken to look for unroofed caves that may occur along gorges in carbonate outcrops, but lie away from known caves. Indeed, there are no known examples of internal cave chemical or clastic deposits now exposed to direct meteoric erosion in the manner described for sedimentary limestones (section 3.1.11). This is not surprising, given the local comparative rarity of these deposits (Appendix B2.9 and section 5.8.10), and the likelihood that they would also be removed by glacial action. Perhaps because most carbonate outcrops are aligned with the physical topography, there are also no known examples of truncated passages that continue on opposite sides of a valley, although there are many examples of such aligned passages on opposite sides of a doline. Thus, in the study area, conspicuous passage removal may only be associated with the upper, and outer, parts of the *known* caves. Table 7.2 gives some 39 possible examples of seven different observation types.

Table 7.2 Examples of (possibly Late Weichselian) cave roof and wall removal

No.	Location	Observation	Type	Grade	Reference
1 Z2	Klausmark Res. Cave UN86477822	Removal of passage between Res. Cave and Through Cave	WW	C	Faulkner and Newton (1995, Fig. 5)
2 Z2	Reppelv Resurgence UN91522835	Removal of connecting passages between caves	RL	C	Faulkner (1981, Fig. 7)
3 Z2	Langskjellighatten UN93405180	Passages removed between Sud–Øvre and Øvre–Laveste caves	RL	B	Author's unpublished cave survey
4 Z2	Aunhattenhule 1–4 UN94564950	Removal of four continuing passages by creation of a cirque (?) at Tarmaunvatnet. Or just formed beneath an IDL plus marine erosion?	PL	C	Author's unpublished cave surveys.
5 Z2	Nedre Landegrotta UN96723940	Dewalling at resurgence entrance	WW or RP?	C	Newton (1999, Survey 12)
6 Z3	Kringlotheia VN01674745	Shortening of both Wet and Dry Caves by valley widening. Or just formed beneath an IDL?	PW	B	Author's unpublished cave survey
7 Z3	Toerfjellhola VN08424982	Removal of upward cave loops by valley lowering, as seen by boulder chokes at passage ends	PL	B	Figure B1.3
8 Z4	Øyåskjeleren VN16529815	Shortening of cliff entrances by valley widening. Or just formed beneath an IDL plus marine erosion?	PW	B	Faulkner (1983, Fig. 27)
9 Z4	Eiterådal Res. Cave VN14477285	Entrance shortened	RP	B	Faulkner (1980, Fig. 3) Frontispiece 2
10 Z4	Kvitfjellgrotta Res. VN15476242	Shortened by valley widening. Or just formed beneath an IDL?	PW	C	Author's unpublished cave survey
11 Z4	Gevirgrotta VN15225148	Passage removal between Surprise Inlet and Longhorn/Shorthorn Caves	PL	B	Figure B1.6
12 Z4	Cliff Cave VN15824605	Entrances shortened by collapse	PW	C	Faulkner and Newton (1990, Fig.7). Photos D1.22 and D1.23
13 Z5	Øyfjellgrotta VP16770005	Removal of connecting passages to short caves at upper entrance	PL	C	Figure B1.10
14 Z5	Møllebekkgrotta 3 VN21137835	Recession of entrance	PW or RP?	B	Author's unpublished cave survey
15 Z5	Geitklauvgrotta VN20607700	Removal of Wasp Nest Passage link to Fearsome Passage	PW	B	Figure B1.11
16 Z5	Geitklauvgrotta	Roof removal at entrance doline	RC	B	Figure B1.11 Photo 7.4

17 Z5	Wide Cave VN22226560	Doline collapse	RC	B	Newton and Faulkner (1992, Fig. 3).
18 Z5	Camp Cave VN21775974	Doline collapse. Also at Upper Camp Cave and Baptists Cave	RC	B	Newton and Faulkner (1992, Fig. 7).
19 Z5	Virgin Hole VN21705920	Doline collapse. Also at Upper Virgin Hole	RC	B	Newton and Faulkner (1992, Fig. 10).
20 Z5	Saeterbekkgrotta VN20644800	Doline collapse	RC	B	Newton and Faulkner (1992, Fig. 4).
21 Z6	Kammelvgrotta VP32122190	Roof collapse at resurgence entrance	RP	C	Sutcliffe and Hobbs (1972)
22 Z6	Kumragrotta VP23772025	Removal of roof at Middle Entrance	RL	A	Photo 7.5
23 Z6	Rokåsgrotta VP20071480	Wall removal at resurgence	WW or RP?	B	Author's unpublished cave sketch
24 Z6	The Big Sink (D2) VN17022995	Roof collapse at entrance	RB	C	Newton (1999, Survey 22).
25 Z6	White Cave VN17073015	Roof collapse at entrance sink	RB	C	Newton (1999, Survey 24).
26 Z6	Dunfjell D8–D15 VN17073025	Entrance collapses	RC	B	Newton (1999, Survey 25).
27 Z7	Mellanselvgrotta VN350691	Shafts into streamway	RC	C	Doj (1993)
28 Z7	Flåflangahullet VN32205868	Many shafts into streamway	RC	B	Unpublished notes by Y. Freij (1991)
29 Z7	Kvannlihola VN28023985	150m surface flow to Nedre Kvannlihola entrance	RL Or RP?	C	Figure B1.14
30 Z8	Jengelgrotta VN35672340	Collapse doline separates Øvre and Nedre sections	RC	B	Faulkner (1987, Fig. 4)
31 ZA	Røssåga Sink Cave VP43880740	Dewalled passage filled with rocks	WW	C	Author's unpublished cave survey. Photo 7.6
32 ZA	Røssågagrotta VP43870760	R1, R2 entrances and link to R3 dewalled by valley widening	WW	B	Author's unpublished cave survey. Photo 7.7
33 ZA	Remnant Cave VP47152258	Walls removed at north end of cave	WW	A	Photo 7.8
34 ZA	Fjellbrygga VP49152190	20m-long, 10m-high, natural arch carrying $10m^3s^{-1}$ stream	PL	A	
35 ZA	Grønndalsgrotta VP54721720	Shortening of resurgence entrance	RP	B	Figure B1.15
36 ZA	Grønndalsgrotta	Krateret collapse into underlying passage	RC	B	Figure B1.15
37 ZB	Bakliagrotta VP51304385	Sink entrance shortening at gorge end	RB	C	Author's unpublished cave survey.
38 KU	Glimåkragrottan VP83670750	Doline collapse between Øvre and Nedre entrances	RC	B	Lindh (1978a)
39 KU	Tjårrogrottorna 14604 72906	Roof removed between Tj2 and Tj3 (Swedish co-ordinates)	RL	C	Faulkner (2000a)

Co-ordinates are to UTM WGS84. HNC and RNC zones and Køli Nappes are listed in the 'No.' column

Observation types:	RL	Roof removal by lowering of valley floor	No.	5
	RC	Roof removal by collapse doline		11
	RB	Roof removal at blind valley entrance		3
	RP	Roof removal at pocket valley entrance		3
	WW	Wall removal by widening of valley		6
	PL	Complete passage removal by valley lowering		5
	PW	Passage removal or shortening by valley widening		6
			Total	39
Observation grade:	A	Almost certainly caused by glacial erosion	No.	3
	B	Probably caused by glacial erosion		21
	C	Possibly caused by glacial erosion		15
			Total	39

Although these examples are easy to list, there may be other explanations for the observed features. Thus, a passage that may appear to have been shortened by the widening of a glaciated valley, may instead have functioned, and developed in size, purely as an input to, or outlet from, a glacial hydraulic system, with little later valley widening. Similarly, caves with thin roofs that have collapsed in places may not have had their roofs eroded by passing icesheets and glaciers: they may have formed just below the surface, with corrosion extending upwards from the inside. The shortening of entrance passages at blind and pocket valley ends may be caused by seasonal weathering during the Holocene, rather than by glacial action. From the observation grade provided below Table 7.2, the author is only very confident that glacial erosion is the process that accounts for the observed feature in three cases, although another 21 cases seem likely and 15 cases seem possible.

Despite some uncertainty about the processes that have created each of the *individual* examples listed in Table 7.2, the general case for the stripping of cave passages by glacial erosion (possibly supplemented by deglacial exokarst dissolution) is overwhelming. The known passages in at least half the study area caves would probably be removed by another glaciation of a similar size to the Weichselian, because their depths are <9m (section 5.2.4). The presence of short rock bridges ('natural arches') that are in limestone, but completely isolated from other karst features, (such as **Fjellbrygga**, ZA, example 34 in Table 7.2) may be accounted for by the glacial removal of previously longer passages. These rock bridges are common phenomena in the study area, but being apparently insignificant as karst features, they are rarely recorded. Some phreatic relict caves were likely shortened considerably by glacial truncation, leaving them in situations unrelated to present hydrology. The destruction of upper cave levels in the study area speleothanatic zones by fracturing and glacial removal is a much faster process than the total *chemical* disintegration observed by Sustersic (1999), being additional to the study area analogue of an ice-dammed lake dissolutional attack on all exposed exokarst and endokarst surfaces.

Glacial erosion and the tectonic, including seismic, creation and widening of fractures are processes that co-operate in sequence to weaken the upper (and outer in valley walls) part of the bedrock. These processes appear to be particularly important for the creation of many shattered cave entrances in valley shoulder locations (CL=S). Where karstic dissolution has already produced caves below the surface, this further weakening of the bedrock leads to *enhanced* glacial erosion, so that carbonate outcrops containing shallow caves are preferentially eroded and lowered, and glacial shear forces lead to the creation of further fractures. Thus, the many shafts into sub-horizontal meandering streamways and dry passages may themselves indicate surface lowering caused by glacial scouring.

Photo 7.4 Geitklauvgrotta entrance
The roof has been removed between the upper cave and the main cave entrance (to left of figure in red)

Photo 7.5 Kumragrotta (Z6)
Removal of the roof at the Middle Entrance

Photo 7.6 Røssåga Sink Cave (ZA)
The present entrance is to the left of the phreatic arch that was dewalled during the Weichselian glaciation and filled with rocks during deglaciation.

Photo 7.7 Røssågagrotta (ZA)
Glacial dewalling and roof collapse at this large former resurgence.

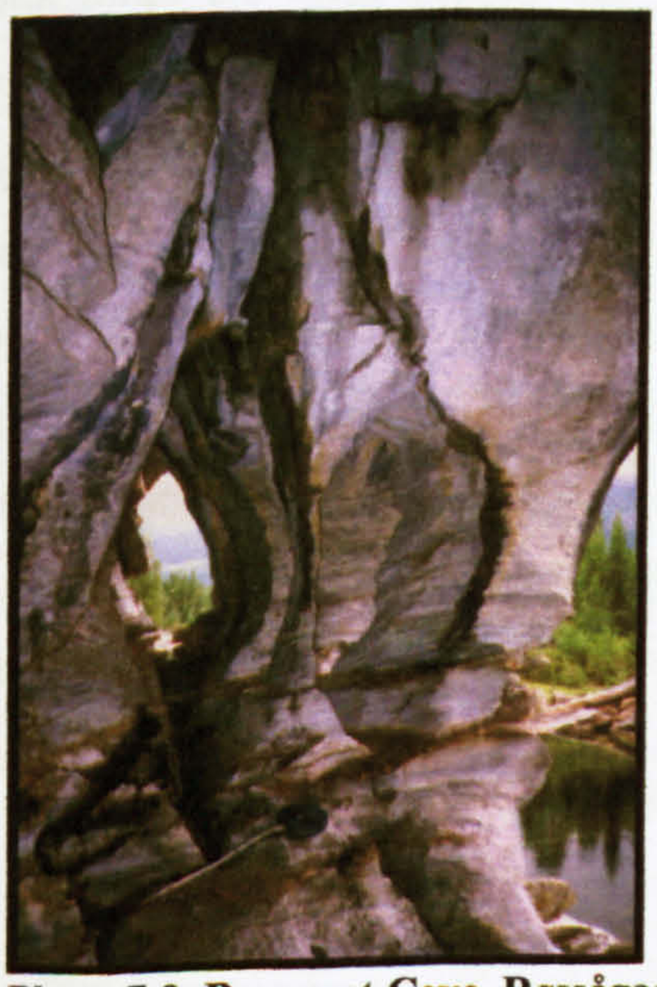

Photo 7.8 Remnant Cave, Røssågadal (ZA)
Outer passages and walls removed by glaciation. Tape measure for scale.

7.3 Cave development model

From Chapter 6 and sections 7.1 and 7.2, it is concluded that the very processes that lead to cave inception are the same processes that cause their destruction. A simple theoretical model describes the relationships between cave existence and the deepening of glacial valleys. For any one valley, if

VL = Mean valley lowering per glaciation

VD_n = Valley depth after n full glacial / deglacial cycles

FD_n = Maximum depth of inception fractures below the valley floor after n cycles

(An inception fracture is defined here as a fracture of sufficient size and geometry that turbulent flows through it exceed the breakthrough point of the Palmer / Dreybrodt model). Then,

VD_n = nVL, and FD_n = nVL/8, assuming that the one-eighth relationship, as derived empirically in section 6.5.2, applied throughout the Quaternary glaciations.

By making the simplifying assumption that the land surface was flat prior to the first major glaciation, it follows that, *for about the first eight major glacial cycles*, all valley floor caves (CL=F) formed by fracture enlargement during deglaciation and the next interglacial were so shallow that they were removed during the subsequent glaciation. Such *single-cycle* caves enlarged phreatically beneath deglacial IDLs with high flow rates during their early formation (section 8.6), with synchronously-formed passage tiers being possible. After deglaciation, some of these caves were left as relicts. Interglacial development of combination caves continued, with relict phreatic passages above upstream vadose passage elements in suitable topographic positions, as deglacial outflows reduced, and as interglacial snowmelt followed an annual cycle. They may have contained relict vadose passages and shafts where headward capture occurred via initially small phreatic conduits. It is unlikely that they would have exhibited significant paragenesis, and could not have contained large chambers with seismically induced collapse. Active mainly vadose caves could also be created.

For n>8, some fractures, and therefore caves, may survive below the surface after the ninth and subsequent glacial cycles. Such *multi-cycle* caves have the potential to become much larger and more complex than single-cycle caves (Figure 7.2), because all their existing passages *with any remaining sediments* will be subjected to further deglacial karstic dissolution, and new, lower, passages can form along new and deeper fractures during subsequent deglacial and interglacial phases. Thus, such caves are more likely to exhibit: tiers of relict phreatic passages, with cross-sections commonly increasing *upwards*; relict vadose passages, away from upstream entrances, which may have experienced later phreatic enlargement; paragenesis above previous clastic sediments; and large chambers with collapsed blocks. If new, lower, passages did *not* form, existing passages may have just enlarged during subsequent deglaciations, until removed by surface lowering. Thus, both single- and multi-cycle caves can contain either single or multiple tiers of passages, complicating diagnosis.

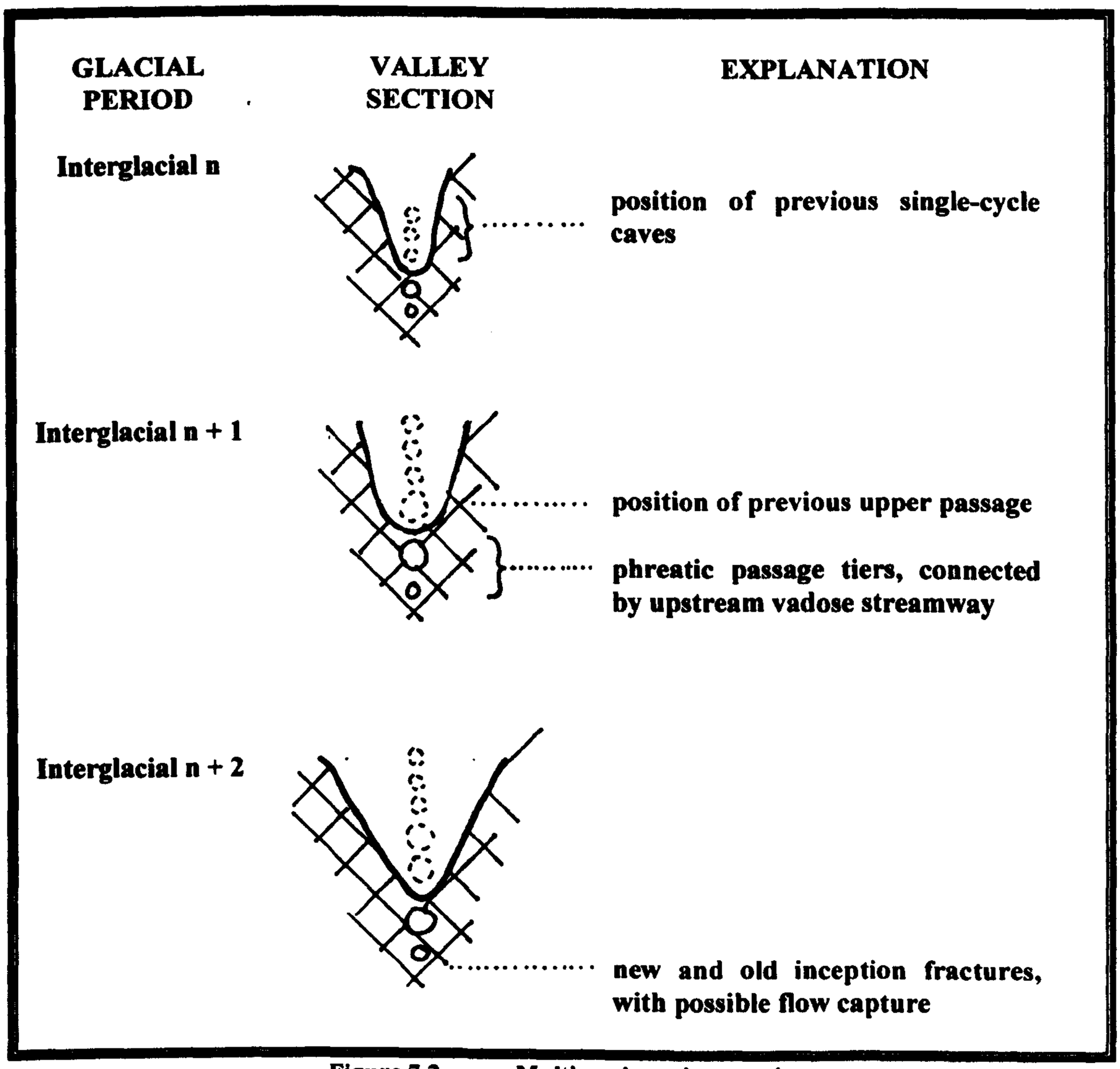

Figure 7.2 Multi-cycle speleogenesis

Because many glacial valleys are aligned with older Tertiary valleys, the transition that enabled the generation of multi-cycle caves at valley floors may have occurred sometime *before* the eighth major glaciation. On the other hand, the one-eighth relationship gives the *maximum* depth reached by inception fractures, and so for many places it would take many more than eight glaciations to create caves deep enough to survive the next erosional cycle.

Figures 7.1 and 7.2 utilise cave location CL=F for simplicity of illustration, although caves can form at all locations beneath ice-dammed lakes. From section 6.5.3, the one-eighth relationship is achieved most frequently if CL=R or S, intermediately if CL=G or W, and least frequently if CL=P or F. However, the glacial removal of bedrock may vary at each cave location and may depend on valley alignment with ice flow direction at glacial maxima. This complicates the interesting competition between the depth of inception fractures and the amount of bedrock removed by each glaciation, and therefore complicates the conditions necessary to achieve multi-cycle caves. Indeed, section 9.8.2 deduces that wall retreats decrease upwards from valley bottoms.

The glacial removal of bedrock probably does not depend on thrust proximity or contact metamorphism, so that the chance of a multi-cycle cave being preserved should increase if T=1 and reduce if R=1, according to their influences on fractures depths (section 6.5.3). This provides another explanation for the rankings of the longest and deepest caves in the study area (which are primarily multi-cycle combination caves) relative to their R and T attributes (section 5.3.6). However, some multi-cycle caves may only survive a few cycles before stochastic reductions in seismic intensity and reduced new fracture depths allow a premature removal by subsequent glacial erosion. Hence, in practice, the oldest age of cave passages may be considerably more variable than the simple theoretical model predicts. In particular, very old passages may still (rarely) remain in locations protected from glacial erosion by their topographic situation.

During interstadials, the icesheet primarily melted at low elevations near the coast (section 8.1.1). Some interstadial ice-dammed lakes may have been created at high altitudes, so that extra dissolution could enlarge existing passages in these situations. It is not known if deglacial earthquakes occur in these conditions, but from section 6.3.1, it seems that high-magnitude seismicity only occurs at deglacial ice margins. As successive deglaciations produce fracture sets commonly extending to greater depths below the contemporary surface than previous ones (within the one-eighth relationship), caves developed during later glaciations are likely to grow to greater sizes, and to survive longer, than caves developed during earlier glaciations.

If the simplifying assumption is made that nine major glacials have occurred in Scandinavia at 100Ka intervals after the Mid Pleistocene Revolution (section 2.3.1), then the existence of multi-cycle caves (which only occur after about eight glacials) should be rare. They may therefore depend on interstadial deglacial erosion, significant glaciations prior to 0.9Ma (such as the long Eburonian from 1.8–1.4Ma and the Menapian at 1.1Ma: section 2.3.1) and the pre-glacial depths of Tertiary valleys (section 2.2.2). This rarity *does* appear to be the case, at least in the study area, and the overwhelming majority of existing caves are suspected to be single-cycle caves.

It might be considered that all caves in the study area can now be classified against the single-cycle and multi-cycle models, according to their internal morphologies and any dating evidence. However, this analysis is best deferred until after the development of the Hydrogeological and Internal Cave Development Models in Chapters 8 and 9.

CHAPTER 8 THE HYDROGEOLOGICAL MODEL

From section 6.2.4, the present caves in central Scandinavia developed as a consequence of the cyclic processes of glaciation, deglaciation and the tectonic formation of fractures, which were repeated many times since, perhaps, the Miocene. The purpose of this chapter is to examine the various hydrological opportunities for the enlargement of fractures into conduits and cave passages that arose during each glacial cycle and to consider, using the latest theories of the physics and chemistry of karst dissolution, the likely timescales for the development of the present caves.

The deglaciation phase is shown to be the most important for cave development, and its characteristics are discussed in general terms from knowledge of the Weichselian glaciation (sections 2.3 and 2.4). The deglacial sequence of the whole study area is derived in Appendix D2, and then the Tosenfjord–Fiplingdal region (Z2–Z7) and its caves are studied in greater detail in Appendix D3. From this analysis, the various glacial conditions, flow regimes and processes that apply to inception fractures, conduits and caves are determined, and enlargement rates in phreatic and vadose conditions are calculated. A common set of processes defines the hydrogeological model of cave development, to which must be overlaid the effects of marine action and modification by ice in some cases. To unravel the various hydrogeological conditions that apply to the study area caves, it is necessary to introduce some topics from a theoretical basis before giving them a practical expression, and to analyse the relevant glacial and geomorphological processes to a greater extent than has so far appeared in the literature discussing the Scandinavian Quaternary.

8.1 The glacial cycle

Two major parameters were most influential during each stadial and interstadial: firstly, the thickness and condition of the ice at each karst area, and secondly, the sea level. The condition of the ice is important because, under cold- or warm-based icesheets and glaciers (Appendices A3.2 and A3.3), existing caves variously contained ice, ice and air, or glacial meltwater. Sea level is important because those caves at altitudes low enough to be depressed isostatically below sea level by the weight of the Scandinavian icesheet at early and late stages of the glacial cycle could experience marine inundation.

8.1.1 Mid to Late Weichselian stadials and interstadials

There is now considerable information available about the Late Weichselian *deglaciation* of the study area (e.g. section 2.3.4; Grønlie, 1975 and section 8.1.4; Andersen and Karlsen, 1986; and various maps of Quaternary geology, e.g. Bergstrøm, 1995). With the removal of the ice burden, Fennoscandia rebounded isostatically at a very fast rate initially, with the elevation increasing inland. Mörner (1979, Fig. 28) showed a peak elevation rate of 50cma^{-1} at the centre of uplift at the end of the Younger Dryas. The tilting shorelines were raised progressively, with the oldest and highest raised shorelines showing the greatest tilt. Sørensen *et al.* (1987) presented land uplift maps for Norway that show YD isobases and

isobases for the maximum Holocene marine transgression at 6500 (when global deglaciation was almost complete), as well as a map for the present annual uplift. Their isolines smooth out scanty observations and uncertain datings, generating isobases that are remarkably linear and parallel in north central Norway. Thus, the coastal area, at a YD isobase of 100m, has risen 100m relative to the YD sea level since the start of the Holocene, and the Caledonide thrust front, at a YD isobase of some 340m, has risen 340m relatively in the same time. A Fennoscandian postglacial uplift map showing fairly smooth uplift rate curves in mma^{-1} from 1892–1991 was presented by Ekman (1996), but no measurements were made in the study area.

Møller (1989) presented a 3D model of Holocene relative sea level changes for northern Norway. Off the Norwegian coast, towards the isostatic hinge-line, marine invasion *initially* overcame the glacio-isostatic uplift. The uplift always outpaced rising sea level at all parts of the indented north central Norway coast, and after the maximum Holocene marine transgression at 6500–6000 elsewhere. At Inndyr, the closest analogue to the north central Norway coastal area, Møller (1989) showed that 38% of the present uplift occurred within the first 1000 years. Svendsen and Mangerud (1987, Fig. 12) drew sea level curves for Trondheim that showed that 53–44% of the present uplift occurred within 1000 years, at isobases equivalent to those going inland at Velfjord.

Information from the last *glaciation* phase and from the glaciation and deglaciation of previous stadials and glacials is much more difficult to obtain, because stratigraphical and dating evidence is commonly altered or destroyed by the glaciation process. From the recent evidence discussed in section 2.3.4, Figures 8.1a and b present highly-conjectural glacial–deglacial scenarios since the Mid Weichselian for the 180m Younger Dryas isobase near Elgfjell (Z4), with an indication of the differences for other relevant YD isobases. These scenarios follow the "yo-yo" glaciation model of Olsen *et al.* (2001b). They should be most accurate for the main deglaciation that was initiated during the Bølling interstadial, because Figure 8.1a (icesheet thickness) is based on the work of Grønlie (1975, as adapted in section 8.1.4), and Figure 8.1b (sea level) is based on the sea level curve near Trondheim by Svendsen and Mangerud (1987).

It is suggested in this thesis that the *form* of these curves was repeated for all glaciations and deglaciations throughout the Mio–Plio–Pleistocene history of the glaciation of the study area. Thus, their upper and lower summer ice-melting curves (Figure 8.1a) and their sea level curves (Figure 8.1b) are assumed to have similar shapes at each relevant isobase, although the thicknesses of the icesheets, the maximum isostatic depressions and their durations varied at each stadial. For the larger stadials, the lower summer ice-melting height was equal to the level of the sea as it encroached inland. For the Little Ice Age, and perhaps for other smaller stadials when the glaciers did not reach the sea, it was determined by summer temperature and glacier dynamics.

The local sea level did not lower to its present level at each interstadial because a significant part of the Scandinavian landmass remained glaciated, or was only unglaciated for a short time. Indeed, Olsen and Grøsfjeld (1999) suggested that sea level averaged 50m above the present level during the Mid Weichselian. Also, the (interglacial) minimum sea level, as measured at the Norwegian coast, probably lowered with each major glaciation, because of the extra isostatic uplift caused by the subsequent unloading by glacial and fluvial erosion.

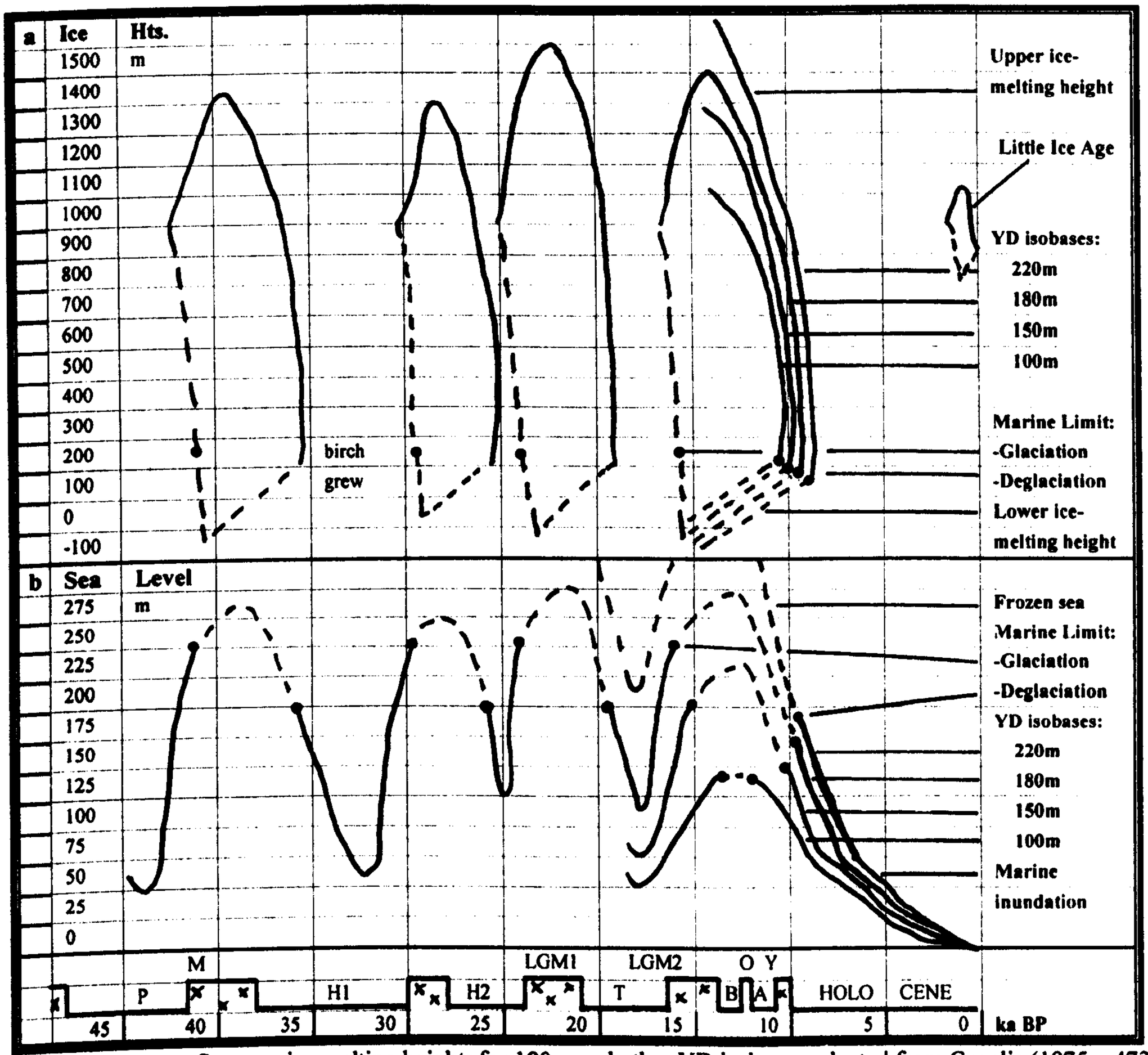

a Summer ice-melting heights for 180m and other YD isobases, adapted from Grønlie (1975, p473)
b Sea level curve for 180m and other YD isobases, adapted from Svendsen and Mangerud (1987)
Stadials (x): M Middle LGM Last Glacial Maximum O Older Dryas Y Younger Dryas
Interstadials: P Pre-Hattfjelldal H Hattfjelldal T Trofors B Bølling A Allerød
Stadial and interstadial timings from Olsen *et al.* (2001b)

Figure 8.1 Conjectural Mid to Late Weichselian stadial cycles for central Scandinavia

Figure 8.1 covers the period from an assumed interstadial at c. 45ka BP through the Last Glacial Maxima (LGM1 and 2) to the present. It does *not* attempt to represent the detailed effects of the various stadials and interstadials between LGM2 and the Younger Dryas (YD), i.e. the Bølling interstadial, the Older Dryas stadial and the Allerød interstadial. [Various authors have called LGM2 the Oldest Dryas, Late

Weichselian Maximum 2 (LWM2), Heinrich event 1 (H1) and the Tampen advance; its maximum may correlate with the Dimlington stadial in Yorkshire, UK (e.g. McCabe *et al.*, 1998)].

8.1.2 The deglaciation marine limit

As discussed in section 2.3.4 and Appendix A3.1, it is accepted herein that the last deglaciation was driven by two summer heat fluxes: warming by sea water that caused both the icesheet to retreat eastwards and the melting sea to encroach up coastal valleys, and direct solar warming that caused the icesheet to melt and ablate from its upper surface.

By locating moraines where the open sea met the land ice, creating deltaic marine terraces, Grønlie (1975, pp456–457, 466–471) recorded the highest sea levels in the valleys south of Mosjøen (Z5). This elevation that the sea reached against the ice margin along the coastal fjords and valleys, when it melted the last remnant of the tidewater valley glacier before retreating because of isostatic elevation, is commonly called the *marine limit* (section 2.4.1), but is henceforth called the *deglaciation* marine limit in this thesis. This limit is important for the enlargement of karst caves that lie below it, with caves at lower altitudes being inundated for longer, as indicated by the sea level curve in Figure 8.1b (sections 8.8.1 and 8.8.2). The deglaciation marine limit depended on the recession of the ice margin *and* on the isobase of the location. It varied from c. 125m at 12000^{14}Ca BP at coastal islands at the 100m YD isobase, via 150m at 10000 at the 150m isobase and c.160m at 9890 at Tosenfjord at the 170m isobase, to 133m at 9080 (Grønlie, 1975) in Vefsndal at the 200m isobase, the farthest east that the sea penetrated in the Holocene. The intermediate 150m-isobase sea level curve in Figure 8.1b shows that all points on and underneath the surface below a present 150m altitude would have been inundated by the sea at the start of the Holocene, *providing that the ice had melted by then at that location*. The deglaciation marine limit in the Eemian interglacial, at the end of the Saalian glaciation, was somewhat higher than that at the end of the Weichselian, from the evidence of a higher eustatic level (Funder, 2000; Huybrechts, 2002; section 2.3.2) and the principle of subsequent erosional isostasy (section 8.1.1).

8.1.3 Other marine limits

It is assumed herein that the curves for each parameter were also self-similar during *glaciation* phases. Following the discussion in Appendix A3.1, the glaciation at each stadial started by winter snow persisting through the next summer, initially at an average altitude appropriate to the study area of c. 1000m. The ice gradually thickened into flowing glaciers, with rising summer upper melting heights, and falling summer lower melting heights. Such a scenario was reported for the neoglaciations of the Okstind mountains in the Little Ice Age (Griffey and Worsley, 1978), when, perhaps, the Holocene almost ended.

It is speculatively hypothesised here that the glaciation curve for the falling *lower* melting height had a similar shape to the deglaciation curve for the falling *upper* melting height (Figure 8.1a). Thus, after the onset of each glaciation cold signal, valley glaciers and mountain icesheets progressively extended

towards the sea, which remained frozen in summer some time after the icesheet reached sea level. However, the icesheet now had a considerable thickness, and at the end of the Eemian "*depression extended ahead of the ice margin*" (Lundqvist, 1986, p288). Hence, the sea encroached significantly inland before its surface froze permanently and there must be *another* marine limit, *not previously explicitly recognised in the literature*, that equals the elevation that the sea reached up each valley before freezing (or before falling eustatically relative to the land) during a transgressive *glaciation* phase. This limit is called the *glaciation marine limit* in this thesis, to distinguish it from the *deglaciation marine limit* that occurred during a regressive phase. If glaciation proceeded whilst the sea remained frozen even in summer from an early stage, then the local glaciation marine limit would be no higher than the local interglacial sea level. However, the depression of the freezing point of sea water to c. -2°C, caused by its solute load (Nesje and Dahl, 2000, p53), would tend to delay such perennial summer freezing. The glaciation marine limit could also be non-existent if eustatic sea levels fell rapidly due to a large build-up of icesheets in northern America and / or Antarctica prior to glaciation in Scandinavia, as suggested by Mangerud (1991) for the start of the Herning stadial (OIS5d), following the Eemian interglacial. Nevertheless, Mangerud (1991) and Fredin (2002) reported that several present coastal caves in southern Norway, which are well above the *deglaciation* marine limit, *were* submerged after the Eemian, because of rapid isostatic depression caused by the YD-sized Herning glaciation in the Early Weichselian.

The concept that the icesheet thickened from the tops of the mountains and annually advanced westward across the study area during each glaciation phase has not been *quantifiably* modelled, and the geometry of the *glaciation* marine limit is presently unknown. However, from the evidence of Mid Weichselian marine-influenced deposits at high elevations, e.g. sediments dated from 35–24ka at 260m near Hattfjelldal in the study area (Olsen *et al.*, 2001b; section 2.3.4), it is clear that this *interstadial* marine limit was 120m above the equivalent local (210m YD isobase) deglaciation marine limit (although the sea did not quite reach this point during deglaciation). This evidence appears credible, because, although marine-influenced deposits from all Mid Weichselian interstadials may have been transported by later ice movements to different elevations, confusing the evidence (a possibility recognised by Olsen and Grøsfjeld, 1999), it does seem probable that their studied deposits were in protected and unmoved positions, because marine deposits were more likely be shifted *downwards* by the radially-moving icesheets or later valley glaciers. The 210m YD isobase may mark the eastward limit of any Weichselian marine impact in the area because there are no eastern caves and few carbonate outcrops below 260m in altitude. This also means that the Swedish part of the study area and the Køli nappes (except those along upper Vefsndal) remained above all Weichselian sea levels.

It is also probable from the survival of Mid Weichselian fine grained sediments and Early Weichselian speleothems dated to 80±9ka in the elevated sea cave **Skjonghelleren** in southern Norway (Appendix 5.1) that that cave was not inundated again by the sea after these depositions, and that it formed at a high sea level even earlier in the Weichselian or before. This suggests that the maximum Weichselian marine

limit occurred relatively soon after the start of the Weichselian glaciation. With no evidence to the contrary, it is concluded that this also applied in the study area, so that the extra 120m above the deglacial marine limit reported near Hattfjelldal is a conservative value to use for the local *glaciation* marine limit. For simplicity therefore, glacial situations G and H were set with an upper limit 120m higher than the local deglacial marine limit (section 5.3.5 and Appendix C2.1).

It is assumed in this thesis that glacial decay during Weichselian interstadials was driven primarily by a rising sea level caused by the melting of ice on other continents. This resulted in ice calving and melting from the Norwegian coast into the fjords and valleys. There was no sharp rise in summer temperature as occurred at the end of the Weichselian, so that ablation at the surface of the inland icesheet was muted farther east. The continuing weight of this ice thus maintained a large isostatic depression, causing the high marine incursions discussed above.

If the principle that "*depression extended ahead of the ice margin*" also applied during the transition from interstadial to stadial conditions, then it seems likely that maximum marine limits were reached during ice build up at the end of each interstadial, rather than at each beginning. These other marine limits may also be indirectly related to the deglacial isobases, but the nature of any relationship is unknown. This thesis assumes that the maximum Weichselian glacial marine limit was everywhere 120m higher than the deglaciation marine limit, for reasons given in section 8.8.3, which also concludes that the maximum Weichselian marine limit did, in fact, occur at the start of the Weichselian glaciation.

The glaciation marine limit and the interstadial limits may also be important for cave development, because all existing karst caves below them were inundated by sea water for periods up to thousands of years at a time, and when this water froze as the ice margin extended beyond the coast (annually during winter, and then perennially), all submerged passages and fractures were subjected to stresses that caused enlargement (section 8.8.3). Because it is assumed that these earlier marine limits were higher than the deglaciation marine limits, more of the caves then existing were affected by marine inundation during early glaciation and interstadial phases than during deglaciation phases, although the timescales of all such inundations reduced with increasing altitude. As with the minimum local sea levels reached during interglacials, all types of marine limits were commonly progressively higher (relative to the underlying basement rocks) for each previous glaciation, from the principle of subsequent erosional isostasy (section 8.1.1). Whether this means that more of the known caves were flooded by sea water during the Saalian and Elsterian deglaciations depends on the extent to which these caves were eroded from the landscape by subsequent glaciations, as discussed in Chapter 7.

8.1.4 Weichselian deglaciation inland: application of the Grønlie formula

Grønlie (1975, p473) devised a parabolic relationship (*"$H=0.75t^2$"*) to give the height, place and time at which the land became ice-free in the central part of the study area at the end of the Weichselian

glaciation, from his study of the geological evidence (e.g. section 2.4.1). His empirical formula must also take into account the dynamics of icesheet evolution, including receding accumulation areas and the increasing velocity of valley glaciers. It is reconstructed by this author to include the isobase:

$$H_u = 1700 + 5(\text{YD Isobase}-220) - 0.75\text{x}10^{-4}\text{x}(13500-t)^2 \text{ m}$$

where H_u = summer upper ice-melting height and t = number of ^{14}Ca BP (Figure 8.2a and b).

This formula assumes that time runs smoothly and does not attempt to resolve the radiocarbon plateaux problem (section 2.4). The ice began to melt in earnest after 13500a BP (at the start of the Bølling interstadial), below the present 1700m altitude (at the 220m YD isobase at Børgefjell) that was already free of ice. After c. 11ka BP, the melting height lowered at roughly 0.5ma^{-1} at all isobases. The formula shows that all ice melted by 8740a BP, even at sea level, as far east as the 220m YD isoline. It also reveals that, at 12, 11, 10 and 9ka BP, all land west of the 220m isoline was clear of ice above 1500, 1200, 800 and 200m respectively. Melting was complete in Svenningdal (at 131m altitude) and in Vefsndal (at 133m) by 9150 and 9080a BP, when the sea melted the *tidewater glacier* from one side, whilst the falling upper ice-melting height caused the remnant ice to melt away on the other side (Grønlie, 1975). The isobase adjustment in the upper melting height formula compensates for both the reducing heat flux from the Atlantic and the increasing isostatic depression in the eastward direction. Despite later improvements in the accuracy of place heights, radiocarbon datings and isobase structures, this reconstruction of Grønlie's formula gives many marine marginal moraine date predictions that are within 300 years of published results. It is therefore used in the form represented above to reconstruct the deglaciation of the study area (Appendices D2 and D3).

The Grønlie (1975) formula was only tested by him in the Vefsn and Northern catchment areas. In the Eastern catchment area, there is evidence that glaciers remained longer than predicted by the formula (Appendix D2.9). In the Western catchment area, the acceleration of icesheet downwasting was much greater than used in this reconstruction, because of the extra warming and calving effects of the sea as it submerged large areas of low-lying and isostatically-depressed land and because of the increased velocity and ice-streaming effects along the fjords. This is clear by considering the low maximum altitudes of the moraines identified by Andersen *et al.* (1981; 1982). However, a simple relationship between isobase, ice melting height and date at the coast cannot be determined from these results, probably because the cooling caused by the Older and Younger Dryas stadials caused significant elevations of the icesheet surface, back towards previous altitudes. In the other catchment areas, these effects can be ignored, because, by analogy with northern America (Cwynar and Spear, 2001), they are probably attenuated inland from the coast. Additionally, the ice-melting height varied between adjacent eastern and western slopes, and this effect was also magnified nearer the coast and at lower altitudes. Thus, the Grønlie formula may give elevations from 0–300m too high for YD isobases below c. 180m in the Western catchment area. Figure 8.2a attempts to extrapolate these effects, suggesting that the lowering icesheet may have exposed low coastal hills up to 1000a earlier than predicted by the formula.

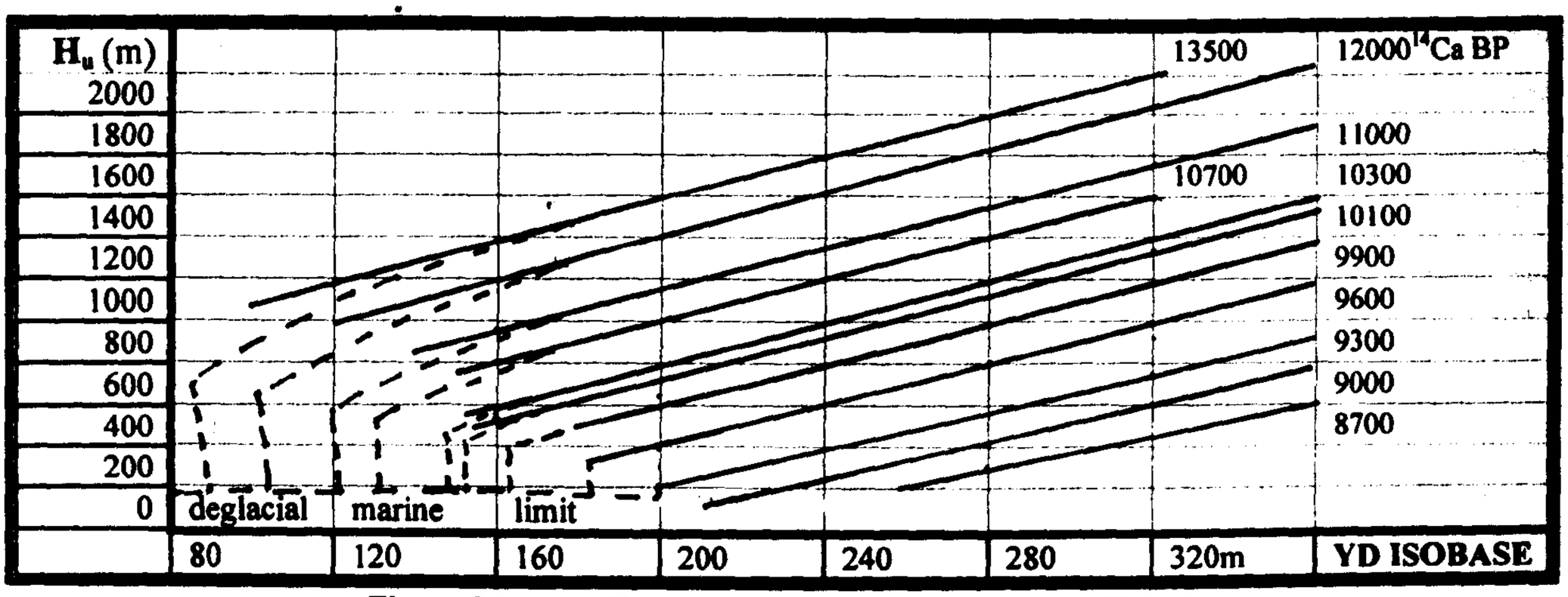

Figure 8.2a Upper ice-melting heights at each YD isobase

According to Grønlie (1975), the *lower melting height* (H_l) caused by the sea melting the glaciers in Vefsndal and Svenningdal also followed a parabolic relationship with time, at least during a shorter time interval. This author's reconstruction of this formula is:

$$H_l = 105 + 0.75 \times 10^{-4} \times (9680-t)^2 \text{ m (Figure 8.2b).}$$

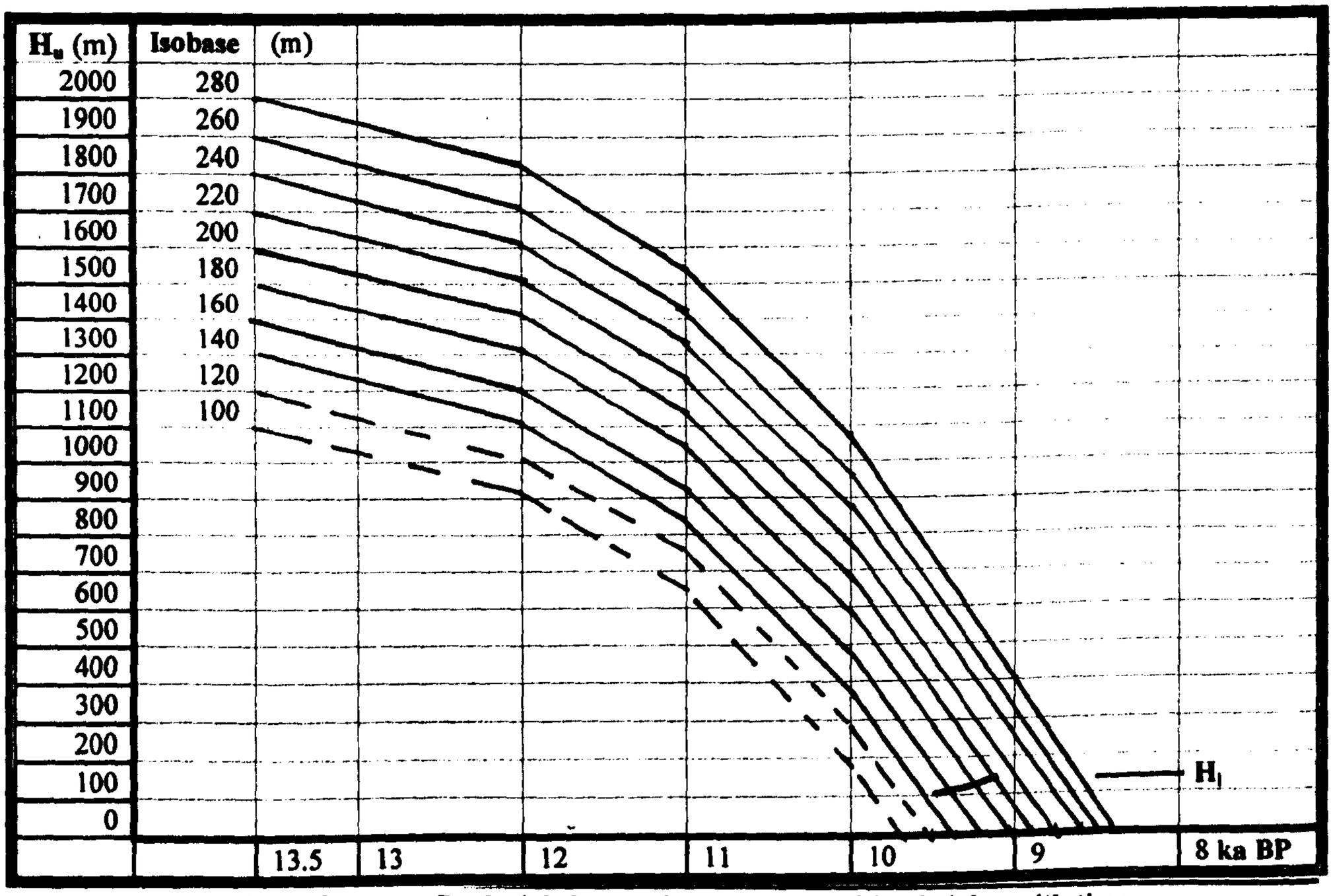

Figure 8.2b Deglacial changes in upper ice-melting heights with time

8.1.5 Ice-dammed lakes

Apparently, the generation of ice-dammed lakes (IDLs) in the Caledonide mountains during deglaciation used to be controversial (e.g. Lundqvist, 1972, p34). However, their existence during the rapidly-warming climate of the early Holocene is regarded as well-established in this thesis, from the descriptions of deglacial IDLs in Scandinavia, northern America and Scotland by Lundqvist (1972 and 1986), Stone and Borns (1986), Andersen and Borns (1994), Donner (1995), Dahl *et al.* (1997; Figure 8.3), Dawson *et al.* (2002) and LaRocque *et al.* (2003). The present rarity of perennial IDLs behind

glaciers and within icesheets is explained by the relative stability of the late Holocene climate and the absence of large-scale non-polar icesheets, so that no environment on earth now provides an analogue for the unstable deglacial conditions of the non-Arctic Caledonides. However, the author observed small short-term 'IDLs' in Z4 during the 1997 spring melt.

Grønlie (1975, pp459–465) recognised non-marine moraines and terraces formed some 10–30m above the levels of present lakes in many places in the Vefsn catchment area. The diagnostic features of these areas of lacustrine sedimentation are stream meanders, groups of isolated tarns, deltas, linear terraces, and lakes with uneven contours. The author is also able to recognise these features on the M711 series maps of the other four catchment areas and therefore regards the deglacial generation of IDLs as widespread throughout the mountains of the study area.

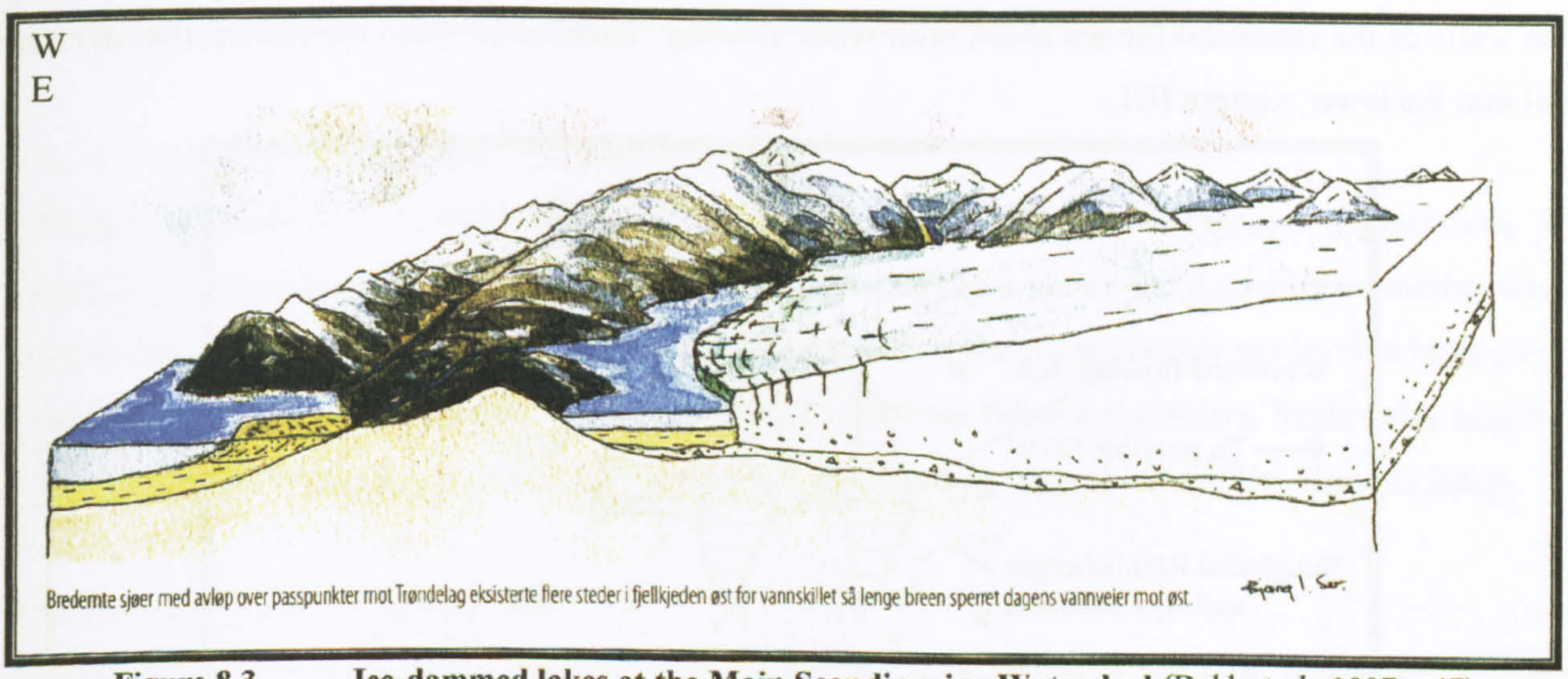

Figure 8.3 Ice-dammed lakes at the Main Scandinavian Watershed (Dahl *et al.*, 1997, p47)

Whereas section 8.1.2 discussed the fact that most caves situated below their local deglaciation marine limit were inundated by *sea water* at the start of the Holocene, succeeding sections show that practically all karst cave sites were inundated by *glacial meltwater* under IDLs for a considerable time during the deglaciation process. Lundqvist (1972) defined an IDL as a body of water whose existence depends on damming by ice that is dynamically active. Tweed and Russell (1999) reviewed the literature on present IDLs and associated jökulhlaup characteristics. Their identifications of IDL types and those of other earlier authors concentrated on the present annual hydrological cycle of IDLs formed adjacent to valley glaciers and on the effects of geothermal heating. They are therefore relevant to specific interglacial conditions, none of which apply to study area caves. This thesis classifies six different types of *deglacial* IDL, plus one situation where IDLs cannot occur, which are defined relative to glacial situations (section 5.3.5). Their characteristics are considerably amplified in section 8.4, but they are briefly introduced here to enable the deglaciation sequences to be described adequately in Appendices D2 and D3:

Coastal western slope	A position where an IDL cannot form, on lower coastal western slopes
Nunatak IDL	The lake surface is above the level of the highest local col (GS=U)
Westward-flowing IDL	The lake surface is west of a major ridge and between the highest local col and the deglaciation marine limit (GS=S, K or G) (Figure 8.3)

Drained IDL	Á previous IDL that drained subglacially
Backward-flowing IDL	The lake surface is east of a major ridge, and between the highest and lowest local cols (GS=T) (Figure 8.3)
Eastward-flowing IDL	The lake surface is east of a major ridge, and between the lowest local col and the deglaciation marine limit (GS=L or H)
Ice margin IDL	A backward- or eastward-flowing IDL at the western extremity of the receding icesheet

These IDL types build on the types defined by Lundqvist (1972) and are partly illustrated in Figures 8.3 and 8.4. These show a stage of deglaciation when the surface of the icesheet has lowered to the level of a col along a ridge oriented N–S. Higher parts of the ridge are exposed in meteoric conditions above the ice. Lower parts (including lower cols) remain covered by ice. Ice-dammed lakes have formed between the walls of the ridge and the ice sheet, with water flowing "backwards" from the eastern IDL over the col into the lower western IDL.

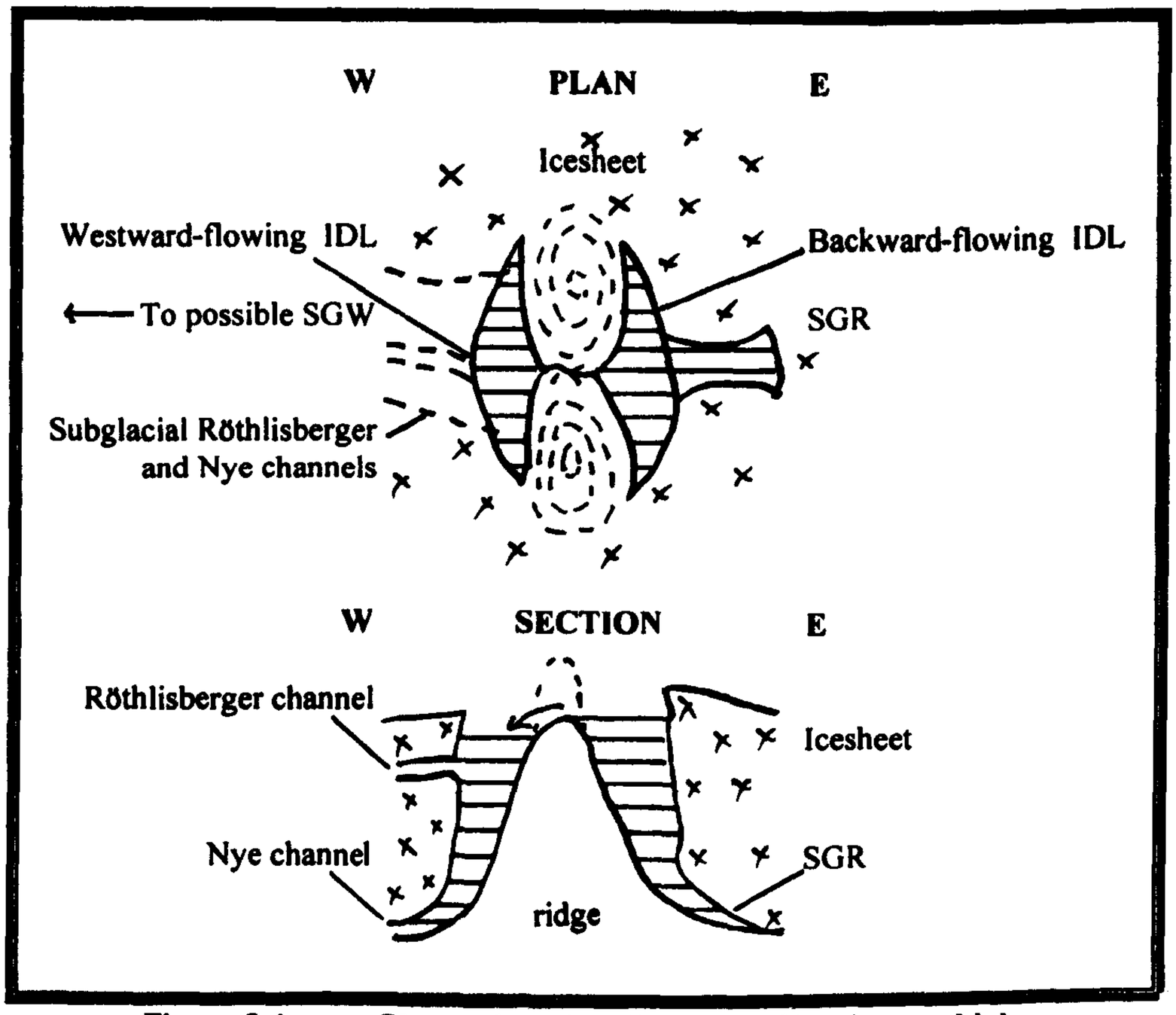

Figure 8.4 **Plan and section diagrams of ice-dammed lakes**

8.1.6 Subglacial reservoirs

An IDL without a continuing Nye channel, i.e. with a vertical back wall of ice, commonly has a depth approximately equal to twenty times the distance from the ice surface down to the water surface, assuming that the water in the IDL is entirely glacial meltwater and ignoring evaporation. The reduced volume occupied by water compared to ice thus allows glacial meltwaters and meteoric waters to 'create their own space' and to flow down and 'disappear' under icesheets and glaciers, by melting more ice, to create *subglacial reservoirs* (SGRs; Figure 8.4). These may lie behind frozen ice margins towards the end of the deglaciation process (e.g. Fisher *et al.*, 2002). Thus, IDLs deepen and enlarge without the necessity of an immediate outlet. Dropstones contained in the ice fall to the base of the IDL or SGR,

potentially impeding underlying cave or conduit entrances. This author supposes that subglacial reservoirs can exist in three forms: *low pressure* (lp-SGR), when the weight of the overlying ice (which must be <200m thick: section 8.1.8) is insufficient to deform the melting base of the ice, and a near-vacuum develops above the meltwater; *high pressure* (hp-SGR), when a Nye channel connects the reservoir (whose upper surface may lie at any depth below the surface of a warm-based icesheet) to an external IDL, keeping the reservoir space full of water; and *air pressure* (ap-SGR), when a drained IDL leads to the reservoir via a Nye channel with mainly vadose flows. The lowest point of an SGR commonly marks the transition from bedrock above the freezing point to bedrock at the pressure melting point of the over-lying icesheet or glacier. SGR formation above the *plastic behaviour limit* (section 8.1.8) can be supplemented by the flow of the icesheet or glacier around obstacles to create cavities (Tweed and Russell, 1999). Subglacial reservoirs are distinct from *subglacial lakes*, which form beneath warm-based icesheets without hydraulic connections to the surface (section 8.4.2).

8.1.7 Subglacial waterways

Subglacial waterways (SGWs) form near the Atlantic coast and at late stages of deglaciation, when subglacial reservoirs coalesce along warm-based valley bottoms above the deglaciation marine limit to create *meltwater subglacial waterways*. If they flow to below the contemporary sea level in Norway, they continue as *brackish subglacial waterways* to the ends of the tidewater glaciers. Such water routes that were active during the deglaciation of Ireland were described as "tunnel valleys" by Knight (2002).

8.1.8 The plastic behaviour limit

According to Badino (2001b; section 3.2.4), most glacial drainage systems lie *above* the bedrock in present thick glaciers and icesheets. Below c. 100–200m (the plastic behaviour limit, PBL), ice moves by plastic flow, closing up any openings, as normally observed in "polar" glaciers (Nesje and Dahl, 2000) and because *"it is conventially assumed that non-temperate ice is an aquiclude"* (Hodgkins, 1997, p957). Significant upward-flowing elements are precluded by the reducing pressure, which raises the freezing point above its likely -2°C. This causes more ice to form on the walls of englacial conduits, choking them off, and ensuring that the Nye and Röthlisberger conduits maintain a general downhill trend. Hence, it is assumed in this thesis that IDLs can only have *active englacial* outlets into Röthlisberger channels in the upper 100–200m of the icesheet, so that the deeper parts of IDLs do not drain away at an early stage.

8.1.9 Proglacial lakes

Proglacial lakes are rather loosely defined in the literature. Whereas those lakes that lie in advance of, and therefore below, a glacial snout are distinguishable from the IDLs described herein, which all lie *above* the main body of a glacier, the two expressions are commonly treated synonymously. In the study area, it appears that all the deglacial valley glaciers ultimately terminated either as tidewater glaciers in Norway, or flowed east into Sweden and out of the area. Thus, probably few caves encountered any proglacial lakes formed by the forward melting of glaciers in valley bottoms.

8.1.10 The influence of deglaciation and seismicity on cave occurrences and dimensions

Section 6.3.1 discussed the evidence that a pulse of earthquakes followed the eastward recession of the ice margin. Figure 8.5 shows that the local isostatic strain was released on the west side of N–S aligned ridges first, so that the intensity of deglacial earthquakes was commonly higher on the west side. The continuing presence of an IDL and the icesheet on the east side also muffled the effect of the earthquakes there. The eastward recession of the ice margin and the different behaviours of IDLs and earthquakes on each side of major ridges in consequence explain the asymmetry in the occurrences and mean dimensions of relict and combination caves that existed before the establishment of present interglacial conditions (sections 5.3.5 and 5.5.6). It is hypothesised that the under-representation of caves (especially relict and combination caves) but with greater mean dimensions on the west side of ridges above the glaciation marine limit (section 5.5.6, Table 5.28) is explained by the production of a smaller number of longer and deeper inception fractures there, with larger apertures, compared with a larger number of smaller and more-scattered fractures on the 'muffled' eastern sides.

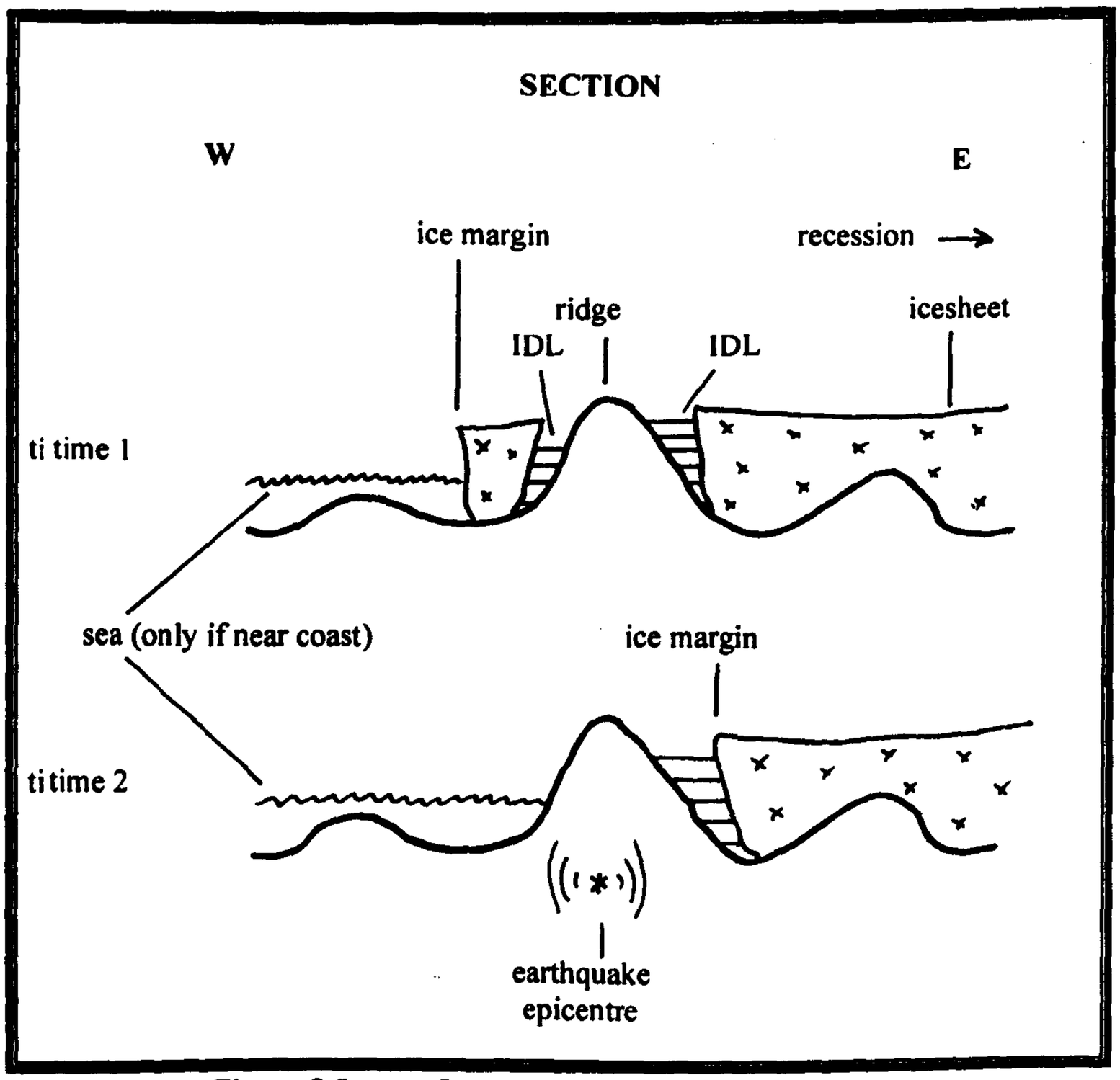

Figure 8.5 Ice margin deglacial earthquakes

The inception fractures were not necessarily created solely during the Weichselian deglaciation: they resulted from the accumulation of fractures created in the same manner from all previous deglaciations. Thus, fracture sets on higher western sides of ridges (GS=S or K) always have larger dimensions than those on eastern sides (GS=T or L), although both are also subjected to surface lowering. [It is not known if there is differential erosion on the western and eastern sides of ridges when they are over-ridden *westwards* by icesheets at glacial maxima]. This provides an additional reason for the commonly small dimensions of the caves at the plateau area of Övre Ältsvattnet (KU; GS=T and L; section 6.5.3).

There is probably a reduced existence time or flow rate for many IDLs on the west compared with IDLs on the east (especially at GS=S), with some quantification given in section 8.4.12. From Figure 8.5, it is also clear that western IDLs cannot exist for long after the time of their local earthquake, whereas there is no such constraint on eastern IDLs. Because the phreatic conditions necessary for the enlargement of the relict passages on the western sides of ridges commonly did not persist after their local earthquake, a greater proportion must have enlarged beneath westward-flowing IDLs *before* the local earthquake, utilising fractures that were created during earlier deglaciations. The occurrence and dimensions of relict caves and passages in central Scandinavian metacarbonates therefore depend on a combination of seismic intensity and persistence of active phreatic conditions. Scalloping on the surfaces exposed by tectonic movement at **Cliff Cave** (Z4; Photo D1.23) indicates that, at least in this cave, deglacial seismicity occurred after submersion beneath an active IDL but before the IDL lowered below the cave. See also Appendix D5.5. In contrast, the absences of scallops on smooth and sharp-edged slickensides in **Elgfjellhola** and **Paradox Cave** (Photos D1.12 and D1.14), both at higher altitudes on Elgfjell (Z4), suggests that the (same) IDL had lowered below their level prior to the time of that inferred deglacial earthquake. The small numbers of above-average-dimension relict caves high on the west of major ridges must be located in positions where active IDLs lasted for significant periods of time. Such an explanation is required to resolve the anomaly that phreatic passages in western glacial situations have larger mean cross-sections, despite the mean western IDL submersion periods being shorter.

For those parts of the study area that are near coastlines, the effects are different. Here, the western under-representation of relict and combination caves below the glaciation marine limit (GS=G or D) coincides with the situations where IDLs cannot form (section 8.1.5). In these western situations, when the ice margin passed overhead, the weight of encroaching sea water (increased in depth by c. 150m compared with now) reduced the pressure change, and so reduced the intensity and muffled the effects of the following earthquakes (Figure 8.5). These consequences increased further with reducing altitude, providing an excellent explanation for the commonly reduced and reducing oc currences and mean lengths and VRs of caves of all hydrological classes as glacial situation lowers from GS=G to D to C (Tables 5.27 and 5.28). In addition, the lower the altitude of a fracture below the deglaciation marine limit, then the longer was its marine inundation, when there was little opportunity for enlargement (Appendix D4.12).

Mean cave lengths and VRs also reduce near *eastern* coastlines for all cave classes from GS=H down to GS=E, again confirming a muffling effect by the sea. However, the dimensions of these caves are commonly larger near *eastern* coastlines than near western coastlines, in contrast to the larger western dimensions above the glaciation marine limit. This indicates that the muffling effect of the Atlantic ocean at western coastlines is greater than the corresponding muffling effect of an IDL (or the sea) plus the continuing icesheet along fjord coasts east of major ridges (Figure 8.5).

The under-representation of MV caves on the west side of major ridges (section 5.5.6) can be explained by assuming that even these caves required a phreatic 'kick start' beneath their IDL, before taking advantage of the fractures created by the Weichselian deglacial earthquakes and enlarging to present dimensions during the Holocene. Section 5.5.6 noted that mainly vadose caves have mean dimensions within 15% of each other at GS=K and L. In fact, their mean length, mean XS and mean volume are still slightly larger to the west, but so are their mean catchment areas. Below the glaciation marine limit, their mean VRs decrease downwards near both western and eastern coastlines, with this dimension slightly larger in eastern situations. Thus, the fracture sets followed by the MV caves (and the streamways of combination caves) follow the same seismicity muffling effects as for phreatic relict caves, although with less pronounced differences. It seems possible, therefore, that inception fractures for both phreatic and vadose caves have similar, and perhaps contemporary, origins, with the type of passage enlargement and its timing dictated by *'phreatic favouring'* or *'vadose favouring'* factors (section 5.6.3).

It is also possible that there were two types of deglacial tectonic activities. The first is the type that immediately followed behind the recession of the ice margin in association with ice-dammed lakes, as discussed above. These earthquakes had local, but significant, asymmetric impacts, within the range of each north to south-aligned valley (i.e. a lateral west to east extent of the order of one kilometre), and were also amplified by steep topography. They started at the Norwegian coast and ceased after the icesheet receded into Sweden. A second type was caused by the continuing, but decaying, isostatic uplift. These tectonic activities probably operated regionally, with symmetrical effects on both sides of major ridges, and continued well into the Holocene as neotectonics. They may have comprised both seismic and aseismic movements. If there were two distinct types of tectonic activity, from their timings, the relict caves resulted primarily from inception fractures created by local earthquakes, and the mainly vadose caves and passages utilised fractures from both local earthquakes and regional tectonism. This would explain why the mean length and vertical range at west and east glacial situations are much more similar in the MV caves. Additionally, MV caves utilised the subset of fractures that provided suitable hydraulic gradients within the local topography, which therefore had more-symmetrical W and E distributions.

8.2 Deglaciation in the study area

Section 8.1 introduced terms and concepts whose relevance to endokarst evolution may not be immediately apparent. Appendix D2 puts these terms into context by deriving the deglacial sequence for the whole study area. Contemporary influences on the karst cave sites are also discussed in general terms. The Tosenfjord–Fiplingdal area deglaciation is presented in more detail in Appendix D3. These reconstructions are considered to be approximate in detail, but correct in principle. They illustrate the recession of the icesheet margin from west to east, and the synchronous thinning of the icesheet downward from the mountain tops. The ice margin lost its sharp, morainal, definition as it retreated eastward out of the Western catchment area, because of the declining influence of heat from the sea and the increasing influence of topography on the lowering and decaying icesheet.

8.3 Earlier glaciations and deglaciations

Whereas the reconstructions in Appendices D2 and D3 are for the final Weichselian deglaciation, this thesis proposes that similar conditions arose at the beginning of all previous interglacials. During Weichselian and earlier *stadial* deglaciations, the ice margin may have progressed a reduced distance inland and stopped at higher upper melting heights before being overtaken by the next glaciation sequence. However, if interstadial summer temperatures did not reach interglacial values, the melting may have been primarily driven by the heat flux from the sea, with less summer ablation. Such a 'bottom-up' deglaciation mode may explain the interstadial ice-free valley floor of Hattfjelldal (section 2.3.4), and would reduce the influence of IDLs during interstadial transitions.

Narrow ice-dammed lakes could also form in summer during *glaciation*, also at about the level of the upper ice-melting height. Such lakes therefore rose *upwards* as glaciation strengthened year by year, until summits were permanently covered by ice. Indeed, Dawson *et al.* (2002) described the formation of a rising and then falling sequence of backward-flowing IDLs during the Younger Dryas glaciation and deglaciation of the Parallel Roads of Glen Roy in the Scottish Caledonides, which reached depths up to 170m. However, if glaciation started with an upper ice-melting height at or above 1000m, few, if any, karst caves in the study area could have been submerged by such glaciation summer lakes. On the other hand, when glaciers grew large enough to block river valleys, IDLs formed behind them in summer (Rudoy, 2002) and flooded any underlying caves. It is also possible to envisage a westward-moving ice margin as the sea cooled during glaciation. However, as discussed in section 6.3.1, any pulse of seismicity associated with such a *glacial* ice margin was likely to be restricted in magnitude, because of the compressive effect of the increasing weight of ice.

Another scenario to consider is when a partially deglaciated interstadial was reversed by a return to stadial conditions. In this case, the growth of perennial ice may have occurred at two levels: from the same 1000m altitude, and by extension of the valley glaciers or by build-up on to an already extensive icesheet. This may be the situation modelled by Arnold *et al.* (2002) for the Hattfjelldal interstadial 1 (section 2.3.4). During the summers of a stadial episode, there are then likely to have been two series of IDLs, and, although probably smaller, the lower series may have functioned in ways compatible with the deglacial IDLs, and experienced both forward and reverse flow conditions, thereby providing additional dissolutional opportunities at existing submerged caves and fractures.

Potential differences in the style of ice-dammed lakes during glaciation and deglaciation under each of cold-based and warm-based conditions may also be relevant. Valen *et al.* (1996) deduced that the floor of **Hamnsundhelleren** (southern Norway) was covered by a lake that was dammed by a fjord glacier at the mouth of the cave during the *onset* of glaciation, supporting the concept of glaciation IDLs. Caves *at higher altitudes* and *nearer the coast* were subjected to immersion beneath advancing and retreating IDLs more frequently than inland caves at lower altitudes during stadial / interstadial sequences, because

lower altitude inland caves were more likely to remain permanently covered by the icesheet. This may explain the large diameter (10m) of **Gåsvasstindhola** (Z4, altitude 778m; Photo 8.1) and the existence of relatively large caves in the Western catchment area, which may have experienced several IDLs as the climate fluctuated through the Older and Younger Dryas stadials (Appendices D5.1–D5.3).

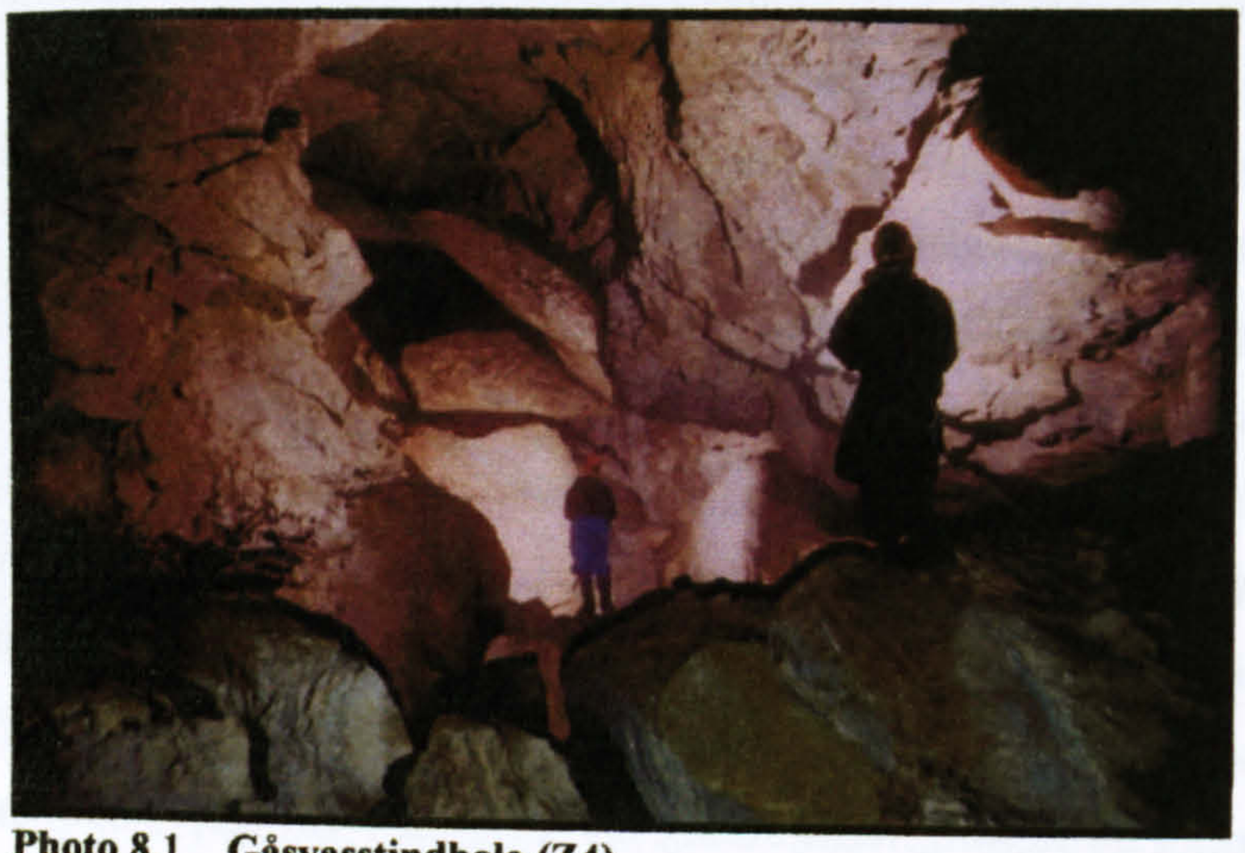

Photo 8.1 Gåsvasstindhola (Z4)
One of the largest passages in the study area

8.4 Glacial conditions and flow regimes

Section 3.2 reviewed the general history of glacial karst research and section 3.3 the development of ideas about glacial karst in Scandinavia. The various glacial sequences that applied at the study area caves and karsts during the many glaciations that central Scandinavia has experienced were considered in some detail in sections 8.1–8.3 and Appendices D1 and D2. This section identifies 11 glacial conditions that cave sites could experience during a cycle from a glacial to an interglacial climate. Whilst describing these conditions, 14 separate flow regimes are derived that could apply at each local cave environment, as summarised in Table 8.1 (section 8.4.12). Sections 8.5–8.9 with Appendix D4 then discuss the effects of these flow regimes on the local karst hydrogeology, and derive the relevant timescales for the gestation and enlargement of karst conduits and cave passages.

8.4.1 Cold-based icesheet

The likelihood that much of the study area was frozen-based at the Last Glacial Maximum (LGM) was discussed in Appendix A3.2. Permafrost could also occur adjacent to valley glaciers during the onset stage, and perhaps also during the decay stage of each stadial, and underlie the narrower valley glaciers. Thus, caves situated in such situations could experience permafrost conditions once or twice at each stadial. Karst caves would then contain frozen water and trapped air in varying proportions. Caves situated high in valley sides adjacent to valley glaciers before the onset of local permafrost would have been subjected to a seasonal high energy erosional environment with severe freeze thaw and high spring melts, i.e. conditions more extreme than those of today. At transitional periods, internal cave environments could be seasonally varying. Klemen and Hättestrand (1999) stated that ribbed moraines surrounding relict landscapes in "west-central Fennoscandia" indicate fracturing of frozen drift sheets during the transition from frozen to thawed conditions during deglaciation.

During the onset of glaciation, caves beneath a cold-based icesheet, but above the glaciation marine limit, might still contain air, plus old, frozen, meteoric water, plus injected glacial ice (as at Castleguard Cave in Canada: Ford, 1987), if they had only experienced permafrost conditions and were below the plastic behaviour limit (PBL). For caves below the glaciation marine limit, the ice may initially have consisted of frozen sea water. However, the temperature at the base of a long-lasting icesheet varied from place to place and time to time, dependent on cold-based and warm-based conditions, whilst remaining close to the pressure melting point (Johnston, 1987; Appendix A3.2). If the immediately overlying icesheet became warm-based at *any* time, then any underlying caves would flood completely with glacial melt, which would force out most of the trapped air, and, in time, replace any pre-existing water, although air, or possibly a near-vacuum (arising from the smaller volume occupied by meltwater in a closed system), could remain in ceiling pockets. The glacial meltwater would then freeze again on a return to permafrost conditions. Because the Weichselian glaciation experienced significant Bond cycle and Dansgaard-Oeschger cycle climate-warming oscillations (section 2.3.3), it seems likely that many caves then in existence in valley floor and other suitable topographic locations (where subglacial lakes were more likely to form) alternated between occupation by glacial ice and by glacial meltwater soon after glaciation, with little trapped air. Caves in locations that did not experience warm-based conditions may have contained both ice and air for long periods of time, until the onset of a deglaciation phase.

It seems that all then-existing caves were potentially occupied by ice at some stage during glaciation, because the maximum distance of a cave passage from the overlying rock surface is always less than 100m (section 5.3.7), which could be the thickness of the permafrosted rock (Appendix A3.4). Because the thickness of the icesheet at the LGM was much greater than the depth of the PBL, the underlying caves could not be integrated with any englacial Röthlisberger channels at the height of each glaciation. Neither could there be any air gaps between the base of the ice and the underlying rock. Thus, ice would be injected at high pressure some way into every available karst orifice, even without an interval of warm-based conditions. The flow regime applicable to caves in cold-based, permafrost, conditions is *occupation by ice*. It is assumed herein that the karst hydraulic condition at the base of an icesheet that is kept at the pressure melting point by glacial movement is similar to that at a cold-based icesheet.

8.4.2 Warm-based icesheet

The existences of *subglacial lakes* at the heart of extensive icesheets and of subglacial groundwaters at their peripheries were discussed in Appendices A3.3 and A3.4. Thus, perennial lakes of topographically varying size commonly form at the bases of full-cover polar icesheets above non-frozen bedrock, which have low hydraulic gradients and very slow circulatory movements. Phreatic inundation by melting of warm-based icesheets to form essentially static subglacial lakes during glacial maxima *may* apply to many karsts in the study area, especially those in valley floor locations. The lengths and frequencies of inundation are commonly unknown, although they may have persisted for many thousands of years.

Subglacial lakes only existed at very high pressures, with no air gaps, because they supported the weight of the floating icesheet. Thus, any cave passage inundated by a subglacial lake would have a high pressure exerted on its walls and internal deposits. It also seems possible that chains of subglacial lakes could form that might, or might not, be connected hydrologically along valley floors.

No direct observations of conditions in a subglacial lake below a warm-based Scandinavian icesheet or glacier are possible, because none are known to exist. The presence of extremely fine clay particles that coat all the surfaces of some Norwegian caves (e.g. in **Tjoarvekrajgge** in northern Norway, and along a 1cm roof notch in **Luktindgrotta**, Z6), may indicate that some, at least, of the submerging lakes were indeed static. These may include subglacial lakes. Other bodies of water that can exist subglacially during deglaciation are discussed separately. The applicable flow regime at a warm-based glacial maximum is *subglacial lake*.

8.4.3 Coastal western slopes

Towards the end of each glaciation, the steep edge of the icesheet receded eastwards at c. 70ma^{-1}, initially across the rather flat bed of the Norwegian Sea, until it reached the Western catchment area. Ice-dammed lakes were not able to form by the melting of the icesheet surface at low altitudes near the coast, because the land there was exposed by the direct melting and calving of the western margin of the icesheet at or above sea level, and the melted ice ran away into the sea. Three timings are relevant (Figure 8.6).

At time 1, the ice margin reached the western side of a minor ridge. Any caves or fractures below the deglaciation marine limit (GS=C or D) were directly invaded by the sea, and an IDL could not form. The applicable flow regime is *marine inundation*. At time 2, the ice margin exposed the higher western slopes of the ridge (GS=G or K). Again, an IDL could not form because the meltwater ran down the slope into the sea. The applicable flow regime is *slope flow*. At time 3, the ice margin crossed the ridge to expose its eastern slope (GS=C, E, H or L). Here, an *ice margin IDL* (section 8.4.10) could form, which initially might be backward-flowing over a col down to the sea, dependent on topography, but which would eventually be replaced by marine incursion up to the deglaciation marine limit. However, a 5km-long east-draining valley could have sustained such an *ephemeral* ice margin IDL for only c. 70a, a period too short to enlarge phreatic conduits to explorable sizes. Hence, relict phreatic passages should not be found in those positions that could only have been submerged beneath coastal western slopes or beneath small ephemeral ice margin IDLs, but mainly vadose caves could perhaps develop there, under interglacial conditions.

The above hypothesis was tested by making the assumption that the ice-melting heights in the Western catchment area were 200m lower at each interval during deglaciation than predicted by the reconstructed Grønlie formula (section 8.1.4). The only dissolutional caves found in the cave database to have formed at a coastal western slope or at an ephemeral IDL situation (i.e. one that is not on the slope of a high peak or ridge that could 'attract' both a nunatak IDL before the arrival of the ice margin and powerful deglacial seismicity) are the hybrid relict **Football Pitch Cave B** (Z1) and the 'mainly vadose' resurgence cave **Olafs Kilden** (Z2). This is strong supporting evidence that nearly all the karst caves were either initiated or formed completely beneath deglacial ice-dammed lakes that were themselves initiated at the nunatak level. Because **Olafs Kilden** is located beside the 720m-deep Bindalsfjord (one of the deepest in Norway: section 2.2.1), its fractures were likely produced by ice marginal seismicity, with subsequent enlargement during the Holocene (Appendix D4.12).

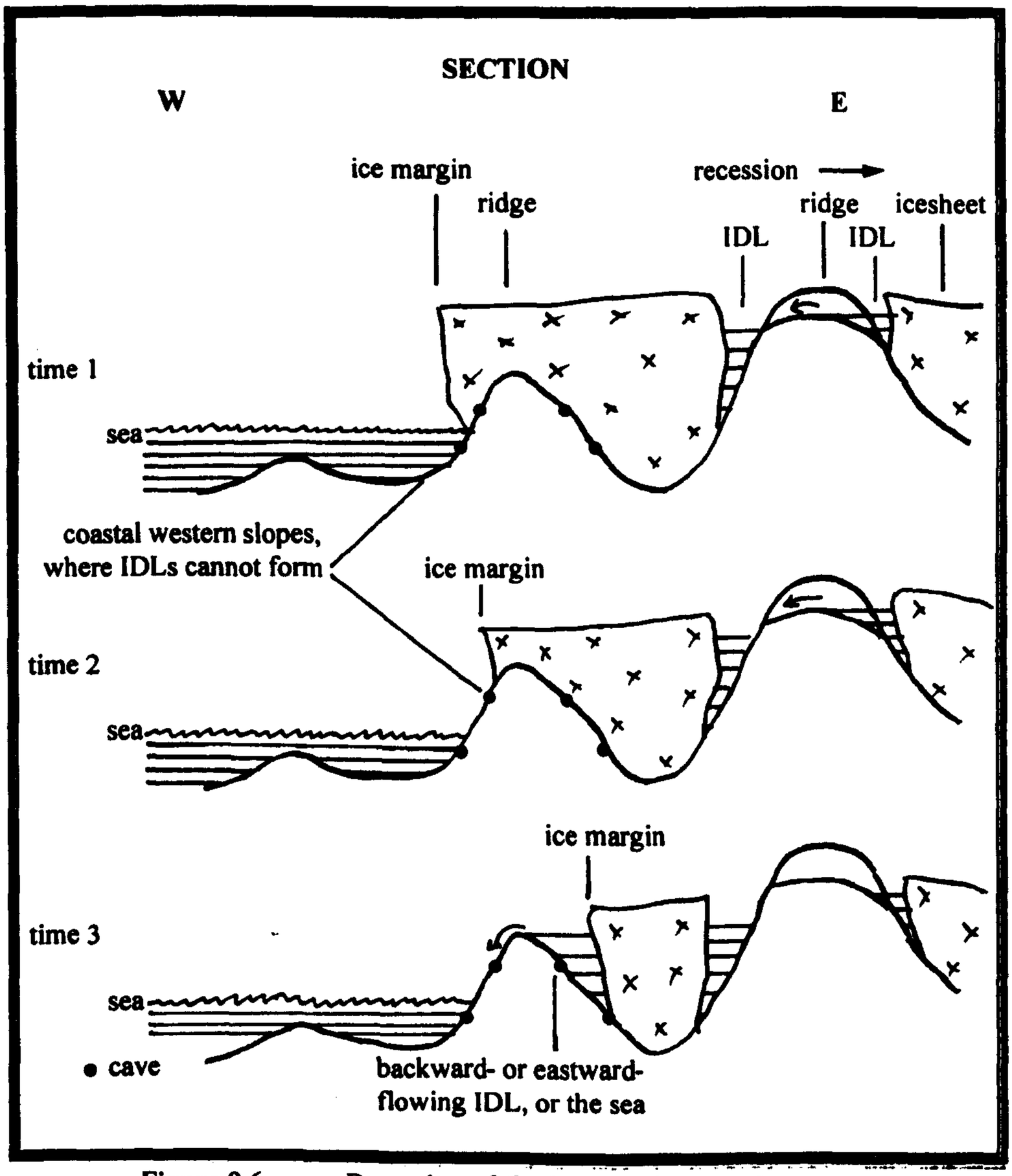

Figure 8.6 **Recession of the ice margin near the coast**

Higher ridges, as also shown in Figure 8.6, formed IDLs *within* the icesheet, as described in the following sections. Thus, there is a fairly complex relationship between altitude, longitude and topography that determines where in Z1, Z2 and Z9 of the Western catchment area IDLs could not form or only ephemeral ice margin IDLs were situated.

8.4.4 Nunatak IDL

At the LGM, the icesheet probably covered all the mountains of the area and no IDLs existed, apart from small, shallow, melting-pools (*supraglacial* lakes) on the surface of the ice each summer. As the icesheet lowered during deglaciation, initially by ablation, individual peaks and ridges became exposed as nunataks. Their rocks were warmed by the sun in summer, causing the immediately-surrounding ice to melt faster than the mass of ice in the icesheet. (The following discussions assume that the air temperature above the icesheet averaged >0°C each summer). Thus, very early in the deglaciation sequence, small, linear, and initially stagnant, lakes were created against the ridge walls, whilst being confined by the main icesheet on the other side, in glacial situation U. Each *nunatak IDL* (Lundqvist, 1972, p32; LaRocque *et al.*, 2003, p77) reached down to solid rock at its base, and potentially continued for some distance as a static Nye channel at the ice-rock contact to an SGR below the surface of the icesheet (Figure 8.7a). The lakes and their water levels lowered away from the summits as the icesheet surface lowered each summer. Any ice in a cave below a nunatak IDL melted as the lake lowered through the level of the cave, and the melted glacial ice gradually drained away as the cave emerged above the level of the IDL, with no significant phreatic flows of water passing through the cave. However, the IDLs probably froze again each winter, when severe freezing at the high altitude could cause extensive frost-shattering, especially when the IDL level was coincident with a cave entrance. The draining of nunatak IDLs by englacial channels was unlikely, because the PBL (sections 3.2.4 and 8.1.8) was initially close to the surface, and the local near-horizontal surface of the icesheet provided few outlet opportunities. Because nunatak IDLs were essentially static, lowered annually and contained little sediment, they left little evidence of their existence after they lowered below the ridges, compared with the lower moraines deposited under IDLs at later stages (Brazier *et al.*, 1998, p300). The applicable flow regimes are *nunatak flow* and *occupation by ice*.

8.4.5 Westward-flowing IDL

The evolution of a westward-flowing IDL from a nunatak IDL to a drained IDL and its relationship to underlying fracture systems and caves at each western glacial situation is described by reference to Figure 8.7. Although new winter snow melted upwards towards the summits during each summer (as now), the surface of the whole icesheet lowered annually by ablation and by melting to form surface flows, as deglaciation proceeded. From the reconstructed Grønlie formula (section 8.1.4), the lowering rate of the upper ice-melting height roughly increased from 30–60cma^{-1} over the period 12000–9000^{14}Ca BP, for all isobases. Thus, more rock became exposed to the sun, and the nunatak IDLs became wider, longer and deeper, but with surfaces that followed the downward trend of the icesheet surface.

The icesheet was commonly lower on the western sides of north-south-aligned ridges because of increased insolation, reduced winter precipitation, reduced accumulation, warming by the sea, warming of bedrock at the receding ice margin and less restricted glacial streaming. Thus, when the lowering surface of the icesheet caused the base of its *eastern* nunatak IDL to coincide with the highest local pass-

point along the ridge on its *western* side (Figure 8.7b and g), the eastern lake-level was stabilised by this outlet pass. Meltwater (supplemented with occasional jökulhlaups, Appendix D4.4) spilled continuously *up-valley* and *'backward'* over the col in summer, to pour down into the lower-level *westward-flowing* IDL. Sporadic overflows of western IDLs also reinforced the increased lowering of the icesheet on the western sides, and contributed to making the warmer western sides *wetter*, with lower plastic behaviour limits. It seems unlikely that reverse flow applied to many IDLs situated on the *western* side of the major ridges: these IDLs typically passed directly from nunatak to westward-flowing.

The ice-dammed lakes were also commonly deeper on the western sides of the main mountain ridges, because their Nye channels were along rock floors also made warmer by the advancing sea and retreating ice margin, by receiving more heat from daily insolation, and by accepting the extra flows from their adjacent backward-flowing IDLs. The first summer outlet was achieved when an epidermic Röthlisberger channel above the PBL found a siphoned route to the surface, creating significant *englacial flow* through the IDL (Figure 8.7b and g). The flow tended to increase as *melt-widening* widened the englacial channel (Tweed and Russell, 1999). At the same time, down-valley glacial Nye channels slowly fed an enlarging high pressure subglacial reservoir at the foot of the IDL whilst the icesheet remained cold-based (hp-SGR: Figure 8.7; section 8.1.6) In winter, the ice-dammed lakes froze from the surface downwards, perhaps also freezing the water in any submerged caves, whilst subjecting their wall-rocks to increased stress and fracturing.

The lowering western IDLs drained 'forward' and 'down-valley' as part of intermittent summer surficial, epidermic, or deeper, glacial drainage systems above the plastic behaviour limit of the ice, in glacial situations S, K and G. The water levels in the earlier (higher) westward-flowing IDLs fluctuated, perhaps hourly, dependent on precipitation, the ice-melting recharge rates, and the deeper subglacial temperature-controlled discharge capacity into subglacial reservoirs. Nye and Röthlisberger channels sporadically fed water to the base of vertical moulins at crevasses, where it rose (perhaps as a fountain: Tweed and Russell, 1999) and overflowed the down-slope surface of the icesheet, which it tended to lower. In other conditions, excess water intermittently overflowed from the IDL on to the icesheet to the west via *ice contact spillways*. Fractures and cave passages situated directly below an active IDL, its subsequent Nye channel or its SGR eventually became incorporated directly into the glacial hydraulic regime.

The western IDLs were commonly smaller in extent than the eastern IDLs, being contained more within the valleys, and persisted for less time because they could not convert into ice margin IDLs. Hence, fractures on E–W spurs that led from major western slopes were likely to be inundated for less time, explaining the rarity of caves with GS=D, G, K and S (sections 5.3.5 and 5.5.6). The extreme rarity of caves at GS=S (Table 5.28) may be because high-level western IDLs remained essentially static, giving few opportunities for phreatic enlargement or for a phreatic 'kick start' for mainly vadose caves.

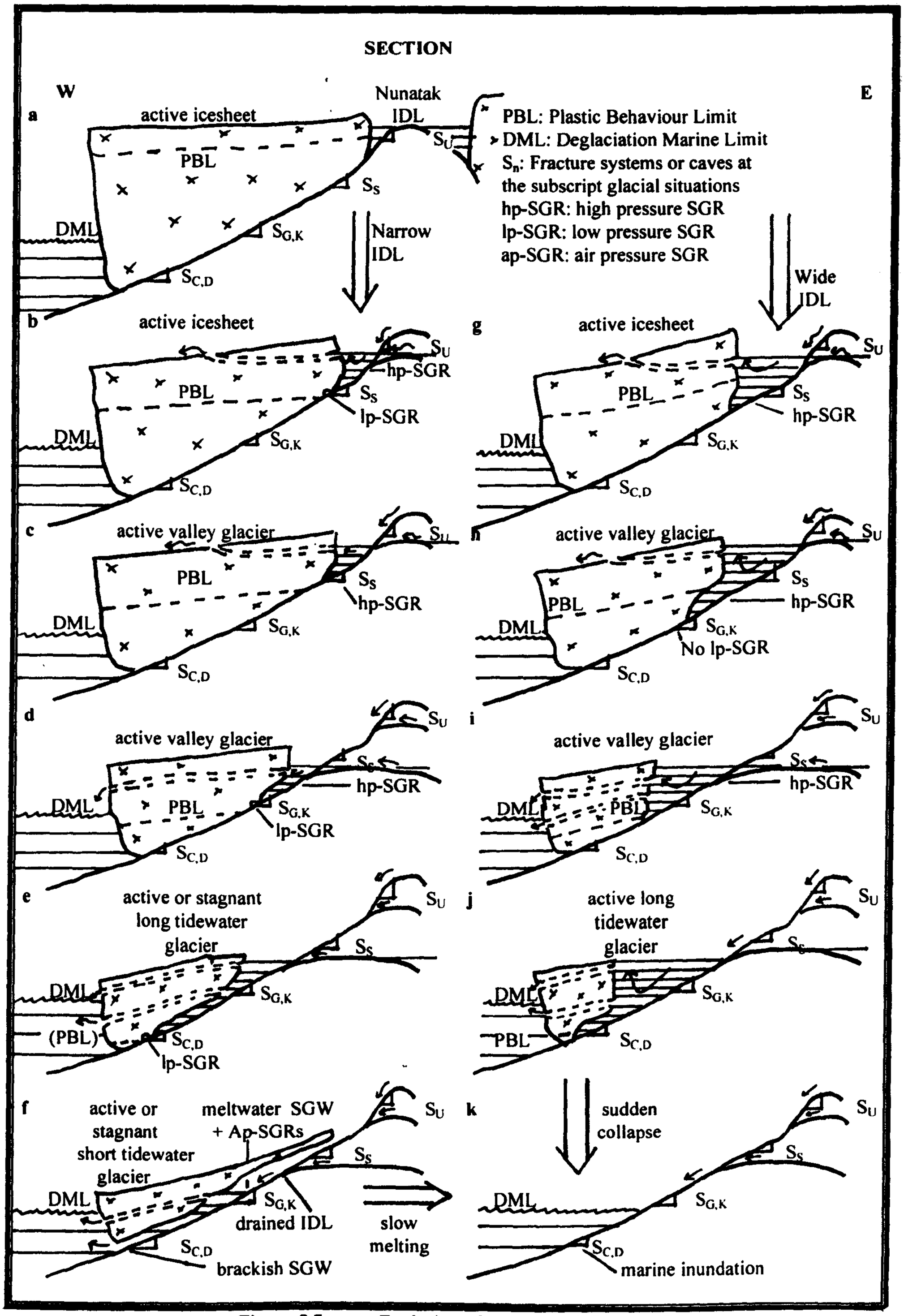

Figure 8.7 Evolution of a westward-flowing IDL

Two extreme examples of IDL evolution need to be analysed: the *narrow IDL* case (n), where the base of the IDL does not reach the PBL: Figure 8.7b–f, and the *wide IDL* case (w), where the IDL base is below the PBL: Figure 8.7g–j. The wide IDL case became increasingly dominant as deglaciation proceeded, especially on the east side of ridges. In the narrow IDL case, if the base of the IDL or hp-SGR reached an inception fracture system, this could create a further small *low pressure* subglacial reservoir (lp-SGR) and *low pressure SGR flow*, where fluid was *sucked* in laminar flow through inception fractures. If post-breakthrough conduits were encountered, these soon enlarged to cause a deepening of the high pressure SGR. Assuming that lp-SGRs could not form below the PBL, they did not form in wide IDLs. Both narrow and wide IDLs provided englacial flows for fracture systems and caves above the PBL, and wide IDLs also provided slower *circulatory flows* below the PBL, as the hp-SGR deepened, and as some water returned towards the englacial outlets above the PBL.

As deglaciation proceeded, the icesheet shrank into separate valley glaciers. When some westward-flowing IDLs lowered themselves down the valleys, they were sporadically held up by ice and moraine debris situated in narrower valley sections. These created temporarily-stable lake levels, typically located directly above the present permanent lakes. There were many such examples west of the MSW in the Northern catchment area and in the eastern limb of the Vefsn catchment area (Grønlie, 1975). The levels of these forward-flowing IDLs also commonly re-adjusted themselves at jökulhlaup events, when, especially at lower altitudes, underlying karst caves were inundated by powerful flows of water. With more land exposed above the IDLs, the *proportion* of flow from direct meteoric precipitation also increased, as did the load carried from glacial sediments. Thus, these sediments were deposited within and washed through any underlying caves, as well as sinking to the bases of the IDLs.

The IDLs reduced in size to occupy the upper valleys above the shrinking valley glaciers, which, in Norway, eventually became receding *tidewater glaciers* near the deglaciation marine limit. Assuming these were always warm-based for some distance inland from the sea, two types can be distinguished: *long* (l), where there was no connection along the valley floor from the Nye channels and SGRs at the head of the glacier to the marine inundation at the glacier snout, and *short* (s), where a brackish SGW ran beneath the whole glacier at its warm base to drain the IDL. Because each type of tidewater glacier could interact with either a narrow or a wide IDL, four combinations were possible: ln, lw, sn and sw. Each combination could also represent an *active* glacier (assumed to be thicker than the depth of the PBL) or a *stagnant* glacier (assumed not to exhibit plastic behaviour), but three of these combinations cannot exist from the definitions. Hence, the five possibilities are: active and stagnant long tidewater glaciers with no valley floor hydrological connections to narrow IDLs (partly cold-based: Figure 8.7e); active long tidewater glaciers with no valley floor hydrological connections to wide IDLs (partly cold-based: Figure 8.7j); and active and stagnant short tidewater warm-based glaciers with a brackish SGW along a valley floor that increasingly comprises meltwater upstream, which may lead to an IDL or to a drained IDL (Figure 8.7f). Appendix D5.3 indicates that a 'short' tidewater glacier could be 10km long near the coast.

Some active and stagnant long tidewater glaciers probably had Röthlisberger flows above the PBL that discharged as waterfalls into the sea (Figure 8.7d, e, i and j). When the increasingly-inclined PBL descended below the sea level (elevated because of isostatic depression of the land) at glacial situations D and C, submarine Röthlisberger discharges were also possible (Figure 8.7e, f, i and j). Because the head of water in the westward-flowing IDLs might still rise above sea level at high stage, the outlets could discharge meltwater as considerable upwellings, just beyond the ends of the fjord glaciers. The flow regimes applicable to all westward-flowing IDLs are *englacial flow, ice contact spillway flow, jökulhlaup flow* and *occupation by ice*. Additionally, narrow IDLs supported *low pressure SGR flow*, and wide IDLs supported *circulatory flow*.

8.4.6 Drained IDL

If the active tidewater glacier did not collapse, but slowly melted away, then the ice deteriorated into stagnant 'dead-ice' when the glacier thickness reduced to less than the PBL (c. 200m; Figure 8.7e and f). Large flows of icemelt were then captured via Nye channel meltwater SGWs, when SGRs coalesced along valley bottoms above sea level. Flow rates increased by melt-widening and mechanical tunnel enlargement (Tweed and Russell, 1999). The SGWs continued as brackish SGWs to the ends of the tidewater glaciers in Norway. The IDL became a *drained IDL*, being replaced by large *air pressure* SGRs (ap-SGRs) at places governed by the local topography (where lakes exist at present). The continuing drained IDL regime had a powerful meltwater SGW running through a large Nye 'tunnel channel' under the base of the remnant tidewater glacier, into a continuing and flooded brackish SGW. There was commonly a continuous airway above the meltwater part of the SGW, with sporadic ap-SGRs along valley floors. These hidden internal SGRs increased in size enormously as their bases lowered down the valley floors and they may have contained significant air pockets below their ice ceilings. In places they later formed *intraglacial* lakes, which were surrounded by static ice, but directly exposed to the atmosphere. The surface of the lowest SGR coincided with the contemporary sea level, creating brackish and tidal conditions in any underlying cave system (Figure 8.7f).

Wide IDLs were more likely to collapse catastrophically, because they were deeper (Figure 8.7j). In this event, a cold-based retaining ice barrier commonly gave way suddenly, perhaps under the warming influence of the advancing sea, to produce a final *proglacial* jökulhlaup or *superflood* (Rudoy, 2002). This could either drain the reservoir through one or more 'tunnel channels', after which the tidewater glacier slowly melted as discussed above, or else the whole ice dam could float away when the hydrostatic head exceeded the over-burden pressure (Figure 8.7k; Walder and Costa, 1996; Tweed and Russell, 1999). The Tosenfjord tidewater glacier probably collapsed catastrophically, because, being aligned NE–SW, it was approached by the sea and the ice margin from low-lying land along its western edge, rather than melting inland along its length (Figures D3.5 and D3.6; Appendices D3.6 and D5.3). Those underlying caves that experienced a proglacial superflood were subjected to a very high, but short-lived, erosional regime, especially those with CL=V, which were in the direct line of the flood.

Thus, IDLs either drained gradually, via ice contact spillways, via meltwater SGWs, or via brackish SGWs (in Norway), or catastrophically, by a collapse of the ice dam. According to Lundqvist (1972), an IDL could not form again if there was a continuous supply of water to the lake basin. Subglacial waterways could reach the sea at the edge of the receding grounded ice shelf, according to the evidence of Follestad (1997) in northern Norway, and of Flinn (1967) at the Scottish coast. This raises the possibility that warm-based icesheets could create SGWs by pressurised internal melting, without connection to an IDL on the surface.

The IDLs and SGRs themselves either eventually disappeared altogether, or remained as the present surface lakes. The only known karst system beneath a surface lake is the source of the resurgence cave **Aunholet** (Z2), beneath the 'vanishing lake' Engjavatn (section 4.2.8). The existence of other permanently submerged caves remains a possibility. The applicable flow regimes are *occupation by ice*, plus *meltwater subglacial waterway* (above the deglaciation marine limit) and *brackish subglacial waterway* (below the deglaciation marine limit).

8.4.7 Submarine

Caves and fractures lying below the glaciation marine limit (GS=C, D, E, G and H) were inundated with sea water before they froze at the onset of glaciation, and so contained little trapped air. During deglaciation, when the ice margin approached a cave located on the west side of a ridge and below the deglaciation marine limit (GS=C and D; section 8.4.3), its internal cave waters became brackish because of tidal effects. Caves below the deglaciation marine limit on the east side of a ridge (GS=E) commonly first became flooded by glacial melt flowing along Nye channels at the base of the icesheet (section 8.4.5; Figure 8.7e and j mirror images) before becoming completely inundated with sea water, perhaps for a second time, as the lower melting height of the tidewater glacier rose and the sea encroached up the valleys at the end of the Younger Dryas (section 8.1.4; Figure 8.7f and k mirror images). **Neptune's Cave** (Z2) is presented as such an example (Appendix D5.3). The continuing extent of the brackish nature of this water after the tidewater glacier melted depended on the fluvial regime in the valley, and the local topography. As isostatic uplift raised the caves with GS=C, D and E to their present altitudes of ≤167m, they were drained of sea water, and exposed to climatic conditions similar to those now operating. The period of inundation by sea water was determined by the cave's altitude, isobase and the local sea level curve. The applicable flow regimes are *marine inundation* and *occupation by ice.*

To summarise the deglaciation of the Western catchment area in particular, many caves became part of powerful englacial hydraulic systems, which initially carried fairly light sediment loads, but were occasionally engulfed by jökulhlaup floods. At least those caves that were near the deglacial marine limit also became part of powerful subglacial waterways, whether above or below contemporary sea level, which carried heavy loads of glacial till. This partly explains the increase in fluvial sediments with lower glacial situation (Appendix B2.10). In both cases of gradual or sudden draining of the final IDL, the end

result was the complete marine inundation of caves below the deglaciation marine limit, and the draining of all the higher caves and fractures (Figure 8.7k).

8.4.8 Backward-flowing IDL

The initiation of a narrow backward-flowing IDL at glacial situation GS=T was described in section 8.4.5. With continuing icesheet downwasting, especially on the western sides of ridges where it was lower, successively lower *spillways* were exposed, so that each backward-flowing IDL adjusted to lower, commonly western, outlets, whilst at the same time becoming larger. The pattern of lowering, expanding, deepening and merging backward-flowing IDLs is illustrated in Figures D2.1–D2.9 for the deglaciation of the whole study area and in Figures D3.1–D3.9 for the Tosenfjord–Fiplingdal area. Because of the depths reached, the 'wide' IDL case soon became dominant, with the IDL bases below the PBL.

Each re-adjustment typically occurred as a catastrophic *jökulhlaup* flood (perhaps accompanied by tectonic deformation: Dawson *et al.*, 2002), which persisted for several minutes or hours, as a new temporarily-stable lake surface formed. Because ridges tend to follow geological structures, there is a general tendency for backward-flowing IDLs to be aligned with cave passages formed in stripe karst. Within each lake (and any underlying cave), flow-switching could occur (e.g. from north to south or from south to north) at each successive lowering, dependent on the relative position of the next active col.

It might be anticipated that there could also be transitional forward *englacial* flows at each level of a backward-flowing IDL, via Röthlisberger outlets above the PBL. These might lower the level of the IDL below the level of the col, and temporarily halt the up-valley reverse flow. During any such transitional stages, restrictions in the size of the IDL outlets by re-freezing, or increases in precipitation or glacial melt, would raise the level of the IDL again, until it partly reverted to reverse flow over the col. However, it seems unlikely that englacial channels drained the backward-flowing IDLs below the levels of the spillways along the ridges, from the evidence of jökulhlaups discussed in Appendix D3. Whilst the level of the icesheet remained above the level of the lowest col (GS=T), a backward-flowing IDL could also not overflow the icesheet itself along ice contact spillways, which would tend to keep the icesheet drier and more horizontal (giving less outlet possibilities) on the eastern sides of ridges, with a PBL nearer the surface. It is also possible that if the altitude difference between successive spillways was sufficiently large, the backward-flowing IDL could lower below the level of a previously-active spillway before the icesheet on the western side lowered enough to expose the next spillway. In this case, the backward-flowing IDL could become temporarily static. It is assumed that this rarely occurred, because of the common small altitude differences between spillways (Appendix D3). Because of the continuous nature and strength of the summer meltwater discharges, it might also be anticipated that reverse flow was greatest near the surface of the IDL, with circulatory flow more likely at depth in a wide IDL. However, this may not be the case, because the density inversion of water below 4°C means that slightly

warmer meteoric water and meltwater may sink into an IDL close to freezing. In Appendix D4.4 it is assumed that the reverse flow speed was 20cms^{-1} at a depth of 240m.

All caves situated east of, and below, the level of the highest local col that are also above the lowest local col (GS=T), and some others lower down, were submerged for varying periods of time by backward-flowing IDLs. They experienced phreatic meltwater flows (in sporadically-varying directions) from the time that a backward-flowing IDL arrived above them, until the time when the level of the lake fell below their own level, when they drained. This concept is demonstrated by the existence of north-facing scallops on Elgfjell. These indicate flow in the opposite direction to that of normal valley drainage (Appendix D3.3), which is only possible beneath a backward-flowing IDL. The applicable flow regimes are *reverse flow, jökulhlaup flow*, and *occupation by ice*. *Low pressure SGR flow* above the PBL of an early narrow backward-flowing IDL was also possible, and *circulatory flow* is uncertain.

8.4.9 Eastward-flowing IDL

After a backward-flowing IDL lowered below the level of the lowest pass, it could then only drain 'forward' and 'down-valley' in glacial situations L, H and E, in various conditions similar to those of a westward-flowing IDL (e.g. Figure 8.7e, f and j). These conditions may be visualised by creating a mirror image of Figure 8.7, but without the early recharge from a backward-flowing IDL.

Eastward-flowing IDLs also stabilised their levels, or drained out completely, via *ice contact spillways*, sporadically into lower-level eastward-flowing IDLs, as they merged within the main body of the icesheet, or as they flowed out beside valley glaciers. Hence, once forward flow was fully entered, fluctuating levels could cause IDL englacial flow to be supplemented by ice contact spillway flow at high stage, controlling the maximum head of the englacial flow. The eastward-flowing IDLs remained trapped against a continuing, more active, icesheet for longer than the westward-flowing IDLs. They therefore commonly also remained full of meltwater for longer, although perhaps in a more static condition, because the lowering of their PBLs lagged behind those of IDLs flowing west. As discussed in section 8.4.3, the possibility of a slope flow regime does not arise on the eastern sides of ridges, but in the Western catchment area, eastward-flowing IDLs could be ephemeral.

From these points, it is clear that *all* inland fractures and caves that lie *east* of a major mountain range in the study area were inundated by a backward- and / or an eastward-flowing ice-dammed lake for a period of time during the late YD or early Holocene, as the IDLs progressively lowered themselves down the valleys during the spring, summer and autumn seasons of a deglaciation phase.

In the Norwegian part of the study area, the water from eastward-flowing IDLs also eventually reached the sea, via valleys aligned S–N and via the fjords aligned E–W. It seems likely that persisting permafrost prevented SGRs from reaching the grounding lines of the glaciers at the inner ends of these fjords whilst

the ice thickness remained greater than the PBL of c. 100–200m. Commonly, individual eastward-flowing IDLs widened then narrowed as they evolved. Collectively, they also widened from west to east across the study area and as time progressed, as a consequence of the lowering of their altitudes and the increase in their melting rates. Thus, the largest eastward-flowing IDLs were created in Sweden, which flowed SE towards the Baltic (Appendix D2). The flow regimes applicable to eastward-flowing IDLs are *ice contact spillway flow, englacial flow* and *occupation by ice*. Wide IDLs also supported *circulatory flow*. There were probably few narrow eastward-flowing IDLs, but those that existed could support *low pressure SGR flow*. They were not associated with many jökulhlaups, because eastward-flowing IDLs tended to become ice-margin IDLs.

8.4.10 Ice margin IDL

Ice margin IDLs are commonly special cases of eastward-flowing IDLs. In the Western catchment area they only formed at low altitudes as ephemeral ice margin IDLs within local east-draining valleys (Figure 8.6). Tidewater glaciers formed the ice margin contact in the *west-draining* valleys. Farther east, and at higher altitudes, ice margin IDLs combined the effects of the eastward-flowing IDLs, formed by the lowering of the icesheet surface, with the effects of the eastward recession of the edge of the icesheet. They therefore had the potential to grow to larger sizes than other IDLs, and to inundate underlying karst caves for longer periods of time. Water flows were in the down-valley direction, towards the ice. In the Vefsn catchment area, large eastward-flowing IDLs became ice margin IDLs when the ice margin reached the valleys of Svenningdal and Eiterådal (Figure D3.6). Water escaped to the north via ice contact spillways between the hillslope and the ice, where the topography sloped down under the icesheet in topographic situations similar to those in southern Quebec described by LaRocque *et al.* (2003). However, the eastern limb of the Vefsn catchment area and most of the Northern catchment area drain westward and therefore could not form large IDLs at the ice contact. It was only when the ice margin passed the MSW into the Eastern catchment area that such IDLs *commonly* grew to very large sizes against the ice margin, as it retreated into Sweden. In turn, ice margin IDLs became drained IDLs (section 8.4.6) slowly or catastrophically, either adjacent to tidewater glaciers, as in Svenningdal and Vefsndal, or near dead-ice areas, as in Sweden. From the above, the flow regimes applicable to ice margin IDLs are *ice contact spillway flow, englacial flow, circulatory flow* and *occupation by ice*. There was probably a maximum of one *jökulhlaup* for each IDL, if it finally drained catastrophically.

8.4.11 Interglacial conditions

The very variable *annual* conditions that have prevailed through the Holocene, as described in Appendix A4.1, and the distribution and character of the present caves (although not their final dimensions), as described in Chapter 5, are assumed to be fairly representative of the last few interglacials. Thus, a proportion of cave passages are 'relict', being perennially air-filled. Others contain vadose streamways, mainly fed from allogenic sinks, which may lead to phreatic sections en route to lower resurgences. Other (as yet unexplored) cave passages may be perennially submerged beneath lakes and tarns.

The predominant flow regime is *interglacial*. Additionally, partial *occupation by ice* affects most caves (both vadose and phreatic) in winter, especially the injection of ice and snow at entrance areas, the partial freezing of streamways, and the internal formation of icicles. Caves below the glaciation marine limit (GS=C, D, E, G and H) experienced *marine inundation* until the sea froze or they were covered by ice at the start of previous glacials. Caves with GS=C, D and E experienced *marine inundation* until raised above sea level by isostatic elevation during an interglacial.

8.4.12 Deglaciation conclusions

Table 8.1 summarises which flow regimes apply to each glacial condition that a cave could experience. From the above discussion, it is clear that much of the land in the study area was flooded by glacial meltwater during deglaciation, so that probably all the studied caves *then existing* (i.e. at least the relict phreatic passages) experienced totally phreatic, dissolutional, conditions beneath backward-flowing and / or forward-flowing IDLs, before being drained to present conditions. Above the deglaciation marine limit, there are rough constancies in this flooding timescale of ~800^{14}Ca on western slopes and of ~1200^{14}Ca on eastern slopes, as each of the caves experienced a pulse of melting as its local ice-dammed lake migrated down-valley, from the reconstructions in Appendices D2 and D3. The actual time taken for an IDL to pass any point is determined by the topography: a long linear ridge aligned N–S without connecting spurs would create a narrow, shallow, IDL that would quickly descend past any submerged karst feature. In the normal case, IDLs formed at the heads of side valleys widened and deepened because of additional heat flux from the upper valley walls. The time a cave remained submerged can commonly be estimated by dividing the presumed initial head of water above the cave by the ice-melting height lowering rate of c. 0.5ma^{-1} (section 8.1.4). This time is independent of the local hillslope.

The SGR bases of wide IDLs probably soon reached along their valley bottoms, even if discharge was only via Röthlisberger channels situated above the PBL, <200m from the surface. However, *all* submerged caves situated both above and below the discharge altitude were likely to be incorporated into the IDL / glacier hydrological flow regime, to some extent. The later high deglacial flow rates of SGWs probably caused many of the existing caves to be scoured by waters charged with heavy loads of till, especially in Sweden, with stochastic mechanisms of frequent blocking and unblocking that varied for each individual cave system. The various IDLs froze downwards to varying depths during each winter of the deglaciation period, so that the water in each of the submerged caves was also potentially subjected to total freezing, at least when the IDL surfaces lowered to near the caves' altitudes. Caves inundated by sea water or brackish water experienced less freezing, because of the depressed freezing points.

The general pattern for shallow caves (the majority of caves in the area) is that they drained and reverted to hydrological conditions similar to those of today as the surfaces of the ice-dammed lakes lowered below their levels. An IDL surface lowering rate of 0.5ma^{-1} should be too fast to leave evidence of the transition from phreatic to vadose flows. Thus, the two apparent relict vadose 'steps' in the floors of both

'The Aven Route' in **Balcony Cave** (Z3; altitude 200m; Faulkner and Newton, 1995, Fig. 12) and **'Fall Aven'** in **Etasjegrotta** (Z4; altitude 300m; Figure B1.8) indicate a hiatus in the rate of melting between 9600 and 9500^{14}Ca BP, from the reconstructed Grønlie formula (section 8.1.4). Such steps are therefore diagnostic of *phreatic to vadose transitions* (in time) and of *vadose to phreatic transitions* (in space) during the deglaciation of caves with upside-down morphology.

Deeper systems, such as **Ytterlihullet** (ZA), remained partially blocked at their resurgences by valley glaciers long after their sink entrances emerged above lake levels. These systems could therefore remain completely flooded for many further years, with meteoric water overflowing their sinks, especially in spring. Nevertheless, because no cave in the study area is deeper than 180m, when the valley glaciers receded, the opportunities for phreatic (Lauritzen, 1986a; section 3.3.2), then vadose, flows soon increased as integrated cave and glacier drainage paths developed above the glacier PBL or along Nye channels, until these deeper systems also reverted to present conditions.

Table 8.1 Applicability of flow regimes to glacial conditions

Glacial Condition / FLOW REGIME	Cold based ice sheet	Warm based ice sheet	C	N IDL	W IDL	D IDL	Sub-marine	B IDL	E IDL	IM IDL	Inter-glacial
Subglacial lake		Yes									
Slope flow			Yes								
Nunatak flow				Yes							
Reverse flow								Yes			
Jökulhlaup flow					Yes			many	rare	Final event	
Ice contact spillway					Yes				Yes	Yes	
Englacial flow					above PBL				above PBL	above PBL	
lp-SGR flow					above PBL[1]			above PBL[1]	above PBL[1]	above PBL[1]	
Circulatory flow					below PBL[2]			?[2] at depth	below PBL[2]	below PBL[2]	
Meltwater SGW						above DML					
Brackish SGW						below DML					
Marine inundation			below DML				below ML				below ML
Interglacial											Yes
Occupation by ice	Yes			*	*	*	*	*	*	*	Partly

Key: lp-SGR Low pressure subglacial reservoir SGW Subglacial waterway
C Coastal western slope N Nunatak W Westward-flowing D Drained
B Backward-flowing E Eastward-flowing IM Ice margin PBL Plastic behaviour limit
DML Deglaciation marine limit ML Marine limit (i.e. glacial or deglacial)
[1]Narrow IDL, via inception fractures only. [2]Wide IDL only. * Winter only, at IDL or sea surface.

8.5 Phreatic cave development

In order to gain some understanding of the range of development histories of the study area caves, the three phases of dissolutional and erosional cave development (Dreybrodt, 1998, Fig. 2-10) need to be considered for each of the 13 liquid flow regimes derived in section 8.4, for the general case of combination caves that contain both relict and active passages (section 5.4.3). The three phases are: an inception–gestation phase, when laminar flow along inception fractures gradually leads to *"breakthrough"*, as described by the Palmer / Dreybrodt model (section 3.1.13); a phreatic enlargement phase, when, after breakthrough, a more rapid enlargement occurs along the whole conduit in turbulent conditions; and a vadose entrenchment phase.

The three phases may each apply to a variety of morphologies, dependent on the previous tectonic and karstic history, as appropriate. For the study area, these are: pre-breakthrough fractures; post-breakthrough fractures, conduits and phreatically-enlarged passages; and post-breakthrough vadose proto-passages and explorable vadose passages. In this context, the term post-breakthrough conduit refers to a phreatic route that is too small to explore.

Before considering each of the above relationships in the glaciated setting of central Scandinavia, further discussion of phreatic karst dissolutional processes is required. It is clear from section 8.4 that phreatic inundation by (at least) ice-dammed lakes and subglacial reservoirs during deglaciation applied to most karsts in the study area, even including those that lay below the deglaciation marine limit. Hence, IDLs, SGRs and possibly subglacial lakes are strong candidates for providing environments in which the first two cave development phases could take place. These environments may, perhaps, be called *nothephreatic*, after the discussion by Osborne (2001c). This section 8.5 therefore attempts to quantify theoretically the physics and chemistry of karst dissolution under glacial conditions for these phreatic development phases, so that the practical implications can be considered in section 8.6 and Appendix D4. Section 8.7 considers vadose development in interglacial conditions.

8.5.1 Calcite dissolution in glacial conditions

The physics and chemistry of the two phreatic cave development phases have been analysed to a considerable degree in the various papers that describe the Palmer / Dreybrodt model (sections 3.1.13–3.1.16). The breakthrough time from laminar to turbulent flow and the conduit enlargement rate thereafter are determined by many natural variables, of which calcite equilibrium solubility, dissolution rate and flow rate are particularly important. Without invoking the involvement of strong acids (for which there is no *universal* evidence for the study area), calcite equilibrium solubility is primarily governed by the initial concentration of CO_2 in the inflowing water, and, to a lesser degree, by the temperature. The calcite dissolution rate is dependent on the contemporary aperture size, the temperature and the hydraulic ratio (section 3.1.14) for laminar flow, or dependent on the flow rate and the length of the conduit for turbulent flow. More importantly, the post-breakthrough dissolution rate is governed by

the degree of saturation of the inflowing water, reaching a maximum rate for unsaturated water that contains *no* dissolved carbonate (Palmer, 1991, Eq. 6). The flow rate is determined by aperture size, conduit length (L), hydraulic gradient (HG: section 3.1.13), and also by the temperature, which controls the fluid viscosity. As noted in section 3.1.13, values of HG greater than unity arise if an additional head is provided by a submerging lake such as an ice-dammed lake, but these can be difficult to determine. Instead, flow rates and water speeds will commonly be estimated to determine the ranges of applicable hydraulic conditions after breakthrough. Prior to breakthrough, flow rates and velocities increase exponentially with time and the use of hydraulic ratio is unavoidable.

Before analysing each of the pre- and post-breakthrough flow regimes, there are two issues to address. Firstly, the published illustrations of the Palmer / Dreybrodt model commonly use rather high temperatures (10°C and above) and relatively high CO_2 partial pressures (1–5% atm.). That is, they rely heavily on organic CO_2 to make dissolution fast enough to achieve breakthroughs in several 10Ka for fractures longer than c. 100m that have low hydraulic gradients in closed phreatic conditions. However, in the phreatic conditions under a glacial submerging lake, there was no contemporary vegetation, and CO_2 levels were at normal atmospheric partial pressures of 0.034% *or lower*, which caused calcite equilibrium solubility under closed conditions to reduce to the range 10–11mgL^{-1}, even at 0°C (Palmer, 1991, Fig. 7). Because short breakthrough times are strongly dependent on high calcite equilibrium solubility (Dreybrodt, 1990, Fig.10), low temperature commonly *reduces* breakthrough time, whereas low P_{CO2} *increases* it (because the solution nears saturation earlier along the fracture, lengthening the time needed for the slower, higher-order, kinetics that act beyond the first-order *penetration length*). These low temperature and low P_{CO2} conditions, the competition between them, the density inversion below 4°C and the temperature inversion of calcite solubility below 0.1% P_{CO2} (Palmer, 1991, Fig. 7) have rarely been modelled for either breakthrough or enlargement (Palmer, pers. comm., 2002; Dreybrodt, pers. comm., 2002).

Secondly, the first published graphs of breakthrough times against hydraulic gradient and hydraulic ratio were restricted to the rather low hydraulic gradients and rather long fracture lengths that combine together to give breakthrough times in excess of 100a. Palmer (1991, Fig. 13) showed that double log plots of breakthrough time against hydraulic ratio for various settings of aperture, P_{CO2} and temperature are families of straight lines from about 100a to beyond 1Ma. Below 100 years, the straight line plots turn into steep curves (Dreybrodt, 1992, Fig. 5). Dreybrodt (1996) provided formulaé to show the "small-scale karstification" relationship between aperture width and hydraulic ratio at which breakthrough at hydraulic structures occurs within 100 years, using first- and higher-order kinetics. However, these were set at 10°C and 5% P_{CO2} and the 'competition' between low P_{CO2} and low temperature was not explored at these large hydraulic ratios.

The extent to which the above two issues are relevant is discussed in sections 8.5.2–8.5.5 and in the analysis of each flow regime in Appendix D4. The study area caves tend to be short, with a mean path length of well under 100m, and so may commonly be candidates for rapid breakthrough and subsequent rapid phreatic enlargement, despite low P_{CO2} in glacial and deglacial conditions.

8.5.2 Enlargement under phreatic conditions

Palmer (1981; 1984a; 1991: Eq. 6 and Fig. 12a and b; 2000b) derived graphs to show how the calcite dissolution rate (illustrated as wall retreat rate) varies with tube radius and length, flow rate, and hydraulic ratio, for laminar flow closed conditions with zero initial concentration. The rate always reaches a theoretical maximum value that is not directly dependent on the equilibrium saturation concentration (perhaps surprisingly) and is also independent of the other physical variables, providing that the tube radius, hydraulic ratio and flow rate are sufficiently large, or that the tube length is sufficiently short. This value is $31.56k/\rho$ cma^{-1}, where ρ is the density of limestone (c. $2.7gcm^{-3}$ for marble) and k is the lowest-order reaction coefficient, which varies with temperature and P_{CO2}. For a system at 10°C with P_{CO2}= 1%, k = c. $0.01mg\text{-}cmL^{-1}s^{-1}$, giving a maximum wall retreat rate of c. $1mma^{-1}$.

The maximum is reached when the solution remains considerably unsaturated at the exit point (commonly below a limiting saturation ratio of 60–70% that is determined by the temperature and P_{CO2}), and occurs if Q/rL or Q/bL exceeds $0.001cms^{-1}$ (where Qcm^3s^{-1} is the flow rate along a conduit of length L cm, r cm is the radius of a cylindrical tube and b cm is the breadth of a planar fissure with a narrow aperture of w cm). Hence, the maximum dissolution rate applies whenever Q>rL/1000 or $Q>bL/1000cm^3s^{-1}$. For the present study, it is more convenient to estimate the mean velocity through a conduit or fissure beneath a submerging lake than the flow rate, for which a knowledge of the applicable hydraulic gradient is required. Hence, noting that $Q=\pi r^2V$ for a cylindrical tube and Q = bwV for a planar fissure (where V cms^{-1} is the mean velocity), the maximum rate occurs when $1000\pi Vr>L$ cm or when 1000Vw>L cm. If the relationship is not true, slower, higher-order dissolution kinetics apply beyond the first-order penetration length until V increases sufficiently at the slowly enlarging exit for "breakthrough" (Dreybrodt, 1990) to occur to fast, first-order, kinetics, commonly accompanied by a transition to turbulent flow with the same maximum wall retreat rate. The dissolution rate is similarly reduced if the recharge contains enough dissolved calcite to cause the saturation ratio limit to be exceeded before the exit.

These conditions apply to many practical situations concerning post-breakthrough conduits, fissures and passages in the study area (where the recharge commonly contains little dissolved calcite). Figure 8.8 illustrates the minimum mean velocity, flow rate and hydraulic ratio required to maintain a maximum wall retreat rate for a tube of a specified radius or for a planar fissure of a specified aperture at various conduit lengths (calculated in centimetres) at 10°C with P_{CO2} = 1%, assuming zero initial dissolved load. The breadth (b) of a fissure is set to 100w cm, so that dissolution at its ends can be ignored.

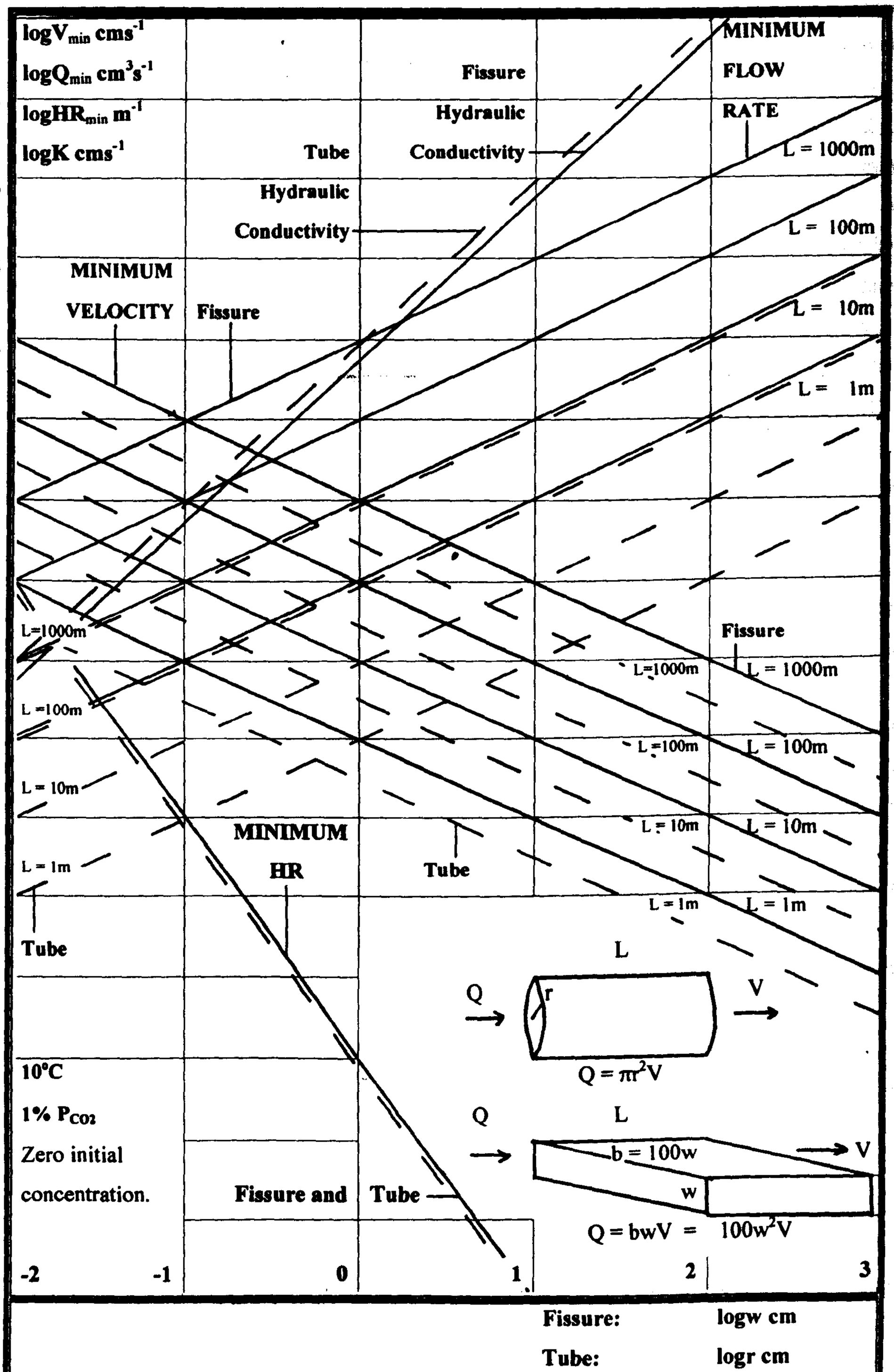

Figure 8.8 **Minimum flow velocities, flow rates and hydraulic ratios to achieve maximum wall retreat rates.** After Palmer (1991)

The velocity and flow rate graphs are plotted as $\log V_{min} = \log(L/1000\pi)-\log r = c. \log L-\log r-3.5$ and $\log V_{min} = \log(L/1000)-\log w = \log L-\log w-3$ and as $\log Q_{min} = \log(L/1000)+\log r = \log L+\log r-3$ and $\log Q_{min} = \log(L/1000)+\log b = \log L+\log(100w)-3 = \log L+\log w-1$. It is deduced from Palmer (1991, Fig. 12a and b) that for both tubes and fissures, $\log HR_{min} = -7-3\log(r \text{ or } w)\ cm^{-1} = -5-3\log(r \text{ or } w)\ m^{-1}$. Hydraulic conductivities for laminar flow are $K=r^2\rho g/8\mu\ cms^{-1}$ for a tube and $K=w^2\rho g/12\mu\ cms^{-1}$ for a fissure, where $g=981 cms^{-2}$ is the gravitational acceleration and $\mu=0.01307\ gm\ cm^{-1}s^{-1}$ at 10°C (Ford and Williams, 1989, p133) is the dynamic viscosity.

The graphs show that four extreme tube dimensions of (a) short (1m) and wide (r=1000cm); (b) long (1000m) and wide (r=1000cm); (c) short (1m) and narrow (r=0.01cm) and (d) long (1000m) and narrow (r=0.01cm) require mean flow velocities of $10^{-4.5}$, $10^{-1.5}$, $10^{0.5}$ and $10^{3.5} cms^{-1}$ to maintain maximum dissolution. The corresponding fissure velocities are 10^{-4}, 10^{-1}, 10^{1} and $10^{4} cms^{-1}$. These velocities also apply when breakthrough occurs at tubes or fractures enlarged to the indicated radii or widths, after a gestation period during which their exit apertures grew by up to three orders of magnitude (Dreybrodt, 1996, Fig. 9). Because there are no applicable thresholds in the calcite dissolution of tubes and fractures (section 3.1.14), if conduits are short enough, then 'breakthrough' from higher- to first-order dissolution occurs at very wide apertures, which, in the extreme, can continue to enlarge at maximum rates in almost static water (if unsaturated), but this probably does not apply within the study area (Appendix D4.1).

Faulkner (2004) considered the relationship between scallops and dissolution rate, concluding that any observable scallop in the wall of a phreatic passage commonly formed when flow was turbulent, the solution remained below the limiting saturation ratio and the limestone in the wall was dissolving at the maximum rate possible, as was limestone in many passages without scallops and in many conduits too small to be entered or even to be observed.

8.5.3 Enlargement at very low temperatures and CO_2 partial pressures

The above discussion mainly concerns dissolution which, in the context of the study area, is at high values of temperature and P_{CO2}. Values of the reaction coefficient, k, for natural limestones provided by Palmer (1991, Table 1) only go down to 5°C with $P_{CO2} = 0.3\%$. These values are plotted as a double log chart in Figure 8.9, and extrapolated to explore the k behaviour at 0°C, with P_{CO2} down to 0.003%. This extrapolation suggests that at 0°C and at normal atmospheric levels of P_{CO2} = c. 0.03%, k = 0.0035, whereas at $P_{CO2} = 0.003\%$, $k = 0.0030 mg\text{-}cmL^{-1}s^{-1}$. These values give maximum wall retreat rates of 0.35 and $0.30 mma^{-1}$, respectively, which could therefore be used as a basis for considering the phreatic enlargement rates of many passages in glacial waters without carbonic acid. They have not yet been verified theoretically or by experiment, although they are reasonable assumptions (Palmer, pers. comm, 2002). It is also assumed herein that the dimension and velocity relationships at 10°C with $P_{CO2} = 1\%$ plotted in Figure 8.8 apply at the glacial values, because the basic shapes of the wall retreat graphs are independent of k (Palmer, 1991).

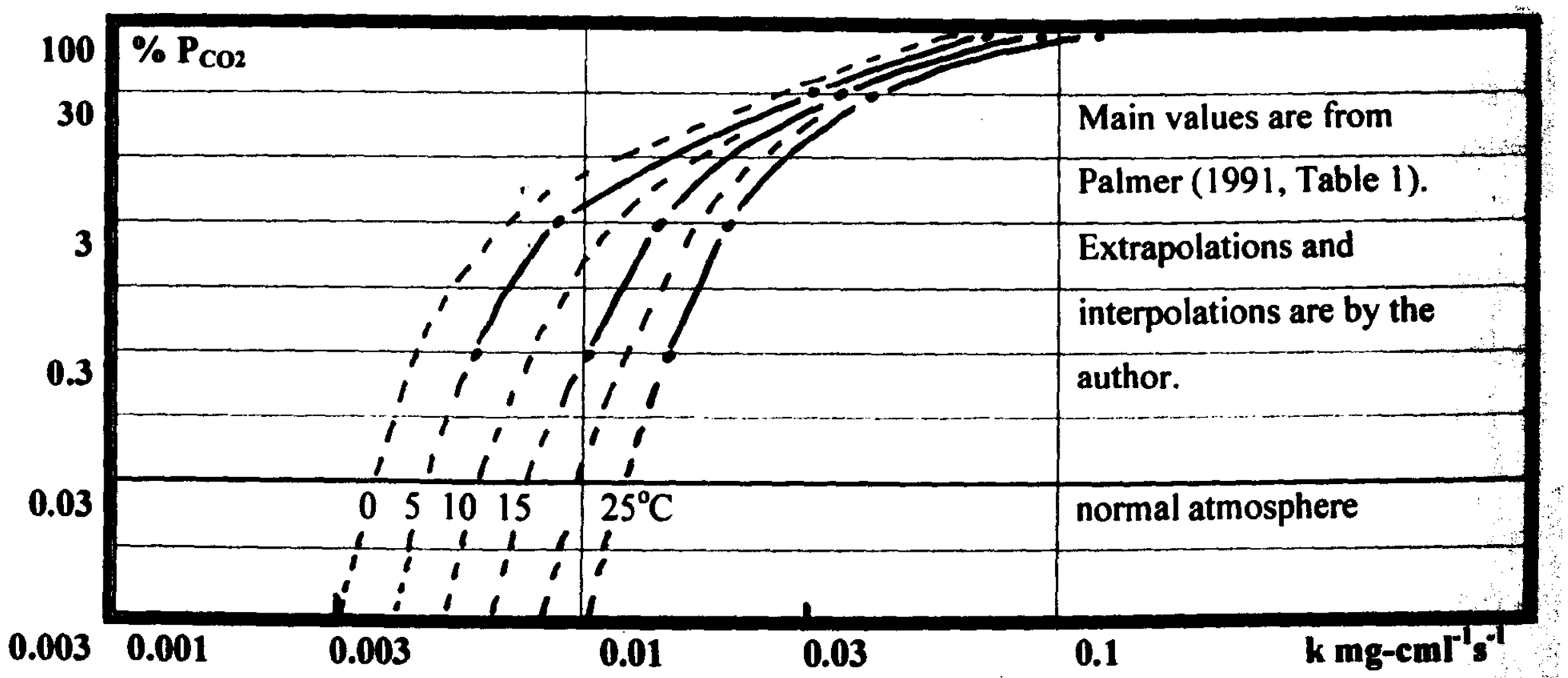

Figure 8.9 Variation of reaction coefficient (k) with temperature and P_{CO2}

The idea that calcite would continue to dissolve in aqueous solutions containing no CO_2 at a relatively high rate was proposed by Plummer, Wigley and Parkhurst (1978). Using synthetic calcite, they measured this rate as $2x10^{-7}$mmoles $cm^{-2}s^{-1}$ at 25°C (p190, Fig. 4; p196, Fig. 7) and $1x10^{-7}$mmoles $cm^{-2}s^{-1}$ at 5°C (p193, Fig. 5 and p196, Fig. 7). These roughly give wall retreat rates of 2 and 1mma^{-1}. (These relatively high values arise because synthetic calcite dissolves with higher reaction rates than natural limestones, which are 'poisoned' by foreign ions: section 3.1.15). For high flow rates and low CO_2 concentrations, the dissolution rate is only dependent on the term k_3 in the PWP equation. This is temperature dependent, but from the equation given by Plummer, Wigley and Parkhurst (1978, p199), it varies little between 5°C and 0°C, and thus the wall retreat rate for *pure calcite* in purely aqueous solutions with high throughput at 0°C can also be taken to be about 1mma^{-1}.

The maximum rates at which *natural* limestones dissolve in phreatic, turbulent, flow is difficult to determine theoretically, because the conditions vary from experiment to experiment. Sjöberg and Rickard (1984, Table 1) obtained dissolution rates for a rotating Carrara marble disc up to $4x10^{-7}$mmoles $cm^{-2}s^{-1}$ at 1°C, in an alkaline solution. A rotating disk laboratory experiment, requested by this author, showed that Jura limestone achieved an equivalent wall retreat rate of 6mm a^{-1} at 10°C and P_{CO2} = 0.1%, when the saturation was below 20% (Dreybrodt, pers. comm., 2002). However, a laminar boundary layer along the surface of the conduit may reduce the dissolution rate by orders of magnitude (e.g. Dreybrodt, 1988, p174). The boundary layer thickness reduces with flow rate, and with projections, which themselves increase the local speed of flow. Thus, the less pure marbles of much of the study area should allow passage enlargement rates to be higher than for other natural limestones, because flakes of mica schist (and other non-carbonate minerals) project into the flow and just float away downstream as the calcite dissolves, providing an extra erosional component to the wall retreat rate. Additionally, in very turbulent conditions, lumps of calcite are knocked from projections by suspended loads, to which they are temporarily added, whilst continuing to dissolve downstream in the unsaturated waters.

Another approach to consider is the practical measurement of present dissolution rates in Caledonide phreatic passages. Lauritzen (1986c) estimated rates in the partially closed phreatic **Glomvatn Underground Outlet** in northern Norway by three methods: the increase in hardness along the flowpath; micro-erosion meter measurements; and weight loss of marble tablets. The mean initial P_{CO2} was not stated, but was probably fairly high, because of local vegetation. The mean annual temperature was assumed to be 2°C (Lauritzen *et al.*, 1985). From the hardness increase, the dissolution rate varied from 10^{-8}–10^{-6}mmoles $cm^{-2}s^{-1}$ (equivalent to a wall retreat rate of 0.1–10mma^{-1}), as the flow rate varied from 1–10m^3s^{-1}, the maximum occurring during a flood in very turbulent conditions. (The flow velocity varied from 5–50cms^{-1}, with an annual mean of 12.5cms^{-1}: Appendix D4.4). Most measurements were in the range 1–7x10^{-7}mmoles $cm^{-2}s^{-1}$. The other two methods indicated rates at the lower end of the total range, but were thought to be under-estimates. Thus, a mean annual wall retreat rate of 1mma^{-1} appears to be a reasonable estimate for this passage.

A final method to estimate maximum wall retreat rates is to consider sump passages within the set of mainly vadose caves analysed in this thesis. Because it is argued in section 9.2.4 that these caves enlarged wholly within the known timescale of the Holocene, estimates of the diameters of the submerged passages in such caves should indicate the rates at which study area caves can enlarge during interglacial conditions. This method is used in Appendix D4.13, to show that Holocene sump wall retreat rates are commonly in the range 0.05–0.10mma^{-1}. Much of this enlargement may be concentrated during the roughly one month period of the annual spring melt (when the water temperature is also close to 0°C).

The above estimates of phreatic wall retreat rates from 0.05–1.0mma^{-1} are used in Appendix D4 to quantify enlargements that are possible during each glacial condition for post-breakthrough conduits. In most cases, it is assumed that the enlargement of a conduit does not affect the hydrology of its submerging lake. During the whole timescale from 11000–9000^{14}Ca BP, each radiocarbon year was equal to 1.4 cal. a on average, although the average varied from 0.5–2.0 cal. a over shorter intervals (Stuiver *et al.*, 1998, Figs. A7–A9), thereby providing more time for enlargement than is immediately apparent.

8.5.4 Previous analysis of short breakthrough times

Breakthrough times (section 3.1.14) can be represented by the product of geometrical, hydraulic and chemical (primarily dependence on P_{CO2}) factors (e.g. Dreybrodt, 1990). Figure 8.10 is a double log chart that shows the relationship between breakthrough time and hydraulic ratio for closed planar fissures at 10°C with initial P_{CO2} = 1% and zero input concentration with *initial* aperture widths (w_0) from 0.001–1.0cm. It is based on Palmer (1991, Fig. 13), which did not attempt to represent the parts of the aperture graphs that become non-linear below breakthrough times of about 100a. However, it is easy to deduce the hydraulic ratio values for each aperture width that give extremely short breakthrough times, because these are the same as the minimum HR values that give maximum wall retreat rates (Figure 8.8). It is assumed that these minimum breakthrough times approach the minimum HRs asymptotically at 10^{-3}a (c.

9 hours) for apertures with widths down to 0.001cm, as indicated on Figure 8.10 with interpolations between these limiting hydraulic ratio values and the linear parts of the graphs. The forms of these curves agree with those presented by Dreybrodt (1992, Fig. 5), who considered the risk of new flow routes developing around reservoir dams on karst (section 3.1.14). That work illustrated the behaviour of individual steep, short, fractures and showed that breakthrough times are reduced to below 100a if aperture sizes are increased sufficiently. Very short breakthrough times are hardly influenced by any variations in the value of the higher-order kinetic constant (Dreybrodt, 1992, Fig. 7), and short fractures that are less than four times the penetration length quickly achieve breakthrough to turbulent flow without utilising higher-order kinetics, as do fractures with unsaturated inflows at high hydraulic ratios (section 3.1.14).

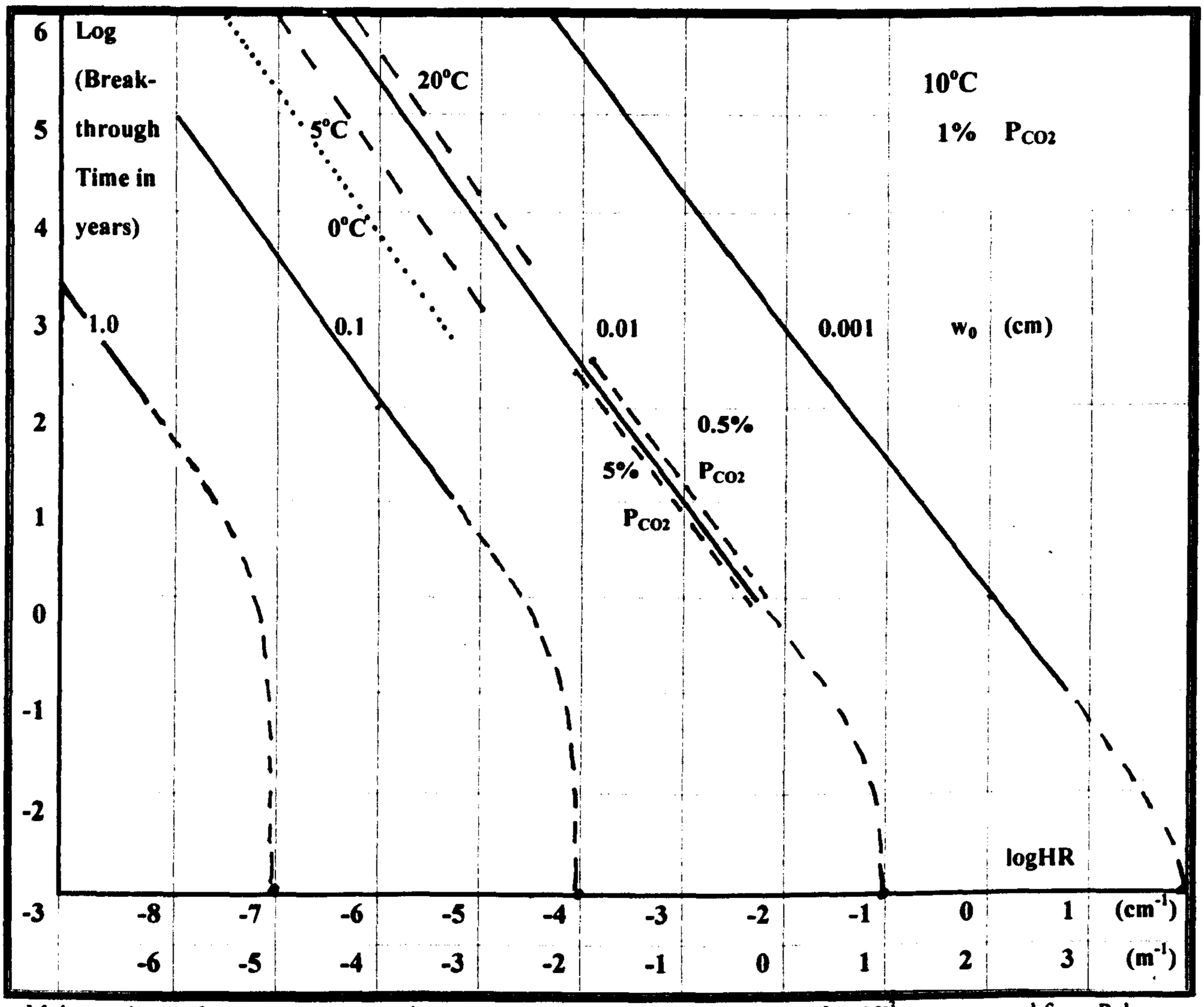

Main graphs are from Palmer (1991, Fig. 13). HR values giving breakthrough after 10^3a are assumed from Palmer (1991, Fig. 12b). Interpolations are by the author.

Figure 8.10 Breakthrough time and hydraulic ratio for planar fissures

Figure 8.10 also shows the reduction and increase in breakthrough time with reduced temperature and reduced P_{CO2} given by Palmer (1991, Fig. 13), with values that partly emulate glacial conditions. The breakthrough time is not greatly increased by reduced P_{CO2} because, as noted by Dreybrodt (pers. comm., 2002), CO_2 is rapidly consumed in pre-breakthough conditions, so that dissolution by water not

containing CO_2 is not very different from dissolution by water initially containing higher levels of CO_2. However, breakthrough times are significantly reduced at lower temperatures because first-order reaction rates are reduced and calcite equilibrium solubility is increased, both effects increasing the first-order peneatration length along the fracture. This author's extrapolation of breakthrough times at 0°C are shown with a dotted line in Figure 8.10. As breakthrough times reduce towards just one year, they appear to become much more *independent* of the calcite equilibrium solubility, although they still depend on aperture, hydraulic ratio and the first-order reaction rate (Dreybrodt, 1992, Fig. 5). This implies that at *very large* hydraulic ratios, breakthrough time becomes even more dependent on temperature than on P_{CO2}, confirming its reduction in glacial conditions. It is thus concluded that breakthrough is always faster in glacial environments if other conditions are unchanged, and the use of Figure 8.10 in Appendix D4 gives hydraulic ratios that are always higher than actually needed to achieve breakthroughs in the times indicated.

8.5.5 Breakthrough in Caledonide metacarbonates

It is clear from section 8.5.4 that there is now considerable knowledge about breakthrough times under a wide range of karstic situations, including those applicable to potential karst aquifers situated beneath dams and reservoirs with significant hydraulic heads. These studies provide analogues for describing some of the conditions beneath subglacial lakes, ice-dammed lakes and subglacial reservoirs. Section 3.1.15 noted that inhibition by aluminosilicates further reduces breakthrough time by introducing 11th order kinetics. This is particularly appropriate in the Caledonides, because of the abundance of mica schist both in adjacent country rocks and within the metalimestones. Another consideration is that some inception surfaces are along contacts between metalimestone and metadolostones or HMC (Appendix A2.7), thereby promoting inception by additional chemical reactions (section 3.1.5). Although mixing corrosion is unimportant for 'normal' breakthrough in unsaturated waters (section 3.1.14), it could possibly occur at the *exit* from a fracture into an IDL, where nearly-saturated water mixes with fresh water in the lake. This would also tend to provide even earlier breakthrough, with the breakthrough point being pushed backwards into the fracture, creating an exit cone with similarities to the entrance cone. All these factors further reduce breakthrough time in glacial settings (section 8.5.4) for the Caledonide marbles. Section 3.1.14 showed that short breakthrough times also cause more complex cave patterns to develop and it is therefore possible that the most complex and multi-tiered caves of the study area were formed by the synchronous enlargement of parallel passages that had reached breakthrough very quickly after suitable hydraulic ratios were achieved (e.g. **Etasjegrotta**, Z4; Figure B1.8).

Chapter 6 reviewed the evidence for the creation of tectonic inception fractures within the metacarbonates of the study area, primarily from tectonic processes associated with the deglaciation phase of each glacial cycle. It is proposed here that, in the general case, some interconnected sets of fractures within the marble were formed beneath active ice-dammed lakes (for example), so that large aperture sizes in combination with high hydraulic ratios enabled flow through them to be *immediately*

turbulent after melting, or after their seismic creation. Such fractures have HRs to the right of the appropriate asymptotic values in Fig. 8.10. Thus, these fracture sets achieved *'tectonic breakthrough'* without the need for first- and / or higher-order dissolution kinetics. Once created, they immediately embarked on the phreatic enlargement phase at the maximum dissolution rate and, given time and continuing recharge, grew into explorable cave passages.

At greater depths, and even within the more highly-fractured near-surface body of the metalimestone, there were other flooded fracture systems that, in combination with their local hydraulic ratio, were too small for *immediate* turbulent flow. The slow, higher-order, dissolution kinetics regime under laminar flow applied to these pre-breakthrough fractures, but some combinations of these fracture widths and hydraulic ratios were sufficiently large for breakthrough to occur within the time that they lay beneath an active submerging lake, as illustrated in Figure 8.10. Such fractures then started to enlarge at the maximum rate during the time that they remained in phreatic conditions. However, there were also other combinations of smaller fractures and hydraulic ratios that could never achieve breakthrough in the time available in each glacial cycle. These fractures enlarged slightly during each deglaciation and might have reached breakthrough after several glacial cycles (and perhaps after enlargement by more tectonic activity), or they might instead have been eroded from the landscape without becoming endokarstic.

The above argument is supported by the many reports of non-carbonate crystalline 'hard rocks' that act as significant near-surface aquifers at a local scale (section 3.1.18). They commonly achieve this capability from the tectonic creation of many interconnected short, planar, fractures. The tectonic processes involved are many and varied, both seismic and aseismic, and may include surface-erosion strain relief, regional horizontal strain arising from plate tectonic forces, and in high latitudes, isostatic uplift after deglaciation.

Table 8.2 summarises some flow parameters associated with fractured hard rock aquifers from the references discussed in section 3.1.18. From this table, the hydraulic conductivities of complete hard rock aquifers lie in the range $1–200x10^{-4}cms^{-1}$. The hard rock flow rates may arise from several fracture zones within the same borehole, but large proportions of these flows are probably accounted for by a few large exit fractures. The hydraulic conductivities of these individual fractures must be higher than that of the rock matrix by several orders of magnitude, giving fracture widths up to the centimetre scale. Because the flow rates lie commonly in the range $5x10^{0}–5x10^{3}cm^{3}s^{-1}$, they could represent lengths up to 100m or even 1000m that would be beyond the breakthrough point if in limestone (Figure 8.8). Such fracture lengths seem feasible, because a discharge rate of $5x10^{3}cm^{3}s^{-1}$ could arise from an annual infiltration of 1m at a catchment area measuring 400m x 400m, i.e. one with a similar length scale. There are no reports suggestive of dissolution in any of the aquifers listed, but as several are developed in silicate rocks, the possibility of some dissolution cannot be excluded. However, it is clear that tectonic fractures provide the primary flow routes.

Table 8.2: Flow parameters in fractured crystalline rocks

Site	Lithology (All non-carbonate)	Max. Hydraulic conductivity cms^{-1} $x10^{-4}$ *	Max. fracture aperture mm	Max. natural flow Ls^{-1}	Reference
Wells and boreholes					
Mirror Lake, NH, USA	Granite		0.7–20		Paillet *et al.* (1987)
Oracle, Arizona	Granite				Paillet *et al.* (1987)
NE Appalachians	Metamorphic	16.5			Randall *et al.*(1988)
Scandinavian shield	Metamorphic	1			Boulton *et al.* (1996)
Swedish Baltic coast	Metamorphic		Open fissures at 150m depth		Carlsten and Stråhle (2001)
Uganda	Granite, schist etc.	100			Howard *et al.*(1992)
S. Norway	Granite, gneiss etc.			5.5	Henriksen (1995)
S. Norway	Granite, gneiss etc.			0.4 (Mean)	Rohr-Torp (1994)
India	Granite	500			Maréchal *et al.* (2004)
World wide review	Precambrian shields			0.005–5 at 5m	Gustafson and Krasny (1994); Krasny (2002)
Norway and Sweden	Metamorphic	10			Banks *et al.*(1996)
Georgetown Island, Maine	Metamorphic			4.6	Mabee (1999)
Mirror Lake, NH	Schist	200			Shapiro (2001)
Pinardville, NH				18.9	Drew *et al.*(2001)
Mine laboratories					
Stripa iron-ore mine, Sweden	Quartz monzonite	$x10^{-5}$ at 340m depth		$x10^{-3}$ at -340m	Witherspoon *et al.* (1981); Dverstorp and Andersson (1989)
Fanay-Augeres uranium mine, France	Granite	320m depth			Long and Billaux (1987); Cacas *et al.* (1990a, 1990b)
Underground Hard Rock Laboratory, Äspö, Sweden	Metamorphic	10			Tsang *et al.* (1996) Gustafson and Krasny (1994)

* From transmissivity of whole 'aquifer' or borehole, measured over several metres at least

Because metalimestones are also capable of brittle fracture, and as they are subjected to the same tectonic events as the other crystalline 'hard rocks', it follows that they are also likely to carry similar fracture systems. Thus, after tectonic activity, marble aquifers should also exhibit similar hydraulic flow rates to those in other crystalline rocks, and some of these will be above the threshold needed for breakthrough conditions in various conduit geometries, as looks likely in the Texas limestones studied by Marrett *et al.* (1999; section 3.1.17), and as realised for the (sedimentary) epikarst by Klimchouk (2000a; section 3.1.8). This argument applies to interglacial conditions, when the ranges of hydraulic ratios in metacarbonate rocks should approximate to those in other crystalline rocks. Large hydraulic ratios also occurred potentially in some conditions during deglacial inundation beneath submerging lakes, so that many fractures in metalimestones could then also exhibit tectonic breakthrough and immediately enlarge at maximum possible rates.

8.6 Analysis of breakthrough and enlargement opportunities

The hypothesis presented in section 8.5 seems so convincing that to consider further the inception–gestation and the enlargement phases for submerged metalimestones, it is probably not necessary to understand completely the physics and chemistry of calcite dissolution under deglacial conditions. Figures 8.8 and 8.10 are therefore used in Appendix D4 to explore a) the extent that gestation along fractures in metalimestones below the various liquid flow regimes could reach the breakthrough point during the time available, and b) the enlargement of post-breakthrough fractures into explorable cave passages in the same conditions and timescales. Because ice-dammed lakes varied in depth up to c. 800m, breakthrough and enlargement occurred at fractures and conduits at most possible cave locations.

8.6.1 Conclusions on breakthrough conditions

The analysis of breakthrough opportunities in Appendix D4 is summarised in Table 8.3. This shows that in the central Scandinavian Caledonides, if breakthrough from laminar to turbulent conditions occurred under the effect of fourth-order dissolutional kinetics, the gestation phase could be completed for various combinations of initial fracture aperture widths and lengths in many differing deglacial flow regimes. In all these regimes, the fractures were submerged beneath ice-dammed lakes, commonly under depths of water much greater than the vertical range of the fracture system. Although a fracture system commonly experienced a restricted succession of flow regimes from the full set of possibilities as its IDL descended to its level (dependent on its glacial situation and cave location), each such regime provided an additive contribution to the gestation phase. Breakthrough could also be reached during interglacial conditions, not under submerging lakes, for various combinations of aperture widths, lengths and vertical ranges.

The standard Palmer / Dreybrodt model was used for glacial conditions, on the assumption that the effect of very low temperature in reducing breakthrough time dominates (especially at high hydraulic gradients) over the effect of very low CO_2 concentration, which tends to increase it. Breakthrough times may therefore be reduced by up to an order of magnitude from those indicated in Figure 8.10, dependent on the accuracy of this assumption. Other possible reductions in breakthrough times caused by uneven fractures or by the introduction of more aggressive water along an enlarging fracture from other, smaller, fractures (section 3.1.14) were not considered. On the other hand, no allowance was made for delays caused by deglacial winter freezing (which would, however, promote fracture widening).

From Table 8.3, there appears to be a very rough inverse relationship between the duration of a glacial flow regime and its flow velocity, providing competition among the hydraulic conditions favourable to breakthrough. It appears that, for cave systems of all lengths in central Scandinavia, all those with initial fracture aperture widths of 1cm or more could reach breakthrough to turbulent flow and dissolutional enlargement at maximum ambient rates within the duration of most flow regimes. Fractures with initial apertures of 0.1cm that are shorter than about 600m had time to reach breakthrough under englacial, low pressure SGR, meltwater subglacial waterway and interglacial flow regimes. Those fractures with smaller initial apertures were much more restricted in the combinations of aperture widths and lengths

(and vertical ranges for interglacial flow) that could reach breakthrough. During interglacial periods, the smaller the initial aperture size, then the closer must the fracture system lie to a valley wall (i.e. in cave locations S, R, and W) to have a hydraulic gradient sufficiently large for breakthrough to be reached in the time available. Because the deglacial and interglacial hydraulic conditions are so different, it is quite possible that fractures that achieved breakthrough during either regime could revert to pre-breakthrough conditions during the other succeeding regime.

Table 8.3 Cave development phases and flow regimes

FLOW REGIME	DURATION ^{14}Ca	FLOW VELOCITY &HEAD cms^{-1}, m	INCEPTION / GESTATION TO BREAKTHROUGH for various initial apertures and lengths	PHREATIC ENLARGEMENT PHASE: total widening and wall retreat rate (mm cal.a^{-1})	VADOSE ENTRENCHMENT PHASE
Subglacial lake	10000?	0.03 –	Not likely	Not likely	Not applicable
Slope flow	70	surface flow	No fractures	No caves	No caves
Nunatak flow	<200	~5?	Not likely	<0.2m 0.35mma^{-1}	Not applicable
Reverse flow	650	20max 0.1m	0.25cm: <250m 0.1cm: <100m	0.6–1.8m. 0.35–1mma^{-1}?	Not applicable
Jökulhlaup flow	hours	< $3x10^3$	Time too short	Contributes, by mechanical erosion	Not applicable
Ice contact spillway	inter-mittent	~20? 0.1m	Insignificant	Concurrent with other flow regimes	Not applicable
Englacial flow	400	~50–60 5–10m	0.1cm: <600m 0.01cm: <17m 0.001cm: <3m	1.1m. ~1.0mma^{-1}?	Not applicable
Lp-SGR flow	<200	? <200m	Special cases	Not applicable	Not applicable
Circulatory flow	<600	<<1–10?	3cm: <1000m 0.2cm: <100m	0.6m. ~0.35mma^{-1}?	Not applicable
Meltwater subglacial waterway	<300	100 10–100m	0.2cm: <1000m 0.01cm: <100m	0.8m. ~1.0mma^{-1}	Could apply at low stage, but of short duration.
Brackish subglacial waterway	<300	<100 to tidal	Less likely than in a meltwater subglacial waterway	0–0.2m. 0–1.0mma^{-1} Rate varied with salinity	Not applicable
Marine inundation	0 – 10000	tidal	Unlikely	Unlikely	(Entrance modification)
Interglacial	10000	0 – 100? Cave VR	0.1cm: 1km, VR=5m 0.01cm: 200mVR=40m 0.001cm:10m,VR=10m	Commonly 1–2m 0.05–0.1mma^{-1} during spring melt in active sumps only	1–5m floor-lowering. 2–12m w'fall recession
Occupation by ice	Perennial / semi-annual	N/A	Enlargement of inception fractures	Roof and wall collapse, and shattering at relict entrances	Roof and wall shattering at entrances

All inception fractures in the metalimestones were produced by processes that may be loosely considered to be tectonic (Chapter 6). Where such interconnected fractures had those combinations of large aperture sizes, short path lengths and / or large vertical ranges that immediately supported turbulent flow, the laminar, gestation, phase was bypassed: *tectonic breakthrough.* Hence, the possible conditions that facilitated breakthrough to turbulent flow and fast, first-order, kinetics were varied and complex. In order

to deduce which set of conditions applied to any one karst system (especially the minimum initial size of the inception fractures), it is necessary to consider all the evidence about the development of the system (including its internal connections and any intermediate entrances) during the evolution of its local landscape, and to consider the various glacial and tectonic processes to which both the landscape and the cave system were subjected. It is also normally necessary to work backwards in time. For example, although it may be possible for an earlier fracture system of a known mainly vadose cave to have just reached breakthrough within a Holocene timeframe, the gestation phase must have been completed earlier than this, to allow time for its subsequent enlargement into an explorable cave.

Despite all the detailed analyses of *chemical inception* possibilities in narrow fractures in Appendix D4, the argument presented in Appendix D4.13 to explain the enlargement of sumps in mainly vadose and combination caves strongly suggests that most explorable caves derive from fractures created from *tectonic inception*, because otherwise the time taken to achieve breakthrough by chemical inception would commonly prevent enlargement to the extent discussed. It is therefore assumed that early deglacial seismicity commonly created fractures with aperture widths a significant fraction of a centimetre, which allowed enlargement of long conduits at maximum rates, either immediately in relict and combination caves beneath active ice-dammed lakes, or subsequently in mainly vadose caves after the establishment of interglacial flow routes.

8.6.2 Conclusions on enlargement conditions

Appendix D4 shows that in both glacial and interglacial environments, most phreatic enlargement (also summarised in Table 8.3), *where and when* it occurs, takes place at rates that are *maximal* for the prevailing temperature and P_{CO2} conditions. This is because in all these situations calcite concentrations remained well below saturation levels, allowing dissolution at maximum rates, as proposed by Palmer (1991). It follows that the diameters of phreatic passages can commonly be used to represent the timescales of enlargement. However, these enlargements took place under successive flow regimes, with observable scallops probably representing the final high-stage flow velocity. From previous discussion, it appears that scallops in relict phreatic passages fall into at least three size groups, with lengths of 20, 8 and 4cm for backward and ice contact spillway, englacial and subglacial waterway flows. This idea has not been studied rigorously, and may need to be extended to a fourth grouping to include interglacial (e.g. Holocene) sump passages.

Appendix D4.13 shows that *all* the active sump passages in the study area could have grown to their present sizes during the Weichselian deglaciation (beneath active ice-dammed lakes) and during the succeeding Holocene interglacial (under present flow conditions). This includes caves in valley floor cave locations (e.g. the caves along the lower Jordbruelv, Z4). It could be surmised that such caves were also submerged beneath subglacial lakes, at glacial maxima. However, presently sumped passages in valley floor locations are not large enough to have been *significantly* enlarged under warm-based

icesheets. Similarly, from Table 5.27, although relict caves with CL=F do have the largest mean cross-section ($4.2m^2$), this is only 30% larger than the overall mean ($3.1m^2$), hardly larger than that for caves with CL=R ($4.0m^2$), and is caused by cave entrances with CL=F being preferentially enlarged by marine action (section 8.8). The reason for the unremarkable sizes of valley floor relict cave passages must be that either these passages did not exist (even as post-breakthrough conduits) prior to the Weichselian deglaciation, or that subglacial dissolution was insignificant, even over timescales of several millennia. The study area combination cave with the largest passage size, **Gåsvasstindhola** (Z4), has a maximum radius of c. 5m. For it to have grown to this dimension at the maximum $0.3mma^{-1}$ rate estimated for the temperature and P_{CO2} conditions of a LGM subglacial lake (section 8.5.3) would have taken c. 17ka in an unsaturated hydraulic regime, which is extremely unlikely (Appendix D4.1). Furthermore, from its altitude of 778m and its CL=R location, it is very unlikely to have been covered by a subglacial lake at all. Consequently, the evidence presented here, and argued on hydrochemical and other grounds in Appendix D4.1, that the phreatic passages in central Scandinavia did not enlarge beneath subglacial lakes, is overwhelming.

During deglaciation, enlargement beneath nunatak ice-dammed lakes at GS=U did not affect many caves, and could not be significant in the time available, because of a maximum wall retreat rate of only $0.35mma^{-1}$. However, enlargements beneath both active and drained IDLs, which may have had flow velocities from 10–$100cms^{-1}$ that were sustained for eight months per year, were *extremely* significant. With the addition of mechanical erosion, some wall retreat rates were probably in the range 0.5–$1.0mma^{-1}$, despite the continuing low P_{CO2} levels. Table 8.3 shows the likely maximum duration of each flow regime at any one cave, although the timescales and estimated enlargements shown cannot simply be summed. However, an absolute maximum passage widening can be estimated from the total time of submersion beneath an active IDL until the final draining of the cave, by assuming a wall retreat rate of $1mma^{-1}$ for the whole period. The caves along the lower Jordbruelv were submerged by an SGR from c. 10850 until c. 9450^{14}Ca BP (Figures D3.1–D3.9), an interval of c. 2200 cal. a (Stuiver *et al.*, 1998, Figs. A7–A9). Thus, they could have grown to diameters up to 4.4m during deglaciation. Hence, although this submersion interval is fairly exceptional, dissolution beneath IDLs explains the existence of most of the relict caves and relict passages in the study area.

The dimensions of all sumps in mainly vadose caves can be explained by dissolution during the time of the spring melt, entirely within the Holocene interglacial. This dissolution occurs at a maximum rate, but commonly only for one month per year, reducing wall retreat rates to 0.05–$0.15mma^{-1}$ (Appendix D4.13). Active sumps in combination caves with very large catchment areas may enlarge at rates $\leq 0.25mma^{-1}$.

A consequence for most of the active sumps in the area is that they have reached *minimum* sizes that are determined by roughly the same periods of enlargement (>10000 cal. a during the Holocene for mainly vadose caves, plus up to 2200 cal. a beneath active IDLs for combination caves) across a wide range of

geographical and altitudinal locations. Because the phreatic passages appear to have developed roughly-circular profiles from flow along the widest parts of the inception fractures, *there should be very few tight sumps!* Indeed few are known from the limited amount of diving, and the minimum diameters of most sumps appear to be 1m for mainly vadose caves, and 2m for combination caves, except where heights are reduced by sediment. However, because the XS/CA ratio of MV caves reduces at higher glacial situations (Table 5.28), sumps above the tree line may be somewhat smaller.

A similar consequence applies to relict (phreatic) passages in relict and combination caves. Most of these enlarged before the start of the Holocene, and were therefore submerged beneath IDLs for up to 2200 cal. a. From the above inference, the enlargement of sump passages during deglaciation was a minimum of 1m, and this should also apply to those passages that drained at the start of the Holocene. Thus, *there should also be very few tight relict phreatic passages!* This explains the general ease of exploration of the caves in the study area, which contain very few 'squeezes' in dry passages, except where there is sediment infill. Indeed, the mean cross-section of all the (phreatic) relict caves of $3.1m^2$ (giving a mean radius of c. 1.0m) is rather consistent across the whole study area.

The comparative rarity of tight sumps and small relict passages strongly confirms that nearly all cave passages enlarged from fractures that achieved (tectonic) breakthrough prior to their submersion below deglacial IDLs or at least prior to the start of the Holocene for MV caves. The low proportions of smaller sumps or passages are assumed to arise from the small number of fractures that only achieved breakthrough *within* the period of IDL inundation or within the Holocene. These conduits subsequently enlarged at the maximum annual rate, but for a shorter time. The cross-sectional areas of most phreatic passages should therefore form a statistical distribution that can be represented by a truly numerical mean. This distribution is not independent of scale, and hence the diameters and cross-sections of phreatic passages are *NOT* fractal quantities. Attributes based on length may also not be fractal, as mean lengths are quite consistent across the zones and various cave classes. This raises the possibility that mean explorable length may be related to mean diameter.

Table 5.28 does not appear to show that mean relict cave cross-sections increase at higher glacial situations. This null finding suggests that not many relict caves were in existence when IDLs formed during interstadial transitions, or else that such interstadial IDLs did not form or did not last very long. The enlargements of phreatic passages with diameters >c. 4m are discussed in section 8.6.3.

Although mainly vadose caves are well-scattered amongst caves of the other two hydrological classes in most zones (section 5.8.9), some valleys and areas seem to have high proportions of mainly vadose caves. These include Saeterfjell (Z2, near Bordvik), Reppen (Z2), Stordal (Z2, which has almost no caves), Hestfjell (Z2, near Svartvatn), Visten (Z3), Vargskar (Z5, east of Blåfjell), Herringbotn (Z6), Fiplingdal (Z7), Sløkskar (Z7, near Store Majavatn), Bleikvassli (ZA) and Övre Ältsvattnet (KU). These are all in

glacial situations above marine limits, except for two in the Western catchment area. The likely explanation is that caves in these valleys were submerged beneath IDLs that remained static for much of their existence (with few outlet possibilities) and / or their active IDLs were rather short-lived. In both cases, the potential to enlarge conduits phreatically was restricted, so that these caves primarily developed under vadose conditions in the Holocene.

8.6.3 Large passages and chambers

Significantly larger passages occur primarily in combination caves. There are none in mainly vadose caves. Section 8.6.2 concluded that relict caves, and relict passages in combination caves, commonly had sufficient time to enlarge to present dimensions whilst beneath ice-dammed lakes during the Weichselian deglaciation. Appendix D4.13 concludes that probably nearly all presently-active sump passages enlarged during deglaciation and the subsequent Holocene interglacial. This section considers the enlargement of large passages with diameters that are too great (i.e. more than c. 4m) to have reached this size during the passing of a submerging IDL, and yet appear to exist in geomorphological locations that preclude them from remaining submerged during the Holocene.

A study of cave surveys showed that some 15 caves have internal passages or chambers with cross-sections in the range 16–50m^2 (i.e., with 'equivalent-square' widths of 4–7m). Chambers near waterfalls and entrance chambers are excluded from this total, because they could be partly enlarged by increased dissolution, or by marine or ice-wedging activities. Commonly, passages with cross-sections of 16–20m^2 are presently relict, retain a predominantly phreatic profile, and their floors are not littered with collapsed angular blocks of limestone, although they may support various types of stream-borne sediments. Larger passages tend to have more rectangular or irregular profiles, and are, almost universally, littered with limestone that is presumed to have fallen from roofs and walls during unloading and deglacial earthquakes (section 6.3.3). Some of these passages also carry streams that may have weathered the collapsed blocks. In the combination caves **Røssågagrotta** (ZA), **Grønndalsgrotta** (ZA), **Östra Jordbäcksgrottan** (ZC) and **Landbrua** (KL), the streams are large or vigorous in summer, and appear to be contributing to passage enlargement across the whole width of the passage, in at least one part of the cave. In other cases, the streams appear to be sluggish misfits that may have had little influence on passage dimensions, as in: Elk Hall, **Sirijordgrotta** (Z4); Megachamber, **Geitklauvgrotta** (Z5); and **Kvannlihola** (Z7). The other large passages are presently relict: Square Chamber, **Bulandsdalgrotta** (Z2); Union Passage and Trunk Passage in **Toerfjellhola** (Z3); **Gåsvasstindhola** (Z4); **Sarvenvårtoehullet** (Z4); **Elgfjellhola** (Z4); and **Klofthølet** (ZC). Two relict caves also have fairly large cross-sections: **Saeterbekkgrotta** (Z5) and **Fossil Cave** (Z7).

There appear to be three main possibilities to explain the large size of the above caves. Firstly, those passages that carry large streams may, indeed, have enlarged under Holocene vadose chemical and mechanical erosion. Three of the four places mentioned above have passage heights that only rise to a

maximum of 5m. From forthcoming discussion in section 8.7, at least 4m of this could be accounted for by Holocene vadose erosion, with the remainder arising from phreatic dissolution beneath an IDL. The enlargement of the mainly phreatic **Røssågagrotta** was probably initiated under an IDL, and continued under phreatic and then deep vadose conditions in the Holocene.

Secondly, the present relict passages, or those with misfit streams, may have remained submerged and experienced phreatic dissolution during a significant part of the Holocene. This could occur if an allogenic stream input provided sufficient flow via a high-level outlet to retain phreatic conditions, whilst a lower-level outlet to the cave remained blocked (perhaps by till), or had not yet grown to a size that could drain the cave. A variant of this mechanism is that, as the bed of the lowest-level outlet channel would have been 3–4m higher at the start of the Holocene (from the evidence of Lauritzen, 1980, as discussed in section 8.7), it could have initially functioned as a small-scale Vauclusian rising, maintaining water levels up to 4m higher than at present, until erosion of its floor gradually caused the outlet passage to revert to vadose conditions. The present existence of several sumped resurgences illustrates this as a continuing mechanism. It may explain the enlargement of Square Chamber in **Bulandsdalgrotta**, which appears to have developed only during and after deglaciation. It also follows that the water levels in all sumps then existing were at least 3–4m higher immediately after deglaciation than they are now. This is a significant proportion of the mean vertical ranges of both mainly vadose caves (3.9m) and combination caves (14.5m) and shows that most caves that are MV at present started the Holocene as fractures and conduits in phreatic conditions.

The third possibility is that part of the enlargement of large passages occurred prior to the Weichselian deglaciation, i.e. beneath IDLs that existed during transitions between Weichselian stadials and interstadials, during the onset of the Weichselian glaciation, during the Saalian deglaciation and / or during long phreatic conditions in the Eemian, or an even earlier interglacial. These mechanisms seem much more likely than the possibility that relict phreatic passages in valley floor positions were enlarged subglacially (which was comprehensively rejected in section 8.6.2). The fact that some of the large passages were already enlarged before they became drained at the start of the Holocene is proved by the occurrence of unweathered slabs of limestone on their floors, which fell there when subjected to high-energy seismic shocks when the ice margin passed overhead during deglaciation. The presence of clay (presumably deposited in subglacial lake conditions) on fallen blocks shows that the containing passage existed during post-Saalian seismicity.

From the above arguments, it seems most likely that the oldest remaining passages in **Toerfjellhola, Gåsvasstindhola**, **Sarvenvårtoehullet, Elgfjellhola** and **Geitklauvgrotta** enlarged during the Saalian deglaciation and the Eemian interstadial, and the oldest remaining passages in **Sirijordgrotta, Gevirgrotta** and **Kvannlihola** date from at least the Holstein interglacial.

8.7 Vadose entrenchment

The inception / gestation and phreatic enlargement phases of cave development during interglacials were summarised in sections 8.6.1 and 8.6.2. The third phase, vadose entrenchment, could only take place during interglacial (and possibly interstadial) flow regimes. During the transition from the final episode of deglaciation to the disappearance of the ice, powerful vadose flows could also occur along meltwater subglacial waterways, but only for ≤420 cal. a (Appendix D4.10). However, the erosional effects of this regime may be indistinguishable from those of the ensuing interglacial meteoric water flow regime, which is also supplemented by powerful flows during spring melt, although parts of **Bulandsdalgrotta** (Z2) appear to have a 'double' vadose profile. Hydraulic gradients changed rapidly and dramatically after deglaciation, promoting inception / gestation and the growth of mainly vadose passages below the level of existing passages. Also, because of the common large extent of glacial valley lowering and widening, the hydrogeology at each cave location also changed significantly at each glacial cycle, again promoting cave development at new, lower, levels. Spring melts increase hydraulic gradients, so that flow can become temporarily phreatic in places, creating anastomoses and floodwater bypasses (section 3.1.16).

Vadose entrenchment is amenable to practical measurement (Appendix A2.6: Table A2.5). Cave surveys were studied by this author to measure the vertical extent of vadose entrenchment below any upper phreatic level in the study area caves, as reported below. These measurements were not taken near waterfalls or at other chambers along streamways unless stated otherwise, because corrosion by waterfalls is much more extensive than along stream passages (section 3.1.16).

8.7.1 Entrenchment in mainly vadose caves

Mainly vadose caves have been surveyed less completely than combination caves because of their 'more trivial' nature, and the difficulties of exploration in the predominantly wet conditions. Hence, few section surveys are available. Nevertheless, it is clear that their passage heights are commonly less than 2m, and rarely reach 3m (as they do in **Col Cave**, Z5), despite mainly vadose caves having slightly larger mean catchment areas (4.7km^2) than combination caves (4.6km^2). These heights are well within the 3–4m expected from the measurements of Lauritzen (1980, above), if erosion at current rates had persisted for 10ka, throughout the Holocene. The probable explanation for their rather limited vertical extent is that the first period of enlargement after breakthrough was phreatic, with a wall retreat rate of only c. 0.05–0.10mma^{-1} (Appendix D4.13), giving an *initial* height increase in the smaller range 0.1–0.2mma^{-1}. The deepest waterfall in a mainly vadose cave is probably only 5m deep (**Saeterfjellhullet**, Z2).

8.7.2 Entrenchment in combination caves

The largest known extent of vadose entrenchment in a combination cave occurs in **Klofthølet** (ZC), which has a vadose canyon up to 10m in height. The mean height of the lower streamway in **Ytterlihullet** (ZA) may exceed this, but its survey is not very precise. In **Øyfjellgrotta** (Z5), both the active streamway and the 'Upper Galleries' (which are presumed to contain relict vadose entrenchments

of phreatic passages, from the sketch provided by Lauritzen, 1983, Fig. 2.1) appear to have entrenched to total depths below their roofs of 7m. **Kvannlihola** (Z7) has a maximum entrenchment of 6m. There are 13 examples of caves where entrenchment reaches 5m. The remainder are less than this.

The explanation for deeper entrenchment along streamways in combination caves than expected from the Lauritzen (1980) measurements is probably that these passages existed in an initially phreatic form before the start of the Holocene, having enlarged towards 2m diameter beneath ice-dammed lakes (section 8.6.2). After draining and an immediate change to vadose conditions, the melt from remnant glaciers, which also sporadically ran through caves under meltwater subglacial waterways, maintained higher flow rates for more months per year than observed at present. Thus, the initial entrenchment rate was higher than that observed from current measurements. The **Klofthølet** canyon was observed by the author to carry a flow of about $2m^3s^{-1}$ during late July, 1997, from a catchment area of c. 10.2 km^2. Thus, this may be an example of caves that sustain high flow rates for longer periods of time than is normal.

The 7m total depth of the relict Upper Galleries in **Øyfjellgrotta** is suggestive that the maximum extent of vadose entrenchment in the Eemian interglacial could have been comparable to that already achieved in the Holocene, and that the present active streamway did not exist before the Weichselian deglaciation (or else its height could have reached c. 14m). Direct study and an accurate cave survey section are required to confirm these conclusions. In **Ytterlihullet**, both the abandoned inlet passage of probable Eemian age and the (Holocene age) upper stream passage have entrenchments of c. 4m. These two passages meet at 'The Duck', so that the greater vertical extent of the lower streamway is likely the result of vadose flows during both the Eemian and the Holocene, coupled with paragenetic enlargement during the Weichselian deglaciation. Relict vadose passages in other caves rarely reach heights of 5m. They are commonly early Holocene streamways that were later bypassed by lower-level post-breakthrough conduits. An upper-level relict vadose passage in **Grønndalsgrotta** (ZA; Figure B1.15), 5m in height, may represent an Eemian flow route.

The deepest internal waterfalls are 15m (near the end of **Ytterlihullet**), 12m (**Tumbledown Pot**, Z7 and **Sotsbäcksgrottan**, KU), 10m (**Övre Bjurälvsgrottan**, KL) and 9m (**Øyfjellgrotta**). Because of the greater corrosion at waterfalls (section 3.1.16), all except the first are comparable with the maximum entrenchment in vadose passages observed above, and probably formed mostly in the Holocene. The 15m waterfall in **Ytterlihullet** probably started its development in the Eemian, as suggested above.

8.7.3 Headward erosion of waterfalls

Another method to confirm that nearly all active stream passages developed primarily during the Holocene is to measure the amount of headward erosion at waterfalls. According to White (1990, p170), these move upstream at a maximum rate of c. $1.2mma^{-1}$, because the face of the waterfall remains covered by a thin film of aggressive water. This condition may apply throughout most of the year in the

study area streamways away from entrance areas (which freeze in winter). Hence, waterfalls that were active for all 10ka of the Holocene have potentially eroded backwards for distances up to 12m. Such headward recession was measured from cave surveys and survey sections where possible, by comparing the roof and floor profiles for cases where it is clear that the waterfall erosion is not impeded by an insoluble barrier. The results showed that headward erosion in combination caves has commonly occurred over distances from 2–10m, with, exceptionally, larger recessions. Thus, part of the lower streamway in **Sirijordgrotta** (Z4) displays headward erosion of 10m, as do streamways in **Elgfjellhola** (Z4) and **Sotsbäcksgrottan** (KU), and waterfalls in **Roaring Cave** (Z5) and **Storskogbekkhullet** (ZA). **Tourist Cave** (Z2) shows 11m; **Hornet Pot** (Z2) and, possibly, steep cascades in **Gevirgrotta** (Z4) show 12m; **Ytterlihullet** (ZA) shows 14m in several places; and **Toerfjellhola** (Z3) possibly shows 15m of headward erosion in one place, with a definite minimum of 5m. It was not possible to estimate headward erosion in mainly vadose caves.

Waterfalls that display significantly <10m recession probably indicate that their passages only achieved vadose conditions some time after the start of the Holocene. Those that have receded significantly >10m may indicate that some of the vadose erosion occurred prior to the Holocene, during an interglacial whose imprint was not removed by paragenetic dissolution beneath a subsequent IDL. This provides supporting evidence that **Ytterlihullet**, for example, was active during the Eemian. **Green Valley Cave** (Z4) and **Gevirgrotta** (Z4) display headward erosions of 8m and 3m at dry waterfalls in *relict* vadose passages. In neither of these cases is it clear whether the waterfalls were active in an earlier interglacial, or were abandoned during the Holocene. Caves at high altitudes and near the coast reverted to vadose conditions early in the deglaciation sequence. Thus, the periods of both vadose floor-lowering and waterfall recession reduced eastwards across the region by as much as 2000^{14}Ca.

8.7.4 Vadose entrenchment during previous interglacials

The rarities of relict vadose passages and of paragenesis above vadose passage elements are noted in Appendices B2.7 and B2.8. These may arise because recharge was less powerful in earlier interglacials. The Eemian and Holsteinian were warmer than the Holocene, with no remnant glaciers and higher levels of forestation (section 2.3.2 and Figure 2.4). Thus, reduced winter precipitation and increased evapotranspiration commonly reduced summer flow rates and durations. Additionally, the stable conditions and relatively high temperatures appear to have lasted for less time during the three previous interglacials. Prior to the Mid Brunhes Event at 430ka, Antarctic interglacials were cooler than during the Holocene (section 2.3.2). If this also applied to the northern hemisphere, periods of summer fluvial activity would be reduced, also reducing vadose development. Thus, the Holocene could represent the optimum conditions for interglacial vadose development during all the 100ka glacial cycles since the Mid Pleistocene Revolution. These factors, coupled with the production of lower fracture densities at the ends of each earlier glacial (section 7.3), mean that the development of vadose passages probably becomes less and less important backwards in time throughout the history of the caves in the study area.

8.8 Formation and modification of caves under marine influence

The deglaciation and other marine limits were discussed in sections 8.1.2 and 8.1.3. This section considers the relationship between the sea and the formation and modification of caves in both carbonate and non-carbonate rocks. The order in which some relevant karst caves in glacial situations GS=C, D, E, G or H were submerged by the sea during the Weichselian deglaciation is presented in Table 8.4, together with estimates of emergence timescales from the sea level curves in Figure 8.1b.

8.8.1 Formation of sea caves and littoral caves in limestone

A few karst caves lie along the coastal strandflat, commonly at altitudes below c. 25m. These are identified as 'coastal caves' in the North Central Norway Cave Database (with CL=C and GS=C). Many of these short caves show little karstic dissolution, but appear to be littoral caves formed by previous wave action with no continuing passage. They include three of the four relict **Brønnøysund Football Pitch Caves** (Z1), **Vistnesoddgrotta** (Z2) and possibly **Tarmaunbotngrottene** (Z2). Their low elevations mean that they were under >100m of sea water at the start of the Holocene; hence, they were not much affected by wedging by YD sea ice. Instead, they were exposed near sea level for ≥1000a during a late phase of the Holocene isostatic rebound. The above-mentioned caves face NE or NW, suggesting that their formation was facilitated by the presence of late Holocene winter sea ice. At least two caves at CL=C appear to be karst caves modified by marine action: **Brønnøysund Football Pitch Cave B** (CT=Hybrid) shows clear signs of the surface erosion of a phreatic tubular passage and **Langfjordgrotta** (Z2) is a resurgence cave partly explored by diving that has a relatively large entrance. (Cave types are only classified as Hybrid if an enlarged entrance is a significant feature of the whole cave).These caves were presumably already enlarged phreatically as part of subglacial waterways during the Weichselian deglaciation (e.g. Appendix D4.10). The probable lack of limestone dissolution by sea water is discussed in Appendix D4.12.

The previous presence of the sea at both coastal and marine-influenced karst caves is sporadically demonstrated by the occurrence of holes bored by marine molluscs in the walls and ceilings of entrance areas (Photo D4.2), although this phenomenon has not been checked exhaustively at relevant caves. More rarely, marine deposits are also found inside caves (Appendix D5.3).

8.8.2 Enlargement of cave entrances that are below the deglaciation marine limit

Caves in the North Central Norway Cave Database with GS=D and E lie below the deglaciation marine limit and above the strandflat. They were inundated by the sea at the end of the Younger Dryas, before being raised to their present altitudes of 30–167m by isostatic uplift. Many exhibit wide, relatively low, sub-horizontal, tapering, rocky entrances that seem disproportionately large when compared with the dimensions of internal passages (Table 8.4). This group of caves includes: **Hubruhola, Green Gorge Cave** and **Marble Arch** (both at Klausmark), **Klausmarkgrotta, Klausmark Resurgence Cave, Aunholet, Skånvikgrotta, Tourist Cave, Svartdalgrotta** (lower entrance), **Evening Cave** (H5) and **Hate Cave** (H8) (both at Hestfjell), **Laveste Langskjellighattengrotta, Jenshola, Mølnvatngrotta**

(Forest Entrance), several caves at the **Arch Cave** complex, **Aunhattenhule 1–3, Nedre Landegrotta and Kalkdalgrotta** (all in Z2); **Risehula 1 and 2** (Z3); **Møllebekkgrotta 1 and 2** (Z5); **Gårdsfjellgrotta** (Z6); plus **Remnant Cave** and, possibly, **Fjellbrygga** (ZA). Beyond the entrance areas, most of these caves contain obviously dissolutional karstic passages. Many function, or have functioned, as resurgences. The near-equivalence of the altitude of the phreatically-formed stream passage in **Svartdalgrotta** (Z2) with the deglaciation marine limit is probably coincidental.

Only relict and combination caves appear to have entrances enlarged by marine action, although some similar caves that are below the deglaciation marine limit do *not* have significantly enlarged entrances, including **Neptune's Cave, Barnacle Cave** and **Draugenshullet** (Z2). The reason may be that the entrances are shafts or they were in protected locations or they did not form until after elevation above the sea. Attached barnacles in these three caves (section 9.6.4) prove that at least *their* internal passages existed prior to emergence. The direct evidence of entrance enlargement from individual caves agrees with the greater mean cross-sections of caves with relict phreatic passages if they lie below the deglaciation marine limit (section 5.5.6) and shows that such caves were already in existence before marine inundation at the start of the Holocene, as do non-laminated deposits of coarse dry sand reported only below the deglacial marine limit in Z2, in the relict phreatic passages of **Aunhattenhullet 2** (GS=D) and of **Søvikgrotta, Nordlysgrotta, Marimyntgrotta** and **Neptune's Cave** (GS=E), suggesting marine ingress into cave entrances that mainly face east, when they coincided with beach levels.

Marine cave entrances at altitudes above 80m experienced a very rapid elevation through sea level in the Preboreal, so that they typically rose 10m in only c. 100a (Figure 8.1b). Lower entrances rose above sea level later, and rose more slowly during emergence. In contrast to the lower littoral caves discussed in section 8.8.1, the only definite littoral cave recorded in limestone above the strandflat is the single chamber **Bordvikgrotta** (Z2), at an altitude of 40m. Several features at the **Arch Cave** complex (Z2), at the relatively low altitude of 60m, may also be littoral caves. It thus appears that, at altitudes higher than 40–60m, the uplift was so fast that there was insufficient time for the sea and ice to form new, presently inland, littoral caves in limestone before they were elevated above wave height.

The extent of the enlargement of pre-existing entrances has a weak relationship with altitude and the duration of submersion. Thus, five entrances to relict and combination caves not obviously enlarged were submerged for a maximum of c. 150 years (although others are exceptions) and enlarged entrances were commonly submerged for many hundreds or thousands of years. Thus, it seems that pre-existing cave entrances were more likely to be enlarged by wave action supplemented by wedging by winter sea ice if they passed *slowly* through the tidal range after long submersion, probably contemporaneously with the production of elevated marine terraces (e.g. Andersen *et al.*, 1982, p44). Large sea caves also formed in non-carbonate rocks above the strandflat (e.g. Sjöberg, 1988). **Marmorhølet** (Z9), in predominantly non-carbonate rocks (despite its internal calcite deposits), is probably a short sea cave created during deglaciation.

Table 8.4 Marine inundation of metacarbonate caves during the Weichselian deglaciation

Time of inun. ^{14}Ca BP	Z.	GS	Local YD iso-base m	Cave(s)	Alt. m	Time of final emer-gence ^{14}Ca BP	Appr. time sub-merged ^{14}Ca	Ent. faces	Notes 1. MV: mainly vadose cave 2. Enlarged entrances (RE if not stated) are suggestive of wave action 3. Sea / littoral caves are commonly non-dissolutional
12000	Z9	E	90	Marmorhølet	113	11500	500	N	Sea cave, formed in non-carbonate
10700	Z2	E	100	Søvikgrotta	64	9000	1700	SW	Slightly enlarged relict entrance. Sand.
10700	Z1	C	110	Football pitch caves	25	4800	5900	NE	1 of 4 is a dissolutional hybrid
10700	Z2	C	110	Vistnesoddgrotta	10	2000	8700	NE	Short littoral cave
10700	Z2	H/E	130	Klausmark caves	120–160	10000	0–700	S,E,E,S	4 enlarged entrances, one at 160m
10300	Z2	E	120	Hubruhola	119	10000	300	N	Enlarged entrance
10300	Z2	E	120	Langkilagrotta	40	6800	3500		
10300	Z2	D	135	Aunholet	60	8300	2000	N	Enlarged entrance
10300	Z2	E	140	Holåsen caves HO1–5	110–135	10000	300	(shafts)	Not enlarged: all MV
10300	Z2	E	140	Bordvikgrotta	40	6500	3800	NW	Single chamber littoral cave
10300	Z2	E	140	Nordlysgrotta	155	10200	100	NE	Sand banks below entrance pitch
10300	Z2	E	140	Marimyntgrotta	155	10200	100	SW	Relict entrance. Sand
10300	Z2	E	140	Skånvikgrotta	77	9000	1300	S	Enlarged entrance
10210	Z2	E	145	Tourist Cave	150	10010	200	N	Enlarged sink entrance
10210	Z2	H/E	145	Svartdalgrotta	180–127	9700	510	NE	Enlarged lower entrance only
10210	Z2	E	145	Neptune's Cave	126	9260	950	E+shafts	Not enlarged. Barnacles. Sand
10210	Z2	E	145	Barnacle Cave	142	9900	310	N	Not enlarged. Barnacles
10210	Z2	E	145	Draugenshullet	137	9600	610	N	Not enlarged. Barnacles
10210	Z2	E	145	Hestfjell H1–4, H6	90–115	9500	710	NW	Not enlarged: all MV
10210	Z2	E	145	Hestfjell caves H5,H8	110, 135	9700	510	NW	Enlarged sink entrances.
10100	Z2	C	155	Tarmaunbotngr. 1–3	5–20	1000	9100	NW	Tectonic and littoral caves
10100	Z2	D	155	L. Langskjellighattengr.	167	10000	100	W	Entrances possibly enlarged
10100	Z2	C	155	Langfjordgrotta	10	1500	8600	NW	Coastal karst sumped resurgence cave
10100	Z2	D	160	Jenshola	145	9800	300	NW	Entrance possibly enlarged. Not MV?
10050	Z3	C	140	Trondjordhula	5	1000	9050	S	Coastal resurgence cave. MV
10050	Z3	D	140	Risehula 1 and 2	50, 53	7800	2250	S	Enlarged relict entrances.
10050	Z2	E	155	Arch Caves R6–R16	60–70	7500	2550	vary	Enlarged ents., except 3 MV caves
10050	Z2	E	155	Mølnvatngrotta	140	9800	250	SW	Enlarged relict Forest Entrance
10050	Z2	C/E	155	5 caves at Saus	21–63	4000	6050		3 are MV. Not enlarged
10050	Z2	D	160	Aunhattenhule 1–4	105–135	9500	550	NW	Enlarged relict ents. to A1–A3. Sand
9900	Z6	E	140	Sildgarngrotta	120	9800	100		
9900	Z6	E	140	Splintågrotta	135	9900	0	E	Not enlarged resurgence entrance
9900	Z6	D	140	Kumragrotta	62	8500	1400		Truncation of entrances
9900	Z2	E	170	Svartdalsholet	160	9850	50	NW+SE	Sea just reached this cave. Not enlarged?
9900	Z2	E	170	Ø. & N. Landegrotta	80, 95	8600	1300	S	Enlarged entrance to lower cave
9800	Z5	H	140	Bollhauggrotta	150	10100	-300	W	Enlarged sink entrance, *but GS=H*
9800	Z6	D	140	Hestdalgrotta	100	9500	300		
9800	Z6	D	140	Through Cave	100	9500	300		
9800	Z2	D	170	Kalkdalgrotta	50	7000	2800	NE	Slightly enlarged relict entrance
9600	Z6	D	140	Gjeitvikgrotta	70	8900	700	W	Not enlarged
9600	Z6	E	140	Berntvikgrotta	40	7200	2400		
9550	Z6	E	140	Høgligrotta	100	9400	150	S	Not enlarged
9500	Z6	E	150	Gårdsfjellgrotta	56	7800	1700	E	Enlarged relict entrance
9300	Z4	H	150	Øyåskjeleren *et al.*	100	9500	-200	NW	Enlarged main relict entrance (*GS=H)*
9300	Z5	H	150	Øyfjellgrotta	180–140	9900	-600	SE	Enlarged lower relict ent. (*GS=H).* Sand
9300	Z5	E	170	N. Laksfors Rising	55	7200	2100	E	Not enlarged sump entrance (=MV)
9300	Z5	E	170	Møllebekkgrotta 1–3	90–79	8600	700	NW,W	Enlarged entrances at M1 and M2
9300	Z5	H	170	Geitklauvgrotta	148	9800	-500	S	Unroofed cave outside, *but GS=H*
9300	Z5	H	170	Lilleelvgrotta	150	9800	-500	N	Enlarged entrance, *but GS=H*
9300	ZA	E	170	Remnant Cave	93	9000	300	E	Cave wall removed
9300	ZA	D	170	Fjellbrygga	110	9300	0	NW	Sea just reached huge 20m long arch
9300	Z6	E	180	Farewell Cave	130	9300	0		Sea just reached cave

The orientations of the enlarged entrances are widely distributed, but the higher percentage (48%) facing NW, N or NE (and hence experiencing more sea ice) compared to 28% facing SW, S or SE may be significant. Some occur in narrow tributary valleys, where ice wedging was especially effective. The majority of these enlarged entrances face the open sea to the west, and the percentage on western slopes (GS=D rather than E) is 33%, which is much greater than the 20% of all relict and combination caves that have GS=D rather than E. Overall, the preferred orientation for the deglacial marine enlargement of pre-existing cave entrances is northwest.

No cave that is clearly mainly vadose appears to have an enlarged entrance (Table 1: the status of **Jenshola**, Z2, is uncertain on both counts). Thus, it is likely that MV caves that lie below the deglaciation marine limit with GS=D and E (and, by extension, those above it) did not exist in their present form at the time of their elevation above sea level (see also sections 9.2.4 and 9.6.5). This observation is partly supported by the absence of reports of sand deposits in such caves. It is concluded that the 'mainly vadose' caves primarily developed within the Holocene.

8.8.3. Enlargement of cave entrances that are above the deglaciation marine limit

Table 8.4 lists five caves that are anomalous in a deglaciation context. From their locations, YD isobases and the time of passing of the ice margin, it appears that the entrances to **Bollhauggrotta** (Z5), **Øyåskjeleren** (Z4; Photo 8.2), **Øyfjellgrotta** (plus Side Chamber and Torrgrotta,), **Lilleelvgrotta** and **Geitklauvgrotta** (Z5) were already too high to be reached by the sea when they were deglaciated. The first four caves have entrances that appear enlarged by marine action, to the same criteria. The entrance to **Geitklauvgrotta** (which is upstream to **Lilleelvgrotta**) is not at all enlarged internally, being a phreatic passage some 1m high by 2m wide. However, there appears to be an unroofed section of cave between this entrance and the end of the upstream **Øvre Geitklauvgrotta** (Photo 7.4). The thin roof may have been removed by glacial movement or by the action of the sea and sea ice, or by a combination. If marine action has modified these caves, and it is difficult to envisage any other agency to account for the enlarged entrances to **Øyåskjeleren** and **Øyfjellgrotta**, then it seems very likely that this occurred when the marine limit was higher than the last deglaciation marine limit. This leads to the possibility that these cave entrances were enlarged during the onset of one or more *glaciation* phases or during a Mid Weichselian interstadial, and were well-enough protected during subsequent glaciation for the enlarged parts of the entrances to have survived. The five cave entrance floors are at altitudes from 100–150m at YD isobases from 140–170m and are well below a possible maximum Weichselian marine limit discussed in section 8.1.3. In contrast to the enlarged entrances below the deglaciation marine limit, all five above the limit are in the eastern glacial situation (GS=H) rather than in the western (GS=G), although the **Bollhauggrotta** and **Øyåskjeleren** entrances *face* west. This may not be significant with a small sample, because 74% of the applicable relict and combination caves are at GS=H rather than G.

There are no other apparently marine-enlarged cave entrance floors above 167m altitude, so that this absence of similarly-styled entrances above the maximum Weichselian marine limit provides supporting evidence for entrance enlargement of phreatic passages below marine limits by sea ice and wave action, although section 8.9.4 discusses entrances that were slightly enlarged by the presence of ice-dammed lakes. Because there is no reported evidence of the etching of entrance walls by condensation corrosion, as discussed in section 3.1.9, and that slow process could only have been active during interglacials, it is concluded that that mechanism could not play a significant role in passage enlargement.

Photo 8.2 Upper cliff entrance to Øyåskjeleren (Z4)
At an altitude of 100m, this entrance was likely enlarged by wave and ice action at a time of *rising* sea level

Cave entrances modified during the *onset* of glaciation were enlarged at a time of *rising* sea level, in contrast to those enlarged during the *falling* sea level of a deglaciation phase. When a sea level that is *falling* encounters a cave entrance, that part of the entrance that remains submerged is protected. Hence, the vertical scale of enlargement is related to the tidal range and wave height: ~5–10m (Figure 8.11a). In fact, the entrances enlarged during deglaciation listed in Table 8.4 are rarely >5m high (although they may extend to a width of 10–20m). However, when a *rising* sea level encounters a cave entrance, a vulnerable roof may remain under attack from the time that the wave height reaches it, until the time when the sea either freezes at its maximum level, or starts to fall relative to the land at a glaciation marine limit (Figure 8.11b). Although the roof collapse rate may be overtaken by the rising sea level and the local isostatic depression rate (possibly $0.5ma^{-1}$ at the onset of glaciation at the coast, section 8.1.1: Figure 8.1b), there is clearly potential for cave entrances to be enlarged vertically by marine action much more during a *glaciation* phase than during a *deglaciation* phase. Caves at GS=H are commonly longer, deeper, and more voluminous than other caves (section 5.5.6: Table 5.28). One reason may be that their inception fractures were enlarged by winter freezing as the rising sea level passed through their elevation at the end of the Eemian and during Weichselian interstadials.

The only karst cave in the whole study area that has an entrance taller than that of the exceptionally tall inland **Grønndalsgrotta** (ZA, 16m) is **Øyfjellgrotta**, whose lower (main) entrance is up to 30m high and c. 15m wide (Figure B1.10). This evidence supports the upward stoping of cave entrances by marine and winter ice activity as a mechanism for entrance enlargement during a *glaciation* phase. The marine invasion of **Øyfjellgrotta** is also supported by a statement by Smart (1984b, p173): "*exotic boulders of*

(up to 6m) *size have been carried in and effectively blocked the system*", and by his mention of sand-sized sediments. Sand deposits in **Sirijordgrotta** (Z4; Valen *et al.*, 1997; entrances not enlarged and not listed in Table 1) and **Øyfjellgrotta**, both at GS=H (eastern slopes below the glaciation marine limit), may have been brought in by the sea at the onset of glaciation, although fluvial or glacio-fluvial deposition remain as possibilities. Above the marine limits, only **Cliff Cave / Invasjonsgrotta** (Z4; laminated deposits of fine sand: Appendix D5.5), **Sotsbäcksgrottan** (KU) and **Korallgrottan** (KL), all at GS=L (eastern slopes) appear to have large sand deposits, which were presumably deposited beneath active IDLs. These findings provide further confirmation that all these caves existed prior to the Holocene.

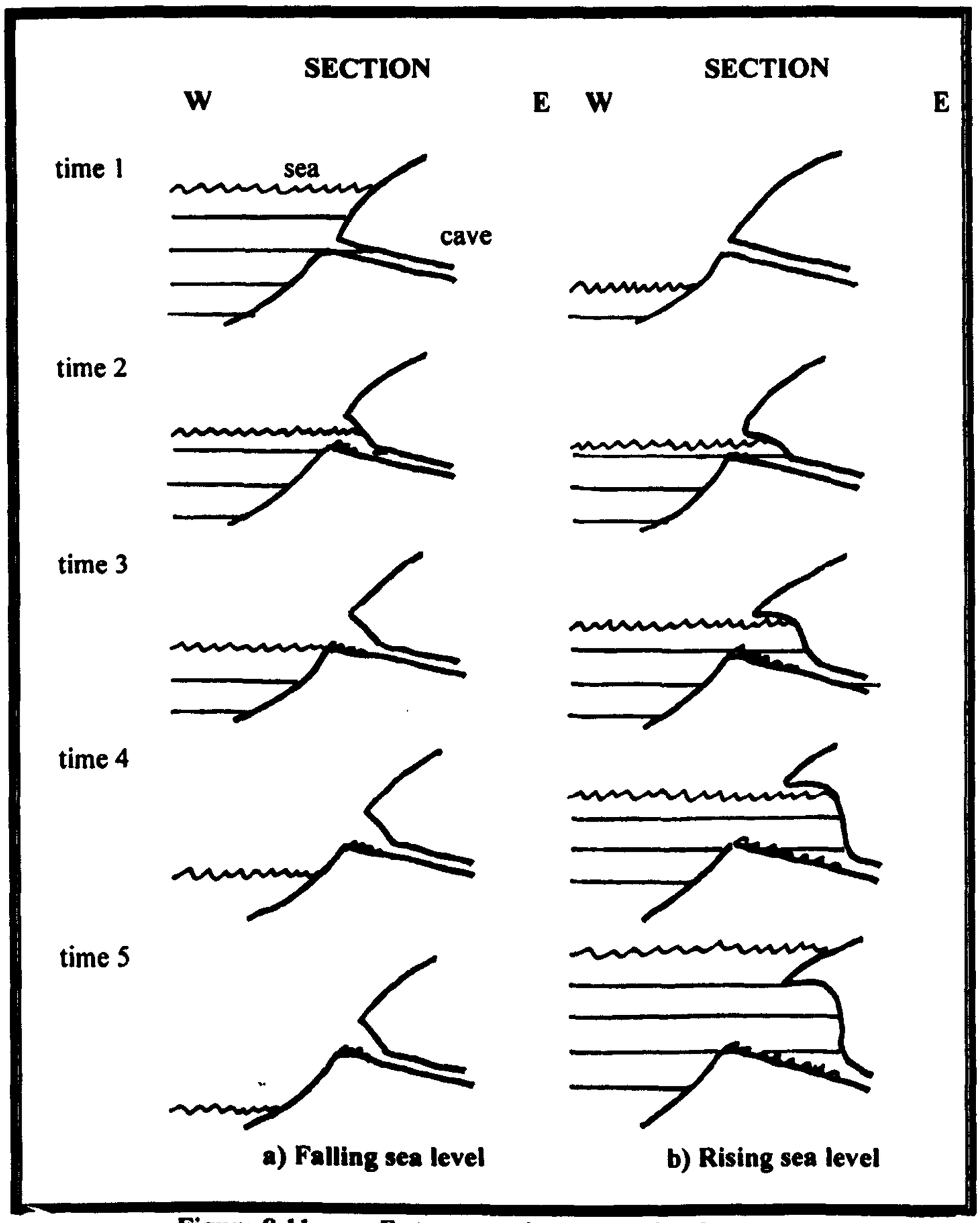

Figure 8.11 Entrance enlargement by the sea

The deglaciation marine limit at **Øyfjellgrotta** was c. 125m, reached at its 150m YD isobase soon after the sea encroached south of Mosjøen at 9300 ^{14}Ca BP (Appendix D2.7). This is some 45m below the 170m level of its main entrance roof, confirming that the enlargement above its floor at 140m must have occurred prior to the final deglaciation. This extra minimum 45m of maximum marine limit is well within the extra 120m discussed earlier so that it seems likely that the interstadial or Early Weichselian sea rise overtook the upward stoping of the **Øyfjellgrotta** entrance, so that the whole cave became submerged.

The upward stoping mechanism also explains the existence of the very large sea caves in non-carbonate rocks along the Nordland coast that are positioned above local deglaciation marine limits (Sjöberg, 1988, Table 2). For example, **Torghatt-hullet** and **Monshola** (Z1, at YD isobases of 115m and 120m) are shown as having entrance floors at 138m and 147m, and roof altitudes as high as 160m. At c. 11500 and 10700^{14}Ca BP, when the YD ice margin passed them, the sea level was at an elevation of c. 135m for each of these caves (Figure 8.1b). Because this level is below the entrance level of each cave, and 25m below roof levels, it seems unlikely that wave action could have formed them during the final Weichselian deglaciation. On the other hand, if they formed or enlarged during the *onset* of the Weichselian glaciation, or during the various interstadials, their maximum roof heights of 160m could define the minimum glaciation or interstadial marine limit applicable to their isobase. Subsequently, such sea caves above the deglaciation marine limit may have changed little in size, being protected by their west-facing aspect beneath a west-moving icesheet. **Torghatt-hullet** could also have been partly enlarged by deglacial meltwater flows at the end of the Weichselian, because it is a through-cave.

By comparing the height of the local deglaciation marine limit with the cave roof altitudes given by Sjöberg (1988, Table 2), his list of 33 caves can be divided into three classes: those formed only during deglaciation, those formed during glaciation and / or during interstadials, and those similarly formed but subsequently enlarged during deglaciation. For the second two classes, the difference between the roof height and the deglaciation marine limit ranges up to 70m, suggesting that an earlier marine limit could have been some 70m higher than the deglaciation marine limit for these coastal caves, which is within the extra 120m discussed in section 8.1.3. It seems likely that this explanation for the formation of sea caves in the study area also applies to the sea caves in northern Norway (e.g. Møller, 1985) and in southern Norway (Appendix A5.1).

Section 8.1.3 suggested that the relative elevations of both marine limits probably fell slightly with successive glaciations. Thus, could there be other karst caves above the maximum Weichselian marine limit whose entrances were modified by the sea during pre-Weichselian glaciations? This seems possible, although such entrance areas would be the first parts of a cave to be removed by subsequent glacial erosion: even if most of a cave survives, its modified entrance may not. Further, the rarity of entrances at altitudes above deglaciation marine limits that were clearly modified by the sea prior to the Weichselian deglaciation suggests that such modified entrance areas cannot survive long periods of glacial erosion, or that such modification becomes indistinguishable from the effects of other processes, or that the caves without enlarged entrances did not exist in their present form at that time. Additionally, the elevation of marine limits backwards in time probably only amounted to 5–10m per glaciation. This would make the marine limits of successive glacials indistinguishable. (See also sections 9.2.3, 9.2.4, 9.6.1 and 9.8).

The main conclusions from this section 8.8 are that at relatively low attitudes below the deglacial marine limit, when there was late and slow emergence above a falling sea level during deglaciation: 'new' littoral caves could form in limestone (and probably in other rocks), giving a late Holocene genesis;

existing karst phreatic entrances could enlarge, with heights ≤5m, suggesting origins prior to the Holocene; and the absence of enlarged entrances to 'mainly vadose' caves suggests that few existed prior to the Holocene. At higher altitudes between the deglacial and glacial marine limit, when there was late and slow submergence below a rising sea level during glaciation: very large sea caves could form in non-carbonate rocks (and probably in limestone, but none are known); and existing karst phreatic entrances could enlarge greatly, with heights ≤30m, suggesting origins prior to the end of the Eemian interglacial.

This study has used published data about marine limits and YD isobases to review influences on speleogenesis and entrance modification. It may also be possible to invert this process and estimate maximum and deglaciation marine limits and relevant isobases more accurately, by a more complete study of both sea cave entrance environments and modified karst cave entrances.

8.9 The effects of ice

Previous sections analysed the effects that meltwater, meteoric water and sea water have on fractures, conduits and passages. However, many caves remain under the influence of *frozen* water for most of a glacial cycle. This section discusses the various endokarstic effects of ice at each stage of glaciation.

8.9.1 Perennial occupation by ice.

As discussed in sections 8.4.1 and 8.4.2, it is likely that air was driven out of many subglacial cave passages for most of a period of glaciation, especially those below the glacial marine limit and those in valley floor locations. If the icesheet experienced a warm base followed by cold-based permafrost, then these caves became fully occupied by ice. Thus, the three conditions of occupation by frozen sea water, occupation by frozen fresh water and partial occupation by ice and air variously applied to the caves, for periods of time perhaps measured in millennia. Flooded inception fractures were subjected to an expansionary force whenever the contained water froze, causing a widening and lengthening of each fracture, thereby promoting later tectonic and dissolutional breakthroughs. Any weaknesses in the surfaces of all passages in any existing submerged caves were exploited by the freezing mechanism, potentially leading to roof falls and the spalling of cave walls when the water subsequently melted, or when the cave was drained. Any caves that were never flooded, only becoming partially occupied by the extrusion of glacial ice into entrance areas, were probably little affected, as it is assumed that the bedrock stresses induced by temperature cycling were of smaller magnitude than occurs annually during interglacials. The perennial occupation of caves by ice does not occur during interglacials, and consequently has no effect on the vadose entrenchment phase.

8.9.2 Semi-annual occupation by ice.

Ice-dammed lakes descended from the heads of valleys during each deglaciation (Appendices D2 and D3). Any ice in fractures and conduit systems melted when the IDL bases reached their levels and this water potentially froze again each winter. It is not known to what depth IDLs froze, and therefore

whether all the water froze in any one cave at any one time (section 8.9.4), although IDLs at higher altitudes might freeze to greater depths because of lower air temperature at higher altitudes and because of their earlier formation whilst more land remained covered by ice. At the very least, every cave, conduit and fracture system experienced an annual pulse of freezing that started when the water level above the cave reduced to a particular height, and continued until the cave slowly emerged above the level of the IDL. A similar scenario can be envisaged for the internal freezing of sea water, for those caves below the deglaciation marine limit, as isostatic uplift slowly brought them above sea level during interglacials. The effects of the annual freezing of submerging water were similar to those described in section 8.9.1 for the freezing of the sea and subglacial lakes, but greatly magnified because of the much higher frequency. The freezing of IDLs also affected all caves or fracture systems because, as section 8.4 showed, all karst caves or their inception fractures were submerged beneath ice-dammed lakes during deglaciation.

After the caves were drained during interglacials, the complete occupation of most caves by winter ice was not possible, but surficial inception fractures must be subjected to annual expansion. Observations show that streamways now freeze annually from their entrances inwards, including sumps. Thus, the upstream and downstream ends of sump passages that are near the surface experience the same effects from semi-annual ice occupation as did caves near the surface of ice-dammed lakes. Otherwise, the air-filled entrance areas of caves, including those undergoing vadose entrenchment, are subjected to frost shattering when the air temperature cycles through 0°C. The winter build-up of ice at resurgence entrances can also create aggressive phreatic conditions during the following spring melt, perhaps exemplified by anastomoses on the roof of the entrance to **Anastomosegrotta** (Z4; Faulkner and Newton, 1990: photo, p109). Internally, draughts can also cause caves to fill with ice, creating spectacular icicles (Photo: endpiece). However, this internal formation of ice probably has a limited effect on passage morphologies.

8.9.3 Glacial movement and caves

The impact of glacial movement on existing caves has rarely been studied. The movement of solid ice into cave entrances as part of external glacial flow has, so far, only been directly observed at Castleguard Cave in Canada (Ford and Williams, 1989, p354). Such ice may bring in injecta of glacial debris, including clastic materials, as seen at the 10m-long, surficial, **Injection Cave** (4B5, Z4; Photo D1.19). If a cave is close to the surface, the ice movement may also cause the geometry of the cave to change. Thus, walls and roofs may move relative to the floor, as seen in the same cave. However, without considerable study, this movement may be indistinguishable from that caused by tectonics associated with later uplift. A cave may also have its roof or a wall removed, as illustrated in Photos 7.4–7.8. Pre-existing speleothem deposits may also be detached, to be removed completely by subsequent deglacial flows.

8.9.4 The enlargement of cave entrances by IDLs

Sections 8.8.2 and 8.8.3 discussed the enlargement of cave entrances as they rose or fell through the local contemporary sea level. It seems likely, therefore, that pre-existing entrances could also be enlarged as the levels of ice-dammed lakes lowered past them during deglaciation, or rose past them at the onset of glaciation. Although IDLs did not generate the power associated with marine waves and tidal movement, they experienced more melting / freezing cycles each year that could cause considerable frost damage, particularly when the surface of the IDL was coincident with a cave opening. Such entrance enlargements may be distinguishable from those caused by the sea, for affected caves at altitudes higher than the deglacial marine limit of c. 125–150m and the glacial marine limit assumed to be at c. 245–270m.

The cave surveys and cave survey sections show that the following caves have sub-horizontal entrances larger than internal passages: **Valleyside Cave, Two Bridges Cave, Bear Cave, Overflow Cave** and **Reppelvgrotta** (Z2); **Låjroe Sink Doline, Låjroegrotta, Cold Wind Cave** and **Dåaranjueniehola** (Z3); **Green Valley Cave, Gevirgrotta, Buktgrotta, Warm Cave, Øvre Sarvejaellagrotta, Etasjegrotta, Road Cave** and **Bjørkåsgrotta** (Z4); **Brubakkgrotta** (Helveteshullet) and **Båtskargrotta** (Z7); **Grønndalsgrotta** (ZA); **Baaagrotta** (ZC); **Stor Grubblandsgrotta, Hjortetakgrotta, Martinusgrotta** and several caves at Övre Ältsvattnet (KU). These caves lie at altitudes from 240–900m. Entrances at shafts and collapse dolines were not reviewed. Roughly half the cave entrances are relict in late summer. All have been widened somewhat compared to continuing passages. Some have also been enlarged vertically, whereas others have not. A reduced vertical enlargement compared to those entrances enlarged by marine action is to be expected, because there is no tidal range in an IDL. All these entrances have collapse material on their floors, but the tapering inwards observed in marine-enlarged entrances (section 8.8.2) is commonly absent: the walls, and the roofs and floors, tend to remain parallel to each other. Only in **The Big Sink** (Z6) and **Baaagrotta** (ZC), two active sink caves well above the marine limits that also have enlarged entrances, do the walls tend to taper inwards. The collapse material may have arisen after enlargement, from a combination of enhanced frost shattering and seismic shocks.

As with the marine-enlarged entrances, *none* of these caves is in the mainly vadose hydrological class. This supports the idea that these entrance enlargements are associated with IDLs, because the IDLs had all been drained before the MV caves enlarged to present sizes. The enlargement of relict and combination cave entrances by the freezing and melting of the surface water in an IDL may be the last act after the flow through the IDL formed the continuing passages. However, it is *not* a universal phenomenon, because many entrances show no sign of enlargement, even when they would have been submerged beneath the same IDL as those that do.

Inland cave entrances taller than c.5m are commonly absent. The only example is the 16m-high resurgence entrance of **Grønndalsgrotta** (ZA, 600m altitude; Photo D1.38). This entrance is *not* widened, and contains much clastic material from a collapse doline shaft to the surface situated 16m

inside the cave (Figure B1.15). However, the roof continues to be 10m high beyond this shaft. It is therefore a candidate for being enlarged by a *rising* IDL, perhaps at the onset of the Weichselian glaciation. An alternative, or additional, mechanism is that vadose entrenchment during the Eemian and the Holocene of an initially Vauclusian exit produced this vertical enlargement (section 9.2.4). The common absence of tall cave entrances may indicate that IDLs did not in fact form significantly at the *onset* of glaciation as otherwise the roofs of more entrances could have been eroded upwards.

Because IDLs lower at a similar rate to that of the constraining icesheet surface, i.e. at c. 0.5ma^{-1} at the start of the Holocene (from the reconstructed Grønlie formula: section 8.1.4), it would only take about four years for the surface of an IDL to descend past a 2m-high cave entrance. This seems too short a time to cause significant widening by freeze-thaw and dissolutional mechanisms if IDLs only froze near the surface, suggesting that IDLs annually froze downwards for several metres, despite evidence from present glaciers that moulins contain meltwater below short frozen surface layers throughout the winter (Jacques Schroeder, pers. comm., 2002). This evidence, and the suggestion that higher IDLs froze deeper (section 8.9.2) is supported by the biased distribution of the 25 caves mentioned above towards the higher western glacial situations, because their percentage occurrences compared with the distribution of all caves are: <u>G</u> 8% (3%); H 0% (7%); <u>K</u> 24% (15%); L 60% (47%); <u>S</u> 4% (1%); and T 4% (13%). (Western GS are underlined). A disproportionately large number (8) lie in the 500–600m altitude range, although eight (including two caves at GS=G) also have altitudes from 240–300m that may have been partially enlarged by a rising sea level at the onset of glaciation if the glaciation marine limit has been set too low. The western favouring is likely assisted by increased temperature cycling on western slopes compared with the eastern slopes that remained more in shadow in the afternoon. Hence, to summarise the phenomenon of enlarged cave entrances, marine enlargement is favoured towards the end of the Holocene at low altitudes at caves facing west, whereas enlargement by IDLs is favoured early during deglaciation at high altitudes at caves that also face west, and there is a band from 300–500m altitude where relatively few caves have enlarged entrances.

This completes the overview of the various hydrogeological processes that influenced the development of Caledonide endokarst. Chapter 9 examines how these processes and surface erosion determined the internal morphological evolution of the karst systems in space and time.

CHAPTER 9 THE INTERNAL MODEL

As discussed in section 5.8.13, Chapter 5 essentially presented the *static* internal model of cave development. From a knowledge of the three main external cave attributes of karst type, glacial situation and cave location it is possible to model and predict the main internal cave attributes, including length, vertical range and volume, and the occurrence frequencies of various cave 'objects', such as chambers and shafts, for the average cave of each cave type of the three hydrological cave classes. This model is broadly the same across all the 'inner' zones and nappes of the whole study area. Internally, the prime influence on the morphology of individual passages is the karst type, and the presence of aquicludes. Chapters 6–8 analysed how the various tectonic and glacial processes that affected the area during the Quaternary and earlier combined together to provide inception fractures that were enlarged into both previously-existing and presently-remaining cave passages by calcite dissolution. The aim of this Chapter is to consider how, and in what sequence, the various internal cave passage elements were constructed. A single *dynamic* model of internal development for caves in vertical stripe karst is presented, followed by consideration of variations caused by the influence of karst type. The tectonic, external, hydrogeological and internal models are then considered together, to deduce the timescale constraints on central Scandinavian cave development.

9.1 Deductions from cave types

Section 5.7.1 compared the cave types representative of the study area with those of Palmer (1991). The elimination of hypogenic cave origins is compatible with the finding that the caves are in close contact with the surface: they are all *epigean*, they can perhaps even be regarded as *epikarstic* (to a broad definition) and they developed synchronously with their landscape (section 3.1.16). Elimination of porous soluble rock and intergranular porosity models is compatible with the known negligible porosity of metalimestones (Appendix A2.2). Whereas Palmer's "bedding partings", gradually sinking streams and diffuse recharge through sandstones are not directly relevant to the study area, these settings are suggestive of suitable environments in which cave inception and development could have occurred. Thus, instead of being along bedding partings, cave development was along *inception surfaces* created by sub-horizontal fractures and joints in all possible karst types (many examples) or by sub-horizontal aquicludes (e.g. **Ytterlihullet**, ZA). Similarly, although there are few examples of gradually sinking streams or diffuse recharge through a caprock in the study area, direct synchronous recharge into the karst at several places beneath ice-dammed lakes in phreatic conditions promoted the development of rectilinear and complex passage arrangements, with *synchronous* dissolution and enlargement of all submerged passages at all levels (many examples). There is only one example of a (relict) cave in horizontal metalimestone below a thin mica schist cap, with dolines: **Akersvanngrotta** (ZB; Figure B1.17). This is an example of what Palmer called an interstratal, rectilinear, maze. It probably developed by diffuse recharge through the mica schist when the Stor Akersvatn level was held up by ice-damming (Appendices D2.3 and D2.6).

Palmer used Onesquethaw Cave (NY, USA) as an example of an epigenic dendritic cave formed in roughly horizontal limestones. Its plan and extended profile are similar to those of **Toerfjellhola** (Z3; Figure B1.3), which has formed in vertical metamorphic stripe karst, although the **Toerfjellhola** profile does not require a vertical exaggeration. This supports the conclusion that caves in vertical stripe karst with orthogonal joint systems commonly have morphologies that appear to be similar to those in horizontal sedimentary limestones. For example, where horizontal joint openings predominate over vertical fractures, passages are sinuous rather than straight, as discussed in section 5.7.1 for horizontally-bedded sedimentary limestones. Palmer (1991) also identified the place where the development of Onesquethaw Cave changed from vadose to phreatic. However, from the discussion in sections 9.2.2–9.2.4, it is argued herein that **Toerfjellhola** developed phreatically *prior* to vadose entrenchment, giving it 'upside-down' morphology in common with other combination caves, but in contrast to the morphology of many classically-described cave systems in sedimentary limestones.

Morphological comparisons with caves in vertical sedimentary limestones may also be useful, but there are few identifying references in the literature. Osborne (1999; sections 3.1.12 and Appendix B2.8) discussed inception 'horizons' in such a setting, noting the importance of lensoid shapes, and tiered passages. However, the "halls and narrows" deduced to be partly-formed by rising artesian or hydrothermal waters (Osborne, 2001c) have no comparable morphological analogues in the study area.

9.2 Caves in vertical stripe karst (VSK)

Monoclinal vertical stripe karst provides the most fundamental structural setting for the morphology of study area caves, from which morphologies in other settings can be derived.

9.2.1 Etasjegrotta, the ultimate example

Etasjegrotta (Z4; Figure B1.8; section 5.7.3) is chosen as the best example of a combination cave formed in monoclinal VSK. Its passages total over 1km in length, but the horizontal extent of the cave from its entrance area to the downstream sump is only some 170m, because the length is distributed across tiered passage elements on about 20 different levels. These have a mean vertical separation of c. 2m, and a minimum separation of only c. 30cm. The cave survey section shows that the upper passages consist of shallow single phreatic loops, commonly with rectangular cross-sections bounded by vertical aquicludes. They are connected by several chambers and by many vertical shafts with a mean horizontal separation of c. 7m, and they sporadically have blocked connections to the surface. The stream flows from the entrance area at the lowest levels of the system, commonly along immature vadose passage elements and vadose-entrenched relict phreatic levels at its upstream end, towards permanently submerged phreatic passages. Because of its complexity and angled, along-strike, relict phreatic 'ramp' passages, the cave is assigned cave type h. The stream resurges at the **Main Rising**, c. 500m south along the strike from the sump, at a large, completely submerged, passage that was dived upstream for 340m at a maximum depth of 20m (Whybro, 1988; Figure B1.9). Relict phreatic passages in **Invasjonsgrotta** lie

above the downstream end of this sump, and have both open and blocked connections to the surface. Thus, the **Etasjegrotta** system contains most of the internal morphological elements that are representative of combination caves in VSK, and is typical *within the study area* as it apparently does not contain paragenetic dissolution above a vadose passage. Most other caves in VSK are expected to have cave development sequences that are subsets of those of **Etasjegrotta**.

9.2.2 The internal model of a cave in VSK

Figure 9.1h represents the vertical section of a complex cave formed in VSK, loosely based on the present **Etasjegrotta–Rockbridge system** (Z4). A series of relict phreatic passages, whose individual profiles comprise a single phreatic loop, overlie a mainly vadose streamway. The absence of passages containing multiple phreatic loops was noted in section 5.7.2. Relict vadose passages are very rare, but where they do occur, they commonly form a dry (and possible flood-overflow) entrance to the system, almost universally at the upstream end of the cave. The present surface stream commonly sinks into immature conduits upstream of the entrance. **Etasjegrotta** is rather exceptional, because it appears to contain a vadose-modified shaft, Fall Aven, near its lower end (section 8.4.12).

The two distinct passage morphologies are strongly suggestive of a very simple two-phase cave enlargement history: firstly phreatic, and secondly, predominantly vadose. Whereas some vadose developments may also suggest a sequence of events (for example, if the original stream-route has been captured via lower-level immature fractures and conduits), a key question concerns the phreatic enlargements. Were the tiered passages enlarged simultaneously, or did they enlarge successively, level by level in a top-down sequence, perhaps controlled by external 'base levels' or geological aquicludes?

The frequency and small mean separation of phreatic passage tiers (2–13m; Table 6.2) eliminates the possibility of any external, base-level, control, supported by the absence of any known relationship between passage elevations and regional topography, as noted by Helldén (1975) for **Sotsbäckgrottan** (KU, Appendix B1.13), and as reported herein (section 5.8.3). Within VSK, the aquicludes commonly align with the foliation, so that horizontal sills are extremely rare, thus eliminating the possibility of sub-horizontal geological control. Hence, the phreatic levels did not enlarge in a strict top-down sequence, with an air surface above the next active level. Instead, they commonly enlarged simultaneously, but not necessarily at the same rates, as part of one submerged phreatic network per cave or group of caves. Less commonly, an upper group of phreatic levels enlarged before a lower group of fractures was formed, or achieved breakthrough dimensions, and then, in a different timescale, both groups enlarged together.

9.2.3 The timing of cave development

Section 8.6.2 considered the enlargement of phreatic passages from knowledge of wall retreat rates and passage dimensions. This section discusses supporting evidence for the conclusions reached. There seem to be only three possible timings for a conduit system to be totally water filled: a) during early cave

development under present and previous interglacial conditions; b) during flooding by large-scale interglacial spring melts; and c) during the various subglacial and IDL conditions.

Considering a), and assuming that the maximum length of an interstadial or interglacial is 10ka, a phreatic passage could theoretically enlarge to a diameter of 20m, at a maximum wall retreat rate of $1mma^{-1}$, i.e. greater than the largest size known, providing that the recharge rate could maintain flowing phreatic unsaturated conditions throughout the year. However, if the mainly phreatic relict caves and the combination caves in the study area did develop to their present sizes during the Holocene and / or earlier interglacials, then there would surely be a relationship between their catchment areas and their cave volumes and mean cross-sections, which does not occur (section 5.8.9). Even if the catchment areas differed slightly during previous interglacials, it is implausible that they could change in such a way as to remove such a relationship. Additionally, because enlarging caves fed from a roughly constant annual recharge eventually drain in their upper levels (Palmer, 1991), there would be consistent vadose entrenchment along *all* the relict phreatic passages, rather than just along the lowest-level phreatic passages. The almost universal absence of upper-level vadose entrenchment away from entrance areas (Appendix B2.7), the consequent rarity of phreatic to vadose transition zones (section 8.4.12), and the very existence of the phreatic relict caves with an almost total absence of vadose relict caves, rule out the possibility of a *gradual* transition from phreatic to vadose conditions, and deny possibility a).

Considering b), although there are undoubtedly frequent (perhaps annual) occasions when *some* individual caves are completely submerged, and such floods are highly aggressive (Appendix B2.2), it is inconceivable that such floods caused the *primary* enlargement of any of the relict or combination caves. Indeed, there are many phreatic relict passages and whole caves in 'topographically impossible' cave locations that could not possibly be submerged under present conditions, and probably not during previous recent interglacials.

The only natural conclusion is that the phreatic passage networks primarily enlarged to their present sizes at time c), before they were drained and experienced interglacial conditions similar to the present. Consequently, the vadose entrenchment phase of the active combination and mainly vadose caves was almost universally restricted to the Holocene. Other evidence for the Holocene timescale for the enlargement of the mainly vadose caves was discussed in section 5.8.9. Phreatic modification or paragenetic enlargement of a pre-existing vadose passage may be regarded as a morphological diagnostic for a cave that has experienced at least two glacial cycles. Although modified passages developed under previously vadose conditions may not be easily recognisable in VSK with vertical aquicludes, the common absence of such evidence is at least *indicative* that any such modified vadose flow-routes were either extremely short-lived during a previous interstadial or interglacial (such as the Eemian, which is unlikely), or else that such passages, and therefore the whole cave above them, were eroded away during the Weichselian stadials. Relict vadose passages would also be eroded away by glacial movement prior to

relict phreatic passages, because they were closer to the upstream cave entrances. Hence, the remaining parts of the present combination caves have only existed for a single glacial cycle in the large majority of cases (a concept discussed in section 7.3). The (phreatic) relict caves are also commonly more epigean than the combination caves, as they only extend to a maximum depth of 40m below the surface (Table 5.20), hinting that most of them also only survived for one glacial cycle.

9.2.4 The top-down, middle-outwards, model (TDMO)

A dynamic internal cave development model is derived by bringing together the ideas presented in Chapters 5–9, to show how a combination cave in VSK could have developed to its present form (Figure 9.1h) via stages illustrated in Figures 9.1a–g, and could develop to a future form, Figure 9.1i.

Initially, consider a shallow valley along the strike of unfractured, non-cavernous, vertically-foliated metamorphic limestone that was stripped to bare rock by glaciation. The metalimestone contained no open joints, 'bedding planes' or inception horizons, and no primary, secondary or tertiary porosity, and therefore did not support an internal 'watertable'. Early Quaternary glaciations did not produce large seismic shocks (section 7.3), so that only small fractures were penetrated when submerged beneath the local ice-dammed lake during deglaciation. After deglaciation, any stream that entered the upper end of the valley flowed along the surface of the limestone. Hence, during both early deglacial and early interglacial periods, only the most superficial and short fractures achieved tectonic or chemical breakthrough, and there was little karstification.

During the sequence of later Quaternary glaciations, the valley deepened, deglacial earthquakes became greater in frequency and magnitude, and some significant systems of orthogonal horizontal and vertical fractures achieved breakthrough, either directly from pressure relief, seismic shocks and slow tectonic movements, or by supplementary chemical dissolution beneath an IDL (Figure 9.1a). The largest fractures were created down to a depth determined by the strength of the seismic activity, following the 'one-eighth' relationship derived in Chapter 7. Below this depth, the fractures were too small to influence karstification in relevant timescales. A study of cave surveys (section 6.5.4) showed that the vertical and horizontal separations of passages and shafts are very variable, with no discernible trends related to depth, within the vertical range of each cave. Some of the fractures enlarged into phreatic conduits and explorable cave passages whilst still submerged by their first IDL, or by the IDL of a subsequent deglaciation (Figure 9.1b). Conduits could also enlarge through narrow ridges of limestone, as at the Klausmark System (Faulkner and Newton, 1995, Figs. 4 and 5), with entrances on the west, east and top of a N–S ridge. During the interglacial following the deglaciation, the cave drained partially, with vadose entrenchment below higher-level phreatic passages that remained relict (Figure 9.1c). The next glaciation lowered the surface of the valley, stripping it bare of small exokarstic features, and may have removed most of the cave passages (Figure 9.1d). If all traces of the cave were removed by the next glaciation, only a *single-cycle* combination cave had been created.

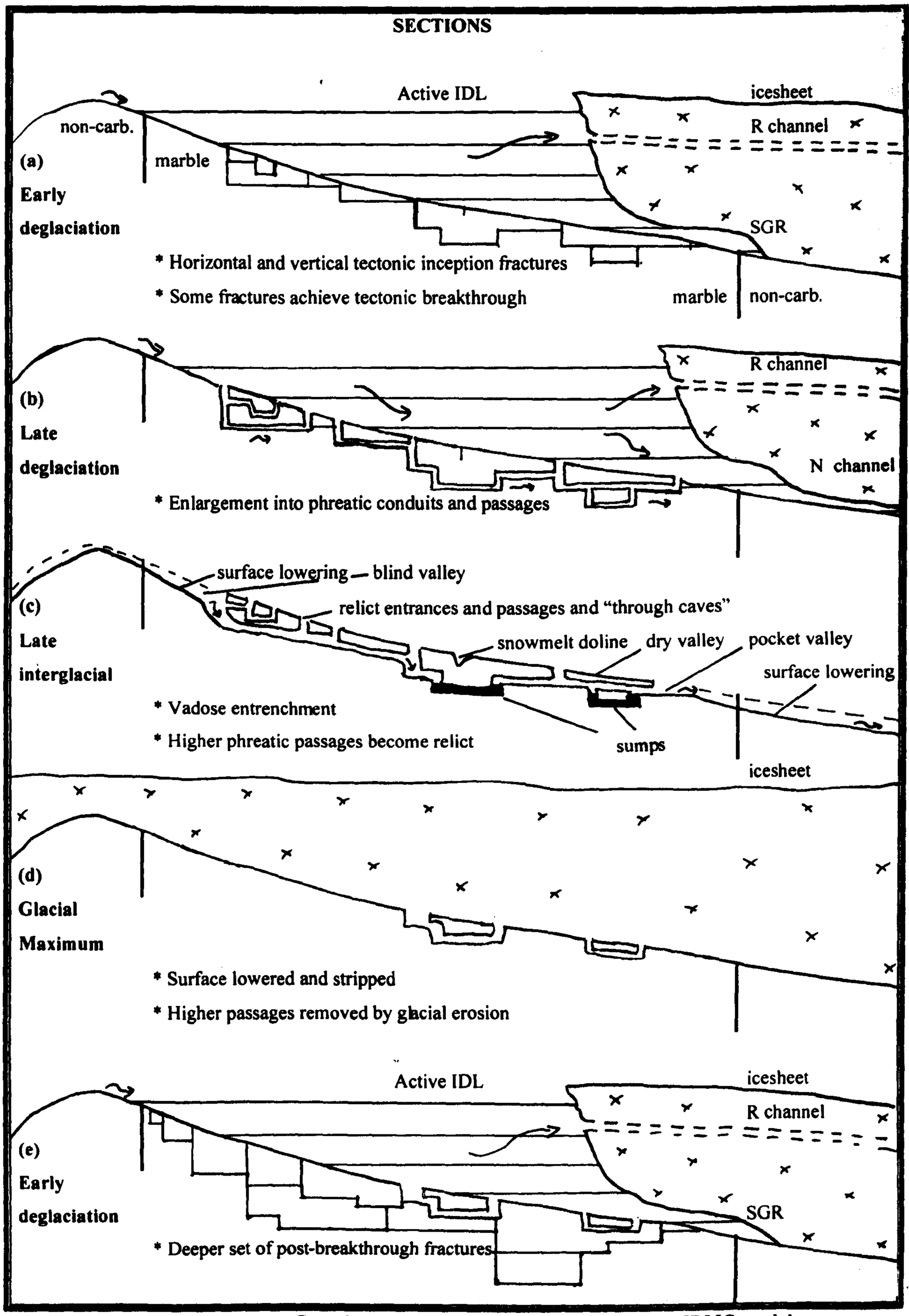

Figure 9.1a–e Cave development in vertical stripe karst: the TDMO model

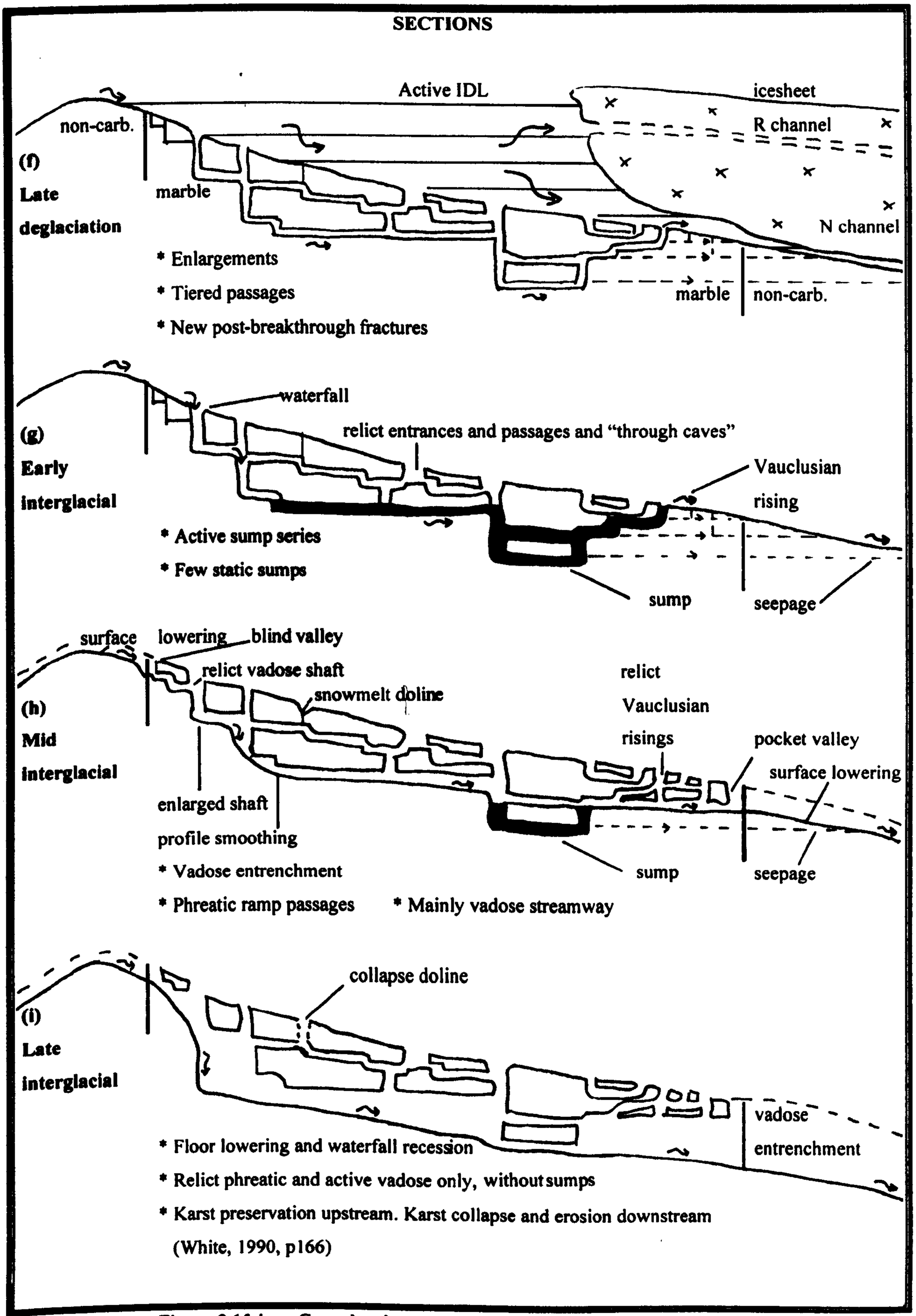

Figure 9.1f–i Cave development in vertical stripe karst: the TDMO model

The above sequence of events could have been repeated many times at each karst location. In the general case for large combination caves, the previous orthogonal network of fractures was reinforced and deepened by the surge of tectonic activity that accompanied deglaciation and isostatic rebound after a significant number of glacial cycles, so that significant new vertical and horizontal post-breakthrough fractures were created *each side of and below the level of any existing cave passages*, to new depths that obeyed the contemporary one-eighth relationship (Figure 9.1e). Some of these fractures enlarged to form tiered phreatic conduits and explorable passages by dissolution under a lowering IDL, as discussed in Chapter 8, whereas other, smaller, fractures just reached breakthrough dimensions (Figure 9.1f).

The cave was drained early in the succeeding interglacial, except that those passages below the level of the outlet remained submerged, commonly creating a long and active series of sumps behind a Vauclusian rising (Figure 9.1g). Statistically, sumps occur with a higher frequency near the resurgence end of a cave, both in the study area *and anywhere in the world,* because this is the *lower* end, where water tends to collect under the influence of gravity. The allogenic stream in the valley commonly sank into the cave as a waterfall at the first shaft, to begin the vadose entrenchment of the upstream phreatic passages. The higher parts of the cave were abandoned as relict entrances, relict passages and 'through caves', with few, if any, static sumps. Some of the surface flow was captured by fractures upstream of the sink entrance, and some water was diverted away from the sumps and the rising via underflow seepages along fractures at small springs lower down the valley (section 7.2.1).

During the interglacial, surface lowering of the valley upstream of the sink (to create a blind valley) and downstream of the rising (to create a pocket valley) was significant in comparison to the vertical range of the cave system (Figure 9.1h). The actual sink could also migrate upstream by headward capture via enlarged fractures, to leave behind relict vadose shafts and short sections of relict upstream vadose passages, in a manner similar to that described by Osborne (1999, Fig. 7). Vadose-enlarged phreatic passages near sink entrances have larger cross-sections than 'downstream' relict phreatic passages, as at **Etasjegrotta** (Z4). Rather exceptionally, modern vadose streams may also invade upper relict passages well-away from their upstream ends, as at **Invasjonsgrotta** (Z4), where a small stream has cut a vadose canyon some 2–3m high into the roof of a relict tube situated above the **Etasjegrotta** to **Vatnhullet** phreas (Figure B1.9).

Above the typical cave, the continuing dry valley experienced very little erosion, except for the creation of solution dolines, where water from snow patches trickled into vertical fissures. In time, these could enlarge into collapse dolines that connected to underlying passage roofs (Figure 9.1i). When the floor of the pocket valley encountered seepage from behind the Vauclusian rising, the fracture enlarged to lower the level of the flooded networks at the base of the cave and drain the rising. Because there is a complete absence of *underflow springs* below present flooded and open resurgence entrances (at least under normal flow conditions), it is assumed that this capturing process was relatively rapid, in agreement with

the shortness of the hydrological paths. The bypassing fractures themselves enlarged into sub-horizontal conduits, sumps and resurgence passages, as at the **Main Rising** termination of the **Etasjegrotta** system that has bypassed a previous Vauclusian rising at **Vatnhullet** (Figure B1.9). If there was no suitable sub-horizontal fracture to provide a bypass route, the Vauclusian rising eventually reduced to an open passage by entrenchment, as would happen in Figure 9.1c (Photo 9.1). Figure 9.1h explains why relict shafts tend to form at system extremities (sections 4.4.3 and Appendix D4.1). This is where the Holocene vadose entrenchments promote upstream and downstream cave development, in contrast to the central parts that commonly remain undisturbed during interglacials.

Photo 9.1 Fiskartjerngrotta (KU)
This cave functions as a resurgence for the epigean, and primarily flooded, system in Skindfjelddal.
The entrance was a Vauclusian rising immediately after deglaciation, before Holocene entrenchment.
The cave has formed in a *ridge* of dark, low metamorphic grade, low angle karst in the Upper Køli nappes.

Within the cave, considerable vadose modification of previously phreatic passages was achieved by the interglacial allogenic stream. Upstream passages were enlarged by waterfalls that rapidly eroded backwards. Downstream, previously phreatic passage profiles were commonly smoothed by turbulent flows that created 'keyhole' -shaped meanders, and the drained phreatic outlets to Vauclusian risings were left as relict ramp passages. The streamway itself became more 'mainly vadose' in character, with less flow along sumps. A long interglacial (such as the Holocene) provided sufficient time for considerable lowering of streamway floors, both on the surface and inside the caves (up to 7m in some combination caves: section 8.7.2). Thus, the common conclusion of interglacial cave development is a combination cave with a large continuous wholly-vadose streamway with no sumps remaining between the sink and the resurgence, beneath relict phreatic passages and beneath upstream relict vadose shafts and downstream relict phreatic ramps (Figure 9.1i). Outside the cave, a significant pocket valley is

commonly created by erosion by the resurging water. **Jegerhullet** (Z4, upstream of **Etasjegrotta)** provides a splendid example of all these features.

According to Dreybrodt (1998, p42; section 3.1.16), the *"breakthrough length"* of the fractures determines the style of caves formed: intensive karstification with many small caves arises if the fracture lengths are small, but fewer, longer, caves develop if the lengths are large. Clearly, caves have formed in the study area across the whole range of these styles, up to path lengths of c. 3.5km. In narrow stripe karsts, the 2D models of calcite dissolution (e.g. Dreybrodt, 1990) should be adequately representative. The common resulting morphology for the longer caves has tiered, symmetrical, rather shallow, phreatic loops with interconnecting vertical shafts and several entrances at both 'upstream' and 'downstream' ends of the cave. The symmetry of the phreatic loops is modified by the surface slope above the cave, so that the 'down-valley' ends of the loops are universally somewhat lower than the 'up-valley' ends. In shallow, strike-aligned, valleys in VSK, water can never find deep outlet points. Only when the outcrop is orthogonal to a deep valley can there be a deep outlet, and then the outlet can only be to the maximum depth allowed by the one-eighth relationship (e.g. 50m below the valley shoulder for VSK in the study area).

The common lack of high-level abandoned or phreatically-modified vadose passages indicates that most (but not all) caves in the study area were single-cycle caves, only developing to their present size during the final glacial cycle. Relict caves did not develop into combination caves because the topographic locations of their entrances precluded invasion by allogenic recharge. It is possible that the highest levels of **Etasjegrotta** (Øvre Etasjegrotta; Figure B1.8) developed in a previous glacial cycle, but remained relict in the following interglacial.

From this discussion, cave development followed a top-down sequence as passages migrated downwards through the sub-surface tectonic fractures, which were enlarged to form phreatic, then vadose, passages through various glacial cycles. Middle-outwards extensions developed at each end of an active cave during interglacials, to complete a general top-down, middle-outwards (TDMO) cave development model. This may be compared with Alpine studies, where Bini (2001) implicitly described a tectonically-driven top-down sequence, and Häuselmann (2002, p36) observed that *"in contrast to the laws of stratigraphy, the youngest cave phases are usually found in depth and the oldest are at the top"*. Removal by glacial and subaerial erosion followed behind, with caves commonly shortened at each end by glaciation prior to any total removal, giving a top-down, extremities-inward, process for cave destruction.

Mainly vadose caves developed during interglacials from those more superficial fractures that achieved late breakthrough when under an IDL, or only reached breakthrough during the interglacial itself, assisted by enlargement by annual freeze-thaw cycles. These fractures resembled the system shown in

Figure 9.1a. In interglacial conditions, phreatic cave enlargement was limited by the annual recharge rate, so that conduits and passages remained submerged until they enlarged sufficiently to be partially drained. Thereafter, their development became mainly vadose, and continued as described above for combination caves, but without an extensive higher level network of relict phreatic passages. This explains the formation of the set of presently-active, mainly vadose caves (section 5.4.2), which, in the study area, only exploit fractures less than 20m from the surface. As these caves have developed entirely within the Holocene interglacial, they are considered to be *half cycle* caves. Good examples of mainly vadose caves occur at Vargskar (Z5), where there is very high allogenic recharge from permanent snowfields on Blåfjell into many active stream caves (e.g. **Drowning Cave**, Table 5.22), and these show that a primarily vadose development of significant passages can occur within an interglacial. Although mainly vadose caves continued to develop in this latest interglacial, they may also represent the earliest type of cave formed in the Scandinavian Caledonides, after the onset of the Mio–Plio–Pleistocene glaciations that started to generate the first superficial fracture sets.

It is assumed that during interstadials the ice primarily melted where it was in contact with the sea (section 8.1.1). Caves below the relevant marine limit were immediately flooded by sea water, which had little *dissolutional* influence on cave development (Appendix D4.12). With only minor lowering of the inland icesheet by ablation and melting, only caves at high altitudes could have been submerged beneath interstadial IDLs. Thus, cave internal morphologies were commonly not modified during interstadials, although passage diameters could enlarge.

9.3 Caves in angled stripe karst

As proposed in section 5.7.3, **Gevirgrotta** (Z4; Figure B1.7) is a good example for combination caves formed in monoclinal angled stripe karst (ASK). From its survey section, it mainly consists of relict single phreatic passage loops at five levels, some being invaded and interconnected by a presently-active vadose streamway that is meandering and steeply descending in its lower part. Thus, although its cave plan is more complex than commonly applies to caves in VSK (because the morphology is guided by the ASK dip of 70–80°W), **Gevirgrotta** also appears to demonstrate a multi-phase development history, with both phreatic and vadose episodes.

Gevirgrotta and **Øyfjellgrotta** (Z5, also formed in ASK) appear to be unique in the study area, because they both contain relict vadose (RV) passages and relict vadose entrenchment along the down-valley ends of phreatic loops. This is a rarity discussed in Appendix B2.7 and section 9.2.2 that suggests entrenchment during the Eemian interglacial. **Gevirgrotta**'s RV elements are the 'muddy pit' and the entrenchments in 'Tooms Revenge' and in 'Upper Inlet Passage'. **Øyfjellgrotta** appears to have large relict passages with very significant vadose deepening along its 'Upper Galleries', according to its cross-sections (Figure B1.10). The approximate 150–180m altitude of these entrenchments in **Øyfjellgrotta** may coincide with the ice-melting height at the local isobase at which a suggested deglacial hiatus

occurred between 9600 and 9500^{14}Ca BP (section 8.4.12), before the arrival of the ice margin at 9300 (Table 8.4), so that the lowest part of the entrenchment may have occurred early in the Holocene.

Those parts of **Gevirgrotta** and **Øyfjellgrotta** that remain from previous glacial erosion probably follow the same TDMO sequence of development, within two glacial cycles. The commentary on the TDMO model in section 9.2.4 is therefore generally applicable to caves in both VSK and ASK, and, thus to most caves in the study area. However, the great majority of combination caves have much simpler cave types and morphologies than those of the type-examples. In the *simplest* single-cycle caves, a single phreatic tube enlarged under an ice-dammed lake, before being drained to a relict cave, or before being invaded and modified to a combination cave under mainly vadose conditions by an allogenic stream during the Holocene.

9.4 Caves in low angle karst

As also discussed in section 5.7.3, caves in low angle karsts (LAK) display a variety of complex forms, so that no one cave is representative. The longest and deepest of these caves are listed in Tables 5.16 and 5.17: **Sotsbäcksgrottan** (KU, Figure B1.21), **Grønndalsgrotta** (ZA, Figure B1.15), **Akersvanngrotta** (ZB, Figure B1.17), **Svartdalgrotta** (Z2, Figure B1.1), and **Ytterlihullet** (ZA, Figure B1.16). Their cave survey sections show that, apart from **Akersvanngrotta** and **Ytterlihullet**, they all comprise a series of primarily relict and probably phreatic passages above a partly graded and active vadose streamway. **Svartdalgrotta** also displays a previously-Vauclusian rising at its relict lower entrance that has now been drained by immature lower conduits leading to its small resurgence. The relict **Akersvanngrotta** was formed entirely phreatically beneath a sub-horizontal mica schist roof, and appears to have been rapidly drained when its local ice-dammed lake fell to the level of the present Akersvatnet, and thus did not experience any allogenic invasion and vadose development. **Ytterlihullet** is perhaps unique in comprising just two main 'inlet' passages that both appear to be phreatically initiated prior to significant vadose entrenchment, without exhibiting many tiers of passages. This is because cave development has been constrained to lie within two layer-parallel aquicludes that commonly provide roof and floor barriers. Thus, caves in LAK also commonly appear to follow a 'TDMO' sequence of passage development. **Akersvanngrotta** and **Ytterlihullet** display this in the simplest form: a single level that has probably extended from one end of the system to the other since inception.

9.5 Caves in complexly folded karst

Because only three caves in the study area are recorded in complexly folded karst (CFK; section 5.3.1), and these all differ in form, no common model can be proposed with confidence. **Kvitfjellgrotta (Z4)**, although only c. 200m long and 22m deep, has a complex series of relict upper-level phreatic passages above a tall meandering stream passage with sump sections (not shown). It lies at a valley shoulder position (CL=S), and its present stream resurges from mainly phreatically-formed tubes high on the side of a deep, glaciated, valley (Photo C2.4). Its (relict) entrance is at the highest point in the cave, about

halfway along its plan length, and thus the cave also fits the TDMO model. No survey has been published for **Nedre Helveteshullet** (Z7), and so no conclusions can be drawn about its formation. The third cave in CFK, **Labyrintgrottan** (ZC, Figure B1.19), comprises mainly relict and inter-linked phreatic passages, with still-active phreatic passages along its stream route that are being explored by diving. Although a cave survey section has not been published, and the author has not visited the whole cave, there appears to be a complete absence of both active and relict vadose passages. The extent that the cave contains levels of relict phreatic passages is difficult to determine. It has a relatively small vertical range of 20m, and several relict entrances. The absence of an (at least) partly vadose streamway in a long (over 2600m) 'active' cave seems to be unique for the area, and suggests that there has been little lowering of the floor of the small valley below its sump resurgence in the time since the local IDL lowered to the level of the lake Över-Uman. The submerged character of much of the present **Labyrintgrottan** stream is probably not a function of its CFK classification: because the cave runs parallel to the strike of the folds, they behave as angled stripe karst for many individual passage elements. Although CFK is rare in the study area, there are at least two long and deep caves in such karst in northern Norway. They appear to violate the TDMO model (Appendix D6.1.1) and they also appear to have more complex internal morphologies than caves formed in homoclinal outcrops, as do **Kvitfjellgrotta** (above) and **Labyrintgrottan** (Figure B1.19).

9.6 Minimum timescale constraints from marine and IDL entrance enlargement

The enlargements of cave entrances that lie below the glaciation and deglaciation marine limits by marine activity as the sea level rose or fell past the entrance positions were described in sections 8.8.2 and 8.8.3. Such enlargements place constraints on the latest possible times of cave inception and development for caves in the lower glacial situations (GS=C, D, E, G or H), although the enlargement of entrances by IDLs at higher situations provides less timescale constraint.

9.6.1 Saalian or earlier development

Sections 8.8.3 considered the theoretical possibility that some old, remnant, cave passages above the Weichselian glaciation marine limit may have been modified by wave action during the onset of the Saalian or an earlier glaciation, but concluded that such modified entrances would be difficult to diagnose. Therefore, it is assumed that time constraints on cave development above GS=G or H cannot be deduced from the *marine* enlargement of entrances.

9.6.2 Eemian or earlier development

If we accept that a *rising* sea level enlarged an existing entrance to **Øyfjellgrotta** (Z5; GS=H; Figure B1.10; section 8.8.3), it follows that its ramping, phreatic, main entrance passage was likely in existence by the end of the Eemian interglacial. Hence, this entrance passage, together with many other relict phreatic passages in the same cave, probably developed to cave dimensions beneath an IDL during the Saalian deglaciation or glaciation, or even earlier. These phreatic passages could then have been further

enlarged, and perhaps new ones developed, beneath IDLs during the Weichselian glaciation and deglaciation. The developments of the vadose passages in **Øyfjellgrotta** are discussed in sections 8.7.2 and 9.3.

9.6.3 Weichselian interstadial or earlier development

None of the other four cave entrances with GS=H (Table 8.4 and section 8.8.3) that are candidates for marine enlargement prior to the final deglaciation are sufficiently tall to have *required* a rising sea level to create them. Indeed, as they are each only 2–3m high, it is only their altitudes above their local deglaciation marine limits that distinguishes them from the enlarged entrances with GS=D or E. Hence, these entrances could have been enlarged as late as during a Weichselian interstadial, when (or if) the sea melted and then froze again, perhaps without much change in isostasy or sea level. In this case, all that can be inferred is that the (mainly phreatic) entrance passages to **Bollhauggrotta** (Z5), **Øyåskjeleren** (Z4), **Lillelvgrotta** (Z5) and **Geitklauvgrotta** (Z5) were all in existence some time before the Weichselian deglacial IDLs formed. Tectonically-moved blocks in the **Bollhauggrotta** entrance provide supporting evidence that this cave existed prior to Weichselian deglacial seismicity. The phreatic parts of these caves were thus significantly developed under older ice-dammed lakes formed at the beginning or end of Weichselian interstadials, or perhaps during Saalian events. If they did originate during the Saalian or earlier, the epigean nature of all these caves that lie close to the surface indicates that they may be the surviving lower levels of older caves subjected to considerable synchronous removal of the overlying limestone.

9.6.4 Development during final deglaciation or earlier

Table 8.4 lists many of the caves that were inundated by sea water during the final Weichselian deglaciation, i.e. those with GS=C, D or E. Those relict and combination caves with marine-enlarged entrances must have had entrance passages in place prior to the passing of the ice margin and the cave's submersion. The relict phreatic passages in such caves were therefore developed to present dimensions under the final Weichselian deglaciation ice-dammed lakes, or earlier. As expected from the description of the TDMO standard cave development model (section 9.2.4), there are no marine-enlarged *vadose* entrances, as, obviously, vadose conditions only came into existence during the Holocene, or only after a cave emerged above sea level. Because there are also no known relict vadose entrance passages dating from the Eemian, there are also no known examples of marine-enlarged Eemian vadose entrances.

A lack of obvious marine modification of an entrance cannot be used alone to infer that the passage development post-dates the post-glacial marine inundation. For example, **Neptune's Cave** (Z2) contains barnacles on the walls of its relict phreatic passages that are dated to 9900±110 ^{14}Ca BP (Table A5.1; Appendix D5.3). This proves that the passage was fully developed prior to submersion, yet none of the four cave entrances show marine enlargement. This may be because three entrances are shaft tops, and the small resurgence entrance (protected by a boulder ruckle) formed after emergence above sea level.

Also, some other unmodified cave entrance altitudes listed in Table 8.4 are so close to the deglaciation marine limit that there was insufficient time for marine enlargement before these caves rose above sea level.

Section 8.9.4 considered the enlargement of cave entrances above marine limits by dissolution and freeze-thaw cycles as ice-dammed lakes lowered or rose past them, and gave many examples over a large range of altitudes. However, an entrance enlarged by a descending IDL does not provide an additional timescale constraint, because the entrance passage probably developed to its internal size beneath the same IDL. A tall entrance, enlarged by a rising IDL, would indicate an entrance passage that was already formed before the onset of glaciation, but there are no confirmed examples of this.

9.6.5 Development after final deglaciation

Section 9.2.4 deduced that all mainly vadose caves developed to present dimensions during the Holocene interglacial. Several MV caves at GS=C, D or E are listed in Table 8.4, including the Holåsen and lower Hestfjell caves (Z2), and none has a confirmed enlarged entrance, thus not contradicting the timescale of development after emergence above the sea. Other enlarged entrance passages have active vadose entrenchment of an originally phreatic tube, commonly, but not always, displaying a 'keyhole' cross-section (e.g. **Green Gorge Cave**, Klausmark, Z2; Photo 9.2). These suggest that after the marine enlargement of the phreatic part of the entrance, the subsequent vadose development has only occurred during the Holocene.

Photo 9.2 Entrance to Green Gorge Cave (Z2)
An originally-phreatic entrance was enlarged by wave action before being entrenched during the Holocene. Photo by P. Hann.

Section 5.5.5 deduced that the active vadose parts of resurgence caves situated at knick points above surface waterfalls (with sink entrances commonly at CL=S) probably developed entirely within the Holocene. If the vadose streamway had originated in the Eemian, then Holocene flow would likely be along a deeper set of fractures, leaving a relict vadose passage above, of which none are known.

9.6.6 Extension to caves above the marine limits

The above sections mainly considered caves that lie *below* the glaciation and deglaciation marine limits. Although caves of all hydrological classes exist in nearly all glacial situations (section 5.5.6), it is only those at lower altitudes that can provide timescale constraints from the marine enlargement of entrances. It is however logical to extend the range of development sequences and timescales to caves that lie above the marine limits as well. Thus, it is concluded that in *all* relict and combination caves at all altitudes, those phreatic passages that are now relict were fully developed *prior* to the end of the final deglaciation, and that *all* mainly vadose caves and the active streamways in the combination caves were only developed to present dimensions *after* the final deglaciation. The extreme rarity of speleothems in mainly vadose caves and other active stream passages (Appendix B2.9) is therefore explained by the short time available for their growth, coupled with dissolution and mechanical destruction during Holocene floods.

9.7 Truncated and half-loop caves

The previous section showed that the TDMO model of cave development can be overlaid with the enlargement of entrances for caves in glacial situations that lie below the marine limits. This section explores the influence that other external cave attributes have on internal cave morphology, especially the apparent truncation of phreatic loops.

Table 9.1 lists caves whose survey sections exemplify many elements of the TDMO model. As expected, these caves are predominantly the more complex cave types, especially type h, and they consist of both relict and combination caves. The list includes examples with R=0 and 1, and with T=0 and 1, and includes all main karst types. The caves occur in all well-populated glacial situations. All cave locations are represented (except CL=C), as are all slope relationships and orientations (except OR=N). This wide spread of external attributes confirms that the full TDMO model applies to combination caves throughout the study area, and subsets of it also apply to relict caves and to mainly vadose caves.

Few cave passages contain *multiple* phreatic loops (section 5.7.2) and the cave survey sections reveal that many caves do not consist of fully-symmetrical single phreatic loops, but contain instead a tiered series of 'half loops', or other 'incomplete' loops. The last column in Table 9.1 provides information on the extent of exploration, the apparent extent of truncation and the open or closed nature of the termination. Only those phreatic loops identified as 'A' are surveyed as fairly-symmetrical complete loops. In four cases exploration is probably incomplete in an 'up-valley' direction ('B'), whereas in seven cases exploration appears incomplete 'down-valley' ('C'). This larger number may arise because down-valley

relict phreatic passages tend to be somewhat smaller than up-valley passages, which can gain size with vadose entrenchment (section 9.2.4). For cases B and C, there may be no truncation of the identified passages, although other passages in the same cave may be truncated.

Table 9.1 Examples of the TDMO model

CAVE	Z	R	T	GS	CL	KT	SR	OR	CT	VR m	Notes
Klausmark System	Z2	1	0	E/H	R	A	N	P	h	50	F(O)
Two Bridges Cave	Z2	1	0	K	W	A	D	P	h	36	B F(O+C) RC
Tourist Cave	Z2	0	0	E	G	A	N	P	g	20	A RV? Shallow loops
Svartdalgrotta	Z2	1	0	E/H	S	L	D	P	h	53	C F(O) RV?
Neptune's Cave	Z2	1	0	E	W	A	D	P	h	33	A F(O) Steep loops
Balcony Cave	Z3	0	0	H	W	A	D	P	f	18	A F(C) RC Shallow loops
Toerfjellhola	Z3	0	0	K	R	V	N	A	h	101	F(C) RV?
Øyåskjeleren	Z4	0	0	H	S	V	N	P	f	15	B F(O) RC Shallow loops
Sirijordgrotta	Z4	0	0	H	G	V	N	P	h	78	F(O) RJ 3 outlet levels
Håpgrotta	Z4	0	0	L	G	A	U	P	h	20	A RV?
Green Valley Cave	Z4	0	0	T	S	V	N	O	e	8	A B RV Shallow loops
Kvitfjellgrotta	Z4	0	0	L	S	C	N	O	h	22	F(O+C)
Pustehola	Z4	0	0	L	W	A	U	P	h	28	C Mainly relict Steep loops
Gevirgrotta	Z4	0	0	L	R	A	N	P	h	27	A RV Shallow loops 3 outlet levels
Gåsvasstindhola	Z4	0	0	T	R	V	N	P	d	13	F(O)
Sarvejaellagrottene	Z4	0	0	L	W	A	U	P	h	55	A RJ RC + vadose trench
Jegerhullet	Z4	0	0	L	F	A	N	P	h	34	C F(C) R RV
Etasjegrotta	Z4	0	0	L	F	V	N	P	h	42	A C Shallow loops
Øyfjellgrotta	Z5	0	0	H	W	A	D	P	h	105	F(O) RJ Large RV?
Møllebekkgrottene	Z5	0	0	E	G	A/V	N	P	g	20	C F(O) V. Shallow loops
Geitklauvgrotta	Z5	0	0	H	G	V	N	P	h	16	E(C) V. Shallow loops
Trench Pot	Z5	0	0	L	W	A	U	P	b	25	F(O) RJ RV
Blåfjellgrotta	Z5	0	0	T	R	V	N	P	h	31	F(C) RJ Shallow loops
Høgligrotta	Z6	0	0	E	S	A	D	P	f	33	F(C) Steep loops
Grønndalsgrotta	ZA	0	0	K	S	L	U	P	g	70	C E(O+C) RV
Sotsbäcksgrottan	KU	0	1	L	P	L	N	A	h	110	C E(C)
Korallgrottan	KL	0	1	L	F	A	N	P	h	144	B F(O)

Key

A	Contains symmetrical phreatic loop(s)
B	Possibly has unexplored 'up-valley' phreatic loop continuations
C	Possibly has unexplored 'down-valley' phreatic loop continuations
D	Phreatic loop(s) are truncated up-valley
E	Phreatic loop(s) are truncated in the middle
F	Phreatic loop(s) are truncated down-valley
(O)	Truncation at an open entrance, or where daylight is visible, or where there is a strong draught
(C)	Truncated passage is closed by a boulder choke or sediment fill
RJ	Rejuvenation during Holocene interglacial
RC	Relict Cave (all other caves are combination caves)
RV	Contains relict vadose passage

Truncation of phreatic loops occurs primarily at the down-valley and rising ends of the caves, although there are three cases of truncation near the middle. In no case does a *major* truncation occur at the up-valley and descending end of a cave, although some shortening of upper (and lower) entrance passages by glacial ice is suspected, e.g. at **Pustehola** (Elgfjell, Z4). The best example of a half-loop cave is **Toerfjellhola** (Z3; Figure B1.3). This has six tiered phreatic passages at the down-valley end of the cave (including the lowest, sump, level) that are all choked near the start of their rising limbs. These passage

terminations lie up to 50m directly beneath a dry valley floor that is littered with scree and huge talus slopes (Appendix D3.3; Photo D3.5).

In both cases of a presently-open and a presently-closed incomplete phreatic loop, it might be considered feasible that truncation could have been produced by large-scale glacial valley deepening or widening, after formation of the passage. Open entrances that emerge at a steep slope (as is commonly the case), or that were enlarged by marine activity, might survive without a significant blockage. However, another possibility is that such phreatic passages only developed as incomplete half-loops, when the cave hydrology was integrated with that of an ice-dammed lake and the remnant icesheet, as discussed in section 8.6 and illustrated in Figures 9.1a,b,e and f. For both possibilities, any continuing 'passages' are now 'virtual', having been removed: glacial truncation removing the limestone containing rising limbs of passages, and the falling limbs of any Röthlisberger conduits disappearing with the melting away of the ice sheet.

In the case of **Toerfjellhola**, at least, the possibility that complete phreatic loops developed before being removed by glacial erosion seems very unlikely on two counts. Firstly, there is no indication that the limestone outcrop continued in the required direction, and secondly, if the valley floor was much higher than at present, then the lowest level passage formed at a distance greater than 50m from the surface, which would be exceptional for caves in VSK, and would violate the one-eighth relationship. Thus, considering also the discussion about the large Tverrfjell IDL in Appendix D3, it seems likely that the phreatic half-loop passages developed to their present sizes under one or more westward-flowing IDLs. Similar arguments also apply to those other caves in Table 9.1 that have incomplete phreatic loops. For example, **Kvitfjellgrotta** (Z4) is located at CL=S above a waterfall, 200m above an orthogonal valley floor (Photo C2.4). It would surely have been eroded away synchronously with valley deepening if it existed before the valley was formed. Hence, the degree of symmetry of phreatic loops in the study area caves is approximately inversely-related to the slope of the surface above the cave, at the time of passage enlargement. This constraint does not follow directly from the one-eighth relationship, because it is possible to envisage almost symmetrical phreatic loops that could be both steeply inclined at each end and yet bound within a fixed distance to a steep external surface slope. These do not occur, because the direct fracture length from the base of each loop to a steeply sloping surface is always less than the path length of a steeply rising set of fractures up to the surface, and breakthrough and enlargement occur at the shorter inception fracture first.

The common lack of vadose entrenchment of the down-valley ends of phreatic loop passages (section 9.2.4) also confirms that a sudden collapse in the level of the IDL was the normal outcome, rather than a gradual lowering, which would have permitted vadose flows through each tiered passage in sequence. This reasoning supports the idea that the large talus slopes that block the rising passage limbs in

Toerfjellhola (Photo D3.5) were carried there by the jökulhlaups from the backward-flowing IDL east of Jordhulefjell (Appendix D3.3), and that they did not simply arise from glacial erosion.

Symmetrical and asymmetrical loops can each occur in any karst type, with any slope relationship, any orientation, and in any cave location. (However, the few loops truncated in the middle only occur with CL=P, G or S). This is not surprising, because the cave location is assigned to the location of the highest cave entrance, at the up-valley end. In the case of the longer, more complex, caves, the topography at the down-valley end of the cave can be quite different. Indeed, the caves in Table 9.1 with asymmetrical phreatic loops ('F') all have down-valley ends at CL=W or F, which commonly differ from the cave locations at the upper ends of the caves. On the other hand, the caves with symmetrical loops ('A') tend to have both ends in similar cave locations.

These observations expand the hypothesis in section 7.1, that the (external) evolution of an epigean central Scandinavian cave is integrated with the geomorphological evolution of its locality. It is now clear that the pre-existing local topography exerts a great influence on the development of the *internal* cave morphology as well. Thus, in order to understand the internal cave development processes, including the symmetry of phreatic loops, it is necessary to consider each cave and its local geomorphology individually.

9.8 Multi-cycle caves

Section 9.2.4 deduced that most caves in the study area developed to their present size only during the last glacial cycle: single-cycle caves. That is, inception fractures created during seismic activity at the Weichselian deglaciation (possibly reinforcing those produced during the Saalian and earlier deglaciations) were mainly enlarged under IDLs during the Weichselian deglaciation, to create the present relict phreatic passages of the relict and combination caves. This development was followed by vadose entrenchment of the lowest phreatic passages in combination caves during the Holocene, and the vadose exploitation of other, low-level, fractures throughout the Holocene in both combination caves and mainly vadose caves. This section considers possible examples of present caves that still contain passages that were developed to explorable sizes during the Saalian deglaciation and Eemian interglacial or earlier: multi-cycle caves.

9.8.1 Diagnostics for multi-cycle caves

As discussed earlier in this thesis, there are several possible attributes of the caves that may be used to determine constraints on development timescales. The most obvious is the direct dating of internal cave chemical, clastic, marine and animal deposits, as a passage must be in existence prior to such material being deposited. This method has been applied in a few study area caves (Appendices A5 and B2.9–B2.12), but the extreme rarity of substantial stalagmitic material has limited its usefulness. Similarly, evidence of dissolution of pre-existing speleothem could indicate a return to phreatic conditions after an

interglacial or interstadial growth phase, but few such reports are known. Indeed, the rarity of large speleothems and flowstones (Appendix B2.9) is itself indicative of the immaturity of most of the caves, as large speleothems take time to grow, and only large speleothems could have survived the large deglacial floods at the end of the Weichselian and earlier glaciations. Thus, the great majority of small stalagmites and stalactites (that commonly reach only 30cm in length) grew entirely during the Holocene.

Other diagnostic indicators are geomorphological, which may be interpreted to provide evidence of the sequence of cave development. Thus, large relict vadose (RV) passages could indicate their development during the Eemian (or an earlier) interglacial, especially if clearly accompanied by subsequent phreatic, paragenetic, or vadose enlargement. The best example in the study area may be the Upper Galleries in **Øyfjellgrotta** (Z5), but these have not been studied by the author. Discordant upper vadose levels or hanging potholes (section 3.2.1) above active streamways would suggest entrenchment in an earlier interglacial, as occurs at **Sirijordgrotta** (Z4; Appendix B2.7; Photo B2.1). However, the absence of large RV passages does not deny the possibility that *phreatic* passages enlarged during the Saalian (or an earlier) deglaciation, as such caves may have remained relict during some succeeding interglacials. Paragenetic enlargement of roof-tubes in phreatic passages is more difficult to interpret in terms of whole glacial cycles. Entrance passage truncation at either end of a cave may be related to the glacial erosion of the surface, if this is known or can be deduced. As considered in section 8.8.3, the enlargement of cave entrances that lie above the deglaciation marine limit must indicate Mid or pre-Weichselian passage formation, especially if the entrance is extremely tall. Isacsson (1999) pointed out that varved clay on fallen blocks indicates a glaciation subsequent to deglacial seismicity. Finally, the dimensions of a cave may be diagnostic of age. For example, the larger is the cross-section of a phreatic passage, then the longer it took to form by dissolution in unsaturated conditions. It follows that older, higher, phreatic passages, which experienced dissolution beneath more deglacial IDLs than younger, lower, passages in a cave, should be larger, if they had not subsequently become sealed at one end. Thus, in multi-cycle caves, phreatic passage diameters should commonly increase upwards (section 7.3). Deep caves may exploit tectonic inception fractures created by several deglacial seismic events. Long and deep caves of great complexity may have experienced more development episodes, and therefore be older, than simpler caves. However, as discussed for the TDMO model, tiered passages may develop synchronously, and thus create complex caves even during a single glacial cycle.

9.8.2 Multi-cycle candidates

Table 9.2 lists study area caves that are potential candidates as multi-cycle caves, by utilising the various diagnostic strands of evidence discussed in section 9.8.1. Detailed studies would be required at each individual cave before firmer conclusions could be reached. **Two Bridges Cave** (Z2), **Sarvejaellagrotta** (Z4) and **Øyåskjeleren** (Z5) are relict caves. All the others are combination caves.

Table 9.2 Multi-cycle candidates

CAVE	Z	R	T	GS	CL	CT	VRm	Evidence	'Age'
Klausmark System	Z2	1	0	EH*	R	h	50	Re-dissolved 'Twiglet' speleothems? Sealed 'Twiggy Passage' may predate lower levels and upstream cave	Saalian degl.
Two Bridges Cave	Z2	1	0	K	W	h	36	Cross-sections increase upwards	Saalian degl.
Tourist Cave	Z2	1	0	E*	G	g	20	Possible RV passage beyond streamway	Saalian degl.
Neptune's Cave	Z2	1	0	E	W	h	33	Cross-sections increase upwards	Saalian degl.
Toerfjellhola	Z3	0	0	K	R	h	101	Union and other Passages may be partly RV. Lower Entrance passages may predate most of cave. Some cross-sections increase upwards. (Appendix D5.2)	Pre-Elsterian ?
Øyåskjeleren	Z4	0	0	H	S	f	15	Marine enlargement of phreatic entrance at end of Eemian	Saalian degl.
Sirijord-grotta	Z4	0	0	H	G	h	78	Arctic Passage probably led to Holstein interglacial outlet. XS increase upwards. Stalagmite date c. 128ka BP (Lauritzen and St.Pierre, 1982). Main Entrance = Eemian outlet	Elsterian degl. Saalian degl.
Eiterådal Res. Cave	Z4	0	0	H	G	b	4	Entrance at similar altitude to Sirijordgrotta Main Entrance: probably also active in Eemian	Saalian degl.
Håpgrotta	Z4	0	0	L	G	h	20	Possible rejuvenation below older 'Safe Entrance'. Cross-section increases upwards.	Saalian degl.
Brown Stains Cave	Z4	0	0	L	W	g	34	Cross-sections increase upwards	Saalian degl.
Sarvenvårtoe hullet	Z4	0	0	L	R	g	24	Cross-sections increase upwards	Saalian degl.
Gevirgrotta	Z4	0	0	L	R	h	27	RV passages at 2 levels (section 9.3): 1. Upper Inlet Passage. 2. Tooms Revenge. Also, 12m headward erosion of steep cascades in Holocene.	Elsterian degl. Saalian degl.
Gåsvasstind-hola	Z4	0	0	T	R	d	13	10m passage diameter of relict phreatic passage, with breakdown. Dissolution beneath multiple IDLs, perhaps during interstadials?	Saalian degl.?
Sarvejaella-grottene	Z4	0	0	L	W	h	55	Possible valley lowering below previous 'Joint Entrance' resurgence.	Saalian degl.
Jegerhullet	Z4	0	0	L	F	h	34	Possible valley lowering below presumed 'Angel's Walk' resurgence.	Saalian degl.
Etasjegrotta system	Z4	0	0	L	F	h	42	XS do not increase upwards. (Appendix D5.5)	Weichsel degl.?
Rockbridge System	Z4	0	0	L	F	f	27	Invasjonsgrotta is primarily relict, but probable Eemian flow route of the Jordbruelv. (Appendix D5.5)	Saalian degl.
Anastomose-grotta	Z4	0	0	L	F	e	20	High level route may be Eemian flow route	Saalian degl.?
Øyfjellgrotta	Z5	0	0	H	W	h	105	Marine enlargement upwards of phreatic entrance at end of Eemian. Large RV 'Upper Galleries' were therefore entrenched one cycle earlier, during Holstein interglacial.	Elsterian degl.
Geitklauv-grotta	Z5	0	0	H	G	h	16	Truncation of 'Wasp Nest Passage' by valley widening. Two stages of phreatic enlargement at Split Arch (Photo D1.29). Eemian marine enlargement of Lilleelvgrotta. Large diameters.	Saalian degl.
Blåfjellgrotta	Z5	0	0	T	R	h	31	Possible valley lowering below relict 'Bold Step Chamber' resurgence.	Saalian degl.
Ytterlihullet	ZA	0	0	S	S	d	180	RV 'Inlet Passage'. 10m entrenchment and 14m headward erosion of waterfalls in Lower Stream Passage.	Saalian degl.

Grønndals-grotta	ZA	0	0	K	S	g	70	RV 'Over etasjen'. Large diameter. Stalagmite date 148–91ka BP (Lauritzen & Gascoyne, 1980).	Saalian degl.
Sotsbäck-grottan	KU	0	1	L	P	h	110	Surface lowering below 3 separate but presumed contemporaneous relict resurgences.	Saalian degl.
Korall-grottan	KL	0	1	L	F	h	144	Flowstone dated between 127–140ka BP (Sundqvist, 2002). Presumed Eemian rising at Ingangsdolinen. Cross-sections increase upwards. Varved clay on some fallen blocks among clean blocks (Isacsson, 1999), who thought that the cave reached its present size c. 1Ma BP.	Elsterian degl.

* Enlarged entrance(s) indicate at least pre-Holocene enlargement of phreatic passages.

The occurrence frequencies of caves in this list are much higher for CL=R and S, and lower for CL=F and P, than for the full set of caves. This bias probably follows the tendency of type h caves (section 5.3.4) and the 12 longest and the 12 deepest caves (section 5.3.6) to occur preferentially in steeper topography. This is where seismic shocks were amplified (section 6.5.3) and where interglacial hydraulic gradients are comparable with those investigated in quarries with rapidly-forming dolines (Gunn and Gagen, 1987; section 3.1.14). It is also concluded that glacial erosion was highest in valley bottoms, so that multi-cycle caves were less likely to remain there. Indeed, it is the half-cycle mainly vadose caves that are concentrated at CL=F (Table 5.27). Additionally, downward and outward glacial erosion at ridges and valley shoulders appears to have been small enough to permit the survival of at least some of their pre-existing passages. Taking the assumed valley floor lowerings at **Sirijordgrotta** (Z4) of 40m and 30m in the Saalian and Weichselian glaciations as being typical for large N–S aligned glacial valleys in the study area (section 7.1), it is assumed that valley wall retreat rates per glaciation decreased upwards from these maximum values.

The 'Age' column in Table 9.2 indicates a minimum age for the first deglacial enlargement of the oldest surviving passages. These are commonly centrally-situated relict phreatic passages closest to the surface. Their first tectonic fractures may have been created at a deglaciation previous to the period indicated. All these caves probably connected previously to even older passages that were at higher levels relative to basement rocks, but which were since eroded away. However, the majority of the enlargement of most remaining relict passages probably occurred under IDLs during the Weichselian deglaciation. Most active passages achieved most of their enlargement during the Holocene. Despite the dimensions and complexity of **Labyrintgrottan** (ZC), there is presently insufficient evidence to confirm that its existing passages developed prior to the Weichselian. The CT column in Table 9.2 shows that the multi-cycle candidates comprise the more complex cave types (d–h), which commonly form the longer caves. There may therefore be a rough proportionality between the length of a cave and its age.

9.9 The dynamic internal cave development model

This Chapter has now described the dynamic TDMO model of internal cave development. This shows that, in the most complete cases, karst caves primarily developed downwards by enlarging inception fractures during alternate periods of sub-IDL phreatic development and interglacial primarily vadose development. The basic principle of the model applies to dissolutional caves in all metamorphic karst types, in all glacial situations, and in all cave locations, everywhere in the study area, for all time since the onset of the late Tertiary glaciations. There is no evidence that any remaining cave passages developed in the Tertiary and were later truncated by Pleistocene glaciations. Reasonable estimates can be made that allow the development of the local topography and the internal structure of a cave to be deduced, and fitted within the timescales of at least the last few glacial cycles. It should not now be necessary to await the dating of internal sediments, if available. Instead, such fortuitous datings can be considered as a check on the scheme derived, rather than as a start-point.

Each cave is involved in a 'race' to develop deeper, before surface erosion (mainly) during glaciation removes its upper levels. The 'half-cycle' mainly vadose caves started this race sometime during the Holocene. They may be the last of a generation of *palaeocaves in the sky* that once existed at higher levels in the same limestone outcrops, but which lost the 'race', having been eroded away before the end of the Weichselian glaciation. Most of the relict (phreatic) and combination (phreatic and vadose) caves of the area have survived so far for just a 'single-cycle', with their uppermost relict phreatic passages enlarging to their present size during the Weichselian glaciation and deglaciation. Again, there may be lost generations of palaeocaves that were once situated above them. The rarity of significant karst cave passages that survived from the Eemian interglacial is in agreement with the extreme rarity of karst caves in the GS=G or H glacial situations that have very tall entrances, as only **Øyfjellgrotta** (Z5) is known. In just a few cases, as postulated in Table 9.2, some present caves can be shown to have survived for more than a single glacial cycle, but in only four cases is it likely that the oldest existing passages experienced *three* major deglaciations. This is in contrast to some caves farther north in Norway, which contain passages that may be over 1Ma old, from stalagmite dating (Appendix A5.3). The probable explanation for the relatively younger age of the oldest passages in the study area is twofold. The area occupies a saddle position between the higher mountains of northern and southern Norway (section 2.3.3). The relief is less dramatic, and hence inception fractures and enlarged cave passages penetrate less deeply, based on the one-eighth relationship. However, the area is also subject to higher glacial erosion, and thus the older pre-existing passages have been removed, both absolutely and proportionately, to greater depths than farther north, restricting the age range.

Although it is hypothesised that the TDMO model of development applied throughout the Mio–Plio–Pleistocene glaciations, because the Holocene is apparently the longest-lasting of the most recent five interglacials (Figure 2.4), and may indeed be the longest-lasting interglacial since the Mid Pleistocene Revolution, the extent of vadose entrenchment in previous interglacials must have been less than is

witnessed in the present active caves. This may go a long way to explain the rarity of large relict vadose passages in the upper levels of the explored caves. It probably also means that the occurrence of, and all the dimensions of, the present caves are greater than for any previous Quaternary interglacial. An additional consideration is that, according to the one-eighth relationship, the depth of inception fractures has increased with the repeated deepening of each glaciated valley (section 7.3), again leading to the conclusion that the present set of caves is deeper, on average, than during any earlier interglacial. Thus, the present caves are larger in every way than those that could be visited in previous interglacials, and may consist of proportionately more vadose enlargement than has occurred at any time since the Mid Pleistocene Revolution.

In the warmer climates before the advent of the late Tertiary glaciations, speleogenesis beneath ice-dammed lakes was not possible, and so the karst caves of Scandinavia were then all mainly vadose in character. Seismic and non-seismic tectonics was not driven by rapid postglacial uplifts, but by more deep-seated and long term processes. Inception fractures probably penetrated less deeply. On the other hand, the evolution of karst caves would have been in tune with the reduced erosion of a more arid landscape, but over much longer periods of time. The result may have been that dendritic mainly vadose caves of cave types a, b, c, and d developed as relatively superficial narrow canyons with sporadic phreatic sections, which were able to entrench below the fracture depth where the topography was favourable. In time, steady-state conditions may have been reached, where the rate of entrenchment kept pace with the rate of surface lowering, so that streamways became deep unroofed grykes in their upper parts.

Five important study area karst systems are analysed with respect to the four models of cave development in Appendix D5. These studies show that a single set of inter-related processes can be used to explain cave existence in the central Scandinavian Caledonides. The strength of the explanation is confirmed because a history of cave development consistent with the gathered evidence is derived in each case, without needing to go beyond the proposed concepts. Chapter 10 illustrates how the same models, with some local extensions, explain karst development in the other Caledonide terranes.

CHAPTER 10 THE CALEDONIDE MODEL

Chapters 5–9 established the various models that describe the inception, development and removal of caves in the previously-glaciated metalimestones of central Scandinavia. This Chapter explores the extent to which these models also apply to karsts within the other glaciated terranes of the Caledonides (Figure A1.1). It is beyond the scope of this thesis to examine these regions to the same level of detail as undertaken in the main study area. They are therefore discussed more briefly in Appendix D6, by considering specific examples known to the author, by sampling on a selective basis, and by literature review. The aim is to establish if there is a *prima facie* case that cave existence in these other areas follows the processes already proposed for central Scandinavia, and to develop a more general model for cave development throughout the metacarbonates of the whole Caledonide system.

10.1 Scandinavia

Appendix D6.1.1 reviews the caves in the valley of Gråtådal and provides a preliminary discussion about four major cave systems in other parts of northern Scandinavia. Although the subsurface cave distances of the caves of Gråtådal lie within the one-eighth relationship (section 6.5.2), the mean cave dimensions are much greater than those of the main study area. The larger mean vertical range is accounted for by the greater tectonism visible in the valley, which probably arises from its considerable depth, and the much greater passage sizes are caused by enhanced recharge from permanent glaciers, especially in the active caves. It is therefore concluded that the caves in Gråtådal developed over the same timescales and glacial cycles as the caves in the main study area, but that post-glacial phreatic enlargement of relict caves persisted for longer, giving them a somewhat larger size. Holocene vadose entrenchment was much more vigorous, creating the very large stream passages that exist today. The roofs of many previous sumps were also raised above water level by a combination of chemical and strong mechanical erosion, and resurgence sumps were lowered by the faster down-cutting of the external pocket valleys, to create more caves of the 'late interglacial' stage of the TDMO model (Figure 9.1i). There may have been no remnant glaciers during the previous interglacial, because of an elevated temperature during the Eemian, so that *glacial recharge enhanced* vadose enlargement did not then occur. This could explain why, although relict vadose passages of possible Eemian age occur in Gråtådal, they are not particularly large.

A contrast can be made between the rather long and deep caves in Gråtådal, and the plateau of Glomfjell, which lies just 15km to the west. Glomfjell comprises some 200km^2 of high-grade metalimestones, also of the Beiarn Nappe (but with commonly a low-angle foliation). However, the caves there only reach c. 500m in length and 50m in depth, and much less in subsurface cave distance (e.g. Corbel, 1953; St. Pierre, 1984). The likely reason is that the plateau setting, with distant, isolated, peaks at c. 1100m above lakes at c. 500m did not provide the conditions for the large deglacial seismic shocks experienced in Gråtådal, despite the area being surrounded by high neotectonic activity (Figure 6.1). Additionally, the lateral extent of the limestone does not reach beyond the plateau itself, and hence does not encounter the

lower valley sides towards Glomfjord, which might otherwise have acted as discharge points. The longer caves appear to be mainly vadose in character, and therefore to have formed within the Holocene. The short relict phreatic caves probably formed beneath an active IDL during Weichselian deglaciation, after Weichselian glacial erosion towards Glomfjord removed most pre-existing karst systems.

The inception and evolution during successive glacials and interglacials of three of the four major systems discussed in Appendix D6.1.1 have yet to be analysed in more detail by any authors. From these brief observations, and from the limited study of the caves in Gråtådal, there seems no reason to suppose that most of the caves in northern Scandinavia in amphibolite grade VSK or ASK have not developed according to the conceptual models proposed for the main study area. Some suitable local interpretations may be required, such as enhanced vadose entrenchment for systems that still experience recharge from glaciers and permanent snowfields.

However, at least three deep caves in northern Norway dramatically breach the proposed one-eighth relationship. Two of these (**Tjoarvekrajgge** and the **Okshola / Kristihola** system) are rather similar, as they occur in only medium metamorphic grade low angle karsts, and they both form maze networks of great total length and significant depth. The deepest cave in central Scandinavia (**Ytterlihullet, ZA;** 180m deep) has also formed in low angle karst (although it is in high-grade metalimestone and still follows the one-eighth relationship). Thus, it seems likely that endokarst formation in low angle marbles is more likely to favour fractures that are aligned with the foliation, and can thus carry water to deep outlets, if the local topography is (stochastically) beneficial. In these cases, the fractures act more like the inception horizons of sedimentary limestones, so that chemical inception may become more important than tectonic inception, especially if the limestone is less-highly metamorphosed.

The case of the **Greftkjelen / Greftsprekka** system is entirely different, because it is formed in complexly-folded marbles of high metamorphic grade. Here, inception does seem to be tectonic, with the synclinal / anticlinal folding enhancing the formation of deep, probably open, joints. It is suggested here that the prime tectonic activity that opened these joints may not be related to the deglacial seismicity that is caused by rapid uplift. Rather, it may be caused by much longer-timescale, possibly aseismic, processes, such as the general uplift of the Scandinavian landmass, or the spreading of the Atlantic Ocean. Thus, with a completely different process involved, the one-eighth relationship does not apply, and such a mechanism may also contribute to the depths of **Tjoarvekrajgge** and **Okshola / Kristihola.**

The dimensions of the largest northern caves are much greater than those in central Scandinavia, and so (probably) are the mean dimensions of all these caves. The likely reason is the significantly greater seismic activity north of Ranafjord (Figure 6.1). Increased frequency and magnitude of neotectonic and postglacial earthquakes means that the one-eighth 'limit' can be approached more closely in more areas, so increasing the overall lengths and densities of inception fractures, thereby providing larger frameworks in which individual cave systems can develop. In particular, the deepest and longest caves

briefly discussed above all lie within regions of greatest neotectonic activity. Because the mountains are higher, it is also likely that caves enlarged beneath deglacial IDLs for longer periods of time, resulting in larger cross-sections. The author also has the impression that there are proportionately more multi-cycle caves in northern Scandinavia, as supported by the greater ages of some dated speleothems (up to 800ka: Table A5.1). These may survive because reduced glacial erosion away from the central 'saddle' area (section 2.3.3) preferentially allowed older, higher, passages to remain farther north. However, Lund and Eraso (1989) remarked that the karst in Glomdalen is (also) shallow, depths mostly being 40–50m.

The discussion about marine limits (sections 8.1.2 and 8.1.3) also applies to northern Norway. The map by Sørensen *et al.* (1987) shows that the YD isostatic uplifts at various karst areas are as follows (south–north): Burfjell, 110m; Røvassdal, 150m; Dunderlandsdal, 180m; Saltdal, 170m; Fauske, 140m; Hellemofjord, 140m. Thus, many local caves below these altitudes potentially have entrances enlarged by marine action. The large (c. 10m high) Resakjelen entrance to **Setergrotta** in Røvassdal, at an altitude of 100m, probably formed at a time of rising sea level at the end of the Eemian, in the manner described in section 8.1.3, with further enlargement during deglaciation. The two huge tapering entrances of **Okshola** and **Kristihola** at 160m altitude (commonly dry with large boulders on their floors) have almost certainly been enlarged by marine activity. They were probably above the reach of storm levels when the sea invaded after the start of the Holocene, because the YD isobase in this area is at about 145m. However, both are good candidates for enlargement upwards by a rising sea level at the end of the Eemian.

The conclusion to be drawn from the overview of karst caves in *southern* Scandinavia (Appendix D6.1.3) is that there is nothing remarkable about them, when compared to the caves in central Scandinavia, despite the poorer quality of the information used. It thus seems reasonable to assume that their cave inception and development followed the same processes described for the main study area. The data also hint that, as well as the maximum subsurface cave distance being determined by the depth of the local valley, the mean length and depth of caves may be similarly influenced.

10.2 New England

The marble caves of New England (Appendix D6.2.3) are commonly contained within small lenses of merokarst with low angles of foliation, giving their surveys a different appearance to those of many caves in north central Norway. The Quaternary glacial history is similar to that of Scandinavia and the area provides much evidence of deglacial IDLs. Deglacial seismicity is confirmed by the existence of many talus and fracture caves and by movements within the karst caves themselves, which are suggestive of tectonic inception. The mean lengths, cross-sections and volumes are rather smaller than in central Scandinavia, but the mean vertical range is comparable and subsurface cave distances consistently lie within the one-eighth relationship. There are proportionately less mainly-vadose caves, but they have larger cross-sections than the MV caves of the main study area, perhaps indicating a longer period of interglacial conditions.

Generally, it is concluded that the relict and combination caves are single-cycle caves. They commonly have less vertical complexity than those in central Scandinavia, and therefore do not contradict the principles of the TDMO model of cave development. The few mainly vadose caves are half-cycle caves, which enlarged to present dimensions after the Wisconsin deglaciation.

10.3 British Isles

In the British Isles, the Caledonide terranes comprise the Dalradian Supergroup in Scotland, Ireland and the isles of Shetland, which are described in Appendix D6.3. The geological setting in the three areas is remarkably similar to that of the Helgeland Nappe Complex in north central Norway, with many long linear outcrops of high metamorphic grade vertical or angled strike karst. The Pleistocene glaciations were probably less intense, especially at Shetland, and deglacial IDLs more short-lived. Evidence of deglacial seismicity is well reported but less widespread, with fewer reports of talus and fracture caves, for example. However, the author has always been successful when looking for signs of tectonic movement in the Scottish marble caves.

Scotland (Appendix D6.3.1–D6.3.3) contains many karst caves in the Dalradian Supergroup, but, although the proportion in each hydrological cave class is similar to that in central Scandinavia, they have much smaller mean dimensions. It is concluded that all the relict, and probably most of the combination, caves are single-cycle caves. They commonly have less vertical complexity than those in central Scandinavia, and do not contradict the principles of the TDMO model of cave development. The mainly vadose caves are half-cycle caves, which enlarged to present dimensions in the Holocene. Because the caves east of the centre of the Devensian icesheets have smaller dimensions than those closer to the centre, it is surmised that the depths of caves and fractures formed below much thinner ice covers are always less than the maximum allowed by the one-eighth relationship, and that they were inundated by IDLs for shorter periods of time.

Only 12 caves are recorded in the Irish Caledonides of NW Ireland and Connemara (Appendix D6.3.4), but there has been little systematic searching for caves there compared with Scandinavia, Scotland and New England. Despite the small sample size and the sparse written record, the approximated mean cave dimensions are of the same order as those in the Scottish Caledonides. It is therefore assumed that all the caves in the Irish Caledonides developed within a single glacial cycle, with any previously-existing higher passages being eroded away during the Devensian (and earlier) glaciations. It is likely that more caves wait to be found, and that the dimensional similarities with Scotland will be strengthened in future.

The absence of endokarst on Shetland (Appendix D6.3.5) may seem paradoxical in the context of the metalimestones of the Caledonides. However, when the models of cave development that are proposed in this thesis are applied to Shetland, the reason becomes clear. An obvious difference with many karstic Caledonide terranes is that the relief on Shetland is very modest. The maximum elevation difference

between the floor and ridge of a limestone valley is only 250m. This means that, based on the one-eighth relationship, the absolute maximum depth of tectonically produced inception fractures is only some 30m, and in many settings, it is much less. Also, Shetland was partly overrun by ice from Scandinavia during the Devensian glaciation, before forming its own local ice cap, which was centred on ridges less than 300m high (Flinn, 1967; Mykura, 1976). The Scandinavian icesheet was certainly 200m thick locally, because it completely overran the nearby Fair Isle. Thus, it appears that the maximum thickness of the ice on Shetland was only in the range 200–300m. This would only permit much lower intensity deglacial seismic shocks than in all the areas previously discussed, making the one-eighth relationship too generous for this setting (as in the eastern part of the Scottish Caledonides, and perhaps in Ireland).

Another difference is that, unlike in most of the other glaciated Caledonide terranes, there are no raised beaches, and the sea level is presently *rising* at Shetland. Valleys are being inundated by the sea, to create inland waterways called '*voes*'. According to Mykura (1976), this submersion has been continuous during the Holocene, and the land has been depressed by 9m since 5500a BP. The reason is that Shetland lies in the forebulge area of both Scandinavia and Scotland, so that as these lands were depressed isostatically during each glaciation, Shetland, with a thinner icesheet, actually rose. The process was then reversed during interglacials, with Shetland falling as Scandinavia and Scotland both re-adjusted upwards. The effect of this interglacial depression of Shetland is to suppress seismicity in its immediate area and to close up any previously-formed fractures. The absence of neotectonic seismicity at the Shetland Platform was noted by Bungum (1989), and can be observed at those web sites that record present and historical earthquakes. Additionally, the smothering effect of the icesheets over Shetland during its enforced isostatic uplift also suppressed seismic activity (Johnston, 1987), as did the proximity of the sea around a relatively small island (c.f. section 8.1.10). Hence, Shetland did not experience the seismic activity necessary for the creation of inception fractures in metalimestones at any time during the last glaciation. It therefore could not enter the phreatic phase of passage enlargement, whatever ice-dammed lakes were created during deglaciation, and, except sporadically in the top 2m of the limestone, has not been able to develop any karst conduits during the Holocene.

Mykura (1976) also reported the occurrence of offshore submerged platforms of probable earlier erosion surfaces at depths of 9, 24, 45 and 82m. These can be explained from the comment made in section 8.1.1 that, as a trend, the crustal rocks of Scandinavia continued to rise relative to sea level during the Quaternary, as glacial and fluvial erosion reduced the weight on the mantle. As a consequence, Shetland continued to fall by at least 82m over the same timescale, from the above evidence. Thus, previous glacial and deglacial conditions at Shetland were the same as those observed for the Devensian. Consequently, karst caves probably *never* developed on Shetland during the Quaternary.

10.4 The Arctic region

The Arctic Caledonides comprise Central East Greenland, North East Greenland, the Northern Greenland Fold Belt, Spitsbergen, and, for completeness, the small island of Bjørnøya, as described in Appendix D6.4. Karst caves have only been reported in North East Greenland sedimentary limestones and in Spitsbergen in both sedimentary and metamorphic limestones. Palaeokarst caves are also reported from both areas, and Spitsbergen exhibits present thermal activity and hydrothermal karstification.

There are three fundamental differences between the Arctic Caledonide environment and that of the other Caledonide areas discussed in this thesis. Firstly, the Proterozoic and early Palaeozoic carbonates commonly experienced less deformation and metamorphism during the Caledonide Orogeny in the Arctic terranes. This would allow greater fracturing, permeability and porosity to greater depths than in the amphibolite facies metalimestones of the HNC in north central Norway, for example. Thus, speleogenesis could be promoted more strongly in the Arctic, and any palaeokarst developed soon after deposition was more able to survive later tectonic events, as appears to be the case.

Secondly, sedimentary deposits (including carbonates) that were subsequently laid down on the Arctic Caledonide rocks survived later glacial and fluvial erosion much better then elsewhere. This author conjectures that this is because glacial erosion is primarily concentrated during *deglaciation*. Thus, in the Arctic Caledonides, with their large icesheets and ice caps that persist during interglacials, paradoxically, there has been less glacial erosion. There was also little fluvial erosion in the late Pleistocene, because of permafrost during interglacials. The consequence of the cover sequences remaining above the Arctic Caledonide carbonates is that these lower rocks were shielded from further karst development (after forming the reported palaeokarsts), whereas the post-Devonian limestones could themselves contain caves. A corollary is that in areas where the upper parts of the Caledonide metalimestones have been eroded away, any pre-Caledonide palaeokarst there that was able to survive metamorphism has also been removed. This is demonstrated by the complete absence of reported palaeokarst at the surface in metalimestones in the other studied Caledonide areas (section 3.1.6).

Thirdly, large-scale glaciations (which started at 7Ma in the Late Miocene in Greenland, according to Larsen *et al.*, 1994) and a permafrost polar climate have continued into the Holocene. The muffling effect of the present and previous icesheet and ice caps probably reduced the deglacial seismicity, thus impeding tectonic inception in the higher-grade metalimestones, reducing karstification in at least those rocks. Permafrost prevents the interglacial vadose entrenchment that forms combination and mainly vadose caves elsewhere. This is demonstrated because there are no recorded vadose passages anywhere in the Arctic Caledonides, except in NE Greenland paleokarsts, which were formed in tropical conditions. Cuffey and Marshall (2000) deduced that a greatly-reduced Greenland Ice Sheet contributed more than 4m to sea level rise during the Eemian, because of the generally warmer global climate. Thus, more carbonate outcrops may have been exposed beyond the local ice caps than at present, and the

permafrost may have been thinner. However, the absence of vadose passages in both Greenland and Spitsbergen suggests that, even during the Eemian, there was little fluvial activity.

In Spitsbergen, there is the additional major factor of hydrothermal karstification. Because of all the above differences, it is inappropriate to expect the caves and karsts of the Arctic Caledonides commonly to fit the models derived in this thesis: cave inception and development in East Greenland and in the Svalbard archipelago need to be addressed from first principles. The large phreatic passages at three levels in the valley walls near Grottedalen, NE Greenland pose interesting questions. Did they form successively, following the erosion of the valley floor downwards? Did they form concurrently along deep inception horizons during either a warmer, earlier, perhaps interglacial, Pleistocene climate? Or did they form whilst submerged beneath early Pleistocene deglacial ice-dammed lakes? (The enlarged size of the main entrance to **Grotte des Quatre** may be explained by IDL, instead of marine, enlargement). A fuller study of the geomorphological evolution of this area under the influence of glaciation, uplift, and seismic shocks is required before these questions can be satisfactorily answered.

10.5 The general Caledonide model for cave development

This section makes comparisons among the various karstic Caledonide terranes, and proposes a general model for their cave development. The data giving mean cave dimensions and internal attributes for each of the Scandinavian, Laurentian and British Caledonides are presented in Tables 10.1 and 10.2. Table 10.3 summarises the observations about each area, together with deductions about applicable processes and controls. Table 10.4 summarises major cave dimensions for each non-Arctic Caledonide terrane and provides relevant glacial and geomorphological data.

10.5.1 Applicability of the models

The preceding sections showed that the four models derived in Chapters 6–9 to represent cave development in central Scandinavia can also be utilised in most other Caledonide terranes that contain metalimestones, with some additional processes being necessary in those areas with special geological and / or climatic characteristics. However, this does not apply in the *Arctic* Caledonides, which experienced a completely different glacial regime throughout the Pleistocene.

The similarities in many mean cave dimensions and in the numbers of entrances, cave streams and sump pools per cave across all areas for each hydrological class suggest that similar processes have operated across all the non-Arctic Caledonide terranes (and not just across central Scandinavia: section 5.8.11), with two extra processes applying to northern Scandinavia, one process applying to Norway and perhaps to Ireland, and a null-process applying to Shetland.

Table 10.1 Caledonide Caves - hydrological classes and major dimensions

CAVE CLASS and AREA	No. of caves in class	% of caves in class	Total cave length in class (m)	% of total cave length in class	Mean cave length (m)	Mean cave VR (m)	Mean cave XS (m^2)	Mean cave volume (m^3)
RELICT								
Gråtådal	13	31	963	13	74	4.7	6.3	168
C. Scandinavia	280	32	9437	13	34	5.9	3.1	131
S. Scandinavia	*11*	*23*	*117*	*3*	*11*	*5.7*	*2.0*	*18*
New England	81	53	1998	22	25	5.3	2.6	75
Scotland	42	28	745	18	18	5.9	1.9	44
Ireland	*8*	*67*	*142*	*34*	*18*	*5.6*	*2.8*	*70*
RC TOTALS	**435**	**34***	**13401**	**13***	**31**	**5.7**	**3.0**	**110**
COMBINATION								
Gråtådal	14	33	4925	67	352	33.6	24.9	3372
C. Scandinavia	360	41	58995	79	164	14.5	4.8	1020
S. Scandinavia	*16*	*34*	*3454*	*81*	*216*	*17.6*	*5.9*	*1902*
New England	52	34	6189	68	117	14.8	3.1	473
Scotland	55	36	2736	64	50	8.9	2.8	175
Ireland	*4*	*33*	*276*	*66*	*69*	*12.5*	*5.1*	*314*
CC TOTALS	**501**	**39***	**76575**	**76***	**153**	**14.5**	**5.0**	**959**
MAINLY VADOSE								
Gråtådal	15	36	1474	20	98	10.2	8.8	808
C. Scandinavia	244	28	6449	9	26	3.9	2.1	62
S. Scandinavia	*20*	*43*	*667*	*16*	*33*	*4.3*	*2.5*	*96*
New England	20	13	900	10	45	10.7	3.4	237
Scotland	55	36	744	18	14	2.9	1.6	25
Ireland	*0*	*0*	*0*	*0*	*0*	*0.0*	*0.0*	*0*
MV TOTALS	**354**	**27***	**10234**	**10***	**29**	**4.4**	**2.4**	**100**
ALL CLASSES								
Gråtådal	42	3.3*	7362	7.3*	175	16.3	13.4	1465
C. Scandinavia	884	68.5*	74881	74.7*	85	8.8	3.5	474
S. Scandinavia	*47*	3.6*	*4238*	4.2*	*90*	*9.1*	*3.5*	*692*
New England	153	11.9*	9087	9.1*	59	9.3	2.9	234
Scotland	152	11.8*	4225	4.2*	28	5.9	2.1	84
Ireland	*12*	0.9*	*418*	0.4*	*35*	*7.9*	*3.6*	*151*
GRAND TOTALS	**1290**	**100**	**100211**	**100**	**78**	**8.8**	**3.6**	**437**

Values for areas with small sample size or lower quality data are shown in italics.
* % of all caves

10.5.2 Rankings of Caledonide terranes

The rankings of maximum and mean cave length, maximum VR, and mean cave cross-section (Table 10.4, columns 2, 3, 4 and 6) are in the same order for each of the five better-documented areas: northern Scandinavia (largest caves, using Gråtådal as an example for mean cave dimensions); central Scandinavia; New England; Scotland; and Shetland (zero caves). Only the ranking of the mean cave VR (column 5) is slightly different, probably because the meticulous recording of small caves in central Scandinavia has reduced this value more than applies elsewhere. This uniformity in ranking of the major cave dimensions suggests that the differences *between* the five areas are greater than the differences *within* each of them, so that each area can be considered in its entirety in comparison with the others. This is in contrast to the *zone*s within the main study area of central Scandinavia, where the absence of

ranking led to the conclusion in section 5.8.11 that not only had each zone experienced a similar history, but that there was uniformity in the effectiveness of the applicable processes.

The placement of southern Scandinavia and Ireland within this scheme is more difficult, because their rankings vary much more for each measured parameter. This may be because, as already noted, the sample sizes are small and the data quality is poorer. Additionally, each of these two areas comprises several geographically-dispersed distinct regions, which would be better considered individually. However, if the quality of this data is improved in future, it is anticipated that these two areas will fit in the rank order shown in Table 10.4, with the mountainous Jotunheimen area ahead of the rest of southern Scandinavia, and Donegal ahead of Connemara in Ireland.

Table 10.2 Caledonide Caves - hydrological classes, entrances, cave streams and sump pools

CAVE CLASS and AREA	No. of caves	SE per cave	RE per cave	DE per cave	Total entrances per cave	CS per cave	SP per cave
RELICT							
Gråtådal	13			1.62	1.62		
C. Scandinavia	280			1.41	1.41		
S. Scandinavia	*11*			*1.27*	*1.27*		
New England	81			1.16	1.16		
Scotland	42			1.21	1.21		
Ireland	*8*			*1.13*	*1.13*		
RC TOTALS	**435**			**1.34**	**1.34**		
COMBINATION							
Gråtådal	14	0.71	0.29	1.07	2.07	2.21	0.43
C. Scandinavia	360	0.50	0.21	0.97	1.68	1.13	0.80
S. Scandinavia	*16*	*0.50*	*0.31*	*1.94*	*2.75*	*1.38*	*1.13*
New England	52	0.38	0.21	0.68	1.27	1.23	0.47
Scotland	55	0.55	0.22	0.71	1.48	1.25	0.47
Ireland	*4*	*0.75*	*0.50*	*0.00*	*1.25*	*1.50*	*1.00*
CC TOTALS	**501**	**0.50**	**0.22**	**0.93**	**1.66**	**1.20**	**0.73**
MAINLY VADOSE							
Gråtådal	15	0.80	0.73	0.67	2.20	1.00	0.20
C. Scandinavia	244	0.58	0.34	0.40	1.32	1.04	0.39
S. Scandinavia	*20*	*0.65*	*0.25*	*0.50*	*1.40*	*1.00*	*0.35*
New England	20	0.80	0.20	1.00	2.00	1.15	0.15
Scotland	55	0.49	0.44	0.29	1.22	1.04	0.25
Ireland	*0*						
MV TOTALS	**354**	**0.59**	**0.36**	**0.43**	**1.39**	**1.04**	**0.34**
ALL CLASSES							
Gråtådal	42	0.52	0.36	1.10	1.98	1.10	0.21
C. Scandinavia	884	0.36	0.18	0.95	1.50	0.75	0.43
S. Scandinavia	*47*	*0.45*	*0.21*	*1.17*	*1.83*	*0.89*	*0.53*
New England	153	0.24	0.10	0.97	1.31	0.58	0.18
Scotland	152	0.37	0.24	0.70	1.31	0.83	0.26
Ireland	*12*	*0.25*	*0.17*	*0.75*	*1.17*	*0.50*	*0.33*
GRAND TOTALS	**1290**	**0.35**	**0.18**	**0.93**	**1.47**	**0.75**	**0.37**

Values for areas with small sample size or lower quality data are shown in italics.

Table 10.3 Caledonide caves and karsts - major observations, processes and controls

Caledonides	Observations	Processes and Controls
Scandinavian		
-Northern	Has the longest, deepest and largest caves, as exemplified in Gråtådal. Mean cave dimensions for the whole of northern Scandinavia are unknown, but they are probably greater than those of central Scandinavia.	Commonly, high local relief caused large deglacial seismic shocks. Exceptionally, **very deep tectonic movement** violates the one-eighth relationship, as can also occur in extensive low angle karsts (which may utilise inception horizons). Locally, **recharge from permanent glaciers** produced larger relict passages, greater vadose entrenchment and fewer sumps. **Entrance enlargement** below marine limits when isostatically depressed.
-Central	The main study area, as reported in Chapters 4–9.	The four 'standard models' described in Chapters 6–9. **Entrance enlargement** below marine limits when isostatically depressed.
-Southern	Less well studied, and small sample size. No caves in VSK. None below marine limits.	Follows the 'standard models', with controls similar to those in central Scandinavia.
Laurentian		
-New England	Reduced cave dimensions (except VR) and proportionately more Relict and less MV caves compared with main study area. No caves in VSK. None below marine limits.	Follows the 'standard models'. These may also apply to caves in metacarbonates of the Grenville-age Canadian Shield.
-Newfoundland	There are no metacarbonate outcrops in this terrane.	Caledonide models do not apply, but could be considered for the sedimentary limestones of the Humber zone.
British		
-Scotland	Reduced cave dimensions, compared with main study area and New England. No caves in low angle karst, and none below marine limits.	Follows the 'standard models', but with smaller phreatic enlargements under shorter-lived IDLs, and less vadose entrenchment from shorter spring melts. The one-eighth relationship is too generous in the east, where the Devensian icesheet was not continuous.
-Ireland	Less well studied, and small sample size. Mean dimensions may be comparable with Scotland. No MV caves.	Probably follows the 'standard models'. Unknown reason for apparent absence of MV caves. Possible **entrance enlargement**.
-Shetland	There are metacarbonate outcrops in this terrane, but no karst caves.	Low relief, thin icesheets, and **continual interglacial isostatic depression** has suppressed tectonic inception and always prevented cave formation.
Arctic		
-CE Greenland	There are metacarbonate outcrops in this terrane, but, as yet, no reports of karst caves.	Unknown, but may be similar to NE Greenland.
-NE Greenland	13 large relict phreatic caves and infilled palaeokarsts reported in low metamorphic grade low angle karsts. Universal permafrost, and adjacent large-scale glaciation.	Early post-depositional infilled **palaeokarst** protected by **overlying sediments**, even during (**moderate**) Caledonide tectonism. Early Pleistocene phreatic development, perhaps using inception horizons and chemical inception. **Permafrost** during interglacials prevents vadose entrenchment. (Glaciation and deglaciation little studied).
-N Greenland	There are probably low-grade low angle karst metacarbonates in this terrane, but, as yet, no reports of karst caves.	Unknown, but may be similar to NE Greenland.
-Spitsbergen	Short relict phreatic caves in low angle karst, infilled palaeokarst, universal permafrost, adjacent large-scale glaciation, and thermal springs reported.	As NE Greenland, plus effects of **hydrothermal karstification.**
- Bjørnøya	There are low angle sedimentary limestones in this terrane, but no reports of karst caves.	Unknown.

Processes and controls in bold are additional to the main processes that apply in central Scandinavia.

Table 10.4 Caledonide caves, glaciation, uplift and local relief difference

CALEDONIDE AREA	Max. cave length (m)	Mean cave length (m)	Max. cave VR (m)	Mean cave VR (m)	Mean cave XS (m^2)	Max. local icesheet thickness (m)	Local Holocene uplift (m)	Max. relief diff. (m)
N. Scandinavia	17000	?	580	?	?	2000–3000	40–200	1655
- (Gråtådal)		175		16.3	13.4	2000	140	1174
C. Scandinavia	5600	85	180	8.8	3.5	1800–2800	120–280	900
New England	900	59	82	9.3	2.9	1500–2500	60–180	790
S. Scandinavia	*560*	*90*	*46*	*9.1*	*3.5*	1200–2400	120–360	1200
Scotland	340	28	48	5.9	2.1	1000	<=40	980
Ireland	*220*	*35*	*25*	*7.9*	*3.6*	500?	15?	>300
Shetland						200–300	-9	250

Values for areas with small sample size or lower quality data are shown in italics.
Refer to earlier texts for references.

10.5.3 Main control on karstification

The prime conclusion of this thesis is that the main control on the extent of karstification in the non-Arctic Caledonides is the weight of each of the various Pleistocene icesheets, for which the thickness of the local icesheet at the Weichselian LGM can be taken as a proxy.

The weight of the icesheets caused isostatic depression, and therefore the previous thickness determined the amount of postglacial uplift. The greater this was, the faster was the initial acceleration of the uplift, by Hooke's Law. This, in combination with the change of local relief (valley bottom to ridge top), determined the magnitude of local deglacial earthquakes. These in turn controlled the density and the depth of tectonic inception fractures that were wide enough to permit breakthrough and enlargement to explorable cave passages within the timescales of the various hydrological regimes that the karst subsequently experienced. Hence, because the Pleistocene glacial–interglacial cycles were globally synchronous, these timescales were approximately the same for all Caledonide terranes, and total explorable cave lengths and vertical ranges are direct functions of previous local icesheet thicknesses. A supplementary mechanism for phreatic enlargement related to icesheet thickness is that the more ice there was to melt at the end of each glaciation, the longer caves and fractures remained submerged under ice-dammed lakes, and the more water flowed through them. Greater flows in turn caused a greater widening of cave passages, increasing their measured cross-section and permitting smaller conduits to enlarge to explorable size, so increasing the measured length of each cave.

The final demonstration of these relationships is presented in Table 10.4, columns 7 and 8. These show that the ranges of both local icesheet thicknesses at the LGM and the local Holocene uplifts for the five better-documented areas follow ranking orders similar to those of the main cave dimensions. Column 9 shows how the applicable maximum topographic relief differences also follow roughly the same trend. It is anticipated that a suitable index of seismicity for each area would give values in the same order. Shetland, the extreme end-member of the series, illustrates the case where deglaciation caused isostatic

depression. This suppressed seismic activity, prevented tectonic inception, and explains the complete lack of karst caves to be found there.

The enigma of the Caledonide marble caves, which has puzzled Scandinavian geologists for over a century, is resolved in this thesis and the key research objectives set in section 1.1 are now satisfied. The inception, development and destruction of the caves in metalimestones in the non-Arctic Caledonides are explicable by the paradigm based on the five models developed in Chapters 6–10, which explain the cave attributes of the main study area described in Chapter 5. The succeeding sections of this Chapter reconsider the main conclusions, discuss outstanding Caledonide questions and propose how the Caledonide model can be extended to other karst areas.

10.6 Main conclusions

This section reviews the main conclusions against the thesis objectives and considers several other major research results. The other important, but less significant, findings arising from this project were discussed throughout Chapters 4–10, and are not repeated here.

10.6.1 Variation of the extent of karstification

Chapter 5 showed that there is no systematic variation of mean cave dimensions across the zones and nappes of the main study area of central Scandinavia, although later deductions suggest that this observation may need to be moderated for those caves in low angle karst, especially those that occur in the lower-grade Køli Nappes in the east of the area. These caves have maximum lengths and vertical ranges that exceed those predictable from the data about the caves in the high-grade and steeply-dipping HNC metalimestones in the major part of the area to the west. Their inception was more likely to be along fractures that are aligned with the foliation, making them more like caves in sedimentary limestones in this respect.

Although a detailed study of variations with altitude and location was not undertaken for caves in the other Caledonide terranes, and would commonly be less reliable because of smaller sample sizes, it seems safe to assume that the larger of these areas also show no systematic *internal* variation. Only in Scotland is there a probable systematic geographical decline in cave dimensions, because of a reduction in the thickness of the relatively small Scottish icesheet from west to east. Hence, most Caledonide areas can be treated as coherent entities regarding the influence that their previous geological history had on cave development. Within the main study area and probably within other Caledonide areas the *cave location* and *glacial situation* (including situation east or west of a major ridge) were commonly more important influences on cave dimensions than other variables. On the other hand, important differences occur *between* the various terranes, and, as shown in section 10.5.2, cave dimensions can be usefully ranked by Caledonide terrane. This suggests that their geological histories, whilst being similar, were not identical in detail.

10.6.2 Processes

It is hereby proposed that cave development in the metamorphic non-Arctic Caledonides commonly followed a four-stage process. Firstly, local seismic and aseismic tectonic movements that accompanied deglacial isostatic uplift, the retreating ice margin and ice-dammed lake jökulhlaups created inception fractures to depths that were commonly within one-eighth of the change of local relief. Secondly, the fractures were enlarged phreatically under contemporary and / or subsequent active ice-dammed lakes in aqueous conditions at very low temperatures and CO_2 partial pressures without necessarily invoking the influence of strong acids (section 10.7.4). Thus, the caves themselves are the observable expression of deglacial tectonic activity. Phreatic enlargement occurred at high flow rates, when a proportion of c. 80000km^3 of glacial meltwater flowed from the study area into the sea at each major deglaciation. Cave dimensions are probably related to the size of the submerging IDL, because large IDLs inundate underlying fracture and conduit systems for longer periods of time. Thirdly, there was primarily vadose entrenchment at the lowest level of many caves during each ensuing interglacial at a maximum rate controlled by the size of the catchment area. Finally, at least the upper and outer parts of the caves were removed by glacial erosion during the next glaciation, but valley-deepening produced ever-deeper inception fractures at the first stage of the next cycle. An additional process for some caves below marine limits in Norway was the enlargement of entrances by marine activity when isostatically depressed.

Put more simply, all cave passages developed from local inception fractures created primarily during deglaciation by seismic, aseismic and unloading processes. The relict phreatic passages and levels arose from *deglacial speleogenesis* beneath ice-dammed lakes. Vadose passages, including any presently-active phreatic sections, developed during *interglacial speleogenesis*. Depending on external topography, the phreatic deglacial and the vadose interglacial flow directions could oppose each other, especially if the cave was submerged by a backward-flowing IDL.

Most *combination caves,* which developed in a Top-Down, Middle-Outwards (TDMO) sequence, are assumed to be single-cycle caves in this thesis. *Relict* caves (universally in the main study area and commonly also single-cycle caves) and relict passages (commonly) retain phreatic forms, because they exist in topographic locations that caused them to escape the vadose entrenchment phase. *Mainly vadose* caves achieved most of their enlargement during the interglacial that followed the demise of the ice-dammed lakes and the final disappearance of the valley glaciers, and are thus referred to as half-cycle caves. Those caves that developed passages too far from the surface to be removed by the subsequent glaciation became multi-cycle caves, with their oldest parts commonly occurring in central positions nearest the surface. However, the 'cyclicity' of the remaining cave could change at each glaciation, as the surface lowered and cave development progressively took place at lower and lower levels above the basement in any metacarbonate outcrop.

The processes and models discussed in Chapters 6–9 provide an explanation for the relationships between caves, carbonate outcrops and topography listed in section 5.8. Because of the epigean nature of the caves, they may perhaps be described as epikarstic (section 3.1.8), but in this case it is an epikarst that can support a wide range of cave morphologies, without any passages lying in the deeper unfractured rock mass. The concept of a 'watertable' has little validity in the metamorphic Caledonides, because water storage and flow is contained within discrete fractures, conduits and cave passages. Cave morphologies and other internal attributes (Appendix B2) are explained by the same processes, which act in concert with the local external geomorphological evolution and the effects of glacial and interglacial climatic and hydrological conditions.

10.6.3 Commonality of processes across the Caledonides

From the evidence presented in Appendix D6, there are many similar relationships among the caves of the various Caledonide areas for which databases were constructed. Thus, there certainly is a *prima facie* case that similar processes have operated in all the non-Arctic Caledonides. However, there are many examples of more complex caves in northern Scandinavia that probably experienced more than the 'standard' processes, and certainly even more that developed over many glacial cycles. On the other hand, caves in all the other Caledonide areas tend to be simpler and smaller than those in central and northern Scandinavia, indicating less development stages over shorter timescales. Shetland provides an extreme example of thin icesheets, reverse isostasy, and negligible seismicity that contributed to a complete absence of endokarst.

Whereas there is no reason to doubt that the four-stage process commonly applied to all parts of the non-Arctic Caledonides, there are several important subsidiary processes that appear to apply only in particular Caledonide terranes. The entrance areas of pre-existing caves could be modified by marine activity during both rising and falling sea levels, if below the applicable marine limit. This almost certainly applied near the coast of north central Norway, and probably applied in northern Norway (Appendix D6.1.1) and at one cave in Ireland (Appendix D6.3.4). Entrance enlargement by ice-wedging at ice-dammed lakes could apply at all non-Arctic terranes. Recharge from permanent interglacial glaciers can explain both larger relict phreatic passages and greater vadose entrenchment with fewer sumps, but only applied in northern Scandinavia. However, recharge from what are now perennial snowfields in central Scandinavia also contributed to the development of significant mainly vadose passages, as probably did the earlier initiation of interglacial vadose processes in New England (and perhaps in Scotland), with a consequential reduction in numbers of sumps. In northern Norway, a very deep, and probably very long-range, tectonic movement may have caused the one-eighth relationship to be exceeded, as did cave development in extensive low angle karsts. In the Arctic Caledonides, sediments overlying the Caledonide metacarbonates protected palaeokarstic caves, and interglacial permafrost prevented vadose entrenchment. Spitsbergen is the only Caledonide area that displays evidence of hydrothermal karstification.

10.6.4. Timescales

As discussed in Chapter 9, the timescales of the various stages are commonly related to the Pleistocene glacial stages. Thus, mainly vadose caves primarily enlarged during the Holocene, combination caves commonly enlarged phreatically at the end of the Weichselian glaciation and experienced vadose entrenchment in the Holocene, and most relict caves only enlarged for a maximum period of c. 2000 cal. a during the last deglaciation. Those few combination caves in the main study area with relict vadose passages and / or obviously relict higher-level resurgence outlets are assumed to have developed their oldest existing passages during the deglaciation of the Saalian, or more rarely during the deglaciation of the Elsterian. It appears that, in central Scandinavia, only parts of **Toerfjellhola** (Z3) may pre-date the Elsterian glaciation, despite noting that Isacsson (1999) suggested that the complex **Korallgrottan** (KL) was fully-formed at the end of the Pliocene (section 3.3.3).

Development timescales for single- and half-cycle caves in the other areas are broadly comparable to those in central Scandinavia. It appears that only in northern Scandinavia are there multi-cycle caves with passages that originated at about the time of the Mid Pleistocene Revolution (1Ma). However, outside the Arctic Caledonides, there is no evidence that any cave passages have survived since before this time.

10.6.5 Key parameters

The discovery that mean cave dimensions in each of the main Caledonide areas fit universally into one ranked order led to the idea that there may be one key factor that determined the extent of endo-karstification in each place. This appears to be substantiated by the finding that the rankings of modelled LGM icesheet thicknesses and their consequent isostatic uplifts are in the same order. Thus, the prime parameter that determined the mean and maximum cave dimensions in each terrane was probably the weight of the recent Pleistocene icesheets, assumed to be represented by the thickness of the Weichselian ice at the LGM. Important subsidiary factors were glacial situation (especially west and east differences), cave location and the change of local relief (from ridge top to glacial-valley bottom), which also influenced the extent and magnitude of neotectonics. Less important factors were the proximity to thrusts and any contact metamorphism of the limestone.

10.6.6 Non-fractal nature of phreatic passage sizes

A counter-intuitive finding is that Caledonide phreatic cave passages have cross-sections with a positive mean value: they do not follow an exponential, fractal, distribution from a small number of explorable passages towards a large number of tiny conduits. The likely explanation is that the caves all followed the processes described in section 10.6.2 and *kept in step with each other*. Thus, after tectonic inception, all fractures were subjected to phreatic enlargement under IDLs for similar periods of time, giving a relatively small variation in the size achieved before they were drained. Similarly, those mainly vadose passages that retained phreatic sections throughout the Holocene experienced phreatic enlargement for the same period of about 10ka. Thus, although few caves of the Caledonide metalimestones achieve the larger dimensions associated with caves in sedimentary limestones, there are very few tight relict

passages or active sumps. This finding does not necessarily apply to vadose passages, where the hydraulic gradient can cause narrow stream canyons to form that are too tight to explore.

10.6.7 Validity of previous theories

As discussed in section 3.3, the previously-proposed timings of speleogenesis in Scandinavia have ranged over most conceivable possibilities, from the postglacial, proglacial, subglacial, interglacial and preglacial theories of earlier authors to the polygenetic ideas of Lauritzen (1984b) and a Miocene age proposed by Haugane and Grønlie (1988). These theories were all based on studies of the longer caves of northern Norway, without considering the significance of the short, superficial, caves and without the analysis of hydrological classes introduced in this thesis. In fact, elements of many of the early theories can now be seen to apply to particular situations that have been discussed herein (with suitable interpretations), but without providing a complete explanation. Thus, 'postglacial' applies to the enlargement of mainly vadose caves in the Holocene and 'proglacial' may be the analogue of phreatic enlargement of relict passages in relict caves and combination caves beneath ice-dammed lakes: the Corbel (1952a) opinion that caves in zone KL formed beneath glacial lakes is supported in this thesis (Appendix D2.4–D2.9). However, the concept that Scandinavian cave development was strongly influenced by a high calcite saturation concentration at low temperature (as assumed by Corbel and other authors) is rejected herein. This thesis assumes that, at the applicable large flow velocities, the water remained unsaturated (even, commonly, in interglacial conditions). Reaction kinetics dominated and conduits enlarged at maximum rates, even if the saturation concentration values remained low in almost pure water.

The idea supported by Jakucs (1977, p121) that Scandinavian caves developed in periglacial conditions in the Holocene is unlikely, based on the commonly warm summer climate (section 2.4). The discussion about breakthrough times and enlargement rates in Chapter 8 showed that speleogenesis under strictly 'subglacial' conditions is extremely unlikely, preventing the mechanism proposed by Horn (1937; 1947). However, if 'sub-IDL' is substituted for 'subglacial', then much of the logic of Horn's argument is supported in this thesis, including his suggestion that joints are created and widened by earthquakes.

Some of the 'interglacial' chronologies (section 3.3.3) may refer to earlier stages in the development of the more complex multi-cycle combination caves, but Miocene and 'preglacial' (which now has to be interpreted as speleogenesis at some time in the Tertiary) ages are ruled out by this thesis because, prior to the establishment of the large glaciations that followed the Mid Pleistocene Revolution (section 2.3.1), the relief was too subdued to permit the creation of deep inception fractures by postglacial earthquakes. Thus, superficial single-cycle caves that developed then were removed by subsequent glacial erosion. Similarly, because the oldest passages in an existing Scandinavian metalimestone cave occur at the top and towards the middle of any cave section (TDMO model), any passage elements that developed during the Tertiary or early Pleistocene were also removed, even if the younger and lower parts of the cave still

exist. Thus, ideas that the large relict phreatic passages developed *before* the deepening of glaciated valleys, when water levels and 'watertables' were supposedly higher, are unnecessarily complicated, ignore glacial erosion, and do not consider possible inception mechanisms. Similarly, theories about interglacial 'base-level' control of speleogenesis are false in the Caledonides, because caves occur randomly at almost any altitude, and there are no base-levels that extend beyond the immediate vicinity of each cave (as realised by Helldén, 1975, at **Sotsbäcksgrottan**; Appendix B1.13). It also follows that the existence of palaeokarst in central Scandinavia dating from *after* the Cretaceous peneplanation (Appendix A1.3.2) is unlikely. Palaeokarst in sedimentary carbonates deposited after the Caledonide orogeny is impossible in the main study area, because such rocks do not exist.

Cave development influenced by relatively fast external events, such as the creation and lowering of ice-dammed lakes, the bypassing of Vauclusian risings and the inundation of the sea, contribute to the TDMO model and to entrance enlargement. As noted in section 3.1.1, these concepts are in sympathy with the Woodward (1961) theory of stream piracy. However, the TDMO model of cave development in high-grade metamorphic limestone stands apart from the Ford and Ewers (1978) Four-state Model of cave development in sedimentary limestones (which depends on fracture frequency and long development timescales), because each tectonically-produced fracture in Caledonide marble is potentially capable of enlarging to a cave passage in a short time during deglaciation. The absence of passages with multiple phreatic loops likely arises from the negligible matrix and fracture porosity of the metalimestone, away from the relatively large fractures produced by deglacial seismicity.

The earlier theories were developed in ignorance of the more recent research about the importance of deglacial seismicity to the fracturing of the 'partially detached thin upper crustal layer' (section 6.2.3) and of the potential importance to speleogenesis of deglacial ice-dammed lakes, whose sizes and depths (facilitated by cold-based ice acting as an aquiclude below the plastic behaviour limit) provide a neat bypass to the problems that early authors sought to explain by deep dissolution beneath palaeo landscapes. Additionally, the quantitative approaches adopted in this thesis, including especially the use of pivot tables, provide revealing relationships among the caves that could not be derived or even guessed at by previous researchers. The four-stage process proposed in section 10.6.2 is considerably simpler than previous theories, and by application of Occam's Razor, is a more likely hypothesis.

The new Alpine paradigms of Audra (1994) and Häuselmann *et al.* (2003), discussed in section 3.2.2, have some parallels in the metamorphic Caledonides, including the influence of tectonic activity and the in-phase relationship of cave development with the deepening of glacial valleys. However, the absence of soutirages in the study area relict phreatic passages supports the conclusion deduced from the commonly 'impossible' locations of such passages that they did not enlarge to present sizes by regular interglacial floods. It would also be interesting to determine whether *Alpine* caves were influenced by dissolution beneath ice-dammed lakes during the many deglaciations that they experienced.

10.7 Outstanding work in the metamorphic Caledonides

Further work could usefully be undertaken to underpin and to expand the conclusions reached in this thesis, as discussed briefly below.

10.7.1 Statistical treatment

Although the thesis relies heavily on the data contained in the various constructed databases and derives some formulae to relate the maximum dimensions of mainly vadose caves to catchment areas (section 5.4.2), there was insufficient time and space to analyse these data with any statistical rigour. The approach has been to use simple arguments based on mean values and ranking orders. A successor project could quantify the derived models mathematically, based on the data contained in the Appendices, and try to find simple formulae to estimate cave dimension distributions from icesheet thicknesses or isostatic uplifts. It may also be possible to quantify mathematically the sectional geometries applicable to the TDMO model under various internal fracture geometries and dimension distributions and under specified external topographic conditions, and compare these with the relationships reported by Worthington (1991; section 3.1.12).

10.7.2 Deglaciation

The deglaciation histories of the study area (Appendix D2) and of the Tosenfjord–Fiplingdal area in particular (Appendix D3) were derived by the manual illustration of the effect of applying the reconstructed Grønlie formula to topographic maps. An approach using GIS techniques and computer simulation would provide a much more accurate depiction and a more precise calculation of inundation timescales by IDLs of each cave in the area. A more comprehensive study of scallop sizes and directions in each cave would also assist the determination of individual cave histories. The glacial conditions and hydrological flow regimes applicable to icesheets described in section 8.4 are probably not exhaustive. A more complete treatment would analyse the internal hydrology of at least four main time-varying glacial configurations: frozen surface + frozen base; frozen surface + warm base; melting surface + frozen base and melting surface + warm base.

10.7.3 Exokarst

This thesis provides scant information about the extent of exokarst in the Caledonide metacarbonates. Most dolines must date from the Holocene, because of glacial erosion. Their commonly modest sizes (up to c. 10m depth and 10m diameter) seem to confirm this. Larger dolines that may have survived one or more glaciations were not considered. It is known from some sedimentary limestones that there can be a correlation between endokarst and its overlying exokarst (Dreybrodt, 1988, p5), although this is unlikely in the case of speleogenesis arising from deep chemical inception. It is untested, but conjectured here, that this correlation also applies to metamorphic limestones. Thus, the depth of dolines may indicate the size of subterranean conduits, and perhaps also the depth of karstification. In this case, the maximum depth of dolines in areas of metalimestone without caves is 2m, as occurs in Shetland.

10.7.4 Dissolution chemistry

Previous theories of cave development considered karst dissolution by carbonic acid and by stronger acids. This thesis demonstrates that at sufficiently large hydraulic ratios, karst breakthrough and enlargement can take place at maximum rates in *pure water*. Thus, section 8.5 considered the physics and chemistry of breakthrough and phreatic enlargement based only on cold aqueous solutions with very little dissolved carbon dioxide. The approach adopted was non-rigorous, and such dissolution in short fractures at high hydraulic gradients would benefit from a proper theoretical and experimental analysis.

In some caves, inception fractures may occur at metadolostone–metalimestone contacts, at HMC–LMC contacts or along contacts between metalimestones and rocks containing sulphides (section 3.1.5). Metadolostones and HMC metalimestones commonly contain Fe impurities (giving a characteristic pink or yellow colour) and Fe may be liberated in the various complex dolomite dissolution reactions. Both situations may eventually lead to H_2SO_4 production via reactions with dissolved sulphates. Hence, in some inception fractures, both breakthrough and enlargement may be further enhanced by strong acid dissolution at low temperatures. Again, a theoretical and experimental treatment should enable applicable breakthrough times and wall retreat rates to be estimated. At the same time, it could be determined experimentally how mica and silica impurities within the metalimestone lithology influence the overall wall retreat rate of cave conduits at various flow velocities. At a practical level, this thesis has also paid scant attention to the cross-sectional profiles of individual cave passages (e.g. Osborne, 1999, Figs. 11 and 17). Thus, it would be useful to study profiles at the various lithological contacts to determine if possible strong acid reactions influence the shape of such profiles and the shapes of any observable inception fractures.

10.7.5 Evolution of Quaternary landscapes

This thesis discusses several examples where the previous depth of glaciated valleys is constrained by the positions of relict resurgences. Thus, the existence and morphology of karst caves may themselves be used to interpret the geomorphological evolution of the Caledonide terranes. In suitably complex caves, their internal morphology may be sufficient for such an interpretation, with evidence from the dating of various internal cave deposits providing extra confirmation. However, not all speleogenetic histories may be soluble from the available evidence, because several possible solutions may lead to the same result in terms of existing passages and surface topography. This is particularly true for the less complex caves at shallow depths. The more complex a cave, then the easier it should be to deduce the evolution of the local landscape with respect it. This *inversion of concepts*, to use cave data to derive Quaternary geomorphological models, may also be usefully applied to other interdisciplinary subjects, including seismic and aseismic tectonics, neotectonics, glacial histories and previous sea levels.

10.8 Extensions of the Caledonide models

This section considers how the models derived in this thesis may be applicable beyond the non-Arctic Caledonides.

10.8.1 Model extension to the Arctic Caledonides

As discussed in section 10.4, the Arctic permafrost areas do not appear to follow the five derived models. However, some aspects of the models could be expected to apply to the cave development that did take place in these terranes when they previously experienced much warmer conditions, early in the Pleistocene or soon after deposition early in the Palaeozoic. The extents to which the models did, or did not, apply then should provide useful information about contemporary environmental conditions.

10.8.2 Model extension to other previously-glaciated metalimestone areas

The extent to which metamorphic stripe karst occurs in other previously-glaciated parts of the world has been little studied, but it is conjectured that the principles derived herein should also apply. This appears to be the case for the caves in Grenville-age metalimestones in the Adirondack Mountains of New York state (Appendix D6.2.4). Ford (1967) described the sinking creeks of Mt. Tupper in Glacier National Park, Canada. The rock is a blue dolomitized limestone marble, forming an angled stripe karst with a dip of 45°. A $0.7m^3s^{-1}$ stream flows for 2km under a mountain ridge to a rising that is 480m below the main sink. The cave passage is probably partly down dip, and may follow marble / non-carbonate inception surfaces. The distance of conduits below the surface can be deduced to be 130m at the Tupper ridge. As the height of the Mt. Tupper summit above the local valley is 1536m, the system obeys the one-eighth relationship. There are no references to caves in metadolomites in Canada, agreeing with the observations about their absence in central Scandinavia.

10.8.3 Model extension to previously-glaciated sedimentary limestone areas

It appears to this author that, after the completion of this thesis, there are now two extreme paradigms that explain karst cave development. The Inception Horizon Hypothesis utilises slow *chemical* inception along deep, long-range, inception horizons in sedimentary limestones to create channels large enough to support continuous laminar flow. Flow rates and dissolution gradually increase until breakthrough occurs, after which phreatic enlargement proceeds at a constant rate until the recharge cannot maintain phreatic conditions above the level of the outlet. Thereafter, development occurs under vadose conditions. This scenario is completely credible for speleogenesis in sedimentary limestones during interglacials, and in regions that do not experience glaciation. The *tectonic* inception theory, introduced in this thesis, explains how near-surface caves can form in high-grade marbles, if they are subjected to repeated and extensive glaciations.

In order to derive a *Unified Model of Karst Development*, bridges between the two paradigms need to be explored. One such bridge is the theory of the epikarst, which also relies on the creation of near-surface tectonic fractures. Other bridges concern cave developments in those sedimentary limestones that were

also subjected to repeated glaciations. Clearly, such karsts should also experience both the creation of tectonic fractures by deglacial earthquakes and phreatic dissolution beneath active ice-dammed lakes. These processes are additional to deep-seated chemical inception and to the primarily vadose entrenchment that occurs during interglacials, as observed at present and for which environment most current theories of speleogenesis have been constructed. Indeed, it seems that all these theories should now be re-visited in the knowledge that ~90% of the Pleistocene (when many caves developed) was glacial, so that conditions over most of the planet were quite different from those at present. Significant terrestrial cave development may also have occurred at the transitions to and from glacial climates.

Areas that would help elucidate a fuller range of cave development processes applicable to *glaciated* sedimentary limestones include those that contain ancient sedimentary limestones relatively close to the Caledonides. Examples include the Cambrian Durness Group carbonates of Scotland, similar limestones in Newfoundland, the Silurian limestones of the island of Gotland, Sweden, sedimentary limestones at Spitsbergen and the Carboniferous limestones in the Yorkshire Dales, Ireland and the northern part of the USA.

Waltham (1977) reported the existence of two main groups of cave passages in the Yorkshire Dales: old, mainly phreatic relict passages, and younger stream passages. Thus, the hydrological classification of Caledonide caves as relict, combination and mainly vadose caves also seems appropriate in Yorkshire. Waltham deduced that, because the older series lie some 50m above the active passages, a major rejuvenation (caused by valley excavation) separated the two main phases of development. Following this thesis, it seems much more likely that the (upper) relict phreatic passages formed under ice-dammed lakes at the successive deglaciations of (e.g.) Easegill, Kingsdale and Chapel-le-Dale, and that the active 'mainly vadose' passages developed during the Holocene and earlier interglacials. Indeed, Waltham also noted the presence of "high-level vadose passages" (presumably relict) and it is their relationships with valley floors that should inform us about the depth of local valley entrenchment at each glaciation. Evidence in support of the idea that the major karst valleys in Yorkshire became submerged beneath IDLs at the end of the Devensian and earlier glaciations is the presence of deep gorges through which their outflowing streams presently pass. These could have been partly formed by jökulhlaups when the Yorkshire Dales IDLs breached the remnant Devensian icesheet to their south.

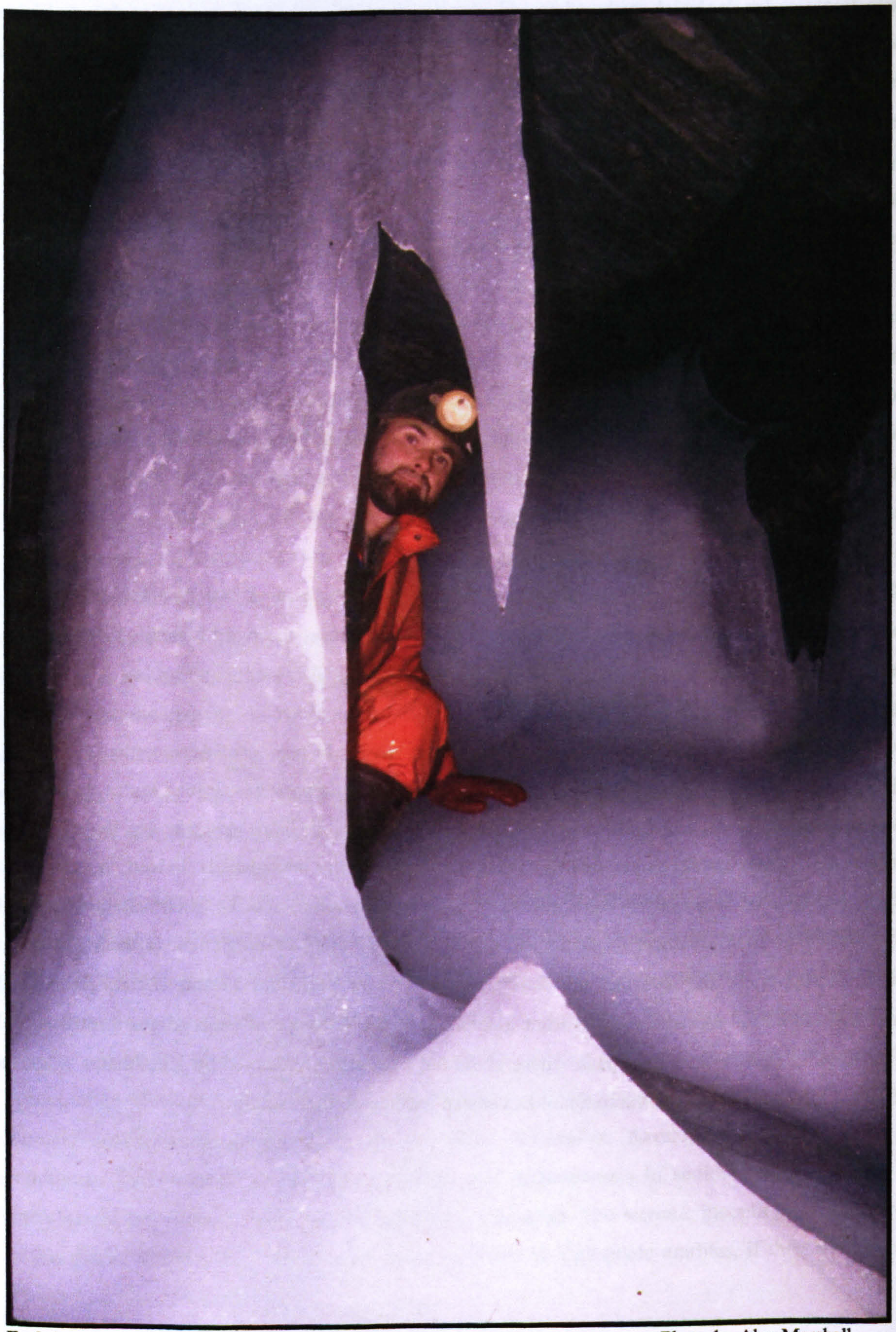

Endpiece **Ice ledge, Etasjegrotta (Z4)** Photo by Alan Marshall

REFERENCES

Adkins, JF, Boyle, EA, Keigwin, L and Cortijo, E. 1997. Variability of the north Atlantic thermohaline circulation during the last interglacial period. Nature **390** 154–156.

Ague, JJ. 2000. Contrasts between pervasive and fracture-controlled fluid flow during crustal metamorphism. Abstracts p8 and seminar notes from Geoscience 2000, 17–20 April 2000. The Geological Society.

Ahnert, F and Williams, PW. 1997. Karst landform development in a three-dimensional theoretical model. Zeitschrift fur Geomorphologie N.F. Suppl.-Bd. **108** 63–80.

Alley, RB. 1998. Icing the north Atlantic. Nature **392** 335–337.

Alley, RB and 10 authors. 1993. Abrupt increase in Greenland snow accumulation at the end of the Younger Dryas event. Nature **362** 527–529.

Andersen, BG. 1980. The deglaciation of Norway after 10,000 BP. Boreas **9** 211–216.

Andersen, BG and Borns, HW. 1997. The Ice Age World. 208pp. Scandinavian University Press.

Andersen, BG and Karlsen, M. 1986. Glacial chronology – recession of the ice margin. 1:5000000. Nasjonalatlas for Norge. Kartblad 2.3.4. Statens kartverk.

Andersen, BG and Mangerud, J. 1989. The last interglacial–glacial cycle in Fennoscandia. Quaternary International **3/4** 21–29.

Andersen, BG, Bøen, F, Nydal, R, Rasmussen, A and Vallevik, PN. 1981. Radiocarbon dates of marginal moraines in Nordland, N. Norway. Geografiska Annaler **63A** (3–4) 155–160.

Andersen, BG, Bøen, F, Rasmussen, A, Rokoengen, K and Vallevik, PN. 1982. The Tjøtta glacial event in southern Nordland, North Norway. Norsk Geologisk Tidsskrift **62** (1) 39–49.

Andersen, BG, Lundqvist, J and Saarnisto, M. 1995a. The Younger Dryas margin of the Scandinavian icesheet - an introduction. Quaternary International **28** 145–146.

Andersen, BG, Mangerud, J, Sørensen, R, Reite, A, Sveian, H, Thoresen, M and Bergström, B. 1995b. Younger Dryas ice-marginal deposits in Norway. Quaternary International **28** 147–169.

Anderson, AJ. 1980. Land uplift in the Gulf of Bothnia and causes of geotectonics of the region 339-340 in Mörner, N-A, Ed. Earth Rheology, Isostasy and Eustasy. Wiley.

André, M-F. 1996. Rock weathering rates in arctic and subarctic environments (Abisko Mountains, Sweden). Zeitschrift fur Geomorphologie **40** (4) 499–517.

André, M-F. 1997. Holocene rockwall retreat in Svalbard: a triple rate evolution. Earth Surface Processes and Landforms **22** 423–440.

André, M-F. 2002. Rates of postglacial rock weathering on glacially scoured outcrops (Abisko – Riksgränsen area, 68°N). Geografiska Annaler **84A** (3&4) 139–150.

Andreo, B, Carrasco, F and Sanz de Galdeano, C. 1997. Types of carbonate aquifers according to the fracturation and the karstification in a southern Spanish area. Environmental Geology **30** (3/4) 163–173.

Arnekleiv, JV and Dolmen, D. 1992. Ferskvanns inveretebrater i noen nord-norske kalksteingrottor. Ent. Tidsskrift **114** 15–26. Goteborg, Sweden.

Arnold, NS, van Andel, TH and Valen, V. 2002. Extent and dynamics of the Scandinavian icesheet during Oxygen Isotope Stage 3 (65,000–25,000 yr BP). Quaternary Research **57** 38-48.

Arvidsson, R. 1996. Fennoscandian earthquakes: whole crustal rupturing related to postglacial rebound. Science **274** 744–746.

Atkinson, TC. 1968. The earliest stages of underground drainage in limestones- a speculative discussion. Proceedings of the British Speleological Association (6) 53–70.

Atkinson, TC. 1977. Diffuse flow and conduit flow in limestone terrain in the Mendip Hills, Somerset (Great Britain). Journal of Hydrology **35** 93–110.

Atkinson, TC. 1983. Growth mechanisms for speleothems in Castleguard Cave, Columbia Ice Field, Alberta, Canada. Arctic and Alpine Research **15** (4) 523–536.

Aub, CF. 1963. Discussion on "Age of Caves by Solution (K. Renwick)". Cave Science **5** (34) 88–90.

Audra, P. 1994. Karsts alpine. Genèse de grands réseaux souterrains. Karstologia Mémoires (5). 279pp.

Audra, P. 2001. French Alps karsts: study methods and recent advances in Häuselmann, P and Monbaron, M. (Eds.) Cave genesis in the Alpine belt. Research Reports **10** Institute of Geography, University of Fribourg, Switzerland. 7–28.

Auler, A. 1995. Lakes as a speleogenetic agent in the karst of Lagoa Santa, Brazil. Cave and Karst Science 21 (3) 105–110.

Badino, G. 2001a. Has deep karst a fractal behaviour? Proceedings of the Thirteenth International Speleological Congress. Paper no. 178. 12pp.

Badino, G. 2001b. Glacial karst phenomenology. Proceedings of the Thirteenth International Speleological Congress. Paper no. 179. 5pp.

Bakalowicz, M. 1984. Water chemistry of some karst environments in Norway. Norsk Geografisk Tidsskrift **38** (3–4) 209–214.

Balashov, VN and Yardley, BWD. 1998. Modelling metamorphic fluid flow with reaction-compaction-permeability feedbacks. American Journal of Science **298** 441–470.

Ballantyne, CK. 1997. Periglacial trimlines in the Scottish Highlands. Quaternary International **38/39** 119–136.
Ballantyne, CK, McCarroll, D, Nesje, A, Dahl, SO and Stone, JO. 1998. The last icesheet in NW Scotland: reconstruction and implications. Quaternary Science Reviews **17** 1149–1184.
Banks, D, Odling, NE, Skarphagen, H and Rohr-Torp, E. 1996. Permeability and stress in crystalline rocks. Terra Nova **8** 223–235.
Barker, AJ and Gayer, RA. 1985. Caledonide – Appalachian tectonic analysis and evolution of related oceans, 126–165 **in** Gayer (1985).
Barker, AJ, Bennett, DG, Boyce, AJ and Fallick, AE. 1998. Deep circulation of meteoric fluids during the final stages of orogenic exhumation. Geoscience 98 (Keele University) Abstracts p75.
Basset, MG. 1985. Silurian stratigraphy and facies development in Scandinavia, 283–292. **in** Gee and Sturt (1985).
Bauer, S, Birk, S, Liedl, R and Sauter, M. 1999. Solutionally enhanced leakage rates of dams in karst regions **in** Palmer, AN, Palmer, MV and Sasowsky, I. (Eds.) Karst Modeling. Karst Waters Institute Special Publication 5. 158–162.
Bauer, S, Liedl, R and Sauter, M. 2003. Modeling of karst aquifer genesis: influence of exchange flow. Water Resources Research **39** (10) SBH6 1–12.
Baumgartner, LP, Gerdes, ML, Person, MA and Roselle, GT. 1996. Porosity and Permeability of Carbonate Rocks during contact metamorphism **in** Jamtveit, B & Yardley, B (Eds.). Fluid flow and transport in Rocks: Mechanisms and Effects. 83–98.
Becker, D. 1980. Karst - en studie av Bjurälvens karst landscap. Naturgeogr. Inst. Stockholms Universitet. Seminarieuppsats (Stencil).
Bentley, CR. 2000. Stirring the icy waters. Nature **403** 610–611.
Berg, G. 1979. Jamnviktsaspekter pa kalkstensvittringen i Kåtavikens karstområde. Sem. Pap. Chem. Inst. Umea Univ. 14pp.
Bergsten, KE. 1976. The genesis of caves in Swedish preCambrian rock. Grottan **11** (1) 4–7.
Bergstrøm, B. 1995. Elsfjord Kvartaergeologisk kart 1927 III–M 1:50,000, med beskrivelse. Norges Geologiske Undersøkelse.
Bergström, J and Gee, DG. 1985. The Cambrian in Scandinavia. 247–272. **in** Gee and Sturt (1985).
Berner, RA and Morse, JW. 1974. Dissolution kinetics of calcium carbonate in sea water IV; theory of calcite dissolution. American Journal of Science **274** 108–134.
Berstad, IM, Einevoll, S and Lauritzen, S-E. 1997. U series dating and stable isotope analysis of some last interglacial speleothems from north Norway. Proceedings of the twelfth International Speleological Congress **1** 53–54.
Berstad, IM, Lundberg, J, Lauritzen, S-E and Linge, HC. 2002. Comparison of the climate during Marine Isotope Stage 9 and 11 inferred from a speleothem isotope record from northern Norway. Quaternary Research **58** 361–371.
Beskow, G. 1929. Sodra Storfjallet im Sudlichen Lappland. Sver. Geol. Unders. C350 21 (5) 335pp. (20–24: Tjårrogrottorna).
Bini, A, Tognini, P and Zuccoli, L. 1998. Rapport entre karst et glaciers durant les glaciations dans les vallées préalpines du sud des Alpes. Karstologia **32** (2) 7–26.
Bini, A. 2001. Consideration on karst in the Italian Alps. **in** Häuselmann, P and Monbaron, M. (Eds.) Cave genesis in the Alpine belt. Research Reports **10** Institute of Geography, University of Fribourg, Switzerland.41–79.
Bitterli, T. 1997. Gravitational downsliding of carbonate masses. Twelfth International Speleological Congress. Field Trip notes.
Bitterli, T and Jeannin, P-Y. 1997. Genesis of a large cave system: the case study of the North of Lake Thun system (Canton Bern, Switzerland). Proceedings of the twelfth International Speleological Congress. Proceedings of the sixth Conference on Limestone Hydrology and Fissured Media. Modelling in Karst Systems. 57–65.
Bond, G and 13 authors. 1992. Evidence for massive discharges of icebergs into the north Atlantic ocean during the last glacial period. Nature **360** 245–249.
Bond, G and 9 authors. 1997. A pervasive millennial-scale cycle in north Atlantic Holocene and glacial climates. Science **278** 1257–1266.
Bond, G and 9 authors. 2001. Persistent solar influence on north Atlantic climate during the Holocene. Science **294** 2130–2136.
Bond, GC and Lotti, R. 1995. Iceberg discharges into the north Atlantic on millennial timescales during the last glaciation. Science **267** 1005–1010.
Bond, G, Broecker, W, Johnsen, S, McManus, J, Labeyrie, L, Jouzel, J and Bonani, G. 1993. Correlations between climate records from north Atlantic sediments and Greenland ice. Nature **365** 143–147.
Bonow, J, Lidmar-Bergström, K and Näslund, J-O. 2000. Palaeosurfaces and major valleys in the Døvre–Rondana area, southern Norway. Abstracts p164 and seminar notes from Geoscience 2000, 17–20 April 2000. The Geological Society.

Borsato, A and Frisia, S. 199? Litho facies and diagenesis as controlling factors in the development of solution caves in dolomite: the example of the Norian Dolomia Principale (Trentino- northern Italy). Publication ?? 95–107.

Bosak, P, Ford, DC, Glazek, J and Horacek, I. (Eds). 1989. Paleokarst: a systematic and regional review. Elsevier.

Bosch, R. 1998. Clastic sediments in karst systems. p8. Abstracts of the Friends of Karst Symposium, Western Kentucky University.

Bottrell, S. 1988. Geological controls on speleogenesis in the marbles of lower Glomdal, Rana, Norway. Cave Science **15** (3) 133–137.

Bottrell, SH, Gunn, J and Lowe, DJ. 2000a. Calcite dissolution by sulphuric acid in Klimchouk, AB, Ford, DC, Palmer, AN and Dreybrodt, W (Eds). 2000. Speleogenesis: Evolution of karst aquifers. National Speleological Society. USA. 156–157.

Bottrell, SH, Gunn, J and Lowe, DJ. 2000b. Some case studies of speleogenesis by sulphuric acid in Klimchouk, AB, Ford, DC, Palmer, AN and Dreybrodt, W (Eds). 2000. Speleogenesis: Evolution of karst aquifers. National Speleological Society. USA. 304–308.

Boulton, GS, Caban, PE, van Gijssel, K, Leijnse, A, Punkari, M and van Weert, FHA. 1996. The impact of glaciation on the groundwater regime of Northwest Europe. Global And Planetary Change **12** (1–4) 397–413.

Boulton, GS, Dongelmans, P, Punkari, M and Broadgate, M. 2001. Palaeoglaciology of an icesheet through a glacial cycle: the European icesheet through the Weichselian. Quaternary Science Reviews**20** 591–625.

Boulton, GS, Slot, T, Blessing, K, Glasbergen, P, Leijnse, T and van Gijssel, K. 1993. Deep circulation of groundwater in over pressurised subglacial aquifers and its geological consequences. Quaternary Science Reviews **12** 739–745.

Bowen, DQ, Phillips, FM, McCabe, AM, Knutz, PC and Sykes, GA. 2002. New data for the Last Glacial Maximum in Great Britain and Ireland. Quaternary Science Reviews**21** 89–101.

Braathen, A, Osmundsen, PT, Nordgulen, Ø, Roberts, D and Meyer, GB. 2002. Orogen-parallel extensions of the Caledonides in northern central Norway: and overview. Norwegian Journal of Geology**82** 225–241.

Braathen, A, Blikra, LH, Berg, SS and Karlsen, F. 2004. Rock-slope failures in Norway; type, geometry, deformation mechanisms and stability. Norwegian Journal of Geology**84** 67–88.

Brahana, JV, Thrailkill, J, Freeman, T and Ward, WC. 1988. Chapter 38. Carbonate Rocks. in Back, W, Rosenshein, JS and Seaber, PR. Eds. Hydrogeology. Geological Society of North America. The Geology of North America v. O-2.

Brattli, B. 1996. Structures and metamorphism at Brygfjell–Simafjell within the Rødingsfjellet Nappe Complex, Nordland, Norway. Norges Geologiske Undersøkelse **431** 19–32.

Brazier, V, Kirkbride, MP and Gordon, JE. 1998. Active ice-sheet deglaciation and ice-dammed lakes in the northern Cairngorm Mountains, Scotland. Boreas **27** 297–310.

Brodie, KH and Rutter, EH. 2000. Deformation mechanisms and rheology: why marble is weaker than quartzite. Journal of the Geological Society, London **157** 1093–1096.

Broecker, WS, Kennett, JP, Flower, BP, Teller, JT, Trumbore, S, Bonani, G and Wolfli, W. 1989. Routing of meltwater from the Laurentide Ice Sheet during the Younger Dryas cold episode. Nature**341** 318–321.

Broecker, WS. 1994. Massive iceberg discharges as triggers for global climate change. Nature **372** 421–424.

Brown, MC, Ford, DC and Wigley, TML. 1971. Ice caves of the Canadian Rockies (Abstract). Caves and Karst **13** (5) p38.

Bryhni, I and Andreasson, P-G. 1985. Metamorphism in the Scandinavian Caledonides 763–782. in Gee and Sturt (1985).

Buhmann, D and Dreybrodt, W. 1985a. The kinetics of calcite dissolution and precipitation in geologically relevant situations of karst areas 1. Open System. Chemical Geology **48** 189–211.

Buhmann, D and Dreybrodt, W. 1985b. The kinetics of calcite dissolution and precipitation in geologically relevant situations of karst areas 2. Closed System. Chemical Geology **53** 109–124.

Buhmann, D and Dreybrodt, W. 1987. Calcite dissolution kinetics in the system H_20–CO_2–$CaCO_3$ with participation of foreign ions. Chemical Geology **64** 89–102.

Bungum, H. 1989. Earthquake occurrence and seismotectonics in Norway and surrounding areas in S Gregerson and PW Basham (Eds), Earthquakes at North-Atlantic Passive Margins: Neotectonics and Postglacial Rebound, 501–519.

Bungum, H, Hokland, BK, Husebye, ES and Ringdal, F. 1979. An exceptional intraplate earthquake sequence in Meløy, northern Norway. Nature **280** 32–35.

Busenberg, E and Plummer, LN. 1982. The kinetics of dissolution of dolomite in CO_2–H_2O systems at 1.5 to 65°C and 0 to 1 atm. P_{CO2}. American Journal of Science **282** 45–78.

Bögli, A. 1964. Mischungskorrosion - ein Beiträg zur Verkarstungsproblem. Erdkunde **18** 83–92. [English translation by E Elder. 1985. Mixture Corrosion - a contribution to the karstification problem. Cave Geology **1** (10) 393–406].

Cao, H, Yang, J and Wang, D. 1999. Paleokarsts in Precambrian and Ordovician carbonates, Kalpin-Shaya Uplift Zone, Tarim Basin, China. Carbonates and Evaporites **14** (2) 200–208.
Carlsten, S and Stråhle, A. 2001. Inte mycket spridkor under Bodagrottorna! Grottan **36** (1) 30–31.
Choppy, J. 1997. La tectonique et la karst. Proceedings of the Twelfth International Speleological Congress **1** 367–368.
Chou, L, Garrels, RM and Wollast, R. 1989. Comparative study of the kinetics and mechanisms of dissolution of carbonate minerals. Chemical Geology **78** 269–282.
Ciry, R. 1959. Une categorie speciale de cavites soutterraines; Les Grottes Cutanees. Ann. de Spel. **14** 23–30.
Clark, PU, Marshall, SJ, Clarke, GKC, Hostetler, SW, Licciardi, JM and Teller, JT. 2001. Freshwater forcing of abrupt climate change during the last glaciation. Science **293** 283–287.
Clark, PU, Alley, RB and Pollard, D. 1999. Northern hemisphere ice-sheet influences on global climate change. Science **286** 1104–1111.
Clark, PU and Mix, AC. 2002. Ice sheets and sea level of the Last Glacial Maximum. Quaternary Science Reviews **21** 1–7.
Cloetingh, S, Reemst, P, Kooi, H and Fanavoll, S. 1992. Intraplate stresses and the post-Cretaceous uplift and subsidence in northern Atlantic basins. Norsk Geologisk Tidsskrift **72** (3) 229–236.
Cogley, JG and McCann, SB. 1971. Chemistry of limestone run off waters in the high arctic (Abstract). Caves and Karst **13** (5) 38–39.
Corbel, J. 1952a. Les Phenomenes Karstiques en Suede. Geografiska Annaler **34** 203–237.
Corbel, J. 1952b. Karst et glaciers en Laponie. Revue Géogr. Lyons. **27** 257–267.
Corbel, J. 1953. Une region karstique de Haute-Laponie, Navnløsfjell. Revue Géogr. Lyons. **28** 329–344.
Corbel, J. 1954. Karst de climat froid. Erdkunde **8**. Bonn.
Corbel, J. 1957. Les Karsts du nord-ouest de l'Europe. Mém. Docums. Inst. Etud. rhodan **12** 501pp.
Corbel, J. 1960. Nouvelles recherches sur les karsts arctiques Scandinaves. Zeitschrift fur Geomorphologie. N.F. Supp. 2 74–78.
Cuffey, KM and Marshall, SJ. 2000. Substantial contribution to sea-level rise during the last interglacial from the Greenland icesheet. Nature **404** 591–594.
Cuffey, KM and Vimeux, F. 2001. Covariation of carbon dioxide and temperature from the Vostok ice core after deuterium-excess correction. Nature **412** 523–527.
Curl, RL. 1958. A statistical theory of cave entrance evolution. National Speleological Society Bulletin **20** 9–22.
Curl, RL. 1960. Stochastic models of cavern development. National Speleological Society Bulletin **22** (1) 66–75.
Curl, RL. 1966a. Scallops and flutes. Transactions of the Cave Research Group of GB **7** 121–160.
Curl, RL. 1966b. Caves as a measure of Karst. Journal of Geology **74** (15) part 2 798–830.
Curl, RL. 1971. Cave conduit competition - 1: Power law models for short tubes (Abstract). Caves and Karst **13** (5) p39.
Curl, RL. 1974. Deducing flow velocity in cave conduits from scallops. National Speleological Society Bulletin **36** (2) 1–5.
Curl, RL. 1986. Fractal Dimensions and Geometrics of Caves. Mathematical Geology **18** (8) 765–785.
Cwynar, LC and Spear, RW. 2001. Late glacial change in the White Mountains of New Hampshire. Quaternary Science Reviews **20** 1265–1274.

Dahl, OD and Nesje, A. 1994. Holocene glacier fluctuations at Hardangerjøkulen, central-southern Norway: a high-resolution composite chronology from lacustrine and terrestrial deposits. The Holocene **4** (3) 269–277.
Dahl, R, Sveian, H and Thoresen, MK. 1997. Nord Trøndelag og Forsen: Geologi og Landscap. Norges Geologiske Undersøkelse. 137pp.
Dallmann, WK. 1986. Polyphase deformation in the Hattfjelldal Nappe, internal zone of the Scandinavian Caledonides, North-Central Norway. Norsk Geologisk Tidsskrift **66** (2) 163–182.
Dallmann, WK. 1987. Sedimentary environment and synsedimentary tectonics in the Hattfjelldal Nappe, North-Central Norway. Norges Geologiske Undersøkelse **410** 25–54.
Dansgaard, W and Duplessy, C-J. 1981. The Eemian interglacial and its termination. Boreas **10** 219–228.
Dansgaard, W and 10 authors. 1993. Evidence for general instability of past climate from a 250-kyr ice-core record. Nature **364** 218–220.
Davenport, CA, Ringrose, PS, Becker, A, Hancock, P and Fenton, C. 1989. Geological investigations of late and post glacial earthquake activity in Scotland in S Gregerson and PW Basham (Eds), Earthquakes at North-Atlantic Passive Margins: Neotectonics and Postglacial Rebound, 175–194.
Davies, JH and von Blanckenburg, F. 1998. Orogenic consequences of slab break off during continental collision. Geoscience 98 Abstracts p161.
Davies, WE. 1960. Origin of caves in folded limestones. National Speleological Society Bulletin **22** (1) 5–18.
Davies, WE. 1961. Glacier caves in Svartisen, Norway. National Speleological Society Bulletin **23** (2) 75–76.
Davis, SN and Moore, GW. 1965. Semidiurnal movement along a bedrock joint in Wool Hollow Cave, California. National Speleological Society Bulletin **27** (4) 133–142.

Davis, SN. 1966. Initiation of groundwater flow in jointed limestone.
National Speleological Society Bulletin **28** (3) 111–118.

Davies, WE and Krinsley, DB. 1960. Caves in N. Greenland.
National Speleological Society Bulletin **22** 114–116.

Dawson, AG, Hampton, S, Fretwell, P, Harrison, S and Greengrass, P. 2002. Defining the centre of glacio-static uplift of the last Scottish ice-sheet: the Parallel Roads of Glen Roy, Scottish Highlands.
Journal of Quaternary Science 17 (5) 527–533.

Dehls, JF, Olesen, O, Bungum, H, Hicks, EC, Lindholm, CD and Riis, F. 2000a. 1:3000000 Neotectonic map: Norway and adjacent areas. 1:3,000,000. Geological Survey of Norway.

Dehls, JF, Olesen, O, Olsen, L and Blikra, LH. 2000b. Neotectonic faulting in northern Norway; the Stuoragurra and Nordmannvikdalen postglacial faults. Quaternary Science Reviews **19** 1447–1460.

Denton, GH. 2000. Does an asymmetric thermohaline-icesheet oscillator drive 100,000-yr glacial cycles?
Journal of Quaternary Science **15** (4) 301–318.

Doj, T. 1985. Korallgrottan - "hål-kometen" slår nye rekord... Grottan **20** (4) 3–13.

Doj, T. 1993. Hattfjelldal September 1990. Grottan **28** (1) 7–10.

Dolmen, D and Arnekleiv, JV. 1990. En zoologisk befaring av karstområder og grotte systemer i Grane og Rana Kommuner, Nordland.
Rapport Zoologisk Series 1990–92. Universitet i Trondheim,Vitenskapsmuseet. 50pp.

Donner, J. 1995. The Quaternary History of Scandinavia. 200pp. Cambridge University Press.

Donner, J. 1996. The Early and Middle Weichselian Interstadials in the Central Area of the Scandinavian Glaciations. Quaternary Science Reviews. **15** 471–479.

Doré, AG. 1992. The Base Tertiary Surface of southern Norway and the northern North Sea.
Norsk Geologisk Tidsskrift **72** (3) 259–266.

Doré, AG and Jensen, LN. 1996. The impact of late Cenozoic uplift and erosion on hydrocarbon exploration: offshore Norway and some other uplifted basins. Global And Planetary Change **12** (1–4) 415–436.

Dowdeswell, JA and Siegert, MJ. 1999. The dimensions and topographic setting of Antarctic subglacial lakes and implications for large-scale water storage beneath continental ice sheets.
Geological Society of America Bulletin **111** (2) 254–263.

Dowdeswell, JA, Elverhøi, A, Andrews, JT and Hebbeln, D. 1999. Asynchronous deposition of ice-rafted layers in the Nordic seas and north Atlantic ocean. Nature **400** 348–351.

Drew, LJ, Schuenemeyer, JH, Armstrong, TR and Sutphin, DM. 2001.
Initial yield to depth relation for water wells drilled into crystalline bedrock - Pinardville Quadrangle, New Hampshire. Groundwater **39** (5) 676–684.

Dreybrodt, W. 1981a. Kinetics of the dissolution of calcite and its application to karstification.
Chemical Geology **31** 245–269.

Dreybrodt, W. 1981b. Mixing corrosion in $CaCO_3$–CO_2–H_2O systems and its role in the karstification of limestone areas. Chemical Geology **32** 221–236.

Dreybrodt, W. 1987. The kinetics of calcite dissolution and its consequences to karst evolution from the initial to the mature state. National Speleological Society Bulletin **49** 31–49.

Dreybrodt, W. 1988. Processes in Karst Systems: Physics, Chemistry and Geology. Springer, New York.

Dreybrodt, W. 1989a. Effect of $MgCO_3$ to the solubility of calcite.
Proceedings of the tenth International Speleological Congress 177–178.

Dreybrodt, W. 1989b. Karst development in its initial state: a model of speleogenesis.
Proceedings of the tenth International Speleological Congress 174–176.

Dreybrodt, W. 1990. The role of dissolution kinetics in the development of karst aquifers in limestone: a model simulation of karst evolution. Journal of Geology **98** (5) 639–655.

Dreybrodt, W. 1992. Dynamics of karstification: A model applied to hydraulic structures in karst terranes.
Applied Hydrogeology **1** (3) 20–32.

Dreybrodt, W. 1996. Principles of early development of karst conduits under natural and man-made conditions revealed by mathematical analysis of numerical models. Water Resources Research **32** (9) 2923–2935.

Dreybrodt, W. 1997. Limestone dissolution rates in karst environments. Proceedings of the twelfth International Speleological Congress. Proceedings of the sixth Conference on Limestone Hydrology and Fissured Media. Modelling in Karst Systems. 45–52. Also in Bulletin d'Hydrogéologie **16** 1998 167–183.

Dreybrodt, W. 1998. Chapter 2. Principles of karst evolution from initiation to maturity and their relation to physics and chemistry **in** Yuan, D and Liu, Z (Editors). Global Karst Correlation.
Final Report of the UNESCO/IUGS International Geological Correlation Program Project 299: Geology, Climate, Hydrology and Karst Formation (1990–1994).

Dreybrodt, W. 2000. Equilibrium chemistry of karst water in limestone terranes
in Klimchouk, AB, Ford, DC, Palmer, AN and Dreybrodt, W (Eds). 2000. Speleogenesis: Evolution of karst aquifers. National Speleological Society. USA. 126–135.

Dreybrodt, W and Buhmann, D. 1991. A mass transfer model for dissolution and precipitation of calcite from solutions in turbulent motion. Chemical Geology **90** 107–122.

Dreybrodt, W and Eisenlohr, L. 2000. Limestone dissolution rates in karst environments **in** Klimchouk, AB, Ford, DC, Palmer, AN and Dreybrodt, W (Eds). 2000. Speleogenesis: Evolution of karst aquifers. National Speleological Society. USA. 136–148.

Dreybrodt, W and Gabrovsek, F. 2000a. Dynamics of the evolution of single karst conduits **in** Klimchouk, AB, Ford, DC, Palmer, AN and Dreybrodt, W (Eds). 2000. Speleogenesis: Evolution of karst aquifers. National Speleological Society. USA. 184–193.

Dreybrodt, W and Gabrovsek, F. 2000b. Influence of fracture roughness on karstification times **in** Klimchouk, AB, Ford, DC, Palmer, AN and Dreybrodt, W (Eds). 2000. Speleogenesis: Evolution of karst aquifers. National Speleological Society. USA. 20–223.

Dreybrodt, W and Siemers, J. 2000. Cave evolution on two-dimensional networks of primary fractures in limestones **in** Klimchouk, AB, Ford, DC, Palmer, AN and Dreybrodt, W (Eds). 2000. Speleogenesis: Evolution of karst aquifers. National Speleological Society. USA. 201–211.

Dreybrodt, W, Lauckner, J, Liu, Z, Svensson, U and Buhmann, D. 1996. The kinetics of the reaction $CO_2 + H_2O \rightarrow H^+ + HCO_3^-$ as one of the rate limiting steps for the dissolution of calcite in the system $H_2O + CO_2 + CaCO_3$. Geochimica et Cosmochimica Acta **60** (18) 3375–3381.

Dreybrodt, W, Romanov, D and Gabrovsek, F. 2001. Karstification below dam sites: a model of increasing leakage from reservoirs **in** Beck, BF and Herring, JG. (Eds.) Geotechnical and environmental applications of karst geology and hydrology. Balkema. 131–137.

Droppa, A. 1986. L'influence des saisons de l'année sur la dénudation karstique. Proceedings of the ninth International Speleological Congress **1** 237–241.

Dublyansky, VN and Dublyansky, YV. 2000. The role of condensation in karst hydrogeology and speleogenesis **in** Klimchouk, AB, Ford, DC, Palmer, AN and Dreybrodt, W (Eds). 2000. Speleogenesis: Evolution of karst aquifers. National Speleological Society. USA. 100–112.

Durham, WB, Bourcier, WL and Burton, EA. 2001. Direct observation of reactive flow in a single fracture. Water Resources Research **37** (1) 1–12.

Dyke, AS, Andrews, JT, Clark, PU, England, JH, Miller, GH, Shaw, J and Veillette, JJ. 2002. The Laurentide and Innuitian ice sheets during the Last Glacial Maximum. Quaternary Science Reviews **21** 9–31.

Earl-Gulet, JR, Mahaney, WC, Sanmugadas, K, Kalm, V and Hancock, RGV. 1998. Middle-Holocene timberline fluctuation: influence on the genesis of Podzols (Spodosols), Norra Storfjället Massif, northern Sweden. The Holocene **8** (6) 705–718.

Egemeier, SJ. 1987. A theory for the origin of Carlsbad Caverns. National Speleological Society Bulletin **49** 73–76.

Ehlers, J. 1996. Quaternary and Glacial Geology. 578 pp.

Einevoll, S and Lauritzen, S-E. 1994. Calibration of stable isotope and temperature signal in the percolation zone of a sub-arctic cave, N. Norway. Cave and Karst Science **21** (1) p9. (abstract)

Eisenlohr, L, Madry, B and Dreybrodt, W. 1997. Changes in the dissolution kinetics of limestone by intrinsic inhibitors adsorbing to the surface. Proceedings of the twelfth International Speleological Congress **2** 81–84.

Eisenlohr, L, Meteva, K, Gabrovsek, F and Dreybrodt, W. 1999. The inhibiting action of intrinsic impurities in natural calcium carbonate minerals to their dissolution kinetics in aqueous $H_2O - CO_2$ solutions. Geochimica et Cosmochimica Acta **63** (7/8) 989–1002.

Ek, C and Gewelt, M. 1985. Carbon dioxide in cave atmospheres. New results in Belgium and comparison with some other countries. Earth Surface Processes and Landforms **10** 173–187.

Ekman, M. 1996. A consistent map of the postglacial uplift of Fennoscandia. Terra Nova **8** 158–165.

Engh, L. 1974. En morphogenetisk studie av ett fjällområde vid Giengeljaure väster om Övre Ältsvattnet i Västerbottens län. PM Länsstyrelsen, Västerbotten

Engh, L. 1977. Karst morphology in subarctic Sweden. Proceedings of the seventh International Speleological Congress 168–170.

Engh, L. 1980. Skandinavisk speleokronologi i ny belysning genom nyupptackta grottor i Vadvevagge. Grottan **15** (1) 3–24.

Engh, R and Sjöberg, R. 1981. Svenska Grottor Nr. 4. Karst och Grottor i svenska fjällen. 58pp.

EPICA community members. 2004. Eight glacial cycles from an Antarctic ice core. Nature **429** 623–628.

Fairchild, IJ. 1989. Dolomitic stromatolite-bearing units with storm deposits from the Vendian of East Greenland and Scotland: a case of facies equivalence **in** Gayer, RA (Ed.) The Caledonide Geology of Scandinavia. Graham and Trotman. 275–283.

Fairchild, IJ and Killawee, JA. 1995. Selective leaching in glacierized terrains and implications for retention of primary chemical signals in carbonate rocks. **in** Water-Rock Interaction. Kharaka and Chudaev. Balkerna, Rotterdam.

Fairchild, IJ, Bradby, L, Sharp, M and Tison, J-L. 1994. Hydrochemistry of carbonate terrains in Alpine glacial settings. Earth Surface Processes and Landforms **19** 33–54.

Fastook, JL and Holmlund, P. 1994. A glaciological model of the Younger Dryas event in Scandinavia. Journal of Glaciology. **40** (134) 125–131.

Faulkner, TL. 1980. Sirijordgrotten, and other caves in Eiterådal, Vefsn, Norway. Trans. British Cave Research Association 7 (2) 53–69.

Faulkner, T. 1981. Swetc CC / Wessex CC Expedition to Norway 1978. Newsletter SwetcCC **16** (1) 3–13.

Faulkner, TL. 1983. Kvannlihola 2 and other caves in Fiplingdal and other areas of Nordland, Norway. Cave Science **10** (3) 117–144.

Faulkner, TL. 1987. Caves of the Jordbruelv and Jordhulefjell, south Nordland, Norway. Cave Science **14** (1) 31–45.

Faulkner, TL. 1988. The Legends and Studies of the Favnvatn Area. Norsk Grotteblad (20) 14–16.

Faulkner, T. 1992. South Nordland 1987 and 1988. Norsk Grotteblad **23** 25–29.

Faulkner, T. 1997. Cave development in metacarbonate rocks. Application to register for a research degree. University of Huddersfield.

Faulkner, T. 1998. Karst and Tectonics Symposium Review. Cave and Karst Science **25** (3) 150–152.

Faulkner, T. 1999a. Order and disorder in the karsts and caves of central Scandinavia. Cave and Karst Science **26** (3) p131.

Faulkner, T. 1999b. Transfer Report: Cave development in metacarbonate rocks. Univ. of Huddersfield 24pp.

Faulkner, T. 2000a. Tjårrogrottorna. Grottan **35** (2) 15–18.

Faulkner, T. 2000b. Metamorphic Limestones in Shetland. Grampian Speleological Society Bulletin **5** (3) 40–46.

Faulkner, T. 2000c. Undersøkelse av kalksteinsgrotter på Helgeland. Årbok for Helgeland 2000 (31) 166–181.

Faulkner, T. 2000d. Caves in metamorphic limestones of the Irish Dalradian Supergroup. Irish Speleology **17** 43–49.

Faulkner, T. 2001. Cave development in central Scandinavia. Proceedings of the thirteenth International Speleological Congress. Paper 155 4pp (Abstract p106).

Faulkner, T. 2003. The hydrogeology of crystalline rocks: pointers to tectonic inception mechanisms in karst. Proceedings of the International Conference on Karst Hydrogeology and Ecosystems. Bowling Green, Kentucky, USA. 3–6 June 2003. (Abstract p20).

Faulkner, T. 2004. Scallops and dissolution rate. Cave and Karst Science **31** (1) 43–44.

Faulkner, T and Newton, G. 1990. Caves of Bjørkåsen and Elgfjell. Cave Science **17** (3) 107–122.

Faulkner, T and Newton, G. 1995. Toerfjellhola and Other Caves at Vevelstad and Brønnøy, Norway. Cave and Karst Science **22** (1) 3–22.

Faulkner, T and St.Pierre, D. 1988. Cave Studies in Norway. Cave Science **15** (3) 91–92.

Faulkner, T and St.Pierre, S. 1977. Expedition to Norway 1974. Swetc Caving Club Occ. Pub. (4). 70pp.

Fein, JB, Graham, CM, Holness, MB, Fallick, AE and Skelton, ADL. 1994. Controls on the mechanisms of fluid infiltration and front advection during regional metamorphism: a stable isotope and textural study of retrograde Dalradian rocks of the SW Scottish Highlands. Journal of Metamorphic Geology **12** 249–260.

Finnesand, SU. 2003. Analyse av overflatekarstformer i Glomfjell området ved Svartisen. Norsk Grotteblad (41) 3–32.

Fisher, TG, Clague, JJ and Teller, JT. 2002. The role of outburst floods and glacial meltwater in subglacial and proglacial landform genesis. Quaternary International **90** (1) 1–4.

Fjeldskaar, W. 1994. The amplitude and decay of the glacial forebulge in Fennoscandia. Norsk Geologisk Tidsskrift **74** (1) 2–8.

Fjeldskaar, W. 2000. An isostatic test of the hypothesis of ice-free mountain areas during the last glaciation. Norsk Geologisk Tidsskrift **80** 51–56.

Fjeldskaar, W, Lindholm, C, Dehls, JF and Fjeldskaar, I. 2000. Postglacial uplift, neotectonics and seismicity in Fennoscandia. Quaternary Science Reviews **19** 1413–1422.

Flinn, D. 1967. Ice front in the North Sea. Nature **215** 1151–1154.

Follestad, BA. 1997. Preliminary report on the research project: Upper and Lower Glomsjø - subglacial waterways or open lakes? Norges Geologiske Undersøkelse **433** 50–51.

Ford, DC. 1965a. The origin of limestone caverns: a model from the central Mendip Hills, England. National Speleological Society Bulletin **27** (4) 109–132.

Ford, DC. 1965b. Stream potholes as indicators of erosion phases in limestone caves. National Speleological Society Bulletin **27** (1) 27–32.

Ford, DC. 1967. Sinking creeks of Mt. Tupper: a remarkable groundwater system in Glacier National Park. Canadian Geographer **11** (1) 49–52.

Ford, DC. 1968. Features of cavern development in Central Mendip. Trans. Cave Research Group of Great Britain **10** (1) 11–25.

Ford, DC. 1971a. Characteristics of limestone solution in the southern Rocky Mountains and Selkirk Mountains, Alberta and British Columbia. Canadian Journal of Earth Sciences **8** 585–609.

Ford, DC. 1971b. Geologic structure and a new explanation for limestone cave genesis. Trans. Cave Research Group of Great Britain **13** (2) 81–94.

Ford, DC. 1977a. Karst and Glaciation in Canada. Proceedings of the seventh International Speleological Congress 188–189.

Ford, DC. 1977b. Genetic classification of solutional cave systems.
Proceedings of the seventh International Speleological Congress 189–192.
Ford, DC. 1983. Effects of glaciations upon karst aquifers in Canada. Journal of Hydrology **61** (1/3) 149–158.
Ford, DC. 1986. Review of glaciation in Canada.
Proceedings of the ninth International Speleological Congress **1** 113–114.
Ford, DC. 1987. Effects of glaciation and permafrost upon the development of karst in Canada.
Earth Surface Processes and Landforms **12** 507–521.
Ford, DC. 1995. Features of karren development in dolostones in Canada. International Symposium of Karren Landforms **14** 1995. (Abstract in Newsletter on Annotated Bibliography (4) 57–58 1996).
Ford, DC. 1998. Perspectives in karst hydrogeology and cavern genesis. Bulletin d'Hydrogéologie **16** 9–29.
Also in Palmer, AN, Palmer, MV and Sasowsky, I. (Eds.)
Karst modeling. Karst Waters Institute Special Publication 5. 17–29.
Ford, DC. 2000. Speleogenesis under unconfined settings
in Klimchouk, AB, Ford, DC, Palmer, AN and Dreybrodt, W (Eds). 2000. Speleogenesis: Evolution of karst aquifers. National Speleological Society. USA. 319–324.
Ford, DC. 2002. Depth of conduit flow in unconfined carbonate aquifers: Comment. Geology **30** (1) p93.
Ford, DC and Ewers, RO. 1978. The development of limestone cave systems in the dimensions of length and depth. Canadian Journal of Earth Sciences **15** 1783–1798.
Ford, DC and Williams, PW. 1989. Karst Geomorphology and Hydrology. 601pp. (London: Chapman and Hall).
Ford, DC, Fuller, PG and Drake, JJ. 1970. Calcite precipitates at the soles of temperate glaciers.
Nature **226** 441–442.
Ford, DC, Lauritzen, S-E and Ewers, RO. 2000. Hardware and software modelling of initial conduit development in karst rocks in Klimchouk, AB, Ford, DC, Palmer, AN and Dreybrodt, W (Eds). 2000. Speleogenesis: Evolution of karst aquifers. National Speleological Society. USA. 175–183.
Ford, DC, Palmer, AW and White, WB. 1988. Chapter 43. Landform development: karst
in Back, W, Rosenshein, JS and Seaber, PR. Eds. Hydrogeology. Geological Society of North America. The Geology of North America v. O-2.
Ford, DC, Schwarcz, HP, Drake, JJ, Gascoyne, M, Harmon, RS and Latham, AG. 1981.
Estimates of the age of the existing relief within the southern Rocky Mountains of Canada.
Arctic and Alpine Research **13** (1) 1–10.
Ford, TD. 1963. The Goyden Pot drainage system, Nidderdale, Yorks.
Trans. Cave Research Group of Great Britain **6** (3) 81–90.
Ford, TD. 1984. Paleokarsts in Britain. Cave Science **11** (4) 246–264.
Ford, TD. 1989. Paleokarst of Britain in Bosak *et al.* (Eds.) Paleokarst - a systematic and regional review.
Elsevier. 51–70.
Ford, TD. 1995. Some thoughts on hydrothermal caves. Cave and Karst Science **22** (3) 107–118.
Ford, TD. 2000. Vein cavities: an early stage in the evolution of the Castleton caves, Derbyshire, UK.
Caves and Karst Science **27** (1) 5–14.
Ford, TD and Worley, NE. 1977a. Phreatic caves and sediments at Matlock.
Proceedings of the seventh International Speleological Congress 194–196.
Ford, TD and Worley, NE. 1977b. Mineral veins and cave development.
Proceedings of the seventh International Speleological Congress 192–194.
Forsberg, CF. 1996. Possible consequences of glacially induced groundwater flow.
Global And Planetary Change **12** (1–4) 387–396.
Forsström, L and Punkari, M. 1997. Initiation of the last glaciation in northern Europe.
Quaternary Science Reviews **16** 1197–1215.
Foslie, S and Strand, T. 1956. Namsvatn med en del av Frayningsfjell.
Norges Geologiske Undersøkelse **196** 82pp.
Fountain, AG, Jacobel, RW, Schlichting, R and Jansson, P. 2005. Fractures as the main pathways of water flow in temperate glaciers. Nature 433 618–620.
Fredin, O. 2002. Glacial inception and quaternary mountain glaciations in Fennoscandia.
Quaternary International **95/96** 99–112.
Freeze, RA and Cherry, JA. 1979. Groundwater. Prentice-Hall 604pp.
Funder, S. 2000. An unusual combination of glacio-eustasy and -isostasy, and the life of an Eemian shelf sea in northern Eurasia. Abstracts p83 and seminar notes from Geoscience 2000, 17–20 April 2000.
The Geological Society.

Gabrovsek, F. 2000. Evolution of early karst aquifers: from simple principles to complex models.
Zalozba ZRC, Ljubljana. 150pp.
Gabrovsek, F and Dreybrodt, W. 2000. Role of mixing corrosion in calcite-aggressive H_2O–CO_2–$CaCO_3$ solutions in the early evolution of karst aquifers in limestone. Water Resources Research **36** (5) 1179–1188.
Gabrovsek, F and Dreybrodt, W. 2001. A model of the early evolution of karst aquifers in limestone in the dimensions of length and depth. Journal of Hydrology **240** 206–224.

Gale, SJ. 1981. The palaeohydraulics of karst drainage systems: fluvial cave-sediment studies. Proceedings of the eighth International Speleological Congress **1** 213–216.

Gale, SJ. 1984. The hydraulics of conduit flow in carbonate aquifers. Journal of Hydrology **70** 309–337.

Gams, I. 1981. Comparative research of limestone solution by means of standard tablets. Proceedings of the eighth International Speleological Congress 273–275.

Gams, I. 1994. Types of Contact Karst. Geografia Fisica e Dinamica Quaternia **17** 34–46.

Gascoyne, M and Nelson, DE. 1983. Growth mechanisms of recent speleothems from Castleguard Cave, Columbia Ice Fields, Alberta, Canada, inferred from a comparison of Uranium-series and Carbon-14 age data. Arctic and Alpine Research **15** (4) 537–542.

Gayer, RA. (Ed.) 1985. The Tectonic Evolution of the Caledonian – Appalachian Orogeny. Vieweg.

Ge, S. 1997. A governing equation for fluid flow in rough fractures. Water Resources Research **33** (1) 53–61.

Gebelein, CD and Hoffmann, P. 1973. Algal origin of dolomite laminations in stromatolite limestones. Journal of Sedimentary Petrology **43** 603–613.

Gee, DG and Sturt, BA (Eds.). 1985. The Caledonide Orogen - Scandinavia and Related Areas. John Wiley. 1250pp.

Gibbons, W and Harris, WL. 1994. A revised correlation of Precambrian rocks in the British Isles. The Geological Society. Special Report (22). 110pp.

Gillieson, D. 1996. Caves: Processes, development and management. Blackwell. 336pp.

Gjessing, J. 1967. Norway's Paleic Surface. Norsk Geografisk Tidsskrift **21** 69–132,

Glasser, NF. 1995. Modelling the effect of topography on ice sheet erosion, Scotland. Geografiska Annaler **77A** (1–2) 67–82.

Glazak, J, Rudnicki, J and Szynkiewicz, A. 1977. Pro-glacial caves. Proceedings of the seventh International Speleological Congress 215–217.

Glennie, EA. 1952. Evidence in caverns of deep freezing during the Ice Age. Cave Research Group of Great Britain Newsletter **37** 3–4.

Glover, RR. 1977. Conceptual model of cave development in a glaciated region. Proceedings of the seventh International Speleological Congress 220–221.

Gorbatschev, R. 1985. Precambrian basement of the Scandinavian Caledonides. 197–212. in Gee and Sturt (1985).

Griffey, NJ and Worsley, P. 1978. The pattern of Neoglacial glacier variations in the Okstindan region of northern Norway during the last three millennia. Boreas **7** 1–17.

Grimsby, B. Undated. Øyfjellgrotta ved Mosjøen. Mosjøen og omegn reisetrafikklag. 7pp.

Groves, CG and Howard, AD. 1994. Minimum hydrochemical conditions allowing limestone cave development. Water Resources Research **30** (3) 607–615.

Grønlie, A. 1975. Geologien I Vefsnbygdene. Vefsn Bygdebok 1975 417–483.

Grønlie, A. 1982. Kovagrotta i Elsfjord. Norsk Grotteblad **9** 19–20.

Gudmundsson, A, Fjeldskaar, I and Gjesdal, O. 2002. Fracture-generated permeability and groundwater yield in Norway. Norges Geologiske Undersøkelse Bulletin **439** 61–69.

Guest, RE, McCaig, AM and Graham, CM. 2000. Retrograde Dolomitisation of Marble. Abstracts p164 and seminar notes from Geoscience 2000, 17–20 April 2000. The Geological Society.

Gulliksen, S, Birks, HH, Possnert, G, Mangerud, J. 1998. A calendar age estimate of the Younger Dryas–Holocene boundary at Kråkenes, western Norway. The Holocene **8** (3) 249–259.

Gunn, J. 1981a. Hydrological processes in karst depressions. Zeitschrift fur Geomorphologie **25** (3) 313–331.

Gunn, J. 1981b. Prediction of limestone solution rates. Earth Surface Processes and Landforms **6** 595–597.

Gunn, J. 1983. Point-recharge of limestone aquifers - a model from New Zealand karst. Journal of Hydrology **61** (1/3) 19–29.

Gunn, J and Gagen, P. 1987. Limestone quarrying and sinkhole development in the English Peak District in Beck, BF and Wilson, WL. (Eds.) Karst Hydrogeology. Balkema. 121–125.

Gustafson, G and Krasny, J. 1994. Crystalline rock aquifers: their occurrence, use and importance. Applied Hydrogeology **94** (2) 64–75.

Gustavson, M. 1988. Mosjøen. Description of the 1:250000 bedrock geological map. Norges Geologiske Undersøkelse. Skrifter 87. 47pp.

Haggerty, R, Fleming, SW, Meigs, LC and McKenna, SA. 2001. Tracer tests in a fractured dolomite. 2. Analysis of mass transfer in single-well injection-withdrawal tests. Water Resources Research **37** (5) 1129–1142.

Hallet, B, Hunter, L and Bogen, J. 1996. Rates of erosion and sediment evacuation by glaciers: A review of field data and their implications. Global And Planetary Change **12** (1–4) 213–235.

Hanna, RB and Rajaram, H. 1998. Influence of aperture variability on dissolutional growth of fissures in karst formations. Water Resources Research **34** (11) 2843–2853.

Hanshaw, BB and Back, W. 1979. Major geochemical processes in the evolution of carbonate aquifer systems. Journal of Hydrology **43** 287–312.

Harland, WB. 1985. Caledonide Svalbard in Gee and Sturt (1985). 999–1016.

Haugane, E and Grønlie, A. 1988.Tertiary Caves in Nordland, Norway. Cave Science **15** (3) 93–97.
Häuselmann, P. 2002. Cave genesis and its relationship to surface processes: investigations in the Siebenhengste region (BE, Switzerland). PhD thesis. Sieben Hengste-Hohgant (6) 168pp.
Häuselmann, P, Jeannin, P-Y, Monbaron, M. 2003. Role of epiphreatic flow and soutirages in conduit morphogenesis: the Bärenschacht example (BE, Switzerland). Zeitschrift fur Geomorphologie **47** (2) 171–190.
Heap, D. 1968. Norway Report for 1967. Kendal Caving Club Journal **3** 11–16.
Heap, D. 1975. William Hulme Grammar School Report of Expedition to Nordland 1974. 27pp.
Hebdon, NJ, Atkinson, TC, Lawson, TJ and Young, IR. 1997. Rate of glacial valley deepening during the late Quaternary in Assynt, Scotland. Earth Surface Processes and Landforms **22** 307–315.
Heinrich, H. 1988. Origin and consequences of cyclic ice rafting in the northeast Atlantic Ocean during the past 130,000 years. Quaternary Research **29** 142–152.
Heki, K. 2001. Seasonal modulation of interseismic strain build-up in northeastern Japan driven by snowloads. Science **293** 89–92.
Helland, A. 1907. Topografisk statistisk beskrivelse over Nordlands amt. Kristiana. Norges Land og Folk **18** (1). Caves: 199–211 Underground streams: 464–476.
Helland, A. 1909. Topografisk statistisk beskrivelse over Nordre Trondhjems amt. Kristiana. Norges Land og Folk **17** (1). Huler: 97–101.
Helldén, U. 1973. Limestone solution intensity in a karst area in Lapland, N. Sweden. Geografiska Annaler **54A** (3–4) 185–196.
Helldén, U. 1974a. A Lapplandisk Karst Area: Hydrology and Morphology. Trans. British Cave Research Association **1** (1) 43–53. [Artfjäll and Sotsbäkkgrotta]
Helldén, U. 1974b. Karst. En studie av Artfjällets karstomarade samt jämförande korrosionsanalyser fran Västspetsbergen och Tjeckoslovakian. Med. fran Lunds Universitets Geografiska Institution. Avhandlinger LXXII 192pp.
Helldén, U. 1975. Sotsbäck Cave. The largest known cavern in Sweden. Trans. British Cave Research Association **2** (1) 13–27.
Henriksen, H. 1995. Relation between topography and well yield in boreholes in crystalline rocks, Sogn and Fjordane, Norway. Groundwater **33** (4) 635–643.
Henriksen, S and Vorren, TO. 1996. Late Cenozoic sedimentation and uplift history on the mid-Norwegian continental shelf. Global And Planetary Change **12** (1–4) 171–199.
Herman, JS, and White, WB. 1985. Dissolution kinetics of dolomite: effects of lithology and fluid flow velocity. Geochimica et Cosmochimica Acta **249** 2017–2026.
Higham, S. 2001. An introduction to the caves of Newfoundland. NE Caver **32** (4) 134–136.
Hicks, EC, Bungum, H and Lindholm, CD. 2000. Seismic activity, inferred crustal stresses and seismotectonics in the Rana region, northern Norway. Quaternary Science Reviews **19** 1423–1436.
Higgins, SR and Hu, X. Self-limiting growth on dolomite: Experimental observations with in situ atomic force microscopy. Geochimica et Cosmochimica Acta 69 (8) 2085–2094.
Hill, CA. 1981. Speleogenesis of Carlsbad Caverns and other caves of the Guadalupe Mountains. Proceedings of the eighth International Speleological Congress 143–144.
Hill, CA. 1995. Sulphur redox reactions: hydrocarbons, native sulphur, Mississippi Valley-type deposits, and sulphuric acid karst in the Delaware Basin, New Mexico and Texas. Environmental Geology **25** (1) 16–24.
Hill, C and Forti, P. 1997. Cave minerals of the World. 463pp.
Hjorthen, PG. 1968. Grotter og grotteforskning i Rana. Norges Geologiske Undersøkelse Småskrift (9) 40pp.
Hodgkins, R. 1997. Glacier hydrology in Svalbard, Norwegian high Arctic. Quaternary Science Reviews **16** 957–973.
Hoel, A. 1906. Den marine graense ved Velfjorden. Christiana Videnskaps-Selskabs Forhandlinger (4) 1–15.
Holbye, U and Lauritzen, S-E. 1983. Stalagmittdateringer fra Greftkjelen. Norsk Grotteblad **11** 34–35.
Holbye, U. 1983a. Greftmarmoren - hvordan folder og sprekker har pavirka grottene. Norsk Grotteblad **11** 25–27.
Holbye, U. 1983b. Grottenes utvikling: en forklaring på grottedannelse giennom flere faser. Norsk Grotteblad **11** 14–24.
Holbye, U. 1983c. Stamlederfaser i grottene ved Greftvatnet. Norsk Grotteblad **11** 28–34.
Holbye, U. 1989. Bowl-karren in the littoral karst of Nord-Arnøy, Norway. Cave Science **16** (1) 19–26.
Holmlund, P and Fastook, J. 1995. A time-dependent glaciological model of the Weichselian Ice Sheet. Quaternary International **27** 53–58.
Holtedahl, H. 1998. The Norwegian Strandflat - a geomorphological puzzle. Norsk Geologisk Tidsskrift **78** (1) 47–66.
Horn, G. 1935. Uber die bildung von karsthöhlen unter einem gletscher. Norsk Geografisk Tidsskrift **5** 494–498.
Horn, G. 1937. Uber einige karsthöhlen in Norwegen. Mitt. Höhl.-u.Karstforsch.1937. 1–15. [English translation by AE Montague. 1951. On certain caves in the karst of Norway. Cave Science **3** (17) 1–12].
Horn, G. 1947. Karsthuler in Nordland. Norges Geologiske Undersøkelse **165** 77pp. [Partial English translation by AD McCrady. 1978. Limestone Caves in Nordland. Cave Geology **1** (5) 123–138].
Hossack, JR. 1985. The role of thrusting in the Scandinavian Caledonides, 97–116. **in** Gayer (1985).

Hossack, JR and Cooper, MA. 1986. Collision tectonics in the Scandinavian Caledonides. Geol. Soc. Special Pub. (19) 287–304.

Howard, AD. 1964. Processes of limestone cave development. International Journal of Speleology **1** (1/2) 47–60.

Howard, AD. 1971. Quantitative measures of cave patterns. Caves and Karst **13** (1) 1–7.

Howard, KWF, Hughes, M, Charlesworth, DL and Ngobi, G. 1992. Hydrogeologic evaluation of fracture permeability in crystalline basement aquifers in Uganda. Applied Hydrogeology **92** (1) 55–65.

Hubbard, B and Hubbard, A. 1998. Bedrock surface roughness and the distribution of subglacially precipitated carbonate deposits: implications for formation at Glacier de Tsanfleuron, Switzerland. Earth Surface Processes and Landforms **23** 262–270.

Hunt, AG and Malin, PE. 1998. Possible triggering of Heinrich events by ice-load-induced earthquakes. Nature **393** 155–158.

Husebye, ES, Bungum, H, Fyen, J and Gjøystdal, H. 1978. Earthquake activity in Fennoscandia between 1497 and 1975 and intraplate tectonics. Norsk Geologisk Tidsskrift **58** 51–68.

Huybrechts, P. 2002. Sea-level changes at the LGM from ice-dynamic reconstructions of the Greenland and Antarctic ice sheets during the glacial cycles. Quaternary Science Reviews **21** 203–231.

Isacsson, G. 1989. Cave deposits during glaciations and interglacials - an example from the Korallgrottan in Middle Sweden. Proceedings of the tenth International Speleological Congress 217–218.

Isacsson, G. 1994. Vad kan man se i Korallgrottan? Grottan **29** (2) 21–23.

Isacsson, G. 1999. Korallgrottan - ett nyckelhål till historien. Jämtlands Grottförening Årsskrift 1999 9–11, 18.

Ive, A. 1980. Caves at Sandnessjøen, 1–4 August 1979. Norsk Grotteblad **2** (6) 27–28.

Jakucs, L. 1977. Morphogenetics of Karst Regions. Bristol: Adam Hilger.

James, NP and Choquette, PW. 1988. Paleokarst. New York. Springer Verlag.

Jamtveit, B, Malthe-Sorensen, A and Austrheim, H. 2000. Permeability production and destruction during retrogressive metamorphism. Abstracts p8 and seminar notes from Geoscience 2000, 17–20 April 2000. The Geological Society.

Jansen, E and Sjøholm, J. 1991. Reconstruction of glaciation over the past 6 M years from ice borne deposits in the Norwegian Sea. Nature **349** 600–603.

Jasinski, H. 1978. Korrosionberäkningar från två karstområden: Mieseken i Tärnafjällen och Lummelunda på Gotland. Nat. geogr. Inst. Lunds Univ. Seminarieuppsats (stencil).

Jeannin, P-Y, Bitterli, T and Häuselmann, P. 2000. Genesis of a large cave system: case study of the North of Lake Thun System (Canton Bern, Switzerland) in Klimchouk, AB, Ford, DC, Palmer, AN and Dreybrodt, W (Eds). 2000. Speleogenesis: Evolution of karst aquifers. National Speleological Society. USA. 338–347.

Jean-Baptiste, P, Petit, J-R, Lipenkov, VY, Raynaud, D and Barkov, NI. 2001. Constraints on hydrothermal processes and water exchange in Lake Vostok from helium isotopes. Nature **411** 460–462.

Jenkins, D. 1959. Report on the Cambridge University Caving Club Expedition to Svartisen, Norway, 1958. Cave Science **4** (29) 206–229.

Johnsen, SJ and 9 authors. 1992. Irregular glacial interstadials recorded in new Greenland ice core. Nature **359** 311–313.

Johnson, RG and Lauritzen, S-E. 1995. Hudson Bay-Hudson Strait jökulhlaups and Heinrich events: a hypothesis. Palaeogeography, Palaeoclimatology, Palaeoecology **117** 123–137.

Johnston, AC. 1987. Suppression of earthquakes by large continental icesheets. Nature **330** 467–469.

Johnstone, GS and Mykura, W. 1989. British Regional Geology: The Northern Highlands of Scotland. HMSO. 219pp.

Kapitsa, AP, Ridley, JK, Robin, G de Q, Siegert, MJ, Zotikov, IA. 1996. A large deep freshwater lake beneath the ice of central East Antarctica. Nature **381** 684–686.

Karlén, W. 1988. Scandinavian glacial and climatic fluctuations during the Holocene. Quaternary Science Reviews **7** 199–209.

Karlén, W and Kuylenstrierna, J. 1996. On solar forcing of Holocene climate: evidence from Scandinavia. The Holocene **6** (3) 359–365.

Karlgren, L. 1962. Vattenkemiska analysmetoder. Kompendium från Limnologiska Inst. Uppsala (Stencile).

Kastning, EH. 1984. Hydrogeomorphic evolution of karsted plateaus in response to regional tectonism. in LaFleur, RG (Ed.) Groundwater as a geomorphic agent. (Boston: Allen and Unwin). 351–382.

Kaufmann, G. 2002. Karst aquifer evolution in a changing water table environment. Water Resources Research **38** (6) 26 1–9.

Kaufmann, G. 2003a. Modelling unsaturated flow in an evolving karst aquifer. Journal of Hydrology **276** 53–70.

Kaufmann, G. 2003b. A model comparison of karst aquifer evolution for different matrix-flow formulations. Journal of Hydrology **283** 281–289.

Kaufmann, G and Braun, J. 1999. Karst aquifer evolution in fractured rocks. Water Resources Research **35** (11) 3223–3238.

Kaufmann, G and Braun, J. 2000. Karst aquifer evolution in fractured, porous rocks. Water Resources Research **36** (6) 1381–1391.

Kautsky, G. 1953. Ett fossilfynd i Susendalen, Nordland. Norges Geologiske Undersøkelse **184** 142–144.

Kejonen, A. 1997. On Finnish Caves. Proceedings of the twelfth International Speleological Congress**4** 93–98.

Keppie, JD. 1985. The Appalachian collage. **in** Gee and Sturt (1985). 1217–1225.

Killawee, JA, Fairchild, IJ, Tison, J-L, Janssens, L and Lorrain, R. 1998. Segregation of solutes and gases in experimental freezing of dilute solutions: implications for natural glacial systems. Geochimica et Cosmochimica Acta **62** (23–24) 3637–3655.

Kirkland, RJ. 1958. The Karst of south Svartisen. Undergraduate dissertation. Trinity College, Cambridge.

Klemen, J and Hättestrand, C. 1999. Frozen-bed Fennoscandian and Laurentide ice sheets during the Last Glacial Maximum. Nature **402** (6757) 63–66.

Klemen, J, Hättestrand, C, Borgström, I and Stroeven, A. 1997. Fennoscandian paleoglaciology reconstructed using a glacial geological inversion model. Journal of Glaciology **43** 283–299.

Klimchouk, A. 1995. Karst morphogenesis in epikarstic zone. Cave and Karst Science **21** (2) 45–50.

Klimchouk, A. 1997a. Artesian speleogenetic setting. Proceedings of the twelfth International Speleological Congress **1** p157 .

Klimchouk, A. 1997b. Nature and principle characteristics of epikarst. Proceedings of the twelfth International Speleological Congress **1** p306.

Klimchouk, AB. 2000a. The formation of epikarst and its role in vadose speleogenesis **in** Klimchouk, AB, Ford, DC, Palmer, AN and Dreybrodt, W (Eds). 2000. Speleogenesis: Evolution of karst aquifers. National Speleological Society. USA. 91–99.

Klimchouk, AB. 2000b. Speleogenesis under deep seated and confined settings **in** Klimchouk, AB, Ford, DC, Palmer, AN and Dreybrodt, W (Eds). 2000. Speleogenesis: Evolution of karst aquifers. National Speleological Society. USA. 244–260.

Klimchouk, AB, Sauro, U and Lazzarotto, M. 1996. Hidden shafts at Sette Communi, Italy. Cave and Karst Science **23** (3) 101–107.

Klimchouk, AB, Ford, DC, Palmer, AN and Dreybrodt, W (Eds). 2000. Speleogenesis: Evolution of karst aquifers. National Speleological Society. USA. 527pp.

Knez, M and Slabe, T. 2001. Unroofing of a cave system - an example from classical karst. Proceedings of the Thirteenth International Speleological Congress. Paper no. 105. 4pp

Knez, M and Slabe, T. 2002. Unroofed caves are an important feature of karst surfaces: examples from the classical karst. Zeitschrift fur Geomorphologie **46** (2) 181–191.

Knight, J. 1999. Geological evidence for neotectonic activity during deglaciation of the southern Sperrin Mountains, Northern Ireland. Journal of Quaternary Science **14** (1) 45–57.

Knight, J. 2002. Bedform patterns, subglacial meltwater events, and late Devensian ice sheet dynamics in north central Ireland. Global and Planetary Change 35 237–253.

Knipe, RJ. 2000. Understanding the micro-macro behaviour of rock fluid systems. Abstract. Geoscience 2000.

Knudsen, NT. 1978. Drainage of an ice dammed lake, Okstinden, Nordland, Norway. Norsk Geografisk Tidsskrift **32** (2) 55–61.

Kollung, S. 1967. Geologiske undersøkelser i sørlige Helgeland og nordlige Namdal. Norges Geologiske Undersøkelse **254** 95pp. Summary 84–93.

Kosa, A. 1989. A type of vertical cave considered as deep karren. Proceedings of the tenth International Speleological Congress 1 109–112.

Krasny, J. 2002. Quantitative hardrock hydrogeology in a regional scale. Norges Geologiske Undersøkelse Bulletin **439** 7–14.

Kukla, G, McManus, JF, Rousseau, D-D and Chuine, I. 1997. How long and stable was the last interglacial? Quaternary Science Reviews 16 605–612.

Laberg, JS and Vorren, TO. 2000. Holocene megaslides on the north Norway continental margin. Abstracts p14 and seminar notes from Geoscience 2000, 17–20 April 2000. The Geological Society.

Lagerström, C. 1980. Scandinavian discoveries in Vadve valley. Descent **46** 5–6.

Lambeck, K and Purcell, AP. 2001. Sea-level change in the Irish Sea since the Last Glacial Maximum: constraints from isostatic modelling. Journal of Quaternary Science **16** (5) 497–506.

Lambeck, K, Esat, TM and Potter, E-K. 2002. Links between climate and sea-levels for the past three million years. Nature **419** 199–206.

Lambeck, K, Yokoyama, Y and Purcell, T. 2002. Into and out of the Last Glacial Maximum: sea-level change during Oxygen Isotope Stages 3 and 2. Quaternary Science Reviews **21** (1–3) 343–360.

LaRocque, A, Dubois, J-MM and Leblon, B. 2003. Characteristics of late-glacial ice-dammed lakes reconstructed in the Appalachians of southern Quebec. Quaternary International **99–100** 73–88.

Larsen, E and Mangerud, J. 1981. Erosion rate of a Younger Dryas cirque glacier at Kråkenes, western Norway. Ann. Glaciol. **2** 153–158.

Larsen, E and Mangerud, J. 1989. Marine caves: on-off signals for glaciations. Quaternary International **3 / 4** 13–19.

Larsen, E, Gulliksen, S, Lauritzen, S-E, Lie, R, Løvlie, R and Mangerud, J. 1987. Cave stratigraphy in western Norway; multiple Weichselian glaciations and interstadial vertebrate fauna. Boreas **16**, 267–292.

Larsen, HC, Saunders, AD, Clift, PD, Beget, J, Wei, W, Spezzaferri, S and ODP Leg 152 Scientific Party. 1994. Seven million years of glaciation in Greenland. Science **264** 952–955.

Lauritsen, Å and Lauritzen, S-E. 1996. Quaternary Cave and Landform Development in the Tysfjord Region, north Norway. Karst Waters Institute Special Publication 2, 73–77.

Lauritzen, S-E. 1977. Grønndalen. Norsk Grotteblad **2** 34–43.

Lauritzen, S-E. 1980. Speleologisk Arbeid i Nord-Norge 1977-1980. Norsk Grotteblad **6** 14–21.

Lauritzen, S-E. 1981a. Hammernesgrottene sett i lys av begrepene om grunnvannspeil og freatiske sløyfer. Norsk Grotteblad **7** 20–23.

Lauritzen, S-E. 1981b. A study of some karst waters in Norway. Norsk Geografisk Tidsskrift **35** (1) 1–19.

Lauritzen, S-E. 1981c. Glaciated karst in Norway. Proceedings of the eighth International Speleological Congress **2** 410–411.

Lauritzen, S-E. 1981d. Statistical symmetry analysis of scallops. National Speleological Society Bulletin **43** 52–55.

Lauritzen, S-E. 1982. The paleocurrents and morphology of Pikhauggrottene, Svartisen, north Norway. Norsk Geografisk Tidsskrift **36** (4) 183–209.

Lauritzen, S-E. 1983. Program and field guide for Arctic and Alpine Karst Symposium, Oslo. 88pp.

Lauritzen, S-E. 1984a. A symposium: arctic & alpine karst. Norsk Geografisk Tidsskrift **38** (3–4) 139–143.

Lauritzen, S-E. 1984b. Evidence of subglacial karstification in Glomdal, Svartisen, Norway. Norsk Geografisk Tidsskrift **38** (3–4) 169–170.

Lauritzen, S-E. 1984c. Speleothem dating in Norway: an interglacial chronology. Norsk Geografisk Tidsskrift **38** (3–4) p198.

Lauritzen, S-E. 1984d. Some estimates of denudation rates in karstic areas of the Saltfjellet– Svartisen region, north Norway. Catena **11** (1) 97–104.

Lauritzen, S-E. 1985. Virveldyrrester og dryppsteins dateringer i karsthuler. Naturana (5). Rana Museum. 27pp.

Lauritzen, S-E. 1986a. Kvithola at Fauske, northern Norway: an example of ice-contact speleogenesis. Norsk Geologisk Tidsskrift **66** (2) 153–161.

Lauritzen, S-E. 1986b. CO_2 content of glacial environments and the likelihood of sub-glacial karstification. Proceedings of the ninth International Speleological Congress **1** 127–130.

Lauritzen, S-E. 1986c. Hydraulic and dissolution kinetics of a phreatic conduit. Proceedings of the ninth International Speleological Congress **1** 20–22.

Lauritzen, S-E. 1988a. Paleokarst in Norway. Cave Science **15** (3) 129–131.

Lauritzen, S-E. 1988b. A geomorphological approach to engineering in karst. IAH 21st Congress, Guilin, China. 1194–1199.

Lauritzen, S-E. 1989a. Fracture Control of Caves in Marble in Norway (abstract only). Cave Science **16** (3) p114.

Lauritzen, S-E. 1989b. Shear, tension or both - a critical view on the prediction potential for caves. Proceedings of the tenth International Speleological Congress 118–120.

Lauritzen, S-E. 1989c. Paleokarst of Norway. in Bosak, P. *et al.* (Eds). Paleokarst. A Systematic and Regional Review. Prague, Academia. 71–76. (Same text as Lauritzen, 1988).

Lauritzen, S-E. 1989d. Scallop dominant discharge. Proceedings of the tenth International Speleological Congress **1** 123–124.

Lauritzen, S-E. 1990a. Autogenic and allogenic denudation in carbonate karst by the multiple basin method: an example from Svartisen, N. Norway. Earth Surface Processes and Landforms **15** 157–167.

Lauritzen, S-E. 1990b. Tertiary Caves in Norway: a Matter of Relief and Size. Cave Science **17** (1) 31–37.

Lauritzen, S-E. 1991a. Uranium series dating of speleothems. A glacial chronology for Nordland, Norway for the last 600 Ka. Striae **34** 127–132.

Lauritzen, S-E. 1991b. Karst resources and their conservation in Norway. Norsk Geografisk Tidsskrift **45** 119–142.

Lauritzen, S-E. 1993. Natural environmental change in karst: the Quaternary record. Catena Supplement **25** 21–40.

Lauritzen, S-E. 1995. High resolution paleo temperature proxy record for the last interglacial based on Norwegian speleothems. Quaternary Research **43** 133–146.

Lauritzen, S-E (Ed.). 1996a. Climatic Change: The Karst Record. Extended Abstracts of the Bergen Conference. Karst Waters Institute Special Publication No. 2. 196pp.

Lauritzen, S-E. 1996b. Karst landforms and caves of Nordland, North Norway. Guide for Excursion 2. Climatic Change: The Karst Record (Bergen Conference). 160pp.

Lauritzen, S-E. 1996c. Calibration of speleothem stable isotopes against historical records: a Holocene temperature curve for north Norway? Karst Waters Institute Special Publication 2, 78–80.

Lauritzen, S-E. 1996d. Interaction between glacier and karst aquifers: Preliminary results from Hilmarfjellet, S. Spitsbergen. Kras i Speleologia (XVII) 17–28

Lauritzen, S-E. 1997. Groundwater recharge in thermoglacial karst springs, S. Spitsbergen. Proceedings of the twelfth International Speleological Congress **2** p320.

Lauritzen, S-E. 1998. Chapter 3. Karst morphogenesis in the arctic: examples from Spitsbergen. in Yuan, D and Liu, Z (Editors). Global Karst Correlation. Final Report of the UNESCO/IUGS International Geological Correlation Program Project 299: Geology, Climate, Hydrology and Karst Formation (1990–1994).

Lauritzen, S-E and Bottrell, SH. 1994. Microbiological activity in Thermoglacial karst springs. Geomicrobiology Journal **12** 161–173.

Lauritzen, S-E and Gascoyne, M. 1980. The first radiometric dating of Norwegian stalagmites - evidence of pre-Weichselian karst caves. Norsk Geografisk Tidsskrift **34** (2) 77–82.

Lauritzen, S-E and Lauritsen, Å. 1995. Different diagnosis of paragenetic and vadose canyons. Cave and Karst Science **21** (2) 55–59.

Lauritzen, S-E and Lundberg, J. 1999. Calibration of the speleothem delta function: an absolute temperature record for the Holocene in northern Norway. The Holocene **9** (6) 659–669.

Lauritzen, S-E and St.Pierre, S. 1982. A stalagmite date from Sirijordgrotten, northern Norway. Norsk Geogr. Tidsskr. **36** (2) 115–116.

Lauritzen, S-E, Abbot, J, Arnesen, R, Crossley, G, Grepperud, D and Ive, A. 1985. Morphology and hydraulics of an active phreatic conduit. Cave Science **12** (4) 139–146.

Lauritzen, S-E, Ford, DC and Schwarcz, HP. 1986. Humic substances in speleothem matrix - Paleoclimatic significance. Proceedings of the ninth International Speleological Congress **2** 77–79.

Lauritzen, S-E, Haugen, JE, Løvlie, R and Gilje-Nielsen, H. 1994. Geochronological potential of isoleucine epimerization in calcite speleothems. Quaternary Research **41**, 52–58.

Lauritzen, S-E, Ive, A and Wilkinson, B. 1983. Mean annual runoff and the scallop flow regime in a subarctic environment. (Svartisen). Cave Science **10** (2) 97–102.

Lauritzen, S-E, Kyselak, J and Løvlie, R. 1991. A new survey of Råggejavri-Raigi and the Hellemofjord karst, Norway. Cave Science 18 (3) 131–137.

Lauritzen, S-E, Løvlie, R, Moe, D and Østbye, E. 1990. Paleoclimate deduced from a multidisciplinary study of a half-million-year-old stalagmite from Rana, Northern Norway. Quaternary Research **34** 306–316.

Lauritzen, S-E, Nese, H, Lie, RW, Lauritsen, Å and Løvlie, R. 1996. Interstadial / Interglacial fauna from Norcemgrotta, Kjøpsvik, N. Norway. Karst Waters Institute Special Publication 2, 89–92.

Laverty, M. 1987. Fractals in karst. Earth Surface Processes and Landforms **12** 475–480.

Lawson, TJ. 1995. An analysis of sediments in caves in the Assynt area, NW Scotland. Cave and Karst Science **22** 23–30.

Lehman, SJ and Keigwin, LD. 1992. Sudden changes in north Atlantic circulation during the last deglaciation. Nature **356** 757–762.

Lidmar-Bergström, K. 1997. A long-term perspective on glacial erosion. Earth Surface Processes and Landforms **22** 297–306.

Liedl, R, Sauter, M, Hückinhaus, D, Clemens, T and Teutsch, G. 2003. Simulation of the development of karst aquifers using a coupled pipe flow model. Water Resources Research **39** (3) SBH 6 1–11.

Lindh, L. 1978a. Rödningsbäckens karstomrade. Grottan **13** (4) 32–34.

Lindh, L. 1978b. Äntligen öppnad - en port till Bjurälvs underjord. Grottan **13** (4) 11–13.

Linge, H, Lauritzen, S-E, Lundberg, J and Berstad, IM. 2001a. Stable isotope stratigraphy of Holocene speleothems: examples from a cave system in Rana, northern Norway. Palaeogeography Palaeoclimatology Palaeoecology **167** 209–224.

Linge, H, Lauritzen, S-E, Baker, A and Proctor, CJ. 2001b. Luminescent growth banding and stable isotope stratigraphy in a stalagmite from northern Norway: preliminary results for the period AD1734 to 955BC. Proceedings of the Thirteenth International Speleological Congress. Paper no. 70. 5pp

Linge, H, Lauritzen, S-E, Lundberg, J. 2001c. Stable isotope stratigraphy of a late last interglacial speleothem from Rana, northern Norway. Quaternary Research **56** 155–164.

Liu, Z and Dreybrodt, W. 1997. Dissolution kinetics of calcium carbonate minerals in $H_2O - CO_2$ solutions in turbulent flow: The role of the diffusion boundary layer and the slow reaction $H_2O + CO_2 <> H^+ + HCO_3^-$. Geochimica et Cosmochimica Acta **61** (14) 2879–2889.

Lototskaya, A and Ganssen, GM. 1999. The structure of termination II (penultimate deglaciation and Eemian) in the North Atlantic. Quaternary Science Reviews **18** 1641–1654.

Loubiere, J-F. 1987. Observations preliminaires sur les cavites de la region du Lac Centrum (NE Groenland). Karstologia **9** 7–16.

Lowe, DJ. 1992a. The origin of limestone caverns: an inception horizon hypothesis. PhD Thesis. Manchester Metropolitan University.

Lowe, DJ. 1992b. A historical review of concepts of speleogenesis. Cave Science **19** (3) 63–90.

Lowe, DJ. 1998. The necessity for inception. Kras i Speleologia. **9** (18) 150–153.

Lowe, DJ. 1999. Why and how are caves "organised": Does the past offer a key to the present. Acta Carsologica. 28/2 (7) 121–144.

Lowe, DJ. 2000a. Development of speleogenetic ideas in the 20th Century: the Early Modern Approach. **in** Klimchouk, AB, Ford, DC, Palmer, AN and Dreybrodt, W (Eds). 2000. Speleogenesis: Evolution of karst aquifers. National Speleological Society. USA. 30–38.

Lowe, DJ. 2000b. Role of stratigraphic elements in speleogenesis: the speleo inception concept **in** Klimchouk, AB, Ford, DC, Palmer, AN and Dreybrodt, W (Eds). 2000. Speleogenesis: Evolution of karst aquifers. National Speleological Society. USA. 65–76.

Lowe, DJ and Gunn, J. 1997. Carbonate Speleogenesis: An Inception Horizon Hypothesis. Acta Carsologica 26/2 38 457–488.

Lowe, DJ and Waltham, AC. 1995. A Dictionary of Karst and Caves. BCRA Cave Studies Series (6) 42pp.

Luetscher, M and Jeannin, P-Y. 2004. Temperature distribution in karst systems: the role of air and water fluxes. Terra Nova **16** 344–350.

Lund, C. 1986. Denudation measurements by the limestone-tablet-method in a sub-arctic area, Glomdalen northern Norway. Proceedings of the ninth International Speleological Congress**1** 241–247.

Lund, C and Eraso, A. 1989. The endogenetic drainage at the karst area of Glomdalen, Melfjord-Utbyggingen, the prediction method and its results. Proceedings of the tenth International Speleological Congress **1** 9–13.

Lund, K, Scott Fogler, H and McCune, CC. 1973. Acidization - I. The dissolution of dolomite in hydrochloric acid. Chemical Engineering Science **28** 691–700.

Lundberg, J. 1987. Fjällmötet - 87. Grottan **22** (3) 26–29.

Lundqvist, J. 1972. Ice-lake types and deglaciation pattern along the Scandinavian mountain range. Boreas **1** 27–54.

Lundqvist, J. 1986. Late Weichselian glaciation and deglaciation in Scandinavia. Quaternary Science Reviews **5** 269–292.

Luetscher, M and Jeannin, P-Y. 2004. Temperature distribution in karst systems: the role of air and water fluxes. Terra Nova **16** 344–350.

Løvlie, R, Gilje-Nilson, H and Lauritzen, S-E. 1988. Revised Magnetostratigraphic Age Estimate of Cave Sediments From Grønligrotta, Norway. Cave Science **15** (3) 105–108.

Løvlie, R, Ellingsen, KL and Lauritzen, S-E. 1995. Paleomagnetic cave stratigraphy from Hellemofjord, n. Norway. Geophysical Journal International **120** 499–515.

Løvlie, R and Lauritzen, S-E. 1996. Late Weichselian paleomagnetic chronostratigraphy of sediments in four cave systems in Nordland, N-Norway. Karst Waters Institute Special Publication 2, 104–106.

Mabee, SB. 1999. Factors influencing well productivity in glaciated metamorphic rocks. Groundwater **37** (1) 88–97.

Mangerud, J. 1991. The Last Ice Age in Scandinavia. Striae. **34** 15–30.

Mangerud, J, Sønstegaard, E and Sejrup, H-P. 1979. Correlation of the Eemian (interglacial) stage and the deep-sea oxygen-isotope stratigraphy. Nature **277** 189–192.

Mangerud, J, Jansen E and Landvik, JY. 1996. Late Cenozoic history of the Scandinavian and Barents Sea ice sheets. Global And Planetary Change **12** (1–4) 11–26.

Maréchal, JC, Dewandel, B and Subrahmanyam, K.2004. Use of hydraulic tests at different scales to characterize fracture network properties in the weather-fractured layer of a hard rock aquifer. Water Resources Research **40** W11508 1–17.

Marrett, R, Ortega, OJ and Kelsey, CM. 1999. Extent of power–law scaling for natural fractures in rock. Geology **27** (9) 799–802.

Marshall, SJ, James, TS and Clarke, GKC. 2002. North American ice sheet reconstructions at the Last Glacial Maximum. Quaternary Science Reviews**21** 175–192.

Maslin, MA, Li, XS, Loutre, M-F and Berger, A. 1998. The contribution of orbital forcing to the progressive intensification of northern hemisphere glaciation. Quaternary Science Reviews**17** 411–426.

Martinez, MI and White, WB. 1999. A laboratory investigation of the relative dissolution rates of the Lirio Limestone and the Isla de Mona dolomite and implications for cave and karst development on Isla de Mona. National Speleological Society Journal of Cave and Karst Studies **61** (1) 7–12.

Matsuoka, N. 2001. Direct observation of frost wedging in Alpine bedrock. Earth Surface Processes and Landforms **26** 601–614.

McCabe, AM. 1997. Geological constraints on geophysical models of relative sea-level change during deglaciation of the western Irish Sea Basin. Journal of the Geological Society, London **154** (4) 601–604.

McCabe, AM and Clark, PU. 2003. Deglacial chronology from County Donegal, Ireland: implications for deglaciation of the British – Irish ice sheet. Journal of the Geological Society, London **160** 847–855.

McCabe, AM, Haynes, JR and MacMillan, N. 1986. Late–Pleistocene tidewater glaciers and glaciomarine sequences from north County Mayo, Republic of Ireland. Journal of Quaternary Science1 (1) 73–84.

McCabe, M, Knight, J and McCarron, S. 1998. Evidence for Heinrich event 1 in the British Isles. Journal of Quaternary Science **13** (6) 549–568.

McKenna, SA, Meigs, LC and Haggerty, R. 2001. Tracer tests in a fractured dolomite. 3. Double-porosity, multiple-rate mass transfer processes in convergent flow tracer tests. Water Resources Research **37** (5) 1143–1154.

McManus, JF, Oppo, DW and Cullen, JL. 1999. A 0.5-million-year record of millennial-scale climate variability in the north Atlantic. Science **283** 971–975.

Meigs, LC and Beauheim, RL. 2001. Tracer tests in a fractured dolomite. 1. Experimental design and observed tracer recoveries. Water Resources Research **37** (5) 1113–1128.

Melezhik, VA, Roberts, D, Pokrovsky, BG, Gorokhov, IM and Ovchinnikova, GV. 1997. Primary isotopic features in metamorphosed Caledonian carbonates: implications for depositional age. Norges Geologiske Undersøkelse **433** 22–23.

Mihevc, A. (Ed.) 1999. Roofless Caves. 7th International Karstological School Karst Research Institute, Postojna, Slovenia. 38pp.

Milanovic, PT. 1981. Karst Hydrogeology. Water Resources Publications. Littleton, Colorado. 434pp.

Moe, D and Johannessen, PJ. 1980. Formation of cavities in calcareous rocks in the littoral zone of northern Norway. Sarsia **65** (3) 227–332.

Morehouse, DF. 1968. Cave development via the sulfuric acid reaction. National Speleological Society Bulletin **30** (1) 1–10.

Muir-Wood, R. 2000. Deglaciation seismotectonics: a principal influence on intraplate seismogenesis at high latitudes. Quaternary Science Reviews **19** 1399–1411.

Mulvaney, L, Wolff, EW and Oates, K. 1988. Sulphuric acid at grain boundaries in Antarctic ice. Nature **331** 247–249.

Murphy, P and Cordingley, J. 1999. Some observations on the occurrence of channel karren-like features in flooded karst conduits in the Yorkshire Dales, UK. Cave and Karst Science **26** (3) 129–130.

Murphy, PJ, Hall, AM and Cordingley, JN. 2000. Anomalous scallop distributions in Joint Hole, Chapel-le-Dale, north Yorkshire, UK. Cave and Karst Science **27** (1) 29–32.

Mykura, W. 1976. British Regional Geology: Orkney and Shetland. HMSO. 149pp.

Mylroie, JE. 1981. Glacial controls of speleogenesis. Proceedings of the eighth International Speleological Congress 689-691. (Same text as below).

Mylroie, JE and Carew, JL. 1986. Minimum duration for speleogenesis. Proceedings of the ninth International Speleological Congress **1** 249–251.

Mylroie, JE and Carew, JL. 1987. Field evidence for the minimum time for speleogenesis. National Speleological Society Bulletin **49** (2) 67–72.

Myrin, N. 2002. Dykning I Korallgrottan. Grottan **37** (2) 35–39.

Møller, JJ. 1985. Coastal caves and their relation to early postglacial shore levels in Lofoten and Vesterålen, north Norway. Norges Geologiske Undersøkelse Bulletin **400** 51–65.

Møller, JJ. 1989. Geometric simulation and mapping of Holocene Relative Sea-Level Changes in northern Norway. Journal of Coastal Research **5** (3) 403–417.

Mörner, N-A. 1979. The Fennoscandian Uplift and Late Cenozoic Geodynamics: Geological Evidence. Geojournal **3** (3) 287–318.

Mörner, N-A. 1980. The Fennoscandian Uplift: geological data and their geodynamical implication 251-284 in Mörner, N-A, Ed. Earth Rheology, Isostasy and Eustasy. Wiley.

Mörner, N-A. (Ed.) 2003. Paleoseismicity of Sweden: a novel paradigm. Stockholm University. 320pp.

Mörner, N-A, Tröften, PE, Sjöberg, R, Grant, D, Dawson, S, Bronge, C, Kvamsdal, O and Sidén, A. 2000. Deglacial paleoseismicity in Sweden: the 9663 BP Iggesund event. Quaternary Science Reviews **19** 1461–1468.

Nadis, S. 1999. Moves are afoot to probe the lake trapped beneath the Antarctic ice. Nature **401** (6750) p203.

Nese, H and Lauritzen, S-E. 1996. Quaternary Stratigraphy of the Storsteinshola cave system, Kjøpsvik, north Norway. Karst Waters Institute Special Publication 2, 116–120.

Nesje, A and Dahl, SO. 1992. Geometry, thickness, and isostatic loading of the late Weichselian Scandinavian Ice-sheet. Norsk Geologisk Tidsskrift **72** (3) 271–273.

Nesje, A, Anda, E, Rye, N, Lien, R, Hole, PA and Blikra, LH. 1987. The vertical extent of the late Weichselian ice sheet in the Nordfjord – Møre area, western Norway. Norsk Geologisk Tidsskrift **67** 125–141.

Nesje, A, Lauritzen, S-E and Dahl, SO. 1989. Volume estimates of Glacial Erosion on the Land Surface in Nordland, Norway. Report. Dept. of Geology, Sect. B. Bergen University. 38pp.

Nesje, A and Dahl, SO. 2000. Glaciers and environmental change. Arnold, London. 203pp.

Newton, G. 1998. Caves of marble 1997. Caves and Caving **79** 221–223.

Newton, G. 1999. Caves of Svartdal and other areas of Sør Helgeland, Norway. Chelsea Spelaeological Society Records **25** 56pp.

Newton, G. 2002. Caves of marble 2001. Chelsea Spelaeological Society Newsletter **44** (2) 19–41.

Newton, G and Faulkner, T. 1992. The Caves of Svenningdal. Chelsea Spelædogical Society Records **21** 37 pp.

Nisell, J. 1986. Karstområdet vid Kåtaviken, en geohydrologisk studie av ett karst område i Væsterbottens fjälltrakter. Umeå univ. Naturgeogr. Inst.

Noel, M and St.Pierre, S. 1984. The paleomagnetism and magnetic fabric of sediments from Grønligrotta and Jordbrugrotta, Norway. Geophys. J.R. astr. Soc. **78** 231–239.

Norberg, L. 1987. Rödingsfjällsbäckens karst område. Grottan **22** (4) 4–6.

Norberg, L, Pettersson, G and Sjöberg, R. 1988. Kåtaviken och Rödingsfjället - en studie av två karstområden. Svenska Grottor. Ser. C. nr. 3. 26pp.

Norberg, L. och Petterson, G. 1988. Karst och grottor i Rödingsfjället - kemi, hydrologi och morfologi. Umeå univ. Naturgeogr. Inst.

Nordell, P-O. 1952. Bjuälvenskarstlandscap. Geogr. Inst. Uppsala Univ. Seminarieuppsats (stencil).

Oerlemans, J. 1991. The role of ice sheets in the Pleistocene climate. Norsk Geologisk Tidsskrift **71** (3) 155–161.

Oldham, A and Oldham, T. 1971. The 1970 Övre Ältsvattnet Expedition - Sweden. The British Caver **55** 22–53.

Olesen, O. 1988. The Stuoragurra Fault, evidence of neotectonics in the Precambrian of Finnmark, northern Norway. Norsk Geologisk Tidsskrift **68** 107–118.

Olesen, O, Gjelle, S, Henkel, Karlsen, TA, Olsen, L and Skogseth, T. 1995. Neotectonics in the Ranafjorden area, northern Norway. Norges Geologiske Undersøkelse Bulletin **427** 5–8.

Olesen, O, Henkel, H, Lile, OB, Mauring, E, Rønning, JS and Torsvik, TH. 1992. Neotectonics in the Precambrian of Finnmark, northern Norway. Norsk Geologisk Tidsskrift **72** 301–306.

Olesen, O, Blikra, LH, Braathen, A, Dehls, JF, Olsen, L, Rise, L, Roberts, D, Riis, F, Faleide, JI and Anda, E. 2004. Neotectonic deformation in Norway and its implications: a review. Norwegian Journal of Geology **84** 3–34.

Olsen, L. 1997. Rapid shifts in glacial extension characterise a new conceptual model for glacial variations during the Mid and Late Weichselian in Norway. Norges Geologiske Undersøkelse Bulletin **433** 54–55.

Olsen, L and Grøsfjeld, K. 1999. Middle and Late Weichselian high relative sea levels in Norway: implications for glacial isostasy and ice-retreat rates. Norges Geologiske Undersøkelse Bulletin **435** 43–51.

Olsen, L, Sveian, H, Bergstrøm, B, Selvik, SF, Lauritzen, S-E, Stokland, Ø and Grøsfjeld, K. 2001a. Methods and stratigraphies used to reconstruct Mid and Late Weichselian palaeoenvironmental and palaeoclimatic changes in Norway. Norges Geologiske Undersøkelse Bulletin **438** 21– 46.

Olsen, L, Sveian, H and Bergstrøm, B. 2001b. Rapid adjustments of the western part of the Scandinavian Ice Sheet during the Mid and Late Weichselian - a new model. Norsk Geologisk Tidsskrift **81** 93–118.

Onac, BP. 1991. Contributions to the knowledge of the north Norway karst. Studia Univ. Babes-Bolya, Geographia. **36** (2) 35–42.

Onac, BP. 1995. Mineralogical data concerning moonmilk speleothems in a few caves from Northern Norway. Acta Carsologica. **24** 429–437.

Onac, BP and Ghergari, L. 1993. Moonmilk mineralogy in some Romanian and Norwegian caves. Cave and Karst Science **20** (3) 107–111.

Onac, BP and Lauritzen, S-E. 1995. On some cave minerals from Northern Norway. International Journal of Speleology **24** (1–4) 67–75.

Oppo, DW, McManus, JF and Cullen, JL. 1998. Abrupt climate events 500,000 to 340,000 years ago: evidence from subpolar north Atlantic sediments Science **279** 1335–1338.

Osborne, RAL. 1986. Cave and landscape chronology at Timor Caves, New South Wales. Journal and Proceedings of the Royal Society of New South Wales **119** 55–75.

Osborne, RA. 1999. The Inception Horizon Hypothesis in vertical to steeply dipping limestone: applications in New South Wales, Australia. Cave and Karst Science **26** (1) 5–12.

Osborne, RAL. 2000. Paleokarst and its significance for speleogenesis in Klimchouk, AB, Ford, DC, Palmer, AN and Dreybrodt, W (Eds). 2000. Speleogenesis: Evolution of karst aquifers. National Speleological Society. USA. 113–123.

Osborne, RAL. 2001a. Australian caves without roofs. Proceedings of the Thirteenth International Speleological Congress. Paper no. 134. 3pp.

Osborne, RAL. 2001b. Non-meteoric speleogenesis: evidence from eastern Australia. Proceedings of the Thirteenth International Speleological Congress. Paper no. 131. 4pp.

Osborne, RAL. 2001c. Halls and Narrows: Network caves in dipping limestone, examples from eastern Australia. Cave and Karst Science **28** (1) 3–14.

Oxaal, J. 1909. Fjeldbygningen i den sydlige del av Børgefjeld og trakterne om Namsvandene. Norges Geologiske Undersøkelse **53** 23pp.

Oxaal, J. 1914. Kalkstenhuler i Rana. Norges Geologiske Undersøkelse **69** (2) 1–46.

Oxaal, J. 1916. Huler of Grønlitypen. Norsk Geologisk Tidsskrift IV 1–5.

Paillet, FL, Hess, AE, Cheng, CH and Hardin, E. 1987. Characterization of fracture permeability with high resolution vertical flow measurements during borehole pumping. Groundwater **25** (1) 28–40.

Palmer, AN. 1972. Dynamics of a sinking stream system: Onesquethaw Cave, New York. National Speleological Society Bulletin **34** (3) 89–110.

Palmer, AN. 1975. The origin of maze caves. National Speleological Society Bulletin **37** (3) 56–76.

Palmer, AN. 1981. Hydrochemical factors in the origin of limestone caves.
Proceedings of the eighth International Speleological Congress 120–122.
Palmer, AN. 1984a. Chapter 8. Geomorphic interpretation of karst features.
in La Fleur, RG (Ed.) Groundwater as a geomorphic agent. 173–209.
Palmer, AN. 1984b. Recent trends in karst geomorphology. Journal of Geological Education**32** 247–253.
Palmer, AN. 1987. Cave levels and their interpretation. National Speleological Society Bulletin 49 50–66.
Palmer, AN. 1988. Solutional enlargement of openings in the vicinity of hydraulic structures in karstregions.
Proceedings of the Second Conference on Environmental Problems in KarstTerranes and Their Solutions. Association of Ground Water Scientists and Engineers. 3–15.
Palmer, AN. 1990. Chapter 8. Groundwater processes in karst terranes.
in Higgins, CG and Coates, DR (Eds.) Groundwater geomorphology: The role of subsurface water in Earth-surface processes and landforms. Geological society of America Special Paper**252** 177–209.
Palmer, AN. 1991. Origin and Morphology of limestone caves. Geological Society of America Bulletin**103** 1–21.
Palmer, AN. 1997. Modelling the evolution and morphology of limestone caves. Proceedings of the twelfth International Speleological Congress. Proceedings of the sixth Conference on Limestone Hydrology and Fissured Media. Modelling in Karst Systems. 41–52.
Also in Bulletin d'Hydrogéologie **16** 1998 157–165.
Palmer, AN. 1999a. Patterns of dissolution porosity in carbonate rocks-conduit patterns.
in Palmer, AN, Palmer, MV and Sasowsky, I. (Eds.) Karst Modeling.
Karst Waters Institute Special Publication 5. 71–78.
Palmer, AN. 1999b. A statistical evaluation of the structural influences on solution-conduit patterns.
in Palmer, AN, Palmer, MV and Sasowsky, I. (Eds.) Karst Modeling.
Karst Waters Institute Special Publication 5. 187–195.
Palmer, AN. 2000a. Hydrogeologic control of cave patterns
in Klimchouk, AB, Ford, DC, Palmer, AN and Dreybrodt, W (Eds). 2000. Speleogenesis: Evolution of karst aquifers. National Speleological Society. USA. 77–90.
Palmer, AN. 2000b. Digital modelling of individual solution conduits
in Klimchouk, AB, Ford, DC, Palmer, AN and Dreybrodt, W (Eds). 2000. Speleogenesis: Evolution of karst aquifers. National Speleological Society. USA. 194–200.
Palmer, TJ, McKerrow, WS and Courie, JW. 1980. Sedimentological evidence for a stratigraphic break in Durness Group. Nature **287** 720–722.
Papadimitriou, S, Kennedy, H, Kattner, G, Dieckmann, GS and Thomas, DN. 2003.
Experimental evidence for carbonate precipitation and CO2 degassing during sea ice formation.
Geochimica et Cosmochimica Acta **68** (8) 1744–1761.
Parkes, MA, Johnston, D, Simms, MJ and Kelly, JG. 1999. Geological guidance of speleogenesis in marble of the Dalradian Supergroup, County Donegal, Ireland. Cave and Karst Science 26 (3) 115–124.
Payne, A and Sugden, D. 1990. Topography and icesheet growth.
Earth Surface Processes and Landforms **15** 625–639.
Peterson, MNA. 1966. Calcite: rates of dissolution in a vertical profile in the central Pacific.
Science **154** 154–1544.
Petit, JR and 19 authors. 1999. Climate and atmospheric history of the past 420000 years from the Vostok ice core, Antarctica. Nature **399** 429–436.
Peulvast, J-P. 1985. Post-orogenic morphotectonic evolution of the Scandinavian Caledonides during the Mesozoic and Cenozoic. 979–998 in Gee and Sturt (1985).
Pezdic, J, Sustersic, F and Misic, M. 1998. On the role of clay-carbonate reactions in speleo-inception.
Acta Carsologica **27** (1) 187–200.
Picknett, RG. 1976. The chemistry of cave waters, advanced discussion, 213–266.
in Ford, TD and Cullingford, CHD (eds.). The Science of Speleology. Academia Press. London. 593 pp.
Picknett, RG and Stenner, RD. 1978. Enhanced calcite solubility in dilute magnesium carbonate solutions.
Trans. British Cave Research Association **5** (1) 47–54.
Plummer, LN and Wigley, TML. 1976. The dissolution of calcite in CO_2-saturated solutions at 25 °C and 1 atmosphere total pressure. Geochimica et Cosmochimica Acta**40** 191–202.
Plummer, LN, Wigley, TML and Parkhurst, DL. 1978. The kinetics of calcite dissolution in CO_2 – water systems at 5° to 60 °C and 0.0 to 1.0 atm. CO_2 . American Journal of Science **278** 179–216.
Price, M. 1996. Introducing groundwater. Second edition. Chapman & Hall, London. 278pp.
Priscu, JC and 11 authors. 1999. Geomicrobiology of subglacial ice above Lake Vostok, Antarctica.
Science **286** 2141–2144.
Puech V & Jeannin P-Y. 1997. Hydraulic behaviour of epikarst.
Proceedings of the twelfth International Speleological Congress **1** 293–296.
Pulina, M. 1984. Glacier karst phenomena in Spitsbergen. Norsk Geogr. Tidsskrift**38** (3/4) 163–168.

Quick, PG. 1994. Vermont Caves: a geologic and historical guide. Paleoflow Press, USA. 74pp.
Quinif, Y. 1998. Dissipation d'énergie et adaptabilité dans les systèmes karstiques. Karstologia **31** (1) 1–11.

Rahmstorf, S. 2002. Ocean circulation and climate during the past 120,000 years. Nature**419** 207–214.
Railton, CL. 1954. Caving in Norway. Trans. Cave Research Group of GB**3** (1) 17–40.
Rajaram, H, Cheung, W and Hanna, B. 1999. Potential influence of aperture variability on the dissolutional enlargement of fissures. **in** Palmer, AN, Palmer, MV and Sasowsky, I. (Eds.) Karst Modeling. Karst Waters Institute Special Publication 5. 120–130.
Randall, AD, Francis, RM, Frimpter, MH and Emery, JM. 1988. Chapter 22. Region 19, Northeastern Appalachians, in Back, W, Rosenshein, JS and Seaber, PR. Eds. Hydrogeology. Geological Society of North America. The Geology of North America v. O2.
Rauch, HW. 1972. The effects of lithology and other hydrogeologic factors on the development of solution porosity in the Middle Ordovician carbonates of central Pennsylvania. Unpublished PhD thesis. Pennsylvania State University.
Rauch, HW and White, WB. 1977. Dissolution kinetics of carbonate rocks 1. Effects of lithology on dissolution rate. Water Resources Research **13** (2) 381–394.
Raymo, ME. 1998. Glacial puzzles. Science **281** 1467–1468.
Rea, BR and Whalley, WB. 1994. Sub glacial observations from Øksfjordjøkelen, north Norway. Earth Surface Processes and Landforms **19** 1–15.
Renwick, K. 1962. Age of Caves by Solution. Cave Science **4** (32) 338–350.
Rekstad, J. 1914. Kalksten fra Nordland. Norges Geologiske Undersøkelse **69** (3) 1 –10.
Rekstad, J. 1917. Vega. Beskrivelse til det geologiske generalkart. Norges Geologiske Undersøkelse **80** 85pp.
Rial, JA. 2004. Abrupt climate change: chaos and order at orbital and millennial scales. Global and Planetary Change **41** 95–109.
Riggs, AC, Carr, WJ, Kolesar, PT and Hoffman, RJ. 1994. Tectonic speleogenesis of Devils Hole, Nevada, and implications for hydrogeology and the development of long, continuous paleoenvironmental records. Quaternary Research **42** 241–254.
Riis, F. 1992. Dating and measurement of erosion, uplift, and subsidence in Norway and the Norwegian shelf in Glacial Periods. Norsk Geologisk Tidsskrift **72** (3) 325–331.
Riis, F. 1996. Quantification of Cenozoic vertical movements of Scandinavia by correlation of morphological surfaces with offshore data. Global And Planetary Change **12** (1–4) 331–357.
Ringrose, PS, Hancock, P, Fenton, C and Davenport, CA. 1991. Quaternary tectonic activity in Scotland **in** A. Forster, MG Culshaw, JC Cripps, JA Little and CF Moon (Eds.) Quaternary Engineering Geology, Geological Society Engineering Special Publication No. 7, 679–686.
Roberts, D. 2000. Reverse-slip offsets and axial fractures in road-cut boreholes from the Caledonides in Finnmark, northern Norway: neotectonic stress orientation fractures. Quaternary Science Reviews **19** 1437–1445.
Roberts, D and Gee, DG. 1985. An introduction to the structure of the Scandinavian Caledonides, 55–68. **in** Gee and Sturt (1985).
Roberts, D, Melezhik, VM and Heldal, T. 2002. Carbonate formations and early NW-directed thrusting in the highest allochthons of the Norwegian Caledonides: evidence of a Laurentian ancestry. Journal of the Geological Society, London **159** 117–120.
Robertson, T, Simpson, JB and Anderson, JGC. 1949. The limestones of Scotland. HMSO. 221pp.
Rohling, EJ, Fenton, M, Jorissen, FJ, Bertrand, P, Ganssen, G and Caulet, JP. 1998. Magnitudes of sea-level lowstands of the past 500000 years. Nature **394** 162–165.
Rohr-Torp, E. 1994. Present uplift rates and groundwater potential in Norwegian hard rocks. Norges Geologiske Undersøkelse Bulletin **426** 47–52.
Romanov, D, Gabrovsek, F and Dreybrodt, W. 2003. The impact of hydrochemical boundary conditions on the evolution of limestone karst aquifers. Journal of Hydrology**276** 240–253.
Rubin, PA, Engel, T, Nardacci, M and Morgan, B. 2002. Geology and paleogeography of Mount Desert Island and surrounding area, Maine **in** ML Nardacci (Ed.) A guide to the geology and caves of the Acadian coast: 2002 NSS Convention, Camden , Maine. 47–91.
Rudberg, S. 1992. Multiple glaciations in Scandinavia - seen in gross morphology or not? Geografiska Annaler **74A** (2–3) 231–243.
Rudberg, S. 1997. Glacial and interglacial erosion in Scandinavian mountains in a W–E comparison including an approach to a quantitative calculation. Zeitschrift fur Geomorphology**41** (2) 183–204.
Ruddiman, WF. 1977. North Atlantic ice-rafting: a major change at 75000 years before present. Science **196** 1208–1211.
Rudoy, AN. 2002. Glacier-dammed lakes and geological work of glacial superfloods in the late Pleistocene, southern Siberia, Altai Mountains. Quaternary International **87** 119–140.
Rutherford, S and D'Hondt, S. 2000. Early onset and tropical forcing of 100,000-year Pleistocene glacial cycles. Nature **408** 72–75.

Sahimi, M. 1995. Flow and transport in porous media and fractured rock. Weinheim, VCH verlagsges. 482pp.
Salomon, J-N. 1999. Le facteur temps dans la karstification. Géomorphologie **3** 195–214.
Sasowsky, ID and White, WB. 1994. The role of stress release fracturing in the development of cavernous porosity in carbonate aquifers. Water Resources Research **30** (12) 3523–3530.
Sauter, M and Liedl, R. 2000. Modelling karst aquifer genesis using a coupled continuum-pipe flow model in Klimchouk, AB, Ford, DC, Palmer, AN and Dreybrodt, W (Eds). 2000. Speleogenesis: Evolution of karst aquifers. National Speleological Society. USA. 212–219.
Sauter, M, Liedl, R, Clemens, T and Huckinghaus, D. 1997. Karst aquifer genesis- modelling. Proceedings of the twelfth International Speleological Congress **2** 107–110.
Schöner, W and Hartl, M. 1996. The 1991 jokulhlaup of Gaesvatnet (SW Spitsbergen). Kras i Speleologia (VII) 29–33.
Schroeder, J and Ford, DC. 1983. Clastic sediments in Castleguard Cave, Columbia Ice Fields, Alberta, Canada. Arctic and Alpine Research **15** (4) 451–461.
Schrøder, I. 1989. Some caves in siliceous rocks in Norway. Cave Science **16** (1) 27–29. Also in Proceedings of the tenth International Speleological Congress 301–303.
Sejrup, HP, Larsen, E, Landvik, J, King, EL, Haflidason, H and Nesje, A. 2000. Quaternary glaciations in southern Fennoscandia: evidence from southwestern Norway and the northern North Sea region. Quaternary Science Reviews **19** 667–685.
Sekhar, M, Mohan Kumar, MS and Sridharan, K. 1994. A leaky aquifer model for hard rock aquifers. Applied Hydrogeology **94** (3) 32–39.
Shaikh, NA, Karis, L, Kampulanien, R, Sundberg, A and Wik, N-G. 1989. Kalksten och dolomit i Sverige. Del 1. Norra Sverige. Rapporter och meddelanden No. 54. Sveriges Geologiske Undersøkelse. Uppsala.
Shapiro, AM. 2001. Effective matrix diffusion in kilometer-scale transport in fractured crystalline rock. Water Resources Research **37** (3) 507–522.
Shoemaker, EM. 1991. On the formation of large subglacial lakes. Canadian Journal of Earth Sciences **28** 1975–1981.
Siegert, MJ and Bamber, JL. 2000. Subglacial water at the heads of Antarctic ice-stream tributaries. Journal of Glaciology **46** (155) 702–703.
Siegert, MJ, Kwok, R, Mayer, C and Hubbard, B. 2000. Water exchange between the subglacial Lake Vostok and the overlying ice sheet. Nature **403** 643–646.
Siegert, MJ, Ellis-Evans, CJ, Tranter, M, Mayer, C, Petit, J-R, Salamatin, A and Priscu, JC. 2001. Physical, chemical and biological processes in Lake Vostok and other Antarctic subglacial lakes. Nature **414** 603–609.
Simms, M. 1999. Holey rocks and boulders in sockets: weird karst from the west of Ireland. Cave and Karst Science **26** (1) p42 (abstract).
Simms, M. 2002. The origin of enigmatic, tubular, lake-shore karren: a mechanism for rapid dissolution of limestone in carbonate-saturated waters. Physical Geography 23 (1) 1–20.
Singurindy, O and Berkowitz, B. 2003. Flow, dissolution, and precipitation in dolomite. Water Resources Research **39** (6) SBH 3 1–13.
Singurindy, O, Berkowitz, B and Lowell, RP. 2004. Carbonate dissolution and precipitation in coastal environments: laboratory analysis and theoretical consideration. Water Resources Research **40** W04401 1–12.
Sippel, RF and Glover, ED. 1964. The solution alteration of carbonate rocks, the effects of temperature and pressure. Geochimica et Cosmochimica Acta **28** 1401–1417.
Sjöberg, EL. 1978. Kinetics and mechanism of calcite dissolution in aqueous solutions at low temperatures. Stockholm Contributions in Geology **32** 1–92
Sjöberg, EL and Rickard, DT. 1984. Temperature dependence of calcite dissolution kinetics between 1 and 62°C at pH 2.7 to 8.4 in aqueous solutions. Geochimica et Cosmochimica Acta **48** 485–493.
Sjöberg, R. 1972. Bjurälven och Södra Storfjället. Grottan 7 (4) 1–6.
Sjöberg, R. 1979. Karstområdet vid Skjelmoen i Norge. Grottan **14** (4) 6–9.
Sjöberg, R. 1980. Svenska Grottor Nr. 2. Grottområdet vid Övre Ältsvattnet. 52pp.
Sjöberg, R. 1981a. Tunnel caves in Swedish non calcareous rocks. Proceedings of the eighth International Speleological Congress 2 652–656.
Sjöberg, R. 1981b. Tunnel Caves in Swedish Archean Rocks. Cave Science **8** (3) 159–167.
Sjöberg, R. 1986a. SSF 20 år = 20 års svensk grottforskning. Grottan **21** (1) 8–11.
Sjöberg, R. 1986b. Caves indicating neotectonic activity in Sweden. Geografiska Annaler. **68A** (4)
Sjöberg, R. 1987a. Neotektonik och grottor i Sverige. Grottan **22** (2) 4–9. [Swedish version of Sjöberg (1986b)].
Sjöberg, R. 1987b. Caves as indicators of neotectonics in Sweden. Zeitschrift fur Geomorphologie N.F. Suppl. Bd63. 141–148.
Sjöberg, R. 1987c. Två vägar till Rödingsfjällsbäcken. Grottan **22** (2) 14–18.
Sjöberg, R. 1988. Coastal Caves Indicating Preglacial Morphology in Norway. Cave Science **15** (3) 99–103.
Sjöberg, R. 1991a. A pro på de norska (och svenska) karst grottornas ålder. Grottan **26** (1) 12–13.
Sjöberg, R. 1991b. Renstängselgrottorna. Grottan **26** (2) 21–23.

Sjöberg, R. 1994. Bedrock caves and fractured rock surfaces in Sweden. PhD Thesis. University of Stockholm. 86 pp etc. [English abstract in Sjöberg, 1996a].
Sjöberg, R. 1996a. Bedrock caves and fractured rock surfaces in Sweden. Cave and Karst Science **23** (3) p128. [English abstract].
Sjöberg, R. 1996b. Tavelsjöbergets blockbrant och hur den kan ha bildats. Grottan **31** (1) 36–40.
Sjöberg, R. 1996c. Seismotektoniken äntligen erkänd !(?). Grottan **31** (2) 4–8.
Sjöberg, R. 1996d. Lervarv, grottor och jordskalv. Grottan **31** (2) 29–31.
Sjöberg, R. 1996e. De "Fem Stora" och speleogförbundets 30-åriga historia. Grottan **31** (4) 39–41.
Sjöberg, R. 1997. Grottor i Sverige över 200m längd. Grottan **32** (1) p17.
Sjöberg, R. 1999a. Forskningsproject kring Bodagrottorna. Grottan **34** (2) 28–34.
Sjöberg, R. 1999b. De stora jordbävningarna i Umeå och INQUA:s Sverige-exkursion 1999. Grottan **34** (3) 4–8.
Sjöberg, R. *et al.* 1971. Övre Ältsvattenexpeditionen 1970. Report. 76pp.
Sjöberg, R. och Engh, R. 1979. Bjuälvens karstlandscap, förslag till naturstig. (Stencil). Stromsunds kommun.
Skjeseth, S. 1957. Norske kilder. Norges Geologiske Undersøkelse Årbok **203** 88–99.
Smart, CC. 1981. Glacier groundwater interaction. Proceedings of the eighth International Speleological Congress 720–723.
Smart, CC. 1983. The hydrology of the Castleguard Karst, Columbia Ice Field, Alberta, Canada. Arctic and Alpine Research **15** (4) 471–486.
Smart, CC. 1984a. Glacier hydrology and the potential for sub glacial karstification. Norsk Geografisk Tidsskrift **38** (3/4) 157–162.
Smart, CC. 1984b. Overflow sedimentation in an alpine cave system. Norsk Geografisk Tidsskrift **38** (3/4) 171–175.
Smart, CC. 1988. A deductive model of karst evolution based on hydrological probability. Earth Surface Processes and Landforms **13** 271–288.
Smart, PL and Whitaker, F. 1988. Controls on the rate and distribution of carbonate bedrock dissolution in the Bahamas. Proceedings of the fourth symposium on the geology of the Bahamas. 313-321.
Smart, PL, Palmer, RJ, Whitaker, F and Wright, VP. 1988. Neptunian dykes and fissure fills: an overview and account of some modern examples in James and Choquette (1988), 149–163.
Smith, DI. 1972. The solution of limestone in an Arctic environment. in Polar Geomorphology: RJ Price and DE Sugden (Eds.) IBG Special Publication 4 187–199.
Smith, MP, Soper, NJ, Higgins, AK, Rasmussen, JA and Craig, LE. 1999. Palaeokarst systems in the Neoproterozoic of eastern North Greenland in relation to extensional tectonics on the Laurentian margin. Journal of the Geological Society, London, **156** 113–124.
Smith, MP. 2000. Cambro–Ordovician stratigraphy of Bjørnøya and north Greenland: constraints on tectonic models for the arctic Caledonides and the Tertiary opening of the Greenland Sea. Journal of the Geological Society, London, **157** 459–470.
Solheim, A, Riis F, Elverhøi A, Faleide JI, Jensen LN, Cloetingh, S. 1996. Impact of glaciations on basin evolution: data and models from the Norwegian margin and adjacent areas - Introduction and summary. Global And Planetary Change **12** (1–4) 1–9.
Sollid, JL and Sørbel, L. 1979. Deglaciation of western central Norway. Boreas **8** 233–239.
Sollid, JL and Torp, B. 1984. Glacial geological map of Norway. 1:1000000. Nasjonalatlas for Norge. Kartblad 2.3.2. Geografisk Institutt, Universitet i Oslo.
Soper, NJ, Strachan, RA, Holdsworth, RE, Gayer, RA and Greiling, RO. 1992. Sinistral transpression and the Silurian closure of Iapetus. Journal of the Geology Society **149** 871–880.
Stauffer, B and 10 authors. 1998. Atmospheric concentration and millennial-scale climate change during the last glacial period. Nature **392** 59–62.
Stenner, RO. 1969. Measurement of aggressiveness of water to $CaCO_3$. Trans. Cave Research Group of Great Britain **11** (3) 175 –200.
Stephansson, O and Carlsson, H. 1980. Seismo-tectonics in Fennoscandia in Mörner, N-A, Ed. Earth Rheology, Isostasy and Eustasy. Wiley. 327–338.
Stephens, MB, Gustavson, M, Ramberg, IB and Zachrisson, E. 1985. The Caledonides of central– north Scandinavia - a tectonostratigraphic overview. in Gee and Sturt (1985).
Stephenson, D and Gould, D. 1995. British Regional Geology: The Grampian Highlands. British Geological Survey. 261pp.
Stewart, IS, Sauber, J and Rose, J. 2000. Glacio-seismotectonics: ice sheets, crustal deformation and seismicity. Quaternary Science Reviews **19** 1367–1389.
Stone, BD and Borns, HW. 1986. Pleistocene glacial and interglacial stratigraphy of New England, Long Island, and adjacent Georges Bank and Gulf of Maine. Quaternary Science Reviews **5** 39–52.
St.Pierre, D. 1966. The caves of Gråtådal, northern Norway. Trans. Cave Research Group of Great Britain **8** (1) 1–64.
St.Pierre, D. 1984. The caves and karst of Glomfjell, Nordland, Norway. Caves and Caving (24) p25.
St.Pierre, D. 1988. A History of Cave Exploration and Study in Norway. Cave Science **15** (3) 139–144.
St.Pierre, D. 2003. Norges lengste og dypeste grotter. Norsk Grotteblad **40** 3–10.

St.Pierre, D and St.Pierre, S. 1969. Caves of Rana, Nordland, Norway.
Trans. Cave Research Group of Great Britain **11** (1) 1–71.
St.Pierre, D and St.Pierre, S.1971.The Caves of Rana, Nordland, Norway - supplementary list.
Trans. Cave Research Group of Great Britain **13** (4) 297–305.
St.Pierre, S. 1967. Cave Studies in Nordland, Norway. Studies in Speleology **1** (5) 275–284.
St.Pierre, S. 1980. Studies in Grønligrotta. Norsk Grotteblad **5** 31–38.
St.Pierre, S. 1988. Morphology and Sediments of the Grønlie–Seter Caves, Norway.
Cave Science **15** (3) 109–116.
St.Pierre, S and St.Pierre, D. 1980. Caves of Velfjord, south Nordland, Norway, with particular reference to Sirijordgrotten. Trans. British Cave Research Association **7** (2) 70–82.
Stuevold, LM and Eldholm, L. 1996. Cenozoic uplift of Fennoscandia inferred from a study of the mid Norwegian margin. Global And Planetary Change **12** (1–4) 359–386.
Stuiver, M and 9 authors. 1998. INTCAL 98 radiocarbon age calibration, 24000–0 cal BP.
Radiocarbon **40** (3) 1041–1083.
Sugden, DE . 2000. Climate change, glaciation and effects on sediment production.
Abstracts p164 and seminar notes from Geoscience 2000, 17–20 April 2000. The Geological Society.
Summerfield, M. 1991. Global Geomorphology. 537pp. Longman.
Sundqvist, H. 2002. Droppstenar från Korallgrottan och Uppsala slott - ett doktorandproject. Grottan **37** (2) 4–9.
Sustersic, F. 1996. The Pure Karst Model. Cave and Karst Science **23** (1) 25–32.
Sustersic, F. 1997. Cave patterns north of the Planinsko polje (Slovenia).
Proceedings of the twelfth International Speleological Congress **1** 117–120.
Sustersic, F. 1998. Interaction between a cave and the lowering karst surface. Acta Carsologica 27/2 **8** 115–138.
Sustersic, F. 1999. Vertical zonation of the speleogenetic space. Acta Carsologica 28/2 11 187–201.
Sutcliffe, R and Hobbs, RS. 1972. Norway Caving Notes. Journal Gritstone Club (4) I–II.
Svendsen, JI and Mangerud, J. 1987. Late Weichselian and Holocene sea-level history for a cross-section of western Norway. Journal of Quaternary Science **2** 113–132.
Svensson, U and Dreybrodt, W. 1992. Dissolution kinetics of natural calcite minerals in CO_2 – water systems approaching calcite equilibrium. Chemical Geology **100** 129–145.
Sverdup, HU. 1935. The temperature of the firn on Isachsen's plateau, and general conclusions regarding the temperature of the glaciers on West-Spitsbergen. Geografiska Annaler. Stockholm.
Sweet, G. 1989. Subcutaneous drainage and cave development in the Interlakes Area, Manitoba, Canada.
Proceedings of the tenth International Speleological Congress **1** 275–277.
Svenonius, F. 1880. En egendomlig dalgang I nordligaste Jämtland. Geol. Foren:s Föhandl. 76–83.
Svenonius, F. 1910. Bjurälfdalens karstlandscap I norra Jämtland. Sveriges Natur Årsbok 73–80.
Sørensen, R, Bakkelid, S and Torp, B. Land Uplift. 1987. 1:5000000. Nasjonalatlas for Norge. Statens kartverk.

Tarhule-Lips, RFA and Ford, DC. 1998. Morphometric studies of bell hole development on Cayman Brac.
Cave and Karst Science **25** (3) 119–130.
Tell, L. 1955. Underjordens vackra värld. Stockholm.
Tell, L. 1974. Fifty typical Swedish Caves. 40pp. Archives of Swedish Speleology (14). Norrköping.
Theakstone, WH. 1964. Recent studies in the Svartisen area. Norsk Geogr. Tidsskr. **19B** 318–334.
Theakstone, WH. 1978. The 1977 drainage of the Austre Okstindbreen ice dammed lake.
Norsk Geogr. Tidsskrift. **32** (4) 159–171.
Theakstone, W. 1988. Glacier caves and subglacial water in Nordland, Norway. Cave Science **15** (3) 121–127.
Thomas, CW, Graham, CM, Ellam, RM and Fallick, AE. 2004. $^{87}Sr/^{86}Sr$ chemostratigraphy of Neoproterozoic Dalradian limestones of Scotland and Ireland: constraints on depositional ages and times scales.
Journal of the Geological Society, London. 161 229–242.
Thorp, PW. 1987. Late Devensian icesheet in the western Grampian, Scotland.
Journal of Quaternary Science **2** 103–112.
Thorsnes, T and Løseth, H. 1991. Tectonostratigraphy in the Velfjord–Tosen region, southwestern part of the Helgeland Nappe Complex, Central Norwegian Caledonides. Norges Geologiske Undersøkelse **421** 1–18.
Thorson, RM. 2000. Glacial tectonics: a deeper perspective. Quaternary Science Reviews **19** 1391–1398.
Thrailkill, JV. 1968. Chemical and hydrologic factors in the excavation of limestone caves.
Geological Society of America Bulletin **79** 19–45.
Tognini, P. 2001. Lombard south alpine karst.
in Häuselmann, P and Monbaron, M. (Eds.) Cave genesis in the Alpine belt.
Research Reports **10** Institute of Geography, University of Fribourg, Switzerland. 7–28.
Torsvik, TH, Carlos, D, Mosar, J, Cocks, LRM and Malme, TN. 2002. Global reconstructions and North Atlantic paleogeography 440Ma to Recent in Eide, EA (coord.): BATLAS – Mid Norway plate reconstruction atlas with global and Atlantic perspectives. Geological Survey of Norway pp1839.
Trudgill, ST. 1985. Limestone geomorphology. (London: Longman).
Trønnes, R and Sundvoll, B. 1995. Isotopic composition, deposition ages and environments of Central Norwegian Caledonian marbles. Norges Geologiske Undersøkelse **427** 44–47.

Tsang, YW and Tsang, CF. 1989. Flow Channelling in a Single Fracture as a Two-Dimensional Strongly Heterogeneous Permeable Medium. Water Resources Research **25** (9) 2076–2080.
Tucker ME and Wright VP. 1990. Carbonate Sedimentology. 482pp. Blackwell Science.
Tweed, FS and Russell, AJ. 1999. Controls on the formation and sudden drainage of glacier-impounded lakes: implications for jökulhlaup characteristics. Progress in Physical Geography **23** (1) 79–110.
Tyc, A. 1997. Epikarstic features in zones affected by periglacial processes. Proceedings of the twelfth International Speleological Congress 1 289–292.

Urbani, F. 2001. Venezuelan caves with palaeoseismical record. Proceedings of the Thirteenth International Speleological Congress. Paper no. 59 (Abstract)
Urushibara-Yoshino, K, Suzuki, H, Goto, N and Takai, T. 1996. The formation of scallops in the Irimizu Cave, northeast Japan. Komazawa Geography **32** 55–67.
Urushibara-Yoshino, K, Suzuki, H, Goto, N, Takai, T and Hirayama, N. 1997. Scallops formation and composition of deposited pebbles in Irimizu Cave, northeast Japan. Journal of the Speleological Society of Japan **22** 71–80.

Valen, V and Lauritzen, S-E. 1989. The sedimentology of Sirijorda Cave, Nordland, northern Norway. Proceedings of the tenth International Speleological Congress **1** 125–126.
Valen, V. 1991. Thesis: Sirijordgrottas Sedimentologiske Historie.Universitet i Bergen. 261pp.
Valen, V, Lauritzen, S-E and Løvlie, R. 1997. Sedimentation in a high-latitude karst cave: Sirijordgrotta, Nordland, Norway. Norsk Geologisk Tidsskrift **77** 233–250.
Valen, V, Larsen, E and Mangerud, J. 1995. High-resolution paleomagnetic correlation of middle Weichselian ice-dammed lake sediments in two coastal caves, western Norway. Boreas **24** 141–153.
Valen, V, Mangerud, J, Larsen, E and Hufthammer, AK. 1996. Sedimentology and stratigraphy in the cave Hamnsundhelleren, western Norway. Journal of Quaternary Science **11** (3) 185–201.
Van Staal, CR, Dewey, JF, MacNiocaill, C and McKerrow, WS. 1998. The Cambrian-Silurian tectonic evolution of the northern Appalachians and British Caledonides: history of a complex, west and southwest Pacific type segment of Iapetus. Geology Society of London Special Publication **143** 199–242.
Vogt, JHL. 1897. Norsk Marmor. Norges Geologiske Undersøkelse **22** 364pp. (Central Norway 240–265).

Walder, JS and Costa, JE. 1996. Outburst floods from glacier-dammed lakes: the effect of mode of lake drainage on flood magnitude. Earth Surface Processes and Landforms **21** 701–723.
Waltham, AC. 1970. Cave development in the limestone of the Ingleborough district. Geographical Journal **136** 574–585.
Waltham, AC. 1971b. Controlling factors in the development of caves. Trans. Cave Research Group of Great Britain **13** (2) 73–80.
Waltham, AC (Ed). 1974. The limestones and caves of north-west England. (Newton Abbot: David and Charles).
Waltham, AC. 1977. Chronology of cave development in the Yorkshire Dales,England. Proceedings of the seventh International Speleological Congress 423–425.
Ward, RC and Robinson, M. 1990. Principles of Hydrology. 365pp. McGraw-Hill.
Warwick, GT. 1956. Caves and Glaciation. Trans. of Cave Research Group of Great Britain **4** (2) 127–158.
Warwick, GT. 1971. Caves and the Ice Age. Trans. of Cave Research Group of Great Britain **13** (2) 123–130.
Wellander, P. 1981. Bjuälvens karstlandscap. Naturinv. Länsstyrelsen i Jämtlands län, naturvårdsenh.
Westerdahl, C. 1974. Vad är gjort och inte gjort i svenska fjällen - en preliminär översikt. Grottan **9** (2) 15–21.
Werenskiold, W. 1922. Frozen earth in Spitsbergen. Geofysiske publikasjoner **2** (10).
Weyl, PK. 1958. The solution kinetics of calcite. Journal of Geology **66** 163–176.
White, WB. 1977. Role of solution kinetics in the development of karst aquifers. in Tolsen and Doyle (Eds.) International Association of Hydrogeologists. Memoirs **12** 503–517.
White, WB. 1979. Water balance, mass balance and timescale for cave system development (Abstract). National Speleological Society Bulletin **41** (4) p115.
White, WB. 1984. Rate processes: chemical kinetics and karst landform development in La Fleur (Ed.) Groundwater as a geomorphic agent. 227–248.
White, WB. 1988. Geomorphology and hydrology of karst terrains. Oxford University Press.
White, WB. 1990. Chapter 7. Surface and near-surface karst landforms. in Higgins, CG and Coates, DR (Eds.) Groundwater geomorphology: The role of subsurface water in Earth-surface processes and landforms. Geological Society of America Special Paper **252** 157–175.
White, WB. 2000a. Development of speleogenetic ideas in the 20th Century: the Modern Period, 1957 to the present. in Klimchouk, AB, Ford, DC, Palmer, AN and Dreybrodt, W (Eds). 2000. Speleogenesis: Evolution of karst aquifers. National Speleological Society. USA. 149–155.
White, WB. 2000b. Dissolution of limestone from field observations in Klimchouk, AB, Ford, DC, Palmer, AN and Dreybrodt, W (Eds). 2000. Speleogenesis: Evolution of karst aquifers. National Speleological Society. USA. 149–155.

White, WB and Longyear, J. 1962. Some limitations on speleo-genetic speculation imposed by the hydraulics of groundwater flow in limestone. National Speleological Society Nittany Grotto Newsletter **10** 155–167.
Whitehouse, RH. 1969. Eldon Pothole Club Expedition to Northern Norway 1968. 2–8.
Whybro, P. 1986. Jordbruelv Dive Reports. Newsletter Cave Diving Group **81** 23–25.
Whybro, P. 1987. Sirijordgrotta Dive Report. Newsletter Cave Diving Group **82** p17.
Whybro, P. 1988. Jordbruelv Dive Reports. Newsletter Cave Diving Group **87** 22–23.
Wigley, TML. 1975. Speleogenesis: a fundamental approach. Proceedings of the sixth International Speleological Congress **3** 317–324.
Wigley, TML and Plummer, LN. 1976. Mixing of carbonate waters. Geochimica et Cosmochimica Acta **40** 989–995.
Wilhelmsson, P. 1997. Fjällguiden. Din guide i Tärnafjällen. 98pp. [Kåtavikens grottstig and Mjölkbäckens grottor 43–48. Tjårrogrottorna p59. Rödingsfjällets grottor 70–71.]
Williams, JE. 1949. Chemical weathering at low temperatures. Geog. Rev. **39** 129–135.
Williams, PW and Dowling, RK. 1979. Solution of marble in Pikikiruna Range, New Zealand. Earth Surface Processes and Landforms **4** 15–36.
Wilson, HE. 1972. British Regional Geology: Northern Island. HMSO. 105pp.
Winkler, HGF. 1976. Petrogenesis of Metamorphic Rocks. 4th Ed. Springer Verlag, NY.
Winograd, IJ, Landwehr, JM, Ludwig, KR, Coplen, TB and Riggs, AC. 1997. Duration and structure of the past four interglaciations. Quaternary Research **48** 141–154.
Wolfe, TE. 1967. The Jordbruen area of northern Norway - an example of high latitude karst. National Speleological Society Bulletin **29** (1) 13–21.
Woodward, HP. 1961. A stream piracy theory of cave formation. National Speleological Society Bulletin **23** (2) 39–58.
Worthington, SRH. 1991. Karst Hydrology of the Canadian Rocky Mountains. PhD Thesis. McMaster Univers
Worthington, SRH. 1994. Flow velocities in unconfined paleozoic carbonate aquifers. Cave and Karst Science **21**(1) 21–22. (Abstract).
Worthington, SRH. 1999. A comprehensive strategy for understanding flow in carbonate aquifers. in Palmer, AN, Palmer, MV and Sasowsky, I. (Eds.) Karst Modeling. Karst Waters Institute Special Publication 5. 30–37.
Worthington, SRH. 2001. Depth of conduit flow in unconfined carbonate aquifers. Geology **29** (4) 335–338.
Worthington, SRH. 2002. Depth of conduit flow in unconfined carbonate aquifers: Reply to comment. Geology **30** (1) 93–94.
Worthington, SRH and Ford, DC. 1995. High sulphate concentrations in limestone springs: an important factor in conduit initiation? Environmental geology **25** (1) 9–15.
Worthington, SRH and Ford, DC. 1997. Borehole Tests for megascale channelling in carbonate aquifers. Proceedings of the twelfth International Speleological Congress **2** 195–198.
Worthington, SRH, Davies, GJ and Ford, DC. 2000a. Matrix, fracture and channel components of storage and flow in a Paleozoic limestone aquifer in Sasowsky, ID and Wicks, CM (Eds).Groundwater flow and contaminant transport in carbonate aquifers. Balkema. 113–128.
Worthington, SRH, Ford, DC and Beddows, PA. 2000b. Porosity and permeability enhancement in unconfined carbonate aquifers in Klimchouk, AB, Ford, DC, Palmer, AN and Dreybrodt, W (Eds). 2000. Speleogenesis: Evolution of karst aquifers. National Speleological Society. USA. 463-472.
Wray, RAL. 1997. Quartzite dissolution: karst or pseudokarst? Cave and Karst Science **24** (2) 81–86.

Yardley, BWD. 1989. Introduction to Metamorphic Petrology. 248pp. Longman.
Yardley, BWD and Balashov, VN. 2000. Porosity-creation and the origin of skams. Abstracts p9 and seminar notes from Geoscience 2000, 17–20 April 2000. The Geological Society.
Yonge, CJ. 1997. Climate Change: The Karst Record - A Conference Review. Cave and Karst Science **24** (2) 65–75. [At Bergen, 1–4 August 1996].

Zupan Hajna, N. 2001. Weathering of cave walls in Martinska Jama, SW Slovenia. Proceedings of the Thirteenth International Speleological Congress. Paper no. 92. 4pp.

Ångström, A. 1958. Sveriges klimat. Gen. Litogr. Anstalt. Stockholm. p155.
Åström, L-E. 1986. Grottor i Sverige. 96pp.

Østbye, E and 6 authors. 1987. Invertebrates of Norwegian Caves. Fauna Norv. Ser. A8 Oslo 43–64.
Øvstedal, J. 1991. Thesis: En hydrologiske og hydrokjemisk beskrivelse av Sirijordas karst akvifer. Universitet i Bergen. 204pp.
Øvstedal, J. and Lauritzen, S-E. 1989. The Sirijorda Karst Aquifer, Nordland, northern Norway. Proceedings of the tenth International Speleological Congress **1** 121–122.

APPENDIX A1 THE CALEDONIAN OROGENY

The geological structure of the Caledonides was briefly described in section 2.1. This Appendix discusses the sequence of events that generated the original Caledonide mountain range, including its outcrops of metamorphic carbonates.

A1.1 Precambrian environments

The Scandinavian Caledonide nappes rest unconformably on the Precambrian Baltic Shield basement. This derives from several earlier orogenies that culminated in the creation of a Proterozoic super-continent. The ages of the rocks in this basement range up to 2800Ma (Archean) in northern Norway, becoming younger farther south. For most of the sequence, the ages are commonly between 1900–1500Ma (Palaeoproterozoic). In southern Norway and southwest Sweden, Grenvillian ages of 1150–930Ma (Mesoproterozoic) are typical (Barker and Gayer, 1985, p131). During the Vendian, the basement was eroded to a gently-sloping peneplain just above sea level, when it experienced the Varanger Ice Age from about 620–580Ma. It then became gradually drowned by the Iapetus Ocean in the Cambrian. During this time, a thin clastic deposition formed the cover rocks that, together with the basement, comprise the Autochthon. The Autochthon is thought to have extended far to the west of the present coast line (Gorbatschev, 1985).

In common with all the Caledonian continental margins, deposition in terranes forming the Scandinavian Caledonides started in several Precambrian sedimentary ensialic basins on thinned continental crust. These basins started to form at about 800–700Ma. Deposition of the Uppermost Allochthon, off what is now the coast of eastern Greenland, may have started as early as 950Ma. The Lower and Middle Allochthon rocks are considered to have been deposited in a shallow marine environment off Baltica, starting in Late Riphean times, perhaps during the Grenvillian stretching that initiated the early rifting of the Iapetus Ocean. Dolostones were deposited to a thickness of 100m in the Risbäck Basin within the study area in the Late Vendian. These are overlain by tillites from the Varanger Ice Age. The Seve rocks were perhaps deposited on the outer margin of a miogeosyncline in the Neoproterozoic, before being later depressed, metamorphosed and thrust eastwards. Hossack and Cooper (1986) included the Seve unit in their "Crystalline Thrust Sheet", believing it to contain mainly basement and other metamorphosed Precambrian rocks. Deposition continued generally into the Devonian, coupled with the many plate tectonic events.

Those Caledonian terranes that currently reside on the eastern seaboard of northern America have the Canadian Shield as a basement. These rocks date from the Grenville Orogeny at about 1000Ma. In eastern Greenland, the Archean and Palaeoproterozoic basement is overlain by rocks that experienced pre-Caledonian orogenies, dating from around 1200–900Ma. The Precambrian environments in the NW of Ireland and NW of Scotland are related, but are rather complex and uncertain. In NW Scotland, a Lewisian Complex (Archean) basement is overlain unconformably by Torridonian Supergroup sandstones dating from about 1000Ma (Barker and Gayer, 1985, pp137,140–143).

The Caledonide terranes of Ireland and Scotland are of interest because the Dalradian Supergroup (Grampian) terrane, which lies between the Great Glen Fault and the Highland Boundary Fault in Scotland, correlates with the eastern part of Shetland, with the Dalradian Supergroup in Donegal, and with the displaced Dalradian terrane in Connemara. Whereas the Grampian terrane and the Uppermost Allochthon of Scandinavia *"have never been correlated, it would be fair to say that they have similar tectonic status and position"* (R. Gayer, University of Cardiff, pers. comm., 1998). This supports the author's initial impression of great similarities in the metacarbonate outcrops and their contained karst caves between the Scottish Dalradian Supergroup and the Helgeland Nappe Complex of Norway.

A1.2 Caledonian deposition, metamorphism and thrusting

The following highly-simplified account of the Caledonian Orogeny is condensed mainly from Barker and Gayer (1985, pp147–160) and Gee and Sturt (1985). The understanding of the orogeny is still being developed, so that conflicts inevitably occur between papers written at different times, even (or especially!) between those written in the last two decades. Indeed, Van Staal *et al.* (1998, pp201–202) asserted that final continental collision can result in a pseudo-simplistic semi-linear orogenic zone that conceals an earlier complicated history and geometry. This history can be impossible to model backwards in time, because multiple pathways may lead to the same final result.

A1.2.1 Cambrian

The spreading of the Iapetus Ocean continued into and throughout much of the Cambrian, by which time it reached a maximum width varying from 6000km to 10000km. On the NW side, a Cambro–Ordovician miogeosynclinal (non-volcanic) carbonate shelf developed in southern hemisphere tropical latitudes, whereas on the SE side, a clastic shelf could have lain farther south, in temperate latitudes. The Uppermost Allochthon originated within the NW Iapetus margin, between an east Greenland terrane and the Grampian terrane, but offshore from Laurentia.

Most of the Cambrian age produced stable drift sequences that stretched for hundreds of kilometres off the passive miogeosynclinal margin of Baltica, as the Iapetus Ocean started to widen. The various shallow marine deposits were regionally uniform along the whole 1800km coastline. The deposition continued on the Autochthon, Parautochthon and Lower Allochthon as thin Cambrian sandstones, and as radioactive and organic rich black shales (Bergstrom and Gee, 1985). The Middle Allochthon remained dominated by its Precambrian basement. The Køli deposition probably started in an oceanic (Iapetus) eugeosynclinal (volcanic) environment during the Cambrian, and continued into the Ordovician in island arc, back arc and fore arc situations.

Iapetus started to close from the Mid to Late Cambrian (Figure A1.1), with later oceanward subduction and landward obduction being postulated on both sides of the ocean. Deformation of the earlier Cambrian deposits started in the Late Cambrian, accompanied by intrusions and metamorphism that produced metasedimentary rocks and metavolcanites in the higher nappes. The first orogenic phase to arise from the closing of the Iapetus Ocean was possibly the Finnmarkian, at the far north of what is now Norway. It continued from the Late Cambrian into the Early Ordovician.

A1.2.2 Ordovician

The Ordovician Period was one of a general marine transgression interrupted by three major regressions that produced shallow water deposits. In the epicontinental seas, 200m-thick carbonates and shales were formed over a stable platform to the east of the Caledonides, as on the Swedish island of Gotland. At Oslo these sediments reached thicknesses of nearly 1100m. There were no deposits on the Autochthon or Parautochthon in the study area, but poorly-correlated Lower Køli rocks were formed in Sweden and central Norway, in an island arc environment to the west.

As Iapetus closed further in the Early Ordovician, oceanic crust was obducted on to Baltica. However, the main event was the Taconic Orogeny on the other side of Iapetus, when various offshore terranes collided with Laurentia. The collisions caused subduction and metamorphism eastwards and southeastwards, and thrusting along the Appalachians to the west or northwest. To the NE, the Grampian Orogeny of Scotland occurred at the same time, whilst, however, the Uppermost Allochthon was probably experiencing only mild deformation.

By Mid to Late Ordovician times, subduction was apparent along the deepening Baltic margin, and more island arcs developed, commencing deposition of volcanic sequences in eugeosynclinal sediments in the higher Køli Nappes (amongst others), which continued into the Early Silurian. Igneous intrusions are substantial in the various allochthons, but not in the platform, proving the later eastward thrusting. The existence of plutonic rocks only in the highest and most far-travelled nappes indicates that the thermal axis for the Caledonide Orogeny lay far to the west of the Baltic Shield.

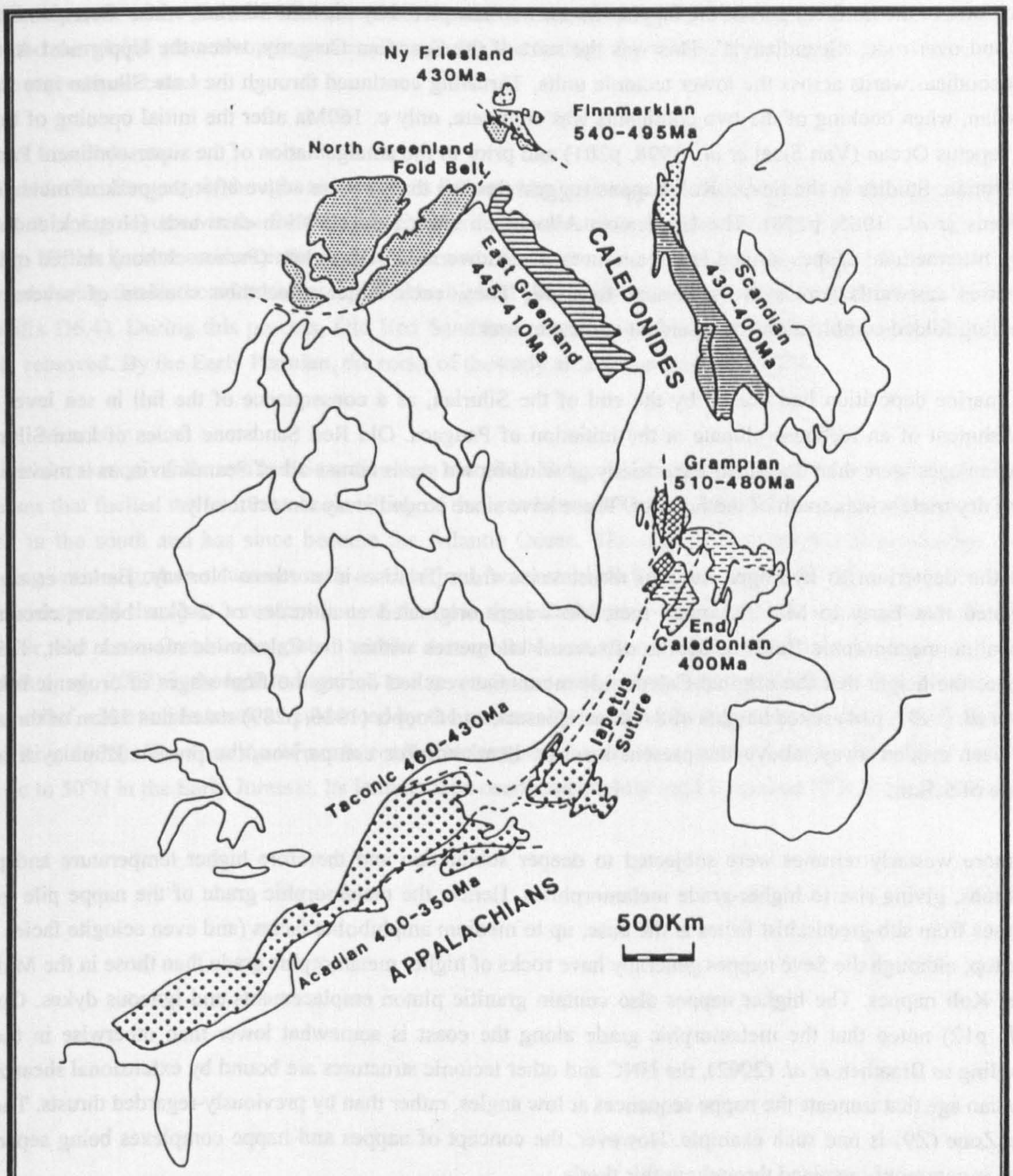

Fig. 1

Regions of the Caledonian-Appalachian Orogen in their pre-Mesozoic drift configurations, showing ages of principal deformation events.

Large dots – Appalachians; dashes – paratectonic British Caledonides; cross-hatch – orthotectonic British Caledonides; closely spaced horizontal lines and triangles – Scandinavian Caledonides; widely spaced horizontal lines – East Greenland Caledonides; small dots – North Green fold belt, Ellesmere Island and West Spitsbergen; open circles – East Spitsbergen.

Figure A1.1 Regions involved in the Caledonian–Appalachian Orogeny.
From Barker and Gayer (1985, Fig. 1)

A1.2.3 Silurian and Devonian

The Silurian Period was one of increasing instability, as the Laurentian plate overrode Baltica obliquely, and the Caledonide Trough deepened to the west. Marine transgressions also promoted carbonate sedimentation environments as clastic source areas submerged along the thrust front. The Lower Køli in central Västerbotten has limestones that date from the Ordovician and Silurian. The Parautochthon and Lower Allochthon have Silurian-dated rocks in Jämtland. The Remdalen rocks in the Middle Køli are of Ordovician or Silurian age. There were also stable carbonate platforms and lagoons during the Mid Silurian along the western margin marine area. Section 3.1.6 discusses evidence of palaeokarst in non-metamorphic limestones that dates back to this or earlier periods.

The closure of the northern part of the Iapetus Ocean was completed by the Mid Silurian, when 'Greenland' collided with, and over-rode, 'Scandinavia'. This was the start of the Scandian Orogeny, when the Uppermost Allochthon thrust southeastwards across the lower tectonic units. Thrusting continued through the Late Silurian into the Early Devonian, when docking of the two continents was complete, only c. 160Ma after the initial opening of the short-lived Iapetus Ocean (Van Staal *et al.*, 1998, p201) and prior to the amalgamation of the super-continent Pangaea in the Permian. Studies in the Seve / Køli nappes suggest that the thrusts were active after the peak of metamorphism (Stephens *et al.*, 1985, p158). The Uppermost Allochthon moved over 800km eastwards (Hossack and Cooper, 1986). Intermediate nappes moved lesser amounts. The Lowermost Allochthon (Parautochthon) shifted only a few kilometres eastwards across the basement foreland. Thus, each major allochthon consists of several nappes containing folded combinations of basement and cover rocks.

Most marine deposition had ceased by the end of the Silurian, as a consequence of the fall in sea level and the establishment of an icehouse climate at the initiation of Pangaea. Old Red Sandstone facies of Late Silurian and Devonian ages were then deposited terrestrially as wind-blown sands across all of Scandinavia, as it moved into the area of dry trade winds south of the Equator. These have since eroded away almost totally.

From the deuterium to hydrogen ratio in thrust veins from Tromsø in northern Norway, Barker *et al.* (1998) calculated that Early to Mid Devonian meteoric waters originated at altitudes of 5–6km before circulating as hypersaline metamorphic fluids at depths of several kilometres within the Caledonide mountain belt. This result indicates the height that the original Caledonide mountains reached during the final stages of orogenic relaxation. Dahl *et al.* (1997, p14) stated heights of 8–10km. Hossack and Cooper (1986, p289) stated that 10km of thrust sheets have been eroded away, above the present level of Jämtland. For comparison, the present Himalayas reach an altitude of 5.5km.

The more westerly terranes were subjected to deeper subduction and therefore higher temperature and pressure conditions, giving rise to higher-grade metamorphism. Hence, the metamorphic grade of the nappe pile generally increases from sub-greenschist facies at the base, up to medium amphibolite facies (and even eclogite facies locally) at the top, although the Seve nappes generally have rocks of higher metamorphic grade than those in the Middle and Lower Køli nappes. The higher nappes also contain granitic pluton emplacements and igneous dykes. Gustavson (1988, p12) noted that the metamorphic grade along the coast is somewhat lower than otherwise in the HNC. According to Braathen *et al.* (2002), the HNC and other tectonic structures are bound by extensional shear zones of Devonian age that truncate the nappe sequences at low angles, rather than by previously-regarded thrusts. The Nesna Shear Zone (Z9) is one such example. However, the concept of nappes and nappe complexes being separated by thrusts is commonly retained throughout this thesis.

Whilst the various Caledonide terranes were being developed and brought together as accreted island arcs, their general position on the surface of the earth was also evolving. According to Van Staal *et al.* (1998, p211), Laurentia and Baltica were both in the southern hemisphere in Early Cambrian times, perhaps straddling 30°S, but with the future Scandinavian coastline of Baltica facing *away from* Laurentia. It was not until the beginning of the Silurian that Baltica had rotated until what was to become Norway faced the future Greenland on the oppositeside of Iapetus. By this time, both continents had moved northwards to straddle the Equator (Torsvik*et al.*, 2002).

After the collision, the plate tectonic energy was directed into various strike-slip fault systems, such as the Great Glen Fault Zone in Scotland. Around 2000km of sinistral movement took place from the Early Devonian to the Early Carboniferous, during which time various Caledonide terranes moved to their present relative positions prior to the start of Atlantic opening. Figure A1.1 shows the configuration of the Caledonian–Appalachian mountain range at this end of the orogeny.

A1.3 Post Caledonian developments

The development of the Caledonides after their formation was described by Peulvast (1985). Torsvik *et al.* (2002) illustrated the global plate tectonic movements, giving the timings for the northward migration of the Caledonides that are reproduced below.

A1.3.1 Late Palaeozoic

The Caledonian Orogeny is thought to have been followed by an increased crustal rigidity, although subsidence and oceanic thinning occurred in the Devonian or Carboniferous around fault zones between Proto-Greenland and Proto-Norway. There is some evidence that, after these vertical movements, a peneplanation of the Caledonide structure occurred during the Carboniferous (except for the highest peaks and massifs, and except in the Arctic Caledonides, Appendix D6.4). During this process, Old Red Sandstone deposits of the Late Silurian and Early Devonian were largely removed. By the Early Permian, the rocks of thestudy area had migrated to 20°N.

A1.3.2 Mesozoic

The initial creation of an uplifted Scandinavian Marginal Bulge is considered to have been driven by the same processes that fuelled the late Palaeozoic rifting of the area between Greenland and Norway to open a new sea. This started in the south and has since become the Atlantic Ocean. The approximate present Scandinavian coastline, including various graben structures such as Oslofjord, was established by the start of the Mesozoic. The uplift was more widespread than just a reactivation of the now rigid Caledonide structures, and continued into the Jurassic. However, the Late Cretaceous global marine transgression as the Atlantic rift system propagated northwards (Torsvik *et al.*, 2002) is thought to have led to a reversal, and reduced any exposed landscape in mid Norway to one of low relief, close to sea level, as evidenced by the universally fine-grained deposition (Doré, 1992; Solheim *et al.*, 1996; Riis, 1996). The location of north central Norway continued to move northwards, from 30°N in the Early Triassic to 50°N in the Early Jurassic. Its latitude then oscillated slightly until it reached 55°N in the Late Cretaceous.

APPENDIX A2 SCANDINAVIAN CARBONATES

The chemistry and processes involved in carbonate deposition, lithification, diagenesis, dolomitization and / or dedolomitization are complex, but were addressed by Tucker and Wright (1990). The effect of metamorphism on these situations is commonly less well known. No attempt was made in that work to explain them, although particular topics have been covered in a few fairly recent research papers. The formation and alteration of carbonates within the Caledonides (and the applicable timescales) had received little detailed scientific study prior to about 1985. Tucker and Wright (1990) included some 1500 references to carbonate sedimentation and related topics, but none referred to carbonates within the nappes of central Scandinavia. Brahana *et al.* (1988) tabulated processes and provided data that pertain to the porosity and permeability of carbonate rocks, including those that are metamorphosed, and made comparisons with non-carbonate rocks. The hydrogeology of carbonates is the result of variable combinations of more than 60 processes and controls. The two processes of dissolution / precipitation and dynamic freshwater flow seem to dominate, so that carbonate rocks show a range of hydraulic conductivities over ten orders of magnitude. This brief review attempts to describe what is known only in the context of the carbonates of the study area.

A2.1 Sedimentation and diagenesis

Tucker and Wright (1990, p419–420) stated that the great majority of sediments were clastic in nature during the Archean. As organic life developed in the oceans, carbonate deposition was initiated and grew. At the end of the Archean, at 2.5Ba, perhaps 1% of all rocks on the Canadian Shield were carbonates, but all of these were dolostones. The Baltic Shield fragments that are bound up in the Palaeozoic nappes of the study area probably date from 1.9–1.5Ba (Appendix A1.1). At the beginning of the Proterozoic eon, sea water temperatures were still high, with the only organisms present being algae, bacteria and fungi. An initial "soda ocean" of Na_2CO_3 became a saline ocean of NaCl and $CaCO_3$ as the oceans cooled following the creation of the Proterozoic super-continent. During the Cambrian re-warming, dolostones rose to become about 20% of all rocks, and limestones another 5%. After this, the dolomite proportion of carbonate formation dropped rapidly from over 80% to under 50% on average, whilst remaining variable. Whereas the preponderance of dolostones in the Precambrian can explain that dolostones, and few limestones, are found in the Lower Allochthon in the study area, there is however a potential conflict with other Caledonide depositions, where in practice metalimestones always predominate over metadolostones in the mapped outcrops (section 4.2.1). Appendix A2.10 attempts to resolve this anomaly.

Two major types of earth climate are recognised: a *greenhouse climate,* when higher temperatures and high sea levels promoted the sedimentation of carbonates in shallow seas; and an *icehouse climate,* during periods of mountain building and glaciation, when low sea levels and increased weathering favoured clastic sedimentation (although pelagic accumulation of carbonates also increased). Just over two complete earth climate cycles have occurred since the start of the Cambrian. During the icehouse climate of the late Proterozoic, Aragonite (A) and High Magnesium Calcite (HMC) were probably the main carbonate precipitates. Diagenesis is the process of cementation and mineral stabilisation. Diagenetic dissolution of fine-grained (micritic) A and HMC in partly-meteoric waters in shallow marine environments and re-precipitation as coarse grained (sparitic) crystals of Low Magnesium Calcite (LMC) probably started and completed soon after initial compaction. Thereafter, slow dolomitization of LMC occurred by dissolution and initial replacement as Calcian Dolomite (CD). The *ultimate* conclusion of this sedimentary dolomitization process is the replacement of previous calcite minerals by Stoichiometric Dolomite (SD). Appendix A2.4 reviews the chemical composition of the various types of carbonates.

With the breaking up of the early super-continent after the Mid Cambrian, the earth entered a greenhouse climate that lasted into the Early Carboniferous. In these warmer conditions, "Aragonite Seas" were replaced by "Calcite Seas", in which calcite precipitated directly as LMC, before starting the slow process of dolomitization. The greenhouse climate also favoured the direct precipitation of dolomites, which are thought to account for up to 70% of carbonate rock formation at this time.

Pelagic deposition was well represented in the Mesozoic and Cenozoic, but less common in the Palaeozoic during the Caledonian Orogeny. Carbonate precipitation varies with the temperature and P_{CO2}, and therefore with the depth

of the sea (although it is little dependent on actual pressure: section 3.1.2) and the various minerals do not precipitate below their *Compensation Depths*. These are: A (2km at Equator now), LMC (5km), and Dolomite (D, >5km?), so that below about 2km, LMC and D are preferred precipitates. Peterson (1966) reported that optical calcite dissolution is constant in Pacific Ocean sea water at 19°N, down to a depth of 3700m, and increases sharply below this depth. The Calcite Compensation Depth (CCD) varies with latitude, which is a proxy for temperature and dissolved CO_2. Tucker and Wright (1990, Fig. 5.3) showed that it reduces rapidly to 1km at c. 55° N and S and (*Ibid.*, p33) implied that, at mid and high latitudes, it reduces to zero, as seawater becomes unsaturated. CCD also varied in geological time: it rose when sea level was high, as during the Eocene and Late Miocene, but fell when sea level was low, as during the Oligocene to Early Miocene and during the Pliocene and Quaternary. These concepts could be important in this study, not because of calcite precipitation during sedimentation, but because they illustrate the possibility of metalimestone dissolution when caves are inundated by the sea (section 8.8) or by various types of freshwater lakes (section 8.6).

Three main carbonate depositional environments were recognised by Tucker and Wright (1990). These are: marine coastal (shallow offshore, carbonate ramps on shelf margins, or reefs plus reef mounds); pelagic (deep marine); and lacustrine. From Appendices A1.1 and A1.2, the majority of Caledonide carbonate deposition was in the marine coastal, miogeosynclinal, environment, which produced rather thin structures. Pelagic, eugeosynclinal, deposition may be applicable for the Ordovician and Silurian sediments in the higher Køli Nappes at the deepening Baltic Trough as Iapetus closed. Dallmann (1987, p45) regarded the rather unique 2000m succession of calcite marbles of the Susna Formation of the Hattfjelldal Nappe (KU: Appendix B1.13) as resedimented allodapic limestones, which experienced mass flow of unlithified calcareous debris over the edge of a tidal flat. This resedimentation occurred during a diagenetic phase prior to any dolomitization. There are no recorded lacustrine carbonates in the study area.

A2.2 Carbonate metamorphism

All metamorphic lithologies exposed at the surface in central Scandinavia experienced at least one cycle of prograde then retrograde *regional metamorphism* and some of these also experienced *contact metamorphism*. During the prograde path, rocks descend at increasing temperature and pressure. The fluid pressure increase leads to a loss of volatiles (mainly H_2O and CO_2), so that the rock dries out and becomes impermeable: *"Fluid flow is down the temperature gradient"* (Ague, 2000, lecture quotation). During the retrograde path, new minerals can only be created if further fluid is acquired, leading to bone-dry rock (Jamtveit *et al.*, 2000). Commonly, when hot dry rock reacts with water it shrinks, creating extra stresses in the fabric and its fractures. The reaction proceeds via an advancing front of wetted cracking fissures in a tree-like pattern. However, if water flow ceases, "crack-healing" occurs.

There has been little attempt in the scientific literature to provide an overview of the formation and development of the Caledonide limestones and dolostones through their generally complex and regionally-varying metamorphic history. Winkler (1976, Chap. 6) provided a general description of the metamorphism of dolomites and limestones and Yardley (1989, Chap. 5) gave a general description of the metamorphism and metasomatism of marbles and calc-silicate rocks. Yardley noted the importance of the composition of the metamorphic fluids in determining the mineral assemblages produced. Baumgartner *et al.* (1996), discussed the significant porosity and permeability of carbonates during contact metamorphism, and introduced the term "metamorphic aquifers". Because calcite is stable under most crustal conditions, pure calcite does not develop new minerals under metamorphism: calcite recrystallises back to calcite. [In the very rare conditions of very high pressures and very low temperatures, aragonite would be the stable species]. Metacalcite usually produces a coarser grain size, and commonly a foliation.

Limestones containing other constituents (such as dolomites and silicates) react extensively with these during metamorphism. Thus, in marly sediments there is a complete spectrum possible between purely carbonate and purely silicate facies that can lead under metamorphism to a broad range of calc-silicate mineralogies. Rocks produced by metasomatic interaction between limestone and silicate rock are known as *skarns*. These occur particularly from the intrusion of granite into marble, and are well represented in the western part of the study area. Indeed, some of the geological maps used do not distinguish between metacarbonates and skarns. At very high temperatures but low pressures, as can occur during contact metamorphism, calcite and quartz react to form the

skarn calcium silicate (wollastonite) by the decarbonation reaction $CaCO_3 + SiO_2 => CaSiO_3 + CO_2$ + porosity. This reaction may occur at 600°C and at pressures up to 200Mpa, when calcite becomes a soft, very ductile, rock (Balashov and Yardley, 1998). Whereas the production of CO_2 as a supercritical fluid under metamorphic conditions is clearly of extreme importance in influencing other chemical reactions involving carbonates during metasomatic processes, the above necessary P-T conditions are not usual for regional metamorphism.

According to Balashov and Yardley (1998) and Yardley and Balashov (2000), thick marble bodies survive to high metamorphic grade, despite being potentially very reactive with nearby siliceous metasediments, because they are extremely impermeable. However, the onset of decarbonation reactions (e.g. during retrograde metamorphism) creates porosity and increases the permeability of calcareous layers. This can permit layer-parallel infiltration of water from surrounding rocks that can promote a run-away reaction to wollastonite. Thus, all carbonate can be used up in at least the outer metre of a large marble body, creating calc-silicate zones at the edge of marble units, especially at low pressure. At high metamorphic grades, any thin (<1m wide) limestones should be completely converted to skarns. (*However, cavernous bands of metalimestone down to 1m thickness exist in, e.g., HNC Z6).* The rates of porosity creation and collapse by creep and fluid back-flow (crack healing) are in dynamic balance, so that structures may spontaneously open or close down during reaction, dependent on conditions such as temperature over-stepping and water supply. At high metamorphic pressures, only the outermost metre of calcite is likely to be metasomatised to wollastonite, as porosity loss by creep dampens out the reaction.

A range of Ca-Mg-silicates can also form in decarbonation reactions in cooler, regional metamorphism, P-T conditions, from carbonates that contain *dolomite.* Yardley (1989, p132) presented a triangular phase diagram for the system $CaO\text{-}SiO_2\text{-}MgO+CO_2+H_2O$, which includes the minerals calcite, dolomite and the three skarn minerals talc, tremolite and diopside, and showed how these vary with metamorphic grade. The chemistry and texture of metamorphic carbonates and silicates can vary at the centimetre and millimetre scale across the layers. A one metre thickness of such rocks could sustain a temperature difference of 1000°C during metamorphism, and therefore support a layered range of chemical reactions and products. Whereas calc-silicate skarns are non-karstic in themselves, it is clear from the above that they can form in association with the karstic metacarbonates, and therefore guide the morphology of karst caves (section 5.7.4).

Yardley (1989) discussed the phase relationships among calcite, dolomite and quartz from the dolomitic marbles of the central Alps. The topics of dolomitization of calcite, retro-dolomitization, and the prograde and retrograde metamorphism of both calcite and dolomite in the Caledonides in the possible presence or absence of Mg-rich H_2O derived from seawater were not addressed there. Presumably all these processes need to be invoked to explain the present variety and mineralogy of the Scandian carbonates.

Because of its importance in understanding cave inception in medium- to high-grade metacarbonates, the possibility of residual porosity and permeability in such lithologies exposed at the surface needs to be considered. There is no possibility of the survival of a memory of peak metamorphic porosity, but, because pressure is reduced on ascent, calcite grains experience an isotopic stress relaxation (BWD Yardley, University of Leeds, 2000, pers. comm.). This tends to increase permeability relative to the low values associated with peak metamorphism, and promote the creation of fractures. However, it must be noted that calcite marbles typically have porosities of <1%, compared to sedimentary micrites and sparites that are in the ranges <2% and 5–10% (Ford and Williams, 1989, p33). Limestone aquifers are said to exhibit *triple porosity* at the pore, fissure and conduit scales (Ford and Williams, 1989, p199; Worthington, 1994). At the pore and fissure scales, metacarbonates commonly have lower hydraulic conductivities than sedimentary carbonates (Ford and Williams, 1989, p135). Hence, from this evidence, it has to be concluded that karst cave inception is less favoured and would occur over much longer timescales in metalimestones than in sedimentary limestones, when both lithologies are set in otherwise equivalent environments.

A2.3 Caledonide carbonate metamorphism

Bryhnie and Andreasson (1985) provided a general overview of metamorphism in the Scandinavian Caledonides. All the major allochthons are known to contain previously-sedimentary carbonates (limestones or dolostones) with metamorphic grades that generally decrease downwards through the nappes, i.e. in the direction west–east. The higher-than-trend grades of the Seve Nappes are an exception. Fossils are known from some of the low-grade lower nappes in the east, and possibly from the Køli Nappes (Kautsky, 1953). [The SGU map Ai75, 23F Fatmomakke NV, shows fossil localities along the carbonate outcrops on the mountain Daunentjakke; these are in the lowest of the Lower Køli Nappes, the Bjørkvatten nappe (KB: Appendix B1.17)]. These lower nappes can retain some primary structure, and probably experienced only one metamorphic event. In contrast, the high-grade highest nappes were multiply metamorphosed (Appendix A2.10). The regional metamorphism in the HNC is supplemented with contact metamorphism in aureoles around syntectonic intrusions. At Velfjord (Z2), this produced pure fine-grained calcitic marbles from which organic material has disappeared (Kollung, 1967; Thorsnes and Løseth, 1991). They commonly have a massive white appearance, and are being quarried in several places (Appendix A4.5).

Weak metamorphism probably started in the Late Proterozoic. With the closing of the Iapetus Ocean, high temperature metamorphism in the Mid Cambrian to Mid Ordovician, at depths up to perhaps 50km, was accompanied by igneous activity, and followed by intermediate pressure metamorphism. The collisional stage of closure from the Mid Silurian into the Devonian saw varying degrees of regional metamorphism along the whole 1800km length of the Scandian orogeny, from high-grade in the south of Norway, to practically-unaltered facies where the nappe sheets were thrust eastwards over the basement. The lowest nappes and the basement also exhibit a higher- to lower-grade metamorphic trend within each other, also in the direction from west to east, providing further evidence that the deepest burial and highest temperatures were well to the west of the present mountain range, whilst the Baltoscandian margin was subducted under the North American plate.

Crustal shortening (up to 400km in southern Norway) and crustal thickening (from 30km initially to 70km, Hossack, 1985, p98) was caused by nappe stacking and by the imbrication of previous sediments (repeated carbonate outcrops in the Uppermost Allochthon being good examples). This facilitated partial melting and deformation at depth, during which earlier structures, including bedding, were commonly obliterated. With the movements eastward up to higher elevations, and then with rapid erosion, many of the former high pressure assemblages experienced considerable pressure relief, causing extensive retrogression in their metamorphism.

Various papers that analyse the structure and metamorphism of particular parts of the study area have been published since about 1985. Thus, Brattli (1996) discussed the RNC south of Korgen and included reactions involving siliceous carbonate rocks. Dallmann (1986) considered polyphase deformation in the Hattfjelldal Nappe (KU), and observed that, in parts, the movement of the HNC over the Upper Køli nappes was achieved by ductile flow of the lower mylonitic limestone group within the Hattfjelldal Nappe. He placed the Hattfjelldal Nappe in KU, whilst at the same time relating its upper group stratigraphically to part of the lower Gjersvik Nappe in the Middle Køli (KG). The relevant parts of the Carbonate Outcrops and Caves Databases (Appendices C1–C5) were thus constructed according to Dallmann (1986).

Dallmann (1987) considered, in detail, the stratigraphy and sedimentary environments of the Hattfjelldal Nappe (KU), in which both calcitic and dolomitic metacarbonates occur extensively (Appendix A2.1). He noted that dolomites (and other rocks) commonly show primary structures, whereas calcites (and other rocks) are dominated by tectonic structures (*Ibid.*, p28), although recrystallisation of the calcite is variable, because, in places, graded bedding is observed as a primary feature (*Ibid.*, pp31, 44). In the transition zone between calcite and dolomite marbles, he observed dedolomitization progressing from fractures, which suggests that partly dolomitized rocks might have been completely dolomitized prior to the last recrystallisation process. Further evidence that at least *some* dolomitization occurred during diagenesis is provided by overlying conglomerates that contain dolomites and by the abundance of micritic and micro-sparitic dolomite crystals. However, other coarse-grained sparitic dolomites indicate epigenetic dolomitization (*Ibid.*, p45).

In metalimestones of the Scottish Dalradian Supergroup, which have similarities with those of the HNC (Appendix A1.1), retrograde dolomitization of calcite during uplift and cooling of a metamorphic complex was reported by Fein *et al.* (1994). In this situation, high temperature epidote amphibolite facies calcites and calc-silicates were infiltrated by H_2O and CO_2 fluids along adjacent veins, which produced mainly lower-greenschist facies dolomite and quartz. Guest *et al.* (2000) noted that dolomite reaction zones in Loch Tay Limestones occur adjacent to faults cutting calcite-rich marbles. They suggested that porosity generation and growth of Fe-enriched calcite rims were both precursors to the retrograde dolomitization that followed the transport of sufficient Mg to nucleation sites. Gillieson (1996, p67) also noted that hydrothermal dolomites tend to be located along fracture zones where warm basin fluids are circulating.

Melezhik *et al.* (1997) used isotopic data to suggest that metacarbonates from the Evenes Group in northern Norway were deposited from 635–615Ma and were metamorphosed at 600±80Ma. These rocks have been correlated to the Køli Nappes, and, alternatively, to the Uppermost Allochthon. Trønnes and Sundvoll (1995) also used isotopic dating on 43 calcite and 5 dolomite samples from the HNC, Køli and Seve in north central Norway, and concluded that the environments of the Late Proterozoic HNC carbonates differed markedly from those of the Ordovician Køli, and of the Vendian or Early Cambrian, Seve carbonates.

A2.4 Chemical composition

Tucker and Wright (1990, pp13, 284, 314, 333, 371–372) identified the chemically stable and meta-stable minerals of common sedimentary carbonates, which are brought together here in Table A2.1.

Table A2.1 Common sedimentary carbonate minerals

Symbol [1]	Mineral	Occurrence	Diagenetic Stability	Mole % Composition	Mg/Ca weight ratio
A [2]	Aragonite	Marine	Metastable	~100% $CaCO_3$ [3]	0.00
C [2]	Pure Calcite	Synthetic		>99% $CaCO_3$	<0.01
LMC	Low Magnesian Calcite	Limestone	Stable	>96% $CaCO_3$ + 1–4% $MgCO_3$	<0.03
HMC	High Magnesian Calcite	Limestone (very rare)	Metastable	>80% $CaCO_3$ + 5–20% $MgCO_3$	0.03–0.18
DL	Dolomitic Limestone	Limestone		~20% CD + 80% LMC	0.07–0.10 (c.f. HMC)
D [2]	Pure Dolomite	?		100% $CaMg(CO_3)_2$, i.e. 54% $CaCO_3$ + 46% $MgCO_3$	0.61
SD	Stoichiometric Dolomite	Dolostone	Stable	>97% $CaMg(CO_3)_2$	0.57–0.65
CD	Calcian Dolomite	Dolostone	Metastable	54–58% $CaCO_3$ + 46–42% $MgCO_3$	0.52–0.57
MD	Magnesian Dolomite	Dolostone	Metastable	44–54% $CaCO_3$ + 56–46% $MgCO_3$	0.65–0.91

[1] As used in this thesis [2] Included for completeness [3] May contain Sr and Pb substitutions

Additionally, siderite ($FeCO_3$) and ankerite (ferroan-rich dolomite) are commonly present in dolostones (Hanshaw and Back, 1979, p294; Ford and Williams, 1989, p14; Tucker and Wright, 1990, p171). Because Fe^{2+} is intermediate in size between Ca^{2+} and Mg^{2+}, it fits readily into the dolomite crystal structure, commonly causing pink or buff colours in weathered outcrops. The speleological literature commonly refers to more general classifications of carbonates (e.g. Klimchouk *et al.*, 2000, p56).

An important question is whether stable forms of *metamorphic* carbonates follow the same classification, although the millimetre-scale inhomogeneities in high-grade metacarbonates complicate the answer. The 43 calcitic marbles from north central Norway, analysed by Trønnes and Sundvoll (1995; Appendix A2.3), have $CaCO_3$ bulk compositions that vary from 82–99%, so that the (unreported) maximum mole $MgCO_3$ compositions are from 1–18%, i.e. approximately within the LMC and HMC ranges. Shaikh *et al.* (1989) reported the petrographic and chemical analyses of many metacarbonate samples from the Swedish part of the study area. The great majority are clearly LMC, some are metadolostones that vary from CD to SD, but significant proportions are reported to contain

both "calcite" and "dolomite". However, the bulk compositions of these mixed samples have (with only one exception) $MgCO_3$ values that vary from 5–19%, similar to the chemical composition of HMC or DL (and only two of these have values in the range 5–11%). Whereas the LMC samples (and the same two HMC / DL samples) contain proportions of silica that vary from 0.4% to 28.7%, *all* the samples with >11% $MgCO_3$ contain at least 9% silica, so that the high proportions of Mg in bulk only occur with significant SiO_2. A very similar picture was provided by Robertson *et al.* (1949), who reported metacarbonate compositions from the Dalradian Supergroup in Scotland. Appendix A2.5 discusses the composition of karst spring waters in the study area, and shows that their Ca / Mg ratios also conform to the ranges established in Table A2.1.

Five metacarbonate samples from cave locations in the study area were analysed chemically at the University of Huddersfield as part of this project (Table A2.2).

Table A2.2 Chemical analysis of study area metacarbonate samples

Sample number	1: 2000081902	2: 2000080203	3: 2000082001	4: 2000082401	5: 98080604
Location	Sarvenvårtoe -hullet (Z4)	Bryggfjeldhullet (ZA)	Elgfjellhola (Z4)	Track Cave (ZA)	Tjuvhelleren (ZB)
Weathered appearance	dark brown, black, orange	yellow/brown, sucritic	light brown	White, clean-washed	pale grey, sucritic
Grain size	coarse	coarse sand	medium	coarse	coarse
Internal appearance	similar + white, with muscovite	buff crystals	purple mm-scale bands	white, + 4mm pale grey bands	homogeneous matrix, with tremolite?
Dil. HCl test	vv	vv	v	vv	a
Visual Identification	HMC	HMC	HMC	LMC	Dolomite
Mole % composition $CaCO_3$[1]	83.0	82.1	84.2	97.5	79.2
Mole % composition $MgCO_3$[1]	17.0	17.9	15.8	2.5	20.8
Insoluble residue %	17.4	12.2	9.2	3.0	8.1
Revised Identification	HMC	HMC	HMC	LMC	DL

[1] ignoring insoluble residue and other species
a audible v vigorous vv very vigorous

Samples 1–3 were chosen to test the author's ability to identify yellow / brown carbonates as HMC in the field, which is confirmed by the fairly uniform $MgCO_3$ values. Sample 4 was a presumed (and confirmed) LMC control sample. Sample 5 was taken from the only cave in the study area that was a candidate for forming in dolomite (section 4.4.5). In fact, its $MgCO_3$ composition is too low for dolomite, despite the occurrence of tremolite within its matrix. It therefore appears to comprise a type of dolomitic limestone, or contains both dolomite and calcite (which would explain the audible dilute HCl reaction). The association of insoluble residue (assumed to comprise mainly silica) with larger $MgCO_3$ values is also observed in these samples.

From this discussion, it follows that the Caledonide metacarbonates probably *do* follow the Tucker and Wright (1990) classification as expressed in Table A2.1, and, additionally, mixtures with dolomite inclusions within a metalimestone have Ca / Mg contents that lie within the HMC / DL range. Thus, although it is not stable in sedimentary limestones, only appearing in young limestones, and *never* in Palaeozoic limestones (VP Wright, University of Cardiff, pers. comm., 2002), it seems likely that metastable HMC occurs quite commonly in the metalimestones of at least Scandinavia and Scotland. The karstic role of metamorphic HMC / DL is discussed in sections 4.4.6 and 5.8.2.

A2.5 Karst water chemistry

Helldén (1975) noted that during the spring melt of the overlying snow, percolation water accounted for up to 60% of the flow from the **Sotsbäcksgrottan** (KU) rising, despite the large size of the allogenic input stream, indicating a well-developed epikarst. It fell back to 1–2% in August. Lauritzen (1981b) reported measures of the aggressiveness of karst waters at c. 100 caves and springs across Norway, using the Stenner (1969) method. There is a negative correlation between the size of springs and total hardness, especially for small springs below the tree line. The smaller the spring, then the greater is the proportion of autogenic recharge. Most (but not all) of the samples were unsaturated with respect to calcium carbonate, as expected with short residence times. (Ford, 1971a, pp606–607, noted that fast-flowing cave streams in Canada may not saturate, nor even gain hardness, along a distance of 1.9km, apparently due to a lack of opportunity for effective turbulent mixing and solute diffusion). Samples from above the tree line have a total hardness in the range 5–75 $CaCO_3$ ppm. The hardness range is 7–120ppm below the tree line. For autogenic exsurgences above the tree line, the aggressiveness is inversely proportional to the hardness, which is also in the range 5–75ppm, indicating atmospheric supply of CO_2. There is no such relationship below the tree line, with hardness varying between 35–120ppm. Here, Lauritzen explained the lack of correlation as being caused by varying amounts of biogenic CO_2 and organic acids from the differing vegetation above each site. The effect of the tree line was also shown in the generally negative correlation between hardness and altitude. (Appendices B2.9 and B2.10 and section 5.6 analyse the relationships between altitude and chemical and fluvial deposits in study area caves). Seasonal variations in hardness vary from very peaky to almost constant, depending on the system. Autogenic exsurgences are more uniform than allogenic or mixed resurgences. The hardness value at the end of August can commonly be taken to approximate to the annual mean.

There is a very good linear correlation between titrated total hardness and the electrical conductance of karst waters, so that conductance can be used as a quick estimator of hardness (as confirmed at **Sirijordgrotta**, Z4 by Øvstedal, 1991, p126). The total hardness in the above-treeline vadose streamway of **Grønndalsgrotta** (ZA) varied downstream from 8–12ppm, whilst always remaining aggressive. This aggressive nature of most Scandinavian karst waters was also reported by Helldén (1975), Bakalowicz (1984), Lund and Eraso (1989) and Øvstedal (1991). Palmer (1991, p11) remarked that nearly all cave streams fed from non-carbonate rocks (which applies in the study area) are undersaturated all year round. The hardnesses of Norwegian karst waters from various studies are summarized in Table A2.3.

Table A2.3 Karst water hardness

Place	Total hardness (ppm)	Method	Notes	Reference
Norwegian springs	10–55	Stenner (1969)	Autogenic, above tree line	Lauritzen (1981b, Fig. 7)
Norwegian springs	9–75	Stenner (1969)	Allogenic, above tree line	Lauritzen (1981b, Fig. 7)
Grønndalsgrotta (ZA)	8–12	Stenner (1969)	Allogenic, above tree line	Lauritzen (1981b, Table 1)
Norwegian springs	65–120	Stenner (1969)	Autogenic, below tree line	Lauritzen (1981b, Fig. 7)
Norwegian springs	15–45	Stenner (1969)	Allogenic, below tree line	Lauritzen (1981b, Fig. 7)
Norway, various	5–70	From Ca^{2+}	18 karst sites in flood	Bakalowicz (1984)
Øyfjellgrotta (Z5)	20	From Ca^{2+}	Spring outlet	Bakalowicz (1984)
Glomvatn, N. Norway	10	From Ca^{2+}	Glomvatn outlet	Bakalowicz (1984)
Deep subglacial	13	Modelling		Lauritzen (1986b)
Sirijordgrotta (Z4)	15–86	Stenner (1969)	Sirijordgrotta rising	Øvstedal (1991)

According to Palmer (1991, Fig. 7), when water is in equilibrium with atmospheric CO_2 (c. 340ppm) in an open system, calcite equilibrium solubility and Ca^{2+} saturation concentration vary from 70–50ppm and 28–20ppm over the temperature range 0–20°C. These are the lowest ranges applicable in present, open, conditions. Thus, the data in Table A2.3 confirm that most allogenic cave streams in Scandinavia are unsaturated. Autogenic karst springs vary from unsaturated to saturated, dependent especially on the extent of vegetation cover.

From a discussion about congruent dolomite dissolution (Appendix A2.8), the Mg/Ca ratios in spring waters commonly correspond to the Mg/Ca ratios in the aquifer bedrock for unsaturated solutions. Fairchild *et al.* (1994) and Fairchild and Killawee (1995) found that Mg/Ca ratios in Alpine glacial meltwaters with <1% dissolved

carbonate were much higher than in the local carbonates, but laboratory experiments showed that the ratio reduced to a constant value (in agreement with Picknett, 1976) as dissolution increased to 2%. A graph of 33 Norwegian carbonate spring waters has one sample close to the calcian dolomite (CD) ratio, none with ratios between CD and HMC / DL, and none with >99% Ca (Lauritzen, 1981b, Fig. 10). The bulk of the samples thus appear to represent various mixtures between the proposed extremes of HMC and LMC. This provides hydrochemical support to the conclusion that mixtures of Caledonide metalimestones and metadolostones always have Mg/Ca ratios in the HMC range (Table A2.1, Appendix A2.4).

In the springs analysed by Lauritzen (1981b), Mg and Ca concentrations respectively varied from 0.1–4.4ppm and from 2–42ppm. The Na concentrations varied from 1–5ppm, reducing with distance from the sea, which suggested derivation from airborne salt spray. Other metal ions were <=1ppm. Hence, the cationic inhibitors are probably unimportant in Norway.

The Lauritzen (1981b) results were supported in a more limited set of tests at 18 sites across Norway by Bakalowicz (1984), who measured the major cations and anions, generally in flood conditions. The *maximum* values recorded for various ionic species are presented in Table A2.4, together with *mean* ionic values taken by Øvstedal (1991) at **Sirijordgrotta** (Z4) in July 1988.

Table A2.4 Ionic species concentrations from across Norway and at Sirijordgrotta

Ion	Ca^{2+}	Ca^{2+}	Mg^{2+}	Mg^{2+}	Na^{+}	Na^{+}	K^{+}	K^{+}	SO_4^{2-}	SO_4^{2-}	Cl^{-}	Cl^{-}	HCO_3^{-}	HCO_3^{-}
Unit	$meqL^{-1}$	ppm	$meqL^{-1}$	ppm	$meqL^{-1}$	ppm	$meqL^{-1}$	ppm	$meqL^{-1}$	ppm	$meqL^{-1}$	ppm	$meqL^{-1}$	ppm
Max	1.4	28	0.44	5	0.20	5	0.14	5	0.18	9	0.05	2	2.1	128
Unit	$mmolL^{-1}$	ppm	$mmolL^{-1}$	ppm	$mmolL^{-1}$	ppm	$mmolL^{-1}$	ppm	$mmolL^{-1}$	ppm	$mmolL^{-1}$	ppm	$mmolL^{-1}$	ppm
R	0.40	16	0.08	2	0.13	3	0.01	0.4	0.02	2	0.06	2	0.9	55
P	0.84	34	0.07	2	0.17	4	0.01	0.4	~0.09	~9	~0.2	~7	1.6	98

Max = maximum individual values from 18 sites across Norway at temperatures from 6.5–9.0°C (Bakalowicz, 1984)
R = mean value at Sirijordgrotta rising at low-flow at temperatures from 5–7°C (Øvstedal, 1991, Station C, Table 6.1 and Appendix A)
P = mean value for Sirijordgrotta percolation waters (Øvstedal, 1991, Station D, Table 6.1 and Appendix A)
L = litre

Ignoring other species, the mean **Sirijordgrotta** compositions are $CaCO_3$ 83 mole % (at the rising at low flow) and 92 mole % (percolation water) and $MgCO_3$ 17 mole % (at the rising at low flow) and 8 mole % (percolation water). These are also within the HMC ranges discussed in Appendix A2.4. Although the **Sirijordgrotta** cave system lies *below* the tree-line, its source streams run over mica schists and granites before sinking *at* the tree-line, so that atmospheric CO_2 levels should apply. Thus, despite the very low July 1988 flows ($50ls^{-1}$ peak) that ran through 600m and 1200m of limestone passages, the resurgence water remained unsaturated, at Ca^{2+} = 16ppm. At higher flow rates, the degree of under-saturation would be higher, so that this cave is a good example of a cave stream that has probably remained aggressive throughout the Holocene. There is no reason to doubt that the above observations, mainly from northern Norway, apply equally well within the study area.

Einevoll and Lauritzen (1994) noted that beneath 50–100m of rock, annual variations in stalactite drip chemistry and cave climate are well damped, giving near constant results. However, most caves in the study area are much closer to the surface.

A2.6 Limestone denudation

Various physical and chemical experiments that measured limestone denudation rates in Scandinavia and elsewhere are shown in Table A2.5. Engh (1980), Gunn (1981b) and White (2000) discussed the inaccuracies of early measurements, and the many factors to be considered in relating dissolution rates to rainfall or to *runoff* (i.e. annual precipitation less evapotranspiration). Droppa (1986) studied dissolution rates in Czechoslovakia, using limestone tablets. He found that corrosion intensity was consistently higher in summer than in winter, except for tablets buried under 20cm of soil, when winter maxima and minima were twice those of summer. White (1984; 1988) and Ford *et al.* (1988) cited Smith and Atkinson (1976) as giving a linear arctic and alpine denudation rate (presumably for

sedimentary limestones) of D=0.025R+7.4mmka^{-1}, where Rmma^{-1} is the runoff. This formula gives a chemical denudation rate of c. 100mmka^{-1} for arctic environments with 2.5ma^{-1} runoff. White (1984; 1988) also argued, from both a theoretical and an observational basis, that annual denudation rate is proportional to runoff, and plotted various curves for groups of temperatures and P_{CO2}. Denudation rate increases with the cube root of P_{CO2}, and by only 30% when the temperature reduces from 25–5°C. White (2000) gave a summary of denudation rate observations.

Table A2.5 Limestone denudation

Place	Rate (mmka^{-1})	Method	Notes	Reference
Kongsfjorden, Spitsbergen	16	Corbel formula (Autogenic + allogenic total)	Water hardness = 105ppm Precip. 350mma^{-1}, evap. 50mma^{-1}, mean temp. -8°C	Corbel (1960)
Norway, various	80–500	Corbel formula	From water hardness	Corbel (1960)
Norrland, Sweden	40	Corbel formula	From water hardness	Corbel (1960)
Misvaer, N. Norway	320	Corbel formula	Water hardness = 80ppm	Corbel (1960)
Svartisen, N. Norway	100–150	Postglacial pedestals	Pedestals 10–15cm thick	Kirkland (1958, p57)
Norway, various	30–50	Micro-erosion meter	Rainwater, above treeline	Lauritzen (1980)
Norway, various	300–400	Micro-erosion meter	In stream beds and caves	Lauritzen (1980)
Svartisen, N. Norway	8–64	Sweeting formula	Hardness = 32–96ppm (Lauritzen, 1981b results)	Lauritzen (1984d)
Glomdal, N. Norway	60–350	Limestone tablet	Under water	Lund (1986)
Glomdal, N. Norway	0.1–4	Limestone tablet	Under soil or vegetation	Lund (1986)
Glomdal, N. Norway	0.1–1	Limestone tablet	Under air	Lund (1986)
Glomdal, N. Norway	27	Bögli formula	Hardness 10–110ppm	Lund and Eraso (1989)
Glomdal, N. Norway	25	Micro-erosion meter	Rainwater, on bare karst	Lauritzen (1990a)
Glomdal, N. Norway	13–23	Veins and pedestals	9ka postglacial dissolution	Lauritzen (1990a)
Glomdal, N. Norway	23–43 Allogenic =8	Linear mixing, multiple basin	From water hardness	Lauritzen (1990a)
Sotsbäcksgrottan (KU, Sweden)	21/28 (modified formula)	Corbel formula, by complexometric titration	Hardness = 20–45ppm Used Karlgren (1962) method	Helldén (1975) Cited by Helldén (1973)
Övre Ältsvattnet (KU, Sweden)	30	?	Cited by Norberg *et al.* (1988, p1).	Engh (1974)
Mieseken (ZC, Sweden)	32	?	Cited by Norberg *et al.* (1988, p1).	Jasinski (1978)
Kåtaviken (ZC, Sweden)	225	?	Hardness = 67–213ppm Cited: Norberg *et al.* (1988). Unreasonable rate?	Nisell (1986)
Kåtaviken (ZC, Sw.)	26	See formula used	Hardness = 8–63ppm	Norberg *et al.* (1988)
Rödingsfjäll (KU, Sweden)	14–19	?	Hardness = 5–45ppm Cited: Norberg *et al.* (1988)	Norberg and Pettersson (1988)
Rödingsfjäll(KU,Sw)	34	See formula used	Hardness =14–17ppm	Norberg *et al.* (1988)
Sirijordgrotta (Z4)	76	Stenner, Corbel	Hardness =15–86ppm	Øvstedal (1991)
Sirijordgrotta (Z4)	124–302	Limestone tablet	In streams	Øvstedal (1991)
Pikikiruna Marble, New Zealand	100	Modified formula	Hardness = 50–120ppm	Williams and Dowling (1979)
Somerset Island, Canada	2	Modified formula. Permafrosted to -300m.	-17°C mean annual tempr. Precip. 129mm. Evap. 39mm Hardness = 36–95ppm	Smith (1972)
Castleguard, Canada	6–15	Unstated formula	Hardness = 20–30ppm	Smart (1983)
27 sites, world wide	1–22	Limestone tablet	Rain, in air	Gams (1981)
27 sites, world wide	1–18	Limestone tablet	Rain, on a dry surface	Gams (1981)
27 sites, world wide	1–44	Limestone tablet	Buried in soil	Gams (1981)

Results of studies of internal cave wall retreat rates in Scandinavia are presented in Table A2.6. According to Palmer (1981; section 3.1.13), the theoretical maximum cave wall retreat rate is c. 1mma^{-1}, i.e. 1000mmka^{-1}. Tables A2.5 and A2.6 show that erosion in some Scandinavian active vadose and phreatic cave passages can approach this rate, despite the reduced flow during the winter months. From micro-erosion meter readings on marble, Lauritzen (1980;

1986c) calculated that active canyons could have developed to a depth of 3–4m during the Holocene. However, if the submerged 6m-diameter passage at the **Glomdal Underground Outlet** enlarged at an estimated present rate of 800mmka^{-1} throughout the Holocene, it would have reached its present size within 4ka, rather than >40ka (section 3.3.3). The presence of the glacially-truncated Middle Entrances with 2m-diameters suggests that the main passage had reached this size before the last deglaciation, reducing the mean Holocene radius enlargement rate to only c. 200mmka^{-1}.

Table A2.6 Phreatic cave wall retreat rates

Place	Rate (mmka^{-1})	Method	Notes	Reference
Glomdal Underground Outlet, N. Norway	200	Hardness increase along tube	Assumed passage geometry	Renwick (1962)
Glomdal Underground Outlet, N. Norway	200–400 200–600	Limestone tablet and micro-erosion meter	Present rate	Lauritzen (1986c) Lauritzen (1990b)
Glomdal Underground Outlet, N. Norway	800	Hardness increase along tube	Present rate	Lauritzen (1986c)
Pikhaug, N. Norway	5–88	Assumed aggressiveness[1]	Present rate	Lauritzen (1982)
Kvithola, N. Norway	100–1000	Theoretical assumption	Relict passage	Lauritzen (1986a)
?	0.5–1.0	Speleothem corrosion	Subglacial[2]	Lauritzen (1990b)
Hammernesgrotta, N. Norway	0.2	Condensation corrosion of relict passage	2mm crusts	Lauritzen (1990b)
Rödingsfjäll (KU, Sw.)	14–87	Assumed aggressiveness[1]	Lauritzen (1982) method	Norberg *et al.* (1988)

[1] Rates from assumptions about maximum total hardness of 50 ppm $CaCO_3$ in non-glacial conditions, and minimum total hardness of 12/20ppm $CaCO_3$ in subglacial conditions. This method is less reliable, because it used a formula based on aggressiveness by Palmer (1981) that was superseded by a formula based on the degree of undersaturation (Palmer, 1991).

[2] The subglacial rate is probably an underestimate by comparison with a cited quartz weathering rate of 4mmka^{-1}.

A2.7 Scandinavian dolostones

Historically, the formation of dolostones containing dolomite minerals has been poorly understood, and there are many unresolved problems and contradictions (e.g. Gillieson, 1996, p67). Both direct precipitation (perhaps in high organic concentrations) and replacement of calcite are possible processes. The known 'dolomite problems' include: a) Despite seawater being supersaturated by dolomite by nearly two orders of magnitude, precipitation is rare at present. Presently-forming dolostones are known, but it is thought that widespread precipitation is inhibited by kinetic factors such as the high ionic strength of sea water (especially sulphate) and fast, inhibiting, LMC precipitation. b) Sea floor calcite should be dolomitized by replacement, but this is rare. c) Although it can be formed at hydrothermal temperatures both artificially and during metamorphism, laboratory synthesis of dolomite from natural waters is impossible at normal temperatures. This arises from the very long reaction rates and long precipitation times, although eventual saturation concentrations are comparable to those of calcite. (Higgins and Hu, 2005, found by experiment that a relatively rapid growth of a single crystal layer inhibits further growth). d) There are few modern analogues of ancient dolostones. e) Although seawater is rich in Mg, a large flow of Mg^{2+} ions would be needed to dolomitize a limestone formation completely.

To summarise, whereas dolomitic minerals behave to an extent like the more reactive calcitic minerals, their very long reaction times means that they can only form over very long timescales [Ma?], and, once formed, they remain stable and resist dissolution also over very long periods of time. Appendices A2.4, A2.5, A2.8 and sections 4.4.5 and 4.4.6 discuss dolostone chemistry and the karstic properties of dolostones within the study area.

There is no documented Scandinavian karst cave existing in a correctly-described metadolostone rock (i.e. one that is D, SD, CD or MD, as defined in Table A2.1). Although Lauritzen (1981c) mentioned the existence of cave systems in dolomite, he did not say where in Norway they occur, nor was a definition of "dolomite" given: he probably meant High Magnesian Calcite (HMC) or Dolomitic Limestone (DL). Ford (1971a, p586) remarked that areas of considerable dolomitization in the Rocky and Selkirk Mountains of Canada yield negligible development of karst landforms. However, Ford (1995) gave a description of some karren landforms on Canadian dolostones.

Where two different limestone lithologies are in contact along the strike, then it is common to find cave entrances formed along this junction. Bottrell (1988) reported caves formed at the junction of grey and yellow metalimestones in Lower Glomdal, northern Norway. He described the grey lithology as being >95% calcitic, with silicate and mica impurities. This is presumably impure Low Magnesian Calcite (LMC). It varies from massive structures to banded structures, with darker bands at scales of 5–100mm. The yellow lithology always contains >20% non-calcitic components and has a very variable composition (including dolomite, in some cases), colour (e.g. brown), and banding (up to a scale of 100mm), and may therefore include HMC or DL. Bottrell found that cave passages exist in both lithologies, but preferentially in the grey limestone. In caves where both types of limestone could be observed, the yellow limestone appeared to act as an aquiclude in some instances. Lower Glomdal lies in the RNC, some 25km north of the study area boundary. See also sections 4.4.5, 4.4.6 and 5.7.3 and Appendix A2.8.

A2.8 Dolostone chemistry

Hill and Forti (1997, pp142–150) discussed the occurrence of various calcium- and magnesium-based carbonate minerals in caves. The dissolution of dolomite in hydrochloric acid was studied using rotating discs by Lund *et al.* (1973). They found that the rate of dissolution of calcite as marble or limestone is c. 100 times greater than that of dolomite for the same concentration, at 25°C. This is in agreement with field experience in the study area: calcitic metacarbonates give a vigorous reaction with dilute HCl, whereas metadolostones give a reaction that is not visible and barely audible (section 4.2.9). Picknett (1976, pp247–248) noted that when dolomite dissolves in carbonic acid, the ratio of Ca to Mg in solution equals that of the solid (congruent dissolution), and a true saturation is attainable. However, in saturated solutions, "magnesian aragonite" [A+HMC?] crystallises out in preference to dolomite at normal temperature, because of a slow rate of deposition, as agreed by Palmer (1991, p15), who stated that dolomite cannot reach *saturation* without driving calcite into supersaturation below 25°C, causing incongruent dissolution. Wigley and Plummer (1976, Fig. 3) described the conditions favouring the replacement of calcite by dolomite in various solutions of dilute sea water at two P_{CO2} concentrations.

Rauch and White (1977) conducted experiments on the dissolution rates of various Ordovician carbonates from the Union Furnace outcrop in Pennsylvania. Their results showed that dissolution rates of carbonate types by carbonic acid at a standard 22% saturation reduce in the order LMC, C, HMC, CD, although this was less certain at low dilution. However, this author suggests that their results would now benefit from a modern re-appraisal to consider: a) the identification of samples against the carbonate classification in Table A2.1; b) the inhibiting effects of SiO_2 and other impurities; and c) their assumption that C and D saturation occur together at equilibrium.

The influence that $MgCO_3$ has on calcite dissolution has been the subject of much debate. Picknett (1976, p247) reported some paradoxical evidence about the solubility of (low) "magnesian calcite" (LMC) compared with that of pure calcite. The solubility of high magnesian calcite (HMC) was also contradictory and confusing and he acknowledged (*Ibid.*, p249) that the contemporary knowledge of Mg^{2+}-related equilibrium constants was unsatisfactory. Thus, Jakucs (1977) found that $MgCO_3$ substantially reduces calcium carbonate dissolution, in contrast to Rauch (1972) and to Picknett and Stenner (1978) who reported enhanced calcite solubility in dilute $MgCO_3$ solutions. However, Dreybrodt (1989a) could find no such increase when he repeated the laboratory experiment. The work reported in section 3.1.15 probably resolves these conflicts.

White (1977) explained the well-known rarity of conduits in *dolomite* aquifers by presenting experimental evidence that, although the dissolution rate is comparable to that of limestone in highly unsaturated solutions, the rate soon falls as saturation increases, and saturation takes several years to achieve. The slowdown in reaction kinetics on increasing saturation takes place much earlier than in calcite (sections 3.1.13–3.1.15), at 1% saturation, so that the critical triggering for conduit development never takes place.

The most comprehensive experiments to study the kinetics of dolomite dissolution were those reported by Busenberg and Plummer (1982). They measured the rates of dissolution of eight samples of stoichiometric dolomite far from equilibrium, using the same procedures that Plummer, Wigley and Parkhurst (1978; section 3.1.3) had used for calcite dissolution. Four of the samples were of sedimentary origin, and four were "hydrothermal" (= metamorphic). They deduced an empirical rate equation to describe the dissolution of dolomite that has similarities

with the PWP equation for calcite, and resolved many previous conflicts and anomalies in the understanding of dolomite chemistry. At low temperatures, the more highly ordered *metamorphic* dolomites always dissolved significantly more slowly than sedimentary dolomites i.e. they had lower forward reaction rates. Further, the metamorphic sample with the highest iron content dissolved the slowest, suggesting that it is the most stable. The slow dissolution rate of all dolomites is accounted for by a strong backward reaction in the presence of increasing bicarbonate ions. The effect is to slow down the reaction, rather than to precipitate a solid phase, so that dolomite dissolution becomes even slower than its initial speed of 100 times slower than calcite dissolution. They also confirmed that, except at the very start of the reaction, the dissolution of dolomite is congruent, i.e. the $CaCO_3$ and Mg CO_3 components react at the same rate, and the Ca/Mg mole ratio tends to unity, in agreement with field experience about the chemistry of springs from dolomite aquifers (Appendix A2.5).

White (1984, pp244–246) explained the more subdued nature of dolomite surface karst from its dissolution behaviour. The saturation concentrations of calcite and dolomite solutions as measured at springs are similar, so that denudation rates are also similar. However, the bulk mass of dissolved limestone comes from the surface, whereas dolomite dissolution occurs throughout the fracture system, commonly without forming large conduits, but generating highly-productive aquifers.

Herman and White (1985) conducted low concentration rotating disc experiments on three dolomite samples, mainly at 25°C: one sedimentary, one metamorphic single crystal, and one coarse-grained metamorphic sample from Fauske in northern Norway. The shapes of their dissolution rate curves were in good general agreement with those of Busenberg and Plummer (1982), although actual dissolution rates were lower by a factor of about two, and the sedimentary sample behaved more like one of Busenberg and Plummer's metamorphic samples. The Fauske dolomite marble dissolved at a rate nearly equal to that of the sedimentary sample, but the single crystal rate was lower.

From the above experimental results, Ford and Williams (1989, pp88–92) proposed a picture of dolomite, HMC and LMC dissolution at the molecular level. There is no information at present on the mechanism of dolomite dissolution under near-saturation conditions (White, 1988, p147). Borsato and Frisia (199?) discussed the unique preferential karstification of Dolomia Principale dolostones in the South Tyrol, Italy. These host cave systems up to 18.5km long. They noted that ordered, stable, stoichiometric dolomites are not common in sedimentary dolostones, which commonly consist of CD, are full of defects, and hence are better candidates for dissolution. Where hydrothermal fluids circulated through fractures, and caused recrystallization of original diagenetic facies, the grain size increased, giving reduced surface area, and in those places the Dolomia Principale is not karstified. Karstification is also lacking in porous and massive facies where intergranular porosity hindered concentrated recharge.

Chou *et al.* (1989) studied the kinetics of the dissolution of the carbonate minerals calcite [LMC?], aragonite, witherite ($BaCO_3$), magnesite ($MgCO_3$) and stoichiometric dolomite. The forward rate curves against pH were similar for the first three minerals, but rate constants for magnesite were three to four orders of magnitude lower (probably due to the difficulty to hydrate $MgCO_3$), and those for dolomite were about one order of magnitude lower. The dissolution kinetics of dolomite are much more complicated compared to the others, with fractional reaction orders. The paper made the important point that minerals with similar solubilities may have very different dissolution rates. Singurindy and Berkowitz (2003) explored the oscillating competition between dissolution and calcite precipitation processes in stoichiometric dolomite (dedolomitization) at various flow rates and pH values. They agreed with earlier research that reaction becomes congruent as the reaction proceeds, and suggested that the earlier preponderance of Ca^{2+} arises from dissolution of calcite in the dolomite sample.

Martinez and White (1999) found that (Calcian) Dolomite from the Isla de Mona (near Puerto Rica) had a lower dissolution rate than LMC (?) from limestone overlying it. Karst development on Mona consists of shafts in the limestone to horizontal openings at the limestone / dolostone contact, with little penetration in the dolostone. The higher dissolution rate of the Mona dolostone compared to a reference dense Ordovician dolostone sample was explained by the *presence of interspersed calcite* (c.f. section 4.2.9 and Appendix A2.4). The global rarity and

subdued nature of karst in dolostone rocks is even more marked in the metadolostones of the study area (sections 4.2.1, 4.4.5 and 5.8.2), although inception at metadolostone / metalimestone contacts is likely (section 3.1.5).

A2.9 Breakthrough and enlargement in metadolostones

From the discussion in section 8.1.10, there seems no reason to suppose that fracture systems were not also generated in the Caledonide *metadolostone* outcrops from seismic activity associated with glacial unloading. A large proportion of these should also be wide enough to sustain turbulent flows that in metalimestones would be beyond the breakthrough point. However, from the review in Appendix A2.8, dolomite only dissolves at a measurable rate when the solution is completely unsaturated. No reference is known to the equilibrium solubility of dolomite at low P_{CO2} and 0°C (as applies during deglaciation), but this is hardly relevant. According to Busenburg and Plummer (1982, Fig. 7), the dissolution rate of dolomite at zero P_{CO2} and 1.5°C is $<0.1x10^{-7}$mmolcm^{-2}s^{-1} for pH>3. Herman and White (1985) gave the maximum (initial) dissolution rate of dolomite as about 1μmolm^{-2}s^{-1} (=10^{-7}mmolcm^{-2}s^{-1}) at 0°C (*but at a P_{CO2} of 1 atmosphere*). Thus, the dolomite rate is comparable to the maximum calcite rate only in the most favourable conditions and the rate becomes negligible after a few hours as the saturation level increases. Hence, compared with calcite, neither breakthrough nor passage enlargement over significant path lengths are likely to occur within the timescales applicable to any Caledonide flow regimes.

These theoretical and laboratory results explain the rarity of karst features in metadolostone outcrops in the study area (section 4.4.5). Small surficial karst features have developed from tectonic fractures, but presumably only under present meteoric conditions during the Holocene. The short **Tjuvhelleren** (ZB), whose bedrock partly comprises a dolostone (Appendix A2.4), probably enlarged to its c. 2m^2 cross-section under an ice-dammed lake above Stor Akersvatn (Appendix D2.3), but only because the path length was very short (4m) and the hydraulic gradient was very high (0.75).

A2.10 Caledonide carbonates: a discussion

In concluding the brief review of the diagenetic, dolomitization and metamorphic history of the central Scandinavian Caledonide carbonates, the anomaly regarding the relative paucity of dolostones in the Proterozoic and Palaeozoic metacarbonates of the study area (when diagenetic processes commonly converted high proportions of carbonates to dolostones: Appendix A2.1) may perhaps be resolved as follows.

Deposition of early carbonates was as A + HMC, or as LMC, or as D directly. In many Caledonide situations there was sufficient time for the full range of diagenetic reactions and recrystallisations to have gone to completion, so that conversion to dolomite would be 100%. In other situations, metamorphism could have occurred too soon after deposition for full dolomitization, and much of these carbonate layers could have remained as calcite. From the work of Dallmann (1987), admittedly in only one area, there is at least some evidence that metamorphism can cause *dedolomitization*. His study was based on rocks in the Køli Nappes, which only experienced low-grade (typically greenschist facies) metamorphism. At the much higher grade metamorphisms suffered by the HNC / RNC and Seve rocks, conversion of dolomite back to calcite ("dedolomite") and skarn minerals may be facilitated and accelerated. Winkler (1976, p173) listed 16 applicable reactions in siliceous dolomites. In six of these, calcite is consumed, and skarns and dolomite are produced. In eight reactions, dolomite is consumed, and calcite produced, together with calc-silicate minerals.

It follows that the rocks in the Uppermost Allochthon and in the Seve nappes may have been subjected to a sufficient number of repeated high-grade metamorphic events over sufficient timescales for dedolomitization to LMC or to HMC / DL to have been completed in many places. A corollary is that calc-silicate rocks would have been produced contemporaneously, and formed intermediate layers within the meta-calcites. This could partly explain the very high frequency of interlayered aquiclude rocks that are found inside the caves of the Uppermost Allochthon, but which are relatively absent from the caves in the Køli Nappes limestones. (Sections 4.3, 4.4 and 5.7.4 consider the roles of non-carbonate rocks in karst and cave morphology). Similarly, the paradoxical higher proportions (section 4.2.1) of dolomites in the Køli Nappes (16%) and Lower Allochthon (96%) could be associated with the reducing metamorphic grade of these nappes, and a consequent reduction in opportunities for dedolomitization.

APPENDIX A3 GLACIAL PROCESSES

The likely timings and extents of glacial events in the study area were considered in section 2.3. The various processes that characterise the onset, existence and culmination of continental icesheets are reviewed in this Appendix.

A3.1 Glaciation and deglaciation

Warwick (1956 and 1971) discussed the onset and decay of glaciation in Britain in the context of cave development with a description that seems partly applicable to Scandinavia. The beginning of each stadial was triggered by a switch to a climate with cooler and drier summers and warmer and wetter winters. An increased amount of precipitation fell as snow in winter, whilst less fallen snow melted in summer. In critical areas on higher ground, a surplus of unmelted snow at the end of successive summers led to an accumulation of unconsolidated snow and ice each winter. At a critical depth, the ice bodies started to flow. Movement was initially guided by valleys, but later, as the icesheet thickened, the flow became radial from the higher mountain areas, where accumulation was most persistent. At the ice front, the supply of fresh ice from the centre was matched by the wastage due to melting. This thinned ice front waxed and waned with the seasons, but generally expanded outwards if the lower temperature persisted, and was also guided by the local topography. The surface was commonly quite dirty at the ice front, as the ice melted around enclosed debris, which was deposited as till. Meltwaters from the front of the ice carried much of this till forward as a fan, choking valley floors with sand and gravel. A zone of permafrost probably lay beyond the ice front at least, and beyond this there was a zone of periglacial conditions, with seasonal variations.

At the end of each glacial, the mean annual temperature rose again, causing the melting to outpace the supply of new ice, and the icesheet to recede. Ice melted first at the highest levels, and the valley bottoms were the last to be clear of ice. Dead-ice remained in topographically low positions, commonly forming up-valley, ice-dammed lakes (IDLs), where large amounts of glacial deposits were laid down. Hence, each Scandinavian glaciation and deglaciation started and ended in the west, near the summits of the Norwegian mountains. Chapter 8 develops this concept, and also discusses the effect of the sea during glaciation and deglaciation.

Oerlemans (1991) discussed the role of icesheets in the Pleistocene climate. Depending on local conditions, snowfall reaches a maximum at annual temperatures between -5 and +5°C. There is a powerful feedback between increasing altitude and ice accumulation, because the icesheet grows even if there is no further cooling (albedo effect). Although isostatic adjustment lags increasing load and decreasing thickness, both movements provide some negative feedback, restricting growth, and then restricting decay. Oerlemans referred to two studies that showed that at glacial maxima, when the Atlantic sea ice restricts moisture supply, precipitation decreases by up to 50% north of 60°N. This has the effect of drying out northern hemisphere icesheets. Icesheets can decay much faster than they grow, but a rapid decay requires destabilising mechanisms as well as a high summer temperature. Ice fronts that calve into the sea or into proglacial lakes can provide this instability and lead to a fast retreat. Geothermal heat input causes higher ice temperatures at the base of the icesheet and subglacial meltwater is produced when the base reaches the pressure melting point. This reduces friction and can lead to sliding on till layers, which may also accelerate the decay. Donner (1995, p96) mentioned that unfrozen sediments were commonly deformed under large icesheets in addition to frozen sediments near the ice margin. Andersen and Borns (1997, p108) remarked that even below a smooth icesheet there can be ice streams in subglacial valleys that drain much of the ice.

A3.2 Cold-based glaciation

It seems likely that permafrost conditions occurred beneath the icesheet near glacial maxima in much of the study area. Studies of pre-Late Weichselian Scandinavian glacial fans by Klemen *et al.* (1997) suggested that the *core* of the Late Weichselian glaciation retained a frozen bed, assisted by reduced frictional heating. Klemen and Hättestrand (1999) studied "ribbed" or "Rogan" moraines (linear moraines orthogonal to the ice flow that are probably formed subglacially) and "relict" landscapes (landforms not modified by overriding icesheets). They similarly deduced that, during the LGM, large core areas of the Laurentide and Fennoscandian icesheets were frozen-based, and therefore

high-domed and stable. Their maps (*Ibid.*, Figs. 1b and 1d) indicate that the frozen-bed limit apparently reached at least to Trofors in the study area, and perhaps as far west as Tosbotn. It shrank during deglaciation, so that in the study area only the Okstind mountains retained a frozen bed by 9500a. However, the extent of the frozen bed is related to the size of the icesheet and Johnston (1987) noted that icesheets tend to maintain bedrock temperatures near the pressure melting point, suggesting that karst rocks in the study area were covered by at least a film of liquid water during part of each glaciation. The reconstruction by Boulton *et al.* (2001, Fig.17) showed that the mountains of Scandinavia, including the study area, experienced basal melting during the Early Weichselian prior to 80ka, but were subsequently characterised by basal freezing. During early icesheet growth, the base is everywhere below the freezing point (*Ibid.*, p619). At the decay of the icesheet, a major ice stream flowed due west across Elgfjell and Jordhulefjell (Z4), suggestive of a warm bed there at that time (*Ibid.*, Fig.15 and p600). However, during deglaciation, the rate of retreat of the ice margin was commonly greater than that of the melting / freezing interface, so that much of the remaining icesheet was still frozen at its base, despite higher annual temperatures.

A3.3 Warm-based glaciation

Warm-based (temperate) glaciers and icesheets move by deformation and by *regelation*, whereby basal ice melts on the higher pressure stoss side of an obstacle and refreezes on the lower pressure lee side. Additionally, it is now known that contemporary *subglacial lakes* exist. A large, deep, freshwater subglacial lake lies below the Antarctic icesheet (Kapitsa *et al.*, 1996; Nadis, 1999). It has bedrock walls and floor, and its upper water surface is at a depth of c. 3743m below Vostok (section 2.3.2), i.e. 255m below sea level. The mean and maximum heads of water in Lake Vostok are 125 and 510m (≥1000m, Siegert *et al.*, 2001). The total hydraulic pressure is equivalent to a head of water c. 3140m above sea level (~350 atmospheres) for the whole lake, on which the local icesheet is floating. For subglacial lakes to be in hydrostatic equilibrium, their ice-water interfaces slope at eleven times the ice surface gradient, but in the opposite direction (Siegert *et al.*, 2001). Lake Vostok is the largest of around 70 identified subglacial lakes beneath the east Antarctic icesheet (Bentley, 2000). It is also possible that neighbouring subglacial lakes could have a hydrological connection with Lake Vostok (Siegert *et al.*, 2001). The model of slow circulation replacement water in such lakes was confirmed by Siegert *et al.* (2000; 2001). They demonstrated that, at Lake Vostok, the basal ice melts on the west and north (up ice flow) side of the lake, whilst the lake water freezes (at -3°C) and builds up into the icesheet base on the east and south, down flow, side. Rotating water circulation patterns were estimated to have speeds of $0.3 mms^{-1}$.

The presence of Lake Vostok and other subglacial lakes at the heart of an icesheet shows that both warm-based and cold-based glaciation can vary locally. The possibility that Lake Vostok is caused by the presence of a hydrothermal rift zone was virtually ruled out by Jean-Baptiste *et al.* (2001), who also deduced that the renewal time of the lake is c. 5000a. Dowdeswell and Siegert (1999) showed that the majority of Antarctic subglacial lakes are located near the centre of the icesheet, where ice surface slope, ice velocity and surface accumulation rates are all low, but a minority lie closer to the Antarctic coast. Pressure melting occurs in the centre because of the ice thickness (2–4km), and occurs nearer the periphery from the heat generated by basal sliding. Apart from Lake Vostok, most lakes are found in areas of relatively low relief (less than 400m elevation in 4km). The authors suggested that present Antarctic subglacial lakes provide an analogue for northern Quaternary icesheets at the height of glaciation. These observations complement those of Klemen and Hättestrand (1999; Appendix A3.2), who suggested that the core of the Scandinavian icesheet had a frozen bed. Shoemaker (1991) calculated that under normal bed-slope conditions and hydraulic transmissivities, local ponding can occur in *any* bed depression. Thus, the variation of cold-based and warm-based glaciation over space and time is an extremely complex problem to resolve. Indeed, there are at least four general cases to consider, because the air and bedrock temperatures can vary almost independently above and below the freezing point of water.

A3.4 Subglacial groundwater

Boulton *et al.* (1993; 1996) modelled the groundwater regimes that existed at the SW margins of the Saalian and Weichselian glaciations along a transect from the Netherlands via southern Sweden into southern Norway. They noted that subglacial meltwater tends to flow radially outwards towards the icesheet margin, forming eskers, except in mountainous terrain, where bed topography is more important (as in most of the study area). Unlike in present, non-glacial, conditions, water at the ice-bed interface and groundwater in aquifers beneath the icesheet both flow as parts of icesheet-wide systems. Where basal melting occurs, the water pressure head approximates to the magnitude of ice pressure, and may produce high pressures and flows in any lower, highly permeable, aquifers. Near to the ice divide, the basal ice does not melt, groundwater heads remain low and no groundwater flows in the frozen zone. In this model, continuous permafrost exists beneath the ice divide in the middle of the icesheet, and beneath the outermost margin of the icesheet, *if this is on land*. Between these two zones of freezing, and beneath sea areas and major rivers, is an extensive zone of melting. The melting rate rises to a maximum of 1–2cma^{-1} just before the permafrost zone that lies beneath, and beyond, the glacier snout. The maximum thickness of the outer continuous permafrost zone, at both maximum and intermediate glaciation, was modelled to be c. 100m. The permafrost thins farther forward of the glacier front and becomes discontinuous at a thickness of c. 50m. [Presumably, the lower limit of each of the permafrost zones would follow, in a subdued form, the topography of the land surface above]. Thus, although existing caves in the study area may have experienced permafrost conditions at various stages of glaciation, any cave passages lying farther than c. 100m from the surface would always contain water, even if surrounded by areas of ice and permafrost. However, section 5.3.7 shows that there are no passages in the study area this far from the surface.

Lauritzen (1996d and 1997) reported an example of a contemporary glacier at south Spitsbergen where almost all the drainage is into an underlying conduit karst. He suggested that the down-ice limit of capture is probably coincident with the transition between a temperate glacier base up-ice and the polar snout of the glacier. The melt-water at the base of the ice above the transition would produce a high hydrostatic pressure above the karst. For glaciation above the *sedimentary* aquifers south of the Baltic Sea, if all the glacial meltwater can be discharged by groundwater flow in these aquifers, as modelled by Forsberg (1996), no base tunnels or eskers form. Otherwise, excess meltwater flows along tunnels and eskers to be discharged at the glacial front. The groundwater remains stagnant beneath the frozen ice divide, with a low head, but at very high effective pressure. At the outer margin, groundwater heads exceed the overburden pressure beneath the permafrost. This can lead to the *hydrofacturing* of bedrock and a strong upward groundwater flow through local gaps in the permafrost, perhaps in areas of former proglacial lakes. The potential importance of these processes for karst development is discussed in section 63 and Chapter 8.

A3.5 Glacial erosion

From section 2.3, the Quaternary was a time of complex and repeated rapid advances and retreats of both whole icesheets and individual valley glaciers, with enormous surface erosion particularly during the deglaciation phases. The response to these glacial fluctuations was more pronounced on the steeper, western, side of the Scandinavian mountains than on the gently-sloping lee side, causing advances and retreats along the fjords. Off the north central Norway study area, the Skjoldryggen end moraine and sediments, which are over 500m thick at the Vøring Plateau (Figure 2.5), continue to, and flow over, the edge of the continental shelf, 250km west of the island of Vega (Andersen and Borns, 1997, Fig. 2–30). A proportion of the sediment presumably derives from *subglacial waterways* (section 8.1.7) that flowed in tunnels under the icesheets and glaciers during the various deglaciations.

Glasser (1995) modelled the effect of topography on the erosion of the Scottish icesheet along a W–E transect at the LGM. Noting that ice deformation rates and ice temperatures are mutually interactive, he distinguished between three basal temperature zones: basal melting, i.e. warm-based everywhere, close to 0°C; basal freezing, which is mainly cold-based but local pressure melting varies the temperature between 0 and -8°C; and cold basal freezing below -8°C, where melting does not occur. He showed that in the western mountainous centre of glaciation, basal melting was associated with thick ice and convergent flow along valleys, causing high erosion rates, and basal freezing occurred along ridges with thinner ice and less erosion. Ice streaming velocities in valleys could reach 225ma^{-1}, three times greater than on adjacent interfluves. Modification of the landscape decreased eastwards, and

high velocities and basal melting resulted in deposition of till rather than high erosion at the lowland eastern end of the transect. Gently undulating topography is characterised by restricted glacial erosion and / or deposition, where the main outline of the preglacial (c.f. 'paleic' in Scandinavia) landscape could survive. This description is similar to that of the effects of glaciation on the landscape in the main study area (section 2.3 and below). The concept of ice-streams along warm-based valleys was supported by Siegert and Bamber (2000), who suggested that enhanced velocities in Antarctica are facilitated by supplies of liquid water from subglacial lakes at the heads of these valleys.

According to Sugden (2000) there is still uncertainty regarding the effect of glacial erosion at passive margins. Cold-based glaciers (below the pressure melting point) can protect valley sides, as evidenced by 14Ma-old sediments still lying on the surface in the Dry Valley area of the Trans-Antarctic Mountains. At the other extreme, warm-based glaciations in NW Scotland have caused a fairly homogeneous areal erosion of 10–50m over the last 2.5Ma. In intermediate cases, localised selective linear erosion can occur with exploitation of existing river valleys deepened by ice to create fjords. Sugden stated that the oldest glaciations may have created the deepest landforms, with evidence of Miocene sediments at the base of some valleys in Antarctica. Thereafter, subsequent ice flows occupy the same glacial valleys. This reasoning was supported by Stuevold and Eldholm (1996), who noted that glacial erosion is probably greatest when eroding into material that is already weathered, as was the case with the Scandinavian paleic surface (section 2.2.1). The offshore sedimentation evidence from Henriksen and Vorren (1996; section 2.2.2), is that major valley deepening and the formation of U-shaped valleys and fjords started from about 3Ma. It seems likely, however, that the most significant deepening of glacial U-shaped valleys in the study area occurred after the Mid Pleistocene Revolution at 0.9Ma, when glacial advances became most extensive.

The overall geomorphological effect of the waxing and waning Plio–Pleistocene glaciations was to emphasise the topographical guidance by rock type and tectonic structure and to create glaciated valleys and over-deepened fjords in the mountains (e.g. Rudberg, 1992). Hebdon *et al.* (1997) also pointed out that during full ice cover, the greatest denudation occurred along valleys aligned with the direction of ice movement. Glacial scouring is commonly aligned with linear and near-vertical metasedimentary units that are commonly furrowed by longitudinal valleys between narrow structural ridges of folded schists, quartzites or metacarbonates, with trends that usually lie between N–S and NE–SW, although E–W glacial through valleys also exist and E–W glacial sculpting is seen at peaks that are over c. 1000m in altitude. Hence, despite the importance of the repeated glaciations over the last 2.8Ma, the topography of the study area remains guided by the Caledonide geology.

The nappe boundaries also continue to influence the study area landscape, with numerous examples being observed. These include the northern limit of the HNC, which is mostly along Ranafjord (gouged out to depths >500m); the three-way junction of the HNC, the RNC and the Køli Nappes under the 'Inland Sea' of Røssvatn that is c. 150km^2 in extent; and high mountain ranges along the sole thrust of the Uppermost Allochthon, where it overrides the Køli Nappes. These ranges form a N–S chain south of Røssvatn, with peaks up to 1700m (HNC / Køli; Photo 4.2), and form a W–E chain along the southern flanks of the Okstind range (RNC / Køli). In Sweden, the individual nappes of the Upper, Middle and Lower Allochthons commonly create a 'stepped' landscape. [The limestone escarpment scenery at Svartisen in northern Norway that is guided by gently dipping outcrops (Kirkland, 1958) is rare in the study area, where outcrops are usually much steeper].

The influence on the glacially-scoured high plateaux was much less marked, as the mean erosion across the *whole of Scandinavia* from all glaciations was interpreted to be only 16m by Peulvast (1985, p992), from data proved by Ruddiman (1977). Rudberg (1997, p198) calculated an average glacial lowering of the paleic surface of a c. 15000km^2 region in the *eastern* part of southern Norway to be c. 25m, a figure similar to one he cited from Helland for the glacially "lost rock" of Scandinavia. His calculation for the average thickness of the glacially lost rock layer at a region of similar size in the *western* part of southern Norway was c. 250m, i.e. ten times as much. From the geomorphological evidence, he deduced that periods with a lowering of the present altitude of glaciation by 500–800m were frequent and long-lasting. A lowering of 800m would fill most presently-empty cirques, fjords, through valleys and Swedish mountain valleys with ice. Lidmar-Bergström (1997) studied the denudation of the Precambrian

shield rocks since the Proterozoic and concluded that the amounts of erosion were 600m maximum during the Mesozoic and Tertiary and 200m maximum for channelled glacial erosion during the Pleistocene [and Pliocene?].

The entrenchment of U-shaped valleys by glaciation has been estimated both by direct methods, as presented in Table A3.1 (which makes a simplifying assumption that Cenozoic glaciations can be represented by ten major 100ka glacial cycles since the Mid Pleistocene Revolution: section 2.3.1) and by dating the earliest growth of stalagmites located in relict cave passages 'hanging' above valley floors, as presented in Table A3.2. The stalagmite date method provides maximum rates, by assuming that speleothem growth can only start after a valley floor has lowered below the level of the passage, as otherwise the passage would be flooded (Ford *et al.*, 1981). Minimum rates are also estimated by assuming that deposition commences within one 100ka glacial cycle. However, this minimum rate would still be too high if the passage formed above the level of its contemporary valley floor, so that it remained relict during subsequent interglacials, as considered likely in Chapters 6–10. The data in Tables A3.1 and A3.2 indicate that glacial valleys in the mountains of Norway, Scotland and Canada can deepen by as much as 60m during each complete glacial cycle (probably dependent on rock type and valley orientation relative to glacial movement) whilst at the same time, glacial erosion can be negligible in areas of low relief. These values are considered further in Chapter 7.

Table A3.1 Valley entrenchment rates, from direct methods

Place	Rate ($mmka^{-1}$)	Glac. Rate c	Max. or Min.	Method	Notes	Reference
All Scandinavia	16	1.6	Scand. mean	16m total mean removal		Peulvast (1985, p992) from data by Ruddiman (1977)
W. Norway	500–600	50–60	mean	YD moraine volumes		Larsen and Mangerud (1981), cited by Lauritzen (1986a)
Hammernesgrotta, N. Norway	240	24	actual	240m of total glacial erosion		Haugane and Grønlie (1988, Fig. 9)
Nordland, Norway	440–450	44–45	mean	Topographic volumes	a	Nesje *et al.* (1989), cited by Lauritzen (1990b)
Nordland, Norway	150–180	15–18	min	Off shore sediment	a	Nesje *et al.* (1989), cited by Lauritzen (1990b)
Norway	60–960 330	6–96 33	range mean	Present glacial erosion	b	Hallet *et al.* (1996, pp217, 220)
N. Sweden Precambrian Base.	>200	>20	max	>200m channelled glacial erosion		Lidmar-Bergström, 1997, p305

a Lauritzen (1990b) assessed mean Norwegian rates to be in the range 150–550$mmka^{-1}$ (i.e. c. 15–55m per glaciation).

b Glacial yields vary from 100–1300 $tonskm^{-2}a^{-1}$. Erosion is fastest beneath large valley glaciers with several tributaries, and can peak during years with large floods or discharges. Smaller yields are obtained from only partially covered basins.

c m per 100ka glacial cycle

A3.6 Holocene weathering

The limestone weathering results (Appendix A2.6) can be compared with the commonly much lower weathering rates measured by André (1996; 1997; 2002) in various rocks exposed to the atmosphere in Scandinavia and in polar environments (Table A3.3). Holocene micro-weathering is consistently weak compared to the effect of glacial lowering. André (1996) concluded that, during the Holocene, azonal chemical and biological processes dominate over "periglacial" processes. André (1997) discussed the Holocene rate of rockwall retreat at Spitsbergen. She found that three processes combine to give mean triple-rates of erosion: biogenic flaking; frost shattering; and postglacial stress relaxation. Postglacial stress relaxation dominated over freeze-thaw processes, as evidenced by deep and widely-opened joints (up to 1.2m), which run parallel to cliff faces and to the former ice flow direction. She also noted that the present surface lowering rate of granite in northern Scandinavia is only $1mmka^{-1}$, but in stratified and / or densely-fissured dolomitic limestone in Finland and Canada, the total Holocene cliff recession rate can exceed 10m, i.e. $1000mmka^{-1}$. However, average Holocene rockwall retreat rates are usually much higher than present rates, indicating an intermittent process. This was supported by lichenometric evidence.

Table A3.2 Valley entrenchment rates, from stalagmite growth above the valley floor

Place	Dewater Age range (ka)	Hang (m)	Rate (mm ka^{-1})	Glac. Rate c	Max. or Min.	Notes	Reference
Grønndalsgrotta (ZA)	148	50	340	34	max		Lauritzen and Gascoyne (1980)
	248	50	200	20	min?		
Greftkjelen, N. Norway	A: 190	205	1080	108	max		Holbye and Lauritzen (1983)
	290	205	700	70	min?		
	B: 179	80	450	45	max		
	279	80	290	29	min?		
Sirijordgrotta (Z4)	128	40	310	31	max		Valen *et al.* (1997)
	228	40	180	18	min?		
Bearjaw Cave, Deadman Pass, Canada	>350	45	<130	<13	max	a	Ford *et al.* (1981)
	>450	45	<100	<10	min?		
	<690	45	>65	>6.5	max		
	<790	45	>60	>6	min?		
Eagle Cave, Crowsnest Pass, Canada	>690	90	130	13	max	a	Ford *et al.* (1981)
	>790	90	110	11	min?		
	<1000	90	90	9	max		
	<1100	90	80	8	min?		
Castleguard Cave, Canada	>690	365	530	53	max	a	Ford *et al.* (1981)
	>790	365	460	46	min?		
Uamh an Claonaite, Assynt, Scotland	>192	205	680	68	max	b	Hebdon *et al.* (1997)
Uamh an Claonaite, Assynt, Scotland	>192	140	470	47	min	b	Hebdon *et al.* (1997)

a In carbonate bedrock in the Rocky Mountains. Stalagmite dates were beyond the U-series range, but constrained by palaeomagnetic and U-isotope ratio constraints. The paper pointed out that a limestone massif with 1000m of relief will be eroded away within 10Ma, if the denudation rate is 100mmka^{-1}.

b Also uses geochronological arguments. Calculations are based on three glacialcycles (300ka). However, four or five glacial cycles may be appropriate instead.

c m per 100ka glacial cycle

Table A3.3 Holocene bedrock weathering rates

Place	Rate (mmka^{-1})	Method	Rock type	Notes	Reference
N. Sweden	0.1–2.0		Amphibolite	a	André (1996)
N. Sweden	0.1–0.7		Quartzophyllite and quartzite	a	André (1996)
N. Sweden	0.2–2.0		Phyllite	a	André (1996)
N. Sweden	1.4–13.7		Dolomite	a	André (1996)
Norway	0.2–1.0		Granite	Earlier study	André (1996)
Spitsbergen	mean 2.8		Marble	Earlier study	André (1996)
Canada	mean 3.3		Limestone	Earlier study	André (1996)
Spitsbergen	mean 2.5		Dolomitic limestone	Earlier study	André (1996)
Spitsbergen	2	Biogenic flaking	Rockwall retreat: Amphibolite		André (1997)
Spitsbergen	70	Frost shattering	Rockwall retreat: Amphibolite		André (1997)
Spitsbergen	160	Frost shattering	Rockwall retreat: Quartzite		André (1997)
Spitsbergen	700	Stress relaxation	Rockwall retreat: Quartzite		André (1997)
N. Sweden	mean 0.2	Proud veins	Homogeneous crystalline		André (2002)
N. Sweden	mean 1	Proud veins	Biotite-rich crystalline		André (2002)
N. Sweden	mean 5	Proud veins	Carbonate sedimentary		André (2002)

a At two study areas that have a contemporary precipitation of 800mma^{-1}, at altitudes of 500m and 1000m, with mean annual temperatures of -1.5°C and -5°C. The rates show postglacial surface lowering.

APPENDIX A4 PRESENT CONDITIONS

This Appendix considers study area characteristics and features that apply at present.

A4.1 Climate

The contemporary climate is dominated by the variable extremes of temperature experienced during the annual cycle. Winter temperatures of -40°C are not uncommon from December to February, especially when still cold air sinks into the valleys. The inland annual average was around -5°C in 1925 (Corbel, 1957, p211). The winter diurnal variation is relatively low, because of the prolonged absence of sunlight. Snow cover builds up across the whole area during winter, reaching a maximum thickness in April everywhere, and can reach tens of metres thickness in the mountains. Corbel presented information (Table A4.1) that showed that the winter becomes more severe moving from south to north across the study area, and at increasing elevation. The highest snowfalls occur some 30km inland from the coast, with a general and gradual decrease towards the east.

Table A4.1 Annual snowfall and precipitation in 1925 (from Corbel, 1957)

Place	Position relative to study area	Altitude (m)	Days of snowfall	Days of snow cover	April snow thickness (m)	Total precipitation (m)
Bessaker	Coast, 30km S.	12	92	103		
Malm	50km inland, 40km S.	250	102	188	0.9	2.5
Hattfjelldal	Central	250	108	210	1.2	2.0
Hattfjelldal	Central	380			2.0	
Grønli	Central, 20km N.	250	121	240	2.3	1.7

Hence, the winter weather is cold, with temperatures rarely above 0°C. The rivers freeze over, and many higher cave entrances are buried under blankets of snow and ice. Within those caves that can be entered, water levels remain at very low stage. Sumps recede back along their containing passages and may even become passable by crawling along frozen surfaces. Elsewhere, ice formations grow and can block open passages, depending on local cave meteorological conditions (e.g. Photo: Endpiece). Because 1925 was near the end of the Little Ice Age, the climate has become warmer since then (section 2.4.5). In particular, the winters were much milder in the late-1990s.

The onset of the spring melt is variable, but commonly starts in May or June, when the temperature rises considerably. Most of the accumulated low-lying and mountain snow melts, and is transported to the sea via swollen mountain streams and valley rivers. The spring melt normally lasts for about one month at very high flow and accounts for a high proportion of the annual discharges. In the areas of stripe karst, some of this water flows underground for short distances with high erosive power. The remnant snow patches left in dolines usually melt, with the water draining away underground. Mountain streams reduce in size or cease completely when the snow fields in their catchment areas disappear. Larger snow fields (and glaciers) may persist all summer, in which case the stream flow is very variable, depending on the height and strength of the sun, and follows a diurnal pattern. In a cool summer, some snow fields may survive until the following winter. Similarly, at high altitudes, cave entrances may remain blocked by snow. However, it is unusual for known caves to be blocked for more than one summer at a time. Once the snow has gone, mountain flora recover quickly and come into bloom and into fruit.

The temperature in the short spring, summer and autumn seasons is very variable, as is the rainfall. The weather may remain unchanged for several weeks, or may change almost daily. An extreme example was experienced in 1997. After a winter with only light snowfalls, perhaps the largest snowfall for 100 years occurred in late May. The snow built up in the mountains to depths of 10–30m, and snow covered the ground beside all the roads. Conditions changed on 1 June and the daytime temperature rose to 15–20°C, accompanied by an enormous spring melt. For the whole of June and July, it only rained on 5 days, and temperatures occasionally peaked at 34°C. Despite this, temporary snowfields persisted at altitudes over 500m, and there was almost complete snow cover above 1000m for

these two months. Sometimes mist rising from a snowfield indicated that the snow was ablating directly into the atmosphere from its top surface, as well as melting as run off. However, July temperatures from 10–13°C in the main valleys are more usual.

During periods of heavy summer rain, rivers and mountain streams can rise in a few hours and become impassable. Hence, it is necessary to check the size of catchment areas before crossing rivers or entering stream caves if there is any possibility of rain. Very large spring and summer floods clearly occur quite frequently, because it is not uncommon for roads to be damaged, and sediments in karst caves can be moved dramatically. The autumn can be a time of dry conditions as temperatures drop, often to below 0°C in the valleys by September. With lower stream flows after the disappearance of the mountain snow, cave waters approach low stage before the onset of complete freezing in late autumn and winter.

Corbel (1957) also presented monthly precipitation charts for seven places in the central and southern parts of the study area. These showed a very consistent pattern in 1925 of high snow fall in January, reducing to the lowest precipitation rates in April and May. Rainfall then increased from June to September, when, presumably, combinations of rain and snow continued at about the January rate until November. December had a somewhat lower precipitation in most places. Going from west to east, annual precipitation varied from 1.0m at Brønnøysund on the coast, via 2.3m at Strompdal some 30km inland, to 0.8m at Leipikvattnet, just inside Sweden. Helldén (1973) gave 0.7m (averaged from 1965–1972) at Hemavan, at an altitude of 450m in the NE, Swedish, part of the study area, where the mean annual temperature is -0.4°C, and the temperature falls 0.6°C for each 100m of altitude (Earl-Goulet *et al.*, 1998). In his study of nearby **Sotsbäcksgrottan** (KU), Helldén (1973) remarked that only five months of the year are frost-free at the cave's altitude of 750m, but there is no permafrost. A minimal underground drainage continues throughout the winter. Lauritzen (1996c) gave the present annual mean temperature at Mo i Rana as 3.5°C. Table A4.2 gives the mean monthly temperatures, precipitation and length of day for the coastal towns of Bodø and Trondheim, which are 120km north and 120km south of the study area.

Table A4.2 **Monthly temperature, precipitation and length of day**
(from the Norwegian Tourist Board, 1992, averaged from 1961–1990).

Month	Bodø tempr. (°C)	Trondheim tempr. (°C)	Bodø precip. (mm)	Trondheim precip. (mm)	Trondheim daylight (h,m)
January	-2.2	-3.1	86	87	4h44
February	-2.2	-2.4	64	70	7h13
March	-0.6	-0.5	68	68	10h15
April	2.5	3.9	52	60	13h32
May	7.2	9.4	46	50	16h43
June	10.4	12.6	54	66	19h44
July	12.5	13.9	92	85	20h21
August	12.3	13.4	88	86	17h43
September	9.0	9.8	123	133	14h29
October	5.3	6.0	147	131	11h22
November	1.2	0.8	100	99	8h08
December	-0.3	-1.6	100	113	5h20
Annual	5 °C	5 °C	1.0m	1.0m	

The values and trends in the above data may not be representative for inland areas. For comparison (from Whitaker's Almanac, 1993, p1193), in England / Wales and in Scotland annual mean temperatures are 10°C and 9°C (both averaged from 1951–1980) and annual rainfalls are 0.9m and 1.4m (both averaged from 1941–1970).

The mean annual rate of evaporation in the study area is estimated at c. 300mma^{-1}, from the temperatures and information presented in Table A4.2 and by Ward and Robinson (1990, p110). Helldén (1973) cited Ångström (1958) who presented Tamm's formula: Evaporation (mma^{-1}) = 221 + 30 x Mean Annual Temperature in °C. On this basis, the annual evaporation at Mo i Rana is 326 mm. Øvstedal (1991) studied the hydrological and hydrochemical

properties of the Sirijord karst aquifer (Z4). Using data loggers, he recorded the hourly air temperature at the main rising for **Sirijordgrotta** (Z4) from July 1988 until October 1989. This showed summer fluctuations from 1–25°C, with typical swings of about 12°C in any 24-hour period. By the end of November 1988, the temperature had drifted down to -28°C, with the fluctuation wavelength commonly being several days rather than 24 hours. The temperature commonly varied between 0°C and -20°C from December 1988 until the end of March 1989.

A4.2 Caves and modern glaciers

At present, neither mapped carbonate outcrops nor known karst caves pass beneath the (commonly small) modern glaciers in the study area. Thus, it is likely that all the karst systems were free of permanent ice cover for at least 2500a. There is no permafrost in the study area, except at an isolated site in the Okstind mountains (Griffey and Worsley, 1978). A few caves receive recharge from small glaciers and perennial snow fields (section D.6.3).

A4.3 Farming and forestry

Within the study area, the main effects of habitation and industry have been small scale farming and logging, even in remote areas and in valleys up to altitudes of several hundred metres. Local communications used to rely on the railway and various types of watercraft along the Norwegian coast and across fjords and lakes. Horses were used along tracks through the forest. The tendency since the 1950s was for the more isolated farms to be abandoned, whilst at the same time modern roads and tracks cut by the state timber company increased public and industrial access to the forested areas. Logging is an industry that was successfully exploited in the area for at least 250 years, following its development by an English company in about 1750. Thus, some of the karst areas lie under stripped forest, and cave entrances may sporadically be blocked by logs and branches. Rapid changes can be caused by just one employee operating modern machinery. Due to farming and forestry, much of the primary forest has been replaced by younger conifers, as evidenced by the larger diameters of the stumps of the old felled trees. Close to farms, cave entrances are sometimes used as places for refuse.

A4.4 Hydroelectric schemes

Many major lakes in the area are dammed for hydroelectric power. The raising of water levels potentially inundates dry cave passages, and this may have happened at one small cave beside Stor Akersvatn (ZC). The outlet from Røssvatn (ZA) is dammed and the water flows into Tustervatn, from where its flow is controlled by electricity authorities in Korgen. In normal conditions, most of the outflow is along a tunnel of 150m^3s^{-1} capacity that was built in c. 1960. In 1997, the overflow discharge along the continuing Røssåga valley was crudely estimated by the author to be 50m^3s^{-1} at the height of the spring melt, from a total catchment area of some 1700km^2. All this water flowed powerfully into a sumped passage, where several jammed logs indicate the strength of the spring melt prior to the construction of the hydroelectric tunnel. The sump heads the mainly phreatic **Røssågagrotta** (ZA; Photos 7.6 and 7.7). This has a passage size in excess of 10m diameter, and resurges at the side of the continuing dry valley. [It is essential to enquire about plans for opening sluice gates before entering caves situated downstream of such hydroelectric schemes]. Assuming an annual precipitation of 1.5m and evaporation of 0.3m, then the *mean* flow rate along the upper Røssåga used to be 57m^3s^{-1}, prior to the construction of the tunnel, when the cave would have taken the normal flow. During floods, water would have also flowed partly on the surface, bypassing this oxbow-type conduit (and others lower down the valley). This passage must represent the highest mean and maximum flow rates for any karst system in Norway. For comparison, the catchment areas for Plurdal and Glomdal in northern Norway are ~80 and ~50km^2.

A4.5 Quarries, mines and tourist caves

Several marble quarries exist in the Norwegian part of the study area, in outcrops of both calcitic and dolomitic metacarbonates. A quarry at Hegge in Velfjord (Z2) de-roofed a short karst cave (S-E Lauritzen, University of Bergen, pers. comm., 1998). Planning permission was sought in 1998 for two new marble quarries at Velfjord that may be close to some undocumented caves and karst features. There are both working and abandoned metal mines, but none are known to be associated with karst caves. There are no local show caves, but 'adventure caving' trips may be arranged with local guides at **Etasjegrotta** (Z4), **Øyfjellgrotta** (Z5), **Kvannlihola** (Z7) and **Korallgrottan** (KL). Norway's only show cave, **Grønligrotta**, is situated near Mo i Rana, just north of the study area.

A4.6 Strandflat

The long strandflat along the Norwegian coastline was studied by Holtedahl (1998), who divided it into three types. Part of the strandflat in Helgeland is characterised as a 50km-wide horizontal shelf with a slope close to zero (Rudberg, 1997, p192; Photo B1.1). It is situated mainly below 20m altitude (approximately 50% being below sea level), with a steep back wall rising to c. 100m, which is also the Late Weichselian marine limit during the maximum isostatic depression. Holtedahl concluded that the Helgeland strandflat must be very mature and therefore developed during times of crustal stability (after the Tertiary uplift), i.e. it developed by glacial and marine erosion coupled with frost-shattering during the interglacials and interstadials of the Plio–Pleistocene. [This author conjectures that, because the elevation of the strandflat above sea level typically occurred only in the last 4ka, its emergence during the long and climatically stable Holocene period, with its uninterrupted isostatic uplift and relatively low sea levels, is *not* typical of earlier interstadials and interglacials, and may indeed be unique. For example, the shorter, warmer, Eemian interglacial period had a eustatic sea level maximum higher than at present (section 2.3.2)].

A4.7 Sea caves

The large sea caves found along the Atlantic coast of the study area were summarised by St.Pierre and St.Pierre (1986, p76). Their heights were studied by Sjöberg (1988), among others. He showed that the altitude of the sea caves follows a linearly increasing trend from south to north which reaches a maximum at the Helgeland coast and then declines linearly farther north. He concluded that this follows a bulge in the postglacial isostatic and neotectonic uplift. However, with the straight and parallel isobase lines now presented by Sørensen *et al.* (1987), this trend seems instead merely to demonstrate the indentation of the central Norwegian coastline (e.g. Figures 1.1 and 2.5). A possible formation process for these caves is presented in section 8.8.

A4.8 Jettegryter: 'Giant Pots'

Jettegryter are rock-mills drilled by large boulders that were swirled around by huge deglacial outflows. They can occur in any rock type, and although there are many in the study area, the only ones known in metalimestone form a group of 20–30 near Stabbfors (ZA). The largest is 12.5m deep with a diameter of 6m (Photo A4.1). No karst caves are associated with these features, but some have captured recent drainage, and some display tectonic movements (section 6.3.3; Table D1.1).

Photo A4.1 Jettegryten near Stabbfors (ZA)
This is a 12.5m-deep non-karstic shaft in metalimestone. It displays neotectonic movement (arrowed) that post-dates its formation during the Weichselian deglaciation of the Røssvatn catchment area.

APPENDIX A5 DATING OF SCANDINAVIAN CAVE SEDIMENTS

This Appendix reviews the work done on dating Scandinavian cave sediments (summarised in Table A5.1) and the deductions made about their cave development histories. Caves in the study area are identifiable by the use of the zone code. The mineralogy of Norwegian cave sediments, particularly authogenic precipitates, was reported by Onac (1995), Onac and Ghergari (1993) and Onac and Lauritzen (1995). The presence of extensive moonmilk deposits was attributed to a present favourable very cold and wet underground microclimate.

A5.1 Radio-carbon dating

The first report of organic deposits was by Hoel (1906), who found marine shells in caves at Aunhatten (Z2). He identified many *Pomatoceros tricuspis and Saxicava pholadis* (a bivalve borer) and one example of *Balanus creratus* in **Aunhattenhullet 2**, at an altitude of 116m. Hoel also found many *Saxicava pholadis* and a fragment of *Pomatoceros tricuspis* in **Aunhattenhullet 3**, at an altitude of 132m. Although these shells were not dated, they presumably lived at the earliest part of the Holocene, when the area was deglaciated at sea level, before isostatic rebound raised the caves to their present levels (section 2.4.6). No remaining evidence of these marine shells was found by this author during the 1998 field trip. However, barnacle shells attached to passage walls, unconsolidated marine shell floor deposits, elk bone and organic sediments in **Neptune's Cave** (Z2, only 13km from Aunhatten), were radiocarbon-dated by Beta Analytic, Miami, as part of this project (Appendix D5.3). The YD age of the barnacles shows that the relict parts of this cave were in existence before this time.

Engh (1980) reported the ^{14}C date of *flowstone* in **Labyrintgrottan** (ZC) to show that the cave pre-dates an age of 18–19ka, and has remained undisturbed since, suggesting an interstadial origin at least. [This date now appears unreliable from the evidence of continuing glacial cover until c. 10100 given in Appendix D2.4]. Lauritzen (1985) reported the ^{14}C dating of brown bear bones from **Revhølet** (ZA), among other animal bone datings from Norway.

Skjonghelleren, a non-carbonate littoral cave in southern Norway, was reported by Larsen *et al.* (1987) and by Larsen and Mangerud (1989) to have formed probably in an early Weichselian period, after taking radiocarbon dates on bone samples from its 15–20m-thick pre-Holocene subglacial sediments. These have three laminated fine-grained deposits, alternating with blocky sediments. The glaciolacustrine clays and silts were correlated with three stadials of full ice cover, dated by their palaeomagnetic properties (Larsen *et al.*, 1987). The blocky beds represent four ice-free interstadials. Other bone fragments from higher layers gave younger dates. U-series dating of speleothems clustered around 30ka at the end of the Ålesund Interstadial; the oldest dated at 80±9ka, proving the cave's existence early in the Weichselian. Correlated sequences were also dated in two nearby coastal caves, **Olahula** and **Hamnsundhelleren** (Valen *et al.*, 1995; 1996). The latter paper considered four depositional phases for glacier-overridden marine abrasion caves: a) ice-free; b) shallow, subaerial, ice-dammed lake, formed during the *onset* of glaciation; c) subglacial lake; d) ice-plugged.

About 10000 ^{14}C-dated bone fragments and skeletons in the pitfall Elk Shaft of **Sirijordgrotta** (Z4) lie in a stratigraphy covering the last 7ka (Table A5.1). Lauritzen and Lauritsen (1995), Lauritzen *et al.* (1996), Lauritsen and Lauritzen (1996) and Nese and Lauritzen (1996) discussed Quaternary cave and landform development at the Kjøpsvik quarries near Tysfjord, northern Norway, where **Norcemgrotta** is the palaeospring for **Storsteinhola**. **Norcemgrotta** displays three or four depositional cycles, the second youngest being at 70ka. Faunal assemblages from one of the sediment horizons fall into two climatically incompatible groups. These are cold fauna (including polar bear, *Ursus maritimus*), suggestive of open-sea contact with a glacier front, and warm fauna (including field mouse), suggestive of a temperate vegetation with grass and trees. ^{14}C dating of these bones at 39–42ka was assumed to be incorrect, because they are overlain by a calcareous concretion dated by U-series techniques to 70±8.5ka. This layer also gave an almost vertical palaeomagnetic direction, which perhaps represents the onset or termination of a palaeomagnetic excursion, such as is thought to have occurred at 70–76ka and at the Blake event at c. 105ka (or 117ka: Valen *et al.*, 1997, p233). The association of the two faunal groups could be explained by either climatic change during deposition, or by a subsequent mixing in the cave, which is compatible with the mass-movement character of the host sediment. The horizon also contained fragments of marine, littoral, invertebrates. A single bear bone from a gravel layer 3m above gave the unlikely ^{14}C LGM date of 20.1±0.3ka.

A5.2 Palaeomagnetic dating

The use of the palaeomagnetic dating method was attempted at several other karst caves. Noel and St.Pierre (1984) found that the magnetic record for clay sediments in **Jordbrugrotta**, northern Norway, was too short to reveal evidence of geomagnetic secular variation. At **Grønligrotta**, they correlated clay sediment with a Swiss lake sediment core, and suggested an age of 9600–6800a. The same sediment bank was tested again by Løvlie *et al.* (1988). Their correlation with the British geomagnetic secular record gave an accumulation period of 9500–8900a, restricting the deposition to ice contact conditions, rather than extending into the subsequent temperate period when the cave would be drained, but would carry an active stream. S St.Pierre (1988) also discussed the morphology and sediments of the **Grønligrotta / Setergrotta** system. A study of clay sediment laminates in **Rågge Javre Raige** at Hellemofjord in northern Norway suggested that deposition took place either from 10.9–10.2ka, or during several subglacial events (Løvlie *et al.*, 1995). The first alternative is within the local final Weichselian glacial retreat from 10.9–9.8ka.

Løvlie and Lauritzen (1996) reported briefly on attempts to correlate palaeomagnetic results from 10 caves in northern Norway, which they assumed were exposed to comparable climatic and depositional histories. Reliable signals were found in four of the caves, which were correlated in fairly great detail, suggesting synchronous sediment accumulations under complete ice cover from LGM2 to the YD. They noted that the thickness of sediment appeared to be proportional to the height above present sea level, but the duration of deposition showed no systematic relationship to altitude.

A5.3 U-series dating

The first definite evidence for a pre-Weichselian karst cave in the study area was provided by Lauritzen and Gascoyne (1980), who dated a flowstone from **Grønndalsgrotta** (ZA) using U-series methods. Between 1980 and 1983, some 44 Norwegian speleothems were dated in this way (Lauritzen, 1984c). The dates tend to cluster into four groups. Because these periods do not always correspond to ice-free surface conditions, they were called *speleothem chronozones*. The probable number of speleothem chronozones was later expanded to ten, dating back to c. 600ka, from a sample of 100 speleothems (Lauritzen, 1991a), and from these data Lauritzen (1993, p29) gave a probability curve for speleothem growth back to 300ka, with a maximum value in the Eemian.

Lauritzen (1995) constructed a palaeo temperature proxy record for the last interglacial from the dating and analysis of speleothems from **Okshola** and **Stordalsgrotta** in northern Norway. He proposed that speleothem growth rate is a proxy parameter for climatic mildness, and that growth can only occur during the absence of full stadial conditions, when caves become flooded, or percolation water freezes. It was observed by comparison between the two caves that speleothem growth was delayed and restricted at higher altitudes, where cold conditions may have persisted longer. Although the **Okshola** Speleothem Chronozone lasted from 150–80ka, optimum growth occurred during the Eemian, from 128–114ka. The paper also noted the general rarity of Norwegian speleothems dating from the mid-Weichselian interval. (This thesis notes the paucity of speleothems in the study area: Appendix B2.9). [From studies of the many actively-growing speleothems in Castleguard Cave, Canada, which is situated beneath the Columbia Ice Field, Atkinson (1983) showed that speleothems can grow without biogenic CO_2, if common-ion effects or incongruent dissolution of dolomite occur. This can apply in mixed gypsum / limestone or limestone / dolomite terrains, and in carbonates with abundant pyrite. Gascoyne and Nelson (1983) proposed, as an alternative mechanism, that the CO_2 source in the groundwater was derived from the oxidation of inactive carbonaceous substances in the bedrock overlying the cave]. An Eemian stalagmite from **Søylegrotta**, near Mo i Rana, was reported by Berstad *et al.* (1997) and another stalagmite from the same cave revealed four interglacial growth periods from c. 630–320ka (Berstad *et al.*, 2002).

Linge *et al.* (2001c) reported dating of another stalagmite from **Hammernesgrotta**, which grew at a fast and constant rate of 1mm every 22a from 123.35–119.5ka. This shows that conditions were highly favourable for speleothem deposition during the late Eemian, when measured $\delta^{18}O$ and $\delta^{13}C$ values and ranges were similar to those of the Holocene, agreeing with the above result from **Okshola**. The growth rate reduced to 1mm every 1475a from 119.5–107.7ka, and to 1mm every 13760a from 107.7–73.3ka (OIS4), after which deposition ceased.

Table A5.1 Dating of Scandinavian cave sediments

Cave	Area	Sediment type	Date	Reference
Radiocarbon dating method (Ages in ^{14}Ca BP)				
Norcemgrotta	N. Norway	bone bear bone	>42–39ka 20.1±0.3ka	Lauritzen *et al.* (1996) Nese and Lauritzen (1996)
Labyrintgrottan	ZC(Sweden)	flowstone	18.2–19.2±0.2ka	Engh (1980)
Revhølet	ZA	bear bone	4420±70	Lauritzen (1985)
Sirijordgrotta, Elk Shaft	Z4	bone	7.3±0.9ka to present	Lauritzen (1991b) Valen *et al.* (1997, p243)
Neptune's Cave	Z2	barnacle shell mollusc shell elk bone organic material	10280±90–380±20* 10010±80–400±20* 5100±70 1780±70	This thesis (unconsolidated) *assumed local reservoir age (unconsolidated)
Skjonghelleren	W. Norway (non-carbonate coastal cave)	bone bone bone bone	32.8±0.8ka 29.6±0.8ka 11.5±0.2ka 10.4±0.2ka	Larsen *et al.* (1987) Larsen and Mangerud (1989)
Hamnsundhelleren	W. Norway	bone bone	32–28ka c. 24.5ka and 9.9±0.1ka	Valen *et al.* (1996)
Palaeomagnetic dating method				
Jordbrugrotta	N. Norway	clay	None	Noel and St.Pierre (1984)
Grønligrotta	N. Norway	clay	9600–6800a	Noel and St.Pierre (1984)
Grønligrotta	N. Norway	same clay	9500–8900a	Løvlie *et al.* (1988)
Rågge Javre Raige	N. Norway	clay	10.9–10.2ka or earlier	Løvlie *et al.* (1995)
4 caves	N. Norway	clays to sands	16/15.5–11.5/10.5ka	Løvlie and Lauritzen (1996)
Norcemgrotta	N. Norway	bone layer	76–70ka	Lauritzen *et al.* (1996)
Sirijordgrotta	Z4	Clay deglacial	Lake Mungo 10.4ka	Valen *et al.* (1997, p249)
Skjonghelleren	W. Norway	clay and silt silt clay	Laschamp (c. 42–36ka) Ålesund onset (c. 33ka) Lake Mungo (c. 30–28ka)	Larsen *et al.* (1987) Larsen and Mangerud (1989)
Olahula Hamnsundhelleren	W. Norway	clay clay	Laschamp Lake Mungo	Valen *et al.* (1995) Valen *et al.* (1996)
U-series dating method				
Greftkjelen	N. Norway	stalagmite	190.2 and 178.8 ± 15ka	Holbye and Lauritzen (1983)
Unspecified	N. Norway	44 speleothems / mollusc shells / vertebrate teeth	800–350ka 200–170ka 130–90ka, 12–0ka	"4 speleothem chronozones" Lauritzen (1984c)
15 caves	N. Norway	100 speleothems	10 chronozones	Lauritzen (1991a; 1993)
Lapphullet	N. Norway	stalagmite	730–350ka	Lauritzen (1986a) Lauritzen *et al.* (1990)
Hammernesgrotta	N. Norway	corroded stalagmite stalagmite	500–21ka 123350–73300a	Lauritzen (1990b) Lauritzen *et al.* (1994) Linge *et al.* (2001c)
Norcemgrotta	N. Norway	calcareous concretions	70±8.5ka	Lauritzen *et al.* (1996) Nese and Lauritzen (1996)
Ockshola Stordalsgrotta	N. Norway N. Norway	flowstone flowstone	145±5–81±4ka 111±10–6.0±0.7ka	Lauritzen (1995)
Søylegrotta	N. Norway	stalagmite	10.41±0.0–0.253±0.002ka	Lauritzen (1996c) Lauritzen and Lundberg (1999)
Søylegrotta	N. Norway	stalagmite	>350ka 144–114ka	Berstad *et al.* (1997)
Søylegrotta	N. Norway	stalagmite	OIS15, 13, 11, 9 (c. 630, 470, 390, 320ka)	Berstad *et al.* (2002)
Grønndalsgrotta	ZA	flowstone	148+23/-20–91+7/-6ka	Lauritzen and Gascoyne (1980)
Sirijordgrotta	Z4	speleothem	128±5ka	Valen *et al.* (1997, p241)
Korallgrottan	KL(Sweden)	speleothem	148–127ka	Sundqvist (2002)
Skjonghelleren	W. Norway	speleothem	80.1±8.7–8.5±0.2ka	Larsen *et al.* (1987)

Caves are grouped under Northern, Central and Southern Scandinavian areas for each dating method

A5.4 Holocene dates

The ^{14}C dating of bone and shell and the use of the palaeomagnetic dating method has resulted in YD or Holocene ages for several faunal deposits, indicating entries into caves after Weichselian deglaciation.

Many speleothems have yielded Holocene dates from U-series dating methods, but these are generally *not* included in Table A5.1. Lauritzen (1996c) sampled a single large (32cm) stalagmite from **Søylegrotta** every 1mm to derive the temperature every 25–30a, from the $\delta^{18}O$ signal. From this information, he derived a smoothed curve from 180–8500a. The shape of the curve is in good agreement with a Holocene temperature curve for south Norway, which was derived from the palynological, botanical and glaciological data of other workers. Lauritzen and Lundberg (1999) revised this curve to produce an absolute temperature record for the Holocene in northern Norway that is in good agreement with a Greenland ice core. Lauritzen *et al.* (1986) showed that brown-to-black banding in speleothems from northern America may contain 2000ppm of organic material derived from humic and fulvic acid from overlying soils, rather than indicate the presence of iron. Linge *et al.* (2001a) demonstrated that $\delta^{18}O$ and $\delta^{13}C$ stalagmite records reflect the local cave microclimate, and are significant, but complex, proxies of the external palaeoclimate. Linge *et al.* (2001b) suggested that the main bands of luminescent organic matter in a Holocene speleothem from **Larshullet** (c. 20km north of the study area) were deposited by soil-flushing during spring snow melts and that the less intense subannual laminae result from heavy autumn rainstorms, so that there is a strong relation between summer soil-zone conditions and stalagmite growth rate.

Within the study area, Holocene dates were obtained from **Sirijordgrotta** (Z4; Lauritzen and St.Pierre, 1982; Valen *et al.*, 1997) and **Korallgrottan** (KL; Sundqvist, 2002). The age of a stalagmitic cap from **Neptune's Cave** (Z2) was indeterminate, but probably of Holocene age (S-E Lauritzen, University of Bergen, pers. comm., 1998).

APPENDIX B1 CAVES IN EACH ZONE

Chapter 4 discussed the database constructed to record the zonal attributes of the carbonate outcrops and Chapter 5 discusses the two cave databases. The purpose of this Appendix is to introduce each zone by describing the longer caves in their local geological context. Some caves in Z2–Z4 provide examples of the various cave development models proposed in this thesis (Appendix D5).

B1.1 HNC Zone 1: The Coastal Area

The HNC and RNC in the Uppermost Allochthon comprise rocks with medium to high metamorphic grades: mainly amphibolite facies, with some being only to greenschist facies locally, and some being altered further by contact metamorphism (e.g. Thorsnes and Løseth, 1991). The coastal area was delineated to cover the low-lying coastal islands, the strandflat and some of the immediate hinterland. The Outcrops Database records 41 carbonate outcrops, with an average maximum altitude of only 27m. Only four very short caves are documented, near the football pitch at the port of Brønnøysund. Three of these appear to have been formed by wave action, but one is a short truncated phreatic tube. Non-carbonate, raised-beach, littoral caves occur at least at seven places along the coast, some being very large. Their altitudes and sizes are indicative of the extent of Quaternary isostasy (section 8.8). A surprising feature of the zone is the mapping of some 160 Quaternary karst features in the area of Tjøtta alone. These are primarily on many tiny islands of low-lying limestone. Two larger limestone islands, S. Herøya and Tenna, were visited on 11 August 2000, when several shallow karst depressions were seen. Additionally, there are several good examples of Size Groups 3 and 4 bowl karren (Holbye (1989; section 4.4) near a brackish-water tarn on Tenna that overlooks the sound Tennsundet (Photo B1.1).

Photo B1.1 Bowl karren and Seven Sisters
Karren, perhaps formed by the sea, in stripe karst on the strandflat at the island of Tenna (Z1). Compass for scale. U-shaped glacial valleys between the Seven Sisters in the background.

B1.2 HNC Zone 2: The Fjord Area: Svartdalgrotta and Neptune's Cave

Svartdalgrotta (Figure B1.1) is the longest cave in Z2 at 899m. The upper entrance is at an altitude of 180m. The cave has a depth of 53m (Newton, 1999), but is atypical for the zone, because it lies within the contact metamorphism aureole of a large pluton of diorite, monzonite and monzodiorite. This has caused the limestone to lose any former steep, striped, foliation so that the foliation dip is only 25°N. The survey and section show that large passages occur mainly at two levels, with down-dip trends. These passages are connected via large shafts and steep ramp-tubes that are probably formed on orthogonal joints. With a catchment area of c. 0.7 km^2, a large stream flows through the lower levels of the cave in summer. Along the cliffs above Svartvatn and only some 400m east of **Svartdalgrotta** is **Neptune's Cave** (Figure B1.2; Appendix D5.3), where marine shells were collected at an altitude of about 120m (Appendix A5.1). These two caves were flooded by the sea to an altitude of c. 150m at about 10250a BP, during the Younger Dryas (Appendix D2.3). The lowest part of **Svartdalgrotta** emerged from the sea some 500a later, and the chamber inside the lower entrance appears to be enlarged by marine activity. The main stream passage grades towards the lower entrance at an altitude of c.140m and the main flow must have left the cave via a

tidal sump, prior to emergence. The present stream exit route through impassable fissures is a recent capture. No marine deposits remain in Svartdalgrotta because the large active stream would remove ancient deposits during flood events, but Newton's description of the cave indicates that the upper passages contain speleothems and moonmilk.

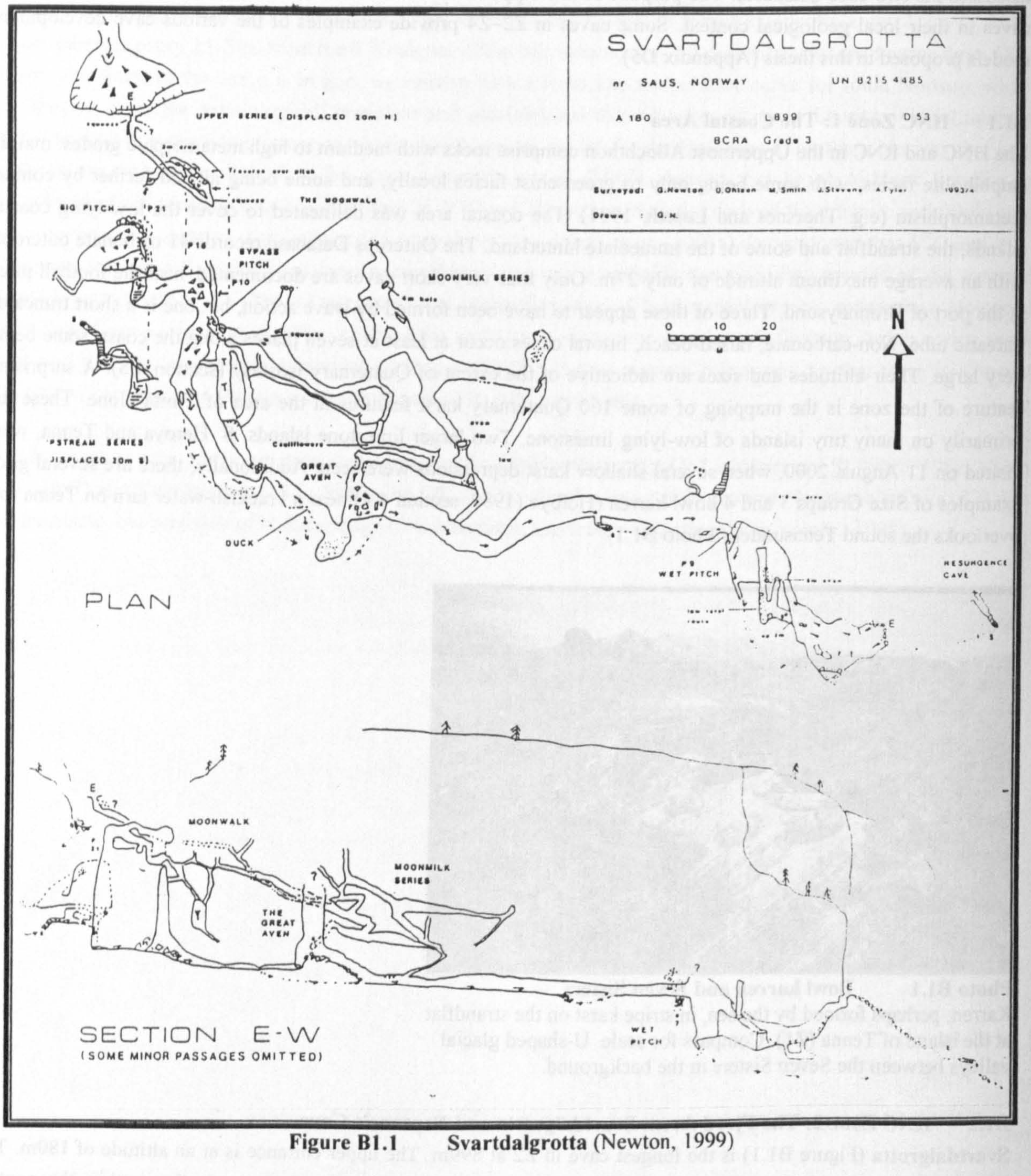

Figure B1.1 Svartdalgrotta (Newton, 1999)

B1.3 HNC Zone 3: The Central Granite Area: Toerfjellhola and Cave of the Cold Wind

The longest cave in the HNC is **Toerfjellhola** (Figure B1.3), with a surveyed length of 1896m and a depth of 101m (Faulkner and Newton, 1995, pp13–16). Its morphology is typical of many HNC caves. The metalimestone is well-banded in grey and white colours, commonly with a vertical foliation. The cave contains several levels of sub-horizontal strike-aligned relict passages stacked vertically above a very active streamway (Photo B1.2) that interconnect by joint-aligned shafts and rifts. There are only a very few (straw) speleothems in the system. The cave lies within an unmapped outcrop measuring perhaps 1000m by 200m that forms a platformal bench above the upper, dry, part of the glaciated valley of the Overengbakk (Photo D3.4). Despite being in Z3, it is some distance from a pluton so that the limestone is consequently unaffected by contact metamorphism. From a study of the cave survey, section and passage cross-sections it appears as if much of the early cave development was phreatic (Appendix

D5.2), because the explored upper series of passages mainly represent the descending parts of several interconnected phreatic loops. These loops are all blocked at boulder chokes beneath surface dry valleys, just as they start to ascend. The resurgence is 500m away in Overengbakkdal (Photo D3.5), 50m below the level of the terminating downstream sump. This valley is remarkable (but not untypical of the area) for the size and extent of its talus slopes and the block stream that occupies the dry valley bottom (Figure B1.3; Photos D3.4 and D3.5). These are surmised herein to have been formed by jökulhlaups that rapidly lowered the levels of ice-dammed lakes to the east (Appendix D3.3).

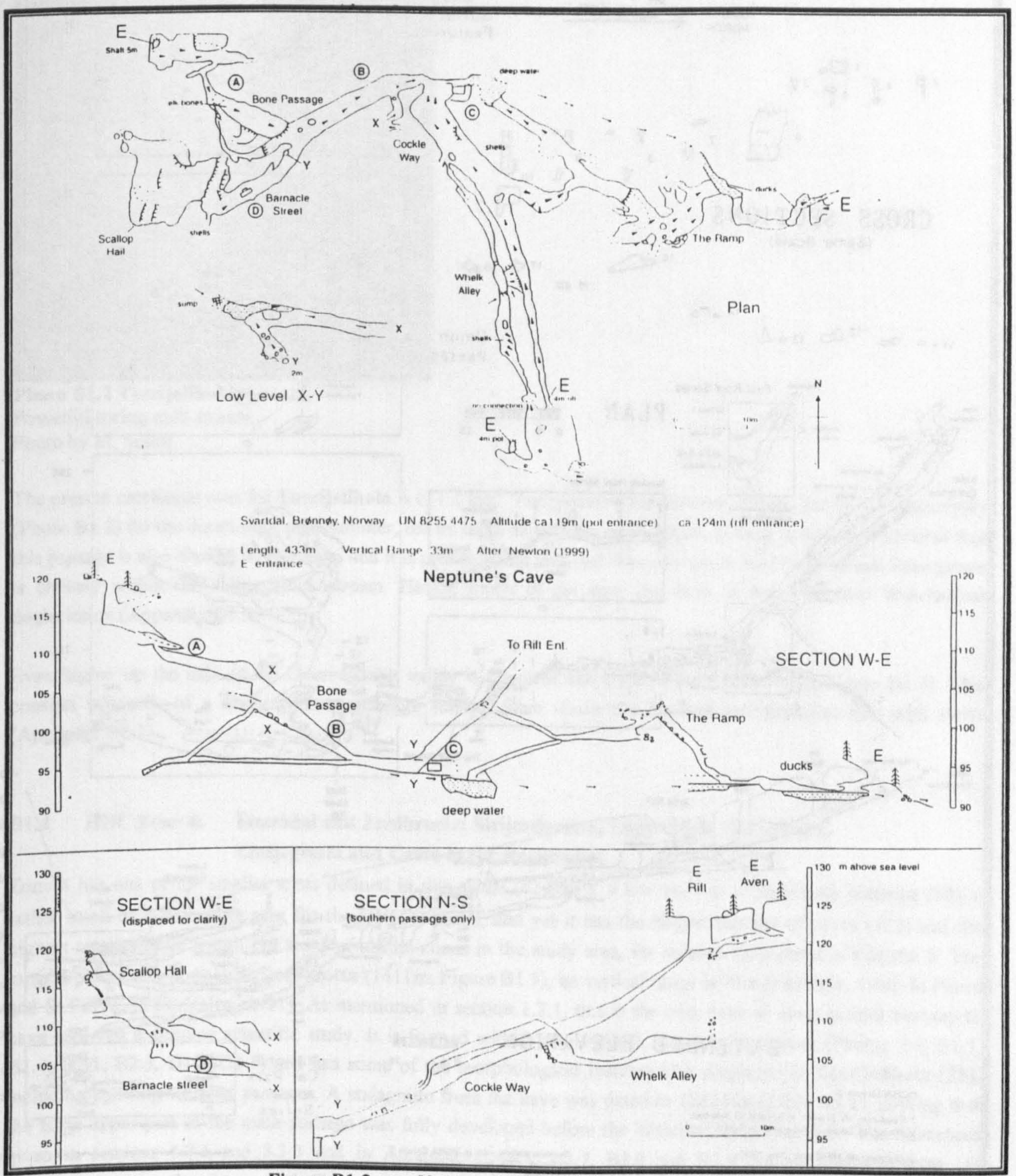

Figure B1.2 Neptune's Cave (After Newton, 1999)

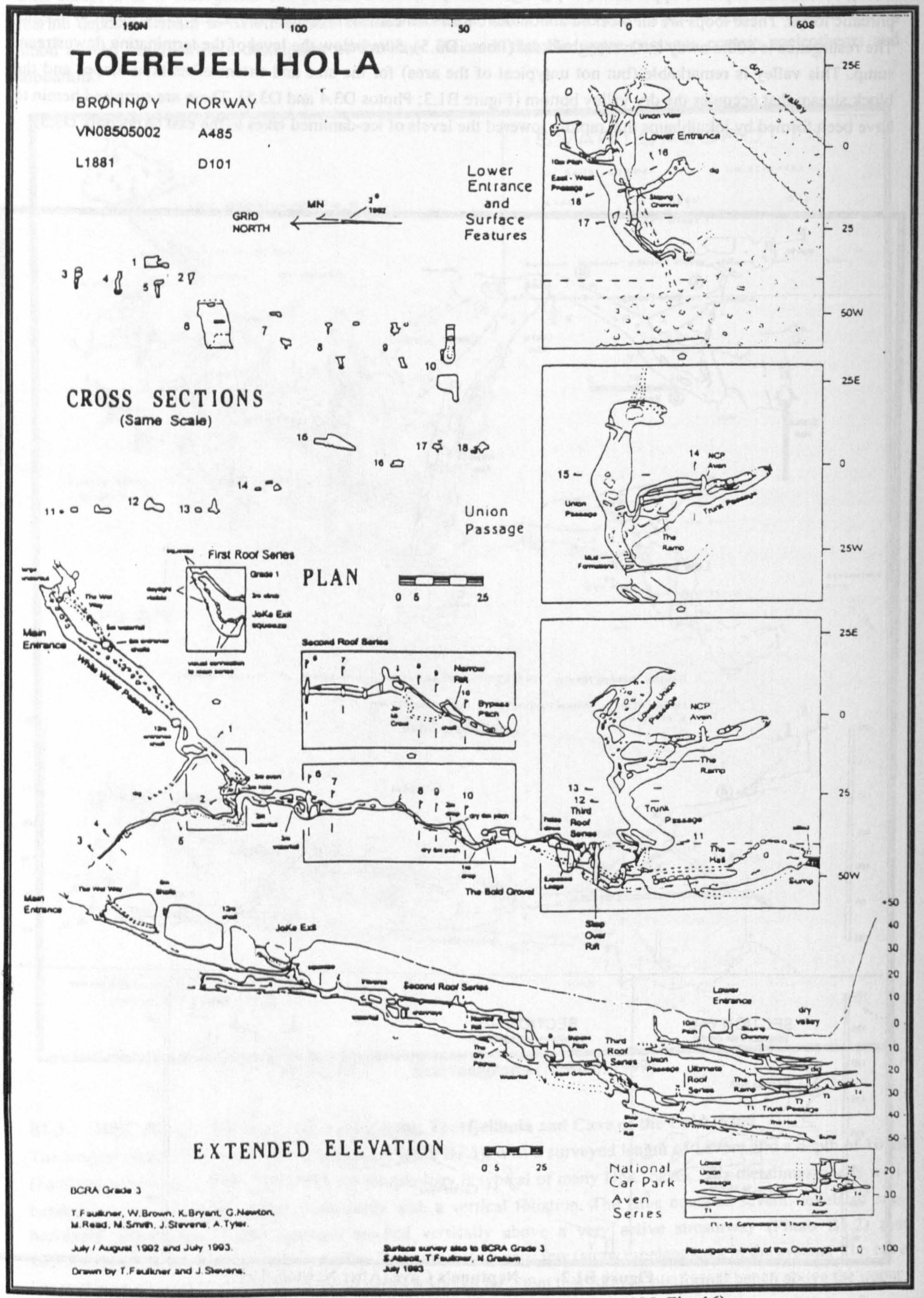

Figure B1.3 Toerfjellhola (Faulkner and Newton, 1995, Fig. 16)

Photo B1.2 Toerfjellhola stream
Powerful spring melt stream.
Photo by M. Smith.

The present catchment area for **Toerfjellhola** is c. 1.1 km^2. The powerful stream runs through the vadose streamway (Photo B1.2) for the duration of each summer, fed by large snowfields on Toerfjell. Diving at the sump revealed that this passage is also choked by boulders, and it is probable that the final 50m descent to the Overengbakk Resurgence is entirely within the valley block stream. Hence, much of the cave pre-dates at least the final Weichselian deglaciation (Appendix D5.2).

Even higher up the side of the Overengbakk valley is **Cave of the Cold Wind** (372m long; Figure B1.4). This consists primarily of a single phreatic passage leading from above the blocked resurgence to two high avens (Appendix D5.1).

B1.4 HNC Zone 4: Eiterådal and Jordbruelv: Sirijordgrotta, Elgfjellhola, Gevirgrotta, Etasjegrotta and Caves at the Rockbridge

Zone 4 has one of the smaller areas defined in this thesis (814km^2), a low number of carbonate outcrops (36), a rather small total carbonate area for the HNC (37km^2), and yet it has the largest number of caves (182) and the highest total passage length (14.5km) of all the zones in the study area, for reasons considered in Chapter 8. The longest cave in the zone is **Sirijordgrotta** (1411m; Figure B1.5); its vertical range is 78m (Faulkner, 1980; St.Pierre and St.Pierre, 1980; Valen, 1991). As mentioned in section 1.7.1, this is the only cave in north central Norway to have received a detailed scientific study. It is formed within near-vertical, banded, limestones (Photos 5.4, B1.3, B1.4, B2.1, B2.3, D1.4–D1.7) and has some of the morphological features also displayed in **Toerfjellhola** (Z3), including stacking of relict passages. A stalagmite from the cave was dated to 128±5ka (Table A5.1), proving that the large upper part of the main passage was fully developed before the Weichselian glaciations. The references given in sections 1.7.1 and 3.3.3 and in Appendices A4.1, B2.7, B2.8 and B2.9 discuss **Sirijordgrotta**, its sediments, water chemistry, and flow rates. In the same valley lies **Eiterådalgrotta** and **Eiterådalgrotta Resurgence Cave**, an epigean system with a total length of some 700m (Frontispiece 2; Photos B1.5 and B1.6).

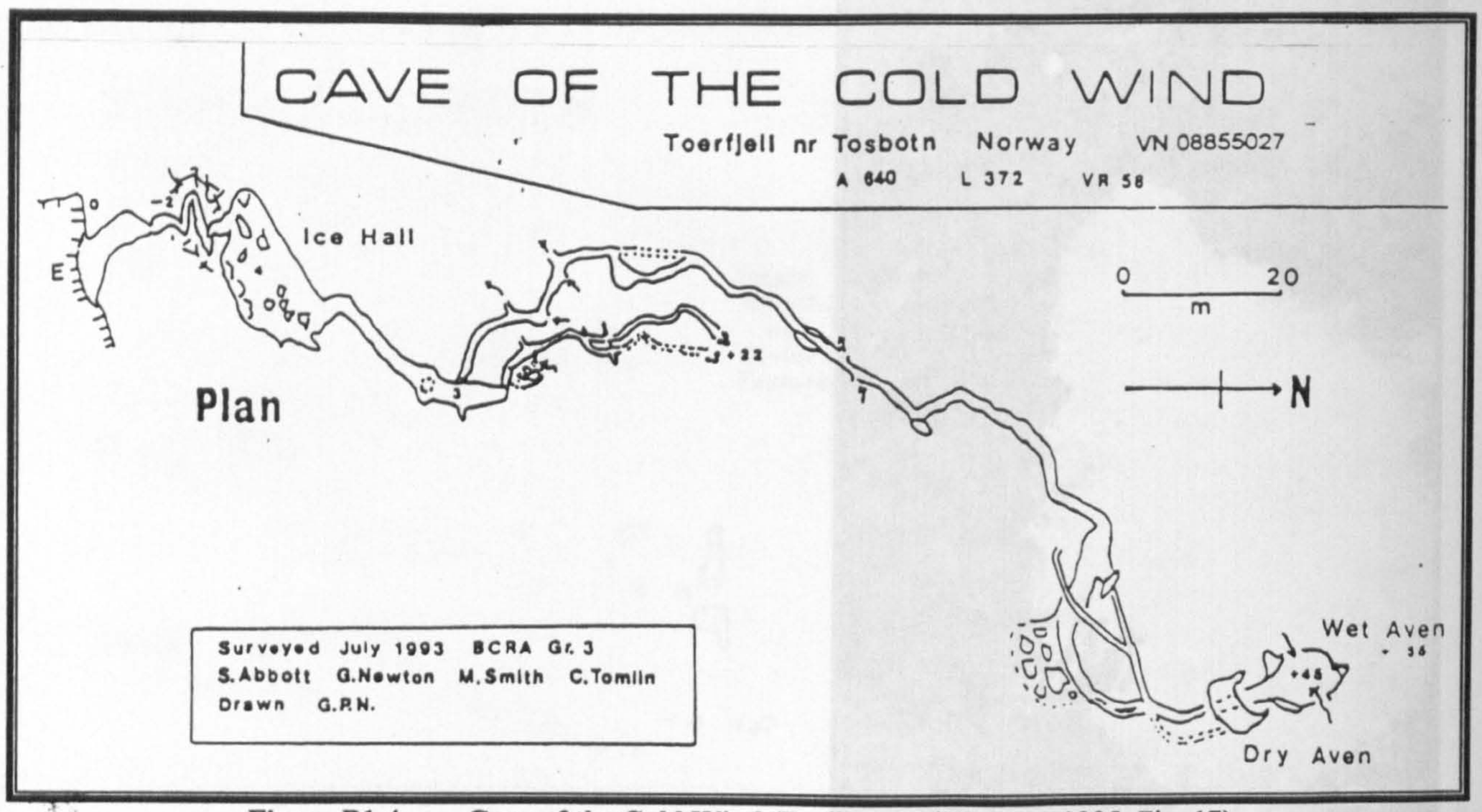

Figure B1.4 Cave of the Cold Wind (Faulkner and Newton, 1995, Fig. 17)

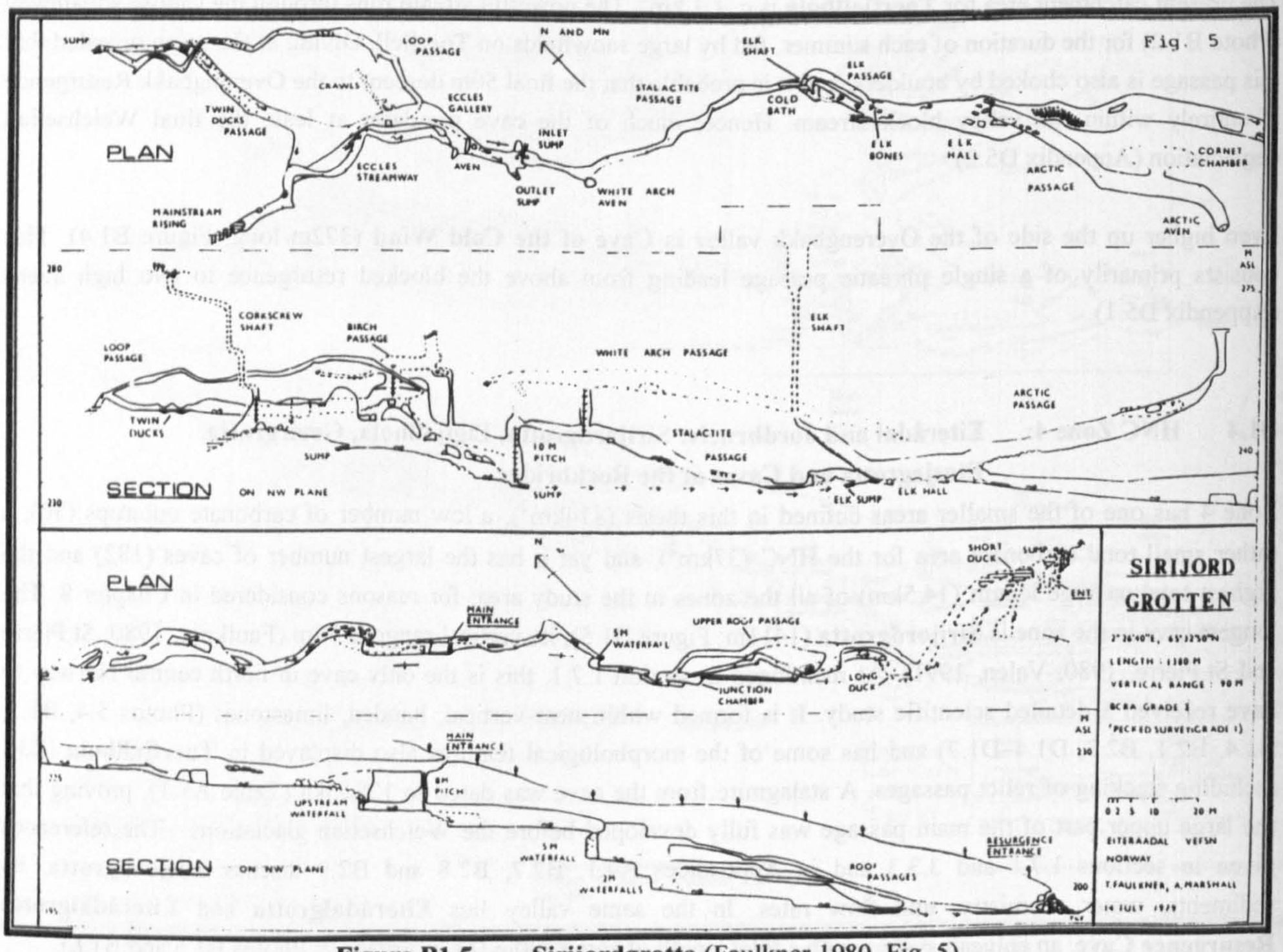

Figure B1.5 Sirijordgrotta (Faulkner 1980, Fig. 5)

An informative part of Z4 is the plateau / cirque of Elgfjell (Faulkner and Newton, 1990). This is an upland area of c. 8km^2 at an altitude of c. 600m, crossed by several long N–S aligned outcrops of metacarbonates. Many small north-draining and south-draining valleys lie parallel to these outcrops. Despite being mapped as contiguous with the carbonate outcrops along the Jordbruelv to the south, the Elgfjell carbonates differ in weathered appearance. Two marble types are seen: a pure grey variety and a yellow / brown striped variety that likely comprises HMC (Table A2.2, samples 1 and 3). These two varieties commonly occur in pairs of linear outcrops, which are either adjacent or separated by up to 50m by schists. The yellow / brown striped marble outcrops are narrower (up to 60m wide) than the grey outcrops, and do not occur in isolation. These observations also apply at Kvitfjell, 12km to the north, and both mountains display complexly-folded karst outcrops (section 4.4.6). The foliation dip and the contact angle with the mica schist country rock varies from 50°W in the central part of Elgfjell to 70–80°W on the steep hill-slopes to the east and south. This contrasts with the vertical foliation in the Jordbruelv valley, to which these same outcrops are mapped as continuing.

The longest cave on Elgfjell is **Gevirgrotta** at 683m. The survey and section (Figure B1.6) show that this cave developed along-strike at three main levels. The upper two are relict shallow phreatic loops that directed water northeastwards to unknown resurgences on the hillside above the highest Gåsvatn lake, at about the level of the upper entrance and at perhaps 8m below this. The lowest level may represent rejuvenation with an active vadose streamway leading to a sump 27m below the upper entrance. The actual present resurgence is 28m below this, which is still some 40m above the lake. In contrast to the caves formed in vertical limestones, the passages are not stacked vertically above each other, but have migrated down the dip towards the west.

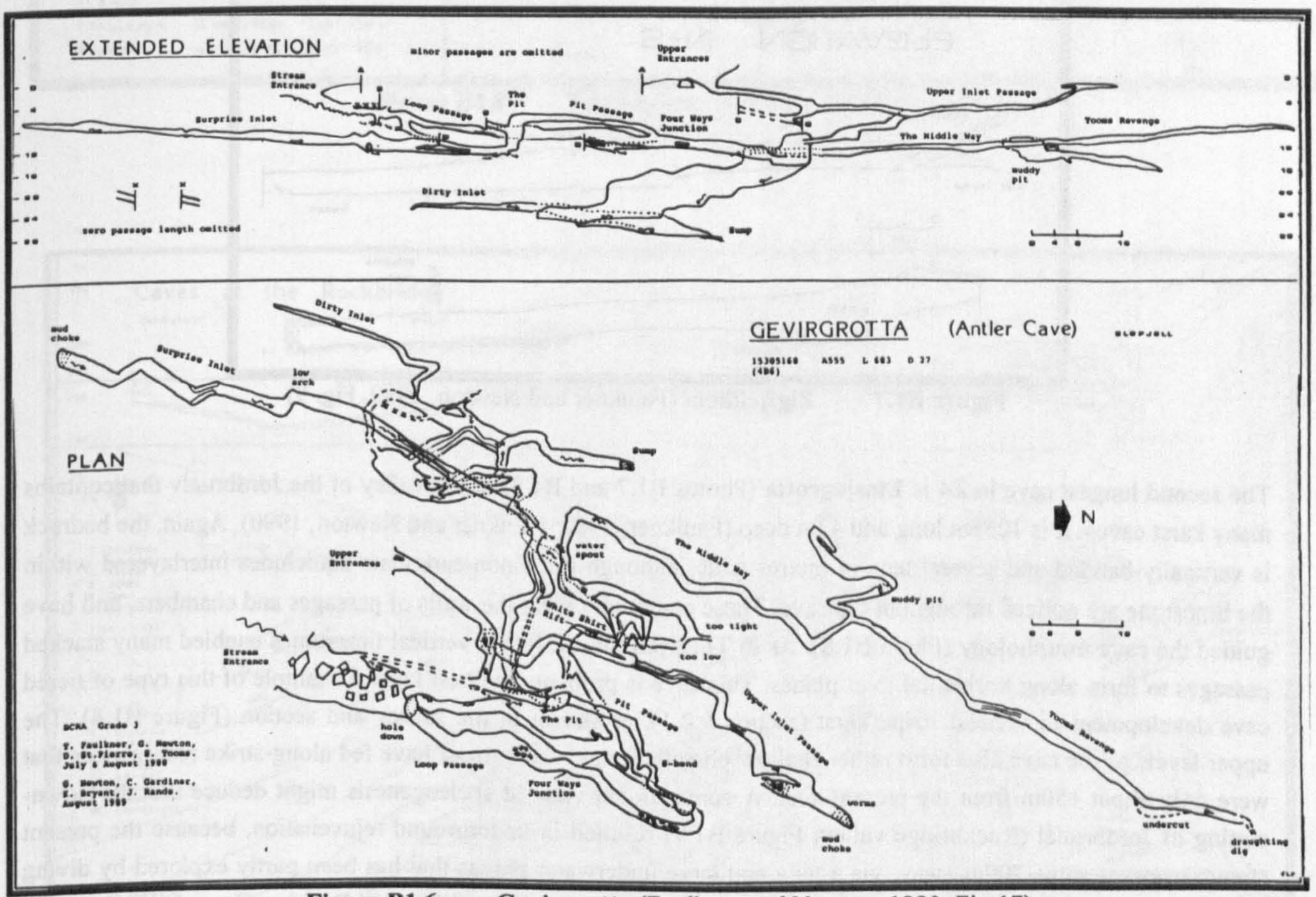

Figure B1.6 **Gevirgrotta** (Faulkner and Newton, 1990, Fig.17)

About 90 caves with a total passage length >5km are known at Elgfjell, some lying at the junction of the two marble types. Many of these caves are relict or carry only misfit streams, as at **Elgfjellhola** (Figure B1.7; Photos 4.4, D1.11, D1.12; Appendix D5.4).

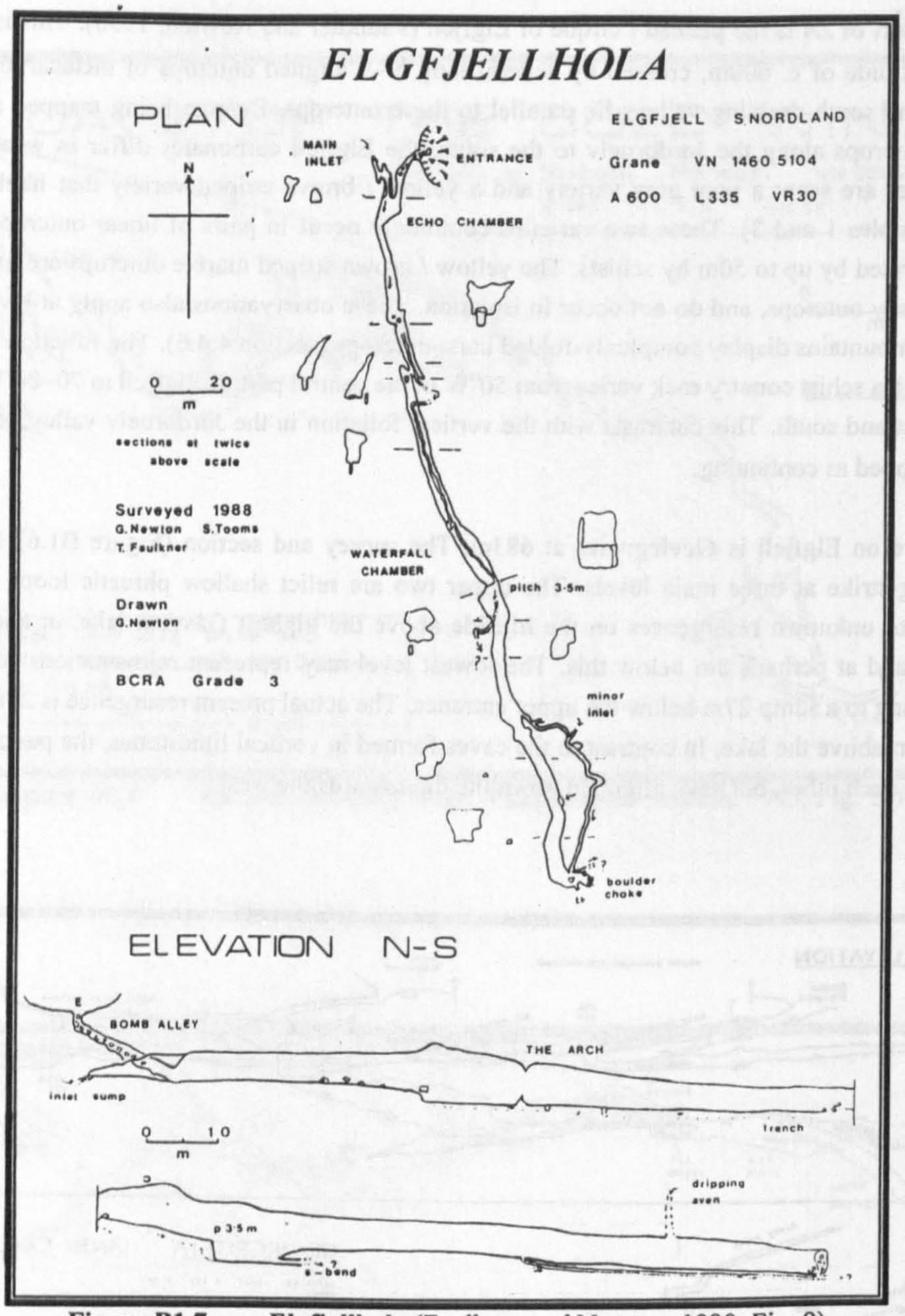

Figure B1.7 **Elgfjellhola** (Faulkner and Newton, 1990, Fig. 9)

The second longest cave in Z4 is **Etasjegrotta** (Photos B1.7 and B1.8) in the valley of the Jordbruelv that contains many karst caves. It is 1055m long and 42m deep (Faulkner, 1987; Faulkner and Newton, 1990). Again, the bedrock is vertically-banded and several tens of metres wide, although thick non-carbonate aquicludes interlayered within the limestone are noticed throughout the cave. These commonly form the walls of passages and chambers, and have guided the cave morphology (Photo B1.8). As in **Toerfjellhola** (Z3), the vertical limestones enabled many stacked passages to form along horizontal joint planes. This cave is probably the best known example of this type of tiered cave development in vertical stripe karst (section 9.2.1), as shown in the survey and section (Figure B1.8). The upper levels of the cave also form rather shallow phreatic loops, which must have fed along-strike resurgences that were only about 150m from the present sink. A conventional view of speleogenesis might deduce that the down-cutting of Jordbrudal (Rockbridge valley; Figure B1.9) resulted in underground rejuvenation, because the present stream resurges some 700m away, via a long and large underwater phreas that has been partly explored by diving from the **Main Rising** and from **Vatnhullet**. The primarily relict and interconnected **Beehive Cave**, **Cliff Cave** and **Invasjonsgrotta** lie above this phreas, indicating a complex speleogenesis that is considered further in Appendix D5.5. South of here, the short cave **Anastomosegrotta** has an anastomatic roof at its low entrance, which probably formed as a distributary maze above a resurgence too small for flood discharge, as described by Palmer (1972; 1984a; section 3.1.16).

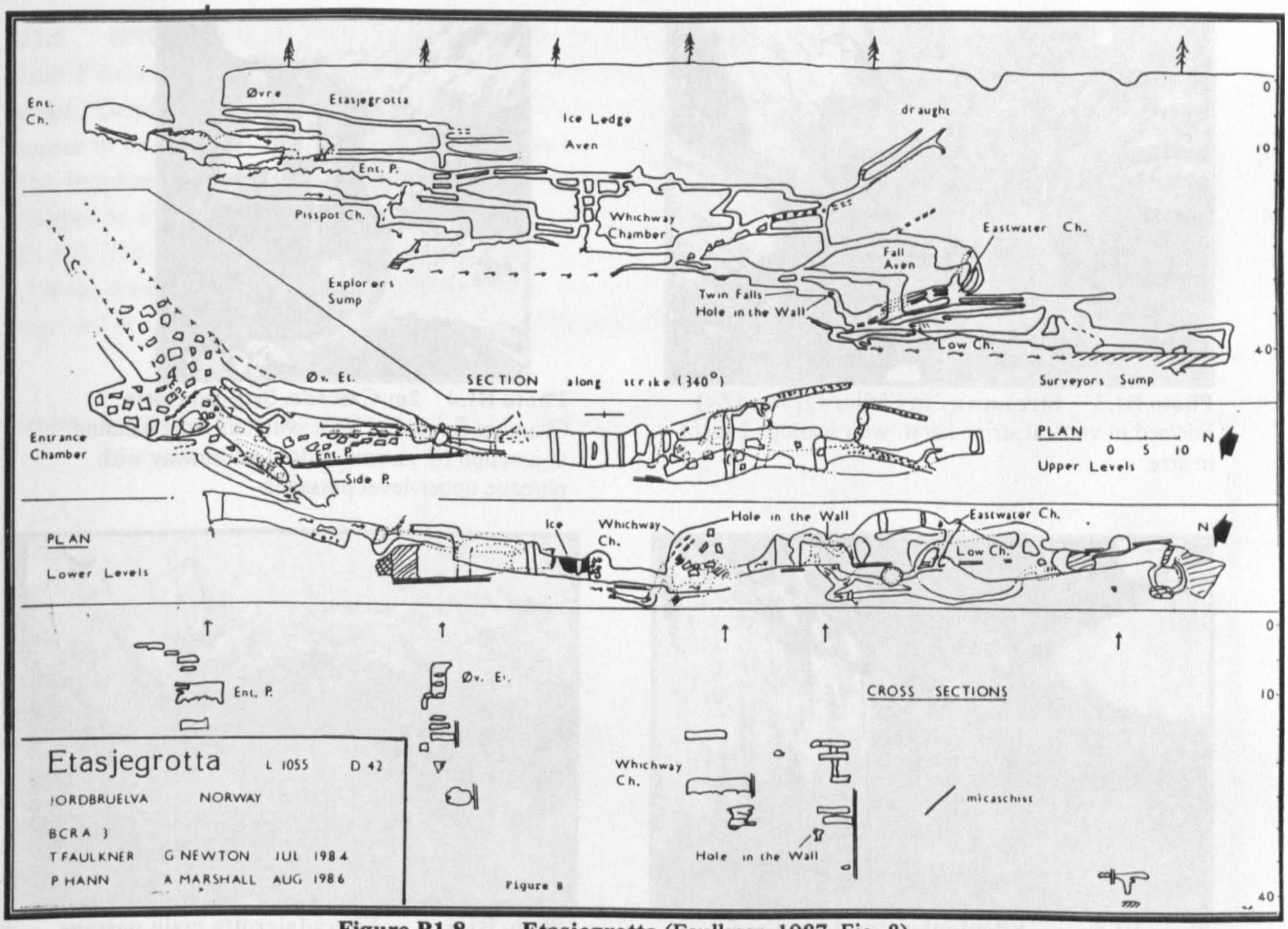

Figure B1.8 Etasjegrotta (Faulkner, 1987, Fig. 8)

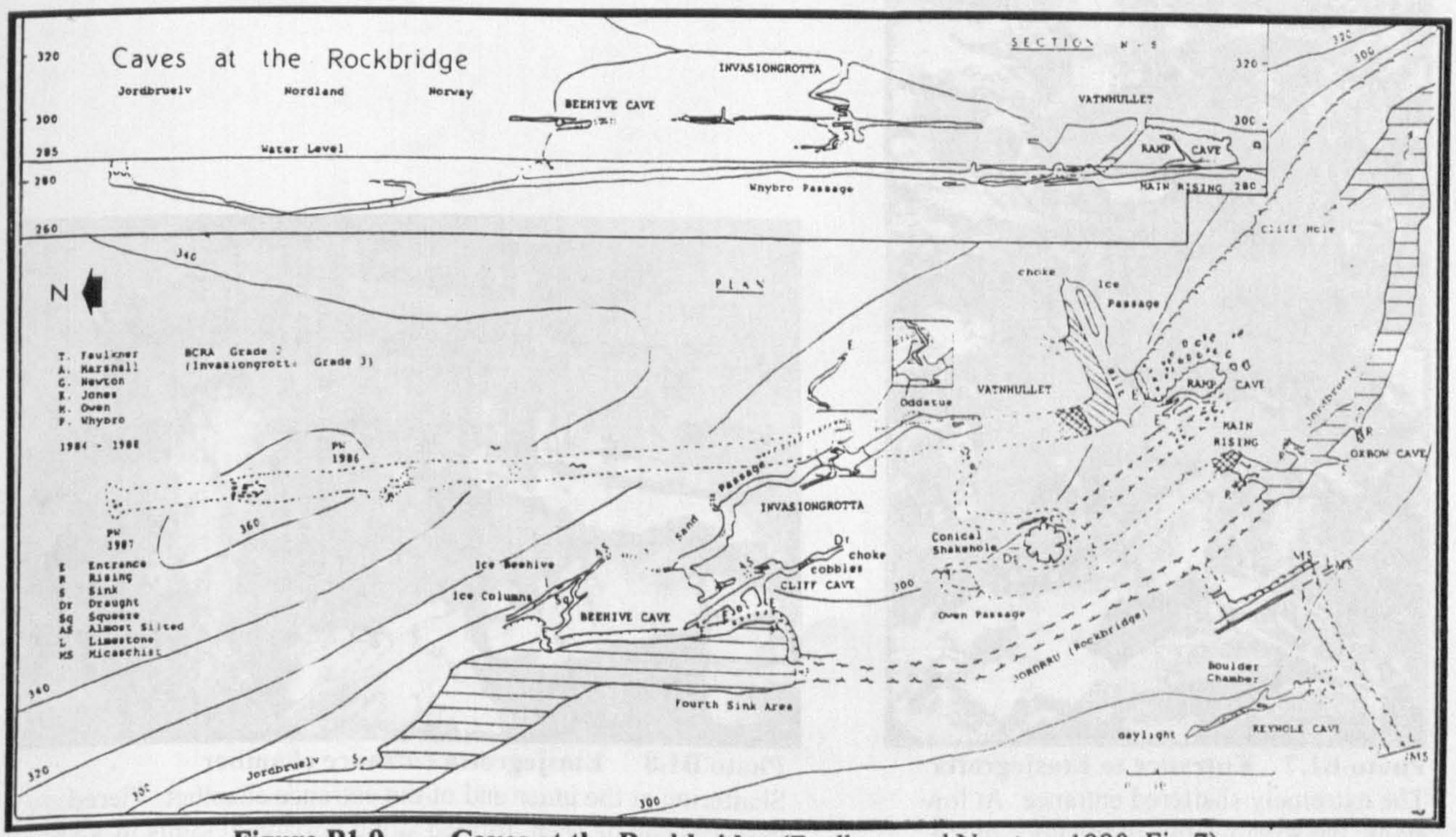

Figure B1.9 Caves at the Rockbridge (Faulkner and Newton, 1990, Fig.7)

Photo B1.3 Streamway in Sirijordgrotta (Z4)
Formed in vertical stripe karst, with scallops 2–3cm in size.

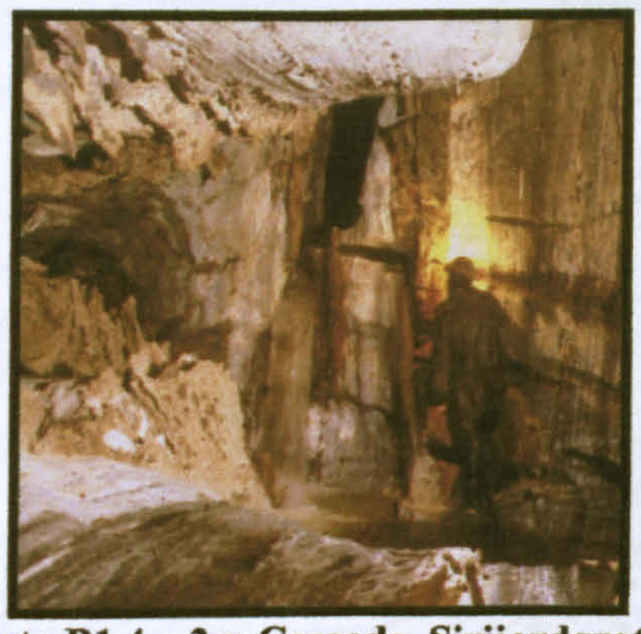

Photo B1.4 2m Cascade, Sirijordgrotta
Chamber formed in VSK with cm-scale banding at junction of narrow vadose streamway with phreatic upper-level passages.

Photo B1.5 Eiterådalgrotta streamway
Vadose entrenchment beside and below phreatic level, with wall along amphibolite within VSK.

Photo B1.6 Eiterådalgrotta main passage
Phreatic level, with amphibolite roof pendants, rounded cobbles and condensation droplets.

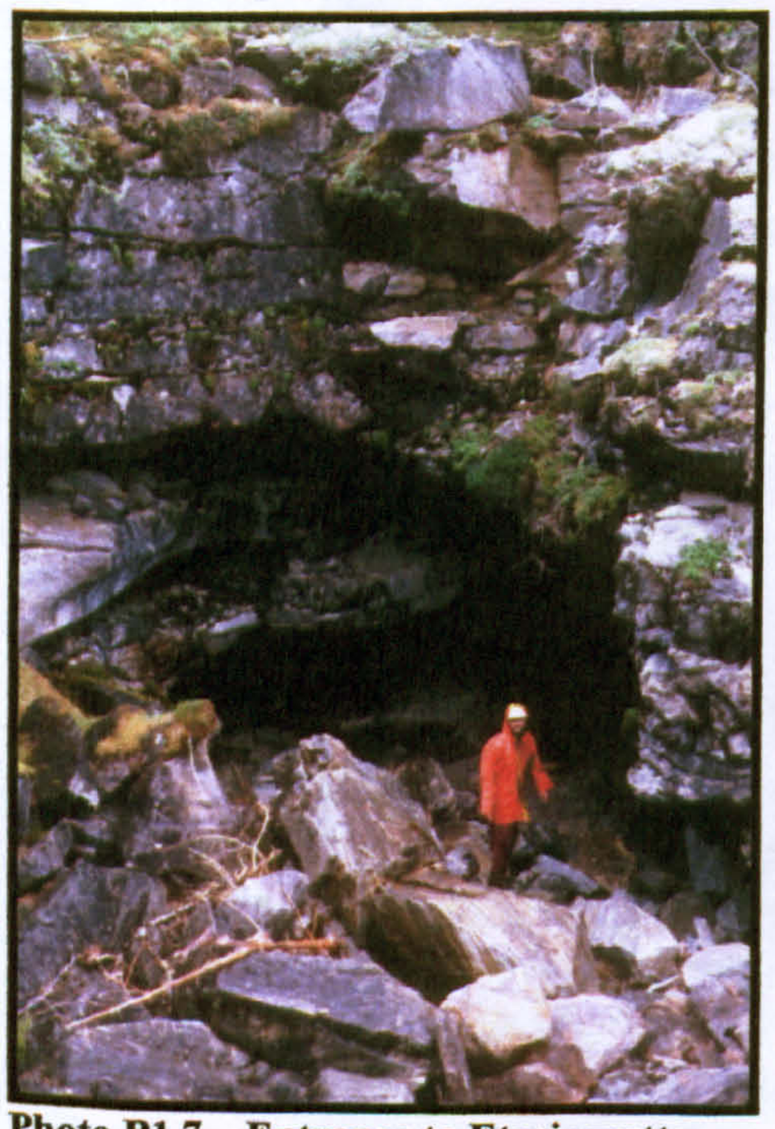

Photo B1.7 Entrance to Etasjegrotta
The extremely shattered entrance. At low stage, the stream sinks in the floor of the preceding gorge.

Photo B1.8 Etasjegrotta entrance chamber
Shattering at the inner end of the entrance chamber. Tiered passages can be seen, formed along horizontal joints in VSK. The vertical wall consists of amphibolite. Photo by A. Marshall.

B1.5 HNC Zone 5: Mosjøen to Fjellryggen: Øyfjellgrotta, Geitklauvgrotta and Blåfjellgrotta

Zone 5 includes a carbonate outcrop that is some 53km long and contains significant caves in many places along its length. Despite being adjacent to a long pluton of granite and granitic diorite for c. 25km, this outcrop does not appear to be affected by contact metamorphism, being well-foliated with mainly vertical grey and white banding. The best-known cave is **Øyfjellgrotta** near Mosjøen, regularly visited by local people (Grimsby, undated) and mapped to a length of 800m and a depth of 105m (Heap, 1968), but only a plan survey was published (Figure B1.10). The cave contains very large upper relict passages above a very large and vigorous streamway. Smart (1984b) compared upper-level sandy sediments in the cave with those at Castleguard Cave in Canada, which he regarded as a 'proximal' equivalent, because both comprise autochthonous stream-laid deposits. See section 8.8.3.

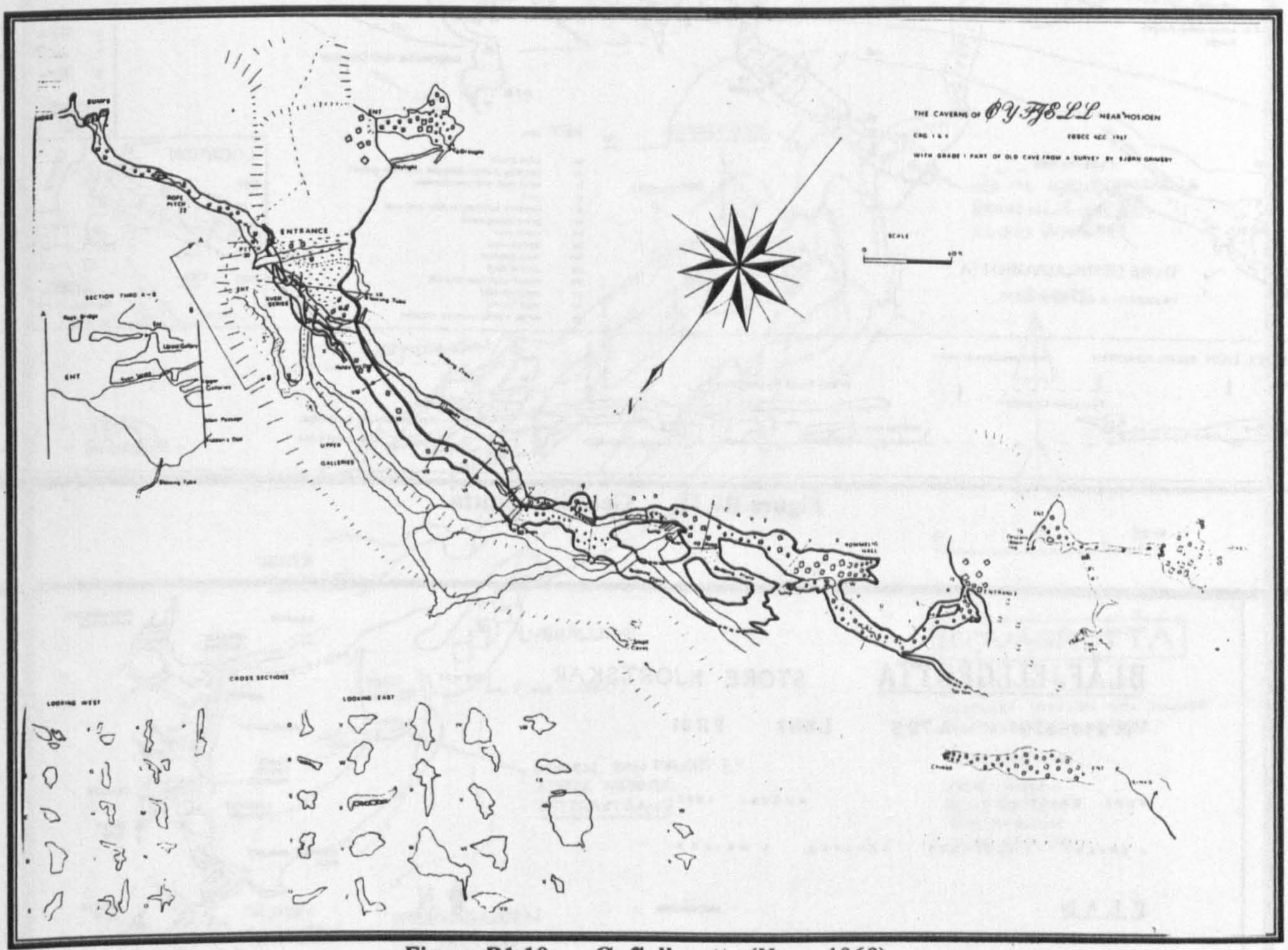

Figure B1.10 Øyfjellgrotta (Heap, 1968)

The longest cave in Z5 is **Geitklauvgrotta** (935m long; Figure B1.11), which was studied in 1997 and 1998 (Photos B2.2, D1.27, D1.28 and D1.29). This important cave is very different from those discussed previously, as it contains a maze of passages within a limited vertical range of only 16m. The length between **Øvre Geitklauvgrotta** and the main cave (Photo 7.4) is a short example of an *Unroofed Cave* (section 3.1.11). Here the two lowest levels of the system have been removed at the valley bottom, probably by glacial action. Surprisingly, the *highest* level, being situated in the valley side, is preserved, as Wasp Nest Passage and as Fearsome Chamber.

The second longest cave is **Blåfjellgrotta** (Newton and Faulkner, 1992; Figure B1.12). This contains 861m of passages that are rather small when compared to the length of the system. The cave, formed in dark, banded, vertical limestones, consists of three shallow phreatic loops that are interconnected via ramps and rifts. Some vertical stacking of passages occurs, but the cave has also developed across the width of the outcrop, which here may reach 200m. Some eight sumps are encountered along the streamway at the lowest level.

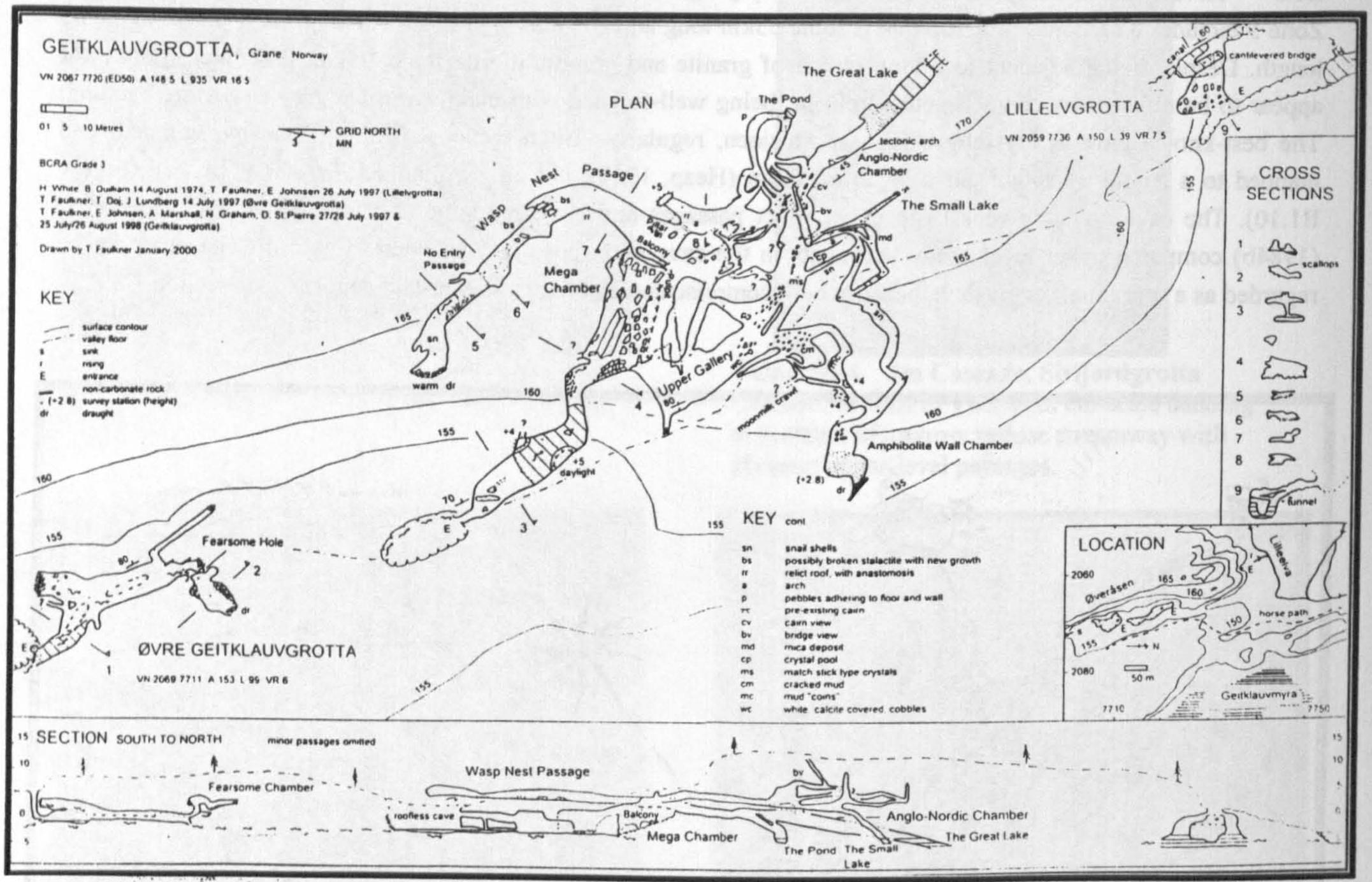

Figure B1.11 Geitklauvgrotta

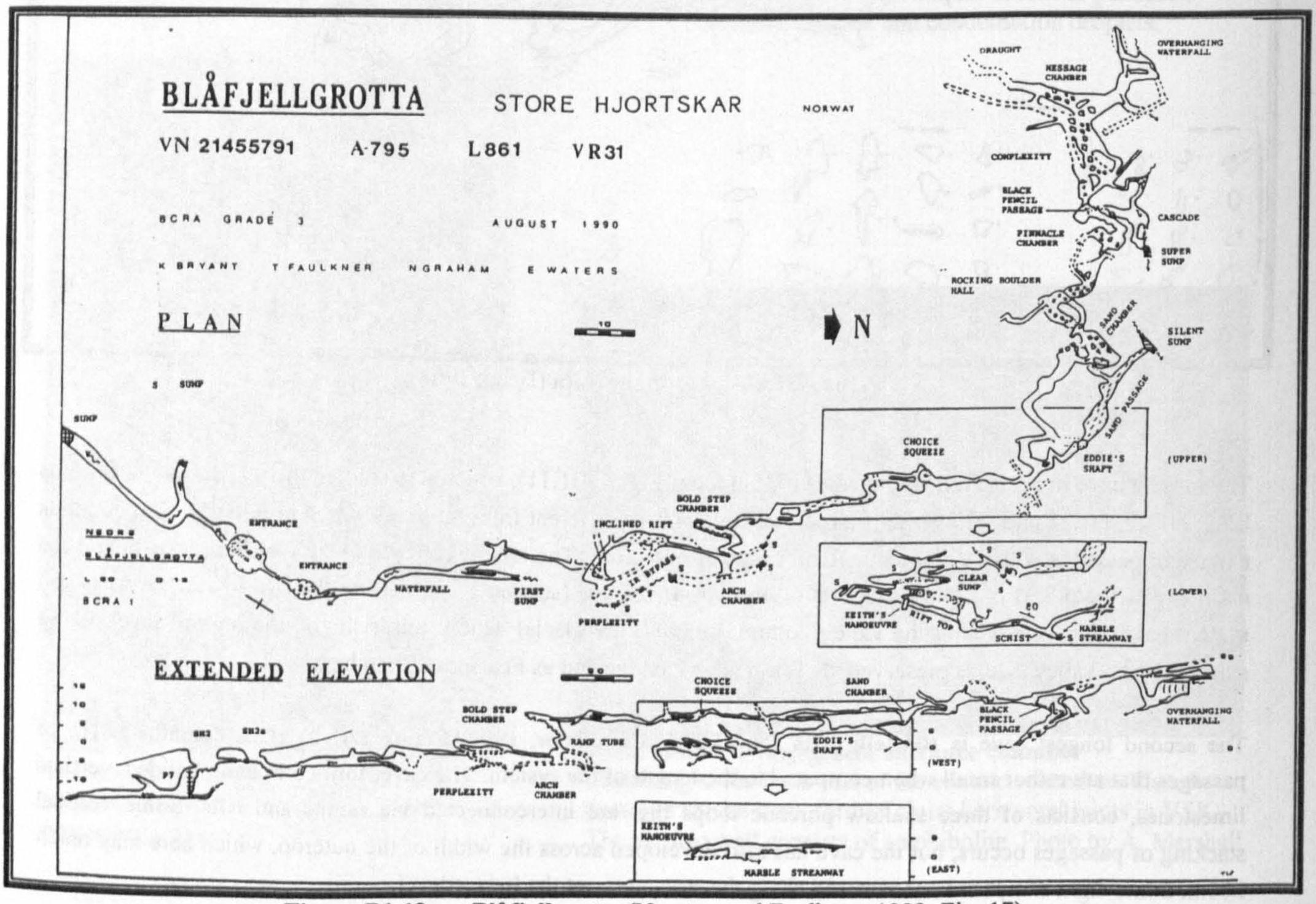

Figure B1.12 Blåfjellgrotta (Newton and Faulkner, 1992, Fig. 17)

B1.6 HNC Zone 6: Hemnes to Dunnfjell: Kovagrotta and Luktindgrotta

Zone 6 has received comparatively little attention from British and other cave explorers, although there is probably unrecorded knowledge about individual caves held by people who live in the Mosjøen area. The longest published survey (c. 650m) is that of **Kovagrotta** (Grønlie, 1982, pp19–20; Figure B1.13). A previously-unreported cave, **Luktindgrotta** (Photo D1.33), was visited in 1997 and 1998. This cave consists of a roomy vadose, strike-aligned, streamway. It presently carries a small misfit stream for c. 500m to a sump that is close to a presumed resurgence in an orthogonal surface valley. At the southern end of the zone, a group of caves at Dunnfjell (Newton, 1999) lie at the upper reaches of the Namsen catchment area.

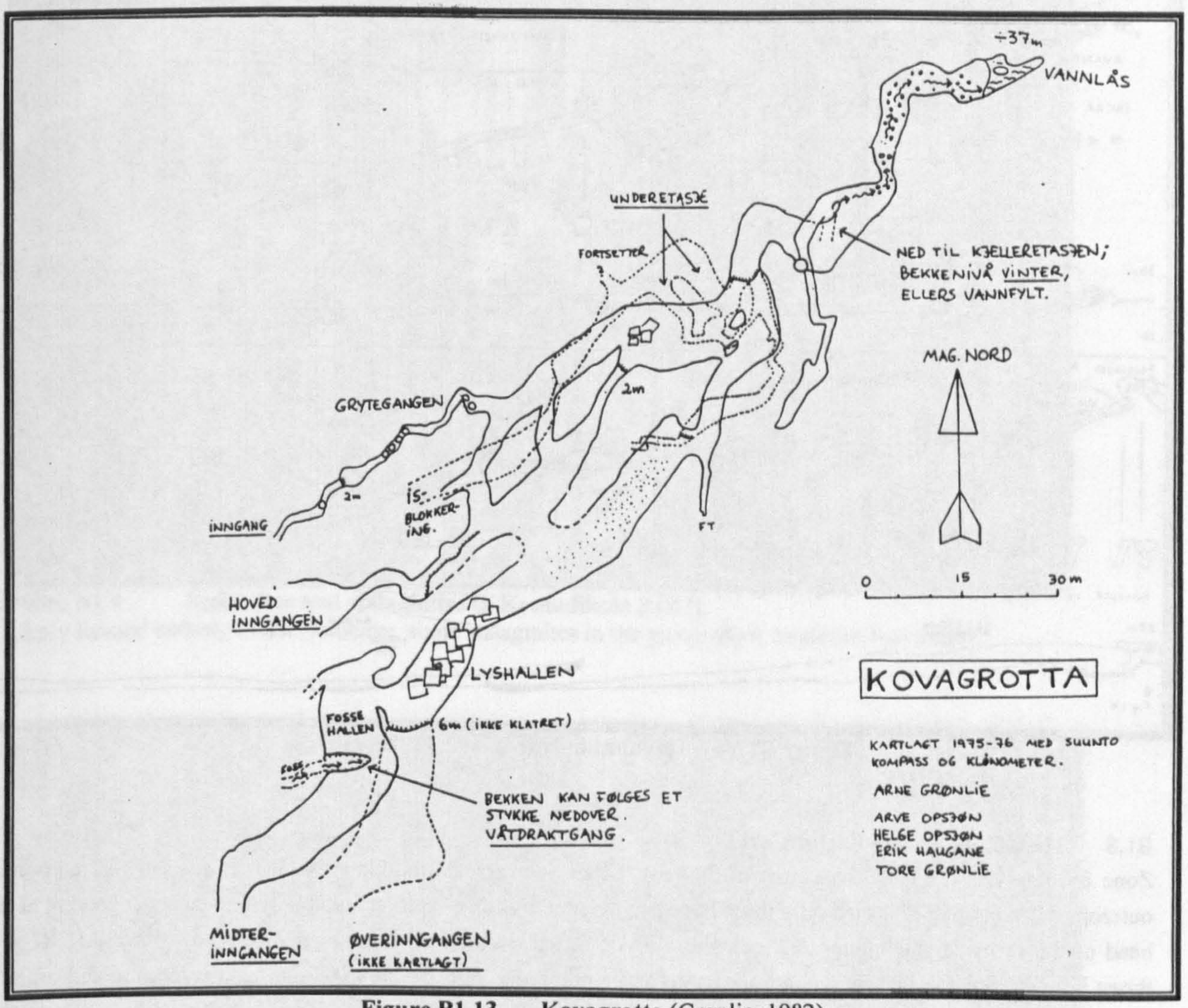

Figure B1.13 Kovagrotta (Grønlie, 1982)

B1.7 HNC Zone 7: Åkervik to Fiplingdal: Kvannlihola

The Carbonate Outcrops Database records a total length of 421km for the carbonates in Z7. Much of the limestone is contained within six highly complex and multiply-interconnected outcrops with many parallel limbs. Each of these outcrops has a total limb length of 20km or more. The outcrop with the longest limb length (42km) contains **Kvannlihola**, the longest cave in the zone (Faulkner, 1983; Figure B1.14). The cave is entered at its resurgence and consists mainly of a single streamway, although a short sump has to be passed after some 200m. The passage enlarges considerably beyond here, has a display of excellent speleothems (Photo B1.9), and then passes an area with a considerable number of collapsed blocks (Photo D1.36). Narrowing above a waterfall (Photo B1.10), the passage displays the clean-washed vertical banding of the limestone at its floor, with a nest of cave pearls near the roof (Photo B1.11) and a large collapsed block at roof level (Photo D1.37). A second waterfall (Photo B1.12) leads to a canal and a sump that is only a short distance from the undived sump in the **Kvannli Sink Cave**. The total length of the connected system would approach 1000m, with a vertical range of c. 30m. The survey reveals that the cave morphology is guided by the presence of thick, interlayered, aquicludes within the vertical limestone. The passage has broken through these aquicludes at Canal Corner, the Top Waterfall, the Greasy Climb and at Sump 1,

shifting to the left (east) on each occasion. Side passages that join the cave at some of these breakthrough points may represent earlier, now abandoned, sinks of the same cave stream. There is no sign of vertical stacking of horizontal passages in this cave, perhaps because much of the cave development was vadose after an initial phreatic phase, which can be deduced from the keyhole shape of the cross-sections. The catchment area is some 2km^2.

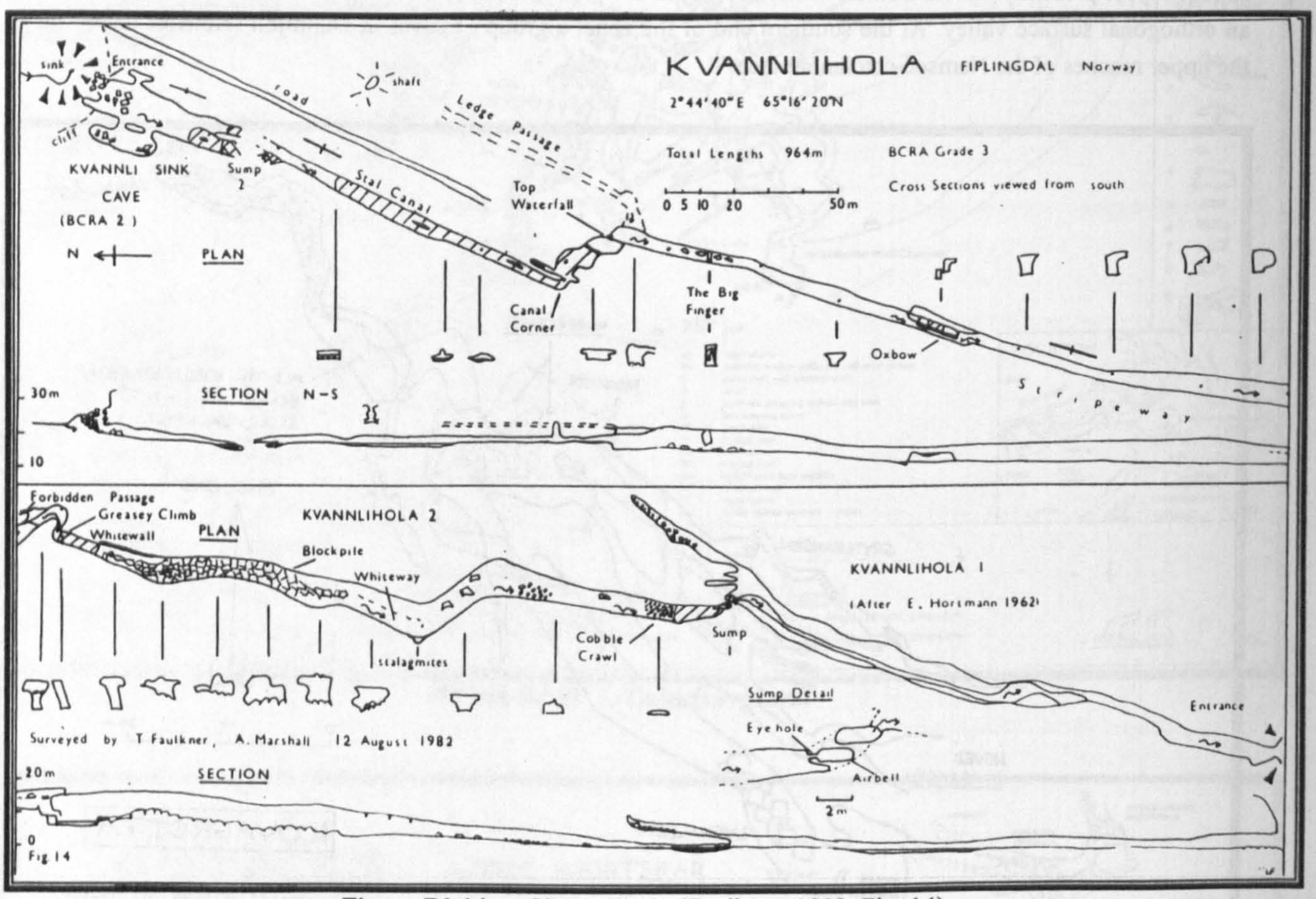

Figure B1.14 Kvannlihola (Faulkner, 1983, Fig. 14)

B1.8 HNC Zone 8: The Eastern Area

Zone 8 comprises the HNC basement in the east, where it overrides the Upper Køli nappes. Only 27 carbonate outcrops are recorded, of which only three have been visited by cave explorers, and only one, near Jengelvatn at the head of the Namsen catchment area, contains fully-reported caves. This outcrop is separated from the HNC sole thrust boundary to the east by a band of gabbro and amphibolite only 500m wide, and abuts a granite and granitic diorite pluton on its west side. Several caves were found here in fractured grey-banded metalimestones that contain numerous impurities within a partially drift covered area (Faulkner, 1987). If **Øvre** and **Nedre Jengelgrotta** could be connected the system would be over 700m long, but due to the remoteness of the area (18km from the nearest road), the published cave surveys are too inadequate to permit an understanding of cave development. S. St.Pierre (in Faulkner, 1987) quoted Oxaal (1910) and Foslie and Strand (1956) in describing a former ice-dammed lake with a surface some 30m above the present level of Jengelvatn. This ice-dammed lake would have flooded at least the lower parts of Jengelgrotta, and other local caves, but the effects of this on the caves and their sediments await study.

B1.9 HNC Zone 9: The Nesna Shear Zone

The NGU 1:50000 Sandnessjøen map shows an internal thrust within the HNC, and this "Nesna Shear Zone" (Braathen *et al.*, 2002) is taken to be that part of the HNC that lies to the north of, and structurally below, this thrust. Z9 lies in the area of Ranafjord, beneath which the HNC overrides the RNC, and includes parts of the islands of Dønna, Løkta and Hugla as well as part of the peninsular of Nordvikfjell. Only 22 carbonate outcrops are recorded, and only one 'carbonate' cave is known, the 25m long **Marmorhølet** on the island of Dønna, visited in August 2000. The cave has formed in calcitic biotite schist. It appears to have a tectonic origin, although its walls are

covered by calcitic formations and crystals that mask the bedrock. The cave is located at the c. 90m YD isobase shown by Sørensen *et al.* (1987). Because its altitude is 113m, it was subjected to marine influence and probable enlargement for a significant time after the ice melted locally during the Younger Dryas (Appendix D2.1).

Photo B1.9 Stalactites and stalagmites in Kvannlihola 2 (Z7)
Likely formed entirely in the Holocene, some stalagmites in the group show rotational movement

Photo B1.10 Streamway in Kvannlihola 2
Formed in monoclinal vertical stripe karst.

Photo B1.11 Cave pearls in Kvannlihola 2
These are at roof level, well-above the stream.

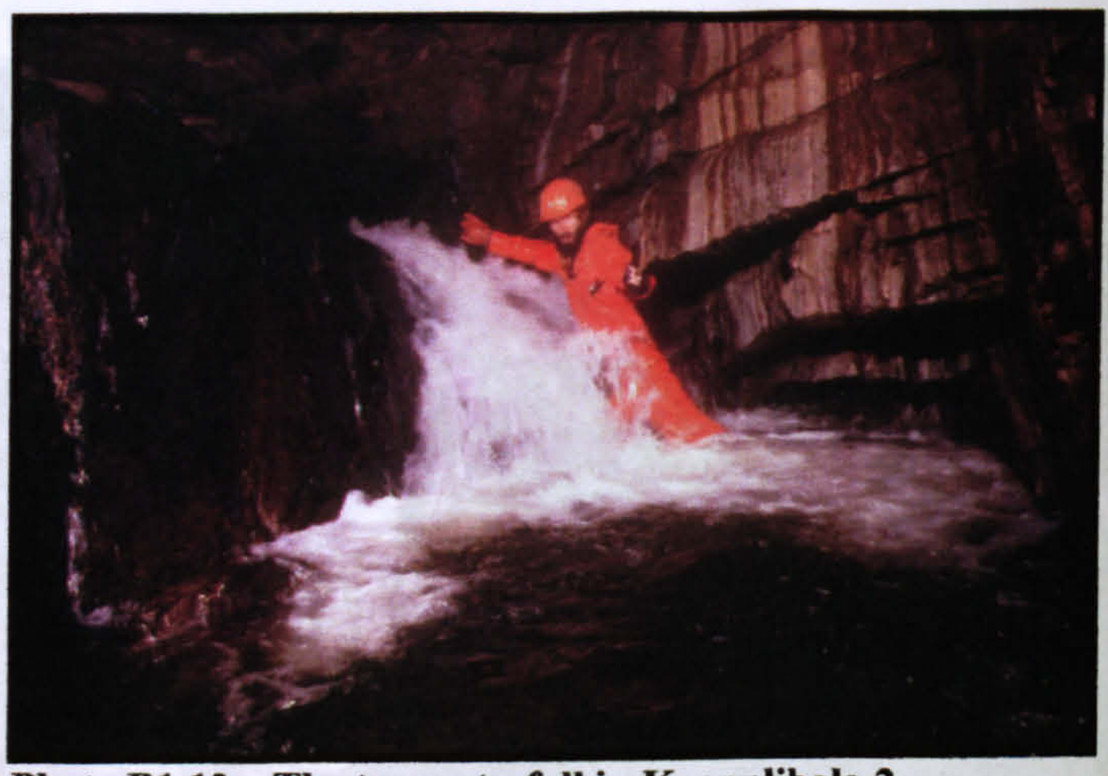

Photo B1.12 The top waterfall in Kvannlihola 2
Formed where the stream has breached a thick layer of amphibolite contained within the vertical stripe karst.

B1.10 RNC Zone A: Bleikvassli Area: Grønndalsgrotta and Ytterlihullet

Metamorphic grade in the RNC is similar to that in the HNC (Appendix B1.1). The longest cave in ZA is **Grønndalsgrotta**, which is 1400m long and 70m deep (Lauritzen, 1977; Figure B1.15; Photo D1.38). It has formed where the Jordåga stream flows underground at a wet shaft from a catchment area of c. 5km^2 in the Okstind mountains. The cave is in a folded metacarbonate mapped as "calcitic and dolomitic marble". Lauritzen described the limestone as being generally relatively impure, with several schist layers that have directed the present watercourse. The foliation dip is mentioned as "varying towards the north". From the diagrams and text it appears that the dip is, in fact, quite low, as the cave seems to have formed at two main levels (along the east–west strike direction), in two types of limestone. The upper "bench of homogeneous marble" contains maze-type passages of phreatic origin; the vadose active river passage has formed in the more impure lower limestone, which is rich in schist "horizons". The upper limestone is floored by a schist flake at Fossprekka, where a waterfall has broken through to the lower level. A similar connection has formed at the Large and Small Rope Shafts, farther downstream. Lauritzen noted the presence of shallow dry valleys beyond abandoned inlets into the cave, and concluded, therefore, that the streamway development followed a model of knick-point recession of the stream along the strike to the east. He also deduced that the cave structure pre-dates the contemporary valley topography.

The cave system that is deeper by far than any other in the study area is **Ytterlihullet** in Bryggfjelldal (Heap, 1975; Figure B1.16), with a depth of 180m and length of 700m. The entrance (marked "Storhola" on the 1:50000 Korgen map) is at an altitude of 817m, below a summit plateau at c. 900m. The catchment area is c. 0.4km^2. The system was visited by the author in wet weather in August 2000 as far as The Duck, when the flow was c. 0.7m^{3}s^{-1}. The foliation dip is 20°W in the Upper Stream Passage, and 40°W at Inlet Passage. Heap described the cave as a typical "Yorkshire pothole": it has a turbulent noisy stream that drops down eight shafts, up to 15m deep, which require ladder or rope to descend.

The meandering and steeply descending streamway is generally along narrow rift passages that display clean-washed blue, grey, orange and white bands in the marble walls. The roof and / or floor are commonly formed along flat, within-foliation, layers of mica schist [or amphibolite?]. Two sumps and a duck can be bypassed, or crawled through. These bypasses and the 1m-diameter tubular tunnel that links to Inlet Passage appear to be perched phreatic diversion conduits, as described by Palmer (1972; 1984a; 1991). The difficult exploration conditions are halted at an undived sump, at an altitude of 637 m. The water eventually rises from a small unexplorable entrance at an altitude of 614 m, some 400m to the SW. Inlet Passage carries only a misfit stream, and terminates beneath a snow-choked collapse doline at a choke of large rocks that hang from the roof and litter the floor. The presence of a surveyor's

pencil in a polythene bag, on a ledge 1m above the floor, showed that there has been no inundation of Inlet Passage between 1974 and 2000. This passage is of similar form to the Upper Stream Passage, but larger. It was clearly developed by the same stream, prior to its capture at the present entrance. At Boulder Hall, slabs of marble have spalled away from the walls, and rest at various angles on the floor, perhaps brought down by earthquakes (Chapter 6). The roof and floor here are 3m apart, and consist of mica schist or amphibolite that *does not* seem to have collapsed. **Ytterlihullet** is clearly atypical for the study area, because both main passages have formed as predominantly vadose developments along passage segments that commonly descend the dip directly in a low angle karst outcrop that is some 2km wide and that is not representative of stripe karst.

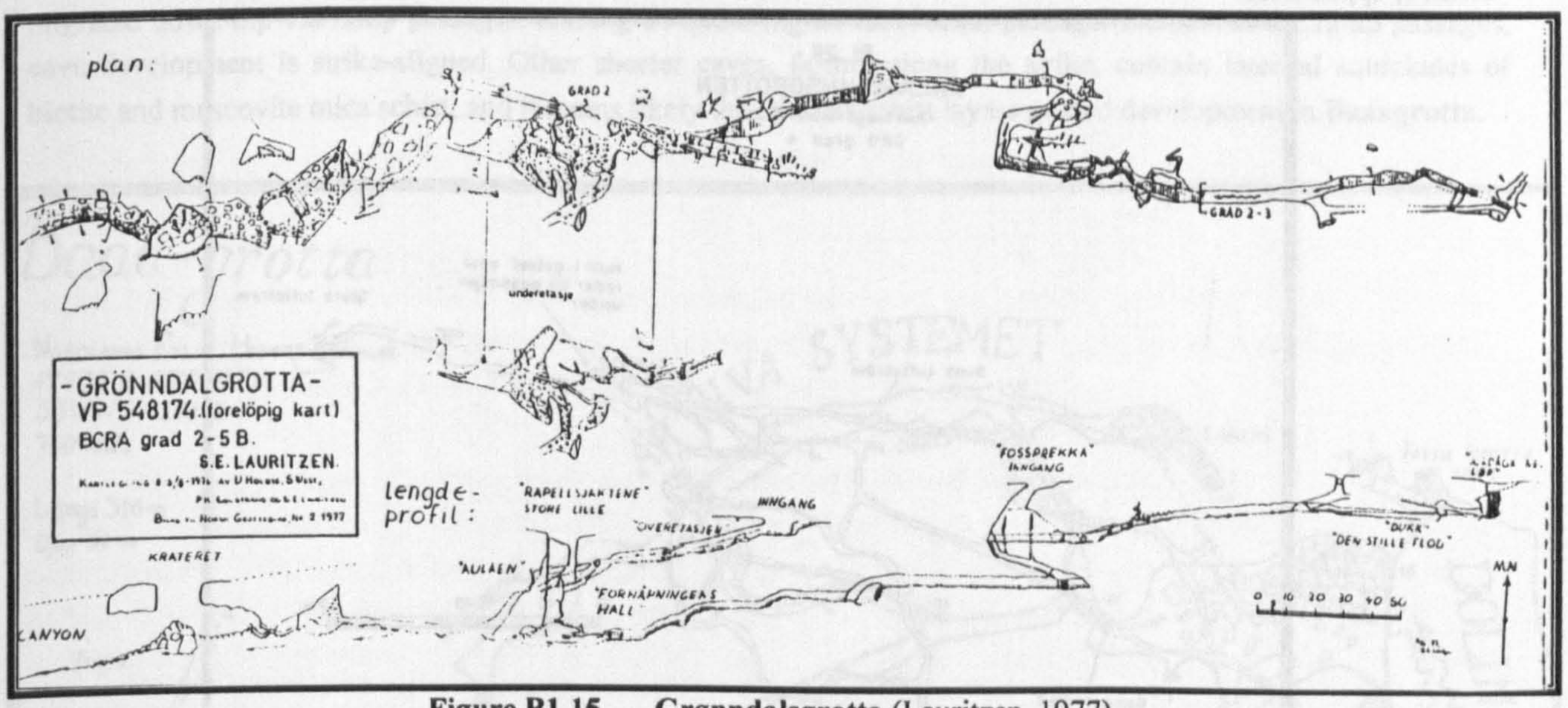

Figure B1.15 Grønndalsgrotta (Lauritzen, 1977)

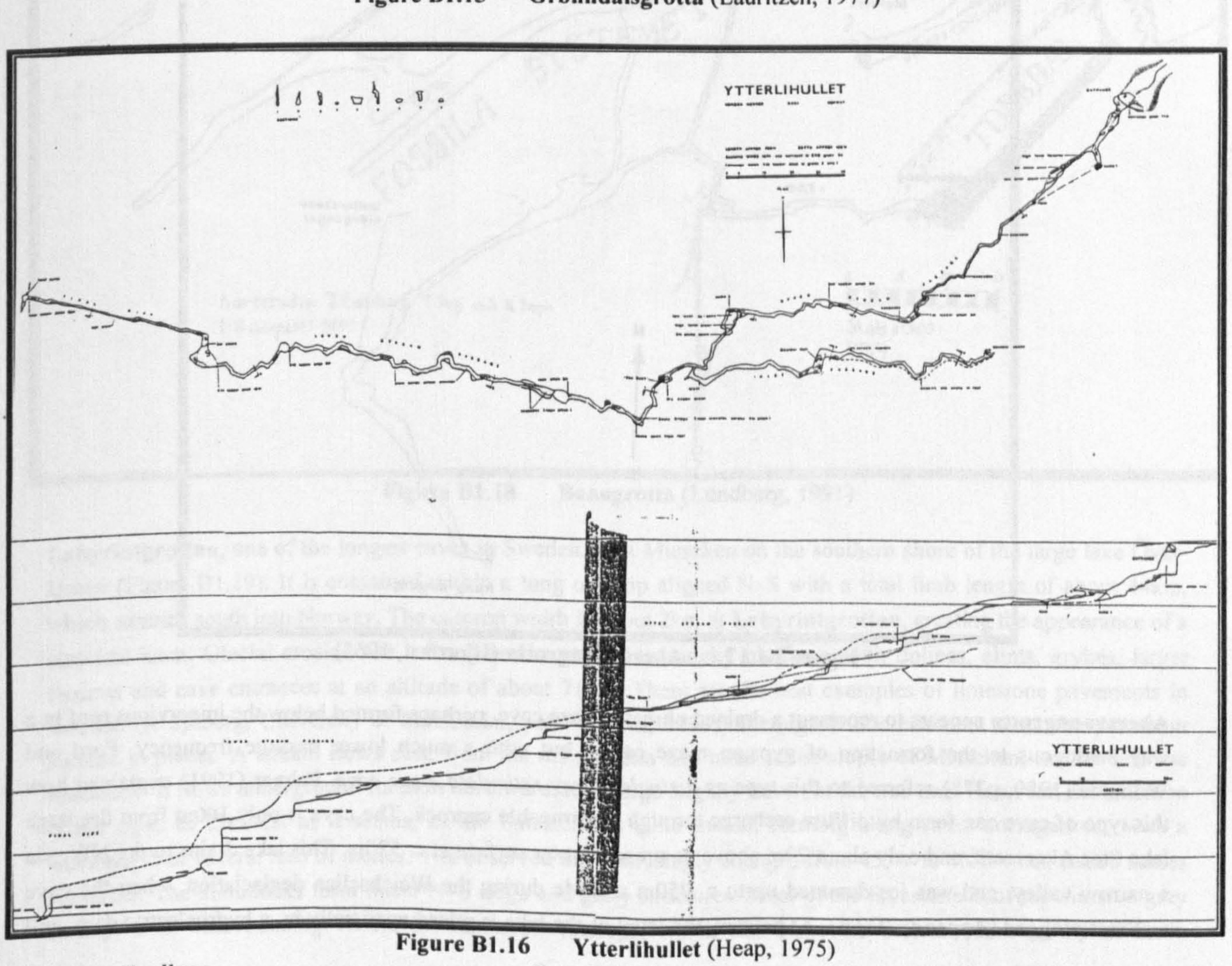

Figure B1.16 Ytterlihullet (Heap, 1975)

B1.11 RNC Zone B: Bjerka and Stor Akersvatn: Akersvanngrotta

The plan survey of **Akersvanngrotta** (Figure B1.17) shows it to be another atypical cave for the study area, as it has formed in metalimestones that are only gently folded and lie beneath a thin cover of mica schist (with surface dolines), forming an *interstratal karst*. The relict cave passages are predominantly horizontal, so that the cave has developed as a rectangular network on one level, presumably by utilising an orthogonal N–S and E–W joint system. Cave passages have a typical height of 2m and width of 1m. The mica schist roof is present throughout the cave. Passages commonly terminate at fills of silt, which, together with sand, also floors much of the cave. Speleothem comprises flowstones and 30cm-high columns. Where the bedrock is water-worn, the limestone has a striped, banded, appearance.

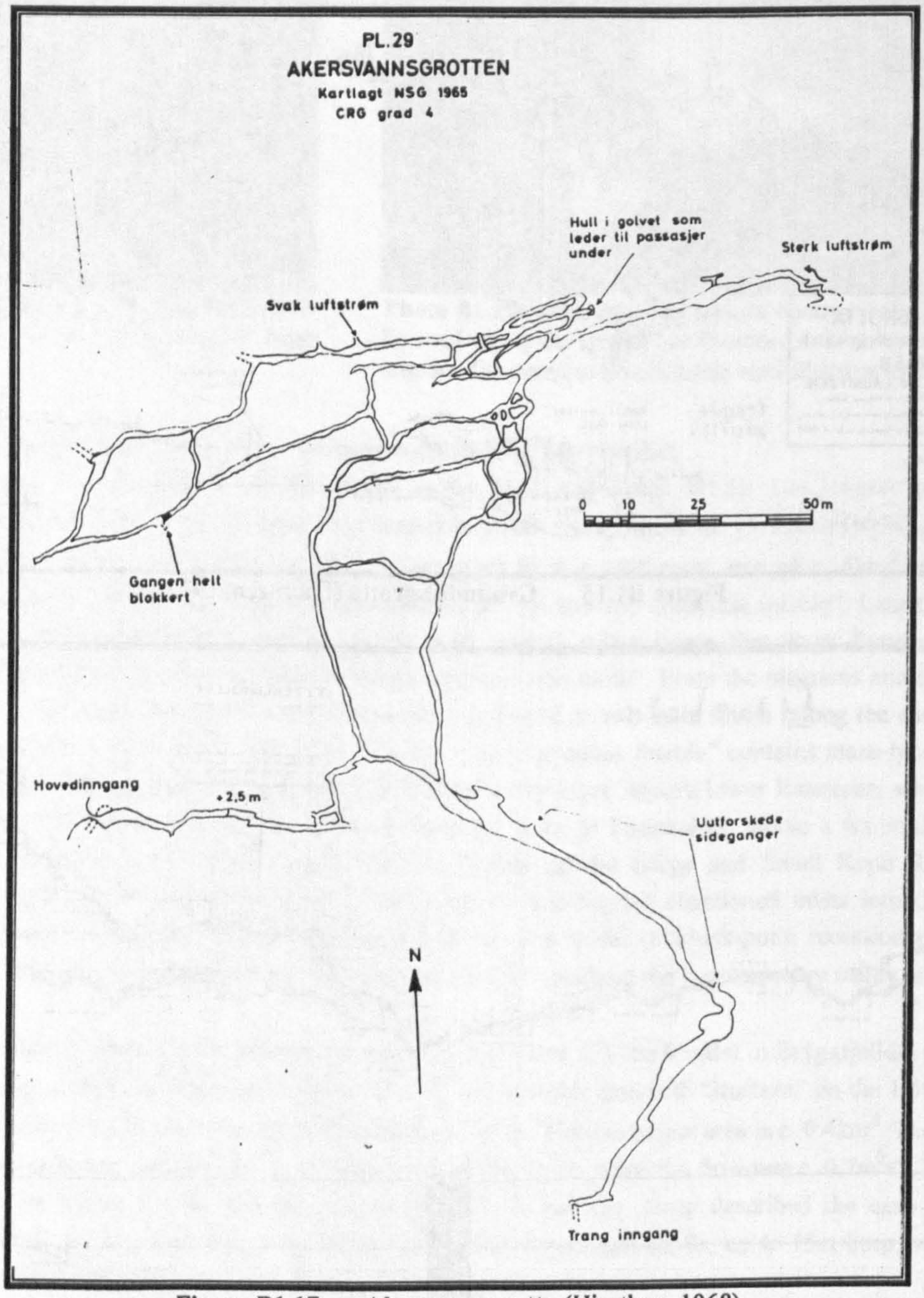

Figure B1.17 Akersvanngrotta (Hjorthen, 1968)

Akersvanngrotta appears to represent a drained phreatic maze cave, perhaps formed below the impervious roof in a way analogous to the formation of gypsum maze caves, but with a much lower passage frequency. Ford and Williams (1989, p278) referred to this type as a *single storey reticulate maze cave*. Palmer (1991) explained how this type of cave can form by diffuse recharge through a permeable caprock. The cave is only 100m from the large lake Stor Akersvatn, and only about 20m above its present water surface at c. 520m. This lake drains to the NW, via a narrow valley, and was ice-dammed up to c. 750m altitude during the Weichselian deglaciation, when the cave was waterlogged (Appendix D2.3). At present, the level of the lake is raised artificially by a hydroelectric dam, and

this has caused limestone and dolostone outcrops to be inundated, possibly including some short caves. However, **Tjuvhelleren**, the only cave candidate in dolomite (section 4.4.5), is at an altitude of 580m and is consequently not inundated at present. It is likely that it, and the cliff in which it is situated, formed when the lake Stor Akersvatn was above this level at various times during the Quaternary.

B1.12 RNC Zone C: Southern and Border Area: Baaagrotta and Labyrintgrottan

Baaagrotta is the longest cave in the Norwegian part of ZC (Figure B1.18). It lies in a fairly linear outcrop of creamy grey coloured, non-banded, metalimestone on Kongsfjell with a 60° strike and an average dip of (probably) c. 50°N. The survey, made by J. Lundberg in 1991, shows a rather simple system in which the active stream has migrated down-dip via ramp passages, leaving behind a higher-level relict passage. Except for the ramp passages, cave development is strike-aligned. Other shorter caves, farther along the strike, contain internal aquicludes of biotite and muscovite mica schist, and it seems likely that similar schist layers guided development in **Baaagrotta**.

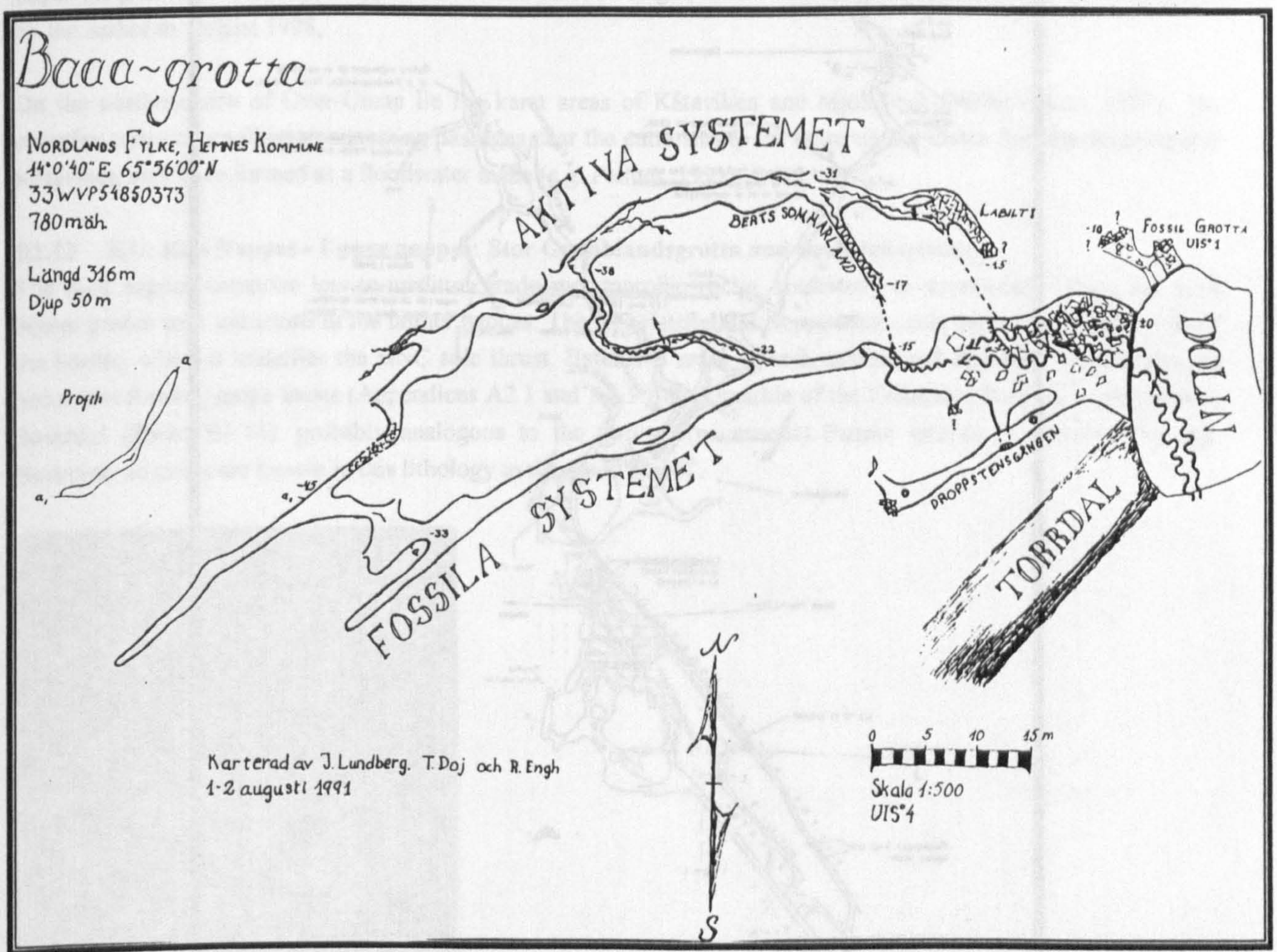

Figure B1.18 **Baaagrotta** (Lundberg, 1991)

Labyrintgrottan, one of the longest caves in Sweden, is at Mieseken on the southern shore of the large lake Över-Uman (Figure B1.19). It is contained within a long outcrop aligned N–S with a total limb length of about 44km, which extends south into Norway. The outcrop width is about 2km at **Labyrintgrottan**, creating the appearance of a classical karst. Glacial erosion has left a bare limestone hummocky platform, with dolines, clints, grykes, larger fissures and cave entrances at an altitude of about 710m. These are the best examples of limestone pavements in Sweden (R Sjöberg, University of Stockholm, pers. comm., 1998), although erratic boulders mask the pavement surface in places. A stream flows east, from the mica gneiss and mica schist slopes of Mieseken, to sink into the limestone. It flows underground for 2km northward, to resurge slightly lower, at the tree line. However, the situation is not quite as classical as it seems, as the limestone is quite folded, forming along-strike corrugations, with a wavelength of several tens of metres. The observed dip confusingly changes from 45°W to 45°E when traced across the strike. The hummocks form linear N–S ridge and gully structures. Most of the limestone is of the massive grey variety, with little banding visible in weathered outcrops, which can make the determination of dip difficult.

However, on the eastern side of the bench, brown, sucritic, limestones [HMC?] predominate. These have high mica content, with some quartz, and contain the entrances to short caves.

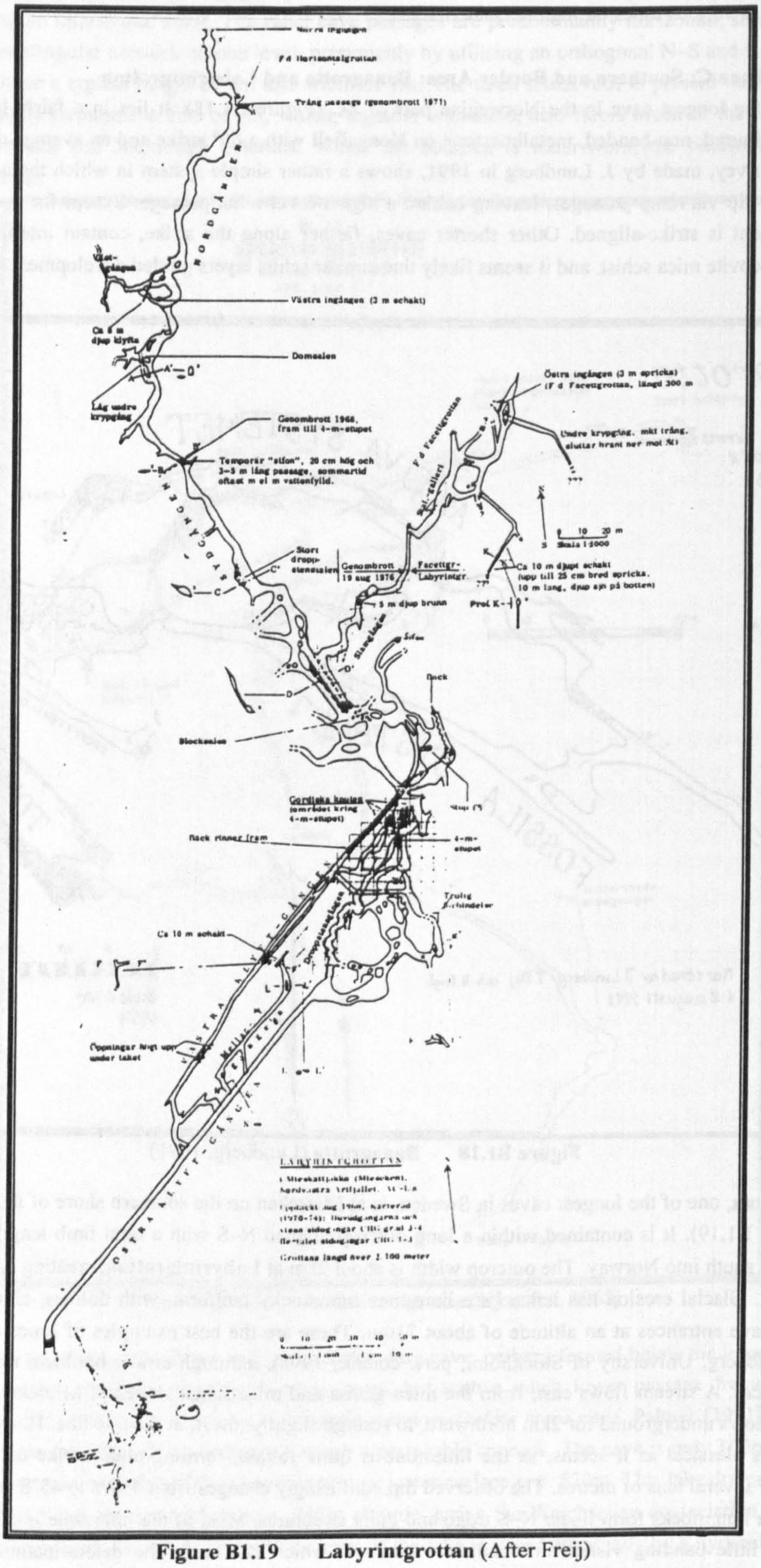

Figure B1.19 Labyrintgrottan (After Freij)

The plan survey of **Labyrintgrottan** was assembled over many years of exploration by Y. Freij. Its measured length is now c. 2600m, having been extended by diving through several upstream sumps at the SSF Mountain Camps in 1998 and 2000. The vertical range is only about 20m. Most of the cave is dry, because the active stream has abandoned most of the explorable passages. Hence, even without a published section, the cave can be seen to combine several horizontal along-strike passages that run to the NE, with sloping orthogonal passages that run to the NW. On the journey from the Facettgrottan entrance into the cave, progress is alternately along horizontal strike passages and via up-and-down ramps that follow the dip, or that follow joints that are normal to the dip. Throughout the cave, the limestone is of the massive grey variety, although towards the south it becomes more banded, with black layers roughly every 2cm. Commonly, these indicate a dip of 45°W. Very few aquiclude layers are seen within the limestone, but slabs of mica schist occur near the roof at the diver's sump at the end of the normally dry Östra Klyftgången. There are several sediments of very fine silt and sand in the cave, indicative of deposition at low flow. However, banks of clastic pebbles up to 5cm in diameter at the sump indicate the force with which water has flowed out in the past. The whole cave appears to have a phreatic origin, from observation of those parts of the cave visited by the author in August 1998,

On the northern side of Över-Uman lie the karst areas of Kåtaviken and Mjölkbäck (Wilhelmsson, 1997). The complex series of small interconnecting passages near the entrances to the large cavern **Östra Jordbäcksgrottan** at Kåtaviken may have formed as a floodwater maze (e.g. Palmer, 1991).

B1.13 KU: Køli Nappes - Upper nappes: Stor Grubblandsgrotta and Sotsbäcksgrottan

The Køli nappes comprise low-to-medium grade metamorphic rocks, commonly to greenschist facies, but with higher grades near intrusions in the higher nappes. The KU Hattfjelldal Nappe exists only on the Norwegian side of the border, where it underlies the HNC sole thrust. Extensive areas of both calcitic and dolomitic metacarbonates occur, not forming stripe karsts (Appendices A2.1 and A2.3.). Pink marble of the Unkerelva Formation crops out in Susendal (Photo B1.13), probably analogous to the famous (cavernous) Fauske marble in northern Norway. However, no caves are known in this lithology in the study area.

Photo B1.13 Pink marble in Susendal

The longest cave in the Hattfjelldal Nappe is **Stor Grubblandsgrotta** (Heap, 1968; Figure B1.20), 1890m long and 50m deep. It appears to have formed partly by successive captures of the Stor Grubblandselv, a relatively large stream with a catchment area of c. 19km^2. It runs southeastwards, from small glaciers on 1300m-high mountains of quartz diorite and trondhjemite at the edge of Z8, to flow over a waterfall on to KU (Photo 4.2). After flowing for 1.3km more over limestones and distinctive white dolostones (Photo 4.3), the water sinks at a pool below another powerful waterfall. The cave itself is visited via a dry entrance 150m south, below the west cliff of the continuing dry valley. It is formed in dark grey folded limestone that variously dips at 30–70°W, with a general strike direction

of N–S. The limestone is cut by many white calcite veins and mica schist layers, and white bedrock, which might be dolomite, occurs in at least one place.

The main streamway probably migrated downwards and westwards (utilising the dip) via six separate tributary passages, which all lead back towards the surface dry valley. Each major junction reached when exploring the cave to the Main Drain has the form of a tube that descends partly down dip, and partly aslant the strike, to reach the roof of a larger orthogonal passage. All six tributary passages are focused on the First Lake of the Main Drain, where they meet. Beyond the Main Drain is a complex maze of incompletely-explored distributary passages, many containing sumps even when dry conditions permit exploration of this part of the cave.

Stor Grubblandsgrotta is probably the most disturbing cave to explore in the whole study area, because of the volume of the stream and the fluctuating water levels. On the day of its discovery, the Grubblandselv overflowed its waterfall sink and continued down the dry valley to sink in the 80m-long **Øvre Grubblandsgrotta**. Inside the main cave, the roaring main stream reached a "temporary saturation level" some 15m above its normal level, as marked on the survey. As with most caves in the study area, **Stor Grubblandsgrotta** is entered very infrequently, the last recorded previous visit being in 1983. No sign of any earlier visit was observed during a brief reconnaissance as far as the Main Drain in August 1998, proving that the whole cave has filled to the roof at least once in the intervening period. As Heap (1968) remarked, the cave may have developed relatively quickly and mainly by mechanical erosion caused by the large flood-discharges of glacial meltwater carrying abrasive materials. Above the First Lake, much of the cave development is vadose, whereas below it, the distributary passages mainly developed phreatically, probably under a considerable hydraulic head. Presumably the various clastic sediments seen throughout the cave are of very recent origin. No speleothems were noted. It is not known how the water penetrates the massive white dolostone layer that lies between the sink and the upstream passages, but perhaps this rock is not a true dolomite (Appendix A2.4).

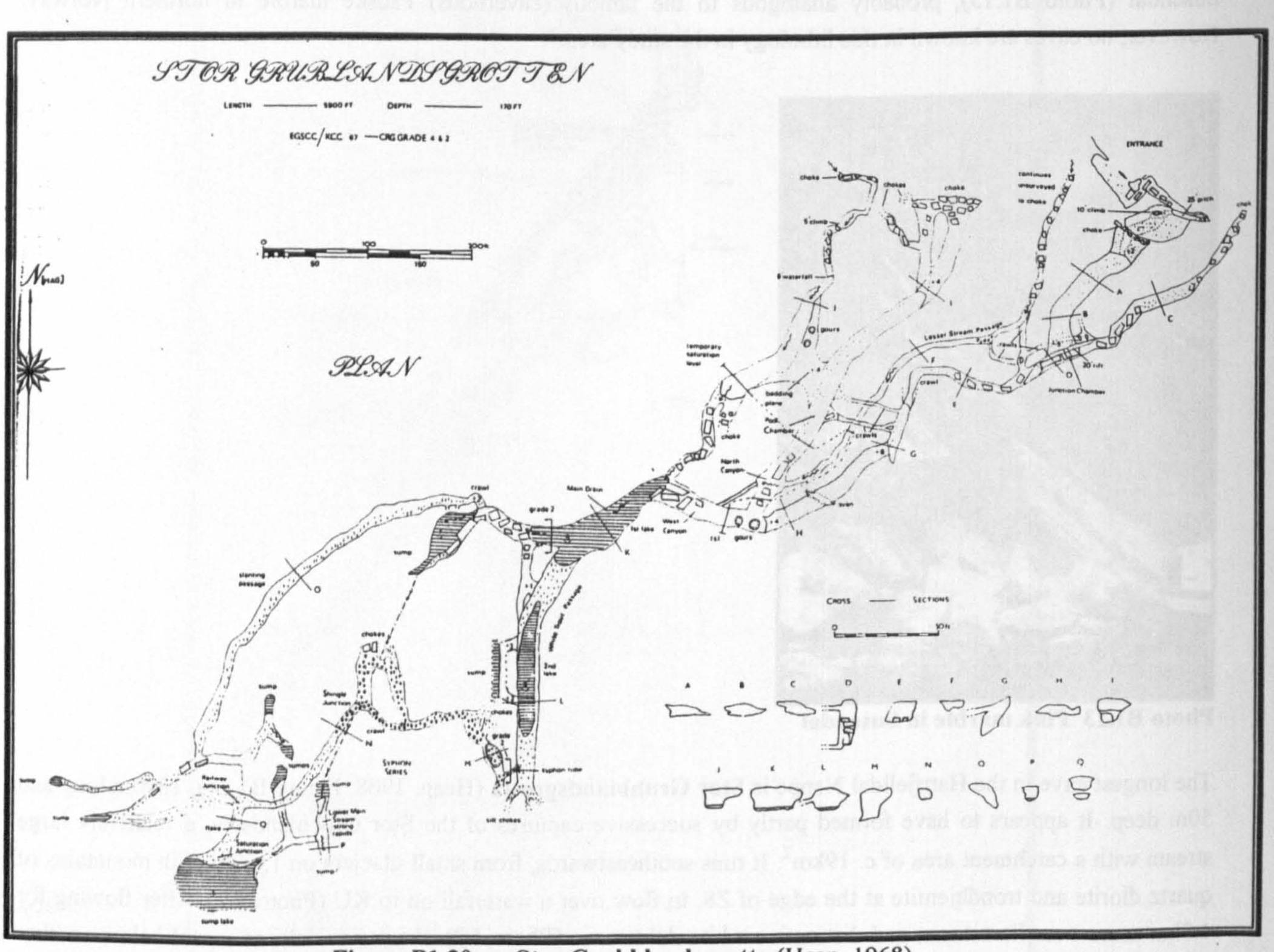

Figure B1.20 Stor Grubblandsgrotta (Heap, 1968)

Several caves occur in the very dark, lower metamorphic grade, limestones of the Akfjell Nappe in KU, also on the Norwegian side of the border. These lie north and east of the lake Favnvatn, and have E–W strikes. Despite long pecked blue lines on the 1:50000 Hjartfjell map, the underground drainage is rather superficial, and exploration is commonly halted at sumps. The longest cave here is the 260m-long **Skinfellvassgrotta** (Faulkner, 1987 and 1988). It is formed in an elongated ridge of dark grey limestone with platy fractures that dips at 70°S, and consists of a strike-aligned inclined rift down to water level, with sumps at each end. The whole karst drainage system is about 1km long, and deep sumps along the phreas can be seen at several other openings and short caves (Photo 9.1). Caves along underground tributaries of the nearby Tverrelv were shown to have formed along the strike, in anticlinal ridges of limestone (Sjöberg, 1979; section 5.7).

On the Swedish side of the border, the KU outcrops continue below the sole thrust zone of the RNC to the Rödingsfjäll karst area (Norberg and Petterson, 1988). This is some 10km south of the **Labyrintgrottan** outcrop in ZC. The sole thrust is commonly marked on the ground by a south-, or southeast-, facing cliff, above the under-thrust Jofjell Nappe of KU. In many places, a single metacarbonate outcrop forms the contact rock in the Jofjell Nappe; in other places this outcrop lies up to 500m south of the contact. Many short caves carry an underground stream that flows steeply down, along the strike of the thrust, below the mountain Rödingsfjäll. This underground drainage route commonly runs parallel to other surface streams. The longest cave system (235m) comprises **Övre** and **Nedre Glimåkragrottorna**, both being entered at the same collapse doline. Here the limestone dips under the thrust at 30°W, and has a varied lithology. Mostly it is dark blue / grey in colour, but a thin yellow / brown layer occurs half way up the 6m-high passage that leads in to the upper cave entrance and also marks the top of a waterfall some 10m inside. The lower cave has formed entirely in the lower layer of blue / grey limestone, which becomes almost black in its tall and narrow entrance rift, closely resembling the limestone in **Skinfellvassgrotta**.

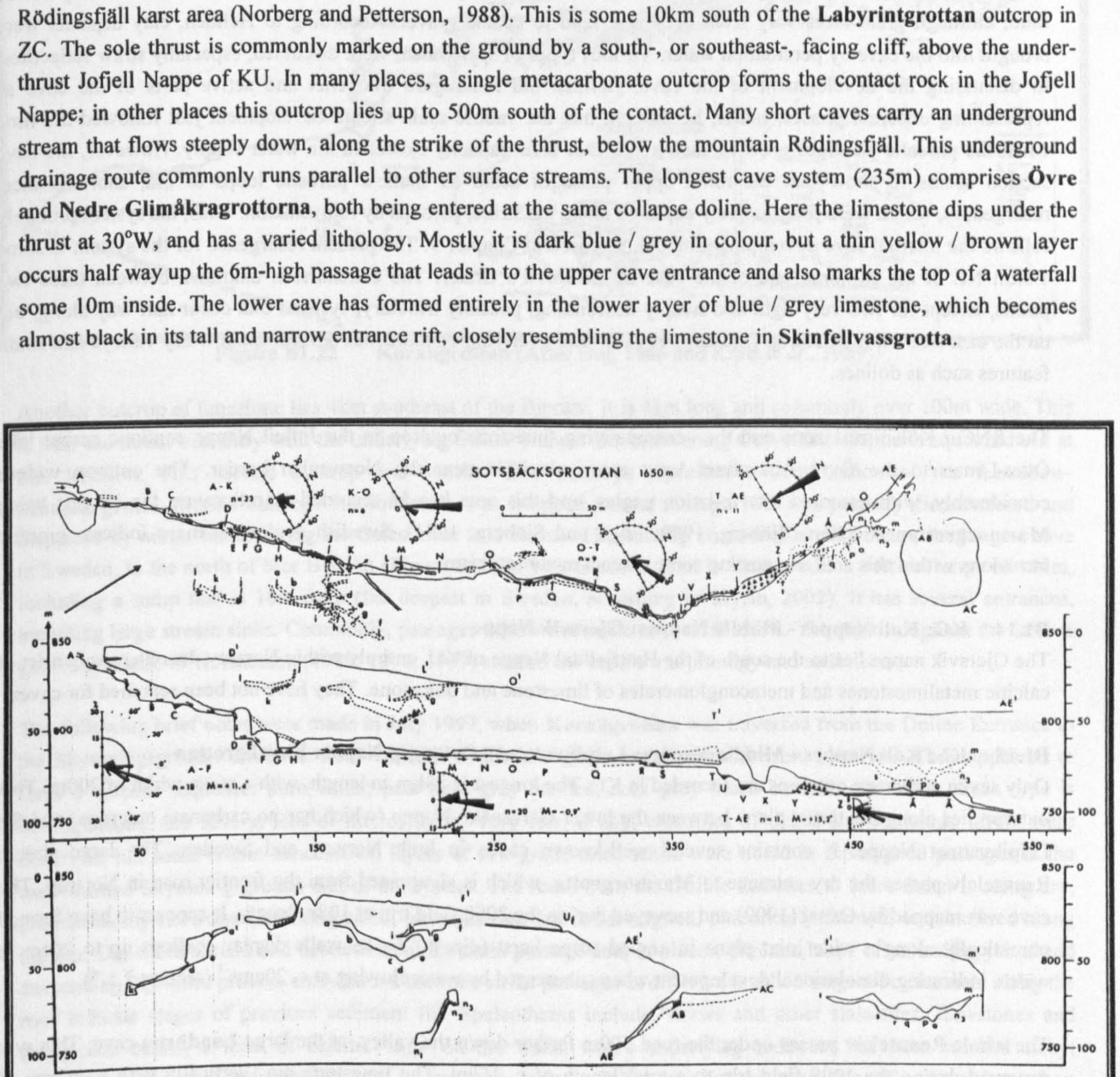

Fig. 4. Sotsbäcks Cave. Dotted lines indicate passages in a different orientation to the master passage A-AE. The rose diagrams above indicate the strike of the beds for the distances A-K, K-O, O-T and T-AE. The rose diagrams below indicate the dip of the bedrock in the direction of the fold axes for the distances A-F, F-T and T-AE. n denotes for the number of measurements and M the mean values of the dip. The arrows indicate water streams and the triangles collapse accumulations (Helldén 1974 b).

Figure B1.21 Sotsbäcksgrottan (Helldén, 1975)

Sotsbäcksgrottan, the second longest cave in KU (Figure B1.21) lies several kilometres to the NE, along the thrust zone and in the same Jofjell Nappe limestone outcrop. This cave, 1850m long and 110m deep, was studied in a thesis (summarised by Helldén, 1975) when it was Sweden's longest explored cave. A powerful stream flows along the large main passage of the cave in spring and summer, from a catchment area of c. 2.5km², which generally follows the strike to the NE. Helldén noted that the limestone is deeply folded, so that the dip fluctuates from 10°W to 50°W, with a mean dip of 35°W. The cave also has several relict passages that are above, and offset to the east (i.e. up dip), of the streamway. Helldén mentioned two main passage forms for these abandoned routes: high and narrow fissures, and phreatically-formed, elliptically-shaped, passages along bedding planes. The cave also contains extensive areas of collapse, which have formed enlarged chambers with vaulted roofs.

Large accumulations of allochthonous sediments occur, especially in the relict passages. These are commonly coarse sand, although grain sizes vary from very fine sand to coarse gravel. According to Helldén, clay deposits were brought into the cave by percolation water. Various types of speleothem were discussed, especially straw stalactites. In discussing the development of the cave, Helldén did not regard the relict and active parts of the cave as representing different phases; rather, he thought that the vadose main stream development just followed the time when the phreatic passages grew to such a size that their capacity exceeded the water supply. However, the cave section seems to show that the relict upper passages acted as shallow phreatic loops to old, short-distance, resurgences, which were progressively captured along the strike, perhaps by rejuvenation. Thus, the system probably follows the internal cave development model proposed in Chapter 9. The present resurgence for the system is some 1.5km NE of the explored end of the cave at the Devil's Crater. The endokarst is unknown between these two points, except for two very tight and steeply-descending, possibly tributary, systems that occur half way along, but on the east side of, the outcrop (Sjöberg, 1991b). The overlying exokarst has several shallow dry valleys and small features such as dolines.

The RNC / Köli thrust zone and the accompanying limestone outcrop in the Jofjell Nappe continue across lake Över-Uman to the Övre Ältsvattnet karst area, which is near the Norwegian border. The outcrop widens considerably, with assumed low foliation angles, and this area has 54 recorded (short) caves, the longest being **Marmorgrottan** at 320m (Sjöberg, 1980; Engh and Sjöberg, 1981). Swedish geological maps indicate granitic intrusions within this area, suggesting some contact metamorphism.

B1.14 KG: Køli Nappes - Middle Nappes: Gjersvik Nappe

The Gjersvik nappe lies to the south of the Hattfjelldal Nappe of KU, entirely within Norway. Its outcrops consist of calcitic metalimestones and metaconglomerates of limestone and dolostone. They have not been searched for caves.

B1.15 KL: Køli Nappes - Middle Nappes: Leipikvattnet / Orklump Nappe: Korallgrottan

Only seven carbonate outcrops are recorded in KL. The longest is 23km in length, with a mean width of 200m. This outcrop lies along the thrust plane between the lower Gelvenåko Nappe (which has no carbonate outcrops) and the Leipikvattnet Nappe. It contains several well-known caves in both Norway and Sweden. The large stream Rennselelv passes the dry entrance to **Marmorgrotta**, which is signposted from the frontier road in Norway. The cave was mapped by Oxaal (1909) and surveyed during the 2000 field trip at 108m length. It appears to have formed phreatically along a wide joint plane in angled stripe karst (dip=80°S). Its walls display scallops up to 20cm in width, indicating dissolutional development when submerged by water flowing at c. 20cms^{-1} (section 3.1.7).

The whole Rennselelv passes under the road 500m farther down the valley, at the large **Landbrua** cave. This was surveyed during the 1998 field trip to a total length of c. 150m. The limestone dips vertically with a change of lithology across the strike, as seen at the cave entrance, which is 6m wide and 2m high. On the south side of the entrance, the limestone is very banded, with pale grey and blue grey colours. There are then some white bands before the limestone becomes more massive on the north side. Inside the cave, the roof forms a phreatic arch, without breakdown. Scallops 2–3cm in diameter point downstream across the whole width of the roof, indicating fast water flows at the latest stage of phreatic development. The cave is terminated by a large deep sump that has been dived to emerge at a rising on the south side of the road (Photo D1.40).

The outcrop continues NE along the intermittently-dry valley of Langslåtten to the Swedish border, where it forms the nationally-famous Bjurälv karst area. The discovery of **Övre Bjurälvsgrottan** was mentioned in section 1.6.4, and the studies about the deep dolines and other karst features are referenced in section 1.7.2. The limestone remains steeply dipping; a dip of 80°S was noted in **Svenoniusgrottan** during the 1997 field study trip. The low-grade metalimestone displays very pale blue / grey bands and is massive in appearance, with few impurities.

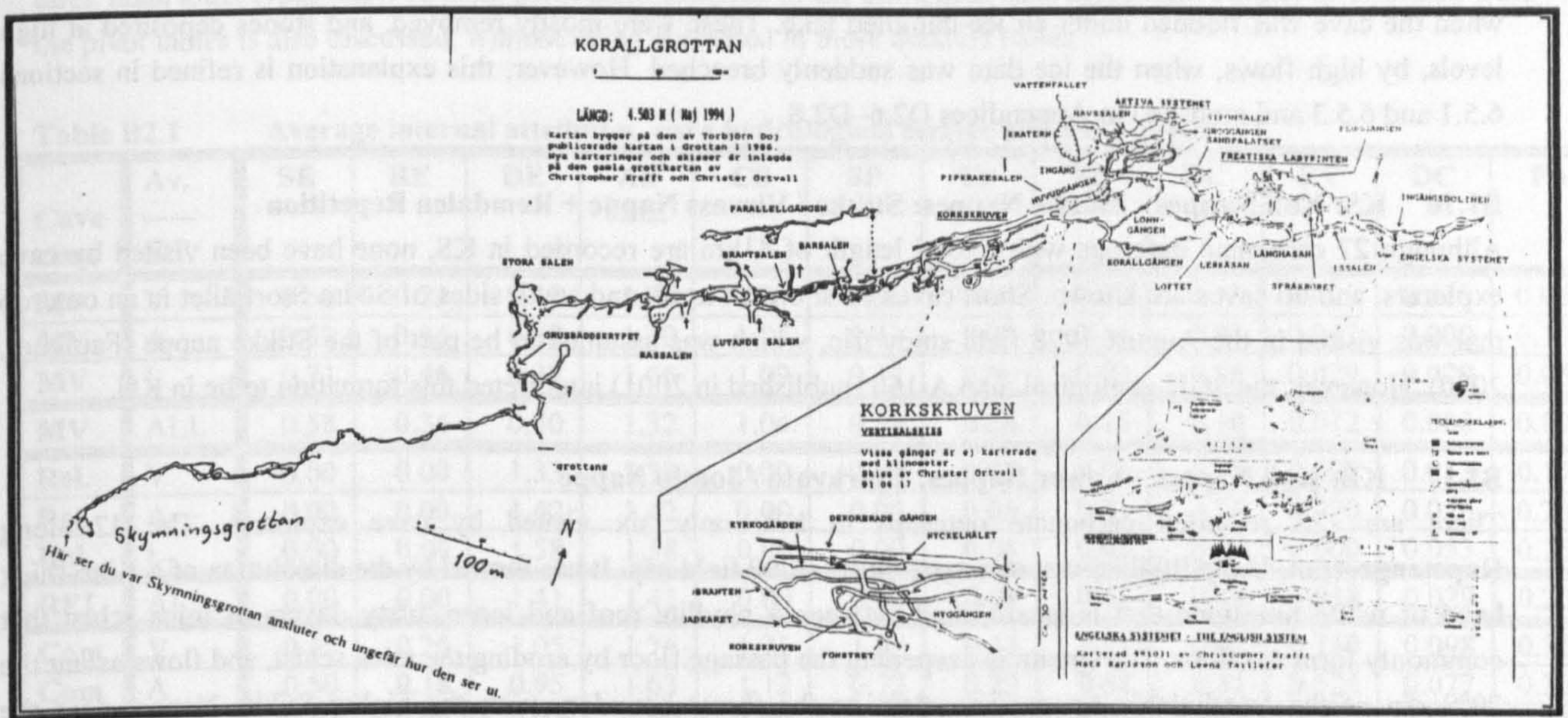

Figure B1.22 **Korallgrottan** (After Doj, 1986 and Kraft *et al.*, 1989)

Another outcrop of limestone lies 4km southeast of the Bjurälv. It is 4km long and commonly over 100m wide. This is near the thrust boundary with the underlying Stikke Nappe: the intervening Gelvenåko Nappe is squeezed out at this location. This second outcrop and another five outcrops represent a continuation of the **Landbru–Marmorgrotta**–Bjurälv outcrop. The limestone was wrapped around through 180° and partially dismembered and displaced by minor faults during the Caledonide fold events. The outcrop contains **Korallgrottan**, the longest cave in Sweden, to the north of Stor Blåsjön (Figure B1.22). This is now 5.6km in length, with a vertical range of 144m, including a sump that is 16m deep (the deepest in Sweden, according to Myrin, 2002). It has several entrances, including large stream sinks. Commonly, passages follow the strike at several levels. The dip throughout the cave is generally about 45°N. Isacsson (1989; 1994; 1999) studied the cave's morphology and sediments.

The following brief notes were made in July 1997, when **Korallgrottan** was traversed from the Doline Entrance to the Skymningsgrottan Entrance. Four varieties of the low-grade metalimestones were observed. They appeared to form a vertical sequence: pure white; pale blue–grey banded; dark grey–black banded; and black. Each type is homogeneous, and several tens of metres thick. Very few, if any, examples of dykes and aquiclude layers were observed, but some within-band brown layers of low-grade mica schist were noted in dip-aligned passages at the well-washed Skymningsgrottan end of the system. The route from the Doline Entrance to Stora Salen is along dry, predominantly horizontal, walking-sized, passages that are strike-aligned, phreatically-formed, and inclined along the dip. Dip-tubes ascend and descend from the main passage and, in places, phreatic loops of ascending joints and descending dip-tubes provide connections between strike passages at different levels. Paragenetic channels along the roof indicate stages of previous sediment fill. Speleothems include: straws and other stalactites; flowstones and stalagmitic banks; a form of calcitic 'cup' on the walls, where underlying sediment has been washed away; concretions of gravel and pebbles; and, in one area, raised calcitic deposits that resemble coins have formed on several near-horizontal blocks in an almost regular pattern. The route out from Stora Salen to the Skymningsgrottan Entrance is along a small and awkward, ascending, vadose streamway, with, in one place, a low static duck. From the survey section, most of the through-route passes well above, and to the south of, the mainly vadose "Active System", which lies between Stora Salen and Sifonsalen. The cave thus seems to represent another example, in dipping limestones, of passage migration down-dip during development, when at least one higher and older resurgence (Doline Entrance) was abandoned. However, the cave morphology is in reality much more complex than

this in the eastern part, as lower passages have developed under phreatic conditions both north and south of the high-level through-route, i.e. both down-dip, and in lower dip-planes.

According to Isacsson (1994), the relict phreatic passages developed before a higher landscape (which provided a larger catchment area) had been eroded away by glacial action. Large quantities of rocks fell from the walls of the main passage during deglacial earthquakes, and varved sediments were laid down at the end of the last glaciation, when the cave was flooded under an ice-dammed lake. These were mostly removed, and stones deposited at high levels, by high flows, when the ice dam was suddenly breached. However, this explanation is refined in sections 6.5.1 and 6.5.3 and modified in Appendices D2.6–D2.8.

B1.16 KS: Køli Nappes - Middle Nappes: Stikke / Virvass Nappe + Remdalen Repetition

Although 27 carbonate outcrops with a total length of 41km are recorded in KS, none have been visited by cave explorers, and no caves are known. Short caves exist on the north and south sides of Södra Storfjället in an outcrop that was visited in the August 1998 field study trip, which was assumed to be part of the Stikke nappe (Faulkner, 2000). However, the SGU geological map Ai160 (published in 2001) interpreted this formation to lie in KU.

B1.17 KB: Køli Nappes - Lower Nappes: Bjørkvatn / Joesjø Nappe

There are 122 recorded carbonate outcrops in KB, only six visited by cave explorers. The 47m-long **Rapstengrottan**, V. Fjällfjället, was surveyed on the 2000 field trip. It has formed by the dissolution of a 1.2m-thick band of white limestone that is sandwiched between a phyllite roof and loose, platy, layers of mica schist that commonly form the floor. The stream is deepening the passage floor by eroding the mica schist, and flows aslant the 20°S dip of the 'sandwich'. An outcrop close to the thrust boundary with the higher Stikke Nappe, near the Sjliengojukke stream (Photo D1.41) and below the mountain Gelvenåko, was visited in August 1988. The dip is commonly 20°N. Two types of limestone were seen: a 2m-thick calcitic layer, banded with pale grey and white colours, and an overlying thinly-banded brown layer that attained a surface width of about 20m. Whereas this rock looked like mica schist, in places it also gave a vigorous reaction with dilute HCl. The grey limestone was followed for some distance along an outcrop only 5m wide. The 25m-long **Renbenshålet** is in this vicinity. Several small dolines and one small rising were also noted. Four outcrops on the mountain Daunentjakke (1291m) were visited in August 1998. These highly-folded limestones have a brown platy micaceous appearance, and give only a faintly visible reaction with dilute HCl. The dip varies from 45°W to vertical. The SGU map indicates one of the outcrops as a fossil locality. The only karst features seen were shallow dolines on the NE lower slopes.

B1.18 SU: Seve Units

The reducing trend of metamorphic grade is reversed in the Seve nappes, with rocks of medium to high grade. Some 84 small outcrops are recorded in SU on the SGU maps, but they do not distinguish between carbonates and calc-silicates for any Seve nappes, and few outcrops have been visited by cave explorers. The area of two mapped tiny outcrops at Blomhöjden was visited on 13 August 1998. No carbonate outcrops and no karst features were seen. There are no known caves in nappes below the Køli Nappes in the study area. The absence of karst caves in the Seve Nappes also holds for the few Seve carbonates that occur in northern Norway, although such caves occur in Sweden to the south (Appendix D6.1.3).

B1.19 SB: Seve Belts (Western, Central and Eastern)

A total length of only 36km in 39 outcrops is recorded in SB. Visits to three sites in August 1998 failed to identify carbonate bedrock.

B1.20 ML: Middle and Lower Allochthons

There are no mapped carbonates in the low-grade Middle Allochthon. The Lower Allochthon has 15 dolostone and 6 limestone outcrops of Ordovician (Tremadoc) age in the study area, but no known caves, although they do occur to the south in both Norway and Sweden (Appendix D6.1.3). During the August 1998 field study trip, one dolomite outcrop was positively identified, but without seeing any karst features. One Ordovician limestone and two other dolomite outcrops were sought but not identified.

APPENDIX B2 INTERNAL CAVE ATTRIBUTES

This Appendix discusses the various internal attributes recorded in the cave databases (as defined in Appendix C2.2), and reviews the influence that the external attributes (section 5.3) and the hydrological cave classes (section 5.4) have on them. Table B2.1 gives the mean values of the internal attributes for each of the cave classes and the three main karst types, derived from pivot table analyses of the combined cave databases. Further information from the pivot tables is also discussed, without being presented in more detailed tables.

Table B2.1 Average internal attributes, cave hydrological classes and karst types

Cave class	Av. —— KT	SE	RE	DE	All ents.	CS	SP	Ch	Sh	BC	RV	DC	FS
MV	V	0.56	0.23	0.47	1.26	1.01	0.36	0.04	0.22	0.17	0.000	0.013	0.051
MV	A	0.59	0.34	0.37	1.30	1.05	0.42	0.03	0.14	0.07	0.017	0.000	0.101
MV	L	0.71	0.46	0.37	1.55	1.09	0.37	0.06	0.03	0.06	0.029	0.029	0.057
MV	ALL	0.58	0.34	0.40	1.32	1.04	0.39	0.04	0.15	0.10	0.012	0.008	0.078
Rel.	V	0.00	0.00	1.33	1.33	0.00	0.00	0.03	0.63	0.13	0.027	0.013	0.173
Rel.	A	0.00	0.00	1.42	1.42	0.00	0.00	0.05	0.41	0.16	0.020	0.026	0.209
Rel.	L	0.00	0.00	1.58	1.58	0.00	0.00	0.08	0.08	0.29	0.000	0.053	0.263
REL	ALL	0.00	0.00	1.41	1.41	0.00	0.00	0.05	0.43	0.18	0.018	0.029	0.204
Com	V	0.45	0.26	1.05	1.76	1.21	1.02	0.31	1.21	0.42	0.110	0.098	0.305
Com	A	0.50	0.18	0.95	1.63	1.12	0.72	0.22	0.61	0.31	0.125	0.077	0.327
Com	L	0.59	0.28	0.93	1.80	1.09	0.78	0.41	0.57	0.22	0.222	0.074	0.315
CC	ALL	0.50	0.21	0.97	1.68	1.13	0.80	0.27	0.74	0.32	0.139	0.083	0.322
All	V	0.34	0.17	0.95	1.46	0.76	0.48	0.13	0.69	0.24	0.047	0.043	0.179
All	A	0.36	0.16	0.95	1.47	0.74	0.42	0.12	0.43	0.20	0.065	0.042	0.233
All	L	0.45	0.24	0.97	1.66	0.76	0.43	0.21	0.28	0.20	0.102	0.055	0.228
ALL	ALL	0.37	0.18	0.95	1.50	0.75	0.43	0.13	0.48	0.21	0.066	0.045	0.217

'All' includes caves in karst types C and X.

B2.1 Cave entrances (SE, RE and DE)

Common cave entrance positions within the landscape were discussed in section 4.4.2. Cave entrance areas are commonly not much larger than continuing passage sizes, although larger chambers that measure up to 5m high by 5m wide (or more) are found in some entrances. These almost invariably display various degrees of frost shattering, so that it has sporadically been necessary to dig through loose rocks with dimensions up to one metre to gain first access to a cave entrance, at any altitude. The possible processes that enlarged such cave entrances are discussed in sections 8.8.2, 8.8.3 and 8.9.4.

Three entrance types are distinguished: sink entrances (SE), resurgence entrances (RE) and relict (dry) entrances (DE). The cave databases and summaries record the numbers of these entrance types for each cave. The total numbers are: SE 323; RE 160; and DE 840; i.e. 0.37, 0.18 and 0.95 per cave, giving a total of 1.50 entrances per cave. These means are very consistent. The DE: SE: RE rank order of entrance types is the same for *all* 'inner' zones, cave types a–h, karst types V, A and L, cave locations and glacial situations (except that situation C has only one SE, and the situation U cave fragments are relict). Combination cave entrances have the same ranking, but mainly vadose caves have more SE than DE, and relict caves only have DE. Thus, the great majority of entrances are relict, with no water flow through them in normal conditions. As there are 662 cave streams in the study area, the mean number of cave streams per cave is only 0.75, of which only about half enter caves directly at an open sink entrance. There are only half as many resurgence entrances as sink entrances, because *all* active caves in the area are ultimately dendritic: there is not one reported case of a karst system that feeds widely-separated risings in normal flow conditions.

There is no systematic variation of any entrance type across the zones. However, there are some very consistent, but small, trends for karst type. For mainly vadose caves, as foliation dip reduces (V:A:L), SE and RE both increase,

and DE primarily decreases, but their total means still increase. The DE trend is reversed in relict caves. Combination caves reflect this 'competition', because their SE increase and DE decrease, whereas RE show no trend. Taking all caves together, entrances of all types commonly increase slightly as foliation dip reduces. SE and RE both increase slightly if R=1 or T=1, whereas DE means decrease. This finding agrees with the 'favouring' of vadose over phreatic development by either R=1 or T=1 (section 5.5.4).

Caves in cave locations R, S and W have less SE (0.23, 0.26 and 0.33) and RE (0.06, 0.12 and 0.13), and, correspondingly, more DE (1.37, 1.26 and 1.05), because of the predominance of relict caves over mainly vadose caves in these locations (section 5.5.5). These trends are reversed for the small samples of mainly vadose caves in these locations. Locations R and S have the largest numbers of total entrances per cave (1.66 and 1.64). SE show a slight increase with higher glacial situations, RE have no trend, and DE show a slight decrease on the eastern sides. SE and RE are always greater in the western glacial counterparts, whereas DE are always greater to the east (especially at GS=E rather than D). The total numbers of entrances are largest at GS=E (1.75) and smallest at GS=S and C (1.16 and 1.27). Entrance frequencies show greater variations when cave location and glacial situation are considered together.

The large number of entrances per kilometre of cave passage (17.7) means that there is one entrance for every 56.6m of passage, arising from the large number of very short caves in the study area. However, many caves possess more than one entrance. It might be expected that the number of entrances would generally increase with cave length, as postulated by Curl (1958) for his study areas in sedimentary limestones in the USA. However, this may not be the case, because the caves with the largest number of recorded entrances (ten, all DE) are **Shelter Cave** (Z4, relict) and **Murevardolabyrinten** (KU, combination), which are only 78m and 275m long. The relict cave with the third-most entrances (six) is **Balcony Cave** (Z3, 175m). Two combination caves also have six entrances: **Roaring Cave** (Z5, 522m) and **Mellanselvgrotta** (Z7, 280m). In fact, SE and RE show no increasing trend with cave type complexity (a–h), ranging between only 0.26–0.44 and 0.06–0.29. This null trend is also followed for both MV caves and combination caves, all karst types, all cave locations (except that SE tend to *increase* with cave type at CL=R) and for all glacial situations (except that RE increase for the lower situations GS=C, D and G). The SE and RE means of both active entrance types are therefore commonly independent of cave length. This is understandable, as few caves have more than one SE, and the maximum number of RE is commonly one. On the other hand, DE *do* increase fairly smoothly with cave type a–h, from 0.65–2.13, and increase similarly within each cave class. Therefore, only the DE increase with length agrees with Curl's postulate. Neither of two other postulates by Curl (1958), i.e. that a) there could be 20 times as many caves without entrances as with entrances (for caves over 15m long), and b) most caves with entrances have already been recorded, are likely to hold in *this* study area. The non-autogenic nature of the karst, and the observation that cave entrances are commonly of similar dimensions to their internal passages, suggest that large proportions of the caves along each part of each visited carbonate outcrop have indeed been entered and recorded. However, because only 14% of the total mapped outcrop length has been visited, some 86% of all caves may remain to be recorded (section 5.2.3).

B2.2 Cave streams (CS)

The maximum numbers of cave streams that flow in each cave during normal summer discharges are shown in the two Cave Databases. These include tributaries, roof inlets, impenetrable inlets and presumed flows at apparently-static sump pools. The overall mean of 0.75 cave streams per cave varies non-systematically from 0.5 to 1.0 across the 'inner' zones, and hardly shows any overall variation with karst type. A slight increase in CS for MV caves as foliation dip reduces agrees with the corresponding increase in SE and RE (Appendix B2.1). However, combination caves show a reduction in CS as KT reduces. The CS means for caves with R=1 or T=1 are slightly higher at 0.80 or 0.93, again agreeing with 'vadose favouring'. Cave locations F and P seem to favour cave streams slightly, as their means are 0.85 and 0.82, whereas R and S have slightly less (0.55 and 0.65), agreeing with their reduced SE and RE. Mean CS increases for higher western glacial situations but shows no trend for eastern situations, and the counterpart rankings are inconsistent.

The cave with the greatest number (five) of cave streams is **Korallgrottan** (KL), which is also the longest cave. Five caves across the study area (with cave types from b–h) each have four cave streams, including one that is a

mainly vadose cave. Ignoring relict caves, which do not have cave streams, the mainly vadose and combination caves have means of only 1.04 and 1.13 cave streams per cave, showing that the overwhelming majority of *active* caves have just one stream. This suggests that, in nearly all cases, *vadose* cave development has occurred under a flow regime similar to the present one. In contrast to the independence of SE and RE with cave type (Appendix B2.1), the number of *cave streams* per cave does increase fairly smoothly with cave type a–h, from 0.64–1.38.

As mentioned in sections 4.2 and 4.4, the geomorphology of the study area is mainly non-karstic because of the small percentage of outcropping carbonate rocks, even at a local valley scale. Hence, most of the catchment areas for most of the caves are on non-carbonate bedrocks. Within the active stream caves, a high proportion of the water that flows back to the surface consists of the *allogenic* recharge water from the catchment areas upstream of the cave sink points. The catchment areas directly over the cave systems vary from c. 0.2km^2 for the longest cave, **Korallgrottan** (which has a total catchment area of c. 3.5km^2), down to the vanishingly small. Hence, the contributions of *autogenic* waters to the contemporary development of active stream passages must be very small. However, the presence of dolines above cave systems shows that percolation water does enter the subcutaneous zone and epikarst, and may drain in to any underlying caves. The volume of this autogenic recharge is highest during and after heavy rain, and during the spring melt of the overlying snow and ice, when it is concentrated via joints and, especially, via the dolines that always drain underground (section 4.4.3). Thus, autogenic recharge makes a disproportionate (and perhaps the only) contribution to present passage enlargement in those higher levels of the cave systems that have been abandoned by down-cutting vadose streamways. Autogenic recharge also provides the percolation water that forms those few speleothems that occur. For most active caves in the study area, flow-through times are very short, because of short cave lengths and / or high hydraulic gradients. One of the longer systems (**Ytterlihullet**, ZA) was tested from sink to rising (horizontal distance 840m, VR 203m) with fluorescein, which passed through in only three hours (Heap, 1975).

The annual weather cycle and the meteorological effects on caves and cave environs are discussed in Appendix A4.1. Very few caves in the study area have been studied at all during winter conditions. Only the limited observations of Helldén (1973) about temperature and precipitation for **Sotsbäcksgrottan** (KU) are known from Sweden. Øvstedal (1991) gave information from data loggers about the **Sirijordgrotta** (Z4) stream waters for a 16 month period. The flow rates measured at the **Sirijordgrotta** spring show that from about early July 1988 until the end of November 1988, a low flow rate of about 20Ls^{-1} was re-established within a week of a non-repeated flood pulse. From December 1988 until the end of April 1989, the recovery period extended to about two weeks and from early February to mid-April 1989, flow rates remained commonly at a minimum 20Ls^{-1} level, presumably due to the melting of some winter snow. From the onset of the spring-melt in May 1989, the flow maintained a rate from 100–200Ls^{-1} between flood pulses, but with diurnal variations of about 50Ls^{-1}. This pattern continued until the end of June 1989, when presumably all the snow in the catchment area had melted. About 40 flood pulses giving discharges up to 1200Ls^{-1} were recorded in the 12 months from July 1988 to June 1989, with the flooding frequency peaking between mid-September 1988 and the end of January 1989.

A very approximate calculation based on these data reveals that **Sirijordgrotta** discharges at a mean annual rate of 100Ls^{-1}, or some 3.4x10^{6}m^{3}a^{-1}. This is made up by: 1.6 (flood events); 1.2 (snow melt); and 0.6m^{3}a^{-1} (base flow). The Cave Database shows a 2km^2 catchment area for the cave, giving an annual run off of 1700mm. Addition of an estimated evaporation rate of 300mma^{-1} (Appendix A4.1) gives an estimated annual precipitation of 2000mm. This is a very reasonable result, as it is equal to the 2000mm for Hattfjelldal (also Appendix A4.1), and thus gives an approximate confirmation of the estimated catchment area. [However, Øvstedal, 1991, p63, measured an area of 1.6km^2 for the catchment, from a map at the scale of 1:5000].

Extremely high floods are common throughout the caves of the study area, and there is evidence that, in some caves, all known passages can fill to the roof. During these events, sediments can move considerable distances, block individual passages, and seal or open cave entrances. The sink entrance to **Øvre Landegrotta** (Z2) was blocked by debris between 1983 and 1997. In **Etasjegrotta** (Z4), the *Hole in the Wall* in the streamway is now blocked by a boulder, and the high-level route to the south end of the cave is choked by sediments. These changes occurred between 1986 and 1998. The sink for **Gjeitvikgrotta** (Z6) was described as "at the foot of a low cliff" (Whitehouse,

1969, p3). In 1997, this cliff was 12m high. Caves at Gullmoen (Z6) mentioned by Helland (1907, p467) could not be found in 1998, and were not known locally. In **White Cave** (Dunnfjell, Z6), large blocks above the pitch, observed in 1997 (G. Newton, cave explorer, pers. comm.), were found to be shifted downstream in 1998, so that cascades over boulders in the lower streamway were replaced by a 3.5m overhanging pitch. At **Stor Grubblandsgrotta** (KU), the lower passages, which were explored in 1967 and 1968, were choked by sediment in 1979, thus preventing access to the lower stream passages (D. Heap, cave explorer, pers. comm.). As noted in Appendix B1.13, all signs of previous visits to this cave were removed by floods before 1998. Whilst it is possible that just one large storm over a wide area between August 1997 and June 1998 caused changes in up to four of the caves mentioned above, it seems more likely that flood events of a size that can open and close cave entrances, and move large amounts of sediment underground, are a regular occurrence. In these respects, some of the active caves in the study area may be compared to the *floodwater caves* of Palmer (1972).

B2.3 Sump pools (SP)

The numbers of sump pools in each cave (where the roof of a passage normally descends below water level in July and August) are recorded in the Cave Databases. A sump that has been visited at each end is shown as two sump pools. The total number is 384, or 0.43 sump pools per cave, which is much less than one sump pool per cave stream, giving even less than one complete sump per cave stream. The mean varies non-systematically across the inner zones from 0.17–0.72, but (as for cave streams) it is almost constant for the different karst types, except that combination caves in vertical stripe karst have a high mean SP of 1.02, in agreement with their higher mean CS, and for both R=0 or 1. Caves with T=1 have a slightly higher mean (0.52). As expected, caves in location F have more sump pools (0.64), whereas caves at CL=P and W have relatively few (0.30 and 0.23). There is also little variation in sump pools in each glacial situation, except that the lower eastern situations E and H have larger means (0.65 and 0.71).

The cave with the highest number of sump pools (15) is **Blåfjellgrotta** (Z5). These all occur in the course of its powerful stream, along a probably-immature stream passage. This can be visited at several places by descending connections from higher-level phreatic crawls and passages. **Stor Grubblandsgrotta** (KU) has eight sump pools that are all situated in the so-called "saturation zone" of the cave. **Labyrintgrottan** (ZC) has six, **Sirijordgrotta** (Z4) and **Korallgrottan** (KL) have five each, and **Ytterlihullet** (ZA) has four sump pools. Some 15 caves have three sump pools each. Most of the remaining active caves of the study area have just one sump pool, which is situated typically at the lowest explored point of the system. Hence, the incidence of sumps along the active streamways of the central Scandinavian caves is probably comparable with other caving regions of the world.

The caves mentioned above with four or more sump pools are all combination caves of cave type h, except **Ytterlihullet** (type d). Only one mainly vadose cave has three sump pools, although some 14 have two each. The overall SP means for the cave classes are relict: 0.0 (as specified), mainly vadose: 0.39 and combination: 0.80, and the lower SP mean for MV caves compared with combination caves is maintained for cave types a, c and d, but not for type b. The SP 'half value' for the mainly vadose caves and their common lack of multiple sump pools seem anomalous, but Appendix D6.1.1 interprets this finding by suggesting that vadose streamways with powerful discharges have fewer sumps, because of chemical and mechanical erosion at roof level. The total numbers of sump pools per cave increase fairly smoothly with cave type a–h, from 0.23–2.18, as occurs with cave streams.

The preponderance of phreatic over vadose passage forms in upper cave levels was noted in section 3.3.2 and in the discussions about individual caves in Appendix B1. Rather conversely, there are very few perched static sumps and ducks (where a pool of water has a small airspace below the passage roof) in these upper phreatic passages, suggesting that any water that may pond in the upper levels of a cave soon drains away to lower levels, because evaporation must be slow in the cold cave atmospheres, even in summer. All the known sumps in all the caves of the study area occur along streamways or at the lower ends of dry passages, where they probably connect with unexplored streamways.

Only a few sumps in the study area have been investigated by diving. The long underwater system at **Vatnhullet** and **Main Rising** (Z4; Appendix B1.4) was dived for 340m upstream towards **Etasjegrotta**, in a large conduit with

complex parallel passages and pillars, via a maximum depth of 20m. The total dived length of this active phreatic system is some 580m (Whybro, 1986; 1988). In **Sirijordgrotta** (Z4), the Upstream Sump was shown to become only 0.3m high after 11m, probably above sediment (Whybro, 1987), and three short ducks in various places can be passed in dry summer conditions. The short first streamway sump in **Kvannlihola** (Z7) was passed by free-diving (Faulkner, 1983). A duck, which is about one third of the way along the streamway in **Ytterlihullet** (ZA), can be passed to complete an exploration of this system. In Sweden, several upstream sumps at **Labyrintgrottan** (ZC) were passed by diving at the SSF 1998 mountain camp, and there is also a short, temporary, sump in the Sydgången passage. The Skymningsgrottan passage in **Korallgrottan** (KL) passes a short low duck. Several of the lowest level sumps in this cave are currently being investigated by diving.

B2.4 Large chambers (Ch)

The number of significant internal chambers (excluding entrance chambers) that are large compared to passage dimensions is shown for each cave in both cave databases. Across the whole study area, the total number of such chambers is 118, i.e. 0.13 per cave. The mean number of chambers per cave varies non-systematically across the inner zones from 0.0–0.4. The mean rises to 0.21 at KT=L, where it is highest for all cave classes. It is independent of contact metamorphism (R), but doubles to 0.27 if T=1. There is no consistent trend with cave location or glacial situation. The shorter mainly vadose and relict caves have means of only 0.04 and 0.05 chambers per cave (their maximum is two), whereas combination caves have double the overall mean at 0.27.

Although the overall means appear to be low, few internal chambers can be expected in caves that do not have internal connections, i.e. cave types S, a and b, which account for 635 (72%) of all the caves, and only 24 are recorded there. For those caves that *do* have connecting levels and passages, the mean becomes 0.4 chambers per cave. The cave with the most chambers (eight) is **Korallgrottan** (KL), and **Svartdalgrotta** (Z2) has five, suggesting that the number of chambers is loosely related to the length of the cave. In fact, the numbers of chambers per cave increase rather erratically with cave type a–h, and probably therefore with length, from 0.03–1.15. The number of chambers per kilometre of cave passage increases with reducing karst dip, despite the few trends apparent in Table B2.1. Most internal chambers and passages with cross-sections larger than $20m^2$ contain large, angular, commonly rectangular, blocks and slabs of unweathered limestone and other non-carbonate rocks that have clearly fallen from the roof and peeled away from the walls (section 6.3.3).

B2.5 Shafts (Sh)

In an attempt to analyse the interconnectedness of cave passages, the number of vertical, or near-vertical, relict entrance shafts and internal, apparently phreatic, shafts and avens are recorded in the two cave databases. The figures do not include shafts at sink entrances nor changes of level along vadose passages. There are 424 such shafts, i.e. 0.48 per cave, which vary in depth from c. 2m (the smallest recorded) up to 55m at the relict entrance to **Djupdalshullet** (KU). The mean number per cave varies across the inner zones from 0.1–1.0, and shows a decreasing trend eastwards, perhaps related to the eastward decline in angle of dip and / or metamorphic grade. The dip relationship is confirmed, because all cave classes commonly have decreasing means in the order V:A:L. For R=1 or T=1 the means decrease to 0.44 and 0.18 from 0.54 at R=0 and T=0. The numbers of shafts per cave are much more at cave locations R (1.13) and S (0.86), and less at P (0.28) and F (0.37). Easterly glacial situations below marine limits have much greater shaft means than their western counterparts, agreeing with their larger vertical ranges (section 5.3.5). From Table B2.1, combination caves have by far the greatest number of shafts and mainly vadose caves by far the least.

Caves that are mainly shafts (CT=S) share some of these trends. By comparing their cave location percentages with those of the full set of caves, 18% of shaft caves are at CL=S, but only 6% of all caves, whereas only 12% of shaft caves are at CL=F, compared with 28% of all caves. It is therefore concluded that caves of type S are not fundamentally different from other karst (dissolutional) caves, and can be considered to be a special case of cave type a.

Toerfjellhola (Z3) contains the most shafts (14) and **Etasjegrotta** (Z4) and **Blåfjellgrotta** (Z5) each contain 13. **Balcony Cave** (Z3) is the relict cave with the most shafts (7). Only four mainly vadose caves have as many as two

shafts. This is suggestive that the number of shafts may also be loosely linked to the length of the cave. However, the longest cave, **Korallgrottan** (KL) in medium grade metalimestone, has no shafts, although this record may arise from the absence of a complete surveyed section. The numbers of shafts per cave increase quite smoothly with cave type a–h, from 0.11– 2.95, probably confirming a relationship with length. The number of internal shafts per kilometre of cave passage decreases with decreasing foliation dip (V: 23, A: 14, L: 6), suggesting that shafts preferentially align with foliation-parallel fractures rather than with orthogonal fractures. A count of the number of unclimbed avens for the whole study area reached less than 30. This again seems a small number, and is probably related to the common small vertical range of most of the caves, and to the general ease of exploration.

B2.6 Boulder chokes (BC)

The total number of internal boulder chokes that hinder or prevent further exploration along passages is 187, i.e. 0.21 per cave, varying from 0.0 to only 0.3 across all the zones. In mainly vadose caves, the means decrease with decreasing foliation dip, but they increase in relict caves. In this case, the MV trend 'wins', because combination caves also show decreases. The mean is almost independent of R and T. It is larger in cave location F (0.28), and smaller at P (0.13) and S (0.09), but has little variation with glacial situation, except for the small sample at GS=S (0.44). As with shafts (Appendix B2.5), combination caves have by far the greatest number of BCs and mainly vadose caves by far the least, suggesting that the boulder chokes were commonly formed during deglacial outflows, before the MV caves enlarged to present sizes.

The cave with the most boulder chokes (seven) is the commonly-flooded **Övre Bjurälvsgrottan** (KL, section 1.6.4 and Appendix B1.15). **Stor Grubblandsgrotta** (KU) has five and **Anastomosegrotta** (Z4) has four. **Remnant Cave** (ZA, relict) also has four BCs and **Rainbow Cave** (Z5, mainly vadose) contains three. No other relict or mainly vadose caves contain more than two boulder chokes. The number of boulder chokes per cave increases rather erratically with cave type a–h, from 0.12–0.79. Thus, there may be a weak relationship with cave length. Whereas many chambers contain fallen and slipped limestone and / or non-carbonate slabs from roofs and walls, these piles seldom accumulate to reach the ceiling and prevent further exploration. This is in contrast to the situation in the UK, for example, where passages are commonly choked by infills of water-worn and collapsed boulders and blocks of limestones and gritstones in a matrix of sediment, such chokes lying beneath tall avens.

B2.7 Relict vadose passages (RV)

Following an observation of the apparent rarity of relict vadose passages, the instances of these passage forms were recorded in the two cave databases. The RV field also includes those cases where a stream that once sank into an apparently vadose entrance has been captured underground in normal summer flow conditions, upstream of the explorable cave. Phreatic passages with dry, narrow, vadose trenches (creating keyhole-shaped profiles) are *not* included. Such trenches almost universally occur in upper-level relict passages situated at the present 'upstream and descending' ends of phreatic loops, as in the combination caves **Tourist Cave** (Z2), **Toerfjellhola** (Z3), **Green Valley Cave** (Z4), **Sarvejaellagrotta** (Z4) and **Kompassgrotta** (Z5). A study of cave surveys showed that the only vadose entrenchments of 'downstream but ascending' ends of relict phreatic loop passages occur in **Gevirgrotta** (Z4) and **Øyfjellgrotta** (Z5; section 9.3). The keyhole profiles in the descending Roof Passages of **Sirijordgrotta** (Z4; Valen, 1991, p151) are representative of the first case, despite them occurring at the lower end of the cave. There are few examples of vadose to phreatic transitions along sub-horizontal passages (c.f. Bitterli and Jeannin, 1997; section 3.1.4) above the active streamways (section 8.4.12). Active vadose passages with indications of discordant higher-level vadose profiles or hanging potholes (section 3.2.1) would suggest vadose entrenchments during two interglacials. The relict vadose passage and shaft inside the main entrance to **Sirijordgrotta** (Z4) is one such example (Photo B2.1). The large streamway in **Øyfjellgrotta** has not been checked for this possibility.

The RV count for the whole study area is only 58, a mean of 0.066 relict vadose passages per cave, confirming the extreme rarity. The means vary non-systematically across the zones, and have the opposite karst type trends to boulder chokes (Appendix B2.6), because the frequencies increase with reducing foliation dip in mainly vadose and combination caves, but reduce in relict caves. The mean is independent of R, but doubles where T=1 (0.11). There is no clear trend with cave location. The frequency is always greater for eastern glacial situations compared with their western counterparts. The RV means increase fairly smoothly with cave type a–h, from 0.01–0.54.

Photo B2.1 Entrance chamber and shaft, Sirijordgrotta (Z4)
The relict vadose entrenchment is probably of Eemian age, when this entrance functioned as a resurgence.

Nearly all the RV passages are contained in combination caves (0.139 per cave). Just two mainly vadose caves (in Z2) are recorded with RV passages (both with probably a Holocene upstream capture), and only five relict caves. Three of these relict caves are in Fiplingdal (Z7). Their RV passages are all probably active during spring melt. The other relict caves are **Balcony Cave** (Z3; section 8.4.12) and **Stupgrottan** (near Kåtavik, ZC). Their RV passage floors probably formed during deglacial melting. A review of cave surveys showed that the only relict cave with a keyhole passage profile is **Fault Cave** (Z4). Its lower vadose entrenchment also probably occurred during deglacial melting. Thus, *the overwhelming majority of relict caves contain no relict vadose passage elements and have therefore developed primarily under phreatic conditions.*

B2.8 Anastomosis and paragenesis

Anastomosis channels are observed in the roofs of many cave passages. This may suggest that the early development phase of many passages was phreatic, i.e. under water with perhaps a large hydraulic head, but the more likely explanation is of dissolution by aggressive flood-water (Palmer, 1991; section 3.1.16). A particularly good example of anastomosis occurs in the roof of the entrance passage in **Anastomosegrotta** (Z4). Farther inside, corroded roof pendants reach 1.5m in length.

There are no known examples of paragenetic passages that either meander or have continuously descending floors in the caves of the study area, which would indicate paragenetic enlargement of an originally *vadose* passage. Valen and Lauritzen (1989) hypothesised that Elk Passage in **Sirijordgrotta** (Z4) enlarged paragenetically by rising water above a diamicton fill at a time when the cave outlet was dammed by ice. The author noted paragenetic roof channels in **Korallgrottan** (KL, Appendix B1.15), but, although other similar roof channels undoubtedly exist, they have not been systematically recorded.

A thorough study of all cave surveys did not find one definite *blind passage*, i.e. a passage that ends at a blind, near horizontal, termination in solid rock. Those passages that appeared at first sight to have this property were later shown to end at a boulder choke, at a sediment infill, or at a narrowing slit. This is in contrast to the recording of blind passages in vertical to steeply dipping sedimentary limestones in NSW, Australia, by Osborne (1999), which he surmised could form along lensoid inception surfaces. Osborne (2001b; 2001c) suggested that the dissolution of these blind passages was by rising hydrothermal waters, a possibility without an analogue in the non-Arctic Caledonide metacarbonates.

B2.9 Chemical deposits (DC)

The reported presence or absence of significant speleothems in each cave is shown in the cave databases by a simple 1 or 0 in the chemical deposits (DC) column. Only 40 of the 884 reported caves (4.5%) contain such stalactites, stalagmites or other chemical deposits, which must therefore be regarded as consistently rare in this area, especially as the zone with the highest incidence (Z2) only reaches 6%. There is no consistent trend across the zones, but the percentage increases as foliation dip reduces in relict caves, whilst reducing in combination caves and in type h caves. It increases slightly to 5.6% if R=1, but hardly changes if T=1. The percentage commonly declines with increasingly high glacial situations (registering a reducing average interglacial temperature, increasing annual snow cover and reducing vegetation), and is commonly greater for eastern rather than western counterparts (perhaps indicating higher summer rainfall on the east of mountain ranges). The controls on chemical deposition must be complex, because if CL=P or R the probabilities are larger (6.4% and 11.3%), but smaller if CL=F (2.4%).

The numbers of caves that contain various types of chemical deposits are approximately recorded as:

Stalactites (incl. straws)	32	Stalagmites	6	Columns	1	Helictites	3
Flowstone	7	Gour pools	2	Corraloids	3	Cave pearls	1
Moonmilk	6	'Cups'	1	'Coins'	1	Wall crystals	1

Since this table relies on information appended to cave surveys and described in reported texts and personal observations, it is probably a slight underestimate of the true position in the known caves. There are some 30 combination caves with significant speleothems, but only eight relict caves and two MV caves. As expected, the probability of a cave containing speleothems increases with cave type a–h, and therefore with length, from 0.6–33%.

The cave with the greatest number of straws and stalactites is probably **Sotsbäcksgrottan** (KU), for which the estimate is 200, with a mean length of 10cm (Helldén, 1975). Straws that are 45cm long occur in **Sud Langskjellighattengrotta** (Z2, revealed during the 1998 field trip). In both **Sirijordgrotta** (Z4) and **Geitklauvgrotta** (Z5), complex and pure white stalactites occur, some having bulbous lower ends (Photo B2.2). **Sirijordgrotta** also contains stalagmites, and stalactites that taper downwards rather like ice cream cornets (Photo B2.3). These appear similar to the bulbous type, but with the extra 'stem'. The only known complete columns occur in **Akersvanngrotta** (ZB), where they reach 30cm in length. In many of the above cases, the chemical deposits have formed in relict upper passages that are quite close to the surface (probably within 10m). Only in a few of the caves have speleothems formed in the higher parts of stream passages, such as the fine grotto in **Kvannlihola** (Z7), which contains both stalactites and stalagmites (Photo B1.9). The extreme rarity of substantial floor and wall deposits of stalagmite and flowstone is significant when considering cave development (section 9.8.1). Apart from a chemical analysis of dripstone waters in **Sirijordgrotta** (Øvstedal, 1991; Appendix A2.5), there are no other published chemical studies. The datings of chemical deposits from the study area are included in Appendix A5.

Photo B2.2 The Wasp Nest, Geitklauvgrotta
A pure white stalactite with a bulbous end.

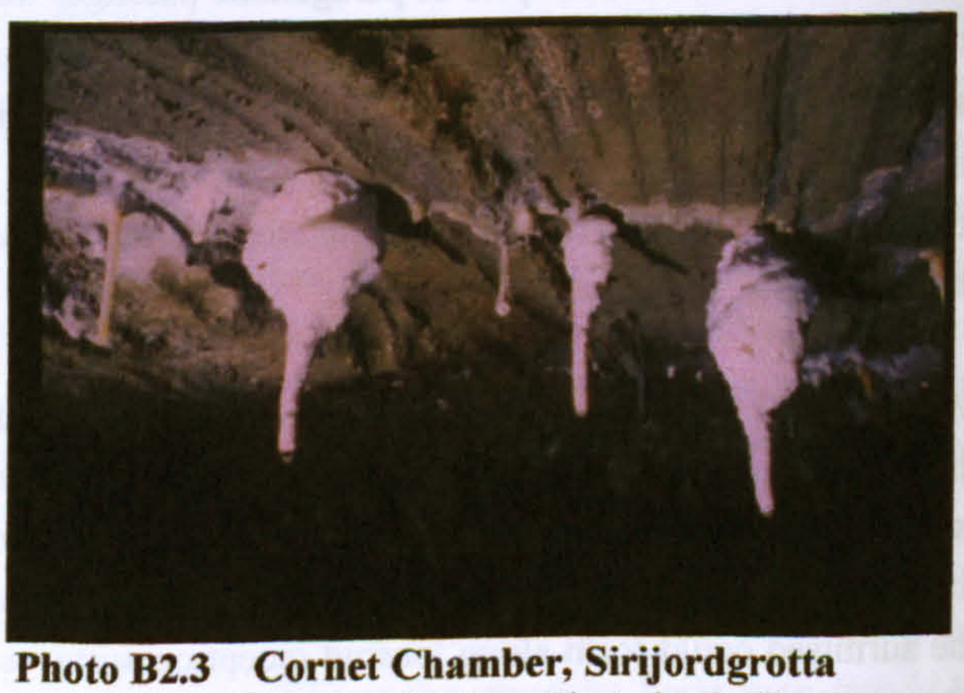

Photo B2.3 Cornet Chamber, Sirijordgrotta
Rare cornet-shaped stalactites. Photo by P. Hann.

B2.10 Fluvial sediments (FS)

In contrast to caves in England and Wales, few caves in the study area contain extensive deposits of moist clays and fine muds away from entrances, although many do contain dry silts, sands, gravels and larger fluvial deposits. The reported presence or absence of significant clastic fluvial sediments in each cave is shown in the cave databases by a simple 1 or 0 in the 'FS' column. A blank entry means that the report and survey include no relevant data about such sediments. Some 192 of the reported caves (22%) contain such clastic deposits, which is probably an underestimate of the true number. The inner zone percentages vary non-systematically from 8–38%, with Z2 having the highest, as it has for chemical deposits. Caves with KT=V have slightly less fluvial sediments overall (18%), but only relict caves show an increasing trend as foliation dip reduces. Type h caves have a *decreasing* trend as KT reduces. There is little change with either R=1 or T=1.

Unlike with the chemical deposits (Appendix B2.9), FS does not vary much with cave location, except that the percentages are high for CL=R and CL=S (44% and 32%) where relict caves dominate and there are few MV caves (section 5.5.5). This strongly suggests that most fluvial sediments derive from deglacial flows and not from annual spring melts or floods. Hence, the present fluvial activity generally acts to flush sediments out of caves, despite observations about the recent blocking of some passages (Appendix B2.2) The FS percentages of each hydrological cave class support this conclusion, because only 8% of MV caves have fluvial sediments, compared with 20% of relict caves and 32% of combination caves.

Combination caves contain more upper levels, which are commonly too high to be affected by present streams, and which emerged first from the deglacial flows. For example, it is clear from studies of sediments in **Sirijordgrotta** (Z4; Valen *et al.*, 1997) that not all caves flood to the roof regularly during interglacials and interstadials. Fluvial sediment percentages decrease smoothly with higher glacial situations, with no east or west dominance. This opposes the trend of increasing catchment area (section 5.3.5), and follows the reduction of temperature, vegetation and soil cover with altitude. Hence, it seems that fluvial sediments are also more likely to be washed completely through cave systems with higher flow rates, and at higher altitudes, where deglacial sediments were also less likely to be deposited. As expected, the probability of a cave to contain fluvial deposits increases with cave type a–h, and therefore with length, from 16–74%.

Four main deposition environments were proposed in **Sirijordgrotta** (Valen *et al.*, 1997): laminated clay deposited subglacially during full ice cover and ice damming; gravel and boulders deposited during high-energy water flows; sands from alternating flow regimes (which section 8.10 suggests may have been deposited by the sea in other caves); and laminated fine sand and silt from almost stagnant conditions. Also, coarse gravel situated beneath stalagmite dated to 128ka BP (section 3.3.3) was thought to represent a high-energy deglaciation event prior to the Weichselian. The clay deposit was tentatively correlated to a Lake Mungo excursion at 28ka BP on palaeomagnetic evidence. The other three deposits were thought to represent catastrophic floods, alternating flow conditions, and stagnant conditions during the final deglaciation. Fluvial sediments were also studied in **Sotsbäcksgrottan** (KU; Helldén, 1975) and **Korallgrottan** (KL; Isacsson, 1989; 1999).

B2.11 Marine deposits

Four caves with entrance altitudes around 120–130m at Velfjord (Z2) are reported to contain various types of marine shell deposits. These must date from the early Holocene, when the land surface was still depressed by the previous weight of the Scandinavian icesheet. Their present altitude indicates the extent of isostatic rebound that has occurred since then, relative to a sea-level that has also risen since the melting of all the Weichselian icesheets in both hemispheres (Chapter 8). **Aunhattenhule 2**, in which Hoel (1906) reported marine shells, was visited by the author during the 1998 field study trip. No sign of these shells remains in the cave. However, a British expedition reported finding barnacles attached to the walls and roofs of three different caves, one of which (**Neptune's Cave**) also contains many marine shells on, and among, gravel sediments on the floor in several places (Newton, 1999). Samples of these deposits were collected in 1998, and later identified at Liverpool Museum. A paper describing them and their significance in the Holocene uplift history of the area will be published separately. Section 8.10 suggests that some thick deposits of dry sand were brought into caves by the sea. Cave development deductions are

made in Appendix D5.3. Kirkland (1958, pp68–70) discussed the marine invasion of some karst caves at south Svartisen (north of the study area), and the possibility of marine sediments.

B2.12 Animal deposits

It is not uncommon to find the bones and skeletons of both large and small animals and birds inside the study area caves, either within other clastic deposits or lying loose in relict passages or, more rarely, calcited to the floor or wall recesses. In the more accessible caves and entrance areas, they may have been left there in recent times by Norwegian or Sami hunters or reindeer herdsmen, who use such caves as shelters. Thus, not all instances of underground bones are mentioned in cave reports. The cave with the most important faunal deposits is undoubtedly **Sirijordgrotta** (Z4). Below the pitfall Elk Shaft, some 10000 bones and fragments were collected and are being identified and dated at the University of Bergen. These have ages up to at least 7500a BP. (Lauritzen, 1991b). At least three caves on Elgfjell (Z4) contain animal bones, some of which are calcited to the floor (Faulkner and Newton, 1990). The remains of field vole, bank vole and willow grouse were found in a side passage in **Jegerhullet** (Z4; Faulkner, 1987).

APPENDIX C1

CENTRAL SCANDINAVIAN CALEDONIDE CARBONATE ROCK OUTCROPS DATABASE

CENTRAL SCANDINAVIAN CALEDONIDE CARBONATE ROCK OUTCROPS: GRAND SUMMARY

PTO for key

Metres

NAPPE COMPLEX AREA Sq. Km	NAPPE COMPLEX	COUNTRY	AV. MAX ALT.	O	R	T	V	D	TOTAL CARB. LENGTH Km	TOTAL VISITED LENGTH Km	AV. WIDTH	TOTAL CARB. AREA Sq. Km	TOTAL DOL. AREA Sq. Km	CARB. AREA %	DOL. AREA %	AV. CARB. AREA Sq. Km	AV. DOL. AREA Sq. Km	AV. VR Length	AV. VR Width	AV. DIP Degs.	TOTAL E	TOTAL F	TOTAL W	TOTAL C	TOTAL L	COMMENTS
UPPERMOST ALLOCHTHON																										
9950	**HNC**	**Norway only**	331	536	257	34	125	16	1911	251.6	190	560.2	10.77	5.63%	0.11%	1.05	0.67	161	54	63	244	196	141	626	47276	
1528	**RNC**	**Norway**	634	65	1	5	25	12	384	51.0	229	101.5	12.61	6.64%	0.83%	1.56	1.05	235	95	42	17	121	33	62	6301	
234	**RNC**	**Sweden**	824	9	0	0	6	0	88	50.0	194	24.2	0.00	#REF!	0.00%	2.69	#DIV/0!	218	65	45	9	2	5	40	4872	**No carbs. near a pluton** **No carbs. near a thrust** **No mapped dolomites**
1762	**RNC**	**Norway+Sweden**	657	74	1	5	31	12	472	101.0	225	125.7	12.61	7.14%	0.72%	1.70	1.05	233	92	42	26	123	38	102	11173	
UPPER ALLOCHTHON																										
3586	**KØLI**	**Norway**	651	60	2	22	13	16	270	29.5	239	90.9	22.09	2.53%	0.62%	1.52	1.38	180	59	44	20	47	21	40	4905	
5750	**KØLI**	**Sweden**	755	192	2	45	17	5	410	64.6	93	72.2	4.24	1.26%	0.07%	0.38	0.85	91	19	41	156	25	38	116	11527	**No carbs. near a pluton**
9336	**KØLI**	**Norway+Sweden**	730	252	4	67	30	21	680	94.1	127	163.1	26.33	1.75%	0.28%	0.65	1.25	112	29	42	176	72	59	156	16432	
46	**SEVE**	**Norway**																								**No mapped carbonates**
4397	**SEVE**	**Sweden**	733	123	0	14	5	0	99	0.4	57	6.6	0.00	0.15%	0.00%	0.05	#DIV/0!	54	11	30	107	0	6	0	0	
4443	**SEVE**	**Norway+Sweden**	733	123	0	14	5	0	99	0.4	57	6.6	0.00	0.15%	0.00%	0.05	#DIV/0!	54	11	30	107	0	6	0	0	**Includes calc-silicates** **No carbs. near a pluton** **No caves reported**
MIDDLE and LOWER ALLOCHTHONS																										
903	**ALL**	**Norway**																								**No mapped carbonates**
5373	**ALL**	**Sweden**	510	21	0	12	4	15	31	0.3	110	5.1	4.90	0.10%	0.09%	0.24	0.33	54	15	33	21	0	1	0	0	
6276	**ALL**	**Norway+Sweden**	510	21	0	12	4	15	31	0.3	110	5.1	4.90	0.08%	0.08%	0.24	0.33	54	15	33	21	0	1	0	0	**No mapped carbonates in Middle Allochthon** **No carbs. near a pluton** **Mainly dolomites** **Some Ord. limestones**
ALL ALLOCHTHONS																										
16013	**TOTALS**	**Norway**	390	661	260	61	163	44	2565	332.1	199	752.6	45.47	4.70%	0.28%	1.14	1.03	170	58	59	281	364	195	728	58482	
15754	**TOTALS**	**Sweden**	734	345	2	71	32	20	627	115.4	83	108.1	9.14	0.69%	0.06%	0.31	0.46	79	17	36	293	27	50	156	16399	
31767	**TOTALS**	**Norway+Sweden**	508	1006	262	132	195	64	3193	447.4	159	860.7	54.61	2.71%	0.17%	0.86	0.85	139	44	52	574	391	245	884	74881	

CENTRAL SCANDINAVIAN CALEDONIDE CARBONATE ROCK OUTCROPS: SUMMARY

Metres

ZONE AREA Sq.Km	NAME OR NAPPE	ZONE	AV. MAX ALT.	O	R	T	V	D	TOTAL CARB. LENGTH Km	TOTAL VISITED LENGTH Km	AV. WIDTH	TOTAL CARB. AREA Sq.Km	TOTAL DOL. AREA Sq.Km	CARB. AREA %	DOL. AREA %	AV. CARB. AREA Sq.Km	AV. DOL. AREA Sq.Km	AV. VR Length	AV. VR Width	AV. DIP Degs.	TOTAL E	TOTAL F	TOTAL W	TOTAL C	TOTAL L	COMMENTS	SHEET	PAGE
UPPERMOST ALLOCHTHON: Helgeland Nappe Complex													*(NORWAY only)*															
276	Coastal Area	Z1	27	41	13	0	3	0	106.2	1.7	432	59.80	0.00	21.67%	0.00%	1.46	#####	26	24	60	0	1	7	4	31	No mapped dolomites	11	1
2056	Fjord Area	Z2	176	193	113	2	39	2	433.6	73.5	169	119.11	0.43	5.79%	0.02%	0.62	0.22	127	54	60	83	28	36	165	10886		12	1 - 5
2002	Central Granite Area	Z3	421	63	26	0	21	0	155.8	28.9	150	33.14	0.00	1.66%	0.00%	0.53	#####	220	60	63	21	20	8	36	3320		13	1 - 2
814	Eiterådal & Jordbruelv	Z4	584	36	10	0	14	1	173.7	44.5	164	36.90	0.24	4.53%	0.03%	1.03	0.24	224	59	73	28	16	15	182	14490	No mapped dolomites	14	1
458	Mosjøen to Fjellryggen	Z5	342	39	15	0	10	5	164.8	46.4	137	37.89	2.58	8.27%	0.56%	0.97	0.52	177	52	73	21	15	8	79	7689		15	1
2228	Hemnes to Dunnfjell	Z6	393	55	38	1	17	4	281.2	29.4	255	106.52	3.52	4.78%	0.16%	1.94	0.88	190	61	65	35	53	23	64	5204		16	1 - 2
1054	Åkervik to Fiplingdal	Z7	606	60	3	7	17	4	421.0	24.8	201	145.80	4.00	13.83%	0.38%	2.43	1.00	219	67	63	45	60	31	87	4806		17	1 - 2
967	Eastern Area	Z8	786	27	24	20	3	0	102.0	1.9	96	11.99	0.00	1.24%	0.00%	0.44	#####	230	33	54	5	3	5	8	825	No mapped dolomites	18	1
95	Northern Area	Z9	116	22	15	4	1	0	72.9	0.5	109	9.03	0.00	9.51%	0.00%	0.41	#####	95	46	59	6	0	8	1	25	No mapped dolomites	19	1
9950	TOTALS / AV. per outcrop	ALL	331	536	257	34	125	16	1911.2	251.6	190	560.19	10.77	5.63%	0.11%	1.05	0.67	161	54	63	244	196	141	626	47276			
1106	AVERAGES per Zone		383	60	29	4	14	2	212.4	28.0	190	62.24	1.20	7.92%	0.13%	1.09	0.32	168	51	63	27	22	16	70	5253			
2228	MAXIMUM per Zone		786	193	113	20	39	5	433.6	73.5	432	145.80	4.00	21.67%	0.56%	2.43	1.00	230	67	73	83	60	36	182	14490			
	% per outcrop				48%	6%	23%	3%													46%							
	AVERAGES per outcrop								3.6													0.37	0.26	1.17	88			
	AVERAGES per visited outcrop									2.0														5.01	378			
	AVERAGES per explored cave																					0.31	0.23		76			

øääöÅØÖ

CENTRAL SCANDINAVIAN CALEDONIDE CARBONATE ROCK OUTCROPS: SUMMARY

Metres

ZONE AREA Sq.Km	NAME OR NAPPE	ZONE	AV. MAX ALT.	O	R	T	V	D	TOTAL CARB. LENGTH Km	TOTAL VISITED LENGTH Km	AV. WIDTH	TOTAL CARB. AREA Sq.Km	TOTAL DOL. AREA Sq.Km	CARB. AREA %	DOL. AREA %	AV. CARB. AREA Sq.Km	AV. DOL. AREA Sq.Km	AV. VR Length	AV. VR Width	AV. DIP Degs.	TOTAL E	TOTAL F	TOTAL W	TOTAL C	TOTAL L	COMMENTS	SHEET	PAGE
UPPERMOST ALLOCHTHON: Rødingsfjell Nappe Complex - Nappes below the Beiarn Nappe																										***(NORWAY)***		
415	**Bleikvassli Area**	**ZA**	595	23	1	3	12	3	188.5	27.1	200	56.81	0.72	13.69%	0.17%	2.47	0.24	213	109	41	15	94	17	37	3920		20	1
712	**Bjerka & Stor Akersvatn**	**ZB**	634	25	0	1	8	9	89.6	8.7	294	26.38	11.89	3.71%	1.67%	1.06	1.32	235	103	37	2	10	9	7	1410	**No carbs. near a pluton**	21	1
401	**Southern & Border**	**ZC**	686	17	0	1	5	0	106.2	15.2	172	18.34	0.00	4.57%	0.00%	1.08	#####	264	66	67	0	17	7	18	971	**No mapped dolomites**	22	1 - 2
																										No carbonates near a pluton		
1528	**TOTALS / AV. per outcrop**	**ALL**	634	65	1	5	25	12	384.3	51.0	229	101.53	12.61	6.64%	0.83%	1.56	1.05	235	95	42	17	121	33	62	6301			
509	**AVERAGES per Zone**		639	22	0	2	8	4	128.1	17.0	222	33.84	4.20	7.32%	0.61%	1.53	0.52	237	93	48	6	40	11	21	2100			
712	**MAXIMUM per Zone**		686	25	1	3	12	9	188.5	27.1	294	56.81	11.89	13.69%	1.67%	2.47	1.32	264	109	67	15	94	17	37	3920			
	% per outcrop				2%	8%	39%	18%													26%							
	AVERAGES per outcrop								5.9													1.86	0.51	0.95	97			
	AVERAGES per visited outcrop									2.0														2.47	251			
	AVERAGES per explored cave																					1.95	0.53		102			
UPPERMOST ALLOCHTHON: Rødingsfjell Nappe Complex - Nappes below the Beiarn Nappe																										***(SWEDEN)***		
234	**Southern & Border**	**ZC**	824	9	0	0	6	0	87.5	50.0	194	24.20	0.00	10.34%	0.00%	2.69	#####	218	65	45	9	2	5	40	4872		22	1 - 2
234	**TOTALS / AV. per outcrop**	**ALL**	824	9	0	0	6	0	87.5	50.0	194	24.20	0.00	10.34%	0.00%	2.69	#####	218	65	45	9	2	5	40	4872	**No mapped dolomites**		
																										No carbonates near a thrust		
234	**AVERAGES per Zone**		824	9	0	0	6	0	87.5	50.0	194	24.20	0.00	10.34%	0.00%	2.69	0.00	218	65	45	9	2	5	40	4872	**No carbonates near a pluton**		
234	**MAXIMUM per Zone**		824	9	0	0	6	0	87.5	50.0	194	24.20	0.00	10.34%	0.00%	2.69	0.00	218	65	45	9	2	5	40	4872			
	% per outcrop				0%	0%	67%	0%													100%							
	AVERAGES per outcrop								9.7													0.22	0.56	4.44	541			
	AVERAGES per visited outcrop									8.3														6.67	812			
	AVERAGES per explored cave																					0.05	0.13		122			
UPPERMOST ALLOCHTHON: Rødingsfjell Nappe Complex - Nappes below the Beiarn Nappe																										***(NORWAY and SWEDEN)***		
415	**Bleikvassli Area**	**ZA**	595	23	1	3	12	3	188.5	27.1	200	56.81	0.72	13.69%	0.17%	2.47	0.24	213	109	41	15	94	17	37	3920	**0**	20	1
712	**Bjerka & Stor Akersvatn**	**ZB**	634	25	0	1	8	9	89.6	8.7	294	26.38	11.89	3.71%	1.67%	1.06	1.32	235	103	37	2	10	9	7	1410	**No carbs. near a pluton**	21	1
635	**Southern & Border**	**ZC**	734	26	0	1	11	0	193.7	65.2	180	42.54	0.00	6.70%	0.00%	1.64	#####	248	66	58	9	19	12	58	5843	**No mapped dolomites**	22	1 - 2
																										No carbonates near a pluton		
1762	**TOTALS / AV. per outcrop**	**ALL**	657	74	1	5	31	12	471.8	101.0	225	125.73	12.61	7.14%	0.72%	1.70	1.05	233	92	42	26	123	38	102	11173		22	1 - 2
587	**AVERAGES per Zone**		655	25	0	2	10	4	157.3	33.7	225	41.91	4.20	8.03%	0.61%	1.72	0.78	232	93	45	9	41	13	34	3724			
712	**MAXIMUM per Zone**		734	26	1	3	12	9	193.7	65.2	294	56.81	11.89	13.69%	1.67%	2.47	1.32	248	109	58	15	94	17	58	5843			
	% per outcrop				1%	7%	42%	16%													35%							
	AVERAGES per outcrop								6.4													1.66	0.51	1.38	151			
	AVERAGES per visited outcrop									3.2														3.28	359			
	AVERAGES per explored cave																					1.21	0.37		110			

CENTRAL SCANDINAVIAN CALEDONIDE CARBONATE ROCK OUTCROPS: SUMMARY

Metres

EXL 034

ZONE AREA Sq.Km	NAME OR NAPPE	ZONE	AV. MAX ALT.	O	R	T	V	D	TOTAL CARB. LENGTH Km	TOTAL VISITED LENGTH Km	AV. WIDTH	TOTAL CARB. AREA Sq.Km	TOTAL DOL. AREA Sq.Km	CARB. AREA %	DOL. AREA %	AV. CARB. AREA Sq.Km	AV. DOL. AREA Sq.Km	AV. VR Length	AV. VR Width	AV. DIP Degs.	TOTAL E	TOTAL F	TOTAL W	TOTAL C	TOTAL L	COMMENTS	SHEET	PAGE
UPPER ALLOCHTHON: Køli Nappes															(Norway)													
731	Upper Køli	All	645	48	2	19	12	15	216.5	24.5	256	79.92	21.89	#####	2.99%	1.67	1.46	195	65	45	13	41	16	32	4414		23	1 - 2
1648	Middle Køli	Gjersvik	667	9	0	2	0	0	29.8	0.0	189	7.16	0.00	0.43%	0.00%	0.80	####	109	34	32	5	0	5	0	0	No R, V or D. No caves reported	24	1
236		Leipikvattnet	660	1	0	1	1	0	17.0	5.0	200	3.40	0.00	1.44%	0.00%	3.40	####	196	70	85	1	6	0	8	491	No R or D	25	1
27		Gelvenåko																								No mapped carbonates	26	1
583		Stikke	526	1	0	0	0	0	4.5	0.0	50	0.22	0.00	0.04%	0.00%	0.22	####	215	20	45	1	0	0	0	0	No R, T, V or D. No caves	27	1 - 2
361	Lower Køli	Bjørkvatten	910	1	0	0	0	1	2.0	0.0	100	0.20	0.20	0.06%	0.06%	0.20	0.20	30	30	##	0	0	0	0	0	No R, T or V. No caves reported	28	1 - 2
3586	TOTALS / AV. per outcrop		651	60	2	22	13	16	269.8	29.5	239	90.90	22.09	2.53%	0.62%	1.52	1.38	180	59	44	20	47	21	40	4905			
598	AVERAGES per Nappe		682	12	0	4	3	3	54.0	5.9	159	18.18	4.42	2.58%	0.61%	1.26	0.83	149	44	52	4	9	4	8	981			
1648	MAXIMUM per Nappe		910	48	2	19	12	15	216.5	24.5	256	79.92	21.89	#####	2.99%	3.40	1.46	215	70	85	13	41	16	32	4414			
	% per outcrop				3%	37%	22%	27%													33%							
	AVERAGES per outcrop								4.5													0.78	0.35					
	AVERAGES per visited outcrop									2.3														3.08	377			
	AVERAGES per explored cave																					1.18	0.53		123			
UPPER ALLOCHTHON: Køli Nappes															(Sweden)													
1683	Upper Køli	All	860	38	2	9	9	3	143.9	47.0	155	43.16	0.96	2.56%	0.06%	1.14	0.32	123	26	34	29	18	28	93	5237	No carbonates near a pluton	23	1 & 3
0	Middle Køli	Gjersvik																								Nappe does not occur in Sweden		
135		Leipikvattnet	546	7	0	5	2	0	15.0	10.0	136	2.56	0.00	1.90%	0.00%	0.37	####	74	30	66	7	2	0	21	6221	No R or D	25	1
76		Gelvenåko																								No mapped carbonates	26	1
1030		Stikke	770	26	0	0	0	0	37.0	0.0	53	2.39	0.00	0.23%	0.00%	0.09	####	77	10	51	24	0	1	0	0	No R, T, V or D. No caves	27	1 & 3
2826	Lower Køli	Bjørkvatten	730	121	0	31	6	2	214.4	7.6	79	24.12	3.28	0.85%	0.12%	0.20	1.64	84	18	38	96	5	9	2	69	No carbonates near a pluton	28	1 - 4
5750	TOTALS / AV. per outcrop		755	192	2	45	17	5	410.3	64.6	93	72.23	4.24	1.26%	0.07%	0.38	0.85	91	19	41	156	25	38	116	11527	No carbonates near a pluton		
958	AVERAGES per Nappe		727	48	1	11	4	1	102.6	16.2	106	18.06	1.06	1.39%	0.04%	0.45	0.98	90	21	50	39	6	10	29	2882			
2826	MAXIMUM per Nappe		860	121	2	31	9	3	214.4	47.0	155	43.16	3.28	2.56%	0.12%	1.14	1.64	123	30	66	96	18	28	93	6221			
	% per outcrop				1%	23%	9%	3%													81%							
	AVERAGES per outcrop								2.1													0.13	0.20					
	AVERAGES per visited outcrop									3.8														6.82	678			
	AVERAGES per explored cave																					0.22	0.33		99			
UPPER ALLOCHTHON: Køli Nappes															(Norway and Sweden)													
2414	Upper Køli	All	740	86	4	28	21	18	360.4	71.5	212	123.08	22.85	5.10%	0.95%	1.43	1.27	163	48	42	42	59	44	125	9651		23	1 - 3
1648	Middle Køli	Gjersvik	667	9	0	2	0	0	29.8	0.0	189	7.16	0.00	0.43%	0.00%	0.80	####	109	34	32	5	0	5	0	0	No R, V or D. No caves reported	24	1
371		Leipikvattnet	561	8	0	6	3	0	32.0	15.0	144	5.96	0.00	1.61%	0.00%	0.75	####	89	35	69	8	8	0	29	6712	No R or D	25	1
103		Gelvenåko																								No mapped carbonates	26	1
1613		Stikke	761	27	0	0	0	0	41.5	0.0	53	2.61	0.00	0.16%	0.00%	0.10	####	82	10	50	25	0	1	0	0	No R, T, V or D. No caves	27	1 - 3
3187	Lower Køli	Bjørkvatten	732	122	0	31	6	3	216.4	7.6	79	24.32	3.48	0.76%	0.11%	0.20	1.16	84	18	38	96	5	9	2	69	No carbonates near a pluton	28	1 -4
9336	TOTALS / AV. per outcrop		730	252	4	67	30	21	680.1	94.1	127	163.13	26.33	1.75%	0.28%	0.65	1.25	112	29	42	176	72	59	156	16432			
1556	AVERAGES per Nappe		692	50	0.8	13.4	6	4.2	136.0	18.8	135	32.63	5.27	1.61%	0.21%	0.65	1.21	105	29	46	35	14	12	31	3286			
3187	MAXIMUM per Nappe		761	122	4	31	21	18	360.4	71.5	212	123.08	22.85	5.10%	0.95%	1.43	1.27	163	48	69	96	59	44	125	9651			
	% per outcrop				2%	27%	12%	8%													70%							
	AVERAGES per outcrop								2.7													0.29	0.23					
	AVERAGES per visited outcrop									3.1														5.20	548			
	AVERAGES per explored cave																					0.46	0.38		105			

CENTRAL SCANDINAVIAN CALEDONIDE CARBONATE ROCK OUTCROPS: SUMMARY

Metres

EXL 034

ZONE AREA Sq.Km	NAME OR NAPPE	ZONE	AV. MAX ALT.	O	R	T	V	D	TOTAL CARB. LENGTH Km	TOTAL VISITED LENGTH Km	AV. WIDTH	TOTAL CARB. AREA Sq.Km	TOTAL DOL. AREA Sq.Km	CARB. AREA %	DOL. AREA %	AV. CARB. AREA Sq.Km	AV. DOL. AREA Sq.Km	AV. VR Length	AV. VR Width	AV. DIP Degs.	TOTAL E	TOTAL F	TOTAL W	TOTAL C	TOTAL L	COMMENTS	SHEET	PAGE
UPPER ALLOCHTHON: Seve Units																												(Norway)
46		Seve Units																								No mapped carbonates	29	1
0		Seve Belts																								Nappes do not occur in Norway		
UPPER ALLOCHTHON: Seve Units																												(Sweden)
1390		Seve Units	740	84	0	11	2	0	62.8	0.3	59	4.09	0.00	0.29%	0.00%	0.05	####	49	10	28	73	0	5	0	0	No R or D. No caves reported	29	1 - 3
3007		Seve Belts	720	39	0	3	3	0	35.8	0.2	52	2.47	0.00	0.08%	0.00%	0.06	####	64	13	33	34	0	1	0	0	No R or D. No caves reported	30	1 - 2
4397	TOTALS / AV. per outcrop		733	123	0	14	5	0	98.6	0.4	57	6.56	0.00	0.15%	0.00%	0.05	####	54	11	30	107	0	6	0	0	No carbonates near a pluton		
	% per outcrop				0%	11%	4%	0%													87%					Includes calc-silicates		
	AVERAGES per outcrop		6						0.8													0.00	0.05			No mapped dolomites		
	AVERAGES per visited outcrop									0.1														0.00	0	No caves reported		
	AVERAGES per explored cave																					#####	#####		#####			
MIDDLE and LOWER ALLOCHTHONS																												(Norway)
903		All																								No mapped carbonates	31	1
MIDDLE and LOWER ALLOCHTHONS																												(Sweden)
																										No mapped carbonates in Middle Allochthon	31	1 - 2
5373	TOTALS / AV. per outcrop		510	21	0	12	4	15	30.9	0.3	110	5.12	4.90	0.10%	0.09%	0.24	0.33	54	15	33	21	0	1	0	0	No carbonates near a pluton		
	% per outcrop				0%	57%	19%	71%													100%					Mainly Dolomites		
	AVERAGES per outcrop								1.5													0.00	0.05			Some Ordovician Limestones		
	AVERAGES per visited outcrop									0.1														0.00	0	No caves reported		
	AVERAGES per explored cave																					#####	#####		#####			

CENTRAL SCANDINAVIAN CALEDONIDE CARBONATE ROCK OUTCROPS: SUMMARY

Metres EXL 034

ZONE AREA Sq.Km	NAME OR NAPPE	ZONE	AV. MAX ALT.	O	R	T	V	D	TOTAL CARB. LENGTH Km	TOTAL VISITED LENGTH Km	AV. WIDTH	TOTAL CARB. AREA Sq.Km	TOTAL DOL. AREA Sq.Km	CARB. AREA %	DOL. AREA %	AV. CARB. AREA Sq.Km	AV. DOL. AREA Sq.Km	AV. VR Length	AV. VR Width	AV. DIP Degs.	TOTAL E	TOTAL F	TOTAL W	TOTAL C	TOTAL L	COMMENTS	SHEET	PAGE
UPPER ALLOCHTHON: Seve Units																										**(Norway)**		
46	**Seve Units**																									**No mapped carbonates**	29	1
0	**Seve Belts**																									**Nappes do not occur in Norway**		
UPPER ALLOCHTHON: Seve Units																										**(Sweden)**		
1390	**Seve Units**	740	84	0	11	2	0		62.8	0.3	59	4.09	0.00	0.29%	0.00%	0.05	####	49	10	28	73	0	5	0	0	**No R or D. No caves reported**	29	1 - 3
3007	**Seve Belts**	720	39	0	3	3	0		35.8	0.2	52	2.47	0.00	0.08%	0.00%	0.06	####	64	13	33	34	0	1	0	0	**No R or D. No caves reported**	30	1 - 2
4397	**TOTALS / AV. per outcrop**	733	123	0	14	5	0		98.6	0.4	57	6.56	0.00	0.15%	0.00%	0.05	####	54	11	30	107	0	6	0	0	**No carbonates near a pluton includes calc-silicates**		
	% per outcrop			0%	11%	4%	0%														87%					**No mapped dolomites**		
	AVERAGES per outcrop	6							0.8													0.00	0.05			**No caves reported**		
	AVERAGES per visited outcrop									0.1														0.00	0			
	AVERAGES per explored cave																					#####	#####		#####			
MIDDLE and LOWER ALLOCHTHONS																										**(Norway)**		
903	**All**																									**No mapped carbonates**	31	1
MIDDLE and LOWER ALLOCHTHONS																										**(Sweden)**		
																										No mapped carbonates in Middle Allochthon	31	1 - 2
5373	**TOTALS / AV. per outcrop**	510	21	0	12	4	15		30.9	0.3	110	5.12	4.80	0.10%	0.09%	0.24	0.33	54	15	33	21	0	1	0	0	**No carbonates near a pluton Mainly Dolomites**		
	% per outcrop			0%	57%	19%	71%														100%					**Some Ordovician Limestones**		
	AVERAGES per outcrop								1.5													0.00	0.05			**No caves reported**		
	AVERAGES per visited outcrop									0.1														0.00	0			
	AVERAGES per explored cave																					#####	#####		#####			

CENTRAL SCANDINAVIAN CALEDONIDE CARBONATE ROCK OUTCROPS: KEY

Heading	Meaning		Units
Map	The Norwegian Statens Kartverk 1:50000 Series M711 map sheet or the Swedish Lantmäteriverket 1:100000 Fjällkartan map sheet		
Nappe Area	The area of the nappe that is located on that map sheet		Sq. Km.
Coordinates in italics	*ED50, Black UTM grid*	A 6-digit coordinate within the outcrop	
Coordinates in standard	WGS84, Blue UTM grid	A 6-digit coordinate within the outcrop for Norwegian 1:50000 maps A 10-digit coordinate within the outcrop for Swedish 1:100000 maps, but with Eastings presented before Northings, to be consistent with UTM.	
Other italics	*The author's best (gu)estimate*		
Av.	The average value per carbonate outcrop, *or per visited outcrop.*		
Max. Alt.	The maximum altitude to which the carbonate outcrop rises.		Metres
Geol. Map Ident.	The type of carbonate outcrop, as identified on the relevant geological map or other reference.		
Sample Ident.	The type of carbonate outcrop, as identified by the author from a carbonate sample collected (usually) from inside a cave situated along the outcrop.		
Outcrop shape	A rough description of the shape of the carbonate outcrop, to assist location.		
O	The number of carbonate outcrops		
R	1 A significant part of the carbonate outcrop has probably been 'remetamorphosed' by high temperature, low pressure, contact metamorphism from an adjacent igneous pluton. This typically removes organic material so that the carbonate rock is refoliated with less prominent bands or becomes predominantly a massive white colour, sometimes with intruded darker dykes and sills. 0 The carbonate outcrop has probably only been subjected to various episodes of regional metamorphism.		
T	1 The carbonate outcrop lies along or near to a major tectonic thrust 0 The carbonate outcrop does not lie along or near to a major tectonic thrust		
V	1 The carbonate outcrop has been visited by cavers searching for caves, or contains at least one properly recorded cave. 0 The carbonate outcrop has not been visited by cavers searching for caves, and does not contain a properly recorded cave.		
D	1 The carbonate outcrop is identified as mainly consisting of dolomite on the relevant geological map or reference. 0 The carbonate outcrop is identified as mainly consisting of calcitic metalimestone on the relevant geological map or reference, or the identification is imprecise or ambiguous.		

CENTRAL SCANDINAVIAN CALEDONIDE CARBONATE ROCK OUTCROPS: KEY

Heading	Meaning	Units
Length	The length of the carbonate outcrop as measured with a ruler on the geological map or other reference.	Metres
Visited length	The length of the carbonate outcrop that has been searched by cavers, or else the probable length of visited outcrop for other properly recorded caves.	Metres
Width	The mean width of the carbonate outcrop as measured with a ruler on the geological map or other reference.	Metres
Carb. Area	The approximate product of the length and width of the carbonate outcrop.	Sq. Km.
Dol. Area	Equals the carbonate area if D = 1. Else zero.	Sq. Km.
VR Length	The maximum vertical range of the carbonate outcrop along its length, if necessary crossing intermediate valleys.	Metres
VR Width	The maximum vertical range of the carbonate outcrop across its width.	Metres
Strike	The strike of the carbonate outcrop as shown on the relevant geological map. Presented in degrees (360 degree circle) from grid north.	Degrees (Circle = 360 degrees)
Dip	The angle of dip of the foliation of the carbonate outcrop and its direction. Usually taken from the relevant geological map, but occasionally taken from measurements inside a cave along the outcrop.	Degrees (Circle = 360 degrees)
#	The number of outcrops for which the dip has been recorded.	
E	1 Most of the outcrop lies east of a major ridge. In uncertain cases, altitudes and moraine alignments are also considered, to retain consistency with Glacial Situation in the cave databases. Many outcrops in Sweden that are away from the Main Scandinavian Watershed are given the value 1. 0 Most of the outcrop lies west of a major ridge. Many outcrops in coastal areas are given the value 0.	
F	The number of karst features shown on the relevant topological map along the outcrop. These include sinks, risings and caves. Underground streams as shown by dotted blue lines are counted as 2 features, a sink and a rising.	
W	The number of significant bodies of water located along the outcrop, i.e. >= 100m x 100m. Rivers, marshes, fjords and bodies of water much larger than the outcrop width are excluded.	
C	The number of explored and adequately reported carbonate caves that lie along the outcrop, as represented in the Central Scandinavian Cave Databases.	
L	The total passage length of the adequately reported caves that lie along the outcrop, as represented in the Central Scandinavian Cave Databases.	Metres

UPPERMOST ALLOCHTHON: Helgeland Nappe Complex: Zone 1 (Coastal Area)

MAP SHEET	MAP NAME & NAPPE AREA	UTM / SWEDISH RN COORD		MAX ALT.	GEOL MAP IDENT	SAMPLE IDENT	OUTCROP SHAPE	O	R	T	V	D	LENGTH	VISITED LENGTH	WIDTH	CARB. AREA	DOL. AREA	VR Length	VR Width	STRIKE	DIP	#	E	F	W	C	L	COMMENTS
																											Metres	
Totals	276			####				41	13	0	3	0	106200	1700	#####	59.80	0.00	####	###		###	29	0	1	7	4	31	There are some 126 more Q karst features in the Tjøtta area, mainly on tiny islands of limestone. Most outrops lie within the strandflat.
%									32%	0%	7%	0%				21.7%	0%					71%	0%					
Averages				27									2590	567	432	1.46	#DIV/0!	26	24		60			0.02	0.17	1	10	
Maxima				100									8000	1000	2000	10.00	0.00	100	100		90			1	5	4	31	
1726 II	***Vega***	PT	*330*	*880*	28	Calcitic		Irregular	1	1	0	0	0	5000	0	2000	10.00	0.00	28	28	130	60	N	0	1	5	0	0	Marshy area
1726 II	***Vega***	PT	*340*	*900*	44	Calcitic		Irregular	1	0	0	0	0	5000	0	400	2.00	0.00	44	24				0	0	0	0	0	
1726 II	***Vega***	PT	*340*	*850*	30	Calcitic		Circular	1	1	0	0	0	400	0	400	0.20	0.00	5	5				0	0	0	0	0	
1726 II	***Vega***	PT	*350*	*890*	33	Calcitic		Irregular	1	0	0	0	0	5000	0	200	1.00	0.00	14	5				0	0	1	0	0	
1726 II	***Vega***	PT	*360*	*850*	57	Calcitic		Arc	1	1	0	0	0	2000	0	200	0.40	0.00	57	40				0	0	0	0	0	
1726 II	***Vega***	UN	*630*	*854*	20	Calcitic		Arc	1	1	0	0	0	2500	0	100	0.25	0.00	20	20				0	0	0	0	0	
1726 II	***Vega***	UN	*630*	*900*	19	Calcitic		Islands	1	0	0	0	0	5000	0	400	2.00	0.00	19	19	100	70	S	0	0	0	0	0	Coastal + islands
1726 II	***Vega***	UN	*660*	*880*	30	Calcitic		Arc	1	1	0	0	0	3000	0	400	1.20	0.00	30	30	10	75	E	0	0	0	0	0	
Area	124	UN	*680*	*880*	19	Calcitic		Irregular	1	0	0	0	0	1500	0	500	0.75	0.00	19	19	10	75	E	0	0	0	0	0	
1725 I	**Brønnøysund**	UN	670	645	20	Calcitic		Linear	1	0	0	0	0	500	0	100	0.05	0.00	20	5	40			0	0	0	0	0	Low lying islands
1725 I	**Brønnøysund**	UN	670	630	20	Calcitic		Linear	1	0	0	0	0	3500	0	1000	3.50	0.00	20	20	80	85	S	0	0	0	0	0	Low lying islands. Dips 45-90. TF98
1725 I	**Brønnøysund**	UN	685	645	20	Calcitic		Linear	1	0	0	0	0	1000	0	500	0.50	0.00	20	20				0	0	0	0	0	Low lying islands
1725 I	**Brønnøysund**	UN	680	630	30	Calcitic		Irregular	1	0	0	0	0	3500	0	400	1.40	0.00	30	30	50	80	E	0	0	0	0	0	Low lying islands. Dips 45-90. TF98
1725 I	**Brønnøysund**	UN	690	630	20	Calcitic		Irregular	1	0	0	0	0	2500	0	300	0.75	0.00	20	20	50	60	E	0	0	0	0	0	Low lying islands
1725 I	**Brønnøysund**	UN	700	620	40	Calcitic		Linear	1	0	0	1	0	8000	*1000*	1000	8.00	0.00	40	40	60	20	S	0	0	1	4	31	By football pitch. Incl. to NE.TF00
1725 I	**Brønnøysund**	UN	655	585	40	Calcitic		Linear	1	0	0	0	0	3000	0	300	1.00	0.00	40	40	160	85	E	0	0	0	0	0	Low lying islands
Area	29	UN	705	595	13	Calcitic		Rectangle	1	0	0	0	0	1500	0	500	0.80	0.00	13	13	60	40	E	0	0	0	0	0	Low lying islands
1827 III	**Sandnessjøen**	UP	775	270	40	Calc++		Triangle	1	0	0	0	0	500	0	100	0.05	0.00	40	40	140	20	S	0	0	0	0	0	Low lying island
1827 III	**Sandnessjøen**	UP	773	257	5	Calc++		Linear	1	0	0	0	0	300	0	100	0.03	0.00	5	5	70	50	S	0	0	0	0	0	Low lying island
1827 III	**Sandnessjøen**	UP	745	255	25	Calc++		Irregular	1	0	0	0	0	1000	0	500	0.50	0.00	25	25				0	0	0	0	0	Low lying island
1827 III	**Sandnessjøen**	UP	755	250	10	Calc++		Irregular	1	1	0	0	0	1000	0	200	0.20	0.00	10	10	35	30	W	0	0	0	0	0	Low lying island
1827 III	**Sandnessjøen**	UP	760	230	10	Calc+gr		Irregular	1	0	0	0	0	500	0	200	0.10	0.00	10	10	20	55	W	0	0	0	0	0	Low lying island
1827 III	**Sandnessjøen**	UP	780	225	10	Calc+gr		Linear	1	1	0	0	0	4000	0	500	2.00	0.00	10	10	30			0	0	0	0	0	Low lying island
1827 III	**Sandnessjøen**	UP	800	230	40	Calc+gr		Irregular	1	1	0	0	0	3000	0	300	1.00	0.00	40	40	55	85	N/S	0	0	0	0	0	Low lying island
1827 III	**Sandnessjøen**	UP	855	245	10	Calcitic		Linear	1	1	0	0	0	1000	0	200	0.20	0.00	10	10	40	70	W	0	0	0	0	0	Low lying island
1827 III	**Sandnessjøen**	UP	880	273	10	Calcitic		Two limbs	1	0	0	0	0	1500	0	50	0.08	0.00	10	10	50	30	N/S	0	0	0	0	0	Low lying coastal
1827 III	**Sandnessjøen**	UP	890	260	10	Calcitic		Linear	1	1	0	0	0	700	0	100	0.07	0.00	10	10	70	90		0	0	0	0	0	Low lying coastal
Area	12	UP	900	279	20	Calcitic		Linear	1	0	0	0	0	300	0	50	0.02	0.00	20	20	70			0	0	0	0	0	Low lying coastal
1826 IV	***Tjøtta***	UP	*750*	*200*	10	Calcitic		Irregular	1	1	0	1	0	3000	500	1000	3.00	0.00	10	10	55	68	N/S	0	0	0	0	0	Low lying island. 4 Q karst. TF00
1826 IV	***Tjøtta***	UP	*740*	*170*	13	Calcitic		Irregular	1	0	0	1	0	4000	200	1000	4.00	0.00	13	13	40	54	W	0	0	0	0	0	Low lying islands. 9 Q karst. TF00
1826 IV	***Tjøtta***	UP	*780*	*220*	15	Calcitic		Irregular	1	1	0	0	0	2500	0	500	1.25	0.00	15	15	55	63	N	0	0	0	0	0	Low lying island
1826 IV	***Tjøtta***	UP	*820*	*180*	33	Calcitic		Linear	1	0	0	0	0	2500	0	100	0.25	0.00	33	33	45	63	N	0	0	0	0	0	Low lying islands. 10 Q karst
1826 IV	***Tjøtta***	UP	*790*	*150*	22	Calcitic		Irregular	1	0	0	0	0	5000	0	1000	5.00	0.00	22	22	40	74	E/W	0	0	0	0	0	Low lying island. 11 Q karst
1826 IV	***Tjøtta***	UP	*790*	*050*	63	Calcitic		Irregular	1	1	0	0	0	3000	0	200	0.60	0.00	63	63	40	40	W	0	0	0	0	0	Low lying island
Area	28	UP	*820*	*130*	40	Calcitic		Linear	1	0	0	0	0	3000	0	200	0.60	0.00	40	40	30	81	W	0	0	0	0	0	Low lying coastal
1826 III	***Vevelstad***	UN	*760*	*750*	60	Calcitic		Arc	1	0	0	0	0	4500	0	500	2.20	0.00	60	60	10	32	E	0	0	0	0	0	
1826 III	***Vevelstad***	UN	*730*	*695*	10	Calcitic		Arc	1	0	0	0	0	1500	0	100	0.15	0.00	10	10	105	54	N	0	0	0	0	0	Low lying coastal
Area	43	UN	*760*	*670*	100	Calcitic		Irregular	1	0	0	0	0	2000	0	1500	3.00	0.00	100	100	160	72	E	0	0	0	0	0	moraine covered
1825 IV	***Velfjord***	UN	*720*	*610*	9	Calcitic		Islands	1	0	0	0	0	5500	0	200	1.10	0.00	9	9				0	0	0	0	0	Low lying islands
1825 IV	***Velfjord***	UN	*760*	*655*	33	Calcitic		Two limbs	1	0	0	0	0	2500	0	200	0.50	0.00	33	33	40	50	E	0	0	0	0	0	
Area	40	UN	*760*	*650*	10	Calcitic		Irregular	1	0	0	0	0	500	0	200	0.10	0.00	10	10				0	0	0	0	0	Low lying islands

UPPERMOST ALLOCHTHON: Helgeland Nappe Complex: Zone 2 (Fjord Area)

MAP SHEET	MAP NAME & NAPPE AREA	UTM / SWEDISH RN COORD			MAX ALT.	GEOL MAP IDENT	SAMPLE IDENT	OUTCROP SHAPE	O	R	T	V	D	LENGTH	VISITED LENGTH	WIDTH	CARB. AREA	DOL. AREA	VR Length	VR Width	STRIKE	DIP	#	E	F	W	C	L	COMMENTS
																									Metres				
Totals	2056				#####				193	113	2	39	2	433600	73500	#####	119.11	0.43	#####	#####		###	78	83	28	36	165	10886	
%										59%	1%	20%	1%				5.79%	0.02%					40%	43%					
Averages					176									2247	1885	169	0.62	0.22	127	54		60			0.15	0.19	4.23	279	
Maxima					849									18000	8000	1500	17.00	0.35	560	412		90			7	8	19	1593	
1725 I	**Brønnøysund**	UN	694	480	140	Calcitic		Linear	1	0	0	0	0	600	0	100	0.06	0.00	100	5	55			0	0	0	0	0	
1725 I	**Brønnøysund**	UN	688	466	75	Calcitic		Triangle	1	0	0	0	0	300	0	100	0.03	0.00	45	20				0	0	0	0	0	
1725 I	**Brønnøysund**	UN	697	463	100	Calcitic		Linear	1	0	0	0	0	200	0	50	0.01	0.00	40	20	170			0	0	0	0	0	Below Holin Hullet
1725 I	**Brønnøysund**	UN	690	455	122	Calcitic		Circular	1	0	0	0	0	400	0	300	0.12	0.00	60	60				0	0	0	0	0	
1725 I	**Brønnøysund**	UN	694	455	140	Calcitic		Linear	1	0	0	0	0	200	0	50	0.01	0.00	100	100	60			0	0	0	0	0	
1725 I	**Brønnøysund**	UN	689	448	88	Calcitic		Circular	1	0	0	0	0	300	0	200	0.05	0.00	40	60				0	0	0	0	0	
Area	62	UN	694	445	200	Calcitic		Linear	1	0	0	0	0	1000	0	100	0.10	0.00	160	40	50	50	E	0	0	0	0	0	
1725 II	**Austra**	UN	620	355	140	Calcitic		Linear	1	0	0	1	0	1000	700	200	0.20	0.00	140	140	150			0	0	0	1	4	Olaf's Kilden
1725 II	**Austra**	UN	638	360	240	Calcitic		Linear	1	0	0	0	0	2500	0	100	0.30	0.00	180	80	50			1	0	0	0	0	
1725 II	**Austra**	UN	640	355	200	Calcitic		Linear	1	0	0	0	0	2000	0	100	0.20	0.00	200	200	50			1	0	0	0	0	
1725 II	**Austra**	UN	683	170	430	Calcitic		Rectangle	1	0	0	0	0	1000	0	200	0.20	0.00	430	100				0	0	0	0	0	
Area	71	UN	670	168	200	Calcitic		Linear	1	0	1	0	0	1200	0	50	0.06	0.00	200	60	150	50	E	0	0	0	0	0	On HNC thrust
1829 III	**Sandnesjøen**	UP	820	299	10	Calcitic		Linear	1	1	0	0	0	1000	0	20	0.02	0.00	10	1	60	50	S	0	0	0	0	0	Dønna
1830 III	**Sandnesjøen**	UP	820	297	20	Calcitic		Linear	1	1	0	0	0	2000	0	30	0.06	0.00	20	5	60		S	0	0	0	0	0	Dønna
1831 III	**Sandnesjøen**	UP	815	295	20	Calcitic		Linear	1	1	0	0	0	300	0	30	0.01	0.00	20	2	60		S	0	0	0	0	0	Dønna
1832 III	**Sandnesjøen**	UP	817	293	50	Calcitic		Linear	1	1	0	0	0	300	0	20	0.01	0.00	50	2	50		S	0	0	0	0	0	Dønna
1833 III	**Sandnesjøen**	UP	838	310	40	Calcitic		Linear	1	1	0	0	0	1200	0	20	0.02	0.00	40	2	60	55	S	0	0	0	0	0	Dønna
1834 III	**Sandnesjøen**	UP	835	307	100	Calcitic		Linear	1	1	0	0	0	400	0	20	0.01	0.00	20	2	60		S	0	0	0	0	0	Dønna
1835 III	**Sandnesjøen**	UP	840	310	60	Calcitic		Linear	1	1	0	0	0	300	0	20	0.01	0.00	20	2	40		S	0	0	0	0	0	Dønna
1836 III	**Sandnesjøen**	UP	830	300	130	Calcitic		Linear	1	1	0	0	0	900	0	30	0.03	0.00	20	5	60	65	S	0	0	0	0	0	Dønna
1836 III	**Sandnesjøen**	UP	840	297	460	Calc+am		Two limbs	1	0	0	0	0	2100	0	100	0.21	0.00	230	40	60	55	S	0	0	0	0	0	Dønna
1837 III	**Sandnesjøen**	UP	875	310	120	Calc+am		Linear	1	0	0	0	0	2000	0	50	0.10	0.00	53	20	60	65	S	1	0	1	0	0	Dønna
1838 III	**Sandnesjøen**	UP	880	310	200	Calc+am		Sinuous	1	0	0	0	0	5000	0	150	0.75	0.00	80	100	45	65	S	1	0	1	0	0	Dønna
1839 III	**Sandnesjøen**	UP	872	298	160	Calc+am		Linear	1	1	0	0	0	700	0	30	0.02	0.00	57	20	45	60	S	1	0	0	0	0	Dønna
1840 III	**Sandnesjøen**	UP	940	352	140	Calcitic		Sinuous	1	1	0	0	0	600	0	50	0.03	0.00	140	20				1	0	0	0	0	Dønna
1841 III	**Sandnesjøen**	UP	940	345	180	Calcitic		Irregular	1	1	0	0	0	1000	0	125	0.13	0.00	180	120	50	80	S	1	0	0	0	0	Dønna
1842 III	**Sandnesjøen**	UP	940	340	330	Calcitic		Irregular	1	1	0	0	0	3000	0	500	1.50	0.00	220	200				1	0	0	0	0	Dønna. Complexly folded
1827 III	**Sandnesjøen**	UP	960	310	30	Calcitic		Linear	1	1	0	0	0	1000	0	100	0.10	0.00	30	5	70	65	S	0	0	0	0	0	Løkta. Continues E?
1827 III	**Sandnesjøen**	UP	965	305	140	Calcitic		Linear	1	1	0	0	0	500	0	50	0.03	0.00	80	20	70			0	0	0	0	0	Løkta. Continues E?
1827 III	**Sandnesjøen**	UP	960	294	220	Calcitic		Linear	1	1	0	0	0	1000	0	50	0.05	0.00	180	20	80			0	0	0	0	0	Løkta. Continues E?
1827 III	**Sandnesjøen**	UP	960	290	100	Calcitic		Linear	1	1	0	0	0	1500	0	50	0.08	0.00	100	10	70			0	0	0	0	0	Løkta. Continues E?
1827 III	**Sandnesjøen**	UP	965	286	40	Calcitic		Linear	1	0	0	0	0	700	0	100	0.07	0.00	40	40	80	65	N	0	0	0	0	0	Løkta. Continues E?
1827 III	**Sandnesjøen**	UP	960	270	40	Calcitic		Linear	1	0	0	0	0	3000	0	300	0.90	0.00	40	40	60	85	S	0	0	0	0	0	Continues E?
1827 III	**Sandnesjøen**	UP	900	230	40	Calcitic		Linear	1	0	0	0	0	4000	0	200	0.80	0.00	40	40	55	80	N/S	0	0	0	0	0	Continues SW?
1827 III	**Sandnesjøen**	UP	930	241	20	Dolom.		Linear	1	0	0	0	1	1500	0	50	0.08	0.08	20	20	60	85	N	0	0	0	0	0	Low lying coastal
1827 III	**Sandnesjøen**	UP	940	246	10	Cal+ms		Linear	1	0	0	0	0	1200	0	100	0.12	0.00	10	10	60			0	0	0	0	0	
1827 III	**Sandnesjøen**	UP	930	237	60	Cal+ms		Linear	1	0	0	0	0	4500	0	50	0.23	0.00	60	40	60	75	S	0	0	0	0	0	Continues SW?
1827 III	**Sandnesjøen**	UP	930	235	100	Calcitic		Linear	1	0	0	0	0	4500	0	50	0.23	0.00	100	20	60	80	N	0	0	0	0	0	Continues SW?
1827 III	**Sandnesjøen**	UP	940	240	40	Calcitic		Linear	1	0	0	0	0	2000	0	50	0.10	0.00	40	10	60	80	N	0	0	0	0	0	
1827 III	**Sandnesjøen**	UP	930	230	100	Calcitic		Linear	1	0	0	0	0	4000	0	100	0.40	0.00	100	40	60	65	S	0	0	0	0	0	
Area	74	UP	928	220	10	Calcitic		Irregular	1	0	0	0	0	1000	0	100	0.10	0.00	10	10	40	75	E	0	0	0	0	0	Low lying coastal

UPPERMOST ALLOCHTHON: Helgeland Nappe Complex: Zone 2 (Fjord Area)

MAP SHEET	MAP NAME & NAPPE AREA	UTM / SWEDISH RN COORD		MAX ALT.	GEOL MAP IDENT	SAMPLE IDENT	OUTCROP SHAPE	O	R	T	V	D	LENGTH (Metres)	VISITED LENGTH	WIDTH	CARB. AREA	DOL. AREA	VR Length	VR Width	STRIKE	DIP	#	E	F	W	C	L	COMMENTS
1826 IV	***Tjøtta***	UP *820*	*120*	60	Calcitic		2 limbs	1	1	0	0	0	6000	0	200	1.20	0.00	60	60	45	77	E/W	0	0	0	0	0	
1826 IV	***Tjøtta***	UP *870*	*205*	60	Calcitic		Linear	1	0	0	0	0	4000	0	50	0.20	0.00	60	10	45			0	0	0	0	0	
1826 IV	***Tjøtta***	UP *880*	*210*	100	Calcitic		Linear	1	0	0	0	0	1000	0	50	0.05	0.00	40	10	45			0	0	0	0	0	
1826 IV	***Tjøtta***	UP *880*	*205*	170	Calcitic		Linear	1	0	0	0	0	4500	0	100	0.45	0.00	70	20	45			0	0	0	0	0	
1826 IV	***Tjøtta***	UP *880*	*200*	100	Dolom.		Linear	1	0	0	0	1	7000	0	50	0.35	0.35	80	60	45	59	W	0	0	0	0	0	white dolomite
1826 IV	***Tjøtta***	UP *920*	*215*	40	Calcitic		Rectangle	1	0	0	0	0	1500	0	200	0.30	0.00	40	40				0	0	0	0	0	
1826 IV	***Tjøtta***	UP *910*	*200*	104	Calcitic		Linear	1	0	0	0	0	3000	0	300	0.90	0.00	104	60	50	81	E/W	0	0	0	0	0	
1826 IV	***Tjøtta***	UP *870*	*130*	560	Calcitic	Calc (2off)	Sinuous	1	1	0	1	0	8000	3500	50	0.40	0.00	560	50	50	60	N	1	0	0	5	605	Søvikgrotta + 4
1826 IV	***Tjøtta***	UP *830*	*110*	360	Calcitic		Sinuous	1	1	0	1	0	4500	1000	50	0.22	0.00	360	80				1	0	0	0	0	
1826 IV	***Tjøtta***	UP *870*	*125*	480	Calcitic		Sinuous	1	1	0	0	0	5500	0	50	0.27	0.00	480	40		59	N	1	0	0	0	0	
1826 IV	***Tjøtta***	UP *885*	*125*	240	Calcitic		Linear	1	1	0	0	0	4000	0	200	0.80	0.00	240	200	70	14	N	1	0	0	0	0	Svarthullet? 2 Q karst features
1826 IV	***Tjøtta***	UP *860*	*090*	12	Calcitic		Irregular	1	0	0	0	0	4000	0	700	2.80	0.00	12	12		23	E	0	0	0	0	0	Low lying island. 1Q, + 4Q on drift
1826 IV	***Tjøtta***	UP *860*	*060*	29	Calcitic		Irregular	1	0	0	0	0	1000	0	1000	1.00	0.00	29	29	180	25	E	0	0	0	0	0	Low lying island. 4 Q karst
1826 IV	***Tjøtta***	UP *905*	*075*	45	Calcitic		Linear	1	1	0	0	0	1200	0	100	0.12	0.00	45	45	30			0	0	0	0	0	Low lying island. 1 Q karst
1826 IV	***Tjøtta***	UP *910*	*070*	44	Calcitic		Linear	1	0	0	0	0	3500	0	200	0.70	0.00	44	44	20			0	0	0	0	0	Low lying island. 1Q + 3Q
1826 IV	***Tjøtta***	UN *820*	*975*	100	Calcitic		Arc	1	0	0	0	0	1200	0	100	0.12	0.00	60	60	55			1	0	0	0	0	
1826 IV	***Tjøtta***	UN *819*	*970*	60	Calcitic		Linear	1	0	0	0	0	1200	0	100	0.12	0.00	60	20	35			0	0	0	0	0	
1826 IV	***Tjøtta***	UN *820*	*970*	160	Calcitic		Linear	1	0	0	0	0	2000	0	100	0.20	0.00	160	60	35			0	0	0	0	0	
1826 IV	***Tjøtta***	UN *840*	*988*	50	Calcitic		Linear	1	0	0	0	0	1000	0	100	0.10	0.00	20	5	50	70	E	0	0	0	0	0	
1826 IV	***Tjøtta***	UP *860*	*015*	13	Calcitic		Irregular	1	0	0	0	0	700	0	100	0.07	0.00	13	13				0	0	0	0	0	Islands. 1 Q karst
1826 IV	***Tjøtta***	UP *880*	*010*	135	Calcitic		Linear	1	1	0	0	0	3500	0	800	2.80	0.00	135	135	150	60	E	0	0	0	0	0	Island. 3 Q karst
Area		165 UP *890*	*010*	43	Calcitic		Irregular	1	1	0	0	0	5000	0	500	2.50	0.00	43	43	5	45	E	1	0	0	0	0	Island. 9 Q karst
1826 III	***Vevelstad***	UN *862*	*932*	*40*			*Unmapped*	1	1	0	1	0	*1000*	100	*20*	*0.02*	*0.00*	*40*	*5*				0	0	0	1	6	Vistnesodden
1826 III	***Vevelstad***	UN *835*	*894*	40	Calcitic		Triangle	1	1	0	0	0	600	0	200	0.12	0.00	5	10				0	2	0	0	0	
1826 III	***Vevelstad***	UN *818*	*880*	10	Calcitic		Linear	1	1	0	0	0	3000	0	100	0.30	0.00	10	10	40			0	0	0	0	0	Low lying coastal
1826 III	***Vevelstad***	UN *850*	*860*	849	Calcitic		Linear	1	1	0	0	0	2500	0	300	0.75	0.00	169	80	30			1	0	1	0	0	
1826 III	***Vevelstad***	UN *880*	*850*	340	Calcitic		Linear	1	1	0	1	0	5500	4000	100	5.50	0.00	340	100	20	60	E	1	0	0	4	105	Langkilelv
1826 III	***Vevelstad***	UN *860*	*850*	520	Calcitic		Tapering	1	1	0	1	0	5500	2000	200	1.10	0.00	140	180	170			1	0	1	2	12	Spruten
1826 III	***Vevelstad***	UN *846*	*801*	*500*	*Calcitic?*		*Unmapped*	1	1	0	1	0	*400*	200	*20*	*0.01*	*0.00*	*116*	*20*				1	0	0	1	30	Swanlake Cave
1826 III	***Vevelstad***	UN *860*	*840*	500	Calcitic		Linear	1	1	0	0	0	600	0	100	0.06	0.00	180	20	170			1	0	0	0	0	
1826 III	***Vevelstad***	UN *865*	*780*	430	Calcitic		Linear	1	1	0	1	0	6500	4500	300	2.00	0.00	430	160	180	75	E	1	1	1	11	961	Klausmarkdal
1826 III	***Vevelstad***	UN *875*	*815*	260	Calcitic		Circular	1	1	0	0	0	400	0	200	0.08	0.00	60	5				1	0	0	0	0	
1826 III	***Vevelstad***	UN *890*	*810*	220	Calcitic		Arc	1	1	0	0	0	5000	0	300	1.50	0.00	40	80	20	54	E	1	0	1	0	0	
1826 III	***Vevelstad***	UN *890*	*820*	100	Calcitic		Linear	1	1	0	0	0	1000	0	200	0.20	0.00	50	5	10			1	0	0	0	0	
1826 III	***Vevelstad***	UN *899*	*870*	300	Calcitic		Linear	1	1	0	0	0	600	0	100	0.06	0.00	300	60	180			0	0	0	0	0	
1826 III	***Vevelstad***	UN *919*	*940*	667	Calcitic		Linear	1	1	0	0	0	1500	0	100	0.15	0.00	467	80	5			1	0	0	0	0	Incl. to N.
1826 III	***Vevelstad***	UN *880*	*765*	120	Calcitic		Arc	1	1	0	1	0	2000	2000	200	0.40	0.00	120	80				0	0	0	0	0	Storfjorden
1826 III	***Vevelstad***	UN *870*	*720*	120	Calcitic		Linear	1	1	0	1	0	1000	*1000*	100	0.10	0.00	120	120	170	81	E	1	0	0	0	0	
1826 III	***Vevelstad***	UN *855*	*710*	400	Calcitic		Linear	1	1	0	0	0	300	0	50	0.02	0.00	10	10	40			0	0	0	0	0	
1826 III	***Vevelstad***	UN *850*	*700*	400	Calcitic		Circular	1	1	0	0	0	200	0	100	0.02	0.00	20	20				1	0	0	0	0	
Area		328 *UN* *905*	*675*	*398*	*Calcitic?*		*Unmapped*	1	1	0	1	0	*1500*	1500	*20*	*0.03*	*0.00*	*238*	*30*	150	80	W	0	1	0	10	1340	Bulandsdal

UPPERMOST ALLOCHTHON: Helgeland Nappe Complex: Zone 2 (Fjord Area)

MAP SHEET	MAP NAME & NAPPE AREA	UTM / SWEDISH RN COORD	MAX ALT.	GEOL MAP IDENT	SAMPLE IDENT	OUTCROP SHAPE	O	R	T	V	D	LENGTH (Metres)	VISITED LENGTH	WIDTH	CARB. AREA	DOL. AREA	VR Length	VR Width	STRIKE	DIP	#	E	F	W	C	L	COMMENTS
1825 IV	*Velfjord*	UN *764 600*	380	Calcitic		Linear	1	1	0	0	0	5000	0	50	0.25	0.00	300	60	40			0	0	0	0	0	
1825 IV	*Velfjord*	UN *813 625*	80	Calcitic		Linear	1	1	0	0	0	200	0	50	0.01	0.00	54	5	20			1	0	0	0	0	
1825 IV	*Velfjord*	UN *810 607*	105	Calcitic		Linear	1	1	0	0	0	600	0	50	0.03	0.00	105	20	50			1	0	0	0	0	
1825 IV	*Velfjord*	UN *810 605*	110	Calcitic		Triangle	1	0	0	0	0	1000	0	200	0.20	0.00	110	20				1	0	0	0	0	
1825 IV	*Velfjord*	UN *785 590*	599	Calcitic		Arc	1	1	0	1	0	1500	1500	100	0.15	0.00	364	60				1	0	0	9	262	Saeterfjellhullet etc. GPN 97,01
1825 IV	*Velfjord*	UN *790 590*	560	Calcitic		Arc	1	0	0	1	0	5000	3500	200	1.00	0.00	560	40	45	50	S	1	0	0	3	359	Klimpengr etc. GPN 97 + local rep.
1825 IV	*Velfjord*	UN *810 590*	280	Calcitic		Linear	1	0	0	1	0	4000	500	300	1.20	0.00	280	66	35	41	E	1	0	0	1	10	Halsengrotta
1825 IV	*Velfjord*	UN *735 560*	40	Calcitic		Several	1	1	0	0	0	500	0	100	0.05	0.00	10	5				1	0	0	0	0	
1825 IV	*Velfjord*	UN *730 545*	40	Calcitic		Linear	1	1	0	0	0	600	0	50	0.03	0.00	20	5	50			1	0	0	0	0	
1825 IV	*Velfjord*	UN *712 525*	5	Calcitic		Circular	1	1	0	0	0	200	0	100	0.02	0.00	5	5				1	0	0	0	0	Low lying coastal
1825 IV	*Velfjord*	UN *725 530*	100	Calcitic		Irregular	1	1	0	0	0	700	0	100	0.07	0.00	80	20				0	0	0	0	0	
1825 IV	*Velfjord*	UN *730 523*	100	Calcitic		Linear	1	1	0	0	0	500	0	100	0.05	0.00	40	20	40			1	0	0	0	0	Low lying coastal
1825 IV	*Velfjord*	UN *713 497*	80	Calcitic		Linear	1	1	0	0	0	300	0	50	0.01	0.00	20	40	5	36	E	0	0	0	0	0	
1825 IV	*Velfjord*	UN *722 509*	10	Calcitic		Circular	1	1	0	0	0	200	0	100	0.02	0.00	10	5				0	0	0	0	0	
1825 IV	*Velfjord*	UN *728 512*	40	Calcitic		Circular	1	1	0	0	0	300	0	100	0.03	0.00	20	10				0	0	0	0	0	
1825 IV	*Velfjord*	UN *730 517*	40	Calcitic		Circular	1	1	0	0	0	100	0	100	0.01	0.00	5	5				0	0	0	0	0	
1825 IV	*Velfjord*	UN *738 521*	60	Calcitic		Linear	1	0	0	0	0	400	0	50	0.02	0.00	5	10	60			0	0	0	0	0	
1825 IV	*Velfjord*	UN *755 530*	220	Calcitic		Two limbs	1	1	0	0	0	2500	0	200	0.50	0.00	190	40		32		0	0	0	0	0	
1825 IV	*Velfjord*	UN *760 520*	300	Calcitic		Linear	1	1	0	1	0	2000	2000	200	0.40	0.00	260	80	60		*E*	0	2	0	9	620	Fjelldal
1825 IV	*Velfjord*	UN *813 550*	160	Calcitic		Arc	1	0	0	1	0	3500	1500	200	0.70	0.00	160	40	180?		*E*	1	0	0	5	107	Bordvikgrotta + Holåsen
1825 IV	*Velfjord*	UN *820 530*	160	Calcitic	Calcitic	Triangle	1	0	0	1	0	1000	500	600	0.60	0.00	136	80	25	*80*	*W*	1	2	4	2	1000	Navan: Nordlysgr.+ Marimyntholet
1825 IV	*Velfjord*	UN *806 520*	200	Calcitic		Linear	1	0	0	1	0	600	600	100	0.06	0.00	200	100	30			1	0	0	0	0	TF00
1825 IV	*Velfjord*	UN *800 515*	200	Calcitic		Rectangle	1	1	0	1	0	500	200	300	0.15	0.00	200	100				1	0	0	1	58	Skånvikgrotta. TF00
1825 IV	*Velfjord*	UN *820 560*	80	Calcitic		Irregular	1	0	0	0	0	3500	0	200	0.70	0.00	80	50	175	50	E	1	0	0	0	0	
1825 IV	*Velfjord*	UN *825 565*	60	Calcitic		Arc	1	0	0	0	0	3000	0	100	0.30	0.00	60	40	170	54	E	0	0	0	0	0	Hallaraunet
1825 IV	*Velfjord*	UN *826 528*	120	Calcitic		Circular	1	0	0	0	0	300	0	200	0.06	0.00	103	103				0	0	0	0	0	
1825 IV	*Velfjord*	UN *830 528*	70	Calcitic		Circular	1	0	0	0	0	250	0	200	0.05	0.00	40	53				1	0	0	0	0	
1825 IV	*Velfjord*	UN *832 528*	70	Calcitic		Circular	1	0	0	0	0	300	0	200	0.06	0.00	30	30				1	0	0	0	0	
1825 IV	*Velfjord*	UN *828 525*	100	Calcitic		Circular	1	0	0	0	0	400	0	300	0.12	0.00	83	40				0	0	0	0	0	
1825 IV	*Velfjord*	UN *805 490*	100	Calcitic		Linear	1	1	0	0	0	750	0	100	0.08	0.00	100	20	20			0	0	0	0	0	
1825 IV	*Velfjord*	UN *830 520*	260	Calcitic		Sinuous	1	0	0	0	0	2000	0	100	0.20	0.00	243	60	110	23	N	0	0	0	0	0	
1825 IV	*Velfjord*	UN *820 494*	100	Calcitic		Linear	1	0	0	0	0	600	0	50	0.03	0.00	23	5	10	32	E	0	0	0	0	0	
1825 IV	*Velfjord*	UN *824 618*	19	Calcitic		Rectangle	1	1	0	0	0	200	0	100	0.02	0.00	19	19				1	0	0	0	0	Low lying coastal
1825 IV	*Velfjord*	UN *822 612*	16	Calcitic		Triangle	1	1	0	0	0	200	0	100	0.02	0.00	16	16				1	0	0	0	0	Low lying coastal
1825 IV	*Velfjord*	UN *845 550*	20	Calcitic		Arc	1	0	0	0	0	1000	0	100	0.10	0.00	20	20				1	0	0	0	0	Low lying coastal
1825 IV	*Velfjord*	UN *850 560*	140	Calcitic		Two limbs	1	1	0	1	0	5000	500	300	1.50	0.00	140	140				0	0	0	1	5	Naustvik: Hallaran
1825 IV	*Velfjord*	UN *850 520*	412	Calcitic		3 limbs	1	0	0	1	0	18000	1000	700	13.00	0.00	400	412		50		1	1	4	1	315	Tourist Cave, Svadhylla
1825 IV	*Velfjord*	UN *795 456*	200	Calcitic		Linear	1	0	0	0	0	1500	0	200	0.30	0.00	200	200	100			0	0	0	0	0	
1825 IV	*Velfjord*	UN *810 454*	260	Calcitic		Linear	1	0	0	0	0	1500	0	50	0.08	0.00	160	20	90			1	0	0	0	0	
1825 IV	*Velfjord*	UN *810 450*	384	Calcitic	Calcitic	Sinuous	1	1	0	1	0	5000	2500	100	0.50	0.00	304	60		25	E	1	0	1	15	1593	Svartdal
1825 IV	*Velfjord*	UN *840 434*	400			*Unmapped*	1	0	0	1	0	*500*	500	*100*	*0.05*	0.00	100	20				0	0	0	4	186	Nonsdal. GPN 97
1825 IV	*Velfjord*	UN *832 460*	340	Calcitic		Arc	1	1	0	1	0	2000	1000	100	0.20	0.00	280	60		45	E	1	0	0	11	449	Hestfjellbotn
1825 IV	*Velfjord*	UN *890 450*	88	Calcitic		Arc	1	1	0	1	0	5500	2000	400	2.20	0.00	73	50	?	80	E/W	1	0	1	5	118	Saus
1825 IV	*Velfjord*	UN *900 490*	80	Calcitic		Linear	1	1	0	0	0	2000	0	200	0.40	0.00	80	80	140	9	E	1	0	0	0	0	
1825 IV	*Velfjord*	*UN 858 420*	*191*			*Unmapped*	1	1	0	1	0	*2500*	2500	*300*	*0.75*	*0.00*	*130*	*40*	50	60	W	1	0	1	19	983	Meinvatn++. Small pluton to east
1825 IV	*Velfjord*	UN *900 400*	292	Calcitic		Irregular	1	0	0	1	0	7000	3000	1500	10.50	0.00	*256*	278		60		1	0	3	0	0	Storvatn. Little investigated
1825 IV	*Velfjord*	UN *860 547*	94	Calcitic		Rectangle	1	1	0	0	0	500	0	300	0.15	0.00	94	40				0	0	0	0	0	Akset cave?
1825 IV	*Velfjord*	UN *925 470*	180	Calcitic		Rectangle	1	1	0	0	0	500	0	300	0.15	0.00	100	165				0	0	0	0	0	
1825 IV	*Velfjord*	UN *865 557*	50	Calcitic		Irregular	1	1	0	0	0	1300	0	100	0.10	0.00	50	50				1	0	0	0	0	Rugås cave?
1825 IV	*Velfjord*	UN *865 565*	40	Calcitic		Rectangle	1	1	0	0	0	300	0	100	0.03	0.00	40	5				1	0	0	0	0	

UPPERMOST ALLOCHTHON: Helgeland Nappe Complex: Zone 2 (Fjord Area)

Metres

MAP SHEET	MAP NAME & NAPPE AREA	UTM / SWEDISH RN COORD		MAX ALT.	GEOL MAP IDENT	SAMPLE IDENT	OUTCROP SHAPE	O	R	T	V	D	LENGTH	VISITED LENGTH	WIDTH	CARB. AREA	DOL. AREA	VR Length	VR Width	STRIKE	DIP	#	E	F	W	C	L	COMMENTS
1825 IV	***Velfjord***	UN *868*	*565*	20	Calcitic		Linear	1	1	0	0	0	300	0	100	0.03	0.00	20	5	160			1	0	0	0	0	Low lying coastal
1825 IV	***Velfjord***	UN *870*	*565*	26	Calcitic		Linear	1	1	0	0	0	600	0	100	0.06	0.00	26	26	160			1	0	0	0	0	Low lying coastal
1825 IV	***Velfjord***	UN *860*	*580*	220	Calcitic		Linear	1	1	0	1	0	3000	200	100	0.30	0.00	220	120	130			1	0	0	0	0	Hegge Quarry. TF00
1825 IV	***Velfjord***	UN *875*	*565*	10	Calcitic		Linear	1	1	0	0	0	1000	0	100	0.10	0.00	10	10	140			1	0	0	0	0	Low lying coastal
1825 IV	***Velfjord***	UN *880*	*560*	25	Calcitic		Rectangle	1	1	0	0	0	1000	0	600	0.60	0.00	25	20				0	0	0	0	0	Low lying coastal
1825 IV	***Velfjord***	UN *890*	*560*	60	Calcitic		Rectangle	1	0	0	0	0	500	0	300	0.15	0.00	57	20				0	0	0	0	0	
1825 IV	***Velfjord***	UN *846*	*593*	60	Calcitic		Linear	1	1	0	1	0	200	200	50	0.01	0.00	10	10	140			0	0	0	2	47	Aunholet
1825 IV	***Velfjord***	UN *848*	*593*	64	Calcitic		Linear	1	1	0	1	0	500	500	50	0.03	0.00	14	5	140			0	1	0	0	0	Engjavatn
1825 IV	***Velfjord***	UN *860*	*587*	160	Calcitic		Linear	1	1	0	0	0	1500	0	100	0.15	0.00	160	36	130			1	0	0	0	0	
1825 IV	***Velfjord***	UN *855*	*600*	252	Calcitic		Linear	1	1	0	0	0	1500	0	200	0.30	0.00	252	60	140			0	0	0	0	0	
1825 IV	***Velfjord***	UN *852*	*606*	40	Calcitic		Linear	1	1	0	0	0	300	0	100	0.03	0.00	40	40	140			0	0	0	0	0	
1825 IV	***Velfjord***	UN *855*	*605*	190	Calcitic		Linear	1	1	0	0	0	900	0	100	0.09	0.00	190	40	140			0	0	0	0	0	
1825 IV	***Velfjord***	UN *863*	*605*	20	Calcitic		Linear	1	1	0	0	0	300	0	100	0.03	0.00	20	20	140			0	0	0	0	0	Low lying coastal
1825 IV	***Velfjord***	UN *865*	*610*	20	Calcitic		Linear	1	1	0	0	0	500	0	100	0.05	0.00	20	20	140	54	E	1	0	0	0	0	Low lying coastal
1825 IV	***Velfjord***	UN *882*	*535*	60	Calcitic		Linear	1	1	0	0	0	400	0	100	0.04	0.00	10	10	130			0	1	0	0	0	Poss. feature
1825 IV	***Velfjord***	UN *887*	*537*	20	Calcitic		Linear	1	1	0	0	0	300	0	100	0.03	0.00	5	10	130			1	0	0	0	0	
1825 IV	***Velfjord***	UN *880*	*550*	50	Calcitic		Linear	1	1	0	0	0	2500	0	100	0.25	0.00	50	50	130	70	E/W	1	0	0	0	0	Bru and Straum caves?
1825 IV	***Velfjord***	UN *900*	*580*	130	Calcitic		Linear	1	0	0	0	0	3500	0	50	0.20	0.00	130	60	150			0	0	0	0	0	
1825 IV	***Velfjord***	UN *905*	*585*	200	Calcitic		Linear	1	0	0	0	0	300	0	50	0.02	0.00	200	5	170	81	E	0	0	0	0	0	
Area	446	UN *907*	*585*	200	Calcitic		Linear	1	0	0	0	0	300	0	50	0.02	0.00	200	5	170			0	0	0	0	0	
1825 III	***Terråk***	UN *795*	*372*	110	Calcitic		Triangle	1	1	0	0	0	600	0	100	0.06	0.00	110	110				0	0	0	0	0	
1825 III	***Terråk***	UN *810*	*370*	360	Calcitic		Arc	1	1	0	0	0	1500	0	100	0.15	0.00	360	140		90		0	0	0	0	0	
1825 III	***Terråk***	UN *840*	*355*	341	Calcitic		Arc	1	1	0	0	0	2500	0	100	0.25	0.00	341	60		72	E	1	0	1	0	0	
1825 III	***Terråk***	UN *848*	*372*	200	Calcitic		Rectangle	1	1	0	0	0	300	0	200	0.06	0.00	155	10	115	63	S	0	0	0	0	0	
1825 III	***Terråk***	UN *855*	*367*	400	Calcitic		Rectangle	1	1	0	0	0	400	0	200	0.08	0.00	100	20	115	63	S	0	0	0	0	0	
1825 III	***Terråk***	UN *920*	*340*	327	Calcitic		Irregular	1	1	0	1	0	7000	4000	1200	8.40	0.00	327	327	170	27	E	0	2	2	1	8	Hongfjell: Unscheduled Cave
1825 III	***Terråk***	UN *928*	*355*	445	Calcitic		Linear	1	1	0	0	0	400	0	100	0.04	0.00	65	20				1	0	0	0	0	
1825 III	***Terråk***	UN *720*	*270*	40	Calcitic		Arc	1	1	0	0	0	1000	0	100	0.10	0.00	40	40	85	72	S	1	0	0	0	0	Low lying coastal
1825 III	***Terråk***	UN *750*	*266*	70	Calcitic		Linear	1	0	0	0	0	1000	0	200	0.20	0.00	70	20	110			1	0	0	0	0	
1825 III	***Terråk***	UN *770*	*245*	20	Calcitic		Arc	1	1	0	0	0	1000	0	200	0.20	0.00	20	20		54	S	0	0	0	0	0	Low lying coastal
1825 III	***Terråk***	UN *790*	*250*	140	Calcitic		Irregular	1	1	0	0	0	1500	0	300	0.45	0.00	140	100		72	W	1	0	0	0	0	
1825 III	***Terråk***	UN *780*	*278*	268	Calcitic		Arc	1	1	0	0	0	1500	0	100	0.15	0.00	268	20				0	0	0	0	0	
1825 III	***Terråk***	UN *805*	*265*	120	Calcitic		Arc	1	1	0	0	0	2500	0	100	0.25	0.00	120	120	90	72	N	1	0	0	0	0	
1825 III	***Terråk***	UN *820*	*280*	440	Calcitic		Linear	1	1	0	0	0	2500	0	100	0.25	0.00	180	60	120	54	N	1	0	0	0	0	
1825 III	***Terråk***	UN *700*	*170*	278	Calcitic		Linear	1	1	1	0	0	2000	0	100	0.20	0.00	278	40			E	1	0	0	0	0	Near HNC thrust
1825 III	***Terråk***	*UN* *744*	*176*	*181*			*Unmapped*	1	1	0	1	0	*300*	300	*50*	*0.01*	*0.00*	*30*	*20*				0	0	0	4	94	Jenshola etc
1825 III	***Terråk***	UN *750*	*200*	134	Calcitic		Rectangle	1	1	0	0	0	1000	0	600	0.60	0.00	134	114		50	E	0	0	0	0	0	
1825 III	***Terråk***	UN *785*	*223*	40	Calcitic		Rectangle	1	1	0	0	0	300	0	200	0.06	0.00	40	40				0	0	0	0	0	
1825 III	***Terråk***	UN *800*	*230*	200	Calcitic		Linear	1	0	0	0	0	1000	0	200	0.20	0.00	200	200	40	54	E	0	0	0	0	0	
1825 III	***Terråk***	UN *815*	*235*	120	Calcitic		Linear	1	1	0	0	0	500	0	100	0.05	0.00	120	20	20			1	0	0	0	0	
1825 III	***Terråk***	UN *820*	*230*	50	Calcitic		Linear	1	1	0	0	0	1000	0	200	0.20	0.00	50	10	20			1	0	0	0	0	
1825 III	***Terråk***	UN *820*	*155*	160	Calcitic		Linear	1	1	0	1	0	1000	1000	200	0.20	0.00	160	120	40			1	0	0	0	0	Jordfalldal. SN96. TF00
1825 III	***Terråk***	UN *860*	*230*	520	Calcitic		Linear	1	1	0	0	0	4000	0	100	0.40	0.00	520	100	35	45	E	0	0	1	0	0	
Area	500	UN *860*	*210*	540	Calcitic	Calcitic	Linear	1	1	0	1	0	17000	8000	1000	17.00	0.00	540	380	40	72	W	1	7	8	16	820	Stordal & Reppen
1824 IV	**Kongsmoen**	UN 780	080	670	Calcitic		Linear	1	1	0	0	0	2000	0	200	0.40	0.00	270	40	160			0	0	0	0	0	
Area	67	UN 800	090	554	Calcitic		Linear	1	1	0	0	0	3500	0	200	0.70	0.00	234	60	150			0	1	1	0	0	

UPPERMOST ALLOCHTHON: Helgeland Nappe Complex: Zone 2 (Fjord Area)

MAP SHEET	MAP NAME & NAPPE AREA	UTM / SWEDISH RN COORD			MAX ALT.	GEOL MAP IDENT	SAMPLE IDENT	OUTCROP SHAPE	O	R	T	V	D	LENGTH (Metres)	VISITED LENGTH (Metres)	WIDTH (Metres)	CARB. AREA	DOL. AREA	VR Length (Metres)	VR Width (Metres)	STRIKE	DIP	#	E	F	W	C	L	COMMENTS
1827 II	**Nesna**	VP	110	380	140	Calcitic		Linear	1	0	0	0	0	4000	0	100	0.40	0.00	140	60	90			0	0	0	0	0	Check Upper Nappe
1827 II	**Nesna**	VP	150	390	46	Calcitic		Linear	1	0	0	0	0	5500	0	200	1.00	0.00	46	20	60			0	0	0	0	0	Check Upper Nappe
1827 II	**Nesna**	VP	030	300	118	Calcitic		Linear	1	0	0	0	0	12000	0	200	2.40	0.00	118	20	75	77	S	1	0	0	0	0	Bends S at E end
1827 II	**Nesna**	VP	050	290	71	Calcitic		Sinuous	1	0	0	0	0	15000	0	100	1.50	0.00	71	60				1	0	0	0	0	
Area	187	VP	180	360	197	Calcitic		Linear	1	0	0	0	0	14000	0	200	2.80	0.00	168	148	70	90		1	0	0	0	0	Bends S at E end
1826 I	**Mosjøen**							Sinuous	1	*0*	0	1	0	12000	2500	200	2.40	0.00	197	60	50	54	W	0	0	1	1	92	Hubrohula. TF00
Area	10																												**No mapped carbonates**
1825 I	***Tosbotn***	UN	*942*	*490*	256	Calcitic		Linear	1	0	0	1	0	2500	2000	100	0.50	0.00	176	60	150	54	E	0	0	0	3	57	Tarmaunbotn (Velfjord)
1825 I	***Tosbotn***	UN	*950*	*490*	252	Calcitic		2 limbs	1	0	0	1	0	8000	7500	50	0.40	0.00	209	20	160	54	E	0	3	1	13	451	Langfj., Aunhatten, Dyrmoen. TF00
1825 I	***Tosbotn***	UN	*950*	*470*	188	Calcitic		Linear	1	0	0	0	0	500	0	50	0.03	0.00	10	20	180			1	1	0	0	0	Juvatn
1825 I	***Tosbotn***	UN	*952*	*470*	270	Calcitic		Linear	1	0	0	0	0	500	0	50	0.03	0.00	100	10	180			0	1	0	0	0	Juvatn
1825 I	***Tosbotn***	UN	*962*	*440*	580	Calcitic		Linear	1	0	0	0	0	3800	0	100	0.38	0.00	320	40	180	72	E	0	0	0	0	0	
1825 I	***Tosbotn***	UN	*960*	*400*	400	Calcitic		Sinuous	1	0	0	1	0	3500	3000	200	0.70	0.00	400	60	160	81	E	1	0	1	2	41	Svartdalsholet
1825 I	***Tosbotn***	UN	*970*	*390*	100	Calcitic	Calcitic	Sinuous	1	0	0	1	0	1500	500	100	0.15	0.00	100	30	160	81	E	1	2	0	2	168	Landegrottene
Area	45	UN	*973*	*390*	100	Calcitic		Sinuous	1	1	0	0	0	1500	0	100	0.15	0	100	20	160	81	E	1	0	0	0	0	
1825 II	***Majafjellet***	UN	*970*	*350*	220	Calcitic		Linear	1	0	0	0	0	1500	0	200	0.30	0.00	220	220	180			0	0	0	0	0	
Area	57																												
1927 III	**Elsfjord**						(South of Ranafjord)																						
Area	44																												**No mapped carbonates**

UPPERMOST ALLOCHTHON: Helgeland Nappe Complex: Zone 3 (Central Granite Area)

Metres

MAP SHEET	MAP NAME & NAPPE AREA	UTM / SWEDISH RN COORD	MAX ALT.	GEOL MAP IDENT	SAMPLE IDENT	OUTCROP SHAPE	O	R	T	V	D	LENGTH	VISITED LENGTH	WIDTH	CARB. AREA	DOL. AREA	VR Length	VR Width	STRIKE	DIP	#	E	F	W	C	L	COMMENTS
Totals	2002		####				63	26	0	21	0	155800	28900	####	33.14	0.00	#####	####		###	33	21	20	8	36	3320	
%								41%	0%	33%	0%				1.66%	0.00%					52%	33%					
Averages			421									2473	1376	150	0.53	#####	220	60		63			0.32	0.13	1.71	158	
Maxima			1000									11000	7000	1500	9.00	0.00	690	340		90			4	2	9	2385	
1826 IV	***Tjøtta***	UP *930 030*	160	Calcitic		Linear	1	0	0	0	0	600	0	100	0.06	0.00	160	20	180			1	0	0	0	0	
1826 IV	***Tjøtta***	UP *933 030*	80	Calcitic		Linear	1	0	0	0	0	300	0	50	0.02	0.00	80	40	10			1	0	0	0	0	
1826 IV	***Tjøtta***	UP *947 050*	40	Calcitic		Linear	1	1	0	0	0	1000	0	50	0.05	0.00	40	40	10			0	0	0	0	0	
1826 IV	***Tjøtta***	UP *950 050*	40	Calcitic		Linear	1	1	0	0	0	2300	0	50	0.11	0.00	40	40	10			0	0	0	0	0	
1826 IV	***Tjøtta***	UN *952 960*	516	Calcitic		2 limbs	1	1	0	1	0	4500	1000	100	0.45	0.00	200	120				1	1	1	0	0	Not fully inv. 2Q. Incl. Mosjøen+Eiterådal.
1826 IV	***Tjøtta***	UN *932 960*	729	Calcitic		Linear	1	1	0	0	0	300	0	50	0.02	0.00	120	20	180			1	0	0	0	0	
Area	46	UN *935 945*	420	Calcitic		Linear	1	1	0	0	0	300	0	50	0.02	0.00	92	10	175			1	0	0	0	0	
1826 III	***Vevelstad***	UN *943 940*	518	Calcitic		Linear	1	0	0	1	0	1700	200	100	0.17	0.00	78	20	10			0	0	0	0	0	Incl. to N.
1826 III	***Vevelstad***	UN *950 920*	702	Calcitic		2 limbs	1	0	0	1	0	3500	2000	100	0.35	0.00	358	156	180	36	W	0	1	2	8	62	Top Bed Cave etc
1826 III	***Vevelstad***	UN *951 900*	460	Calcitic		Linear	1	0	0	0	0	1000	0	50	0.05	0.00	160	20	180			0	0	0	0	0	
1826 III	***Vevelstad***	UN *950 840*	560	Calcitic		3 limbs	1	0	0	0	0	3000	0	200	0.60	0.00	560	100	180		W	0	0	0	0	0	
Area	34	UN *950 820*	165	Calcitic		Triangle	1	0	0	0	0	1200	0	200	0.30	0.00	165	100	180	63	W	1	0	0	0	0	
1825 III	**Terråk**																										**No mapped carbonates**
Area	20																										
1824 IV	**Kongsmoen**																										**No mapped carbonates**
Area	322																										3 possible small features
1824 III	**Harran**																										**No mapped carbonates**
Area	86																										2 possible small features
1827 II	**Nesna**	VP 100 280	140	Calcitic		Linear	1	0	0	0	0	8500	0	100	0.85	0.00	140	40	50	59	E	0	0	0	0	0	
1827 II	**Nesna**	VP 020 220	126	Calcitic		Linear	1	1	0	0	0	3500	0	200	0.70	0.00	126	60	60			1	0	0	0	0	
1827 II	**Nesna**	VP 050 230	126	Calc+lst		Irregular	1	0	0	0	0	2500	0	1500	4.00	0.00	126	126				1	0	0	0	0	Cont. under water
1827 II	**Nesna**	VP 080 250	340	Calc+lst		Irregular	1	1	0	0	0	9000	0	1000	9.00	0.00	340	340	40	45	E	0	0	1	0	0	
Area	120	VP 080 230	460	Calcitic		Linear	1	1	0	0	0	7000	0	200	1.40	0.00	380	120	20			0	0	1	0	0	Incl. to SW (Mosjøen)
1826 I	***Mosjøen***	VP *010 200*	60	Calcitic		Linear	1	1	0	0	0	5000	0	200	1.00	0.00	60	60	30	41	E	1	0	0	0	0	1 Quat. karst
1826 I	***Mosjøen***	UP *983 130*	160	Calcitic		Linear	1	0	0	0	0	1000	0	100	0.10	0.00	80	20	55			0	0	0	0	0	
1826 I	***Mosjøen***	VP *020 095*	720	Calcitic		Arc	1	0	0	0	0	2500	0	300	0.75	0.00	598	100	60	45	S	0	0	0	0	0	
1826 I	***Mosjøen***	UP *960 980*	140	Calcitic		Linear	1	1	0	0	0	500	0	100	0.05	0.00	140	20				0	0	0	0	0	Sørfjordgrotta reported
1826 I	***Mosjøen***	UP *980 050*	500	Calcitic		Linear	1	0	0	0	0	1200	0	100	1.20	0.00	50	40	170			0	0	0	0	0	
1826 I	***Mosjøen***	UP *995 022*	640	Calcitic		Linear	1	0	0	0	0	1000	0	100	0.10	0.00	240	40	110	59	N	0	0	0	0	0	
1826 I	***Mosjøen***	UP *995 020*	600	Calcitic		Linear	1	0	0	0	0	1000	0	100	0.10	0.00	300	100	110	59	N	0	0	0	0	0	
1826 I	***Mosjøen***	UP *998 065*	660	Calcitic		Linear	1	0	0	0	0	1000	0	100	0.10	0.00	160	160				1	0	0	0	0	
Area	132	VP *000 040*	700	Calcitic		4 limbs	1	0	0	0	0	11000	0	100	1.10	0.00	360	100				0	0	1	0	0	4 Quat. karst (Neverdal)
1826 II	***Eiterådal***	UN *956 830*	500	Calcitic		Linear	1	0	0	1	0	2000	1000	100	0.20	0.00	500	20	5	45	E	0	0	1	0	0	Impen. sink + res.
1826 II	***Eiterådal***	UN *957 810*	340	Calcitic		Linear	1	0	0	0	0	3000	0	100	0.30	0.00	340	60	175	45	E	0	0	0	0	0	
1826 II	***Eiterådal***	UN *960 840*	360	Calcitic		Linear	1	0	0	1	0	2000	1500	100	0.20	0.00	360	60	5		E	0	0	0	3	98	Bønnå
1826 II	***Eiterådal***	UN *970 858*	*500*			*Unmapped*	1	1	0	1	0	*800*	*800*	*50*	*0.04*	*0.00*	*120*	*40*				0	0	0	1	50	Multi Entr. System
Area	323	UN *970 843*	*215*			*Unmapped*	1	1	0	1	0	*1500*	1000	*50*	*0.08*	*0.00*	*85*	*40*	40	90		0	4	0	0	0	TF98

UPPERMOST ALLOCHTHON: Helgeland Nappe Complex: Zone 3 (Central Granite Area)

Metres

MAP SHEET	MAP NAME & NAPPE AREA	UTM / SWEDISH RN COORD		MAX ALT.	GEOL MAP IDENT	SAMPLE IDENT	OUTCROP SHAPE	O	R	T	V	D	LENGTH	VISITED LENGTH	WIDTH	CARB. AREA	DOL. AREA	VR Length	VR Width	STRIKE	DIP	#	E	F	W	C	L	COMMENTS
1825 I	***Tosbotn***	UN	*950*	*630*	400	Calcitic		Linear	1	0	0	0	0	1500	0	100	0.15	0.00	400	100	20	54		1	0	0	0	0	
1825 I	***Tosbotn***	UN	*953*	*635*	280	Calcitic		Linear	1	0	0	0	0	600	0	100	0.06	0.00	80	20	10	54		1	0	0	0	0	
1825 I	***Tosbotn***	UN	*955*	*637*	240	Calcitic		Linear	1	0	0	0	0	300	0	100	0.03	0.00	60	20	10	54		1	0	0	0	0	
1825 I	***Tosbotn***	UN	*963*	*640*	120	Calcitic		Triangle	1	1	0	0	0	600	0	100	0.06	0.00	10	10		72	E	0	0	0	0	0	
1825 I	***Tosbotn***	UN	*962*	*625*	100	Calcitic		Linear	1	1	0	0	0	900	0	100	0.09	0.00	100	80	10	72	E	1	0	0	0	0	
1825 I	***Tosbotn***	UN	*965*	*625*	100	Calcitic		Linear	1	1	0	0	0	600	0	100	0.06	0.00	100	80	180	72	E	0	0	0	0	0	
1825 I	***Tosbotn***	UN	*966*	*640*	240	Calcitic		Linear	1	1	0	0	0	2200	0	50	0.10	0.00	240	40	170	72	E	0	1	0	0	0	
1825 I	***Tosbotn***	UN	*980*	*614*	420	Calcitic		Linear	1	1	0	1	0	7000	2250	50	0.35	0.00	160	40	160	72	E	0	0	0	0	0	Strompdal. SN92
1825 I	***Tosbotn***	UN	*952*	*590*	560	Calcitic		Linear	1	0	0	1	0	4000	1000	100	0.40	0.00	560	60	180	54	E	1	0	0	2	28	Klavbekk
1825 I	***Tosbotn***	UN	*960*	*615*	300	Calcitic		Linear	1	0	0	0	0	400	0	100	0.04	0.00	300	10	180	63	E	1	0	0	0	0	
1825 I	***Tosbotn***	UN	*965*	*590*	420	Calcitic		Linear	1	0	0	1	0	7000	7000	400	2.80	0.00	420	140	180	72	E	1	4	0	9	466	Tettingsdal
1825 I	***Tosbotn***	UN	*974*	*600*	340	Calcitic		Linear	1	1	0	1	0	3000	500	50	0.15	0.00	340	40	180	72	E	0	3	0	1	20	Keith's 1990 Cave
1825 I	***Tosbotn***	UN	*990*	*590*	340	Calcitic		Linear	1	1	0	0	0	500	0	100	0.05	0.00	80	20	180	63	E	1	0	0	0	0	
1825 I	***Tosbotn***	VN	*065*	*610*	620	Calcitic		Linear	1	1	0	0	0	1500	0	200	0.30	0.00	87	40	40	45	E	0	2	0	0	0	
1825 I	***Tosbotn***	UN	*973*	*500*	820	Calcitic		Linear	1	0	0	0	0	5500	0	50	0.25	0.00	500	60	160	63	E	0	0	1	0	0	
1825 I	***Tosbotn***	VN	*003*	*515*	940	Calcitic		Circular	1	1	0	0	0	300	0	300	0.08	0.00	80	30			E	0	0	0	0	0	n. Snøfjell cave reported
1825 I	***Tosbotn***	VN	*010*	*485*	*520*			*Unmapped*	1	1	0	1	0	*1500*	1500	*200*	*0.30*	*0.00*	*120*	*50*	30			1	0	0	4	205	Låjroe
1825 I	***Tosbotn***	VN	*030*	*470*	120	Calcitic		Linear	1	1	0	1	0	500	50	100	0.05	0.00	80	40				1	0	0	0	0	Leirådal
1825 I	***Tosbotn***	VN	*070*	*410*	1000	Calcitic		Sinuous	1	0	0	0	0	9000	0	100	0.90	0.00	477	20				1	0	0	0	0	
1825 I	***Tosbotn***	VN	*070*	*520*	580	Calcitic		Linear	1	0	0	1	0	2500	2500	100	0.25	0.00	437	40	180	63	E	0	0	0	1	6	Godvassdal.
1825 I	***Tosbotn***	VN	*073*	*513*	300			*Unmapped*	1	0	0	1	0	500	500	10	0.00	0.00	60	5	180	90		0	0	0	0	0	TF00
1825 I	***Tosbotn***	VN	*082*	*528*	700			*Unmapped*	1	0	0	1	0	*100*	100	*50*	0.00	0.00	60	40	20	90		0	0	0	0	0	TF00. Waterfall Rising
1825 I	***Tosbotn***	VN	*085*	*500*	*700*			*Unmapped*	1	0	0	1	0	*1000*	1000	*200*	*0.20*	*0.00*	*240*	*60*	15	90		0	4	0	7	2385	Toerfjell
1825 I	***Tosbotn***	VN	*106*	*550*	720	Calcitic		Rectangle	1	0	0	0	0	200	0	50	0.01	0.00	50	10		63	W	0	0	0	0	0	
1825 I	***Tosbotn***	VN	*003*	*400*	780	Calcitic		Sinuous	1	1	0	1	0	5500	1500	150	0.80	0.00	690	100		54	E	0	0	0	0	0	KB: SN 96. Incl. to S
1825 I	***Tosbotn***	VN	*070*	*460*	220	Calcitic		Linear	1	1	0	0	0	1000	0	100	0.10	0.00	140	40	170			0	0	0	0	0	
1825 I	***Tosbotn***	VN	*075*	*460*	240	Calcitic		Linear	1	0	0	0	0	1000	0	100	0.10	0.00	40	40	150	72	E	0	0	0	0	0	
1825 I	***Tosbotn***	VN	*080*	*440*	220	Calcitic		Linear	1	1	0	1	0	1500	1500	200	0.30	0.00	80	80	150			0	0	0	0	0	Tosdalen. SN92
1825 I	***Tosbotn***	VN	*098*	*420*	400	Calcitic		Linear	1	0	0	1	0	2000	*1000*	*50*	0.20	0.00	200	60	160			0	0	0	0	0	GPN01
1825 I	***Tosbotn***	VN	*100*	*420*	440	Calcitic		Linear	1	0	0	1	0	2400	*1000*	*50*	0.24	0.00	140	60	160			0	0	0	0	0	GPN01
Area	415	VN	*112*	*400*	960	Calcitic		Linear	1	0	0	0	0	2500	0	100	0.25	0.00	460	40	180			0	0	0	0	0	
1825 II	***Majafjellet***	UN	*990*	*310*	720	Calcitic		Sinuous	1	0	0	0	0	5000	0	200	1.00	0.00	530	100				0	0	0	0	0	
Area	344																												
1824 I	**Namskogan**																												**No mapped carbonates**
Area	38																												
1927 III	**Elsfjord**																												**No mapped carbonates**
Area	122																												1 Quat. karst

UPPERMOST ALLOCHTHON: Helgeland Nappe Complex: Zone 4 (Eiterådal and Jordbruelv)

Metres

MAP SHEET	MAP NAME & NAPPE AREA		UTM / SWEDISH RN COORD		MAX ALT.	GEOL MAP IDENT	SAMPLE IDENT	OUTCROP SHAPE	O	R	T	V	D	LENGTH	VISITED LENGTH	WIDTH	CARB. AREA	DOL. AREA	VR Length	VR Width	STRIKE	DIP	#	E	F	W	C	L	COMMENTS
Totals	814				#####				36	10	0	14	1	173700	44500	####	36.9	0.24	####	####		1539	21	28	16	15	182	14490	
%										28%	0%	39%	3%				4.53%	0.03%					58%	78%					
Averages					584									4825	3179	164	1.03	0.24	224	59		73			0.4	0.4	13.0	1035	
Maxima					1000									50000	25000	1000	12.00	0.24	687	300		90			6	13	110	9091	
1927 II	**Nesna**																												**No mapped carbonates**
Area	4																												
1826 I	***Mosjøen***	VP	*050*	*195*	380	Calcitic		Linear	1	1	0	0	0	1000	0	100	0.10	0.00	380	60	40			1	0	0	0	0	
1826 I	***Mosjøen***	VP	*050*	*190*	360	Calcitic		Linear	1	1	0	0	0	1000	0	1000	0.10	0.00	360	40	40			1	0	0	0	0	
1826 I	***Mosjøen***	VP	*075*	*205*	687	Calcitic		Linear	1	0	0	0	0	3500	0	100	0.35	0.00	687	60	20	41	E	1	1	0	0	0	
1826 I	***Mosjøen***	VP	*020*	*127*	500	Calcitic		Multi limbs	1	0	0	0	0	4500	0	100	0.45	0.00	200	60		77	W	1	0	0	0	0	
1826 I	***Mosjøen***	VP	*040*	*115*	300	Calcitic		Sinuous	1	0	0	0	0	1800	0	100	0.18	0.00	200	20	140	81	WE	1	0	0	0	0	
1826 I	***Mosjøen***	VP	*120*	*160*	420	Calcitic		Linear	1	0	0	0	0	2500	0	200	0.50	0.00	420	40	50	90		1	0	0	0	0	
1826 I	***Mosjøen***	VP	*130*	*160*	300	Calcitic		Linear	1	0	0	0	0	4000	0	100	0.40	0.00	300	80	50	81	W	0	0	0	0	0	
1826 I	***Mosjøen***	VP	*090*	*095*	648	Calcitic		Sinuous	1	0	0	0	0	4500	0	200	0.50	0.00	448	80				0	0	0	0	0	
1826 I	***Mosjøen***	VP	*082*	*080*	600	Calcitic		Arc	1	0	0	0	0	2500	0	200	0.50	0.00	330	20	180			0	0	0	0	0	
1826 I	***Mosjøen***	VP	*094*	*080*	560	Calcitic		Linear	1	0	0	0	0	1000	0	100	0.10	0.00	100	40	180			0	0	0	0	0	
1826 I	***Mosjøen***	VP	*100*	*070*	761	Calcitic		Linear	1	0	0	0	0	2500	0	200	0.50	0.00	141	40	20			0	0	0	0	0	
1826 I	***Mosjøen***	VP	*105*	*070*	720	Calcitic		Linear	1	0	0	0	0	4200	0	200	0.84	0.00	220	60	170	50	W	1	0	0	0	0	
1826 I	***Mosjøen***	VP	*100*	*030*	680	Calcitic		Sinuous	1	0	0	0	0	2500	0	200	0.50	0.00	130	60	140			1	0	0	0	0	
1826 I	***Mosjøen***	VP	*130*	*009*	670	Calcitic		Linear	1	0	0	0	0	1000	0	100	0.10	0.00	270	20	140			1	0	0	0	0	
1826 I	***Mosjøen***	VN	*160*	*970*	331	Calcitic		3 limbs	1	0	0	0	0	26000	0	200	5.20	0.00	159	140	180	72	W	1	2	0	0	0	4 Quat. karst. SN96. Incl. to S
1826 I	***Mosjøen***	VN	*165*	*980*	140	Calcitic		Linear	1	0	0	1	0	500	250	50	0.03	0.00	60	60	150	90		1	0	0	3	356	Øyåskjeleren et al
Area	320	VN	*175*	*960*	238	Calcitic		Sinuous	1	0	0	0	0	8500	0	100	0.85	0.00	158	20	170	63	W	1	0	0	0	0	Incl. to S (Eiterådal)
1826 II	***Eiterådal***	VN	*110*	*770*	400	Calcitic		Linear	1	1	0	0	0	500	0	100	0.50	0.00	69	20	0			1	0	0	0	0	
1826 II	***Eiterådal***	VN	*115*	*747*	350	Calcitic		Linear	1	1	0	0	0	300	0	50	0.02	0.00	5	5	0			1	0	0	0	0	
1827 II	***Eiterådal***	VN	*116*	*740*	370	Calcitic		Linear	1	1	0	0	0	200	0	50	0.01	0.00	18	5	0			1	0	0	0	0	
1826 II	***Eiterådal***	VN	*145*	*750*	400	Calcitic	Calcitic	Linear	1	0	0	1	0	11000	5500	500	5.50	0.00	220	220	180	75	W	1	6	0	11	2522	Eiterådal
1826 II	***Eiterådal***	VN	*160*	*750*	400	Calcitic		Linear	1	1	0	1	0	10000	500	100	1.00	0.00	200	40	180	54	W	0	0	0	0	0	TF97
1826 II	***Eiterådal***	VN	*158*	*713*	260	Calcitic		Linear	1	1	0	1	0	3000	2000	50	0.15	0.00	60	20	180	45	W	0	1	0	1	5	Holbekkgrotta
Area	296	VN	*168*	*709*	*430*			*Unmapped*	1	1	0	1	0	*500*	*250*	*50*	*0.03*	0.00	*40*	*20*				0	0	0	1	150	Disappointment Cave. TF00
1825 I	***Tosbotn***	VN	*148*	*629*	*1000*			*Unmapped*	1	0	0	1	0	*1000*	1000	10	*0.01*	*0.00*	*350*	*5*	180	90		1	0	0	5	37	Kvitfjell - 1
1825 I	***Tosbotn***	VN	*149*	*627*	*1000*			*Unmapped*	1	0	0	1	0	*1000*	1000	4	*0.00*	*0.00*	*350*	*4*	180	85	E	1	0	0	2	20	Kvitfjell - 3
1825 I	***Tosbotn***	VN	*152*	*622*	*900*			*Unmapped*	1	0	0	1	0	*900*	900	20	*0.02*	*0.00*	*300*	*20*	20	45	E	1	0	0	0	0	Kvitfjell - 4. Short unexp. caves
1825 I	***Tosbotn***	VN	*155*	*625*	*940*		Calc. (4off)	*Unmapped*	1	0	0	1	0	*600*	600	50	*0.03*	*0.00*	*200*	*20*	180	80	E	1	0	0	10	504	Kvitfjell - 7
1825 I	***Tosbotn***	VN	*129*	*493*	*800*			*Unmapped*	1	0	0	1	0	*500*	500	*40*	*0.02*	*0.00*	*40*	*10*	170	90		1	0	0	1	10	Collapsed Cave 1
1825 I	***Tosbotn***	VN	*126*	*495*	*780*			*Unmapped*	1	0	0	1	0	*500*	500	*40*	*0.02*	*0.00*	*60*	*10*	170	90		1	0	0	1	8	Collapsed Cave 2
1825 I	***Tosbotn***	VN	*120*	*510*	840	Calcitic		Arc	1	0	0	1	0	3500	3500	100	0.35	0.00	156	40	160	90		1	0	1	21	876	Jordhulefjell
1825 I	***Tosbotn***	VN	*130*	*505*	900	Calcitic		Linear	1	0	0	0	0	1500	0	100	0.15	0.00	80	60	140			1	0	0	0	0	Jordhulefjell
1825 I	***Tosbotn***	VN	*150*	*500*	894	Calc/Dol	Calc. (5 off)	Multi limbs	1	0	0	1	0	50000	25000	100	5.00	0.00	614	150	180	90		1	6	1	110	9091	Elgfjell - Jordbruelv + E. Jordhulefjell
Area	140	VN	*170*	*500*	633			*Sinuous*	1	0	0	1	0	4000	3000	100	0.65	0.00	310	80	30	60	W	1	0	0	16	911	Sarvejaella - S. Slopes (east)
1927 III	**Elsfjord**	VP	220	260	845	Calc+gr.		Irregular	1	1	0	0	0	12000	0	1000	12.00	0.00	362	300				1	0	13	0	0	{gneiss? Cal. Orogeny p.153. Incl SW
Area	30	VP	210	250	600	Dolom.		Tapering	1	1	0	0	1	1200	0	200	0.24	0.24	60	200				1	0	0	0	0	**South of Ranafjord only**
1925 IV	***Svenningdal***																												**No mapped carbonates**
Area	24																												

UPPERMOST ALLOCHTHON: Helgeland Nappe Complex: Zone 5 (Mosjøen to Fjellryggen)

MAP SHEET	MAP NAME & NAPPE AREA		UTM / SWEDISH RN COORD		MAX ALT.	GEOL MAP IDENT	SAMPLE IDENT	OUTCROP SHAPE	O	R	T	V	D	LENGTH	VISITED LENGTH	WIDTH	CARB. AREA	DOL. AREA	VR Length	VR Width	STRIKE	DIP	#	E	F	W	C	L	COMMENTS
																											Metres		
Totals		458			#####				39	15	0	10	5	164800	46400	####	37.894	2.58	####	####		####	20	21	15	8	79	7689	
%										38%	0%	26%	13%				8.3%	0.56%					51%	54%					
Averages					342									4226	4640	137	0.97	0.52	177	52		73			0.38	0.21	7.90	769	
Maxima					980									53000	31000	600	21.00	1.20	730	261		90			6	2	56	5995	
1826 I	***Mosjøen***		VP *180 140*		436	Calcitic	(& Dol?)	3 limbs	1	1	0	1	0	5000	1100	400	2.00	0.00	436	136	25	68	W	0	0	1	2	70	Bollhgr.+Nordvetgr. (Gustavson?). TF00
1826 I	***Mosjøen***		VP *120 075*		383	Calcitic		Linear	1	0	0	0	0	1600	0	50	0.08	0.00	383	40	20			1	0	0	0	0	
1826 I	***Mosjøen***		VP *120 050*		280	Calcitic		Linear	1	0	0	0	0	1000	0	50	0.05	0.00	20	20	170			0	0	0	0	0	
1826 I	***Mosjøen***		VP *150 024*		770	Calcitic		Sinuous	1	0	0	0	0	2000	0	100	0.20	0.00	240	20	90	32	S	0	0	0	0	0	
1826 I	***Mosjøen***		VP *150 021*		750	Calcitic		Sinuous	1	0	0	0	0	2500	0	100	0.25	0.00	150	20				0	0	0	0	0	
1826 I	***Mosjøen***		VP *150 018*		720	Calcitic		Arc	1	0	0	0	0	1500	0	100	0.15	0.00	140	20				0	0	0	0	0	
1826 I	***Mosjøen***		VP *160 008*		440	Calcitic		Arc	1	0	0	0	0	2000	0	100	0.20	0.00	100	40		68	E	1	0	0	0	0	
1826 I	***Mosjøen***		VP *170 000*		500	Calcitic		Irregular	1	0	0	1	0	3000	1500	600	1.80	0.00	500	160	110	72	S	1	1	0	6	985	Øyfjellgrotta et al
	Area	89	VN *180 968*		140	Calcitic		Linear	1	0	0	0	0	3000	0	50	0.15	0.00	140	10	160	63	W	1	0	0	0	0	
1826 II	***Eiterådal***		VN *175 990*		120	Calcitic		Linear	1	0	0	0	0	1000	0	100	0.10	0.00	120	100	160			1	0	0	0	0	
	Area	2																											**No mapped carbonates**
1926 IV	***Fustvatn***		VP *191 131*		156	Dolom.	Calcitic?	Linear	1	1	0	0	1	3000	0	200	0.60	0.60	119	80	165	90		1	0	0	0	0	Calc. blocks in stream
1926 IV	***Fustvatn***		VP *230 064*		500	Calcitic		Linear	1	1	0	0	0	2000	0	50	0.10	0.00	400	20	65			0	0	0	0	0	
1926 IV	***Fustvatn***		VP *190 045*		326	Calcitic		Sinuous	1	0	0	0	0	3000	0	100	0.30	0.00	240	20				1	0	0	0	0	Incl. to NE (Mosjøen)
1926 IV	***Fustvatn***		VP *200 040*		320	Dolom.		2 limbs	1	0	0	0	1	4000	0	100	0.40	0.40	240	50		75	W	1	0	0	0	0	
1926 IV	***Fustvatn***		VP *204 035*		180	Dolom.	Calcitic	Irregular	1	1	0	0	0	800	0	200	0.16	0.00	80	60				1	0	0	0	0	Sucritic, yellow. Vig. with dil. HCl.
1926 IV	***Fustvatn***		VP *190 030*		280			Irregular	1	0	0	1	1	4000	*500*	300	1.20	1.20	260	220		80	W	0	0	0	0	0	Andåsgr. + 2 UH caves. Incl. to NE
1926 IV	***Fustvatn***		VP *196 025*		90	Calcitic		Tapering	1	0	0	0	0	600	0	50	0.03	0.00	50	10				0	0	0	0	0	
1926 IV	***Fustvatn***		VP *187 007*		40	Calcitic		Triangle	1	0	0	0	0	200	0	100	0.02	0.00	20	20	140	70	E	0	0	0	0	0	
1926 IV	***Fustvatn***		VP *187 002*		100	Calcitic		Linear	1	0	0	0	0	500	0	100	0.05	0.00	60	10	150	55	E	0	0	0	0	0	
1926 IV	***Fustvatn***		VP *195 010*		166	Calcitic		Irregular	1	1	0	0	0	2500	0	500	1.25	0.00	60	60				0	0	0	0	0	
1926 IV	***Fustvatn***		VN *189 940*		100	Calcitic		Linear	1	0	0	0	0	500	0	50	0.02	0.00	20	20	180			1	0	0	0	0	
1926 IV	***Fustvatn***		VN *192 940*		60	Calcitic		Linear	1	0	0	0	0	1000	0	50	0.05	0.00	40	40	180			1	0	0	0	0	
1926 IV	***Fustvatn***		VN *200 975*		260	Calcitic		Sinuous	1	1	0	0	0	3000	0	50	0.15	0.00	130	20	140	80	W	0	0	0	0	0	
1926 IV	***Fustvatn***		VN *200 980*		260	Calcitic		Sinuous	1	1	0	0	0	3500	0	50	0.18	0.00	130	60	150	75	W	1	0	0	0	0	
1926 IV	***Fustvatn***		VN *203 940*		260	Calcitic		Linear	1	1	0	0	0	2000	0	50	0.10	0.00	130	20	180			0	0	0	0	0	
1926 IV	***Fustvatn***		VN *204 940*		273	Calcitic		Linear	1	1	0	0	0	2500	0	50	0.12	0.00	123	20	180			0	0	0	0	0	
1926 IV	***Fustvatn***		VN *205 940*		260	Calcitic		2 limbs	1	1	0	0	0	3000	0	50	0.15	0.00	60	20	180			1	0	0	0	0	Incl. S (Trofors)
1926 IV	***Fustvatn***		VN *210 952*		240	Calcitic		Linear	1	1	0	0	0	3000	0	100	0.30	0.00	180	80	180			1	1	1	0	0	Radios Cave?
1926 IV	***Fustvatn***		VN *210 990*		321	Calcitic		Tapering	1	1	0	1	0	8500	*500*	500	4.25	0.00	261	261	160	90		0	6	2	2	295	Bokkflåggrotta+5m cave
1926 IV	***Fustvatn***		VN *230 982*		300	Dolom.	D possible	Sinuous	1	0	0	1	1	4500	*500*	50	0.23	0.23	220	20	180			0	0	0	1	5	Cave in a parallel band
1926 IV	***Fustvatn***		VN *235 980*		400	Dolom.	Calc. + Do	Linear	1	0	0	1	0	4500	200	50	0.23	0.00	130	20	180	75	E	1	0	0	0	0	Karst rising at base of cliff
1926 IV	***Fustvatn***		VN *236 980*		340	Dolom.		Linear	1	0	0	0	1	3000	0	50	0.15	0.15	70	20	180			0	0	0	0	0	
1926 IV	***Fustvatn***		VN *239 980*		540	Calcitic		Sinuous	1	0	0	0	0	10000	0	50	0.50	0.00	360	20		90		1	0	0	0	0	
1926 IV	***Fustvatn***		VN *246 990*		391	Calcitic		Sinuous	1	0	0	0	0	4500	0	50	0.23	0.00	141	20				1	0	0	0	0	
	Area	127	VN *248 990*		420	Calcitic		Sinuous	1	1	0	0	0	4000	0	50	0.20	0.00	170	20		60	E	1	0	0	0	0	
1926 III	***Trofors***		VN *200 800*		980	Calcitic	Calc (3 off	c. Linear	1	0	0	1	0	53000	31000	400	21.00	0.00	730	200	180	75	W	1	4	2	56	5995	Møllebekk-Vargskar-Fjellryggen. 1Q. *
	Area	140	VN *227 899*		*440*			*Unmapped*	1	1	0	1	0	*400*	400	*10*	*0.00*	*0.00*	*40*	*10*	5	90		0	1	0	1	80	Ravatnhullet
1925 IV	***Svenningdal***		VN *223 530*		*430*		Calcitic	*Unmapped*	1	1	0	1	0	*700*	700	*250*	*0.14*	*0.00*	*70*	*20*	30	80	W	1	0	0	4	40	Litle Hjortskar: TF97 & 98
	Area	100	VN *210 495*		360	Calcitic	Calc (2 0ff	2 limbs	1	0	0	1	0	10000	10000	100	0.80	0.00	140	40	20	70	W	1	2	2	7	219	Saeterbekk etc. TF97

* Eastern edge of northern half of outcrop is along a granitic pluton

UPPERMOST ALLOCHTHON: Helgeland Nappe Complex: Zone 6 (Hemnes to Dunfjell)

MAP SHEET	MAP NAME & NAPPE AREA	UTM / SWEDISH RN COORD		MAX ALT.	GEOL MAP IDENT	SAMPLE IDENT	OUTCROP SHAPE	O	R	T	V	D	LENGTH	VISITED LENGTH	WIDTH	CARB. AREA	DOL. AREA	VR Length	VR Width	STRIKE	DIP	#	E	F	W	Metres C	Metres L	COMMENTS
Totals	2228			####				55	38	1	17	4	281150	29350	#####	106.52	3.52	#####	####		###	24	35	53	23	64	5204	
%									69%	2%	31%	7%				4.78%	0.16%					44%	64%					
Averages				393									5112	1726	255	1.94	0.88	190	61		65			0.96	0.42	3.76	306	
Maxima				900									53000	7800	3000	25.00	2.50	630	400		90			9	8	24	1192	
1824 IV	**Kongsmoen**																											**No mapped carbonates**
Area	66																											
1824 III	**Harran**																											**No mapped carbonates but 15 Q karst features!**
Area	153																											
1825 I	**Tosbotn**																											**No mapped carbonates**
Area	8																											
1825 II	**Majafjell**																											**No mapped carbonates**
Area	200																											
1824 I	**Namsskogan**																											**No mapped carbonates**
Area	449																											
1824 II	**Skorovatn**	UM	930	810	270	Calcitic		Linear	1	0	0	0	0	4000	0	250	1.00	0.00	76	76	60			1	0	1	0	0	
Area	20																											
1927 III	**Elsfjord**	VP	385	464	80	Calcitic		Triangle	1	1	0	0	0	500	0	100	0.05	0.00	80	80	60	36	S	0	0	0	0	0	**South of Ranafjord only**
1927 III	**Elsfjord**	VP	410	467	*140*		Calcitic	*Unmapped*	1	1	0	1	0	*150*	150	*300*	*0.05*	*0.00*	*20*	*67*	40	40	E	0	0	0	1	265	Gjeitvikgrotta
1927 III	**Elsfjord**	VP	359	454	*100*			*Unmapped*	1	0	0	1	0	*200*	*200*	*50*	*0.01*	*0.00*	*100*	*10*				1	0	0	1	35	Berntvikgrotta
1927 III	**Elsfjord**	VP	404	456	*100*			*Unmapped*	1	1	0	0	0	*500*	*0*	*50*	*0.02*	*0.00*	*40*	*40*				0	0	0	0	0	Cliff Cave (Unexplored)
1927 III	**Elsfjord**	VP	392	448	90	Calcitic		Rectangle	1	0	0	0	0	300	0	200	0.06	0.00	40	40	45	45	S	0	0	0	0	0	
1927 II	**Korgen**	VP	*460*	*470*	*167*	*?*		*Unmapped*	1	1	1	1	0	*1000*	1000	*20*	*0.02*	*0.00*	*167*	*20*	90	60	N	1	2	0	1	120	Gårdsfjellgrotta. Near HNC
1927 III	**Elsfjord**	VP	385	420	140	Calcitic		Linear	1	0	0	0	0	2000	0	100	0.20	0.00	140	20	180	54	W	0	0	0	0	0	
1927 III	**Elsfjord**	VP	340	390	316	Calcitic		Rectangle	1	1	0	0	0	700	0	200	0.14	0.00	56	30	30			1	0	0	0	0	2 Quat. karst features
1927 III	**Elsfjord**	VP	290	364	776	Calcitic		Arc	1	0	0	0	0	2000	0	100	0.20	0.00	216	60		59	W	1	0	0	0	0	{Cont. W. In basement (Cal. Orog.p153)
1927 III	**Elsfjord**	VP	305	355	660	Calcitic		Linear	1	0	0	0	0	1500	0	300	0.45	0.00	280	140	40			1	0	0	0	0	
1927 III	**Elsfjord**	VP	230	220	598	Calcitic	Calcitic	Irregular	1	1	0	1	0	4000	100	3000	12.00	0.00	558	400	180	80	E	0	5	0	1	90	Incl. Kumragrotta (Fustvatnet)
1927 III	**Elsfjord**	VP	260	300	540	Dolom.		Sinuous	1	0	0	1	1	12500	1000	200	2.50	2.50	480	100		68	W	1	0	0	0	0	Gullmogr.: Helland. Not found! TF98
1927 III	**Elsfjord**	VP	330	330	420	Calcitic	Calcitic	Tapering	1	0	0	1	0	19000	5500	500	9.50	0.00	420	240	20	90		1	0	4	4	1192	Splintågr+Kovagr+Sildgamgr+21Q. *
1927 III	**Elsfjord**	VP	285	250	420	Calcitic		Rectangle	1	1	0	0	0	600	0	200	0.06	0.00	80	120	80			0	1	0	0	0	
1927 III	**Elsfjord**	VP	350	300	636	Calcitic	Some Dol.	Irregular	1	1	0	1	0	10000	1000	2500	25.00	0.00	630	200	40	41	E	0	8	4	3	450	T. Doj.19 Q. R. Selvåg cave
1927 III	**Elsfjord**	VP	360	340	350	Dolom.		Sinuous	1	1	0	0	1	3500	0	200	0.70	0.70	350	20				0	0	0	0	0	Dolomite quarry at Seljelia
1927 III	**Elsfjord**	VP	320	210	620	Calcitic	Calc. (3 of	Multilimbs	1	1	0	1	0	15000	1000	100	1.50	0.00	620	100	30	70	W	1	2	0	5	830	Kammelv.
Area	275	VP	360	210	580	Calcitic		Sinuous	1	0	0	0	0	5200	0	200	1.00	0.00	340	100				1	1	0	0	0	Incl. S (Fustvatnet)

* Encloses small gabbro plutons

UPPERMOST ALLOCHTHON: Helgeland Nappe Complex: Zone 6 (Hemnes to Dunfjell)

																												Metres	
MAP SHEET	MAP NAME & NAPPE AREA	UTM / SWEDISH RN COORD			MAX ALT.	GEOL MAP IDENT	SAMPLE IDENT	OUTCROP SHAPE	O	R	T	V	D	LENGTH	VISITED LENGTH	WIDTH	CARB. AREA	DOL. AREA	VR Length	VR Width	STRIKE	DIP	#	E	F	W	C	L	COMMENTS
1926 IV	***Fustvatn***	VP	*197*	*210*	160	Calcitic		Linear	1	0	0	0	0	900	0	50	0.05	0.00	20	20	40	80	E	1	0	0	0	0	
1926 IV	***Fustvatn***	VP	*196*	*200*	70	Dolom.	Dolomite	Linear	1	0	0	1	1	1400	200	50	0.07	0.07	10	10	40	90		1	0	0	1	5	Øygårdgrotta in adjacent Calcitic lst.
1926 IV	***Fustvatn***	VP	*270*	*210*	200	Calcitic		Linear	1	0	0	0	0	1000	0	50	0.05	0.00	80	20	50	65	E	1	0	0	0	0	
1926 IV	***Fustvatn***	VP	*260*	*200*	143	Calcitic		Linear	1	0	0	0	0	2000	0	100	0.20	0.00	63	63	50			1	0	0	0	0	
1926 IV	***Fustvatn***	VP	*250*	*140*	420	Calcitic	Calc (3 off	Multi limbs	1	1	0	1	0	16000	1500	1000	16.00	0.00	378	328		45	S	1	9	1	9	749	Hellfjell. 25Q. Concent. outcr. Varying dips
1926 IV	***Fustvatn***	VP	*282*	*120*	100	Calcitic		Linear	1	0	0	0	0	1000	0	100	0.10	0.00	73	20	180			0	0	0	0	0	
1926 IV	***Fustvatn***	VP	*285*	*120*	143	Calcitic		Linear	1	0	0	0	0	1000	0	100	0.10	0.00	105	10	10	60	W	0	0	0	0	0	
1926 IV	***Fustvatn***	VP	*287*	*113*	88	Calcitic		Circular	1	0	0	0	0	500	0	500	0.25	0.00	48	48	170	60	W	0	0	0	0	0	
1926 IV	***Fustvatn***	VP	*283*	*030*	460	Calcitic		Linear	1	1	0	0	0	2000	0	100	0.20	0.00	140	40	180			1	8	0	0	0	
1926 IV	***Fustvatn***	VP	*288*	*040*	300	Calcitic		Linear	1	0	0	0	0	1000	0	50	0.05	0.00	60	20	20			1	5	0	0	0	
1926 IV	***Fustvatn***	VP	*290*	*040*	320	Calcitic		Linear	1	1	0	0	0	1500	0	50	0.08	0.00	100	20	20			1	0	0	0	0	
1926 IV	***Fustvatn***	VP	*292*	*040*	190	Calcitic		Arc	1	1	0	0	0	1000	0	50	0.05	0.00	90	20				1	0	0	0	0	
1926 IV	***Fustvatn***	VP	*290*	*030*	370	Calcitic		2 limbs	1	1	0	0	0	2000	0	100	0.20	0.00	70	20	20			1	2	0	0	0	
1926 IV	***Fustvatn***	VN	*290*	*960*	700	Calcitic		Arc	1	1	0	0	0	3500	0	50	0.18	0.00	100	20				1	0	0	0	0	
1926 IV	***Fustvatn***	VN	*290*	*940*	700	Calcitic		2 limbs	1	1	0	0	0	6000	0	200	1.20	0.00	300	60	20			1	2	0	0	0	
1926 IV	***Fustvatn***	VN	*300*	*990*	520	Calcitic		Linear	1	1	0	0	0	1500	0	200	0.30	0.00	100	40	180	60	W	1	0	1	0	0	
1926 IV	***Fustvatn***	VN	*304*	*980*	480	Calcitic		Sinuous	1	1	0	0	0	2000	0	100	0.20	0.00	80	40				1	0	0	0	0	
1926 IV	***Fustvatn***	VN	*306*	*980*	400	Calcitic		2 limbs	1	1	0	0	0	9000	0	100	0.90	0.00	240	40		70	W	1	2	0	0	0	
1926 IV	***Fustvatn***	VP	*303*	*040*	160	Calcitic		Arc	1	1	0	0	0	2500	0	100	0.25	0.00	80	20				1	2	0	0	0	
1926 IV	***Fustvatn***	VP	*350*	*060*	700	Calcitic		Multi limbs	1	1	0	1	0	32000	4000	250	8.00	0.00	500	80				0	2	3	5	130	Herringbotn. 7 Q . Incl. to S. Dips 45-70
1926 IV	***Fustvatn***	VP	*350*	*030*	626	Dolom.		Sinuous	1	1	0	0	1	5000	0	50	0.25	0.25	426	40				0	0	0	0	0	
1926 IV	***Fustvatn***	VP	*350*	*050*	580	Calcitic		Sinuous	1	1	0	0	0	8000	0	100	0.80	0.00	380	40				0	0	0	0	0	
1926 IV	***Fustvatn***	VN	*338*	*950*	490			*Unmapped*	1	1	0	1	0	*500*	500	3	0.00	0.00	40	1	20	90		0	0	0	4	145	SN82: Herringbotn
1926 IV	***Fustvatn***	VN	*340*	*948*	540	Calcitic		Linear	1	1	0	0	0	1000	0	50	0.05	0.00	80	20	20			0	0	0	0	0	
1926 IV	***Fustvatn***	VN	*345*	*960*	520	Calcitic		Linear	1	1	0	0	0	500	0	50	0.02	0.00	100	10	20			0	0	0	0	0	
1926 IV	***Fustvatn***	VN	*375*	*980*	900	Calcitic		Linear	1	1	0	0	0	1000	0	50	0.05	0.00	200	10	30			0	0	0	0	0	
1926 IV	***Fustvatn***	VP	*366*	*190*	350	Calcitic		Arc	1	1	0	0	0	1200	0	50	0.06	0.00	150	20				1	0	0	0	0	
1926 IV	***Fustvatn***	VP	*364*	*170*	400	Calcitic		Linear	1	1	0	0	0	600	0	50	0.03	0.00	20	20	180			1	2	0	0	0	
Area	454	VP	*365*	*170*	380	Calcitic		Linear	1	1	0	0	0	500	0	50	0.02	0.00	20	20	180			1	0	0	0	0	
1926 III	***Trofors***	VN	*235*	*703*	*340*			*Unmapped*	1	1	0	1	0	*400*	400	*50*	*0.02*	*0.00*	*20*	*5*				1	0	0	2	6	Wet Crawls (Stengvass)
1926 III	***Trofors***	VN	*236*	*740*	698	Calcitic	Calcitic	c. Linear	1	1	0	1	0	53000	7800	50	2.60	0.00	414	40	180	80	W	1	0	8	24	1068	+lakes.Doj94.GPN90,97,01:Dunfjell+Sv.TF98.*
1926 III	***Trofors***	VN	*257*	*830*	560	Calcitic		Linear	1	1	0	0	0	3000	0	50	0.15	0.00	120	20	180			1	0	0	0	0	2 Quat karst features
1926 III	***Trofors***	VN	*260*	*780*	280	Calcitic		Linear	1	1	0	0	0	3500	0	100	0.35	0.00	240	40	20			1	0	0	0	0	
1926 III	***Trofors***	VN	*300*	*820*	620	Calcitic		Linear	1	1	0	1	0	15000	1000	600	9.00	0.00	580	100	20	90		0	0	0	1	94	Gluggvasselvgr. 2 Quart karst
Area	220	VN	*255*	*720*	260	Calcitic	Calcitic	Linear	1	1	0	1	0	13000	2000	800	10.00	0.00	160	160	180	30	W	1	0	0	2	25	Gr. Doline Ca, Farewell Ca. Incl to S
1925 IV	***Svenningdal***																												**No extra mapped carbonates**
Area	112																												
1927 II	**Korgen**																												**No extra mapped carbonates**
Area	19																												
1925 III	***Majavatn***	VN	*180*	*150*	440	Calcitic		Linear	1	1	0	1	0	4500	2000	50	0.23	0.00	150	10	10	85	E	1	0	1	0	0	Steinelv
Area	244																												* Within granite N. of Holmvassåsen.
1924 IV	***Røyrvik***																												**No mapped carbonates**
Area	8																												

UPPERMOST ALLOCHTHON: Helgeland Nappe Comple: Zone 7 (Åkervik to Fiplingdal)

Metres

MAP SHEET	MAP NAME & NAPPE AREA		UTM / SWEDISH RN COORD		MAX ALT.	GEOL MAP IDENT	SAMPLE IDENT	OUTCROP SHAPE	O	R	T	V	D	LENGTH	VISITED LENGTH	WIDTH	CARB. AREA	DOL. AREA	VR Length	VR Width	STRIKE	DIP	#	E	F	W	C	L	COMMENTS
Totals	1054				####				60	3	7	17	4	421000	24800	#####	145.8	4.00	#####	####		###	35	45	60	31	87	4806	
%										5%	12%	28%	7%				13.83%	0.38%					58%	75%					
Averages					606									7017	1459	201	2.43	1.00	219	67		63			1.00	0.52	5.12	283	
Maxima					1200									42000	4000	1000	35.00	1.80	780	547		90			21	8	44	2261	
NOTE:	MOST CARBONATES IN ZONE 7 IN TROFORS / SVENNINGDAL / HATTFJELLDAL ARE PART OF ONE HIGHLY COMPLEX AND MULTIPLY INTERCONNECTED OUTCROP																												
1926 IV	***Fustvatn***																												**No mapped carbonates**
Area	4																												
1926 III	***Trofors***	VN	*360*	*860*	813	Calcitic		Multilimbs	1	0	0	1	0	26000	1500	1000	26.00	0.00	653	240	180	90		0	2	2	5	83	Almdalselv, Rauvatn. 2Q karst
1926 III	***Trofors***	VN	*300*	*750*	640	Calcitic		Linear	1	0	0	0	0	9500	0	50	0.45	0.00	140	20	20			0	0	0	0	0	
1926 III	***Trofors***	VN	*350*	*730*	767	Calcitic	Calc (2 off)	Multilimbs	1	0	0	1	0	35000	4000	1000	35.00	0.00	667	547	20	45	E	1	5	4	14	1227	Svartvassdal,Rømmar
1926 III	***Trofors***	VN	*390*	*790*	820	Calcitic		Linear	1	0	0	0	0	4500	0	200	0.90	0.00	160	60	30			0	0	1	0	0	
1926 III	***Trofors***	VN	*400*	*795*	700	Calcitic		Linear	1	0	0	0	0	4500	0	50	0.20	0.00	100	10	40			0	0	0	0	0	
1926 III	***Trofors***	VN	*400*	*790*	640	Calcitic		Irregular	1	0	0	0	0	2000	0	500	1.00	0.00	17	57	40			1	0	1	0	0	
1926 III	***Trofors***	VN	*390*	*735*	660	Calcitic		Sinuous	1	0	0	0	0	9000	0	100	0.90	0.00	260	20				0	1	0	0	0	
1926 III	***Trofors***	VN	*310*	*660*	640	Calcitic		2 limbs	1	1	0	1	0	9000	1000	150	1.50	0.00	540	160				1	2	1	0	0	Incl. N. Båfjell. SN 84
1926 III	***Trofors***	VN	*340*	*670*	400	Calcitic		Linear	1	0	0	1	0	2500	*1000*	500	1.25	0.00	260	60	30			1	1	0	0	0	Stormogrotta
1926 III	***Trofors***	VN	*360*	*680*	440	Calcitic		Linear	1	0	0	0	0	4000	0	50	0.20	0.00	340	10	30			0	0	0	0	0	
Area	252	VN	*400*	*700*	534	Calcitic		Multilimbs	1	0	0	0	0	20000	0	200	4.00	0.00	414	80				1	0	0	0	0	
1925 IV	***Svenningdal***	VN	*290*	*600*	400	Calcitic		Linear	1	0	0	0	0	500	0	200	0.10	0.00	20	20				0	0	0	0	0	S. Båfjell
1925 IV	***Svenningdal***	VN	*350*	*640*	633	Calcitic		Irregular	1	0	0	1	0	3000	*1000*	200	2.00	0.00	233	233				1	2	0	0	0	Kvannholan Sink
1925 IV	***Svenningdal***	VN	*360*	*645*	600	Calcitic		2 limbs	1	0	0	1	0	4000	*2000*	100	0.40	0.00	220	20	40			1	2	0	2	69	Tuvbekken
1925 IV	***Svenningdal***	VN	*290*	*560*	1020	Calcitic		Irregular	1	0	0	1	0	8000	*2000*	100	0.80	0.00	620	100		75	S	0	0	0	6	472	Kappskar: SN90. Prospects SE?
1925 IV	***Svenningdal***	VN	*300*	*450*	880	Calcitic		Multilimbs	1	0	0	1	0	42000	1400	600	25.00	0.00	580	140	25	80	W	1	21	8	44	2261	Fiplingdal+Flåflangahullet
1925 IV	***Svenningdal***	*VN*	*348*	*576*	*620*	Calcitic		*Unmapped*	1	0	0	1	0	*1000*	1000	*50*	*0.05*	*0.00*	*80*	*10*				1	2	0	3	207	Litle Fiplingdal
1925 IV	***Svenningdal***	VN	*390*	*610*	660	Calcitic		Linear	1	0	0	0	0	8000	0	600	4.80	0.00	420	420	20			1	0	0	0	0	
1925 IV	***Svenningdal***	VN	*330*	*475*	440	Calcitic		Linear	1	0	0	0	0	12500	0	50	0.60	0.00	74	20	30	80	W	1	0	0	0	0	
Area	409	VN	*360*	*480*	840	Calcitic		c. Linear	1	1	0	1	0	18000	1000	50	0.90	0.00	440	40	25	70	W	0	0	0	1	50	Nyrudhola
1925 III	***Majavatn***	VN	*195*	*140*	260	Calcitic		Linear	1	0	0	0	0	1000	0	100	0.10	0.00	20	10	10			1	0	0	0	0	
1925 III	***Majavatn***	VN	*230*	*300*	380	Calcitic		Linear	1	0	0	0	0	3000	0	100	0.30	0.00	75	20	30			0	0	0	0	0	
1925 III	***Majavatn***	VN	*220*	*200*	345	Calcitic		Arc	1	0	0	0	0	7000	0	200	0.35	0.00	72	20		90		1	0	1	0	0	
1925 III	***Majavatn***	VN	*300*	*315*	1200	Calcitic		Sinuous	1	1	0	1	0	13500	4000	100	1.35	0.00	780	100		90		0	3	3	5	96	Sløkskar: SN84. Incl. to N
Area	144	VN	*280*	*280*	724	Calcitic		Linear	1	0	0	0	0	2000	0	100	0.20	0.00	224	20	180	90		0	0	0	0	0	
1926 I	***Røssvatnet***																												**No mapped carbonates**
Area	63																												

UPPERMOST ALLOCHTHON: Helgeland Nappe Complex: Zone 7 (Åkervik to Fiplingdal)

Metres

MAP SHEET	MAP NAME & NAPPE AREA	UTM / SWEDISH RN COORD	MAX ALT.	GEOL MAP IDENT	SAMPLE IDENT	OUTCROP SHAPE	O	R	T	V	D	LENGTH	VISITED LENGTH	WIDTH	CARB. AREA	DOL. AREA	VR Length	VR Width	STRIKE	DIP	#	E	F	W	C	L	COMMENTS
1926 II	***Hattfjelldal***	VN *490 910*	696	Dolomite		Sinuous	1	0	1	0	1	4000	0	200	0.80	0.80	316	80				1	0	0	0	0	#6. On internal thr. Dips 37 - 76
1926 II	***Hattfjelldal***	VN *500 870*	486	Calcite	Calcitic	Linear	1	0	0	1	0	6500	100	500	3.25	0.00	106	80	40	38	W	1	4	0	2	124	#7 Faulted. Åkervik. TF00
1926 II	***Hattfjelldal***	VN *420 865*	500	Calcite		Sinuous	1	0	1	0	0	1600	0	50	0.08	0.00	120	10		10	S	1	0	0	0	0	#7.On internal thrust
1926 II	***Hattfjelldal***	VN *420 860*	500	Calcite		Sinuous	1	0	1	0	0	1600	0	50	0.08	0.00	120	20		32	S	1	0	0	0	0	#7.Between internal thrusts
1926 II	***Hattfjelldal***	VN *420 855*	753	Calcite		Multilimbs	1	0	1	1	0	5000	1000	100	0.50	0.00	373	100		73	S	1	0	0	0	0	#7.On int. thrust. No clifftop hole. TF00
1926 II	***Hattfjelldal***	VN *420 853*	832	Calcite		Sinuous	1	0	0	0	0	2000	0	50	0.10	0.00	452	20				1	0	0	0	0	#7
1926 II	***Hattfjelldal***	VN *435 850*	607	Calcite		Sinuous	1	0	0	0	0	2500	0	100	0.25	0.00	227	20		35	S	1	0	0	0	0	#7
1926 II	***Hattfjelldal***	VN *440 850*	609	Calcite		Sinuous	1	0	0	0	0	3000	0	200	0.60	0.00	229	20		30	S	1	0	0	0	0	#7
1926 II	***Hattfjelldal***	VN *445 850*	540	Calcite		Arc	1	0	0	0	0	2500	0	50	0.12	0.00	160	20		40	S	1	0	0	0	0	#7
1926 II	***Hattfjelldal***	VN *420 830*	758	Calcite		Linear	1	0	0	0	0	2000	0	100	0.20	0.00	178	10	40	80	W	1	0	0	0	0	#7
1926 II	***Hattfjelldal***	VN *418 820*	680	Calcite		Linear	1	0	0	0	0	2000	0	50	0.10	0.00	50	5	40	75	W	1	0	0	0	0	#7
1926 II	***Hattfjelldal***	VN *430 830*	624	Mar+m.g.		Linear	1	0	0	0	0	2500	0	400	1.00	0.00	154	100	35			1	0	0	0	0	#5
1926 II	***Hattfjelldal***	VN *465 848*	446	Calcite		Linear	1	0	0	0	0	300	0	100	0.03	0.00	60	10	50	90		1	0	0	0	0	#7
1926 II	***Hattfjelldal***	VN *460 842*	442	Calcite		Linear	1	0	0	0	0	1800	0	50	0.10	0.00	62	10	50	75	E	1	0	0	0	0	#7
1926 II	***Hattfjelldal***	VN *460 840*	468	Calcite		Linear	1	0	0	0	0	1800	0	100	0.18	0.00	88	10	50	75	E	1	0	0	0	0	#7
1926 II	***Hattfjelldal***	VN *440 825*	600	Calcite		Multilimbs	1	0	0	1	0	8000	500	100	0.80	0.00	220	80				1	2	0	0	0	#7. Sink + res. SN97
1926 II	***Hattfjelldal***	VN *460 830*	630	Calcite		Linear	1	0	0	0	0	2500	0	50	0.12	0.00	70	40	60			1	0	0	0	0	#7
1926 II	***Hattfjelldal***	VN *435 798*	746	Calcite		Sinuous	1	0	0	0	0	1600	0	100	0.16	0.00	76	20		18	S	0	0	1	0	0	#7
1926 II	***Hattfjelldal***	VN *411 760*	700	Calcite		Linear	1	0	0	0	0	1500	0	50	0.08	0.00	40	5	35	72	W	1	0	0	0	0	#7
1926 II	***Hattfjelldal***	VN *416 760*	660	Calcite		Linear	1	0	0	0	0	500	0	50	0.02	0.00	20	20	45			1	0	0	0	0	#7
1926 II	***Hattfjelldal***	VN *440 777*	680	Mar+m.g.		Linear	1	0	0	0	0	8000	0	100	0.80	0.00	65	20	45	40	E	1	0	1	0	0	#5
1926 II	***Hattfjelldal***	VN *449 800*	710	Calcite		Linear	1	0	0	0	0	1600	0	100	0.16	0.00	20	10	40	50	W	1	0	0	0	0	#7
1926 II	***Hattfjelldal***	VN *470 820*	610	Mar+m.g.		Linear	1	0	0	0	0	3500	0	300	1.00	0.00	230	60	30			1	2	0	0	0	#5
1926 II	***Hattfjelldal***	VN *417 740*	480	Calcite		Linear	1	0	0	0	0	700	0	50	0.07	0.00	20	5	20			1	2	0	0	0	#7
1926 II	***Hattfjelldal***	VN *420 740*	551	Calcite		Multilimbs	1	0	0	0	0	8500	0	100	1.00	0.00	111	40		60	E	1	0	3	0	0	#7
1926 II	***Hattfjelldal***	VN *460 790*	638	Calcite		Multilimbs	1	0	0	1	0	9000	3000	300	2.70	0.00	148	40	40	50	E	1	7	0	5	217	#7 Gryteselv. Heap 68, Doj 91
1926 II	***Hattfjelldal***	VN *450 750*	590	Calcite		Multilimbs	1	0	0	0	0	25000	0	500	12.50	0.00	450	90				1	2	2	0	0	#7. Dip varies
1926 II	***Hattfjelldal***	VN *450 760*	590	Mar+m.g.		Linear	1	0	0	0	0	5500	0	500	2.80	0.00	190	40	25	55	E	1	0	0	0	0	#5
1926 II	***Hattfjelldal***	VN *440 720*	480	Dolomite		Linear	1	0	0	0	1	4000	0	200	0.80	0.80	110	20	30	65	W	1	0	2	0	0	#6
1926 II	***Hattfjelldal***	VN *420 677*	360	Dolomite		Linear	1	0	0	0	1	3000	0	200	0.60	0.60	200	60	30	81	E	0	0	0	0	0	#6
1926 II	***Hattfjelldal***	VN *480 750*	460	Dolomite		Linear	1	0	1	1	1	6000	100	300	1.80	1.80	210	150	35	80	W	1	0	0	0	0	**#6. Dol. quarry on int. thr.**
1926 II	***Hattfjelldal***	VN *448 700*	617	Mar+m.g.		Multilimbs	1	0	1	1	0	25000	200	100	2.50	0.00	477	160	35	70	W	0	0	1	0	0	#5 and #7. Long limb on int thr. TF98
1926 II	***Hattfjelldal***	VN *466 730*	334	Calcite		Linear	1	0	0	0	0	1000	0	100	0.10	0.00	34	20	25	70	W	1	0	0	0	0	#7. Dark
1926 II	***Hattfjelldal***	VN *470 730*	310	Mar+m.g.		Linear	1	0	1	0	0	1500	0	300	0.45	0.00	150	150	35	70	W	1	0	0	0	0	#5. On internal thrust
Area	180	VN *485 770*	600	Calcite		Multilimbs	1	0	0	0	0	16000	0	100	1.60	0.00	220	50	25	70	W	1	0	0	0	0	#7. Dark
1925 I	***Susendal***																										
Area	2																										

UPPERMOST ALLOCHTHON: Helgeland Nappe Complex: Zone 8 (Eastern Area)

																										Metres	
MAP SHEET	MAP NAME & NAPPE AREA	UTM / SWEDISH RN COORD			MAX ALT.	GEOL MAP IDENT	SAMPLE IDENT	OUTCROP SHAPE	O	R	T	V	D	LENGTH	VISITED LENGTH	WIDTH	CARB. AREA	DOL. AREA	VR Length	VR Width	STRIKE	DIP	#	E	F	W	C	L	COMMENTS
Totals	967				####				27	24	20	3	0	102000	1900	####	11.99	0	####	###		###	11	5	3	5	8	825	
%										89%	74%	11%	0%				1.24%	0.00%					41%	19%					
Averages					786									3778	633	96	0.44	#DIV/0!	230	33		54			0.11	0.19	2.67	275	
Maxima					1220									26000	1000	500	5.20	0.00	750	250		80			2	2	8	825	
1824 III	**Harran**																												**No mapped carbonates**
Area	21																												**No mapped carbonates**
1824 I	**Namskogen**																												
Area	98																												**No mapped carbonates**
1925 IV	**Svenningdal**																												
Area	45																												
1925 III	***Majavatn***	VN	*334*	*310*	800	Calcitic		Linear	1	1	0	0	0	800	0	100	0.08	0.00	70	10	30			1	0	0	0	0	+ 3 tiny outcrops
1925 III	***Majavatn***	VN	*300*	*176*	860	Calcitic		Arc	1	1	0	0	0	4000	0	100	0.40	0.00	440	20	45		W	0	0	0	0	0	
1925 III	***Majavatn***	VN	*300*	*175*	760	Calcitic		Linear	1	1	0	0	0	1000	0	100	0.10	0.00	240	10	45		W	0	0	0	0	0	
1925 III	***Majavatn***	VN	*320*	*170*	820	Calcitic		Linear	1	1	1	0	0	5500	0	200	1.10	0.00	270	80	60	30	W	1	2	1	0	0	On HNC Thrust
1925 III	***Majavatn***	VN	*350*	*200*	1060	Calcitic		Sinuous	1	1	1	0	0	1000	0	100	0.10	0.00	140	60			W	1	0	0	0	0	Near HNC Thrust
Area	266	VN	*355*	*235*	680	Calcitic	with moraine	Rectangular	1	1	1	1	0	3500	1000	500	0.40	0.00	50	250				1	1	0	8	825	Jengelvatn: near thrust
1924 IV	***Røyrvik***	VN	*203*	*070*	680	Calcitic		Linear	1	0	0	0	0	1500	0	100	0.15	0.00	24	20	20	70	W	0	0	0	0	0	
1924 IV	***Røyrvik***	VN	*205*	*065*	700	Calcitic		Arc	1	1	0	0	0	1400	0	100	0.14	0.00	104	20		70	W	0	0	0	0	0	
1924 IV	***Røyrvik***	VN	*220*	*080*	889	Calcitic		Arc	1	1	0	0	0	10000	0	200	1.80	0.00	309	100		80	E	0	0	1	0	0	Incl. Majavatn
1924 IV	***Røyrvik***	VN	*265*	*092*	880	Calcitic		Linear	1	1	0	0	0	800	0	50	0.04	0.00	25	10	30			0	0	0	0	0	
Area	110	VN	*230*	*010*	810	Calcitic		Sinuous	1	0	1	1	0	26000	600	200	5.20	0.00	210	100				0	0	2	0	0	On HNC Thrust. Incl. Majavatn &
1824 II	**Skorovatn**																												**No mapped carbonates**
Area	44																												
1926 II	***Hattfjelldal***	VN	*448*	*665*	800	Myl. calc		Sinuous	1	1	1	0	0	1000	0	50	0.05	0.00	340	20		56	W	0	0	0	0	0	#26. On internal thr.
1926 II	***Hattfjelldal***	VN	*480*	*710*	940	Myl. calc		Sinuous	1	1	1	1	0	8000	300	50	0.40	0.00	570	20		48	W	0	0	1	0	0	#26. On internal thr. TF98
1926 II	***Hattfjelldal***	VN	*480*	*697*	600	Myl. calc		Sinuous	1	1	1	0	0	3000	0	50	0.15	0.00	200	10		58	W	0	0	0	0	0	#26. On internal thr.
1926 II	***Hattfjelldal***	VN	*480*	*693*	620	Myl. calc		Sinuous	1	1	1	0	0	3000	0	50	0.15	0.00	220	10		54	W	0	0	0	0	0	#26. On internal thr.
1926 II	***Hattfjelldal***	VN	*490*	*713*	600	Myl. calc		Sinuous	1	1	1	0	0	3000	0	50	0.15	0.00	200	10		34	W	0	0	0	0	0	#26. On internal thr.
1926 II	***Hattfjelldal***	VN	*500*	*720*	560	Myl. calc		Sinuous	1	1	1	0	0	1000	0	50	0.05	0.00	180	10				0	0	0	0	0	#26. On internal thr.
1926 II	***Hattfjelldal***	VN	*480*	*687*	671	Myl. calc		Sinuous	1	1	1	0	0	2500	0	50	0.12	0.00	191	10		58	W	0	0	0	0	0	#26. On internal thr.
1926 II	***Hattfjelldal***	VN	*480*	*681*	1220	Myl. calc		Sinuous	1	1	1	0	0	6000	0	50	0.30	0.00	750	10				0	0	0	0	0	#26. On internal thr. Dips 42 - 61
1926 II	***Hattfjelldal***	VN	*486*	*654*	1100	Myl. calc		Sinuous	1	1	1	0	0	500	0	50	0.02	0.00	90	10				0	0	0	0	0	#26. On internal thr.
1926 II	***Hattfjelldal***	VN	*490*	*664*	1100	Myl. calc		Multilimbs	1	1	1	0	0	9000	0	50	0.45	0.00	600	10		40	W	0	0	0	0	0	#26. On internal thr.
1926 II	***Hattfjelldal***	VN	*500*	*700*	700	Myl. calc		Sinuous	1	1	1	0	0	500	0	50	0.02	0.00	70	10				0	0	0	0	0	#26. On internal thr.
1926 II	***Hattfjelldal***	VN	*510*	*697*	842	Myl. calc		Linear	1	1	1	0	0	1000	0	50	0.05	0.00	62	10	35			0	0	0	0	0	#26. On internal thr.
1926 II	***Hattfjelldal***	VN	*530*	*880*	460	Myl. calc		Sinuous	1	1	1	0	0	3000	0	50	0.15	0.00	460	10				0	0	0	0	0	#26. On internal thr.
1926 II	***Hattfjelldal***	VN	*524*	*804*	520	Myl. calc		Linear	1	1	1	0	0	500	0	50	0.02	0.00	40	10	125			0	0	0	0	0	#26. On internal thr.
Area	90	VN	*520*	*730*	540	Myl. calc		Multilimbs	1	1	1	0	0	1000	0	50	0.05	0.00	100	10				0	0	0	0	0	#26.On HNC Thr.base
1925 I	***Susendalen***																												**No mapped carbonates**
Area	250																												
1925 II	***Borgefjell***	VN	430	290	1000	Calcitic		Sinuous	1	0	1	0	0	3500	0	100	0.35	0.00	260	40				1	0	0	0	0	On HNC thrust
Area	43																												

UPPERMOST ALLOCHTHON: Helgeland Nappe Complex: Zone 9 (Northern Area)

																											Metres	
MAP SHEET	MAP NAME & NAPPE AREA	UTM / SWEDISH RN COORD			MAX ALT.	GEOL MAP IDENT	SAMPLE IDENT	OUTCROP SHAPE	O	R	T	V	D	LENGTH	VISITED LENGTH	WIDTH	CARB. AREA	DOL. AREA	VR Length	VR Width	STRIKE	DIP	#	E	F	W	C	L	COMMENTS
Totals	95				####				22	15	4	1	0	72900	500	####	9.03	0.00	####	####		###	16	6	0	8	1	25	
%										68%	18%	5%	0%				9.51%	0.00%					73%	27%					
Averages					116									3314	500	109	0.41	#####	95	46		59			0.00	0.36	1.00	25	
Maxima					600									10000	500	250	2.00	0.00	225	200		90			0	2	1	25	
1827 III	**Sandnesjøen**	UP	880	370	85	Calc++		Linear	1	1	0	0	0	8000	0	50	0.40	0.00	75	75	60	25 S	0	0	1	0	0	
1827 III	**Sandnesjøen**	UP	925	388	90	Calc++		Multi limbs	1	1	0	0	0	1500	0	100	0.15	0.00	90	10			1	0	0	0	0	Donna
1827 III	**Sandnesjøen**	UP	915	380	40	Calc++		Linear	1	1	0	0	0	2000	0	100	0.20	0.00	40	40	60	35 S	1	0	0	0	0	
1827 III	**Sandnesjøen**	UP	895	368	120	Calc++		Linear	1	1	0	0	0	2000	0	200	0.40	0.00	120	60	60	40 S	1	0	0	0	0	
1827 III	**Sandnesjøen**	UP	875	363	225	Calc++		Multi limbs	1	1	0	0	0	2000	0	100	0.20	0.00	225	40		50 S	0	0	0	0	0	
1827 III	**Sandnesjøen**	UP	880	360	160	Calc++		Arc	1	1	0	0	0	1000	0	100	0.10	0.00	130	40			0	0	0	0	0	
1827 III	**Sandnesjøen**	UP	875	355	200	Calc++		Linear	1	0	0	1	0	3000	500	50	0.15	0.00	200	20	60	80 S	0	0	0	1	25	Marmorholet: 500m N. TF00
1827 III	**Sandnesjøen**	UP	900	355	194	Calc++		Linear	1	1	0	0	0	6000	0	250	1.50	0.00	194	80	60	90	1	0	1	0	0	
1827 III	**Sandnesjøen**	UP	895	350	180	Calc++		Linear	1	1	0	0	0	5000	0	50	0.30	0.00	180	20	60	65 S	1	0	0	0	0	
1827 III	**Sandnesjøen**	UP	850	343	10	Calc++		Linear	1	0	0	0	0	1500	0	50	0.08	0.00	10	5	60	85 S	0	0	0	0	0	Low lying coastal
1827 III	**Sandnesjøen**	UP	870	340	40	Calc++		Sinuous	1	1	0	0	0	5000	0	50	0.20	0.00	30	5		85 N	0	0	0	0	0	
1827 III	**Sandnesjøen**	UP	900	340	40	Calc++		Linear	1	1	1	0	0	10000	0	200	2.00	0.00	40	40	60	60 S	0	0	2	0	0	On Lower Nappe thrust top
1827 III	**Sandnesjøen**	UP	805	330	27	Calc++		Linear	1	1	0	0	0	400	0	50	0.02	0.00	27	27	60	30 S	0	0	0	0	0	
1827 III	**Sandnesjøen**	UP	800	320	37	Calc++		Linear	1	0	0	0	0	3000	0	100	0.30	0.00	37	37	60		0	0	2	0	0	Low lying coastal
1827 III	**Sandnesjøen**	UP	820	320	76	Calc++		Linear	1	1	0	0	0	6000	0	100	0.60	0.00	76	10	60	80 S	0	0	2	0	0	Low lying coastal
1827 III	**Sandnesjøen**	UP	880	330	20	Calc++		Linear	1	0	1	0	0	1000	0	50	0.05	0.00	20	20	70	65 S	0	0	0	0	0	
1827 III	**Sandnesjøen**	UP	960	410	60	Calc++		Linear	1	1	0	0	0	2500	0	50	0.13	0.00	60	20	70	50 S	0	0	0	0	0	On Lower Nappe thrust top
1827 III	**Sandnesjøen**	UP	970	399	50	Calc++		Sinuous	1	1	0	0	0	1000	0	50	0.05	0.00	40	10			0	0	0	0	0	Løkta. Incl. to NE
1827 III	**Sandnesjøen**	UP	970	390	65	Calc++		Linear	1	0	0	0	0	4000	0	150	0.60	0.00	65	20	70	N	0	0	0	0	0	Løkta
1827 III	**Sandnesjøen**	UP	970	380	42	Calc++		Irregular	1	0	1	0	0	2000	0	200	0.40	0.00	42	42	65	60 S	0	0	0	0	0	Løkta. Incl. to NE
1827 II	**Nesna**	VP	050	410	600	Calc++		Arc	1	1	0	0	0	2000	0	100	0.20	0.00	180	180	90	41 N	0	0	0	0	0	Løkta. Incl. to NE
1927 IV	**Sjona**	VP	320	510	200	Calc +		Arc	1	0	1	0	0	4000	0	250	1.00	0.00	200	200			1	0	0	0	0	Hugla.
Area	95																											On HNC thrust.
																												Sjona / Elsfjord: HNC north of Ranafjord only

UPPERMOST ALLOCHTHON: Rødingsfjell Nappe Complex - Nappes below the Beiarn Nappe: Zone A (Bleikvassli Area) (NORWAY ONLY)

MAP SHEET	MAP NAME & NAPPE AREA		UTM / SWEDISH RN COORD		MAX ALT.	GEOL MAP IDENT	SAMPLE IDENT	OUTCROP SHAPE	O	R	T	V	D	LENGTH	VISITED LENGTH	WIDTH	CARB. AREA	DOL. AREA	VR Length	VR Width	STRIKE	DIP	#	E	F	W	C	L	COMMENTS
																								Metres						
Totals		415			#####				23	1	3	12	3	188500	27100	####	56.81	0.72	####	####		###	13	15	94	17	37	3920	
%										4%	13%	52%	13%				13.69%	0.17%					57%	65%						
Averages					595									8196	2258	200	2.47	0.24	213	109		41			4.1	0.7	3.1	327	
Maxima					980									50000	9000	600	15.00	0.32	738	630		65			18	10	8	2149	
1927 III	**Elsfjord**		VP 410	360	738	Calcitic		2 limbs	1	0	1	1	0	8000	*1000*	200	1.60	0.00	738	80	180		W	0	0	2	1	5	On RNC Thrust top. T. Doj caves
Area		26	VP 404	265	600	Calcitic		Linear	1	0	1	1	0	8000	*200*	100	0.80	0.00	118	80	168	28	W	0	4	1	0	0	On RNC Thrust top. Sump in next band. *
1926 IV	***Fustvatn***		VP *400*	*100*	763	Cal+Dol		Sinuous	1	0	1	1	0	20000	2000	600	12.00	0.00	273	163	180	40	W	1	12	10	2	10	On RNC Thr. top. 4 Q. Incl. Røssvatn. TF98
1926 IV	***Fustvatn***		VP *416*	*200*	540	Calcitic		Linear	1	0	0	0	0	1500	0	50	0.08	0.00	20	20	180			0	0	2	0	0	
1926 IV	***Fustvatn***		VP *418*	*200*	590	Calcitic		Linear	1	0	0	0	0	2500	0	50	0.12	0.00	65	10	180	45	W	0	0	0	0	0	
1926 IV	***Fustvatn***		VP *418*	*170*	720	Calcitic		Sinuous	1	0	0	0	0	1500	0	50	0.08	0.00	40	10		25	W	1	0	0	0	0	
1926 IV	***Fustvatn***		VP *418*	*160*	640	Calcitic		Sinuous	1	0	0	0	0	400	0	50	0.02	0.00	20	10				1	2	0	0	0	
1926 IV	***Fustvatn***		VP *413*	*150*	600	Dolom.		Sinuous	1	0	0	0	1	6500	0	50	0.32	0.32	200	20	180	55	W	1	2	0	0	0	
1926 IV	***Fustvatn***		VP *415*	*150*	500	Dolom.		Sinuous	1	0	0	0	1	5000	0	50	0.25	0.25	40	20	180	40	W	1	0	0	0	0	
1926 IV	***Fustvatn***		VP *416*	*140*	500	Calcitic		Sinuous	1	0	0	0	0	2500	0	50	0.12	0.00	40	20				1	0	0	0	0	
Area		20	VP *416*	*090*	520	Dolom.		Arc	1	0	0	0	1	1500	0	100	0.15	0.15	80	80		45	W	1	1	0	0	0	Near Tosbotnåsen
1927 II	**Korgen**		VP 430	250	620	Calcitic	Calc. (2 of	Linear	1	0	0	1	0	17000	*4000*	500	8.50	0.00	220	100	180	65	W	1	12	1	4	159	Doj 95. 4 Q at N. Incl.Storskog (Røssv.).TF97&98
1927 II	**Korgen**		VP 444	357	500	Calcitic	Some D	Linear	1	0	0	1	0	18000	*1000*	300	5.40	0.00	500	80	180	20	W	1	12	0	0	0	16 Q. 1m D cave. TF98
1927 II	**Korgen**		VP 450	250	340	Calcitic		Linear	1	0	0	0	0	3000	0	200	0.60	0.00	160	80	160	40	W	1	4	0	0	0	
1927 II	**Korgen**		VP 470	230	360	Calcitic		2 limbs	1	0	0	1	0	8000	1500	200	1.60	0.00	280	60				1	4	0	2	99	Helland. Fjellbrygga. Remnant Cave. TF97, 00
1927 II	**Korgen**		VP 510	230	950	Calcitic		Irregular	1	0	0	1	0	6000	3000	500	4.00	0.00	620	630		40	W	0	10	0	7	1039	Ytterlihullet etc. Heap74, GC82. TF00**
Area		120	VP 535	240	980	Calcitic		Circular	1	1	0	0	0	1200	0	500	1.00	0.00	180	180				1	0	0	0	0	
1926 I	***Røssvatnet***		VP *470*	*110*	840	Dol / Calc		Complex	1	0	0	1	0	50000	9000	300	15.00	0.00	440	260		45	W	0	18	0	7	238	Heap 74, TF97+ Grønnelvgrotta (UH). TF00 ***
1926 I	***Røssvatnet***		VP *435*	*077*	441	Cal&Dol		Arc	1	0	0	1	0	1000	400	100	0.10	0.00	141	40	25	*40*	W	1	2	0	4	200	Røssågagrotta. TF 97 & 98
1926 I	***Røssvatnet***		VP *461*	*192*	260			*Unmapped*	1	0	0	1	0	*500*	*500*	*50*	*0.02*	*0.00*	*20*	*5*				1	0	0	1	10	Doj 1991. pc to TLF
1926 I	***Røssvatnet***		VP *465*	*200*	240	Cal&Dol		Linear	1	0	0	1	0	1800	500	100	0.15	0.00	40	10				1	2	0	1	11	TF97. Jettegryter TF00
1926 I	***Røssvatnet***		VP *550*	*180*	960	Cal&Dol		Complex	1	0	0	1	0	23000	*4000*	200	4.60	0.00	560	450				0	9	1	8	2149	NGK 74,76. Grønndalgr. Incl. Korgen
Area		249	VP *500*	*140*	491	Cal&Dol		Irregular	1	0	0	0	0	1600	0	300	0.30	0.00	100	100				0	0	0	0	0	Peninsular

Storskog caves are included in Korgen

What does "Calcitic and dolomitic marble" actually mean?

* Crosses E6. Or in HNC? TF98.

** Bjurå area is not near granite.

*** NW of outcrop is beside a granite pluton.

UPPERMOST ALLOCHTHON: Rødingsfjell Nappe Complex - Nappes Below the Beiarn Nappe: Zone B (Bjerka and Stor Akersvatn Area) (NORWAY ONLY)

MAP SHEET	MAP NAME & NAPPE AREA	UTM / SWEDISH RN COORD	MAX ALT.	GEOL MAP IDENT	SAMPLE IDENT	OUTCROP SHAPE	O	R	T	V	D	LENGTH (Metres)	VISITED LENGTH	WIDTH	CARB. AREA	DOL. AREA	VR Length	VR Width	STRIKE	DIP	#	E	F	W	C	L	COMMENTS
Totals	712		#####				25	0	1	8	9	89600	8700	####	26.38	11.89	####	####		###	12	2	10	9	7	1410	**No carbonates near a pluton**
%								0%	4%	32%	36%				3.71%	1.67%					48%	8%					
Averages			634									3584	1088	294	1.06	1.32	235	103		37			0.4	0.4	0.9	176	
Maxima			1220									16500	3500	1500	6.50	3.75	740	620		90			2	2	3	900	
1927 II	**Korgen**	VP 620 231	*660*	Calc. mica schist		*Unmapped*	1	0	0	1	0	*700*	700	*20*	*0.14*	*0.00*	*100*	*10*	28	38	W	0	2	0	3	380	Leirskarelvgrotta
1927 II	**Korgen**	VP 620 470	520	Calcitic		Linear	1	0	0	0	0	7000	0	200	1.40	0.00	140	60	110	35	N	0	0	0	0	0	Incl. Storakersvatnet
1927 II	**Korgen**	VP 500 450	500	Calcitic		Linear	1	0	0	1	0	3000	1000	100	0.30	0.00	160	40	100	90		0	0	2	0	0	TF98. Limestone not found
1927 II	**Korgen**	VP 525 440	650	Calcitic		Irregular	1	0	0	1	0	2500	1000	100	0.25	0.00	320	40				0	2	0	0	0	3 Quat. karst features. TF98. Limestone not found
1927 II	**Korgen**	VP 540 444	570	Calcitic		Irregular	1	0	0	0	0	1800	0	200	0.14	0.00	10	10				0	0	0	0	0	
1927 II	**Korgen**	VP 513 438	431	Calc. m:	Calcitic	*Unmapped*	1	0	0	1	0	*500*	500	*30*	*0.02*	0.00	*60*	*15*	60	70	S	0	0	0	2	126	Bakliagrotta. TF98
1927 II	**Korgen**	VP 465 435	300	Dolom.		Irregular	1	0	0	0	1	800	0	300	0.24	0.24	300	300	120	80	N	0	0	0	0	0	
1927 II	**Korgen**	VP 443 425	200	Dolom.		Linear	1	0	1	0	1	1500	0	100	0.15	0.15	200	100	20	60	W	1	0	0	0	0	SN97. Rising on RNC Thr. at road
1927 II	**Korgen**	VP 460 420	400	Calcitic		Linear	1	0	0	0	0	1500	0	200	0.30	0.00	400	10	70			0	2	0	0	0	
1927 II	**Korgen**	VP 465 415	720	Dolom.		Sinuous	1	0	0	1	1	16500	3500	100	1.65	1.65	720	40				0	0	0	0	0	Vekthaugen. TF98
1927 II	**Korgen**	VP 500 405	700	Calcitic		Sinuous	1	0	0	0	0	5000	0	200	1.00	0.00	260	60				0	1	0	0	0	
1927 II	**Korgen**	VP 520 400	660	Calcitic		Linear	1	0	0	0	0	1000	0	100	0.10	0.00	160	10	170			0	0	0	0	0	
1927 II	**Korgen**	VP 526 397	566	Calcitic		Triangle	1	0	0	0	0	400	0	100	0.04	0.00	66	66				0	0	0	0	0	
Area	448	VP 535 395	420	Calcitic		Irregular	1	0	0	0	0	400	0	400	0.10	0.00	120	120				0	0	0	0	0	
1926 I	***Røssvatnet***																										**Under ice**
Area	10																										
2027 III	**Storakersvat**	VP 720 440	800	Dolomite		Irregular	1	0	0	0	1	1500	0	300	0.45	0.45	209	140				0	0	0	0	0	**(Norway**, W. of E79 and S. of Study Area boundary)
2027 III	**Storakersvat**	VP 725 427	825	Dolomite		Irregular	1	0	0	0	1	1500	0	300	0.45	0.45	205	125				0	0	0	0	0	**(No mapped carbonates in Sweden)**
2027 III	**Storakersvat**	VP 740 420	800	Calcite	Calcite	Irregular	1	0	0	1	0	5000	*500*	400	2.00	0.00	320	140		0		0	0	1	1	*900*	Akersvanngrotta
2027 III	**Storakersvat**	VP 750 420	920	Dolomiti	Dol + Calc	Irregular	1	0	0	0	1	5000	0	400	2.00	2.00	440	60		0		0	0	0	0	0	Crosses road
2027 III	**Storakersvat**	VP 750 380	571	Calcite		Peninsular	1	0	0	0	0	1500	0	800	1.20	0.00	91	91				0	0	2	0	0	1 flooded cave?
2027 III	**Storakersvat**	VP 760 380	670	Dolomiti	Dolomite	Peninsular	1	0	0	1	1	2500	500	1500	3.75	3.75	190	190		0		0	0	2	1	4	Near tracks. Tjuvhelleren. TF98
2027 III	**Storakersvat**	VP 740 370	570	Calcite		Island	1	0	0	0	0	1500	0	400	0.60	0.00	90	90				0	0	0	0	0	
2027 III	**Storakersvat**	VP 800 380	760	Calcite		Linear	1	0	0	0	0	4000	0	100	0.40	0.00	230	40	25			1	0	0	0	0	Ivargrotta (UH list)
2027 III	**Storakersvat**	VP 710 350	630	Dolomite		Irregular	1	0	0	0	1	9000	0	300	2.70	2.70	150	120		20	S	0	0	1	0	0	
2027 III	**Storakersvat**	VP 700 350	1220	Calcite		Irregular	1	0	0	0	0	13000	0	500	6.50	0.00	740	620		20	S	0	2	1	0	0	K16 prospect. ? 32 km walk!
Area	247	VP 740 240	789	Dolomite		Arc	1	0	0	1	1	2500	*1000*	200	0.50	0.50	200	80		30	W	0	1	0	0	0	Intermittent doline: DStP
2026 IV	**Hjartfjell**																										**Under ice**
Area	7																										

UPPERMOST ALLOCHTHON: Rödingsfjäll Nappe Complex - Nappes Below the Beiarn Nappe: Zone C (Southern and Border Area): NORWAY TOTALS

Metres

MAP SHEET	MAP NAME & NAPPE AREA	UTM / SWEDISH RN COORD	MAX ALT.	GEOL MAP IDENT	SAMPLE IDENT	OUTCROP SHAPE	O	R	T	V	D	LENGTH	VISITED LENGTH	WIDTH	CARB. AREA	DOL. AREA	VR Length	VR Width	STRIKE	DIP	#	E	F	W	C	L	COMMENTS
Totals	401		####				17	0	1	5	0	106200	15200	####	18.34	0.00	####	####		###	3	0	17	7	18	971	**No carbonates near a pluton**
%								0%	6%	30%	0%				4.57%	0.00%					18%	0%					**No mapped dolomites**
Averages			686									6247	2980	172	1.08	######	264	66		67			1.0	0.4	3.5	190	
Maxima			1340									21000	7000	300	4.20	0.00	956	300		70			7	6	8	812	

UPPERMOST ALLOCHTHON: Rødingsfjell Nappe Complex - Nappes Below the Beiarn Nappe: Zone C (Southern and Border Area): SWEDEN TOTALS

MAP SHEET	MAP NAME & NAPPE AREA	UTM / SWEDISH RN COORD	MAX ALT.	GEOL MAP IDENT	SAMPLE IDENT	OUTCROP SHAPE	O	R	T	V	D	LENGTH	VISITED LENGTH	WIDTH	CARB. AREA	DOL. AREA	VR Length	VR Width	STRIKE	DIP	#	E	F	W	C	L	COMMENTS
Totals	234		####				9	0	0	6	0	87500	50000	####	24.20	0.00	####	###		##	2	9	2	5	40	4872	**No carbonates near a thrust**
%								0%	0%	67%	0%				10.34%	0.00%					22%	100%					**No carbonates near a pluton**
Averages			824									9722	8333	194	2.69	######	218	65		45			0.2	0.6	6.7	812	**No mapped dolomites**
Maxima			1100									44500	18000	350	15.00	0.00	580	140		45			2	3	18	3347	

UPPERMOST ALLOCHTHON: Rødingsfjell Nappe Complex - Nappes Below the Beiarn Nappe: Zone C (Southern and Border Area): NORWAY AND SWEDEN TOTALS

MAP SHEET	MAP NAME & NAPPE AREA	UTM / SWEDISH RN COORD	MAX ALT.	GEOL MAP IDENT	SAMPLE IDENT	OUTCROP SHAPE	O	R	T	V	D	LENGTH	VISITED LENGTH	WIDTH	CARB. AREA	DOL. AREA	VR Length	VR Width	STRIKE	DIP	#	E	F	W	C	L	COMMENTS
Totals	635		####				26	0	1	11	0	193700	65200	####	42.54	0.00	####	####		###	5	9	19	12	58	5843	**No carbonates near a pluton**
%								0%	4%	43%	0%				6.70%	0.00%					19%	35%					**No mapped dolomites**
Averages			734									7450	5874	180	1.64	######	248	66		58			0.7	0.5	5.2	526	
Maxima			1340									44500	18000	350	15.00	0.00	956	300		70			7	6	18	3347	

Outcrops which cross the Norwegian - Swedish border are shown separately under Norway and Sweden

UPPERMOST ALLOCHTHON: Rødingsfjell Nappe Complex - Nappes Below the Beiarn Nappe: Zone C (Southern and Border Area): Norway only

Metres

MAP SHEET	MAP NAME & NAPPE AREA	UTM / SWEDISH RN COORD	MAX ALT.	GEOL MAP IDENT	SAMPLE IDENT	OUTCROP SHAPE	O	R	T	V	D	LENGTH	VISITED LENGTH	WIDTH	CARB. AREA	DOL. AREA	VR Length	VR Width	STRIKE	DIP	#	E	F	W	C	L	COMMENTS
1926 I	***Røssvatnet***	VP *530 030*	980	Cal&Dol	x	Multilimbs	1	0	0	1	0	13000	*4500*	100	1.30	0.00	600	80	70	70	N	0	7	6	8	812	Gåsvassgr. etc GC, Heap, Doj, SN97
1926 I	***Røssvatnet***	VP *590 020*	680	Cal&Dol	x	Linear	1	0	0	0	0	13000	0	200	2.60	0.00	300	100	60		N	0	0	0	0	0	
1926 I	***Røssvatnet***	VP *630 074*	390	Cal&Dol	x	Linear	1	0	0	0	0	700	0	200	0.14	0.00	10	10	60			0	0	0	0	0	
1926 I	***Røssvatnet***	VN *533 980*	420	Cal&Dol	x	Linear	1	0	0	0	0	1000	0	200	0.20	0.00	40	10	50			0	0	0	0	0	
1926 I	***Røssvatnet***	VN *535 978*	409	Cal&Dol	x	Square	1	0	0	0	0	300	0	300	0.09	0.00	30	30				0	0	0	0	0	Peninsular
1926 I	***Røssvatnet***	VN *560 990*	540	Cal&Dol	x	Linear	1	0	0	0	0	6000	0	100	0.60	0.00	160	40	55			0	0	0	0	0	
1926 I	***Røssvatnet***	VP *590 010*	480	Cal&Dol	x	Linear	1	0	0	0	0	2000	0	200	0.40	0.00	100	40	55			0	0	0	0	0	
Area	93	VP *635 020*	580	Cal&Dol	x	Linear	1	0	0	0	0	1000	0	100	0.10	0.00	200	20	50			0	0	1	0	0	Continues NE
2027 III	**Storakersvatnet**																										
Area	50																										
2026 IV	***Hjartfjellet***	VP *726 150*	980	Cal&Dol	x	Sinuous	1	0	0	1	0	9500	1500	100	0.95	0.00	440	40				0	2	0	5	23	SN96: Lst. shown 1 km S.
2026 IV	***Hjartfjellet***	VP *750 120*	760	Cal&Dol	x	Multilimbs	1	0	0	1	0	21000	7000	200	4.20	0.00	376	80		70	N	0	3	0	5	136	SN96
2026 IV	***Hjartfjellet***	VP *695 103*	520	Cal&Dol	x	Linear	1	0	0	1	0	2000	1500	100	0.20	0.00	136	40				0	0	0	0	0	SN96
2026 IV	***Hjartfjellet***	VP *700 100*	460	Cal&Dol	x	Linear	1	0	0	0	0	1500	0	300	0.45	0.00	76	40				0	0	0	0	0	**(W. of E79 and S. of Study Area boundary)**
2026 IV	***Hjartfjellet***	VP *780 110*	740	Cal&Dol	x	Sinuous	1	0	0	0	0	6000	0	300	1.80	0.00	356	60				0	0	0	0	0	
2026 IV	***Hjartfjellet***	VP *775 092*	*500*		x	*Unmapped*	1	0	0	1	0	*700*	700	*20*	*0.01*	0.00	*40*	*10*				0	2	0	0	0	TF97: Sinks + risings
2026 IV	***Hjartfjellet***	VP *750 070*	1340	Cal&Dol	x	Irregular	1	0	0	0	0	20000	0	200	4.00	0.00	956	300			N	0	2	0	0	0	
Area	222	VP *780 050*	1200	Cal&Dol	x	Irregular	1	0	1	0	0	4500	0	200	0.90		600	200				0	0	0	0	0	On RNC Thrust base. WvS mapping
2027 II	**Kaldvatnet**	VP 977 390	690	Calcitic	x	Sinuous	1	0	0	0	0	4000	0	100	0.40	0.00	60	20		60	W	0	1	0	0	0	
Area	36																										

What does "Calcitic and dolomitic marble" actually mean?

UPPERMOST ALLOCHTHON: Rødingsfjell Nappe Complex - Nappes Below the Beiarn Nappe: Zone C (Southern and Border Area): Sweden only

MAP SHEET	MAP NAME & NAPPE AREA	UTM / SWEDISH RN COORD	MAX ALT.	GEOL MAP IDENT	SAMPLE IDENT	OUTCROP SHAPE	O	R	T	V	D	LENGTH	VISITED LENGTH	WIDTH	CARB. AREA	DOL. AREA	VR Length	VR Width	STRIKE	DIP	#	E	F	W	C	L	COMMENTS
2027 III	**Storakersvatnet**	VP *830 210*	1100	Cal&Dol		Multilimbs	1	0	0	1	0	18000	*18000*	200	3.60	0.00	580	60	5			1	0	2	4	150	Slukgrottan to N. Arttjåro
2027 III	**Storakersvatnet**	VP *839 238*	900			*Unmapped*	1	0	0	1	0	*2000*	*2000*	*50*	*0.10*	0.00	*20*	*5*	10			1	0	0	1	14	Schaktgrottan
Area	52	VP *850 240*	960	Cal&Dol	Calcitic	Multilimbs	1	0	0	1	0	44500	*17000*	350	15.00	0.00	440	140	40	45	E/W	1	0	3	12	3347	Labyrintgr. etc. Incl.Hjartfjell, Kaldvatn, corner
2026 IV	***Hjartfjellet***																										Carbonates included on Storakersvatn
Area	70																										
2027 II	**Kaldvatnet**	VP 910 340	780	Cal&Dol	Calcitic	Linear	1	0	0	1	0	7500	*7500*	300	2.25	0.00	220	140	90	45	N	1	0	0	18	1021	Kåtaviken. Incl. Storakersvatn
2027 II	**Kaldvatnet**	VP 930 330	620	Cal&Dol		Linear	1	0	0	0	0	1500	0	200	0.30	0.00	60	60	50			1	0	0	0	0	**Geology incl. from Werner von Screiber**
2027 II	**Kaldvatnet**	VP 930 320	700	Cal&Dol		Linear	1	0	0	0	0	3500	0	200	0.70	0.00	180	40	40			1	0	0	0	0	
2027 II	**Kaldvatnet**	VP 950 340	800	Cal&Dol		2 limbs	1	0	0	1	0	2500	*2500*	100	0.25	0.00	180	60				1	0	0	4	200	Mjölkbäck
2027 II	**Kaldvatnet**	VP 960 350	820	Cal&Dol		3 limbs	1	0	0	1	0	3000	*3000*	50	0.50	0.00	60	20				1	2	0	1	140	Fisktjarnsgrottan (Cave on west of ridge)
Area	112	VP 910 280	740	Cal&Dol		Linear	1	0	0	0	0	5000	0	300	1.50	0.00	220	60	15			1	0	0	0	0	

For D%, see SGU Rapporter (54) p176

UPPER ALLOCHTHON: Køli Nappes - Upper Køli (Fauske / Gasak / Akfjell / Hattfjelldal / Jofjell / Krutfjell Nappes): KU: NORWAY TOTALS

Metres

MAP SHEET	MAP NAME & NAPPE AREA	UTM / SWEDISH RN COORD	MAX ALT.	GEOL MAP IDENT	SAMPLE IDENT	OUTCROP SHAPE	O	R	T	V	D	LENGTH	VISITED LENGTH	WIDTH	CARB. AREA	DOL. AREA	VR Length	VR Width	STRIKE	DIP	#	E	F	W	C	L	COMMENTS
Totals	731		####				48	2	19	12	15	216500	24500	#####	79.92	21.89	####	####		###	31	13	41	16	32	4414	
%								4%	40%	25%	31%				10.93%	2.99%					65%	27%					
Averages			645									4510	2042	256	1.7	1.46	195	65		45			0.85	0.33	2.67	368	
Maxima			1020									30000	5500	2000	32.00	9.00	580	532		73			8	4	9	2862	

UPPER ALLOCHTHON: Køli Nappes - Upper Køli (Fauske / Gasak / Akfjell / Hattfjelldal / Jofjell / Krutfjell Nappes): KU: SWEDEN TOTALS

MAP SHEET	MAP NAME & NAPPE AREA	UTM / SWEDISH RN COORD	MAX ALT.	GEOL MAP IDENT	SAMPLE IDENT	OUTCROP SHAPE	O	R	T	V	D	LENGTH	VISITED LENGTH	WIDTH	CARB. AREA	DOL. AREA	VR Length	VR Width	STRIKE	DIP	#	E	F	W	C	L	COMMENTS
Totals	1683		####				38	2	9	9	3	143900	47000	####	43.16	0.96	####	###		###	8	29	18	28	93	5237	**No carbonates near a pluton**
%								5%	24%	24%	8%				2.56%	0.06%					21%	76%					
Averages			860									3787	5222	155	1.14	0.32	123	26		34			0.47	0.74	10	582	
Maxima			1392									24000	24000	2000	24.00	0.40	842	132		60			7	14	32	2448	

UPPER ALLOCHTHON: Køli Nappes - Upper Køli (Fauske / Gasak / Akfjell / Hattfjelldal / Jofjell / Krutfjell Nappes): KU: NORWAY AND SWEDEN TOTALS

MAP SHEET	MAP NAME & NAPPE AREA	UTM / SWEDISH RN COORD	MAX ALT.	GEOL MAP IDENT	SAMPLE IDENT	OUTCROP SHAPE	O	R	T	V	D	LENGTH	VISITED LENGTH	WIDTH	CARB. AREA	DOL. AREA	VR Length	VR Width	STRIKE	DIP	#	E	F	W	C	L	COMMENTS
Totals	2414		####				86	4	28	21	18	360400	71500	#####	123.08	22.85	#####	####		###	39	42	59	44	125	9651	
%								5%	33%	24%	21%				5.10%	0.95%					45%	49%					
Averages			740									4191	3405	212	1.43	1.27	163	48		42			0.69	0.51	5.95	460	
Maxima			1392									30000	24000	2000	32.00	9.00	842	532		73			8	14	32	2862	

UPPER ALLOCHTHON: *Køli Nappes - Upper Køli (Fauske / Gasak / Akfjell / Hattfjelldal / Jofjell / Krutfjell Nappes): KU: Norway only*

See Caledonide Orogeny p905: Krutfjell Mega Lens is a higher grade nappe emplaced within the Køli. There are no mapped carbonates within the Krutfjell nappe, *but there is a feature at VN 615945, under the road!*

Akfjell and Hattfjelldal Nappes are placed in KU according to Dallmann (1986)

Metres

MAP SHEET	MAP NAME & NAPPE AREA	UTM / SWEDISH RN COORD	MAX ALT.	GEOL MAP IDENT	SAMPLE IDENT	OUTCROP SHAPE	O	R	T	V	D	LENGTH	VISITED LENGTH	WIDTH	CARB. AREA	DOL. AREA	VR Length	VR Width	STRIKE	DIP	#	E	F	W	C	L	COMMENTS
1926 II	***Hattfjelldal***	VN *509 920*	500	Calcite		Linear	1	0	1	0	0	900	0	50	0.05	0.00	120	20	30	34	W	1	0	0	0	0	#50. Near Køli Thrust top
1926 II	***Hattfjelldal***	VN *515 913*	480	Calcite		Linear	1	0	1	0	0	1000	0	50	0.05	0.00	100	20	110	55	S	1	0	0	0	0	#50. On Køli Thrust top
1926 II	***Hattfjelldal***	VN *530 880*	460	Myl. Calc		Sinuous	1	1	1	0	0	2500	0	50	0.10	0.00	80	5		60	W	1	0	0	0	0	#45b. On Køli Thrust top
1926 II	***Hattfjelldal***	VN *560 840*	460	Calcite		Sinuous	1	0	0	0	0	4500	0	200	0.90	0.00	80	40		12	W	0	0	2	0	0	#50. **Jofjell Nappe + Krutfjell Nappe**
1926 II	***Hattfjelldal***	VN *580 780*	500	Calcite		Multilimbs	1	0	0	0	0	7000	0	500	3.50	0.00	120	40	0	46	W	0	0	2	0	0	#50
1926 II	***Hattfjelldal***	VN *581 750*	390	Calcite		Linear	1	0	0	0	0	400	0	50	0.02	0.00	40	20	0			0	0	0	0	0	#50
1926 II	***Hattfjelldal***	VN *595 740*	420	Dolomite		Irregular	1	0	0	0	1	1000	0	200	0.20	0.20	37	37		55	S	0	0	0	0	0	#49
1926 II	***Hattfjelldal***	VN *510 682*	800	Calcite		Sinuous	1	0	1	0	0	2000	0	100	0.20	0.00	190	100				1	0	1	0	0	#42. On Køli Thrust top
1926 II	***Hattfjelldal***	VN *510 668*	760	Calcite		Linear	1	0	1	0	0	2000	0	100	0.20	0.00	60	40	160	73	W	1	0	0	0	0	#42. On Køli Thrust top
1926 II	***Hattfjelldal***	VN *530 700*	780	Calcite		Tapering	1	0	1	1	0	16000	*4000*	2000	32.00	0.00	542	532	180	38	W	1	8	0	6	484	#42. On Køli & int. thr. Heap/Doj. Djup. Continues S.
1926 II	***Hattfjelldal***	VN *525 760*	600	Myl. calc		Sinuous	1	0	1	0	0	4000	0	50	0.20	0.00	380	10		26	W	0	0	0	0	0	#41. On Køli Thrust top
1926 II	***Hattfjelldal***	VN *530 760*	560	Calcite		Sinuous	1	0	1	0	0	7000	0	200	1.40	0.00	320	80	180	30	W	0	2	1	0	0	#42. On Køli Thrust top
1926 II	***Hattfjelldal***	VN *550 650*	440	Calcite		Irregular	1	0	0	0	0	500	0	300	0.15	0.00	120	120	60	55	N	0	0	0	0	0	#34. **Hattfjelldal Nappe**
1926 II	***Hattfjelldal***	VN *540 770*	440	Dolomite		Linear	1	0	0	0	1	700	0	50	0.04	0.04	120	5	180	45	WE	0	0	0	0	0	#44
1926 II	***Hattfjelldal***	VN *553 753*	560	Calcite		Multilimbs	1	0	1	1	0	14000	*500*	200	2.80	0.00	320	40	180	37	WE	0	2	0	0	0	#42.Grey. Nappe base.Prestegårdsskogen.TF98
1926 II	***Hattfjelldal***	VN *535 825*	520	Dolomite		Sinuous	1	0	0	0	1	2000	0	100	0.20	0.20	140	10		55	W	0	0	0	0	0	#44
1926 II	***Hattfjelldal***	VN *540 790*	568	Dolomite		Sinuous	1	0	0	0	1	4000	0	200	0.80	0.80	118	20	170	24	W	0	0	0	0	0	#44
1926 II	***Hattfjelldal***	VN *554 680*	420	Red calc		Multilimbs	1	0	0	1	0	5500	1000	50	0.20	0.00	140	40		31	W	0	0	0	0	0	#43. TF00
1926 II	***Hattfjelldal***	VN *550 730*	580	Dolomite		Multilimbs	1	0	0	0	1	6000	0	300	1.80	1.80	350	40		39	W	0	1	0	0	0	#44
1926 II	***Hattfjelldal***	VN *554 690*	374	Dolomite		Linear	1	0	0	0	1	1000	0	50	0.05	0.05	94	20	180	31	W	0	0	0	0	0	#44
1926 II	***Hattfjelldal***	VN *560 680*	428	Dolomite		Irregular	1	0	0	0	1	3500	0	600	2.00	2.00	188	60		70	N	0	0	0	0	0	#44
1926 II	***Hattfjelldal***	VN *558 697*	370	Calcite		Linear	1	0	0	0	0	600	0	200	0.12	0.00	30	30	180	70	W	0	0	0	0	0	#42. Grey
1926 II	***Hattfjelldal***	VN *580 670*	560	Dolomite		Irregular	1	0	1	1	1	9000	*1000*	1000	9.00	9.00	280	120		63	S	0	2	0	0	0	#44. On Nappe base. Heap: Impenetrable syst.
1926 II	***Hattfjelldal***	VN *580 654*	688	Red calc		Rectangle	1	0	1	0	0	1000	0	300	0.30	0.00	188	108		45	W	0	0	0	0	0	#43. On Nappe base.Thick
1926 II	***Hattfjelldal***	VN *596 660*	620	Red calc		Sinuous	1	0	1	0	0	4500	0	100	0.45	0.00	310	40		38	W	0	0	0	0	0	#43. On Nappe base.Thick
1926 II	***Hattfjelldal***	VN *598 660*	480	Dolomite		Linear	1	0	0	0	1	1500	0	100	0.15	0.15	170	20	180	37	W	0	0	0	0	0	#44
1926 II	***Hattfjelldal***	VN *605 663*	536	Dolomite		Sinuous	1	0	1	0	1	3000	0	100	0.30	0.30	215	40				0	0	0	0	0	#44. On Nappe base
1926 II	***Hattfjelldal***	VN *602 677*	390	Dolomite		Linear	1	0	1	0	1	500	0	100	0.50	0.50	30	10	130			0	0	0	0	0	#44. On Nappe base
Area	193	VN *550 800*	579	Calcite		2 limbs	1	0	0	0	0	1500	0	200	0.30	0.00	79	60		31	W	0	0	0	0	0	#42
1925 I	***Susendalen***	VN *500 580*	700	Calcite		Tapering	1	0	1	1	0	1500	700	700	1.00	0.00	160	140				1	0	0	0	0	Grey. On Køli Thrust top. **Hattfjelldal Nappe**
1925 I	***Susendalen***	VN *510 580*	750	Dol&Cal	Calcitic	Tapering	1	0	1	1	1	4500	1300	500	2.25	2.25	250	160		30		1	0	1	3	230	On Køli Thr top. Kvalpskard.Heap74.TF98.DipE&S
1925 I	***Susendalen***	VN *510 570*	720	Calcite	Cal+Dol	Tapering	1	0	1	1	0	3500	1500	1000	3.50	0.00	320	100		50	W	1	4	0	9	2862	Stor Grubblandsgrotta etc. Thrust top at west.
Area	215	VN *550 600*	700	Dolomite		Sinuous	1	0	0	1	1	11500	1000	1000	3.30	3.30	360	300				0	3	1	0	0	SN97 - superficial flows
1925 II	**Børgefellet**																										**No carbonates**
Area	7																										
2026 IV	***Hjartfjellet***	VP 665 *030*	764	Calcite		Arc	1	0	1	0	0	4000	0	100	0.40	0.00	164	80				0	0	0	0	0	On Køli Thrust top. **Akfjell and Krutfjell Nappes**
2026 IV	***Hjartfjellet***	VP *750 036*	1000	Calcite		Sinuous	1	0	0	0	0	6500	0	100	0.65	0.00	350	20				0	0	0	0	0	
2026 IV	***Hjartfjellet***	VP *800 037*	830	Calcite		Linear	1	0	0	0	0	1000	0	100	0.10	0.00	41	20				1	0	0	0	0	Olfjell legends: Olfjelltjornagrotta?
2026 IV	***Hjartfjellet***	VP *800 030*	1000	Calcite		Sinuous	1	0	0	1	0	8500	500	100	0.85	0.00	344	100	100	30	N	1	4	1	3	136	Martinus area
2026 IV	***Hjartfjellet***	VP *800 025*	676	Calcite		Sinuous	1	0	0	1	0	4000	3500	100	0.40	0.00	20	20	90	70	S	1	4	1	4	332	Skinfelldal
2026 IV	***Hjartfjellet***	VP *700 010*	1020	Calcite		Multilimbs	1	0	1	1	0	30000	*4000*	200	6.00	0.00	580	200	80	45	N	0	4	4	2	6	Thr at W end (Røssvatn).Akfjell. 2 WvS+. Jup.
2026 IV	***Hjartfjellet***	VP *680 010*	960	Dol.Cong		Linear	1	0	0	0	1	6000	0	200	1.20	1.20	460	40	85			0	0	0	0	0	
2026 IV	***Hjartfjellet***	VP *760 010*	989	Calcite		Linear	1	0	0	0	0	8000	0	100	0.00	0.00	300	40	85			1	1	2	0	0	1 W. von Schreiber feature + cave?
2026 IV	***Hjartfjellet***	VP *760 000*	800	Calcite		Sinuous	1	0	0	0	0	3000	0	50	0.15	0.00	170	20				0	0	0	0	0	1 W. von Schreiber feature
2026 IV	***Hjartfjellet***	VN *745 994*	580	Calcite		Linear	1	0	0	0	0	500	0	50	0.02	0.00	20	20	95			0	0	0	0	0	
2026 IV	***Hjartfjellet***	VN *773 997*	740	Calcite		Linear	1	0	0	0	0	400	0	50	0.02	0.00	20	5	75			0	0	0	0	0	
2026 IV	***Hjartfjellet***	VN *770 983*	820	Calcite		Arc	1	0	0	1	0	7500	5500	200	1.50	0.00	300	80	90	60	N/S	0	4	0	5	364	Heap 74, DStP70, Sjöberg 79, Selvaag pc 1998
2026 IV	***Hjartfjellet***	VN *810 960*	840	Calcite		Linear	1	0	0	0	0	2000	0	100	0.20	0.00	140	20	85			0	0	0	0	0	
Area	141	VN 773 *925*	*866*			*Linear*	*1*	0	*0*	*0*	*0*	*6000*	0	*50*	*0.30*	*0.00*	*326*	*10*	*90*			0	2	0	0	0	Assumed from prospects. 1 WvS
2026 III	***Krutvatnet***	VN *720 818*	960	Dol&Cal		Arc	1	1	0	0	1	1000	0	100	0.10	0.10	80	20				0	0	0	0	0	Is it Dolomite?
Area	172																										
2025 IV	**Skardmodalen**																										**No carbonates**
Area	3																										

UPPER ALLOCHTHON: Køli Nappes - Upper Køli (Fauske / Gasak / Akfjell / Hattfjelldal / Jofjell / Krutfjell Nappes): KU: Sweden only

Metres

MAP SHEET	MAP NAME & NAPPE AREA	UTM / SWEDISH RN	COORD		MAX ALT.	GEOL MAP IDENT	SAMPLE IDENT	OUTCROP SHAPE	O	R	T	V	D	LENGTH	VISITED LENGTH	WIDTH	CARB. AREA	DOL. AREA	VR Length	VR Width	STRIKE	DIP	#	E	F	W	C	L	COMMENTS
2026 IV	***Hjartfjellet***	VP	*850*	*090*	1392	Calcite	Calcitic	Multilimbs	1	0	1	1	0	16000	*6500*	50	0.80	0.00	842	60	45	60	W	0	0	0	11	603	**Akfjell Nappe.** On Køli Thrust top. Rødingsfjall
2026 IV	***Hjartfjellet***	VP	*830*	*030*	760	Calcite		Irregular	1	0	0	0	0	2000	0	100	0.20	0.00	150	40				1	0	0	0	0	Jofjell Geol. Map. SGU c778
2026 IV	***Hjartfjellet***	VN	*820*	*960*	740	Calcite		Linear	1	0	0	0	0	1000	0	100	0.00	0.00	40	40	90			0	0	0	0	0	Nappe as VwS
2026 IV	***Hjartfjellet***	VN	*825*	*945*	830	Lst & Dol		Linear	1	0	0	0	0	500	0	30	0.02	0.00	20	5				1	0	0	0	0	From Ai160
2026 IV	***Hjartfjellet***	VN	*840*	*952*	900	Lst & Dol		Linear	1	0	0	0	0	500	0	50	0.03	0.00	60	5				0	0	0	0	0	From Ai160
Area	67	VN	*850*	*945*	920	Calcite		Sinuous	1	0	0	0	0	3000	0	100	0.30	0.00	100	20				1	0	0	0	0	Geology includes Werner von Schreiber mapping (1987)
2026 III	***Krutvatnet***	VN	*831*	*830*	700	Lst&Dol		Linear	1	0	0	0	0	200	0	50	0.01	0.00	20	5				0	0	0	0	0	From Ai160
2026 III	***Krutvatnet***	VN	*840*	*844*	920	Lst&Dol		Linear	1	0	0	0	0	500	0	50	0.03	0.00	50	5				0	0	0	0	0	From Ai160
2026 III	***Krutvatnet***	VN	*850*	*853*	940	Lst&Dol		Irregular	1	0	1	0	0	1000	0	100	0.10	0.00	90	20				1	0	0	0	0	From Ai160
2026 III	***Krutvatnet***	VN	*842*	*830*	760	Lst&Dol		Sinuous	1	0	0	0	0	500	0	50	0.03	0.00	20	5				0	0	0	0	0	From Ai160
2026 III	***Krutvatnet***	VP	825	770	1020	Lst & Dol		Arc	1	0	1	0	0	1400	0	100	0.14	0.00	60	5	35	30	W	0	0	0	0	0	From Ai160
2026 III	***Krutvatnet***	VN	840	720	720	Calcite		Sinuous	1	0	0	0	0	1000	0	50	0.05	0.00	40	10				1	0	0	0	0	From Ai161
Area	140	VN	860	670	860	Calcite		Arc	1	0	1	0	0	300	0	50	0.02	0.00	40	5				1	0	0	0	0	From Ai161. Between thrusts
2025 IV	**Skardmodalen**																												**No carbonate outcrops**
Area	16																												
2027 II	**Kaldvatnet**	VP	910	210	1120	Hellden	Calcitic	Multilimbs	1	0	1	1	0	9000	*7000*	300	2.70	0.00	600	80	0-60		20 N	1	2	2	13	2448	**Jofjell/Fauske Nappe?** On Thr. top. Sotsbäcksgr. etc.
Area	144	WP	040	300	1060	Calcitic		Sinuous	1	1	1	1	0	24000	*24000*	300	7.20	0.00	540	100				1	7	14	32	823	On Thrust top. Ö. Altsvatnet+ Brandsfjäll.
25EF	**Umfors NE**	14760		73420	810	Calcitic		Irregular	1	1	0	1	0	12000	0	2000	24.00	0.00	129	40				1	6	1	23	920	**Fauske Nappe?** Övre Altsvatn (contiguous with above)
Area	96																												(Area bounded by 1474 to 1478, north of 7322 only)
25G	**Ammarnäs NE**	14805		73440	880	Calcitic		Arc	1	0	0	1	0	5000	0	200	1.00	0.00	160	20				0	0	0	0	0	Frei 1968
Area	168																												(Area north of 7322 only)
25EF	**Umfors SW**	14520		73210	1000	Lst & Dol		Sinuous	1	0	1	1	0	4000	*2000*	40	0.16	0.00	144	40	45	25	N	1	0	0	3	118	On Køli Thrust top. Gielasvaratjgr.+Dutch.
	592																												(Area bounded by 1450 to 1478 and 7300 to 7322)
25G	**Ammarnäs SE**																												**No carbonate outcrops**
Area	132																												(Area bounded by 7300 to 7322)
Ai160	24EF **Tärnaby**	14605		73000	700	D+Ankarite		Irregular	1	0	0	0	1	2000	0	100	0.20	0.20	100	60				1	0	0	0	0	See SGU (54) p184 & Jofjell Geol. Map
Ai160	24EF **Tärnaby**	14615		72990	800	D+Ankarite		Lozenge	1	0	0	0	1	1200	0	300	0.36	0.36	100	132				1	0	0	0	0	See SGU (54) p184 & Jofjell Geol. Map
Ai160	24EF **Tärnaby**	14640		72990	680	D+Ankarite		Ellipse	1	0	0	0	1	1000	0	400	0.40	0.40	45	20				1	0	1	0	0	See SGU (54) p184 & Jofjell Geol. Map
Ai160	24EF **Tärnaby**	14660		72960	802	Lst & Dol		Arc	1	0	0	0	0	3000	0	200	0.60	0.00	102	20				1	0	0	0	0	
Ai160	24EF **Tärnaby**	14604		72906	620	Calcitic	(Beskens)	Arc	1	0	0	1	0	2500	500	50	0.13	0.00	30	10	140	30	S	1	1	4	4	135	Tjårrogrottan1-4.TF98
Ai160	24EF **Tärnaby**	14585		72910	720	Lst & Dol		Sinuous	1	0	0	0	0	2000	0	50	0.10	0.00	40	10				1	0	1	0	0	
Ai160	24EF **Tärnaby**	14520		72880	900	Cal&Dol	(Beskens)	Sinuous	1	0	1	1	0	13000	2000	100	1.30	0.00	135	40				1	2	0	0	0	Near int. thrust.TF98.Lst.insig.SGU(54) p188.
Ai160	24EF **Tärnaby**	14507		72875	770	Lst & Dol		Irregular	1	0	0	0	0	300	0	100	0.03	0.00	5	5				1	0	0	0	0	
Ai160	24EF **Tärnaby**	14510		72860	900	Lst & Dol		Sinuous	1	0	1	0	0	2000	0	80	0.16	0.00	135	10	45	38	W	1	0	1	0	0	Near internal thrust
Ai160	24EF **Tärnaby**	14580		72898	720	Lst & Dol		Arc	1	0	0	0	0	500	0	50	0.03	0.00	20	5				1	0	0	0	0	
Ai160	24EF **Tärnaby**	14580		72896	720	Lst & Dol		Arc	1	0	0	0	0	600	0	50	0.03	0.00	20	5				1	0	0	0	0	
Ai160	24EF **Tärnaby**	14580		72895	720	Lst & Dol		Sinuous	1	0	0	0	0	500	0	50	0.03	0.00	20	5				1	0	2	0	0	
Ai160	24EF **Tärnaby**	14565		72850	980	Lst & Dol		Arc	1	0	0	0	0	2000	0	100	0.20	0.00	140	20				1	0	1	0	0	
Ai160	24EF **Tärnaby**	14568		72850	920	Lst & Dol		Diamond	1	0	0	0	0	500	0	150	0.08	0.00	5	35				1	0	0	0	0	
Ai160	24EF **Tärnaby**	14550		72770	990	Calcitic	(Beskens)	Sinuous	1	0	0	1	0	22500	*5000*	100	2.25	0.00	270	40		25	N	1	0	1	7	190	Rajagrottan etc. Sinks and rising at 14610 72830
Area	264	14720		72950	700	Lst & Dol		Sinuous	1	0	0	0	0	6500	0	50	0.33	0.00	200	20				1	0	0	0	0	(Area bounded by 1450 to 1475 and 7275 to 7300 only)
Ai161	24EF **Tärnaby**	14504		72648	890	Calcite		Linear	1	0	0	0	0	200	0	50	0.01	0.00	30	2				1	0	0	0	0	
Ai161	24EF **Tärnaby**	14501		72638	1030	Calcite		Linear	1	0	0	0	0	200	0	50	0.01	0.00	10	2				0	0	0	0	0	
Area	24	14508		72640	980	Calcite		Linear	1	0	0	0	0	600	0	50	0.03	0.00	90	10				1	0	0	0	0	(Area bounded by 1450 to 1475 and 7250 to 7275 only)
Ai163	24EF **Tärnaby**	14750		72935	800	Calcitic		Arc	1	0	0	0	0	900	0	100	0.09	0.00	80	20		40	W	1	0	0	0	0	In 4 sections
Area	40																												(Area bounded by 1475 to 1500 and 7275 to 7300 only)

UPPER ALLOCHTHON: Køli Nappes - Middle Køli - Gjersvik Nappe: KG (NORWAY ONLY)

Metres

MAP SHEET	MAP NAME & NAPPE AREA	UTM / SWEDISH RN COORD	MAX ALT.	GEOL MAP IDENT	SAMPLE IDENT	OUTCROP SHAPE	O	R	T	V	D	LENGTH	VISITED LENGTH	WIDTH	CARB. AREA	DOL. AREA	VR Length	VR Width	STRIKE	DIP	#	E	F	W	C	L	COMMENTS
Totals	1648		####				9	0	2	0	0	29800	0	####	7.16	0.00	###	###		###	6	5	0	5	0	0	**No carbonates near a pluton**
%								0%	22%	0%	0%				0.43%	0.00%					67%	56%					**No visited carbonates**
Averages			667									3311	#DIV/0!	189	0.80	######	109	34		32			0.00	0.56	###	###	**No mapped dolomites**
Maxima			840									7000	0	500	3.50	0.00	201	130		70			0	2	0	0	**No caves reported**
1824 III	**Harran**																										**No carbonate outcrops**
Area	146																										
1823 IV	**Grong**																										**No carbonate outcrops**
Area	67																										
1824 I	**Namsskogan**																										**No carbonate outcrops**
Area	40																										
1824 II	**Skorovatn**																										**No carbonate outcrops**
Area	602																										
1823 I	**Andorsjøen**																										**No carbonate outcrops**
Area	60																										Map not seen
1925 III	***Majavatn***	VN	*300*	*120*	620	L & D Cong.	Arc	1	0	1	0	0	7000	0	200	1.40	0.00	201	40		70	W	0	0	1	0	0	North end near Køli Thrust top. Continues S.
1925 III	***Majavatn***	VN	*300*	*105*	527	L & D Cong.	Linear	1	0	0	0	0	1400	0	100	0.14	0.00	37	10	20			0	0	0	0	0	
Area	84	VN	*370*	*110*	540	Calcitic	Linear	1	0	0	0	0	7000	0	100	0.70	0.00	99	10	60	30	W	0	0	2	0	0	Includes continuation on Børgefjell
1924 IV	***Røyrvik***	VN	*290*	*010*	640	L & D Cong.	Linear	1	0	0	0	0	7000	0	500	3.50	0.00	195	130	5	30	W	1	0	1	0	0	
Area	288	VM	272	900	510	Calcitic	Arc	1	0	0	0	0	1600	0	50	0.08	0.00	92	20		25	W	1	0	0	0	0	Marked on 1:100,000 54D Solid. Or phyllite?
1924 III	**Tunnsjøen**	VM	210	690	720	L & D Cong.	Linear	1	0	0	0	0	3000	0	350	1.00	0.00	126	60	50	20	E	0	0	1	0	0	
Area	248																										
1925 II	***Børgefjellet***	VN	*440*	*217*	820	Calcite	Linear	1	0	0	0	0	600	0	200	0.12	0.00	100	20	50			1	0	0	0	0	
1925 II	***Børgefjellet***	VN	*440*	*212*	790	Calcite	2 limbs	1	0	1	0	0	1500	0	100	0.15	0.00	90	10		15	N	1	0	0	0	0	Near Gjersvik Thrust base
Area	66	VN	*495*	*343*	840	Calcite	Linear	1	0	0	0	0	700	0	100	0.07	0.00	40	5	70		N	1	0	0	0	0	
1924 I	**Jomafjellet**																										**No carbonate outcrops**
Area	42																										
1924 II	**Limingen**																										**No carbonate outcrops**
Area	5																										

UPPER ALLOCHTHON: Køli Nappes - Middle Køli - Orklump / Leipikvattnet Nappe: KL (NORWAY): TOTALS

MAP SHEET	MAP NAME & NAPPE AREA	UTM / SWEDISH RN COORD	MAX ALT.	GEOL MAP IDENT	SAMPLE IDENT	OUTCROP SHAPE	O	R	T	V	D	LENGTH	VISITED LENGTH	WIDTH	CARB. AREA	DOL. AREA	VR Length	VR Width	STRIKE	DIP	#	E	F	W	C	L	COMMENTS
																			Metres								
Totals	236		###				1	0	1	1	0	17000	5000	###	3.40	0.00	###	##		##	1	1	6	0	8	491	**No carbonates near a pluton**
%								0%	100%	100%	0%				1.44%	0.00%					100%	100%					**No mapped dolomites**
Averages			660									17000	5000	200	3.40	#DIV/0!	196	70		85			6.0	0.0	8	491	
Maxima			660									17000	5000	200	3.40	0.00	196	70	75	85	0		6	0	8	491	Also see Helland1909 p98

UPPER ALLOCHTHON: Køli Nappes - Middle Køli - Orklump / Leipikvattnet Nappe: KL (SWEDEN): TOTALS

Totals	135		####				7	0	5	2	0	15000	10000	###	2.56	0.00	###	###		###	5	7	2	0	21	6221	**No carbonates near a pluton**
%								0%	71%	29%	0%				1.90%	0.00%					71%	100%					**No mapped dolomites**
Averages			546									2143	5000	136	0.37	#DIV/0!	74	30		66			0.29	0.00	10.50	3111	
Maxima			740									6500	6500	300	1.30	0.00	280	60		80			2	0	14	5683	

UPPER ALLOCHTHON: Køli Nappes - Middle Køli - Orklump / Leipikvattnet Nappe: KL (NORWAY AND SWEDEN): TOTALS

Totals	371		####				8	0	6	3	0	32000	15000	####	5.96	0.00	###	###		###	6	8	8	0	29	6712	**No carbonates near a pluton**
%								0%	75%	38%	0%				1.61%	0.00%					75%	100%					**No mapped dolomites**
Averages			561									4000	5000	144	0.75	#DIV/0!	89	35		69			1.00	0.00	9.67	2237	
Maxima			740									17000	6500	300	3.40	0.00	280	70		85			6	0	14	5683	

THE 8 CARBONATE OUTCROPS REPRESENT ONE SINGLE OUTCROP THAT HAS BEEN DISMEMBERED BY FOLDING AND FAULTING

UPPER ALLOCHTHON: Køli Nappes - Middle Køli - Orklump / Leipikvattnet Nappe: KL (NORWAY)

MAP SHEET	MAP NAME & NAPPE AREA	UTM / SWEDISH RN COORD	MAX ALT.	GEOL MAP IDENT	SAMPLE IDENT	OUTCROP SHAPE	O	R	T	V	D	LENGTH	VISITED LENGTH	WIDTH	CARB. AREA	DOL. AREA	VR Length	VR Width	STRIKE	DIP	#	E	F	W	C	L	COMMENTS
1924 IV	**Røyrvik**																										
Area	45																										
1924 III	**Tunnsjoen**																										**No carbonate outcrops**
Area	78																										
1924 I	**Jomafjellet**	VM 500 970	660	Calcite	Calcitic	Linear	1	0	1	1	0	17000	5000	200	3.40	0.00	196	70	75	85		1	6	0	8	491	On Thrust. Marmorgr., Landbrua etc. TF97,00
Area	93																										
1924 II	**Limingen**																										**No carbonate outcrops**
Area	20																										

UPPER ALLOCHTHON: Køli Nappes - Middle Køli - Orklump / Leipikvattnet Nappe: KL (SWEDEN)

1924 I	**Jomafjellet**	VM 560 990	540	Calcite		Linear	1	0	1	1	0	6500	6500	200	1.30	0.00	72	40	70	80	S	1	2	0	14	523	Near thr. Bjurälv. SGU (54) p364
Ai74	**Jomafjellet**	VM 583 998	490	Calcite		Linear	1	0	0	0	0	500	0	50	0.02	0.00	10	5	70			1	0	0	0	0	
Ai74	**Jomafjellet**	VN 593 002	475	Calcite		Linear	1	0	0	0	0	500	0	50	0.02	0.00	7	2	70	75	S	1	0	0	0	0	
Ai74	**Jomafjellet**	VM 625 990	540	Calcite		Linear	1	0	1	0	0	2000	0	300	0.60	0.00	72	60	20	70	W	1	0	0	1	15	On int. thr. at S end. SGU (54)p364. 4km gr.
Ai74	**Jomafjellet**	VM 625 975	520	Calcite		Linear	1	0	1	0	0	500	0	50	0.02	0.00	20	20	50			1	0	0	0	0	On Thrust
Ai74	**Jomafjellet**	VM 600 968	520	Calcite		Irregular	1	0	1	0	0	1000	0	200	0.20	0.00	54	40		60	N	1	0	0	0	0	On int. thrust.
Area	95	VM 600 960	740	Calcite		Linear	1	0	1	1	0	4000	3500	100	0.40	0.00	280	40	60	45	N	1	0	0	6	5683	On Thrust. Korallgrottan etc, TF00
1924 II	**Limingen**																										**No carbonate outcrops**
Area	40																										

UPPER ALLOCHTHON: Kalí Nappes - Middle Kalí - Gelvenákko Nappe (NORWAY): TOTALS **Metres**

MAP SHEET	MAP NAME & NAPPE AREA	UTM / SWEDISH RN COORD	MAX ALT.	GEOL MAP IDENT	SAMPLE IDENT	OUTCROP SHAPE	O	R	T	V	D	LENGTH	VISITED LENGTH	WIDTH	CARB. AREA	DOL. AREA	VR Length	VR Width	STRIKE	DIP	#	E	F	W	C	L	COMMENTS
Totals	27																										
%																											
Averages																											
Maxima																											

UPPER ALLOCHTHON: Kalí Nappes - Middle Kalí - Gelvenákko Nappe (SWEDEN): TOTALS

Totals	76																										
%																											
Averages																											
Maxima																											

UPPER ALLOCHTHON: Kalí Nappes - Middle Kalí - Gelvenákko Nappe (NORWAY AND SWEDEN): TOTALS

Totals	103																										
%																											
Averages																											
Maxima																											

There are no mapped carbonate outcrops in this nappe

UPPER ALLOCHTHON: Kalí Nappes - Middle Kalí - Gelvenákko Nappe (NORWAY)

MAP SHEET	MAP NAME & NAPPE AREA	UTM / SWEDISH RN COORD	MAX ALT.	GEOL MAP IDENT	SAMPLE IDENT	OUTCROP SHAPE	O	R	T	V	D	LENGTH	VISITED LENGTH	WIDTH	CARB. AREA	DOL. AREA	VR Length	VR Width	STRIKE	DIP	#	E	F	W	C	L	COMMENTS
1924 IV	**Røyrvik**																										**No carbonate outcrops**
Area	9																										
1924 I	**Jomafjellet**																										**No carbonate outcrops**
Area	18																										

UPPER ALLOCHTHON: Kalí Nappes - Middle Kalí - Gelvenákko Nappe (SWEDEN)

MAP SHEET	MAP NAME & NAPPE AREA	UTM / SWEDISH RN COORD	MAX ALT.	GEOL MAP IDENT	SAMPLE IDENT	OUTCROP SHAPE	O	R	T	V	D	LENGTH	VISITED LENGTH	WIDTH	CARB. AREA	DOL. AREA	VR Length	VR Width	STRIKE	DIP	#	E	F	W	C	L	COMMENTS
1925 II	**Børgefjellet**																										**No carbonate outcrops**
Area	2																										
1924 I	**Jomafjellet**																										**No carbonate outcrops**
Area	35																										
2025 III	**Ranseren**																										**No carbonate outcrops**
Area	29																										
Ai 74	Z1 Frostviken																										**No carbonate outcrops (Area bounded by 1425 to 1450 and 7200 to 7211 only)**
Area	10																										

UPPER ALLOCHTHON: Kall Nappes - Middle Kall - Virvass / Stikke Nappe and Remdalen Repitition: KS (NORWAY): TOTALS — Metres

MAP SHEET	MAP NAME & NAPPE AREA	UTM / SWEDISH RN COORD	MAX ALT.	GEOL MAP IDENT	SAMPLE IDENT	OUTCROP SHAPE	O	R	T	V	D	LENGTH	VISITED LENGTH	WIDTH	CARB. AREA	DOL. AREA	VR Length	VR Width	STRIKE	DIP	#	E	F	W	C	L	COMMENTS
Totals	583		###				1	0	0	0	0	4500	0	##	0.22	0.00	###	##		##	1	1	0	0	0	0	No R, T, V or D. No caves reported
%								0%	0%	0%	0%				0.04%	0.00%					100%	100%					
Averages			526									4500	#DIV/0!	50	0.22	#####	215	20		45			0.0	0.0	###	###	
Maxima			526									4500	0	50	0.22	0.00	215	20		45			0	0	0	0	

UPPER ALLOCHTHON: Kall Nappes - Middle Kall - Virvass / Stikke Nappe and Remdalen Repitition: KS (SWEDEN): TOTALS

MAP SHEET	MAP NAME & NAPPE AREA	UTM / SWEDISH RN COORD	MAX ALT.	GEOL MAP IDENT	SAMPLE IDENT	OUTCROP SHAPE	O	R	T	V	D	LENGTH	VISITED LENGTH	WIDTH	CARB. AREA	DOL. AREA	VR Length	VR Width	STRIKE	DIP	#	E	F	W	C	L	COMMENTS
Totals	1030		#####				26	0	0	0	0	36950	0	####	2.39	0.00	####	###		###	6	24	0	1	0	0	No R, T, V or D. No caves reported
%								0%	0%	0%	0%				0.23%	0.00%					23%	92%					
Averages			770									1421	#DIV/0!	53	0.09	#####	77	10		51			0.00	0.04	###	###	
Maxima			1080									12000	0	100	1.20	0.00	330	40		80			0	1	0	0	

UPPER ALLOCHTHON: Kall Nappes - Middle Kall - Virvass / Stikke Nappe and Remdalen Repitition: KS (NORWAY AND SWEDEN): TOTALS

MAP SHEET	MAP NAME & NAPPE AREA	UTM / SWEDISH RN COORD	MAX ALT.	GEOL MAP IDENT	SAMPLE IDENT	OUTCROP SHAPE	O	R	T	V	D	LENGTH	VISITED LENGTH	WIDTH	CARB. AREA	DOL. AREA	VR Length	VR Width	STRIKE	DIP	#	E	F	W	C	L	COMMENTS
Totals	1613		#####				27	0	0	0	0	41450	0	####	2.61	0.00	####	###		###	7	25	0	1	0	0	No R, T, V or D. No caves reported
%								0%	0%	0%	0%				0.16%	0.00%					26%	93%					
Averages			761									1535	#DIV/0!	53	0.10	#####	82	10		50			0.00	0.04	###	###	
Maxima			1080									12000	0	100	1.20	0.00	330	40		80			0	1	0	0	

UPPER ALLOCHTHON: Kalí Nappes - Middle Kalí - Virvass / Stikke Nappe and Remdalen Repitition: KS (NORWAY)

Metres

MAP SHEET	MAP NAME & NAPPE AREA	UTM / SWEDISH RN COORD		MAX ALT.	GEOL MAP IDENT	SAMPLE IDENT	OUTCROP SHAPE	O	R	T	V	D	LENGTH	VISITED LENGTH	WIDTH	CARB. AREA	DOL. AREA	VR Length	VR Width	STRIKE	DIP	#	E	F	W	C	L	COMMENTS
1823 IV	**Grong**																											**No carbonate outcrops**
Area	3																											
1924 IV	**Skorovatn**																											**No carbonate outcrops**
Area	6																											
1823 I	**Andorsjøen**																											**No carbonate outcrops**
Area	11																											Map not seen
1924 IV	**Røyrvik**																											**No carbonate outcrops**
Area	9																											
1924 III	**Tunnsjøen**	VM	355	675	526	Calcite		Sinuous	1	0	0	0	0	4500		0	50	0.22	0.00	215	20		45	N	1	0	0	0	0	Contig. with first outcrop in Sweden
Area	166																											
1923 IV	**Nordli**																											**No carbonate outcrops**
Area	56																											
1926 II	**Hattfjelldal**																											**No carbonate outcrops**
Area	15																											
1925 I	**Susendalen**																											**No carbonate outcrops**
Area	52																											
1925 II	**Bergefjellet**																											**No carbonate outcrops**
Area	34																											
1924 I	**Jomafjellet**																											**No carbonate outcrops**
Area	20																											
1924 II	**Limingen**																											**No carbonate outcrops**
Area	6																											
1923 I	**Murusjøen**																											**No carbonate outcrops**
Area	8																											
2026 III	**Krutvatnet**																											**No carbonate outcrops**
Area	41																											
2025 IV	**Skardmodalen**																											**No carbonate outcrops**
Area	156																											

UPPER ALLOCHTHON: Kall Nappes - Middle Kall - Virvass / Stikke Nappe and Remdalen Repitition: KS (SWEDEN)

Metres

MAP SHEET	MAP NAME & NAPPE AREA	UTM / SWEDISH RN COORD		MAX ALT.	GEOL. MAP IDENT	SAMPLE IDENT	OUTCROP SHAPE	O	R	T	V	D	LENGTH	VISITED LENGTH	WIDTH	CARB. AREA	DOL. AREA	VR Length	VR Width	STRIKE	DIP	#	E	F	W	C	L	COMMENTS
1924 III	**Tunnsjoen**	VM	375 660	480	Calcite		Sinuous	1	0	0	0	0	2000	0	50	0.10	0.00	70	20		20	N	1	0	0	0	0	Contig. with above
1924 III	**Tunnsjoen**	VM	370 650	480	Calcite		Sinuous	1	0	0	0	0	600	0	50	0.03	0.00	60	5				1	0	0	0	0	
1924 III	**Tunnsjoen**	VM	370 647	500	Calcite		Sinuous	1	0	0	0	0	1500	0	50	0.05	0.00	80	10		25	N	1	0	0	0	0	Crossed by "Hålbäcken"
1924 III	**Tunnsjoen**	VM	370 630	600	Calcite		Sinuous	1	0	0	0	0	3500	0	50	0.18	0.00	180	10				1	0	0	0	0	Limestone not found. TF98
1924 III	**Tunnsjoen**	VM	368 630	600	Calcite		Sinuous	1	0	0	0	0	1700	0	50	0.09	0.00	170	10				1	0	0	0	0	
1924 III	**Tunnsjoen**	VM	370 627	520	Calcite		Sinuous	1	0	0	0	0	800	0	50	0.04	0.00	40	10				1	0	0	0	0	Portfjällbäck sinks: JFG p56 1997. *
1924 III	**Tunnsjoen**	VM	370 612	620	Calcite		Arc	1	0	0	0	0	500	0	50	0.02	0.00	20	5				1	0	0	0	0	Limestone not found. TF98
Area	14	VM	373 610	640	Calcite		Arc	1	0	0	0	0	400	0	50	0.02	0.00	10	10				1	0	0	0	0	Limestone not found. TF98
1925 II	**Bergefjellet**																											**No carbonate outcrops**
Area	2																											
1924 I	**Jomafjellet**	VM	513 840	580	Calcite		Linear	1	0	0	0	0	150	0	50	0.01	0.00	20	5				1	0	0	0	0	
Area	92																											* See SGU (54) p366 and RM database.
1924 II	**Limingen**																											**No carbonate outcrops**
Area	173																											
2026 III	**Krutvatnet**																											**No carbonate outcrops**
Area	20																											
2025 IV	**Skardmodalen**	VN	843 470	890	Calcite		Linear	1	0	0	0	0	600	0	50	0.03	0.00	40	5	180			0	0	0	0	0	From Ai73. In the Remdalen Repitition.
2025 IV	**Skardmodalen**	VN	823 455	960	Calcite		Sinuous	1	0	0	0	0	1000	0	50	0.05	0.00	120	5				1	0	0	0	0	From Ai73. In the Remdalen Repitition.
2025 IV	**Skardmodalen**	VN	782 445	800	Calcite		Arc	1	0	0	0	0	700	0	50	0.03	0.00	50	5				1	0	0	0	0	From Ai73. In the Remdalen Repitition.
2025 IV	**Skardmodalen**	VN	790 440	850	Calcite		Linear	1	0	0	0	0	1000	0	50	0.05	0.00	130	10	20			1	0	0	0	0	From Ai73. In the Remdalen Repitition.
2025 IV	**Skardmodalen**	VN	815 430	940	Calcite		Multilimbs	1	0	0	0	0	12000	0	100	1.20	0.00	330	40		50	W	1	0	1	0	0	From Ai73. In the Remdalen Repitition.
2025 IV	**Skardmodalen**	VN	826 450	960	Calcite		Arc	1	0	0	0	0	1000	0	100	0.10	0.00	120	5				1	0	0	0	0	From Ai73. In the Remdalen Repitition.
2025 IV	**Skardmodalen**	VN	785 400	830	Calcite		Linear	1	0	0	0	0	300	0	50	0.01	0.00	30	5	10			1	0	0	0	0	From Ai73. In the Remdalen Repitition.
2025 IV	**Skardmodalen**	VN	786 400	860	Calcite		Linear	1	0	0	0	0	400	0	50	0.02	0.00	40	5	30			1	0	0	0	0	From Ai73. In the Remdalen Repitition.
2025 IV	**Skardmodalen**	VN	750 370	930	Calcite		Linear	1	0	0	0	0	300	0	50	0.01	0.00	70	5	20	80	N	1	0	0	0	0	From Ai73. In the Remdalen Repitition.
2025 IV	**Skardmodalen**	VN	761 375	760	Calcite		Arc	1	0	0	0	0	600	0	50	0.03	0.00	30	5				1	0	0	0	0	From Ai73. In the Remdalen Repitition.
2025 IV	**Skardmodalen**	VN	785 380	940	Calcite		Linear	1	0	0	0	0	1500	0	50	0.08	0.00	60	5	180			1	0	0	0	0	From Ai73. In the Remdalen Repitition.
2025 IV	**Skardmodalen**	VN	822 370	880	Calcite		Linear	1	0	0	0	0	1600	0	50	0.08	0.00	90	5	170			1	0	0	0	0	From Ai73. In the Remdalen Repitition.
Area	185	VN	778 470	1080	Calcite		Arc	1	0	0	0	0	600	0	50	0.03	0.00	80	20				1	0	0	0	0	From Ai73. In the Remdalen Repitition.
2025 III	**Ranseren**	VN	758 364	880	Calcite		Sinuous	1	0	0	0	0	500	0	50	0.02	0.00	60	10		60	N	1	0	0	0	0	From Ai73. In the Remdalen Repitition.
2025 III	**Ranseren**	VN	790 343	810	Calcite		Arc	1	0	0	0	0	1000	0	50	0.05	0.00	80	10				1	0	0	0	0	From Ai73. In the Remdalen Repitition.
2025 III	**Ranseren**	VN	810 343	940	Calcite		Linear	1	0	0	0	0	200	0	50	0.01	0.00	20	20				0	0	0	0	0	From Ai73. In the Remdalen Repitition.
Area	262	VN	790 325	690	Calcite		Sinuous	1	0	0	0	0	2500	0	20	0.05	0.00	5	5		70	S	1	0	0	0	0	4 strips along quartzite
25G	**Ammarnäs NE**																											**No carbonate outcrops**
Area	80																											North of 7322 only
25EF	**Umfors SW**																											**No carbonate outcrops**
Area	4																											(Area bounded by 1450 to 1478 and 7300 to 7322 only)
Ai160	24EF Tärnaby																											**No carbonate outcrops**
Area	48																											(Area bounded by 1450 to 1475 and 7275 to 7300 only)
Ai161	24EF Tärnaby																											**No carbonate outcrops**
Area	40																											(Area bounded by 1450 to 1475 and 7250 to 7275 only)
Ai 74	Z1 Frostviken																											**No carbonate outcrops**
Area	70																											(Area bounded by 1425 to 1450 and 7200 to 7211 only)
Ai42	Z1 Frostviken																											**No carbonate outcrops**
Area	32																											(Area bounded by 1425 to 1450 and 7175 to 7200 only)
Ai163	24EF Tärnaby																											**No carbonate outcrops**
Area	8																											(Area bounded by 1475 to 1500 and 7275 to 7300 only)

UPPER ALLOCHTHON: Køli Nappes - Lower Køli - Joesjø / Bjørkvatten /Junkerdals Nappe: KB (NORWAY): TOTALS

Metres

MAP SHEET	MAP NAME & NAPPE AREA	UTM / SWEDISH RN COORD	MAX ALT.	GEOL MAP IDENT	SAMPLE IDENT	OUTCROP SHAPE	O	R	T	V	D	LENGTH	VISITED LENGTH	WIDTH	CARB. AREA	DOL. AREA	VR Length	VR Width	STRIKE	DIP	#	E	F	W	C	L	COMMENTS
Totals	361		###				1	0	0	0	1	2000	0	100	0.20	0.20	######	##		#	0	0	0	0	0	0	**No R, T or V.**
%								0%	0%	0%	100%				0.06%	0.06%					0%	0%					**No caves reported**
Averages			910									2000	#DIV/0!	100	0.20	0.20	30	30		###			0.0	0.0	##	##	
Maxima			910									2000	0	100	0.20	0.20	30	30		0			0	0	0	0	

UPPER ALLOCHTHON: Køli Nappes - Lower Køli - Joesjø / Bjørkvatten /Junkerdals Nappe: KB (SWEDEN): TOTALS

Totals	2826		####				121	0	31	6	2	214400	7600	####	24.12	3.28	#####	####		###	60	96	5	9	2	69	**No carbonates near a pluton**
%								0%	26%	5%	2%				0.85%	0.12%					50%	79%					
Averages			730									1772	1267	79	0.20	1.64	84	18		38			0.04	0.07	0	12	
Maxima			1280									16000	5000	200	3.20	3.20	480	150		90			2	5	1	44	

UPPER ALLOCHTHON: Køli Nappes - Lower Køli - Joesjø / Bjørkvatten /Junkerdals Nappe: KB (NORWAY AND SWEDEN): TOTALS

Totals	3187		####				122	0	31	6	3	216400	7600	####	24.32	3.48	#####	####		###	60	96	5	9	2	69	**No carbonates near a pluton**
%								0%	25%	5%	2%				0.76%	0.11%					49%	79%					
Averages			732									1774	1267	79	0.20	1.16	84	18		38			0.04	0.07	0	12	
Maxima			1280									16000	5000	200	3.20	3.20	480	150		90			2	5	1	44	

UPPER ALLOCHTHON: Køli Nappes - Lower Køli - Joesjø / Bjørkvatten /Junkerdals Nappe: KB (NORWAY)

Metres

MAP SHEET	MAP NAME & NAPPE AREA	UTM / SWEDISH RN COORD	MAX ALT.	GEOL MAP IDENT	SAMPLE IDENT	OUTCROP SHAPE	O	R	T	V	D	LENGTH	VISITED LENGTH	WIDTH	CARB. AREA	DOL. AREA	VR Length	VR Width	STRIKE	DIP	#	E	F	W	C	L	COMMENTS
1923 IV	**Nordli**																										**No carbonate outcrops**
Area	9																										
1926 II	**Hattfjelldal**																										**No carbonate outcrops**
Area	17																										
1924 II	**Limingen**																										**No carbonate outcrops**
Area	16																										
1923 I	**Murusjøen**																										**No carbonate outcrops**
Area	77																										
2026 IV	**Hjartfellet**																										**No carbonate outcrops**
Area	22																										
2026 III	**Krutvatnet**																										**No carbonate outcrops**
Area	121																										
2025 IV	**Skardmodalen**	VN 670 590	910	Dol&Cal		Sinuous	1	0	0	0	1	2000	0	100	0.20	0.20	30	30				0	0	0	0	0	Is it Dolomite?
Area	99																										

UPPER ALLOCHTHON: Køli Nappes - Lower Køli - Joesjø / Bjørkvatten /Junkerdals Nappe: KB (SWEDEN)

MAP SHEET	MAP NAME & NAPPE AREA	UTM / SWEDISH RN COORD			MAX ALT.	GEOL MAP IDENT	SAMPLE IDENT	OUTCROP SHAPE	O	R	T	V	D	LENGTH	VISITED LENGTH	WIDTH	CARB. AREA	DOL. AREA	VR Length	VR Width	STRIKE	DIP	#	E	F	W	C	L	COMMENTS
1924 I	**Jomafjellet**	VM	620	885	560	Calcite		Linear	1	0	1	0	0	600	0	50	0.03	0.00	60	5	50			1	0	0	0	0	Near thrust. Not found. TF98.
1924 I	**Jomafjellet**	VM	618	835	480	Calcite		Linear	1	0	0	0	0	1000	0	50	0.05	0.00	50	5	170			1	0	0	0	0	
1924 I	**Jomafjellet**	VM	585	825	600	Calcite		Linear	1	0	0	0	0	700	0	50	0.03	0.00	20	5	180	25	W	1	0	0	0	0	
Area	17	VM	590	815	600	Calcite		Linear	1	0	0	0	0	500	0	50	0.02	0.00	10	5	20			1	0	0	0	0	
1924 II	**Limingen**	VM	582	802	720	Calcite		Sinuous	1	0	0	0	0	500	0	50	0.02	0.00	60	10				1	0	0	0	0	
1924 II	**Limingen**	VM	594	746	660	Calcite		Sinuous	1	0	0	0	0	400	0	50	0.02	0.00	80	20				1	0	0	0	0	
1924 II	**Limingen**	VM	456	594	660	Calcite		Linear	1	0	0	0	0	250	0	50	0.01	0.00	40	5	180	20	W	1	0	0	0	0	
1924 II	**Limingen**	VM	420	578	580	Calcite		Linear	1	0	1	0	0	1200	0	50	0.06	0.00	100	10	90	20	N	1	0	0	0	0	On thrust
Area	50	VM	440	572	640	Calcite		Sinuous	1	0	0	0	0	2000	0	50	0.10	0.00	140	10		15	N	1	0	0	0	0	
2026 IV	**Hjartfellet**																												**No extra carbonate outcrops**
Area	7																												
2026 III	***Krutvatnet***	VN	*820*	*900*	630	Lst&Dol		Sinuous	1	0	1	0	0	3000	0	200	0.15	0.00	146	30	5	40	E	1	0	0	0	0	From Ai160. Internal thrust
2026 III	***Krutvatnet***	VN	*820*	*880*	520	Lst&Dol		Linear	1	0	0	0	0	700	0	50	0.04	0.00	36	1	45			1	0	0	0	0	From Ai160. Internal thrust
Area	42	VN	*800*	*873*	876	Dol&Cal		Linear	1	0	1	0	1	1500	0	50	0.08	0.08	196	5	50	42	E	1	0	0	0	0	From Ai160. Internal thrust
2025 IV	**Skardmodalen**	VN	840	610	1200	Calcite		Linear	1	0	1	0	0	400	0	50	0.02	0.00	40	40		60	W	0	0	0	0	0	From Ai161
2025 IV	**Skardmodalen**	VN	830	583	780	Calcite		Linear	1	0	0	0	0	250	0	50	0.01	0.00	40	5			E	0	0	0	0	0	From Ai161
2025 IV	**Skardmodalen**	VN	778	570	780	Calcite		Arc	1	0	1	0	0	500	0	50	0.03	0.00	100	40		40	N	0	0	0	0	0	From Ai161. Internal thrust
Area	56	VN	800	552	900	Calcite		Arc	1	0	1	0	0	1500	0	50	0.08	0.00	320	10		45	E	0	0	0	0	0	From Ai161. Internal thrust
2025 III	**Ranseren**	VN	853	330	780	Calcite		Linear	1	0	0	0	0	500	0	50	0.02	0.00	80	10	30	35	W	1	0	0	0	0	
2025 III	**Ranseren**	VN	787	220	810	Calcite		Linear	1	0	1	0	0	700	0	50	0.03	0.00	40	10	60			1	0	0	0	0	On Bjørkvatten Thrust top
2025 III	**Ranseren**	VN	795	216	940	Calcite		Irregular	1	0	1	0	0	300	0	50	0.01	0.00	160	40				1	0	0	0	0	On Bjørkvatten Thrust top
2025 III	**Ranseren**	VN	810	180	800	Calcite		Sinuous	1	0	1	0	0	5500	0	100	0.55	0.00	330	40		20	W	1	0	0	0	0	On Bjørkvatten Thrust top
2025 III	**Ranseren**	VN	860	180	970	Calcite		Arc	1	0	0	1	0	10000	*1000*	100	1.00	0.00	250	20		20	S	1	2	0	1	44	2 limbs on Ai76. Rapstengrottan.TF00
2025 III	**Ranseren**	VN	800	137	1025	Calcite		Linear	1	0	0	0	0	400	0	50	0.02	0.00	10	10	40	30	W	0	0	0	0	0	
2025 III	**Ranseren**	VN	780	125	920	Calcite		Linear	1	0	1	0	0	800	0	50	0.04	0.00	10	10	70	30	N	0	0	0	0	0	On Bjørkvatten Thrust top
2025 III	**Ranseren**	VN	755	116	930	Calcite		Linear	1	0	0	0	0	500	0	50	0.02	0.00	30	5	80	30	N	0	0	0	0	0	
2025 III	**Ranseren**	VN	742	110	930	Calcite		Sinuous	1	0	1	1	0	8000	*5000*	50	0.40	0.00	330	20	250	20	N	0	0	0	1	25	Thr.top.Renbenshålet.TF98.5m wide
Area	98	VN	760	110	920	Calcite		Sinuous	1	0	0	0	0	7000	0	100	0.70	0.00	200	20		30	N	0	0	2	0	0	
25G	**Ammarnäs NE**	14968		73550	1060	Lst & Dol		Rectangle	1	0	0	0	0	400	0	200	0.08	0.00	60	20	30			0	0	0	0	0	Junkerdals Nappe
25G	**Ammarnäs NE**	14960		73540	960	Lst & Dol		Irregular	1	0	0	0	0	2000	0	200	0.40	0.00	80	40				0	0	0	0	0	
25G	**Ammarnäs NE**	14935		73500	760	Lst & Dol		Sinuous	1	0	0	0	0	3000	0	200	0.60	0.00	80	20				1	0	0	0	0	
25G	**Ammarnäs NE**	14940		73500	820	Lst & Dol		Sinuous	1	0	0	0	0	3000	0	200	0.60	0.00	100	20				1	0	0	0	0	
25G	**Ammarnäs NE**	14960		73495	900	Lst & Dol		Sinuous	1	0	0	0	0	3000	0	200	0.60	0.00	140	40				0	0	0	0	0	
Area	180																												North of 7322
25G	**Ammarnäs SE**	15040		73180	800			Arc	1	0	1	0	0	5000	0	100	0.50	0.00	200	100				1	0	0	0	0	Joesjø Nappe. SGU (54) p181.
Area	204																												Bounded by 7300 to 7322
Ai74	Z1 **SipmekeSV-**	14290		72110	680	Calcite		Sinuous	1	0	0	0	0	1200	0	50	0.06	0.00	80	20		45	N	1	0	0	0	0	(Area from 1425 to 1450 and 7200 to 7211 only)
Ai74	Z1 **SipmekeSV-**	14310		72113	600	Calcite		Arc	1	0	0	0	0	400	0	50	0.02	0.00	20	20		30	N	1	0	0	0	0	
Ai74	Z1 **SipmekeSV-**	14275		72080	630	Calc+Dol		Irregular	1	0	1	0	0	2000	0	100	0.20	0.00	50	10		45	N	1	0	0	0	0	On Bjørkv. Thr. top. SGU (54) p362
Ai74	Z1 **SipmekeSV-**	14278		72058	660	Calcite		Linear	1	0	0	0	0	200	0	50	0.01	0.00	20	5	180	35	W	1	0	0	0	0	
Ai74	Z1 **SipmekeSV-**	14290		72050	720	Calcite		Sinuous	1	0	1	0	0	500	0	50	0.02	0.00	20	20		45	S	1	0	0	0	0	On Bjørkvatten Thrust top
Ai74	Z1 **SipmekeSV-**	14300		72045	720	Calcite		Arc	1	0	1	0	0	400	0	50	0.02	0.00	10	10				1	0	0	0	0	On Bjørkvatten Thrust top
Ai74	Z1 **SipmekeSV-**	14310		72047	760	Calcite		Arc	1	0	1	0	0	500	0	50	0.02	0.00	40	20		50	W	1	0	0	0	0	On Bjørkvatten Thrust top
Ai74	Z1 **SipmekeSV-**	14363		72027	670	Calcite		Sinuous	1	0	0	0	0	300	0	50	0.01	0.00	10	10		60	S	1	0	0	0	0	
Ai74	Z1 **SipmekeSV-**	14370		72027	660	Calcite		Linear	1	0	0	0	0	300	0	50	0.01	0.00	20	5	80	35	S	1	0	0	0	0	
Ai74	Z1 **SipmekeSV-**	14373		72023	640	Calcite		Sinuous	1	0	0	0	0	300	0	50	0.01	0.00	20	5		25	S	1	0	0	0	0	
Ai74	Z1 **SipmekeSV-**	14380		72023	600	Calcite		Linear	1	0	0	0	0	600	0	50	0.03	0.00	40	5	125	25	S	1	0	0	0	0	
Ai74	Z1 **SipmekeSV-**	14385		72024	540	Calcite		Linear	1	0	0	0	0	200	0	50	0.01	0.00	30	5	70	20	S	1	0	0	0	0	
Ai74	Z1 **SipmekeSV-**	14340		72020	660	Calcite		Sinuous	1	0	1	0	0	5000	0	100	0.50	0.00	69	20		25	S	1	0	0	0	0	On Bjørkvatten Thrust top

UPPER ALLOCHTHON: Køli Nappes - Lower Køli - Joesjø / Bjørkvatten /Junkerdals Nappe: KB (SWEDEN)

MAP SHEET	MAP NAME & NAPPE AREA	UTM / SWEDISH RN COORD		MAX ALT.	GEOL MAP IDENT	SAMPLE IDENT	OUTCROP SHAPE	O	R	T	V	D	LENGTH	VISITED LENGTH	WIDTH	CARB. AREA	DOL. AREA	VR Length	VR Width	STRIKE	DIP	#	E	F	W	C	L	COMMENTS
															Metres													
Ai74	Z1 **SipmekeSV-**	14380	72010	580	Calcite		Irregular	1	0	1	0	0	4500	0	200	0.90	0.00	71	71		10	S	1	0	0	0	0	On Bjørkvatten Thrust top
Ai74	Z1 **SipmekeSV-**	14420	72010	700	Calcite		Linear	1	0	0	0	0	1000	0	100	0.10	0.00	191	10	90			1	0	0	0	0	
Ai74	Z1 **SipmekeSV-**	14430	72008	700	Calcite		Linear	1	0	0	0	0	1200	0	50	0.06	0.00	191	5	80			1	0	0	0	0	
Ai74	Z1 **SipmekeSV-**	14446	72020	760	Calcite		Sinuous	1	0	0	0	0	700	0	50	0.03	0.00	40	40		30	S	1	0	0	0	0	
Ai74	Z1 **SipmekeSV-**	14450	72008	750	Calcite		Linear	1	0	0	0	0	400	0	50	0.02	0.00	60	5	60			1	0	0	0	0	
Area	140	14453	72008	780	Calcite		Linear	1	0	1	0	0	200	0	50	0.01	0.00	160	20	60			1	0	0	0	0	Near Bjørkvatten Thrust top
Ai42	Z1 **Frostviken N**	14270	71950	500	Calcite		Linear	1	0	0	0	0	600	0	50	0.03	0.00	51	5	70			1	0	0	0	0	(Area from 1425 to 1450 and 7175 to 7200 only)
Ai42	Z1 **Frostviken N**	14270	71948	520	Calcite		Linear	1	0	0	0	0	700	0	50	0.03	0.00	71	10	65			1	0	0	0	0	
Ai42	Z1 **Frostviken N**	14270	71945	520	Calcite		Linear	1	0	0	0	0	500	0	50	0.02	0.00	71	5	60			1	0	0	0	0	
Ai42	Z1 **Frostviken N**	14280	71960	560	Calcite		Linear	1	0	0	0	0	500	0	50	0.02	0.00	60	10	75			1	0	0	0	0	
Ai42	Z1 **Frostviken N**	14280	71953	580	Calcite		Linear	1	0	0	0	0	500	0	50	0.02	0.00	20	5	75			1	0	0	0	0	
Ai42	Z1 **Frostviken N**	14280	71950	580	Calcite		Linear	1	0	0	0	0	400	0	50	0.02	0.00	20	5	70			1	0	0	0	0	
Ai42	Z1 **Frostviken N**	14285	71958	620	Calcite		Linear	1	0	0	0	0	500	0	50	0.02	0.00	60	40	85			1	0	0	0	0	
Ai42	Z1 **Frostviken N**	14295	71965	660	Calcite		Linear	1	0	0	0	0	300	0	50	0.01	0.00	60	10	90	30	N	1	0	0	0	0	
Ai42	Z1 **Frostviken N**	14305	71965	680	Calcite		Linear	1	0	0	0	0	800	0	50	0.04	0.00	20	5	90	35	N	1	0	0	0	0	
Ai42	Z1 **Frostviken N**	14320	71965	640	Calcite		Sinuous	1	0	0	0	0	1500	0	50	0.07	0.00	20	10		35	N	1	0	0	0	0	
Ai42	Z1 **Frostviken N**	14340	71974	660	Calcite		Linear	1	0	0	0	0	300	0	50	0.01	0.00	20	5	85	35	N	1	0	0	0	0	
Area	86	14260	71905	480	Calcite		Linear	1	0	1	0	0	600	0	50	0.03	0.00	20	20	40	30	N	1	0	0	0	0	Near Køli Thr. base
Ai160	24EF:**Tärnaby**	14500	72960	620	Dol&Cal		Sinuous	1	0	1	0	1	16000	0	200	3.20	3.20	140	50				1	0	5	0	0	
Ai160	24EF:**Tärnaby**	14680	72950	510	?		Arc	1	0	0	0	0	1500	0	200	0.30	0.00	60	40				1	0	0	0	0	From 1929 Geol. map
Ai160	24EF:**Tärnaby**	14680	72930	480	Lst&Dol		Arc	1	0	0	0	0	500	0	50	0.03	0.00	25	5				1	0	0	0	0	
Ai160	24EF:**Tärnaby**	14660	72860	870	Calcitic		Sinuous	1	0	1	0	0	14000	0	200	2.80	0.00	311	150				1	0	0	0	0	Södra Storfj. Geol.Map.SGU (54)p187.*
Ai160	24EF:**Tärnaby**	14665	72830	800	Lst&Dol		Sinuous	1	0	1	0	0	4000	0	100	0.40	0.00	120	20	0	65	W	1	0	0	0	0	
Ai160	24EF:**Tärnaby**	14675	72825	750	Lst&Dol		Arc	1	0	1	0	0	1000	0	50	0.05	0.00	25	5				1	0	0	0	0	
Ai160	24EF:**Tärnaby**	14670	72775	900	Lst&Dol		Multi limbs	1	0	1	0	0	8000	0	100	0.80	0.00	240	120				1	0	0	0	0	
Ai160	24EF:**Tärnaby**	14730	72875	720	Lst&Dol		Rectangular	1	0	0	0	0	300	0	100	0.03	0.00	70	30			W	1	0	0	0	0	
Ai160	24EF:**Tärnaby**	14540	72925	600	?		Linear	1	0	0	0	0	1500	0	200	0.30	0.00	123	20	70			1	0	0	0	0	From 1929 Geol. map
Area	300	14740	72760	460	?		Linear	1	0	0	0	0	400	0	50	0.02	0.00	10	60	100	20	W	1	0	0	0	0	(Area from 1450 to 1475 and 7275 to 7300 only)
Ai161	24EF:**Tärnaby**	14625	72750	865	Calcitic	(Beskens)	Arc	1	0	1	0	0	500	0	50	0.03	0.00	20	5		30	N	1	0	0	0	0	(Area from 1450 to 1475 and 7250 to 7275 only)
Ai161	24EF:**Tärnaby**	14540	72660	820	Calcitic		Triangular	1	0	0	0	0	300	0	50	0.02	0.00	30	5		30	N	1	0	0	0	0	
Ai161	24EF:**Tärnaby**	14590	72605	640	Calcitic		Sinuous	1	0	0	0	0	1000	0	50	0.05	0.00	30	10		30	N	0	0	0	0	0	
Ai161	24EF:**Tärnaby**	14663	72740	700	?		Linear	1	0	0	0	0	1500	0	100	0.15	0.00	55	5	15			1	0	0	0	0	Ai161 differs
Ai161	24EF:**Tärnaby**	14660	72665	960	Lst & Dol		Sinuous	1	0	0	0	0	3500	0	100	0.35	0.00	240	40				1	0	0	0	0	+11 tiny outcrops shown on the Södra
Ai161	24EF:**Tärnaby**	14680	72680	800	?		Arc	1	0	0	0	0	2500	0	200	0.50	0.00	140	20				0	0	0	0	0	Storfjallet Geol. map. Ai161 differs
Ai161	24EF:**Tärnaby**	14640	72635	840	Lst		Linear	1	0	0	0	0	2500	0	200	0.50	0.00	100	40	110			1	0	0	0	0	SGU (54) p193
Ai161	24EF:**Tärnaby**	14680	72620	860	Lst		Linear	1	0	0	0	0	1200	0	100	0.12	0.00	20	50	80			1	0	0	0	0	SGU (54) p193. Ai161 differs
Ai161	24EF:**Tärnaby**	14635	72600	910	Lst		Arc	1	0	0	0	0	3500	0	100	0.35	0.00	180	5				0	0	0	0	0	
Ai161	24EF:**Tärnaby**	14530	72610	890	Lst & Dol		Linear	1	0	0	0	0	500	0	50	0.03	0.00	20	10		32	W	1	0	0	0	0	
Area	456	14595	72520	880	Lst & Dol		Linear	1	0	0	0	0	1000	0	100	0.10	0.00	30	30	15			0	2	0	0	0	Not on Ai161

* Limestone not seen by RM (2003)

UPPER ALLOCHTHON: Køli Nappes - Lower Køli - Joesjø / Bjørkvatten /Junkerdals Nappe: KB (SWEDEN)

Metres

MAP SHEET	MAP NAME & NAPPE AREA	UTM / SWEDISH RN COORD		MAX ALT.	GEOL MAP IDENT	SAMPLE IDENT	OUTCROP SHAPE	O	R	T	V	D	LENGTH	VISITED LENGTH	WIDTH	CARB. AREA	DOL. AREA	VR Length	VR Width	STRIKE	DIP	#	E	F	W	C	L	COMMENTS
Ai75	23EF **Fatmo. N**	14745	72485	780	Calcitic		Sinuous	1	0	0	0	0	700	0	100	0.07	0.00	5	5		45	N	1	0	0	0	0	
Ai75	23EF **Fatmo. N**	14740	72472	760	Calcitic		Sinuous	1	0	0	0	0	3000	0	50	0.15	0.00	202	5				1	0	0	0	0	
Ai75	23EF **Fatmo. N**	14570	72440	880	Calcitic		Linear	1	0	0	0	0	1500	0	50	0.08	0.00	60	5	180	60	E	0	0	0	0	0	
Ai75	23EF **Fatmo. N**	14575	72450	963	Calcitic		Linear	1	0	0	0	0	1500	0	50	0.08	0.00	113	5	175			0	0	0	0	0	
Ai75	23EF **Fatmo. N**	14575	72435	910	Calcitic		Linear	1	0	0	0	0	1000	0	50	0.05	0.00	20	5	175	65	W	0	0	0	0	0	
Ai75	23EF **Fatmo. N**	14725	72455	740	Calcitic		Sinuous	1	0	0	0	0	2500	0	50	0.12	0.00	20	5		35	N	1	0	0	0	0	
Ai75	23EF **Fatmo. N**	14720	72440	1030	Calcitic		Sinuous	1	0	0	0	0	8000	0	50	0.40	0.00	210	5				0	0	0	0	0	
Ai75	23EF **Fatmo. N**	14735	72420	1240	Calcitic	Sample	Sinuous	1	0	0	1	0	5000	1000	50	0.24	0.00	440	5	180	90		0	1	0	0	0	Fossil locality. Karstic. TF98
Ai75	23EF **Fatmo. N**	14740	72420	1280	Calcitic		Sinuous	1	0	0	1	0	4000	100	50	0.20	0.00	480	5				1	0	0	0	0	TF98. Lower part seen
Ai75	23EF **Fatmo. N**	14745	72425	740	Calcitic		Sinuous	1	0	0	1	0	1000	300	50	0.05	0.00	100	5				1	0	0	0	0	TF98
Ai75	23EF **Fatmo. N**	14742	72406	1060	Calcitic		Sinuous	1	0	0	1	0	1000	200	50	0.05	0.00	120	20	180	90		0	0	0	0	0	TF98
Ai75	23EF **Fatmo. N**	14542	72320	840	Calcitic		Linear	1	0	0	0	0	1500	0	50	0.08	0.00	78	5	20	85	W	1	0	0	0	0	
Ai75	23EF **Fatmo. N**	14685	72315	880	Calcitic		Sinuous	1	0	0	0	0	300	0	50	0.02	0.00	40	5		50	W	0	0	0	0	0	
Ai75	23EF **Fatmo. N**	14685	72310	900	Calcitic		Linear	1	0	0	0	0	200	0	50	0.01	0.00	10	5	30	50	W	0	0	0	0	0	
Ai75	23EF **Fatmo. N**	14640	72270	580	Calcitic		Linear	1	0	0	0	0	700	0	50	0.04	0.00	20	5	30			1	0	0	0	0	
Area	516	14645	72265	620	Calcitic		Triangle	1	0	0	0	0	200	0	100	0.02	0.00	67	5				1	0	0	0	0	(Area from 1450 to 1475 and 7225 to 7250 only)
Ai76	23EF **Fatmo. S**	14495	72235	850	Calcite		Arc	1	0	0	0	0	600	0	50	0.03	0.00	90	5				1	0	0	0	0	(Area from 1450 to 1475 and 7200 to 7225 only)
Ai76	23EF **Fatmo. S**	14652	72245	660	Calcitic		Arc	1	0	0	0	0	500	0	50	0.02	0.00	107	10				1	0	0	0	0	(Incl. 4 sq km on Ai 102)
Ai76	23EF **Fatmo. S**	14530	72198	680	Calcitic		Arc	1	0	0	0	0	700	0	50	0.03	0.00	20	10		20	N	1	0	0	0	0	
Ai76	23EF **Fatmo. S**	14540	72200	712	Calcitic		Sinuous	1	0	0	0	0	6000	0	100	0.60	0.00	32	10		40	N	1	0	0	0	0	SGU (54) p195
Ai76	23EF **Fatmo. S**	14590	72190	740	Calcitic		Linear	1	0	0	0	0	2000	0	50	0.10	0.00	130	5	70	20	N	1	0	0	0	0	
Ai76	23EF **Fatmo. S**	14620	72201	800	Calcitic		Linear	1	0	0	0	0	1500	0	50	0.08	0.00	60	6	50			1	0	0	0	0	
Area	234	14547	72187	630	Calcitic		Linear	1	0	0	0	0	600	0	50	0.03	0.00	20	10	90	30	N	1	0	0	0	0	Fossil locality.
Ai163	24EF:**Tärnaby**	14800	72950	660	?		Arc	1	0	1	0	0	4000	0	200	0.80	0.00	160	100				1	0	0	0	0	Both ends on thrs. Lst. not seen. TF98
Ai163	24EF:**Tärnaby**	14880	72940	560	Calcitic		Sinuous	1	0	1	0	0	2000	0	150	0.30	0.00	80	5		20	W	1	0	1	0	0	Internal thrust
Ai163	24EF:**Tärnaby**	14783	72790	840	Calcitic		Irregular	1	0	1	0	0	200	0	100	0.02	0.00	20	20				0	0	0	0	0	Internal thrust
Ai163	24EF:**Tärnaby**	14780	72770	680	Calcitic		Linear	1	0	1	0	0	400	0	50	0.02	0.00	20	5		75	W	1	0	0	0	0	Internal thrust
Area	200																											(Area from 1475 to 1500 and 7275 to 7300 only)
Ai162	24EF:**Tärnaby**	14755	72742	490	Calcitic		Linear	1	0	0	0	0	300	0	50	0.02	0.00	10	10				1	0	0	0	0	
Ai162	24EF:**Tärnaby**	14760	72735	460	Calcitic		Linear	1	0	0	0	0	400	0	50	0.02	0.00	20	20				1	0	1	0	0	
Ai162	24EF:**Tärnaby**	14775	72715	440	Calcitic		Linear	1	0	0	0	0	200	0	50	0.01	0.00	20	2				1	0	0	0	0	
Ai162	24EF:**Tärnaby**	14775	72705	440	Calcitic		Linear	1	0	0	0	0	400	0	50	0.02	0.00	20	2				1	0	0	0	0	
Ai162	24EF:**Tärnaby**	14770	72695	500	Calcitic		Arc	1	0	0	0	0	400	0	50	0.02	0.00	20	5				1	0	0	0	0	
Ai162	24EF:**Tärnaby**	14760	72700	600	?		Arc	1	0	0	0	0	1600	0	200	0.32	0.00	80	40				1	0	0	0	0	Not shown on Ai162
Ai162	24EF:**Tärnaby**	14790	72700	505	?		Linear	1	0	0	0	0	1400	0	200	0.80	0.00	25	25	170			1	0	0	0	0	Not shown on Ai162
Ai162	24EF:**Tärnaby**	14766	72685	490	Calcitic		Linear	1	0	0	0	0	500	0	100	0.05	0.00	30	2		30	W	1	0	0	0	0	
Area	190	14780	72655	480	Calcitic		Linear	1	0	0	0	0	200	0	50	0.01	0.00	40	20		35	W	1	0	0	0	0	(Area from 1475 to 1500 and 7250 to 7275 only)
Ai 77	23EF **Fatmo. N**	14765	72370	740	Calcitic		Sinuous	1	0	0	0	0	1000	0	50	0.35	0.00	60	10		85	W	1	0	0	0	0	
Area	50																											(Area from 1475 to 1500 and 7225 to 7250 only)

UPPER ALLOCHTHON: Seve Units - Seve Units: SU (NORWAY): TOTALS

Metres

MAP SHEET	MAP NAME & NAPPE AREA	UTM / SWEDISH RN COORD	MAX ALT.	GEOL MAP IDENT	SAMPLE IDENT	OUTCROP SHAPE	O	R	T	V	D	LENGTH	VISITED LENGTH	WIDTH	CARB. AREA	DOL. AREA	VR Length	VR Width	STRIKE	DIP	#	E	F	W	C	L	COMMENTS
Totals	46																										**No carbonates in Norway**
%																											
Averages																											
Maxima																											

UPPER ALLOCHTHON: Seve Units - Seve Units: SU (SWEDEN): TOTALS

MAP SHEET	MAP NAME & NAPPE AREA	UTM / SWEDISH RN COORD	MAX ALT.	GEOL MAP IDENT	SAMPLE IDENT	OUTCROP SHAPE	O	R	T	V	D	LENGTH	VISITED LENGTH	WIDTH	CARB. AREA	DOL. AREA	VR Length	VR Width	STRIKE	DIP	#	E	F	W	C	L	COMMENTS
Totals	1390		####				84	0	11	2	0	62800	250	####	4.09	0.00	####	###		###	31	73	0	5	0	0	**Includes calc-silicates**
%								0%	13%	2%	0%				0.29%	0.00%					37%	87%					**No carbonates near a pluton**
Averages			740									748	125	59	0.05	#####	49	10		28			0.00	0.06	0	0	**No caves reported**
Maxima			1097									3500	150	100	0.35	0.00	200	20		40			0	2	0	0	

UPPER ALLOCHTHON: Seve Units - Seve Units: SU (NORWAY AND SWEDEN): TOTALS

MAP SHEET	MAP NAME & NAPPE AREA	UTM / SWEDISH RN COORD	MAX ALT.	GEOL MAP IDENT	SAMPLE IDENT	OUTCROP SHAPE	O	R	T	V	D	LENGTH	VISITED LENGTH	WIDTH	CARB. AREA	DOL. AREA	VR Length	VR Width	STRIKE	DIP	#	E	F	W	C	L	COMMENTS
Totals	1436		####				84	0	11	2	0	62800	250	####	4.09	0.00	####	###		###	31	73	0	5	0	0	**Includes calc-silicates**
%								0%	13%	2%	0%				0.28%	0.00%					37%	87%					**No carbonates near a pluton**
Averages			740									748	125	59	0.05	#####	49	10		28			0.00	0.06	0	0	**No caves reported**
Maxima			1097									3500	150	100	0.35	0.00	200	20		40			0	2	0	0	

NOTE: THE SGU MAPS DO NOT DISTINGUISH BETWEEN MARBLE AND CALC-SILICATE ROCKS IN THE SEVE.

UPPER ALLOCHTHON: Seve Units - Seve Units: SU (NORWAY):

MAP SHEET	MAP NAME & NAPPE AREA	UTM / SWEDISH RN COORD	MAX ALT.	GEOL MAP IDENT	SAMPLE IDENT	OUTCROP SHAPE	O	R	T	V	D	LENGTH	VISITED LENGTH	WIDTH	CARB. AREA	DOL. AREA	VR Length	VR Width	STRIKE	DIP	#	E	F	W	C	L	COMMENTS
1924 IV	**Røyrvik**																										**No carbonate outcrops**
Area	6																										
1924 II	**Limingen**																										**No carbonate outcrops**
Area	1																										
1923 I	**Murusjøen**																										**No carbonate outcrops**
Area	39																										

UPPER ALLOCHTHON: Seve Units - Seve Units: SU (SWEDEN)

MAP SHEET	MAP NAME & NAPPE AREA	UTM / SWEDISH RN COORD	MAX ALT.	GEOL MAP IDENT	SAMPLE IDENT	OUTCROP SHAPE	O	R	T	V	D	LENGTH	VISITED LENGTH	WIDTH	CARB. AREA	DOL. AREA	VR Length	VR Width	STRIKE	DIP	#	E	F	W	C	L	COMMENTS
1924 II	**Limingen**																										**No carbonate outcrops**
Area	185																										
1923 I	**Murusjøen**																										**No carbonate outcrops**
Area	33																										
2025 III	**Ranseren**																										**No carbonate outcrops**
Area	13																										
Ai74	Z1 **Sipmeke SV**	14300 72095	660	c or c-s		Arc	1	0	1	0	0	300	0	50	0.01	0.00	60	5				1	0	0	0	0	In narrow thrust zone
Ai74	Z1 **Sipmeke SV**	14310 72104	625	c or c-s		Linear	1	0	1	0	0	600	0	50	0.03	0.00	5	5	40			1	0	0	0	0	In narrow thrust zone
Ai74	Z1 **Sipmeke SV**	14315 72105	620	c or c-s		Linear	1	0	1	0	0	900	0	50	0.04	0.00	40	5	40			1	0	0	0	0	In narrow thrust zone
Ai74	Z1 **Sipmeke SV**	14318 72105	625	c or c-s		Linear	1	0	1	0	0	400	0	50	0.02	0.00	5	5	40			1	0	0	0	0	In narrow thrust zone
Ai74	Z1 **Sipmeke SV**	14310 72102	625	c or c-s		Linear	1	0	1	0	0	400	0	50	0.02	0.00	5	5	40			1	0	0	0	0	In narrow thrust zone
Ai74	Z1 **Sipmeke SV**	14307 72100	640	c or c-s		Linear	1	0	1	0	0	300	0	50	0.01	0.00	10	10	70			1	0	0	0	0	In narrow thrust zone
Ai74	Z1 **Sipmeke SV**	14305 72090	640	c or c-s		Arc	1	0	1	0	0	800	0	50	0.04	0.00	40	10				1	0	0	0	0	Near Seve Thr. base
Ai74	Z1 **Sipmeke SV**	14365 72095	760	c or c-s		Linear	1	0	1	0	0	600	0	50	0.03	0.00	20	10	120	20	N	1	0	0	0	0	Near Seve Thr. base
Ai74	Z1 **Sipmeke SV**	14370 72088	760	c or c-s		Sinuous	1	0	1	0	0	2500	0	100	0.25	0.00	80	20		10	N	1	0	0	0	0	Near Seve Thr. base
Ai74	Z1 **Sipmeke SV**	14378 72082	770	c or c-s		Linear	1	0	1	0	0	200	0	50	0.01	0.00	10	10	125	10	N	1	0	0	0	0	Near Seve Thr. base
Ai74	Z1 **Sipmeke SV**	14379 72083	770	c or c-s		Arc	1	0	1	0	0	300	0	50	0.01	0.00	5	5		15	N	1	0	0	0	0	Near Seve Thr. base
Ai74	Z1 **Sipmeke SV**	14343 72058	760	c or c-s		Linear	1	0	0	0	0	200	0	50	0.01	0.00	40	20	80			1	0	0	0	0	
Ai74	Z1 **Sipmeke SV**	14340 72052	770	c or c-s		Arc	1	0	0	0	0	200	0	50	0.01	0.00	10	5				1	0	0	0	0	
Ai74	Z1 **Sipmeke SV**	14348 72057	765	c or c-s		Arc	1	0	0	0	0	400	0	50	0.04	0.00	5	5				1	0	0	0	0	
Ai74	Z1 **Sipmeke SV**	14342 72050	760	c or c-s		Arc	1	0	0	0	0	200	0	50	0.01	0.00	20	5				1	0	0	0	0	c or c-s = calcitic marble
Ai74	Z1 **Sipmeke SV**	14345 72043	700	c or c-s		Linear	1	0	0	0	0	500	0	50	0.02	0.00	20	20	100			1	0	0	0	0	or calc-silicate rocks
Ai74	Z1 **Sipmeke SV**	14359 72043	750	c or c-s		Linear	1	0	0	0	0	200	0	50	0.01	0.00	10	10	160			1	0	0	0	0	
Area	70	14380 72030	560	c or c-s		Linear	1	0	0	0	0	200	0	50	0.01	0.00	50	5	70			1	0	0	0	0	(Area from 1425 to 1450 and 7200 to 7211 only)
Ai42	Z1 **Frostviken N**	14400 71932	1000	c or c-s		Linear	1	0	0	0	0	1000	0	100	0.10	0.00	200	20	110			0	0	0	0	0	
Ai42	Z1 **Frostviken N**	14405 71932	1024	c or c-s		Linear	1	0	0	0	0	1000	0	100	0.10	0.00	100	10	115			0	0	0	0	0	
Ai42	Z1 **Frostviken N**	14420 71928	900	c or c-s		Arc	1	0	0	0	0	700	0	50	0.03	0.00	60	10				1	0	1	0	0	
Ai42	Z1 **Frostviken N**	14420 71920	900	c or c-s		Arc	1	0	0	0	0	700	0	50	0.03	0.00	40	10		25	E	1	0	0	0	0	
Ai42	Z1 **Frostviken N**	14448 71920	940	c or c-s		Arc	1	0	0	0	0	1200	0	100	0.12	0.00	140	10				1	0	0	0	0	
Ai42	Z1 **Frostviken N**	14488 71898	960	c or c-s		Linear	1	0	0	0	0	1000	0	100	0.10	0.00	40	10	110			0	0	0	0	0	
Ai42	Z1 **Frostviken N**	14480 71892	960	c or c-s		Arc	1	0	0	0	0	600	0	50	0.03	0.00	20	5				0	0	0	0	0	
Ai42	Z1 **Frostviken N**	14425 71880	880	c or c-s		Linear	1	0	0	0	0	300	0	50	0.01	0.00	10	10	80			1	0	0	0	0	
Ai42	Z1 **Frostviken N**	14411 71860	1097	c or c-s		Sinuous	1	0	0	0	0	500	0	50	0.02	0.00	97	20				0	0	0	0	0	
Ai42	Z1 **Frostviken N**	14460 71842	1010	c or c-s		Arc	1	0	0	0	0	600	0	100	0.06	0.00	10	10				1	0	0	0	0	
Ai42	Z1 **Frostviken N**	14470 71833	1020	c or c-s		Linear	1	0	0	0	0	600	0	100	0.06	0.00	60	10	130			1	0	0	0	0	
Ai42	Z1 **Frostviken N**	14472 71830	1020	c or c-s		Linear	1	0	0	0	0	500	0	50	0.02	0.00	20	20	130			1	0	0	0	0	
Ai42	Z1 **Frostviken N**	14335 71838	780	c or c-s		Linear	1	0	0	0	0	500	0	50	0.02	0.00	20	20	125			0	0	0	0	0	
Ai42	Z1 **Frostviken N**	14335 71836	760	c or c-s		Linear	1	0	0	0	0	600	0	50	0.03	0.00	20	20	125			0	0	0	0	0	
Ai42	Z1 **Frostviken N**	14325 71828	710	c or c-s		Linear	1	0	0	0	0	400	0	50	0.02	0.00	10	5	60	5	S	0	0	0	0	0	
Ai42	Z1 **Frostviken N**	14330 71826	710	c or c-s		Linear	1	0	0	0	0	400	0	50	0.02	0.00	10	5	60			0	0	0	0	0	
Ai42	Z1 **Frostviken N**	14330 71823	710	c or c-s		Linear	1	0	0	0	0	400	0	50	0.02	0.00	10	5	60			0	0	0	0	0	
Area	482	14330 71821	710	c or c-s		Linear	1	0	0	0	0	400	0	50	0.02	0.00	10	5	60	25	S	0	0	1	0	0	(Area from 1425 to 1450 and 7175 to 7200 only)

UPPER ALLOCHTHON: Seve Units - Seve Units: SU (SWEDEN)

Metres

MAP SHEET	MAP NAME & NAPPE AREA	UTM / SWEDISH RN COORD	MAX ALT.	GEOL MAP IDENT	SAMPLE IDENT	OUTCROP SHAPE	O	R	T	V	D	LENGTH	VISITED LENGTH	WIDTH	CARB. AREA	DOL. AREA	VR Length	VR Width	STRIKE	DIP	#	E	F	W	C	L	COMMENTS
AI44	Z1 Frostviken S	14260 71692	700	c or c-s		Linear	1	0	0	0	0	400	0	50	0.02	0.00	5	5	70	25	S	1	0	0	0	0	
AI44	Z1 Frostviken S	14325 71705	680	c or c-s		Linear	1	0	0	0	0	400	0	50	0.02	0.00	10	10	95	30	S	1	0	0	0	0	
AI44	Z1 Frostviken S	14370 71708	720	c or c-s		Sinuous	1	0	0	0	0	3500	0	100	0.35	0.00	90	20				1	0	0	0	0	
AI44	Z1 Frostviken S	14380 71705	720	c or c-s		Arc	1	0	0	0	0	500	0	50	0.02	0.00	20	20				1	0	0	0	0	
AI44	Z1 Frostviken S	14370 71705	740	c or c-s		Sinuous	1	0	0	0	0	2000	0	100	0.20	0.00	100	10				1	0	0	0	0	
AI44	Z1 Frostviken S	14370 71700	740	c or c-s		Sinuous	1	0	0	0	0	2000	0	50	0.10	0.00	100	10				1	0	0	0	0	
AI44	Z1 Frostviken S	14370 71698	700	c or c-s		Sinuous	1	0	0	0	0	1500	0	50	0.08	0.00	60	10				1	0	0	0	0	
AI44	Z1 Frostviken S	14350 71675	790	c or c-s		Linear	1	0	0	0	0	800	0	50	0.04	0.00	90	10	75	40	N	1	0	0	0	0	
AI44	Z1 Frostviken S	14370 71680	660	c or c-s		Sinuous	1	0	0	0	0	2500	0	50	0.12	0.00	10	10				1	0	0	0	0	
AI44	Z1 Frostviken S	14390 71695	760	c or c-s		Sinuous	1	0	0	0	0	1500	0	50	0.08	0.00	10	10				1	0	0	0	0	
AI44	Z1 Frostviken S	14390 71693	780	c or c-s		Linear	1	0	0	0	0	600	0	100	0.06	0.00	20	10	120			1	0	0	0	0	
AI44	Z1 Frostviken S	14390 71692	780	c or c-s		Linear	1	0	0	0	0	1000	0	50	0.05	0.00	40	5	115			1	0	0	0	0	
AI44	Z1 Frostviken S	14390 71690	780	c or c-s		Sinuous	1	0	0	0	0	2500	0	100	0.25	0.00	100	20				1	0	2	0	0	
AI44	Z1 Frostviken S	14390 71680	740	c or c-s		Sinuous	1	0	0	0	0	1800	0	100	0.18	0.00	60	10				1	0	0	0	0	
AI44	Z1 Frostviken S	14410 71680	680	c or c-s		Sinuous	1	0	0	0	0	800	0	50	0.04	0.00	20	10		30	N	1	0	0	0	0	
AI44	Z1 Frostviken S	14318 71655	780	c or c-s		Linear	1	0	0	0	0	700	0	50	0.03	0.00	120	20	165			1	0	0	0	0	
AI44	Z1 Frostviken S	14320 71655	790	c or c-s		Arc	1	0	0	0	0	500	0	50	0.02	0.00	170	10				1	0	0	0	0	
AI44	Z1 Frostviken S	14322 71657	760	c or c-s		Arc	1	0	0	0	0	200	0	50	0.01	0.00	120	10				1	0	0	0	0	
AI44	Z1 Frostviken S	14325 71656	820	c or c-s		Linear	1	0	0	0	0	400	0	50	0.02	0.00	200	10	10			1	0	0	0	0	
AI44	Z1 Frostviken S	14330 71650	800	c or c-s		Arc	1	0	0	0	0	400	0	50	0.02	0.00	140	10				1	0	0	0	0	
AI44	Z1 Frostviken S	14338 71642	730	c or c-s		Arc	1	0	0	0	0	700	0	50	0.03	0.00	130	10				1	0	0	0	0	
AI44	Z1 Frostviken S	14340 71641	730	c or c-s		Linear	1	0	0	0	0	500	0	50	0.02	0.00	130	10	90			1	0	0	0	0	
AI44	Z1 Frostviken S	14390 71632	600	c or c-s		Arc	1	0	0	0	0	1500	0	100	0.15	0.00	60	10		15	N	1	0	0	0	0	
AI44	Z1 Frostviken S	14390 71622	540	c or c-s		Linear	1	0	0	0	0	1000	0	100	0.10	0.00	25	5	90	40	N	1	0	0	0	0	
AI44	Z1 Frostviken S	14405 71627	610	c or c-s		Arc	1	0	0	0	0	1000	0	100	0.10	0.00	70	10		40	W	1	0	1	0	0	
AI44	Z1 Frostviken S	14412 71610	580	c or c-s		Linear	1	0	0	0	0	700	0	50	0.03	0.00	40	5	20	30	W	1	0	0	0	0	
AI44	Z1 Frostviken S	14410 71603	580	c or c-s		Linear	1	0	0	0	0	600	0	50	0.03	0.00	10	5	70	30	N	1	0	0	0	0	
AI44	Z1 Frostviken S	14435 71680	700	c or c-s		Arc	1	0	0	0	0	700	0	50	0.03	0.00	60	10				1	0	0	0	0	
AI44	Z1 Frostviken S	14440 71679	700	c or c-s		Arc	1	0	0	0	0	700	0	50	0.03	0.00	60	5				1	0	0	0	0	
AI44	Z1 Frostviken S	14440 71665	640	c or c-s		Linear	1	0	0	0	0	700	0	50	0.03	0.00	30	5	100			1	0	0	0	0	
AI44	Z1 Frostviken S	14436 71660	700	c or c-s		Arc	1	0	0	0	0	600	0	50	0.03	0.00	60	5		35	W	1	0	0	0	0	
AI44	Z1 Frostviken S	14450 71645	680	c or c-s		Linear	1	0	0	0	0	700	0	50	0.03	0.00	20	5	85	30	N	1	0	0	0	0	
AI44	Z1 Frostviken S	14435 71620	720	c or c-s		Linear	1	0	0	0	0	1000	0	50	0.05	0.00	100	10	180			1	0	0	0	0	
AI44	Z1 Frostviken S	14490 71690	540	c or c-s		Linear	1	0	0	0	0	700	0	50	0.03	0.00	20	5	50	25	N	1	0	0	0	0	
AI44	Z1 Frostviken S	14475 71675	700	c or c-s		Arc	1	0	0	0	0	700	0	50	0.03	0.00	100	5		35	N	1	0	0	0	0	
AI44	Z1 Frostviken S	14473 71663	570	c or c-s		Linear	1	0	0	0	0	500	0	50	0.02	0.00	5	5	40	30	W	1	0	0	0	0	
AI44	Z1 Frostviken S	14480 71663	570	c or c-s		Linear	1	0	0	1	0	400	100	50	0.02	0.00	5	5	30	30	W	1	0	0	0	0	Limestone not found. TF98
AI44	Z1 Frostviken S	14480 71660	600	c or c-s		Linear	1	0	0	1	0	700	150	50	0.03	0.00	10	10	45			1	0	0	0	0	Limestone not found. TF98
AI44	Z1 Frostviken S	14475 71650	700	c or c-s		Linear	1	0	0	0	0	700	0	50	0.03	0.00	100	10	60			1	0	0	0	0	
AI44	Z1 Frostviken S	14470 71643	660	c or c-s		Linear	1	0	0	0	0	700	0	50	0.03	0.00	5	5	75	40	N	1	0	0	0	0	
AI44	Z1 Frostviken S	14290 71543	700	c or c-s		Linear	1	0	0	0	0	500	0	50	0.02	0.00	40	10	90	30	N	1	0	0	0	0	
AI44	Z1 Frostviken S	14290 71542	700	c or c-s		Linear	1	0	0	0	0	500	0	50	0.02	0.00	40	10	90	30	N	1	0	0	0	0	
AI44	Z1 Frostviken S	14290 71541	680	c or c-s		Linear	1	0	0	0	0	500	0	50	0.02	0.00	60	10	90	30	N	1	0	0	0	0	
AI44	Z1 Frostviken S	14300 71550	760	c or c-s		Linear	1	0	0	0	0	500	0	50	0.02	0.00	60	10	50	30	N	1	0	0	0	0	
AI44	Z1 Frostviken S	14300 71552	760	c or c-s		Linear	1	0	0	0	0	400	0	50	0.02	0.00	20	10	45	30	N	1	0	0	0	0	
AI44	Z1 Frostviken S	14308 71550	700	c or c-s		Linear	1	0	0	0	0	300	0	50	0.01	0.00	17	5	50	30	N	1	0	0	0	0	
AI44	Z1 Frostviken S	14310 71550	700	c or c-s		Linear	1	0	0	0	0	300	0	50	0.01	0.00	17	5	50	30	N	1	0	0	0	0	
Area	607	14315 71545	700	c or c-s		Linear	1	0	0	0	0	400	0	50	0.02	0.00	17	5	50	30	N	1	0	0	0	0	(Area from 1425 to 1450 and 7150 to 7175 only)

UPPER ALLOCHTHON: Seve Units - Seve Units: SU (SWEDEN)

Metres

MAP SHEET	MAP NAME & NAPPE AREA	UTM / SWEDISH RN COORD		MAX ALT.	GEOL MAP IDENT	SAMPLE IDENT	OUTCROP SHAPE	O	R	T	V	D	LENGTH	VISITED LENGTH	WIDTH	CARB. AREA	DOL. AREA	VR Length	VR Width	STRIKE	DIP	#	E	F	W	C	L	COMMENTS
Ai44	Z1 **Frostviken** S	14260	71692	700	c or c-s		Linear	1	0	0	0	0	400	0	50	0.02	0.00	5	5	70	25	S	1	0	0	0	0	
Ai44	Z1 **Frostviken** S	14325	71705	680	c or c-s		Linear	1	0	0	0	0	400	0	50	0.02	0.00	10	10	95	30	S	1	0	0	0	0	
Ai44	Z1 **Frostviken** S	14370	71708	720	c or c-s		Sinuous	1	0	0	0	0	3500	0	100	0.35	0.00	90	20				1	0	0	0	0	
Ai44	Z1 **Frostviken** S	14380	71705	720	c or c-s		Arc	1	0	0	0	0	500	0	50	0.02	0.00	20	20				1	0	0	0	0	
Ai44	Z1 **Frostviken** S	14370	71705	740	c or c-s		Sinuous	1	0	0	0	0	2000	0	100	0.20	0.00	100	10				1	0	0	0	0	
Ai44	Z1 **Frostviken** S	14370	71700	740	c or c-s		Sinuous	1	0	0	0	0	2000	0	50	0.10	0.00	100	10				1	0	0	0	0	
Ai44	Z1 **Frostviken** S	14370	71698	700	c or c-s		Sinuous	1	0	0	0	0	1500	0	50	0.08	0.00	60	10				1	0	0	0	0	
Ai44	Z1 **Frostviken** S	14350	71675	790	c or c-s		Linear	1	0	0	0	0	800	0	50	0.04	0.00	90	10	75	40	N	1	0	0	0	0	
Ai44	Z1 **Frostviken** S	14370	71680	660	c or c-s		Sinuous	1	0	0	0	0	2500	0	50	0.12	0.00	10	10				1	0	0	0	0	
Ai44	Z1 **Frostviken** S	14390	71695	760	c or c-s		Sinuous	1	0	0	0	0	1500	0	50	0.08	0.00	10	10				1	0	0	0	0	
Ai44	Z1 **Frostviken** S	14390	71693	780	c or c-s		Linear	1	0	0	0	0	600	0	100	0.06	0.00	20	10	120			1	0	0	0	0	
Ai44	Z1 **Frostviken** S	14390	71692	780	c or c-s		Linear	1	0	0	0	0	1000	0	50	0.05	0.00	40	5	115			1	0	0	0	0	
Ai44	Z1 **Frostviken** S	14390	71690	780	c or c-s		Sinuous	1	0	0	0	0	2500	0	100	0.25	0.00	100	20				1	0	2	0	0	
Ai44	Z1 **Frostviken** S	14390	71680	740	c or c-s		Sinuous	1	0	0	0	0	1800	0	100	0.18	0.00	60	10				1	0	0	0	0	
Ai44	Z1 **Frostviken** S	14410	71680	680	c or c-s		Sinuous	1	0	0	0	0	800	0	50	0.04	0.00	20	10		30	N	1	0	0	0	0	
Ai44	Z1 **Frostviken** S	14318	71655	780	c or c-s		Linear	1	0	0	0	0	700	0	50	0.03	0.00	120	20	165			1	0	0	0	0	
Ai44	Z1 **Frostviken** S	14320	71655	790	c or c-s		Arc	1	0	0	0	0	500	0	50	0.02	0.00	170	10				1	0	0	0	0	
Ai44	Z1 **Frostviken** S	14322	71657	760	c or c-s		Arc	1	0	0	0	0	200	0	50	0.01	0.00	120	10				1	0	0	0	0	
Ai44	Z1 **Frostviken** S	14325	71656	820	c or c-s		Linear	1	0	0	0	0	400	0	50	0.02	0.00	200	10	10			1	0	0	0	0	
Ai44	Z1 **Frostviken** S	14330	71650	800	c or c-s		Arc	1	0	0	0	0	400	0	50	0.02	0.00	140	10				1	0	0	0	0	
Ai44	Z1 **Frostviken** S	14338	71642	730	c or c-s		Arc	1	0	0	0	0	700	0	50	0.03	0.00	130	10				1	0	0	0	0	
Ai44	Z1 **Frostviken** S	14340	71641	730	c or c-s		Linear	1	0	0	0	0	500	0	50	0.02	0.00	130	10	90			1	0	0	0	0	
Ai44	Z1 **Frostviken** S	14390	71632	600	c or c-s		Arc	1	0	0	0	0	1500	0	100	0.15	0.00	60	10		15	N	1	0	0	0	0	
Ai44	Z1 **Frostviken** S	14390	71622	540	c or c-s		Linear	1	0	0	0	0	1000	0	100	0.10	0.00	25	5	90	40	N	1	0	0	0	0	
Ai44	Z1 **Frostviken** S	14405	71627	610	c or c-s		Arc	1	0	0	0	0	1000	0	100	0.10	0.00	70	10		40	W	1	0	1	0	0	
Ai44	Z1 **Frostviken** S	14412	71610	580	c or c-s		Linear	1	0	0	0	0	700	0	50	0.03	0.00	40	5	20	30	W	1	0	0	0	0	
Ai44	Z1 **Frostviken** S	14410	71603	580	c or c-s		Linear	1	0	0	0	0	600	0	50	0.03	0.00	10	5	70	30	N	1	0	0	0	0	
Ai44	Z1 **Frostviken** S	14435	71680	700	c or c-s		Arc	1	0	0	0	0	700	0	50	0.03	0.00	60	10				1	0	0	0	0	
Ai44	Z1 **Frostviken** S	14440	71679	700	c or c-s		Arc	1	0	0	0	0	700	0	50	0.03	0.00	60	5				1	0	0	0	0	
Ai44	Z1 **Frostviken** S	14440	71665	640	c or c-s		Linear	1	0	0	0	0	700	0	50	0.03	0.00	30	5	100			1	0	0	0	0	
Ai44	Z1 **Frostviken** S	14436	71660	700	c or c-s		Arc	1	0	0	0	0	600	0	50	0.03	0.00	60	5		35	W	1	0	0	0	0	
Ai44	Z1 **Frostviken** S	14450	71645	680	c or c-s		Linear	1	0	0	0	0	700	0	50	0.03	0.00	20	5	85	30	N	1	0	0	0	0	
Ai44	Z1 **Frostviken** S	14435	71620	720	c or c-s		Linear	1	0	0	0	0	1000	0	50	0.05	0.00	100	10	180			1	0	0	0	0	
Ai44	Z1 **Frostviken** S	14490	71690	540	c or c-s		Linear	1	0	0	0	0	700	0	50	0.03	0.00	20	5	50	25	N	1	0	0	0	0	
Ai44	Z1 **Frostviken** S	14475	71675	700	c or c-s		Arc	1	0	0	0	0	700	0	50	0.03	0.00	100	5		35	N	1	0	0	0	0	
Ai44	Z1 **Frostviken** S	14473	71663	570	c or c-s		Linear	1	0	0	0	0	500	0	50	0.02	0.00	5	5	40	30	W	1	0	0	0	0	
Ai44	Z1 **Frostviken** S	14480	71663	570	c or c-s		Linear	1	0	0	1	0	400	100	50	0.02	0.00	5	5	30	30	W	1	0	0	0	0	Limestone not found. TF98
Ai44	Z1 **Frostviken** S	14480	71660	600	c or c-s		Linear	1	0	0	1	0	700	150	50	0.03	0.00	10	10	45			1	0	0	0	0	Limestone not found. TF98
Ai44	Z1 **Frostviken** S	14475	71650	700	c or c-s		Linear	1	0	0	0	0	700	0	50	0.03	0.00	100	10	60			1	0	0	0	0	
Ai44	Z1 **Frostviken** S	14470	71643	660	c or c-s		Linear	1	0	0	0	0	700	0	50	0.03	0.00	5	5	75	40	N	1	0	0	0	0	
Ai44	Z1 **Frostviken** S	14290	71543	700	c or c-s		Linear	1	0	0	0	0	500	0	50	0.02	0.00	40	10	90	30	N	1	0	0	0	0	
Ai44	Z1 **Frostviken** S	14290	71542	700	c or c-s		Linear	1	0	0	0	0	500	0	50	0.02	0.00	40	10	90	30	N	1	0	0	0	0	
Ai44	Z1 **Frostviken** S	14290	71541	680	c or c-s		Linear	1	0	0	0	0	500	0	50	0.02	0.00	60	10	90	30	N	1	0	0	0	0	
Ai44	Z1 **Frostviken** S	14300	71550	760	c or c-s		Linear	1	0	0	0	0	500	0	50	0.02	0.00	60	10	50	30	N	1	0	0	0	0	
Ai44	Z1 **Frostviken** S	14300	71552	760	c or c-s		Linear	1	0	0	0	0	400	0	50	0.02	0.00	20	10	45	30	N	1	0	0	0	0	
Ai44	Z1 **Frostviken** S	14308	71550	700	c or c-s		Linear	1	0	0	0	0	300	0	50	0.01	0.00	17	5	50	30	N	1	0	0	0	0	
Ai44	Z1 **Frostviken** S	14310	71550	700	c or c-s		Linear	1	0	0	0	0	300	0	50	0.01	0.00	17	5	50	30	N	1	0	0	0	0	
Area		607	14315	71545	700	c or c-s	Linear	1	0	0	0	0	400	0	50	0.02	0.00	17	5	50	30	N	1	0	0	0	0	(Area from 1425 to 1450 and 7150 to 7175 only)

UPPER ALLOCHTHON: Seve Belts (SWEDEN ONLY): TOTALS

Metres

MAP SHEET	MAP NAME & NAPPE AREA	UTM / SWEDISH RN COORD		MAX ALT.	GEOL MAP IDENT	SAMPLE IDENT	OUTCROP SHAPE	O	R	T	V	D	LENGTH	VISITED LENGTH	WIDTH	CARB. AREA	DOL. AREA	VR Length	VR Width	STRIKE	DIP	#	E	F	W	C	L	COMMENTS
Totals	3007			####				39	0	3	3	0	35840	180	####	2.47	0.00	####	###		###	25	34	0	1	0	0	**Includes calc-silicates**
%									0%	8%	8%	0%				0.08%	0.00%					64%	87%					**No carbonates near a pluton**
Averages				720									919	60	52	0.06	#DIV/0!	64	13		33			0.00	0.03	0	0	**No mapped dolomites**
Maxima				1110									5000	100	100	0.50	0.00	320	60		80			0	1	0	0	**No caves reported**

UPPER ALLOCHTHON: Seve Belts - Western Belt of SB

MAP SHEET	MAP NAME & NAPPE AREA	UTM / SWEDISH RN COORD		MAX ALT.	GEOL MAP IDENT	SAMPLE IDENT	OUTCROP SHAPE	O	R	T	V	D	LENGTH	VISITED LENGTH	WIDTH	CARB. AREA	DOL. AREA	VR Length	VR Width	STRIKE	DIP	#	E	F	W	C	L	COMMENTS
Ai75	23EF **Fatmo. NV**																											**No carbonate outcrops**
Area	26																											(Area from 1450 to 1475 and 7225 to 7250 only)
Ai76	23EF **Fatmo. SV**																											**No carbonate outcrops**
Area	231																											(Area from 1450 to 1475 and 7200 to 7225 only)
Ai102	22F **Risbäck NV**																											**No carbonate outcrops**
Area	9																											(Area from 1450 to 1475 and 7175 to 7200 only)
Ai163	24EF:**Tärnaby**	14920	72765	1042	c or c-s		Linear	1	0	0	0	0	1000	0	70	0.07	0.00	42	40	90	15	W	1	0	0	0	0	
Area	228																											(Area from 1475 to 1500 and 7275 to 7300 only)
Ai162	24EF:**Tärnaby**																											**No carbonate outcrops**
Area	200																											(Area from 1475 to 1500 and 7250 to 7275 only)
Ai77	23EF **Fatmo. NC**	14775	72300	1110	c or c-s		Sinuous	1	0	0	0	0	5000	0	100	0.50	0.00	290	60		35	W	1	0	0	0	0	
Area	60																											(Area from 1475 to 1500 and 7225 to 7250 only)
Ai78	23EF **Fatmo. SO**																											**No carbonate outcrops**
Area	2																											(Area from 1475 to 1500 and 7200 to 7225 only)

UPPER ALLOCHTHON: Seve Belts - Central Belt of SB

Ai76	23EF **Fatmo. SV**																											**No carbonate outcrops**
Area	48																											(Area from 1450 to 1475 and 7200 to 7225 only)
Ai102	22F **Risbäck NV**																											**No carbonate outcrops**
Area	6																											(Area from 1450 to 1475 and 7175 to 7200 only)
Ai162	24EF:**Tärnaby**	14940	72575	940	c or c-s		Sinuous	1	0	0	0	0	1700	0	70	0.12	0.00	110	10		30	W	1	0	1	0	0	
Ai162	24EF:**Tärnaby**	14945	72585	940	c or c-s		Linear	1	0	0	0	0	300	0	50	0.02	0.00	60	5				1	0	0	0	0	
Ai162	24EF:**Tärnaby**	14950	72580	960	c or c-s		Sinuous	1	0	0	0	0	3000	0	70	0.21	0.00	150	20		20	N	1	0	0	0	0	
Ai162	24EF:**Tärnaby**	14975	72600	997	c or c-s		Sinuous	1	0	0	0	0	3500	0	70	0.25	0.00	147	60		45	W	1	0	0	0	0	
Area	150	14984	72610	860	c or c-s		Linear	1	0	0	0	0	500	0	50	0.03	0.00	40	20		80	E	1	0	0	0	0	(Area from 1475 to 1500 and 7250 to 7275 only)
Ai77	23EF **Fatmo. NC**	14860	72480	900	c or c-s		Sinuous	1	0	1	0	0	3500	0	100	0.35	0.00	140	20		40	W	0	0	0	0	0	Near Thrust on belt base
Ai77	23EF **Fatmo. NC**	14850	72460	1000	c or c-s		Sinuous	1	0	0	0	0	2000	0	100	0.20	0.00	230	20		30	W	0	0	0	0	0	
Area	89	14809	72360	1000	c or c-s		Sinuous	1	0	0	0	0	2000	0	50	0.10	0.00	320	20		35	W	0	0	0	0	0	(Area from 1475 to 1500 and 7225 to 7250 only)
Ai78	23EF **Fatmo SO**																											**No carbonate outcrops**
Area	63																											(Area from 1475 to 1500 and 7200 to 7225 only)

c or c-s = calcitic or calc-silicate

UPPER ALLOCHTHON: Seve Belts - Eastern Belt of SB

MAP & NAPPE AREA Sq. Km			UTM / SWEDISH RN COORD		MAX ALT.	GEOL MAP IDENT	SAMPLE IDENT	OUTCROP SHAPE	O	R	T	V	D	LENGTH	VISITED LENGTH	WIDTH	CARB. AREA Sq. Km	DOL. AREA Sq. Km	VR Length	VR Width	STRIKE Degs.	DIP	# Degs.	E	F	W	C	L	COMMENTS
																													Metres
Ai76	23EF	**Fatmo.SV**																											**No carbonate outcrops**
Area		78																											(Area from 1450 to 1475 and 7200 to 7225 only)
Ai102	22F	**Risbäck NV**	14520	71878	880	c or c-s		Sinuous	1	0	0	0	0	700	0	50	0.04	0.00	60	10		25	W	1	0	0	0	0	
Ai102	22F	**Risbäck NV**	14512	71764	620	c or c-s		Linear	1	0	0	1	0	700	30	70	0.05	0.00	40	10	40			1	0	0	0	0	Limestone not found. TF98
Ai102	22F	**Risbäck NV**	14562	71906	1060	c or c-s		Sinuous	1	0	0	0	0	200	0	50	0.01	0.00	20	5				0	0	0	0	0	
Ai102	22F	**Risbäck NV**	14560	71886	1000	c or c-s		Sinuous	1	0	0	0	0	400	0	50	0.02	0.00	160	20				0	0	0	0	0	
Ai102	22F	**Risbäck NV**	14560	71855	640	c or c-s		Arc	1	0	0	0	0	500	0	50	0.03	0.00	80	20		20	W	1	0	0	0	0	
Ai102	22F	**Risbäck NV**	14650	71935	620	c or c-s		Sinuous	1	0	0	1	0	900	50	50	0.05	0.00	40	20		60	W	1	0	0	0	0	Limestone not found. TF98
Ai102	22F	**Risbäck NV**	14647	71883	640	c or c-s		Arc	1	0	0	0	0	300	0	30	0.01	0.00	40	5		40	N	1	0	0	0	0	
Ai102	22F	**Risbäck NV**	14660	71876	660	c or c-s		Sinuous	1	0	0	0	0	500	0	50	0.03	0.00	20	5		20	N	1	0	0	0	0	
Ai102	22F	**Risbäck NV**	14670	71886	670	c or c-s		Arc	1	0	0	0	0	600	0	60	0.04	0.00	30	10		40	N	1	0	0	0	0	
Ai102	22F	**Risbäck NV**	14620	71786	780	c or c-s		Sinuous	1	0	0	0	0	800	0	50	0.04	0.00	60	5		20	W	1	0	0	0	0	
Ai102	22F	**Risbäck NV**	14654	71774	740	c or c-s		Sinuous	1	0	0	0	0	300	0	50	0.02	0.00	20	5		20	W	1	0	0	0	0	
Ai102	22F	**Risbäck NV**	14667	71784	620	c or c-s		Linear	1	0	1	0	0	600	0	50	0.03	0.00	10	5	110	35	S	1	0	0	0	0	Near Seve Thrust base
Ai102	22F	**Risbäck NV**	14670	71750	660	c or c-s		Arc	1	0	0	0	0	500	0	30	0.02	0.00	20	5				1	0	0	0	0	
Ai102	22F	**Risbäck NV**	14672	71750	640	c or c-s		Arc	1	0	0	0	0	400	0	50	0.02	0.00	10	5				1	0	0	0	0	Partly on Ai 103
Ai102	22F	**Risbäck NV**	14675	71755	610	c or c-s		Linear	1	0	0	0	0	500	0	30	0.02	0.00	20	5	35	10	W	1	0	0	0	0	
Ai102	22F	**Risbäck NV**	14715	71788	490	c or c-s		Linear	1	0	0	0	0	500	0	30	0.02	0.00	30	5	5			1	0	0	0	0	
Area		499	14716	71788	500	c or c-s		Arc	1	0	0	0	0	300	0	20	0.01	0.00	20	5				1	0	0	0	0	(Area from 1450 to 1475 and 7175 to 7200 only)
Ai103	22F	**Risbäck SV**	14535	71735	490	c or c-s		Arc	1	0	0	0	0	200	0	50	0.01	0.00	12	5				1	0	0	0	0	
Ai103	22F	**Risbäck SV**	14615	71660	460	c or c-s		Arc	1	0	0	0	0	400	0	50	0.02	0.00	10	5		60	N	1	0	0	0	0	
Ai103	22F	**Risbäck SV**	14625	71665	520	c or c-s		Arc	1	0	0	0	0	300	0	30	0.01	0.00	20	10		40	N	1	0	0	0	0	
Ai103	22F	**Risbäck SV**	14645	71680	610	c or c-s		Arc	1	0	0	0	0	600	0	50	0.03	0.00	30	5				1	0	0	0	0	
Ai103	22F	**Risbäck SV**	14652	71680	605	c or c-s		Sinuous	1	0	0	0	0	500	0	50	0.03	0.00	40	5		35	N	1	0	0	0	0	
Ai103	22F	**Risbäck SV**	14652	71665	590	c or c-s		Arc	1	0	0	0	0	700	0	30	0.02	0.00	70	25		15	N	1	0	0	0	0	
Ai103	22F	**Risbäck SV**	14650	71640	470	c or c-s		Linear	1	0	0	1	0	400	100	50	0.02	0.00	20	5	120	40	S	1	0	0	0	0	Only buried boulder = Carb. TF98
Ai103	22F	**Risbäck SV**	14650	71590	475	c or c-s		Linear	1	0	0	0	0	300	0	30	0.01	0.00	25	5	20			1	0	0	0	0	
Ai103	22F	**Risbäck SV**	14647	71585	480	c or c-s		Arc	1	0	0	0	0	40	0	50	0.02	0.00	5	5				1	0	0	0	0	
Area		430	14635	71540	590	c or c-s		Arc	1	0	0	0	0	400	0	50	0.02	0.00	10	5				1	0	0	0	0	(Area from 1450 to 1475 and 7150 to 7175 only)
Ai123	23G	**Dikanäs**																											**No carbonate outcrops**
Area		12																											(Area from 1500 to 1525 and 7200 to 7225 only)
Ai162	24EF:	**Tärnaby**																											**No carbonate outcrops**
Area		25																											(Area from 1475 to 1500 and 7250 to 7275 only)
Ai77	23EF	**Fatmo. NO**																											**No carbonate outcrops**
Area		289																											(Area from 1475 to 1500 and 7225 to 7250 only)
Ai78	23EF	**Fatmo. SC**	14765	72065	620	c or c-s		Linear	1	0	0	0	0	500	0	50	0.02	0.00	20	5	140	20	W	1	0	0	0	0	
Area		200																											(Area from 1475 to 1500 and 7200 to 7225 only)
Ai104	22F	**Risbäck NO**																											**No carbonate outcrops**
Area		37																											(Area from 1475 to 1500 and 7175 to 7200 only)
Ai122	23G	**Dikanäs**	15070	72290	605	c or c-s		Linear	1	0	1	0	0	300	0	25	0.01	0.00	10	15				1	0	0	0	0	
Area		325																											(Area from 1500 to 1525 and 7225 to 7250 only)

MIDDLE and LOWER ALLOCHTHONS: ML (NORWAY): TOTALS

Metres

MAP SHEET	MAP NAME & NAPPE AREA	UTM / SWEDISH RN COORD	MAX ALT.	GEOL MAP IDENT	SAMPLE IDENT	OUTCROP SHAPE	O	R	T	V	D	LENGTH	VISITED LENGTH	WIDTH	CARB. AREA	DOL. AREA	VR Length	VR Width	STRIKE	DIP	#	E	F	W	C	L	COMMENTS
Totals	903																										**No carbonate outcrops in Norway**
%																											
Averages																											
Maxima																											

MIDDLE and LOWER ALLOCHTHONS: ML (SWEDEN): TOTALS

MAP SHEET	MAP NAME & NAPPE AREA	UTM / SWEDISH RN COORD	MAX ALT.	GEOL MAP IDENT	SAMPLE IDENT	OUTCROP SHAPE	O	R	T	V	D	LENGTH	VISITED LENGTH	WIDTH	CARB. AREA	DOL. AREA	VR Length	VR Width	STRIKE	DIP	#	E	F	W	C	L	COMMENTS
Totals	5373		#####				21	0	12	4	15	30900	320	####	5.12	4.90	####	###		###	15	21	0	1	0	0	**Mainly Dolomites**
%								0%	57%	19%	71%				0.10%	0.09%					71%	100%					**Some Ordovician Limestones**
Averages			510									1471	80	110	0.24	0.33	54	15		33			0.00	0.05	0	0	**No carbonates near a pluton**
Maxima			728									7000	100	500	2.40	2.40	228	100		45			0	1	0	0	**No caves reported**

MIDDLE and LOWER ALLOCHTHONS: ML (NORWAY AND SWEDEN): TOTALS

MAP SHEET	MAP NAME & NAPPE AREA	UTM / SWEDISH RN COORD	MAX ALT.	GEOL MAP IDENT	SAMPLE IDENT	OUTCROP SHAPE	O	R	T	V	D	LENGTH	VISITED LENGTH	WIDTH	CARB. AREA	DOL. AREA	VR Length	VR Width	STRIKE	DIP	#	E	F	W	C	L	
Totals	6276		#####				21	0	12	4	15	30900	320	####	5.12	4.90	####	###		###	15	21	0	1	0	0	**Mainly Dolomites**
%								0%	57%	19%	71%				0.08%	0.08%					71%	100%					**Some Ordovician Limestones**
Averages			510									1471	80	110	0.24	0.33	54	15		33			0.00	0.05	0	0	**No carbonates near a pluton**
Maxima			728									7000	100	500	2.40	2.40	228	100		45			0	1	0	0	**No caves reported**

There are no mapped carbonates in the Middle Allochthon

MIDDLE and LOWER ALLOCHTHONS: ML (NORWAY)

MAP SHEET	MAP NAME & NAPPE AREA	UTM / SWEDISH RN COORD	MAX ALT.	GEOL MAP IDENT	SAMPLE IDENT	OUTCROP SHAPE	O	R	T	V	D	LENGTH	VISITED LENGTH	WIDTH	CARB. AREA	DOL. AREA	VR Length	VR Width	STRIKE	DIP	#	E	F	W	C	L	COMMENTS
1924 IV	**Royrvik**																										**No carbonate outcrops**
Area	29																										
1925 I	**Susendal**																										**No carbonate outcrops**
Area	121																										
1925 II	**Børgefjellet**																										**No carbonate outcrops**
Area	445																										
1924 I	**Jomafjellet**																										**No carbonate outcrops**
Area	139																										
2025 IV	**Skardmodalen**																										**No carbonate outcrops**
Area	66																										
2025 III	**Ranseren**																										**No carbonate outcrops**
Area	103																										

MIDDLE and LOWER ALLOCHTHONS: ML (SWEDEN)

MAP SHEET	MAP NAME & NAPPE AREA	UTM / SWEDISH RN COORD	MAX ALT.	GEOL MAP IDENT	SAMPLE IDENT	OUTCROP SHAPE	O	R	T	V	D	LENGTH	VISITED LENGTH	WIDTH	CARB. AREA	DOL. AREA	VR Length	VR Width	STRIKE	DIP	#	E	F	W	C	L	COMMENTS
2025 IV	**Skardmodalen**																										**No carbonate outcrops**
Area	4																										
2025 III	**Ranseren**																										**No carbonate outcrops**
Area	89																										
25G	**Ammarnäs SE**																										**No carbonate outcrops**
Area	36																										Bounded by 7300 to 7322
Ai161	24EF:**Tärnaby**																										**No carbonate outcrops**
Area	8																										(Area from 1450 to 1475 and 7250 to 7275 only)
Ai74	Z1 **Sipmeke SV-SO**																										**No carbonate outcrops**
Area	30																										(Area from 1425 to 1450 and 7200 to 7211 only)
Ai75	23EF **Fatmo. NV**																										**No carbonate outcrops**
Area	55																										(Area from 1450 to 1475 and 7225 to 7250 only)
Ai102	22F **Risbäck NV**																										**No carbonate outcrops**
Area	79																										(Area from 1450 to 1475 and 7175 to 7200 only)
Ai103	22F **Risbäck SV**																										**No carbonate outcrops**
Area	155																										(Area from 1450 to 1475 and 7150 to 7175 only)
Ai163	24EF:**Tärnaby**																										**No carbonate outcrops**
Area	40																										(Area from 1475 to 1500 and 7275 to 7300 only)
Ai77	23EF **Fatmo. NO**																										**No carbonate outcrops**
Area	120																										(Area from 1475 to 1500 and 7225 to 7250 only)
Ai78	23EF **Fatmo. SO**	14893 72135	540	Dolomite		Arc	1	0	0	0	1	500	0	50	0.02	0.02	20	5			1	0	0	0	0		
Ai78	23EF **Fatmo. SO**	14890 72120	550	Dolomite		Lozenge	1	0	0	0	1	1000	0	200	0.20	0.20	10	5	20	10 W	1	0	0	0	0		
Ai78	23EF **Fatmo. SO**	14901 72125	540	Dolomite		Arc	1	0	0	0	1	300	0	50	0.01	0.01	20	5			1	0	0	0	0		
Ai78	23EF **Fatmo. SO**	14917 72120	540	Dolomite		Arc	1	0	0	1	1	1200	100	50	0.06	0.06	40	5			1	0	0	0	0		Limestone not found. No karst. TF98
Ai78	23EF **Fatmo. SO**	14919 72120	530	Dolomite		Arc	1	0	0	1	1	600	100	50	0.03	0.03	10	5			1	0	0	0	0		TF98. No karst. Faintly audible with dil. HCl
Area	341	14940 72050	680	Dolomite		Linear	1	0	0	0	1	300	0	50	0.01	0.01	40	5	10		1	0	0	0	0		(Area from 1475 to 1500 and 7200 to 7225 only)
Ai104	22F **Risbäck NO**	14760 71880	600	Dolomite		Sinuous	1	0	1	1	1	5000	100	50	0.25	0.25	130	60		30 W	1	0	0	0	0		Near thrusts. Limestone not found. TF98
Ai104	22F **Risbäck NO**	14775 71800	728	Dolomite		Irregular	1	0	1	0	1	3000	0	200	0.60	0.60	228	100		45 W	1	0	0	0	0		On Lower Allochthon thr. top. SGU (54) p197
Area	562																										(Area from 1475 to 1500 and 7175 to 7200 only)
Ai105	22F **Risbäck SO**						(Lower Allochthon only)																				**No carbonate outcrops**
Area	591																										(Area from 1475 to 1500 and 7150 to 7175 only)
Ai122	23G **Dikanäs NV**	15055 72260	520	Dolomite		Arc	1	0	1	0	1	700	0	150	0.11	0.11	20	10	5	25 W	1	0	0	0	0		Internal thrust
Area	300																										(Area from 1500 to 1525 and 7225 to 7250 only)
Ai123	23G **Dikanäs SV**	15212 72190	520	Dolomite		Arc	1	0	1	0	1	1000	0	50	0.05	0.05	80	10	175	25 W	1	0	0	0	0		Internal thrust
Area	613																										(Area from 1500 to 1525 and 7200 to 7225 only)
Ai84	22G **Vilhelmina NV**	15105 71885	360	Ord. Ist: Tremadoc		Arc	1	0	1	0	0	700	0	50	0.04	0.00	20	5			1	0	0	0	0		Internal thrust
Ai84	22G **Vilhelmina NV**	15128 71880	380	Ord. Ist: Tremadoc		Sinuous	1	0	0	0	0	200	0	50	0.01	0.00	20	5		40 S	1	0	0	0	0		**Topo map is not published**
Ai84	22G **Vilhelmina NV**	15135 71880	430	Ord. Ist: Tremadoc		Sinuous	1	0	1	0	0	1000	0	50	0.05	0.00	20	5		30 S	1	0	0	0	0		Internal thrust
Area	625																										(Area from 1500 to 1525 and 7175 to 7200 only)
Ai85	22G **Vilhelmina SV**	15018 71624	420	Ord. Ist: Tremadoc		Arc	1	0	1	1	0	400	20	50	0.02	0.00	90	5		25 S	1	0	0	0	0		Internal thrust. Limestone not found. TF98
Area	625																										(Area from 1500 to 1525 and 7150 to 7175 only)
Ai124	23G **Dikanäs NO**	15385 72490	380	Dolomite		Arc	1	0	0	0	1	1200	0	50	0.06	0.06	30	5		30 W	1	0	0	0	0		
Ai124	23G **Dikanäs NO**	15390 72490	380	Dolomite		Arc	1	0	0	0	1	1000	0	50	0.05	0.05	20	5		40 W	1	0	0	0	0		
Ai124	23G **Dikanäs NO**	15350 72310	465	Dolomite		Sinuous	1	0	1	0	1	7000	0	350	2.40	2.40	55	20		35 W	1	0	0	0	0		Internal thrust
Ai124	23G **Dikanäs NO**	15380 72330	470	Dolomite		Lozenge	1	0	1	0	1	1500	0	500	0.75	0.75	80	30		45 N	1	0	1	0	0		Internal thrust
Ai124	23G **Dikanäs NO**	15350 72280	500	Dolomite		Sinuous	1	0	1	0	1	3000	0	100	0.30	0.30	90	10		45 W	1	0	0	0	0		Internal thrust
Area	500																										(Area from 1525 to 1550 and 7225 to 7250 only)
Ai125	23G **Dikanäs SO**	15380 72150	650	Ord. Ist: Tremadoc		Linear	1	0	1	0	0	800	0	100	0.08	0.00	100	20	70	40 N	1	0	0	0	0		Internal thrust
Area	400																										(Area from 1525 to 1550 and 7200 to 7225 only)
Ai86	22G **Vilhelmina NO**	15315 71790	520	Ord. Ist: Tremadoc		Arc	1	0	1	0	0	500	0	50	0.03	0.00	20	5		30 S	1	0	0	0	0		Internal thrust. Near Caledonide thrust front
Area	200																										(Area from 1525 to 1550 and 7175 to 7200 only)

APPENDIX C2 KEY TO CAVE DATABASES

This Appendix describes the various cave attribute fields used in the cave databases, as discussed particularly in sections 53 and 5.6 and in Appendix B2.

C2.1 External cave attribute fields

Heading	Meaning	Value	Comments	Units
Coordinates			For each cave, a 2-alpha + 6- or 8-figure UTM grid reference commonly defines its location. These were taken from a published reference or from personal checking. In the 1998 field trip, such checking was assisted by the use of a Garmin 12 GPS system that could be relied on to give a co-ordinate accurate to 100m. Final determination of an 8-figure co-ordinate was then made from all available information, including altitude. The fourth digit of each East and North field is commonly set to either 0 or 5, so that accuracy to ±25m is attempted. The use of other fourth digit numbers is usually reserved to distinguish between several proximal cave entrances. Coordinates given to the nearest 10m are from GPS readings in year 2000, or are relative to another cave coordinate, or are from the local economic map.	
Coordinates in italics	*ED50, Black UTM grid*		6 or 8 digit coordinates. The original M711 series 1:50000 maps used a black UTM grid based on European Datum (ED50) in UTM grid zone 33.	
Coordinates in regular font	WGS84, Blue UTM grid		6 or 8 digit coordinates for sites based on Norwegian 1:50000 maps. From about the late 1980s, purchased M711 series maps commonly used a blue UTM grid based on World Geodetic System 1984 (WGS84), also in grid zone 33. A typical conversion is as follows: $E_{WGS}=E_{ED}-66m$; $N_{WGS}=N_{ED}-202m$. Special care is required in the use of the GPS for each type of map. In Norway, *Navigational Set Up* is set to *Position Format*: UTM/UPS and *Map Datum*: European 50 or WGS84. In practice, the instrument used always gave co-ordinates for the WGS84 datum. The 2000 field trip benefited from improved GPS accuracy, as a random perturbation signal was removed earlier that year. For each Swedish cave that can be mapped on a bordering 1:50000 Norwegian M711 series map, the 2-alpha + 6- or 8-figure UTM grid reference defines its location for that map. These grid references were commonly translated manually from published references based on the Swedish grid system, or from personal checking. In the 1998 field trip, such checking was assisted by the use of a Garmin 12 GPS system that was set up as though in Norway, where appropriate.	
Coordinates in regular font	Swedish 10-digit RN system		Where a bordering Norwegian map is not available, a Swedish 1:100000 Fjällkartan map was used, and the cave position recorded using the Swedish 10-digit RN system, but with Eastings presented before Northings to be consistent with UTM. The fifth digits of the East and North fields define a 100m square and hence an accuracy of ±50m is attempted for these cave locations. In order to use the GPS with the Fjällkartan maps, *Navigational Set Up* is set to *Position Format*: Swedish Grid and *Map Datum*: RT90. It was only necessary to use Swedish maps in the Övre Ältsvattnet (KU) and Södra Storfjället (KU) areas.	
Other italics			The author's best (gu)estimate	

Heading	Meaning	Value	Comments	Units
Alt.	Altitude		The altitude for each cave was taken from published references or from personal observation assisted by the use of a Pretel Altiplus D2 digital altimeter. When used in the field, this was set to an easily-identified altitude (usually a road or a lake), as read from the appropriate map, and the time noted. Readings at cave locations were then recorded and timed. On return to an identified altitude, a new reading for this altitude was noted with the time, to determine the drift due to change in air pressure. The altitudes for the cave locations were then corrected using a linear interpolation of the change during the day. When, in one area, it was possible to compare 1997 measured altitudes with those measured again in 1998, the altitude differences were: 0, +1, +2, +3, 0, +1, -1m. Hence, altitudes are commonly recorded to the nearest metre, and are probably accurate to better than ±5m, when compared to the maps in use.	
Alt.	Altitude		Sink caves and Through caves: the highest point (the highest entrance if several).	Metres
			Resurgence caves: the lowest point (water level).	Metres
			Relict caves: floor level at entrance	Metres
Kommune			The administrative district within the Norwegian or Swedish county.	
Area			A geographical description of the cave's locality.	
Lst. Strike and Dip			The strike and dip of the carbonate foliation is usually taken from personal measurements made inside the cave, or from published survey information, rather than from such data marked on geological maps, which may differ. If the values vary within the cave, then a typical value is quoted. [Some Scandinavian geological maps quote dip in 400 grad circles].	Degrees (Circle = 360°)
OW	Outcrop Width		The width of the carbonate outcrop across the strike at the cave location is commonly taken from geological maps or from personal observation. Accurate probably to within a factor of 2.	Metres
Ext. Colour			The colour of the weathered face of the limestone sample. Many internal cave samples of carbonate bedrock were also tested with dilute HCl: these are almost universally calcitic. Those with a yellow, weathered, appearance are assumed to comprise HMC or DL.	
Other Int. Rock			Where internal cave samples of any aquiclude rock were studied, such as from a schist wall or from a dyke forming a non-solutional barrier, then identifications by the author or a colleague are given.	
R	'Remetamorphosed'	1	The carbonate outcrop containing the cave has probably been 'remetamorphosed' (with loss of foliation) by high temperature, low pressure, contact metamorphism from an adjacent igneous pluton. The cave lies within the contact aureole, less than 250m from the pluton.	
		0	The carbonate outcrop lies away from any igneous pluton.	
T	Thrust	1	The carbonate outcrop containing the cave lies along or near to a major tectonic thrust.	
		0	The carbonate outcrop does not lie along or near to a major tectonic thrust.	

Heading	Meaning	Value	Comments	Units
GS	Glacial Situation	C	A coastal cave along the Atlantic-facing strandflat (commonly below 25m). The cave has been invaded by the sea for much of the Holocene. Includes littoral caves, formed without dissolution, and sea caves, which may have experienced dissolution.	
		D	The cave is situated west of a major ridge and between the strandflat and the deglaciation marine limit (section 8.1.2). The cave was invaded by the sea at least at the start of the Holocene, prior to major isostatic uplift (section 8.4.7). This limit varied from c. 125m at 12000 14Ca BP at YD isobase 100m off the coast, via 150m at 10000 at YD isobase 150m at Langfjord, to 133m at 9080 at YD isobase 200m at Svenningdal. Most of these caves function, or have functioned, as resurgences.	
		E	The cave is situated east of a major ridge and between the strandflat and the deglaciation marine limit.	
		G	The cave is situated west of a major ridge and between the deglaciation marine limit and the probable glaciation marine limit. At the start of a previous glacial, the cave would have been invaded by the sea, which would then freeze perennially inside the cave. The glaciation marine limit is difficult to determine, as its evidence may be destroyed by the subsequent glaciation. It is assumed to be everywhere 120m higher than the deglaciation marine limit (section 8.1.3).	
		H	The cave is situated east of a major ridge and between the deglaciation marine limit and the probable glaciation marine limit.	
		K	The cave is situated west of a major ridge and between the glaciation marine limit and the level of the lowest local col. The cave was probably only immersed by a westward, forward-flowing, ice-dammed lake (IDL) during deglaciation (section 8.4.5).	
		L	The cave is situated east of a major ridge and between the glaciation marine limit and the level of the lowest local col. The cave was probably only immersed by backward and eastward, forward-flowing, IDLs during deglaciation (sections 8.4.8 and 8.4.9).	
		S	The cave is situated west of a major ridge and between the levels of the lowest and the highest local col. The cave was probably only immersed by westward, forward-flowing, IDLs during deglaciation (section 8.4.5).	
		T	The cave is situated east of a major ridge and between the levels of the lowest and the highest local col. The cave was probably only immersed by backward-flowing IDLs during deglaciation (section 8.4.8).	
		U	An uppermost situation, above the level of the highest local col, so that the cave could only have been immersed beneath a static nunatak IDL during the Holocene deglaciation (section 8.4.4).	
CL	Cave Location	C	Coastal cave, as under Glacial Situation above.	
		F	Valley Floor cave	
		W	Hanging Valley Wall cave	
		R	Ridge Crest cave	
		S	Valley Shoulder cave, referred as a "Sva" position in parts of the study area (e.g. Photos C2.4, C2.5 and C2.6).	
		G	Gently sloping surface cave, where 20m contours are over 100m apart, excluding paleic surfaces.	
		P	Paleic surface cave, as inferred from Rudberg (1997). Only applies in the eastern part of the area.	
		Note:	The above 7 classes are based on a classification proposed by Lauritzen (1981c and 1990b) with the addition of types C, R and G, which are necessary to include the extreme topographical locations that occur in the study area. The cave location classification is strongly linked to surface topography and, except for the P and C extremes, only weakly linked to altitude. For inland caves, a judgement is applied to the appropriate valley to consider. For active caves in minor side valleys, the appropriate valley is usually taken to be the major glaciated valley to which the cave stream flows.	

Heading	Meaning	Value	Comments	Units
KT	Karst Type	V or VSK	Vertical stripe karst. The generally homoclinal angle of dip varies commonly between 81° and 90° (e.g. Photos B1.10 and B1.12) and the outcrop is much longer than its width. The widest outcrop in the group is c. 800m in width, in Z7 (section 4.2.3).	
		A or ASK	Angled stripe karst. The generally homoclinal angle of dip varies commonly between 31° and 80° (Photo C2.1) and the outcrop, or the outcrop limb of a complex outcrop, is much longer than its width.	
		L or LAK	Low angle karst. The angle of dip is 30° degrees or less, may be varying or homoclinal, and the outcrop is quite broad in relation to its length.	
		C or CFK	Complexly folded karst, at a scale so that folds are visible or may be inferred within a cave. Surprisingly, only three such caves are recorded: **Kvitfjellgrotta** (Z4), **Nedre Helveteshullet** (Z7) and **Labyrintgrottan** (ZA). This type is probably under-represented, especially in short caves. Carbonate outcrops also sporadically display CFK, as at the central part of Elgfjell (Z4) and as shown in Photos C2.2–C2.4.	
		X	Unknown karst type	
SR	Slope relationship	D	The dip of the foliation is down slope	
		N	The dip of the foliation is not related to the slope. This always applies to vertical stripe karst, and to angled stripe karst and low angle karst if the cave is in location R or F.	
		U	The dip of the foliation is upslope	
		X	Unknown relationship	
OR	Strike orientation	P	The outcrop strike is parallel to the topographical structure, a judgement being made about local scale.	
		A	The outcrop strike is angled to the topography	
		O	The outcrop strike is orthogonal to the topography	
		N	The outcrop strike is not related to the topography	
		X	Unknown relationship	
CA	Catchment Area		The approximate surface catchment area for each cave was obtained by 'eyeballing', or by making measurements with a ruler on, each applicable topographical map. A regional interpretation was used, so that, in general, a cave entrance on the side of a valley is shown as having the catchment area for the whole valley upstream of it. In order to permit the use of logarithmic charts, the smallest catchment areas are recorded as 0.01km^2. An accuracy of perhaps ±30% is expected for these data. Because the catchment areas vary by over four orders of magnitude, any statistical analysis on them should be little affected by this range of approximation.	km^2
Ref. No	Reference number		As used by referenced authors	

Photo C2.1 Entrance to Krokgrotta (Z4), Eiterådal
A resurgence cave formed in angled stripe karst.

Photo C2.2 Complexly folded karst
Recumbent folds near Skånvik (Z2).

Photo C2.3 Double anticline
Road cutting beside lake Över-Uman (ZC).
Narrow marble layers within mica schist.

Photo C2.4 Kvitfjell resurgences (Z4)
Two separate resurgences (arrowed), 3m apart and 200m above the main valley floor but only 30m below the skyline. The cave systems are at the valley shoulder, in cave location S. The limestone in the upper right corner of the picture exhibits complex folding, which is rare within the study area.
Trevor Faulkner

Photo C2.5 Sørlielvgrotta (Z4), Elgfjell
The sink entrance is at cave location S.

Photo C2.6 Naeverskardhullet Waterfall (ZA)
The water flows from an unexplored potential through-cave at CL=S
June 2005

C2.2 Internal cave attributes fields

Heading	Meaning	Value	Comments	Units
CT	Cave Type	S	Predominantly a single shaft	
	See also section 5.2.5.	a	Single linear passage, including those with simple staircase profiles	
		b	Single meandering passage, including those with simple staircase profiles	
		c	One level rectilinear network	
		d	One level dendritic network, including those with simple staircase profiles	
		e	Tiered linear passages, connected by shafts	
		f	Multilevel rectilinear network	
		g	Multilevel dendritic, including those with distributary passages	
		h	Complex multilevel network with steeply sloping (phreatic) passages	
		Hy	Hybrid cave: formed by an obvious combination of at least two of the possible Tectonic, Littoral and Dissolutional processes. Excludes long solutional caves with entrances modified by marine action.	
		I	Interstratal cave: apparently not solutional, but perhaps formed by collapse into a solutional void beneath.	
		J	Jettegryten: a 'giant pot', formed by swirling stones during powerful deglacial outflows. Most are formed in non-carbonate rocks, but only jettegryter in carbonates are recorded here. Not included in dimensional analysis.	
		L	Littoral cave: probably formed primarily by wave action, supplemented by ice wedging	
		R	Collapsed roof cave: apparently has solutional walls and floor, but with a roof of collapsed blocks along its length, which was perhaps initially formed as a 'gull' feature.	
		T	Tectonic cave: in carbonate bedrock, but with little apparent dissolution, and an opening created apparently by bedrock movement	
		Note:	Refer to Ford and Williams (1989, Table 7.1, p243: Some classifications of solution caves). Classifications S and a–h (which generally increase in complexity) use approach A3: internal characteristics. These are identifiable quickly from cave surveys, and do not pre-judge the method of cave or passage formation. Classifications Hy, I, J, L, R and T make assumptions about the process of formation, and apply to a few known caves in the study area.	
LENG.	Cave Length		Cave Length is taken from published survey or other reported information. In the Norwegian part of the study area, at least, the usual convention is to include in the length the sum of the survey legs (including laddered shafts) with manual additions and corrections for oxbows, side passages, avens, pits and survey duplications. Lengths should be accurate to a few metres for BCRA Grade 3 (or better) surveys, which are measured using a tape measure. The accuracy may be ±25% or worse for Grade 1 and 2 surveys, which rely on estimates of length made outside and inside the cave. Generally, the longer caves are surveyed to a higher grade, although parts of these caves may be surveyed to a lower accuracy. Open passages are normally explored as far as humanly possible, because cave explorers are motivated to maximise the reported cave length. Caves are commonly recorded down to 5m length or depth. Unpassed boulder chokes are quite rare in these caves (only c. 25 were counted in the Norwegian part of the study area) and hence it is passage size, sediment fill and water level that commonly limit exploration. Thus, there is probably some consistency in the reporting of cave length.	

Heading	Meaning	Value	Comments	Units
VR	Cave Vertical Range		The vertical difference between the highest and lowest explored points in a cave, which may equal the cave 'depth'. Cave vertical range is more difficult to measure accurately than length, and in many caves estimates of vertical range on sub-horizontal survey legs were agreed between the surveyor and his assistant, rather than by use of instruments, as this could double the time to measure each leg. Where possible, vertical ranges were checked using information from topographical maps and by reference to water levels. They are probably accurate to 10%. For the less deep caves, cave reports may not state the vertical range. In this case, an estimate was made from general field experience, and such data placed in the database in *italics*. These estimates are probably accurate to ±5m.	
XS	Cave Cross-Section		A rapidly-formed estimate of the mean cross-section of all the passages in a cave was commonly made by 'eyeballing' published cave surveys and by considering other reported information. This may be accurate to ±30%. If there is no adequate information to do this, rather than leave the field blank, which would further derogate any statistical analysis, a crude estimate was made from practical field experience, and shown in the database in *italics*. The total number of caves for which cross-sections have been crudely estimated is c. 200, i.e. c. 27% (Sweden: c. 90, i.e. c. 60%). This applies mainly to the shorter caves without adequate surveys, and so these cross-sections may only be accurate to +100/-50%. [The author tends to *under-estimate* cross-sections that are not measured]. For cave surveys drawn from data calculated by a spreadsheet (see below) the mean cross-section is derived from the ratio of the total cave volume to the total cave length (i.e. VOL./LENG.), giving a probable accuracy of ±10%. These cross-sections are presented in **bold** in the cave databases. The cross-sections refer to the explorable parts of passages, which might therefore be larger if there were no clastic sediments.	m^2
VOL.	Cave Volume		The approximate cave volume is commonly recorded as the product of the cave length and the mean cross-section (LENG. x XS). Accuracy may vary from ±30% to +100/-50%. Some recent cave surveys were drawn from data calculated by a spreadsheet that also calculates total cave volume from the volumes of individual survey legs. These volumes are presented in **bold**, with a probable accuracy of ±10%.	m^3
Min. HG	Minimum Hydraulic Gradient		Hydraulic gradient (HG) is an important parameter for determining flow characteristics and dissolutional behaviour within karst conduits, especially during cave inception and phreatic enlargement (Chapter 8). To determine the exact internal HG for all the >1000 caves of the study area would be an enormous task, and instead a short-cut approach was adopted to gain some understanding of the range of HGs that might apply. The ***minimum*** HG for each cave is recorded automatically in the cave database by simply representing it as the ratio of vertical range (VR) to the total cave length (i.e. VR/LENG.), expressed as a percentage. For a simple cave tube that has one upper and one lower entrance, this value equals exactly the correct HG (which is defined here as the ratio of the hydraulic head to the path length along a tube), because total cave length is represented by the sum of the survey legs, which therefore includes twists and turns along the passage, and upward and downward sections along their slopes. Alternative passages increase the measured total cave length in more complex caves and so reduce the value of the HG calculated by this method, giving a minimum HG (assuming that the head remains equal to the VR). However, as shown in section 5.2.5, over half the caves of the study area are of the single passage types, and probably most of the others do not have a true HG that is more than a factor of 2 or 3 greater than this calculated value. Hence, it is hoped that this easy method of estimation gives consistent results of practical utility. From its definition, HG can range from 0% for a horizontal tube of any length up to 100% for a vertical shaft of any depth. However, the calculated minimum HG is not related to the HG that would apply if a cave was submerged totally below water during some stages of the glacial cycle, as discussed in Chapter 8.	%
C	Caves	n	The number of explored and adequately-reported carbonate caves. (1 per utilised reference).	
		-	If blank, the cave is not represented in totals and summaries.	
SE	Sink Entrance	n	The number of such entrances, including places where daylight is visible. Entrances within the same doline are counted as separate entrances.	
RE	Resurgence Ent.	n	The number of such entrances, including places where daylight is visible. Entrances within the same doline are counted as separate entrances.	
DE	Relict (Dry) Ent.	n	The number of such entrances, including places where daylight is visible. Entrances within the same doline are counted as separate entrances.	

Heading	Meaning	Value	Comments	Units
CS	Cave Streams	n	The maximum number of cave streams flowing in the cave during normal summer discharges, including tributaries, roof inlets, impenetrable inlets and presumed flows at apparently static sumps. Active caves have n>0.	
RC	Relict Cave	CS=0	The whole cave is normally dry in summer	
SP	Sump Pools	n	The number of sump pools in the cave. (2 for a sump explored at each end). A sump pool is defined here as the place where the roof of a cave passage descends below normal water level in July and August. More of the passage may 'sump' during spring melt between April and June, and during floods. Some sumps near entrances dry out in winter. Each sump pool is active, i.e. it has a visible water flow, unless noted separately as a static sump. Very few of the many sumps have been dived, especially in Norway.	
Ch	Chambers:	n	The number of significant internal chambers in the cave that are large compared to passage dimensions, excluding entrance chambers.	
		0	The cave does not contain such a chamber.	
Sh	Shafts	n	The number of significant vertical or near vertical shafts in the cave, including relict entrance shafts, but excluding pitches along vadose passages and at sink entrances. The value includes all other explored and unexplored avens and pits.	
		0	The cave does not contain avens or pits.	
BC	Boulder Chokes	n	The number of internal chokes of boulders or large blocks of bedrock in the cave, excluding at entrances and where daylight is visible. Each such choke hinders or prevents further exploration	
		0	The cave does not contain any boulder chokes.	
Sh	Shafts	n	The number of significant vertical or near vertical shafts in the cave, including relict entrance shafts, but excluding pitches along vadose passages and at sink entrances.	
RV	Relict Vadose	n	The number of apparently abandoned vadose passages in the cave, as observed during normal summer discharges. The value may include vadose-appearing entrances, where the stream has sunk underground upstream of the explorable cave.	
		0	The cave does not contain apparently relict vadose passages.	
MV	Mainly Vadose	1	The cave passages appear to have developed primarily under vadose conditions, including active phreatic sections without relict upper levels, and short, mainly submerged, caves. Commonly only applies to cave types S,a,b,c,d and Hy, and only if CR>0.	
		0	The cave contains relict phreatic passages or phreatic upper levels.	
DC	Chemical Deposits	1	The cave is reported to contain significant stalactite and / or stalagmite growth.	
		0	The cave contains little speleothem growth, or none has been reported.	
FS	Fluvial Sediments	1	The cave is reported to contain significant fluvial sediments	
		0	The cave is reported to contain little fluvial sediments	
		-	The cave report is silent about fluvial sediments	
P	Personally visited	1	The cave has been visited Personally by the author, at least to the entrance.	
		-	The cave has not been visited by the author	
SG	Survey Grade	n	The Survey Grade represents the BCRA grade for each published or available cave survey used in this thesis.	

APPENDIX C3

NORTH CENTRAL NORWAY CAVE DATABASE

UPPERMOST ALLOCHTHON: Helgeland Nappe Complex: Zone 1 (Coastal Area): TOTALS

	ALT.			LST.	LST.	OW	EXT.	OTHER	R	T	GS	CL	KT	SR	OR	CA	REF.	CAVE	CT	LENG.	VR	XS	VOL.	Min.	C	SE	RE	DE	CS	SP	Ch	Sh	BC	RV	MV	DC	FS	P	SG	PRIME
				STRIKE	DIP		COLOUR	INT. ROCK									NO.	NAME						HG %																REFERENCES
Totals	###				##	####			0	0						###			31	##	####	195	##	4	0	0	4	0	0	0	0	0	0	0	0	0	0	4	
Av. per cave	24				23	1000			0.0	0.0						0.1			8	2	5.5	49	34		0.0	0.0	1.0	0.0	0.0	0.0	0.0	0.0	0.0	0.0	0.0	0.0	1.0	
Minima	20				20	1000										0.10			4	2	2.0	11	18		0	0	1	0	0	0	0	0	0	0				
Maxima	25				30	1000										0.1			11	3	15.0	150	50		0	0	1	0	0	0	0	0	0	0				

(Dip measured in 4 caves)

Glacial Situations:

	#	Length
C	4	31
D	0	0
E	0	0
G	0	0
H	0	0
K	0	0
L	0	0
S	0	0
T	0	0
U	0	0
Totals	4	31

Karst Types:

	#	Length
V	0	0
A	0	0
L	4	31
C	0	0
X	0	0
Totals	4	31

Cave Locations:

	#	Length
C	4	31
F	0	0
W	0	0
R	0	0
S	0	0
G	0	0
P	0	0
Totals	4	31

Cave Types:

	#	Length
S	0	0
a	0	0
b	0	0
c	0	0
d	0	0
e	0	0
f	0	0
g	0	0
h	0	0
Hy	1	6
I	0	0
J	0	0
L	3	25
R	0	0
T	0	0
Totals	4	31

Relict Caves:

#	Length
4	31

MV Caves:

#	Length
0	0

Combination Caves:

#	Length
0	0

UPPERMOST ALLOCHTHON: Helgeland Nappe Complex: Zone 1 (Coastal Area)

Caves are grouped by carbonate outcrop

Western catchment area

	ALT.			LST.	LST.	OW	EXT.	OTHER	R	T	GS	CL	KT	SR	OR	CA	REF.	CAVE	CT	LENG.	VR	XS	VOL.	Min.	C	SE	RE	DE	CS	SP	Ch	Sh	BC	RV	MV	DC	FS	P	SG	PRIME
				STRIKE	DIP		COLOUR	INT. ROCK									NO.	NAME						HG %																REFERENCES
Vega			**1726 II**																																					
Brønnøysund			**1725 I**																																					
UN	6995	4625	160 Sømna Bjøru	Littoral cave, not in limestone						(I)								**Holinn Hullet**	(L)	L 150		VR 10																	1	1	Unpublished. TF96
UN	6505	5605	138 Brønnøy Torghatten	Littoral cave, not in limestone						(I)								**Torghattenhullet**	(L)	L 160		VR 51																	1		St.P & St.P 1980. Sjøberg 1988
Velfjord			***1825 IV***																																					
UN	*7140*	*6405*	20 Brønnøy	Brønnøysund	35	30 W	1000			0	0	C	C	L	U	P	0.10	**F'ball Pitch Ca.A**	L	4	2	3.0	12	50	1	0	0	1	0	0	0	0	0	0	0	0	0	1	1	St.Pierre & St.Pierre 1980.TF00
UN	*7127*	*6409*	25 Brønnøy	Brønnøysund	135	20 S	1000			0	0	C	C	L	U	P	0.10	**F'ball Pitch Ca.B**	Hy	6	2	2.0	11	36	1	0	0	1	0	0	0	0	0	0	0	0	0	1	1	St.Pierre & St.Pierre 1980.TF00
UN	*7127*	*6408*	25 Brønnøy	Brønnøysund	135	20 S	1000			0	0	C	C	L	U	P	0.10	**F'ball Pitch Ca.C**	L	11	2	2.0	22	18	1	0	0	1	0	0	0	0	0	0	0	0	0	1	1	St.Pierre & St.Pierre 1980.TF00
UN	*7128*	*6406*	25 Brønnøy	Brønnøysund	135	20 S	1000			0	0	C	C	L	U	P	0.10	**F'ball Pitch Ca.D**	L	10	3	15.0	150	30	1	0	0	1	0	0	0	0	0	0	0	0	0	1	1	St.Pierre & St.Pierre 1980.TF00
Sandnesjøen			**1827 III**																																					No known refs.
Tjøtta			**1826 IV**																																					No known refs.
Vevelstad			***1826 III***																																					
UN	*7428*	*7208*	54 Brønnøy Mosfjell	Littoral cave, not in limestone						(M)								**Cave at Mo**	(L)	L 16 + 25		VR 14																	1	1	TF00
UN	*7412*	*7061*	58 Brønnøy Mosfjell	Littoral cave, not in limestone						(M)								**Cave near Tiksm**	(L)	L 38		D c.10																	1	1	TF00
UN	*774*	*689*	147 Brønnøy Skåren	Littoral cave, not in limestone						(I)								**Mons Hola**	(L)	L160		VR 25																	1	1	Pettersen 1980.Sjøberg 88.TF96
Velfjord			**1825 IV**																																					No known refs.

UPPERMOST ALLOCHTHON: Helgeland Nappe Complex: Zone 2 (Fjord Area): TOTALS

External Cave Attributes

	UTM COORDS	ALT.	KOMMUNE	AREA	LST. STRIKE	LST. DIP	CW	EXT. COLOUR	OTHER INT. ROCK	R	T	GE	CL	KT	SR	OR	CA	REF. NO.	CAVE NAME
Totals		###				###	####			115	0						###		
Av. per cave		182				57	244			0.7	0.0						2.0		
Minima		3				5	5										0.01		
Maxima		580				90	1200										40.0		

Internal Cave Attributes

	CT	LENG.	VR	XS	VOL.	Min. HG %	C	SE	RE	DE	CS	SP	Ch	Sh	BC	RV	MV	DC	FS	P	SG	PRIME REFERENCES
Totals		10686	###	#####	50635	####	165	60	36	##	##	78	19	70	41	13	62	10	62	79		
Av. per cave		66	7.7	3.8	308	22		0.4	0.2	0.9	0.8	0.5	##	0.4	0.2	0.1	0.4	0.1	0.4	0.5		
Minima		2	1	1.0	3	3		0	0	0	0	0	0	0	0	0						
Maxima		899	53	31.5	5394	100		2	2	6	4	5	4	7	2	2						

(Dip measured in 43 caves)

Glacial Situations:

	#	Length
C	10	162
D	13	478
E	51	4283
G	26	1449
H	28	2124
K	17	1525
L	20	865
S	0	0
T	0	0
U	0	0
Totals	165	10686

Karst Types:

	#	Length
V	25	1355
A	115	7065
L	12	2117
C	0	0
X	13	349
Totals	165	10686

Cave Locations:

	#	Length
C	10	162
F	67	3320
W	38	2472
R	16	1520
S	7	1043
G	27	2369
P	0	0
Totals	165	10686

Cave Types:

	#	Length
S	9	96
a	59	1061
b	41	1963
c	10	738
d	11	1021
e	3	986
f	3	457
g	8	1257
h	9	2859
Hy	7	380
I	0	0
J	0	0
L	3	32
R	0	0
T	2	36
Totals	165	10686

Relict Caves:

#	Length
45	1696
45	1696

MV Caves:

#	Length
62	1653
62	1653

Combination Caves:

#	Length
58	7636

UPPERMOST ALLOCHTHON: Helgeland Nappe Complex: Zone 2 (Fjord Area)

Caves are grouped by carbonate outcrop

UTM COORDS	ALT.	KOMMUNE	AREA	LST. STRIKE	LST. DIP	OW	EXT. COLOUR	OTHER INT. ROCK	External Cave Attributes: R	T	GE	CL	KT	SR	OR	CA	REF. NO.	CAVE NAME	Internal Cave Attributes: CT	LENG.	VR	XS	VOL.	Min. HG %	C	SE	RE	DE	CS	SP	Cb	Sb	SC	RV	MV	DC	FS	P	SG	PRIME REFERENCES
Brønnøysund		**1725 I**																																					**No known refs.**
Austra		**1725 II**																																					
UN 6207 3505	12	Sømna	Vennesund			200	White		0	0	C	C	X	X	P	0.1		Olaf's Kilden	a	4	2	1.5	6	50	1	0	1	0	1	1	0	0	0	0	1	0	1	1	1	TF00
																		cave		On mountain west of Vennesund?																		A. Rasmussen pc 1998
Sandnesjøen		**1827 III**																																					**No known refs.**
Tjøtta		***1826 IV***																																					* Passable boulder choke
UP *8485 1305*	64	Alstahaug	Seven Sisters	50	60 N	200	White		1	0	E	F	A	N	P	2.0		Sevikgr. (=Svarthullet?	h	400	10	2.0	800	3	1	0	0	2	1	0	0	1	1	1	0	0	1	1	3	Ive 1980. A.Rasmussen pc 98.TF97.*
UP *8510 1305*	130	Alstahaug	Seven Sisters	70	N	200			1	0	H	F	A	N	P	2.0		Trankt Bekkegr.	b	30	*5*	*1.0*	*30*	17	1	1	0	0	1	0	0	*0*	*0*	*0*	1	0	0	0		Schnæder 1983
UP *8575 1330*	362	Alstahaug	Seven Sisters	65	70 N	200	White	Schist	1	0	L	F	A	N	P	0.5		Grotte Aug. 82	e	*60*	*40*	*3.0*	*180*	67	1	0	0	2	0	0	0	1	2	*0*	0	1	1	1		Schnæder 1983. TF97
UP *857 126*	320	Alstahaug	Seven Sisters		N	*100*			1	0	L	R	A	N	P	1.0		Skredhullet	d	*100*	*20*	*2.0*	*200*	20	1	1	0	0	1	0	0	0	*0*	*0*	0	0	1	0		Ive1980. How long?
UP *857 125*	325	Alstahaug	Seven Sisters		N	*100*			1	0	L	R	A	N	P	1.0		Sink pothole	a	*15*	10	2.0	30	67	1	1	0	0	1	0	0	0	0	0	0	0	1	0		Ive 1980
UP *856 126*	325	Alstahaug	Seven Sisters															Doline med trekk																				Schnæder 1983
UP 85x 115		*Alstahaug*	*Seven Sisters*															*Svarthullet*		*UH List: L270*																			*Helland 1907. p205*
Vevelstad		***1826 III***																																					
UN *8620 9315*	10	Vevelstad	Visten (S)			*10*			1	0	C	C	V	N	A	1.0	VN1	Vistnesoddgrotta	L	6	2	4.0	24	33	1	0	0	1	0	0	0	0	0	0	0	0	0	1	1	Faulkner&Newton 1995. Sea cave?
UN *8860 8650*	40	Vevelstad	Visten (S)		E	100			1	0	E	W	A	D	P	0.5	VL1	Langklagrotta	b	18	4	2.0	36	22	1	0	0	2	0	0	0	2	0	0	0	0		0		Faulkner&Newton 1995
UN *8790 8475*	140	Vevelstad	Visten (S)		E	200			1	0	H	F	A	N	P	2.0	VL2	Staulangrotta	b	10	1	1.0	10	10	1	0	1	0	1	1	0	0	0	0	1	0		1	1	Faulkner&Newton 1995
UN *8795 8440*	210	Vevelstad	Visten (S)	30	E	200			1	0	H	S	A	U	P	1.0	VL3	Dry Waterfall Cave	a	60	5	4.0	240	8	1	1	0	0	1	1	0	0	0	0	0	0	1	1	1	Faulkner&Newton 1995
UN *8795 8440*	205	Vevelstad	Visten (S)	30	E	200			1	0	H	S	A	U	P	1.0	VL4	Dry Waterfall Res.	a	17	2	4.0	68	12	1	0	1	0	1	1	0	0	0	0	0	0	1	1	1	Faulkner&Newton 1995
UN *863 847*	300	Vevelstad	Visten (S)			1200			1	0	L	W	X	X	X	0.5	VT1	cave	a	6	3	1.5	9	50	1	0	0	1	0	0	0	0	0	0	0	0		0		Faulkner&Newton 1995
UN *858 845*	280	Vevelstad	Visten (S)			1200			1	0	L	F	X	X	X	1.0	VT2	Sprutten Res. Cave	a	6	*1*	1.0	6	17	1	0	1	0	1	0	0	0	0	0	*1*	0		0		Faulkner&Newton 1995
UN *8455 8020*	350	Vevelstad	Klausmarkdal			5			1	0	L	W	V	N	O	1.0		Svanlake Cave	b	30	10	4.0	120	33	1	1	0	3	1	1	0	3	0	0	0	0		1	1	Faulkner&Newton 1995
UN *8615 8135*	330	Vevelstad	Klausmarkdal			300			1	0	L	W	V	N	P	0.3		Nilsiltindgrotta	b	8	1	2.0	16	13	1	0	0	2	1	0	0	1	1	0	0	0		1	1	Faulkner&Newton 1995
UN *8610 8110*	310	Vevelstad	Klausmarkdal			300			1	0	L	W	V	N	P	0.5		Storhaugvatngr.	a	19	10	2.0	38	53	1	1	0	0	1	0	0	0	0	0	1	0		1	1	Faulkner&Newton 1995
UN *8620 8010*	180	Vevelstad	Klausmarkdal			250			1	0	H	R	V	N	P	0.7		Trap Cave	b	105	20	2.0	210	19	1	1	0	1	1	0	0	0	0	1	1			1	3	Faulkner&Newton 1995. Moonmilk
UN *8625 7980*	160	Brønnøy	Klausmarkdal			250			1	0	H	W	V	N	P	2.0		Green Gorge Cave	g	60	12	4.0	240	20	1	0	1	0	1	2	0	2	1	0	0	1		1	3	Faulkner&Newton 1995
UN *8625 7980*	180	Brønnøy	Klausmarkdal			250			1	0	H	W	V	N	P	2.0		Cave Above	S	7	3	3.0	21	43	1	1	0	0	1	0	0	0	1	0	0	0		0	1	Faulkner&Newton 1995
UN *8630 7955*	180	Brønnøy	Klausmarkdal	180	90	250			1	0	H	W	V	N	P	1.5		Twin Stream Cave	d	106	12	2.0	212	11	1	0	0	1	2	0	0	0	0	1	0	0	1	1	2	Faulkner&Newton 1995
UN *8645 7925*	140	Brønnøy	Klausmarkdal			300			1	0	E	F	V	N	P	1.0		Marble Arch Sink	a	3	3	9.0	27	100	1	1	0	1	1	0	0	0	1	0	0	0	1			Faulkner&Newton 1995
UN *8650 7866*	167	Brønnøy	Klausmarkdal		75 E	300			1	0	H	R	A	N	P	1.5		JOBshullet	h	320	46	4.0	1280	14	1	1	0	4	1	1	1	7	0	0	0	1		1	3	Faulkner&Newton 1995
UN *8657 7851*	131	Brønnøy	Klausmarkdal	170	60 E	300			1	0	E	R	A	N	P	1.5		Klausmarkgrotta	h	230	11	6.0	1380	5	1	0	0	1	1	3	0	2	0	0	0	1	1	1	3	Faulkner&Newton 1995
UN *8655 7842*	123	Brønnøy	Klausmarkdal		E	300			1	0	E	F	A	N	P	1.5		Klausmark Res. Ca.	h	93	17	4.0	372	18	1	0	1	2	1	2	0	2	0	0	0	0		1	3	Faulkner&Newton 1995
UN *8655 7842*	120	Brønnøy	Klausmarkdal		E	300			1	0	E	F	A	N	P	1.5		Through Cave	b	10	2	3.0	30	20	1	1	1	0	1	0	0	0	0	0	0	0		1	1	Faulkner&Newton 1995
UN *9098 6675*	380	Brønnøy	Bulandsdal	170	90	15			1	0	K	F	V	N	P	2.0	B0	Ø. Bulandsdalgrotta	c	58	8	3.0	174	14	1	1	0	0	1	0	1	0	1	0	0	0	1	1	1	Faulkner&Newton 1995
UN *9065 6705*	345	Brønnøy	Bulandsdal			15			1	0	K	F	V	N	P	2.0	B1	Resurgence Cave	a	12	1	1.0	12	8	1	0	1	0	1	0	0	0	0	0	1	0	0	1		Faulkner&Newton 1995
UN *9060 6720*	340	Brønnøy	Bulandsdal	160	90	15			1	0	K	F	V	N	P	2.3	B2	Bulandsdalgrotta	e	326	11	3.0	978	3	1	1	0	2	1	0	1	0	0	0	0	0	1	1	3	Faulkner&Newton 1995
UN *9056 6738*	330	Brønnøy	Bulandsdal														B3	Wayne's Exit		As B2																		Faulkner&Newton 1995
UN *9050 6740*	335	Brønnøy	Bulandsdal														B4	Tributary Res.																				Faulkner&Newton 1995
UN *9052 6745*	325	Brønnøy	Bulandsdal														B5	sink																				Faulkner&Newton 1995
UN *9045 6755*	300	Brønnøy	Bulandsdal			15			1	0	K	F	V	N	P	2.8	B6	Valleyside Cave	d	35	7	10.0	350	20	1	0	1	0	1	1	0	1	1	0	0	0	1	1	1	Faulkner&Newton 1995
UN *9040 6765*	260	Brønnøy	Bulandsdal		W	20			1	0	K	W	A	D	P	3.0	B7	Bulandselvgrotta	b	176	29	2.0	352	16	1	0	1	0	1	0	1	0	0	0	0	0		1	3	Faulkner&Newton 1995
UN *9045 6770*	300	Brønnøy	Bulandsdal	150	80 W	20			1	0	K	W	A	D	P	1.5	B7a	Two Bridges Cave	h	395	36	3.0	1185	9	1	0	0	2	0	0	0	0	0	0	0	0	1	1	3	Faulkner&Newton 1995
UN *9035 6775*	270	Brønnøy	Bulandsdal		W	20			1	0	K	W	A	D	P	1.5	B8	Shakehole Cave	b	100	20	8.0	800	20	1	1	0	0	2	0	0	0	1	0	0	0	1	0	2	Faulkner&Newton 1995
UN *9035 6780*	280	Brønnøy	Bulandsdal		*W*	20			1	0	K	W	*A*	*D*	P	1.5	B9	Next up Cave	a	53	5	*3.0*	159	9	1	1	0	0	1	0	0	0	0	0	*1*	0		0		Faulkner&Newton 1995
UN *9033 6785*	270	Brønnøy	Bulandsdal		*W*	20			1	0	K	W	*A*	*D*	P	1.5	B10	Hornet Pot	g	160	36	4.0	640	23	1	1	0	0	1	1	1	1	0	0	0	0		1	3	Faulkner&Newton 1995
UN *9033 6785*	270	Brønnøy	Bulandsdal		*W*	20			1	0	K	W	*A*	*D*	P	1.5	B11	Hornet Hole	b	25	3	*2.0*	50	12	1	1	0	1	1	0	0	0	0	0	1	0		0	1	Faulkner&Newton 1995
UN *9025 6790*	230	Brønnøy	Bulandsdal														B12	Billberry Sink																				Faulkner&Newton 1995
UN *9030 6770*	220	Brønnøy	Bulandsdal														B13	Wet Sink Entrance																				Unexplored. Faulkner&Newton 1995
UN *9025 6775*	210	Brønnøy	Bulandsdal														B14	Rising																				Faulkner&Newton 1995

UPPERMOST ALLOCHTHON: Helgeland Nappe Complex: Zone 2 (Fjord Area) — **Caves are grouped by carbonate outcrop** — **Western catchment area**

UTM COORDS			ALT.	KOMMUNE	AREA	LST. STRIKE	LST. DIP	GW	EXT. COLOUR	OTHER INT. ROCK	External Cave Attributes: R	T	GE	GL	KT	SR	OR	CA	REF. NO.	CAVE NAME	Internal Cave Attributes: CT	LENG.	VR	XS	VOL.	Min. HB %	C	SE	RE	DE	CS	SP	CN	SN	BC	RV	MV	DC	FS	P	SG	PRIME REFERENCES
Vefsfjord				***1826 IV***																																						
UN	7900	5910	270	Brønnøy	Sæterfjell		S	150			1	0	L	W	A	U	A	0.2	SA5	Sæterfjell Resurgence	a	10	1	1.0	10	10	1	0	1	0	1	1	0	0	0	0	1	0		0		Newton 1999
UN	7890	5910	300	Brønnøy	Sæterfjell		S	150			1	0	L	W	A	U	A	0.2	SA6	Snowplug Sink	a	21	8	1.0	21	38	1	1	0	0	1	0	0	0	0	0	1	0		0	2	Newton 1999
UN	7880	5910	300	Brønnøy	Sæterfjell		S	150			1	0	L	W	A	U	A	0.2	SA7	Sæterfjellhullet	d	180	20	1.5	270	11	1	1	0	0	2	1	2	0	1	0	1	0		0	2	Newton 1999
UN	7875	5910	300	Brønnøy	Sæterfjell		S	150			1	0	L	W	A	U	A	0.2	SA8	Slab Sink	a	8	3	1.0	8	38	1	1	0	0	1	0	0	0	0	0	1	0		0		Newton 1999
UN	7870	5910	295	Brønnøy	Sæterfjell		S	150			1	0	L	W	A	U	A	0.2	SA9	Keyhole Sink	a	8	2	1.0	8	25	1	1	0	0	1	0	0	0	0	0	1	0		0		Newton 1999
UN	7910	5900	350	Brønnøy	Sæterfjell														SA11	Suicide Resurgence																					Newton 2002
UN	7900	5900	355	Brønnøy	Sæterfjell		S	150			1	0	L	W	A	U	A	0.2	SA12	Suicide Pot	S	15	9	2.0	30	60	1	0	0	1	1	0	0	1	1	0	0	0		0	1	Newton 2002
UN	7890	5890	420	Brønnøy	Sæterfjell		S	150			1	0	L	W	A	U	A	0.2	SA13	Lost Sink 2	a	5	3	1.0	5	60	1	1	0	0	1	0	0	0	0	0	1	0		0		Newton 2002
UN	7880	5885	450	Brønnøy	Sæterfjell		S	150			1	0	L	W	A	U	A	0.2	SA14	Lost Sink 1	a	5	3	1.0	5	60	1	1	0	0	1	0	0	0	0	0	1	0		0		Newton 2002
UN	7790	5860	580	Brønnøy	Sæterfjell		E	150			1	0	L	W	A	U	A	0.01	SA15	Summit Shafts	S	10	5	1.0	10	50	1	0	0	2	0	0	0	2	0	0	0	0		0		Newton 2002
UN	77x	58x		Brønnøy	Sæterfjell															caves		South of Sæterfjell																			Vevelstad Kommune pc 1998
UN	7930	5900	290	Brønnøy	Sæterfjell		S	200			0	0	L	R	A	N	O	0.25	SA1/2	Klimpengrotta	f	225	25	2.0	450	11	1	2	0	0	4	0	0	0	0	0	0	1	0	2	Newton 1999
UN	7930	5895	290	Brønnøy	Sæterfjell		S	200			0	0	L	R	A	N	O	0.25	SA3	Lidi Klimpengrotta	c	128	13	2.0	256	10	1	2	0	0	4	0	0	0	0	0	0	1	0	2	Newton 1999
UN	7930	5895	290	Brønnøy	Sæterfjell		S	200			0	0	L	R	A	N	O	0.25	SA4	choked sink	a	6	2	1.0	6	33	1	1	0	0	1	0	0	0	0	0	1	0	1	0	2	Newton 1999
UN	*809*	*588*	40	Brønnøy	Sæterfjell		E	300			1	0	E	F	A	N	A	3.0	SA10	Halsengrotta	a	10	*3*	*4.0*	*40*	30	1	0	0	2	0	0	0	0	0	0	0	0		0		Nilsson1967. Lundin, pc to DStP 86
UN	*7560*	*5155*	250	Sømna	Fjelldal		*E*	200			1	0	G	W	A	N	P	1.5	F1	Lisivatngrotta (ULC)	g	256	18	4.0	1024	7	1	1	0	2	0	*1*	0	0	0	0	0	0		0	3	Newton 1999
UN	*7530*	*5110*	210	Sømna	Fjelldal		*E*	200			1	0	G	F	A	N	P	1.0	F2	Marsh Sink	d	34	2	1.5	51	6	1	1	0	0	1	1	0	0	0	1	0	0		0	2	Newton 1999
UN	*7515*	*5130*	215	Sømna	Fjelldal		*E*	200			1	0	G	F	A	N	P	3.5	F3	Dry Vall. Dol. Res. Cave	g	60	5	2.0	120	8	1	0	1	1	1	1	0	0	0	0	0	0		0	2	Newton 1999
UN	*7515*	*5130*	215	Sømna	Fjelldal		*E*	200			1	0	G	F	A	N	P	3.5	F4	Dry Vall. Dol. Mid. Cave	a	5	2	1.0	5	40	1	1	0	0	1	1	0	0	1	0	1	0		0	1	Newton 1999
UN	*7515*	*5130*	215	Sømna	Fjelldal		*E*	200			1	0	G	F	A	N	P	3.7	F5	Dry Vall. Dol. Sink Cave	b	134	25	5.0	670	19	1	0	0	2	1	1	0	0	1	1	0	0		0	2	Newton 1999
UN	*7515*	*5140*	205	Sømna	Fjelldal		*E*	200			1	0	G	F	A	N	P	3.7	F6	Dry Valley Cave	a	50	*20*	*10.0*	*500*	40	1	0	0	2	0	0	0	0	1	0	0	0		0		St. Pierre 1977. Newton 1999
UN	*7515*	*5150*	195	Sømna	Fjelldal		*E*	200			1	0	G	F	A	N	P	4.0	F7	Robber's Cave	a	33	*10*	*2.0*	*66*	30	1	0	0	1	0	0	0	0	1	0	0	0	1	0		St. Pierre 1977. Newton 1999
UN	*7515*	*5160*	190	Sømna	Fjelldal		*E*	200			1	0	G	F	A	N	P	4.0	F8	Engelv Resurgences	c	40	*2*	*3.5*	*140*	5	1	0	2	0	1	1	0	0	0	0	1	0		0		St. Pierre 1977. Newton 1999
UN	*7700*	*5385*	140	Sømna	Fjelldal		*E*	*100*			1	0	D	F	A	N	P	0.5	F9	Hattenhullet	S	8	8	*10.0*	*80*	100	1	0	0	1	0	0	0	0	1	0	0	0		0		Newton 1999
UN	*7670*	*5255*	80	Sømna	Fjelldal														F10	east valley resurgence																					Newton 1999
UN	*8140*	*5530*	110	Brønnøy	Holåsen		*E*	250			1	0	E	F	A	N	P	0.05	HO1	crawl	a	19	3	2.0	38	16	1	0	0	3	1	0	0	0	0	0	0	0		0	2	Newton 1999
UN	*8140*	*5510*	135	Brønnøy	Holåsen		*E*	250			1	0	E	F	A	N	P	0.03	HO2	Lower Keyhole Cave	b	12	2	2.0	24	17	1	0	0	2	1	0	0	0	2	0	0	0		0	2	Newton 1999
UN	*8140*	*5510*	135	Brønnøy	Holåsen		*E*	250			1	0	E	F	A	N	P	0.03	HO3	Keyhole Cave	b	27	3	2.0	54	11	1	0	0	1	1	0	0	0	1	0	0	0		0	2	Newton 1999
UN	*8140*	*5510*	135	Brønnøy	Holåsen		*E*	250			1	0	E	F	A	N	P	0.03	HO4	Upper Keyhole Cave	b	44	4	2.0	88	9	1	0	0	4	1	0	0	0	0	0	0	0		0	2	Newton 1999
UN	*8180*	*5410*	40	Brønnøy	Holåsen		*E*	250			0	0	E	F	A	N	P	3.5	HO5	Bordvikgrotta	L	5	4	10.0	50	80	1	0	0	1	0	0	0	0	0	0	0	0		1		Newton 1999
UN	*8200*	*5274*	185	Brønnøy	Navan															Cleft Sink																					TF00
UN	*8115*	*5262*	155	Brønnøy	Navan															Rockwall Sink																					TF00
UN	*8110*	*5271*	155	Brønnøy	Navan	*90*	*30*	*N*	400	V. coarse	ms, a	0	0	E	G	L	N	O	1.0		Nordlysgrotta	e	*600*	*30*	*8.0*	4800	5	1	0	0	1	1	1	0	1	1	*1*	0	0	1	1	3	TF97. TF00. Surveyed as 423m:SN04.
UN	*8111*	*5266*	138	Brønnøy	Navan	*90*	*30*	*N*	400		a	0	0	E	G	L	N	O	1.0		Marinmyrgrotta	d	*400*	*10*	*10.0*	4000	3	1	0	0	1	1	1	0	0	0	*0*	0	0	1	1	3	TF00. Surveyed as 611m: SN04.
UN	*8131*	*5271*	110	Brønnøy	Navan															Masterstonglia Res. Ca.		Tight 4m-long tube above rising																					TF00. SN04.
UN	*8105*	*5230*	121	Brønnøy	Navan															Tadpole Cave		Low resurgence entrance with tadpoles, >4m long.																					Unexplored. SN04
UN	*8004*	*5167*	77	Sømna	Skånvik				200			1	0	E	W	X	X	P	3.5		Skånvikgrotta	Hy	58	25	24.9	1444	43	1	0	1	0	1	0	0	1	0	0	0	0	1	1	3	Incompl .Helland(1907,p200).TF00
UN				Brønnøy	Hallaraunet																																				St.Pierre & St.Pierre 1980
UN	*826*	*560*	70	Brønnøy	Annbukta															Svedhuis		30 m cave to be quarried away.																					A. Rasmussen pc 1998
UN	*842*	*552*	30	Brønnøy	Annbukta															many holes		and 30m cave outside quarry area																					AR and M. Solbakk pc 1998
UN	*8225*	*4590*	150	Brønnøy	Svartdal	*25*	*80*	E	200			0	0	E	G	A	N	P	0.5	SV9	Tourist Cave	g	315	20	3.0	945	6	1	1	1	2	1	2	0	4	1	*1*	0	1		0	3	Newton 1999
UN	*8510*	*5610*	25	Brønnøy	Naustvik			N	250			1	0	C	C	A	N	P	0.2		Hellaren	*a*	*5*	*2*	*3.0*	15	40	1	0	0	2	0	0	0	0	0	0	0	0		2		StP & StP 1980. Hoel 1906. *

ms mica schist
a amphibolite

* or littoral?

UPPERMOST ALLOCHTHON: Helgeland Nappe Complex: Zone 2 (Fjord Area)

Caves are grouped by carbonate outcrop

Western catchment area

UTM COORDS			ALT.	KOMMUNE	AREA	LST. STRIKE	LST. DIP		OW	EXT. COLOUR	OTHER INT. ROCK	External Cave Attributes: R	T	GS	CL	KT	SR	OR	CA	REF. NO.	CAVE NAME	Internal Cave Attributes: CT	LENG.	VR	XS	VOL.	Min. HG %	C	SZ	RE	DE	CS	SP	Ch	Sh	SC	RV	MV	DC	PS	P	SG	PRIME REFERENCES
Vestfjord					***1825 IV***	***cont.***																																					
UN	*8120*	*4505*	250	Brønnøy	Svartdal		*40*	*S*	200			0	0	H	G	A	N	P	0.1	SV15	**Black Silt Cave**	a	10	3	*2.0*	20	30	1	0	0	*1*	1	1	0	0	0	0	0	0	1	0	1	Newton, 2002
UN	*8120*	*4505*	250	Brønnøy	Svartdal		*40*	*S*	200			0	0	H	G	A	N	P	0.1	SV16	**Chris's Playpen**	a	10	2	4.0	40	20	1	1	0	0	1	0	0	0	0	0	0	0	1	0	1	Newton 2002
UN	*8120*	*4505*	250	Brønnøy	Svartdal		*40*	*S*	200			0	0	H	G	A	N	P	0.1	SV17	**Cliff Tube**	a	3	*1*	*1.0*	3	33	1	0	0	1	0	0	0	0	0	0	0	0		0		Newton 2002
UN	*8215*	*4485*	180	Brønnøy	Svartdal		25	N	200	White	cs	1	0	H	S	L	D	P	0.25	SV1	**Svartdalgrotta**	h	899	53	6.0	5394	5.9	1	0	0	2	1	2	4	7	1	*1*	0	1	1	1	3	Newton 1999
UN	*8210*	*4485*	190	Brønnøy	Svartdal		5	*N*	200			1	0	H	S	L	D	P	0.7	SV2	**The Black Hole**	h	39	12	4.0	156	31	1	0	0	1	2	2	0	0	0	0	0	0	1	0	2	Newton 1999. 2 Sumps are static
UN	*8225*	*4465*	190	Brønnøy	Svartdal			N	200			1	0	H	S	L	D	P	0.2	SV3	**Midge Pot**	S	10	7	*2.0*	20	70	1	1	0	0	1	0	0	0	0	0	1	0		0		Newton 1999
UN	*8225*	*4465*	190	Brønnøy	Svartdal			N	200			1	0	H	S	L	D	P	0.2	SV4	**Valdskifthullet**	S	15	7	*2.0*	30	47	1	1	0	0	1	0	0	0	0	0	1	0		0	1	Newton 1999
UN	*8255*	*4475*	126	Brønnøy	Svartdal	130	45	N	200	Wh R Bl E	ig	1	0	E	W	A	D	P	0.2	SV5	**Neptune's Cave**	h	433	33	6.0	2598	8	1	0	1	3	1	3	0	3	1	*0*	0	1	1	1	3	Newton 1997 and 1999
UN	*8260*	*4450*	142	Brønnøy	Svartdal	50	40	S	200			1	0	E	W	A	U	P	0.1	SV6	**Barnacle Cave**	a	20	2	2.0	40	10	1	0	0	1	0	0	0	0	0	0	0	0	1	1	1	Newton 1999
UN	*8260*	*4440*	150	Brønnøy	Svartdal			*E*	100			1	0	E	W	*L*	D	P	0.1	SV18	**Midget Cave**	a	54	10	3.0	162	19	1	1	0	0	1	3	2	2	0	0	0	0	1	0	2	Newton 2002
UN	*8275*	*4435*	140	Brønnøy	Svartdal			*E*	100			1	0	E	W	*L*	D	P	0.1	SV19	**Pond Cave**	a	15	2	*3.0*	*45*	13	1	*0*	*0*	*1*	*0*	*0*	0	0	*0*	0	*0*	0		0	2	Newton 2002
UN	*8285*	*4440*	137	Brønnøy	Svartdal	30	20	E	100			1	0	E	W	L	D	P	0.3	SV7	**Draugeneshullet**	h	50	13	4.0	200	26	1	0	0	4	0	0	0	1	1	0	0	0	1	1	2	Newton 1999
UN	*8290*	*4440*	129	Brønnøy	Svartdal	70	20	S	100			1	0	E	W	L	U	P	0.5	SV8a	**Gorge Cave 1**	a	9	4	2.0	18	44	1	0	1	0	1	0	0	0	0	0	1	0	1	1		Newton 1999
UN	*8290*	*4440*	128	Brønnøy	Svartdal			S	100			1	0	E	W	L	U	P	0.5	SV8b	**Gorge Cave 2**	a	11	4	2.0	22	36	1	0	0	2	0	0	0	0	0	0	0	0	1	1		Newton 1999
UN	*8323*	*4442*	60	Brønnøy	Svartdal				200			1	0	E	F	L	*U*	P	1.0	SV20	**Summer Holiday Ca.**	c	15	3	*2.0*	30	20	1	0	0	1	0	0	0	1	0	0	0	0	1	0	1	Newton, 2002
UN	*8350*	*4310*	370	Brønnøy	Nonsdal				*100*			0	0	K	F	X	N	*P*	0.9	SV10	**Upper Rising**	b	25	1	*1.5*	38	4	1	0	1	0	1	0	0	0	0	0	1	0		0		Newton 1999, 2002
UN	*8370*	*4310*	340	Brønnøy	Nonsdal				*100*			0	0	K	F	X	N	*P*	0.9	SV11	**Hag-grotta**	g	54	15	4.0	216	28	1	1	1	0	1	0	0	1	0	0	0	0		0	2	Newton 1999, 2002
UN	*8380*	*4320*	330	Brønnøy	Nonsdal				*100*			0	0	K	F	X	N	*P*	1.0	SV12	**Side Cave**	a	25	2	*2.0*	*50*	8	1	0	1	0	1	0	0	0	0	0	1	0		0		Newton 1999
UN	*8390*	*4330*	300	Brønnøy	Nonsdal															SV13	**resurgence**																					Newton 1999
UN	*8410*	*4330*	290	Brønnøy	Nonsdal				*100*			0	0	K	R	X	N	*P*	0.3	SV14	**Bear Cave**	a	62	6	2.0	124	10	1	0	0	1	0	0	0	0	2	0	0	0	1	0	2	Newton 1999
UN	8350	4495	90	Brønnøy	Hestfjell		*50*	E	150			1	0	E	F	A	N	P	0.7	H1	**Dave's Cave**	a	6	1	*1.5*	*9*	17	1	0	0	1	1	0	1	0	0	0	1	0		0	1	Newton 1999, 2002
UN	8365	4505	105	Brønnøy	Hestfjell		*50*	E	150			1	0	E	F	A	N	P	0.7	H2	**Morning Cave**	d	42	5	4.0	168	12	1	0	0	1	1	2	0	1	0	1	1	0	1	0	2	Newton 1999, 2002
UN	8355	4507	105	Brønnøy	Hestfjell		*50*	E	150			1	0	E	F	A	N	P	0.7	H3	**Tooth Cave**	d	45	5	4.0	180	11	1	0	0	1	1	2	0	1	0	1	1	0		0	2	Newton 1999, 2002
UN	8355	4508	105	Brønnøy	Hestfjell		*50*	E	150			1	0	E	F	A	N	P	0.7	H4	**Canyon Cave**	d	34	6	3.0	102	18	1	1	0	1	1	1	0	2	0	0	1	0		0	2	Newton 1999, 2002
UN	8360	4508	110	Brønnøy	Hestfjell		*50*	E	150			1	0	E	F	A	N	P	0.6	H5	**Evening Cave**	g	50	10	4.0	200	20	1	1	0	1	1	2	0	0	0	0	0	0	1	0	2	Newton 1999, 2002
UN	8345	4515	115	Brønnøy	Hestfjell		*50*	E	150			1	0	E	F	A	N	P	0.5	H6	**Blood Cave**	b	35	4	*2.0*	70	11	1	0	1	0	1	1	0	0	0	1	0		0	1	Newton 1999, 2002
UN	8355	4530	160	Brønnøy	Hestfjell		*50*	E	150			1	0	H	F	A	N	P	0.5	H7	**70 Metre Cave**	b	70	12	3.0	210	17	1	1	1	1	1	0	0	1	0	0	1	0		0	2	Newton 1999, 2002
UN	8355	4520	135	Brønnøy	Hestfjell		*50*	E	150			1	0	E	F	A	N	P	0.4	H8	**Hate Cave**	b	130	15	3.0	390	12	1	1	0	0	1	0	0	0	0	0	0	0		0	2	Newton 1999, 2002
UN	8340	4560	195	Brønnøy	Hestfjell		*50*	E	150			1	0	H	F	A	N	P	0.4	H9	**Top Sink Cave**	a	16	2	*2.0*	32	13	1	1	0	0	1	0	0	0	0	0	1	0		0		Newton 1999, 2002
UN	8338	4558	195	Brønnøy	Hestfjell		*50*	E	150			1	0	H	F	A	N	P	0.4	H10	**H10**	a	16	2	*2.0*	32	13	1	0	0	2	0	0	0	0	0	0	0	0		0	1	Newton 2002
UN	8345	4540	175	Brønnøy	Hestfjell		*50*	E	150			1	0	H	F	A	N	P	0.4	H11	**H11**	a	5	2	*2.0*	*10*	40	1	0	0	1	1	0	0	0	0	0	1	0		0		Newton 2002
UN	*8912*	*4555*	63	Brønnøy	Saus			E	400	White		1	0	E	W	A	D	P	1.5	SS1	**Earshot Sink Cave**	b	52	5	6.0	312	10	1	1	0	0	1	0	0	0	1	0	1	0	1	0	2	Faulkner & Newton 1995
UN	*9040*	*4660*	60	Brønnøy	Saus			E	400			1	0	E	W	A	D	P	0.5	SS2	**Sildhullet**	a	26	*5*	2.0	52	19	1	0	0	1	0	0	0	0	2	0	0	0	1	0	2	Newton 1999
UN	*9010*	*4610*	21	Brønnøy	Saus		80	E	400			1	0	C	C	A	N	P	40.0	SS3	**Oxbow Cave**	b	8	2	2.0	16	25	1	1	1	0	1	0	0	0	0	0	1	0		1	1	Newton 1999
UN	*9060*	*4640*	17	Brønnøy	Saus													P		SS8	**tight rising**																					Newton 1999
UN	*9020*	*4615*	22	Brønnøy	Saus		80	E	400			1	0	C	C	A	N	P	40.0	SS9	**Deep Rising**	a	2	2	4.0	8	100	1	0	1	0	1	1	0	0	0	0	1	0		1		Newton 1999
UN	*861*	*447*	40	Brønnøy	Saus			N	400			1	0	E	G	A	N	P	0.1	SS10	**Gate Cave**	d	30	*2*	*2.0*	*60*	7	1	0	0	3	0	0	0	*0*	*0*	*0*	0	0		0		Newton 1999

UPPERMOST ALLOCHTHON: Helgeland Nappe Complex: Zone 3 (Fjord Area) — Caves are grouped by carbonate outcrop — Western catchment area

UTM COORDs			ALT.	KOMMUNE	AREA	LST. STRIKE	LST. DIP		OW	EXT. COLOUR	OTHER INT. ROCK	R	T	GR	CL	KT	SR	OR	CA	REF. NO.	CAVE NAME	CT	LENGTH	VR	XS	VOL.	Min. HD %	C	SE	RE	DE	CS	SP	Ch	Sh	BC	RV	MV	DC	PS	P	SG	PRIME REFERENCES
Valfjord				**1825 IV**	**cont.**																																					
UN	8535	4290	200	Brønnøy	Rognvardseiv			W	300			0	0	H	F	A	N	P	0.3	R1	Striped Pot	b	35	11	6.0	210	31	1	0	0	1	1	1	1	1	1	1	0	0	1	0	3	Newton 2002
UN	8540	4280	190	Brønnøy	Rognvardseiv			W	300			0	0	H	F	A	N	P	0.3	R2	Pies Pot	S	9	3	2.0	18	33	1	0	0	1	1	0	0	0	0	0	0	1	0	0	1	Newton 2002
UN	8545	4270	185	Brønnøy	Rognvardseiv			W	300			0	0	H	F	A	N	P	0.3	R3	Slippery Cave	f	102	5	3.0	306	5	1	0	0	1	1	5	0	0	0	0	0	1	0	2	Newton 2002
UN	8550	4260	180	Brønnøy	Rognvardseiv			W	300			0	0	H	F	A	N	P	0.3	R4	The Sewer	a	10	1	2.0	20	10	1	1	1	0	1	0	0	0	0	1	0	0		Newton 2002
UN	8560	4260	180	Brønnøy	Rognvardseiv			W												R5	Main Resurgence																					Newton 2002
UN	8550	4370	70	Brønnøy	Rognvardseiv			W	300			0	0	E	G	A	N	P	0.03	R16	Submarine Cave	b	22	2	2.0	44	9	1	0	0	1	1	0	0	1	0	0	0	0	0	2	Newton 2002
UN	8580	4335	55	Brønnøy	Rognvardseiv			W												R14	Arch Cave Res.																					Newton 2002
UN	8580	4330	60	Brønnøy	Rognvardseiv			W	300			0	0	E	F	A	N	P	1.0	R13	Maze Cave	c	90	5	4.0	360	6	1	0	0	6	0	0	0	0	0	0	0	0	0	3	Newton 2002
UN	8580	4330	65	Brønnøy	Rognvardseiv			W	300			0	0	E	F	A	N	P	1.0	R12	Un-named Cave	a	8	2	8.0	64	25	1	0	0	1	0	0	0	0	1	0	0	0	0	3	Newton 2002
UN	8580	4330	60	Brønnøy	Rognvardseiv			W	300			0	0	E	F	A	N	P	1.0	R11	Arch Cave	f	130	10	4.0	520	8	1	0	0	1	1	4	0	4	0	0	0	0	1	0	3	Newton 2002
UN	8580	4330	60	Brønnøy	Rognvardseiv			W	300			0	0	E	F	A	N	P	1.0	R10	Shelf Cave	a	7	2	6.0	42	29	1	0	0	1	0	0	0	0	0	0	0	0	0	0	3	Newton 2002
UN	8580	4330	60	Brønnøy	Rognvardseiv			W	300			0	0	E	F	A	N	P	1.0	R9	Side Cave	b	19	4	4.0	76	21	1	0	0	1	0	0	0	0	1	0	0	0	0	3	Newton 2002
UN	8582	4310	70	Brønnøy	Rognvardseiv			W	300			0	0	E	F	A	N	P	1.0	R8	Terrace Cave	a	15	1	4.0	60	7	1	0	0	2	0	0	0	0	0	0	0	0	0	3	Newton 2002
UN	8580	4320	65	Brønnøy	Rognvardseiv			W	300			0	0	E	F	A	N	P	1.0	R7	Arch Cave Sink	a	25	4	5.0	125	16	1	1	0	0	1	0	0	0	0	0	1	0	0	2	Newton 2002
UN	8580	4315	65	Brønnøy	Rognvardseiv			W	300			0	0	E	F	A	N	P	1.0	R6B	Oxbow Resurgence	a	18	1	2.0	36	6	1	0	1	0	1	0	0	0	0	0	1	0	0	1	Newton 2002
UN	8580	4315	65	Brønnøy	Rognvardseiv			W	300			0	0	E	F	A	N	P	1.0	R6A	Oxbow Sink	a	20	4	2.0	40	20	1	1	0	1	1	0	0	1	1	0	1	0	0	1	Newton 2002
UN	*856*	*425*	185	Bindal	Meinvatn	40		W	300	White		1	0	H	G	A	U	P	1.0	S2	Skytlergravgrotta	b	56	21	4.0	224	38	1	0	0	1	1	0	2	3	0	2	0	0	0	3	Faulkner & Newton 1995
UN	*855*	*425*	190	Bindal	Meinvatn			W	300			1	0	H	G	A	U	P	1.0	S3	Floytehule	b	70	*5*	2.0	140	7	1	1	0	0	1	2	0	0	0	0	1	0	0	1	Faulkner & Newton 1995
UN	*858*	*423*	170	Bindal	Meinvatn			W	300			1	0	H	F	A	N	P	1.2	S4	Ø. Meinvatngrotta	b	20	3	2.0	40	15	1	0	0	1	1	0	0	1	0	0	1	0	0	1	Faulkner & Newton 1995
UN	*857*	*421*	150	Bindal	Meinvatn			W	300			1	0	E	G	A	U	P	1.5	S5	Meinvatn Kilde Hule	b	25	*3*	2.0	50	12	1	0	0	1	1	1	0	*1*	0	0	1	0	0		Faulkner & Newton 1995
UN	*8580*	*4175*	140	Bindal	Meinvatn	50	60	W	300			1	0	E	F	A	N	P	1.8	S6	Meinvatngrotta	g	302	16	8.0	2416	6	1	0	0	4	1	1	0	0	0	1	0	1	1	1	3	Faulkner & Newton 1995
UN				Brønnøy	Akset																																				St.Pierre & St.Pierre 1980
UN				Brønnøy	Bru																																				St.Pierre & St.Pierre 1980
UN				Brønnøy	Straum																																				St.Pierre & St.Pierre 1980
UN				Brønnøy	Rugås																																				St.Pierre & St.Pierre 1980
UN	*8480*	*5930*	60	Brønnøy	Engjavatn			*E*	50			1	0	D	G	A	N	P	1.5		Aunholet	Hy	27	4	4.0	108	15	1	0	1	0	1	2	0	1	0	0	1	0	1	1	St.Pierre 1979
UN			*60*	Brønnøy	Engjavatn			*E*	50			1	0	D	G	A	N	P	*0.2*		Crawl Cave	b	20	*1*	2.0	40	5	1	1	0	0	1	0	0	0	1	0	1	0		0	St.Pierre 1979
UN	*866*	*578*	*20*	Brønnøy	Hegge																Hegge Quarry Cave		Now quarried away																			St.Pierre 1984

External Cave Attributes — Internal Cave Attributes

cs = chlorite schist — ig = igneous origin: micagneiss or alkali felspar granite?

Tarmaunbotnet caves are listed under Tosbton

UPPERMOST ALLOCHTHON: Helgeland Nappe Complex: Zone 2 (Fjord Area)

Caves are grouped by carbonate outcrop — Western catchment area

External Cave Attributes (LST. STRIKE … REF. NO.); Internal Cave Attributes (CT … SG)

UTM COORDS			ALT.	KOMMUNE	AREA	LST. STRIKE	LST. DIP	OW	EXT. COLOUR	OTHER INT. ROCK	R	T	GE	CL	KT	SR	OR	CA	REF. NO.	CAVE NAME	CT	LENG.	VR	XS	VOL.	Min. HG %	C	SE	RE	DE	CS	SP	Ch	Sh	BC	RV	MV	DC	FS	F	SG	PRIME REFERENCES
Terråk				*1825 III*																																						
UN	762	367	50	Bindal	Hovøya															Bear Skull Cave																						AR pc to TLF 1998
UN	845	367	250	Bindal	Tuvfjell															shaft		South of Urdstjorna (or Øvre Urdstjorna?)																				Local report to TLF 1998
UN	9190	3560	320	Bindal	Hongfjell		E	1000			1	0	K	W	A	U	A	0.4	S7	Unscheduled Cave	b	8	2	2.0	16	25	1	0	0	1	0	0	0	0	0	0	0	0		0	2	Faulkner & Newton 1995
UN	9220	3140	3	Bindal	Reppen			400			1	0	C	C	X	X	P	1.0		Johngrotta	a	15	1	1.0	15	7	1	0	0	1	0	0	0	0	0	0	0	0	0	1		Faulkner 1978
UN	9220	3140	0	Bindal	Reppen															Rapsteingrotta																						Helland 1907
UN	9220	3110	400	Bindal	Reppen			400			1	0	K	S	V	N	P	0.7		Rapstein Sink	a	3	2	2.0	6	67	1	0	0	1	0	0	0	0	0	0	0	0		1		Faulkner 1978. On fjord shoulder
UN	9135	2615	190	Bindal	Reppen	40	80 E	600			1	0	G	F	A	N	P	0.6	R1	Reppgrotta	b	50	3	2.0	100	6	1	0	0	1	1	1	0	0	0	0	1	0		1	1	Faulkner 1978
UN	9155	2620	220	Bindal	Reppen		E	600			1	0	G	F	A	N	P	2.0	R2	Oxbow Cave	a	10	1	2.0	20	10	1	1	1	0	1	0	0	0	0	0	1	0		1		Faulkner 1978
UN	9165	2650	240	Bindal	Reppen			600			1	0	G	G	V	N	P	1.8	R3	Reppelvgrotta	c	15	5	5.0	75	33	1	0	0	1	1	1	0	0	0	0	1	0		1	1	Faulkner 1978. Sump is static.
UN	9160	2655	250	Bindal	Reppen			600			1	0	G	G	V	N	P	1.8	R4	Ø. Reppelvgrotta	c	100	5	2.0	200	5	1	0	0	1	1	0	1	0	1	0	0	0	1	1	1	Faulkner 1978
UN	9160	2655	250	Bindal	Reppen			600			1	0	G	G	V	N	P	1.8	R5/6	Arch/Mainstream C.	c	80	4	3.0	240	5	1	0	0	2	2	2	0	0	0	0	1	0	1	1	1	Faulkner 1978
UN	9160	2655	250	Bindal	Reppen	40	90	600			1	0	G	G	V	N	P	1.8	R7	Overflow Cave	c	150	5	2.0	300	3	1	0	0	1	1	2	0	0	0	0	0	0		1	1	Faulkner 1978. 1sump is static.
UN	9160	2655	250	Bindal	Reppen			600			1	0	G	G	V	N	P	1.8	R8	Depression Cave	d	15	3	2.0	30	20	1	0	0	1	1	0	0	0	0	0	1	0		1	1	Faulkner 1978
UN	9160	2665	270	Bindal	Reppen			600			1	0	G	G	V	N	P	1.7	R9	Bone Cave	a	50	3	3.0	150	6	1	0	0	1	0	0	0	0	0	0	0	0	1	1		Faulkner 1978
UN	9200	2900	310	Bindal	Reppen			1000			1	0	K	G	V	N	P	1.5	R10	Top Sink	a	8	4	1.0	8	50	1	1	0	0	1	0	0	0	1	0	1	0	1	1	1	Faulkner 1978
UN	9175	2885	290	Bindal	Reppen			1000			1	0	G	G	V	N	P	1.6	R11	Fir Tree Sink	a	30	4	2.0	60	13	1	1	0	0	1	0	0	0	1	0	1	0	1	0	1	Faulkner 1978
UN	9125	2850	280	Bindal	Reppen			600			1	0	G	F	V	N	P	0.5	R20	Reppfjellgrotta 1	b	70	3	2.0	140	4	1	1	1	1	1	0	0	0	0	0	1	0		1	1	Faulkner 1978
UN	9125	2850	275	Bindal	Reppen			600			1	0	G	F	V	N	P	0.5	R23	Reppfjellgrotta 2	b	45	3	2.0	90	7	1	1	1	2	1	0	0	0	0	0	1	0		1	1	Faulkner 1978
UN	8600	2105	320	Bindal	Stordal			1000			1	0	H	W	V	N	P	0.5		Aunsaetra Hullet	S	14	6	4.0	56	43	1	0	0	1	1	0	0	1	0	0	1	0		1	1	Unpublished TF96
UN	8305	1745	50	Bindal	Stordal	20	70 W	200	Wh+mica	Musc.	0	0	D	G	A	N	P	1.8		Kalkdalgrotta	b	165	16	2.1	330	10	1	0	0	1	0	0	1	0	0	0	0	0	1	1	3	Unpublished TF97
UN	7459	1755	175	Bindal	Svartåsheia			50			1	0	G	G	X	N	X	0.7		Svartås Doline	S	8	5	10.0	80	63	1	1	0	0	1	0	0	0	1	0	1	0		1	1	Unpublished TF97
UN	7459	1757	172	Bindal	Svartåsheia			50			1	0	G	G	X	N	X	0.7		Svartåsgrotta 1	b	30	6	1.5	45	20	1	0	0	1	0	0	0	1	0	0	0	0		1	1	Unpublished TF97
UN	7456	1757	162	Bindal	Svartåsheia															Svartås Rising																						Unpublished TF97
UN	7452	1772	153	Bindal	Svartåsheia			50			1	0	D	G	X	N	X	2.0		Svartåsgrotta 2	a	26	5	2.0	52	19	1	1	0	1	1	1	0	1	0	0	1	0		1	1	Unpublished TF97
UN	7452	1781	145	Bindal	Svartåsheia			50			1	0	D	F	X	N	X	2.0		Jensahola	b	30	5	2.0	60	17	1	0	1	0	1	1	0	0	0	0	1	0		1	1	Unpublished TF97
				Bindal	Tjomlia															cave																						Helland. 1907. p200
										Musc. = muscovite schist																																
Kongsmoen				**1824 IV**																																						No known Refs
Neena				**1827 II**																																						
VP	1771	3610	119	Leirfjord	Randalen	180	60 E	200	Wh/grey/d	ms	1	0	E	G	A	N	P	16.0		Hubrohola	Hy	92	10	6.0	552	11	1	0	0	2	1	1	0	0	0	0	0	0	1	1	3	TF00
										ms = mica schist										Other caves?																						Helgeland leaflet 1992 p18
Tosbotn				*1825 I*																																						
UN	9370	5104	5	Brønnøy	Langfjord		E	100			0	0	C	C	A	U	P	14.0		Tarmaunbotngrotta 1	L	21	4	6.0	126	19	1	0	0	2	1	1	0	0	0	0	0	0		1	1	Unpublished. TF96. Sump is static.
UN	9370	5104	15	Brønnøy	Langfjord		E	100			0	0	C	C	A	U	P	14.0		Tarmaunbotngrotta 2	T	10	2	2.0	20	20	1	0	0	1	0	0	0	0	1	0	0	0		1	1	Unpublished. TF96. Or marine?
UN	9370	5104	20	Brønnøy	Langfjord		E	100			0	0	C	C	A	U	P	14.0		Tarmaunbotngrotta 3	T	26	4	6.0	156	15	1	0	0	1	0	0	0	0	1	0	0	0		1	1	Unpublished. TF96. Or marine?
UN	9347	5202	179	Brønnøy	Langfjord	155	70 E	50			0	0	G	R	A	N	P	0.1		Ø. Langskjellighattengr	b	72	9	7.0	504	13	1	0	0	2	0	0	0	0	0	0	0	0	1	1	1	Hoel, 1907. UH List 1974
UN	9351	5196	185	Brønnøy	Langfjord	155	70 E	50			0	0	G	R	A	N	P	0.1		Sud Langskjellihatteng	b	70	4	2.0	140	6	1	0	0	1	0	0	0	0	0	0	0	1	1	1	1	Unpublished. TF96
UN	9348	5203	167	Brønnøy	Langfjord	155	E	50			0	0	D	R	A	N	P	0.1		L. Langskjellighattengr	c	62	14	8.0	496	23	1	0	0	3	0	0	0	0	0	0	0	0	1	1	1	Hoel, 1907. UH List 1974
UN	940	515		Brønnøy	Langfjord															Elk Trap																						M. Solbakk pc 1996
UN	9375	5130	10	Brønnøy	Langfjord	150	70 E	50			0	0	C	C	A	U	P	2.0		Langfjordgrotta	a	65	9	6.0	390	14	1	0	1	1	1	2	0	0	0	0	0	0		1		St.Pierre&St.Pierre1980. AR pc2000
UN	9415	5010	30	Brønnøy	Langfjord		E	50	Grey / wh		0	0	D	G	A	U	P	0.2		Fjelldalsvatngrotta*	b	12	3	3.0	36	25	1	1	0	0	1	0	0	0	0	0	1	0		1		St.Pierre &St.Pierre 1979
UN	9464	4970	105	Brønnøy	Langfjord	155	E	50			0	0	D	R	A	N	P	0.2		Aunhattenhullet 1	Hy	42	6	31.5	1323	14	1	0	0	1	0	0	0	0	0	0	0	0	1	1	3	Hoel, 1907. St.P & St.P 1980. TF00
UN	9466	4971	116	Brønnøy	Langfjord	155	E	50			0	0	D	R	A	N	P	0.2		Aunhattenhullet 2	Hy	50	5	5.6	280	10	1	0	0	1	0	0	0	0	0	0	0	1	1	1	3	Hoel, 1907. St.P & St.P 1980. TF00
UN	9466	4967	132	Brønnøy	Langfjord	155	50 E	50			0	0	D	R	A	N	P	0.2		Aunhattenhullet 3	Hy	23	7	12.0	276	30	1	0	0	1	0	0	0	0	0	0	0	0	1	1	3	Hoel, 1907. St.P & St.P 1980. TF00
UN	9465	4967	135	Brønnøy	Langfjord	155	E	50			0	0	D	R	A	N	P	0.2		Aunhattenhullet 4	a	10	1	1.2	12	10	1	0	0	1	0	0	0	0	0	0	0	0	1	1	1	Unpublished. TF96. TF00
UN	9505	4880	150	Brønnøy	Langfjord		E	200			0	0	D	F	A	N	P	12.0		Dyrmoengrotta	b	3	1	2.0	6	33	1	0	1	0	1	0	0	0	0	0	1	0	1	1		St.Pierre &St.Pierre 1979
UN	952	480	175	Brønnøy	Langfjord		E	300			0	0	G	F	A	N	P	7.0		Meintjenna Sink Cave	a	8	1	3.0	24	13	1	1	0	0	1	1	0	0	0	0	1	0	0	1	1	Unpublished. TF96
UN	952	480	180	Brønnøy	Langfjord		E	300			0	0	G	F	A	N	P	7.0		Meintjenna Dry Cave	b	12	3	2.0	24	25	1	0	0	1	0	0	0	0	0	0	0	0	1	1	1	Unpublished. TF96
UN	952	480	175	Brønnøy	Langfjord		E													Svartijenna Sump Pool																						Unpublished. TF96
UN	952	480	185	Brønnøy	Langfjord		E	300			0	0	G	F	A	N	P	7.0		Rift Cave	a	22	8	8.0	176	36	1	0	0	1	0	0	0	0	0	0	0	0		1	1	Unpublished. TF96
UN	9630	3675	160	Brønnøy	Lande		E	200			0	0	E	W	A	D	P	0.3	L2	Svartdalsholet	a	35	4	5.0	175	11	1	0	0	2	0	0	0	0	0	0	0	0	1	0	2	Newton 1999
UN	9631	3650	120	Brønnøy	Lande		E	200			0	0	E	W	A	D	P	0.3	L3	Rockbridge	a	6	1	2.0	12	17	1	1	1	0	1	0	0	0	0	0	0	0		0		Newton 1999
UN	9680	3972	95	Brønnøy	Lande		E	100			0	0	E	F	A	N	P	2.0	L1b	Øvre Landegrotta	b	80	5	15.0	1200	6	1	1	0	0	1	1	0	0	0	0	0	0	1	1		St.Pierre 1984
UN	9680	3960	80	Brønnøy	Lande	2	80 E	100	Dark grey	schist	0	0	E	F	A	N	P	2.0	L1a	Nedre Landegrotta	Hy	88	9	15.0	1320	10	1	0	1	0	1	1	0	0	0	0	0	0	1	1	3	Newton 1999
																				* assumed to be Rubbish Tip Cave (TF96)																						Includes some caves in Velfjord
Mejafjellet				**1825 II**																																						1 outcrop. No known refs.

UPPERMOST ALLOCHTHON: Helgeland Nappe Complex: Zone 3 (Central Granite Area): TOTALS

	ALT.	LST. DIP	OW	R	T	CA	LENG.	VR	XS	VOL.	Min. HG %	C	SE	RE	DE	CS	SP	Ch	Sh	BC	RV	MV	DC	FS	P
Totals	###	###	####	6	0	###	3320	###	####	16251	###	36	10	8	47	25	6	4	35	9	3	13	0	12	20
Av. per cave	387	50	332	0.2	0.0	2.1	92	10	2.2	451	36		0.3	0.2	1.3	0.7	0.2	0.1	1.0	0.3	0.1	0.4	0.0	0.3	0.6
Minima	5	31	50			0.10	2	1	1.0	2	5		0	0	0	0	0	0	0	0	0				
Maxima	680	90	700			25.0	1896	101	6.0	11376	100		2	1	6	4	1	2	14	3	1				

(Dip measured in 10 caves)

Glacial Situations:

	#	Length
C	1	38
D	3	80
E	1	85
G	0	0
H	5	207
K	16	2497
L	10	413
S	0	0
T	0	0
U	0	0
Totals	36	3320

Karst Types:

	#	Length
V	7	2291
A	25	824
L	0	0
C	0	0
X	4	205
Totals	36	3320

Cave Locations:

	#	Length
C	1	38
F	4	131
W	18	1043
R	6	1930
S	6	170
G	1	8
P	0	0
Totals	36	3320

Cave Types:

	#	Length
S	3	58
a	16	290
b	8	256
c	1	10
d	0	0
e	0	0
f	3	372
g	1	372
h	1	1896
Hy	2	60
I	0	0
J	0	0
L	0	0
R	0	0
T	1	6
Totals	36	3320

Relict Caves:

	#	Length
	15	413
Totals	15	413

MV Caves:

	#	Length
	13	222
Totals	13	222

Combination Caves:

	#	Length
Totals	8	2685

UPPERMOST ALLOCHTHON: Helgeland Nappe Complex: Zone 3 (Central Granite Area)

Caves are grouped by carbonate outcrop

Western catchment area

External Cave Attributes / Internal Cave Attributes

UTM COORDS	ALT.	KOMMUNE	AREA	LST. STRIKE	LST. DIP	OW	EXT. COLOUR	OTHER INT. ROCK	R	T	GS	CL	KT	SR	OR	CA	REF. NO.	CAVE NAME	CT	LENG.	VR	XS	VOL.	Min. HG %	C	SE	RE	DE	CS	SP	Ch	Sh	BC	RV	MV	DC	FS	P	SG	PRIME REFERENCES
Tjøtta		**1826 IV**																																						No known references
Vevelstad		***1826 III***																																						
UN 9500 9300	560	Vevelstad	Visten (N)		36 W	200			0	0	K	S	A	N	O	0.1	VS1	Karma Sutra Cave	c	10	5	1.0	10	50	1	1	0	1	1	1	0	0	0	0	1	0	1	1	1	Faulkner&Newton 1995
UN 9515 9300	565	Vevelstad	Visten (N)		36 W	200			0	0	K	S	A	N	O	0.1	VS2	Going Cave	a	10	6	1.0	10	60	1	1	0	0	1	0	0	0	0	0	1	0		1		Faulkner&Newton 1995
UN 9500 9220	400	Vevelstad	Visten (N)		36 W	600			0	0	K	W	A	D	O	1.0	VS3	Top Bed Cave	a	5	3	1.0	5	60	1	0	1	0	1	0	0	0	0	0	1	0		1		Faulkner&Newton 1995
UN 9530 9230	470	Vevelstad	Visten (N)		36 W	600			0	0	K	W	A	D	O	0.2	VS4	Arch Cave	a	8	4	1.0	8	50	1	0	0	1	0	0	0	0	0	0	0	0		0		Newton 1999
UN 9515 9240	400	Vevelstad	Visten (N)		36 W	600			0	0	K	W	A	D	O	0.2	VS8	Keyhole Resurgence	a	8	3	1.0	8	38	1	0	1	0	1	0	0	0	0	0	1	0		0		Newton 1999
UN 9570 9180	595	Vevelstad	Visten (N)		W	200			0	0	K	W	A	N	P	0.3	VS5	Hopeless Hole	b	8	2	1.0	8	25	1	0	0	1	1	0	0	0	0	0	1	0		0	1	Newton 1999
UN 9570 9135	680	Vevelstad	Visten (N)		W	200			0	0	K	G	A	N	P	0.1	VS6	Collapsed Cave	a	8	2	1.0	8	25	1	1	1	0	1	0	0	0	0	0	1	0		0	1	Newton 1999
UN 9555 9100	550	Vevelstad	Visten (N)		W	200			0	0	K	S	A	U	P	0.4	VS7	The Oubliette	a	5	3	1.0	5	60	1	1	0	0	1	0	0	0	0	0	1	0		0		Newton 1999
																		VS5, VS6 and VS7 are from the Eiterådal sheet																						
Nesna		**1827 II**																																						No known references
Mosjøen		***1826 I***																																						
UP 988 189	10	Leirfjord	Alsten															karst x 1																						Mosjøn Quat. Map
VP 010 030	400	Alstahuag	Stortuva															karst x 4																						Mosjøen Quat. Map
UP 980 980		Alstahuag	Sorfjorden															Sørfjordgrotta		200m cave to a sump.																				A. Rasmussen pc 1998

UPPERMOST ALLOCHTHON: Helgeland Nappe Complex: Zone 3 (Central Granite Area)

Caves are grouped by carbonate outcrop

Western catchment area

UTM COORDS	ALT.	KOMMUNE	AREA	LST. STRIKE	LST. DIP	CAVE NAME	CT	LENG.	VR	XS	VOL.	Min. HG %	C	SE	RE	DE	CS	SP	Ch	Sh	BC	RV	MV	DC	FS	P	SG	PRIME REFERENCES
External Cave Attributes							**Internal Cave Attributes**																					
Elterådal ***1826 II***																												* 1 bc is passable
UN *9610 8235*	5	Vevelstad	Bønnå		E	**Trondjordhula**	b	38	*5*	*2.0*	*76*	13	1	0	1	0	1	0	0	0	0	0	1	0	1	0	1	Faulkner&Newton 1995
UN *9605 8250*	50	Vevelstad	Bønnå		E	**Risehula 1**	Hy	30	5	1.0	30	17	1	0	0	2	0	0	0	2	2	0	0	0	1	0	3	Faulkner&Newton 1995. *
UN *9605 8250*	53	Vevelstad	Bønnå		E	**Risehula 2**	Hy	30	4	4.0	120	13	1	0	0	1	0	0	0	2	0	0	0	0	1	0	3	Faulkner&Newton 1995
UN *9705 8585*	370	Vevelstad	Bønnå			**Multi Entrance Syst.**	b	50	5	*2.0*	*100*	10	1	0	0	3	0	0	0	3	0	0	0	0		0	1	Faulkner&Newton 1995
					50																							

There are unmapped caves of considerable length on Storfjellet

Lomsdal-Visten Rep. 2/2004

Tosbotn ***1825 I***																												
UN *952 593*	420	Brønnøy	Klavbekkda	180	54 E	**Klavbekk Rising**	S	3	3	*3.0*	9	100	1	0	1	0	1	1	0	1	0	0	1	0	0	0		Faulkner &Newton 1995
UN *952 590*	440	Brønnøy	Klavbekkda	180	54 E	**Thunder Pot**	a	25	10	*3.0*	75	40	1	1	0	0	1	1	0	0	0	0	0	0	0	0	1	Faulkner &Newton 1995
UN *9670 6025*	240	Brønnøy	Tettingsdal		E	**Black Space Cave**	a	9	3	1.0	9	33	1	0	0	1	0	0	0	0	0	0	0	0		1		Faulkner &Newton 1995
UN *9660 6025*	240	Brønnøy	Tettingsdal		E	**Rift Cave**	a	10	5	5.0	50	50	1	0	0	3	0	0	0	1	0	0	0	0		1		Faulkner &Newton 1995
UN *9680 6020*	200	Brønnøy	Tettingsdal		E	**Balcony Cave**	f	175	18	2.0	350	10	1	0	0	6	0	0	0	7	0	1	0	0	1	1	3	Faulkner &Newton 1995
UN *9685 6025*	160	Brønnøy	Tettingsdal		E	**Nettle Pot**	a	85	34	2.0	170	40	1	0	0	2	1	0	0	1	0	0	0	0		1	3	Faulkner &Newton 1995
UN *967 592*	230	Brønnøy	Tettingsdal		E	**cave**	b	10	*3*	1.0	10	30	1	0	0	1	0	0	0	0	0	0	*0*	0		0		Faulkner &Newton 1995
UN *9685 5865*	205	Brønnøy	Tettingsdal		E	**Sandy Cave**	a	3	1	1.0	3	33	1	0	0	1	0	0	0	0	0	0	*0*	0		1		Faulkner &Newton 1995
UN *9620 5790*	310	Brønnøy	Tettingsdal		E	**Pylon Cave**	f	137	14	4.0	548	10	1	0	0	2	1	1	1	0	0	0	0	0		0	1	Faulkner &Newton 1995
UN *9618 5780*	311	Brønnøy	Tettingsdal		E	**Øst-Vat Grotta**	b	35	15	*2.0*	70	43	1	0	0	1	0	0	0	0	0	0	*0*	0	1	0	3	Faulkner &Newton 1995
UN *9615 5775*	312	Brønnøy	Tettingsdal		E	**Top Sink**	a	2	1	*1.0*	2	50	1	1	0	0	1	0	0	0	0	0	1	0		0		Faulkner &Newton 1995
UN *9735 6105*	140	Brønnøy	Tettingsdal		E	**Keith's 1990 Cave**	b	20	3	2.0	40	15	1	1	1	0	1	0	0	0	0	0	1	0		0	1	Faulkner &Newton 1995
VN *0040 5145*	930	Brønnøy	n. Snøfjell			**unexplored cave**																					M. Solbakk pc 1998
VN *0110 4865*	520	Brønnøy	Leiråvatn			**Låjroe Sink Doline**	S	50	10	4.0	200	20	1	1	0	4	1	0	0	1	0	0	0	0	1	1		Unpublished TF96
VN *0105 4840*	475	Brønnøy	Leiråvatn			**Låjroegrotta**	f	60	7	3.0	180	12	1	0	0	1	1	0	0	0	2	0	0	0	1	1	2	Unpublished TF96
VN *0105 4840*	487	Brønnøy	Leiråvatn			**Øvre Låjroegrotta**																						**Unexplored.** TF96
VN *0175 4765*	420	Brønnøy	Leiråvatn	30		**Kringlotheia Wet Cave**	b	60	5	2.0	120	8	1	0	1	3	1	0	0	0	0	0	0	0		1	1	Unpublished TF96
VN *0175 4765*	420	Brønnøy	Leiråvatn	30		**Kringlotheia Dry Cave**	b	35	3	2.0	70	9	1	0	0	2	0	0	0	0	0	0	0	0		1	1	Unpublished TF96
VN *0814 5286*	583	Brønnøy	Godvassda	20	90	**Godvassdalgrotta**	T	6	3	2.0	12	50	1	0	0	1	0	0	0	0	0	0	0	0	0	1		TF00
VN *0814 5286*	596	Brønnøy	Godvassdal			**Waterfall Rising**	1 cubic metre per second from sump above waterfall																					TF00
VN *0835 4980*	425	Brønnøy	Toerfjell			**Edge Cave**	S	5	5	3.0	15	100	1	0	0	1	0	0	0	0	0	0	0	0		1		Faulkner &Newton 1995
VN *0835 4987*	440	Brønnøy	Toerfjell			**Doline Cave**	a	5	3	1.0	5	60	1	0	0	1	0	0	0	0	0	0	0	0	1	1		Faulkner &Newton 1995
VN *0850 5002*	485	Brønnøy	Toerfjell	15	90	**Toerfjellhola**	h	1896	101	6.0	11376	5.3	1	2	0	4	2	1	1	14	3	*1*	0	0	1	1	3	Faulkner &Newton 1995
VN *0885 5027*	640	Brønnøy	Toerfjell			**Cave of Cold Wind**	g	372	58	6.0	2232	15.6	1	0	0	1	4	0	2	2	1	1	0	0	1	1	3	Faulkner &Newton 1995
VN *0893 5030*	680	Brønnøy	Toerfjell			**Squeeze Cave**																						Faulkner &Newton 1995
VN *0867 5000*	500	Brønnøy	Toerfjell			**High Cave**	a	2	1	1.0	2	50	1	0	0	1	0	0	0	1	0	0	0	0	0	1		Faulkner &Newton 1995
VN *0870 5006*	530	Brønnøy	Toerfjell			**Blocked Cave**	a	5	3	3.0	15	60	1	0	1	0	1	0	0	0	1	0	1	0		1		Faulkner &Newton 1995
VN *0880 5006*	580	Brønnøy	Toerfjell	55	31 E	**Dåsranjuenjehola**	a	100	15	3.0	300	15	1	0	0	2	1	1	0	0	0	0	1	0	1	1		Faulkner &Newton 1995
		Brønnøy	Tosdal			**Tosentunnel cave**	Filled with concrete during construction																					R. Selvaag pc 2000

Majafjellet **1825 II**
Elsfjord **1927 III**

No known refs.

VP 272 372	600	Hemnes	Svartholtop.			**karst x 1**		No mapped carbs																				Elsfjord Q. Map.

UPPERMOST ALLOCHTHON: Helgeland Nappe Complex: Zone 4 (Eiterådal and Jordbruelv): TOTALS

	ALT.	LST. DIP	OW	R	T	CA	LENG.	VR	XS	VOL.	Min. HG %	C	SE	RE	DE	CS	SP	Ch	Sh	SC	RV	MV	DC	FS	P
Totals	###	###	####	2	0	###	14490	####	#####	76258	###	182	30	15	242	93	50	20	156	35	10	16	7	38	155
Av. per cave	570	79	87	0.0	0.0	2.0	80	9.24	2.9	419	33		0.2	0.1	1.3	0.5	0.3	0.1	0.9	0.2	0.1	0.1	0.0	0.2	0.9
Minima	100	45	0.3			0.01	1	1	0.5	1	1		0	0	0	0	0	0	0	0	0				
Maxima	940	90	500			30.0	1411	78	20.0	16932	100		2	1	10	3	5	3	13	4	2				

(Dip measured in 105 caves)

Glacial Situations:

	#	Length
C	0	0
D	0	0
E	0	0
G	1	5
H	13	2683
K	1	150
L	132	10308
S	0	0
T	33	1330
U	2	14
Totals	182	14490

Karst Types:

	#	Length
V	92	7345
A	88	6790
L	0	0
C	1	205
X	1	150
Totals	182	14490

Cave Locations:

	#	Length
C	0	0
F	34	5064
W	57	2428
R	35	2841
S	29	1227
G	27	2930
P	0	0
Totals	182	14490

Cave Types:

	#	Length
S	32	355
a	42	1029
b	62	2307
c	7	1584
d	13	1079
e	2	346
f	7	1246
g	7	1434
h	9	5038
Hy	0	0
I	0	0
J	0	0
L	0	0
R	0	0
T	1	72
Totals	182	14490

Relict Caves:

#	Length
99	3104
99	3104

MV Caves:

#	Length
16	210
16	210

Combination Caves:

#	Length
67	11176

UPPERMOST ALLOCHTHON: Helgeland Nappe Complex: Zone 4 (Eiterådal and Jordbruelv)

Caves are grouped by carbonate outcrop

Vefsn catchment area

External Cave Attributes / Internal Cave Attributes

UTM COORDS	ALT.	KOMMUNE	AREA	LST. STRIK	LST. DIP	OW	EXT. COLOUR	OTHER INT. ROCK	R	T	GB	CL	KT	SR	OR	CA	REF. NO.	CAVE NAME	CT	LENG.	VR	XS	VOL.	Min. HG %	C	SE	RE	DE	CS	SP	Ch	Sh	SC	RV	MV	DC	FS	P	SG	PRIME REFERENCES
Mosjøen			**1826 I**																																					
VN 1680 9635	100	Vefsn	Royåsen	130	90	50			0	0	H	S	V	N	P	0.1		Byåskjeleren	f	300	15	1.0	300	5	1	0	0	4	0	0	1	3	0	0	0	0		1	2	Faulkner 1983
VN 1680 9630	110	Vefsn	Royåsen	130	90	50			0	0	H	S	V	N	P	0.1		Skulle Cave	S	6	5	1.0	6	83	1	0	0	1	0	0	0	1	0	0	0	0	1	1	2	Faulkner 1983
VN 1680 9625	110	Vefsn	Royåsen	130	90	50			0	0	H	S	V	N	P	0.1		Bridge Pot	f	50	10	2.0	100	20	1	0	0	1	0	0	0	3	0	0	0	0	1	1	2	Faulkner 1983
VN 155 940	240	Vefsn	Grovholten															karst x 4																						Mosjøen Quat. Map
VN 156 935	250	Vefsn	Stortverråga															draughting sink																						R. Selvåg pc98 Or VN159926?
Eiterådal			**1826 II**																																					
VN 1515 7115	210	Vefsn	Eiterådal		W	500			0	0	H	G	A	U	P	0.2	E2	Ice Hole	S	5	3	1.0	5	60	1	0	0	1	0	0	0	1	0	0	0	0		1	1	Faulkner 1980
VN 1520 7110	190	Vefsn	Eiterådal		W	500			0	0	H	W	A	U	P	0.2	E3	Krokgrotta	b	100	18	3.0	300	18	1	0	1	1	1	1	0	0	0	0	0	0		1	3	Faulkner 1980
VN 1450 7195	260	Vefsn	Eiterådal		W	500			0	0	H	G	A	U	P	1.5	E4	Through Cave	a	15	4	2.0	30	27	1	1	0	1	1	2	0	1	0	0	0	0		1	1	Faulkner 1980
VN 1455 7305	237	Vefsn	Eiterådal	4	75 W	500			0	0	H	G	A	U	P	1.3	E9	Eiterådalgr. Res. Ca.	b	45	4	10.0	450	9	1	0	1	1	1	1	0	0	0	0	0	0	1	1	3	Faulkner 1980. TF97
VN 1450 7340	257	Vefsn	Eiterådal	174	74 W	500	White	Am.	0	0	H	G	A	U	P	0.6	E11	Eiterådalgrotta	g	661	25	12.0	7932	4	1	1	0	4	2	1	0	5	0	0	0	0		1	3	Faulkner 1980. TF97
VN 1510 7085	275	Vefsn	Eiterådal	140	90	500			0	0	H	G	V	N	P	2.0	E13	Sirijordgrotta*	h	1411	78	12.0	16932	5.5	1	0	1	3	2	5	3	6	0	0	0	1	1	1	3	Faulkner 1980. Valen et al. (1991)
VN 1540 7015	259	Vefsn	Eiterådal		W	500			0	0	H	R	A	N	P	1.6	E17	Brynhildgrotta 1	c	15	3	2.0	30	20	1	0	0	1	0	0	0	0	0	0	0	0		1	1	Unpublished. TF97
VN 1570 6940	269	Vefsn	Eiterådal	120	60 W	500			0	0	H	R	A	N	P	1.5	E18	Brynhildgrotta 2	c	41	10	8.0	328	24	1	0	0	2	0	0	0	1	1	0	0	0	1	1	1	Unpublished. TF97
VN 1510 7125	260	Vefsn	Eiterådal		W	500			0	0	H	G	A	U	P	0.1	E20	Laragrotta	a	19	10	6.0	114	53	1	0	0	1	0	0	0	0	0	0	0	0	1	1		Faulkner 1987
VN 1485 7115	260	Vefsn	Eiterådal			500			0	0	H	G	A	U	P	0.1	E21	Surprise Cave	a	15	2	1.0	15	13	1	0	0	2	0	0	0	0	0	0	0	0	0	1		Faulkner 1987
VN 1470 7090	270	Vefsn	Eiterådal		W	500			0	0	L	G	A	U	P	0.5	E22	Håpgrotta	h	195	20	5.0	975	10	1	0	0	2	1	1	2	2	1	1	0	0	1	1	3	Faulkner 1987
VN 1560 7205	200	Vefsn	Eiterådal		W	50			1	0	G	F	A	N	P	3.0	E1	Holbekkgrotta	a	5	2	1.0	5	40	1	0	1	0	1	0	0	0	0	0	1	0	0	1		Faulkner 1980
VN 168 705	435	Vefsn	Eiterådal			50			1	0	K	W	X	X	P	1.0	E19	Disappointment Cave	b	150	10	3.0	450	7	1	1	1	0	1	0	0	0	0	0	0	0		0		Faulkner 1980. Not found TF00

Am. = amphibolite

*Altitude at Elk Shaft, GS at Main Entrance

UPPERMOST ALLOCHTHON: Helgeland Nappe Complex: Zone 4 (Elsterdal and Jordbruvely)

Caves are grouped by carbonate outcrop

Vefsn catchment area

UTM COORDS	ALT.	KOMMUNE	AREA	LST. STRIK	LST. DIP	OW	EXT. COLOUR	OTHER INT. ROCK	R	T	GB	CL	KT	SR	OR	CA	REF. NO.	CAVE NAME	CT	LENGL	VR	XS	VOL.	Mix. HG %	C	BE	RE	DE	CS	SP	CN	Sh	BC	RV	MV	DC	FS	P	SG	PRIME REFERENCES
Tesboto		***1825 I***																																						
VN *1475* *6295*	923	Grane	Kvitfjellet - 1	180	90	10			0	0	T	W	V	N	O	0.7		Interesting Hole	S	5	4	6.0	30	80	1	0	0	1	0	0	0	1	1	0	0	0	0	1		Unpublished. TF97
VN *1475* *6290*	908	Grane	Kvitfjellet - 1	180	90	10			0	0	T	W	V	N	O	0.7		Matti's Hole	S	6	5	15.0	90	83	1	0	0	1	0	0	0	1	1	0	0	0	0	1		Unpublished. TF97
VN *1475* *6290*	893	Grane	Kvitfjellet - 1	180	90	10			0	0	T	W	V	N	O	0.7		Rectangular Hole	a	8	4	4.0	32	50	1	0	0	2	0	0	0	1	0	0	0	0	0	1		Unpublished. TF97
VN *1475* *6290*	876	Grane	Kvitfjellet - 1	180	90	10			0	0	T	W	V	N	O	0.7		Resurgence Cave	a	10	1	1.0	10	10	1	0	1	0	1	0	0	0	0	0	0	0	0	1		Unpublished. TF97
VN *1475* *6270*	812	Grane	Kvitfjellet - 1	180	90	10			0	0	L	W	V	N	O	0.8		Odd's Hole	S	8	8	2.0	16	100	1	0	0	1	0	0	0	1	1	0	0	0	0	1		Unpublished. TF97
VN *1485* *6265*	759	Grane	Kvitfjellet - 3	1	85 E	4			0	0	L	W	V	N	O	0.8		Johannes Hole	S	10	10	3.0	30	100	1	0	0	1	0	0	0	1	1	0	0	0	0	1		Unpublished. TF97
VN *1485* *6260*	746	Grane	Kvitfjellet - 3	180	85 E	4			0	0	L	W	V	N	O	0.8		Shattered Shaft	S	10	10	3.0	30	100	1	0	0	1	0	0	0	1	1	0	0	0	0	1		Unpublished. TF97
VN *1520* *6220*	630	Grane	Kvitfjellet - 4	20	45 E													Dry Cave																					Unexplored. TF97
VN *1520* *6220*	625	Grane	Kvitfjellet - 4	20	45 E													Sink Cave 1																					Unexplored. TF97
VN *1520* *6220*	620	Grane	Kvitfjellet - 4	20	45 E													Sink Cave 2																					Unexplored. TF97
VN *1560* *6300*	900	Grane	Kvitfjellet - 7	170	90	50	Pale yell	bs	0	0	T	S	V	N	O	1.0		Green Valley Cave	e	108	8	3.5	378	7	1	0	0	4	1	0	0	3	0	1	0	0	1	1	3	Unpublished. TF97&98. HMC?
VN *1555* *6298*	885	Grane	Kvitfjellet - 7	10	80 E	50	Grey/yell/br		0	0	T	S	A	N	O	1.0		Sandy Cave	a	17	6	2.0	34	35	1	0	0	2	1	0	0	0	0	0	0	0	1	1		Unpublished. TF97&98. HMC?
VN *1554* *6293*	879	Grane	Kvitfjellet - 7	180	90	50			0	0	T	S	V	N	O	1.0		Collapsed Cave	S	15	15	2.0	30	100	1	0	0	1	0	0	0	0	0	0	0	0	1	1		Unpublished. TF97&98
VN *1552* *6290*	855	Grane	Kvitfjellet - 7	180	90	50			0	0	L	S	V	N	O	1.0		Sfinxhullet	b	103	25	4.4	453	24	1	0	0	2	1	0	0	2	0	0	0	0	1	1	3	Unpublished. TF97&98
VN *1552* *6289*	850	Grane	Kvitfjellet - 7	5	80 E	50			0	0	L	S	A	N	O	1.0		Snow Hole	S	5	5	1.0	5	100	1	0	0	1	0	0	0	0	0	0	0	0	0	1		Unpublished. TF97&98
VN *1552* *6274*	825	Grane	Kvitfjellet - 7	180	45 E	50			0	0	L	S	A	N	O	1.2		Snow Sink	S	10	5	1.0	10	50	1	0	0	2	1	0	0	2	0	0	0	0	0	1		Unpublished. TF97&98
VN *1550* *6275*	826	Grane	Kvitfjellet - 7			50			0	0	L	S	A	N	O	1.0		Dug Hole	S	5	5	1.0	5	100	1	0	0	1	0	0	0	0	0	0	0	0	0	1		Unpublished. TF98
VN *1549* *6268*	809	Grane	Kvitfjellet - 7	20	80 E	50	Grey	bs+d	0	0	L	S	C	N	O	1.3		Kvitfjellgrotta	h	205	22	*2.5*	*513*	11	1	0	0	1	1	3	0	0	1	0	0	0	1	1	3	Unpublished. TF97&98
VN *1555* *6262*	787	Grane	Kvitfjellet - 7	170	90	50	Grey / wh		0	0	L	S	V	N	O	1.4		Valley Resurgence 1	f	33	3	1.1	36	9	1	0	1	0	1	1	0	0	0	0	0	0	0	1	1	Unpublished. TF97&98
VN *1556* *6262*	782	Grane	Kvitfjellet - 7	170	90	50			0	0	L	S	V	N	O	1.4		Valley Resurgence 2	a	3	1	0.5	2	33	1	0	1	0	1	0	0	0	0	0	0	0	0	1		Unpublished. TF97&98
VN *1290* *4925*	780	Grane	Jordhulefjell	170	90	*40*			0	0	T	G	V	N	P	0.1	J1	Collapsed Cave 1	a	10	3	3.0	30	30	1	1	0	0	1	0	0	0	1	0	0	0		1		Faulkner 1987
VN *1255* *4945*	730	Grane	Jordhulefjell	170	90	*40*			0	0	T	G	V	N	P	0.2	J2	Collapsed Cave 2	a	8	2	3.0	24	25	1	1	0	0	1	0	0	0	1	0	0	0		1		Faulkner 1987
VN *1210* *5085*	731	Grane	Jordhulefjell	150	90	100	Grey		0	0	T	R	V	N	P	2.0	J3	Kidney Lake Res.	a	1	1	1.0	1	100	1	0	1	0	1	1	0	0	0	0	1	0		1	1	Faulkner 1987
VN *1205* *5085*	770	Grane	Jordhulefjell	150	90	100	Grey		0	0	T	R	V	N	P	0.8	J5	Kidney Lake Cave	b	114	16	6.0	684	14	1	0	0	2	0	0	0	0	0	0	0	0		1	3	Faulkner 1987
VN *1200* *5090*	780	Grane	Jordhulefjell	150	90	100	Grey		0	0	T	R	V	N	P	0.8	J6	Through Cave	b	40	4	2.0	80	10	1	0	0	2	0	0	0	0	0	0	0	0		1	2	Faulkner 1987
VN *1195* *5100*	785	Grane	Jordhulefjell	150	90	100	Grey		0	0	T	R	V	N	P	0.8	J8	Jordhulefjellhullet	f	290	23	4.0	1160	8	1	0	0	5	2	0	0	5	0	0	0	0		1	2	Faulkner 1987
VN *1190* *5105*	795	Grane	Jordhulefjell	150	90		Grey										J9a	shaft																					Faulkner 1987
VN *1190* *5105*	790	Grane	Jordhulefjell	150	90	100	Grey		0	0	T	R	V	N	P	0.8	J10c	Through Cave	b	12	2	2.0	24	17	1	0	0	2	0	0	0	0	0	0	0	0		1	1	Faulkner 1987
VN *1195* *5115*	780	Grane	Jordhulefjell	150	90	100			0	0	T	R	V	N	P	0.8	J11	Crescent Cave	b	30	3	3.0	90	10	1	0	0	1	0	0	0	0	0	0	0	0		1		Faulkner 1987
VN *1185* *5120*	810	Grane	Jordhulefjell	150	90	100			0	0	T	R	V	N	P	0.7	J12	Twin Shafts	S	18	12	4.0	72	67	1	0	0	2	0	0	0	2	1	0	0	0		2		Faulkner 1987
VN *1185* *5125*	810	Grane	Jordhulefjell	150	90	100			0	0	T	R	V	N	P	0.7	J13	Slanting Shaft	a	16	6	1.0	16	38	1	0	0	1	0	0	0	1	0	0	0	0		1		Faulkner 1987
VN *1185* *5125*	810	Grane	Jordhulefjell	150	90	100			0	0	T	R	V	N	P	0.7	J14	Pit Cave	b	43	6	4.0	172	14	1	0	0	1	0	0	0	1	0	0	0	0		1		Faulkner 1987
VN *1180* *5140*	820	Grane	Jordhulefjell	150	90												J15	Two short caves																					Faulkner 1987
VN *1175* *5145*	840	Grane	Jordhulefjell	150	90	100			0	0	T	R	V	N	P	0.7	J16	Fault Cave	d	119	16	6.0	714	13	1	0	0	1	0	0	0	2	0	0	0	0	1	1	3	Faulkner 1987
VN *1165* *5150*	850	Grane	Jordhulefjell	160	90	100			0	0	T	R	V	N	P	0.7	J17	choked shaft	S	7	7	*4.0*	28	100	1	0	0	1	0	0	0	1	0	0	0	0		1		Faulkner 1987
VN *1155* *5170*	860	Grane	Jordhulefjell	160	90	100			0	0	T	R	V	N	P	0.7	J18	Moonmilk Cave	b	24	2	3.0	72	8	1	0	0	2	0	0	0	0	0	0	0	1		1		Faulkner 1987. Moonmilk.
VN *1150* *5180*	860	Grane	Jordhulefjell	160	90	100			0	0	T	R	V	N	P	0.6	J19	shaft	S	8	8	4.0	32	100	1	0	0	1	0	0	0	1	0	0	0	0		1		Faulkner 1987
VN *1150* *5185*	860	Grane	Jordhulefjell	160	90	100			0	0	T	R	V	N	P	6.0	J20	Deep Rift	S	10	10	5.0	50	100	1	0	0	1	0	0	0	1	0	0	0	0		1		Faulkner 1987
VN *1145* *5195*	860	Grane	Jordhulefjell	160	90	100			0	0	T	R	V	N	P	0.6	J21	Short Through Cave	b	*10*	2	3.0	30	20	1	0	0	2	0	0	0	0	0	0	0	0		1		Faulkner 1987
VN *1155* *5200*	860	Grane	Jordhulefjell	165	90	100			0	0	T	R	V	N	P	0.6	J22	Dug Cave	b	27	10	6.0	162	37	1	0	0	1	1	1	0	0	0	0	0	0		1		Faulkner 1987
VN *1155* *5210*	860	Grane	Jordhulefjell	165	90	100			0	0	T	R	V	N	P	0.5	J23	Tarn Cave	b	27	*4*	*4.0*	108	15	1	0	0	1	0	0	0	1	0	0	0	0		1		Faulkner 1987
VN *1120* *5340*	780	Grane	Jordhulefjell	180	90	5			0	0	T	G	V	N	P	0.4	J24	Strike Cave 1	a	25	8	6.0	150	32	1	0	0	1	0	0	0	1	0	0	0	0		1		Faulkner 1987
VN *1120* *5345*	775	Grane	Jordhulefjell	180	90	5			0	0	T	G	V	N	P	0.4	J25	Strike Cave 2	a	40	15	12.0	480	38	1	0	0	2	0	0	0	0	0	0	0	0		1		Faulkner 1987
VN *1120* *5365*	740	Grane	Jordhulefjell	180	90	5			0	0	T	G	V	N	P	0.6	J26	Strike Cave 3	S	9	9	*6.0*	54	100	1	0	0	1	0	0	0	0	0	0	0	0		1		Faulkner 1987
VN *1120* *5375*	735	Grane	Jordhulefjell	180	90	5			0	0	T	G	V	N	P	0.6	J27	Strike Cave 4	a	6	2	*2.0*	12	33	1	0	0	1	0	0	0	0	0	0	0	0		1		Faulkner 1987

bs = biotite schist d = dolomite

HMC = High Magnesian Calcite

UPPERMOST ALLOCHTHON: Helgeland Nappe Complex: Zone 4 (Ellerådal and Jordbruelv)

Caves are grouped by carbonate outcrop

Velfjord catchment area

UTM COORDS			ALT.	KOMMUNE	AREA	LIST. STRIKE	LIST. DIP	GW	EXT. COLOUR	OTHER INT. ROCK	R	T	GS	CL	KT	SR	OR	CA	REF. NO.	CAVE NAME	CT	LENG.	VR	XS	VOL.	Sin. HG %	C	SE	RE	DE	CS	SP	Ch	Sh	SC	RV	MV	DC	FS	P	SG	PRIME REFERENCES
											External Cave Attributes										Internal Cave Attributes																					
Tosbotn				*1826 I*	*cont.*																																					
VN	*1445*	*5109*	610	Grane	Elgfjell - Vall. 2			10	Grey		0	0	L	F	V	N	P	0.03	2N1	Scorpion Pot	b	58	12	1.0	58	21	1	0	0	1	1	0	0	1	0	0	0	0		1	3	Faulkner & Newton 1990
VN	*1445*	*5120*	600	Grane	Elgfjell - Vall. 2			10	Grey		0	0	L	F	V	N	P	0.04	2N2	cave	b	6	2	1.0	6	33	1	0	0	1	1	1	0	0	0	0	1	0		1	1	Faulkner & Newton 1990
VN	*1445*	*5126*	595	Grane	Elgfjell - Vall. 2	180	90	10	Grey		0	0	L	F	V	N	P	0.05	2N3	Fourways cave	g	33	5	1.0	33	15	1	0	0	3	1	2	0	0	0	0	0	0		1	1	Faulkner & Newton 1990
VN	*1446*	*5127*	595	Grane	Elgfjell - Vall. 2	180	90	10	Grey		0	0	L	F	V	N	P	0.05	2N4	cave	b	8	3	1.0	8	38	1	0	0	1	1	1	0	0	1	0	1	0		1	1	Faulkner & Newton 1990
VN	*1444*	*5132*	590	Grane	Elgfjell - Vall. 2			10	Grey		0	0	L	F	V	N	P	0.05	2N5	sink	S	3	3	*1.0*	3	100	1	1	0	0	1	0	0	0	1	0	1	0		1		Faulkner & Newton 1990
VN	*1448*	*5134*	590	Grane	Elgfjell - Vall. 2			10	Grey		0	0	L	F	V	N	P	0.1	2N6	Shatter Pot	b	70	9	2.0	140	13	1	0	0	1	1	1	0	1	0	0	0	0		1	1	Faulkner & Newton 1990
VN	*1449*	*5146*	580	Grane	Elgfjell - Vall. 2			10	Grey		0	0	L	F	V	N	P	0.1	2N7	Funnel Pot	b	24	5	*2.0*	48	21	1	0	0	1	0	0	0	0	0	0	0	0	1	1		Faulkner & Newton 1990
VN	*1480*	*5080*	495	Grane	Elgfjell - Vall. 3			*10*	Grey		0	0	L	W	V	N	P	0.1	3S1	Crowbar Cave	a	3	*2*	1.0	3	67	1	0	0	1	0	0	0	0	0	0	0	0		0		Faulkner & Newton 1990
VN	*1472*	*5080*	510	Grane	Elgfjell - Vall. 3			5	Grey		0	0	L	F	V	N	P	0.1	3S2	Boulder Sink	b	20	8	1.0	20	40	1	1	0	0	1	0	0	0	1	0	0	0		0		Faulkner & Newton 1990
VN	*1471*	*5083*	530	Grane	Elgfjell - Vall. 3			5	Grey		0	0	L	W	V	N	P	0.1	3S3	crawl	a	2	*1*	1.0	2	50	1	0	0	1	0	0	0	0	0	0	0	0		0		Faulkner & Newton 1990
VN	*1476*	*5089*	544	Grane	Elgfjell - Vall. 3			5	Grey		0	0	L	W	V	N	P	0.1	3S4	shafts	S	16	10	*2.0*	32	63	1	0	0	2	0	0	0	2	0	0	0	0		1		Faulkner & Newton 1990. TF00
VN	*1478*	*5097*	597	Grane	Elgfjell - Vall. 3	20	70 W	30	Grey		0	0	L	G	A	D	P	0.1	3S5	The Big Pitch	S	18	16	6.0	108	89	1	0	0	1	1	1	0	1	0	0	0	0		1		Faulkner & Newton 1990. TF00
VN	*1465*	*5102*	594	Grane	Elgfjell - Vall. 3	20	70 W	30	Yell. / br.	Grey	0	0	L	F	A	N	P	0.1	3S6	Elgfjellhola	a	335	30	20.0	6700	9	1	1	0	0	1	0	0	1	1	0	0	0	1	1	3	F. & N. 1990. HMC? TF00. SN04
VN	*1475*	*5109*	620	Grane	Elgfjell - Vall. 3	20	60 W	30	*Yellow*		0	0	L	G	A	N	P	0.1	3S7	Mouth Cave *	b	25	3	1.0	25	12	1	0	0	1	0	0	0	0	0	0	0	0		1		Faulkner & Newton 1990
VN	*1473*	*5092*	587	Grane	Elgfjell - Vall. 3	20	60 W	1	ms	*Grey*	0	0	L	S	A	D	P	0.1	3S8	Secret Stream Cave	T	72	29	16.0	1152	40	1	0	0	1	1	0	0	0	0	0	0	0	1	1	3	F. & N. 1990. TF00. SN04
VN	*1475*	*5115*	625	Grane	Elgfjell - Vall. 3	20	60 W	5	Grey		0	0	L	G	A	N	P	0.1	3S9	Small Bridge Cave	S	16	9	2.0	32	56	1	0	0	1	0	0	0	1	0	0	0	0		0	1	Faulkner & Newton 1990
VN	*1471*	*5087*	572	Grane	Elgfjell - Vall. 3	25	60 W	80	Grey	*Yellow*	0	0	L	F	A	N	P	0.2	3S10	Paradox Cave	b	75	15	12.0	900	20	1	1	0	0	1	1	0	0	0	0	0	0	1	1	3	TF00. Surveyed as 90m: SN04 *
VN	*1482*	*5079*	586	Grane	Elgfjell - Vall. 3				Grey+Yell.										3S11	Three shafts		3m (choked), 2m (choked) and 5m to unexpored crawls																				TF00
VN	*1457*	*5121*	619	Grane	Elgfjell - Ridge	26	60 W	30	Yell. / br.	Grey	0	0	L	G	A	D	P	0.1	R0	crawl cave	b	10	*2*	1.0	10	20	1	0	0	1	0	0	0	0	0	0	0	0		1		F. & N. 1990. TF00. HMC?
VN	*1464*	*5123*	622	Grane	Elgfjell - Ridge	180	86 W	80	Yell. / br.		0	0	L	G	A	N	P	0.1	R1	Ridge Pot	*g*	140	13	1.0	140	9	1	0	0	2	0	0	0	4	1	0	0	0	1	1	1	F. & N. 1990. TF00. HMC?
VN	*1460*	*5123*	623	Grane	Elgfjell - Ridge	180	90	80	Yell. / br.		0	0	L	G	V	N	P	0.1	R2	Spiesstuehullet	f	100	26	4.0	400	26	1	0	0	3	2	1	0	4	1	0	0	1	1	1	3	F. & N. 1990. TF00. HMC?
VN	*1463*	*5135*	630	Grane	Elgfjell - Ridge	180	90	80	Yell. / br.		0	0	L	G	V	N	P	0.1	R3	Ice House Pot	*d*	45	15	*2.0*	90	33	1	0	0	1	0	0	0	2	0	0	0	0		1	1	Faulkner & Newton 90. HMC?
VN	*1460*	*5144*	619	Grane	Elgfjell - Ridge	175	65 W	120	Yell. / br.	Grey	0	0	L	R	A	N	P	0.0	R4	Ridge Cave	c	260	15	2.0	520	6	1	0	0	4	1	1	0	4	0	0	0	0		1	1	F. & N. 1990. TF00. HMC?
VN	*1470*	*5162*	620	Grane	Elgfjell - Ridge		*W*	120	Yell. / br.		0	0	L	R	A	N	P	0.0	R5	Knoll Pot	*b*	42	13	2.0	84	31	1	0	0	2	0	0	0	3	0	0	0	0		1	1	Faulkner & Newton 90. HMC?
VN	*1470*	*5160*	620	Grane	Elgfjell - Ridge		*W*	120	Yell. / br.		0	0	L	R	A	N	P	0.0	R5a	Narrow Shaft	S	5	5	1.0	5	100	1	0	0	1	0	0	0	1	0	0	0	0		1		Faulkner & Newton 90. HMC?
VN	*1472*	*5162*	620	Grane	Elgfjell - Ridge		*W*	120	Yell. / br.		0	0	L	R	A	N	P	0.0	R6	Disappointment Pot	b	9	4	1.0	9	44	1	0	0	1	0	0	0	0	0	0	0	0		1	1	Faulkner & Newton 90. HMC?
VN	*1460*	*5153*	615	Grane	Elgfjell - Ridge		*W*	120	Yell. / br.		0	0	L	W	A	D	P	0.0	R7	Draughting Cave 1	b	15	4	*1.0*	15	27	1	0	0	1	0	0	0	1	0	0	0	0		0	1	Faulkner & Newton 90. HMC?
VN	*1459*	*5157*	606	Grane	Elgfjell - Ridge		*W*	120	Yell. / br.		0	0	L	W	A	D	P	0.0	R8	Draughting Cave 2	S	6	6	*1.0*	6	100	1	0	0	1	0	0	0	1	1	0	0	0		0	1	Faulkner & Newton 90. HMC?
VN	*1457*	*5151*	605	Grane	Elgfjell - Ridge		*W*	120	Yell. / br.		0	0	L	W	A	D	P	0.0	R9	Draughting Cave 3	b	*6*	*2*	*1.0*	6	33	1	0	0	1	0	0	0	0	0	0	0	0		0	1	Faulkner & Newton 90. HMC?
VN	*1458*	*5153*	605	Grane	Elgfjell - Ridge		*W*	120	Yell. / br.		0	0	L	W	A	D	P	0.0	R10	Draughting Cave 4	b	*6*	*2*	*1.0*	6	33	1	0	0	1	0	0	0	0	0	0	0	0		0	1	Faulkner & Newton 90. HMC?
VN	*1459*	*5155*	605	Grane	Elgfjell - Ridge		*W*	120	Yell. / br.		0	0	L	W	A	D	P	0.0	R11	Draughting Cave 5	b	*7*	*2*	*1.0*	7	29	1	0	0	1	0	0	0	0	0	0	0	0		0	1	Faulkner & Newton 90. HMC?
VN	*1471*	*5177*	585	Grane	Elgfjell - Ridge		*W*	*120*	Yell. / br.		0	0	L	W	A	N	P	0.1	R12	Low Cliff Crawls	*d*	32	2	*1.0*	32	6	1	0	0	1	1	0	0	0	0	0	0	0		1	1	Faulkner & Newton 90. HMC?
VN	*1471*	*5183*	570	Grane	Elgfjell - Ridge		*W*	*120*	Yell. / br.		0	0	L	W	A	N	P	0.1	R13	Triangular Cave	*d*	24	2	*1.0*	24	8	1	0	0	1	1	0	0	0	0	0	0	0		1	1	Faulkner & Newton 90. HMC?
VN	*1463*	*5143*	625	Grane	Elgfjell - Ridge		*W*	120	Yell. / br.		0	0	L	W	A	D	P	0.0	R14	Halfway Cave	b	25	3	*1.0*	25	12	1	0	0	1	1	1	0	0	0	0	0	0		0	1	Faulkner & Newton 90. HMC?
VN	*146*	*515*	615	Grane	Elgfjell - Ridge		*W*	120	Yell. / br.		0	0	L	W	A	D	P	0.0	R15	Rainy Day Cave	*b*	38	*3*	*2.0*	76	8	1	0	0	2	0	0	0	0	0	0	0	0		0	1	Faulkner & Newton 90. HMC?

ms = mica schist

* May be part of 4S1

* Sump is static

HMC = High Magnesian Calcite

UPPERMOST ALLOCHTHON: Helgeland Nappe Complex: Zone 4 (Efterådal and Jordbrueiv) — Caves are grouped by carbonate outcrop — Vefsn catchment area

UTM COORDS		ALT.	KOMMUNE	AREA	LST. STRIK	LST. DIP	OW	EXT. COLOUR	OTHER INT. ROCK	R	T	QB	CL	KT	SR	OR	CA	REF. NO.	CAVE NAME	CT	LENG.	VR	XS	VOL.	Min. HG %	C	SE	RE	DE	CS	SP	Ch	Sh	BC	RV	MV	DC	FS	P	SG	PRIME REFERENCES
Toeboen				***1925 I cont.***																																					
VN	*1483*	*5086*	592	Grane	Elgfjell - Vall. 4	20	60 W	100	Grey		0	0	L	W	A	U	P	0.0	4S1	Shelter Cave	d	78	3	8.0	624	4	1	0	0	10	0	0	0	0	0	0	0		1	1	Faulkner & Newton 1990. TF00
VN	*1480*	*5117*	596	Grane	Elgfjell - Vall. 4	20	60 W	100	White		0	0	L	W	A	U	P	0.0	4S2	Musk Cave	b	150	30	*4.0*	600	20	1	0	0	1	0	0	0	0	0	0	0		0		Faulkner & Newton 1990
VN	*1485*	*5103*	596	Grane	Elgfjell - Vall. 4														4S2a	Snowfield Cave		Unexplored passage at base of icy 2m climb down. Could be 4S2?																			TF00
VN	*1486*	*5103*	596	Grane	Elgfjell - Vall. 4														4S2b	Choked Rift		Definitely choked 3m down, so probably not 4S2a.																			SN04
VN	*1504*	*5081*	548	Grane	Elgfjell - Vall. 4	20	60 W	50	Grey	*Brown*	0	0	L	S	A	D	P	0.3	4S3	Through Cave	b	32	2	2.0	64	6	1	0	0	2	0	0	0	0	0	0	0		1	1	F. & N. 1990. TF00. SN04
VN	*1503*	*5081*	550	Grane	Elgfjell - Vall. 4	20	60 W	50	Yellow	Grey	0	0	L	S	A	D	P	0.3	4S4	Two Sticks Cave *	b	25	1	1.0	25	4	1	0	0	1	0	0	0	0	0	0	0		1		F. & N. 1990. TF00. SN04
VN	*1482*	*5111*	604	Grane	Elgfjell - Vall. 4		60 W	100	Grey		0	0	L	W	A	U	P	0.0	4S5	Pustehoia	h	306	28	2.0	616	9	1	0	0	1	2	0	0	2	0	0	1		1	3	Faulkner & Newton 1990. TF00
VN	*1487*	*5118*	600	Grane	Elgfjell - Vall. 4	180	*60 W*	80	Grey		0	0	L	W	A	U	P	0.0	4S6	Ca. of Brown Stains	g	230	34	4.0	920	15	1	0	0	2	2	0	0	5	1	2	0	0	1	1	3	F. & N. 1990. TF00. SN04
VN	*1484*	*5121*	608	Grane	Elgfjell - Vall. 4														4S6a	Shaft		Unclimbed; c. 3m deep. Above end of Hidden Streamway in 4S6.																			TF00
VN	*1482*	*5129*	615	Grane	Elgfjell - Vall. 4		*W*	*5*	Grey		0	0	L	W	A	U	P	0.0	4S7	Reindeer Rift	a	14	13	*2.0*	28	93	1	0	0	1	0	0	0	2	0	0	0	0		0		Faulkner & Newton 1990
VN	*1482*	*5130*	610	Grane	Elgfjell - Vall. 4		*W*	*5*	Grey		0	0	L	W	A	U	P	0.0	4S8	Moss Pot	a	11	8	*1.0*	11	73	1	0	0	1	0	0	0	0	0	0	0	0		0		Faulkner & Newton 1990
VN	*1490*	*5125*	591	Grane	Elgfjell - Vall. 4	180	90	100	Grey		0	0	L	W	V	N	P	0.0	4S9	Slit Pot	b	41	23	*4.0*	164	56	1	0	0	1	0	0	1	1	1	0	0	0	1	1	3	Faulkner & Newton 1990. TF00
VN	*1487*	*5136*	590	Grane	Elgfjell - Vall. 4	180	90	30	Grey		0	0	L	W	V	N	P	0.0	4S10	Disappointment Ca.	a	6	1	1.0	6	17	1	0	0	1	0	0	0	0	0	0	0	0	1	0	1	Faulkner & Newton 1990
VN	*1480*	*5130*	600	Grane	Elgfjell - Vall. 4			0.3			0	0	L	W	*V*	N	P	0.0	4S11	Fern Rift	a	10	6	2.0	20	60	1	0	0	1	0	0	0	0	0	0	0	0		0	1	Faulkner & Newton 1990
VN	*1503*	*5085*	554	Grane	Elgfjell - Vall. 4		70 W	50	Grey		0	0	L	R	A	N	P	0.3	4AS1	Camp View Cave **	d	190	12	2.0	380	6	1	0	0	3	1	1	0	1	0	0	0	0	1	1	3	F. & N. 1990. TF00. SN04. *
VN	*1506*	*5106*	576	Grane	Elgfjell - Vall. 4	170	70 W	100	Grey	Yellow	0	0	L	R	A	N	P	0.0	4AS2	Sarvenvårtoehullet	g	315	24	6.0	1890	8	1	0	0	1	1	1	0	1	3	0	0	0	1	1	3	Faulkner & Newton 1990. TF00
VN	*150*	*518*	510	Grane	Elgfjell - Vall. 4			*20*			0	0	L	W	*V*	*N*	P	0.3	4N1	Streamway 1	b	10	*2*	*1.0*	10	20	1	1	0	0	1	0	0	0	0	0	1	0		1		Faulkner & Newton 1990
VN	*150*	*518*	510	Grane	Elgfjell - Vall. 4			*20*			0	0	L	W	*V*	*N*	P	0.3	4N2	Streamway 2	b	10	*2*	*1.0*	10	20	1	1	0	0	1	0	0	0	0	0	1	0		1		Faulkner & Newton 1990
VN	*150*	*518*	510	Grane	Elgfjell - Vall. 4			*20*			0	0	L	W	*V*	*N*	P	0.3	4N3	Streamway 3	b	10	*2*	*1.0*	10	20	1	1	0	0	1	0	0	0	0	0	1	0		1		Faulkner & Newton 1990
VN	*1504*	*5137*	555	Grane	Elgfjell - Vall. 4	5	70 W	15	Grey		0	0	L	F	A	N	P	0.2	4AN1	Twisting Stream Ca.	d	200	12	1.0	200	6	1	0	0	2	1	1	1	0	1	0	0		1	1	Faulkner & Newton 1990 **
VN	*1510*	*5140*	565	Grane	Elgfjell - Vall. 4	180	70 W	15			0	0	L	S	A	D	P	0.2	4AN2	Blind Shafts	S	15	5	2.0	30	33	1	0	0	4	1	0	0	4	0	0	0	0		1		Faulkner & Newton 1990
VN	*1514*	*5128*	565	Grane	Elgfjell - Vall. 4	180	70 W	*15*	Grey		0	0	L	S	A	D	P	0.2	4B1	Extended Cave	d	28	4	2.0	56	14	1	0	0	2	1	1	1	0	0	0	0	0		1	1	Faulkner & Newton 1990
VN	*1514*	*5131*	565	Grane	Elgfjell - Vall. 4	180	70 W	*15*	Grey		0	0	L	S	A	D	P	0.2	4B2	Warm Cave	d	17	4	2.0	34	24	1	0	0	1	1	0	0	0	0	0	0	0		1	1	Faulkner & Newton 1990
VN	*1517*	*5150*	559	Grane	Elgfjell - Vall. 4	20	70 W	15	Grey		0	0	L	R	A	N	P	0.2	4B3	Snow Cave	a	20	5	3.0	60	25	1	0	0	1	0	0	0	0	0	0	0	0	1	1	1	Faulkner & Newton 1990. TF00
VN	*1517*	*5152*	555	Grane	Elgfjell - Vall. 4	20	70 W	15	Grey		0	0	L	R	A	N	P	0.2	4B4	Barrel Cave	d	33	2	2.0	66	6	1	0	0	2	0	0	0	0	0	0	0	0	1	1	1	F. & N. 1990. TF00. SN04
VN	*1520*	*5157*	554	Grane	Elgfjell - Vall. 4	20	70 W	25	Grey		0	0	L	R	A	N	P	0.2	4B5	Through Cave	b	10	*1*	1.0	10	10	1	0	0	2	0	0	0	0	0	0	0		1		Faulkner & Newton 1990. TF00
VN	*1530*	*5168*	555	Grane	Elgfjell - Vall. 4	20	80 W	30	Grey		0	0	L	R	A	N	P	0.2	4B6	Gevirgrotta	h	683	27	3.0	2049	4	1	1	0	1	3	2	0	1	0	1	0	0	1	1	3	Faulkner & Newton 1990
VN	*1523*	*5165*	549	Grane	Elgfjell - Vall. 4	20	70 W	30	Grey		0	0	L	R	A	N	P	0.2	4B7	Shorthorn Cave	f	34	5	1.0	34	15	1	0	0	1	0	0	0	2	0	0	0	0		1	2	Faulkner & Newton 1990. TF00
VN	*1522*	*5165*	549	Grane	Elgfjell - Vall. 4	20	70 W	30	Grey		0	0	L	R	A	N	P	0.2	4B8	Longhorn Cave	b	85	5	1.0	85	6	1	0	0	2	0	0	0	0	0	0	0	0		1	2	Faulkner & Newton 1990
VN	*1545*	*5195*	505	Grane	Elgfjell - Vall. 4	10	70 W	30	*Grey*		0	0	L	W	A	N	P	0.3	4B9	Antler Res. Pot	S	8	7	*1.0*	8	88	1	0	0	1	1	0	0	1	0	0	0	0		0		Faulkner & Newton 1990
VN	*1501*	*5279*	540	Grane	Gåsvasstind														G0	Choked Sink																				SN04
VN	*1516*	*5314*	660	Grane	Gåsvasstind			*200*			0	0	L	W	*V*	*N*	P	0.8	G1	Snake Pit	b	40	16	3.0	120	40	1	0	0	1	1	0	0	1	0	0	0	0		0	1	Faulkner & Newton 1990. SN04
VN	*1514*	*5312*	643	Grane	Gåsvasstind														G1a	Snake Pit Rising		9m of ascending crawl																			SN04
VN	*1509*	*5370*	880	Grane	Gåsvasstind			*200*			0	0	T	S	*V*	*N*	P	0.1	G2	Summit Cave	S	14	14	3.0	42	100	1	0	0	1	0	0	0	1	0	0	0	0		0		Faulkner & Newton 1990
VN	*1522*	*5417*	770	Grane	Gåsvasstind			120			0	0	T	R	*V*	*N*	P	1.0	G3	Sink Cave	b	10	2	3.0	30	20	1	1	0	1	1	1	0	0	0	0	1	0		1		Faulkner & Newton 1990
VN	*1525*	*5420*	778	Grane	Gåsvasstind			120			0	0	T	R	*V*	*N*	P	1.0	G4/5	Gåsvasstindhola	d	243	13	20.0	4860	5	1	0	1	1	1	1	0	2	1	0	0	0	1	1		Faulkner & Newton 1990
VN	*1550*	*5355*	844	Grane	Gåsvasstind														G6	Outcrop Top Pot		10m deep, c. 15m long, needs 5m ladder and long belay																			SN04
VN	*1537*	*5343*	796	Grane	Gåsvasstind														G7	Windbreak Cave		15m of across-strike crawls, parallel to cliff																			SN04
VN	*1534*	*5339*	776	Grane	Gåsvasstind														G8	Rocky Cave		15m of low crawl																			SN04
VN	*1590*	*5470*	660	Grane	Gåsvassdal															oxbow cave																				Newton 1999 p48
VN	*1660*	*5220*	540	Grane	Gåsvassdal															short vertical cave																				Newton 1999 p48

* Probably west entrance of 4S3
** Shaft Entrance

* Sump is static. (Dry in 2000)
** Passable bc?

UPPERMOST ALLOCHTHON: Helgeland Nappe Complex: Zone 4 (Ellerdal and Jordbrueiv) — **Caves are grouped by carbonate outcrop** — **Vefsn catchment area**

	UTM COORDS		ALT.	KOMMUNE	AREA	LST. STRIKE	LST. DIP		OW	EXT. COLOUR	OTHER INT. ROCK	External Cave Attributes: R	T	GS	CL	KT	SR	OR	CA	REF. NO.	CAVE NAME	CT	Internal Cave Attributes: LENG.	VR	XS	VOL.	Min. HG %	C	SE	RE	DE	CS	SP	Ch	Sh	BC	RV	MV	DC	PB	P	SC	PRIME REFERENCES
Toeboin			***1625 I***		***cont.***																																							
VN	*1506*	*5060*	541	Grane	Elgfjell - Vall. 5			*W*	*10*		gouge	0	0	L	W	A	U	P	0.1	5S1	Crystal Cave	a	*10*	*3*	*3.0*	*30*	30	1	0	0	1	0	0	0	0	0	0	0	0		1		TF00
VN	*1505*	*5061*	543	Grane	Elgfjell - Vall. 5			*W*	*10*			0	0	L	W	A	U	P	0.1	5S2	Tube Cave	b	*10*	*3*	*3.0*	*30*	30	1	0	0	1	0	0	0	0	0	0	0	0	1	1		TF00
VN	*1543*	*5139*	560	Grane	Elgfjell - Vall. 5			*W*	*10*			0	0	L	G	A	N	P	0.2	5N1	cave	b	5	*1*	*1.0*	5	20	1	0	0	1	0	0	0	0	0	0	0	0		0		Faulkner & Newton 1990
VN	*1567*	*5153*	545	Grane	Elgfjell - Vall. 5			*W*	*10*			0	0	L	S	A	D	P	0.2	5N2	cave	b	5	*1*	*1.0*	5	20	1	0	0	1	0	0	0	0	0	0	0	0		0		Faulkner & Newton 1990
VN	*1557*	*5162*	530	Grane	Elgfjell - Vall. 5	175	60	W	10	Grey		0	0	L	F	A	N	P	0.2	5N3	Buktgrotta	b	180	25	2.0	360	14	1	1	0	1	1	1	0	2	0	2	0	0		1	3	Faulkner & Newton 1990
VN	*1530*	*5143*	585	Grane	Elgfjell - Vall. 5															5N4	Tight Shaft		2m deep																				TF00 and SN04
VN	*1532*	*5147*	578	Grane	Elgfjell - Vall. 5															5N5	Injection Cave		12m long with glacially-injected blocks																				TF00
VN	*1491*	*4955*	408	Grane	Elgfjell -S.Slope	175	80	W	*10*	Yell. br	Grey	0	0	L	W	A	D	P	1.0	SS1	Contorted Cave	b	10	*2*	*2.0*	20	20	1	1	0	0	1	0	0	0	0	0	0	0		1		Faulkner & Newton 1990, TF00
VN	*1521*	*4960*	510	Grane	Elgfjell -S.Slope	175	80	W	*10*			0	0	L	S	A	D	P	0.1	SS2	Karren Cave 1	S	5	5	2.0	10	100	1	0	0	1	0	0	0	1	0	0	0	0		1		Faulkner & Newton 1990
VN	*1521*	*4963*	510	Grane	Elgfjell -S.Slope			*W*	*10*			0	0	L	S	A	D	P	0.1	SS3	Karren Cave 2	S	4	4	2.0	8	100	1	0	0	1	0	0	0	1	0	0	0	0		1		Faulkner & Newton 1990
VN	*1518*	*4997*	510	Grane	Elgfjell -S.Slope			*W*	*10*			0	0	L	S	A	D	P	0.1	SS4	Karren Valley Shaft	S	10	10	2.0	20	100	1	0	0	1	0	0	0	1	0	0	0	0		1		Faulkner & Newton 1990
VN	*1533*	*4927*	360	Grane	Elgfjell -S.Slope			*S*	*10*	White		0	0	L	F	A	N	P	3.5	SS5	Elgfjellsvgrotta	d	50	10	2.0	100	20	1	2	0	0	1	0	1	0	0	0	1	0		1	1	Faulkner & Newton 1990
VN	*1540*	*4927*	350	Grane	Elgfjell -S.Slope			*S*	*10*			0	0	L	F	A	N	P	3.5	SS6	Alligator Cave	a	44	*5*	2.0	88	11	1	0	0	1	1	2	0	0	0	0	1	0		1	1	Faulkner & Newton 1990
VN	*1555*	*4920*	340	Grane	Elgfjell -S.Slope			*S*	*10*			0	0	L	F	A	N	P	3.5	SS7	Lake Cave 1	b	15	*3*	2.0	30	20	1	1	0	0	1	0	0	0	0	0	1	0		1	1	Faulkner & Newton 1990
VN	*1570*	*4930*	330	Grane	Elgfjell -S.Slope			*S*	*10*			0	0	L	F	A	N	P	3.5	SS8	Lake Cave 2	b	6	1	2.0	12	17	1	1	0	0	1	0	0	0	0	0	1	0		1	1	Faulkner & Newton 1990
VN	*1572*	*5006*	508	Grane	Elgfjell -S.Slope	135	80	W	8			0	0	L	S	A	N	P	0.5	SS9	Sørfjellvgrotta	a	70	15	3.0	210	21	1	1	1	0	1	0	0	0	0	0	0	0	1	2	1	Faulkner & Newton 1990, TF00
VN	*1600*	*5100*	560	Grane	Elgfjell - Sarvej.			*W*	*10*			0	0	L	W	A	D	P	0.3	S1	Overhanging Pit	S	10	9	1.0	10	90	1	1	0	0	1	0	0	0	0	0	0	0		1		Faulkner & Newton 1990
VN	*1600*	*5130*	540	Grane	Elgfjell - Sarvej.			*W*	*10*			0	0	L	W	A	D	P	0.4	S2	Through Cave	a	5	*1*	*1.0*	5	20	1	0	0	2	0	0	0	0	0	0	0	0		1		Faulkner & Newton 1990
VN	*1610*	*5157*	470	Grane	Elgfjell - Sarvej.			*W*	*10*			0	0	L	W	A	U	P	0.5	S3	Sump Cave	a	5	*2*	*1.0*	5	40	1	1	0	0	1	1	0	0	0	0	0	0		1		Faulkner & Newton 1990
VN	*1593*	*5163*	520	Grane	Elgfjell - Sarvej.	40		*W*	*50*	Grey		0	0	L	W	A	U	P	0.1	S4	Øvre Sarvejaellagr.	b	71	20	2.0	142	28	1	0	0	1	0	0	0	1	0	0	0	0		1	1	Faulkner & Newton 1990
VN	*1596*	*5163*	520	Grane	Elgfjell - Sarvej.			*W*	*50*	Grey		0	0	L	W	A	U	P	0.1	S5	Steve's Entrance	c	28	5	*1.0*	28	18	1	0	0	1	0	0	0	0	0	0	0	0		1	1	Faulkner & Newton 1990
VN	*1597*	*5165*	520	Grane	Elgfjell - Sarvej.			*W*	*50*	Grey		0	0	L	W	A	U	P	0.1	S6	Geoff's Entrance	a	7	3	*1.0*	7	43	1	0	0	1	0	0	0	1	0	0	0	0		1	1	Faulkner & Newton 1990
VN	*1594*	*5170*	518	Grane	Elgfjell - Sarvej.			*W*	*50*	Grey		0	0	L	W	A	U	P	0.1	S7	Sarvejaellagrotta	h	411	31	1.5	617	8	1	0	0	3	0	0	1	5	0	0	0	0		1	3	Faulkner & Newton 1990
VN	*1595*	*5179*	505	Grane	Elgfjell - Sarvej.		60	W	*50*	Grey		0	0	L	W	A	U	P	0.1	S9	Stream Sink	S	28	11	1.0	28	39	1	1	0	0	1	0	0	0	0	0	0	0		1	1	Faulkner & Newton 1990
VN	*1598*	*5181*	493	Grane	Elgfjell - Sarvej.		60	W	*50*	Grey		0	0	L	W	A	U	P	0.1	S10	Aural Passage	b	12	6	1.0	12	50	1	0	0	1	0	0	0	1	0	0	0	0		1	1	Faulkner & Newton 1990
VN	*1600*	*5182*	490	Grane	Elgfjell - Sarvej.	30	60	W	*50*	Grey		0	0	L	W	A	U	P	0.1	S11	Last Rising Passage	b	16	5	1.0	16	31	1	0	0	1	1	0	0	1	0	0	0	0		1	1	Faulkner & Newton 1990
VN	*1603*	*5184*	480	Grane	Elgfjell - Sarvej.	30	60	W	*50*	Grey		0	0	L	W	A	U	P	0.1	S12	Zig Zag Cave	b	110	35	2.0	220	32	1	0	0	3	1	0	0	3	2	0	0	0		1	1	Faulkner & Newton 1990. *
VN	*1622*	*5067*	580	Grane	Elgfjell - Sarvej.		70	W	1	Brown		0	0	L	G	A	U	P	0.1	S14	Grykagrotta	b	28	2	*1.0*	28	7	1	0	0	2	0	0	0	0	0	0	0	0		1		Faulkner & Newton 1990
VN	*1615*	*5080*	600	Grane	Elgfjell - Sarvej.															S15	shaft		In 8m-wide band of grey marble. Narrow and undescended. 6m deep?																				TF00
VN	*1644*	*5061*	581	Grane	Elgfjell - Sarvej.															S16	hole		In 1m-wide band of brown marble																				TF00
VN	*1553*	*5046*	560	Grane	Elgfjell - Sarvej.															S17	small cave		In 5m-wide band of yellow marble. Unentered.																				TF00
VN	*1635*	*5015*	550	Grane	Elgfjell -S.Slope				*10*	Grey		0	0	L	S	A	N	P	0.2	SS10	Fewmet Cave	a	10	*1*	*1.0*	10	10	1	0	0	1	0	0	0	0	0	0	0	0		0		Faulkner & Newton 1990
VN	*1645*	*4995*	510	Grane	Elgfjell -S.Slope				*10*			0	0	L	W	A	N	P	0.3	SS11	Jolly Roger Cave	h	120	35	*2.0*	240	29	1	0	0	2	1	0	0	*2*	0	0	0	0	1	0	1	Faulkner & Newton 1990
VN	*168*	*501*	580	Grane	Elgfjell -S.Slope		80	W	10	Grey		0	0	L	S	A	N	P	0.1	SS13	Through Cave	b	10	*2*	*2.0*	20	20	1	0	0	2	0	0	0	0	0	0	0	0		0		Faulkner & Newton 1990. TF00
VN	*168*	*500*	560	Grane	Elgfjell -S.Slope		80	W	10	Grey		0	0	L	S	A	N	P	0.2	SS14	Gethsemane Cave	g	40	*10*	*2.0*	80	25	1	0	0	2	0	0	0	*2*	0	0	0	0		0		Faulkner & Newton 1990. TF00

* 1 bc is passable

UPPERMOST ALLOCHTHON: Helgeland Nappe Complex: Zone 4 (Elterådal and Jordbruselv)

Caves are grouped by carbonate outcrop

Vefsn catchment area

UTM COORDS			ALT.	KOMMUNE	AREA	LST. STRIKE	LST. DIP	OW	EXT. COLOUR	OTHER INT. ROCK	R	T	GS	CL	KT	SR	OR	CA	REF. NO.	CAVE NAME	CT	LENG.	VR	XS	VOL.	Mia. HG %	C	SE	RE	DE	CS	SP	Ch	Sh	BC	RV	MV	DC	FS	P	SG	PRIME REFERENCES
Tosbotn				***1825 I***	***cont.***																																					
VN	*1310*	5265	940	Grane	E. Jordhulefjell			*10*			0	0	U	G	V	N	P	0.5		cave	a	7	2	2.0	14	29	1	0	0	1	0	0	0	0	1	0	0	0		1		Faulkner & Newton 1990
VN	*1315*	5260	940	Grane	E. Jordhulefjell			*10*			0	0	U	G	V	N	P	0.5		cave	a	7	2	2.0	14	29	1	0	0	1	0	0	0	0	1	0	0	0		1		Faulkner & Newton 1990
VN	*1534*	4800	475	Grane	Jordbruselv			100			0	0	L	W	V	N	P	0.1		Archway Cave	a	30	20	4.0	120	67	1	0	0	1	0	0	0	0	1	0	0	0		1	1	Faulkner & Newton 1990
VN	*1534*	4780	430	Grane	Jordbruselv			100			0	0	L	W	V	N	P	0.1		Ice Crawl Cave	a	18	2	1.5	27	11	1	0	0	2	0	0	0	0	0	0	0	0		1	1	Faulkner & Newton 1990
VN	*1534*	4773	430	Grane	Jordbruselv	180	90	100			0	0	L	W	V	N	P	0.1		Crawl Cave	a	23	3	1.0	23	13	1	0	0	1	0	0	0	0	0	0	0	0	0	1	1	1	Faulkner & Newton 1990
VN	*1535*	4755	400	Grane	Jordbruselv			100			0	0	L	W	V	N	P	0.2		T-Pot	d	20	10	2.0	40	50	1	0	0	1	0	0	0	1	0	0	0	0		1	1	Faulkner 1987
VN	*1530*	4740	365	Grane	Jordbruselv			100			0	0	L	W	V	N	P	0.2		Boulder Stream Sink	b	16	*2*	*1.0*	*16*	13	1	1	0	0	1	0	0	0	0	0	1	0		1	1	Faulkner 1987
VN	*1572*	4722	381	Grane	Jordbruselv	165	80 W	100	Grey white		0	0	L	F	A	N	P	0.2		Jegerhullet	h	650	34	5.0	3250	5	1	0	1	5	1	0	2	5	1	1	0	1	1	1	3	Faulkner 1987
VN	*1580*	4690	335	Grane	Jordbruselv	170	(80 W)													Waterfall Hole																					Faulkner & Newton 1987
VN	*1582*	4680	330	Grane	Jordbruselv	160	90	100	Grey	Amphib.	0	0	L	F	V	N	P	3.0		Etasjegrotta	h	1055	42	3.0	3165	4.0	1	1	0	2	2	2	2	13	0	*1*	0	0	1	1	3	Faulkner 1987. TF97&98. *
VN	*1572*	4670	320	Grane	Jordbruselv			100			0	0	L	F	V	N	P	3.0		Dry Valley Cave	a	60	12	1.0	60	20	1	0	0	1	0	0	0	0	0	0	0	0		1		Faulkner 1987
VN	*1580*	4660	310	Grane	Jordbruselv			100			0	0	L	F	V	N	P	3.0		Ledge Opening	a	13	1	1.0	13	8	1	0	0	1	0	0	0	0	0	0	0	0		1		Faulkner 1987
VN	*1590*	4630	295	Grane	Jordbruselv			100			0	0	L	F	V	N	P	30.0		Beehive Cave	c	61	4	2.0	122	7	1	0	0	1	0	0	0	0	0	0	0	0	1	1	1	Faulkner 1987
VN	*1590*	4605	310	Grane	Jordbruselv	150	90	100			0	0	L	W	V	N	P	1.0		Keyhole Cave	a	50	4	2.0	100	8	1	0	0	2	1	0	0	0	0	0	0	0		1	1	Faulkner 1987
VN	*1600*	4620	318	Grane	Jordbruselv	160	90	100		Quartz	0	0	L	F	V	N	P	30.0		Invasjonsgr./Cliff Ca.	f	439	27	1.5	659	6	1	0	0	4	1	0	1	0	0	1	0	1	1	1	3	Faulkner & Newton 90.TF97&98
VN	*1596*	4610	300	Grane	Jordbruselv	160	90	100	Grey white		0	0	L	F	V	N	P	30.0		Vannhull./Main Rising	c	650	35	6.0	3900	5	1	0	1	1	1	2	0	2	0	0	0	0		1	2	Faulkner & Newton 90, Whybro
VN	*1600*	4610	293	Grane	Jordbruselv	160	90	100			0	0	L	F	V	N	P	30.0		Ramp Cave	g	15	8	2.0	30	53	1	0	1	1	1	1	0	1	0	0	0	0		1	1	Faulkner 1987
VN	*1600*	4606	293	Grane	Jordbruselv			100			0	0	L	F	V	N	P	30.0		Halfmoon Cave	b	40	2	*1.0*	40	5	1	0	0	2	0	0	0	0	0	0	0	0		1		Faulkner & Newton 1990
VN	*1610*	4595	287	Grane	Jordbruselv	135	90	100			0	0	L	F	V	N	P	30.0		Upper River Cave	a	10	3	4.0	40	30	1	0	0	1	1	0	0	0	0	0	0	0		1		Unpublished. TF97
VN	*1610*	4595	287	Grane	Jordbruselv			100			0	0	L	F	V	N	P	30.0		River Cave	a	45	6	6.0	270	13	1	0	0	1	1	1	0	0	0	0	0	0		1	1	Faulkner 1987
VN	*1615*	4580	285	Grane	Jordbruselv			100			0	0	L	F	V	N	P	30.0		The Alcoves	a	6	1	1.0	6	17	1	1	0	0	1	0	0	0	0	0	1	0		1		Faulkner 1987
VN	*1640*	4525	295	Grane	Bjørkåsen			100			0	0	L	F	V	N	P	0.5		Bjørkåstjerngrotta	b	56	5	1.0	56	9	1	1	0	0	1	0	0	0	0	0	0	0		1	1	Faulkner 1987
VN	*1660*	4480	290	Grane	Bjørkåsen			300			0	0	L	F	V	N	P	1.0		Restday Cave	b	55	4	1.0	55	7	1	0	0	1	1	0	0	0	0	0	0	0		0	1	Faulkner 1987
VN	*1653*	4430	310	Grane	Bjørkåsen			100			0	0	L	G	V	N	P	0.0		Road Cave	b	25	6	1.0	25	24	1	0	0	1	1	1	0	0	0	0	0	0		1	1	Faulkner & Newton 1990
VN	*1654*	4412	289	Grane	Bjørkåsen	20	90	100	White	a/m.	0	0	L	F	V	N	P	11.0		Anastomosegrotta	e	238	20	5.0	1190	8	1	0	0	1	1	0	3	3	4	0	0	1	1	1	3	Faulkner & Newton 1990. TF97
VN	*1620*	4353	395	Grane	Bjørkåsen			100			0	0	L	G	V	N	P	0.5		Shaft Caves	S	40	15	4.0	160	38	1	0	0	6	0	0	0	6	0	0	0	0		1	1	Faulkner & Newton 1990
VN	*1540*	4275	520	Grane	Bjørkåsen			100			0	0	L	S	V	N	P	0.1		Third Session Cave	b	10	2	1.0	10	20	1	1	0	0	1	0	0	0	0	0	0	0		0		Faulkner & Newton 1990
VN	*1690*	4450	284	Grane	Bjørkåsen			200	White		0	0	L	F	V	N	P	11.0		Bjørkåsgrotta	c	529	7	5.0	2645	1	1	1	0	2	2	3	1	0	0	0	0	0	1	1	3	Faulkner & Newton 1990. TF97
VN	*1700*	4445	274	Grane	Bjørkåsen															Sumped Sink																					Unpublished. TF97
VN	*1713*	4470	280	Grane	Bjørkåsen			200			0	0	L	F	V	N	P	11.0		Bjørkås Rising	a	10	2	1.0	10	20	1	0	1	0	1	1	0	0	0	0	1	0		1		Faulkner & Newton 1990
VN	*1580*	4840	450	Grane	Bienjenbeektie			80			0	0	L	R	V	N	P	0.1		Bienjenbeektigrotta	b	30	2	1.0	30	7	1	0	0	2	0	0	0	0	0	0	0	0		0	1	Faulkner 1987
VN	*1583*	4843	450	Grane	Bienjenbeektie			80			0	0	L	R	V	N	P	0.1		Bienjenbeektihullet	S	20	10	3.0	60	50	1	0	0	1	0	0	0	1	0	0	0	0		1	1	Faulkner & Newton 1990
VN	*1595*	4830	465	Grane	Bienjenbeektie			80			0	0	L	W	V	N	P	0.1		Bienjenbeektl Cave	b	5	*1*	*1.0*	5	20	1	0	0	1	0	0	0	0	0	0	0	0		1		Faulkner & Newton 1990
VN	*1605*	4822	464	Grane	Bienjenbeektie															Stone Fungus Cave		40m of crawls and larger passage																				SN04
VN	*1600*	4810	464	Grane	Bienjenbeektie															Col Pot		8m-climb down hole to 27m-long phreatic passage																				SN04

a/m = amphibolite / mylonite

* Fall Aven = RV?

UPPERMOST ALLOCHTHON: Helgeland Nappe Complex: Zone 5 (Moajaen to Fjellryggen): TOTALS

UTM COORDS	ALT.	KOMMUNE	AREA	LST. STRIKE	LST. DIP	OW	EXT. COLOUR	OTHER INT. ROCK	R	T	GS	CL	KT	SR	OR	CA	REF. NO.	CAVE NAME	CT	LENG.	VR	XS	VOL.	Min. HG %	C	SE	RE	DE	CB	SP	Ch	Sh	BC	RV	MV	DC	FS	P	SC	PRIME REFERENCES
Totals	####			##	####				7	0						###				7689	####	####	40600	####	79	35	11	73	73	58	15	41	20	4	33	2	12	49		
Av. per cave	450			76	674				0.1	0.0						1.8				97	9.75	3.1	514	26		0.4	0.1	0.9	0.9	0.7	0.2	0.5	0.3	0.1	0.4	0.0	0.2	0.6		
Minima	55			45	10											0.10				1	1	0.5	1	2		0	0	0	0	0	0	0	0	0						
Maxima	880			90	1500											4.0				935	105	15.0	12000	100		2	1	4	4	15	3	13	3	2						

(Dip measured in 29 caves)

Karst Types:

	#	Length
V	43	5206
A	34	2463
L	0	0
C	0	0
X	2	20
Totals	79	7689

Cave Locations:

	#	Length
C	0	0
F	32	1345
W	34	3421
R	3	919
S	1	15
G	9	1969
P	0	0
Totals	79	7689

Glacial Situations:

	#	Length
C	0	0
D	2	10
E	5	654
G	0	0
H	11	2100
K	3	400
L	41	2784
S	0	0
T	17	1781
U	0	0
Totals	79	7689

Cave Types:

	#	Length
S	5	40
a	22	705
b	32	1781
c	4	293
d	5	944
e	2	122
f	2	305
g	2	743
h	3	2586
Hy	2	160
I	0	0
J	0	0
L	0	0
R	0	0
T	0	0
Totals	79	7689

Relict Caves:

#	Length
15	417

15	417

MV Caves:

#	Length
33	1416

33	1416

Combination Caves:

#	Length
31	5856

UPPERMOST ALLOCHTHON: Helgeland Nappe Complex: Zone 5 (Moajsen to Fjellryggen)

Caves are grouped by carbonate outcrop

Vefsn catchment area

UTM COORDS	ALT.	KOMMUNE	AREA	LST. STRIKE	LST. DIP	OW	EXT. COLOUR	OTHER INT. ROCK	R	T	GS	CL	KT	SR	OR	CA	REF. NO.	CAVE NAME	CT	LENG.	VR	XS	VOL.	Min. HG %	C	SE	RE	DE	CS	SP	Ch	Sh	BC	RV	MV	DC	FS	P	BG	PRIME REFERENCES
Moajsen			***1826 I***																																					
VP 1733 1438	344	Vefsn	Storeveten	160	80 W	800	*		0	0	K	F	A	N	P	0.2		Nordvetgrotta	b	30	10	3.0	90	33	1	1	1	0	2	1	0	0	2	0	0	1	0	0	1	1	Unexplored.TF00.
VP 1818 1325	153	Vefsn	Storeveten	90	80 N	100	*		1	0	H	R	A	N	P	0.5		Bollihauggrotta	b	40	3	6.0	240	8	1	1	1	0	1	0	0	0	1	0	0	0	0	1	1	3	TF97. Surveyed to 90m: SN04
VP 1838 1312	133	Vefsn	Storeveten															Bollihaug Res. Cave		Too low after c. 12m																			1	SN04
VP 1685 0025	180	Vefsn	Øyfjell	135	70 S	600			0	0	H	W	A	D	P	2.0		Øyfjeligrotta*	h	800	105	15.0	12000	13	1	0	0	3	1	5	2	1	1	1	0	0	1	1	4	Heap 1967/68. SEL 1983. (Main ent.)
VP 1685 0025	140	Vefsn	Øyfjell	135	70 S	600			0	0	H	W	A	D	P	2.0		Side Chamber	c	50	5	5.0	250	10	1	0	0	2	0	0	0	0	0	0	0	0	0	1	0	4	Heap 1967/68
VP 1670 0025	160	Vefsn	Øyfjell	135	70 S	600			0	0	H	W	A	D	P	2.0		small cave	a	10	2	2.0	20	20	1	0	0	3	1	0	0	0	0	0	0	0	0		0	4	Heap 1967/68. UH list
VP 1665 0025	200	Vefsn	Øyfjell	135	70 S	600			0	0	H	W	A	D	P	2.0		Sink Cave	a	30	3	5.0	150	10	1	0	0	1	1	0	0	0	1	0	0	0	1	0	4	Heap 1967/68
VP 1665 0030	200	Vefsn	Øyfjell	135	70 S	600			0	0	H	W	A	D	P	2.0		Torrgrotta	c	75	10	3.0	225	13	1	0	0	1	1	0	1	0	3	0	0	0	1	0	4	Heap 1967/68. UH list
VP 170 002	80	Vefsn	Øyfjell	135	70 S	600			0	0	E	F	A	N	P	2.0		Nedre Øyfjeligrotta	b	20	2	2.0	40	10	1	0	1	0	1	1	0	0	0	0	1	0		0			U. Holbye 1974 list. Grimsby
							* Dolostone? (Gustavson)																																		
Fustvatn			***1926 IV***																																					
VN 215 945	100	Vefsn	Bjørnåga															Radios Cave																						T. Doj pc 1997
VP 206 003	120	Vefsn	Bjørnåga			400			0	0	D	F	V	N	P	0.2		cave	a	5	1	1.0	5	20	1	1	0	0	1	0	0	0	0	0	1	0		0		Doj 1991. pc 1997
VN 2235 9575	280	Vefsn	Bjørnåga			400			1	0	K	G	V	N	P	1.2		Bokdfågrotta	f	290	30	3.0	870	10	1	1	0	0	1	1	0	0	0	0	0	0		0		Doj 1991. pc 1997
VP 1825 470	160	Vefsn	Dolstadås															Dolstadåsgrotta?		Blocked to protect children? In dolomite? Near Kjerkelia? Not found TF00																				U. Holbye list 1974. Or at 188040?
VP		Vefsn	Dolstadås															Flatåsgrotta?																					
VP 20x 02x	150	Vefsn	Dolstadås													0.3		Andåsgrotta		200		Secret Cave!																	U. Holbye list 1974
VP 216 010	120	Vefsn	Bjørnåga			100			0	0	D	F	X	N	P	0.5		cave	a	5	1	1.0	5	20	1	1	0	0	1	0	0	0	0	0	1	0		0		U. Holbye list 1974
																																							Doj 1991. pc 1997. In dolomite?
Trofors			***1926 III***																																					
VN 2005 8030	55	Grane	Laksfors	180	90	1500			0	0	E	F	V	N	P	3.0		N. Laksfors Rising	f	15	6	2.0	30	40	1	0	1	0	1	1	0	1	0	0	1	0	0	1	1	Faulkner&St.Pierre 1977
VN 2113 7841	88	Grane	Laksfors	160	80 W	1000		Amphibolite	0	0	E	G	A	N	P	2.0	M1	Mellebekkgrotta	g	382	20	3.3	1261	5	1	1	0	3	2	3	0	0	0	2	0	0	1	1	3	Faulkner&St.Pierre 1977. TF00
VN 2116 7854	84	Grane	Laksfors	150	90	1000			0	0	E	G	V	N	P	2.0	M2	Mellebekkgrotta 2	Hy	121	12	5.7	690	10	1	0	0	2	1	2	0	0	0	0	0	0		1	3	Unpublished. TF97, 00
VN 2129 7854	78	Grane	Laksfors	170	90	1000	Grey Wh	Garnet ms	0	0	E	G	V	N	P	2.0	M3	Mellebekkgrotta 3	e	116	6	3.4	394	5	1	0	0	1	1	1	0	0	0	0	0	1	0	1	3	Unpublished. TF97,00. Moonmilk
VN 2069 7711	153	Grane	Laksfors	150	80 W	800	Pale grey	Hornblend?	0	0	H	G	A	U	P	3.5		Øvre Geitkdauvgr.	d	99	6	9.1	901	6	1	1	0	0	1	0	0	0	2	0	0	0		1	3	Unpublished. TF97
VN 2067 7720	148	Grane	Laksfors	160	90	800	Pale grey	a-c + bio. sc	0	0	H	G	V	N	P	3.5		Geitkdauvgrotta	h	935	16	8.3	7761	1.7	1	1	0	0	1	5	2	4	3	0	0	1	1	1	3	Unpublished. TF97&98. *
VN 2059 7736	150	Grane	Laksfors	145	60 E	1000	Grey	Garn. bio sc	0	0	H	G	A	U	P	3.5		Lillelvgrotta	Hy	39	17	9.5	371	44	1	0	0	1	1	2	0	0	0	0	0	0		1	3	Faulkner&St.Pierre1977. TF97
VN 2315 7015	370	Grane	Trofors															Kleppen Sink																					Unexplored. TF97
VN 2237 6610	417	Grane	Trofors		W	800			0	0	L	W	A	U	P	0.7		Lost and Found Cave	b	23	10	1.0	23	43	1	0	0	1	1	0	0	1	0	0	1	0		1		Unpublished. TF97&98
VN 2235 6605	406	Grane	Trofors	170	45 W	800		Musc. schist	0	0	L	W	A	U	P	0.7		Trench Pot	b	138	25	3.0	414	18	1	1	0	2	1	0	1	2	0	1	0	0		1	3	Unpublished. TF97&98
VN 2240 6599	396	Grane	Trofors		W	800			0	0	L	W	A	U	P	0.7		Long Slit	d	8	5	1.0	8	63	1	0	0	2	1	0	0	0	0	0	0	0		1	1	Unpublished. TF98
VN 2220 6570	388	Grane	Trofors	10	80 W	800			0	0	L	F	A	N	P	1.0		Upper Wide Cave	a	3	2	2.0	6	67	1	1	0	0	1	0	0	0	0	0	0	0		1		Unpublished. TF97
VN 223 658	360	Grane	Trofors		W	800			0	0	L	F	A	N	P	1.0	ST2	Wide Sink	a	8	3	4.0	32	38	1	1	0	0	1	0	0	0	0	0	0	0		1	1	Faulkner&Newton 1992
VN 2230 6580	360	Grane	Trofors		W	800			0	0	L	F	A	N	P	1.0	ST1	Wide Cave	b	65	6	4.0	260	9	1	0	0	3	1	0	0	0	0	0	0	0		1	3	Faulkner&Newton 1992
VN 223 658	370	Grane	Trofors		W	800			0	0	L	F	A	N	P	1.0	ST3	Eddie's Pot	S	8	5	2.0	16	63	1	1	0	0	1	0	0	0	0	0	1	0		1	1	Faulkner&Newton 1992
VN 2270 8990	300	Grane	Ravatn			10			1	0	K	F	V	N	P	2.2		Ravatnhuliet	a	80	15	10.0	800	19	1	1	1	0	1	0	0	0	0	0	0	0		1	1	Faulkner&Newton 1992
							a-c = amphibolite-cataclasite																																	* All sumps are static
Svenningdal			***1925 IV***																																					
VN 1885 5290	880	Grane	Gaasvatn		W	100			0	0	T	S	X	X	P	0.4		Through Cave	b	15	2	2.0	30	13	1	0	0	2	0	0	0	0	1	0	0	0		0		Faulkner 1987
VN 2205 6355	431	Grane	Stavassdal															Joint Crawl																					4m deep. Unexplored. TF97
VN 2230 6273	463	Grane	Stavassdal															Tree Hole																					3m deep. Unexplored. TF97
VN 2186 6021	497	Grane	Vargskar		W	1000			0	0	L	F	A	N	P	3.0	V1	Jim's Cave	b	10	2	1.0	10	20	1	0	0	1	0	0	0	0	0	0	0	0		0	1	Newton&Faulkner 1992
VN 2184 6018	502	Grane	Vargskar		W	1000			0	0	L	W	A	N	P	3.0	V2	Drowning Cave	b	174	9	1.0	174	5	1	1	0	0	4	1	0	0	0	0	1	0	1	0	3	Newton&Faulkner 1992. *
VN 2187 6010	515	Grane	Vargskar		W	1000			0	0	L	W	A	N	P	3.0	V3	Track Cave	c	66	15	2.0	132	23	1	2	0	0	2	0	0	0	1	0	1	0		0	2	Newton&Faulkner 1992
VN 2180 5998	536	Grane	Vargskar		W	1000			0	0	L	W	A	N	P	3.0	V4	Elusive Cave	b	60	15	1.0	60	25	1	1	0	0	1	0	0	0	0	0	1	0		0	1	Newton&Faulkner 1992
VN 2185 5994	537	Grane	Vargskar			1000			0	0	L	W	V	N	P	3.0	V5	Camp Cave	b	133	6	2.0	266	5	1	2	0	0	1	1	0	0	0	0	0	0		1	3	Newton&Faulkner 1992
VN 2185 5992	537	Grane	Vargskar			1000			0	0	L	W	V	N	P	3.0	V5A	Upper Camp Cave	b	13	2	1.0	13	15	1	1	1	0	1	0	0	0	0	0	1	0		1	1	Newton&Faulkner 1992
VN 2185 5990	537	Grane	Vargskar			1000			0	0	L	W	V	N	P	3.0	V6	Baptist's Cave	d	288	20	2.0	576	7	1	0	0	1	1	4	0	1	0	0	0	0		1	3	Newton&Faulkner 1992. *
VN 2173 5963	595	Grane	Vargskar			1000			0	0	L	W	V	N	P	2.6	V7	Roaring Cave	d	522	40	4.0	2088	8	1	2	0	4	3	1	2	2	0	0	0	0		0	3	Newton&Faulkner 1992
VN 2154 5969	630	Grane	Vargskar			1000			0	0	L	W	V	N	P	2.5	V8	Three Entrance Cave	b	156	15	4.0	624	10	1	1	0	3	1	0	1	0	0	0	0	0	1	1	3	Newton&Faulkner 1992
VN 2179 5967	580	Grane	Vargskar			1000			0	0	L	F	V	N	P	2.8	V9	Daylight Cave	b	12	3	2.0	24	25	1	1	1	0	1	0	0	0	0	0	1	0		0	1	Newton&Faulkner 1992
VN 2176 5959	594	Grane	Vargskar			1000			0	0	L	F	V	N	P	2.8	V10	Neglected cave	b	31	6	1.0	31	19	1	1	0	0	1	0	0	0	0	0	1	0		0	2	Newton&Faulkner 1992
VN 2139 5945	710	Grane	Vargskar			1000			0	0	T	W	V	N	P	2.3	V11	Trickle Pot	b	30	7	1.0	30	23	1	0	0	1	0	0	0	0	0	0	0	0	1	0	1	Newton&Faulkner 1992

UPPERMOST ALLOCHTHON: Helgeland Nappe Complex: Zone 5 (Mosjøen to Fjellryggen)

Caves are grouped by carbonate outcrop

Vefsn catchment area

	UTM COORDS		ALT.	KOMMUNE	AREA	LST. STRIKE	LST. DIP	OW	EXT. COLOUR	OTHER INT. ROCK	External Cave Attributes: R	T	GB	CL	KT	SR	OR	CA	REF. NO.	CAVE NAME	Internal Cave Attributes: CT	LENG.	VR	XS	VOL.	Mis. HG %	C	SE	RE	DE	CS	SP	Ch	Sh	BC	RV	MV	DC	FS	P	BG	PRIME REFERENCES
Svenningdal				***1925 IV***	***cont.***																																						
VN	*2151*	*5941*	685	Grane	Vargskar			1000			0	0	L	W	V	N	P	2.3	V12	Razor Cave	d	27	3	1.0	27	11	1	0	0	1	1	0	0	0	0	0	1	0		0	1	Newton&Faulkner 1992
VN	*2175*	*5941*	625	Grane	Vargskar			1000			0	0	L	F	V	N	P	2.7	V13	Kompassgrottene	g	361	18	5.0	1805	5	1	0	0	1	2	2	0	0	0	0	0	0		0	3	Newton&Faulkner 1992
VN	*2179*	*5941*	625	Grane	Vargskar			1000			0	0	L	W	V	N	P	2.7	V14	Virgin Hole	b	63	15	4.0	252	24	1	1	0	0	1	1	1	1	0	0	1	0		1	2	Newton&Faulkner 1992
VN	*2179*	*5938*	626	Grane	Vargskar			1000			0	0	L	W	V	N	P	2.7	V15	Upper Virgin Hole	b	45	8	4.0	180	16	1	0	1	0	1	0	0	0	0	0	1	0		1	1	Newton&Faulkner 1992
VN	*2156*	*5920*	680	Grane	Vargskar			1000			0	0	L	W	V	N	P	2.0	V16	Bridge Pot	c	102	20	2.0	204	20	1	1	0	1	1	1	0	0	0	0	0	0		0	2	Newton&Faulkner 1992
VN	*2150*	*5902*	735	Grane	Vargskar			1000			0	0	T	W	V	N	P	2.0	V17	Lower Rainbow Cave	b	12	5	4.0	48	42	1	0	0	1	1	0	0	1	1	0	1	0		1	1	Newton&Faulkner 1992
VN	*2176*	*5888*	710	Grane	Vargskar			1000			0	0	T	F	V	N	P	1.7	V18	Unnamed Sink	a	8	1	2.0	16	13	1	1	0	0	1	1	0	0	0	0	1	0		0	1	Newton&Faulkner 1992
VN	*2145*	*5883*	760	Grane	Vargskar			1000			0	0	T	W	V	N	P	1.2	V19	Rainbow Cave	b	160	22	4.0	640	14	1	0	0	1	1	0	1	1	3	0	1	0		1	2	Newton&Faulkner 1992
VN	*2160*	*5882*	745	Grane	Vargskar			1000			0	0	T	W	V	N	P	1.3	V20	Cairn Pot	b	113	15	2.0	226	13	1	0	0	1	1	1	0	1	0	0	1	0		0	2	Newton&Faulkner 1992
VN	*2156*	*5876*	750	Grane	Vargskar			1000			0	0	T	W	V	N	P	1.2	V21	Upper Cairn Cave 1	b	21	3	2.0	42	14	1	1	0	0	1	1	0	0	0	0	1	0		0	1	Newton&Faulkner 1992
VN	*2156*	*5876*	750	Grane	Vargskar			1000			0	0	T	W	V	N	P	1.2	V22	Upper Cairn Cave 2	a	6	2	2.0	12	33	1	1	1	0	1	0	0	0	0	0	1	0		0	1	Newton&Faulkner 1992
VN	*2171*	*5861*	750	Grane	Vargskar			1000			0	0	T	F	V	N	P	1.7	V23	Brown Marble Cave	b	33	4	1.0	33	12	1	0	0	1	0	0	0	0	0	0	0	0		0	1	Newton&Faulkner 1992
VN	*2167*	*5842*	770	Grane	Vargskar			1000			0	0	T	F	V	N	P	1.5	V24	Unfinished Cave	b	24	3	1.0	24	13	1	0	0	1	0	0	0	0	0	0	0	0		0	1	Newton&Faulkner 1992
VN	*2140*	*5865*	790	Grane	Vargskar			1000			0	0	T	W	V	N	P	1.2	V25	Col Cave	a	208	15	1.0	208	7	1	0	0	1	1	0	0	1	1	0	1	0		1	2	Newton&Faulkner 1992
VN	*2164*	*5830*	777	Grane	Vargskar			1000			0	0	T	F	V	N	P	1.5	V26	Lake Cave	b	23	3	1.0	23	13	1	0	0	1	1	0	0	0	0	0	1	0		1	1	Newton&Faulkner 1992
VN	*2176*	*5885*	597	Grane	Vargskar			1000			0	0	L	F	V	N	P	2.8	V27	Sandpaper Cave	b	15	2	1.0	15	13	1	0	0	1	1	0	0	0	0	0	1	0		0	1	Newton&Faulkner 1992
VN	*2145*	*5791*	795	Grane	St. Hjortskar	30	90	700			0	0	T	R	V	N	P	1.5	SH2A	Blåfjelligrotta	h	861	31	2.0	1722	4	1	0	1	0	2	15	3	13	0	0	0	0	1	1	3	Newton&Faulkner 1992
VN	*2144*	*5791*	794	Grane	St. Hjortskar	30	90	700			0	0	T	F	V	N	P	1.5	SH2	Nedre Blåfjelligrotta	b	50	13	4.0	200	26	1	0	0	1	1	1	0	1	1	0	0	0		1	1	Newton&Faulkner 1992
VN	*2138*	*5777*	771	Grane	St. Hjortskar			700			0	0	T	F	V	N	P	1.5	SH5/6	Cascade Pot	b	144	11	2.0	288	8	1	0	0	3	1	1	0	2	0	0	1	0		1	3	Newton&Faulkner 1992
VN	*2137*	*5765*	760	Grane	St. Hjortskar			700			0	0	T	F	V	N	P	1.5	SH7	hole	S	3	3	1.0	3	100	1	0	0	1	1	0	0	0	0	0	1	0		1		Newton&Faulkner 1992
VN	*2136*	*5751*	735	Grane	St. Hjortskar	30	80 W	700			0	0	T	F	A	N	P	2.0	SH10	Oxbow Cave	b	50	3	1.5	75	6	1	0	1	0	1	2	0	0	0	0	1	0		1	1	Newton&Faulkner 1992
VN	*2120*	*5713*	680	Grane	St. Hjortskar	38	90	700			0	0	L	F	V	N	P	2.5	SH13	St. Hjortskargrotta	b	36	10	2.0	72	28	1	1	0	0	1	1	0	0	0	0	1	0		1	1	Newton&Faulkner 1992
VN	*2115*	*5705*	660	Grane	St. Hjortskar			700			0	0	L	F	V	N	P	2.5	SH14	Choked Rift	S	3	3	1.0	3	100	1	0	0	1	0	0	0	0	0	0	0	0		1		Newton&Faulkner 1992
VN	*1945*	*4500*	260	Grane	Fjellryggen			100			0	0	L	G	V	N	P	0.5		Svartjern Rising	a	1	1	0.5	1	100	1	0	1	0	1	0	0	0	0	0	1	0		1		Faulkner&Newton 1990
VN	*1942*	*4475*	290	Grane	Fjellryggen			100			0	0	L	W	V	N	P	0.5		Svartjernhullet	S	16	16	1.0	16	100	1	0	0	1	0	0	0	1	0	0	0	0		1	1	Faulkner&Newton 1990
VN	*1942*	*4450*	310	Grane	Fjellryggen			100			0	0	L	W	V	N	P	0.4		Tregrotiene	b	22	2	1.0	22	9	1	0	0	3	0	0	0	0	0	0	0	0		1	1	Faulkner&Newton 1990
VN	*1942*	*4433*	350	Grane	Fjellryggen			100			0	0	L	W	V	N	P	0.4		Stream Hole	S	10	10	2.0	20	100	1	1	0	0	1	0	0	0	0	0	0	0		1	1	Faulkner&Newton 1990
VN	*2000*	*4507*	250	Grane	Fjellryggen	30		100			0	0	L	F	V	N	P	0.6		Marmorgrotta	a	90	12	8.0	720	13	1	1	0	0	1	2	0	0	1	0	0	0	1	1	3	Faulkner&Newton 1990
VN	*2000*	*4430*	370	Grane	Fjellryggen		*W*	100			0	0	L	R	A	N	P	0.2		Sparkly Cave	a	18	*3*	*1.0*	*18*	17	1	0	0	1	1	0	0	0	0	0	0	0		0	1	Faulkner&Newton 1990
VN	*2250*	*5335*	404	Grane	L. Hjortskar	20	90	250			1	0	L	W	V	N	P	0.1	LH1	Coffee Break Sink	a	2	1	0.5	1	50	1	1	0	0	1	0	0	0	0	0	1	0		1		Unpublished. TF97&97
VN	*2240*	*5325*	400	Grane	L. Hjortskar	30	60 W	250	Various		1	0	L	W	A	U	P	0.1	LH2	Sunbeam Cave	b	20	10	5.0	100	50	1	0	0	4	1	0	1	4	0	0	0	0		1		Unpublished. TF97&98
VN	*2255*	*5325*	386	Grane	L. Hjortskar	30	80 W	250			1	0	L	W	A	U	P	0.1	LH3	Litle Hjortskargrotta	a	10	4	1.5	15	40	1	0	0	1	0	0	0	0	0	0	0	0		1	1	Unpublished. TF97&98
VN	*2235*	*5290*	369	Grane	L. Hjortskar		W	250			1	0	L	W	A	U	P	0.3	LH5	Main Stream Sink	a	8	5	2.0	16	63	1	1	0	0	1	0	0	0	0	0	1	0		1		Unpublished. TF97&98
VN	*2140*	*5045*	333	Grane	Saeterbekk	30	60 W	100	Wh., Gre	Biotite ms	0	0	L	F	A	N	P	0.5	SA0	White Limestone Ca.	a	6	3	1.0	6	50	1	0	0	1	1	0	0	0	1	0	0	0		1	1	Unpublished. TF97
VN	*2093*	*4867*	346	Grane	Saeterbekk	15	75 W												SA1	Main Sink																							Newton&Faulkner 1992
VN	*2065*	*4830*	349	Grane	Saeterbekk	20	70 W	100			0	0	L	F	A	N	P	4.0	SA2a	Draughting Talus Ca.	a	11	3	0.5	6	27	1	0	0	1	0	0	0	0	0	0	0	0		1	1	Unpublished. TF97
VN	*2072*	*4820*	347	Grane	Saeterbekk	10	60 W	100	Wh., Gre	Mica	0	0	L	F	A	N	P	4.0	SA2	Saeterbekkgrotta	a	153	9	15.0	2295	6	1	0	0	1	0	0	0	0	0	0	0	0		1	3	Newton&Faulkner 1992. TF97
VN	*2072*	*4820*	347	Grane	Saeterbekk		W	100			0	0	L	F	A	N	P	4.0	SA3	N. Saeterbekkgrotta	a	18	3	15.0	270	17	1	0	0	2	0	0	0	0	0	0	0	0		1	1	Newton&Faulkner 1992. TF97
VN	*2050*	*4810*	331	Grane	Saeterbekk		W	100			0	0	L	F	A	N	P	4.0	SA4	Resurgence Canal	a	9	3	4.0	36	33	1	0	1	0	1	1	0	0	0	0	1	0		1	1	Newton&Faulkner 1992. TF97
VN	*2055*	*4810*	329	Grane	Saeterbekk														SA5	Second Sink																							Unpublished. TF97
VN	*2065*	*4810*	319	Grane	Saeterbekk	20	80 W												SA6	Second Resurgence																							Unpublished. TF97
VN	*2005*	*4560*	230	Grane	Fjellryggen		W	*30*			0	0	H	F	A	N	P	1.5	W1	Wildmarkskaffehull. 1	a	16	*2*	*1.0*	*16*	13	1	0	0	1	0	0	0	0	0	0	0	0		0		Faulkner&Newton 1990
VN	*1995*	*4555*	240	Grane	Fjellryggen														W2	Wildmarkskaffehull. 2																							Faulkner&Newton 1990
VN	*1990*	*4545*	245	Grane	Fjellryggen		W	*30*			0	0	H	G	A	N	P	1.5	W3	Wildmarkskaffehull. 3	e	6	*2*	*1.0*	*6*	33	1	0	0	1	0	0	0	0	0	0	0	0		0		Faulkner&Newton 1990

UPPERMOST ALLOCHTHON: Helgeland Nappe Complex: Zone 6 (Hemnes to Dunfjell): TOTALS

External Cave Attributes | Internal Cave Attributes

UTM COORDS	ALT.	KOMMUNE	AREA	LST. STRIKE	LST. DIP	OW	EXT. COLOUR	OTHER INT. ROCK	R	T	GB	CL	KT	SR	OR	CA	REF. NO.	CAVE NAME	CT	LENG.	VR	XS	VOL.	Min. HG %	C	SE	RE	DE	CS	SP	Ch	Sh	BC	RV	MV	DC	FB	P	BC	PRIME REFERENCES
Totals	**###**				**##**	**###**			34	1						**###**			5204	**###**	**####**	26423	**###**	64	22	12	62	49	29	5	26	13	2	14	1	7	39		
Av. per cave	331				66	254			0.5	0.0						5.4			81	9	3.6	413	23		0.3	0.2	1.0	0.8	0.5	0.1	0.4	0.2	0.0	0.2	0.0	0.1	0.8		
Minima	40				31	3										0.05			3	1	0.3	2	2		0	0	0	0	0	0	0	0	0						
Maxima	515				90	3000										145.0			650	80	10.0	3600	100		1	1	4	2	2	2	3	2	1						

(Dip measured in 21 caves)

Karst Types:

	#	Length
V	11	1452
A	49	3511
L	0	0
C	0	0
X	4	241
Totals	64	5204

Cave Locations:

	#	Length
C	0	0
F	29	1852
W	11	1135
R	2	620
S	5	933
G	17	664
P	0	0
Totals	64	5204

Glacial Situations:

	#	Length
C	0	0
D	4	605
E	8	948
G	0	0
H	2	665
K	19	1085
L	31	1901
S	0	0
T	0	0
U	0	0
Totals	64	5204

Cave Types:

	#	Length
S	5	29
a	30	857
b	12	1005
c	5	486
d	3	965
e	2	85
f	1	233
g	4	1064
h	2	480
Hy	0	0
I	0	0
J	0	0
L	0	0
R	0	0
T	0	0
Totals	64	5204

Relict Caves: # 16, Length 387

MV Caves: # 14, Length 297

Combination Caves: # 34, Length 4520

UPPERMOST ALLOCHTHON: Helgeland Nappe Complex: Zone 6 (Hemnes to Dunfjell)

Caves are grouped by carbonate outcrop

External Cave Attributes | Internal Cave Attributes

UTM COORDS	ALT.	KOMMUNE	AREA	LST. STRIKE	LST. DIP	OW	EXT. COLOUR	OTHER INT. ROCK	R	T	GB	CL	KT	SR	OR	CA	REF. NO.	CAVE NAME	CT	LENG.	VR	XS	VOL.	Min. HG %	C	SE	RE	DE	CS	SP	Ch	Sh	BC	RV	MV	DC	FB	P	BC	PRIME REFERENCES
Skoravatn			**1824 II**																																					
Elsfjord and Korgen			**1927 III and 1927 II**																																					
VP	4080	4680	59	Hemnes	Hemnesøya	40	40 E												Nedre Gjeltvikgr.																						No known references
VP	4090	675	70	Hemnes	Hemnesøya		E	300			1	0	D	W	A	U	P	0.1	Gjeltvikgrotta	d	265	5	7.0	1855	2	1	0	1	2	1	1	1	0	1	0	0	0	1	1	4	Excl. Kumragrotta (Fustvatn)
VP	4115	4670	126	Hemnes	Hemnesøya	50													Gjeltvik Sink																						Unpublished. TF97
VP	404	456	100	Hemnes	Hemnesøya														Cliff Cave																						EPC Journal 1969
VP	3595	4545	40	Hemnes	Hemnesøya			50			0	0	E	W	X	X	X	0.5	Berntvikgrotta	b	35	10	1.0	35	29	1	0	0	1	1	0	0	0	0	0	0	0	1	0		Unexplored. TF97
VP	4605	4705	56	Hemnes	Hemnesøya	90	60 N	20		Skarn?	1	1	E	W	A	N	O	3.0	Gårdsfjellgrotta	g	120	15	10.0	1200	13	1	0	0	1	1	2	0	1	0	0	0	0		1	4	Unexplored. EPC Journal 1969
VP	340	390	300	Vefsn	Elsfjord														karst x 2																						EPC Journal 1969. TF97
VP	229	240	70	Vefsn	Dreyja														Gullmogrottene		In dolomite?																					Elsfjord Quat. Map
VP	344	371	120	Vefsn	Elsfjord			300			0	0	E	W	V	N	P	0.3	Sildgarngrotta	d	500	30	5.0	2500	6	1	0	0	1	1	0	0	0	0	0	0	0		0		Heiland p467. Not found TF98
VP	3340	3515	235	Vefsn	Elsfjord			700			0	0	H	S	V	N	P	2.0	Kovagrotta	g	650	37	5.0	3250	6	1	0	0	4	1	1	1	3	0	1	0	0	1	0		U. Holbye pc 1991 & 97
VP	3381	3523	135	Vefsn	Elsfjord	50	90	700	Grey	Dolostone	0	0	E	S	V	N	P	2.0	Splintgrotta	g	30	4	3.0	90	13	1	0	1	0	2	1	0	1	0	0	0	1	0	4	NG(9)82 19-20. A.Gronlie pc 98. *
VP	2859	3005	275	Vefsn	Elsfjord			500			0	0	L	G	V	N	P	0.4	Litlfjelltjorngrotta	a	12	5	2.0	24	42	1	1	0	0	1	0	1	0	0	0	1	0		1		Unexplored. TF98
VP	280	300	300	Vefsn	Elsfjord														karst x 21																						Unpublished.TF98
VP	340	300	200	Vefsn	Elsfjord														karst x 19																						Elsfjord Quat. Map
VP	37x	33x	330	Vefsn	Elsfjord														cave																						Elsfjord Quat. Map
VP	352	324	90	Vefsn	Elsfjord														Jernbanngrotta		Artificial																						R. Selvaag pc 1996
VP	3520	3235	100	Vefsn	Elsfjord		E	800			0	0	D	F	A	N	N	2.3	Hestdalgrotta	*a*	50	*10*	*2.0*	*100*	20	1	*1*	0	0	*1*	*1*	*0*	*0*	*0*	*0*	*0*	*0*		0		Hortmann pc to DSIP.Artificial
VP	352	324	100	Vefsn	Elsfjord		E	800			0	0	D	F	A	N	N	2.3	Through Cave	*a*	200	*10*	*2.0*	*400*	5	1	*1*	*1*	0	*1*	*0*	*0*	*0*	*0*	*0*	*0*	*0*		0		Doj 1991. pc 1997
VP	3820	3495	280	Vefsn	Elsfjord			3000			0	0	K	F	X	N	N	21.0	Kinnforsen	*d*	200	*20*	*3.0*	*600*	10	1	1	*0*	0	*1*	*1*	*0*	*0*	*0*	*0*	*0*	*0*		0		Doj 1991. pc 1997
VP	3215	2195	305	Vefsn	Kammelv	14	50 W	200			1	0	L	F	A	N	P	5.0	Kammelv Sink	a	10	2	3.0	30	20	1	1	0	0	1	0	0	0	0	0	0	0		1	1	GC Jnl (4) I-III 1972
VP	3220	2210	295	Vefsn	Kammelv	30	70 W	200	Grey	*	1	0	L	F	A	N	P	5.0	Kammelvgrotta	c	170	10	6.0	1020	6	1	0	1	2	1	0	0	1	0	0	0	1	1	3	GC Jnl (4) I-III 1972
VP	3220	2215	300	Vefsn	Kammelv	30		200			1	0	L	F	A	N	P	5.0	Dry Passage	b	30	5	4.0	120	17	1	0	0	2	0	0	0	0	0	0	0	0		0	3	GC Jnl (4) I-III 1972
VP	3225	2200	302	Vefsn	Kammelv	30	80 W	200	Off white	Amphibolit	1	0	L	R	A	N	P	5.0	Lulelindgrotta	b	600	80	6.0	3600	13.3	1	0	0	1	1	1	0	0	0	0	1	1	1	3	Unpublished. TF97&98
VP	3230	2205	301	Vefsn	Kammelv			200			1	0	L	R	A	N	P	5.0	Øst Lulelindgrotta	a	20	4	1.0	20	20	1	0	0	1	0	0	0	0	1	0	0	0		1		Unpublished.TF98

* skarn or quartz feldspathic schist?

* Grytegangen = AV?

UPPERMOST ALLOCHTHON: Helgeland Nappe Complex: Zone 6 (Hammas to Dunfjell) — Caves are grouped by carbonate outcrop — **Vefsn catchment area**

UTM COORDS		ALT.	KOMMUNE	AREA	LST. STRIKE	LST. DIP	OW	EXT. COLOUR	OTHER INT. ROCK	R	T	GS	CL	KT	SR	OR	CA	REF. NO.	CAVE NAME	CT	LENG.	VR	XS	VOL.	Min. HG %	C	SE	NE	DE	CS	SP	Ch	Sh	BC	RV	MV	DC	FS	P	Bd	PRIME REFERENCES
External Cave Attributes																			**Internal Cave Attributes**																					
Fustvatn			***1926 IV***																																					
VP	*1950*	*1985*	50	Vefsn	Drevja	40	90	5	Buff Wh	0	0	E	G	V	N	N	0.1		Øygårdgrotta	a	5	1	1.0	5	10	1	0	1	0	1	0	0	0	0	0	0	0	0	1	1	TF98. Adjacent to massive Dol.
VP	*2385*	*2045*	62	Vefsn	Drevja	180	80 E	*50*	Grey Wh	Musc.sch.	1	0	D	G	A	N	N	7.0		Kumragrotta	b	*90*	*8*	*10.0*	*900*	9	1	1	1	1	1	0	0	0	0	0	0	0		1	1	St.Pierre 1973. TF97
VP	*2015*	*1500*	318	Vefsn	Hellfjell	135	40 S	50	Grey Wh		1	0	K	G	A	D	P	3.0		Rokkegrotta	a	*60*	*9*	*4.0*	*240*	15	1	1	1	0	1	0	0	0	*0*	0	1	0		1	1	Unexplored. TF97
VP	*2044*	*1467*	325	Vefsn	Hellfjell	120	45 S	50			1	0	K	G	A	D	P	0.8		Loop Cave	c	*30*	*3*	*10.0*	*300*	10	1	1	0	0	1	0	0	0	1	0	0	0		1	3	TF97. Surveyed to 225m: SN04
VP	*2053*	*1465*	337	Vefsn	Hellfjell															rift		c. 6m deep																		SN04
VP	*2053*	*1464*	339	Vefsn	Hellfjell	120	S	50			1	0	K	G	A	D	P	0.8		Dripsteinhola	h	*200*	*30*	*6.0*	*1200*	15	1	0	0	1	0	0	0	0	*0*	0	0	0	1	1	Unpublished. TF97
VP	*2055*	*1461*	333	Vefsn	Hellfjell															rift		c. 12m deep																		SN04
VP	*2057*	*1457*	329	Vefsn	Hellfjell		S	50			1	0	K	G	A	D	P	0.8		Daylight Cave	a	*20*	*5*	*1.0*	*20*	25	1	0	0	2	0	0	0	0	0	0	0	0		1	1	Unpublished. TF97
VP	*2059*	*1456*	328	Vefsn	Hellfjell		S	50			1	0	K	G	A	D	P	0.8		Jammed Hole	S	*3*	*3*	*2.0*	*6*	100	1	0	0	1	0	0	0	0	0	0	0	0		1		Unpublished. TF97
VP	*2060*	*1453*	325	Vefsn	Hellfjell		S	50			1	0	K	G	A	D	P	0.8		Jammed Cave	S	*3*	*3*	*2.0*	*6*	100	1	0	0	1	0	0	0	0	0	0	0	0		1		Unpublished. TF97
VP	*2061*	*1454*	319	Vefsn	Hellfjell	120	45 S	50	Grey		1	0	K	G	A	D	P	2.0		Snowmelt Sink Ca.	c	*100*	*5*	*1.0*	*100*	5	1	0	0	1	1	2	0	1	0	0	0	0		1	1	Unpublished. TF97
VP	*2061*	*1453*	319	Vefsn	Hellfjell		S	50	Buff gre	Metapelite	1	0	K	G	A	D	P	2.0		The Subway	c	*100*	*10*	*2.0*	*200*	10	1	0	0	1	1	1	0	0	0	0	0	0		1	1	Unpublished. TF97. Sump is static.
VP	*2420*	*1270*	100	Vefsn	Hellfjell	120	45 S	100			0	0	E	S	A	D	P	1.0		Hagligrotta	f	233	33	6.3	1468	14	1	0	0	1	1	1	0	3	0	0	0	0	1	1	3	Unpublished. TF97, 00
VP	*270*	*150*	200	Vefsn	Hellfjell			100												25 karst features																				Fustvatn Quat. Map
VN	*3385*	*9515*	485	Grane	Herringbotn			3			1	0	K	W	V	N	P	0.7	H2	Upper Arch Cave	a	79	*10*	*2.0*	*158*	13	1	1	1	0	1	0	0	0	0	0	0	0		1		Faulkner 1983
VN	*3385*	*9505*	485	Grane	Herringbotn	20	90	3			1	0	K	W	V	N	P	0.7	H3	Arch cave	a	29	4	1.0	29	14	1	1	0	1	1	0	0	1	0	0	1	0		1	2	Faulkner 1983
VN	*3389*	*9495*	485	Grane	Herringbotn	20	90	3			1	0	K	W	V	N	P	0.7	H4	Short Drop Cave	a	22	5	2.0	44	23	1	1	0	1	1	0	0	0	1	0	0	0		1	2	Faulkner 1983
VN	*3389*	*9495*	480	Grane	Herringbotn	20	90	3			1	0	K	W	V	N	P	0.7	H5	Pool Cave	a	15	6	2.0	30	40	1	1	0	0	1	1	0	0	0	0	1	0		1	2	Faulkner 1983
VN	*33x*	*94x*	460	Vefsn	Herringbotn															3 caves																				R. Selvsag pc 1998
VN	*3415*	*9595*	460	Vefsn	Herringbotn		*W*	100			1	0	K	F	A	N	P	2.0	H6	Gjaberg Sink	b	6	2	1.0	6	33	1	1	0	0	1	0	0	0	0	0	1	0		1	2	Faulkner 1983
VN	*3415*	*9600*	465	Vefsn	Herringbotn	25	*W*	100			1	0	K	F	A	N	P	2.0	H7	Gjaberggrotta	a	75	5	2.0	150	7	1	0	0	2	1	0	0	1	0	0	1	0		1	2	Faulkner 1983
VN	*3420*	*9610*	440	Vefsn	Herringbotn		*W*	100			1	0	K	F	A	N	P	2.0	H7a	Canal Cave	a	10	2	2.0	20	20	1	1	1	0	1	0	0	0	0	0	1	0		1		Faulkner 1983
VN	*3495*	*9720*	380	Vefsn	Herringbotn		*W*	100			1	0	K	F	A	N	P	3.0	H8	Branches Cave	a	19	3	2.0	38	16	1	1	0	0	1	0	0	0	0	0	1	0		1	2	Faulkner 1983
VN	*3495*	*9730*	360	Vefsn	Herringbotn		45 W	100			1	0	K	F	A	N	P	18.0	H9	Gneiss & Lst. Cave	a	20	6	1.0	20	30	1	0	0	2	1	0	0	0	1	0	1	0		1		Faulkner 1983
Trofors			***1926 III***																																					
VN	*260*	*815*	450	Grane	Trofors															2 x karst																				Trofors Quat. Map
VN	*2355*	*7030*	340	Grane	Trofors			*50*			1	0	L	G	X	N	N	2.0		Wet Crawl1 (Stengvass)	a	3	1	1.0	3	33	1	0	1	0	1	0	0	0	0	0	1	0		1		Unpublished. TF97
VN	*2360*	*7020*	330	Grane	Trofors			*50*			1	0	L	G	X	N	N	2.0		Wet Crawl2 (Stengvass)	a	3	1	1.0	3	33	1	0	1	0	1	0	0	0	0	0	1	0		1		Unpublished. TF97
VN	*285*	*803*	300	Grane	Glugvatn			800			1	0	K	F	V	N	P	145.0	G1	Gluggvasselvgrotta	b	94	5	8.0	752	5	1	1	1	1	1	0	0	1	0	0	0	0		1	2	Faulkner 1983
VN	*300*	*825*	380	Grane	Glugvatn															2 x karst																				Trofors Quat. Map
VN	*2525*	*7050*	120	Grane	Trofors	180	31 W	500	Wh grey		1	0	E	S	A	U	P	0.3		Green Doline Cave	a	5	2	0.3	2	40	1	0	0	1	0	0	0	0	1	0	0	0		1	1	Unpublished. TF97
Svenningdal			***1925 IV***																																					
VN	*2445*	*6045*	250	Grane	Svenningskard		*W*	*50*			1	0	H	S	A	U	P	10.5	SV2	Waterfall cave	b	15	3	*2.0*	30	20	1	*0*	*0*	*1*	*0*	0	0	*0*	*0*	*0*	0	0	0		0	Newton & Faulkner 1992
VN	*2448*	*5998*	280	Grane	Svenningskard		*W*	*50*			1	0	L	W	A	U	P	0.2	SV3	Legover Pot	S	10	6	*2.0*	*20*	60	1	0	0	2	*0*	0	0	*1*	*0*	*0*	0	0	0		0	Newton & Faulkner 1992
VN	*2445*	*5982*	285	Grane	Svenningskard		*W*	*50*			1	0	L	W	A	U	P	0.2	SV4	Midge Pot 1	b	30	10	*2.0*	*60*	33	1	*1*	0	0	*1*	0	0	*0*	*0*	*0*	0	0	0		0	Newton & Faulkner 1992
VN	*2445*	*5982*	285	Grane	Svenningskard		*W*	*50*			1	0	L	W	A	U	P	0.2	SV5	Midge Pot 2	b	30	10	*2.0*	*60*	33	1	*1*	0	0	*1*	0	0	*0*	*0*	*0*	0	0	0		0	Newton & Faulkner 1992
VN	*2550*	*6515*	130	Grane	Svenningskard		*W*	1500			1	0	E	F	A	N	P	2.2	SV1	Farewell Cave	b	20	4	4.0	80	20	1	0	0	1	0	0	0	0	0	0	0	0		1	Newton & Faulkner 1992

UPPERMOST ALLOCHTHON: Helgeland Nappe Complex: Zone 6 (Hemnes to Dunfjell) Caves are grouped by carbonate outcrop Namsen catchment area

UTM COORDS			ALT.	KOMMUNE	AREA	LST. STRIKE	LST. DIP		OW	EXT. COLOUR	OTHER INT. ROCK	R	T	GS	CL	KT	SR	OR	CA	REF. NO.	CAVE NAME	CT	LENG.	VR	XS	VOL.	Min. HG %	C	SE	RE	DE	CS	SP	Ch	Sh	BC	RV	MV	DC	FS	P	BG	PRIME REFERENCES
Majavatn				***1925 III***																																							
VN	*166*	*272*	320	Grane	*Dunnfjell*				200			0	0	L	G	*A*	D	P	1.0	D16	Roadhead Rift Caves	S	10	4	*2.0*	*20*	40	1	0	0	2	0	0	0	0	0	0	0	0		0		Newton, 2002
VN	*167*	*272*	330	Grane	*Dunnfjell*				200			0	0	L	G	*A*	D	P	1.0	D17	Roadhead Sink	a	5	1	*2.0*	*10*	20	1	1	0	0	1	0	0	0	0	1	0		0		Newton, 2002
VN	*167*	*272*	325	Grane	*Dunnfjell*				200			0	0	L	G	*A*	D	P	1.0	D18	Roadhead Flood Sink	a	10	1	*2.0*	*20*	10	1	0	0	1	1	0	0	0	0	1	0		0		Newton, 2002
VN	*1708*	*2985*	460	Grane	*Dunnfjell*				200			0	0	L	G	*A*	D	P	0.1	D35	Old Sink Cave	a	10	2	*2.0*	*20*	20	1	0	0	1	1	0	0	0	0	0	0		0	1	Newton, 2002
VN	*1695*	*2990*	440	Grane	*Dunnfjell*	4	90		200	White		0	0	L	F	V	N	P	5.0	D1	The Big Resurgence	e	16	4	2.0	32	25	1	0	0	1	1	1	0	0	1	0	0		1	2	Newton 1999. TF98
VN	*1720*	*3010*	470	Grane	*Dunnfjell*	180	70	W	200	White		0	0	L	F	A	N	P	4.7	D2	The Big Sink	a	55	12	10.0	550	22	1	1	0	0	1	1	0	0	0	0	0		1	2	Newton 1999. TF98
VN	*1720*	*3010*	475	Grane	*Dunnfjell*			W	200			0	0	L	F	A	N	P	4.7	D3	Little Bit on the Side	a	22	3	2.0	44	14	1	0	0	1	0	0	0	1	1	0	0	0	0	2	Newton 1999
VN	*1710*	*3010*	470	Grane	*Dunnfjell*			W	200			0	0	L	F	A	N	P	4.6	D4	Black Cave	h	280	35	6.0	1680	13	1	0	0	1	1	2	0	0	1	1	0	0	0	2	Newton 1999
VN	*1711*	*3011*	470	Grane	*Dunnfjell*			W	200			0	0	L	F	A	N	P	4.6	D19	Not Black Cave 1	a	12	3	9.0	108	25	1	0	0	1	0	0	0	0	1	0	0	0	1	1	TF98
VN	*1711*	*3011*	470	Grane	*Dunnfjell*			W	200			0	0	L	F	A	N	P	5.6	D20	Not Black Cave 2	a	10	1	1.0	10	10	1	0	0	1	0	0	0	0	0	0	0	0	1	1	TF98
VN	*1715*	*3020*	470	Grane	*Dunnfjell*	15	80	W		White	Biotite sch	0	0	L	F	A	N	P	4.5	D5	White Cave	g	264	27	6.0	1584	10	1	1	0	2	1	1	2	1	2	0	0	0	1	2	Newton 1999, 2002. TF98
VN	*1720*	*3015*	475	Grane	*Dunnfjell*															D6	Resurgences																						Newton 1999. TF98
VN	*1720*	*3025*	475	Grane	*Dunnfjell*															D7	Flood Sink		Entrance to deep water																				Newton 1999
VN	*1715*	*3025*	475	Grane	*Dunnfjell*															D21	Mini Cenote		Flood overflow?																				Newton, 2002
VN	*1720*	*3025*	475	Grane	*Dunnfjell*															D8	Resurgence																						Newton 1999
VN	*1720*	*3030*	475	Grane	*Dunnfjell*															D9	Flood Resurgence		Entrance to deep water																				Newton 1999
VN	*1720*	*3030*	480	Grane	*Dunnfjell*			W	200			0	0	L	F	A	N	P	4.3	D10	Overflow Cave	a	33	7	*3.0*	*99*	21	1	0	0	3	1	2	0	2	0	0	0	0	0	2	Newton 1999
VN	*1720*	*3035*	480	Grane	*Dunnfjell*	30	70	W	200	White		0	0	L	F	A	N	P	4.3	D11	Ice Cave	e	69	8	10.0	690	12	1	0	0	2	1	2	0	2	1	0	0	0	1	2	Newton 1999. TF98
VN	*1720*	*3035*	490	Grane	*Dunnfjell*			W	200			0	0	L	F	A	N	P	4.3	D12	Sink Cave	a	14	4	10.0	140	29	1	1	0	0	1	1	0	0	0	0	0	0	0	2	Newton 1999
VN	*1720*	*3040*	490	Grane	*Dunnfjell*															D13	Resurgence																						Newton 1999
VN	*1720*	*3040*	490	Grane	*Dunnfjell*			W	200			0	0	L	F	A	N	P	4.3	D14	Flood Resurgence	a	25	5	*5.0*	*125*	20	1	0	0	3	1	2	0	3	0	0	0	0	0	2	Newton 1999. Sumps are static.
VN	*1720*	*3045*	490	Grane	*Dunnfjell*			W	200			0	0	L	F	A	N	P	4.3	D15	Dog Leg cave	c	86	8	4.0	*344*	9	1	0	0	3	1	2	0	1	0	0	0	0	0	2	Newton 1999, 2002. TF98
VN	*1715*	*3050*	495	Grane	*Dunnfjell*															D22	Cliff Doline																						Newton, 2002
VN	*1717*	*3050*	495	Grane	*Dunnfjell*															D23	Big Doline																						Newton, 2002
VN	*1717*	*3052*	495	Grane	*Dunnfjell*															D24	Side Valley Sink																						Newton, 2002
VN	*1717*	*3052*	495	Grane	*Dunnfjell*															D25	Side Valley Rising																						Newton, 2002
VN	*1717*	*3052*	495	Grane	*Dunnfjell*															D26	Wing Rising																						Newton, 2002
VN	*1717*	*3056*	500	Grane	*Dunnfjell*			W	200			0	0	L	F	A	N	P	4.3	D27	Wing Cave	b	25	3	2.0	50	12	1	0	0	1	1	1	0	1	0	0	0	0	0	2	Newton, 2002
VN	*1717*	*3070*	505	Grane	*Dunnfjell*															D28	Damned Dig Sink																						Newton, 2002
VN	*1720*	*3075*	505	Grane	*Dunnfjell*															D29	Interim Sink																						Newton, 2002
VN	*1712*	*3076*	505	Grane	*Dunnfjell*			W	200			0	0	L	F	A	N	P	4.2	D30	Martins Sink	S	3	3	*2.0*	*6*	100	1	0	0	1	0	0	0	0	0	0	0	0	0		Newton, 2002
VN	*1725*	*3080*	510	Grane	*Dunnfjell*															D31	Top Rising																						Newton, 2002
VN	*1730*	*3085*	510	Grane	*Dunnfjell*			W	200			0	0	L	F	A	N	P	4.1	D32	Arch Cave	a	4	1	*2.0*	*8*	25	1	0	0	1	0	0	0	0	0	0	0	0	0		Newton, 2002
VN	*1725*	*3090*	515	Grane	*Dunnfjell*			W	200			0	0	L	F	A	N	P	4.1	D33	Growling Cave	b	30	4	*3.0*	*90*	13	1	0	0	1	1	1	0	1	0	0	1	0	0		Newton, 2002
VN	*1700*	*3095*	515	Grane	*Dunnfjell*															D34	Top Sink																						Newton, 2002

Susendalen **1925 I** One outcrop. No known refs.

Borgefjellet **1925 II** One outcrop. No known refs.

UPPERMOST ALLOCHTHON: Helgeland Nappe Complex: Zone 7 (Åkervik to Fiplingdal): TOTALS

	ALT.	LST. DIP	OW	R	T	CA	LENG.	VR	XS	VOL.	Min. HG %	C	SE	RE	DE	CS	SP	Ch	Sk	BC	RV	MV	DC	FS	P
Totals	####	##	####	6	0	###	4806	###	####	36368	####	87	44	19	54	72	41	3	38	14	7	41	4	7	57
Av. per cave	526	82	855	0.1	0.0	5.7	55	6.4	4.2	416	30		0.5	0.2	0.6	0.8	0.5	0.0	0.4	0.2	0.1	0.5	0.0	0.1	0.7
Minima	175	45	50			0.10	1	1	0.3	1	2		0	0	0	0	0	0	0	0	0				
Maxima	770	90	2500			44.0	889	30	40.0	13335	100		2	1	4	3	3	2	4	2	1				

(Dip measured in 25 caves)

Glacial Situations:

	#	Length
C	0	0
D	0	0
E	0	0
G	3	366
H	4	69
K	19	971
L	61	3400
S	0	0
T	0	0
U	0	0
Totals	87	4806

Karst Types:

	#	Length
V	53	2340
A	30	2159
L	0	0
C	1	100
X	3	207
Totals	87	4806

Cave Locations:

	#	Length
C	0	0
F	20	720
W	2	90
R	0	0
S	1	50
G	58	3629
P	6	317
Totals	87	4806

Cave Types:

	#	Length
s	15	162
a	34	956
b	22	1267
c	8	803
d	3	1096
e	2	130
f	3	392
g	0	0
h	0	0
Hy	0	0
I	0	0
J	0	0
L	0	0
R	0	0
T	0	0
Totals	87	4806

Relict Caves: #	Length	MV Caves: #	Length	Combination Caves: #	Length
19	365	41	1241		
19	365	41	1241	27	3200

UPPERMOST ALLOCHTHON: Helgeland Nappe Complex: Zone 7 (Åkervik to Fiplingdal)

Caves are grouped by carbonate outcrop

Vefsn catchment area

Trofors — *1926 III*

UTM COORDS	ALT.	KOMMUNE	AREA	LST. STRIKE	LST. DIP	OW	EXT. COLOUR	OTHER INT. ROCK	R	T	GE	CL	KT	SR	OR	CA	REF. NO.	CAVE NAME	CT	LENG.	VR	XS	VOL.	Min. HG %	C	SE	RE	DE	CS	SP	Ch	Sk	BC	RV	MV	DC	FS	P	BG	PRIME REFERENCES
VN 2810 7225	320	Grane	Trofors	165	90	600		Ortho -	0	0	K	F	V	N	P	22.0		Almdalselvhullet	f	52	14	2.0	104	27	1	1	0	0	1	1	0	2	1	0	0	0		1	1	Unpublished. TF96
VN 2810 7225	315	Grane	Trofors	165	90	600		amphib	0	0	K	F	V	N	P	22.0		Blade Crawl	a	6	1	0.3	2	17	1	1	0	0	1	0	0	0	0	0	1	0		1		Unpublished. TF96
VN 2805 7220	308	Grane	Trofors	165	90	600			0	0	K	F	V	N	P	22.0		Almdalselv Res. C	a	4	2	2.0	8	50	1	0	1	0	1	1	0	0	0	0	0	0		1		Unpublished. TF96
VN 3745 8505	480	Grane	Glugvatn			1000			0	0	K	F	V	N	N	0.2	G7	Rauvatngrotta	a	13	2	1.0	13	15	1	1	0	0	1	2	0	0	0	0	0	0		0	2	Faulkner 1983
VN 3750 8510	470	Grane	Glugvatn			1000			0	0	K	F	V	N	N	0.2	G8	N. Rauvatngrotta	c	8	1	1.0	8	13	1	0	1	1	1	1	0	0	0	0	0	0		0	2	Faulkner 1983
VN 3720 7930	560	Grane	Glugvatn	60	60 W	900			0	0	K	G	A	D	N	3.0	G4	Rammergrotta	c	150	6	4.0	600	4	1	1	0	2	1	1	2	2	0	0	0	0	1	1	2	Faulkner 1983
VN 3720 7955	540	Grane	Glugvatn	50	W	900			0	0	K	G	A	D	N	3.0	G5	N. Rammergrotta	c	120	10	2.0	240	8	1	1	0	1	1	1	0	0	0	0	0	0		1	3	Faulkner 1983
VN 34x 72x	540	Grane	Svartvassdal															Bron		(17)																				Doj 1991. pc to TLF 1997
VN 34x 72x	540	Grane	Svartvassdal															Finnbekkspreikka		(20)																				Doj 1991. pc to TLF 1997
VN 34x 72x	540	Grane	Svartvassdal															Choked Hole		(2)																				Doj 1991. pc to TLF 1997
VN 3397 6953	320	Grane	Svartvassdal		E	2500			0	0	L	G	A	D	N	2.0		Brubekkgr./Helvetesh.	f	300	20	6.0	1800	7	1	1	0	0	1	2	0	0	0	1	0	1	1	0	3	Heap 1979. Doj 1993. Moonmilk.
VN 3390 6925	291	Grane	Svartvassdal	20	A	2500	White grey*		0	0	L	G	C	N	N	2.0		Nedre Helveteshullet	d	100	10	3.0	300	10	1	0	0	1	2	2	0	0	0	0	0	0		1		Doj 1997. TF97
VN 3380 6915	300	Grane	Svartvassdal	20	45 E	2500	White grey		0	0	L	G	A	D	N	0.5		Soff's Cave	a	14	2	0.5	7	14	1	0	0	1	0	0	0	0	0	0	0	0	1	1	1	Unpublished. TF97
VN		Grane	Svartvassdal															Svartvass Big Sink		(150)																				Doj 1994. pc to TLF
VN 349 700	290	Grane	Svartvassdal		E	1200			0	0	L	G	A	D	P	38.0		Vacra Slukat	b	28	9	6.0	168	32	1	2	0	0	1	0	0	0	0	0	0	0		0		Doj 1990
VN 349 698	270	Grane	Svartvassdal															Svartvass. Jordbru																						Doj.Grottan 28(1)p8 1993
VN 347 696	260	Grane	Svartvassdal		E	1200			0	0	L	W	A	D	P	38.0		Fossil Cave	a	80	2	40.0	3200	3	1	0	0	1	0	0	0	0	0	0	0	0		0		Doj 1995. pc to TLF 1997
VN 3460 6910	190	Grane	Svartvassdal		E	2500			0	0	H	F	A	N	P	38.0		Kylvelvet N.	b	25	2	4.0	100	8	1	0	1	0	1	0	0	0	1	0	1	0		0		Doj 1990
VN 3460 6903	190	Grane	Svartvassdal		E	2500			0	0	H	F	A	N	P	38.0		Kylvelvet S.	b	25	2	4.0	100	8	1	0	0	1	1	2	0	0	0	0	1	0		0		Doj 1990
VN 346 690	190	Grane	Svartvassdal		E	2500			0	0	H	F	A	N	P	38.0		Lillvelvet	b	5	1	4.0	20	20	1	1	1	0	1	0	0	0	0	0	1	0		0		Doj 1990
VN 345 687	175	Grane	Svartvassdal		E	2500			0	0	H	F	A	N	P	44.0		Alvkantsutlodet	b	14	1	4.0	56	7	1	0	1	0	1	1	0	0	0	0	1	0		1		Doj.Grottan 28(1)p7 1993
VN 351 693	250	Grane	Svartvassdal		E	2500			0	0	G	G	A	N	N	3.0		Mellanselvgrotta	b	280	10	10.0	2800	4	1	1	1	4	1	2	0	4	0	0	0	0		0	2	Doj.Grottan 28(1)p10 1993. *
VN 3503 6906	240	Grane	Svartvassdal		E	2500			0	0	G	G	A	N	N	3.0		Blå Kallen	b	48	5	8.0	384	10	1	0	0	1	1	0	0	0	0	0	0	0		0		Doj.Grottan 28(1)p10 1993
VN 3502 6906	240	Grane	Svartvassdal		E	2500			0	0	G	G	A	N	N	3.0		N. Mellanselvgr.	b	38	10	8.0	304	26	1	1	0	0	1	0	0	0	0	0	1	0		0		Doj.Grottan 28(1)p9 1993
VN 3395 6680	140	Grane	Austervefsn															Stormogrotta		(231)																				Doj. 1990. 93m (or 13m?) deep

A= anticline

* muscovite schist + calc-silicate

* Photo shows folding

UPPERMOST ALLOCHTHON: Helgeland Nappe Complex: Zone 7 (Återvik to Fiplingdal)

Caves are grouped by carbonate outcrop

Vefsn catchment area

External Cave Attributes | Internal Cave Attributes

UTM COORDS		ALT.	KOMMUNE	AREA	LST. STRIKE	LST. DIP	OW	EXT. COLOUR	OTHER INT. ROCK	R	T	GR	CL	KT	SR	OR	CA	REF. NO.	CAVE NAME	CT	LENG.	VR	XS	VOL.	Min. HG %	C	BE	RE	DE	CS	SP	Ch	Sh	BC	RV	MV	DC	FS	P	SC	PRIME REFERENCES
Svenningdal			***1926 IV***																																						* Sump dries out in winter.
																																									** 1 sump is static
VN	*351*	*647*	470	Grane	Austervefsn																Kvannholan Sink																				Doj. Grottan28 (1) på 1993
VN	*3623*	*6342*	535	Grane	Austervefsn	40		200			0	0	L	G	A	N	P	1.5		Treuddsgrottan	a	45	*5*	*3.0*	*135*	11	1	1	0	1	1	1	0	0	0	0	1	0		0	1	Doj. Grottan28 (1) 9-10 1993
VN	*3625*	*6350*	530	Grane	Austervefsn	40		200			0	0	L	G	A	N	P	1.5		Morrhålet	a	24	*5*	*3.0*	*72*	21	1	0	0	1	0	0	0	0	0	0	0	0		0	1	Doj. Grottan28 (1) 9-10 1993
VN	*3625*	*6360*	525	Grane	Austervefsn																Tuvbekken Res. Arch																				Doj. Grottan28 (1) 9-10 1993
VN	*2745*	*5620*	343	Grane	Kappskar	40	90													K0	Square Entrance Cave																				Unexplored. TF97
VN	*2772*	*5623*	378	Grane	Kappskar	80	60	S	500			0	0	K	F	A	N	P	15.0	K1	Bottom Rising	b	31	*3*	*4.0*	*124*	10	1	0	1	0	1	1	0	0	0	0	1	0		1	1	Newton&Faulkner 1992. TF97
VN	*2780*	*5624*	380	Grane	Kappskar	100	80	S	500			0	0	K	F	A	N	P	15.0	K2	Bottom Sink	b	30	*4*	*4.0*	*120*	13	1	1	0	0	1	1	0	0	0	0	1	0		1	1	Newton&Faulkner 1992. TF97
VN	*2784*	*5624*	386	Grane	Kappskar			S	500			0	0	K	F	A	N	P	15.0	K3	B Cave	b	16	2	*2.0*	32	13	1	0	0	1	0	0	0	0	0	0	0	0		1	1	Newton&Faulkner 1992. TF97
VN	*2796*	*5624*	385	Grane	Kappskar	130	75	S	500	Wh., Grey		0	0	K	F	A	N	P	15.0	K4	Memorial Cave / A Cave	c	126	5	4.0	504	4	1	1	1	0	1	2	0	0	0	0	1	0		1	3	Newton&Faulkner 1992. TF97. *
VN	*2790*	*5625*	390	Grane	Kappskar			S	500			0	0	K	F	A	N	P	15.0	K5	Whirlpool Cave	d	107	6	4.0	428	6	1	0	0	1	2	1	0	0	0	0	1	0		1	2	Newton&Faulkner 1992. TF97
VN	*2815*	*5617*	400	Grane	Kappskar			S	500			0	0	K	F	A	N	P	15.0	K6	Kappskarelvgrotta	c	162	10	12.0	1944	6	1	1	0	0	1	2	0	4	2	0	0	0		1	3	Newton&Faulkner 1992. TF97. **
VN	*315*	535		Grane	Kappskar																Prospects																				Local reports (NG visited 1990)
VN	*3480*	*5755*	570	Grane	Lille Fiplingdal				*50*			0	0	L	G	X	N	A	2.0		Lilleengåsgrotta	b	130	14	3.0	390	11	1	1	0	0	1	0	1	1	1	1	0	1		0	3	Faulkner 1987
VN	*3485*	*5775*	560	Grane	Lille Fiplingdal				*50*			0	0	L	G	X	N	A	2.0		Flood resurgence	a	62	1	3.0	186	2	1	0	0	1	1	0	0	0	0	1	0		0	1	Faulkner 1987
VN	*3490*	*5780*	550	Grane	Lille Fiplingdal				*50*			0	0	L	G	X	N	A	2.0		Mantrap	a	*15*	*4*	*3.0*	*45*	27	1	0	0	1	1	0	0	1	0	0	1	0		0	1	Faulkner 1987
VN	*3220*	*5888*	770	Grane	Lille Fiplingdal			*N*	500			0	0	L	*P*	A	D	N	0.7	10	Fläflangahullet	a	100	10	9.0	900	10	1	1	1	3	1	0	0	3	0	0	0	0		0	1	Frei 1991 9-11
VN	*3315*	*5256*	705	Grane	Småtjorndal															9	Beaviketsesluket																				Frei 1991 7-8
VN	*3247*	*5132*	720	Grane	Småtjorndal																Prinsessans sluk																				Frei 1991 5-7
VN	3232	*5110*	710	Grane	Småtjorndal				1000			0	0	L	G	V	N	P	0.7	7	Prinsessan	a	60	5	2.0	120	8	1	0	0	1	1	0	0	0	0	0	1	0		0	2	Frei 1991 4-7
VN	3232	*5110*	710	Grane	Småtjorndal				1000			0	0	L	G	V	N	P	0.7		Torrfåra	a	10	5	1.0	10	50	1	1	0	0	1	0	0	0	0	0	1	0		0	2	Frei 1991 4-6
VN	3232	*5110*	710	Grane	Småtjorndal				1000			0	0	L	G	V	N	P	0.7	6	Drinkhålet	S	5	5	1.0	5	100	1	1	0	0	1	0	0	0	0	0	1	0		0	2	Frei 1991 4-6
VN	*3180*	*4955*	655	Grane	Småtjorndal				1000			0	0	L	G	V	N	P	3.0		Guhkisegrotta	b	20	2	1.5	30	10	1	1	1	0	1	0	0	0	0	0	1	0		0		Frei 1991 p2
VN	*3095*	*4855*	750	Grane	Småtjorndal				800			0	0	L	W	V	N	P	0.1	2	Orana Schakthålan	a	10	3	0.4	4	30	1	0	0	3	0	0	0	2	0	0	0	0		0	1	Frei 1991 p3
VN	*3105*	*4815*	695	Grane	Småtjorndal				800			0	0	L	G	V	N	P	0.3	1	Blocksluket	a	3	2	0.3	1	67	1	1	0	0	1	0	0	0	1	0	1	0		0	1	Frei 1991 p3
VN	*3100*	*4785*	675	Grane	Fipling -Tøimskar				800			0	0	L	G	V	N	P	0.5	T24	5m Pot	S	5	5	4.0	20	100	1	1	0	0	1	0	0	0	0	0	0	0		1		Faulkner 1983
VN	*3095*	*4780*	660	Grane	Fipling -Tøimskar	30	90		800			0	0	L	G	V	N	P	0.5	T23	Doorway Cave	b	182	5	2.0	364	3	1	1	0	2	1	1	0	0	0	0	1	0		1	2	Faulkner 1983
VN	*3085*	*4765*	650	Grane	Fipling -Tøimskar				800			0	0	L	G	V	N	P	0.5	T17	Camp Cave	a	15	5	10.0	150	33	1	0	0	1	0	0	0	0	0	0	0	0	1	1		Faulkner 1983
VN	*3070*	*4750*	650	Grane	Fipling -Tøimskar				800			0	0	L	G	V	N	P	3.0	T15	Narrow Canyon	b	10	3	*1.0*	*10*	30	1	0	0	1	0	0	0	0	0	1	0	0		0		Faulkner 1983. Relict vadose
VN	*3060*	*4730*	640	Grane	Fipling -Tøimskar				800			0	0	L	G	V	N	P	3.0	T13	Loose Rift	S	12	7	*2.0*	*24*	58	1	1	0	0	1	0	0	0	2	0	0	0		0		Faulkner 1983
VN	*3060*	*4730*	640	Grane	Fipling -Tøimskar				800			0	0	L	G	V	N	P	3.0	T13a	Small Hole	a	6	3	*1.0*	*6*	50	1	0	0	1	0	0	0	0	0	0	0	0		0		Faulkner 1983
VN	*3050*	*4720*	640	Grane	Fipling -Tøimskar				800			0	0	L	G	V	N	P	3.0	T12	Flake Pot	S	15	10	*1.0*	*15*	67	1	0	0	1	1	0	0	1	0	0	1	0		0		Faulkner 1983
VN	*3050*	*4720*	640	Grane	Fipling -Tøimskar				800			0	0	L	G	V	N	P	3.0	T11	Bridged Doline	S	*10*	*6*	*4.0*	*40*	60	1	0	0	1	0	0	0	1	0	0	0	0		1		Faulkner 1983
VN	*3050*	*4715*	640	Grane	Fipling -Tøimskar				800			0	0	L	G	V	N	P	3.0	T9	Stream Sink	S	5	5	2.0	10	100	1	1	0	0	1	0	0	0	0	0	1	0		1		Faulkner 1983
VN	*3045*	*4705*	635	Grane	Fipling -Tøimskar				800			0	0	L	G	V	N	P	3.0	T2	Daylight Shaft	S	5	4	2.0	10	80	1	0	0	1	1	0	0	1	0	0	1	0		1		Faulkner 1983
VN	*3045*	*4705*	635	Grane	Fipling -Tøimskar				800			0	0	L	G	V	N	P	3.0	T1	Waterfall Doline	S	11	8	4.0	44	73	1	0	0	1	1	0	0	1	0	0	1	0		1		Faulkner 1983
VN	*3020*	*4640*	620	Grane	Fipling -Tøimskar				800			0	0	L	G	V	N	P	0.4	T84	Spray Cave	c	15	5	2.0	30	33	1	1	0	0	1	0	0	0	0	0	1	0		1	2	Faulkner 1983
VN	*3015*	*4635*	620	Grane	Fipling -Tøimskar				800			0	0	L	G	V	N	P	0.4	T83	Hummock Cave	a	10	1	1.0	10	10	1	0	0	1	0	0	0	0	0	0	0	0		1		Faulkner 1983
VN	*2970*	*4550*	620	Grane	Fipling - Båtskar				800			0	0	L	G	V	N	P	0.4	B16	Arch Passage	a	20	*10*	*15.0*	*300*	50	1	0	0	1	0	0	0	1	0	0	0	0		1		Faulkner 1983
VN	*2965*	*4545*	600	Grane	Fipling - Båtskar				800			0	0	L	G	V	N	P	0.4	B14	Rectangular Hole	a	*10*	*5*	*10.0*	*100*	50	1	0	0	1	0	0	0	0	0	0	0	0		1		Faulkner 1983
VN	*2960*	*4535*	600	Grane	Fipling - Båtskar	20	90		800			0	0	L	G	V	N	P	0.4	B12	Vicgrotta	e	70	25	*1.0*	*70*	36	1	0	0	1	1	0	0	1	0	0	1	0		1	2	Faulkner 1983
VN	*2960*	*4535*	600	Grane	Fipling - Båtskar	20	90		800	White	Schist	0	0	L	G	V	N	P	0.4	B11	Tumbledown Pot	e	60	25	*2.0*	*120*	42	1	1	0	0	1	0	0	1	0	0	1	0		1	2	Faulkner 1983
VN	*2955*	*4520*	585	Grane	Fipling - Båtskar				800			0	0	L	G	V	N	P	0.4	B4	Two Level Cave	f	40	8	*1.5*	*60*	20	1	0	0	1	1	0	0	2	1	0	0	0	1	1	2	Faulkner 1983
VN	*2950*	*4500*	570	Grane	Fipling - Båtskar				800			0	0	L	G	V	N	P	0.5	B2	Triangular Hole	S	10	10	*1.0*	*10*	100	1	0	0	1	0	0	0	1	0	0	0	0		1		Faulkner 1983
VN	*2950*	*4495*	570	Grane	Fipling - Båtskar	15	90		800			0	0	L	G	V	N	P	0.5	B1	Båtskargrotta	c	210	*10*	*4.0*	*840*	5	1	0	0	2	3	3	0	0	0	0	0	1	0	2	2	Faulkner 1983
VN	*2950*	*4495*	570	Grane	Fipling - Båtskar				800			0	0	L	G	V	N	P	0.5	B1a	Båtskar Sink 1	S	8	5	*2.0*	*16*	63	1	1	0	0	1	0	0	0	1	0	1	0		1		Faulkner 1983
VN	*2950*	*4495*	570	Grane	Fipling - Båtskar				800			0	0	L	G	V	N	P	0.5	B1b	Båtskar Sink 2	a	3	*1*	*1.0*	*3*	33	1	1	0	0	1	0	0	0	0	0	1	0		1		Faulkner 1983
VN	*2950*	*4495*	570	Grane	Fipling - Båtskar				800			0	0	L	G	V	N	P	0.5	B1c	Båtskar Sink 3	S	4	*2*	*2.0*	*8*	50	1	1	0	0	1	0	0	0	0	0	1	0		1		Faulkner 1983
VN	*2950*	*4495*	570	Grane	Fipling - Båtskar				800			0	0	L	G	V	N	P	0.5	B1d	Båtskar Sink 4	a	14	*4*	*1.0*	*14*	29	1	1	0	0	1	0	0	0	0	0	1	0		1		Faulkner 1983
VN	*2940*	*4425*	550	Grane	Fipling - Båtskar				800			0	0	L	G	V	N	P	0.8	B20	Two Shafts	S	7	4	*2.0*	*14*	57	1	0	0	2	0	0	0	2	0	0	0	0		2		Faulkner 1983
VN	*2940*	*4425*	550	Grane	Fipling - Båtskar				800			0	0	L	G	V	N	P	0.8	B21	Båtskar South Rising	S	*3*	*3*	*6.0*	*18*	100	1	0	1	0	1	1	0	0	0	0	1	0		1		Faulkner 1983
VN	*2910*	4355	575	Grane	Fipling - Båtskar															B0	Deer Pen Cave (?)																				Doj. 1991. pc to TLF? TF98
VN	*2625*	*4075*	440	Grane	Øvre Fiplingdal				500			0	0	L	G	V	N	P	1.8		Kvannli Sink Cave	a	75	10	10.0	750	13	1	1	1	0	0	1	1	0	0	1	0	0	0	0	1	2	Faulkner 1983
VN	*2810*	*4005*	410	Grane	Øvre Fiplingdal	15	90		300			0	0	L	G	V	N	P	2.0		Kvannlihola	d	889	19	15.0	13335	2.1	1	0	1	0	1	3	0	0	1	0	0	1	1	1	3	Faulkner 1983
VN	*2810*	*3990*	385	Grane	Øvre Fiplingdal				300			0	0	L	G	V	N	P	2.5		Nedre Kvannlihola	a	30	5	*5.0*	*150*	17	1	1	0	0	1	0	0	0	1	0	0	0		1		Faulkner 1983

UPPERMOST ALLOCHTHON: Helgeland Nappe Complex: Zone 7 (Återvik to Fiplingsdal) — Caves are grouped by carbonate outcrop — Vefsn and Northern catchment areas

UTM COORDS		ALT.	KOMMUNE	AREA	LST. STRIKE	LST. DIP	OW	EXT. COLOUR	OTHER INT. ROCK	R	T	GE	CL	KT	SR	OR	CA	REF. NO.	CAVE NAME	CT	LENG.	VR	XS	VOL.	Min. HG %	C	SE	RE	DE	CS	SP	Ch	Sh	BC	RV	MV	DC	FS	P	SC	PRIME REFERENCES
Svanningdal			**1925 IV**	**cont.**																																				* Possibly a separate outcrop.
VN	3120 4785	660	Grane	Fipling -Tømmerkar			800			0	0	L	G	V	N	P	0.7	T33	Underground Flow	a	10	2	2.0	20	20	1	1	0	0	1	0	0	0	1	0	1	0		1		Faulkner 1983. *
VN	3095 4745	640	Grane	Fipling -Tømmerkar	30	90	800			0	0	L	G	V	N	P	0.7	T38	Upper TBC	a	14	3	2.0	28	21	1	1	1	0	1	0	0	0	0	1	0		1		Faulkner 1983
VN	3095 4745	640	Grane	Fipling -Tømmerkar	30	90	800			0	0	L	G	V	N	P	0.7	T39	Tømmerkar Stream Cave	a	160	12	2.0	320	8	1	1	0	0	1	0	0	0	0	0	1	0		1	2	Faulkner 1983
VN	3090 4740	640	Grane	Fipling -Tømmerkar	30	90	800			0	0	L	G	V	N	P	0.7	T40	Dry Cave	a	41	6	2.0	82	15	1	0	0	1	0	0	0	0	0	1	0	0		1	2	Faulkner 1983. Relict vadose
VN	3080 4705	620	Grane	Fipling -Tømmerkar	30	90	800			0	0	L	G	V	N	P	1.0	T48	High Flow Cave	b	50	9	2.5	125	18	1	0	0	1	1	1	0	0	0	0	1	0		1	2	Faulkner 1983
VN	3055 4695	615	Grane	Fipling -Tømmerkar			800			0	0	L	G	V	N	P	3.5	T65	Parallel Rifts	c	12	5	3.0	36	42	1	0	0	2	1	2	0	2	0	0	1	0		1		Faulkner 1983
VN	3060 4685	610	Grane	Fipling -Tømmerkar			800			0	0	L	G	V	N	P	3.5	T66	Oxbow Cave	b	10	1	2.0	20	10	1	1	1	0	1	0	0	0	0	0	0	0		1		Faulkner 1983
VN	3060 4680	610	Grane	Fipling -Tømmerkar			800			0	0	L	G	V	N	P	4.0	T68	Watery Cave	a	2	1	1.0	2	50	1	1	0	0	1	1	0	0	0	0	1	0		1		Faulkner 1983
VN	3045 4640	590	Grane	Fipling -Tømmerkar														T73	Unexplored Cave																				Faulkner 1983
VN	3400 4445	480	Grane	East Fiplingdal	30	W	50			1	0	K	S	A	D	P	0.3		Nyrudhola	S	50	30	15.0	750	60	1	0	0	1	0	0	0	4	0	1	0	0		1		Faulkner 1983. Relict vadose
Majavatn			**1925 III**																																			* Dip from Geology map
VN	2975 3135	720	Grane	Slakskar	20	90	200			1	0	K	F	V	N	P	0.3	S1	The Rat Run	b	35	8	1.0	35	23	1	0	1	0	1	0	0	0	0	0	1	0		1	2	* Faulkner 1987
VN	2980 3095	709	Grane	Slakskar	20	90	200			1	0	K	F	V	N	P	1.5	S4	South Shore Cave	a	8	2	1.0	8	25	1	1	0	0	1	0	0	0	0	0	1	0		1	2	Faulkner 1987
VN	2985 3105	705	Grane	Slakskar	20	90	200			1	0	K	F	V	N	P	1.5	S5	Lake Sink Cave	b	45	6	6.0	270	18	1	1	0	1	1	1	0	1	0	0	1	0	1	1	2	Faulkner 1987
VN	2950 3100	702	Grane	Slakskar	20	90	200			1	0	K	F	V	N	P	1.5	S8	Lake Resurgence 1	a	7	1	1.0	7	14	1	0	1	0	1	1	0	0	0	0	1	0		1		Faulkner 1987
VN	2980 3110	702	Grane	Slakskar	20	90	200			1	0	K	F	V	N	P	1.5	S9	Lake Resurgence 2	a	1	1	1.0	1	100	1	0	1	0	1	1	0	0	0	0	1	0		1		Faulkner 1987
Hattfjelldal			**1926 II**																																			
VN	5075 6875	460	Hattfjelldal	Åkervik		60	W	500			0	0	L	G	A	U	P	2.7		Øvre Åkervikgrotta	b	50	10	12.0	600	20	1	1	1	0	1	0	0	0	0	0	0	0	0		1	1	Unpublished. TF98
VN	5105 6865	430	Hattfjelldal	Åkervik	180	60	W	500	Pale brown		0	0	L	G	A	U	P	2.7		Åkervikgrotta	a	74	10	15.0	1110	14	1	1	1	0	1	0	0	0	0	0	0	0	0		1	3	Grottan28 (2)7-9 1993.TF98.TF00
VN	4615 7940	575	Hattfjelldal	Gryteselvdal			E	600	Banded		0	0	L	P	A	N	P	2.0		Gryteselvgrotta	b	180	21	6.0	1080	12	1	1	0	0	1	0	0	0	0	0	0	0	0		0		Heap. Jnl KCC (4) p4 1989. UH list
VN	4495 7810	540	Hattfjelldal	Gryteselvdal			E	500			0	0	L	P	A	D	P	1.0		Bytasschakket	S	12	10	2.0	24	83	1	0	0	1	0	0	0	1	0	0	0	0	0		0		Doj 1991. pc to TLF 97
VN	446 775	540	Hattfjelldal	Gryteselvdal			E	100			0	0	L	P	A	D	P	2.5		Adelskål Crack	a	5	1	1.0	5	20	1	0	0	1	0	0	0	0	0	0	0	0	0		0		Doj 1991. pc to TLF 97
VN	4445 7740	545	Hattfjelldal	Gryteselvdal			E	100			0	0	L	P	A	D	P	0.3		Small sink cave	a	5	1	2.0	10	20	1	1	0	0	1	0	0	0	0	0	1	0	0		0		Doj 1991. pc to TLF 97
VN	4414 7705	645	Hattfjelldal	Gryteselvdal			E	100			0	0	L	P	A	D	P	1.0		Cave below sink	b	15	2	2.0	30	13	1	0	0	1	0	0	0	0	0	0	0	0	0		0		Doj 1991. pc to TLF 97
Susendalen			**1925 I**																																			One outcrop. No known refs.

UPPERMOST ALLOCHTHON: Helgeland Nappe Complex: Zone 8 (Eastern Area): TOTALS

UTM COORDS	ALT.	KOMMUNE	AREA	LST. STRIKE	LST. DIP	OW	EXT. COLOUR	OTHER INT. ROCK	R	T	GS	CL	KT	SR	OR	CA	REF. NO.	CAVE NAME	CT	LENG.	VR	XS	VOL.	Min. HG %	C	SE	RE	DE	CS	SP	Ch	Sh	BC	RV	MV	DC	FS	P	SG	PRIME REFERENCES
									External Cave Attributes										Internal Cave Attributes																					
Totals	###				###	###			8	8						####				825	##	#####	3889	##	8	5	1	3	7	2	1	1	0	0	3	1	1	8		
Av. per cave	684				30	800			1.0	1.0						0.2				103	9	2.3	486	17		0.6	0.1	0.4	0.9	0.3	0.1	0.1	0.0	0.0	0.4	0.1	0.1	1.0		
Minima	660				30	800										0.20				4	1	1.0	4	4		0	0	0	0	0	0	0	0	0						
Maxima	735				30	800										0.3				460	45	6.0	2760	33		1	1	1	2	2	1	1	0	0						

(Dip measured ir 8 caves)

Glacial Situations:

	#	Length
C	0	0
D	0	0
E	0	0
G	0	0
H	0	0
K	0	0
L	8	825
S	0	0
T	0	0
U	0	0
Totals	**8**	**825**

Karst Types:

	#	Length
V	0	0
A	0	0
L	8	825
C	0	0
X	0	0
Totals	**8**	**825**

Cave Locations:

	#	Length
C	0	0
F	0	0
W	2	280
R	0	0
S	0	0
G	6	545
P	0	0
Totals	**8**	**825**

Cave Types:

	#	Length
S	0	0
a	4	30
b	1	30
c	0	0
d	2	515
e	0	0
f	1	250
g	0	0
h	0	0
Hy	0	0
I	0	0
J	0	0
L	0	0
R	0	0
T	0	0
Totals	**8**	**825**

Relict Caves:

#	Length
2	14
2	**14**

MV Caves:

#	Length
3	71
3	**71**

Combination Caves:

#	Length
3	**740**

UPPERMOST ALLOCHTHON: Helgeland Nappe Complex: Zone 8 (Eastern Area)

Caves are grouped by carbonate outcrop

Namsen catchment area

UTM COORDS	ALT.	KOMMUNE	AREA	LST. STRIKE	LST. DIP	OW	EXT. COLOUR	OTHER INT. ROCK	R	T	GS	CL	KT	SR	OR	CA	REF. NO.	CAVE NAME	CT	LENG.	VR	XS	VOL.	Min. HG %	C	SE	RE	DE	CS	SP	Ch	Sh	BC	RV	MV	DC	FS	P	SG	PRIME REFERENCES
									External Cave Attributes										Internal Cave Attributes																					
Majavatn		***1925 III***																																						
VN 34x 22x		Grane	Jengelvatn															Holes with fish																						Aa. Eivinsen pc 2000
VN 3560 2375	735	Grane	Jengelvatn		30 W	800			1	1	L	W	L	N	P	0.2		Gale Crawl Cave	b	30	5	1.0	30	17	1	1	0	0	1	0	0	0	0	0	0	0		1	1	Faulkner 1987
VN 3565 2375	715	Grane	Jengelvatn		30 W	800			1	1	L	W	L	N	P	0.2		Øvre Jengelgrotta	f	250	10	4.0	1000	4	1	1	0	1	1	2	0	0	0	0	0	0		1	1	Faulkner 1987
VN 3575 2360	680	Grane	Jengelvatn		30 W	800			1	1	L	G	L	N	P	0.3		Nedre Jengelgrotta	d	460	45	6.0	2760	10	1	1	0	0	1	0	1	1	0	0	0	1		1	1	Faulkner 1987
VN 3585 2355	675	Grane	Jengelvatn		30 W	800			1	1	L	G	L	N	P	0.3		cave	a	6	2	2.0	12	33	1	0	0	1	0	0	0	0	0	0	0	0		1		Faulkner 1987
VN 3585 2350	670	Grane	Jengelvatn		30 W	800			1	1	L	G	L	N	P	0.3		cave	a	8	2	2.0	16	25	1	0	0	1	0	0	0	0	0	0	0	0		1		Faulkner 1987
VN 3565 2330	660	Grane	Jengelvatn		30 W	800			1	1	L	G	L	N	P	0.2		Green Steps Cave	d	55	5	1.0	55	9	1	1	0	0	2	0	0	0	0	0	1	0	1	1	1	Faulkner 1987
VN 3545 2325	675	Grane	Jengelvatn		30 W	800			1	1	L	G	L	N	P	0.2		Snow Tunnel Cave	a	4	1	1.0	4	25	1	1	0	0	1	0	0	0	0	0	1	0		1		Faulkner 1987
VN 3555 2320	660	Grane	Jengelvatn		30 W	800			1	1	L	G	L	N	P	0.2		Resurgence 2	a	12	2	1.0	12	17	1	0	1	0	1	0	0	0	0	0	1	0		1	1	Faulkner 1987
VN 39x 25x		Grane	St. Kjukkel.															Deep shafts with ice																						Aa. Eivinsen pc 2000

Røyrivk	**1924 IV**	**No known references**
Hattfjelldal	**1926 II**	**No known references**
Børgefjellet	**1925 II**	**One outcrop. No known refs.**

UPPERMOST ALLOCHTHON: Helgeland Nappe Complex : Zone 9 (Northern Area): TOTALS

UTM COORDS	ALT.	KOMMUNE	AREA	LST. STRIKE	LST. DIP	OW	EXT. COLOUR	OTHER INT. ROCK	R	T	GS	CL	KT	SR	OR	CA	REF. NO.	CAVE NAME	CT	LENG.	VR	XS	VOL.	Min. HG %	C	SE	RE	DE	CS	SP	Ch	Sh	BC	RV	MV	DC	FS	P	SG	PRIME REFERENCES
												External Cave Attributes							Internal Cave Attributes																					
Totals	###				##	###			0	0						####				25	##	#####	250	##	1	0	0	1	0	0	0	0	0	0	0	1	0	1		
Av. per cave	113				80	0			0.0	0.0						0.2				25	5	10.0	250	20		0.0	0.0	1.0	0.0	0.0	0.0	0.0	0.0	0.0	0.0	1.0	0.0	1.0		
Minima	113				80	0										0.20				25	5	10.0	250	20		0	0	1	0	0	0	0	0	0						
Maxima	113				80	0										0.2				25	5	10.0	250	20		0	0	1	0	0	0	0	0	0						

(Dip measured in 1 caves)

Glacial Situations:

	#	Length
C	0	0
D	0	0
E	1	25
G	0	0
H	0	0
K	0	0
L	0	0
S	0	0
T	0	0
U	0	0
Totals	1	25

Karst Types:

	#	Length
V	0	0
A	0	0
L	0	0
C	0	0
X	1	25
Totals	1	25

Cave Locations:

	#	Length
C	0	0
F	0	0
W	1	25
R	0	0
S	0	0
G	0	0
P	0	0
Totals	1	25

Cave Types:

	#	Length
S	0	0
a	0	0
b	0	0
c	0	0
d	0	0
e	0	0
f	0	0
g	0	0
h	0	0
Hy	0	0
I	0	0
J	0	0
L	1	25
R	0	0
T	0	0
Totals	1	25

Relict Caves:

#	Length
1	25
1	**25**

MV Caves:

#	Length
0	0
0	**0**

Combination Caves:

#	Length
0	**0**

UPPERMOST ALLOCHTHON: Helgeland Nappe Complex : Zone 9 (Northern Area)

Caves are grouped by carbonate outcrop

Western catchment area

UTM COORDS	ALT.	KOMMUNE	AREA	LST. STRIKE	LST. DIP	OW	EXT. COLOUR	OTHER INT. ROCK	R	T	GS	CL	KT	SR	OR	CA	REF. NO.	CAVE NAME	CT	LENG.	VR	XS	VOL.	Min. HG %	C	SE	RE	DE	CS	SP	Ch	Sh	BC	RV	MV	DC	FS	P	SG	PRIME REFERENCES
												External Cave Attributes							Internal Cave Attributes																					
Sandnessjøen	**1827 III**																																							Dip from Geology map
UP 8940 3587	113	Dønna	Vågsvågen	60	80 S	0	Brown	cbs	0	0	E	W	X	N	N	0.2		**Marmorholet**	L	25	5	10.0	250	20	1	0	0	1	0	0	0	0	0	0	0	1		1	1	DStP 1967 (Card index). TF00
								cbs = calcitic biotite schist - not limestone bedock																																
Nesna	**1827 II**																																							No known references
Elsfjord	**1927 III**	(HNC north of Ranafjord)																																						No known references

UPPERMOST ALLOCHTHON: Rødingsfjell Nappe Complex - Nappes below Beiarn Nappe: Zone A (Bleikvassli Area): TOTALS

External Cave Attributes

UTM COORDS	ALT.	KOMMUNE	AREA	LST. STRIKE	LST. DIP	OW	EXT. COLOUR	OTHER INT. ROCK	R	T	GS	CL	KT	SR	OR	CA	REF. NO.	CAVE NAME
Totals	####				####	####			2	3						#####	(Excluding Røsvatn)	
Av. per cave	437				41	496			0.1	0.1						5.5	(Excluding Røsvatn)	
Minima	93				10	30										0.10		
Maxima	817				90	1500										1700.0		

(Dip measured in 23 caves)

Internal Cave Attributes

	CT	LENG.	VR	XS	VOL.	Min. HG %	C	SE	RE	DE	CS	SP	Ch	Sh	BC	RV	MV	DC	FS	P	SG	PRIME REFERENCES
Totals		3920	###	#####	31976	###	37	15	7	35	28	22	8	8	11	3	8	0	9	24		
Av. per cave		106	13	5.6	864	24		0.4	0.2	0.9	0.8	0.6	0.2	0.2	0.3	0.1	0.2	0.0	0.2	0.6		
Minima		5	1	1.0	5	5		0	0	0	0	0	0	0	0	0						
Maxima		1400	180	28.4	14000	100		2	1	5	2	4	2	4	4	1						

Glacial Situations:

	#	Length
C	0	0
D	1	20
E	1	79
G	0	0
H	1	11
K	17	2528
L	16	582
S	1	700
T	0	0
U	0	0
Totals	**37**	**3920**

Karst Types:

	#	Length
V	2	55
A	18	638
L	16	3217
C	0	0
X	1	10
Totals	**37**	**3920**

Cave Locations:

	#	Length
C	0	0
F	12	464
W	4	100
R	0	0
S	4	2205
G	17	1151
P	0	0
Totals	**37**	**3920**

Cave Types:

	#	Length
S	3	20
a	14	296
b	4	222
c	5	434
d	7	1205
e	0	0
f	1	60
g	3	1683
h	0	0
Hy	0	0
I	0	0
J	0	0
L	0	0
R	0	0
T	0	0
Totals	**37**	**3920**

Relict Caves:

#	Length
11	879
11	**879**

MV Caves:

#	Length
8	167
8	**167**

Combination Caves:

#	Length
18	**2874**

UPPERMOST ALLOCHTHON: Rødingsfjell Nappe Complex - Nappes below Beiarn Nappe: Zone A (Bleikvassli Area)

Caves are grouped by carbonate outcrop

Northern and Vefsn catchment areas

External Cave Attributes (R – REF. NO.); Internal Cave Attributes (CT – SG)

UTM COORDS	ALT.	KOMMUNE	AREA	LST. STRIKE	LST. DIP	OW	EXT. COLOUR	OTHER INT. ROCK	R	T	GS	CL	KT	SR	OR	CA	REF. NO.	CAVE NAME	CT	LENG.	VR	XS	VOL.	Min. HG %	C	SE	RE	DE	CS	SP	Ch	Sh	SC	RV	MV	DC	FS	P	SG	PRIME REFERENCES
Elsfjord		**1927 III**																																						
VP 4135 3720	660	Hemnes	Elsfjord	180	W	200			0	1	L	S	A	N	P	0.1		**Sloping Shaft**	S	5	5	*1.0*	5	100	1	0	0	1	*0*	0	*0*	1	0	0	0	*0*	*0*	0		Doj 1991. pc to TLF
VP 41x 36x		Hemnes	Elsfjord	10	W													**Selhorngrotta**																						U. Holbye List 1974. Helland p472
VP 4005 3350	680	Hemnes	Elsfjord	180	W											0.5		**20 caves**		Up to 30m long																				Doj 1991. pc to TLF
Fustvatn		***1926 IV***																																						
VP *4085 1940*	570	Vefsn	Trollbotn				Yellow											**Ravine Cave**	(R)																					**Unexplored.** TF98
VP *4085 1950*	544	Vefsn	Trollbotn	180	W	400			0	1	K	G	A	N	P	1.5		**Thrust Res. Cave**	a	5	1	1.0	5	20	1	0	1	0	1	0	0	0	0	0	1	0		1		**(Unexplored).** Wet. TF98
VP *4115 1850*	619	Vefsn	Trollbotn		W	500			0	1	K	G	A	D	P	0.3		**Sharp Flake Shaft**	S	5	5	1.0	5	100	1	0	0	1	0	0	0	1	0	0	0	0	0	1		Unpublished. TF98
VP *4140 1920*	560	Vefsn	Trollbotn															**Langvatngrotta**																						**Unexplored.** Very low. TF98
VP *410 190*	560	Vefsn	Trollbotn															**4 karst features**																						Fustvatnet Quat. Map
Korgen		**1927 II**																																						
VP 430 330	460	Hemnes	Korgen															**4 x karst**																						Korgen Quat. Map
VP 4335 2575	435	Hemnes	Korgen		65 W	700			0	0	L	G	A	U	N	0.8		**cave**	a	*5*	*1*	*1.0*	*5*	20	1	0	*1*	0	1	0	0	0	0	0	0	0		0		Doj 1995. pc to TLF
VP 450 360	140	Hemnes	Korgen															**7 x karst**																						Korgen Quat. Map
VP 440 340	220	Hemnes	Korgen															**6 x karst**																						Korgen Quat. Map
VP 440 220	400	Hemnes	Korgen															**3 x karst**																						Korgen Quat. Map
VP 4715 2258	93	Hemnes	Røssåga	160	20 W	600		amph.	0	0	E	F	L	N	N	1700		**Remnant Cave**	c	79	6	4.1	**324**	8	1	0	0	5	0	0	1	0	4	0	0	0		1	3	TF00
VP 4710 2235	93	Hemnes	Røssåga															**Marmorslottet**		signposted rock shelters																				TF00
VP 4915 2190	110	Hemnes	Bryggfjelldal		*W*	100			0	0	D	F	*L*	N	P	23.0		**Fjellbrygga**	a	20	10	20.0	400	50	1	1	1	0	1	0	0	0	0	0	0	0		1		Helland. p472 1907. UH List. TF00
VP 5125 2075	295	Hemnes	Bryggfjelldal		40 W	100			0	0	K	F	A	N	N	15.0		**Bjurå Res. Cave**	b	22	*3*	*4.0*	*88*	14	1	0	1	1	1	1	0	0	0	0	1	0	1	0	1	GC Journal (6)67-69 1985
VP 5125 2075	295	Hemnes	Bryggfjelldal		40 W	100			0	0	K	F	A	N	N	15.0		**Ring Cave**	a	12	*4*	*2.0*	*24*	33	1	1	0	0	1	1	0	0	0	0	0	0		0	1	GC Journal (6)67-69 1985
VP 5140 2070	300	Hemnes	Bryggfjelldal		40 W	100			0	0	K	F	A	N	N	15.0		**Bjurå Pothole**	c	90	*5*	*1.5*	*135*	6	1	0	0	1	1	1	2	1	0	0	0	0	1	0	1	GC Journal (6)67-69 1985
VP 5140 2045	320	Hemnes	Bryggfjelldal		40 W	100			0	0	K	G	A	D	N	3.5		**Slegdabekkgrotta**	c	100	20	3.0	300	20	1	0	0	1	1	4	1	0	0	0	0	0		0	1	GC Journal (6)67-69 1985
VP 5053 2244	530	Hemnes	Bryggfjelldal													(1.8)		**Jordåga Res. Cave**		0.3 cumecs. 4m above rising. 3m is explorable.																			1	TF00. SN04
VP 5094 2243	591	Hemnes	Bryggfjelldal	360	20 N	1500	White		0	0	K	W	L	U	N	1.6		**Track Cave**	g	15	10	1.0	15	67	1	1	0	0	1	0	0	0	0	0	0	0	0	1	2	TF00. Explored to 26m: SN04*
VP 5092 2255	617	Hemnes	Bryggfjelldal													(1.6)		**Bryggfjeld Res. Cave**		3m+ draughting duck																				TF00. SN04
VP 5093 2287	677	Hemnes	Bryggfjelldal	70	20 N	1500	Buff/gr		0	0	K	S	L	U	N	1.0		**Bryggfjeldhullet**	d	100	30	*4.0*	400	30	1	1	0	0	2	0	1	0	0	0	0	0		1	3	Heap 1974. TF00. Surveyed to 126m:SN04
VP 5176 2279	817	Hemnes	Bryggfjelldal	150	20-4C W	1500	*		0	0	S	S	L	D	N	0.4		**Ytterithullet***	d	700	180	8.0	5600	25.7	1	1	0	0	2	4	2	0	1	1	0	0		1	4	Heap 1974. TF00. Inlet Passage = RV?
VP 5206 2211	746	Hemnes	Bryggfjelldal													(0.2)		**Ladalen Sink Cave**		20 l/sec. Tiny, but pushable																				**Unexplored.** TF00
VP 5189 2208	696	Hemnes	Bryggfjelldal	30	(20 W)											(0.2)		**Ladalen Res. Cave**		2m wide X 0.3m high - enterable!																				**Unexplored.** TF00
VP 535 205	700	Hemnes	Bryggfjelldal															**Knicksen karst**		Shallow wet stream caves																				NG (3/4) 34-35 1977.

* blue / grey / white / orange

* GS of entrance

* Sound of stream inside cave

UPPERMOST ALLOCHTHON: Rødingsfjell Nappe Complex - Nappes below Beiarn Nappe: Zone A (Bleikvassli Area) Caves are grouped by carbonate outcrop **Northern catchment area**

UTM COORDS	ALT.	KOMMUNE	AREA	LST. STRIKE	LST. DIP	OW	EXT. COLOUR	OTHER INT. ROCK	R	T	GS	CL	KT	SR	OR	CA	REF. NO.	CAVE NAME	CT	LENG.	VR	XS	VOL.	Min. HG %	C	SE	RE	DE	CS	SP	Ch	Sh	BC	RV	MV	DC	FS	P	SG	PRIME REFERENCES
Rossvatnet 1926 I																																								
VP 4387 1880	364	Hemnes	Bleikvassli		20 W	900			0	0	L	G	L	U	N	5.0		Storskogbekk Sink	S	10	3	1.0	10	30	1	1	0	0	1	0	0	0	1	0	1	0		1		Unpublished. TF98
VP 4394 1878	359	Hemnes	Bleikvassli	50	10 W	900	Buff	cgms	0	0	L	G	L	U	N	5.0		Storskogbekkhullet	a	84	26	23.4	1966	31	1	1	0	0	1	1	0	0	1	1	0	0	1	1	3	Unpublished. TF98
VP 4410 1880	350	Hemnes	Bleikvassli	180	20 W	900	Buff	a + d	0	0	L	W	L	U	N	5.0		Storskoggrotta	f	60	10	4.0	240	17	1	0	0	1	0	0	0	0	1	0	0	0	1	1	1	Unpublished. TF98
VP 4169 0916	433	Hemnes	Bleikvassli	10	45 W	100		*	0	0	L	G	A	N	P	4.0	TBAG	Tosbotnåsgrotta	c	78	5	2.0	156	6	1	0	0	2	0	0	0	0	0	0	0	0	1	3	TF97.Surveyed to 108m: SN04
VP 4172 0924	438	Hemnes	Bleikvassli														TBAG	Middle Cave		58m long																		3	SN04
VP 4177 0936	430	Hemnes	Bleikvassli														TBAG	Calm Cave		42m long to deep silent pool																		3	SN04
VP 4187 0994	412	Hemnes	Bleikvassli														TBAG	Cave at Rising		45m long to resurgence sump																		2	SN04
VP 4195 1085	377	Hemnes	Bleikvassli	160	45 W	300	Grey	*	1	0	L	G	A	N	P	9.0		Storholetjorngrotta	a	45	3	3.0	135	7	1	1	0	0	1	1	0	0	0	0	1	0	1	1	1	Unpublished. TF97.
VP 4215 1140	390	Hemnes	Bleikvassli	170	45 W	30			1	0	L	G	A	N	P	12.0		River Oxbow	a	10	1	1.0	10	10	1	1	1	0	1	0	0	0	0	0	1	0		1		Unpublished. TF97
VP 4390 0890	310	Hemnes	Bleikvassli	80	90	900			0	0	L	G	V	N	P	0.3		Jordbrugrotta	b	30	5	1.0	30	17	1	0	0	2	1	0	0	1	0	0	1	0		0		Heap. 1974 p7-9
VP 4390 0890	310	Hemnes	Bleikvassli	80	90	900			0	0	L	G	V	N	P	0.3		Cliff Foot Cave	d	25	3	1.0	25	12	1	0	0	1	1	2	0	0	0	0	1	0		0		Heap. 1974 p7-9
VP 4365 0720	340	Hemnes	Bleikvassli	25	40 W	400			0	0	L	F	A	N	P	1500.0		Corner Canal	d	20	4	8.0	160	20	1	0	0	2	1	1	0	0	0	0	1	0		1	1	Unpublished. TF97
VP 507 163	440	Hemnes	Bleikvassli	150	W	300			0	0	K	G	A	N	N	20.0		Grønnelvgrotta	b	30	10	4.0	120	33	1	1	0	0	1	0	0	0	0	0	0	0		0		U. Holbye List 1974
VP 4390 0750	300	Hemnes	Bleikvassli															Sumped Resurgence																					TF97
VP 4396 0760	304	Hemnes	Bleikvassli	25	40 W	300			0	0	L	F	A	N	P	1500.0		Ressåga Sink Cave	a	25	6	10.0	250	24	1	1	0	0	1	1	0	0	0	0	0	0	1	1	2	Helland p467. Unpublished. TF97
VP 4395 0780	302	Hemnes	Bleikvassli		40 W	300	Grey Wh.		0	0	L	F	A	N	P	1500.0	R1/R2	Ressågagrotta	b	140	7	28.4	3976	5	1	0	0	2	1	2	0	0	0	0	0	0	1	1	3	Unpublished. TF97
VP 4396 0796	300	Hemnes	Bleikvassli		40 W	300			0	0	L	F	A	N	P	1500.0	R3	Ressåga Res. Cave	a	25	5	20	500	20	1	0	1	0	1	1	0	0	0	0	0	0		1	2	Unpublished. TF97
VP 4405 795	300	Hemnes	Bleikvassli		40 W	300	Wh+bands		0	0	L	F	A	N	P	0.3		Øst Ressågagrotta	a	10	3	6.0	60	30	1	0	0	1	0	0	0	0	0	0	0	0		1		Unpublished. TF97
VP 461 192	260	Hemnes	Bleikvassli			30			0	0	L	F	X	N	P	0.8		cave	a	10	2	1.0	10	20	1	1	0	0	1	0	0	0	0	0	0	0		0		Doj 1991. pc to TLF
VP 4656 1917	182	Hemnes	Bleikvassli	180	60 W	100			0	0	H	F	A	N	P	1700.0		Double Entrance Ca.	d	11	2	2.0	22	18	1	2	0	0	1	0	0	0	0	0	0	0	0	1	1	TF00
VP 4674 1906	218	Hemnes	Bleikvassli	145			Grey Wh.									(1700)		Stabbfors Jettegryter	(J)	20-30 jettegryter in limestone in this area. Deepest is 12m50, with 6m x 6m diameter.																			TF00
VP 5320 2009	755	Hemnes	Tverfjellet		(30 W)													Naeverskard Sink		Sink and resurgence entrances are 200m apart on surface. VR 70m.																			Unexplored. TF00
VP 5298 2011	685	Hemnes	Tverfjellet		(30 W)													Naeverskardhullet		Incomplete exploration of 200m in two stream passages on 17 July 2004																			TF00. SN04
VP 5273 2023	564	Hemnes	Tverfjellet															resurgence cave		0.5m X 0.5 m entrance, 50 m from sink																			Unexplored. TF00
VP 529 179	700	Hemnes	Grøndal															cave		Only a small unenterable sink seen (TF00)																			Unexplored. Local report to TLF 1997
VP 5483 1848	777	Hemnes	Grøndal		(45 W)													sink cave		2 l/sec. Rises at small tarn																			Unexplored. TF00
VP 552 177	650	Hemnes	Grøndal													(5)		Jordågrotta																			U. Holbye List 1974
VP 551 177	650	Hemnes	Grøndal		N	500			0	0	K	G	L	U	P	5.0		Torr Jordbru	a	20	2	4.0	80	10	1	0	0	2	0	0	0	0	0	0	0	0		0		U. Holbye List 1974
VP 552 177	650	Hemnes	Grøndal		N	500			0	0	K	W	L	U	P	5.0		Torr Grotte	a	5	2	4.0	20	40	1	0	0	1	0	0	0	0	0	0	0	0		0		U. Holbye List 1974
VP 552 177	650	Hemnes	Grøndal		N	500			0	0	K	W	L	U	P	5.0		Jordbru	a	20	2	4.0	80	10	1	0	0	2	1	0	0	0	0	0	0	0		0		U. Holbye List 1974
VP 5480 1740	800	Hemnes	Grøndal	70	30 N	500			0	0	K	S	L	U	P	5.0		Grønndalegrotta	g	1400	70	10.0	14000	5.0	1	1	1	5	1	2	1	4	0	1	0	0	1	1	5	NG (2) 34-43 1977. UH List. TF00. *
VP 5499 1748	642	Hemnes	Grøndal	70	N	500			0	0	K	G	L	U	P	5.0		Revtuelet	g	268	15	4.0	1072	8	1	0	0	1	0	0	0	0	0	1	0	0	1	1		NG (2) 34-43 1977. UH List. TF00. *
VP 5499 1748	642	Hemnes	Grøndal	70	N	500			0	0	K	G	L	U	P	5.0		Isgrotta	d	99	5	4.0	400	5	1	0	0	1	0	0	0	0	1	0	0	0		1		NG (2) 34-43 1977. UH List. TF00. *
VP 5501 1749	639	Hemnes	Grøndal	70	N	500			0	0	K	G	L	U	P	5.0		200m Grotta	d	250	15	4.0	1000	6	1	0	0	1	0	0	0	0	1	0	0	0		1		NG (2) 34-43 1977. UH List. TF00. *
VP 5504 1748	637	Hemnes	Grøndal	70	N	500			0	0	K	G	L	U	P	5.0		Bekkehølet	c	87	5	4.0	348	6	1	0	0	1	1	0	0	0	0	0	0	0		1		NG (2) 34-43 1977. UH List. TF00. *
VP 555 155	600	Hemnes	Grønfjell															cave																			E. Johnsen 1976. pc to TLF
VP 556 162	500	Hemnes	Grønfjell															cave																			E. Johnsen 1976. pc to TLF

a + d = amphibolite + dolomite
* near dolostone?

* NG (3/4) 34-35 1977.

UPPERMOST ALLOCHTHON: Rødingsfjell Nappe Complex - Nappes below Beiarn Nappe: Zone B (Bjørka and Stor Akersvatn Area): TOTALS

	UTM COORDS	ALT.	KOMMUNE	AREA	LST. STRIKE	LST. DIP	OW	EXT. COLOUR	OTHER INT. ROCK	R	T	GS	CL	KT	SR	OR	CA	REF. NO.	CAVE NAME	CT	LENG.	VR	XS	VOL.	Min. HG %	C	SE	RE	DE	CS	SP	Ch	Sh	BC	RV	MV	DC	FS	P	SG	PRIME REFERENCES
										External Cave Attributes										Internal Cave Attributes																						
Totals		####				##	####			0	0						###				1410	###	#####	7330	###	7	5	1	5	4	2	1	2	1	0	2	1	2	7		
Av. per cave		530				66	403			0.0	0.0						4.4				201	11	7.4	1047	24		0.7	0.1	0.7	0.6	0.3	0.1	0.3	0.1	0.0	0.3	0.1	0.3	1.0		
Minima		402				0	20										0.10				4	3	1.0	8	2		0	0	0	0	0	0	0	0	0						
Maxima		620				90	1500										8.5				900	28	30.0	3270	75		3	1	2	1	1	1	1	1	0						

(Dip measured in 3 caves)

Karst Types:

	#	Length
V	1	17
A	4	489
L	2	904
C	0	0
X	0	0
Totals	7	1410

Cave Types:

	#	Length
S	0	0
a	2	37
b	1	109
c	2	904
d	1	150
e	0	0
f	0	0
g	0	0
h	0	0
Hy	0	0
I	1	210
J	0	0
L	0	0
R	0	0
T	0	0
Totals	7	1410

Relict Caves:

#	Length
3	1114

MV Caves:

#	Length
2	170

Combination Caves:

#	Length
2	126

Glacial Situations:

	#	Length
C	0	0
D	0	0
E	0	0
G	0	0
H	0	0
K	7	1410
L	0	0
S	0	0
T	0	0
U	0	0
Totals	7	1410

Cave Locations:

	#	Length
C	0	0
F	3	380
W	0	0
R	0	0
S	1	4
G	3	1026
P	0	0
Totals	7	1410

UPPERMOST ALLOCHTHON: Rødingsfjell Nappe Complex - Nappes below Beiarn Nappe: Zone B (Bjørka and Stor Akersvatn Area) Caves are grouped by carbonate outcrop **Northern catchment area**

	UTM COORDS	ALT.	KOMMUNE	AREA	LST. STRIKE	LST. DIP	OW	EXT. COLOUR	OTHER INT. ROCK	R	T	GS	CL	KT	SR	OR	CA	REF. NO.	CAVE NAME	CT	LENG.	VR	XS	VOL.	Min. HG %	C	SE	RE	DE	CS	SP	Ch	Sh	BC	RV	MV	DC	FS	P	SG	PRIME REFERENCES
										External Cave Attributes										Internal Cave Attributes																						
Korgen			**1927 II**																																						
VP			Hemnes	Leirskarddal		-													Kildegrotta																							EPC 71. DStP? RS pc
VP			Hemnes	Leirskarddal															Weetabixgrotta		(30)																					EPC 71
VP	6190	2305	560	Hemnes	Leirskarddal	28	38 W	*20*	Brown Wh	Schist	0	0	K	F	A	N	P	8.5		Leirskarelvgrotta	I	210	*10*	*8.0*	*1680*	5	1	0	0	1	0	0	0	0	1	0	0	0		1	1	GC Journal (6)67-69 1985. TF97. *
VP	6195	2305	580	Hemnes	Leirskarddal		W	*20*			0	0	K	F	A	N	P	8.5		Gully Sinks	d	150	*5*	*3.0*	*450*	3	1	3	0	0	1	0	0	0	0	1	0		1	1	GC Journal (6)67-69 1985
VP	623	233	620	Hemnes	Leirskarddal		W	*20*			0	0	K	F	A	N	P	8.5		Choked Flood Sink	a	20	*3*	*1.0*	*20*	15	1	1	0	0	1	0	0	0	0	1	0		1	1	GC Journal (6)67-69 1985
VP			Hemnes	Bjørka															cave?																						EPC? TD?
VP	5130	4385	430	Rana	Rostafjellet	60	70 S	*30*	White/mic	Bio.schi	0	0	K	G	A	N	P	2.2		Bakilagrotta	b	109	28	30.0	3270	26	1	1	0	0	1	1	0	0	0	0	0	0	1	1	1	Unpub. TF98
VP	5115	4395	402	Rana	Rostafjellet	150	90	*30*			0	0	K	G	V	N	P	2.2		Nedre Bakilagrotta	a	17	7	6.0	102	41	1	0	1	1	1	1	0	1	0	0	0	0	0	1	1	Unpub. TF98
VP	515	445	400	Rana	Rostafjellet														3 x karst																						Korgen Quat. Map. TF98

* Formed in calcitic schist

Storakersvatnet			**2027 III**																																						
VP	7330	4185	540	Rana	Storakersv.		0	1200	Pale brow	cgms	0	0	K	G	L	N	N	1.0	77	Akersvanngrotta *	c	900	20	2.0	1800	2.2	1	0	0	2	0	0	1	0	0	*0	0	1	1	1	4	Hjorten, 1968 pp28,30. TF98
VP	740	420		Rana	Storakersv.															Sigurdsgrotta																						Hjorten. 1968. p30
VP	*800*	*380*	*580*	Rana	Storakersv.															Ivargrotta																						U. Holbye List 1974. D=20
VP	7875	3900	580	Rana	Storakersv.		0	1500	Pale grey	Tremoli	0	0	K	S	L	N	N	0.1	78	Tjuvhelleren (=Huset?)	c	4	3	2.0	8	75	1	0	0	1	0	0	0	1	0	0	0	0	0	1		Hjorten. 1968. p30. Dol. cave! TF98.
VP	75x	33x		Rana	Storakersv.															100m doline																						Hjorten. 1968. p30
VP	77x	36x		Rana	Storakersv.															Grunnvatnet "Hull"																						Hjorten. 1968. p30
VP	7410	2550	590	Hemnes	Grasvatnet															Intermittent Doline																						Horn. 1947. p70. In dolomite?

cgms = calcitic garnet muscovite schist. * Also called Ingegrotta and Jo-grotta. The dip varies.

UPPERMOST ALLOCHTHON: Rødingsfjell Nappe Complex - Nappes below Beiarn Nappe: Zone C (Southern and Border Area): TOTALS

	ALT.								External Cave Attributes										Internal Cave Attributes																								
	UTM COORDS	ALT.	KOMMUNE	AREA	LST. STRIK	LST. DIP	OW	EXT. COLOU	OTHER INT. ROCK	R	T	GS	CL	KT	SR	OR	CA	REF. NO.	CAVE NAME	CT	LENG.	VR	XS	VOL.	Min. HG %	C	SE	RE	DE	CS	SP	Ch	Sh	BC	RV	MV	DC	FS	P	SG	PRIME REFERENCES
Totals		###				##	###			0	0						####				971	###	####	10922	####	18	6	5	13	13	7	2	7	9	1	3	1	4	16		
Av. per cave		640				50	117			0.0	0.0						3.6				54	14	5.4	607	45		0.3	0.3	0.7	0.7	0.4	0.1	0.4	0.5	0.1	0.2	0.1	0.2	0.9		
Minima		550				20	100										0.50				2	1	0.5	2	10		0	0	0	0	0	0	0	0	0						
Maxima		800				70	200										10.2				316	60	30.0	6300	100		1	1	2	1	3	1	2	4	1						

(Dip measured 6 caves)

Karst Types:

	#	Length
V	0	0
A	11	813
L	2	135
C	0	0
X	5	23
Totals	18	971

Cave Locations:

	#	Length
C	0	0
F	2	8
W	4	17
R	0	0
S	1	26
G	11	920
P	0	0
Totals	18	971

Cave Types:

	#	Length
S	3	15
a	7	133
b	3	297
c	2	145
d	0	0
e	0	0
f	0	0
g	0	0
h	1	316
Hy	0	0
I	2	65
J	0	0
L	0	0
R	0	0
T	0	0
Totals	18	971

Relict Caves:

#	Length
5	90

MV Caves:

#	Length
3	36

Combination Caves:

#	Length
10	845

Glacial Situations:

	#	Length
C	0	0
D	0	0
E	0	0
G	0	0
H	0	0
K	14	618
L	1	6
S	3	347
T	0	0
U	0	0
Totals	18	971

UPPERMOST ALLOCHTHON: Rødingsfjell Nappe Complex - Nappes below Beiarn Nappe: Zone C (Southern and Border Area)

Northern catchment area

	UTM COORDS	ALT.	KOMMUNE	AREA	LST. STRIK	LST. DIP	OW	EXT. COLOU	OTHER INT. ROCK	R	T	GS	CL	KT	SR	OR	CA	REF. NO.	CAVE NAME	CT	LENG.	VR	XS	VOL.	Min. HG %	C	SE	RE	DE	CS	SP	Ch	Sh	BC	RV	MV	DC	FS	P	SG	PRIME REFERENCES
Rossvatnet		***1926 I***																																							
VP	*5485 0373*	780	Hemnes	Liljell	40	*N*	200			0	0	S	G	A	N	P	1.5		**Basagrotta**	h	316	50	2.5	790	16	1	1	0	0	1	0	1	0	4	0	0	1	1	0	3	Doj 1991. pc to TLF+survey
VP	*5410 0345*	710	Hemnes	Liljell	40	50 N	200	Grey		0	0	S	S	A	N	P	2.5		**Gåsvassholet**	a	26	*5*	*3.0*	*78*	19	1	1	0	0	1	0	0	*0*	*0*	*0*	0	0		1	Doj 1991. pc to TLF. TF97
VP	*5385 0330*	671	Hemnes	Liljell	70	70 N	200		Biot. schist	0	0	S	F	A	N	P	2.5		**Gåsvasholet Res.**	I	5	3	1.0	5	60	1	0	1	0	1	0	0	0	1	0	0	0	0		1	Unpub. TF97
VP	*5210 0240*	630	Hemnes	Liljell		*S*	100			0	0	K	G	A	N	N	10.0		**Gåsvasgrotta**	I	*60*	*20*	*2.0*	*120*	33	1	0	0	1	1	0	0	2	1	0	0	0	0	0	Heap. 1974 p7-9. GCJ (6) p89
VP	*515 022*	580	Hemnes	Liljell	80	70 S	100	Grey	Musc. schis	0	0	K	G	A	N	N	10.2		**Klofthelet**	b	210	60	30.0	6300	28.6	1	0	0	1	1	2	0	0	0	1	0	0	0	1	2	GC Journal (6) 68-69 1985. TF97
VP	*515 022*	550	Hemnes	Liljell		*S*	100			0	0	K	G	A	N	N	10.2		**Windtunnel**	a	60	20	5.0	300	33	1	0	0	2	0	0	0	0	0	0	0	0	0	1	2	GC Journal (6) 68-69 1985
VP	*5140 0200*	580	Hemnes	Liljell		20 N	100	Grey		0	0	K	G	L	N	N	10.2		**Gåsvaselvgrotta** *	c	130	13	20.0	2600	10	1	0	1	1	1	3	1	0	1	0	0	0	1	1	2	GC Journal (6) 68-69 1985
VP	*5145 0200*	550	Hemnes	Liljell	60	20 N	100			0	0	K	G	L	N	N	10.2		**Rock Bridge**	a	5	3	10.0	50	60	1	1	1	0	1	0	0	0	0	0	0	0	0	1	2	GC Journal (6) 68-69 1985
Hjartfjell		***2026 IV***																	* = Ice Cave																						
VP	*7260 1505*	800	Hemnes	Hekkeltjell			100			0	0	L	G	X	X	N	1.2		**Holbekkgrotta**	a	6	2	4.0	24	33	1	0	0	1	1	1	0	0	0	0	0	0	0	1		Unpublished.TF96. *
VP	*7450 1550*	620	Hemnes	Artfjell			100			0	0	K	W	X	N	N	0.8		**Speltfjelldal Res.**	a	2	1	1.0	2	50	1	0	1	0	1	1	0	0	0	0	1	0	0	1		Unpublished.TF96
VP	*7645 1515*	695	Hemnes	Artfjell			100			0	0	K	W	X	N	N	0.5		**Artfjell North Sink 1**	S	9	4	2.0	18	44	1	0	0	2	0	0	0	2	0	0	0	0	0	1		Unpublished.TF96
VP	*7645 1515*	695	Hemnes	Artfjell			100			0	0	K	W	X	N	N	0.5		**Artfjell North Sink 2**	S	3	3	2.0	6	100	1	0	0	2	0	0	0	2	1	0	0	0	0	1		Unpublished.TF96
VP	*7635 1520*	660	Hemnes	Artfjell			100			0	0	K	W	X	N	N	0.5		**Dead Dear Hole**	S	3	3	2.0	6	100	1	0	0	1	0	0	0	1	0	0	0	0	1	1		Unpublished.TF96
VP	*6980 1075*	590	Hemnes	Steikfjell		*N*	100			0	0	K	G	A	U	P	0.9		**Drippy Shaft**	b	11	9	1.0	11	82	1	1	0	0	1	0	0	0	1	0	0	0	0	1		Unpublished.TF96
VP	*6985 1080*	600	Hemnes	Steikfjell		*N*	100			0	0	K	G	A	U	P	0.9		**Snow Cross Cave**	c	15	4	2.0	30	27	1	0	0	2	0	0	0	0	0	0	0	0	0	1	1	Unpublished.TF96
VP	*6995 1085*	625	Hemnes	Steikfjell	60	*N*	100			0	0	K	G	A	U	P	0.9		**Steikfjellgrotta**	b	76	40	6.0	456	53	1	1	0	0	1	0	0	0	0	0	0	1	1	1	Unpublished.TF96
VP	*7005 1075*	590	Hemnes	Steikfjell	90	70 N	100			0	0	K	G	A	U	P	0.9		**Rift Sink**	a	31	10	4.0	124	32	1	1	0	0	1	0	0	0	0	0	1	0	0	1	Unpublished.TF96
VP	*7575 1235*	800	Hemnes	Artfjell	80	*N*	100			0	0	K	F	A	N	P	1.0		**Wet Crawl Cave**	a	3	1	0.5	2	33	1	0	1	0	1	0	0	0	0	0	1	0	*0	1	Unpublished.TF96
VP	*7720 0925*	457	Hemnes	Olfjell															**Sumped Rising**																			*		Unpublished.TF97
Kaldvatnet		**2027 II**	(South of Kaldvatnet only)																																						

No known references

UPPER ALLOCHTHON: Kall Nappes - Upper Kall: KU (Fausko/Gassok/Akkjell/Hattfjelldal/Jofjell/Krutfjell Nappes): TOTALS

	UTM COORDS	ALT.	KOMMUNE	AREA	LST. STRIKE	LST. DIP	OW	EXT. COLOUR	OTHER INT. ROCK	R	T	GB	CL	KT	SR	OR	CA	REF. NO.	CAVE NAME	CT	LENG.	VR	XS	VOL.	Min. HG %	C	SE	RE	DE	CS	SP	Ch	Sh	BC	RV	MV	DC	FS	P	SG	PRIME REFERENCES
Totals		###				###	###			0	18						###				4414	###	####	37445	####	32	15	6	22	30	27	5	6	9	3	3	2	8	16		
Av. per cave		578				38	950			0.0	0.6						8.6				138	13	7.3	1170	24		0.5	0.2	0.7	0.9	0.8	0.2	0.2	0.3	0.1	0.1	0.1	0.3	0.6		
Minima		423				0	100										0.10				3	1	1.0	3	3		0	0	0	0	0	0	0	0	0					
Maxima		750				70	1900										21.0				1890	55	20.0	11340	100		2	1	4	2	8	2	3	5	3					

(Dip measured in 16 caves)

Glacial Situations:

	#	Length
C	0	0
D	0	0
E	0	0
G	0	0
H	0	0
K	5	140
L	25	4044
S	2	230
T	0	0
U	0	0
Totals	32	4414

Karst Types:

	#	Length
V	0	0
A	20	3254
L	12	1160
C	0	0
X	0	0
Totals	32	4414

Cave Locations:

	#	Length
C	0	0
F	16	3328
W	9	714
R	0	0
S	2	230
G	5	142
P	0	0
Totals	32	4414

Cave Types:

	#	Length
S	1	30
a	9	360
b	14	1244
c	1	260
d	2	111
e	2	230
f	0	0
g	1	12
h	2	2167
Hy	0	0
I	0	0
J	0	0
L	0	0
R	0	0
T	0	0
Totals	32	4414

Relict Caves: # 3, Length 155

MV Caves: # 3, Length 18

Combination Caves: # 26, Length 4241

UPPER ALLOCHTHON: Kall Nappes - Upper Kall: KU (Fausko/Gassok/Akkjell/Hattfjelldal/Jofjell/Krutfjell Nappes)

Caves are grouped by carbonate outcrop

Vefsn catchment area

	UTM COORDS	ALT.	KOMMUNE	AREA	LST. STRIKE	LST. DIP	OW	EXT. COLOUR	OTHER INT. ROCK	R	T	GB	CL	KT	SR	OR	CA	REF. NO.	CAVE NAME	CT	LENG.	VR	XS	VOL.	Min. HG %	C	SE	RE	DE	CS	SP	Ch	Sh	BC	RV	MV	DC	FS	P	SG	PRIME REFERENCES
Raasvatnet				**1926 I**																																					
																																									No known references
																																								1 prospect *in Krutfjell Nappe*
Hattfjelldal				***1926 II***																																					
VN	*55x*	*75x*	340	Hattfjelldal	Hattfjelldal				Grey										Presteglrdaskogen																							Doj pc to TLF
VN	*518*	*665*	600	Hattfjelldal	Vefsnmolia														3 Reingrdsbekk caves																							Doj Grottan 28 (1) p10 1993
VN	*51x*	*66x*	600	Hattfjelldal	Vefsnmolia														Skogstubekk small caves																							Heap 74 p16, 79 p4. Doj 93a
Susendalen				***1925 I***																																					
VN	*51x*	*65x*	600	Hattfjelldal	Susendal				Grey										Brennhut																							U. Holbye List 1974. On 1926 II
VN	*524*	*630*	600	Hattfjelldal	Susendal			*W*	1800	Grey		0	1	L	W	A	U	P	0.8	Djupdalshullet	*a*	240	55	15.0	3600	22.9	1	1	0	0	1	3	2	0	0	0	0	1	0	2 / 3	Heap 1985. Survey
VN	*52x*	*62x*	600	Hattfjelldal	Susendal			*W*	1800	Grey		0	1	L	W	A	U	P	0.2	Nord Fossbekkgrotta	*g*	*12*	10	*4.0*	*48*	83	1	0	0	1	1	0	0	*0*	*0*	*0*	0	0		0		Heap 1979 p4
VN	*525*	*626*	600	Hattfjelldal	Susendal			*W*	1600	Grey		0	1	L	W	A	U	P	0.8	Fossbekkgrotta	*b*	120	18	*4.0*	*480*	15	1	0	0	1	1	0	0	*0*	*0*	*0*	0	1		0		Heap 1979 p4
VN	*526*	*623*	600	Hattfjelldal	Susendal			*W*	1600	Grey		0	1	L	W	A	U	P	0.1	Sør Fossbekkgrotta 1	*b*	30	*5*	*4.0*	*120*	17	1	*1*	0	0	*1*	0	*0*	*0*	*0*	*0*	0	*0*		0		Heap 1979 p4
VN	*526*	*623*	600	Hattfjelldal	Susendal			*W*	1600	Grey		0	1	L	W	A	U	P	0.1	Sør Fossbekkgrotta 2	*b*	22	*5*	*4.0*	*88*	23	1	*1*	0	0	*1*	0	*0*	*0*	*0*	*0*	*0*	*0*		0		Heap 1979 p4
VN	*532*	*623*	430	Hattfjelldal	Susendal			*W*	1600	Grey		0	1	L	W	A	U	P	0.2	Sør Fossbekkgrotta 3	*b*	60	*10*	*4.0*	*240*	17	1	*1*	0	0	*1*	0	*0*	*0*	*0*	*0*	*0*	*0*		0		Heap 1979 p4
VN	*5205*	*5945*	555	Hattfjelldal	Susendal	34	40	E	900	Black	schist?	0	1	L	W	A	D	P	8.0	Kvalpskardelvgrotta 1	b	40	5	10.0	400	13	1	1	1	0	1	0	0	0	0	0	0	0	1	1	Heap 1974 p16. TF98
VN	*5195*	*5945*	570	Hattfjelldal	Susendal	90	20	S	900			0	1	L	W	L	N	P	8.0	Kvalpskardelvgrotta 2	b	40	4	4.0	160	10	1	0	0	4	0	0	0	0	0	0	0	0	1	1	Heap 1974 p16. TF98
VN	*5182*	*5951*	560	Hattfjelldal	Susendal														Meander Cave		c. 67m of stream passage, tributary to main valley																				SN04
VN	*5180*	*5962*	595	Hattfjelldal	Susendal				900										Kvalpskardelvgrotta 3		42m resurgence cave to sump																				TF98. SN04
VN	*5146*	*5972*	622	Hattfjelldal	Susendal		50	*W*	900	Black	calc. sc	0	1	L	W	*L*	*N*	P	8.0	Kvalpskardelvgrotta 4*	b	150	10	20.0	3000	7	1	0	1	1	1	0	0	0	0	0	0	0		1	3	TF98. Surveyed as 127m: SN04

* Coords. of West Entrance

UPPER ALLOCHTHON: Kall Nappes - Upper Kall: KU (Feuska/Gasak/Aktjeli/Hattfjelldal/Joffeli/Krutfjell Nappes)

Caves are grouped by carbonate outcrop

Northern and Vefsn catchment areas

UTM COORDS		ALT.	KOMMUNE	AREA	External Cave Attributes: LST. STRIKE	LST. DIP	OW	EXT. COLOUR	OTHER INT. ROCK	Internal Cave Attributes: R	T	GS	CL	KT	SR	OR	CA	REF. NO.	CAVE NAME	CT	LENG.	VR	XS	VOL.	Min. HG %	C	SE	RE	DE	CS	SP	Ch	Sh	BC	RV	MV	DC	FS	P	SG	PRIME REFERENCES
Susendalen				***1925 I cont.***																																						
VN	*505 568*	500	Hattfjelldal	Susendal		W	1500			0	1	L	F	*A*	N	N	0.8		Øverst Grubblandsgrotta	*b*	90	36	*2.0*	*180*	40	1	0	0	1	0	0	1	0	0	0	0	0		0		Heap 1979 p4
VN	*505 565*	500	Hattfjelldal	Susendal		W	1500			0	1	L	F	*A*	N	N	0.8		South Sink	*a*	10	6	*2.0*	*20*	60	1	1	0	0	1	0	0	0	0	0	0	0		0		Heap 1979 p4
VN	*5085 5710*	480	Hattfjelldal	Susendal		W	1500			0	1	L	F	*A*	N	N	19.0		Øvre Grubblandsgrotta	b	80	30	*6.0*	*480*	38	1	1	0	0	1	0	0	0	0	1	0	0		1		KCC Jnl (3) 68 & (4) 69. UH list
VN	*5080 5705*	492	Hattfjelldal	Susendal	180	50 W	1500	Dark gr	dolomit	0	1	L	F	*A*	N	N	19.0		Stor Grubblandsgrotta	h	1890	50	6.0	11340	3	1	0	0	2	2	8	2	3	5	3	0	0	1	1	2 / 4	KCC Jnl (3) 68 & (4) 69. UH list. TF98
VN	*506 566*	*475*	Hattfjelldal	Susendal															Sjakt (Tillop 1)																						KCC Jnl (3) 68 & (4) 69. UH list
VN	*506 566*	*475*	Hattfjelldal	Susendal															Grotta (Tillop 2)																						KCC Jnl (3) 68 & (4) 69. UH list
VN	*5100 5695*	470	Hattfjelldal	Susendal		W	1500			0	1	L	F	*L*	N	N	21.0		Hjortetakkgrotta	h	277	15	10.0	2770	5	1	0	0	1	1	3	0	2	0	0	0	0	1	0	4	Heap 1985. Survey. Sumps are all static.
VN	*5115 5690*	460	Hattfjelldal	Susendal		W	1500			0	1	L	F	*L*	N	N	21.0		Elvgrotta	b	50	5	15.0	750	10	1	0	*1*	0	1	1	0	0	0	0	0	0	0	1		Heap 1985. Area sketch
VN	*5115 5685*	448	Hattfjelldal	Susendal	40	20 W	1500			0	1	L	F	L	N	N	21.0		Mellom Grubblandsgrotta	b	150	20	15.0	2250	13	1	0	0	2	1	0	0	0	0	0	0	0	1	1		KCC Jnl (3) 68 & (4) 69. UH list. TF97
VN	*5115 5680*	445	Hattfjelldal	Susendal															Hamargrotta																						Heap 1985. Area sketch
VN	*5120 5670*	*425*	Hattfjelldal	Susendal	80	20 N	1500			0	1	L	F	L	N	N	21.0		Lille Grubblandsgrotta	a	15	3	15.0	225	20	1	1	1	0	1	1	0	0	0	0	0	0	1	1		Heap 1985. Area sketch. TF97
VN	*5135 5660*	423	Hattfjelldal	Susendal		0	1500	Grey		0	1	L	F	L	N	N	21.0		Nedre Grubblandsgrotta	b	300	14	15.0	4500	5	1	1	0	0	1	1	0	0	0	0	0	0		1		KCC Jnl (3) 68 & (4) 69. UH list.TF97
VN	*5160 5645*	402			125	(70 S)													Nedre Grubblands Risings																						Sumped. TF97

HNC Thrust front is c. 1 km from all cave sites.

Hjartfjell				***2026 IV***																																						
VP	*800 037*	800	Hattfjelldal	Oltjell															Oltjelltjornagrotta																						Faulkner 1987. NG (20) 14-16. 1988
VP	*7895 0260*	680	Hattfjelldal	Oltjell	100	30 N	500			0	0	L	G	L	N	P	5.0	Sk5	Ø. Oltjelltjernbekkgr.	d	25	5	2.0	50	20	1	2	0	0	1	0	0	0	0	0	0	0	0		1	1	Faulkner 1987. NG (20) 14-16. 1988
VP	*7895 0260*	675	Hattfjelldal	Oltjell	100	30 N	500			0	0	L	G	L	N	P	5.0	Sk6	A. Oltjelltjernbekkgr.	a	25	5	2.0	50	20	1	0	0	1	0	0	0	0	0	0	0	0	0		1	1	Faulkner 1987. NG (20) 14-16. 1988
VP	*7895 0270*	670	Hattfjelldal	Oltjell	100	30 N	500			0	0	L	G	L	N	P	5.0	Sk7	Martinusgrotta	d	86	10	2.0	172	12	1	0	1	1	1	1	0	0	0	0	0	0		1	1	Faulkner 1987. NG (20) 14-16. 1988
VN	*6560 9910*	504	Hattfjelldal	Favnvatn															Jupmelvandgrotta		10m-long sink cave. Could be extended																						Heap 5-6 1974. SN04
VN	*6547 9904*	500	Hattfjelldal	Favnvatn															Jupmelvand Res. Cave		c. 23m of passages to a deep sump																						SN04
VN	*660 991*	580	Hattfjelldal	Favnvatn															Kvighola		Not found on 15 July 2004																						Faulkner 1987. NG (20) 14-16. 1988
VP	*6985 0075*	680	Hattfjelldal	Favnvatn	90	45 N	100			0	0	K	G	A	U	P	1.0		cave	a	3	1	1.0	3	33	1	0	0	1	1	0	0	0	0	0	1	0		1		Akfjell. Faulkner 1987
VP	*7015 0075*	690	Hattfjelldal	Favnvatn	90	45 N	100			0	0	K	G	A	U	P	1.0		cave	a	3	1	1.0	3	33	1	0	0	1	1	0	0	0	0	0	1	0		1		Akfjell. Faulkner 1987
VP	*758 0020*	690	Hattfjelldal	Favnvatn															cave																						von Schreiber. pc to TLF 1987
VP	*767 0021*	670	Hattfjelldal	Favnvatn															cave																						von Schreiber. pc to TLF 1987
VP	*7950 0255*	666	Hattfjelldal	Skinnfjell	90		200			0	0	L	F	A	N	P	15.5	Sk1	Skindfeldal Sink Ca.	e	30	10	4.0	120	33	1	0	0	1	1	0	0	1	1	0	0	0	1	1	2	Faulkner 1987
VP	*8010 0260*	660	Hattfjelldal	Skinnfjell	90	70 S	200			0	0	L	F	A	N	P	16.0	Sk2	Skinnfellvassgrotta	c	260	15	10.0	2600	6	1	0	0	1	1	3	0	0	0	0	0	0	1	1	2	Faulkner 1987
VP	*8025 0255*	655	Hattfjelldal	Skinnfjell	100	20 S	200			0	0	L	F	L	N	P	16.0	Sk3	Skremtholet	b	12	3	10.0	120	25	1	0	0	2	1	2	0	0	0	0	1	0	0	1	2	Faulkner 1987
VP	*8035 0255*	650	Hattfjelldal	Skinnfjell	100	20 S	200			0	0	L	F	L	N	P	16.0	Sk4	Fiskartjerngrotta	a	30	4	10.0	300	13	1	0	1	0	1	1	0	0	1	0	0	0	1	1	2	Faulkner 1987
VP	*7215 0070*	774	Hattfjelldal	Favnvatn															cave																						Faulkner 1987
VP	*740 0010*	710	Hattfjelldal	Favnvatn															cave																						von Schreiber. pc to TLF 1987
VN	*741 997*	680	Hattfjelldal	Favnvatn															cave																						von Schreiber. pc to TLF 1987
VN	*7940 9890*	750	Hattfjelldal	Favnvatn	90	50 N	200			0	0	S	S	A	U	P	3.3	B	Trollhuliet/Brakfjeldhu.	e	200	*20*	*10.0*	*2000*	10	1	1	0	0	1	0	0	0	0	0	0	1		0		Heap 74. Sjöberg. Grottan 14 (4) 1979. *
VN	*7935 9885*	740	Hattfjelldal	Favnvatn	90	70 S	200			0	0	S	S	A	U	P	3.3	C	Vest Trollhuliet	S	30	*30*	*4.0*	*120*	100	1	1	0	0	1	0	0	0	0	0	0	0		0		Sjöberg. Grottan 14 (4) 1979. *
VN	*792 988*	740	Hattfjelldal	Favnvatn															cave																						Faulkner. NG (20) 14-16. 1988
VN	*781 985*	650	Hattfjelldal	Favnvatn															cave																						Faulkner. NG (20) 14-16. 1988
VN	*7710 9850*	555	Hattfjelldal	Favnvatn														D	Tverelv resurgence		From joints																				StPierre&StPierre 1971. Sjöberg 1979
VN	*7680 9835*	550	Hattfjelldal	Favnvatn			200			0	0	K	F	*A*	N	P	5.5	E	Tverelvgrotta	*a*	*20*	*4*	*10.0*	*200*	20	1	1	0	0	1	0	0	0	1	0	0	0		0		StPierre&StPierre 1971. Sjöberg 1979
VN	*7550 9855*	520	Hattfjelldal	Favnvatn			100			0	0	K	F	*A*	N	P	7.0	F	Dry Valley Cave	*b*	100	*10*	*10.0*	*1000*	10	1	0	0	1	1	2		0	0	0	0	0		0		StPierre&StPierre 1971. Sjöberg 1979
VN	*7530 9865*	510	Hattfjelldal	Favnvatn														G	Tributary resurgence		Flooded																				StPierre&StPierre 1971. Sjöberg 1979
VN	*74x 99x*	540	Hattfjelldal	Favnvatn			100			0	0	K	F	*A*	N	P	3.5		Blågrotta	*a*	14	3	4.0	56	21	1	1	0	0	1	1	0	0	0	0	0	0	0	0		R. Selvåg pc, 1998. Not found SN04
VN	*773 925*	790	Hattfjelldal	Favnvatn															cave																						von Schreiber. pc to TLF 1987

Kaldvatnet **2027 II**

* In same anticline.

No known references

UPPER ALLOCHTHON: Kall Nappes - Middle Kall: KG - Gjersvik Nappe

Caves are grouped by carbonate outcrop

Majavatn	**1925 III**	**No known references**
Reyrvik	**1924 IV**	**No known references**
Tunnsjøen	**1924 III**	**No known references**
Børgefjellet	**1925 II**	**No known references**

UPPER ALLOCHTHON: Kali Nappes - Middle Kali: KL -Orklump / Leipikvatnet Nappe: TOTALS

UTM COORDS	ALT.	KOMMUNE	AREA	LST. STRIKE	LST. DIP	OW	EXT. COLOUR	OTHER INT. ROCK	R	T	GS	CL	KT	SR	OR	CA	REF. NO.	CAVE NAME	CT	LENG.	VR	XS	VOL.	Min. HG %	C	SE	RE	DE	CS	SP	Ch	Sh	BC	RV	MV	DC	FS	P	BC	PRIME REFERENCES
Totals	####				##	####			0	8						###				491	###	####	4490	###	8	2	1	8	7	8	1	2	3	0	3	0	4	3		
Av. per cave	480				85	388			0.0	1.0						37.3				61	3.5	5.3	561	9		0.3	0.1	1.0	0.9	1.0	0.1	0.3	0.4	0.0	0.4	0.0	0.5	0.4		
Minima	460				80	300										4.50				10	1	1.5	20	3		0	0	0	0	0	0	0	0	0						
Maxima	520				90	400										42.0				188	6	15.8	2970	20		1	1	2	1	3	1	1	3	0						

(Dip measured in 2 caves)

Glacial Situations:

	#	Length
C	0	0
D	0	0
E	0	0
G	0	0
H	0	0
K	8	491
L	0	0
S	0	0
T	0	0
U	0	0
Totals	8	491

Karst Types:

	#	Length
V	1	188
A	7	303
L	0	0
C	0	0
X	0	0
Totals	8	491

Cave Locations:

	#	Length
C	0	0
F	8	491
W	0	0
R	0	0
S	0	0
G	0	0
P	0	0
Totals	8	491

Cave Types:

	#	Length
S	0	0
a	2	50
b	0	0
c	2	178
d	4	263
e	0	0
f	0	0
g	0	0
h	0	0
Hy	0	0
I	0	0
J	0	0
L	0	0
R	0	0
T	0	0
Totals	8	491

Relict Caves:

#	Length
1	70
1	70

MV Caves:

#	Length
3	60
3	60

Combination Caves:

#	Length
4	361

UPPER ALLOCHTHON: Kali Nappes - Middle Kali: KL -Orklump / Leipikvatnet Nappe

Caves are grouped by carbonate outcrop

Eastern catchment area

Røyrvik 1924 IV — No known references

Jomafjellet 1924 I

UTM COORDS	ALT.	KOMMUNE	AREA	LST. STRIKE	LST. DIP	OW	EXT. COLOUR	OTHER INT. ROCK	R	T	GS	CL	KT	SR	OR	CA	REF. NO.	CAVE NAME	CT	LENG.	VR	XS	VOL.	Min. HG %	C	SE	RE	DE	CS	SP	Ch	Sh	BC	RV	MV	DC	FS	P	BC	PRIME REFERENCES
VM 482 963	460	Røyrvik	Vallerdalen			400			0	1	K	F	A	N	P	42.0		Jordgulvgrotta	a	30	1	4.0	120	3	1	0	0	1	1	1	0	0	0	0	1	0		0		Schrader 1982 list. PB pc 090999
VM 482 963	460	Røyrvik	Vallerdalen			400			0	1	K	F	A	N	P	42.0		Sjøgrotta	d	10	2	2.0	20	20	1	0	0	1	1	0	0	1	0	0	1	0		0		P. Blombergsson pc 090999
VM 4845 9625	480	Røyrvik	Vallerdalen			400			0	1	K	F	A	N	P	42.0		Fiskdolinen	d	25	4	2.0	50	16	1	0	0	1	1	1	0	0	0	0	0	0		0		P. Blombergsson pc 090999, 041099
VM 4870 9625	480	Røyrvik	Vallerdalen			400			0	1	K	F	A	N	P	42.0		Torrdalgrotta	a	20	2	2.0	40	10	1	0	0	2	1	2	0	0	0	0	1	0		0		P. Blombergsson pc 090999, 041099
VM 4880 9630	475	Røyrvik	Vallerdalen	56	90	400	Blue&Wh		0	1	K	F	V	N	P	42.0		Landbrua*	d	188	6	15.8	2970	3	1	1	1	0	1	3	0	0	0	0	0	0	1	1	3	* Speleo 16 (1) p18 1981. TF98
VM 4880 9630	475	Røyrvik	Vallerdalen															Kortgrotta																						U. Holbye List 1974
VM 4915 9645	485	Røyrvik	Vallerdalen			400			0	1	K	F	A	N	P	42.0		Marmorsalen	c	70	5	10.0	700	7	1	0	0	1	0	0	1	0	3	0	0	0	1	0	1	P. Blombergsson pc 030199, 041099
VM 4928 9652	480	Røyrvik	Vallerdalen	65	80 S	400	Wh. Grey		0	1	K	F	A	N	P	42.0		Marmorgrotta / Marmorkjerka	c	108	3	4.9	529	3	1	0	0	1	1	1	0	0	0	0	0	0	1	1	3	* TF98. TF00. SN04
VM 46x 96x	500	Røyrvik	Vallerdalen															Nygårdgrottan																						U. Holbye List 1974.
VM 5202 9762	515	Røyrvik	Vallerdalen															Stormoengrotta	9m long, with sound of stream, and nearby Cleft Entrance (4m).																					TF98. SN04
VM 5267 9791	520	Røyrvik	Vallerdalen			300			0	1	K	F	A	N	P	4.5		Vallerdalgrotta	d	40	5	1.5	60	13	1	1	0	1	1	0	0	1	0	0	0	0	1	1	3	TF98. Extended to 344m: SN04

GS below border pass at 540m

* Also called: Landbro/Jordbrua/Marmorbrua

Caves are grouped by carbonate outcrop

* Oxaal, 1909. Helland, 1909.

UPPER ALLOCHTHON: Kali Nappes - Middle Kali: KS -Virvass / Stikke Nappe

Krutvatnet 2026 III — No known references

Skardmodalen 2025 IV — No known references

APPENDIX C4

CENTRAL SWEDISH CALEDONIDES CAVE DATABASE

UPPERMOST ALLOCHTHON: Rödingsfjell Nappe Complex - Nappes below the Beiarn Nappe: Zone C (Southern and Border Area): TOTALS

Refer to North Central Norway Cave Database for Key

External Cave Attributes | **Internal Cave Attributes**

UTM / SWEDISH RN COORDS	ALT.	KOMMUNE	AREA	LST. STRIK	LST. DIP	OW	EXT. COLOUR	OTHER INT. ROCK	R	T	GS	CL	KT	SR	OR	CA	REF. NO.	CAVE NAME	CT	LENG.	VR	XS	VOL.	Min. HG %	C	SE	RE	DE	CS	SP	Ch	Sh	BC	RV	MV	DC	FS	P	SG	PRIME REFERENCES
Totals	####			##		####			0	0							###		4872	###	####	16353	###	40	13	3	31	28	11	9	11	3	3	1	3	12	11		
Av. per cave	698			43		763			0.0	0.0							2.4		122	9	2.1	409	22		0.3	0.1	0.8	0.7	0.3	0.2	0.3	0.1	0.1	0.0	0.1	0.3	0.3		
Minima	560			35		50											0.20		4	1	1.0	4	1		0	0	0	0	0	0	0	0	0						
Maxima	900			45		2000											9.0		2600	45	6.0	10400	60		2	1	3	4	6	2	6	2	2						

(Dip measured in 10 caves)

Karst Types:

	#	Length
V	0	0
A	34	2198
L	0	0
C	1	2600
X	5	74
Totals	40	4872

Cave Locations:

	#	Length
C	0	0
F	0	0
W	11	880
R	0	0
S	0	0
G	7	141
P	22	3851
Totals	40	4872

Glacial Situations:

	#	Length
C	0	0
D	0	0
E	0	0
G	0	0
H	0	0
K	0	0
L	14	3437
S	1	140
T	25	1295
U	0	0
Totals	40	4872

Cave Types:

	#	Length
S	0	0
a	25	487
b	6	210
c	1	60
d	1	140
e	0	0
f	2	95
g	0	0
h	5	3880
Hy	0	0
I	0	0
J	0	0
L	0	0
R	0	0
T	0	0
Totals	40	4872

Relict Caves:

#	Length
17	271

MV Caves:

#	Length
1	11

Combination Caves:

#	Length
22	4590

UPPERMOST ALLOCHTHON: Rödingefjäll Nappe Complex - Nappes below the Belarn Nappe: Zone C (Southern and Border Area)

Caves are grouped by carbonate outcrop

Eastern catchment area

UTM / SWEDISH RN COORDS	ALT.	KOMMUNE	AREA	LST. STRIK	LST. DIP	OW	EXT. COLOUR	OTHER INT. ROCK	R	T	GS	CL	KT	SR	OR	CA	REF. NO.	CAVE NAME	CT	LENGL	VR	XS	VOL.	Min. HG %	C	SE	RE	DE	CS	SP	Ch	Sh	BC	RV	MV	DC	FS	P	SG	PRIME REFERENCES
Storakersvatnet / *Hjartfjell*			**2027 III / *2026 IV***																					**AC: Västerbottensian**																
VP 830 209	840	Storuman	Mieseken			300			0	0	L	P	A	N	P	4.0	2421	**Slukgrottan 1**	*b*	30	12	*2.0*	*60*	40	1	1	0	0	1	1	0	0	0	0	0	0	0		0		Grottan 12 (3) p5 1977
VP 830 207	830	Storuman	Mieseken			300			0	0	L	P	A	N	P	4.0	2422	**Slukgrottan 2**	*b*	60	10	6.0	360	17	1	1	0	0	2	0	1	0	0	0	0	0	0		0		Grottan 12 (3) p5 1977
VP *828 195*	*860*	Storuman	Mieseken			200			0	0	T	P	A	X	P	0.8	2425	**N. Arttjärro-tunnein**	*a*	15	2	3.0	60	13	1	0	0	1	0	0	0	0	0	0	0	0	0		0		R. Magnusson database+pc
VP *827 190*	900	Storuman	Mieseken			200			0	0	T	P	A	N	P	0.2	2424	**Arttj.-tunn.(Renskelettgr.)**	*f*	45	10	2.0	90	22	1	0	0	1	0	0	2	2	0	0	0	0	1	0	1	Grottan 11 (2) p34 1976
VP 839 238	900	Storuman	Mieseken			*50*			0	0	T	P	X	N	P	0.2	2420	**Schaktgrottan**	*a*	14	6	*4.0*	*56*	43	1	0	0	1	1	0	1	1	0	0	0	0		0		Grottan 11 (2) p34 1976
VP 8490 2770	660	Storuman	Mieseken			2000			0	0	L	P	X	X	P	1.2	2482	**Björkskogsgrottan 1**	*a*	10	*2*	*2.0*	*20*	20	1	0	0	*1*	0	0	0	0	0	0	0	0		0		R. Magnusson database+pc
VP 8490 2770	660	Storuman	Mieseken			2000			0	0	L	P	X	X	P	1.2	2482	**Björkskogsgrottan 2**	*a*	20	10	*4.0*	*80*	50	1	0	0	*1*	0	0	0	0	0	0	0	0		0		R. Magnusson database+pc
VP 84984 27260		Storuman	Mieseken														37	**Två Stenar**		**= Björkskogsgrottan 1?**																			Grottan 35 (3) p13
VP 84994 27035		Storuman	Mieseken														36	**Trycktunnein**																					Grottan 35 (3) p13
VP 84918 26849	720	Storuman	Mieseken	30	45 W	2000			0	0	L	P	A	U	P	2.5	2605	**Pärigrottan**	h	290	31	2.0	580	11	1	0	0	1	1	2	0	0	0	0	0	0	1	1	1/4	Grottan 23 (3) p17 1988. TF98
VP 84784 26838		Storuman	Mieseken														22	**Taggsprickan**			(4)																		Grottan 35 (3) p13
VP 860 270	*650*	Storuman	Mieseken			2000			0	0	L	P	X	X	P	1.5		**Unmapped cave 1**	*b*	20	10	*1.0*	*20*	50	1	*1*	0	0	1	*0*	*0*	0	0	0	0	0	*0*		0		Grottan 33 (1) p23 1998
VP 857 269	*660*	Storuman	Mieseken			2000			0	0	L	P	X	X	P	1.5		**Unmapped cave 2**	*a*	10	*2*	*1.0*	*10*	20	1	0	0	*1*	*0*	0	*0*	0	0	0	0	0	*0*		0		Grottan 33 (1) p23 1998
VP 85332 26827	690	Storuman	Mieseken														38	**Labyrintgrottan rising**																					Grottan 35 (3) p13
VP 85309 26746		Storuman	Mieseken														25	**Bäckgrottan**		2 shafts																			Grottan 35 (3) p13
VP 85114 26728		Storuman	Mieseken														3	**Labyrintgrottan N. entrance**																					Grottan 35 (3) p13
VP 85001 26712		Storuman	Mieseken														21	**Snölegegrottan**		(4+)																			Grottan 35 (3) p13
VP 85080 26622		Storuman	Mieseken														2	**Labyrintgrottan W. entrance**																					Grottan 35 (3) p13
VP 85165 26584	715	Storuman	Mieseken	40	45 E/W	2000	Grey		0	0	L	P	C	N	P	2.5	1752	**Labyrintgrottan / Facettgr.**	h	2600	20	4.0	10400	0.8	1	0	0	3	1	6	*2*	6	0	*2*	0	1	1	1	3	+ Grottan 11 (2) p31 1976. TF98
VP 85068 26515		Storuman	Mieseken														19	**Djup Dolin**		5m cave at bottom																			Grottan 35 (3) p13
VP 85692 26546		Storuman	Mieseken															**Dolin**																					Grottan 35 (3) p13
VP 85611 26444		Storuman	Mieseken															**Dolin med hål i botten**																					Grottan 35 (3) p13
VP 86137 26360		Storuman	Mieseken															**Flera stora djupa dolliner**																					Grottan 35 (3) p13
VP 85240 26463		Storuman	Mieseken														20	**Kämpahålet**		tight 3m shaft																			Grottan 35 (3) p13
VP 84419 26446		Storuman	Mieseken														33	**Falska Inloppsgrottan**		(18)																			Grottan 35 (3) p13
VP 85233 26407		Storuman	Mieseken														23	**Schakt**			(5)																		Grottan 35 (3) p13
VP 85051 26396		Storuman	Mieseken														14	**Spricka**		small passage																			Grottan 35 (3) p13
VP 85271 26367	725	Storuman	Mieseken		45 W	2000	Brown	musc	0	0	L	P	A	N	P	2.0	845	**Brunagrottan**	a	15	3	1.0	15	20	1	0	0	1	0	0	0	0	0	0	0	0	1	1		Grottan 8 (2)p11 1973.TF98. HMC?
VP 85262 26331		Storuman	Mieseken														9	**Bruna överhänget**																					Grottan 35 (3) p13
VP 85249 26316	725	Storuman	Mieseken		45 W	2000			0	0	L	P	A	N	P	2.0	11	**Kaninhålet**	a	5	3	1.0	5	60	1	0	0	1	1	0	0	0	0	0	0	0	1	1		Grottan 35 (3) p13. TF98
VP 85008 26258		Storuman	Mieseken														15	**Spricka**			(4)																		Grottan 35 (3) p13
VP 85082 26191		Storuman	Mieseken														7	**Stupgrannen**			(6)																		Grottan 35 (3) p13
VP 84972 26187		Storuman	Mieseken														16	**Avlångt schakt**			(3)																		Grottan 35 (3) p13
VP 84985 26185		Storuman	Mieseken														13	**Avlångt schakt**			(5)																		Grottan 35 (3) p13
VP 85022 26158		Storuman	Mieseken														12	**Schakt**																					Grottan 35 (3) p13
VP 85053 26158	740	Storuman	Mieseken			2000			0	0	L	P	*A*	N	P	1.4	1374	**Västra (Stora) Tvillingstupet**	h	275	38	2.0	550	14	1	0	0	1	2	0	0	1	2	0	0	0	1	1	3	Grottan 13 (1) p37 1978. TF98
VP 85070 26157	740	Storuman	Mieseken			2000			0	0	L	P	*A*	N	P	1.4	1374	**Östra (Lilla) Tvillingstupet**	a	17	10	*1.0*	*17*	59	1	1	0	0	1	0	0	0	0	0	1	1	1		Grottan 8 (2) p11 1973. TF98
VP 84950 26087		Storuman	Mieseken														17	**Flyttblocksdolinen**			(4)																		Grottan 35 (3) p13
VP 84970 26086		Storuman	Mieseken														24	**Dralryggsschaktet**			(2)																		Grottan 35 (3) p13
VP 84936 26010		Storuman	Mieseken														18	**Vackra minikarrensprickan**																					Grottan 35 (3) p13
VP 84608 25912		Storuman	Mieseken														26	**Tre stuk**																					Grottan 35 (3) p13
VP 84449 25869		Storuman	Mieseken														35	**Gula Grottan**																					Grottan 35 (3) p13
VP 84891 25841		Storuman	Mieseken														8	**Falska Tvillingstupen**																					Grottan 35 (3) p13
VP 84646 25587		Storuman	Mieseken														315	**Scoutgrottan**		(72)	(19)																			Grottan 23 (4) p12 1988. RM dB
VP 84645 25586		Storuman	Mieseken														34	**Blicksprickan**		(8+)																					Grottan 35 (3) p13
VP 84663 25418	810	Storuman	Mieseken			1600			0	0	L	P	*A*	X	P	0.6	28	**De Leende Munnarnas Schakt**	f	50	25	1.5	75	50	1	0	0	1	1	0	0	1	0	0	0	0		0	1	Grottan 30 (2) 22-23 95.
VP 84699 25376		Storuman	Mieseken														29	**Ranbenagropen**		(6+)																					Grottan 35 (3) p13
VP 84629 25355		Storuman	Mieseken														32	**Horisontella grottan**		(11)	(3)																				Grottan 35 (3) p13
VP 84698 25275		Storuman	Mieseken														30	**Lilla Salen**																					Grottan 35 (3) p13
VP 84703 25224	790	Storuman	Mieseken														31	**Labyrintgrottan sink**																					Grottan 35 (3) p13
VP 8720 2540	*700*	Storuman	Mieseken			200			0	0	L	P	*A*	X	P	1.5	2427	**Rectangelgrottan**	*b*	35	*5*	*1.0*	35	14	1	*1*	0	0	1	0	0	0	0	0	0	0	0		0		Grottan 25 (2) p18 1990+RM pc

musc = muscovite schist

UPPERMOST ALLOCHTHON: Rödingsfjäll Nappe Complex - Nappes below the Belarn Nappe: Zone C (Southern and Border Area)

Caves are grouped by carbonate outcrop

Eastern catchment area

UTM / SWEDISH RN COORDS			ALT.	KOMMUNE	AREA	LST. STRIK	LST. DIP	OW	EXT. COLOUR	OTHER INT. ROCK	R	T	GS	CL	KT	SR	OR	CA	REF. NO.	CAVE NAME	CT	LENG.	VR	XS	VOL.	Min. HG %	C	SE	RE	DE	CS	SP	Ch	Sh	BC	RV	MV	DC	FS	P	SG	PRIME REFERENCES
External Cave Attributes																				**Internal Cave Attributes**																							
Kaldvatnet			**2027 II**																																							
VP	8890	3395	565	Storuman	Kåtaviken		*N*	700	Grey/Wh.		0	0	T	G	A	U	P	0.3	1424?	**Noaksesongrotta**	*a*	11	*2*	*1.0*	*11*	18	1	0	0	1	1	*0*	*0*	0	0	0	1	*0*		0		Grottan 2 (2) p17 1967. *
VP			*560*	Storuman	Kåtaviken		*N*	700	Grey/Wh.		0	0	T	G	A	U	P	*1.0*		**Bredvikengrotta 1**	*a*	8	*1*	*2.0*	*16*	13	1	0	0	*1*	*0*	*0*	*0*	0	0	0	0	*0*		0		Grottan 2 (2) p17 1967. *
VP			*560*	Storuman	Kåtaviken		*N*	700	Grey/Wh.		0	0	T	G	A	U	P	*1.0*		**Bredvikengrotta 2**	*a*	*15*	*2*	*2.0*	*30*	13	1	0	0	*1*	*0*	*0*	*0*	0	0	0	0	*0*		0		Grottan 2 (2) p17 1967. *
VP			*560*	Storuman	Kåtaviken		*N*	700	Grey/Wh.		0	0	T	G	A	U	P	*1.0*		**Bredvikengrotta 3**	*a*	*15*	*2*	*2.0*	*30*	13	1	0	0	*1*	*0*	*0*	*0*	0	0	0	0	*0*		0		Grottan 2 (2) p17 1967. *
VP			*560*	Storuman	Kåtaviken		*N*	700	Grey/Wh.		0	0	T	G	A	U	P	*1.0*		**Bredvikengrotta 4**	*a*	22	*3*	*2.0*	*44*	14	1	0	0	*1*	*0*	*0*	*0*	0	0	0	0	*0*		0		Grottan 2 (2) p17 1967. *
VP	9045	3390	550	Storuman	Kåtaviken	50	(5(N)		Grey/Wh.										1306	**Larsson Kalla**																						Svenska Grottor nr. C3. *
VP	9050	3395	560	Storuman	Kåtaviken	80	35 N	700	Grey/Wh.		0	0	T	G	A	U	P	1.0	1306	**Larssons Grotta**	a	30	*2*	*1.0*	*30*	7	1	1	0	0	1	0	0	0	0	0	0	0		0	1	Svenska Grottor nr. C3. *
VP	9055	3395	560	Storuman	Kåtaviken	60	38 N	700	Grey/Wh.		0	0	T	G	A	U	P	1.0	2430	**Liftgrottan**	b	40	10	*1.0*	*40*	25	1	1	0	0	1	0	0	0	0	0	0	0		0	1	Svenska Grottor nr. C3. *
VP	9075	3395	580	Storuman	Kåtaviken			200	Grey/Wh.		0	0	T	W	A	U	P	1.0	2431	**Dolingrotta**	*a*	5	*1*	*1.0*	*5*	20	1	0	0	*1*	*0*	*0*	*0*	0	0	0	0	*0*		0		R. Magnusson database. *
VP	9160	3405	620	Storuman	Kåtaviken	180	45 W	200	Grey/Wh.		0	0	T	W	A	U	P	1.5	2433	**Forshallarna**	a	64	10	4.0	256	16	1	1	0	0	1	0	0	0	0	0	0	1	1	2	Svenska Grottor nr. 4. *
VP	9145	3400	600	Storuman	Kåtaviken			200	Grey/Wh.		0	0	T	W	A	U	P	1.5	2432	**V.Jordbäckens utloppsgr.**	a	5	*1*	4.0	20	20	1	0	1	0	1	1	0	0	0	0	0	0		1		Svenska Grottor nr. C3. *
VP	9160	3405	631	Storuman	Kåtaviken	90	45 N	200	Grey/Wh.		0	0	T	W	A	U	P	1.5	2434	**Vita Tunnein**	b	25	3	1.0	25	12	1	0	0	1	0	0	0	0	0	0	0	1	0	1	2	Svenska Grottor nr. 4. *
VP	9185	3415	650	Storuman	Kåtaviken	90	45 N	200	Grey/Br.	1,2	0	0	T	W	A	U	P	5.0	1380	**Ös. Jordbäcksgr./Krokgr.**	h	460	45	5.0	2300	10	1	0	0	3	4	1	0	0	1	0	0	0	1	1	1/3	Grottan 13 (4) 14-15.S.G. nr.C3. *
VP	9210	3420	675	Storuman	Kåtaviken			200	Grey/Wh.		0	0	T	W	A	U	P	5.0	2435	**Stupgrottan**	a	30	12	2.0	60	40	1	0	0	1	0	0	1	0	0	0	1	0	1	1	Tärna Fjellguiden 43-48 1997. *$
VP	9210	3420	675	Storuman	Kåtaviken			200	Grey/Wh.		0	0	T	W	A	U	P	5.0	2436	**Lilihålen**	*a*	6	*1*	*2.0*	*12*	17	1	0	0	2	*0*	*0*	*0*	0	0	0	0	*0*		0		R. Magnusson database. *
VP	9220	3430	681	Storuman	Kåtaviken	90	45 N	200	Grey/Wh.		0	0	T	W	A	U	P	5.0	2437	**Korkskruvsgrottan**	h	255	30	1.0	255	12	1	1	0	0	1	0	2	0	0	0	0	0	1	1	2	Svenska Grottor nr. C3. *
VP	9230	3430	680	Storuman	Kåtaviken			200	Grey/Wh.		0	0	T	W	A	U	P	5.0	2438	**Dolinhålet 1**	*a*	4	*1*	*1.0*	*4*	25	1	*0*	*0*	*1*	*0*	*0*	*0*	0	0	0	0	*0*		0		R. Magnusson database. *
VP	9230	3430	680	Storuman	Kåtaviken			200	Grey/Wh.		0	0	T	W	A	U	P	5.0	2439	**Lilla Korkskruvsgrottan**	*a*	12	*2*	*2.0*	*24*	17	1	*0*	*0*	*1*	*0*	*0*	*0*	0	0	0	0	*0*		0		R. Magnusson database. *
VP	9230	3430	680	Storuman	Kåtaviken			200	Grey/Wh.		0	0	T	W	A	U	P	5.0	2440	**Dolinhålet 2**	*a*	14	*2*	*2.0*	*28*	14	1	*0*	*0*	*1*	*0*	*0*	*0*	0	0	0	0	*0*		0		R. Magnusson database. *
VP	9505	3450	810	Storuman	Mjölkbäck		*N*	100			0	0	T	P	*A*	N	P	1.0	2631	**Nedre Promenadtunnlarna**	*a*	40	*5*	*2.0*	*80*	13	1	2	0	0	1	*0*	*0*	*0*	*0*	*0*	*0*	0	*0*		0	?	Tärna Fjellguiden 43-48 1997
VP	9505	3460	820	Storuman	Mjölkbäck		*N*	100			0	0	T	P	*A*	N	P	1.0	2630	**Öv / St Promenadtunnein**	*a*	50	*5*	*3.0*	*150*	10	1	0	0	*1*	1	*0*	*0*	*0*	*0*	*0*	*0*	0	*0*		0	?	Tärna Fjellguiden 43-48 1997
VP	9525	3460	805	Storuman	Mjölkbäck		*N*	100			0	0	T	P	*A*	N	P	9.0	2629	**Mjölkbäcksisbyrinten**	*c*	60	*10*	2.0	*120*	17	1	*1*	*1*	0	1	*0*	*0*	*0*	*0*	*0*	*0*	0	*0*		0	?	Grottan 3 (2) 14-15 1968
VP	9540	3460	800	Storuman	Mjölkbäck														2632	**Lilla Grottan**																						R. Magnusson database
VP	9545	3450	760	Storuman	Mjölkbäck		*N*	100			0	0	T	P	*A*	N	P	9.0	2628	**Mjölkbäcksgrottan**	*a*	50	5	2.0	*100*	10	1	0	1	0	1	*0*	*0*	*0*	*0*	*0*	*0*	0	*0*	1	0	?	Tärna Fjellguiden 43-48 1997
VP	9685	3625	810	Storuman	Mjölkbäck		*W*	100			0	0	S	P	A	U	P	1.0	792	**Fiskljusgrottan**	*d*	140	10	2.0	*280*	7	1	1	0	0	1	0	*0*	*0*	*0*	*0*	*0*	0	*0*		0	?	Grottan 4 (2) p10 1969
VP	9410	3175	610	Storuman	Mjölkbäck			50											13	**Kalkstenshallar**																						Tärna Fjellguiden 43-48 1997

1: Biotite schist 2: Muscovite schist

* Lst. identification by Nisell (1986)

$ Relict vadose

Umfors and Tärnaby **26EF**

No known refs in RNC

UPPER ALLOCHTHON: Koli Nappes - Upper Koli (Fauske / Gasak / Joljell Nappes): KU: TOTALS

Refer to North Central Norway Cave Database for Key

External Cave Attributes

	UTM / SWEDISH RN COORDS	ALT.	KOMMUNE	AREA	LST. STRIKE	LST. DIP	OW	EXT. COLOUR	OTHER INT. ROCK	R	T	GS	CL	KT	SH	OR	CA	REF. NO.	CAVE NAME
Totals		####				###	####			27	39						###		
Av. per cave		766				37	2248			0.3	0.8						6.1		
Minima		595				10	40										0.10		
Maxima		926				60	4000										30.0		

(Dip measured in 28 caves)

Internal Cave Attributes

	CT	LENG.	VR	XS	VOL.	Min. HG %	C	SE	RE	DE	CS	SP	Ch	Sh	BC	RV	MV	DC	FS	P	SG	PRIME REFERENCES
Totals		5237	###	#####	28777	###	93	48	31	73	79	28	15	18	12	9	37	5	9	14		
Av. per cave		56	7	2.2	309	27		0.5	0.3	0.8	0.8	0.3	0.2	0.2	0.1	0.1	0.4	0.1	0.1	0.2		
Minima		3	1	0.5	2	3		0	0	0	0	0	0	0	0	0						
Maxima		1850	110	20.0	18500	100		3	2	10	3	3	4	9	3	6						

Glacial Situations:

	#	Length
C	0	0
D	0	0
E	0	0
G	0	0
H	0	0
K	0	0
L	44	3209
S	11	603
T	38	1425
U	0	0
Totals	93	5237

Karst Types:

	#	Length
V	0	0
A	24	1058
L	69	4179
C	0	0
X	0	0
Totals	93	5237

Cave Locations:

	#	Length
C	0	0
F	0	0
W	5	368
R	0	0
S	0	0
G	7	195
P	81	4674
Totals	93	5237

Cave Types:

	#	Length
S	11	108
a	43	654
b	15	614
c	6	258
d	6	246
e	4	304
f	0	0
g	2	463
h	6	2590
Hy	0	0
I	0	0
J	0	0
L	0	0
R	0	0
T	0	0
Totals	93	5237

	Relict Caves: #	Relict Caves: Length	MV Caves: #	MV Caves: Length	Combination Caves: #	Combination Caves: Length
	19	334	37	755		
Totals	19	334	37	755	37	4148

UPPER ALLOCHTHON: Köli Nappes - Upper Köli (Fauske / Gasak / Jofjell Nappes): KU

Caves are grouped by carbonate outcrop — **Eastern catchment area**

UTM / SWEDISH RN COORDS	ALT.	KOMMUNE	AREA	LST. STRIKE	LST. DIP	OW	EXT. COLOUR	OTHER INT. ROCK	R	T	GS	CL	KT	SR	OR	CA	REF. NO.	CAVE NAME	CT	LENG.	VR	XS	VOL.	Min. HG %	C	SE	RE	DE	CS	SP	Ch	Sh	BC	RV	MV	DC	FS	P	SG	PRIME REFERENCES
Hjartfjället		***2026 IV***	**AC: Västerbottenslan**						Note confusion between *numbering systems* of the two main references.												I have generally kept to that in SG nr. C3																			
VP *8490 0870*	900	Storuman	Rödingsfjället	45	60 W	400	Wh/grey		0	1	S	P	A	U	P	1.0	1375/2	Grytsluket med Övregr.	e	100	7	1.0	100	7	1	1	0	1	1	1	1	0	1	0	0	0		0	1	Grottan 13 (4) 32-33 1978. *
VP *8475 0860*	885	Storuman	Rödingsfjället				Wh/grey										5	utlopp (kalla)																						Grottan 22 (2) 14-18 1987. *
VP *8460 0845*	875	Storuman	Rödingsfjället	45	60 W	400	Wh/grey		0	1	S	P	A	U	P	1.1	479/6	Apparatsluket	a	10	*2*	*4.0*	*40*	20	1	1	0	0	1	0	0	0	0	0	*1*	0		0		Grottan 22 (2) 14-18 1987. *
VP *8455 0840*	870	Storuman	Rödingsfjället	45	60 W	400	Wh/grey		0	1	S	P	A	U	P	1.1	463?/7	Tvarkallen	a	20	*2*	*4.0*	*80*	10	1	0	1	0	1	0	0	0	0	0	*1*	0		0	1	Grottan 22 (2) 14-18 1987. *
VP *8455 0840*	870	Storuman	Rödingsfjället				Wh/grey										8	Tvarsluket																						Svenska Grottor nr. C3. *
VP *8455 0840*	865	Storuman	Rödingsfjället				Wh/grey										9	Dolinkallan																						Svenska Grottor nr. C3. *
VP *8450 0850*	870	Storuman	Rödingsfjället	45	60 W	400	Wh/grey		0	1	S	P	A	U	P	1.1	2604/10	Attangrottan	S	10	5	*4.0*	*40*	50	1	1	0	0	1	0	0	0	0	0	1	0		0		Grottan 22 (2) 14-18 1987. *
VP *8455 0835*	860	Storuman	Rödingsfjället	45	60 W	400	Wh/grey		0	1	S	P	A	U	P	1.1	11	Vattenfallsgrottan	b	80	*10*	*4.0*	*320*	13	1	0	1	0	1	0	0	0	0	0	0	0		0	1	Grottan 22 (2) 14-18 1987. *
VP *8505 0865*	920	Storuman	Rödingsfjället				Wh/grey										12	sluk och utlopp																						Svenska Grottor nr. C3. *
VP *8425 0810*	776	Storuman	Rödingsfjället	45	60 W	300	Wh/grey		0	1	S	P	A	U	P	1.5	1483/14	Niagarasluket	S	15	10	20.0	300	67	1	1	0	0	1	0	0	0	1	0	0	0		1		Grottan 22 (3) 26-29 1987. TF98. *
VP *8420 0800*	760	Storuman	Rödingsfjället				Wh/grey										1978/15	Övergivna sluket																						Svenska Grottor nr. C3. *
VP *8410 0800*	760	Storuman	Rödingsfjället				Wh/grey										16	Kamgrottan																						Svenska Grottor nr. C3. *
VP *8405 0800*	780	Storuman	Rödingsfjället				Wh/grey										17																						Svenska Grottor nr. C3. *
VP *8375 0770*	702	Storuman	Rödingsfjället	45	31 W	200	Grey		0	1	S	W	A	U	P	2.0	1377/18a	Övre Glimåkragrottan	b	80	5	*4.0*	*320*	6	1	1	1	0	1	0	0	0	0	0	0	0		1	1	Grottan 13 (4) p34 1978. TF98.*
VP *8375 0770*	708	Storuman	Rödingsfjället	45	31 W	200	Dark grey		0	1	S	W	A	U	P	2.0	1378/18b	Nedre Glimåkragrottan	e	155	30	5.0	775	19	1	1	0	0	2	1	0	0	0	0	0	0		1	3	Grottan 13 (4) p34 1978. TF98.*
VP *8380 0770*	710	Storuman	Rödingsfjället				Wh/grey										1492	Höstgrottan (=2057)																						Grottan 22(2) p26 1987. *
VP *8375 0770*	710	Storuman	Rödingsfjället	45	60 W	200	Wh/grey		0	1	S	W	A	U	P	2.0	1376/19	Grytrannegrottan	b	30	3	*4.0*	*120*	10	1	1	1	0	1	0	0	0	0	0	0	0		0	1	Grottan 22 (2) 14-18 1987. *
VP *8385 0750*	672	Storuman	Rödingsfjället				Wh/grey										20	utlopp																						Svenska Grottor nr. C3. *
VP *8355 0755*	637	Storuman	Rödingsfjället	68	31 N	200	Blue/grey		0	1	S	W	A	U	P	1.6	1496/21	Raugrottan (=2052)	b	95	25	5.0	475	26	1	0	1	0	1	1	0	0	0	0	0	0		1	3	Grottan 23 (1) p35 1988. TF98. *
VP *8355 0755*	630	Storuman	Rödingsfjället				Wh/grey										1517/22	Vantans grotta (=2054)		(4)																				Svenska Grottor nr. C3. *
VP *8355 0755*	630	Storuman	Rödingsfjället			200	Wh/grey		0	1	S	W	A	U	P	1.6	23	Gömstället grotta (=2053)	a	8	1	*1.0*	*8*	13	1	0	0	*1*	0	0	*0*	*0*	*0*	*0*	*0*	*0*		0		Svenska Grottor nr. C3. *
VP *8355 0755*	630	Storuman	Rödingsfjället				Wh/grey										1521/24	Pipgrottan (=2055)		(8)																				Svenska Grottor nr. C3. *
VP *8350 0750*	624	Storuman	Rödingsfjället				Wh/grey										1522/25	Kom upp stallet (=2056)																						Svenska Grottor nr. C3. TF98. *
VP *???? ????*	???	Storuman															1526	Två Stenar		(8)																				Rune Magnusson Database
VP *822 065*	740	Storuman	Olfjället														319	Olfjallsgrottan		(35)																				Rune Magnusson Database
VP *820 066*	800	Storuman	Olfjället														316	Olfjallsporten																				Rune Magnusson Database

* Lst. ident. by Norberg et al. (1988)

Umfors and Tärnaby — **25EF** — (Area bounded by 1451 to 1474 and 7295 to 7323 only)

14511	73199	926	Storuman	Artfjäll	45	25 N	40	Grey		0	1	T	P	L	N	P	0.8	2643	Gielasvaratjgrottan	h	105	12	2.0	210	11	1	1	0	6	2	1	2	0	0	*6*	0	0		1	4/5	Grottan 26 (2) 24-30 1991. TF98
14509	73199	908	Storuman	Artfjäll			40			0	1	T	P	L	N	P	0.8		10 m cave	a	10	4	2.0	20	40	1	0	0	1	1	1	0	0	0	0	0	0		1		Grottan 26 (2) 24-30 1991. TF98
14570	73194	905	Storuman	Artfjäll	180	10 W	40			0	1	T	P	L	U	P	0.2		Dutchman's Hole	a	3	2	0.5	2	67	1	0	0	1	1	0	0	0	0	0	1	0	0	1		Unpublished. TF98 (WS)

Kaldvatnet — **2027 II** — **AC: Västerbottenslan**

VP 9210	2160	836	Storuman	Sotsbäck	0 - 6	20 N	300	Grey		0	1	L	P	L	N	A	2.5	1751	Sotsbäcksgrottan	h	1850	110	10.0	18500	5.9	1	1	0	2	2	0	4	0	3	0	0	1	1	1	3/5	Tr. BCRA 2 (1) 13-27 1975. TF98. *
VP 9210	2160	830	Storuman	Sotsbäck		20 N	300	Grey		0	1	L	P	L	N	A	2.5	2633	Lergrottan	a	60	15	10.0	800	25	1	0	0	1	0	0	0	0	0	0	0	0	1	0	3	Svenska Grottor nr. 4. p37. *
VP 9210	2170	840	Storuman	Sotsbäck		20 N	300	Grey		0	1	L	P	L	N	A	2.5	2634	Roegrottan	a	40	2	1.0	40	5	1	0	0	1	0	0	0	0	0	0	0	1	0	1	Grottan 4 (2) p10 1969+RM dB. *
VP 9210	2170	840	Storuman	Sotsbäck				Grey										2636	Smågrottan		(5)														0	0	0	0			Rune Magnusson database. *
VP 9210	2170	840	Storuman	Sotsbäck			300	Grey		0	1	L	P	L	N	A	2.5	2635	T-grottan	a	16	2	*1.0*	*16*	13	1	1	0	0	1	0	0	*0*	*0*	*0*	*0*	*0*		0		Grottan 25 (2) 12-16 1990. *
VP 9180	2210	860	Storuman	Sotsbäck															unexplored cave		TF98: Could not find:						all mica schist?												Grottan 25 (2) p18 1990. * .
VP 9225	2230	790	Storuman	Sotsbäck			300	Grey		0	1	L	P	L	N	A	0.7	1379	Blåbärsgr./Djupa Br.1	h	150	45	2.0	300	30	1	0	0	2	1	0	0	1	0	0	0	0		0	1	Grottan 13 (4) 30-31 1978. *
VP *9235 2220*	*770*	Storuman	Sotsbäck			300	Grey		0	1	L	P	L	N	A	0.7		Baksluket (near Sink 2)	a	10	3	1.0	10	30	1	1	0	0	1	0	0	0	0	0	0	0	1	0		Grottan 26 (2) p19 1991. *
VP 9235	2230	770	Storuman	Sotsbäck			300	Grey		0	1	L	P	L	N	A	0.8	2640	V-grottan	a	60	5	0.5	30	8	1	0	0	1	1	0	0	0	0	0	0	0	1	0		Grottan 26 (2) 28-29 1991+RM dB. *
VP 9275	2220	675	Storuman	Sotsbäck			300	Grey/Br.		0	1	L	P	L	N	A	*3.0*	2638	Branthallen (RF1)	a	40	19	*3.0*	120	48	1	1	0	0	1	0	0	0	0	0	0	1	0	5	Grottan 26 (2) 21-23 1991. *
VP 9275	2220	710	Storuman	Sotsbäck			300	Grey/Br.		0	1	L	P	L	N	A	*3.0*	2637	Ranstangselgrottorna (RF2	g	143	31	1.0	143	22	1	1	0	0	1	0	2	1	0	1	0	0	1	0	5	Grottan 26 (2) 21-23 1991. *
VP 9245	2220	760	Storuman	Sotsbäck			300	Grey		0	1	L	P	L	N	A	1.0	2639	Fossila utloppsgrottan	*a*	19	*2*	*2.0*	*38*	11	1	0	0	1	0	0	0	*0*	*0*	*0*	*0*	*0*		0		Grottan 26 (2) p20 1991. *
VP 9320	2275	660	Storuman	Sotsbäck	22	45 N	200	Grey		0	1	L	G	A	N	A	3.3	1381	(Nedre) Djupa Brunnen 2	S	40	26	1.5	60	65	1	0	0	*1*	0	0	1	*1*	*0*	*0*	0	*0*		0		Grottan 2 (2) p9 '67+25(2)p12 '90. *
VP 9320	2295	655	Storuman	Sotsbäck			200	Grey		0	1	L	G	A	N	A	3.3	2641	Nedersta Djupa Brunnen	S	10	10	*1.0*	*10*	100	1	0	0	1	1	0	0	*1*	*0*	*0*	0	*0*		1		Rune Magnusson database. *
VP 9350	2315	610	Storuman	Sotsbäck			200	Grey		0	1	L	G	A	N	A	4.5	2642	Sotsbäckens utlopp	a	10	1	2.0	20	10	1	0	1	0	1	1	0	0	0	0	0	0		1		Grottan 25 (2) p9 1990. TF98. *
VP			Storuman	Sotsbäck				Grey											Snirkelgrottan		(12)																			Grottan 25 (2) 12-16 1990. *
VP			Storuman	Sotsbäck				Grey											Bengrottan		(20)																			Grottan 25 (2) 12-16 1990. *
VP			Storuman	Sotsbäck				Grey											Stupidyftan		(15)	(8)																		Grottan 25 (2) 12-16 1990. *
VP			Storuman	Sotsbäck				Grey											Blockhålet		(6)																			Grottan 25 (2) 12-16 1990. *
VP			Storuman	Sotsbäck				Grey											Rengärdeshasalen		(5)																			Grottan 25 (2) 12-16 1990. *
VP			Storuman	Sotsbäck				Grey											Plattgrottorna		(15)																			Grottan 25 (2) 12-16 1990. *

NB: Hallden (1975) mentioned that there are 30 caves, including the very small, which exist in the Sotsbäck area.

* Lst. ident. by Hallden (1974)

UPPER ALLOCHTHON: Köli Nappes - Upper Köli (Fauske / Gasak / Joljell Nappes): KU

Caves are grouped by carbonate outcrop

Eastern catchment area

Kaldvatnet 2027 II AC: Västerbottenslan cont.

UTM / SWEDISH RN COORDS		ALT.	KOMMUNE	AREA	LST. STRIKE	LST. DIP	OW	EXT. COLOUR	OTHER INT. ROCK	R	T	GE	CL	KT	SR	OR	CA	REF. NO.	CAVE NAME	CT	LENG.	VR	XS	VOL.	Min. HG %	C	SE	RE	DE	CS	SP	Ch	Sh	BC	RV	MV	DC	FS	P	SG	PRIME REFERENCES
External Cave Attributes																				Internal Cave Attributes																					
VP 9830	2725	850	Storuman	Brandsfjället		N	200			0	1	T	P	A	U	N	1.5		Brandsfjällsgrottan	a	15	2	2.0	30	13	1	1	1	0	1	0	0	0	0	0	1	0		0		Grottan 11 (3) p19 1976
VP 9825	2690	790	Storuman	Brandsfjället															Mindregrottan																						Grottan 11 (3) p19 1976
WP 0775	4110	734	Storuman	Övre Åltsvattnet	80	W	4000			1	0	L	P	L	N	N	0.1	837/M1		a	10	1	0.6	6	10	1	0	1	0	1	0	0	0	0	0	1	0		0		Svenska Grottor Nr. 2
WP 0780	4110	734	Storuman	Övre Åltsvattnet	80	W	4000			1	0	L	P	L	N	N	0.1	839/M2		e	14	2	0.5	7	14	1	0	1	1	1	0	0	0	0	0	0	0		0		Svenska Grottor Nr. 2
WP 0785	4110	734	Storuman	Övre Åltsvattnet		W	4000			1	0	L	P	L	N	N	2.5	841/M3		c	8	1	0.5	4	13	1	1	1	2	1	0	0	0	0	0	1	0		0	2	Svenska Grottor Nr. 2
WP 0795	4110	760	Storuman	Övre Åltsvattnet		W	4000			1	0	T	P	L	N	N	2.5	843/M4		a	8	1	0.5	4	13	1	1	0	0	1	1	0	0	0	0	0	0		0	3	Svenska Grottor Nr. 2
WP 0795	4115	760	Storuman	Övre Åltsvattnet		W	4000			1	0	T	P	L	N	N	2.5	847/M5		b	27	3	0.5	14	11	1	0	0	7	0	0	0	0	0	0	0	0	1	0	3	Svenska Grottor Nr. 2
WP 072	405	700	Storuman	Övre Åltsvattnet		W	4000			1	0	L	P	L	N	N	2.5	789	Kofjeldalen	S	3	3	2.0	6	100	1	0	0	1	1	0	0	1	0	0	0	0		0		SG2 + R. Magnusson database. *
WP 0800	4120	760	Storuman	Övre Åltsvattnet		W	4000			1	0	T	P	L	N	N	2.5	797/M6	Tunnelgrottan	a	45	4	4.0	180	9	1	1	1	1	1	0	0	1	0	0	1	0		0	3	Svenska Grottor Nr. 2
WP 0806	4125	770	Storuman	Övre Åltsvattnet		W	4000			1	0	T	P	L	N	N	2.5	817/M7		d	45	4	2.0	90	9	1	0	0	3	1	0	1	0	1	1	1	0		0	3	Svenska Grottor Nr. 2
WP 0805	4125	770	Storuman	Övre Åltsvattnet		W	4000			1	0	T	P	L	N	N	2.5	819/M7a		a	10	1	0.5	5	10	1	0	0	1	0	0	0	0	0	0	0	0		0		Svenska Grottor Nr. 2
WP 0815	4130	775	Storuman	Övre Åltsvattnet		W	4000			1	0	T	P	L	N	N	2.5	745/M8	2 low resurgences	c	10	1	1.0	10	10	1	0	2	0	1	1	0	0	0	0	1	0		0		R. Magnusson database
WP 0810	4135	775	Storuman	Övre Åltsvattnet		W	4000			1	0	T	P	L	N	N	2.5	747/M9		b	32	2	0.5	16	6	1	0	0	1	1	2	0	0	0	0	1	0		0	3	Svenska Grottor Nr. 2
WP 0815	4135	775	Storuman	Övre Åltsvattnet		W	4000			1	0	T	P	L	N	N	2.5	749/M10		a	12	2	1.0	12	17	1	1	0	0	1	1	0	0	0	0	1	0		0	3	Svenska Grottor Nr. 2
WP 0820	4135	775	Storuman	Övre Åltsvattnet		W	4000			1	0	T	P	L	N	N	2.5	M10a	Kryptunnel	a	10	1	0.5	5	10	1	0	0	2	0	0	0	0	0	0	0	0		0		Svenska Grottor Nr. 2
WP 0845	4145	770	Storuman	Övre Åltsvattnet		W	4000		Q + ms	1	0	T	P	L	N	N	1.3	827/M11	Murevardolabyrinten	h	275	10	2.0	550	4	1	0	0	10	1	2	1	9	0	0	0	0		0	3	Svenska Grottor Nr. 2
WP 0845	4145	770	Storuman	Övre Åltsvattnet		W	4000			1	0	T	P	L	N	N	1.3	M11a		a	4	1	0.5	2	25	1	0	0	1	0	0	0	0	0	0	0	0		0		Svenska Grottor Nr. 2
WP 0840	4140	770	Storuman	Övre Åltsvattnet		W	4000			1	0	T	P	L	N	N	1.3	829/M12	Temporarily dry outflow	a	17	2	1.0	17	12	1	0	1	0	1	1	0	0	0	0	0	0		0		Grottan 15(4) p3 1980
WP 0900	4175	810	Storuman	Övre Åltsvattnet		W	4000			1	0	T	P	L	N	N	1.0	831/M13a		b	18	2	2.0	36	11	1	0	1	0	1	0	0	0	0	0	1	1		0		Svenska Grottor Nr. 2
WP 0900	4175	810	Storuman	Övre Åltsvattnet		W	4000			1	0	T	P	L	N	N	1.0	833/M13b		b	12	2	1.5	18	17	1	1	0	0	1	0	0	0	0	0	1	0		0		Svenska Grottor Nr. 2
WP 0910	4180	815	Storuman	Övre Åltsvattnet		W	4000			1	0	T	P	L	N	N	1.0	835/M14		a	11	2	6.0	66	18	1	1	0	0	1	0	0	0	0	0	1	0		0		Svenska Grottor Nr. 2
WP 0910	4180	815	Storuman	Övre Åltsvattnet		W	4000			1	0	T	P	L	N	N	1.0	M15	Naturlig Bro	d	15	2	1.0	15	13	1	0	0	1	0	0	0	0	0	0	0	0	1	0		Grottan 15(4) p3 1980
WP 0920	4025	740	Storuman	Övre Åltsvattnet		W	4000			0	0	L	P	L	N	N	9.0	781/O1	Djuptjarnabäck. Utloppsgr.	a	3	2	6.0	18	67	1	0	1	0	1	1	0	0	0	0	1	0		0		Svenska Grottor Nr. 2
WP 0940	4000	720	Storuman	Övre Åltsvattnet		W	4000			0	0	L	P	L	N	N	9.0	815/O2		d	5	1	0.5	3	20	1	0	0	3	0	0	0	0	1	0	0	0		0		Svenska Grottor Nr. 2
WP 0940	4010	725	Storuman	Övre Åltsvattnet		W	4000			0	0	L	P	L	N	N	9.0	783/O3	Karnivorgr. / Bredhallarna	h	80	10	4.0	320	13	1	1	1	0	1	3	0	2	0	0	0	0		0	4	Grottan 15(4) p3 1980. SW dip.
WP 0965	4030	725	Storuman	Övre Åltsvattnet		W	4000			0	0	L	P	L	N	N	9.0	813/O4		a	10	3	1.0	10	30	1	0	0	1	0	0	0	0	0	0	0	0		0		Svenska Grottor Nr. 2
WP 0950	4040	730	Storuman	Övre Åltsvattnet		W	4000			0	0	L	P	L	N	N	9.0	785/O6/O	Djuptjarnabäckloppets Sluk	d	68	2	3.0	204	3	1	1	0	1	3	3	0	0	0	0	1	0		0	4	Grottan 15(4) p3 1980
WP 0960	4040	730	Storuman	Övre Åltsvattnet		W	4000			0	0	L	P	L	N	N	9.0	799/O7		a	6	1	0.5	3	17	1	0	0	1	0	0	0	0	0	0	0	0		0		Svenska Grottor Nr. 2
WP 0950	4045	730	Storuman	Övre Åltsvattnet		W	4000			0	0	L	P	L	N	N	9.0	801/O8		a	15	1	1.0	15	7	1	0	1	1	1	0	0	0	0	0	1	0		0		Svenska Grottor Nr. 2
WP 0950	4045	730	Storuman	Övre Åltsvattnet		W	4000			0	0	L	P	L	N	N	9.0	803/O9		a	6	1	0.5	3	17	1	1	0	0	1	0	0	0	0	0	1	0		0		Svenska Grottor Nr. 2
WP 0950	4045	730	Storuman	Övre Åltsvattnet		W	4000			0	0	L	P	L	N	N	9.0	805/O10		a	9	1	0.5	5	11	1	0	1	0	1	0	0	0	0	0	1	0		0		Svenska Grottor Nr. 2
WP 0950	4045	730	Storuman	Övre Åltsvattnet		W	4000			0	0	L	P	L	N	N	9.0	807/O11		a	10	1	0.5	5	10	1	1	0	0	1	0	1	0	0	0	1	0		0		Svenska Grottor Nr. 2
WP 0980	4080	734	Storuman	Övre Åltsvattnet		W												O12	Naturlig Bro																						Svenska Grottor Nr. 2
WP 0930	4110	748	Storuman	Övre Åltsvattnet		W												809/O13	Flooded Sink																						Svenska Grottor Nr. 2
WP 0915	4100	740	Storuman	Övre Åltsvattnet		W	4000			0	0	L	P	L	N	N	1.0	811/O14		a	10	1	0.5	5	10	1	0	1	0	1	0	0	0	0	0	1	0		0		Svenska Grottor Nr. 2
WP 0950	4040	730	Storuman	Övre Åltsvattnet				Secret Cave										787	Hemliga Grottan																						Svenska Grottor Nr. 2

Q= Quartz

ms= micaschist

Most caves are c. 1km from the thrust.

Contact metamorphism inferred from 1:200,000 geology map (1929), 1:400,000 geology map (1955) and from Svenska Grottor No. 2 Fig.1 (1980)

Also: Grottan 28 (1) p4

1993: Longest and Deepest

* Uncertain position. 1 km west?

UPPER ALLOCHTHON: Köli Nappes - Upper Köli (Feuske / Gasak / Joåeli Nappes): KU

Caves are grouped by carbonate outcrop

UTM / SWEDISH RN COORDS		ALT.	KOMMUNE	AREA	LST. STRIKE	LST. DIP	OW	EXT. COLOUR	OTHER INT. ROCK	R	T	GS	CL	KT	SR	OR	CA	REF. NO.	CAVE NAME	CT	LENG.	VR	XS	VOL.	Min. HG %	C	SE	RE	DE	CS	SP	Ch	Sh	BC	RV	MV	DC	FS	P	SG	PRIME REFERENCES
External Cave Attributes																				**Internal Cave Attributes**																			**Eastern catchment area**
Umfors (North East)				**25EF**			**AC: Västerbottenslan**																																		
14747	73444	780	Storuman	Övre Ältsvattnet			4000			0	0	T	P	A	*U*	N	0.5	769/O	Ranskallegrottan	a	5	2	*1.0*	5	40	1	0	0	1	1	0	0	1	0	0	1	0		0		Svenska Grottor Nr. 2
14754	73446	695	Storuman	Övre Ältsvattnet	65	57 N	4000			0	0	L	P	A	N	N	0.4	771/G1	Kanjongrottan	h	130	30	*2.0*	*260*	23	1	0	0	1	1	0	0	1	1	0	1		0	3	Svenska Grottor Nr. 2. Moonmilk.
14751	73447	720	Storuman	Övre Ältsvattnet			4000			0	0	L	P	A	N	N	0.4	775/G2	Kvannegrotta	b	40	*3*	*0.5*	*20*	8	1	1	0	0	1	0	0	0	0	1	0		0		Svenska Grottor Nr. 2
14753	73449	720	Storuman	Övre Ältsvattnet														777/G3a	Vattenfallsgrottan																				Svenska Grottor Nr. 2
14753	73449	720	Storuman	Övre Ältsvattnet			4000			0	0	L	P	A	N	N	0.4	777/G3b	Vattenfallsgrottsluket	b	15	3	*1.0*	*15*	20	1	1	0	0	1	0	0	0	0	1	0		0		Grottan 15(4) p3 1980
14750	73447	740	Storuman	Övre Ältsvattnet			4000			0	0	L	P	A	N	N	0.4	773/G5	Övre Gusebaktegrottan	c	55	*5*	*1.0*	*55*	9	1	0	1	0	1	0	0	0	0	1	0		0		Grottan 15(4) p3 1980
14744	73404	745	Storuman	Övre Ältsvattnet														D																					Svenska Grottor Nr. 2
14740	73395	800	Storuman	Övre Ältsvattnet			2400	BGB		1	0	T	P	L	N	N	8.0	793/S1	Marmorgrottan	g	320	10	9.0	*2880*	3	1	0	1	2	1	1	0	0	0	0	0	1		0	4	Grottan 15(4) p3 1980
14739	73394	805	Storuman	Övre Ältsvattnet		W	2400		Schist	1	0	T	P	L	N	N	8.0	795/S2	Stora Gapsjukkesluket	b	50	*5*	2.0	100	10	1	1	0	0	1	1	0	0	0	0	0	0		0		Grottan 15(4) p4 1980
14741	73394	805	Storuman	Övre Ältsvattnet			2400			1	0	T	P	L	N	N	8.0	797/S3	Blockgrottan	d	85	*9*	*2.0*	*170*	11	1	0	0	1	1	2	1	0	1	0	0	0		0	3	Svenska Grottor Nr. 2. Static sumps.
14739	73393	810	Storuman	Övre Ältsvattnet	150	W	2400			1	0	T	P	L	N	N	8.0	849/S4	Rödinggrottan	b	10	4	*1.0*	*10*	40	1	0	1	0	1	0	0	0	1	0	0	0		0		Svenska Grottor Nr. 2
14739	73394	805	Storuman	Övre Ältsvattnet			2400			1	0	T	P	L	N	N	8.0	851/S5		e	35	2	*1.0*	*35*	6	1	0	0	1	0	0	0	0	0	0	0	0		0		Svenska Grottor Nr. 2
14739	73394	805	Storuman	Övre Ältsvattnet													8.0	853/S6																					Svenska Grottor Nr. 2
14739	73393	810	Storuman	Övre Ältsvattnet			2400			1	0	T	P	L	N	N	8.0	828/E	Lilla Stalaktithålet	a	5	*2*	*0.5*	*3*	40	1	0	0	1	0	0	0	0	0	1	0		0		Grottan 15(4) p4 1980
14740	73395	800	Storuman	Övre Ältsvattnet			2400			0	0	T	P	L	N	N	8.0	812	Lilla Grottan	a	7	2	1.0	7	29	1	1	0	0	1	0	0	0	0	0	0		0		Svenska Grottor Nr. 2
14740	73395	800	Storuman	Övre Ältsvattnet			2400			0	0	T	P	L	N	N	8.0	814	Lilla Hålan	a	4	2	1.0	4	50	1	0	0	*1*	0	0	0	0	0	0	0		0		Svenska Grottor Nr. 2
14739	73392	810	Storuman	Övre Ältsvattnet			2400			0	0	T	P	L	N	N	8.0	855/S7		b	10	2	1.0	10	20	1	0	0	1	0	0	0	0	0	0	0	0		0	3	Svenska Grottor Nr. 2
14739	73391	820	Storuman	Övre Ältsvattnet			2400			0	0	T	P	L	N	N	8.0	857/S8		c	20	3	1.0	20	15	1	3	1	0	1	0	0	0	0	0	0	1	0	0	3	Svenska Grottor Nr. 2
14743	73423	700	Storuman	Övre Ältsvattnet			4000			0	0	L	P	L	N	N	30.0	859/R1		a	20	*8*	*1.0*	*20*	40	1	0	0	*1*	0	0	0	0	0	0	0	0		0		Svenska Grottor Nr. 2
14743	73423	700	Storuman	Övre Ältsvattnet			4000			0	0	L	P	L	N	N	30.0	865/R2		S	5	5	*1.0*	5	100	1	0	*1*	0	1	0	0	0	0	0	1	0		0		Svenska Grottor Nr. 2
14743	73423	700	Storuman	Övre Ältsvattnet													30.0	866/R3	sink																				Svenska Grottor Nr. 2
14743	73423	700	Storuman	Övre Ältsvattnet			4000			0	0	L	P	L	N	N	30.0	867/R4		a	6	2	*1.0*	*6*	33	1	0	0	*1*	0	0	0	0	1	0	0	0		0		Svenska Grottor Nr. 2
14744	73423	695	Storuman	Övre Ältsvattnet			4000			0	0	L	P	L	N	N	30.0	868/R5		d	28	*4*	*1.0*	*28*	14	1	1	0	0	1	0	0	0	0	0	1	0		0		Svenska Grottor Nr. 2
14745	73423	695	Storuman	Övre Ältsvattnet														869/R6																					Svenska Grottor Nr. 2
14745	73423	695	Storuman	Övre Ältsvattnet														757/R7																					Svenska Grottor Nr. 2
14748	73425	685	Storuman	Övre Ältsvattnet			4000			0	0	L	P	L	N	N	30.0	808/R8	Kombinerat sluk/utlopp	a	10	2	*1.0*	*10*	20	1	3	1	0	1	1	0	0	0	0	1	0		0		Grottan 15(4) p7 1980
14748	73424	690	Storuman	Övre Ältsvattnet			4000			0	0	L	P	L	N	N	30.0	864/R9	Halsskärargrottan	b	35	2	1.0	35	6	1	1	1	0	1	0	0	0	0	0	1	0		0		Grottan 16(1) 14-15 1981
14751	73422	700	Storuman	Övre Ältsvattnet			4000			1	0	L	P	L	N	N	30.0	836/R10	Strömgårds Grotta	a	10	4	*1.0*	*10*	40	1	1	0	0	1	0	0	0	0	0	1	0		0		Svenska Grottor Nr. 2
14747	73423	695	Storuman	Övre Ältsvattnet			4000			0	0	L	P	L	N	N	30.0	800/R11		a	15	2	*1.0*	*15*	13	1	1	0	0	1	0	0	0	0	0	1	0		0		Svenska Grottor Nr. 2

BGB Blue grey black striped

Tärnaby				**24EF**			**AC: Västerbottenslan**												(Area bounded by 1451 to 1474 and 7266 to 7295 only)																							
14603	72906	603	Storuman	Södra Storfjället	140	45 S	100	White		0	1	L	G	A	N	P	1.5		Tjärrogrottan 1	a	10	4	1.0	10	40	1	1	0	0	1	1	0	0	0	0	1	0		1	1	} Beskow 20-24 1929
14603	72905	598	Storuman	Södra Storfjället	140	31 S	100	White	ms	0	1	L	G	A	N	P	1.5	2644	Tjärrogrottan 2 (Övre)	b	80	4	1.0	80	5	1	0	1	1	1	1	0	0	0	0	1	0		1	1	} Grottan 4 (2) p16 1969, 7(4) 4-6 1972
14603	72905	598	Storuman	Södra Storfjället	140	31 S	100	White		0	1	L	G	A	N	P	1.5		Tjärrogrottan 3	a	10	2	4.0	40	20	1	1	1	0	1	0	0	0	0	0	1	0		1		} Tärna Fjälguiden p59 1997.
14603	72905	595	Storuman	Södra Storfjället	140	31 S	100	White		0	1	L	G	A	N	P	1.5	2645	Tjärrogrottan 4 (Nedre)	a	35	2	4.0	140	6	1	1	1	0	1	0	0	0	0	0	1	0		1		} TF98, RM 2003
1453x	7277x	*900*	Storuman	Södra Storfjället		*25 N*	200			0	1	T	P	L	U	P	*4.0*		Förgrotta	c	25	5	2.0	50	20	1	1	0	1	1	0	0	0	1	0	0	0		0	3	Grottan 7 (4) 4-6 1972
14538	72774	*900*	Storuman	Södra Storfjället		*25 N*	200			0	1	T	P	L	U	P	*4.0*	318	Rajagrottan*	c	140	10	2.0	280	7	1	1	1	2	1	0	0	0	0	0	0	0		0	3	Grottan 4(2) p16 1969 & 7(4) 4-6 1972
1455x	7277x	*900*	Storuman	Södra Storfjället		*25 N*	200			0	1	T	P	L	U	P	2.7		Slukhalen 1	S	5	5	*3.0*	*15*	100	1	1	0	0	1	0	0	0	0	0	0	0		0		Grottan 7 (4) 4-6 1972
1455x	7277x	*900*	Storuman	Södra Storfjället		*25 N*	200			0	1	T	P	L	U	P	2.7		Slukhalen 2	S	5	5	*3.0*	*15*	100	1	1	0	0	1	0	0	0	0	0	0	0		0		Grottan 7 (4) 4-6 1972
1455x	7277x	*900*	Storuman	Södra Storfjället		*25 N*	200			0	1	T	P	L	U	P	2.7		Slukhalen 3	S	5	5	*3.0*	*15*	100	1	1	0	0	1	0	0	0	0	0	0	0		0		Grottan 7 (4) 4-6 1972
1455x	7277x	*900*	Storuman	Södra Storfjället		*25 N*	200			0	1	T	P	L	U	P	2.7		Slukhalen 4	S	5	5	*3.0*	*15*	100	1	1	0	0	1	0	0	0	0	0	0	0		0		Grottan 7 (4) 4-6 1972
1455x	7277x	*900*	Storuman	Södra Storfjället		*25 N*	200			0	1	T	P	L	U	P	2.7		Slukhalen 5	S	5	5	*3.0*	*15*	100	1	1	0	0	1	0	0	0	0	0	0	0		0		Grottan 7 (4) 4-6 1972

ms mica schist

* Coords. from Henriksson and Magnusson (2003)

UPPER ALLOCHTHON: Köli Nappes - Middle Köli - Oviumpi / Leipihvatnet Nappe: KL: TOTALS

Refer to North Central Norway Cave Database for Key

External Cave Attributes | Internal Cave Attributes

UTM / SWEDISH RN COORDS	ALT.	KOMMUNE	AREA	LST. STRIK	LST. DIP	OW	EXT. COLOUR	OTHER INT. ROCK	R	T	GB	CL	KT	SR	OR	CA	REF. NO.	CAVE NAME	CT	LENG.	VR	XS	VOL.	Min. HG %	C	SE	RE	DE	CB	SP	Ch	Sh	BC	RV	MV	DC	FS	P	BG	PRIME REFERENCES
Totals	####				###	####			0	21						###				6221	###	#####	30432	###	21	11	4	13	21	13	10	3	7	0	4	2	5	2		
Av. per cave	510				54	160			0.0	1.9						14.0				286	11	3.4	1449	32		0.5	0.2	0.6	1.0	0.6	0.5	0.1	0.3	0.0	0.2	0.1	0.2	0.1		
Minima	475				45	50										0.80				3	1	0.5	3	3		0	0	0	0	0	0	0	0	0						
Maxima	620				80	500										20.0				5600	144	10.0	28000	100		3	1	1	5	5	8	1	7	0						

(Dip measured in 4 caves)

Karst Types:

	#	Length
V	0	0
A	21	6221
L	0	0
C	0	0
X	0	0
Totals	21	6221

Cave Locations:

	#	Length
C	0	0
F	18	6153
W	1	35
R	0	0
S	0	0
G	2	33
P	0	0
Totals	21	6221

Cave Types:

	#	Length
S	3	21
a	6	101
b	8	251
c	3	248
d	0	0
e	0	0
f	0	0
g	0	0
h	1	5600
Hy	0	0
I	0	0
J	0	0
L	0	0
R	0	0
T	0	0
Totals	21	6221

Relict Caves:

#	Length
4	50

MV Caves:

#	Length
4	73

Combination Caves:

#	Length
13	6098

Glacial Situations:

	#	Length
C	0	0
D	0	0
E	0	0
G	0	0
H	0	0
K	2	33
L	16	6158
S	0	0
T	3	30
U	0	0
Totals	21	6221

UPPER ALLOCHTHON: Köli Nappes - Middle Köli - Orklump / Leipikvattnet Nappe: KL

Caves are grouped by carbonate outcrop

Eastern catchment area

UTM / SWEDISH RN COORDS	ALT.	KOMMUNE	AREA	LST. STRIK	LST. DIP	OW	EXT. COLOUR	OTHER INT. ROCK	R	T	GS	CL	KT	SR	OR	CA	REF. NO.	CAVE NAME	CT	LENG.	VR	XS	VOL.	Min. HG %	C	SE	RE	DE	CS	SP	Ch	Sh	BC	RV	MV	DC	FS	P	SG	PRIME REFERENCES
Jomasfjellet		**1924 I**	**Z: Jämtland**																																					**Speleo 16 (1) 18-21 1981**
VM 5545 9915	510	Strömsund	Bjurälv	70	*S*	300			0	1	L	F	A	N	P	19.0	1372	**Övre Bjurälvsgrottan**	c	200	15	4.0	800	8	1	1	0	0	1	0	2	0	7	0	0	0	1	0	2	Grottan 13 (4) 11-13 1978
VM 55x 99x	*510*	Strömsund	Bjurälv	70	*S*	300			0	1	L	F	A	N	P	19.0	1373	**Övre Bjurälvssluken**	S	4	4	*1.0*	*4*	100	1	1	0	0	1	0	0	0	0	0	0	0	0	0		Rune Magnusson database
VM 5575 9915	510	Strömsund	Bjurälv	70	*S*	300			0	1	L	F	A	N	P	19.0	617/10	**U-grottan**	*a*	20	3	0.7	14	15	1	0	0	1	0	0	0	0	0	0	0	0	0		0		Grottan 7 (4) 1-4 1972 *
VM 5610 9930	498	Strömsund	Bjurälv	60	80 S	300	Pale blue gre	None	0	1	L	F	A	N	P	19.0	26/6	**Svenonius Grottan**	a	55	3	10.0	550	5	1	0	0	1	1	1	0	0	0	0	0	0	0	1	Grottan 7 (4) 1-4 1972
VM 5690 9945	495	Strömsund	Bjurälv	70	*S*	200			0	1	L	F	A	N	P	20.0	4	**Stora Dolinsjön**	S	7	7	*4.0*	*28*	100	1	0	0	1	1	1	0	1	0	0	0	0		0	Grottan 32 (4) 31-32 1997
VM 5725 9955	495	Strömsund	Bjurälv	70	*S*	100			0	1	L	F	A	N	P	20.0	317/11	**De Åtta = Valvgrottan?**	b	16	1	1.5	24	6	1	0	0	1	1	0	0	0	0	0	1	0		0	Grottan 7 (4) 1-4 1972
VM 5740 9960	490	Strömsund	Bjurälv	70	*S*	100			0	1	L	F	A	N	P	20.0	1237	**Dolin 3A: Spegelgrottan?**	b	35	1	*2.0*	*70*	3	1	0	0	1	1	1	0	0	0	0	1	0	1	0	Grottan 21 (3) 22-23 1986 *
VM 5740 9960	490	Strömsund	Bjurälv	70	*S*	100			0	1	L	F	A	N	P	20.0		**Dolin 3 cave**	a	5	*1*	*1.0*	*5*	20	1	0	0	1	0	0	0	0	0	0	0	0		0	Grottan 21 (3) 22-23 1986
VM 5740 9960	490	Strömsund	Bjurälv	70	*S*	100			0	1	L	F	A	N	P	20.0		**Marmortunneln (Dolin 2B)**	c	30	*5*	*3.0*	*90*	17	1	0	1	0	1	1	0	0	0	0	0	0	1	0	Grottan 21 (3) 22-23 1986
VM 5740 9970	490	Strömsund	Bjurälv	70	*S*	100			0	1	L	F	A	N	P	20.0	634	**Stenbron**	a	3	*2*	*10.0*	*30*	67	1	1	1	0	1	0	0	0	0	0	0	0	0	0	Grottan 7 (4) p1 1972
VM 5755 9955	480	Strömsund	Bjurälv	70	*S*	100			0	1	L	F	A	N	P	20.0	591/2	**Isgrottan**	S	10	10	*10.0*	*100*	100	1	0	0	1	0	0	0	*1*	0	0	0	0	0	0	Grottan 14 (3) p4 1979
VM 576 996	*490*	Strömsund	Bjurälv	70	*S*	100			0	1	L	F	A	N	P	20.0		**Lergrottan**	b	26	3	*6.0*	*156*	12	1	0	0	1	1	2	0	1	0	0	0	0	1	0	1 Grottan 32 (4) 17-18 1997 *
VM 576 996	*490*	Strömsund	Bjurälv	70	*S*	100			0	1	L	F	A	N	P	20.0	1298	**Banangrottan ++**	b	4	1	*1.0*	*4*	25	1	*1*	*0*	*0*	1	*1*	0	0	0	0	1	0	0	0	JGF Årsskrift p52 1999
VM 5765 9965	475	Strömsund	Bjurälv	70	*S*	100			0	1	L	F	A	N	P	20.0	1	**Festinsgrotta + sump**	b	108	*5*	*4.0*	*432*	5	1	0	1	1	1	1	0	0	0	0	0	0	0	0	Grottan 32 (4) 31-32 1997
VM 6270 9895	480	Strömsund	Stora Blåsjön		*W*	500			0	1	K	G	A	N	P	3.0		**4 kilometersgrottan**	b	15	*3*	*2.0*	*30*	20	1	0	0	1	0	0	0	0	0	0	0	0		0	P. Blombergsson 090999
VM ?	*500*	Strömsund	Stora Blåsjön	70	*45 N*	*100*			0	1	L	W	A	X	X	3.0		**Grottan söder Leipikmon +**	b	35	*4*	*1.0*	*35*	11	1	1	0	0	1	0	0	0	0	0	0	1		0	Grottan 12 (2) p20 1977
VM ?		Strömsund	Stora Blåsjön															**Hallkhålet**		(20)		(2)																		JGF Årsskrift p52 1999
VM ?	*560*	Strömsund	Stora Blåsjön	70		*100*			0	1	T	F	*A*	N	X	3.0		**Såggrottan**	b	12	*3*	*0.5*	*6*	25	1	1	0	0	1	0	0	0	0	0	0	0		0	Grottan 26 (2) p13 1991
VM ?	*560*	Strömsund	Stora Blåsjön	70														**Kylskåpet**																					Grottan 26 (2) p10 1991
VM ?		Strömsund	Stora Blåsjön															**Rentjurens öde**		(15)		(3)																		JGF Årsskrift p55 1999
VM ?	*560*	Strömsund	Stora Blåsjön	70		*100*			0	1	T	F	*A*	N	X	*3.0*	567	**Angagrottan/Kladdhålet**	a	3	*2*	*1.0*	*3*	67	1	0	0	*1*	1	0	0	0	0	0	0	0		0	Grottan 26 (2) p10,12 1991
VM ?		Strömsund	Stora Blåsjön															**Stenskivehålet**		(10)		(5)																		JGF Årsskrift p55 1999
VM ?		Strömsund	Stora Blåsjön															**Övre Koralislukat**		(10)																				JGF Årsskrift p51 1999
VM 5920 9575	603	Strömsund	Stora Blåsjön	60	45 N	100	Vary high to l	Low gr. ms	0	1	L	F	A	N	P	3.5	570	**Koraligrottan/Sky/Klyftgr.***	h	5600	144	5.0	28000	2.6	1	3	0	1	5	5	8	*0*	*0*	0	0	1	1	1	3 Grottan 26 (2) 91, 29 (2) 94 *
VM ?		Strömsund	Stora Blåsjön															**Tvåschakts grottan**		(20)		(10)																		JGF Årsskrift p56 1999
VM 593 959	620	Strömsund	Stora Blåsjön	60	45 N	100			0	1	T	F	A	N	P	0.8	2052	**Blå Kanjonen**	a	15	8	1.0	15	53	1	1	0	0	1	0	0	0	0	0	0	0	0		0	Rune Magnusson dB + pc
VM ?		Strömsund	Stora Blåsjön															**Lyan**		(190)		Near Klyftgrottan																		JGF Årsskrift p51 1999
VM 6160 9710	475	Strömsund	Stora Blåsjön	65		50			0	1	K	G	A	N	P	1.0		**Holibäcken caves**	c	18	2	*2.0*	*36*	11	1	1	1	1	1	0	0	0	0	0	1	0		0	P. Blombergsson 090999 *

* Altitude of highest entrance
\+ = Leipikmonsgrotta? (JGF Årsskrift p51 1999)
++ Assumed to be "Grotta I Bjurdal" (Rune Magnusson database)

Bjurälv GS from border pass at 540m at Ingenmansland
Stora Blåsjönn GS from road pass at 530m at Nysätern
Bjurälv valley is c.300m from the thrust

* JGF Årsskrift 51-57 1999

Limingen **1924 II** **Z: Jämtland** — **No known references**

Murusjöen **1923 I** **Z: Jämtland** — **No known references**

UPPER ALLOCHTHON: Köli Nappes - Middle Köli - Virvass / Stikke Nappe and Remdalen Repitition: KS: TOTALS

Refer to North Central Norway Cave Database for Key

UTM / SWEDISH RN COORDS	ALT.	KOMMUNE	AREA	LST. STRIK	LST. DIP	OW	EXT. COLOUR	OTHER INT. ROCK	R	T	GS	CL	KT	SR	OR	CA	REF. NO.	CAVE NAME	CT	LENG	VR	XS	VOL	Min. HG %	C	SE	RE	DE	CS	SP	Ch	Sh	BC	RV	MV	DC	FS	P	SG	PRIME REFERENCES
				External Cave Attributes															Internal Cave Attributes																					
Totals	####				###	####			0	0						####				0	###	###	0	###	0	0	0	0	0	0	0	0	0	0	0	0	0	0	0	
Av. per cave	####				###	####			###	###						####				###	###	###	###	###		##	##	###	##	##	###	###	##	##	##	###	###	###		
Minima	0				0	0										0.00				0	0	0.0	0	0		0	0	0	0	0	0	0	0	0						
Maxima	0				0	0										0.0				0	0	0.0	0	0		0	0	0	0	0	0	0	0	0						

(Dip measured in 0 caves)

Glacial Situations:

	#	Length
C	0	0
D	0	0
E	0	0
G	0	0
H	0	0
K	0	0
L	0	0
S	0	0
T	0	0
U	0	0
Totals	0	0

Karst Types:

	#	Length
V	0	0
A	0	0
L	0	0
C	0	0
X	0	0
Totals	0	0

Cave Locations:

	#	Length
C	0	0
F	0	0
W	0	0
R	0	0
S	0	0
G	0	0
P	0	0
Totals	0	0

Cave Types:

	#	Length
S	0	0
a	0	0
b	0	0
c	0	0
d	0	0
e	0	0
f	0	0
g	0	0
h	0	0
Hy	0	0
I	0	0
J	0	0
L	0	0
R	0	0
T	0	0
Totals	0	0

Relict Caves:

	#	Length
	0	0
Totals	0	0

MV Caves:

	#	Length
	0	0
Totals	0	0

Combination Caves:

	#	Length
Totals	0	0

UPPER ALLOCHTHON: Köli Nappes - Middle Köli - Virvass / Stikke Nappe and Remdalen Repitition: KS

Caves are grouped by carbonate outcrop

Eastern catchment area

Outcrop / Coords	Map / Kommune	Area	Zone	Ref. No. / Cave name	Notes	Prime references
Tunnsjöen	1924 III		Z: Jämtland			
VM 3550 6225 720	Stromsund	Björkvattnet		2093 Portfjällegrottorna	Non carbonate 'cave'	Grottan 22 (3) p39 1987. TF98
	Stromsund	Björkvattnet		624/1472	Portfjällbäck goes underground	JGF 28,56 1997. RM Database.
Jomafjellet	1924 I		Z: Jämtland			No known references
Kraitvatnet	2026 III		AC: Västerbottenslän			No known references
Skardmodalen	2025 IV		AC: Västerbottenslän			No known references
Ranseren	2025 III		Z: Jämtland			No known references
Tärnaby	24EF		AC: Västerbottenslän		(Area bounded by 1451 to 1474 and 7266 to 7295 only)	No known references
Umfors (North East)	26EF		AC: Västerbottenslän		(Area bounded by 1474 to 1500 and 7325 to 7350 only)	No known references

UPPER ALLOCHTHON: Köli Nappes - Lower Köli - Joesjö / Björkvatten Nappe: KB: TOTALS

Refer to North Central Norway Cave Database for Key

External Cave Attributes / Internal Cave Attributes

UTM / SWEDISH RN COORDS	ALT.	KOMMUNE	AREA	LST. STRIKE	LST. DIP	OW	EXT. COLOUR	OTHER INT. ROCK	R	T	GS	CL	KT	SR	OR	CA	REF. NO.	CAVE NAME	CT	LENG.	VR	XS	VOL.	Min. HG %	C	SE	RE	DE	CS	SP	Ch	Sh	BC	RV	MV	DC	FS	P	SG	PRIME REFERENCES
Totals	###				##	###			0	1						###				69	###	####	142	###	2	2	0	1	2	2	0	0	0	0	2	0	0	1		
Av. per cave	860				20	150			0.0	0.5						0.3				35	7	2.1	71	19		1.0	0.0	0.5	1.0	1.0	0.0	0.0	0.0	0.0	1.0	0.0	0.0	0.5		
Minima	800				20	100										0.10				25	3	2.0	50	12		1	0	0	1	1	0	0	0	0						
Maxima	920				20	200										0.5				44	11	2.1	92	25		1	0	1	1	1	0	0	0	0						

(Dip measured in 2 caves)

Glacial Situations:

	#	Length
C	0	0
D	0	0
E	0	0
G	0	0
H	0	0
K	0	0
L	0	0
S	0	0
T	2	69
U	0	0
Totals	**2**	**69**

Karst Types:

	#	Length
V	0	0
A	0	0
L	2	69
C	0	0
X	0	0
Totals	**2**	**69**

Cave Locations:

	#	Length
C	0	0
F	1	44
W	0	0
R	0	0
S	0	0
G	0	0
P	1	25
Totals	**2**	**69**

Cave Types:

	#	Length
S	0	0
a	0	0
b	1	44
c	0	0
d	1	25
e	0	0
f	0	0
g	0	0
h	0	0
Hy	0	0
I	0	0
J	0	0
L	0	0
R	0	0
T	0	0
Totals	**2**	**69**

Relict Caves:

#	Length
0	0
0	**0**

MV Caves:

#	Length
2	69
2	**69**

Combination Caves:

#	Length
0	**0**

UPPER ALLOCHTHON: Köli Nappes - Lower Köli - Joesjö / Björkvatten Nappe: KB

Caves are grouped by carbonate outcrop

Eastern catchment area

External Cave Attributes / Internal Cave Attributes

UTM / SWEDISH RN COORDS	ALT.	KOMMUNE	AREA	LST. STRIKE	LST. DIP	OW	EXT. COLOUR	OTHER INT. ROCK	R	T	GS	CL	KT	SR	OR	CA	REF. NO.	CAVE NAME	CT	LENG.	VR	XS	VOL.	Min. HG %	C	SE	RE	DE	CS	SP	Ch	Sh	BC	RV	MV	DC	FS	P	SG	PRIME REFERENCES
VN 8566 1831	800	Vilhemina	V. Fjällfjället		20 S	200	White	*	0	0	T	F	L	D	P	0.5	1300	Rapstengrottan	b	44	11	2.1	92	25	1	1	0	0	1	1	0	0	0	0	1	0		1	3	RM Database + pc. TF00
VN 7540 1145	920	Vilhemina	Gelvenåko		20 N	100	"Eyes"		0	1	T	P	L	N	N	0.1		Renbenshålet	d	25	3	2.0	50	12	1	1	0	1	1	1	0	0	0	0	1	0		0		P. Blombergsson pc 090999 *

* Floor: muscovite mica schist. Roof: muscovite phyllite

* JGF Årsskrift 51-57 1999

				PRIME REFERENCES
Jomafjellet	1924 I	Z: Jamtland		No known references
Limingen	1924 II	Z: Jamtland		No known references
Hjartfjellet	2026 IV	AC: Västerbottenslan		No known references
Krutvatnet	2026 III	AC: Västerbottenslan		No known references
Ranseren	2025 III	AC: Västerbottenslan and Z: Jämtland		

					PRIME REFERENCES
Frostviken NO	Z1	AI42	Z: Jämtland		No known references
Umfors and Tärnaby		24EF	AC: Västerbottenslan	(Area bounded by 1451 to 1474 and 7295 to 7323 only)	No known references
Tärnaby		24EF	AC: Västerbottenslan	(Area bounded by 1451 to 1474 and 7266 to 7295 only)	No known references
Tärnaby (South West)		24EF	AC: Västerbottenslan	(Area bounded by 1451 to 1474 and 7250 to 7266 only)	No known references
Fatmomakke NV		23EF	AC: Västerbottenslan		No known references
Fatmomakke SV		23EF	AC: Västerbottenslan		No known references
Umfors (North East)		25EF	AC: Västerbottenslan	(Area bounded by 1474 to 1500 and 7325 to 7350 only)	No known references
Tärnaby (North East)		24EF	AC: Västerbottenslan	(Area bounded by 1474 to 1500 and 7275 to 7300 only)	No known references
Tärnaby (South East)		24EF	AC: Västerbottenslan	(Area bounded by 1475 to 1500 and 7250 to 7275 only)	No known references
Fatmomakke NO		23EF	AC: Västerbottenslan		No known references

									External Cave Attributes											Internal Cave Attributes																								
UTM / SWEDISH RN COORDS	ALT.	KOMMUNE	AREA	LST. STRIKE	LST. DIP	OW	EXT. COLOUR	OTHER INT. ROCK	R	T	GS	CL	KT	SR	OR	CA	REF. NO.	CAVE NAME	CT	LENG.	VR	XS	VOL.	Min. HG %	C	SE	RE	DE	CS	SP	Ch	Sh	BC	RV	MV	DC	FS	P	SG	PRIME REFERENCES

UPPER ALLOCHTHON: Seve Units - Seve Units

Limingen	**1924 III**					**No known references**
Murusjöen	**1923 I**					**No known references**
Sipmeke SV-SO	**Z1**	**Ai74**	**AC: Västerbottenslan and Z: Jämtland**			**No known references**
Frostviken NO	**Z1**	**Ai42**	**Z: Jämtland**			**No known references**
Frostviken SO	**Z1**	**Ai44**	**Z: Jämtland**			**No known references**
Umfors (SE)	**25EF**		**AC: Västerbottenslan**	(Area bounded by 1474 to 1500 and 7300 to 7325 only)		**No known references**

UPPER ALLOCHTHON: Seve Units - Western Belt

Fatmomakke NO	**23EF**	**Ai77**	**AC: Västerbottenslan**			**No known references**

UPPER ALLOCHTHON: Seve Units - Central Belt

Fatmomakke NO	**23EF**	**Ai77**	**AC: Västerbottenslan**			**No known references**

UPPER ALLOCHTHON: Seve Units -Eastern Belt

Risbäck NV	**22F**	**Ai 102**	**AC: Västerbottenslan and Z: Jämtland**	} Underground streams: Lermobäckarna at Sandneset		JGF p28 1997
Risbäck SV	**22F**	**Ai 103**	**Z: Jämtland**	} (Where is this?)		JGF p28 1997
Fatmomakke SO	**23EF**	**Ai78**	**AC: Västerbottenslan**			**No known references**

MIDDLE ALLOCHTHON

No known carbonates

LOWER ALLOCHTHON

Fatmomakke SO	**23EF**	**Ai78**	**AC: Västerbottenslan**			**No known references**
Risback NO	**22F**	**Ai104**	**AC: Västerbottenslan**			**No known references**
??? NV	**22G**	**Ai84**	**AC: Västerbottenslan**			**No known references**
??? SV	**22G**	**Ai85**	**AC: Västerbottenslan**			**No known references**
??? NO	**22G**	**Ai86**	**AC: Västerbottenslan**			**No known references**

APPENDIX C5

COMBINED CENTRAL SCANDINAVIAN CAVE DATABASES: SUMMARIES

COMBINED CENTRAL SCANDINAVIA CAVE DATABASES: SUMMARY - TOTALS

	ZONE	External Cave Attributes R	T	Internal Cave Attributes LENG.	VOL.	C	SE	RE	DE	CS	SP	Ch	Sh	BC	RV	MV	DC	FS	P	COMMENTS
UPPERMOST ALLOCHTHON: Helgeland Nappe Complex																				**HNC does not occur in Sweden**
Z1	**Coastal Area**	0	0	31	195	4	0	0	4	0	0	0	0	0	0	0	0	0	4	Football pitch caves
Z2	**Fjord Area**	115	0	10886	50835	165	60	36	153	131	78	19	70	41	13	62	10	62	79	
Z3	**Central Granite Area**	6	0	3320	16251	36	10	8	47	25	6	4	35	9	3	13	0	12	20	
Z4	**Eiterådal & Jordbruelv**	2	0	14490	76258	182	30	15	242	93	50	20	156	35	10	16	7	38	155	
Z5	**Mosjøen to Fjellryggen**	7	0	7689	40600	79	35	11	73	73	58	15	41	20	4	33	2	12	49	
Z6	**Hemnes to Dunfjell**	34	1	5204	26423	64	22	12	62	49	29	5	26	13	2	14	1	7	39	
Z7	**Åkervik to Fiplingdal**	6	0	4806	36368	87	44	19	54	72	41	3	38	14	7	41	4	7	57	
Z8	**Eastern Area**	8	8	825	3889	8	5	1	3	7	2	1	1	0	0	3	1	1	8	Jengelvatn only
Z9	**Northern Area**	0	0	25	250	1	0	0	1	0	0	0	0	0	0	0	1	0	1	Marmorholet only
	Totals for HNC	178	9	47276	251068	626	206	102	639	450	264	67	367	132	39	182	26	139	412	
UPPERMOST ALLOCHTHON: Rødingsfjell Nappe Complex - Nappes below the Beiarn Nappe																				**Only Zone C occurs in Sweden**
ZA	**Bleikvassli Area**	2	3	3920	31976	37	15	7	35	28	22	8	8	11	3	8	0	9	24	Excl. 1700 sq km Røssvatn
ZB	**Bjerka & Stor Akersvatn**	0	0	1410	7330	7	5	1	5	4	2	1	2	1	0	2	1	2	7	
ZC	**Southern & Border Area**	0	0	5843	27275	58	19	8	44	41	18	11	18	12	4	4	4	16	27	
	Totals for RNC	2	3	11173	66580	102	39	16	84	73	42	20	28	24	7	14	5	27	58	
UPPER ALLOCHTHON: Køli Nappes																				
KU	**Fauske etc**	27	57	9651	66222	125	63	37	95	109	55	20	24	21	12	40	7	17	32	
KG	**Gjersvik**																			**No known references**
KL	**Orklump / Leipikvattnet**	0	29	6712	34922	29	13	5	21	28	21	11	5	10	0	7	2	9	5	
	Gelvenåko																			**No mapped carbonates**
KS	**Virvass / Stikke**																			**Sweden only. No caves**
KB	**Joesjø / Bjørkvatn**	0	1	69	142	2	2	0	1	2	2	0	0	0	0	2	0	0	1	**Sweden only**
	Totals for Køli	27	87	16432	101286	156	78	42	117	139	78	31	29	31	12	49	9	26	38	
UPPER ALLOCHTHON: Seve Nappes																				**No known references**
MIDDLE ALLOCHTHON																				**No mapped carbonates**
LOWER ALLOCHTHON																				**No known references**
	GRAND TOTALS	207	99	74881	418934	884	323	160	840	662	384	118	424	187	58	245	40	192	508	

øääöÅØÖ

COMBINED CENTRAL SCANDINAVIA CAVE DATABASES: SUMMARY - AVERAGES

	ZONE	ALT.	LST. DIP	OW	External Cave Attributes R	T	CA	LENG.	VR	XS	VOL.	Min. HG %	C TOT.	SE	RE	DE	CS	SP	Ch	Sh	BC	RV	MV	DC	FS	P	COMMENTS
UPPERMOST ALLOCHTHON: Helgeland Nappe Complex																											
Z1	**Coastal Area**	24	23	1000	0.0	0.0	0.1	8	2.3	5.5	49	34	4	0.0	0.0	1.0	0.0	0.0	0.0	0.0	0.0	0.0	0.0	0.0	0.0	1.0	Football pitch caves
Z2	**Fjord Area**	182	57	244	0.7	0.0	2.0	66	7.7	3.8	308	22	165	0.4	0.2	0.9	0.8	0.5	0.1	0.4	0.2	0.1	0.4	0.1	0.4	0.5	
Z3	**Central Granite Area**	387	50	332	0.2	0.0	2.1	92	10.3	2.2	451	36	36	0.3	0.2	1.3	0.7	0.2	0.1	1.0	0.3	0.1	0.4	0.0	0.3	0.6	
Z4	**Eiterådal & Jordbruelv**	570	79	87	0.0	0.0	2.0	80	9.2	2.9	419	33	182	0.2	0.1	1.3	0.5	0.3	0.1	0.9	0.2	0.1	0.1	0.0	0.2	0.9	
Z5	**Mosjøen to Fjellryggen**	450	76	674	0.1	0.0	1.8	97	9.7	3.1	514	26	79	0.4	0.1	0.9	0.9	0.7	0.2	0.5	0.3	0.1	0.4	0.0	0.2	0.6	
Z6	**Hemnes to Dunfjell**	331	66	254	0.5	0.0	5.4	81	9.0	3.6	413	23	64	0.3	0.2	1.0	0.8	0.5	0.1	0.4	0.2	0.0	0.2	0.0	0.1	0.6	
Z7	**Åkervik to Fiplingdal**	526	82	855	0.1	0.0	5.7	55	6.4	4.2	418	30	87	0.5	0.2	0.6	0.8	0.5	0.0	0.4	0.2	0.1	0.5	0.0	0.1	0.7	
Z8	**Eastern Area**	684	30	800	1.0	1.0	0.2	103	9.0	2.3	486	17	8	0.6	0.1	0.4	0.9	0.3	0.1	0.1	0.0	0.0	0.4	0.1	0.1	1.0	Jengelvatn only
Z9	**Northern Area**	113	80	0	0.0	0.0	0.2	25	5.0	10.0	250	20	1	0.0	0.0	1.0	0.0	0.0	0.0	0.0	0.0	0.0	0.0	1.0	0.0	1.0	Marmorholet only
	Totals for HNC	####	###	####	178	9	####	47276	####	###	251068	###	626	206	102	639	450	264	67	367	132	39	182	26	139	412	
	Average per cave	409	70	355	0.28	0.01	2.81	76	8.5	3.4	401	28	1	0.3	0.2	1.0	0.7	0.4	0.1	0.6	0.2	0.1	0.3	0.0	0.2	0.7	
UPPERMOST ALLOCHTHON: Rødingsfjell Nappe Complex - Nappes below the Beiarn Nappe																											
ZA	**Bleikvassli Area**	437	41	496	0.0	0.0	5.5	106	13.3	5.6	864	24	37	0.4	0.2	0.9	0.8	0.6	0.2	0.2	0.3	0.1	0.2	0.0	0.2	0.6	Excl. 1700 sq km Røssvatn
ZB	**Bjerka & Stor Akersvatn**	530	66	403	0.0	0.0	4.4	201	10.9	7.4	1047	24	7	0.7	0.1	0.7	0.6	0.3	0.1	0.3	0.1	0.0	0.3	0.1	0.3	1.0	
ZC	**Southern & Border Area**	680	122	562	0.0	0.0	2.8	101	10.6	3.2	470	29	58	0.3	0.1	0.8	0.7	0.3	0.2	0.3	0.2	0.1	0.1	0.1	0.3	0.5	
	Totals for RNC	####	###	####	2	3	####	11173	####	###	66580	###	102	39	16	84	73	42	20	28	24	7	14	5	27	58	
	Average per cave	582	58	527	0.02	0.03	3.88	110	11.6	4.3	653	27	1	0.4	0.2	0.8	0.7	0.4	0.2	0.3	0.2	0.1	0.1	0.0	0.3	0.6	
UPPER ALLOCHTHON: Køli Nappes																											
KU	**Fauske etc**	718	Upper	37	1672	0.2	0.5	6.7	77	8.4	3.5	530	26	125	0.5	0.3	0.8	0.9	0.4	0.2	0.2	0.2	0.1	0.3	0.1	0.1	0.3	
KG	**Gjersvik**		Middle																								**No known references**
KL	**Orklump / Leipikvattnet**	502	Middle	64	116	0.0	1.0	20.4	231	8.8	3.9	1204	26	29	0.4	0.2	0.7	1.0	0.7	0.4	0.2	0.3	0.0	0.2	0.1	0.3	0.2	
	Gelvenåko		Middle																								**No mapped carbonates**
KS	**Virvass / Stikke**		Middle																								**Sweden only. No caves**
KB	**Joesjø / Bjørkvatn**	860	Lower	20	150	0.0	0.5	0.3	35	7.0	2.1	71	19	2	1.0	0.0	0.5	1.0	1.0	0.0	0.0	0.0	0.0	1.0	0.0	0.0	0.5	**Sweden only**
	Totals for Køli	####	###	####	27	87	####	16432	####	###	101286	###	156	78	42	117	139	78	31	29	31	12	49	9	26	38	
	Average per cave	680	40	1363	0.17	0.56	9.17	105	8.4	3.6	649	26	1	0.5	0.3	0.8	0.9	0.5	0.2	0.2	0.2	0.1	0.3	0.1	0.2	0.2	
UPPER ALLOCHTHON: Seve Nappes																											**No known references**
MIDDLE ALLOCHTHON																											**No mapped carbonates**
LOWER ALLOCHTHON																											**No known references**
	GRAND TOTALS	####	###	####	207	99	####	74881	####	###	418934	###	884	323	160	840	662	384	118	424	187	58	245	40	192	508	
	AVERAGE PER CAVE	476	64	553	0.23	0.11	4.06	85	8.8	3.5	474	27	1	0.4	0.2	1.0	0.7	0.4	0.1	0.5	0.2	0.07	0.3	0.05	0.2	0.6	

COMBINED CENTRAL SCANDINAVIA CAVE DATABASES: SUMMARY - MINIMA

				External Cave Attributes			Internal Cave Attributes													
	ZONE	ALT.	LST. DIP	OW	CA	LENG.	VR	XS	VOL.	Min. HG %	SE	RE	DE	CS	SP	Ch	Sh	BC	RV	COMMENTS
UPPERMOST ALLOCHTHON: Helgeland Nappe Complex																				
Z1	Coastal Area	20	20	1000	0.10	4	2	2.0	11.0	18.2	0	0	1	0	0	0	0	0	0	Football pitch caves
Z2	Fjord Area	3	5	5	0.01	2	1	1.0	3.0	2.5	0	0	0	0	0	0	0	0	0	
Z3	Central Granite Area	5	31	50	0.10	2	1	1.0	2.0	5.3	0	0	0	0	0	0	0	0	0	
Z4	Eiterådal & Jordbruelv	100	45	0.3	0.01	1	1	0.5	1.0	1.3	0	0	0	0	0	0	0	0	0	
Z5	Mosjøen to Fjellryggen	55	45	10	0.10	1	1	0.5	0.5	1.7	0	0	0	0	0	0	0	0	0	
Z6	Hemnes to Dunfjell	40	31	3	0.05	3	1	0.3	1.5	1.9	0	0	0	0	0	0	0	0	0	
Z7	Åkervik to Fiplingdal	175	45	50	0.10	1	1	0.3	1.0	1.6	0	0	0	0	0	0	0	0	0	
Z8	Eastern Area	660	30	800	0.20	4	1	1.0	4.0	4.0	0	0	0	0	0	0	0	0	0	Jengelvatn only
Z9	Northern Area	113	80	0.0	0.20	25	5	10.0	250.0	20.0	0	0	1	0	0	0	0	0	0	Marmorholet only
	Minimum per cave	3	5	0.0	0.01	1	1	0.3	0.5	1.3	0	0	0	0	0	0	0	0	0	
UPPERMOST ALLOCHTHON: Rødingsfjell Nappe Complex - Nappes below the Beiarn Nappe																				
ZA	Bleikvassli Area	93	10	30	0.10	5	1	1.0	5.0	5.0	0	0	0	0	0	0	0	0	0	
ZB	Bjerka & Stor Akersvatn	402	0	20	0.10	4	3	1.0	8.0	2.2	0	0	0	0	0	0	0	0	0	
ZC	Southern & Border Area	550	20	50	0.20	2	1	0.5	1.5	0.8	0	0	0	0	0	0	0	0	0	
	Minimum per cave	93	0	20	0.10	2	1	0.5	1.5	0.8	0	0	0	0	0	0	0	0	0	
UPPER ALLOCHTHON: Kali Nappes																				
KU	Fauske etc	423 Upper	0	40	0.10	3	1	0.5	1.5	2.6	0	0	0	0	0	0	0	0	0	No known references
KG	Gjersvik	Middle																		
KL	Orklump / Leipikvattnet	460 Middle	45	50	0.80	3	1	0.5	3.0	2.6	0	0	0	0	0	0	0	0	0	No mapped carbonates
	Gelvenåko	Middle																		Sweden only. No caves
KS	Virvass / Stikke	Middle																		Sweden only
KB	Joesjø / Bjørkvatn	800 Lower	20	100	0.10	25	3	2.0	50.0	12.0	1	0	0	1	1	0	0	0	0	
	Minimum per cave	423	0	40	0.10	3	1	0.5	1.5	2.6	0	0	0	0	0	0	0	0	0	
UPPER ALLOCHTHON: Seve Nappes																				No known references
MIDDLE ALLOCHTHON																				No mapped carbonates
LOWER ALLOCHTHON																				No known references
	OVERALL MINIMA	3	0	0.0	0.01	1	1	0.3	0.5	0.8	0	0	0	0	0	0	0	0	0	

COMBINED CENTRAL SCANDINAVIA CAVE DATABASES: SUMMARY - MAXIMA

	ZONE	ALT.	LST. DIP	OW	CA	LENG.	VR	XS	VOL.	Min. HG %	SE	RE	DE	CS	SP	Ch	Sh	BC	RV	COMMENTS
		External Cave Attributes				Internal Cave Attributes														
UPPERMOST ALLOCHTHON: Helgeland Nappe Complex																				
Z1	Coastal Area	25	30	1000	0.1	11	3	15	150	50	0	0	1	0	0	0	0	0	0	Football pitch caves
Z2	Fjord Area	580	90	1200	40.0	899	53	32	5394	100	2	2	6	4	5	4	7	2	2	
Z3	Central Granite Area	680	90	700	25.0	1896	101	6	11376	100	2	1	6	4	1	2	14	3	1	
Z4	Elterådal & Jordbruselv	940	90	500	30.0	1411	78	20	16932	100	2	1	10	3	5	3	13	4	2	
Z5	Moejøen to Fjellryggen	880	90	1500	4.0	935	105	15	12000	100	2	1	4	4	15	3	13	3	2	
Z6	Hemnes to Dunfjell	515	90	3000	145.0	650	80	10	3600	100	1	1	4	2	2	2	3	2	1	
Z7	Åkervik to Fiplingdal	770	90	2500	44.0	889	30	40	13335	100	2	1	4	3	3	2	4	2	1	
Z8	Eastern Area	735	30	800	0.3	460	45	6	2760	33	1	1	1	2	2	1	1	0	0	Jengelvatn only
Z9	Northern Area	113	80	0	0.2	25	5	10	250	20	0	0	1	0	0	0	0	0	0	Marmorholet only
	Maximum per cave	940	90	3000	145.0	1896	105	40	16932	100	2	2	10	4	15	4	14	4	2	
UPPERMOST ALLOCHTHON: Rødingsfjell Nappe Complex - Nappes below the Beiarn Nappe																				
ZA	Bleikvassli Area	817	0	1500	1700.0	1400	180	28	14000	100	2	1	5	2	4	2	4	4	1	
ZB	Bjerka & Stor Akersvatn	620	0	1500	8.5	900	28	30	3270	75	3	1	2	1	1	1	1	1	0	
ZC	Southern & Border Area	900	70	2000	10.2	2600	60	30	10400	100	2	1	3	4	6	2	6	4	2	
	Maximum per cave	900	70	2000	1700.0	2600	180	30	14000	100	3	1	5	4	6	2	6	4	2	
UPPER ALLOCHTHON: Kall Nappes																				
KU	Fauske etc	926	Upper	60	30.0	1890	110	20	18500	100	3	2	10	3	8	4	9	5	6	No known references
KG	Gjersvik		Middle																	
KL	Orklump / Leipikvattnet	620	Middle	80	42.0	5600	144	16	28000	100	3	1	2	5	5	8	1	7	0	
	Gelvenåko		Middle																	No mapped carbonates
KS	Virvasa / Stikke		Middle																	Sweden only. No caves
KB	Joesja / Bjørkvatn	920	Lower	20	0.5	44	11	2	92	25	1	0	1	1	1	0	0	0	0	Sweden only
	Maximum per cave	926	80	4000	42.0	5600	144	20	28000	100	3	2	10	5	8	8	9	7	6	
UPPER ALLOCHTHON: Seve Nappes																				No known references
MIDDLE ALLOCHTHON																				No mapped carbonates
LOWER ALLOCHTHON																				No known references
	OVERALL MAXIMA	940	90	4000	1700.0	5600	180	40	28000	100	3	2	10	5	15	8	14	7	6	

sääöÅØÕ

NORTH CENTRAL NORWAY CAVE DATABASE: SUMMARY - TOTALS

	ZONE	External Cave Attributes R	T	Internal Cave Attributes LENG.	VOL.	C	SE	RE	DE	CS	SP	Ch	Sh	BC	RV	MV	DC	FS	P	COMMENTS	SHEET	PAGE
UPPERMOST ALLOCHTHON: Helgeland Nappe Complex																						
Z1	**Coastal Area**	0	0	31	195	4	0	0	4	0	0	0	0	0	0	0	0	0	4	Football pitch caves	1	1
Z2	**Fjord Area**	115	0	10886	50835	165	60	36	153	131	78	19	70	41	13	62	10	62	79		2	1 - 6
Z3	**Central Granite Area**	6	0	3320	16251	36	10	8	47	25	6	4	35	9	3	13	0	12	20		3	1 - 2
Z4	**Eiterådal & Jordbruelv**	2	0	14490	76258	182	30	15	242	93	50	20	156	35	10	16	7	38	155		4	1 - 6
Z5	**Mosjøen to Fjellryggen**	7	0	7689	40600	79	35	11	73	73	58	15	41	20	4	33	2	12	49		5	1 - 3
Z6	**Hemnes to Dunfjell**	34	1	5204	26423	64	22	12	62	49	29	5	26	13	2	14	1	7	39		6	1 - 3
Z7	**Åkervik to Fiplingdal**	6	0	4806	36368	87	44	19	54	72	41	3	38	14	7	41	4	7	57		7	1 - 3
Z8	**Eastern Area**	8	8	825	3889	8	5	1	3	7	2	1	1	0	0	3	1	1	8	Jengelvatn only	8	1
Z9	**Northern Area**	0	0	25	250	1	0	0	1	0	0	0	0	0	0	0	1	0	1	Marmorholet only	9	1
	Totals for HNC	178	9	47276	251068	626	206	102	639	450	264	67	367	132	39	182	26	139	412			
UPPERMOST ALLOCHTHON: Rødingsfjell Nappe Complex - Nappes below the Beiarn Nappe																						
ZA	**Bleikvassli Area**	2	3	3920	31976	37	15	7	35	28	22	8	8	11	3	8	0	9	24	Excl. 1700 sq km Røssvatn	10	1 - 3
ZB	**Bjerka & Stor Akersvatn**	0	0	1410	7330	7	5	1	5	4	2	1	2	1	0	2	1	2	7		11	1
ZC	**Southern & Border Area**	0	0	971	10922	18	6	5	13	13	7	2	7	9	1	3	1	4	16		12	1
	Totals for RNC	2	3	6301	50227	62	26	13	53	45	31	11	17	21	4	13	2	15	47			
UPPER ALLOCHTHON: Køli Nappes																						
KU	**Fauske etc**	0	18	4414	37445	32	15	6	22	30	27	5	6	9	3	3	2	8	18		13	1 - 2
KG	**Gjersvik**																			**No known references**	13	1
KL	**Orklump / Leipikvattnet Gelvenåko**	0	8	491	4490	8	2	1	8	7	8	1	2	3	0	3	0	4	3	Marmorgrotta etc **No mapped carbonates**	14	1
KS	**Virvass / Stikke**																			**No known references**	14	1
KB	**Joesjø / Bjørkvatn**																			**No mapped carbonates**		
	Totals for Køli	0	26	4905	41935	40	17	7	30	37	35	6	8	12	3	6	2	12	21			
UPPER ALLOCHTHON: Seve Nappes																				**No mapped carbonates**		
MIDDLE ALLOCHTHON																				**No mapped carbonates**		
LOWER ALLOCHTHON																				**No mapped carbonates**		
	GRAND TOTALS	180	38	58482	343230	728	249	122	722	532	330	84	392	165	46	201	30	166	480			

øääöÅØÖ

NORTH CENTRAL NORWAY CAVE DATABASE: SUMMARY - AVERAGES

	ZONE	ALT.	LST. DIP	OW	R	T	CA	LENG.	VR	XS	VOL.	Min. HG %	C TOT.	SE	RE	DE	CS	SP	Ch	Sh	BC	RV	MV	DC	FS	P	COMMENTS	SHEET	PAGE
		External Cave Attributes						Internal Cave Attributes																					
UPPERMOST ALLOCHTHON: Helgeland Nappe Complex																													
Z1	Coastal Area	24	23	1000	0.0	0.0	0.1	8	2.3	5.5	49	34	4	0.0	0.0	1.0	0.0	0.0	0.0	0.0	0.0	0.0	0.0	0.0	0.0	1.0	Football pitch caves	1	1
Z2	Fjord Area	182	57	244	0.7	0.0	2.0	66	7.7	3.8	308	22	165	0.4	0.2	0.9	0.8	0.5	0.1	0.4	0.2	0.1	0.4	0.1	0.4	0.5		2	1 - 6
Z3	Central Granite Area	387	50	332	0.2	0.0	2.1	92	10.3	2.2	451	36	36	0.3	0.2	1.3	0.7	0.2	0.1	1.0	0.3	0.1	0.4	0.0	0.3	0.6		3	1 - 2
Z4	Eiterådal & Jordbruelv	570	79	87	0.0	0.0	2.0	80	9.2	2.9	419	33	182	0.2	0.1	1.3	0.5	0.3	0.1	0.9	0.2	0.1	0.1	0.0	0.2	0.9		4	1 - 6
Z5	Mosjøen to Fjellryggen	450	76	674	0.1	0.0	1.8	97	9.7	3.1	514	26	79	0.4	0.1	0.9	0.9	0.7	0.2	0.5	0.3	0.1	0.4	0.0	0.2	0.6		5	1 - 3
Z6	Hemnes to Dunfjell	331	66	254	0.5	0.0	5.4	81	9.0	3.6	413	23	64	0.3	0.2	1.0	0.8	0.5	0.1	0.4	0.2	0.0	0.2	0.0	0.1	0.6		6	1 - 3
Z7	Åkervik to Fiplingdal	526	82	855	0.1	0.0	5.7	55	6.4	4.2	418	30	87	0.5	0.2	0.6	0.8	0.5	0.0	0.4	0.2	0.1	0.5	0.0	0.1	0.7		7	1 - 3
Z8	Eastern Area	684	30	800	1.0	1.0	0.2	103	9.0	2.3	486	17	8	0.6	0.1	0.4	0.9	0.3	0.1	0.1	0.0	0.0	0.4	0.1	0.1	1.0	Jengelvatn only	8	1
Z9	Northern Area	113	80	0	0.0	0.0	0.2	25	5.0	10.0	250	20	1	0.0	0.0	1.0	0.0	0.0	0.0	0.0	0.0	0.0	0.0	1.0	0.0	1.0	Marmorholet only	9	1
	Totals for HNC	####	###	####	0	178	9	####	47276	####	###	251068	####	626	206	102	639	450	264	67	367	132	39	182	26	139	412			
	Average per cave	409	70	355	0.28	0.01	2.81	76	8.5	3.4	401	28	1	0.3	0.2	1.0	0.7	0.4	0.1	0.6	0.2	0.1	0.3	0.0	0.2	0.7			
UPPERMOST ALLOCHTHON: Rødingsfjell Nappe Complex - Nappes below the Beiarn Nappe																													
ZA	Bleikvassli Area	437	41	496	0.1	0.1	5.5	(Excluding Røssva	106	13.3	5.6	864	24	37	0.4	0.2	0.9	0.8	0.6	0.2	0.2	0.3	0.1	0.2	0.0	0.2	0.6	Excl. 1700 sq km Røssva	10	1 - 3
ZB	Bjerka & Stor Akersvatn	530	66	403	0.0	0.0	4.4		201	10.9	7.4	1047	24	7	0.7	0.1	0.7	0.6	0.3	0.1	0.3	0.1	0.0	0.3	0.1	0.3	1.0		11	1
ZC	Southern & Border Area	640	50	117	0.0	0.0	3.6		54	13.9	5.4	607	45	18	0.3	0.3	0.7	0.7	0.4	0.1	0.4	0.5	0.1	0.2	0.1	0.2	0.9		12	1
	Totals for RNC	####	###	####	2	3	####	(Excluding Røss (E	6301	###	###	50227	####	62	26	13	53	45	31	11	17	21	4	13	2	15	47			
	Average per cave	507	45	375	0.03	0.05	4.8	(Excluding Røss (E	102	13.2	5.7	810	30	1	0.4	0.2	0.9	0.7	0.5	0.2	0.3	0.3	0.1	0.2	0.0	0.2	0.8			
UPPER ALLOCHTHON: Køli Nappes																													
KU	Fauske etc	578	Uppe	38	950	0.0	0.6	8.6	138	13.2	7.3	1170	24	32	0.5	0.2	0.7	0.9	0.8	0.2	0.2	0.3	0.1	0.1	0.1	0.3	0.6		13	1 - 2
KG	Gjersvik		Middle																									No known references	13	1
KL	Orklump / Leipikvattnet	480	Midd	85	388	0.0	1.0	37.3	61	3.5	5.3	561	9	8	0.3	0.1	1.0	0.9	1.0	0.1	0.3	0.4	0.0	0.4	0.0	0.5	0.4	Marmorgrotta etc	14	1
	Gelvenåko		Middle																									No mapped carbonates		
KS	Virvass / Stikke		Middle																									No known references	14	1
KB	Joesjø / Bjørkvatn		Lower																									No mapped carbonates		
	Totals for Køli	####	###	####	0	26	####	4905	###	###	41935	####	40	17	7	30	37	35	6	8	12	3	6	2	12	21			
	Average per cave	559	43	838	0.00	0.65	14.31	123	11.3	6.9	1048	21	1	0.4	0.2	0.8	0.9	0.9	0.2	0.2	0.3	0.1	0.2	0.1	0.3	0.5			
UPPER ALLOCHTHON: Seve Nappes																											No mapped carbonates		
MIDDLE ALLOCHTHON																											No mapped carbonates		
LOWER ALLOCHTHON																											No mapped carbonates		
	GRAND TOTALS	####	###	####	180	38	####	(Excluding Røsvat	58482	####	###	343230	####	728	249	122	722	532	330	84	392	165	46	201	30	166	480			
	AVERAGE PER CAVE	425	66	78	0.25	0.05	3.61	(Excluding Røsvat	80	9.0	3.8	471	28	1	0.3	0.2	1.0	0.7	0.5	0.1	0.5	0.2	0.1	0.3	0.0	0.2	0.7			

øääöÅØÖ

NORTH CENTRAL NORWAY CAVE DATABASE: SUMMARY - MINIMA

	ZONE	ALT.	LST. DIP	OW	CA	LENG.	VR	XS	VOL.	Min. HG %	SE	RE	DE	CS	SP	Ch	Sh	BC	RV	COMMENTS	SHEET	PAGE
						External Cave Attributes					Internal Cave Attributes											
UPPERMOST ALLOCHTHON: Helgeland Nappe Complex																						
Z1	**Coastal Area**	20	20	1000	0.10	4	2	2.0	11	18	0	0	1	0	0	0	0	0	0	Football pitch caves	1	1
Z2	**Fjord Area**	3	5	5	0.01	2	1	1.0	3	3	0	0	0	0	0	0	0	0	0		2	1 - 6
Z3	**Central Granite Area**	5	31	50	0.10	2	1	1.0	2	5	0	0	0	0	0	0	0	0	0		3	1 - 2
Z4	**Eiterådal & Jordbruelv**	100	45	0	0.01	1	1	0.5	1	1	0	0	0	0	0	0	0	0	0		4	1 - 7
Z5	**Mosjøen to Fjellryggen**	55	45	10	0.10	1	1	0.5	1	2	0	0	0	0	0	0	0	0	0		5	1 - 3
Z6	**Hemnes to Dunfjell**	40	31	3	0.05	3	1	0.3	2	2	0	0	0	0	0	0	0	0	0		6	1 - 3
Z7	**Åkervik to Fiplingdal**	175	45	50	0.10	1	1	0.3	1	2	0	0	0	0	0	0	0	0	0		7	1 - 3
Z8	**Eastern Area**	660	30	800	0.20	4	1	1.0	4	4	0	0	0	0	0	0	0	0	0	Jengelvatn only	8	1
Z9	**Northern Area**	113	80	0	0.20	25	5	10.0	250	20	0	0	1	0	0	0	0	0	0	Marmorhotet only	9	1
	Minimum per cave	3	5	0	0.01	1	1	0.3	1	1	0	0	0	0	0	0	0	0	0			
UPPERMOST ALLOCHTHON: Rødingsfjell Nappe Complex - Nappes below the Beiarn Nappe																						
ZA	**Bleikvassli Area**	93	10	30	0.10	5	1	1.0	5	5	0	0	0	0	0	0	0	0	0		10	1 - 3
ZB	**Bjerka & Stor Akersvatn**	402	0	20	0.10	4	3	1.0	8	2	0	0	0	0	0	0	0	0	0		11	1
ZC	**Southern & Border Area**	550	20	100	0.50	2	1	0.5	2	10	0	0	0	0	0	0	0	0	0		12	1
	Minimum per cave	93	0	20	0.10	2	1	0.5	2	2	0	0	0	0	0	0	0	0	0			
UPPER ALLOCHTHON: Køli Nappes																						
KU	**Fauske etc**	423	Upper	0	0.10	3	1	1.0	3	3	0	0	0	0	0	0	0	0	0		13	1 - 2
KG	**Gjersvik**		Middle																	**No known references**	13	1
KL	**Orklump / Leipikvattnet**	460	Middle	80	4.50	10	1	1.5	20	3	0	0	0	0	0	0	0	0	0	Marmorgrotta etc	14	1
	Geivenåko		Middle																	**No mapped carbonates**		
KS	**Virvass / Stikke**		Middle																	**No known references**	14	1
KB	**Joesjø / Bjørkvatn**		Lower																	**No mapped carbonates**		
	Minimum per cave	423		0	0.10	3	1	1.0	3	3	0	0	0	0	0	0	0	0	0			
UPPER ALLOCHTHON: Seve Nappes																				**No mapped carbonates**		
MIDDLE ALLOCHTHON																				**No mapped carbonates**		
LOWER ALLOCHTHON																				**No mapped carbonates**		
	OVERALL MINIMA	3		0	0.01	1	1	0.3	1	1	0	0	0	0	0	0	0	0	0			

sääöÅØÖ

NORTH CENTRAL NORWAY CAVE DATABASE: SUMMARY - MAXIMA

	ZONE	ALT.	LST. DIP	OW	CA	LENG.	VR	XS	VOL.	Min. HG %	SE	RE	DE	CS	SP	Ch	Sh	BC	RV	COMMENTS	SHEET	PAGE
		External Cave Attributes				Internal Cave Attributes																
	UPPERMOST ALLOCHTHON: Helgeland Nappe Complex																					
Z1	**Coastal Area**	25	30	1000	0	11	3	15	150	50	0	0	1	0	0	0	0	0	0	Football pitch caves	1	1
Z2	**Fjord Area**	580	90	1200	40	899	53	32	5394	100	2	2	6	4	5	4	7	2	2		2	1 - 6
Z3	**Central Granite Area**	680	90	700	25	1896	101	6	11376	100	2	1	6	4	1	2	14	3	1		3	1 - 2
Z4	**Elterådal & Jordbruelv**	940	90	500	30	1411	78	20	16932	100	2	1	10	3	5	3	13	4	2		4	1 - 6
Z5	**Mosjøen to Fjellryggen**	880	90	1500	4	935	105	15	12000	100	2	1	4	4	15	3	13	3	2		5	1 - 3
Z6	**Hemnes to Dunfjell**	515	90	3000	145	650	80	10	3600	100	1	1	4	2	2	2	3	2	1		6	1 - 3
Z7	**Åkervik to Fiplingdal**	770	90	2500	44	889	30	40	13335	100	2	1	4	3	3	2	4	2	1		7	1 - 3
Z8	**Eastern Area**	735	30	800	0	460	45	6	2760	33	1	1	1	2	2	1	1	0	0	Jengelvatn only	8	1
Z9	**Northern Area**	113	80	0	0	25	5	10	250	20	0	0	1	0	0	0	0	0	0	Marmorholet only	9	1
	Maximum per cave	940	90	3000	145	1896	105	40	16932	100	2	2	10	4	15	4	14	4	2			
	UPPERMOST ALLOCHTHON: Radingsfjell Nappe Complex - Nappes below the Beiarn Nappe																					
ZA	**Bleikvassli Area**	817	90	1500	1700.0	1400	180	28	14000	100	2	1	5	2	4	2	4	4	1		10	1 - 3
ZB	**Bjerka & Stor Akersvatn**	620	90	1500	8.5	900	28	30	3270	75	3	1	2	1	1	1	1	1	0		11	1
ZC	**Southern & Border Area**	800	70	200	10.2	316	60	30	6300	100	1	1	2	1	3	1	2	4	1		12	1
	Maximum per cave	817	90	1500	1700.0	1400	180	30	14000	100	3	1	5	2	4	2	4	4	1			
	UPPER ALLOCHTHON: Kali Nappes																					
KU	**Fauske etc**	750	Upper	70	1800	1890	55	20	11340	100	2	1	4	2	8	2	3	5	3		13	1 - 2
KG	**Gjersvik**		Middle																	No known references	13	1
KL	**Orklump / Leipikvattnet**	520	Middle	90	400	188	6	16	2970	20	1	1	2	1	3	1	1	3	0	Marmorgrotta etc	14	1
	Gelvenåko		Middle																	No mapped carbonates		
KS	**Virvass / Stikke**		Middle																	No known references	14	1
KB	**Joesjø / Bjørkvatn**		Lower																	No mapped carbonates		
	Maximum per cave	750		90	1800	1890	55	20	11340	100	2	1	4	2	8	2	3	5	3			
	UPPER ALLOCHTHON: Seve Nappes																			No mapped carbonates		
	MIDDLE ALLOCHTHON																			No mapped carbonates		
	LOWER ALLOCHTHON																			No mapped carbonates		
	OVERALL MAXIMA	940		90	3000	1700.0	1896	180	40	16932	100	3	2	10	4	15	4	14	5	3			

sääöÅØÕ

CENTRAL SWEDISH CALEDONIDES CAVE DATABASE SUMMARY - TOTALS

External Cave Attributes: R, T. Internal Cave Attributes: LENG., VOL., C, SE, RE, DE, CS, SP, Ch, Sh, BC, RV, MV, DC, FS, P.

	ZONE	R	T	LENG.	VOL.	C	SE	RE	DE	CS	SP	Ch	Sh	BC	RV	MV	DC	FS	P	COMMENTS	SHEET	PAGE
	UPPERMOST ALLOCHTHON: Helgeland Nappe Complex																			HNC does not occur in Sweden		
	UPPERMOST ALLOCHTHON: Rödingsfjell Nappe Complex - Nappes below the Beiarn Nappe: Zone A and Zone B																			Zones A and B do not occur in Sweden		
	UPPERMOST ALLOCHTHON: Rödingsfjell Nappe Complex - Nappes below the Beiarn Nappe: Zone C (Southern and Border Area)																					
ZC	Totals for RNC	0	0	4872	16353	40	13	3	31	28	11	9	11	3	3	1	3	12	11		1	1 - 3
	UPPER ALLOCHTHON: Køli Nappes																					
KU	Fauske etc	27	39	5237	28777	93	48	31	73	79	28	15	18	12	9	37	5	9	14		2	1 - 4
KG	Gjersvik																			Nappe does not occur in Sweden		
KL	Orklump / Leipikvattnet	0	21	6221	30432	21	11	4	13	21	13	10	3	7	0	4	2	5	2		3	2
	Gelvenåko																			No mapped carbonates	4	1
KS	Virvass / Stikke																			No caves	5	1
KB	Joesje / Bjørkvatn	0	1	69	142	2	2	0	1	2	2	0	0	0	0	2	0	0	1			
	Totals for Køli	27	61	11527	59351	116	61	35	87	102	43	25	21	19	9	43	7	14	17			
	UPPER ALLOCHTHON: Seve Nappes																			No known references	6	1
	MIDDLE ALLOCHTHON																			No mapped carbonates	6	1
	LOWER ALLOCHTHON																			No known references	6	1
	GRAND TOTALS	27	61	16399	75704	156	74	38	118	130	54	34	32	22	12	44	10	26	28			

săåõÅØÕ

CENTRAL SWEDISH CALEDONIDES CAVE DATABASE

SUMMARY - AVERAGES

ZONE	ALT.		LST. DIP	OW	R	T	CA	LENG.	VR	XS	VOL.	Min. HG %	C TOT.	SE	RE	DE	CS	SP	Ch	Sh	BC	RV	MV	DC	FS	P	COMMENTS	SHEET	PAGE
	External Cave Attributes							Internal Cave Attributes																					
UPPERMOST ALLOCHTHON: Helgeland Nappe Complex																											HNC does not occur in Sweden		
UPPERMOST ALLOCHTHON: Rödingsfjell Nappe Complex - Nappes below the Beiarn Nappe: Zone A and Zone B																											Zones A and B do not occur in Sweden		
UPPERMOST ALLOCHTHON: Rödingsfjell Nappe Complex - Nappes below the Beiarn Nappe: Zone C (Southern and Border Area)																													
ZC Totals for RNC	###		###	####	0	0	###	4872	###	###	16353	###	40	13	3	31	28	11	9	11	3	3	1	3	12	11		1	1 - 3
Average per cave	698		43	763	0.0	0.0	2.4	122	9	2.1	409	22	1	0.3	0.1	0.8	0.7	0.3	0.2	0.3	0.1	0.1	0.0	0.1	0.3	0.3			
UPPER ALLOCHTHON: Kall Nappes																													
KU Fauske etc	766	Upper	37	2248	0.3	0.8	6.1	56	7	2	309	27	93	0.5	0.3	0.8	0.8	0.3	0.2	0.2	0.1	0.1	0.4	0.1	0.1	0.2		2	1 - 4
KG Gjersvik		Middle																									Nappe does not occur in Sweden		
KL Ordump / Leipikvattnet	510	Middle	54	160	0.0	1.9	14.0	296	10.8	3.4	1449	32	21	0.5	0.2	0.6	1.0	0.6	0.5	0.1	0.3	0.0	0.2	0.1	0.2	0.1		3	2
Gelvenåko		Middle																									No mapped carbonates		
KS Virvass / Stikke		Middle																									No caves	4	1
KB Joesjø / Bjørkvatn	860	Lower	20	150	0.0	0.5	0.3	35	7.0	2.1	71	19	2	1.0	0.0	0.5	1.0	1.0	0.0	0.0	0.0	0.0	1.0	0.0	0.0	0.5		5	1
Totals for Kall	###		###	####	27	61	###	11527	###	###	59351	###	116	61	35	87	102	43	25	21	19	9	43	7	14	17			
Average per cave	721		38	1833	0.23	0.53	7.39	99	7.5	2.4	512	27	1	0.5	0.3	0.8	0.9	.0.4	0.2	0.2	0.2	0.1	0.4	0.1	0.1	0.1			
UPPER ALLOCHTHON: Seve Nappes																											No known references	6	1
MIDDLE ALLOCHTHON																											No mapped carbonates	6	1
LOWER ALLOCHTHON																											No known references	6	1
GRAND TOTALS	###		###	####	27	61	###	16399	###	###	75704	###	156	74	38	118	130	54	34	32	22	12	44	10	26	28			
AVERAGE PER CAVE	715		39	1559	0.17	0.39	6.12	105	7.9	2.4	485	26	1	0.5	0.2	0.8	0.8	0.3	0.2	0.2	0.1	0.1	0.3	0.1	0.2	0.2			

øåäöÅØÖ

CENTRAL SWEDISH CALEDONIDES CAVE DATABASE — SUMMARY - MINIMA

						External Cave Attributes				Internal Cave Attributes																				
	ZONE		ALT.			LST. DIP	OW							CA			LENG.	VR	XS	VOL.	Min. HG %	SE	RE	DE	CS	SP	Ch	Sh	BC	RV	COMMENTS	SHEET	PAGE
	UPPERMOST ALLOCHTHON: Helgeland Nappe Complex																													HNC does not occur in Sweden		
	UPPERMOST ALLOCHTHON: Rödingsfjell Nappe Complex - Nappes below the Beiarn Nappe: Zone A and Zone B																													Zones A and B do not occur in Sweden		
	UPPERMOST ALLOCHTHON: Rödingsfjell Nappe Complex - Nappes below the Beiarn Nappe: Zone C (Southern and Border Area)																															
ZC	Minima for RNC		560			35	50							0.20			4	1	1	4	1	0	0	0	0	0	0	0	0	0		1	1 - 3
	UPPER ALLOCHTHON: Kall Nappes																															
KU	Fauske etc		595			10	40							0.10			3	1	1	2	3	0	0	0	0	0	0	0	0	0	Nappe does not occur in Sweden	2	1 - 4
KG	Gjersvik																															
KL	Orklump / Leipikvattnet		475			45	50							0.80			3	1	1	3	3	0	0	0	0	0	0	0	0	0		3	2
	Geivenåko																													No mapped carbonates		
KS	Virvass / Stikke																													No caves	4	1
KB	Joesjø / Bjørkvatn		800			20	100							0.10			25	3	2	50	12	1	0	0	1	1	0	0	0	0		5	1
	Minima for Kall		475			10	40							0.10			3	1	1	2	3	0	0	0	0	0	0	0	0	0			
	UPPER ALLOCHTHON: Seve Nappes																													No known references	6	1
	MIDDLE ALLOCHTHON																													No mapped carbonates	6	1
	LOWER ALLOCHTHON																													No known references	6	1
	OVERALL MINIMA		475			10	40							0.10			3	1	1	2	1	0	0	0	0	0	0	0	0	0			

ääöÅØÖ

CENTRAL SWEDISH CALEDONIDES CAVE DATABASE — SUMMARY - MAXIMA

	ZONE	ALT. (External Cave Attributes)	LST. DIP	OW	CA	LENG. (Internal Cave Attributes)	VR	XS	VOL.	Min. HG %	SE	RE	DE	CS	SP	Ch	Sh	BC	RV	COMMENTS	SHEET	PAGE
	UPPERMOST ALLOCHTHON: Helgeland Nappe Complex																			HNC does not occur in Sweden		
	UPPERMOST ALLOCHTHON: Rödingsfjell Nappe Complex - Nappes below the Beiarn Nappe: Zone A and Zone B																			Zones A and B do not occur in Sweden		
	UPPERMOST ALLOCHTHON: Rödingsfjell Nappe Complex - Nappes below the Beiarn Nappe: Zone C (Southern and Border Area)																					
ZC	**Maxima for RNC**	900	45	2000	9	2600	45	6	10400	60	2	1	3	4	6	2	6	2	2		1	1 - 3
	UPPER ALLOCHTHON: Keli Nappes																					
KU	**Fauske etc**	926	60	4000	30	1850	110	20	18500	100	3	2	10	3	3	4	9	3	6		2	1 - 4
KG	**Gjersvik**																			Nappe does not occur in Sweden		
KL	**Orkdump / Leipikvattnet**	620	80	500	20	5600	144	10	28000	100	3	1	1	5	5	8	1	7	0		3	2
	Gelvenåko																			No mapped carbonates		
KS	**Virvass / Stikke**																			No caves	4	1
KB	**Joesjø / Bjørkvatn**	920	20	200	1	44	11	2	92	25	1	0	1	1	1	0	0	0	0		5	1
	Maxima for Keli	926	80	4000	30	5600	144	20	28000	100	3	2	10	5	5	8	9	7	6			
	UPPER ALLOCHTHON: Seve Nappes																			No known references	·6	1
	MIDDLE ALLOCHTHON																			No mapped carbonates	6	1
	LOWER ALLOCHTHON																			No known references	6	1
	OVERALL MAXIMA	926	80	4000	30	5600	144	20	28000	100	3	2	10	5	6	8	9	7	6			

sääöÅØÖ

COMBINED CENTRAL SCANDINAVIA CAVE DATABASES: SUMMARY FOR TYPES AND LOCATIONS

		NUMBERS OF CAVES																PERCENTAGES FOR EACH ZONE														
ZONE:		Z9	Z1	Z2	Z3	Z4	Z5	Z6	Z7	Z8	ZA	ZB	ZC	KU	KL	KS	KB	ALL	Z9	Z1	Z2	Z3	Z4	Z5	Z6	Z7	Z8	ZA	ZB	ZC	KU	KL	KS	KB	ALL
GLACIAL SITUATIONS	C	0	4	10	1	0	0	0	0	0	0	0	0	0	0		0	15	0%	100%	6%	3%	0%	0%	0%	0%	0%	0%	0%	0%	0%	0%		0%	1.7%
	D	0	0	13	3	0	2	4	0	0	1	0	0	0	0		0	23	0%	0%	8%	8%	0%	3%	6%	0%	0%	3%	0%	0%	0%	0%		0%	2.6%
	E	1	0	51	1	0	5	8	0	0	1	0	0	0	0		0	67	100%	0%	31%	3%	0%	6%	13%	0%	0%	3%	0%	0%	0%	0%		0%	7.6%
	G	0	0	26	0	1	0	0	3	0	0	0	0	0	0		0	30	0%	0%	16%	0%	1%	0%	0%	3%	0%	0%	0%	0%	0%	0%		0%	3.4%
	H	0	0	28	5	13	11	2	4	0	1	0	0	0	0		0	64	0%	0%	17%	14%	7%	14%	3%	5%	0%	3%	0%	0%	0%	0%		0%	7.2%
	K	0	0	17	16	1	3	19	19	0	17	7	14	5	10		0	128	0%	0%	10%	44%	1%	4%	30%	22%	0%	46%	100%	24%	4%	34%		0%	14.5%
	L	0	0	20	10	132	41	31	61	8	16	0	15	69	16		0	419	0%	0%	12%	28%	73%	52%	48%	70%	100%	43%	0%	26%	55%	55%		0%	47.4%
	S	0	0	0	0	0	0	0	0	0	1	0	4	13	0		0	18	0%	0%	0%	0%	0%	0%	0%	0%	0%	3%	0%	7%	10%	0%		0%	2.0%
	T	0	0	0	0	33	17	0	0	0	0	0	25	38	3		2	118	0%	0%	0%	0%	18%	22%	0%	0%	0%	0%	0%	43%	30%	10%		100%	13.3%
	U	0	0	0	0	2	0	0	0	0	0	0	0	0	0		0	2	0%	0%	0%	0%	1%	0%	0%	0%	0%	0%	0%	0%	0%	0%		0%	0.2%
TOTAL		1	4	165	36	182	79	64	87	8	37	7	58	125	29		2	884	100%	100%	100%	100%	100%	100%	100%	100%	100%	100%	100%	100%	100%	100%		100%	100.0%
ZONE % OF ALL		0.1	0.5	18.7	4.1	20.6	8.9	7.2	9.8	0.9	4.2	0.8	6.6	14.1	3.3		0.2	100.0																	
CAVE LOCATIONS	C	0	4	10	1	0	0	0	0	0	0	0	0	0	0		0	15	0%	100%	6%	3%	0%	0%	0%	0%	0%	0%	0%	0%	0%	0%		0%	1.7%
	F	0	0	67	4	34	32	29	20	0	12	3	2	16	26		1	246	0%	0%	41%	11%	19%	41%	45%	23%	0%	32%	43%	3%	13%	90%		50%	27.8%
	W	1	0	38	18	57	34	11	2	2	4	0	15	14	1		0	197	100%	0%	23%	50%	31%	43%	17%	2%	25%	11%	0%	26%	11%	3%		0%	22.3%
	R	0	0	16	6	35	3	2	0	0	0	0	0	0	0		0	62	0%	0%	10%	17%	19%	4%	3%	0%	0%	0%	0%	0%	0%	0%		0%	7.0%
	S	0	0	7	6	29	1	5	1	0	4	1	1	2	0		0	57	0%	0%	4%	17%	16%	1%	8%	1%	0%	11%	14%	2%	2%	0%		0%	6.4%
	G	0	0	27	1	27	9	17	58	6	17	3	18	12	2		0	197	0%	0%	16%	3%	15%	11%	27%	67%	75%	46%	43%	31%	10%	7%		0%	22.3%
	P	0	0	0	0	0	0	0	6	0	0	0	22	81	0		1	110	0%	0%	0%	0%	0%	0%	0%	7%	0%	0%	0%	38%	65%	0%		50%	12.4%
TOTAL		1	4	165	36	182	79	64	87	8	37	7	58	125	29		2	884	100%	100%	100%	100%	100%	100%	100%	100%	100%	100%	100%	100%	100%	100%		100%	100.0%
KARST TYPES	V	0	0	25	7	92	43	11	53	0	2	1	0	0	1		0	235	0%	0%	15%	19%	51%	54%	17%	61%	0%	5%	14%	0%	0%	3%		0%	26.6%
	A	0	0	115	25	88	34	49	30	0	18	4	45	44	28		0	480	0%	0%	70%	69%	48%	43%	77%	34%	0%	49%	57%	78%	35%	97%		0%	54.3%
	L	0	4	12	0	0	0	0	0	8	16	2	2	81	0		2	127	0%	100%	7%	0%	0%	0%	0%	0%	100%	43%	29%	3%	65%	0%		100%	14.4%
	C	0	0	0	0	1	0	0	1	0	0	0	1	0	0		0	3	0%	0%	0%	0%	1%	0%	0%	1%	0%	0%	0%	2%	0%	0%		0%	0.3%
	X	1	0	13	4	1	2	4	3	0	1	0	10	0	0		0	39	100%	0%	8%	11%	1%	3%	6%	3%	0%	3%	0%	17%	0%	0%		0%	4.4%
TOTAL		1	4	165	36	182	79	64	87	8	37	7	58	125	29		2	884	100%	100%	100%	100%	100%	100%	100%	100%	100%	100%	100%	100%	100%	100%		100%	100.0%
CAVE TYPES	S	0	0	9	3	32	5	5	15	0	3	0	3	12	3		0	90	0%	0%	5%	8%	18%	6%	8%	17%	0%	8%	0%	5%	10%	10%		0%	10.2%
	a	0	0	59	16	42	22	30	34	4	14	2	32	52	8		0	315	0%	0%	36%	44%	23%	28%	47%	39%	50%	38%	29%	55%	42%	28%		0%	35.6%
	b	0	0	41	8	62	32	12	22	1	4	1	9	29	8		1	230	0%	0%	25%	22%	34%	41%	19%	25%	13%	11%	14%	16%	23%	28%		50%	26.0%
	c	0	0	10	1	7	4	5	8	0	5	2	3	7	5		0	57	0%	0%	6%	3%	4%	5%	8%	9%	0%	14%	29%	5%	6%	17%		0%	6.4%
	d	0	0	11	0	13	5	3	3	2	7	1	1	8	4		1	59	0%	0%	7%	0%	7%	6%	5%	3%	25%	19%	14%	2%	6%	14%		50%	6.7%
	e	0	0	3	0	2	2	2	2	0	0	0	0	6	0		0	17	0%	0%	2%	0%	1%	3%	3%	2%	0%	0%	0%	0%	5%	0%		0%	1.9%
	f	0	0	3	3	7	2	1	3	1	1	0	2	0	0		0	23	0%	0%	2%	8%	4%	3%	2%	3%	13%	3%	0%	3%	0%	0%		0%	2.6%
	g	0	0	8	1	7	2	4	0	0	3	0	0	3	0		0	28	0%	0%	5%	3%	4%	3%	6%	0%	0%	8%	0%	0%	2%	0%		0%	3.2%
	h	0	0	9	1	9	3	2	0	0	0	0	6	8	1		0	39	0%	0%	5%	3%	5%	4%	3%	0%	0%	0%	0%	10%	6%	3%		0%	4.4%
	Hy	0	1	7	2	0	2	0	0	0	0	0	0	0	0		0	12	0%	25%	4%	6%	0%	3%	0%	0%	0%	0%	0%	0%	0%	0%		0%	1.4%
	I	0	0	0	0	0	0	0	0	0	0	1	2	0	0		0	3	0%	0%	0%	0%	0%	0%	0%	0%	0%	0%	14%	3%	0%	0%		0%	0.3%
	J	0	0	0	0	0	0	0	0	0	0	0	0	0	0		0	0	0%	0%	0%	0%	0%	0%	0%	0%	0%	0%	0%	0%	0%	0%		0%	0.0%
	L	1	3	3	0	0	0	0	0	0	0	0	0	0	0		0	7	100%	75%	2%	0%	0%	0%	0%	0%	0%	0%	0%	0%	0%	0%		0%	0.8%
	R	0	0	0	0	0	0	0	0	0	0	0	0	0	0		0	0	0%	0%	0%	0%	0%	0%	0%	0%	0%	0%	0%	0%	0%	0%		0%	0.0%
	T	0	0	2	1	1	0	0	0	0	0	0	0	0	0		0	4	0%	0%	1%	3%	1%	0%	0%	0%	0%	0%	0%	0%	0%	0%		0%	0.5%
TOTAL CAVES		1	4	165	36	182	79	64	87	8	37	7	58	125	29		2	884	100%	100%	100%	100%	100%	100%	100%	100%	100%	100%	100%	100%	100%	100%		100%	100.0%
RELICT CAVES	RC	1	4	45	15	99	15	16	19	2	11	3	22	22	5		0	279	100%	100%	27%	42%	54%	19%	25%	22%	25%	30%	43%	38%	18%	17%		0%	31.6%
MAINLY VADOSE	MV	0	0	62	13	16	33	14	41	3	8	2	4	40	7		2	245	0%	0%	38%	36%	9%	42%	22%	47%	38%	22%	29%	7%	32%	24%		100%	27.7%
COMBINATION CAVES	CC	0	0	58	8	67	31	34	27	3	16	2	32	63	17		0	360	0%	0%	35%	22%	37%	39%	59%	31%	38%	49%	29%	56%	50%	59%		0%	40.7%

COMBINED CENTRAL SCANDINAVIA CAVE DATABASES: SUMMARY FOR TYPES AND LOCATIONS

		TOTAL CAVE LENGTHS: METRES																PERCENTAGES FOR EACH ZONE															
	ZONE:	Z9	Z1	Z2	Z3	Z4	Z5	Z6	Z7	Z8	ZA	ZB	ZC	KU	KL	KS	KB	ALL	Z9	Z1	Z2	Z3	Z4	Z5	Z6	Z7	Z8	ZA	ZB	ZC	KU	KL	KS	KB	ALL
GLACIAL SITUATIONS	C	0	31	162	38	0	0	0	0	0	0	0	0	0	0		0	231	0%	100%	1%	1%	0%	0%	0%	0%	0%	0%	0%	0%	0%	0%		0%	0.3%
	D	0	0	478	80	0	10	605	0	0	20	0	0	0	0		0	1193	0%	0%	4%	2%	0%	0%	12%	0%	0%	1%	0%	0%	0%	0%		0%	1.6%
	E	25	0	4283	85	0	654	948	0	0	79	0	0	0	0		0	6074	100%	0%	39%	3%	0%	9%	18%	0%	0%	2%	0%	0%	0%	0%		0%	8.1%
	G	0	0	1449	0	5	0	0	366	0	0	0	0	0	0		0	1820	0%	0%	13%	0%	0%	0%	0%	8%	0%	0%	0%	0%	0%	0%		0%	2.4%
	H	0	0	2124	207	2683	2100	665	69	0	11	0	0	0	0		0	7859	0%	0%	20%	6%	19%	27%	13%	1%	0%	0%	0%	0%	0%	0%		0%	10.5%
	K	0	0	1525	2497	150	400	1085	971	0	2528	1410	618	140	524		0	11848	0%	0%	14%	75%	1%	5%	21%	20%	0%	64%	100%	11%	1%	8%		0%	15.8%
	L	0	0	865	413	10308	2764	1901	3400	825	582	0	3443	7253	6158		0	37912	0%	0%	8%	12%	71%	36%	37%	71%	100%	15%	0%	59%	75%	92%		0%	50.6%
	S	0	0	0	0	0	0	0	0	0	700	0	487	833	0		0	2020	0%	0%	0%	0%	0%	0%	0%	0%	0%	18%	0%	8%	9%	0%		0%	2.7%
	T	0	0	0	0	1330	1761	0	0	0	0	0	1295	1425	30		69	5910	0%	0%	0%	0%	9%	23%	0%	0%	0%	0%	0%	22%	15%	0%		100%	7.9%
	U	0	0	0	0	14	0	0	0	0	0	0	0	0	0		0	14	0%	0%	0%	0%	0%	0%	0%	0%	0%	0%	0%	0%	0%	0%		0%	0.0%
TOTAL		25	31	10886	3320	14490	7689	5204	4806	825	3920	1410	5843	9651	6712		69	74881	100%	100%	100%	100%	100%	100%	100%	100%	100%	100%	100%	100%	100%	100%		100%	100.0%
ZONE % OF ALL		0.0	0.0	14.5	4.4	19.4	10.3	6.9	6.4	1.1	5.2	1.9	7.8	12.9	9.0		0.1	100.0																	
CAVE LOCATIONS	C	0	31	162	38	0	0	0	0	0	0	0	0	0	0		0	231	0%	100%	1%	1%	0%	0%	0%	0%	0%	0%	0%	0%	0%	0%		0%	0.3%
	F	0	0	3320	131	5084	1345	1852	720	0	464	380	8	3326	6644		44	23300	0%	0%	30%	4%	35%	17%	36%	15%	0%	12%	27%	0%	34%	99%		64%	31.1%
	W	25	0	2472	1043	2428	3421	1135	90	280	100	0	897	1082	35		0	13008	100%	0%	23%	31%	17%	44%	22%	2%	34%	3%	0%	15%	11%	1%		0%	17.4%
	R	0	0	1520	1930	2841	919	620	0	0	0	0	0	0	0		0	7830	0%	0%	14%	58%	20%	12%	12%	0%	0%	0%	0%	0%	0%	0%		0%	10.5%
	S	0	0	1043	170	1227	15	933	50	0	2205	4	26	230	0		0	5903	0%	0%	10%	5%	8%	0%	18%	1%	0%	56%	0%	0%	2%	0%		0%	7.9%
	G	0	0	2369	8	2930	1989	664	3629	545	1151	1026	1061	337	33		0	15742	0%	0%	22%	0%	20%	26%	13%	76%	66%	29%	73%	18%	3%	0%		0%	21.0%
	P	0	0	0	0	0	0	0	317	0	0	0	3851	4674	0		25	8867	0%	0%	0%	0%	0%	0%	0%	7%	0%	0%	0%	66%	48%	0%		36%	11.8%
TOTAL		25	31	10886	3320	14490	7689	5204	4806	825	3920	1410	5843	9651	6712		69	74881	100%	100%	100%	100%	100%	100%	100%	100%	100%	100%	100%	100%	100%	100%		100%	100.0%
KARST TYPES	V	0	0	1355	2291	7345	5206	1452	2340	0	55	17	0	0	186		0	20249	0%	0%	12%	69%	51%	68%	28%	49%	0%	1%	1%	0%	0%	3%		0%	27.0%
	A	0	0	7085	824	6790	2463	3511	2159	0	636	489	3011	4312	6524		0	37786	0%	0%	65%	25%	47%	32%	67%	45%	0%	16%	35%	52%	45%	97%		0%	50.5%
	L	0	31	2117	0	0	0	0	0	825	3217	904	135	5339	0		69	12637	0%	100%	19%	0%	0%	0%	0%	0%	100%	82%	64%	2%	55%	0%		100%	16.9%
	C	0	0	0	0	205	0	0	100	0	0	0	2800	0	0		0	2905	0%	0%	0%	0%	1%	0%	0%	2%	0%	0%	0%	44%	0%	0%		0%	3.9%
	X	25	0	349	205	150	20	241	207	0	10	0	97	0	0		0	1304	100%	0%	3%	6%	1%	0%	5%	4%	0%	0%	0%	2%	0%	0%		0%	1.7%
TOTAL		25	31	10886	3320	14490	7689	5204	4806	825	3920	1410	5843	9651	6712		69	74881	100%	100%	100%	100%	100%	100%	100%	100%	100%	100%	100%	100%	100%	100%		100%	100.0%
CAVE TYPES	S	0	0	96	58	355	40	29	162	0	20	0	15	138	21		0	934	0%	0%	1%	2%	2%	1%	1%	3%	0%	1%	0%	0%	1%	0%		0%	1.2%
	a	0	0	1081	290	1029	705	857	956	30	296	37	620	1014	151		0	7046	0%	0%	10%	9%	7%	9%	16%	20%	4%	8%	3%	11%	11%	2%		0%	9.4%
	b	0	0	1963	256	2307	1781	1005	1267	30	222	109	507	1858	251		44	11600	0%	0%	18%	8%	16%	23%	19%	26%	4%	6%	8%	9%	19%	4%		64%	15.5%
	c	0	0	738	10	1584	293	486	803	0	434	904	205	518	426		0	6401	0%	0%	7%	0%	11%	4%	9%	17%	0%	11%	64%	4%	5%	6%		0%	8.5%
	d	0	0	1021	0	1079	944	965	1096	515	1205	150	140	357	263		25	7760	0%	0%	9%	0%	7%	12%	19%	23%	62%	31%	11%	2%	4%	4%		36%	10.4%
	e	0	0	986	0	346	122	85	130	0	0	0	0	534	0		0	2203	0%	0%	9%	0%	2%	2%	2%	3%	0%	0%	0%	0%	6%	0%		0%	2.9%
	f	0	0	457	372	1246	305	233	392	250	60	0	95	0	0		0	3410	0%	0%	4%	11%	9%	4%	4%	8%	30%	2%	0%	2%	0%	0%		0%	4.6%
	g	0	0	1257	372	1434	743	1064	0	0	1683	0	0	475	0		0	7028	0%	0%	12%	11%	10%	10%	20%	0%	0%	43%	0%	0%	5%	0%		0%	9.4%
	h	0	0	2859	1896	5038	2596	480	0	0	0	0	4196	4757	5600		0	27422	0%	0%	26%	57%	35%	34%	9%	0%	0%	0%	0%	72%	49%	83%		0%	36.6%
	Hy	0	6	380	60	0	160	0	0	0	0	0	0	0	0		0	606	0%	19%	3%	2%	0%	2%	0%	0%	0%	0%	0%	0%	0%	0%		0%	0.8%
	I	0	0	0	0	0	0	0	0	0	0	210	65	0	0		0	275	0%	0%	0%	0%	0%	0%	0%	0%	0%	0%	15%	1%	0%	0%		0%	0.4%
	J	0	0	0	0	0	0	0	0	0	0	0	0	0	0		0	0	0%	0%	0%	0%	0%	0%	0%	0%	0%	0%	0%	0%	0%	0%		0%	0.0%
	L	25	25	32	0	0	0	0	0	0	0	0	0	0	0		0	82	100%	82%	0%	0%	0%	0%	0%	0%	0%	0%	0%	0%	0%	0%		0%	0.1%
	R	0	0	0	0	0	0	0	0	0	0	0	0	0	0		0	0	0%	0%	0%	0%	0%	0%	0%	0%	0%	0%	0%	0%	0%	0%		0%	0.0%
	T	0	0	36	6	72	0	0	0	0	0	0	0	0	0		0	114	0%	0%	0%	0%	0%	0%	0%	0%	0%	0%	0%	0%	0%	0%		0%	0.2%
TOTAL CAVES		25	31	10886	3320	14490	7689	5204	4806	825	3920	1410	5843	9651	6712		69	74881	100%	100%	100%	100%	100%	100%	100%	100%	100%	100%	100%	100%	100%	100%		100%	100.0%
RELICT CAVES	RC	25	31	1696	413	3104	417	387	365	14	879	1114	361	489	120		0	9417	100%	100%	16%	12%	21%	5%	7%	8%	2%	22%	79%	6%	5%	2%		0%	12.6%
MAINLY VADOSE	MV	0	0	1653	222	210	1416	297	1241	71	167	170	47	773	133		69	6469	0%	0%	15%	7%	1%	18%	6%	26%	9%	4%	12%	1%	8%	2%		100%	8.6%
COMBINATION CAVES	CC	0	0	7535	2685	11176	5856	4520	3200	740	2874	126	5435	8389	6459		0	58995	0%	0%	69%	81%	77%	76%	87%	67%	90%	73%	9%	93%	87%	96%		0%	78.8%

COMBINED CENTRAL SCANDINAVIA CAVE DATABASES:

SUMMARY FOR TYPES AND LOCATIONS

		MEAN CAVE LENGTHS: METRES																
	ZONE:	Z9	Z1	Z2	Z3	Z4	Z5	Z6	Z7	Z8	ZA	ZB	ZC	KU	KL	KS	KB	ALL	No.
No. of caves		1	4	165	36	182	79	64	87	8	37	7	58	125	29		0		884
GLACIAL	C		8	16	38													15	15
SITUATIONS	D			37	27		5	151			20							52	23
	E	25		84	85		131	119			79							91	67
	G			56		5			122									61	30
	H			76	41	206	191	333	17		11							123	64
	K			90	156	150	133	57	51		149	201	44	28	52			93	128
	L			43	41	78	67	61	56	103	36		230	105	385			90	419
	S										700		122	64				112	18
	T					40	104						52	38	10		35	50	118
	U					7												7	2
TOTAL MEAN		25	8	66	92	80	97	81	55	103	106	201	101	77	231		35	85	884
CAVE	C		8	16	38													15	15
LOCATIONS	F			50	33	149	42	64	36		39	127	4	208	256		44	95	246
	W	25		65	58	43	101	103	45	140	25		60	77	35			66	197
	R			95	322	81	306	310										126	62
	S			149	28	42	15	187	50		551	4	26	115				104	57
	G			86	8	109	221	39	63	91	68	342	59	28	17			80	197
	P								53				175	58			25	81	110
TOTAL MEAN		25	8	66	92	80	97	81	55	103	106	201	101	77	231		35	85	884
KARST	V			54	327	80	121	132	44		28	17			188			86	235
TYPES	A			61	33	77	72	72	72		35	122	67	98	233			79	480
	L		8	176						103	201	452	68	66			35	100	127
	C					205			100				2600					966	3
	X	25		27	51	150	10	60	69		10		10					33	39
TOTAL MEAN		25	8	66	92	80	97	81	55	103	106	201	101	77	231		35	85	884
CAVE	S			11	19	11	8	6	11		7		5	12	7			10	90
TYPES	a			18	18	25	32	29	28	8	21	19	19	20	19			22	315
	b			48	32	37	56	84	58	30	56	109	56	64	31		44	50	230
	c			74	10	226	73	97	100		87	452	68	74	85			112	57
	d			93		83	189	322	365	258	172	150	140	45	66		25	132	59
	e			329		173	61	43	65					89				130	17
	f			152	124	178	153	233	131	250	60		48					148	23
	g			157	372	205	372	266			561			158				251	28
	h			318	1898	560	865	240					699	595	5600			703	39
	Hy		6	54	30		80											50	12
	I											210	33					92	3
	J																		0
	L	25	8	11														12	7
	R																		0
	T			18	8	72												29	4
TOTAL MEAN		25	8	66	92	80	97	81	55	103	106	201	101	77	231		35	85	884
RELICT CAVES	RC	25	8	38	28	31	28	24	19	7	80	371	16	22	24			34	279
MAINLY VADOSE	MV			27	17	13	43	21	30	24	21	85	12	19	19		35	26	245
COMBINATION CAVES	CC			130	336	167	180	133	119	247	160	63	170	133	380			164	380

NORTH CENTRAL NORWAY CAVE DATABASE: SUMMARY FOR TYPES AND LOCATIONS

		NUMBERS OF CAVES																PERCENTAGES FOR EACH ZONE															
ZONE:		Z9	Z1	Z2	Z3	Z4	Z5	Z6	Z7	Z8	ZA	ZB	ZC	KU	KL	KS	KB	ALL	Z9	Z1	Z2	Z3	Z4	Z5	Z6	Z7	Z8	ZA	ZB	ZC	KU	KL	KS	KB	ALL
GLACIAL SITUATIONS	C	0	4	10	1	0	0	0	0	0	0	0	0	0	0			15	0%	100%	6%	3%	0%	0%	0%	0%	0%	0%	0%	0%	0%	0%				2.1%
	D	0	0	13	3	0	2	4	0	0	1	0	0	0	0			23	0%	0%	8%	8%	0%	3%	6%	0%	0%	3%	0%	0%	0%	0%				3.2%
	E	1	0	51	1	0	5	8	0	0	1	0	0	0	0			67	100%	0%	31%	3%	0%	6%	13%	0%	0%	3%	0%	0%	0%	0%				9.2%
	G	0	0	26	0	1	0	0	3	0	0	0	0	0	0			30	0%	0%	16%	0%	1%	0%	0%	3%	0%	0%	0%	0%	0%	0%				4.1%
	H	0	0	28	5	13	11	2	4	0	1	0	0	0	0			64	0%	0%	17%	14%	7%	14%	3%	5%	0%	3%	0%	0%	0%	0%				8.8%
	K	0	0	17	16	1	3	19	19	0	17	7	14	5	8			126	0%	0%	10%	44%	1%	4%	30%	22%	0%	46%	100%	78%	16%	100%				17.3%
	L	0	0	20	10	132	41	31	61	8	16	0	1	25	0			345	0%	0%	12%	28%	73%	52%	48%	70%	100%	43%	0%	6%	78%	0%				47.4%
	S	0	0	0	0	0	0	0	0	0	1	0	3	2	0			6	0%	0%	0%	0%	0%	0%	0%	0%	0%	3%	0%	17%	6%	0%				0.8%
	T	0	0	0	0	33	17	0	0	0	0	0	0	0	0			50	0%	0%	0%	0%	18%	22%	0%	0%	0%	0%	0%	0%	0%	0%				6.9%
	U	0	0	0	0	2	0	0	0	0	0	0	0	0	0			2	0%	0%	0%	0%	1%	0%	0%	0%	0%	0%	0%	0%	0%	0%				0.3%
TOTAL		1	4	165	36	182	79	64	87	8	37	7	18	32	8			728	100%	100%	100%	100%	100%	100%	100%	100%	100%	100%	100%	100%	100%	100%				100.0%
ZONE % OF ALL		0.1	0.5	22.7	4.9	25.0	10.9	8.8	12.0	1.1	5.1	1.0	2.5	4.4	1.1			100.0																	
CAVE LOCATIONS	C	0	4	10	1	0	0	0	0	0	0	0	0	0	0			15	0%	100%	6%	3%	0%	0%	0%	0%	0%	0%	0%	0%	0%	0%				2.1%
	F	0	0	67	4	34	32	29	20	0	12	3	2	16	8			227	0%	0%	41%	11%	19%	41%	45%	23%	0%	32%	43%	11%	50%	100%				31.2%
	W	1	0	38	18	57	34	11	2	2	4	0	4	9	0			180	100%	0%	23%	50%	31%	43%	17%	2%	25%	11%	0%	22%	28%	0%				24.7%
	R	0	0	16	6	35	3	2	0	0	0	0	0	0	0			62	0%	0%	10%	17%	19%	4%	3%	0%	0%	0%	0%	0%	0%	0%				8.5%
	S	0	0	7	6	29	1	5	1	0	4	1	1	2	0			57	0%	0%	4%	17%	16%	1%	8%	1%	0%	11%	14%	6%	6%	0%				7.8%
	G	0	0	27	1	27	9	17	58	6	17	3	11	5	0			181	0%	0%	16%	3%	15%	11%	27%	67%	75%	46%	43%	61%	16%	0%				24.9%
	P	0	0	0	0	0	0	0	6	0	0	0	0	0	0			6	0%	0%	0%	0%	0%	0%	0%	7%	0%	0%	0%	0%	0%	0%				0.8%
TOTAL		1	4	165	36	182	79	64	87	8	37	7	18	32	8			728	100%	100%	100%	100%	100%	100%	100%	100%	100%	100%	100%	100%	100%	100%				100.0%
KARST TYPES	V	0	0	25	7	92	43	11	53	0	2	1	0	0	1			235	0%	0%	15%	19%	51%	54%	17%	61%	0%	5%	14%	0%	0%	13%				32.3%
	A	0	0	115	25	88	34	49	30	0	18	4	11	20	7			401	0%	0%	70%	69%	48%	43%	77%	34%	0%	49%	57%	61%	63%	88%				55.1%
	L	0	4	12	0	0	0	0	0	8	16	2	2	12	0			56	0%	100%	7%	0%	0%	0%	0%	0%	100%	43%	29%	11%	38%	0%				7.7%
	C	0	0	0	0	1	0	0	1	0	0	0	0	0	0			2	0%	0%	0%	0%	1%	0%	0%	1%	0%	0%	0%	0%	0%	0%				0.3%
	X	1	0	13	4	1	2	4	3	0	1	0	5	0	0			34	100%	0%	8%	11%	1%	3%	6%	3%	0%	3%	0%	28%	0%	0%				4.7%
TOTAL		1	4	165	36	182	79	64	87	8	37	7	18	32	8			728	100%	100%	100%	100%	100%	100%	100%	100%	100%	100%	100%	100%	100%	100%				100.0%
CAVE TYPES	S	0	0	9	3	32	5	5	15	0	3	0	3	1	0			76	0%	0%	5%	8%	18%	6%	8%	17%	0%	8%	0%	17%	3%	0%				10.4%
	a	0	0	59	16	42	22	30	34	4	14	2	7	9	2			241	0%	0%	36%	44%	23%	28%	47%	39%	50%	38%	29%	39%	28%	25%				33.1%
	b	0	0	41	8	62	32	12	22	1	4	1	3	14	0			200	0%	0%	25%	22%	34%	41%	19%	25%	13%	11%	14%	17%	44%	0%				27.5%
	c	0	0	10	1	7	4	5	8	0	5	2	2	1	2			47	0%	0%	6%	3%	4%	5%	8%	9%	0%	14%	29%	11%	3%	25%				6.5%
	d	0	0	11	0	13	5	3	3	2	7	1	0	2	4			51	0%	0%	7%	0%	7%	6%	5%	3%	25%	19%	14%	0%	6%	50%				7.0%
	e	0	0	3	0	2	2	2	2	0	0	0	0	2	0			13	0%	0%	2%	0%	1%	3%	3%	2%	0%	0%	0%	0%	6%	0%				1.8%
	f	0	0	3	3	7	2	1	3	1	1	0	0	0	0			21	0%	0%	2%	8%	4%	3%	2%	3%	13%	3%	0%	0%	0%	0%				2.9%
	g	0	0	8	1	7	2	4	0	0	3	0	0	1	0			26	0%	0%	5%	3%	4%	3%	6%	0%	0%	8%	0%	0%	3%	0%				3.6%
	h	0	0	9	1	9	3	2	0	0	0	0	1	2	0			27	0%	0%	5%	3%	5%	4%	3%	0%	0%	0%	0%	6%	6%	0%				3.7%
	Hy	0	1	7	2	0	2	0	0	0	0	0	0	0	0			12	0%	25%	4%	6%	0%	3%	0%	0%	0%	0%	0%	0%	0%	0%				1.6%
	I	0	0	0	0	0	0	0	0	0	0	1	2	0	0			3	0%	0%	0%	0%	0%	0%	0%	0%	0%	0%	14%	11%	0%	0%				0.4%
	J	0	0	0	0	0	0	0	0	0	0	0	0	0	0			0	0%	0%	0%	0%	0%	0%	0%	0%	0%	0%	0%	0%	0%	0%				0.0%
	L	1	3	3	0	0	0	0	0	0	0	0	0	0	0			7	100%	75%	2%	0%	0%	0%	0%	0%	0%	0%	0%	0%	0%	0%				1.0%
	R	0	0	0	0	0	0	0	0	0	0	0	0	0	0			0	0%	0%	0%	0%	0%	0%	0%	0%	0%	0%	0%	0%	0%	0%				0.0%
	T	0	0	2	1	1	0	0	0	0	0	0	0	0	0			4	0%	0%	1%	3%	1%	0%	0%	0%	0%	0%	0%	0%	0%	0%				0.5%
TOTAL CAVES		1	4	165	36	182	79	64	87	8	37	7	18	32	8			728	100%	100%	100%	100%	100%	100%	100%	100%	100%	100%	100%	100%	100%	100%				100.0%
RELICT CAVES	RC	1	4	45	15	99	15	16	19	2	11	3	5	3	1			239	100%	100%	27%	42%	54%	19%	25%	22%	25%	30%	43%	28%	9%	13%				32.8%
MAINLY VADOSE	MV	0	0	62	13	16	33	14	41	3	8	2	3	3	3			201	0%	0%	38%	36%	9%	42%	22%	47%	38%	22%	29%	17%	9%	38%				27.6%
COMBINATION CAVES	CC	0	0	58	8	67	31	34	27	3	18	2	10	26	4			288	0%	0%	35%	22%	37%	39%	53%	31%	38%	49%	29%	58%	81%	50%				39.6%

NORTH CENTRAL NORWAY CAVE DATABASE: SUMMARY FOR TYPES AND LOCATIONS

		TOTAL CAVE LENGTHS: METRES															PERCENTAGES FOR EACH ZONE														
ZONE:		Z9	Z1	Z2	Z3	Z4	Z5	Z6	Z7	Z8	ZA	ZB	ZC	KU	KL	KS	KB	ALL	Z9	Z1	Z2	Z3	Z4	Z5	Z6	Z7	Z8	ZA	ZB	ZC	KU	KL	KS	KB	ALL
GLACIAL SITUATIONS	C	0	31	162	38	0	0	0	0	0	0	0	0	0	0			231	0%	100%	1%	1%	0%	0%	0%	0%	0%	0%	0%	0%	0%	0%			0.4%
	D	0	0	478	80	0	10	605	0	0	20	0	0	0	0			1193	0%	0%	4%	2%	0%	0%	12%	0%	0%	1%	0%	0%	0%	0%			2.0%
	E	25	0	4283	85	0	654	948	0	0	79	0	0	0	0			6074	100%	0%	39%	3%	0%	9%	18%	0%	0%	2%	0%	0%	0%	0%			10.4%
	G	0	0	1449	0	5	0	0	366	0	0	0	0	0	0			1820	0%	0%	13%	0%	0%	0%	0%	8%	0%	0%	0%	0%	0%	0%			3.1%
	H	0	0	2124	207	2683	2100	665	69	0	11	0	0	0	0			7859	0%	0%	20%	6%	19%	27%	13%	1%	0%	0%	0%	0%	0%	0%			13.4%
	K	0	0	1525	2497	150	400	1085	971	0	2528	1410	618	140	491			11815	0%	0%	14%	75%	1%	5%	21%	20%	0%	64%	100%	84%	3%	100%			20.2%
	L	0	0	865	413	10308	2764	1901	3400	825	582	0	6	4044	0			25108	0%	0%	8%	12%	71%	36%	37%	71%	100%	15%	0%	1%	92%	0%			42.9%
	S	0	0	0	0	0	0	0	0	0	700	0	347	230	0			1277	0%	0%	0%	0%	0%	0%	0%	0%	0%	18%	0%	36%	5%	0%			2.2%
	T	0	0	0	0	1330	1761	0	0	0	0	0	0	0	0			3091	0%	0%	0%	0%	9%	23%	0%	0%	0%	0%	0%	0%	0%	0%			5.3%
	U	0	0	0	0	14	0	0	0	0	0	0	0	0	0			14	0%	0%	0%	0%	0%	0%	0%	0%	0%	0%	0%	0%	0%	0%			0.0%
TOTAL		25	31	10686	3320	14490	7689	5204	4806	825	3920	1410	971	4414	491			58482	100%	100%	100%	100%	100%	100%	100%	100%	100%	100%	100%	100%	100%	100%			100.0%
ZONE % OF ALL		0.0	0.1	18.6	5.7	24.8	13.1	8.9	8.2	1.4	6.7	2.4	1.7	7.5	0.8			100.0																	
CAVE LOCATIONS	C	0	31	162	38	0	0	0	0	0	0	0	0	0	0			231	0%	100%	1%	1%	0%	0%	0%	0%	0%	0%	0%	0%	0%	0%			0.4%
	F	0	0	3320	131	5084	1345	1852	720	0	464	380	8	3328	491			17103	0%	0%	30%	4%	35%	17%	36%	15%	0%	12%	27%	1%	75%	100%			29.2%
	W	25	0	2472	1043	2428	3421	1135	90	280	100	0	17	714	0			11725	100%	0%	23%	31%	17%	44%	22%	2%	34%	3%	0%	2%	16%	0%			20.0%
	R	0	0	1520	1930	2841	919	620	0	0	0	0	0	0	0			7830	0%	0%	14%	58%	20%	12%	12%	0%	0%	0%	0%	0%	0%	0%			13.4%
	S	0	0	1043	170	1227	15	933	50	0	2205	4	26	230	0			5903	0%	0%	10%	5%	8%	0%	18%	1%	0%	56%	0%	3%	5%	0%			10.1%
	G	0	0	2369	8	2930	1989	664	3629	545	1151	1026	920	142	0			15373	0%	0%	22%	0%	20%	26%	13%	76%	66%	29%	73%	95%	3%	0%			26.3%
	P	0	0	0	0	0	0	0	317	0	0	0	0	0	0			317	0%	0%	0%	0%	0%	0%	0%	7%	0%	0%	0%	0%	0%	0%			0.5%
TOTAL		25	31	10686	3320	14490	7689	5204	4806	825	3920	1410	971	4414	491			58482	100%	100%	100%	100%	100%	100%	100%	100%	100%	100%	100%	100%	100%	100%			100.0%
KARST TYPES	V	0	0	1355	2291	7345	5206	1452	2340	0	55	17	0	0	188			20249	0%	0%	12%	69%	51%	68%	28%	49%	0%	1%	1%	0%	0%	38%			34.6%
	A	0	0	7065	824	6790	2463	3511	2159	0	638	489	813	3254	303			28309	0%	0%	65%	25%	47%	32%	67%	45%	0%	16%	35%	84%	74%	62%			48.4%
	L	0	31	2117	0	0	0	0	0	825	3217	904	135	1160	0			8389	0%	100%	19%	0%	0%	0%	0%	0%	100%	82%	64%	14%	26%	0%			14.3%
	C	0	0	0	0	205	0	0	100	0	0	0	0	0	0			305	0%	0%	0%	0%	1%	0%	0%	2%	0%	0%	0%	0%	0%	0%			0.5%
	X	25	0	349	205	150	20	241	207	0	10	0	23	0	0			1230	100%	0%	3%	6%	1%	0%	5%	4%	0%	0%	0%	2%	0%	0%			2.1%
TOTAL		25	31	10686	3320	14490	7689	5204	4806	825	3920	1410	971	4414	491			58482	100%	100%	100%	100%	100%	100%	100%	100%	100%	100%	100%	100%	100%	100%			100.0%
CAVE TYPES	S	0	0	96	58	355	40	29	162	0	20	0	15	30	0			805	0%	0%	1%	2%	2%	1%	1%	3%	0%	1%	0%	2%	1%	0%			1.4%
	a	0	0	1061	290	1029	705	857	956	30	296	37	133	360	50			5804	0%	0%	10%	9%	7%	9%	16%	20%	4%	8%	3%	14%	8%	10%			9.9%
	b	0	0	1963	256	2307	1781	1005	1267	30	222	109	297	1244	0			10481	0%	0%	18%	8%	16%	23%	19%	26%	4%	6%	8%	31%	28%	0%			17.9%
	c	0	0	738	10	1584	293	486	803	0	434	904	145	260	178			5835	0%	0%	7%	0%	11%	4%	9%	17%	0%	11%	64%	15%	6%	36%			10.0%
	d	0	0	1021	0	1079	944	965	1096	515	1205	150	0	111	263			7349	0%	0%	9%	0%	7%	12%	19%	23%	62%	31%	11%	0%	3%	54%			12.6%
	e	0	0	986	0	346	122	85	130	0	0	0	0	230	0			1899	0%	0%	9%	0%	2%	2%	2%	3%	0%	0%	0%	0%	5%	0%			3.2%
	f	0	0	457	372	1246	305	233	392	250	60	0	0	0	0			3315	0%	0%	4%	11%	9%	4%	4%	8%	30%	2%	0%	0%	0%	0%			5.7%
	g	0	0	1257	372	1434	743	1084	0	0	1683	0	0	12	0			6565	0%	0%	12%	11%	10%	10%	20%	0%	0%	43%	0%	0%	0%	0%			11.2%
	h	0	0	2859	1898	5038	2596	480	0	0	0	0	316	2167	0			15352	0%	0%	26%	57%	35%	34%	9%	0%	0%	0%	0%	33%	49%	0%			26.3%
	Hy	0	6	380	60	0	160	0	0	0	0	0	0	0	0			606	0%	18%	3%	2%	0%	2%	0%	0%	0%	0%	0%	0%	0%	0%			1.0%
	I	0	0	0	0	0	0	0	0	0	0	210	65	0	0			275	0%	0%	0%	0%	0%	0%	0%	0%	0%	0%	15%	7%	0%	0%			0.5%
	J	0	0	0	0	0	0	0	0	0	0	0	0	0	0			0	0%	0%	0%	0%	0%	0%	0%	0%	0%	0%	0%	0%	0%	0%			0.0%
	L	25	25	32	0	0	0	0	0	0	0	0	0	0	0			82	100%	82%	0%	0%	0%	0%	0%	0%	0%	0%	0%	0%	0%	0%			0.1%
	R	0	0	0	0	0	0	0	0	0	0	0	0	0	0			0	0%	0%	0%	0%	0%	0%	0%	0%	0%	0%	0%	0%	0%	0%			0.0%
	T	0	0	36	6	72	0	0	0	0	0	0	0	0	0			114	0%	0%	0%	0%	0%	0%	0%	0%	0%	0%	0%	0%	0%	0%			0.2%
TOTAL CAVES		25	31	10686	3320	14490	7689	5204	4806	825	3920	1410	971	4414	491			58482	100%	100%	100%	100%	100%	100%	100%	100%	100%	100%	100%	100%	100%	100%			100.0%
RELICT CAVES	RC	25	31	1698	413	3104	417	387	365	14	879	1114	90	155	70			8762	100%	100%	16%	12%	21%	5%	7%	8%	2%	22%	79%	9%	4%	14%			15.0%
MAINLY VADOSE	MV	0	0	1653	222	210	1416	297	1241	71	167	170	36	18	60			5561	0%	0%	15%	7%	1%	18%	6%	26%	9%	4%	12%	4%	0%	12%			9.5%
COMBINATION CAVES	CC	0	0	7535	2685	11176	5656	4520	3200	740	2874	126	845	4241	361			44159	0%	0%	69%	81%	77%	76%	87%	67%	90%	73%	9%	87%	96%	74%			75.5%

NORTH CENTRAL NORWAY CAVE DATABASE: SUMMARY FOR TYPES AND LOCATIONS

		MEAN CAVE LENGTHS: METRES																
	ZONE:	Z9	Z1	Z2	Z3	Z4	Z5	Z6	Z7	Z8	ZA	ZB	ZC	KU	KL	KS	KB	ALL	No.
No. of caves		1	4	165	36	182	79	64	87	8	37	7	18	32	8	0	0		728
GLACIAL	C		8	16	38													15	15
SITUATIONS	D			37	27		5	151			20							52	23
	E	25		84	85		131	119			79							91	67
	G			56		5			122									61	30
	H			76	41	206	191	333	17		11							123	64
	K			90	156	150	133	57	51		149	201	44	28	61			94	126
	L			43	41	78	67	61	56	103	36		6	162				73	345
	S										700		116	115				213	6
	T					40	104											62	50
	U					7												7	2
TOTAL MEAN		25	8	66	92	80	97	81	55	103	106	201	54	138	61			80	728
CAVE	C		8	16	38													15	15
LOCATIONS	F			50	33	149	42	64	36		39	127	4	208	61			75	227
	W	25		65	58	43	101	103	45	140	25		4	79				65	180
	R			95	322	81	306	310										126	62
	S			149	28	42	15	187	50		551	4	26	115				104	57
	G			88	8	109	221	39	63	91	68	342	84	28				85	181
	P								53									53	6
TOTAL MEAN		25	8	66	92	80	97	81	55	103	106	201	54	138	61			80	728
KARST	V			54	327	80	121	132	44		28	17			188			86	235
TYPES	A			61	33	77	72	72	72		35	122	74	163	43			71	401
	L		8	176						103	201	452	68	97				150	56
	C					205			100									153	2
	X	25		27	51	150	10	60	69		10		5					36	34
TOTAL MEAN		25	8	66	92	80	97	81	55	103	106	201	54	138	61			80	728
CAVE	S			11	19	11	8	6	11		7		5	30				11	76
TYPES	a			18	18	25	32	29	28	8	21	19	19	40	25			24	241
	b			48	32	37	56	84	58	30	56	109	99	89				52	200
	c			74	10	226	73	97	100		87	452	73	260	89			124	47
	d			93		83	189	322	365	258	172	150		56	66			144	51
	e			329		173	61	43	65					115				146	13
	f			152	124	178	153	233	131	250	60							158	21
	g			157	372	205	372	266			561			12				253	26
	h			318	1896	560	865	240					316	1084				569	27
	Hy											210	33					50	12
	I											210	33					92	3
	J																		0
	L	25	8	11														12	7
	R																		0
	T			18	6	72												29	4
TOTAL MEAN		25	8	66	92	80	97	81	55	103	106	201	54	138	61			80	728
RELICT CAVES	RC	25	8	38	28	31	28	24	19	7	80	371	18	52	70			37	239
MAINLY VADOSE	MV			27	17	13	43	21	30	24	21	85	12	6	20			28	201
COMBINATION CAVES	CC			130	336	167	189	133	119	247	160	63	85	163	90			153	288

ssâsÀØÖ

CENTRAL SWEDISH CALEDONIDES CAVE DATABASE: SUMMARY FOR TYPES AND LOCATIONS

		NUMBERS OF CAVES																PERCENTAGES FOR EACH ZONE													
	ZONE	Z9	Z1	Z2	Z3	Z4	Z5	Z6	Z7	Z8	ZA	ZB	ZC	KU	KL	KS	KB	ALL	Z9	Z1	Z2	Z3	Z4	Z5	Z6	Z7	Z8	ZA	ZB	ZC	KU	KL	KS	KB	ALL
GLACIAL SITUATIONS	C												0	0	0		0	0												0%	0%	0%		0%	0.0%
	D												0	0	0		0	0												0%	0%	0%		0%	0.0%
	E												0	0	0		0	0												0%	0%	0%		0%	0.0%
	G												0	0	0		0	0												0%	0%	0%		0%	0.0%
	H												0	0	0		0	0												0%	0%	0%		0%	0.0%
	K												0	0	2		0	2												0%	0%	10%		0%	1.3%
	L												14	44	16		0	74												35%	47%	76%		0%	47.4%
	S												1	11	0		0	12												3%	12%	0%		0%	7.7%
	T												25	38	3		2	68												63%	41%	14%		100%	43.6%
	U												0	0	0		0	0												0%	0%	0%		0%	0.0%
TOTAL													40	93	21		2	156												100%	100%	100%		100%	100.0%
ZONE % OF ALL													25.6	59.6	13.5		1.3	100.0																	
CAVE LOCATIONS	C												0	0	0		0	0												0%	0%	0%		0%	0.0%
	F												0	0	18		1	19												0%	0%	86%		50%	12.2%
	W												11	5	1		0	17												28%	5%	5%		0%	10.9%
	R												0	0	0		0	0												0%	0%	0%		0%	0.0%
	S												0	0	0		0	0												0%	0%	0%		0%	0.0%
	G												7	7	2		0	16												18%	8%	10%		0%	10.3%
	P												22	81	0		1	104												55%	87%	0%		50%	66.7%
TOTAL													40	93	21		2	156												100%	100%	100%		100%	100.0%
KARST TYPES	V												0	0	0		0	0												0%	0%	0%		0%	0.0%
	A												34	24	21		0	79												85%	26%	100%		0%	50.6%
	L												0	69	0		2	71												0%	74%	0%		100%	45.5%
	C												1	0	0		0	1												3%	0%	0%		0%	0.6%
	X												5	0	0		0	5												13%	0%	0%		0%	3.2%
TOTAL													40	93	21		2	156												100%	100%	100%		100%	100.0%
CAVE TYPES	S												0	11	3		0	14												0%	12%	14%		0%	9.0%
	a												25	43	6		0	74												63%	46%	29%		0%	47.4%
	b												6	15	8		1	30												15%	16%	38%		50%	19.2%
	c												1	6	3		0	10												3%	6%	14%		0%	6.4%
	d												1	6	0		1	8												3%	6%	0%		50%	5.1%
	e												0	4	0		0	4												0%	4%	0%		0%	2.6%
	f												2	0	0		0	2												5%	0%	0%		0%	1.3%
	g												0	2	0		0	2												0%	2%	0%		0%	1.3%
	h												5	6	1		0	12												13%	6%	5%		0%	7.7%
	Hy												0	0	0		0	0												0%	0%	0%		0%	0.0%
	I												0	0	0		0	0												0%	0%	0%		0%	0.0%
	J												0	0	0		0	0												0%	0%	0%		0%	0.0%
	L												0	0	0		0	0												0%	0%	0%		0%	0.0%
	R												0	0	0		0	0												0%	0%	0%		0%	0.0%
	T												0	0	0		0	0												0%	0%	0%		0%	0.0%
TOTAL CAVES													40	93	21		2	156												100%	100%	100%		100%	100.0%
RELICT CAVES	RC												17	19	4		0	40												43%	20%	19%		0%	25.6%
MAINLY VADOSE	MV												1	37	4		2	44												3%	40%	19%		100%	28.2%
COMBINATION CAVES	CC												22	37	13		0	72												55%	40%	62%		0%	46.2%

CENTRAL SWEDISH CALEDONIDES CAVE DATABASE: SUMMARY FOR TYPES AND LOCATIONS

	ZONE	TOTAL CAVE LENGTHS: METRES Z9	Z1	Z2	Z3	Z4	Z5	Z6	Z7	Z8	ZA	ZB	ZC	KU	KL	KS	KB	ALL	PERCENTAGES FOR EACH ZONE Z9	Z1	Z2	Z3	Z4	Z5	Z6	Z7	Z8	ZA	ZB	ZC	KU	KL	KS	KB	ALL
GLACIAL SITUATIONS	C												0	0	0	0	0													0%	0%	0%	0%	0.0%	
	D												0	0	0	0	0													0%	0%	0%	0%	0.0%	
	E												0	0	0	0	0													0%	0%	0%	0%	0.0%	
	G												0	0	0	0	0													0%	0%	0%	0%	0.0%	
	H												0	0	0	0	0													0%	0%	0%	0%	0.0%	
	K												0	0	33	0	33													0%	0%	1%	0%	0.2%	
	L												3437	3209	6158	0	12804													71%	61%	99%	0%	78.1%	
	S												140	603	0	0	743													3%	12%	0%	0%	4.5%	
	T												1295	1425	30	69	2819													27%	27%	0%	100%	17.2%	
	U												0	0	0	0	0													0%	0%	0%	0%	0.0%	
TOTAL													4872	5237	6221		69 16399													100%	100%	100%		100%	100.0%
ZONE % OF ALL													29.7	31.9	37.9		0.4 100.0																		
CAVE LOCATIONS	C												0	0	0	0	0													0%	0%	0%	0%	0.0%	
	F												0	0	6153	44	6197													0%	0%	99%	64%	37.8%	
	W												880	368	35	0	1283													18%	7%	1%	0%	7.8%	
	R												0	0	0	0	0													0%	0%	0%	0%	0.0%	
	S												0	0	0	0	0													0%	0%	0%	0%	0.0%	
	G												141	195	33	0	369													3%	4%	1%	0%	2.3%	
	P												3851	4674	0	25	8550													79%	89%	0%	36%	52.1%	
TOTAL													4872	5237	6221		69 16399													100%	100%	100%		100%	100.0%
KARST TYPES	V												0	0	0	0	0													0%	0%	0%	0%	0.0%	
	A												2198	1058	6221	0	9477													45%	20%	100%	0%	57.8%	
	L												0	4179	0	69	4248													0%	80%	0%	100%	25.9%	
	C												2600	0	0	0	2600													53%	0%	0%	0%	15.9%	
	X												74	0	0	0	74													2%	0%	0%	0%	0.5%	
TOTAL													4872	5237	6221		69 16399													100%	100%	100%		100%	100.0%
CAVE TYPES	S												0	108	21	0	129													0%	2%	0%	0%	0.8%	
	a												487	654	101	0	1242													10%	12%	2%	0%	7.6%	
	b												210	614	251	44	1119													4%	12%	4%	64%	6.8%	
	c												60	258	248	0	566													1%	5%	4%	0%	3.5%	
	d												140	246	0	25	411													3%	5%	0%	36%	2.5%	
	e												0	304	0	0	304													0%	6%	0%	0%	1.9%	
	f												95	0	0	0	95													2%	0%	0%	0%	0.6%	
	g												0	463	0	0	463													0%	9%	0%	0%	2.8%	
	h												3880	2590	5600	0	12070													80%	49%	90%	0%	73.6%	
	Hy												0	0	0	0	0													0%	0%	0%	0%	0.0%	
	I												0	0	0	0	0													0%	0%	0%	0%	0.0%	
	J												0	0	0	0	0													0%	0%	0%	0%	0.0%	
	L												0	0	0	0	0													0%	0%	0%	0%	0.0%	
	R												0	0	0	0	0													0%	0%	0%	0%	0.0%	
	T												0	0	0	0	0													0%	0%	0%	0%	0.0%	
TOTAL CAVES													4872	5237	6221		69 16399													100%	100%	100%		100%	100.0%
RELICT CAVES	RC												271	334	50	0	655													6%	6%	1%	0%	4.0%	
MAINLY VADOSE	MV												11	755	73	69	908													0%	14%	1%	100%	5.5%	
COMBINATION CAVES	CC												4590	4148	6098	0	14836													94%	79%	98%	0%	90.5%	

CENTRAL SWEDISH CALEDONIDES CAVE DATABASE: SUMMARY FOR TYPES AND LOCATIONS

		MEAN CAVE LENGTHS: METRES																
	ZONE	Z9	Z1	Z2	Z3	Z4	Z5	Z6	Z7	Z8	ZA	ZB	ZC	KU	KL	KS	KB	ALL	No.
No. of caves													40	93	21		2		156
GLACIAL	C																		0
SITUATIONS	D																		0
	E																		0
	G																		0
	H																		0
	K														17			17	2
	L												246	73	385			173	74
	S												140	55				62	12
	T												52	38	10		35	41	68
	U																		0
TOTAL MEAN													122	58	298		35	105	156
CAVE	C																		0
LOCATIONS	F														342		44	326	19
	W												80	74	35			75	17
	R																		0
	S																		0
	G												20	28	17			23	16
	P												175	58			25	82	104
TOTAL MEAN													122	56	298		35	105	156
KARST	V																		0
TYPES	A												85	44	298			120	79
	L													61			35	60	71
	C												2600					2600	1
	X												15					15	5
TOTAL MEAN													122	56	298		35	105	156
CAVE	S													10	7			9	14
TYPES	a												19	15	17			17	74
	b												35	41	31		44	37	30
	c												60	43	83			57	10
	d												140	41			25	51	8
	e													76				76	4
	f												48					48	2
	g													232				232	2
	h												776	432	5600			1008	12
	Hy																		0
	I																		0
	J																		0
	L																		0
	R																		0
	T																		0
TOTAL MEAN													122	56	298		35	105	156
RELICT CAVES	RC												16	18	13			16	40
MAINLY VADOSE	MV												11	20	18		35	21	44
COMBINATION CAVES	CC												209	112	469			206	72

APPENDIX C6

GRÅTÅDAL (NORTH NORWAY) CAVE DATABASE

GRÅTÅDAL (NORTH NORWAY) CAVE DATABASE:

UPPERMOST ALLOCHTHON: Beiar nappe

External Cave Attributes

UTM COORDS.	ALT.	KOMMUNE	AREA	LST. STRIK	LST. DIP	OW	EXT. COLOUR	OTHER INT. ROCK	R	T	GS	CL	KT	SR	OR	CA	REF. NO.	CAVE NAME
Totals	####	42			#	##			0	0						##		
Av. per ca	370				#	0			##	##						0.0		
Minima	117				0	0										0		
Maxima	961				0	0										0		

(Dip measured in 0 caves)

Internal Cave Attributes

	CT	LENG.	VR	XS	VOL.	Min. HG %	C	SE	RE	DE	CS	SP	Ch	Sh	BC	AV	MV	DC	FS	P	SG	PRIME REFERENCES
Totals		7362	####	####	61519	##	42	22	15	46	46	9	0	0	0	7	15	0	0	9		
Av. per ca		175	16.3	13.4	1465	0		0.5	0.4	1.1	1.1	0.2	0.0	0.0	0.0	0.2	0.4	0.0	0.0	0.2		
Minima		2	1	0.7	2	0		1	1	1	0	0	0	0	0	1						
Maxima		1190	140	60.0	14400	0		2	1	5	10	3	0	0	0	1						

Glacial Situations:

	#	Length
C	0	0
D	0	0
E	0	0
G	0	0
H	0	0
K	0	0
L	0	0
S	0	0
T	0	0
U	0	0
Totals	0	0

Karst Types:

	#	Length
V	11	4497
A	30	2815
L	0	0
C	0	0
X	1	50
Totals	42	7362

Cave Locations:

	#	Length
C	0	0
F	0	0
W	0	0
R	0	0
S	0	0
G	0	0
P	0	0
Totals	0	0

Cave Types:

	#	Length
S	6	26
a	13	162
b	8	1404
c	4	237
d	5	2102
e	0	0
f	1	390
g	4	2990
h	0	0
Hy	0	0
I	0	0
J	0	0
L	0	0
R	0	0
T	1	51
Totals	42	7362

Relict Caves:

	#	Length
	13	963
Totals	13	963

MV Caves:

	#	Length
	15	1474
Totals	15	1474

Combination Caves:

	#	Length
Totals	14	4925

ëåðÅÄØÖé

GRÅTÅDAL (NORTH NORWAY) CAVE DATABASE:

Caves are grouped by carbonate outcrop

				External Cave Attributes														Internal Cave Attributes																						
UTM COORDS.	ALT.	KOMMUNE	AREA	LST. STRIK	LST. DIP	OW	EXT. COLOUR	OTHER INT. ROCK	R	T	GR	CL	KT	SH	OR	CA	REF. NO.	CAVE NAME	CT	LENG.	VR	XS	VOL.	Min. HG %	C	SE	RE	DE	CS	SP	Ch	Sh	BC	AV	MV	DC	FS	P	SG	PRIME REFERENCES
UPPERMOST ALLOCHTHON: Beiar nappe																																								
Beiardalen	**2028 I**		**and Arstaddalen**	**2028 IV**														**Grâtådal marble band is adjacent to an internal thrust**																						
	390		Central Beiardalen - Tulleråga										A					Hemінghytt Kjerka	a	12	4	30.0	360		1	1			1	0										St. Pierre, 1966
	384		Central Beiardalen - Tulleråga										A					Tulleråga Resurgence	b	233	*6*	5.0	1165		1		1	1	1	1						1				St. Pierre, 1966
	390		Central Beiardalen - Troåga										A					Eventyrgr./Kjeller-Sal	c	200	5	2.0	400		1		1	5	1	2						1				St. Pierre, 1966
			Central Beiardalen - Heståga															Knutkjelen		Possible collapsed cavern																			St. Pierre, 1966
	460		Central Beiardalen - Heståga										V					Heståga System	g	1190	40	8.0	9520		1			5	1	3				1					Duffot, 1963; A. Johnsen, 1988
	308		Lille Gråtåga										V					Isgrotta	b	203	4	2.0	406		1			2	0	0								1	Swetc CC Occ. Pub (3) 1973
	270		Lille Gråtåga										V					Jordbruhullet	b	108	30	60.0	6480		1	1	1	1	1	0					1			1	St. Pierre, 1966
	252		Lille Gråtåga										V					Stormdalhullet	d	720	51	20.0	14400		1		1		3	0								1	St. Pierre, 1966
	240		Lille Gråtåga										V					Lower Stormdalhullet	b	45	5	20.0	900		1	1	1		1	0					1			1	St. Pierre, 1966
	275		Lille Rønåga										A					Steinågrotta	b	700	*60*	*2.0*	1400		1	1	1		1	0					1				Swetc CC Occ. Pub (4) 1977+
	275		Lille Rønåga										A					Rockbridge 1	a	6	2	*2.0*	12		1	1	1		1	0					1				St. Pierre, 1966
	275		Lille Rønåga										A					Rockbridge 2	a	6	2	*2.0*	12		1	1	1		1	0					1				St. Pierre, 1966
	275		Lille Rønåga										A					Rockbridge 3	a	6	2	*2.0*	12		1	1	1		1	0					1				St. Pierre, 1966
	315		Store Rønåga										V					Satisfaction Cave**	d	910	55	5.0	4550		1	2	1	3	4	0				1				1	Swetc CC Occ. Pub (3) 1973
	285		Store Rønåga										V					Rønålihullet***	g	1120	140	10.0	11200		1	1	1	3	10	0				1				1	Swetc CC Occ. Pub (3) 1973
	240		Store Rønåga										V					Tunnel Cave	a	58	*8*	25.0	1450		1	1	1		1	0					1			1	St. Pierre, 1966
	210		Store Rønåga										V					Waterfall Cave	d	87	*5*	1.5	131		1			1	0	0				1					St. Pierre, 1966. *
	258		Store Rønåga										V					Short Tunnel Cave	a	11	*7*	3.5	39		1	1	1		1	0					1				St. Pierre, 1966
	243		Svart Lake										A					Øverste Svartvannegr	a	9	*3*	0.7	6		1	1			1	0					1				St. Pierre, 1966
	189		Svart Lake										A					Øvre Svartvannegrott	g	660	96	3.0	1980		1			2	3	1				1				1	St. Pierre, 1966. Tectonic rift
	147		Svart Lake										A					Nedre Svartvannsgro	d	150	*5*	2.2	330		1			3	0	0									St. Pierre, 1966
			Svart Lake															Flooded resurgence																						St. Pierre, 1966
	245		Løvstad										A					Løvstadgrotta	d	235	12	8.0	1880		1			1	1	2								1	Swetc CC Occ. Pub (3) 1973
	320		Simleelven										A					Johnsen's Cave	f	390	*13*	2.0	780		1			1	0	0				1					St. Pierre, 1966. *
	336		Simleelven										A					Ladder Cave	c	17	6	1.2	20		1			2	0	0									St. Pierre, 1966
	333		Simleelven										A					Ledge Cave	c	10	3	1.0	10		1			1	0	0									St. Pierre, 1966
			Simleelven															Fourth Cave																						
	320		Simleelven										A					Crack No. 1	c	10	2	5.0	50		1			1	0	0									St. Pierre, 1966
	315		Simleelven										A					Disappointment Cave	a	*2*	*1*	*1.0*	2		1			1	0	0									St. Pierre, 1966
	320		Simleelven										A					Cave opp. Johnsen's	a	4	2	1.0	4		1			1	0	0									St. Pierre, 1966
	360		Central Gråtådalen										A				U1	Kyskåga Cave	b	20	6	2.0	40		1			1	1	0					1				St. Pierre, 1966
	450		Central Gråtådalen										A				1A	Sink-hole	S	3	3	36.0	108		1	1			1	0									St. Pierre, 1966
	450		Central Gråtådalen										A				1B	Lille Jordbruhullet	g	20	10	*2.0*	40		1			2	0	0									St. Pierre, 1966
	450		Central Gråtådalen										A				2.1	Sink 1	S	5	5	60.0	300		1	1			1	0									St. Pierre, 1966
	450		Central Gråtådalen										A				2.2	Sink 2	S	5	5	60.0	300		1	1			1	0									St. Pierre, 1966
	450		Central Gråtådalen										A				2.3	Sink 3	S	5	5	60.0	300		1	1			1	0									St. Pierre, 1966
	450		Central Gråtådalen										A				2.4	Sink 4	S	5	5	60.0	300		1			1	0	0									St. Pierre, 1966
			Upper Gråtådalen														U2	cave		3m-high entrance to collapsing vadose streamway, at junction of grey and yellow marbles																					St. Pierre, 1966
			Upper Gråtådalen														U2	rockbridge		Beyond the resurgence of this cave																					St. Pierre, 1966
	810		Upper Gråtådalen										A				U3	Snow patches cave	a	6	*2*	*2.0*	12		1	2			2	0									St. Pierre, 1966
	810		Upper Gråtådalen										A				U3	3m pot	S	3	3	1.0	3		1	1			1	0					1				St. Pierre, 1966
	810		Upper Gråtådalen										V				U4	Skjelåtind collapsed c	b	45	8	4.0	180		1	1	1	2	1	0					1				St. Pierre, 1966

* includes Seggafjøset (410m), Grotte de la Cheval Fou (660m) and Dry Cave (120m)

** includes Unnamed Cave (340m) and Birch Pole Cave (80m)

*** includes Smiths cavern, Øvre Rønålihullet and Pendant Cave

* Partly vadose relict cave

+ Ca. and Caving (3) 1979 p20

GRÅTÅDAL (NORTH NORWAY) CAVE DATABASE:

Caves are grouped by carbonate outcrop

UTM COORDS.	ALT.	KOMMUNE	AREA	LST. STRIK	LST. DIP	OW	EXT. COLOUR	OTHER INT. ROCK	R	T	GS	CL	KT	SR	OR	CA	REF. NO.	CAVE NAME	CT	LENG.	VR	XS	VOL.	Min. HG %	C	SE	RE	DE	CS	SP	Ch	Sh	BC	AV	MV	DC	FS	P	SG	PRIME REFERENCES
								External Cave Attributes												Internal Cave Attributes																				
UPPERMOST ALLOCHTHON: Beiar nappe																																								
Arstaddalen	2028 IV	cont.																																						
	117		Central Beiardalen										A					Reingard Resurgence	a	3	1	1.0	3		1		1		1	0										St. Pierre, 1966
	200		Central Beiardalen										A					Pengekjelen	T	51	51	45.0	2295		1			1	1	0										St. Pierre, 1966. Tectonic rift
			Central Beiardalen															Leirâmoen cave		Cave similar to Pengekjelen																				St. Pierre, 1966
	492		Upper Beiardalen										A					The Bear Den	a	15	2	1.0	15		1			1	0	0										St. Pierre, 1966
	961		Upper Beiardalen										A					Cliff Cave	a	24	6	1.0	24		1	1			1	0					1					St. Pierre, 1966
			Upper Beiardalen															Caves near Bogvandet																						St. Pierre, 1966
	420		Tollådal										X					Tollådalgrotta	b	50	3	2.0	100		1			4	0	0				1						Swetc CC Occ. Pub (3) 1973*

* Partly vadose relict cave

APPENDIX C7

SOUTHERN SCANDINAVIAN CALEDONIDES CAVE DATABASE

SOUTHERN SCANDINAVIAN CALEDONIDES CAVE DATABASE: SUMMARY - TOTALS

			External Cave Attributes			Internal Cave Attributes																			
ALLOCHTHON	NAPPES	ALT.	R	T		LENG.	VR	XS	VOL.	C	SE	RE	DE	CS	SP	Ch	Sh	BC	RV	MV	DC	FS	P	COMMENTS
Upper	Køli (Norway)	####	0	0		1853	####	####	14880	13	5	2	17	12	11	0	0	0	1	6	0	0	0	
Upper	Seve (Sweden)	####	0	0		423	####	####	447	5	1	0	9	2	2	0	0	0	0	0	0	0	0	
Lower	(Norway)	####	0	0		1420	####	####	16117	15	9	5	20	16	4	0	0	0	0	6	0	0	8	
Lower	(Sweden)	####	0	0		542	####	####	1099	14	6	3	9	12	8	0	0	0	0	8	0	0	0	
Totals		####	0	0		4238	####	####	32543	47	21	10	55	42	25	0	0	0	1	20	0	0	8	

SUMMARY - AVERAGES

Upper	Køli (Norway)	235	0	0		143	11.8	3.9	1145		0.4	0.2	1.3	0.9	0.8	0.0	0.0	0.0	0.1	0.5	0.0	0.0	0.0	
Upper	Seve (Sweden)	586	0	0		85	10.8	1.8	89		0.2	0.0	1.8	0.4	0.4	0.0	0.0	0.0	0.0	0.0	0.0	0.0	0.0	
Lower	(Norway)	991	0	0		95	11.8	5.4	1074		0.6	0.3	1.3	1.1	0.3	0.0	0.0	0.0	0.0	0.4	0.0	0.0	0.5	
Lower	(Sweden)	352	0	0		39	3.3	1.8	79		0.4	0.2	0.6	0.9	0.6	0.0	0.0	0.0	0.0	0.6	0.0	0.0	0.0	
Average per cave		549	0	0		90	9.1	3.5	692		0.4	0.2	1.2	0.9	0.5	0.0	0.0	0.0	0.0	0.4	0.0	0.0	0.2	

SUMMARY - MINIMA

Upper	Køli (Norway)	70	0	0		7	2.0	0.5	4		1	1	1	0	0	0	0	0	1	0	0	0	0	
Upper	Seve (Sweden)	500	0	0		3	1.0	1.0	3		1	0	1	0	0	0	0	0	0	0	0	0	0	
Lower	(Norway)	450	0	0		5	1.0	0.3	2		1	1	1	0	0	0	0	0	0	0	0	0	0	
Lower	(Sweden)	300	0	0		4	1.0	0.5	4		1	1	1	0	0	0	0	0	0	0	0	0	0	
Minima		70	0	0		3	1.0	0.3	2		1	0	1	0	0	0	0	0	0	0	0	0	0	

SUMMARY - MAXIMA

Upper	Køli (Norway)	540	0	0		560	30.0	12.0	6000		1	1	6	2	5	0	0	0	1	0	0	0	0	
Upper	Seve (Sweden)	618	0	0		360	40.0	4.0	360		1	0	2	1	1	0	0	0	0	0	0	0	0	
Lower	(Norway)	1220	0	0		432	46.0	20.0	8640		2	1	4	5	1	0	0	0	0	0	0	0	0	
Lower	(Sweden)	400	0	0		130	10.0	4.0	260		1	1	3	1	1	0	0	0	0	0	0	0	0	
Maxima		1220	0	0		560	46.0	20.0	8640		2	1	6	5	5	0	0	0	1	0	0	0	0	

ššåõÅØÕ

SOUTHERN SCANDINAVIAN CALEDONIDES CAVE DATABASE

UPPER ALLOCHTHON: Kall Nappes - Upper Kall: KU (Gula Nappe, or Trondheim Nappe Complex)) (NORWAY ONLY): TOTALS

External Cave Attributes | Internal Cave Attributes

UTM / SWEDISH RN COORDS	ALT.	KOMMUNE	AREA	LST. STRIK	LST. DIP	OW	EXT. COLOUR	OTHER INT. ROCK	R	T	GS	CL	KT	SR	OR	CA	REF. NO.	CAVE NAME	CT	LENG.	VR	XS	VOL.	Min. HG %	C	SE	RE	DE	CS	SP	Ch	Sh	BC	RV	MV	DC	FS	P	SG	PRIME REFERENCES
Totals	####	13			#	##			0	0							##			1853	###	####	####	##	13	5	2	17	12	11	0	0	0	1	6	0	0	0	
Av. per cave	235				#	0			##	##							##			143	11.8	3.9	1145	0		0.4	0.2	1.3	0.9	0.6	0.0	0.0	0.0	0.1	0.5	0.0	0.0	0.0	
Minima	70				0	0											0			7	2	0.5	4	0		1	1	1	0	0	0	0	0	1					
Maxima	540				0	0											0			560	30	12.0	6000	0		1	1	6	2	5	0	0	0	1					

(Dip measured in 0 caves)

Glacial Situations:

	#	Length
C	0	0
D	0	0
E	0	0
G	0	0
H	0	0
K	0	0
L	0	0
S	0	0
T	0	0
U	0	0
Totals	0	0

Karst Types:

	#	Length
V	0	0
A	4	710
L	3	1070
C	0	0
X	6	73
Totals	13	1853

Cave Locations:

	#	Length
C	0	0
F	0	0
W	0	0
R	0	0
S	0	0
G	0	0
P	0	0
Totals	0	0

Cave Types:

	#	Length
S	1	10
a	3	28
b	3	135
c	0	0
d	3	730
e	0	0
f	0	0
g	3	950
h	0	0
Hy	0	0
I	0	0
J	0	0
L	0	0
R	0	0
T	0	0
Totals	13	1853

Relict Caves:

#	Length
2	21

MV Caves:

#	Length
6	297

Combination Caves:

#	Length
5	1536

SOUTHERN SCANDINAVIAN CALEDONIDES CAVE DATABASE

sàäöÀØÖ

Caves are grouped by carbonate outcrop

External Cave Attributes | Internal Cave Attributes

UTM / SWEDISH RN COORDS	ALT.	KOMMUNE	AREA	LST. STRIKE	LST. DIP	OW	EXT. COLOUR	OTHER INT. ROCK	R	T	GS	CL	KT	SR	OR	CA	REF. NO.	CAVE NAME	CT	LENG.	VR	XS	VOL.	Min. HG %	C	SE	RE	DE	CS	SP	Ch	Sh	BC	RV	MV	DC	FS	P	SG	PRIME REFERENCES
UPPER ALLOCHTHON: Kall Nappes - Upper Kall: KU (Gula Nappe, or Trondheim Nappe Complex)) (NORWAY ONLY)																																							
		Snåsa	Bergåsen															Mandhuliet		NW of Renset																				CRG NI (125) p16 1971
		Snåsa	Bergåsen															Bisporten																						CRG NI (125) p16 1971
		Snåsa	Bergåsen															Kirkeporten		Not a cave - a narrow gap																				CRG NI (125) p16 1971
	200	Snåsa	Bergåsen										X					Schenings Hule	a	11	*5*	*6*	66		1			1	0	0										Speleo 16 (1) p18 1981
		Steinkjer	Ogndal														8	sink																						JGF 37-40 1998
		Steinkjer	Ogndal														9	Folkvagn grotta																						JGF 37-40 1998
	330	Steinkjer	Ogndal										L				6,8,10	Gaulstadgrotta	d	560	30	*10*	5600		1	1	1	1	1	3										SwetcCC Occ Pub (3) 14-15 '72 *
	330	Steinkjer	Ogndal														7	smågrottor																						JGF 37-40 1998
		Steinkjer	Ogndal														5	cave		c. 340m long																				T. Doj (pc, 1992). JGF 37-40 1998
		Steinkjer	Ogndal														4	Jättegrytegrotta																						JGF 37-40 1998
		Steinkjer	Ogndal														1,2,3?	cave		c. 300m long																				T. Doj (pc, 1992). JGF 37-40 1998
	400	Steinkjer	Ogndal										L					Storgaulstadhøgdahulene	S	10	10	*4*	40		1			1	0	0										SwetcCC Occ Pub (3) 14-15 '72
		Verdal	Levanger															cave		c. 100m long																				NG (38) 18-19 2002
	250	Verdal	Tromsdalen										A					Storhalet in Ramsåsen	g	300	*30*	*7*	2100		1	1		1	1	0		$		1						NG (38) 18-19 2002. JGF 37-40 '98
	250	Verdal	Tromsdalen										A					Svartfossgrotta	g	150	*15*	*2*	300		1	1			1	1										NG (38) 18-19 2002
	250	Verdal	Tromsdalen										A					Benkberggrotta/Knällkrose	*d*	160	*15*	*2*	320		1	1			1	1					1					NG (38) 18-19 2002. JGF 37-40 '98
	250	Verdal	Tromsdalen										A					Fossekjeftgrotta	*b*	100	*10*	*4*	400		1			1	1	1					1					NG (38) 18-19 2002
		Verdal	Tromsdalen															cave		Over 100m long																				NG (38) 18-19 2002
		Verdal	Tromsdalen															caves		10 caves over 20m long																				NG (38) 18-19 2002
	100	Bjugn	Gjølgavatn										X				1	Hvitmarmorgrotta	a	10	*3*	*1*	10		1	1			1	0					1					NG (14) 12-13 1984
	70	Bjugn	Gjølgavatn										X				2	Gjølgaligrotta	b	25	*4*	*1*	25		1			3	1	0										NG (14) 12-13 1984
	80	Bjugn	Gjølgavatn										X				3	Grikegrotta	b	10	*2*	*1*	10		1			1	1	0					1					NG (14) 12-13 1984
	150	Bjugn	Gjølgavatn										X				4	Svartvannsgrotta	a	7	*2*	*0.5*	3.5		1			1	1	0					1					NG (14) 12-13 1984
	190	Bjugn	Gjølgavatn										X				5	Kammagrotta	d	10	*2*	0.5	5		1			1	1	0					1					NG (14) 12-13 1984

$ 10m diam., 20m deep entrance

* T. Doj (pc, 1992)
Caves and Caving (80) p33 1993
JGF 37-40 1998. JGF 44-45 1999

UPPER ALLOCHTHON: Kall Nappes - Upper Kall: KU (Gula Nappe, or Trondheim Nappe Complex)
OR Seve Nappes - Sulitjelma Nappe?

	540	Fraena	Molde				White						L					Trollkyrkegrotta	g	500	25	*12*	6000		1		1	6	2	5										BPC Survey 1965 +

\+ Grottan 36 (2) 27-33 2001

SOUTHERN SCANDINAVIAN CALEDONIDES CAVE DATABASE

Refer to North Central Norway Cave Database for Key

UPPER ALLOCHTHON: Seve Nappes (SWEDEN ONLY): TOTALS

Column headings: UTM | ALT. | KOMMUNE | AREA | LST. STRIK | LST. DIP | OW | EXT. COLOUR | OTHER INT. ROCK | External Cave Attributes: R | T | GS | CL | KT | SR | OR | CA | REF. NO. | CAVE NAME | Internal Cave Attributes: CT | LENG. | VR | XS | VOL. | Min. HG % | C | SE | RE | DE | CS | SP | Ch | Sh | BC | RV | MV | DC | FS | P | SG | PRIME REFERENCES

	ALT.	KOMMUNE	LST. DIP	OW	R	T	CA	LENG.	VR	XS	VOL.	Min. HG %	C	SE	RE	DE	CS	SP	Ch	Sh	BC	RV	MV	DC	FS	P
Totals	####	5	#	##	0	0	##	423	###	9.0	447	##	5	1	0	9	2	2	0	0	0	0	0	0	0	0
Av. per cave	586		#	0	##	##	##	85	10.8	1.8	89	0		0.2	0.0	1.8	0.4	0.4	0.0	0.0	0.0	0.0	0.0	0.0	0.0	#
Minima	500		0	0			0	3	1	1.0	3	0		1	0	1	0	0	0	0	0	0				
Maxima	618		0	0			0	360	40	4.0	360	0		1	0	2	1	1	0	0	0	0				

(Dip measured ir 0 caves)

Glacial Situations:

	#	Length
C	0	0
D	0	0
E	0	0
G	0	0
H	0	0
K	0	0
L	0	0
S	0	0
T	0	0
U	0	0
Totals	0	0

Karst Types:

	#	Length
V	0	0
A	0	0
L	5	423
C	0	0
X	0	0
Totals	5	423

Cave Locations:

	#	Length
C	0	0
F	0	0
W	0	0
R	0	0
S	0	0
G	0	0
P	0	0
Totals	0	0

Cave Types:

	#	Length
S	1	7
a	2	6
b	0	0
c	1	50
d	0	0
e	0	0
f	0	0
g	1	360
h	0	0
Hy	0	0
I	0	0
J	0	0
L	0	0
R	0	0
T	0	0
Totals	5	423

Relict Caves:

#	Length
3	13
3	13

MV Caves:

#	Length
0	0
0	0

Combination Caves:

#	Length
2	410

UPPER ALLOCHTHON: Seve Nappes (SWEDEN ONLY)

UTM	ALT.	KOMMUNE	AREA	KT	REF. NO.	CAVE NAME	CT	LENG.	VR	XS	VOL.	C	SE	DE	CS	SP	PRIME REFERENCES
13734 70501		Östersund	Bergsjö		8	Bergsjögrottan $		185m long, 18m deep									Grottan 24 (2) 23-27 1989. RM list *
13699 70397	470	Östersund	Åreskutan		1	Fävikshålet		90m-long relict cave									Grottan 24 (2) 23-27 1989. RM list **
13702 70397	420	Östersund	Åreskutan		2	Fäviksångrottan		60m long, 4m deep, relict cave									Grottan 24 (2) 23-27 1989. RM list
		Östersund	Åreskutan			Mossgrottan		6m-long									JGF Årsskrift p23 1997
13692 70393	*600*	Östersund	Åreskutan	*L*		Naturlig bro	a	3	2	*2.0*	6	1		2	*0*	*0*	RM list
13691 70404	610	Östersund	Åreskutan	*L*	3	Kvarnbäckslabyrinten/Ned	g	360	40	*1.0*	360	1	1	2	1	1	Grottan 24 (2) 23-27 1989. RM list
13690 70403	618	Östersund	Åreskutan	*L*	3	Övre Kvarnbäcksgrottan	c	50	6	*1.0*	50	1		2	1	1	Grottan 24 (2) 23-27 1989. RM list
13685 70411	*600*	Östersund	Åreskutan	*L*	4	Gömslesschaktet	S	7	5	4.0	28	1		1	0	0	Grottan 24 (2) 23-27 1989. RM list
13694 70408	*500*	Östersund	Åreskutan	*L*		Valvbrogrottan	a	3	*1*	*1.0*	3	1		*2*	*0*	*0*	RM list
		Östersund	Åreskutan		5	Grytor (and mines?)											Grottan 24 (2) 23-27 1989
		Östersund	Åreskutan		6	Ullån grottor											Grottan 24 (2) 23-27 1989
		Östersund	Åreskutan		7	Rävgrotta											Grottan 24 (2) 23-27 1989
13771 70250		Östersund	Ristafall			N. Ristafalletsgrottan		5m long									RM list
13771 70249		Östersund	Ristafall			M. Ristafalletsgrottan 1		35m long									RM list. JGF Årsskrift p45 1999
13771 70249		Östersund	Ristafall			M. Ristafalletsgrottan 2		10m long									RM list
		Östersund	Ristafall			Isgrottorna											JGF Årsskrift p18 1997

$ Includes Dynamitgrottan. Also called Kallgrottan

* JGF Årsskrift p37 1999
**JGF Årsskrift p26 1998

SOUTHERN SCANDINAVIAN CALEDONIDES CAVE DATABASE

Refer to North Central Norway Cave Database for Key

LOWER ALLOCHTHON: NORWAY

External Cave Attributes

UTM / SWEDISH RN COORDS	ALT.	KOMMUNE	AREA	LST. STRIK	LST. DIP	OW	EXT. COLOUR	OTHER INT. ROCK	R	T	GS	CL	KT	SR	OR	CA	REF. NO.
Totals	#####	15			#	##			0	0						##	
Av. per cave	990.9				#	0			##	##						##	
Minima	450				0	0										0	
Maxima	1220				0	0										0	

(Dip measured 0 caves)

Internal Cave Attributes

	CT	LENG.	VR	XS	VOL.	Min. HG %	C	SE	RE	DE	CS	SP	Ch	Sh	BC	RV	MV	DC	FS	P	SG	PRIME REFERENCES
Totals		1420	###	####	####	##	15	9	5	20	16	4	0	0	0	0	6	0	0	8		
Av. per cave		95	11.8	5.4	1074	0		0.6	0.3	1.3	1.1	0.3	0.0	0.0	0.0	0.0	0.4	0.0	0.0	0.5		
Minima		5	1	0.3	2	0		1	1	1	0	0	0	0	0	0						
Maxima		432	46	20.0	8640	0		2	1	4	5	1	0	0	0	0						

Glacial Situations:

	#	Length
C	0	0
D	0	0
E	0	0
G	0	0
H	0	0
K	0	0
L	0	0
S	0	0
T	0	0
U	0	0
Totals	0	0

Karst Types:

	#	Length
V	0	0
A	13	1407
L	0	0
C	0	0
X	2	13
Totals	15	1420

Cave Locations:

	#	Length
C	0	0
F	0	0
W	0	0
R	0	0
S	0	0
G	0	0
P	0	0
Totals	0	0

Cave Types:

	#	Length
S	2	13
a	2	22
b	3	75
c	0	0
d	2	399
e	3	239
f	0	0
g	1	432
h	1	210
Hy	0	0
I	0	0
J	0	0
L	0	0
R	1	30
T	0	0
Totals	15	1420

Relict Caves:

#	Length
4	65
4	65

MV Caves:

#	Length
6	121
6	121

Combination Caves:

#	Length
5	1234

Vest-Jotunheimen ***1518 111***

External Cave Attributes

UTM / SWEDISH RN COORDS	ALT.	KOMMUNE	AREA	LST. STRIK	LST. DIP	OW	EXT. COLOUR	OTHER INT. ROCK	R	T	GS	CL	KT	SR	OR	CA	REF. NO.	CAVE NAME
		Lom	Bøvertun															Overgrotta
MP 480 330	1220	Lom	Bøvertun										A					Dummhølet (Dummhøgr. 2)
		Lom	Bøvertun															Fidergrotta
	1125	Lom	Bøvertun										A					Smutthullet (Sveitserosten
	1134	Lom	Bøvertun										A					Hannesgrotta (Sveitserosten
MP 484 332	1170	Lom	Bøvertun										A					Spiralgrotta (Dummhøgr. 1)
MP 486 333	1120	Lom	Bøvertun										A					Orgelpipa (Sveitserosten
		Lom	Bøvertun															Jotunhallen
	1050	Lom	Bøvertun										A				11-15	Øvre Elvegrotta
	1015	Lom	Bøvertun										A				9,10	Tørrgrotta
	1005	Lom	Bøvertun										A				8	Tributary Stream "Cave"
	1005	Lom	Bøvertun										A				7	Second Rockbridge
	990	Lom	Bøvertun										A				4,5,6	Nedre Elvegrotta
	970	Lom	Bøvertun										A				3	Through Cave
	960	Lom	Bøvertun										A				2	Offshoot Cave
	950	Lom	Bøvertun										A				1	Dummbrua
	700	Hedmark	Jordet										X					Toregrave
	450	Hedmark	Jordet										X					8m Rift
		Finse	Hardanger.															Steinlon
		Finse	Hardanger.															Ovnsbreen

Internal Cave Attributes

CAVE NAME	CT	LENG.	VR	XS	VOL.	Min. HG %	C	SE	RE	DE	CS	SP	Ch	Sh	BC	RV	MV	DC	FS	P	SG	PRIME REFERENCES
Overgrotta		57m long																				NG (6) 22-26 1980
Dummhølet (Dummhøgr. 2)	e	193	25	3.0	579		1			4	1	0										NG (3/4) p33, 50-52 1977 *
Fidergrotta																						NG (6) 22-26 1980
Smutthullet (Sveitserosten	b	11	6	0.3	3		1			1	0	0										NG (6) 22-26 1980 *
Hannesgrotta (Sveitserosten	e	16	10	0.4	6		1			1	0	0										NG (6) 22-26 1980 *
Spiralgrotta (Dummhøgr. 1)	h	210	20	4.0	840		1	2		1	5	1										NG (3/4) p33, 50-52 1977
Orgelpipa (Sveitserosten	e	30	12	0.4	12		1			2	0	0										NG (3/4) p33, 50-52 1977
Jotunhallen		132m long, 10m wide, 5m high																				NG (6) 22-26 1980 *
Øvre Elvegrotta	g	432	46	20.0	8640		1	1		4	2	1								1		SwetcCC OccPub 4 16-18 1977+
Tørrgrotta	d	158	*10*	*3.0*	474		1			2	1	1								1		SwetcCC OccPub 4 16-18 1977+
Tributary Stream "Cave"	R	30	*4*	*2.0*	60		1		1	1	1	0					1			1		SwetcCC OccPub 4 16-18 1977
Second Rockbridge	a	10	*4*	*10.0*	100		1	1	1		1	0					1			1		SwetcCC OccPub 4 16-18 1977
Nedre Elvegrotta	d	241	*20*	*20.0*	4820		1	1	1	3	1	0								1		SwetcCC OccPub 4 16-18 1977+
Through Cave	a	12	3	*6.0*	72		1	1	1		1	0					1			1		SwetcCC OccPub 4 16-18 1977
Offshoot Cave	b	10	1	1.5	15		1	1			1	1					1			1		SwetcCC OccPub 4 16-18 1977
Dummbrua	b	54	5	*9.0*	486		1	1	1		1	0					1			1		SwetcCC OccPub 4 16-18 1977+
Toregrave	S	*5*	3	*0.3*	2		1	1			1	0					1					CRG NI (125) p26 1971 +
8m Rift	S	8	8	*1.0*	8		1			1	0	0										CRG NI (125) p26 1971 +
Steinlon																						NG (6) 22-26 1980
Ovnsbreen																						NG (6) 22-26 1980

PARAUTOCHTHON and AUTOCHTHON: *Sedimentary cover rocks*

Not considered

UTM / SWEDISH RN COORDS	ALT.	KOMMUNE	AREA	CAVE NAME	PRIME REFERENCES
			Oslo	caves	NG (6) 22-26 1980
			Drammen	caves	NG (6) 22-26 1980
			Skrimfjell	caves	NG (6) 22-26 1980

SOUTHERN SCANDINAVIAN CALEDONIDES CAVE DATABASE

Refer to North Central Norway Cave Database for Key

LOWER ALLOCHTHON: SWEDEN: TOTALS

	ALT.	KOMMUNE	LST. DIP	OW	R	T	CA	LENG.	VR	XS	VOL.	Min. HG %	C	SE	RE	DE	CS	SP	Ch	Sh	BC	RV	MV	DC	FS	P
			#	##			###																			
Totals	#####	14	#	0	0	0	0.0	542	###	####	1099	##	14	6	3	9	12	8	0	0	0	0	8	0	0	0
Av. per cave	352.1		0	0	##	##	0	39	3.3	1.8	79	0		0.4	0.2	0.6	0.9	0.6	0.0	0.0	0.0	0.0	0.6	0.0	0.0	0.0
Minima	300		0	0			0	4	1	0.5	4	0		1	1	1	0	0	0	0	0	0				
Maxima	400							130	10	4.0	260	0		1	1	3	1	1	0	0	0	0				

(Dip measured 0 caves)

Glacial Situations:

	#	Length
C	0	0
D	0	0
E	0	0
G	0	0
H	0	0
K	0	0
L	0	0
S	0	0
T	0	0
U	0	0
Totals	0	0

Karst Types:

	#	Length
V	0	0
A	0	0
L	14	542
C	0	0
X	0	0
Totals	14	542

Cave Locations:

	#	Length
C	0	0
F	0	0
W	0	0
R	0	0
S	0	0
G	0	0
P	0	0
Totals	0	0

Cave Types:

	#	Length
S	0	0
a	3	39
b	5	194
c	3	128
d	2	138
e	0	0
f	0	0
g	0	0
h	0	0
Hy	1	43
I	0	0
J	0	0
L	0	0
R	0	0
T	0	0
Totals	14	542

Relict Caves:

#	Length
2	18
2	18

MV Caves:

#	Length
8	249
8	249

Combination Caves:

#	Length
4	275

LOWER ALLOCHTHON: SWEDEN

UTM / SWEDISH RN COORDS	ALT.	KOMMUNE	AREA	LST. STRIK	LST. DIP	OW	EXT. COLOUR	OTHER INT. ROCK	R	T	GS	CL	KT	SR	OR	CA	REF. NO.	CAVE NAME	CT	LENG.	VR	XS	VOL.	Min. HG %	C	SE	RE	DE	CS	SP	Ch	Sh	BC	RV	MV	DC	FS	P	SG	PRIME REFERENCES
14310 70803	400	Krokom	Hotagen										L					Björnråkskällaren	b	21	5	2.0	42		1	1			1	0					1					JGF Årsskrift pp47,49 1998.RM list
14318 70815	400	Krokom	Hotagen										L					Iskällaren	b	8	3	1.0	8		1	1			1	1					1					JGF Årsskrift pp11,49 1998
14244 70715	390	Krokom	Hotagen										L					Gysengrotta 2	b	70	10	2.0	140		1	1			1	1					1					JGF Årsskrift pp25,49 1998.RM list
14245 70703	390	Krokom	Hotagen										L					Gysengrotta 3	b	40	3	1.0	40		1	1			1	1					1					JGF Årsskrift pp25,49 1998.RM list
14243 70704	390	Krokom	Hotagen										L					Gysengrotta 1	b	55	5	2.0	110		1	1			1	1					1					JGF Årsskrift pp25,49 1998.RM list
14025 70429	400	Krokom	Kaxås										L					Djupbäcksgrottorna	Hy	43	3	2.0	86		1			3	1	0					1					JGF Årsskrift p47 1998. RM list
14025 70429	400	Krokom	Kaxås															cave 1		3m long																				JGF Årsskrift p19 1997
14025 70429	400	Krokom	Kaxås															cave 2		? long																				JGF Årsskrift p19 1997
14025 70429	400	Krokom	Kaxås															cave 3		12m long																				JGF Årsskrift p19 1997
14143 70335	320	Krokom	Ånge										L					Lungrets underjordsbäck	a	4	2	1.0	4		1	1			1	0					1					JGF Årsskrift pp11,50 1998
14124 70391	320	Krokom	Ånge										L					Nästågrottan	d	8	1	1.0	8		1		1	2	1	0					1					JGF Årsskrift p50 1998
14124 70391	320	Krokom	Ånge										L					Tegelgrottan	c	80	3	3.0	240		1			1	1	1										JGF Årsskrift 59-62 1997; p51 1998
14131 70400	320	Krokom	Ånge										L					Västra Torrågrottan (utlöpp	a	25	3	4.0	100		1		1		1	1										Grottan 34 (3) 10-13 1999.*
14131 70400	320	Krokom	Ånge										L					Östra Torrågrottan	d	130	2	2.0	260		1			1	1	1										Grottan 24 (2) 18-23 1989.**
14130 70395	310	Krokom	Ånge										L					Berge Kalkbrottsgrotta	a	10	3	0.5	5		1			1	0	0										Grottan 32 (4) 34-36 1997. *
13859 70233	380	Östersund	Mörsil															Underjordisk Svartbäcken			15m deep																			RM list
13902 70211	350	Östersund	Mörsil										L					Gisteråsgrottan	c	40	2	1	40		1		1		1	1										Grottan 24 (2) 18-23 1989. RM list
13902 70207		Östersund	Mörsil															Gisteråsluket		3m long, 1m deep																				RM list
	300	Östersund	Storsjön										L					Verkögrottan	c	8	1	2	16		1			1	0	0										JGF Årsskrift 82-83 1997

* JGF Årsskrift p51 1998

PARAUTOCHTHON and AUTOCHTHON: *Sedimentary cover rocks* — Not considered

APPENDIX C8

NORTH AMERICAN CALEDONIDES CAVE DATABASE

NORTH AMERICAN CALEDONIDES CAVE DATABASE: VERMONT/ WESTERN MASSACHUSETTS (Berkshire)

VERMONT / WESTERN MASSACHUSETTS (Berkshire): TOTALS

External Cave Attributes / Internal Cave Attributes

STATE AND COUNTY	ALT.	QUAD OR TOWN	AREA	LST. STRIKE	LST. DIP	OW	EXT. COLOUR	OTHER INT. ROCK	R	T	GS	CL	KT	SR	OR	CA	REF. NO.	CAVE NAME	CT	LENG.	VR	XS	VOL.	Min. HG %	C	SE	RE	DE	CS	SP	Ch	Sh	BC	AV	MV	DC	FS	P	SG	PRIME REFERENCES
Totals	####	31		#	##				0	0						####				9087	###	#####	35791	###	153	36	15	148	88	24	0	0	0	6	20	0	0	5		
Av. per cave	385			#	0				##	##						0.0				59	9.3	2.9	234	0		0.2	0.1	1.0	0.6	0.2	0.0	0.0	0.0	0.0	0.1	0.0	0.0	0.0		
Minima	278			0	0											0.00				2	1	0.5	2	0		1	1	0	0	0	0	0	0	1						
Maxima	450			0	0											0.0				900	82	18.0	5400	0		3	1	5	3	3	0	0	0	1						

(Dip measured in 0 caves)

Glacial Situations:

	#	Length
C	0	0
D	0	0
E	0	0
G	0	0
H	0	0
K	0	0
L	0	0
S	0	0
T	0	0
U	0	0
Totals	0	0

Karst Types:

	#	Length
V	0	0
A	18	1370
L	79	6332
C	0	0
X	56	1385
Totals	153	9087

Cave Locations:

	#	Length
C	0	0
F	0	0
W	0	0
R	0	0
S	0	0
G	0	0
P	0	0
Totals	0	0

Cave Types:

	#	Length
S	8	196
a	56	842
b	33	1121
c	17	1172
d	13	851
e	1	42
f	14	1893
g	3	578
h	4	2277
Hy	0	0
I	4	115
J	0	0
L	0	0
R	0	0
T	0	0
Totals	153	9087

Relict Caves:

	#	Length
	81	2024
Totals	81	2024

MV Caves:

	#	Length
	20	900
Totals	20	900

Combination Caves:

	#	Length
Totals	52	6163

Caves are grouped by carbonate outcrop

External Cave Attributes / Internal Cave Attributes

Orwell / Middlebury Limestone / Ira Formation - Whipple Marble / Walloomsac Formation — *Middle Ordovician*

STATE AND COUNTY	ALT.	QUAD OR TOWN	AREA	LST. STRIKE	LST. DIP	OW	EXT. COLOUR	OTHER INT. ROCK	R	T	GS	CL	KT	SR	OR	CA	REF. NO.	CAVE NAME	CT	LENG.	VR	XS	VOL.	Min. HG %	C	SE	RE	DE	CS	SP	Ch	Sh	BC	AV	MV	DC	FS	P	SG	PRIME REFERENCES
VT Addison		Middlebury	Otter Creek										L					Horse Farm Road Cave	c	486	10	2.0	972		1	1	1	1	1	0										Pingree, June 2002
VT Addison		Monkton	Ferrisburg										X					Rokeby Cave	d	100	10	3.0	300		1	1	1	1	1	0					1					Quick, 1994
VT Rutland		W. Rutland	Herrick Mt.										L					Ira Cave	c	67	2	4.0	268		1		1		1	0										Quick, 1994
MA Berkshire	292	West Stockbrid	Williamsville										A					Eldon French Cave	g	243	25	2.0	486		1	3			3	0								1		Howcroft, 1997. Complex folds. TF98
MA Berkshire	292	West Stockbrid	Williamsville										A					Eldon's Annex Cave	f	16	2	1.0	16		1			1	0	0										Howcroft, Plante, June 1997
MA Berkshire	315	West Stockbrid	Williamsville										A					Silver Cave	d	43	10	1.0	43		1	2			2	1										Howcroft, Plante, June 1997
MA Berkshire	315	West Stockbrid	Williamsville										A					Gold Cave	a	14	9	1.0	14		1			1	0	0										Howcroft, Plante, June 1997
MA Berkshire	315	West Stockbrid	Williamsville										A					Porky Hole	a	3	3	1.0	3		1			1	0	0										Plante, June 1997

NORTH AMERICAN CALEDONIDES CAVE DATABASE: VERMONT/ WESTERN MASSACHUSETTS (Berkshire)

Caves are grouped by carbonate outcrop

STATE AND COUNTY	ALT.	QUAD OR TOWN	AREA	External Cave Attributes: LST. STRIKE	LST. DIP	OM	EXT. COLOUR	OTHER INT. ROCK	R	T	GE	CL	KT	SH	OR	CA	REF. NO.	Internal Cave Attributes: CAVE NAME	CT	LENG.	VR	XS	VOL.	Min. HB %	C	SE	RE	DE	CS	SP	Ch	Sh	BC	AV	SV	SC	FS	P	SG	PRIME REFERENCES
Baldens-Beacon (Chipman) Formation: Vermont																		***Lower Ordovician***																				
VT	Addison		Orwell	Orwell									X					Leonard's Cave	d	25	2	1.0	25		1		1	0	0										Quick, 1994
VT	Addison		Cornwall	Piper Crossing									L					Piper Crossing Cave	b	9	4	2.0	18		1		1	0	0										Quick, 1994
VT	Addison		Cornwall	Cornwall									L					Rimmond Cave	c	20	5	0.5	10		1		1	1	0										Quick, 1994
VT	Addison		Middlebury	Otter Creek									X					Baldese Falls Cave	b	120	20	6.0	720		1	1	1	5	1	2					1					Quick, 1994
VT	Addison		Middlebury	Weybridge Hill									L					Weybridge Cave	h	456	39	8.0	3864		1	1			1	0										Not marble, of invasionsgrotte
VT	Rutland		Dorset	Cave Woods									X					Camp Spring Cave	b	12	3	4.0	48		1	1	1	1	1	0					1					Quick, 1994
VT	Rutland		Dorset	Purgatory Plateau									L					Boulder Cave	d	64	23	8.0	512		1	1		1	2	0					1					Quick, 1994
VT	Rutland		Dorset	Purgatory Plateau									X					Peculier Well	S	10	6	2.0	20		1			1	1	0					1					Quick, 1994
VT	Rutland		Dorset	Purgatory Plateau									L					Mole Root Cave	d	15	3	1.0	15		1	1		0	1	0					1					Quick, 1994
VT	Rutland		Dorset	Purgatory Plateau									L					Purgatory System	g	183	82	6.0	1098		1			2	3	0					1					Max. distance to surface = c.40m
VT	Rutland		Dorset	Purgatory Plateau									L					Brian's Cave	a	52	17	4.0	208		1	1			1	0					1					Quick, 1994
VT	Rutland		Dorset	Purgatory Plateau									L					South vent	a	7	2	1.0	7		1			1	0	0										Quick, 1994
VT	Rutland		Dorset	Purgatory Plateau									L					Deer Cave	f	105	22	4.0	420		1			1	1	0										Quick, 1994. Palmer fissure passages
VT	Rutland		Dorset	Purgatory Plateau									L					Hunter Cave	h	356	65	5.0	1780		1			1	1	0										Quick, 1994, Sept 2001. Unknown surf. dist.
VT	Rutland		Dorset	Purgatory Plateau									L					Thin Man's Cave	a	13	7	2.0	28		1	1			1	0					1					Quick, 1994
VT	Rutland		Dorset	Purgatory Plateau									L					Hanging Boulder Cave	b	18	4	2.0	36		1	1		0	1	0					1					Quick, 1994
VT	Rutland		Dorset	Purgatory Plateau									L					Dave's Porcupine Cave	I	34	9	3.0	102		1			1	1	0										Quick, 1994
VT	Rutland		Dorset	Dorset Mt.									L					Chimney Cave	d	104	44	10.0	1040		1			1	1	0										Quick, 1994
VT	Rutland		Dorset	Dorset Mt.									L					North-End Cave 1	a	18	2	4.0	72		1			2	0	0										Quick, 1994
VT	Rutland		Dorset	Dorset Mt.									L					North-End Cave 2	a	12	1	3.0	36		1			1	0	0										Quick, 1994
VT	Rutland		Sudbury	Brandon									X					Brandon Perkie Den	a	15	1	3.0	45		1			1	0	0										Quick, 1994
VT	Rutland		Sudbury										L					Bear Bones Cave	a	24	14	1.0	24		1			1	0	0										Quick, 1994
VT	Rutland		Sudbury										L					1867 Cave	b	62	16	6.0	372		1			1	1	0					1					Quick, 1994
VT	Rutland		Sudbury										L					Cave in the Vales 1	a	13	3	2.0	26		1		1		1	0										Quick, 1994
VT	Rutland		Sudbury										L					Cave in the Vales 2	b	24	3	2.0	48		1			1	0	0										Quick, 1994
VT	Rutland		Sudbury										L					Cave in the Vales 3	a	8	1	2.0	16		1			1	0	0										Quick, 1994
VT	Bennington		Pownal	Bennington									X					Carpenter Hill Cave	d	28	12	4.0	112		1			1	0	0										Quick, 1994
VT	Bennington		Pownal	Bennington									L					Mount Anthony Cave	f	117	22	8.0	702		1	1			1	0										Quick, 1994
VT	Bennington		Pownal	Bennington									L					Bobcat Cave	f	71	18	6.0	426		1			1	1	0										Quick, 1994
VT	Bennington		Pownal	Bennington									L					Everett Cave	b	97	10	4.0	388		1			1	1	2										Quick, 1994
VT	Bennington		Pownal	Pownal									X					Lost Flashlight Cave	b	10	4	1.0	10		1			1	0	0										Keough, Sept. 1999
VT	Bennington		Pownal	Pownal									X					Ellis Hollow Cave	S	13	8	1.0	13		1			1	0	0										Keough, Sept. 1999
VT	Bennington		Pownal	Pownal									X					Halseys Hole Cave	b	16	8	1.0	16		1			1	0	0										Keough, Sept. 1999
VT	Bennington		Pownal	Pownal									X					Hot Rocks Cave	b	6	3	1.0	6		1			1	0	0										Keough, Sept. 1999
VT	Bennington		Pownal	Pownal									X					Axe Handle Cave 1	b	2	1	1.0	2		1	1			1	0										Keough, Sept. 1999
VT	Bennington		Pownal	Pownal									X					Axe Handle Cave 2	b	8	1	1.0	8		1	1			1	0										Keough, Sept. 1999
VT	Bennington		N. Pownal	Bennington									X					Pit of Misery	S	40	13	1.0	40		1			1	0	0										Quick, 1994
VT	Bennington		Bennington	West Mountain									X					Bear Cave	b	15	4	4.0	60		1			1	0	0										Quick, 1994
VT	Bennington		Arlington	West Mountain									X					W. Mt. South Knob West Cave	a	16	5	10.0	160		1			1	0	0										Quick, 1994
VT	Bennington		Arlington	West Mountain									X					W. Mt. South Knob East Cave	a	16	8	10.0	160		1			1	0	0										Quick, 1994
VT	Bennington		Arlington	Red Mountain									X					Red Mountain Pit	S	61	50	6.0	366		1			1	0	0										Quick, 1994. 50m distance to surface
VT	Bennington		Arlington	Red Mountain									X					Knot Cave	a	70	30	4.0	280		1			1	1	0										Quick, 1994
VT	Bennington		Arlington	Red Mountain									X					Chock Stone Cave	f	60	20	2.0	120		1	1			1	0										Keough, March 1999
VT	Bennington		W. Rupert	Sandgate									L					Beartown Spring Cave	b	30	5	4.0	120		1		1		1	1										Quick, 1994
VT	Bennington		W. Rupert	Sandgate									X					Beartown Hollow Perkie NW Den	a	18	1	2.0	36		1			2	0	0										Quick, 1994
VT	Bennington		W. Rupert	Sandgate									X					Beartown Hollow Perkie E Den	c	22	2	2.0	44		1		1		1	0										Quick, 1994
VT	Bennington		Manchester	Mt. Equinox									X					Equinox Cave	a	21	5	2.0	42		1			1	0	0										Quick, 1994
VT	Bennington		Manchester	Mt. Equinox									L					Little / Skinner Hollow Cave	f	420	45	4.0	1680		1			2	1	0										Quick, 1994, Dec. 2001. Keogh Mar 2001
VT	Bennington		Manchester	Mt. Equinox									L					Per-Severance Cave	f	256	52	6.0	1536		1	1			1	0										Racicot *et al.*, Dec.1999. Surf. dist. = 60m
VT	Bennington		Manchester	Mt. Equinox									L					Moses Tablets Cave	S	10	8	2.0	20		1			1	0	0										Racicot, Sept. 1999
VT	Bennington		Manchester	Mt. Equinox									X					Prow Cave Sink	S	21	6	18.0	378		1	1			1	0										Quick, 1994. Open rift
VT	Bennington		Manchester	Mt. Equinox									X					Prow South Cave	a	6	1	2.0	12		1			1	0	0										Quick, 1994
VT	Bennington		Manchester	Mt. Equinox									X					Cook Hollow Cave 1	a	6	1	2.0	12		1			1	0	0										Quick, 1994
VT	Bennington		Manchester	Mt. Equinox									X					Cook Hollow Cave 2	a	6	1	2.0	12		1			1	0	0										Quick, 1994
VT	Bennington		Manchester	Mt. Equinox									X					Walk In Den	a	10	2	2.0	20		1			1	0	0										Quick, 1994
VT	Bennington		Dorset	Rutland									L					Falls Cliff Cave	f	98	21	2.0	196		1			1	1	0									1	Quick, 1994. TF96
VT	Bennington		Dorset	Rutland									L					North Falls Cave	a	10	5	1.0	10		1	1			1	0										Quick, 1994
VT	Bennington		Dorset	Rutland									L					Pothotes Cave	a	10	3	1.0	10		1			1	0	0										Quick, 1994
VT	Bennington		Dorset	Cave Woods									L					Cave Woods West Cave	a	6	2	3.0	18		1			1	0	0										Quick, 1994
VT	Bennington		Dorset	Cave Woods									L					Cave Woods East Cave	a	12	3	3.0	36		1			1	0	0										Quick, 1994

NORTH AMERICAN CALEDONIDES CAVE DATABASE: VERMONT/ WESTERN MASSACHUSETTS (Berkshire)

Caves are grouped by carbonate outcrop

STATE AND COUNTY	ALT.	QUAD OR TOWN	AREA	LST. STRIK	LST. DIP	OW	EXT. COLOUR	OTHER INT. ROCK	R	T	GE	CL	KT	SH	OR	CA	REF. NO.	CAVE NAME	CT	LENG.	VR	XS	VOL.	Min. HG %	C	SE	RE	DE	CS	SP	Ch	Sh	BC	AV	MV	DC	FS	P	SC	PRIME REFERENCES
Bolders-Bascom (Chipman) Formation: W. Massachusetts																			***Lower Ordovician***																				
MA	Berkshire	306	North Adams	N. Adams S.									X					Richmond Cave	I	62	22	8.0	496		1		1	0	0											Plante, Sept. 1993
MA	Berkshire	288	North Adams	N. Adams S.									X					Wilson's Cave	I	13	6	3.0	39		1		1	0	0											Plante, Sept. 1993
MA	Berkshire	276	North Adams	N. Adams S.									X					Wilson's Cave 2	I	6	3	0.5	3		1		1	0	0											Plante, Sept. 1993
MA	Berkshire	390	Lanesborough	Diss. Brook									X					Constitution Cave	c	20	3	2.0	40		1		2	0	0											Plante, June 1992
MA	Berkshire	426	Lanesborough	Hollow Brook									L					Coffin Cave	c	60	*4*	2.5	150		1		3	0	0											Plante, June 1993
MA	Berkshire	390	Lanesborough	Hollow Brook									L					Coon Hollow Cave	g	152	*10*	5.0	760		1		1	1	2				1							Plante, June 1993
MA	Berkshire	405	Lanesborough	Hollow Brook									L					Coon Hollow Res. Cave 3	c	10	1	1.5	15		1		1		1	1										Plante, June 1993
MA	Berkshire	405	Lanesborough	Hollow Brook														Coon Hollow Pit																					Plante, June 1993
MA	Berkshire	405	Lanesborough	Hollow Brook									L					Dolo Cave	c	60	*3*	1.0	60		1		1	1	0											Plante, June 1993
MA	Berkshire		Lanesborough	?									*L*					Berkshire Cavern	d	229	30	3.0	687		1		1	2	1											Plante, March 2000. Location not stated
MA	Berkshire	342	Egremont	Jug End									L					Bat's Den Cave	f	225	10	1.0	225		1		3	0	0				1							Plante, June 1991
MA	Berkshire	342	Egremont	Jug End									L					Crystal Pool Cave	c	33	3	6.0	198		1		1	0	0											Plante, June 1991
MA	Berkshire	342	Egremont	Jug End									L					Pothole Cave	b	48	3	1.0	48		1	1		1	1						1					Plante, June 1991
MA	Berkshire	332	Egremont	Jug End									L					Marble Hole Cave	a	*10*	3	*1.0*	*10*		1	1		1	0											Plante, June 1991
MA	Berkshire	332	Egremont	Jug End									L					Growling Bear Cave	e	42	3	*1.0*	*42*		1		1	1	1											Plante, June 1991
MA	Berkshire	332	Egremont	Jug End									L					Will's Well	a	20	*3*	*1.0*	*20*		1		1	0	0											Plante, June 1991
Shelburne Marble																			***Lower Ordovician***																				
VT	Chittenden		Burlington	Winooski River									L					Lime Kiln Cave 1	a	13	2	6.0	78		1		1	0	0											Quick, 1994
VT	Chittenden		Burlington	Winooski River									L					Lime Kiln Cave 2	a	6	1	*2.0*	*12*		1		1	0	0											Quick, 1994
VT	Chittenden		Burlington	Winooski River														Lime Kiln Cave 3																					
VT	Chittenden		Burlington	Winooski River														Lime Kiln Cave 4																					
VT	Chittenden		Burlington	Winooski River									L					Lime Kiln Cave 5	a	5	2	*3.0*	*15*		1		1	0	0											Quick, 1994
VT	Chittenden		Burlington	Winooski River									L					Winooski River Gorge Cave	b	26	18	4.0	104		1		1	0	0											Quick, 1994
VT	Rutland		Dorset	Dorset Mt.									L					Quarry Cave / Slugge's Cave	b	200	*10*	3.0	600		1		1	1	0											Quick, 1994
VT	Rutland		W. Rutland	Susie Peak									X					Calvin Cave	a	42	15	4.0	168		1		1	1	1											Quick, 1994
VT	Rutland		Proctor	Proctor Village									L					Proctor Village Cave	a	19	4	2.0	38		1		1	0	0											Quick, 1994
VT	Rutland		Proctor	Florence									L					Gully Cave	b	8	2	2.0	16		1		1	0	0											Quick, 1994
VT	Rutland		Proctor	Florence									L					Florence Quarry No. 1	a	5	*1*	*2.0*	*10*		1		1	0	0											Quick, 1994
VT	Bennington		Manchester	Green Peak									L					Aeolus Bat Cave	h	900	65	6.0	5400		1		1	1	1											Photo p24:size, breakdown. Keogh Dec 00*
VT	Bennington		Dorset	Green Peak									L					Cliff Hole	c	50	4	2.0	100		1		1	0	0											Quick, 1994. No natural entrance
VT	Bennington		Dorset	Green Peak									L					Mud Hole Cave	a	11	5	1.0	11		1		1	0	0											Keough, March 1999
VT	Bennington		Dorset	Gulf Brook									L					Sweeny Brook Cave	c	69	7	1.0	69		1		1	1	1											Quick, 1994
VT	Bennington		Dorset	Gulf Brook									L					Deer Trail Cave	c	95	7	1.0	95		1	1	2	1	0											Quick, 1994
VT	Bennington		Dorset	Gulf Brook									L					Bruised Rib Cave	c	53	9	3.0	159		1		1	2	0											Quick, 1994
VT	Bennington		Dorset	Rutland									L					Tallow Cave	b	60	16	4.0	240		1		1	1	1											Quick, 1994
VT	Bennington		Dorset	Rutland									L					Tallow Spur Cave 1	a	3	*1*	*1.0*	3		1		1	0	0											Quick, 1994
VT	Bennington		Dorset	Rutland									L					Tallow Spur Cave 2	a	3	*1*	*1.0*	3		1		1	0	0											Quick, 1994
VT	Bennington		Dorset	Rutland									L					Tallow Spur Cave 3	a	6	*1*	*1.0*	*6*		1		1	0	0											Quick, 1994
VT	Bennington		Dorset	Rutland									L					Tallow Spur Cave 4	a	10	2	*1.5*	*15*		1		1	1	1											Quick, 1994
VT	Bennington		Dorset	Rutland									L					Bone Room Cave	a	10	2	2.0	20		1		1	0	0											Quick, 1994
VT	Bennington		Dorset	Rutland									L					Webster's Bones Cave	b	37	10	1.5	56		1		1	1	0											Quick, 1994
MA	Berkshire	440	Lanesborough	Diss. Brook									A					Elephant's Den Cave	c	48	*4*	1.0	48		1		1	0	0											Plante, June 1992
MA	Berkshire	450	Lanesborough	Diss. Brook									A					Baker's Quarry Cave	d	70	12	1.5	105		1	1		1	0				1							Plante, June 1992
MA	Berkshire	440	Lanesborough	Diss. Brook									A					Disappearing Brook Ca. N.	d	20	1	1.2	24		1		1	1	1											Plante, June 1992
MA	Berkshire	440	Lanesborough	Diss. Brook									A					Disappearing Brook Ca. S.	a	15	2	1.2	18		1	1		2	1				1							Plante, June 1992
MA	Berkshire	435	Lanesborough	Diss. Brook									A					Nowornever Cave	b	24	1	1.2	29		1		1	1	0				1							Plante, June 1992
MA	Berkshire	450	Lanesborough	Diss. Brook									A					Convention Cave	f	60	6	1.6	96		1	1		3	1											Plante, June 1992
MA	Berkshire	420	Lanesborough	Diss. Brook									A					Drag Rock Cave	f	60	4	1.5	*90		1		1	1	1											Plante, June 1992
MA	Berkshire	430	Lanesborough	Diss. Brook									A					Found Cave	d	110	10	3.0	330		1	1	1	3												Plante, June 1992
MA	Berkshire	375	Lanesborough	Hollow Brook									L					Brookside Cave	d	10	1	1.0	10		1	2		2	0					1						Plante, June 1993
MA	Berkshire	415	Lanesborough	Hollow Brook									L					Temper Hole	a	5	2	*2.0*	*10*		1	1		1	0					1						Plante, June 1993
MA	Berkshire	378	Lanesborough	Hollow Brook									L					Blanket Cave	b	15	2	1.5	23		1	1		1	0					1						Plante, June 1993
MA	Berkshire	405	Lanesborough	Hollow Brook									L					Bill Blakney's Cave	a	*5*	*2*	*2.0*	*10*		1	1		1	0					1						Plante, June 1993

* Chuck Porter pc 101102

NORTH AMERICAN CALEDONIDES CAVE DATABASE: VERMONT/ WESTERN MASSACHUSETTS (Berkshire)

Caves are grouped by carbonate outcrop

									External Cave Attributes											Internal Cave Attributes																			
STATE AND COUNTY	ALT.	QUAD OR TOWN	AREA	LST. STRIKE	LST. DIP	OW	EXT. COLOUR	OTHER INT. ROCK	R	T	GS	CL	KT	SH	OR	CA	REF. NO.	CAVE NAME	CT	LENG.	VR	XS	VOL.	Min. Ht.	C	SE	RE	DE	CS	SP	Ch	Sh	BC	AV	MV	DC	FS	P	SG	PRIME REFERENCES
Clarendon Springs Formation																			***Upper Cambrian***																				
VT	Franklin		Alburg Springs	Fortin Farm									X						Highgate Springs Cave 1	a	30	5	5.0	150		1		2	0	0										Quick, 1994
VT	Franklin		Alburg Springs	Fortin Farm									X						Highgate Springs Cave 2	a	10	5	4.0	40		1		2	0	0										Quick, 1994
VT	Chittenden		Colchester	Indian Brook									X						Colchester Cave 1	b	23	2	*1.5*	35		1	1	2	1	0					1					Quick, 1994
VT	Chittenden		Colchester	Indian Brook									X						Colchester Cave 2	b	21	2	*1.5*	32		1	1	1	1	0					1					Quick, 1994
VT	Chittenden		Colchester	Indian Brook									X						Colchester Cave 3	b	26	2	*1.5*	39		1		1	0	0					1					Quick, 1994
VT	Rutland		Wallingford SW	Mt. Tabor									A						Morris Cave	h	563	66	2.0	1126		1		1	3	3								1		Sump reaches to >66m below surface?TF98
VT	Rutland		Wallingford SW	Mt. Tabor									A						West Satellite Cave	a	9	2	*2.0*	*18*		1		1	0	0										Quick, 1994
VT	Rutland		Wallingford SW	Mt. Tabor									A						East Satellite Cave	b	13	2	*2.0*	*26*		1		1	0	0										Quick, 1994
VT	Rutland		Wallingford SW	Mt. Tabor									A						Spider Cave	b	30	2	*2.0*	*60*		1		1	0	0										Quick, 1994
Winooski Dolomite																			***Middle Cambrian***																				
VT	Rutland		Rutland	Clarendon									L						Nag's Den	a	7	*2*	*2.0*	*14*		1		1	0	0										Quick, 1994
VT	Rutland		Rutland	Clarendon									L						Cold River Cave	a	11	4	1.0	11		1	1		1	0										Quick, 1994
VT	Rutland		Rutland	Clarendon									L						Green Frog Cave	b	20	*4*	1.0	20		1		1	0	0										Quick, 1994
VT	Rutland		Brandon	Brandon									A						Johnston Pit	S	29	12	2.0	58		1		1	0	0										Quick, 1994. Dip 80W
Dunham Dolomite																			***Lower Cambrian***																				
VT	Addison		South Mt.	The Cobble									X						Bristol Cave	d	33	5	2.0	66		1		1	0	0										Quick, 1994
VT	Addison		South Mt.	The Cobble									X						Barrel Cave	b	30	4	1.0	30		1		1	0	0										Quick, 1994
VT	Addison		South Mt.	The Cobble									X						Cobble Cave	a	8	*1*	*2.0*	*16*		1		1	0	0										Quick, 1994
VT	Addison		South Mt.	The Cobble									X						Flat Room Cave	b	47	2	4.0	188		1		1	0	0										Quick, 1994
VT	Addison		Bristol	Baldwin Creek									X						Porcupine Cave 1	a	3	*1*	*1.0*	*3*		1		1	0	0										Quick, 1994
VT	Addison		Bristol	Baldwin Creek									X						Porcupine Cave 2	a	22	2	*1.0*	*22*		1		1	0	0										Quick, 1994
VT	Addison		Bristol	Baldwin Creek									X						Porcupine Cave 3	a	10	2	*2.0*	*20*		1		1	0	0										Quick, 1994
VT	Addison		Bristol	Baldwin Creek									X						Porcupine Cave 4	b	15	2	*2.0*	30		1		1	0	0										Quick, 1994
Mendon Formation - Forestdale Marble																			***Lower Cambrian***																				
VT	Rutland		Brandon	Chaffe Mt.									L						Nichwaclett Cave	f	198	13	4.0	792		1		3	0	0								1		Quick, 1994. TF2002
VT	Rutland		Brandon	Chaffe Mt.									L						Chaffe Mountain 1 Cave	a	21	9	1.0	21		1		1	1	0										Keogh, Mar 2000
VT	Rutland		Brandon	Chaffe Mt.									L						Chaffe Mountain 2 Cave	a	98	6	12.0	1176		1	1	4	1	0					1	1		1		Quick, 1994. TF2002
VT	Rutland		Brandon	Chaffe Mt.									X						Wheeler Farm Cave	S	12	9	4.0	48		1		1	0	0										Quick, 1994
VT	Rutland		Brandon	Chaffe Mt.									L						Philadelphia Cave	f	135	21	3.0	405		1		2	0	0										Quick, 1994. Tectonic cave?
VT	Rutland		Brandon	Chaffe Mt.									X						Gee's Cave	b	33	10	2.0	66		1		1	0	0										Keogh, Mar 2000
Tyson Formation																			***Basal Cambrian***																				
VT	Windsor		Killington Peak	Plymouth Union									X						Plymouth West Cave	a	18	4	4.0	72		1		2	0	0										Quick, 1994
VT	Windsor		Killington Peak	Plymouth Union									X						Plymouth South Cave	f	72	8	6.0	432		1		1	0	0										Quick, 1994
Readsboro Formation - Sherman marble																			***Precambrian***																				
VT	Rutland		Wallingford SW	Mt. Tabor									X						Devil's Den	c	24	1	1.0	24		1		1	1	0										Quick, 1994
VT	Rutland		Wallingford SW	Mt. Tabor									X						Devil's Cliff 1	a	10	2	*2.0*	*20*		1		1	0	0										Quick, 1994
VT	Rutland		Wallingford SW	Mt. Tabor									X						Devil's Cliff 2	a	8	1	*2.0*	*16*		1		1	0	0										Quick, 1994
VT	Bennington		Wilmington	Readsboro									X						Red Fox Cave	c	15	5	2.0	30		1		1	1	0										Quick, 1994

NORTH AMERICAN CALEDONIDES CAVE DATABASE: VERMONT/ WESTERN MASSACHUSETTS (Berkshire)

External Cave Attributes — Caves are grouped by carbonate outcrop — Internal Cave Attributes

STATE	AND COUNTY	ALT.	QUAD OR TOWN	AREA	LST. STRIKE	LST. DIP	OW	EXT. COLOUR	OTHER INT. ROCK	R	T	GR	CL	KT	SH	OX	CA	REF. NO.	CAVE NAME	CT	LENG.	VR	XS	VOL.	Min. HG %	C	SE	NE	DE	CS	SP	Ch	Sh	SC	AV	MV	DC	FS	P	SG	PRIME REFERENCES
Unknown and miscellaneous formations																			*unknown age of bedrock*																						
VT	Windham																		Easter Cave		186m long																				Higham, June, 1997
VT	Addison																		Mack Farm Cave		14m long crawl																				NE Caver 23 (2) 2002 p42
VT	Rutland																		Pico Cave		23m long. Altitude 864m																				Moore, June 1999
VT	Rutland		Pittsford																Pittsford Ice Cave		169m long. 25m VR																				Higham, June, 2001
VT	?																		Maidstone Caves																						
NY	Washington		Poultney River										L						Carver Falls Cave	c	40	9	6.0	240		1			1	0	0										Porter, March 2000
MA	Berkshire																		Pettibone Falls Cave		191m long																				Higham, June, 1997
MA	Berkshire																		Great Radium Springs Cave		480m long																				Higham, June, 1997
MA	Berkshire												X						Frying Pan Spring Cave	b	16	5	6.0	96		1	1		3	1	0										Howcroft, June 1997
MA	Berkshire												X						Hot Pot	a	3	2	2.0	8		1			1	0	0										Howcroft, June 1997
MA	?																		McMasters																						
CT	Litchfield																		Twins Lakes Cave		261m long																				Higham, June, 1997
CT	Litchfield			New Milford															Tory Cave		Giant sinkhole entrance, 30 feet in diameter																				Foote, Sept. 1999
MA	Berkshire	320	Alford	Alford Brook															Devil's Den Cave		Interstratal cave in phyllite above calcitic tectonic breccia. 48m long																				Plante, Sept. 1994

APPENDIX C9

SCOTTISH DALRADIAN SUPERGROUP CAVE DATABASE

SCOTTISH DALRADIAN SUPERGROUP CAVE DATABASE:

SUMMARY - TOTALS

			External Cave Attributes			Internal Cave Attributes																			
GROUP	SUBGROUP	ALT.	R	T		LENG.	VR	XS	VOL.	C	SE	RE	DE	CS	SP	Ch	Sh	BC	AV	MV	DC	FS	P	COMMENTS
Argyll	Tayvallich	###	0	0		485	####	####	1181	33	9	8	27	20	0	0	0	0	0	11	0	0	0	
Appin	Blair Atholl	###	0	0		658	####	####	999	40	11	10	30	32	13	0	0	0	0	14	0	0	6	
Appin	Ballachulish - Appin	###	0	0		982	####	####	3036	29	14	4	19	29	7	0	0	0	0	13	0	0	2	
Appin	Ballachulish - Ballachulish	###	0	0		2100	####	####	7584	50	23	14	30	45	20	0	0	0	1	17	0	0	13	
Totals		###	0	0		4225	####	####	12800	152	57	36	106	126	40	0	0	0	1	55	0	0	21	

SUMMARY - AVERAGES

Argyll	Tayvallich	398	0	0		15	4.6	2.1	36		0.3	0.2	0.8	0.6	0.0	0.0	0.0	0.0	0.0	0.3	0.0	0.0	0.0	
Appin	Blair Atholl	378	0	0		16	3.4	1.3	25		0.3	0.3	0.8	0.8	0.3	0.0	0.0	0.0	0.0	0.4	0.0	0.0	0.2	
Appin	Ballachulish - Appin	305	0	0		34	7.8	2.5	105		0.5	0.1	0.7	1.0	0.2	0.0	0.0	0.0	0.0	0.4	0.0	0.0	0.1	
Appin	Ballachulish - Ballachulish	261	0	0		42	7.6	2.6	152		0.5	0.3	0.6	0.9	0.4	0.0	0.0	0.0	0.0	0.3	0.0	0.0	0.3	
Average per cave		330	0	0		28	5.9	2.1	84		0.4	0.2	0.7	0.8	0.3	0.0	0.0	0.0	0.0	0.4	0.0	0.0	0.1	

SUMMARY - MINIMA

Argyll	Tayvallich	260	0	0		2	1.0	0.2	1		1	1	1	0	0	0	0	0	0	0	0	0	0	
Appin	Blair Atholl	150	0	0		1	1.0	0.2	1		1	1	1	0	1	0	0	0	0	0	0	0	0	
Appin	Ballachulish - Appin	75	0	0		3	1.0	0.3	1		1	1	1	0	1	0	0	0	0	0	0	0	0	
Appin	Ballachulish - Ballachulish	81	0	0		1	1.0	0.2	1		1	1	1	0	1	0	0	0	1	0	0	0	0	
Minima		75	0	0		1	1.0	0.2	1		1	1	1	0	0	0	0	0	0	0	0	0	0	

SUMMARY - MAXIMA

Argyll	Tayvallich	700	0	0		50	20.0	8.0	216		1	1	3	2	0	0	0	0	0	0	0	0	0	
Appin	Blair Atholl	740	0	0		100	11.0	4.0	200		1	1	3	2	2	0	0	0	0	0	0	0	0	
Appin	Ballachulish - Appin	610	0	0		170	29.0	10.0	700		1	1	3	3	2	0	0	0	0	0	0	0	0	
Appin	Ballachulish - Ballachulish	895	0	0		340	48.0	10.0	1680		2	1	3	3	4	0	0	0	1	0	0	0	0	
Maxima		895	0	0		340	48.0	10.0	1680		2	1	3	3	4	0	0	0	1	0	0	0	0	

SCOTTISH DALRADIAN SUPERGROUP CAVE DATABASE

Refer to North Central Norway Database for Key

NOTE: DOES NOT INCLUDE INFORMATION IN THE APPIN CAVE GUIDE SUPPLEMENT OF OCTOBER 2003, NOR THE GRID POSITIONS GIVEN IN GSG 2 (1) MARCH 2004 P7.

ARGYLL GROUP: Teyvallich Subgroup: TOTALS

External Cave Attributes

	GRID. REF.	ALT.	COUNTY	AREA	LST. STRIK	LST. DIP	OW	EXT. COLOUR	OTHER INT. ROCK	R	T	GE	CL	KT	SR	OR	CA	REF. NO.
						#	##										##	
Totals		####	33			#	0			0	0						##	
Av. per cave		396				0	0			##	##						0	
Minima		260				0	0										0	
Maxima		700																

(Dip measured in 0 caves)

Internal Cave Attributes

	CAVE NAME	CT	LENG.	VR	XS	VOL.	Min. HG %	C	SE	RE	DE	CS	SP	Ch	Sh	SC	AV	MV	DC	FS	P	SG	PRIME REFERENCES
Totals			485	###	####	1181	##	33	9	8	27	20	0	0	0	0	0	11	0	0	0		
Av. per cave			15	4.6	2.1	36	0		0.3	0.2	0.8	0.6	0.0	0.0	0.0	0.0	0.0	0.3	0.0	0.0	0.0		
Minima			2	1	0.2	1	0		1	1	1	0	0	0	0	0	0						
Maxima			50	20	8.0	216	0		1	1	3	2	0	0	0	0	0						

Glacial Situations:

	#	Length
C	0	0
D	0	0
E	0	0
G	0	0
H	0	0
K	0	0
L	0	0
S	0	0
T	0	0
U	0	0
Totals	0	0

Karst Types:

	#	Length
V	0	0
A	0	0
L	0	0
C	0	0
X	33	485
Totals	33	485

Cave Locations:

	#	Length
C	0	0
F	0	0
W	0	0
R	0	0
S	0	0
G	0	0
P	0	0
Totals	0	0

Cave Types:

	#	Length
S	6	33
a	13	81
b	4	116
c	4	82
d	3	75
e	1	40
f	1	38
g	1	20
h	0	0
Hy	0	0
I	0	0
J	0	0
L	0	0
R	0	0
T	0	0
Totals	33	485

Relict Caves:

	#	Length
	14	156
Totals	14	156

MV Caves:

	#	Length
	11	163
Totals	11	163

Combination Caves:

	#	Length
Totals	8	166

SCOTTISH DALRADIAN SUPERGROUP CAVE DATABASE

Refer to North Central Norway Database for Key

Caves are grouped by carbonate outcrop

GRID. REF.	ALT.	COUNTY	AREA	External Cave Attributes: LST. STRIK	LST. DIP	OW	EXT. COLOUR	OTHER INT. ROCK	R	T	GE	CL	KT	SR	OR	CA	REF. NO.	CAVE NAME	Internal Cave Attributes: CT	LENG.	VR	XS	VOL.	Mla. HG %	C	SE	RE	DE	CS	SP	Ch	Sh	BC	AV	MV	DC	FS	P	BG	PRIME REFERENCES
ARGYLL GROUP: Tayvallich Subgroup: Tayvallich Limestone																																								
1:50000 Landranger Sheet 55 Lochgilphead																																								
NM 875 085	270	Argyll	Glen Domhain										X					Tunnalt Cave 1	S	5	5	*1*	5		1			1	0											Scotland Underground, 1984
NM 875 085	270	Argyll	Glen Domhain										X					Tunnalt Cave 2	S	4	4	*1*	4		1			1	0											Scotland Underground, 1984
NM 916 029	270	Argyll	Loch Awe										X					Fincham River Cave	b	27	2	8.0	216		1	1	1		1											S. Highlands Cave Guide, 1988
ARGYLL GROUP: Tayvallich Subgroup: Loch Tay Limestone																																								
1:50000 Landranger Sheet 50 Glen Orchy																																								
NN 307 268	700	Perth	Strath Fillan										X					Top Sink Cave	g	20	7	3.0	60		1			2	1											S. Highlands Cave Guide, 1988
NN 307 268	690	Perth	Strath Fillan										X					Resurgence Cave	c	12	2	1.0	12		1		1		1							1				GSG Bulletin 2(3) 1992 18-20
NN 307 268	680	Perth	Strath Fillan										X					Window Cave	a	7	2	4.0	28		1	1		1	1							1				S. Highlands Cave Guide, 1988
NN 316 272	490	Perth	Strath Fillan										X					Dubhcraig Subway	b	50	10	2.0	100		1	1	1		1							1				GSG Bulletin 2(3) 1992 18-20
NN 316 272	500	Perth	Strath Fillan										X					Klingon Finger Cave	c	15	3	1.0	15		1		1	2	1											GSG Bulletin 2(3) 1992 18-20
1:50000 Landranger Sheet 51 Loch Tay																																								
NN 516 214	430	Perth	Balquhidder															Secret Cave		10m-long trial adit																					S. Highlands Cave Guide, 1988
NN 514 250	500	Perth	Glen Dochart										X					Resurgence Cave	a	8	2	6.0	48		1		1		1											S. Highlands Cave Guide, 1988
NN 516 255	535	Perth	Glen Dochart										X					Shelling Stream Cave	b	19	2	1.0	19		1			1	1							1				S. Highlands Cave Guide, 1988
NN 516 255	535	Perth	Glen Dochart										X					Fox Hole	c	5	1	0.2	1		1			1	0											S. Highlands Cave Guide, 1988
NN 515 255	540	Perth	Glen Dochart										X					Pepper Pot	d	30	10	2.0	60		1			1	1							1				S. Highlands Cave Guide, 1988
NN 515 266	425	Perth	Glen Dochart															Rabbit Warren		13m cave in earth																					S. Highlands Cave Guide, 1988
NN 515 266	425	Perth	Glen Dochart															Earth Cave		8m cave in earth																					S. Highlands Cave Guide, 1988
NN 515 266	425	Perth	Glen Dochart										X					Lucky Dig	d	25	2	2.0	50		1			1	1							1				S. Highlands Cave Guide, 1988
NN 519 278	275	Perth	Glen Dochart										X					Woodside Cave	a	6	1	0.5	3		1	1			1											S. Highlands Cave Guide, 1988
NN 509 309	430	Perth	Glen Dochart										X					Birch Cave	a	5	1	0.4	2		1		1		1							1				S. Highlands Cave Guide, 1988
NN 564 297	300	Perth	Glen Dochart										X					Cameo Cave	d	20	9	2.0	40		1	1	1	1	1											S. Highlands Cave Guide, 1988
NN 565 297	300	Perth	Glen Dochart										X					Boulder Cave	a	4	2	*1.0*	4		1	1			1							1				S. Highlands Cave Guide, 1988
NN 568 298	300	Perth	Glen Dochart										X					Shakehole Cave	a	9	4	*2.0*	18		1			1	0											S. Highlands Cave Guide, 1988
NN 568 298	300	Perth	Glen Dochart										X					Grassy Sink Hole	a	5	*4*	1.0	5		1			1	0											S. Highlands Cave Guide, 1988
NN 585 214	320	Perth	Strathyre										X					North Fissure Cave	e	40	20	5.0	200		1			1	0											S. Highlands Cave Guide, 1988
NN 585 214	312	Perth	Strathyre										X					Vertical Cleft Cave	a	6	4	2.0	12		1			1	0											S. Highlands Cave Guide, 1988
NN 584 209	395	Perth	Strathyre										X					Deer Fence Hole	S	5	5	*1.0*	5		1			1	0											S. Highlands Cave Guide, 1988
NN 584 208	395	Perth	Strathyre										X					Sloping Rift Pot	S	10	8	*1.0*	10		1			1	0											S. Highlands Cave Guide, 1988
NN 584 208	380	Perth	Strathyre										X					Walk-In Cave	a	17	*3*	*2.0*	34		1			3	0											S. Highlands Cave Guide, 1988
NN 584 208	380	Perth	Strathyre										X					Ice Stal Cave	a	*3*	*1*	*3.0*	9		1			1	0											S. Highlands Cave Guide, 1988
NN 609 323	260	Perth	Loch Tay										X					Stream Cave	a	5	*1*	*1.0*	5		1		1		1							1				S. Highlands Cave Guide, 1988
NN 616 323	380	Perth	Loch Tay										X					Uamh nan Otwen	b	20	4	3.0	60		1	1			1											S. Highlands Cave Guide, 1988
NN 616 323	260	Perth	Loch Tay										X					Nettle Pot	S	6	6	*4.0*	24		1			1	0											S. Highlands Cave Guide, 1988
NN 616 323	260	Perth	Loch Tay										X					Blind Sink	S	3	3	*4.0*	12		1			1	0											S. Highlands Cave Guide, 1988
NN 616 323	260	Perth	Loch Tay										X					Active Streamsink	a	2	2	*1.0*	2		1	1		1	1							1				S. Highlands Cave Guide, 1988
NN 631 336	400	Perth	Loch Tay										X					Gin-Trap Cave	c	50	10	0.3	15		1			1	2											S. Highlands Cave Guide, 1988
NN 653 342	380	Perth	Loch Tay										X					Potential Dig Cave	a	4	2	*2.0*	8		1	1			1							1				S. Highlands Cave Guide, 1988
NN 757 431	215	Perth	Loch Tay															Acharn Cave		30m-long man-made cave																					S. Highlands Cave Guide, 1988
1:50000 Landranger Sheet 44																																								
NO 394 792	450	Angus	Glen Esk										X					Gryps Cave	f	38	10	2.5	95		1			1	0											GSG Bulletin 5(2) 1999 p15

SCOTTISH DALRADIAN SUPERGROUP CAVE DATABASE

Refer to North Central Norway Database for Key

APPIN GROUP: Blair Atholl Subgroup: TOTALS

External Cave Attributes

GRID. REF.	ALT.	COUNTY	AREA	LST. STRIK	LST. DIP	OW	EXT. COLOUR	OTHER INT. ROCK	R	T	GS	CL	KT	BR	OR	CA	REF. NO.	CAVE NAME
Totals	####	40			#	##			0	0						##		
Av. per cave	378				#	0			##	##						##		
Minima	150				0	0										0		
Maxima	740				0	0										0		

(Dip measured in 0 caves)

Internal Cave Attributes

	CT	LENG.	VR	XS	VOL.	Min. HG %	C	SE	RE	DE	CS	SP	Ch	Sh	BC	AV	MV	DC	FS	P	SG	PRIME REFERENCES
Totals		658	###	####	999	##	40	11	10	30	32	13	0	0	0	0	14	0	0	6		
Av. per cave		16	3.4	1.3	25	0		0.3	0.3	0.8	0.8	0.3	0.0	0.0	0.0	0.0	0.4	0.0	0.0	0.2		
Minima		1	1	0.2	1	0		1	1	1	0	1	0	0	0	0						
Maxima		100	11	4.0	200	0		1	1	3	2	2	0	0	0	0						

Glacial Situations:

	#	Length
C	0	0
D	0	0
E	0	0
G	0	0
H	0	0
K	0	0
L	0	0
S	0	0
T	0	0
U	0	0
Totals	0	0

Karst Types:

	#	Length
V	3	30
A	11	259
L	0	0
C	0	0
X	26	369
Totals	40	658

Cave Locations:

	#	Length
C	0	0
F	0	0
W	0	0
R	0	0
S	0	0
G	0	0
P	0	0
Totals	0	0

Cave Types:

	#	Length
S	5	32
a	16	145
b	11	238
c	1	18
d	3	35
e	1	40
f	0	0
g	3	150
h	0	0
Hy	0	0
I	0	0
J	0	0
L	0	0
R	0	0
T	0	0
Totals	40	658

Relict Caves:

	#	Length
	10	93
Totals	10	93

MV Caves:

	#	Length
	14	182
Totals	14	182

Combination Caves:

	#	Length
Totals	16	383

SCOTTISH DALRADIAN SUPERGROUP CAVE DATABASE

Refer to North Central Norway Database for Key

Caves are grouped by carbonate outcrop

GRID. REF.	ALT.	COUNTY	AREA	External Cave Attributes: LST. STRIK	LST. DIP	OW	EXT. COLOUR	OTHER INT. ROCK	R	T	GE	CL	KT	SR	ON	CA	REF. NO.	CAVE NAME	Internal Cave Attributes: CT	LENG.	VR	XS	VOL.	Min. HG %	C	SE	RE	DE	CS	SP	Cb	Sh	BC	AV	MV	DC	FS	P	SG	PRIME REFERENCES
APPIN GROUP: Blair Atholl Subgroup: Islay Limestone																																							
1:50000 Landranger Sheet 60 Islay																			***1¼ inch Geological Survey Sheet 13 Islay and Jura***																				
NR 413 585	*150*	Argyll	Islay										X					Shining Stone Sink	S	11	6	*2.0*	22		1	1		1											GSG Bulletin 4(2) 1983 p29
NR 413 585	*150*	Argyll	Islay										X					White Splash Cave	a	4	3	*2.0*	8		1		1	0											GSG Bulletin 4(2) 1983 p29
NR 411 580	162	Argyll	Islay										X					Uamh Allt nan Allallaidh	a	6	1	*1.0*	6		1	1		1						1					Scotland Underground
NR 410 580	*150*	Argyll	Islay										X					Dry Rising Cave	b	18	3	*1.0*	18		1		1	0											GSG Bulletin 4(2) 1983 p29
NR 410 580	150	Argyll	Islay										X					Kilennan Resurgence Cave 3	a	3	1	*1.0*	3		1		1	1						1					Scotland Underground
NR 410 579	150	Argyll	Islay										X					Kilennan Resurgence Cave 2	a	2	1	*1.0*	2		1		1	1						1					Scotland Underground
NR 411 579	150	Argyll	Islay										X					Kilennan Resurgence Cave 1	a	1	1	*1.0*	1		1		1	1	1					1					Scotland Underground
NR 411 579	*150*	Argyll	Islay										X					Through Trip	a	6	*1*	*1.0*	6		1			2	0										GSG Bulletin 4(2) 1983 p29
NR 410 577	*150*	Argyll	Islay										X					Friendly Adder Pot	S	5	5	*1.0*	5		1			1	0										GSG Bulletin 4(2) 1983 p29
APPIN GROUP: Blair Atholl Subgroup: Blair Atholl Limestone (Strath Fionan Dark Limestone)																																							
1:50000 Landranger Sheet 51 Loch Tay																																							
NN 747 561	331	Perth	Foss										A					Foss Rising	a	18	2	1.5	27		1		1		1	2					1				Caves of Schichallion, 1980
NN 745 562	355	Perth	Foss										A					Foss Cave 1	g	100	11	2.0	200		1			1	1	1							1		Caves of Schichallion, 1980
NN 745 562	355	Perth	Foss										A					Foss Cave 2	b	20	*3*	2.0	40		1	1		1	2								1		Caves of Schichallion, 1980
NN 744 562	357	Perth	Foss															Foss Cave 3																					Caves of Schichallion, 1980
NN 744 562	357	Perth	Foss															Foss Cave 3A																					Caves of Schichallion, 1980
NN 744 562	360	Perth	Foss										A					Foss Cave 4	b	24	3	4.0	96		1	1	1		1								1		Caves of Schichallion, 1980
NN 743 562	365	Perth	Foss										A					Foss Cave 5	b	20	2	2.0	40		1			1	1	1							1		Caves of Schichallion, 1980
NN 739 560	382	Perth	Foss										A					Boom Pot	d	7	5	0.3	2		1			1	0										Caves of Schichallion, 1980
NN 738 561	392	Perth	Foss										A					Top Dig cave	d	20	8	1.5	30		1			1	1										Caves of Schichallion, 1980
NN 735 562	400	Perth	Foss										A					Tuonela Cave	a	16	2	0.5	8		1		1		1	1				1					Caves of Schichallion, 1980
NN 714 573	325	Perth	Foss										X					Tom Tit Hole	g	25	*2*	*0.5*	13		1			2	1	1									Scotland Underground, 1984
NN 748 547	412	Perth	Foss										X					MPC Pot	S	7	4	*1.0*	7		1			1	0										Caves of Schichallion, 1980
NN 6990 5688	376	Perth	Lassintullich										X					Lassintullich Rising Cave	a	3	1	*1.0*	3		1		1		1					1					Caves of Schichallion, 1980
NN 6998 5662	417	Perth	Lassintullich										X					Lassintullich Cave 1	e	40	9	1.0	40		1			1	2	1									Caves of Schichallion, 1980
NN 6998 5660	422	Perth	Lassintullich										X					Lassintullich Cave 2	a	14	4	1.0	14		1			1	1										Caves of Schichallion, 1980
NN 6999 5658	422	Perth	Lassintullich										X					Lassintullich Cave 3	a	4	1	0.2	1		1	1			1	1									Caves of Schichallion, 1980
NN 6999 5657	427	Perth	Lassintullich										X					Lassintullich Cave 4 and 5	b	34	3	0.6	20		1	1	1	3	1					1					Caves of Schichallion, 1980
NN 7009 5644	454	Perth	Lassintullich										X					Tom na Fuine Res. Cave	b	4	1	1.0	4		1		1		1					1					Caves of Schichallion, 1980
NN 7013 5635	473	Perth	Lassintullich										X					Uamh Tom na Fuine	b	18	2	1.0	18		1	1			1					1					Caves of Schichallion, 1980
NN 6995 5680	389	Perth	Lassintullich										X					Lockhole Cave 1	g	25	6	1.0	25		1			1	1										Caves of Schichallion, 1980
NN 7000 5675	394	Perth	Lassintullich										X					Lockhole Main Sink	a	5	1	1.0	5		1	1			1					1					Caves of Schichallion, 1980
NN 7006 5669	397	Perth	Lassintullich										X					Lockhole Cave 2	a	16	1	1.0	16		1	1		1	1					1					Caves of Schichallion, 1980
NN 7009 5668	399	Perth	Lassintullich										X					U-Boat Cave	b	26	2	4.0	104		1	1	1		1					1					Caves of Schichallion, 1980
NN 703 538	535	Perth	Tom a'Mhor-fhir										X					Uamh an Poll-Sneachda	b	30	6	1.2	36		1			1	1	1				1					Caves of Schichallion, 1980
NN 706 535	510	Perth	Tom a'Mhor-fhir										X					Uamh Ease Tom a'Mhor-fhir	c	18	1	0.3	5		1			1	1	1									Caves of Schichallion, 1980
NN 706 535	499	Perth	Tom a'Mhor-fhir										X					Uamh Tom a'Mhor-fhir	b	38	2	2.0	78		1			1	1	1									Caves of Schichallion, 1980
NN 709 534	395	Perth	Tom a'Mhor-fhir										X					Zebra Pot	b	6	5	0.4	2		1			1	1										Caves of Schichallion, 1980
NN 719 585	215	Perth	Foss															McGregors Cave	Non-carbonate rock shelter																					Caves of Schichallion, 1980
1:50000 Landranger Sheet 43 Braemar																			***1 inch Geological Survey Sheet 64 Kingussie and 1:50000 Sheet 55E Pitlochry***																				
NO 035 795	740	Perth	Glen Loch										A					Beinn Iutharn Mhor Shaft	S	4	4	1.0	4		1			1	0								1		GSG Bulletin 4(3) 1997 p17
NN 986 689	625	Perth	Loch Valigan										*V*					Stream Sink	d	8	*3*	*2.0*	16		1	1		1	1	1									S. Highlands Cave Guide, 1988
NN 986 689	625	Perth	Loch Valigan										*V*					Vertical Dig	S	5	5	*0.2*	1		1			1	0										S. Highlands Cave Guide, 1988
NN 985 688	620	Perth	Loch Valigan										*V*					Loch Valigan Shakehole Cave	a	17	11	*2.0*	34		1			1	0										S. Highlands Cave Guide, 1988
NN 982 687	620	Perth	Loch Valigan															Blaeberry Resurgence	Diving required																					S. Highlands Cave Guide, 1988

SCOTTISH DALRADIAN SUPERGROUP CAVE DATABASE

Refer to North Central Norway Database for Key

Caves are grouped by carbonate outcrop

GRID. REF.	ALT.	COUNTY	AREA	LST. STRIK	LST. DIP	OW	EXT. COLOUR	OTHER INT. ROCK	External Cave Attributes: R	T	GS	CL	KT	SR	OR	CA	REF. NO.	CAVE NAME	Internal Cave Attributes: CT	LENG.	VR	XS	VOL.	Min. HG %	C	SE	RE	DE	CS	SP	Ch	Sh	BC	AV	MV	DC	PS	P	SG	PRIME REFERENCES
APPIN GROUP: Blair Atholl Subgroup: Inchrory Limestone Formation																																							
1:60000 Landranger Sheet 36 Grantown, Aviemore and Caringorm																																							
NJ 1625 2020	360	Banff	Glen Avon																Knoc-lochy Well		Unexplored large resurgence																		Marked on map
NJ 1726 1011	595	Banff	Glen Avon																Sink Holes		Unexplored																		J. Mendum, pc, 1997
NJ 1780 0960	600	Banff	Glen Avon																Swallow Holes		Unexplored. On w. of Carn Bad a'Ghuail to 1818 0834																		J. Mendum, pc, 1997
1:60000 Landranger Sheet 37 Strathdon																					***1:60000 Geological Survey Sheet 75E Glenbuchat***																	
NJ 2975 2923	455	Banff	Glen Fiddich											A					Elf House Cave	a	20	2	1.0	20		1	1	0											GSG Bulletin 2(2) 1992 9-10
NJ 295 285	490	Banff	Glen Fiddich											A					Slab Cave	a	10	2	2.0	20		1	1	1											GSG Bulletin 2(2) 1992 9-10
NJ 2767 2608	450	Banff	Glen Suie																Large Sink		Unexplored. And at 2764 2598, 2756 2565. In Ballachulish Subgroup																		J. Mendum, pc, 1997

SCOTTISH DALRADIAN SUPERGROUP CAVE DATABASE

Refer to North Central Norway Database for Key

APPIN GROUP: Ballachulish Subgroup: A - Appin Limestone: TOTALS

External Cave Attributes

	GRID. REF.	ALT.	COUNTY	AREA	LST. STRIKE	LST. DIP	OW	EXT. COLOUR	OTHER INT. ROCK	R	T	GS	CL	KT	SR	OR	CA	REF. NO.	CAVE NAME
Totals		####	29			#	##			0	0						##		
Av. per cave		305				#	0			##	##						##		
Minima		75				0	0										0		
Maxima		610				0	0										0		

(Dip measured in 0 caves)

Internal Cave Attributes

	CT	LENG.	VR	XS	VOL.	Min. HG %	C	SE	RE	DE	CS	SP	Ch	Sh	BC	AV	MV	DC	FS	P	SG	PRIME REFERENCES
Totals		982	###	####	3036	##	29	14	4	19	29	7	0	0	0	0	13	0	0	2		
Av. per cave		34	7.8	2.5	105	0		0.5	0.1	0.7	1.0	0.2	0.0	0.0	0.0	0.0	0.4	0.0	0.0	0.1		
Minima		3	1	0.3	1	0		1	1	1	0	1	0	0	0	0						
Maxima		170	29	10.0	700	0		1	1	3	3	2	0	0	0	0						

Glacial Situations:

	#	Length
C	0	0
D	0	0
E	0	0
G	0	0
H	0	0
K	0	0
L	0	0
S	0	0
T	0	0
U	0	0
Totals	**0**	**0**

Karst Types:

	#	Length
V	7	362
A	21	609
L	0	0
C	0	0
X	1	11
Totals	**29**	**982**

Cave Locations:

	#	Length
C	0	0
F	0	0
W	0	0
R	0	0
S	0	0
G	0	0
P	0	0
Totals	**0**	**0**

Cave Types:

	#	Length
S	7	89
a	10	135
b	3	60
c	4	138
d	2	214
e	3	346
f	0	0
g	0	0
h	0	0
Hy	0	0
I	0	0
J	0	0
L	0	0
R	0	0
T	0	0
Totals	**29**	**982**

Relict Caves:

#	Length
5	171
5	**171**

MV Caves:

#	Length
13	170
13	**170**

Combination Caves:

#	Length
11	**641**

SCOTTISH DALRADIAN SUPERGROUP CAVE DATABASE

Refer to North Central Norway Database for Key

Caves are grouped by carbonate outcrop

External Cave Attributes | Internal Cave Attributes

GRID. REF.	ALT.	COUNTY	AREA	LST. STRIKE	LST. DIP	OW	EXT. COLOUR	OTHER INT. ROCK	R	T	GS	CL	KT	SH	OR	CA	REF. NO.	CAVE NAME	CT	LENG.	VR	XS	VOL.	Min. HG %	C	SE	RE	DE	CS	SP	Ch	Sh	BC	AV	MV	DC	FS	P	SG	PRIME REFERENCES
APPIN GROUP: Subgroup unassigned: Cuthill Limestone Member																																							
1:50000 Landranger Sheet 37 Strathdon																																							***1:50000 Geological Survey Sheet 85E Glenfiddich***
NJ 42x 50x	*140*	Banff	Keith															Quarry Caves	3 small caves in solid limestone																				GSG Bulletin 2(2) 1992 9-10
APPIN GROUP: Ballachulish Subgroup: A - Appin Limestone																																						
1 inch Sheet 46 Loch Linnhe																																						***1 inch Geological Survey Sheet 53 Ben Nevis***
NN 042	620	255	Inverness	Onich									X					Onich Hole	S	11	8	2.0	22		1		1	0												Appin Cave Guide, 1978
NN 078	575	75	Argyll	W. Laroch									A					Gorteneorn Cave 1	a	11	*1*	*2.0*	22		1	1		1						1						Scotland Underground, 1984
NN 078	575	75	Argyll	W. Laroch									A					Gorteneorn Cave 2	S	3	3	*2.0*	6		1	1		1						1						Scotland Underground, 1984
NN 078	575	75	Argyll	W. Laroch									A					Gorteneorn Cave 3	S	*20*	6	*2.0*	40		1	1		1						1						Scotland Underground, 1984
NN 078	575	75	Argyll	W. Laroch									A					Gorteneorn Cave 4	a	3	1	1.0	3		1	1		1						1						Scotland Underground, 1984
NN 013	563	350	Argyll	Glen Duror														Uamh nan Eas an Con	Rockshelter																				Appin Cave Guide, 1978
NN 0122	5555	320	Argyll	Glen Duror									V					Hibernian Cave	c	30	6	2.0	60		1			1	0											GSG Bulletin 2(1) 1991 p21
NN 0126	5546	322	Argyll	Glen Duror									V					Draught Caledonian	e	155	29	3.0	465		1		1		3	2								1		GSG Bulletin 2(1) 1991 p22
NN 011	553	240	Argyll	Glen Duror									V					Uamh Ord Mor	a	6	1	1.0	6		1		1		1	1				1						GSG Bulletin 5(3) 2000 p35
NN 0107	5520	240	Argyll	Glen Duror									V					Treefeller's Pot	S	16	8	2.0	32		1	1			1					1						GSG Bulletin 2(1) 1991 p20
NM 964	522	150	Argyll	Bealach														Natural Arch																						Appin Cave Guide, 1978
NM 964	522	150	Argyll	Bealach									A					Fish-hooks Cave	S	16	14	*1.0*	16		1			3	0											Appin Cave Guide, 1978
NM 964	522	150	Argyll	Bealach									A					South Cave	a	12	6	1.0	12		1			1	1											Appin Cave Guide, 1978
NM 979	519	190	Argyll	Bealach									A					Rose Cave	c	25	3	2.0	50		1	1			2					1						GSG Bulletin 4(5) 1998 p42
NM 9815	5198	120	Argyll	Bealach									V					Uamh an Dige	a	5	3	2.0	10		1	1			1					1						Appin Cave Guide, 1978
NM 9820	5189	128	Argyll	Bealach									V					Uamh an Dullean Briste	e	106	16	3.0	318		1			1	0										1		Appin Cave Guide, 1978
NM 9754	5153	250	Argyll	Bealach									A					Banged Resurgence	b	4	1	*0.3*	1		1		1		1					1						Appin Cave Guide, 1978
NM 9745	5151	270	Argyll	Bealach									V					Uamh an T'Sellich	d	44	9	*2.0*	88		1			2	1											Appin Cave Guide, 1978
NM 971	511	330	Argyll	Bealach									A					Rock Shelter 1	a	30	12	*5.0*	150		1	1			1											Appin Cave Guide, 1978
NM 970	510	320	Argyll	Bealach									A					Rock Shelter 2	a	15	10	*5.0*	75		1	1			1											Appin Cave Guide, 1978
NM 9899	5081	310	Argyll	Bealach									A					Claon Uamh	c	70	18	10.0	700		1			1	2	1										Appin Cave Guide, 1978
NM 9697	5079	310	Argyll	Bealach									A					Rock Shelter 3	a	15	15	*5.0*	75		1	1			1											Appin Cave Guide, 1978
NM 9645	5031	268	Argyll	Glenamuckrach									A					Glenamuckrach Pot	S	15	8	*2.0*	30		1	1			1					1						Appin Cave Guide, 1978
NM 9646	5026	255	Argyll	Glenamuckrach									A					Glenamuckrach Pot Rising	c	13	2	*2.0*	26		1			1	1	1				1						Appin Cave Guide, 1978
NN 035	512	610	Argyll	Coire Mulrooney									A				M1	Uamh a' Chomaichag (Owl Hole	d	170	*5*	*2.0*	340		1	1		1	1	1										Appin Cave Guide, 1978
NN 035	511	580	Argyll	Coire Mulrooney									A				M2	Allt Priomh Uamh (Main Stream	b	36	8	2.0	72		1	1	1		2					1						Appin Cave Guide, 1978
NN 034	510	580	Argyll	Coire Mulrooney									A				M3	Uamh nan Seobhrach (Primrose	e	85	11	*3.0*	255		1			3	1											Appin Supplement, 2003
NN 034	509	550	Argyll	Coire Mulrooney									A				M4	Tromham Uamh 1	a	30	3	3.0	90		1			2	1					1						Appin Supplement, 2003
NN 034	509	550	Argyll	Coire Mulrooney									A				M5	Tromham Uamh 2	a	8	*2*	*2.0*	16		1	*1*			1					1						Appin Cave Guide, 1978
NN 034	509	550	Argyll	Coire Mulrooney									A				M6	Tromham Uamh 3	b	20	10	*2.0*	40		1			1	1	1										Appin Cave Guide, 1978
NN 033	509	549	Argyll	Coire Mulrooney									A				M7	Poll Polt	S	8	8	*2.0*	16		1			1	0											Appin Cave Guide, 1978

SCOTTISH DALRADIAN SUPERGROUP CAVE DATABASE

Refer to North Central Norway Database for Key

APPIN GROUP: Ballachulish Subgroup: B - Ballachulish Limestone: TOTALS

External Cave Attributes | Internal Cave Attributes

GRID. REF.	ALT.	COUNTY	AREA	LST. STRIK	LST. DIP	OW	EXT. COLOUR	OTHER INT. ROCK	R	T	GS	CL	KT	SR	OR	CA	REF. NO.	CAVE NAME	CT	LENG.	VR	XS	VOL.	Min. HG %	C	SE	RE	DE	CS	SP	Ch	Sh	BC	AV	MV	DC	FS	P	SG	PRIME REFERENCES
Totals	####	50			#	##			0	0							##			2100	###	####	7584	##	50	23	14	30	45	20	0	0	0	1	17	0	0	13		
Av. per cave	261				#	0			##	##							##			42	7.6	2.8	152	0		0.5	0.3	0.6	0.9	0.4	0.0	0.0	0.0	0.0	0.3	0.0	0.0	0.3		
Minima	81				0	0											0			1	1	0.2	1	0		1	1	1	0	1	0	0	0	1					
Maxima	895				0	0											0			340	48	10.0	1680	0		2	1	3	3	4	0	0	0	1					

(Dip measured in 0 caves)

Karst Types:

	#	Length
V	7	254
A	40	1756
L	0	0
C	0	0
X	3	90
Totals	50	2100

Cave Types:

	#	Length
S	10	145
a	12	285
b	16	456
c	4	357
d	4	141
e	1	21
f	0	0
g	2	375
h	1	340
Hy	0	0
I	0	0
J	0	0
L	0	0
R	0	0
T	0	0
Totals	50	2100

Relict Caves: # 13, Length 325

MV Caves: # 17, Length 229

Combination Caves: # 20, Length 1546

Glacial Situations:

	#	Length
C	0	0
D	0	0
E	0	0
G	0	0
H	0	0
K	0	0
L	0	0
S	0	0
T	0	0
U	0	0
Totals	0	0

Cave Locations:

	#	Length
C	0	0
F	0	0
W	0	0
R	0	0
S	0	0
G	0	0
P	0	0
Totals	0	0

SCOTTISH DALRADIAN SUPERGROUP CAVE DATABASE

Refer to North Central Norway Database for Key

Caves are grouped by carbonate outcrop

GRID. REF.	ALT.	COUNTY	AREA	LST. STRIK	LST. DIP	OW	EXT. COLOUR	OTHER INT. ROCK	R	T	GS	CL	KT	SH	OR	CA	REF. NO.	CAVE NAME	CT	LENG.	VR	XS	VOL.	Min. HG %	C	SE	RE	DE	CS	SP	Ch	Sh	BC	AV	MV	DC	FS	P	SG	PRIME REFERENCES
				External Cave Attributes																Internal Cave Attributes																					
APPIN GROUP: Ballachulish Subgroup: B - Ballachulish Limestone																																							
1 inch Sheet 46 Loch Linnhe																				***1 inch Geological Survey Sheet 53 Ben Nevis***																	
NM 966 519	61	Argyll	Bealach										A					Castor and Pollux Caves	a	8	1	0.2	2		1	2			2						1				Appin Cave Guide, 1978
NM 963 515	161	Argyll	Bealach										A					Uamh an Tobar Dhubh	e	21	10	*4.0*	84		1		1	1	1	1							1		Appin Cave Guide, 1978
NM 9616 5159	163	Argyll	Bealach															Slate Hole		4m deep fissure in slate																			Appin Cave Guide, 1978
NM 962 513	215	Argyll	Bealach										A					Uamh nan Claig-lonn	g	280	48	6.0	1680		1	2			2	3							1		GSG Bulletin 1(1) 1969 p17
NM 961 512	215	Argyll	Bealach										A					Hogmanay Hole	a	5	2	2.0	10		1		1		1						1				Appin Supplement, 2003
NM 960 511	225	Argyll	Bealach										A					Argus Hole	b	27	6	*1.0*	27		1			2	0										Scotland Underground, 1984
NM 960 511	223	Argyll	Bealach										A					Lady Di's Hole	S	6	6	1.0	6		1			1	0										Appin Cave Guide, 1978
NM 9765 5135	185	Argyll	Bealach										A					Uamh an Sgoltaich Fhada 4	a	15	1	2.0	30		1		1		1	1					1				GSG Bulletin 1(1) 1969 22-24
NM 9770 5119	190	Argyll	Bealach										A					Uamh an Sgoltaich Fhada 3	a	55	4	2.0	110		1	1		1	1	1									Appin Cave Guide, 1978
NM 9769 5115	195	Argyll	Bealach										A					Uamh an Sgoltaich Fhada 2	a	10	1	*1.0*	10		1		1		1						1				Appin Cave Guide, 1978
NM 9753 5097	210	Argyll	Bealach										A					Uamh an Sgoltaich Fhada 1	d	30	5	*1.0*	30		1			1	1	1					1				Appin Cave Guide, 1978
NM 9725 5053	237	Argyll	Bealach										A					Hairpin Hole	d	8	1	*0.5*	4		1			1	1						1				Appin Cave Guide, 1978
NM 9695 5029	246	Argyll	Glenamuckrach										A					Gillette Hole	S	8	8	*2.0*	16		1	1			1						1				Appin Cave Guide, 1978
NM 9689 5020	240	Argyll	Glenamuckrach										A					Uamh Raineach	b	55	12	*4.0*	220		1	1			1						1		1		Appin Cave Guide, 1978
NM 9673 5008	210	Argyll	Glenamuckrach										A					Excavated Shaftehole	b	10	2	1.0	10		1			1	1	2					1				Scotland Underground, 1984
NM 9673 5008	235	Argyll	Glenamuckrach										A					Uamh an Cloinne	a	32	1	1.0	32		1		1		1	1					1				Scotland Underground, 1984
NM 9670 5004	230	Argyll	Glenamuckrach										A					Uamh nan Guthan	d	43	3	*1.5*	65		1	1	1	1	1								1		Appin Cave Guide, 1978
NM 9667 4999	252	Argyll	Glenamuckrach										A					Poll Losgainn	S	6	5	4.0	24		1	1			1						1		1		Appin Cave Guide, 1978
NM 9664 5000	241	Argyll	Glenamuckrach										A					Uamh nan Losgainn	b	15	2	*2.0*	30		1		1		1	1						1	1		Appin Cave Guide, 1978
NM 9630 4975	213	Argyll	Glenamuckrach										A					Long Drop Cave	g	95	23	4.0	380		1	1			3	4							1		Appin Cave Guide, 1978
NM 9589 4953	176	Argyll	Glenamuckrach										A					Uamh Steall na Burich	b	52	5	4.0	208		1		1		1	1							1		Appin Cave Guide, 1978
NM 9485 4910	250	Argyll	Glenstockdale										V					Cave of the Heifer's Outwash	c	180	9	2.0	360		1	2		3	2										Appin Cave Guide, 1978 +
NM 9478 4908	205	Argyll	Glenstockdale										V					Short Circuit Cave	b	12	2	*1.0*	12		1			2	0										Appin Cave Guide, 1978
NM 9468 4901	190	Argyll	Glenstockdale										V					Glenstockdale Cave	b	23	3	4.0	92		1	1			1										Appin Cave Guide, 1978
NM 9465 4895	175	Argyll	Glenstockdale										V					Glenstockdale Rising	b	10	3	2.0	20		1		1		1	1									Appin Cave Guide, 1978
NM 940 484	220	Argyll	Glenstockdale										V					Champagne Hole	a	7	2	1.0	7		1	1			1							1			Appin Cave Guide, 1978
NN 031 503	335	Argyll	Coire Mulrooney										A				C1	Allt Coire Challum Cave	a	9	*3*	*1.0*	9		1			2	0									Scotland Underground, 1984
NN 0305 5017	375	Argyll	Coire Mulrooney										A				C5	Cave of the Great Leg-Pulling	S	23	9	*1.0*	23		1			1	0									GSG Bulletin 4(5) 1985 p34
NN 0304 4984	300	Argyll	Coire Mulrooney										A				S15	Poll Seomar (Chamber Pot)	h	340	40	4.0	1360		1	1			2					1			1	GSGBull4(4)85 p28,5(1)86 9-10
NN 032 499	250	Argyll	Coire Mulrooney										A				S14	Magnum Pot	S	12	10	*10.0*	120		1			1	0									GSG Bulletin 4(4) 1985 p23
NN 030 498	300	Argyll	Coire Mulrooney										A				S12	Clearmidge Hole	S	20	18	3.0	60		1	1			1									GSG Bulletin 4(5) 1985 p37
NN 0370 4995	255	Argyll	Coire Mulrooney										A					Fly Plague Hole	S	60	15	*2.0*	120		1			1	0									GSG Bulletin 5(3) 1987 28-29
NN 0294 4984	260	Argyll	Coire Mulrooney										A				S11	The Snake Pit	b	32	11	*1.0*	32		1	1			2									GSG Bulletin 4(5) 1985 p35
NN 029 497	257	Argyll	Coire Mulrooney										A				S8	Allt Coire Shelleach Cave 4	a	15	*2*	*2.0*	30		1			1	0									GSG Bulletin 4(4) 1985 19-23
NN 029 497	260	Argyll	Coire Mulrooney										A				S5	Allt Coire Shelleach Cave 3	S	1	1	*0.5*	1		1			1	0									GSG Bulletin 4(4) 1985 19-23
NN 030 496	335	Argyll	Coire Mulrooney										A				S4	Allt Coire Shelleach Cave 1	b	45	*2*	*2.0*	90		1			1	0							1		Appin Supplement, 2003
NN 0298 4980	350	Argyll	Coire Mulrooney										A				S3	Uamh Coire Shelleach	c	150	10	8.0	1200		1			2	1							1		Appin Cave Guide, 1978
NN 028 495	385	Argyll	Coire Mulrooney										A					AHS Cave	b	18	6	3.0	54		1			1	0									GSG Bulletin 4(4) 1998 p10
NN 032 497	230	Argyll	Coire Mulrooney										V				S2	Root Tunnel	a	5	1	0.2	1		1		1		1						1			GSG Bulletin 1(1) 1969 p14
NN 032 497	230	Argyll	Coire Mulrooney										V				S1	Allt Coire Shelleach Cave 2	c	17	3	2.0	34		1			2	0							1		Appin Cave Guide, 1978
NN 029 493	290	Argyll	Coire Mulrooney										A				S17	Dundiggin Hole	a	80	*10*	*4.0*	320		1			1	0									GSG Bulletin 4(4) 1985 p21
NN 027 488	185	Argyll	Glen Creran										A				8	SinkPot	S	3	2	1.0	3		1	1			1						1			GSG Bulletin 1(1) 1969 11-19
NN 0269 4876	180	Argyll	Glen Creran										A				7	Upper Black Rift Cave	b	34	*5*	1.0	34		1			1	1									GSG Bulletin 1(1) 1969 11-19
NN 0267 4869	177	Argyll	Glen Creran										A				6	Black Rift Cave	b	51	20	1.5	77		1	1			1									GSG Bulletin 5(4) 1988 10-17
NN 0263 4863	160	Argyll	Glen Creran										A				5	Black Rift Rising	b	10	3	3.0	30		1		1		1	1								GSG Bulletin 5(4) 1988 10-17
NN 0263 4863	160	Argyll	Glen Creran										A				4	Lower Black Rift Sink	c	10	3	0.5	5		1	1			1	1								GSG Bulletin 5(4) 1988 10-17
NN 0266 4860	134	Argyll	Glen Creran										A				3	Lost Memory Cave	b	56	*10*	*1.0*	56		1	1	1		2									GSG Bulletin 5(4) 1988 10-17
NN 0258 4856	127	Argyll	Glen Creran										A				1	Lower Black Rift Resurgence	b	6	2	0.3	2		1		1		1						1			GSG Bulletin 1(1) 1969 11-19

* Refs defined in GSG Bulletin 1 (1) 1969 15-16

+ GSG Bulletin 4(2) 1983 p28

SCOTTISH DALRADIAN SUPERGROUP CAVE DATABASE

Refer to North Central Norway Database for Key

Caves are grouped by carbonate outcrop

GRID. REF.	ALT.	COUNTY	AREA	External Cave Attributes: LST. STRIK	LST. DIP	OW	EXT. COLOUR	OTHER INT. ROCK	R	T	GS	CL	KT	SH	OR	CA	REF. NO.	CAVE NAME	Internal Cave Attributes: CT	LENG.	VR	XS	VOL.	Min. HG %	C	SE	RE	DE	CS	SP	Ch	Sh	BC	AV	MV	DC	FS	P	SG	PRIME REFERENCES
APPIN GROUP: Ballechulish Subgroup: B - Ballechulish Limestone																																							
1 inch Sheet 46 Loch Linnhe cont.																			***1 inch Geological Survey Sheet 53 Ben Nevis***																			
NN 009 575	100	Argyll	Glen Duror	Probably in quartz diorite														Kentallon Kleft+Silver Hole		100m-long fissure cave. 15m deep																			Appin Supplement, 2003
NN 153 563	655	Argyll	Glen Coe	Not carbonate														Ossian's Cave																					Appin Cave Guide, 1978
1:50000 Landranger Sheet 42 Glen Garry																																						
NN 513 821	700	Inverne	Loch Lagan										X					Circular Pool	S	6	3	10	60		1		1		1	1					1				GSG Bulletin 1(5) 1991 15-18
NN 502 799	700	Inverne	Loch Lagan										X					Long Walk Cave	a	24	15	9	216		1	1			1										S. Highlands Cave Guide, 1988
NN 463 746	895	Inverne	Loch Lagan										X					Cave of the High Ground	d	60	10	3	180		1	1		1	1										GSG Bulletin 1(5) 1991 15-18

APPENDIX D1 NEOTECTONICS IN CENTRAL SCANDINAVIA

This Appendix provides the author's uncorroborated evidence of neotectonic activity in the study area, as discussed in section 6.3.3. Each of the 56 observations is described in Table D1.1, many being supported by Photos D1.1–D1.41. The observations are classified into five types defined by the author and are presented in a format similar to that used by Olesen *et al.* (2004), using the same five observation grades, and record the size and direction of movement. However, no checks were made that neotectonic faults at the surface meet the five criteria listed by Stewart *et al.* (2000, p1378) for distinguishing between true faults and the products of glacial erosion.

The use of the term 'neotectonics' has been interpreted very widely here, and may include the following effects: (1) superficial movements; (2) movements that may be supplemented by the effects of ice wedging; (3) gravitational mass slip movements, possibly at steep shafts near valley sides; (4) lateral corrasion at floor level causing wall collapse (Ford, 1965a, p122), perhaps triggered by seismic activity; (5) pressure release after a cave is drained of deep water or after powerful streams subside; (6) simple gravitational collapse of cave ceilings (although this seems unlikely as roof spans rarely exceed 10m); (7) shear stress of over-passing icesheets and glaciers (section 3.2.2); (8) stress release caused by the presence of the cave itself, perhaps seismically triggered; and (9) liquefaction and slumping of laminated sediments.

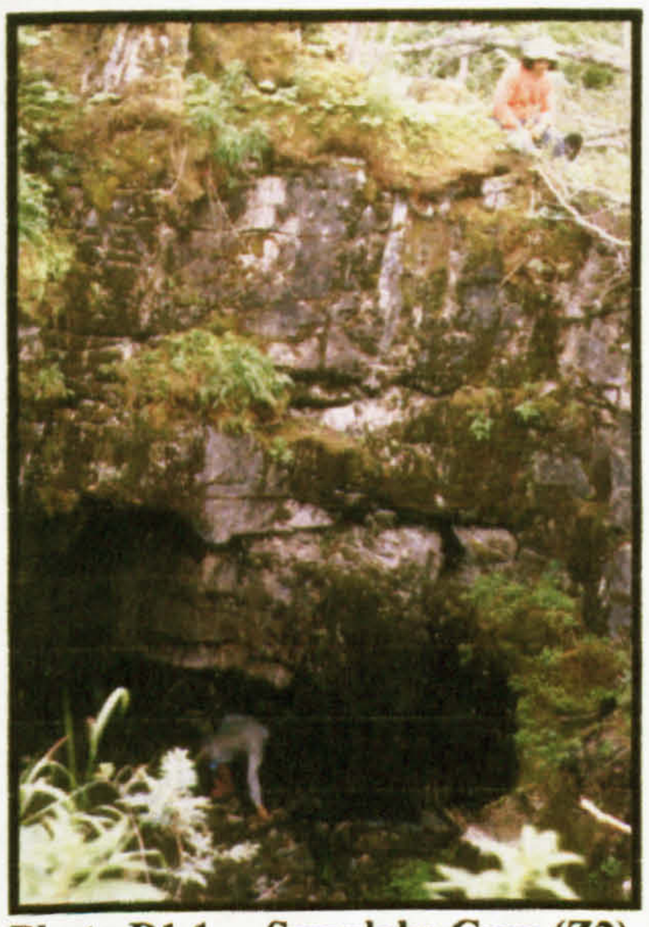

Photo D1.1 Swanlake Cave (Z2)
Along-strike horizontal movement (arrowed) with vertical settlement

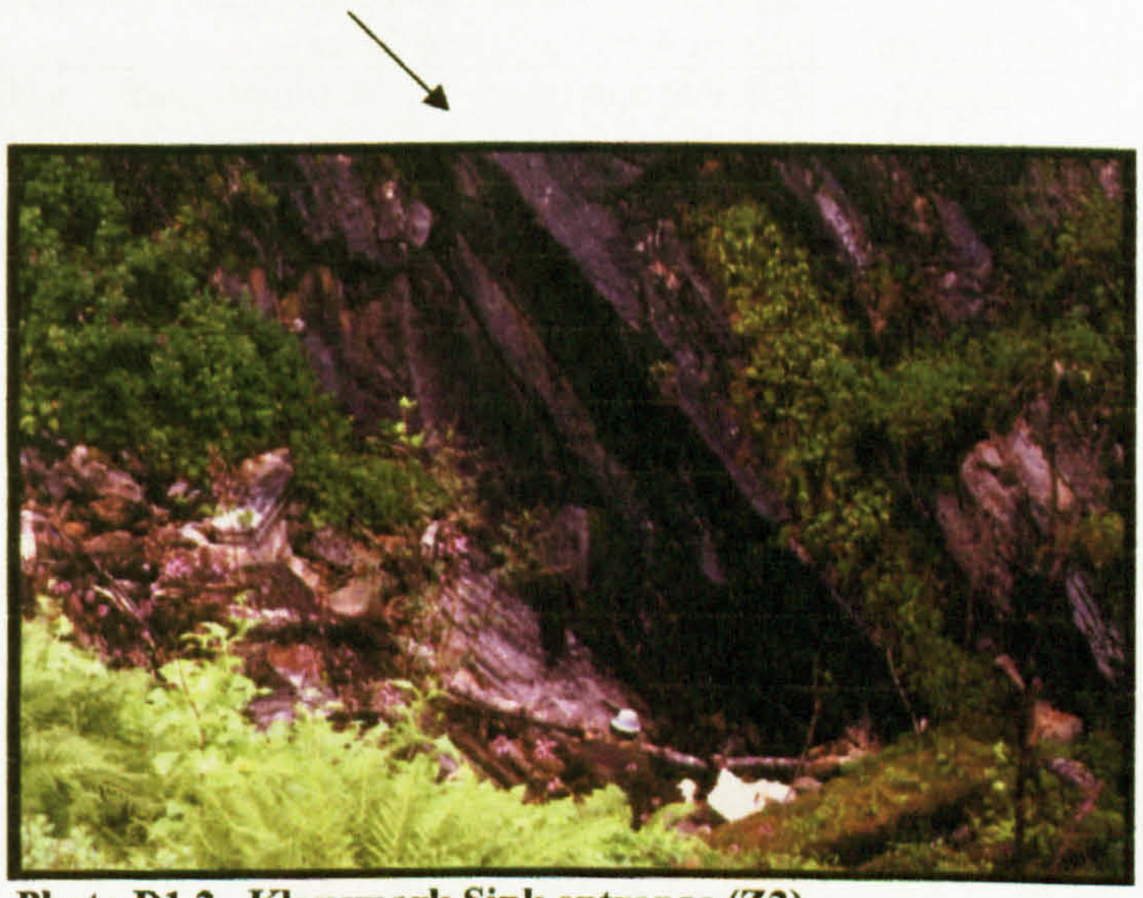

Photo D1.2 Klausmark Sink entrance (Z2)
Smooth surfaces along movement (arrowed) within foliation of angled stripe karst. Person wearing hat for scale.

Photo D1.3 Hornet Pot, Bulandsdal (Z2)
Fractures and movements at base of Hornet Shaft.

Table D1.1 Evidence of neotectonic movements from central Scandinavian karsts

No.	Location	Observation	Type	Size	Grade	Comment
1 Z2	Swanlake Cave UN84478000	Possible horizontal movement north, along strike, plus vertical settlement	M	5cm H	C	Photo D1.1
2 Z2	Klausmark Sink UN86457835	Smooth surfaces along movement within foliation of steep angled stripe karst	M	15cm A	B	Photo D1.2
3 Z2	Bulandsdalgrotta UN90536700	Clean limestone blocks on floor of Square Chamber. This is well away from the entrances.	F	–	B	
4 Z2	Hornet Pot, Bulandsdal UN90256765	~3cm vertical movement down, on wall at foot of Hornet Pitch. Appears to be more extensive than just spalling.	M	3cm V	C	Photo D1.3
5 Z2	Indråsen quarry UN84005510	Shattered nature of top 3m of marble	M	5cm H	C	Photo 6.1
6 Z2	Tarmaunbotn-grottene UN93625084	3 caves at altitudes of 5, 15 and 20m, apparently formed by mass movement down side of ridge. The caves have angular passage profiles with little or no karst dissolution	T	1–2m A	B	Movement probably occurred below sea level, unless recent
7 Z2	Mølnvatngrotta UN85724155	Clean limestone blocks on floor of Waterfall Chamber, near Forest Entrance	F	–	B	
8 Z2	Johngrotta UN92123120	Shattered and moved slabs of complexly folded limestone in wall of Tosenfjord at sea level	M	30cm A	C	Photo 3.1
9 Z3	Godvassdal-grotta VN08075266	6m-long tectonic cave with a triangular cross-section, apparently formed by mass movement and rotation of roof *upwards* to create the cave.	T	1m H	A	Photo D1.10
10 Z3	Durmålstind canyon VN09404460	Possible movement in *calc silicate gneiss,* within vertical foliation	M	15cm ? H	C	Photo D3.2
11 Z4	Sirijordgrotta, Twin Ducks P. VN15027065	Possible horizontal movement on right hand side of figure.	M	10cm H	C	Photo D1.4
12	Sirijordgrotta, Eccles Gallery	Clear horizontal movement at first, lower, roof.	M	15cm H	B	Photo D1.5
13	Sirijordgrotta, Arctic Passage	Movement at floor level of upper (Arctic) passage	M	10cm H	B	Photo D1.6
14	Sirijordgrotta, upstream w'fall	Movements of walls by rotation of 1m-wide vertical slab	M	5cm+ V	B	Photo D1.7
15 Z4	Green Valley Cave, Kvitfjell VN15526280	Relative movement at vertical fracture within vertical foliation of the marble at a 2.5m-deep shaft entrance.	M	25m m V	C	Or dissolutional?
16 Z4	Kidney Lake Cave VN11975065	Relict phreatic passage of typical 2m diameter in VSK. Midway is horizontal movement of roof to the right, probably along original inception fracture.	M	15cm H	A	Photo D1.8
17 Z4	Gåsvasstindhola VN15175400	Fallen blocks of limestone in very large chambers, away from entrances, with fractured N wall.	F	–	B	Photo D1.9
18 Z4	Elgfjellhola, Elgfjell VN14525084	Horizontal movement of ~25 cm to W, across near side of top of shaft, as viewed from far side. Large fracture movement in vertical plane at N64°E, 2m N of the shaft, is seen all the way round passage walls, including an 11 cm 'step' across a wall scallop. A sharp 1mm-thick fault gouge 'wafer' protrudes up to 50mm at the fracture. A 2nd vertical fracture occurs 2.3m N of the first, also showing movement and a 'wafer'. 3m farther N is a 3rd fracture with less clear movement but with wafer blades up to 30cm in extent, and 3mm thick, hanging from the E wall. N of the cave entrance are fractures at N72°E that cross limestone *and* adjacent mica schist, with wafers, but with no obvious movement.	M	25cm H 11cm H	A	Photo D1.11 Photo D1.12
19 Z4	Paradox Cave, Elgfjell VN14715087	Sub-horizontal neotectonic movement along vertical fracture that clearly occurred after the passage had enlarged to its present size.	M	20cm H	A	Photo D1.20
20 Z4	Secret Stream Cave, Elgfjell VN14625077	Large mainly tectonic cave formed at marble contact where a hummock of mica schist has split and W wall has rotated *upwards* to create a 3m-wide opening.	T	3m H	B	Photo D1.13. Or collapse into dissolutional void?

21 Z4	Brown Stains Cave, Elgfjell VN14835110	Sub-horizontal fracture movement across roof of Upper Entrance.	M	2cm H	C	Photo D1.16
22 Z4	Upper Entrance to Brown Stains Cave, Elgfjell VN14835110	Across-foliation vertical fracture set in limestone, at same bearing as fractures in Elgfjellhola, on surface above entrance. Calcitic 'wafer' fault gouges 2–6mm in thickness protrude up to 1cm, but surfaces have a shiny veneer that resists dilute HCl. One fracture shows a movement of 2 cm, apparently post-dating formation of some karren, as shown by the splitting of a flow of coffee by a wafer. This fracture is visible inside entrance, but has not influenced passage morphology.	M	2cm H	A	Fragile protruding wafer must be post-glacial, formed by extrusion or remaining after dissolutional lowering of the karst surface. Photos D1.17, D1.18
23 Z4	Injection Cave, Elgfjell VN15135137	Movement of roof in short, superficial, dry, phreatic cave that also exhibits rocks brought in by injected ice. Ice heave is also a possibility	M	10cm V	C	Photo D1.19
24 Z4	Cliff at Valley 5N, Elgfjell VN15325150	Horizontal mass movement outward of a 2m-thick metalimestone slab between two fractures at the surface cliff. Proto-conduits at upper fracture.	M	20cm H	A	Photo D1.14
25 Z4	Sarvejaellagrotta VN15865150	Vertical movement at Joint Entrance along vertical, across-strike fracture	M	10cm V	C	Photo D1.15
26 Z4	Jegerhullet VN15644702	Movement within foliation in Slot Chamber	M	10cm V	B	Photo D1.21
27 Z4	Etasjegrotta VN15744660	Fallen limestone blocks and open horizontal joints, up to 35m from entrance in Entrance Chamber, and 80m from entrance in Whichway Chamber.	F	–	B	Photo B1.8
28 Z4	Jordbruelv Wfall VN15724640	Neotectonic horizontal joints in VSK that provide a focus for tectonic inception	M	15cm H	B	*Frontispiece 1*
29 Z4	Cliff Cave entrance area, Jordbruelv VN15824605	Horizontal and vertical fractures and slips, with shattered towers of limestone. The view out of Cliff Cave shows 50cm-thick floor of the phreatic passage opened horizontally ~1m along strike, as shown by matching indentations and colourings, plus crushed rocks on unmoved parts of both walls.	M	30cm H 1m H	A	Photo D1.22 Photo D1.23
30 Z4	Invasjonsgrotta VN15924600	Laminations of fine sand at Oddstue that dip at 30°W, with possible liquefaction features. This is the first report of liquefaction in a karst cave in Scandinavia.	S	–	B	Appendix D5.5 Photo D5.1
31 Z4	Vatnhullet ent. VN15884590	A relict Vauclusian rising, with evidence of horizontal movements in VSK	M	10cm H	C	Photo D1.24
32 Z4	Near Ramp Cave, Jordbru VN15924590	Simple slips at shattered marble above a short shattered cave, also near Vatnhullet	M	10cm H	C	Photo D1.25
33 Z4	Bjørkåsgrotta, Interview Room VN16824430	Fallen limestone blocks, near entrance.	F	–	B	Photo D1.26
34 Z4	Anastomosegr. VN16484492	Collapsed wall slabs up to 3m long x 70cm x 50cm from east wall of upper passage, 70m from the entrance.	F	–	B	
35 Z5	Geitklauvgrotta VN20607700	Horizontally moved wall section, 1m thick, in Stream Passage	M	20cm H	B	Photo D1.27
36	Geitklauvgrotta	Clean fallen angled limestone blocks in large Megachamber (5m high, 10m wide, 20m long), 70m from the entrance	F	–	B	Photo D1.28
37	Geitklauvgrotta, Anglo-Nordic Chamber	Split in narrow arch that is a remnant of a smaller phreatic passage. Vertical and horizontal displacements of 13/17 and 25mm. The arch is 105m from the entrance, and is therefore protected from seasonal frost action. However, it could have been affected by subglacial freezing.	M	25mm A	A	Photo D1.29
38	Geitklauvgrotta, Loop Series	Vertical fracture in vertical wall, 5mm wide at base, tapering to closure 1m above.	M	5mm H	A	
39 Z5	Mølnbekk, near Laksfors. VN20408445	4cm movement within vertical foliation and with fault gouge wafers, in bed of surface stream on marble.	M	5cm V	C	Photo D1.30

40 Z5	Cascade Pot (SH6) Blåfjell VN21305757	2m-wide vertical block of settled limestone. The block is orthogonal to the strike	M	5cm V	C	Photo D1.31
41 Z6	Kammelv Sink VP32152195	1m-thick horizontal slab of limestone has moved across roof of passage	M	20cm H	B	Photo D1.32
42 Z6	Luktindgrotta VP32252200	Prominent horizontal fracture near roof, and lower fractures at 1m intervals	M	? H	C	Photo D1.33
43 Z7	Almdalselv VN27787170	Vertical fracture at junction between schist and limestone	M	? V	C	Photo D1.34
44 Z7	Almdalselv gorge, Trofors VN28027205	Near-vertical movements aligned with strike-oriented gorge	M	? V	C	Photo D1.35
45 Z7	Kvannlihola VN28023985	Limestone block pile in large chamber between two sumps, well-protected from seasonal frost action	F	–	A	Photo D1.36
46	Kvannlihola, Stalactite Grotto	Sloping stalagmite and possible moved roof	D	10cm H	C	Photo B1.9
47	Kvannlihola, upstream of the Big Finger	Sloping fracture with horizontal movement in both walls.	M	5cm H	C	Photo D1.37
48 Z8 / ZA	S. of Korgen, W side of E6 VP40452645	Thrust zone at HNC/RNC boundary shows movements, crushed rocks, slickensides and voids. Stress relief may be initiated by road and tunnel construction. (C.f. Roberts, 2000, p1439)	M	10–20 cm A (+H)	A	Photo 4.1
49 ZA	Stabbfors Jettegryter VP46671886	'Giant Pots' in metalimestone. Some have diagonal fractures and movements of ~30cm, some lying beneath metamorphic boudins	M	30cm A	B	Photo A4.1
50 ZA	Ytterlihullet VP51762279	Collapsed marble wall slabs in Boulder Hall, Inlet Passage, well away from possible entrances. The passage roof (and floor) consists of mica schist or amphibolite that *does not* seem to have collapsed.	F	–	B	Or collapse after pressure release when water subsided?
51 ZA	Grønndalsgrotta VP54721720	Large shifted slabs at Resurgence Entrance. Three fractures normal to foliation. Slab thickness 2–3m	M	30cm H	B	Photo D1.38
52 ZA	Bekkehølet VP55201728	The entrance passage is centred on a vertical fracture.	M	2cm H	B	Photo D1.39
53 KU	Sotsbäcksgrotta n VP92102160	Slab breakdown	F	–	B	Helldén (1975, Fig. 4)
54 KL	Landbrua Resurgence VM48809630	Fractures and small horizontal movements at roof level above resurgence	M	3cm H	C	Photo D1.40
55 KL	Korallgrottan VM59209575	Many rocks from the walls fill the bottom of Huvudgången by several metres	F	–	A	Isacsson (1994)
56 KS	Sjliengojukke waterfall VN74601183	Reverse fault with ~50cm throw within foliation of calcareous phyllite. This is 1km NW of Renbenshålet, which is in a marble outcrop in KB.	M	50cm A	B	Photo D1.41

Co-ordinates are to UTM WGS84. HNC and RNC zones and Køli Nappes are listed in the 'No.' column

Observation types:	D	Disturbed speleothems	No.	1
	F	Fallen blocks from walls and ceiling		11
	M	Movement along fracture		40
	T	Tectonic Cave		3
	S	Slumped sediment with liquefaction		1
			Total	56
Movement size key:	H	Horizontal	No.	27
	V	Vertical		10
	A	Angled		7
	-	Not applicable		12
			Total	56
Observation grade (from Stewart *et al.*, 2000, p1378):			No.	12
	A	Almost certainly neotectonic		24
	B	Probably neotectonic		20
	C	Possibly neotectonic		0
	D	Probably not neotectonic		0
	E	Very unlikely to be neotectonic	Total	56

Photo D1.4 Twin Ducks Passage, Sirijordgrotta
Sub-horizontal tectonic movements above and to right of the figure.

Photo D1.5 Eccles Gallery, Sirijordgrotta (Z4)
Shattered passage, with horizontal tectonic movement near roof.

Photo D1.6 Arctic Passage, Sirijordgrotta
Horizontal tectonic movement at base of upper passage.

Photo D1.7 Upstream waterfall, Sirijordgrotta
Rotational tectonic movement at non-carbonate barrier.

Photo D1.8 Kidney Lake Cave (Z4)
Relict phreatic passage, with ~2m diameter. A prominent horizontal neotectonic movement bisects the passage, probably resulting from seismic amplification because the cave lies in a ridge. Although this movement occurred after the passage enlarged to it present size, cave inception probably took advantage of a similar movement at the end of the Saalian deglaciation. Photo by P. Hann.

Photo D1.9 Chamber in Gåsvasstindhola (Z4)
Fallen ceiling blocks in one of the largest chambers in the study area.

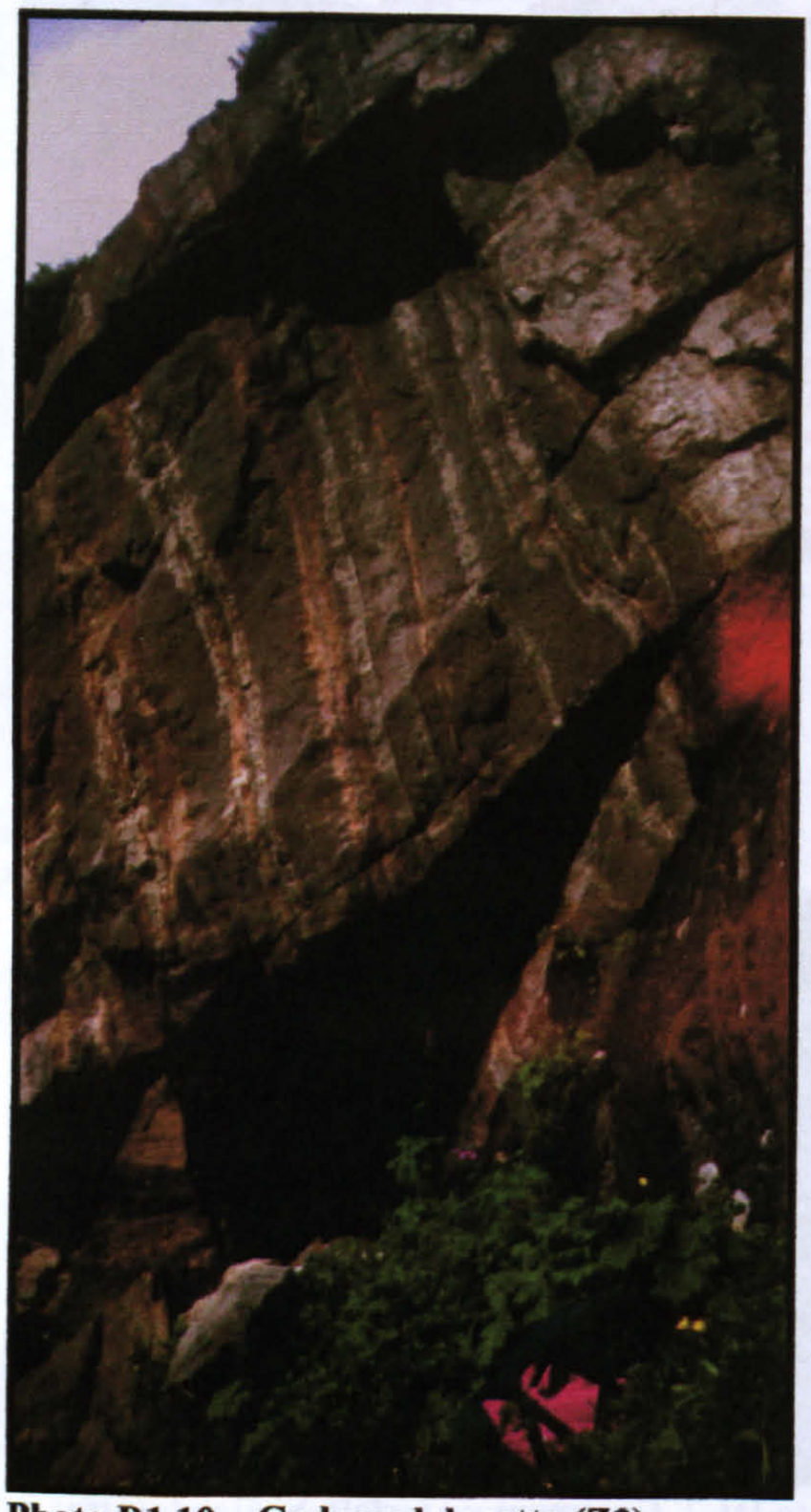

Photo D1.10 Godvassdalgrotta (Z3)
A tectonic cave, formed in stripe karst by apparent rotation of roof upwards.

Photo D1.11 Shaft in Elgfjellhola (Z4)
Sub-horizontal neotectonic movement across top of shaft on upstream (far) side. Ladder for scale.

Photo D1.12 Scallop in Elgfjellhola (Z4)
11cm neotectonic movement at scallop, which occurred after formation of the passage.

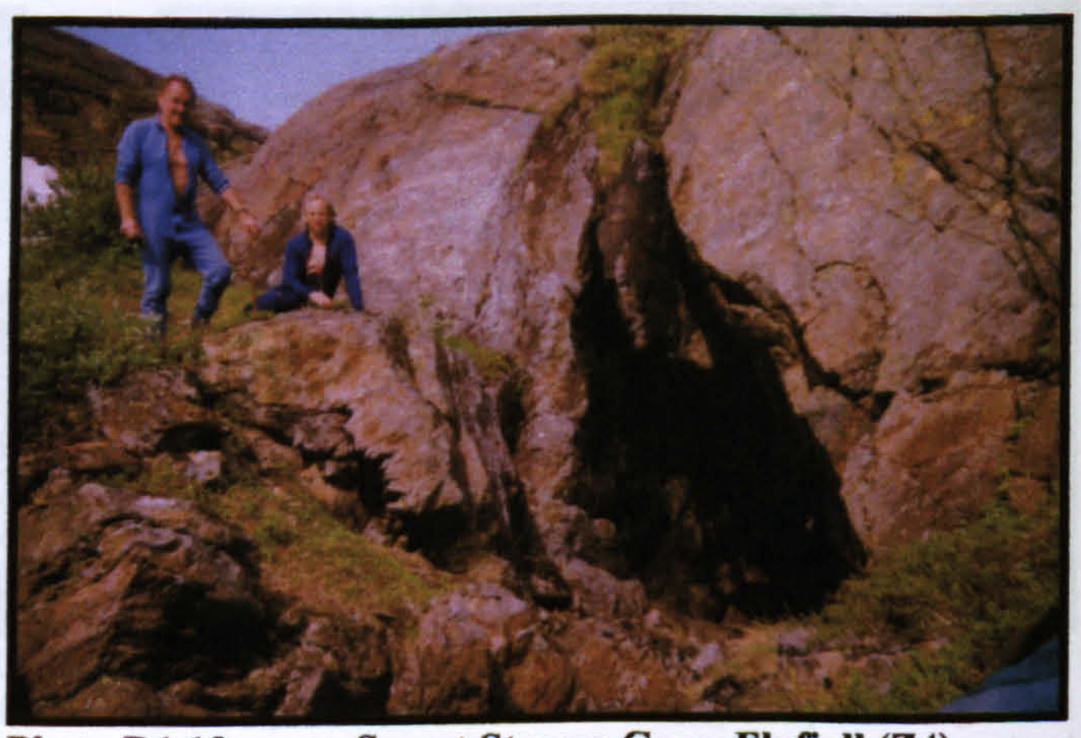

Photo D1.13 Secret Stream Cave, Elgfjell (Z4)
Primarily a tectonic cave, formed at junction of mica schist and marble. The mica schist has split and rotated upwards. The pick-axe head is a relic of previous mining activity.

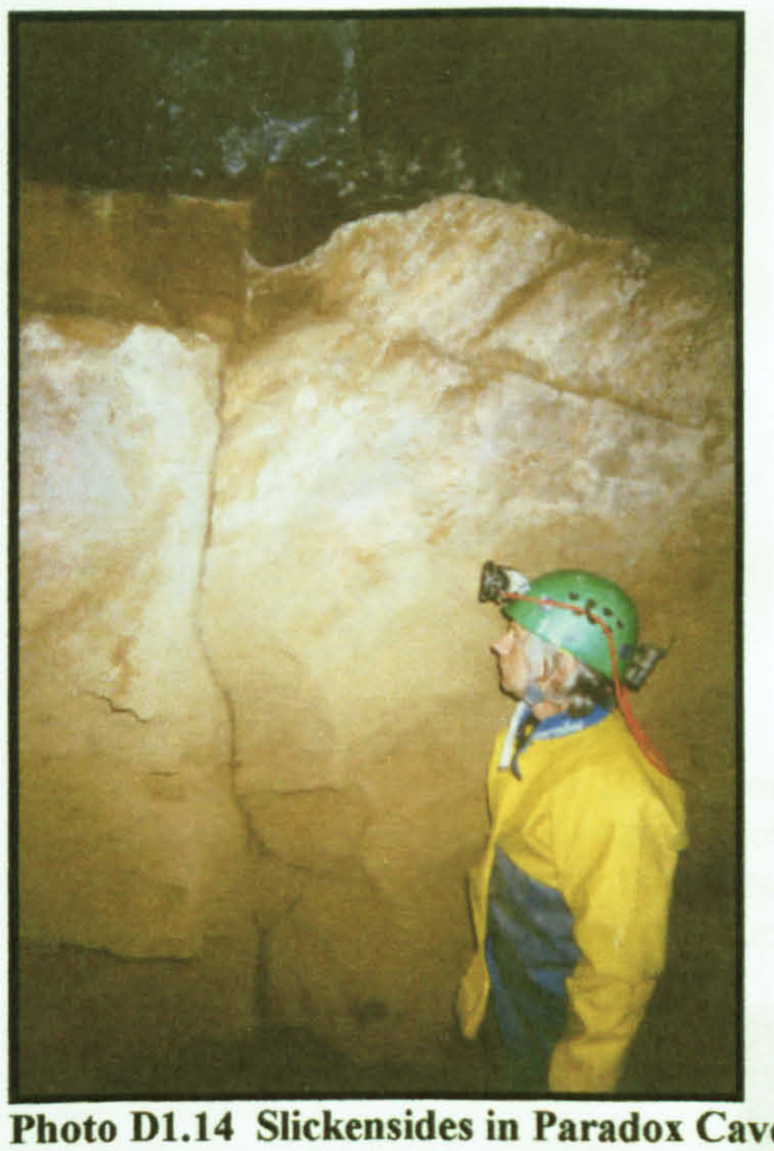

Photo D1.14 Slickensides in Paradox Cave, Elgfjell
Neotectonic movement of ~20cm after enlargement of passage to its present size, probably synchronous with movements in the nearby **Elgfjellhola** (Photos D1.11 and D1.12).

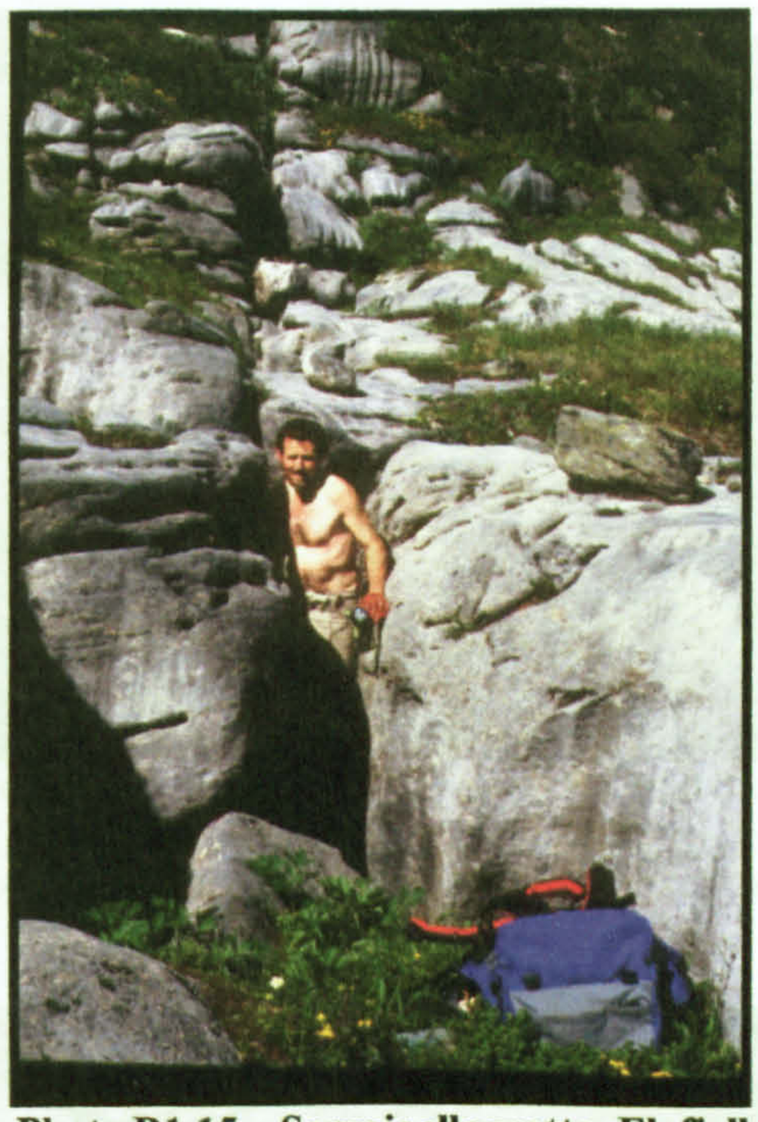

Photo D1.15 Sarvejaellagrotta, Elgfjell
Joint Entrance, formed at vertical movement along vertical, across-strike, fracture.

Photo D1.16 Brown Stains Cave, Elgfjell
Prominent sub-horizontal fracture bisects upper part of cave entrance.

Photo D1.17 Above Brown Stains Cave
Vertical movement with *fault gouge, near rucksack in* Photo 6.15. Compass for scale.

Photo D1.18 Diverging flow
Diverging flow of coffee across vertical fracture (Photo 6.16), suggesting that movement occurred after the surface flow had been established.

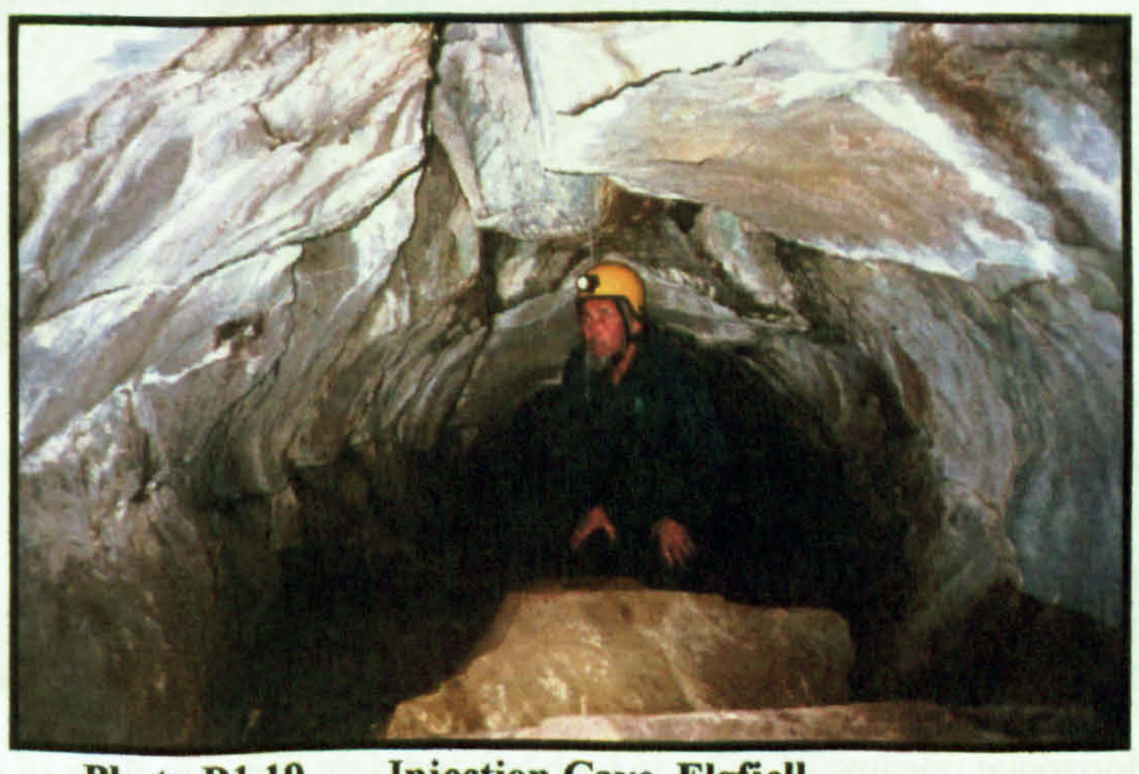

Photo D1.19 Injection Cave, Elgfjell
Rock movements and blocks injected by glacial ice at this superficial cave.

Photo D1.20 Horizontal tectonic movement on Elgfjell
Mass movement outward (after glacial smoothing) of 2m-thick slab of metalimestone, with proto-conduits at upper fracture.

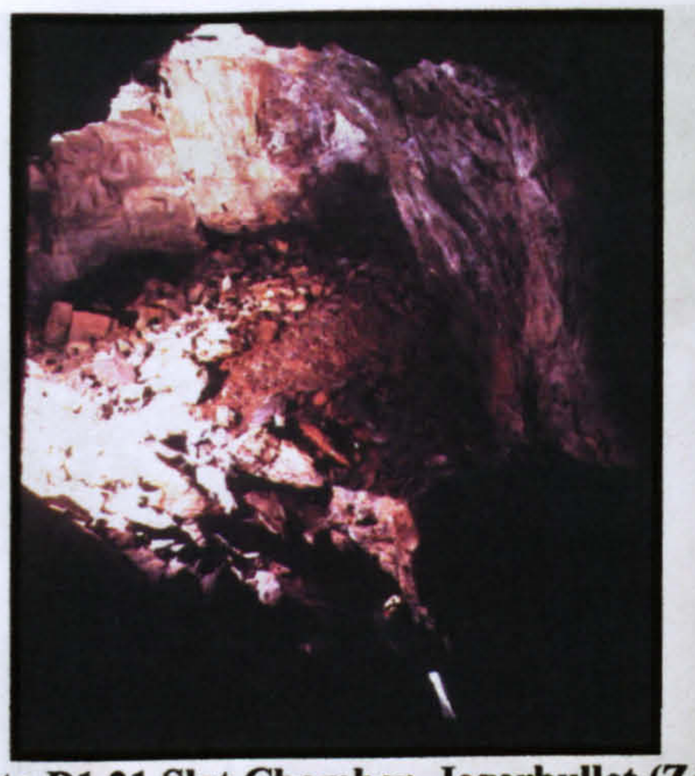

Photo D1.21 Slot Chamber, Jegerhullet (Z4)
Movement within foliation, above sediments that block former resurgence. Person at lower slot for scale.

Photo D1.22 Cliff Cave (Z4) entrances
Shattered cliffs and towers of limestone near the Rockbridge, Jordbruelv. Figure for scale.

Photo D1.23 Cliff Cave entrance from inside
Horizontal opening of c. 1m to both left and right that split floor of phreatic passage to create a box-like profile. This is the largest known neotectonic movement in the study area.

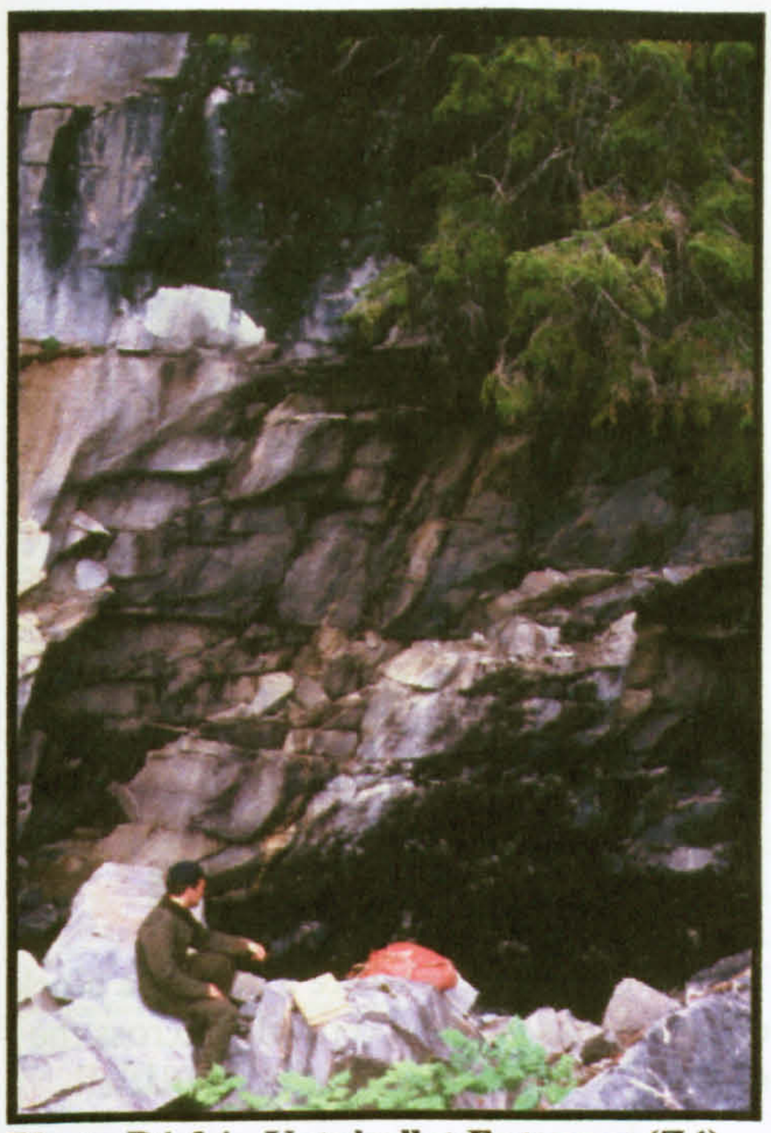

Photo D1.24 Vatnhullet Entrance (Z4)
A relict Vauclusian rising, with horizontal movements in VSK.

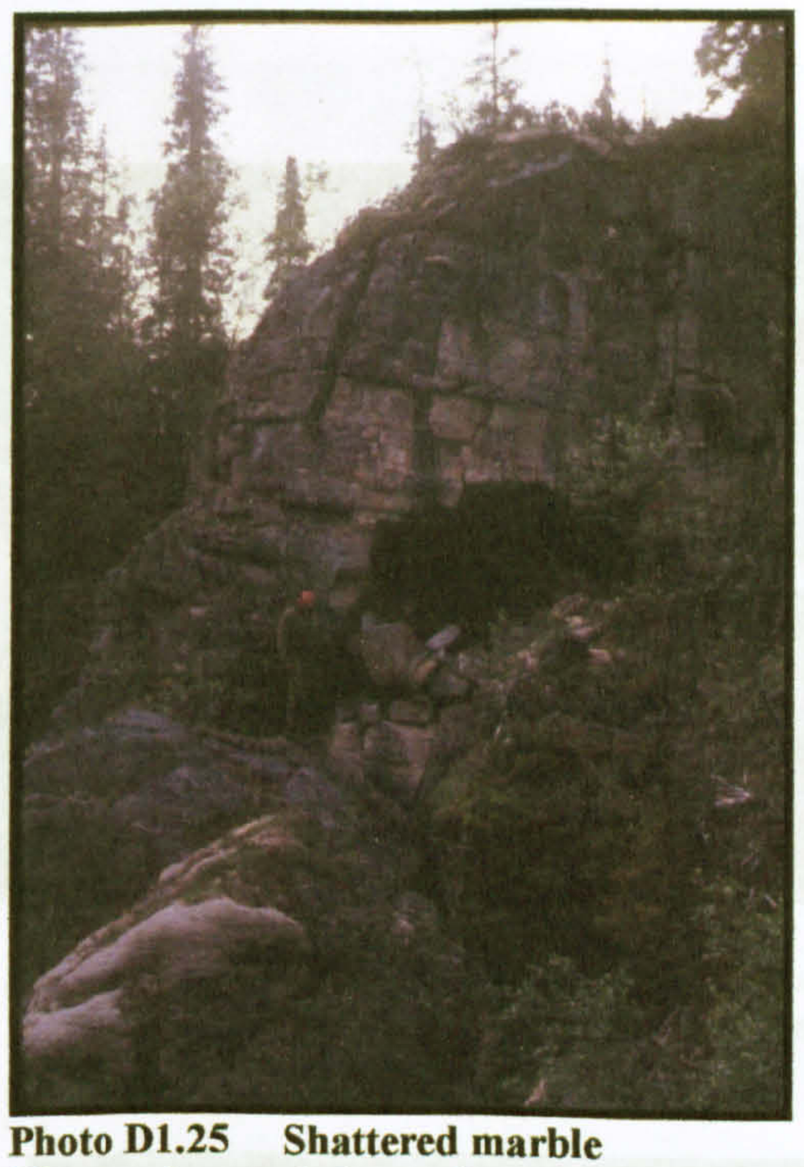

Photo D1.25 Shattered marble
Slip openings and short relict cave near Vatnhullet, at the end of the Rockbridge dry valley.

Photo D1.26 Bjørkåsgrotta (Z4)
Large fallen slabs in entrance chamber.
Photo by P. Hann.

Photo D1.27 Geitklauvgrotta streamway (Z5)
1m-thick wall section has moved right c. 20cm.
Photo by A. Marshall.

Photo D1.28 Megachamber, Geitklauvgrotta
Angled limestone blocks 70m from the entrance, and therefore little influenced by annual freezing. Probably collapsed during Weichselian deglacial seismicity.

Photo D1.29 Split arch in Geitklauvgrotta
The arch is a remnant wall of an earlier smaller (Saalian deglaciation?) phreatic passage. The displacement of ~20mm probably occurred synchronously with collapses in Megachamber.

Photo D1.30 Neotectonism in streambed (Z5)
Vertical movement of ~4cm, with fault gouge wafers, near Laksfors, Vefsndal

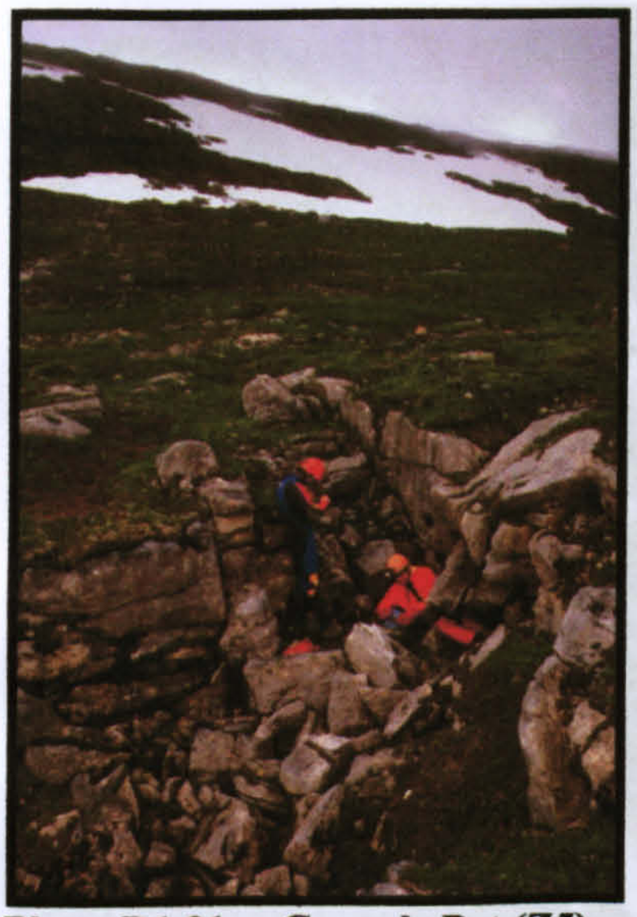

Photo D1.31 Cascade Pot (Z5)
The cave entrance is where a 2m-wide block of marble has lowered vertically, across the strike of VSK at Store Hjortskar, Blåfjell.

Photo D1.32 Kammelv Sink (Z6)
1m-thick slab has moved horizontally across roof of entrance.

Photo D1.33 Luktindgrotta (Z6)
Prominent horizontal fracture near roof in angled stripe karst, with lower fractures at 1m intervals. Photo by A. Marshall.

Photo D1.34 Almdalselv cliffs (Z7)
Vertical fracture at cliff wall vertical junction of darker schist and lighter marble.

Photo D1.35 Almdalselv gorge
Near-vertical movements aligned with strike-aligned gorge formed in VSK.

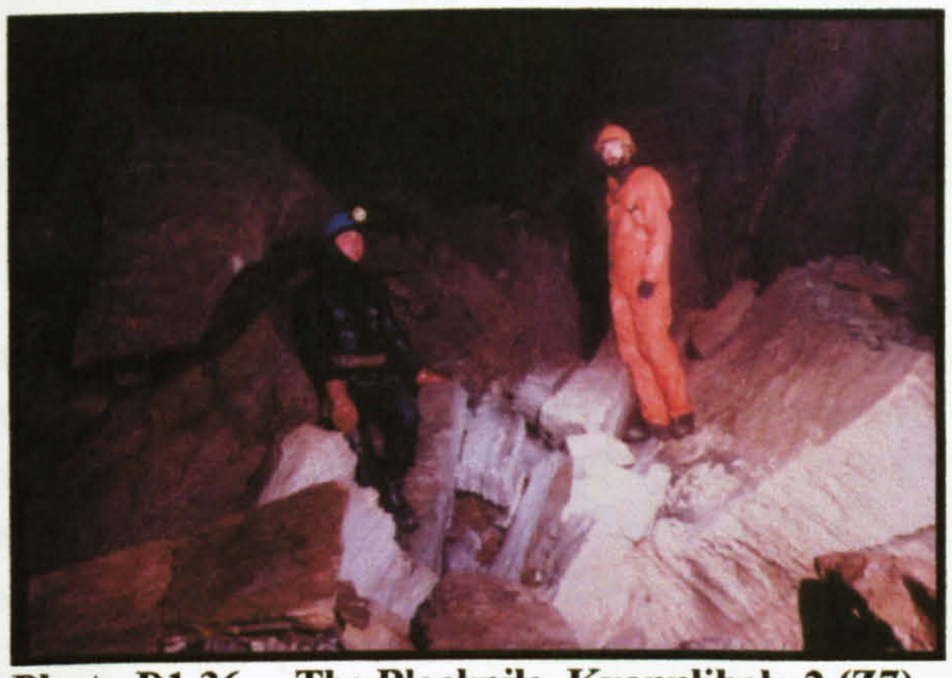

Photo D1.36 The Blockpile, Kvannlihola 2 (Z7)
Well-away from freeze-thaw influences, this collapse likely occurred during early Holocene earthquakes.

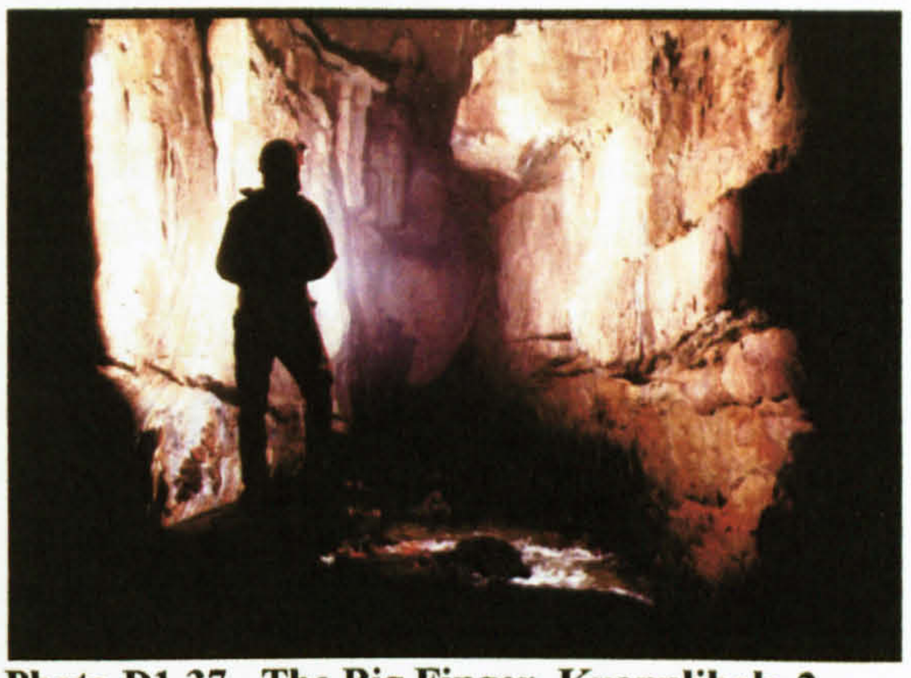

Photo D1.37 The Big Finger, Kvannlihola 2
The collapse of this large block probably happened at the same time as the collapse at the Blockpile. The sloping fractures in the walls show movements of several centimetres.

Photo D1.38 Grønndalsgrotta (ZA)
Three vertical fractures created shifted slabs some 2–3m thick at the resurgence entrance.

Photo D1.39 Bekkehølet, Grønndal (ZA)
Vertical neotectonic fracture inside entrance. Torch for scale.

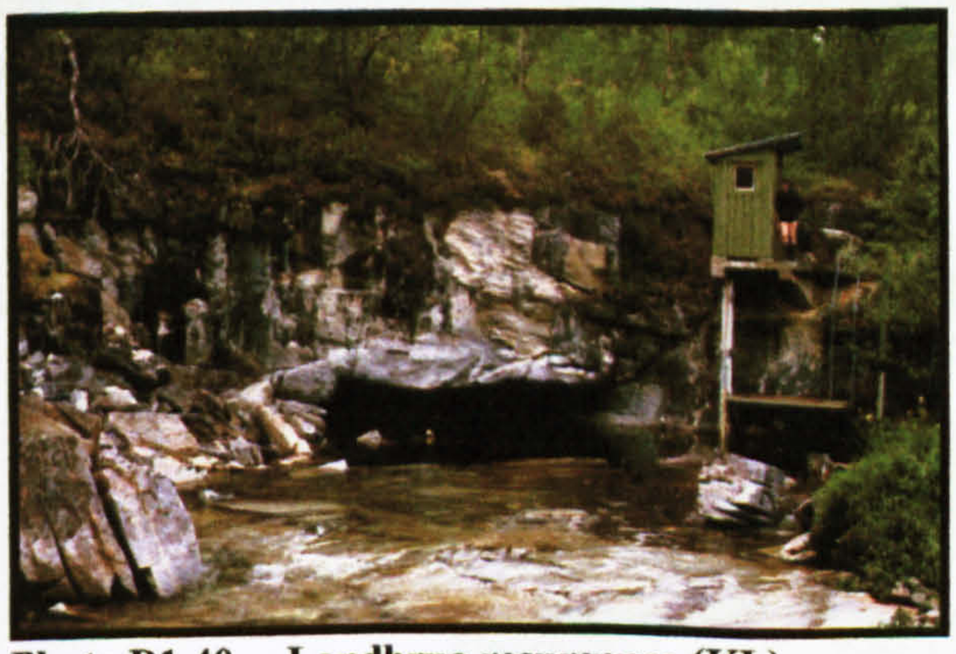

Photo D1.40 Landbrua resurgence (KL)
Fractures and small horizontal movements at roof level above the resurgence.

Photo D1.41 Sjliengojukke waterfall (KS)
Reverse fault with ~50cm throw within foliation of calcareous phyllite (in Sweden).

APPENDIX D2 DEGLACIATION OF THE WHOLE STUDY AREA

This Appendix puts the terms and concepts introduced in section 8.1 into context by deriving the deglacial sequence for the whole study area. Contemporary influences on the karst cave sites are also discussed in general terms. The Tosenfjord–Fiplingdal area deglaciation is considered in more detail in Appendix D3.

Figures D2.1–D2.9 are small-scale models of the deglaciation that show the encroachment of the sea, the movement of the ice margin and the evolution of ice-dammed lakes. They are based on the study area map (Figure 1.1) and are derived from the reconstructed Grønlie (1975) formula for ice-melting height (section 8.1.4; as adapted in Figure 8.2a for the Western catchment area only), from the published ^{14}C dates of various ice margin moraines, and from the author's construction of YD isobase lines that are extrapolations and interpolations from the map of Sørensen *et al.* (1987). These isolines are also in general agreement with altitude / age information provided by Grønlie (1975). Their direction is N25°E, which is similar to geological trends in parts of the study area. To be consistent, the upper ice-melting heights are stated for most dates at a common 180m YD isobase. The profiles assume that the upper ice-melting height rose by c. 100m for each 20m increase in isobase (i.e. for each 15km farther east) at any point in time, and lowered by c. 50m every 100a after 10000^{14}Ca BP at any isobase. (The icesheet surface was roughly horizontal during deglaciation). Different colours are used to differentiate between nunataks, ice-dammed lakes, the ice margin and sea water or meteoric lakes. Uncoloured areas west of the ice margin are completely deglaciated. Those to the east are covered by the remaining icesheet. The maps do not attempt to show directions of ice flow, nor the more transitory ice margin IDLs.

D2.1 Deglaciation at c. 12000^{14}Ca BP: Figure D2.1

At c. 12000, practically the whole area inland from the ice margin along the coast was still covered by the icesheet and the only (possibly) karst cave invaded by the sea was **Marmorhølet** (Z9), on the island of Dønna. The only coastal mountains to stand out as nunataks above the 900m (or lower) ice-melting height at the 100m isobase were the Seven Sisters (Z2). These formed static nunatak IDLs that became westward- and backward-flowing as the ice surface lowered, the latter flooding **Grotte Aug. 82** and then **Søvikgrotta**. Near the 180m YD isobase, only Brurskanken stood out as a nunatak, above the ice-melting height of c. 1300m. Farther east, the Okstind mountains were deglaciated above c. 1400m, and the mountains of Børgefjell above c. 1500m. These nunataks formed narrow static IDLs in glacial situation U, none of which extended far enough down the mountain sides to immerse any nearby caves, because the highest cave was some 300m below the ice-melting height at this time.

D2.2 Deglaciation at 10700^{14}Ca BP: Figure D2.2

By 10700, the sea reached the Seven Sisters and moved inland to about halfway along Velfjord, covering much of the land that is now well above sea level. **Grotte Aug. 82** became drained but the four **Football Pitch Caves** at Brønnøysund (Z1), **Søvikgrotta** and **Vistnesoddgrotta** (Z2), and probably **Green Gorge Cave, Marble-Arch**, and the lower entrances to the **JOBshullet / Klausmark System**, all in Klausmarkdal (Z2), were inundated by sea water. Appendix D4.12 discusses the effects of marine inundation. With the ice-melting height at the 180m YD isobase now at c. 900m, more nunatak, and some westward- and backward-flowing, ice-dammed lakes formed along the upper ridges of the area's major catchment divides that were now exposed above the icesheet. In the Vefsn, Northern and Eastern catchment areas, some caves along the Herringselv (Z6), **Ytterlihullet** (ZA), **Grønndalsgrotta** and **Leirskarelvgrotta** (ZB), the caves at Kåtaviken and Mjölkbäck (ZC), and **Stor Grubblandsgrotta** and caves at Rödingsfjäll (KU) became flooded by these IDLs.

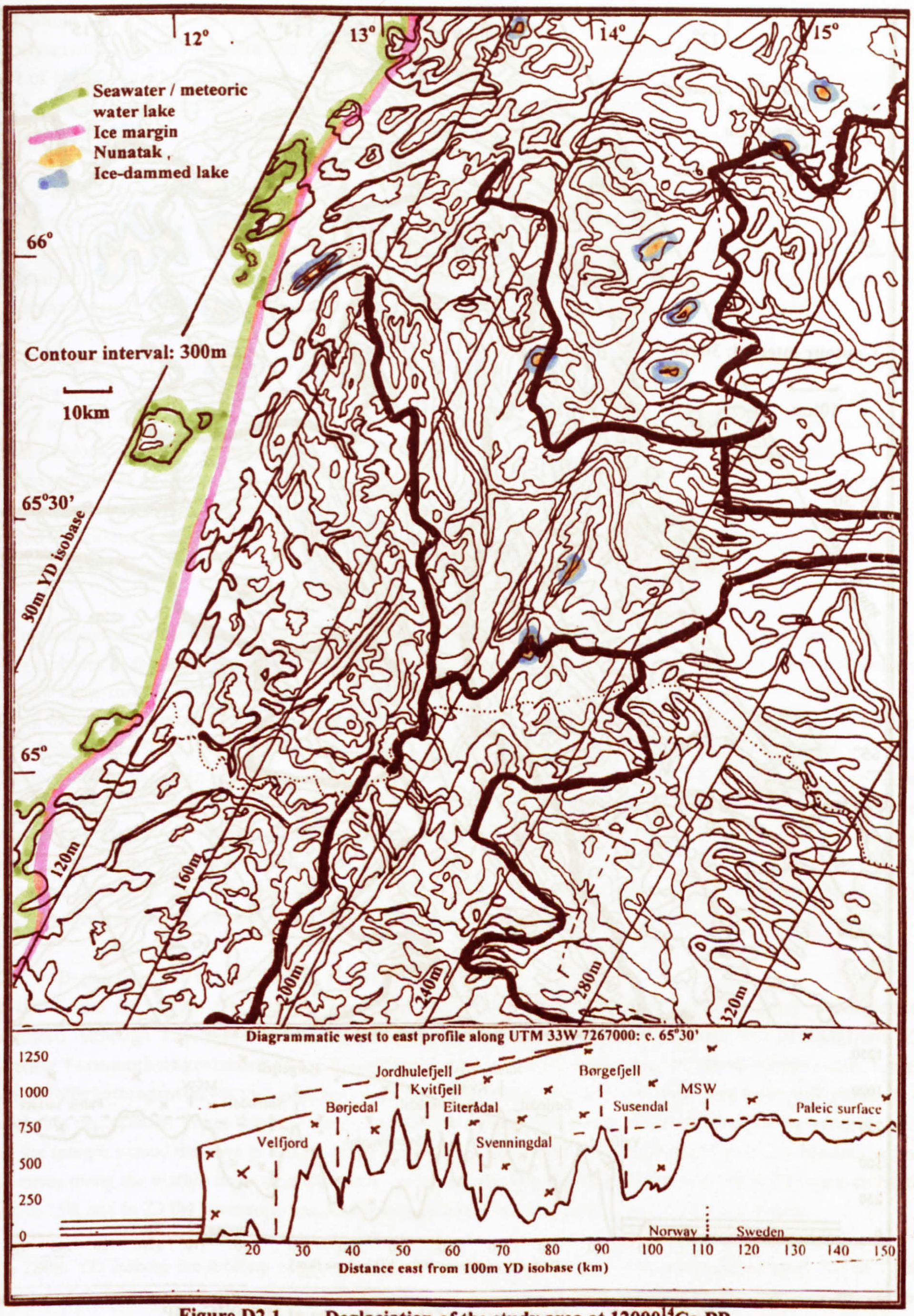

Figure D2.1 **Deglaciation of the study area at 12000^{14}Ca BP**
(180m YD isobase ice melting height: c. 1300m)

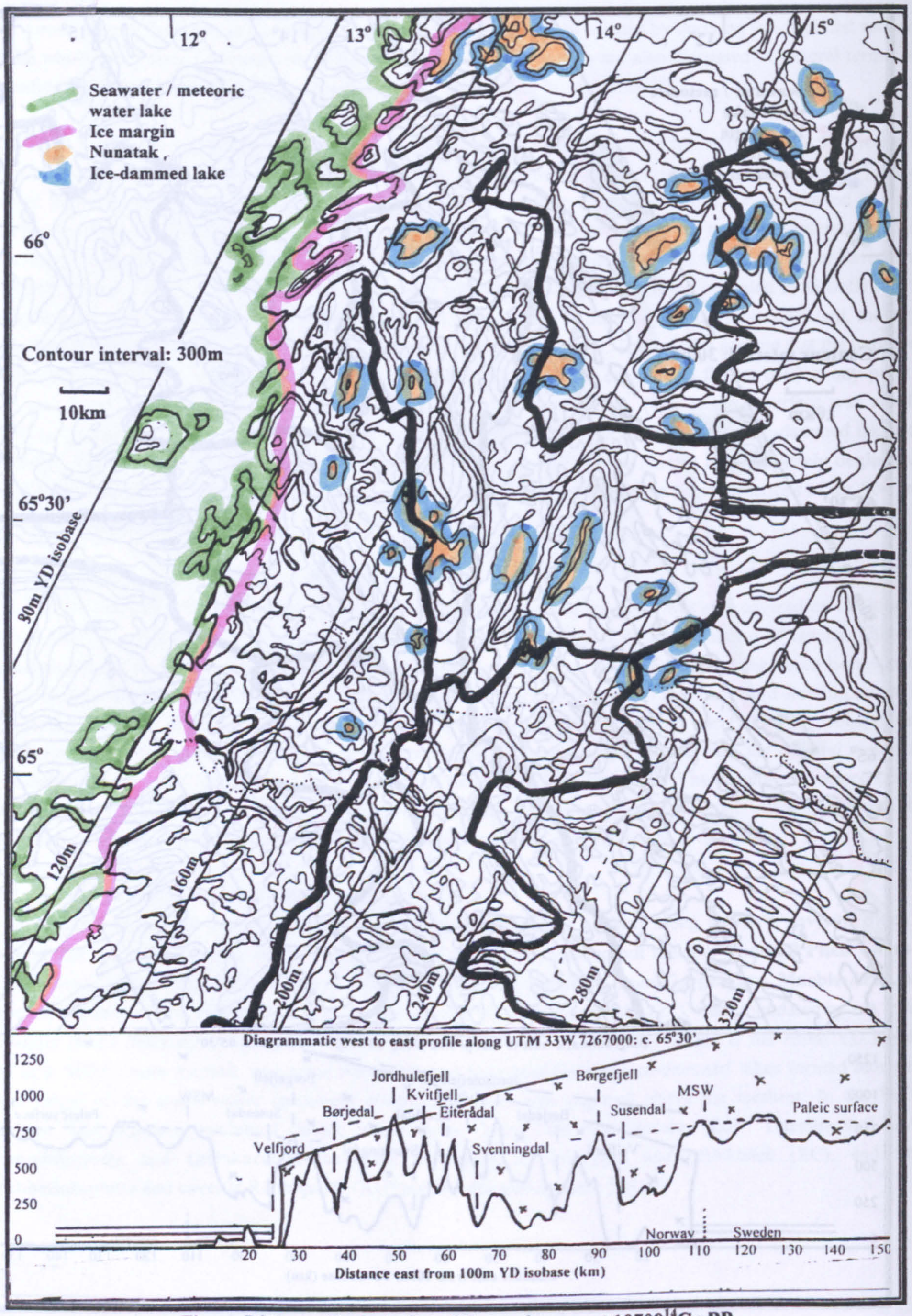

Figure D2.2 Deglaciation of the study area at 10700^{14}Ca BP
(180m YD isobase ice melting height: c. 900m)

D2.3 Deglaciation at 10300^{14}Ca BP: Figure D2.3

The sea covered most of Velfjord, Ursfjord and Bindalsfjord (Z2) by 10300. This marine invasion probably included **Hubruhola** and **Langkilagrotta**, followed soon after by **Aunholet** and the caves near Bordvik: **Bordvikgrotta**, **Nordlysgrotta**, **Marimyntgrotta** and **Skånvikgrotta**. The presence of extensive sand banks below the entrance shaft of **Nordlysgrotta** confirms that it lay below the deglaciation marine limit. By c. 10200, the sea covered the lower part of **Svartdalgrotta** and other caves at Svartvatn, including **Neptune's Cave**, **Barnacle Cave** and **Draugenshullet**, where marine inundation is proved by the presence of barnacles on their walls (Appendix D5.3).

The ice-melting height was now c. 750m at the 180m isobase. The backward-flowing IDLs became much wider and some coalesced into one large and deep lake west of Svenningdal in the Vefsn catchment area that probably reached to the Svenningdal valley itself (Appendix D3). The caves at Herringselv (Z6) and **Grønndalsgrotta** (ZA) at GS=K experienced inundations below IDLs that migrated from nunatak to westward-flowing, whereas **Stor Grubblandsgrotta** (KU, GS=L) was covered by a nunatak, backward- and then eastward-flowing IDL.

Those caves situated totally above 750m altitude at the 180m YD isobase (rising to 950m at the 220m YD isobase inside Sweden) were by now drained and experienced flow regimes (or dry conditions) similar to those at present. Deeper systems that straddled the upper ice-melting height experienced variable flow regimes that depended on the extent of blocking of their resurgences by the icesheet (section 8.4.12). The 180m-deep **Ytterlihullet** (ZA, GS=S), with an altitude of 817m near the 180m YD isobase, is an example of this phenomenon because its outlet was likely to have been restricted by the area's largest glacier (section 6.5.3) for a further 360a. Indeed, a possible overflow beyond its present sink entrance into an entrance at the upstream end of Tributary Passage may partly explain the large size of that passage.

The mountains along the Main Scandinavian Watershed (MSW) increasingly emerged above the icesheet, starting at lower isobases in the north (where the international border turns through 90°). Narrow, initially static, nunatak ice-dammed lakes formed along both sides of the MSW ridge at elevations from 850–1050m (at YD isobases of 200–240m), to repeat the process of enlargement and merger that had begun along the mountains west of Svenningdal some 400a earlier. Thus, **Akersvanngrotta** (ZB, GS=K) and caves at Rödingsfjäll (KU, GS=S) were submerged beneath nunatak and then westward-flowing IDLs and the outlets from the mountains along the Norwegian / Swedish border area were towards, and into, Norway. **Labyrintgrottan** and other caves at Mieseken (ZC), and caves at Skinnfjell, Övre Ältsvattnet and **Sotsbäcksgrottan** (KU), which are all at GS=L or T, became submerged below nunatak and then backward-flowing IDLs, whose outlets to the west or north became controlled by a succession of high pass-points along the MSW. Indeed, some of the waters that passed through **Labyrintgrottan**, **Sotsbäcksgrottan** and the caves at Övre Ältsvattnet must have also passed through **Akersvanngrotta**!

D2.4 Deglaciation at 10100^{14}Ca BP: Figure D2.4

At 10100, the ice margin reached to the ends of the shorter fjords, and about halfway along Vefsnfjord and Ranafjord, although Tosenfjord remained filled with ice. The sea submerged the inner end of Langfjord (Z2), covering **Tarmaunbotngrottene 1–3** and **Langfjordgrotta**, and at the same time, **Jenshola**, farther south. **Laveste Langskjellighattengrotta**, above Langfjord, is probably the highest cave in the study area to be influenced by the sea during deglaciation. It has three entrances, at altitudes from 160 to 167m, and its lowest part descends to 153m. The ice margin passed the cave at 10130, when the local sea level was at 158m (Appendix D5.3). **Mølnvatngrotta** and caves along the marble outcrop to the north, caves at Saus, and **Aunhattenhule 1–4** (all in Z2) were covered at 10050±250, and in Z3 the ice margin passed **Trondjordhula**, and **Risehula 1 and 2** soon afterwards.

The 180m YD isobase ice-melting height was now reduced to c. 650m, and new ice-dammed lakes NE of Trofors submerged the caves along the Glugvasselv (Z6) and in Svartvassdal (Z7). **Øyåskjeleren** (Z4) and **Øyfjellgrotta** (Z5) were submerged below an eastward-flowing ice-dammed lake that formed to the SW of Mosjøen. Along the Swedish border area, the ice-melting height lowered to c. 850m at the 220m YD isobase, the ice-dammed lakes enlarged, particularly along the eastern side of the MSW, and the caves at the highest altitudes at Mieseken and Rödingsfjäll started to drain. **Landbrua**, **Marmorgrotta** and other caves along the Rennselelv (KL) in Norway near isobase 260m were over 500m below a new nunatak IDL at an initial altitude of c. 1050m.

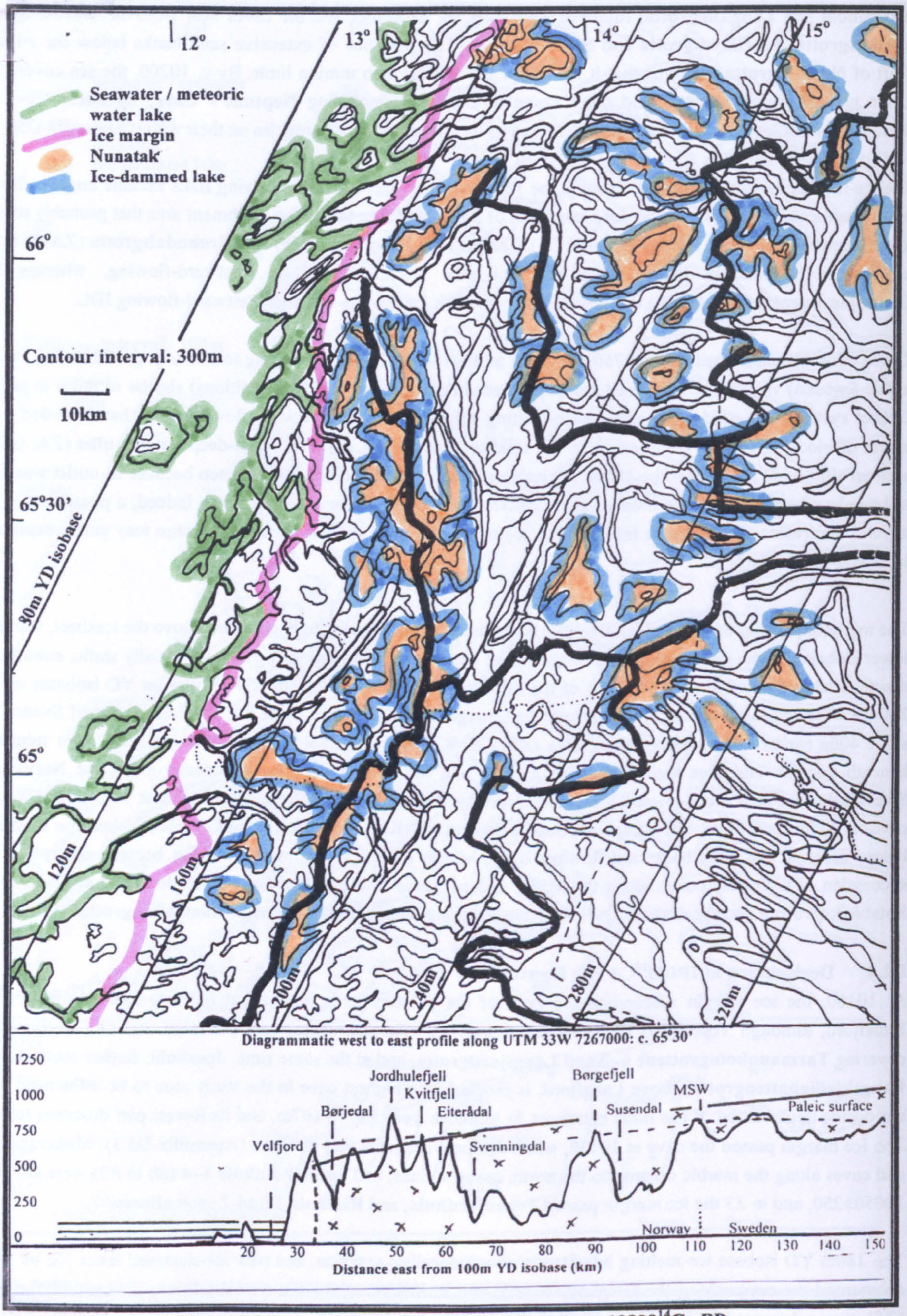

Figure D2.3 **Deglaciation of the study area at 10300^{14}Ca BP**
(180m YD isobase ice melting height: c. 750m)

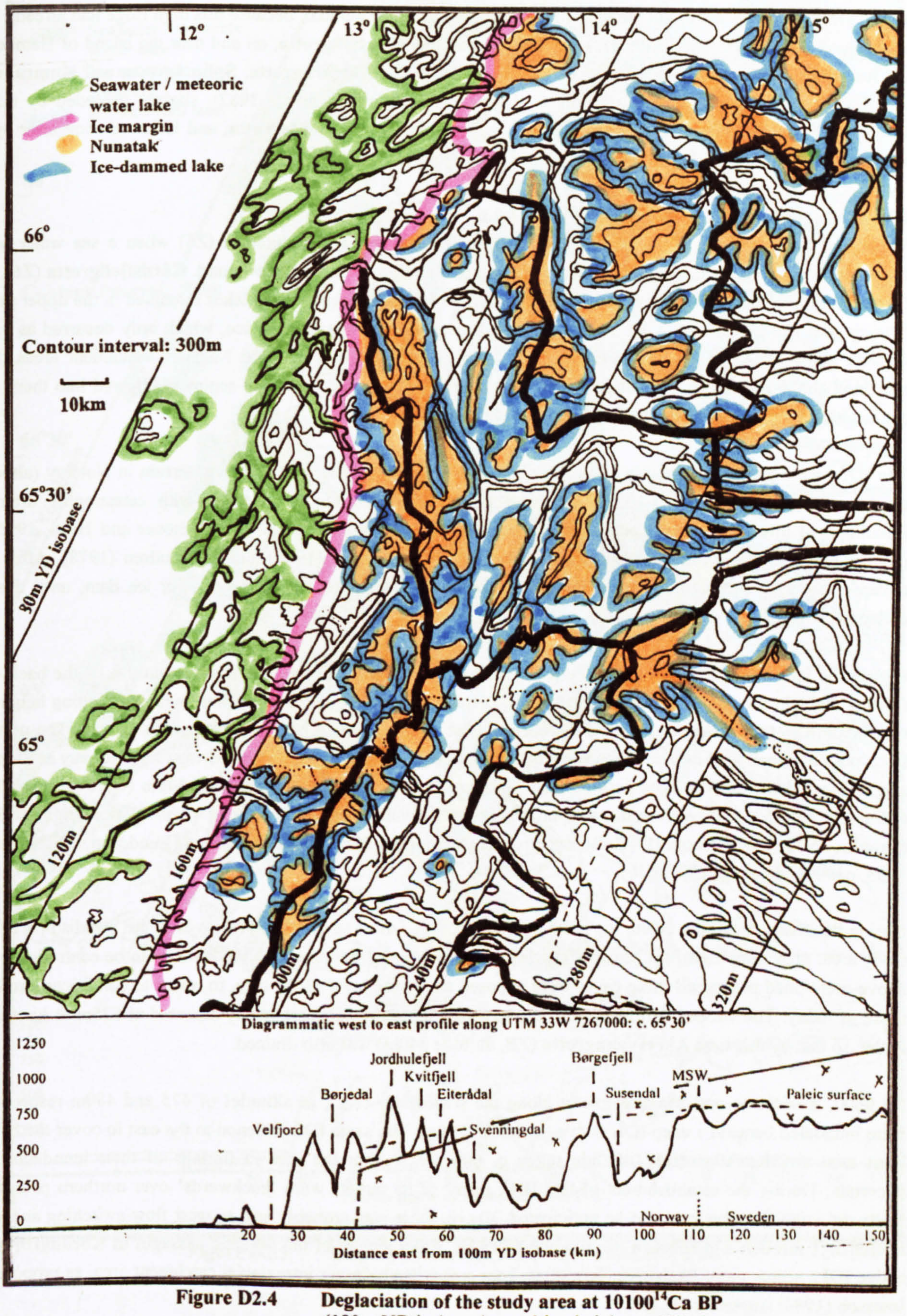

Figure D2.4 **Deglaciation of the study area at 10100^{14}Ca BP**
(180m YD isobase ice melting height: c. 650m)

D2.5 Deglaciation at 9900^{14}Ca BP: Figure D2.5

By about 9900, the ice margin had retreated across most of the Western catchment area. It was about to 'jump' across the intervening mountain range to reach Svenningdal and Eiterådal, because this high ridge had already been deglaciated downwards (Appendix D3). **Gjeitvikgrotta** and **Berntvikgrotta**, on and near the island of Hemnes on the south side of Ranafjord, were covered by the sea, as were **Sildgarngrotta**, **Splintågrotta** and **Kumragrotta** near Elsfjord (all in Z6). Tosenfjord melted at 9890±230 (Andersen *et al.*, 1982), slightly preceded by marine inundation from the west at **Svartdalsholet** and at **Øvre** and **Nedre Landegrotta**, and followed soon after by the inundation of **Kalkdalgrotta** on the other side of Tosenfjord (all in Z2).

D2.6 Deglaciation at 9600^{14}Ca BP: Figure D2.6

Vefsnfjord melted as far as Mosjøen by 9550, flooding the nearby **Høgligrotta** (Z6) when a sea water sound connected Vefsnfjord to Elsfjord. Only the inner end of Ranafjord remained ice-bound. **Gårdsfjellgrotta** (Z6), also on the island of Hemnes, was invaded at 9500. Northward-flowing ice-dammed lakes remained in the upper part of Svenningdal and along Fiplingdal. Most of the high ground here was clear of ice, which only occurred as valley glaciers below 350m at the 180m YD isobase. Farther east, in the Vefsn and Northern catchment areas, IDLs remained above present lake positions, when very large discharges of water and sediments flowed into them from deglaciation centres over Børgefjell and Okstind (Grønlie, 1975, p465).

The IDLs were generally unstable and more short-lived in the steeper, west-draining, terrain in Norway (although they typically existed for c. 1000a: section 8.4.12). They commonly collapsed with catastrophic drainings (jökulhlaups) through rapidly-eroded glacial channels on to outwash terraces (e.g. Schöner and Hartl, 1996). A modern example at an Okstind glacier was discussed by Theakstone (1978) and by Knudsen (1978). After each collapse, the lake surface commonly fell to a lower level, controlled by the next lower ice dam, until this too collapsed in its turn.

During the later melting, when up-valley ice melted before down-valley glacier ice (section 2.4.1), the backward-flowing IDLs in the Eastern catchment area (at YD isobases up to 280m, and therefore with ice-melting heights up to c. 850m) grew to enormous sizes in Sweden, whilst still being held back by the residual icecap. The northern IDLs possibly coalesced into one lake at Tärnaby (the Gäuta Ice Lake), which flowed west into Norway at Røssvatn and at Stor Akersvatn via three pass-points ("spillways": Rudoy, 2002) at heights of 540m (Övre Jovatn), 550m (Tängvatn) and 535m (Över-Uman), and an IDL above Arevatn overflowed west to Vefsndal at a height of 677m (Grønlie, 1975, p465). Large IDLs also occurred at Borga, Stor Blåsjön and Frostviken (Lundqvist, 1972; Donner, 1995, p109; Dahl *et al.*, 1997, p46).

During its enlargement, the Gäuta Ice Lake probably covered most of the northern caves in the Swedish part of the study area, providing high-flow phreatic conditions. However, by the time its level lowered to be controlled by the above-mentioned passes, all these caves were exposed above the level of the lake, to revert to conditions similar to those of today. The westward-flowing IDL above Stor Akersvatn was temporarily dammed at 525m at its western outlet, so that by this time **Akersvanngrotta** (ZB, altitude 540m) was also drained.

By 9600, **Landbrua** and **Marmorgrotta** along the Rennselelv (KL), at altitudes of 475 and 480m respectively, were inundated beneath a deep IDL with a surface at 750m. The same IDL widened to the east to cover the Bjurälv karst area and **Korallgrottan** (altitude range c. 603–459m), but the precise timings of their inundations are uncertain. During the establishment of this IDL, many of its outlets were 'backwards' over northern passes, but westward englacial flow can also be anticipated. Hence, there was probably east to west flow-switching and water interchange through and between the submerged caves. Enlargement of the phreatic passages in **Korallgrottan** by active IDLs seems more likely than formation from a previously-larger interglacial catchment area, as proposed by Isacsson (1994; Appendix B1.15).

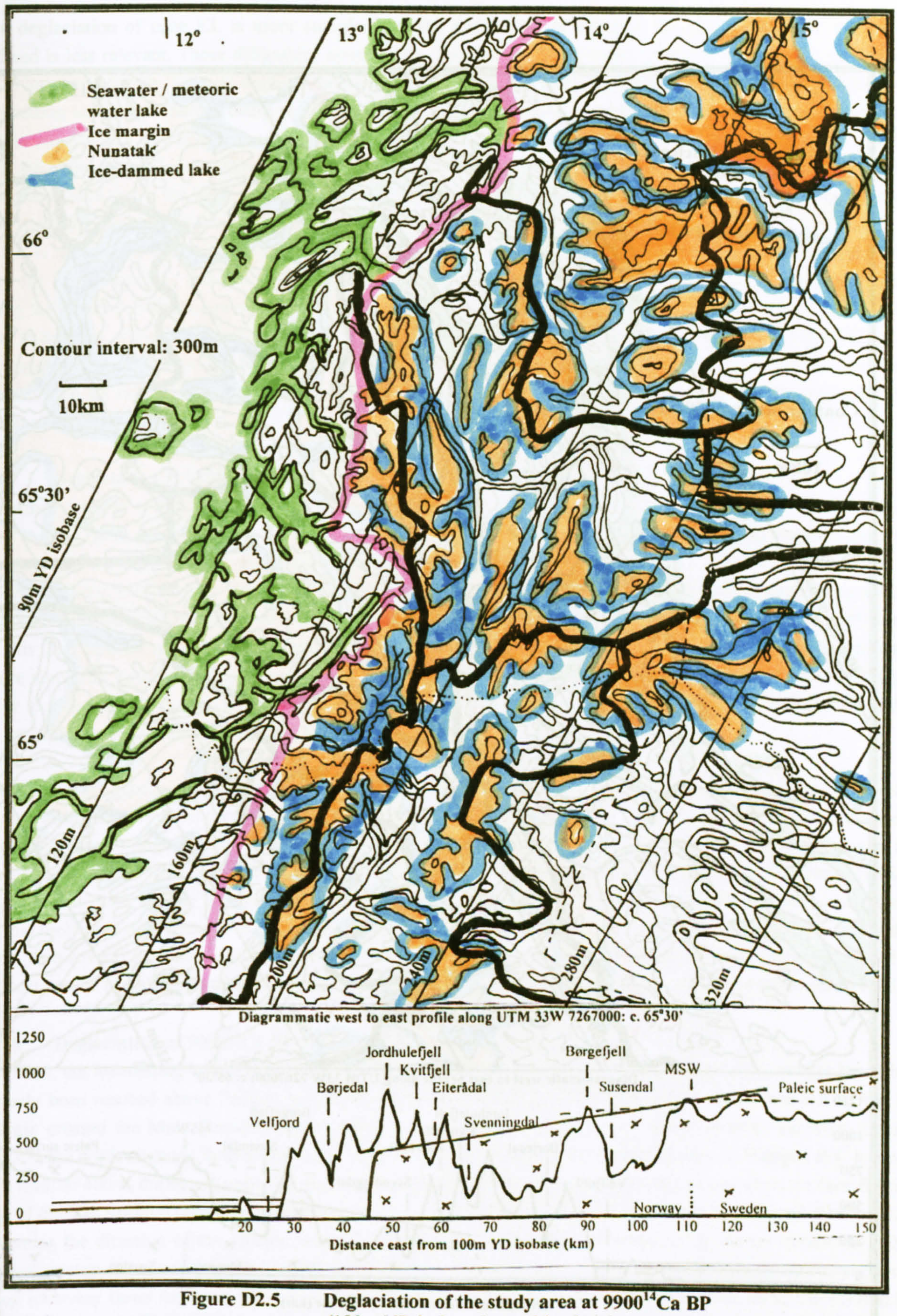

Figure D2.5 **Deglaciation of the study area at 9900^{14}Ca BP**
(180m YD isobase ice melting height: c. 550m)

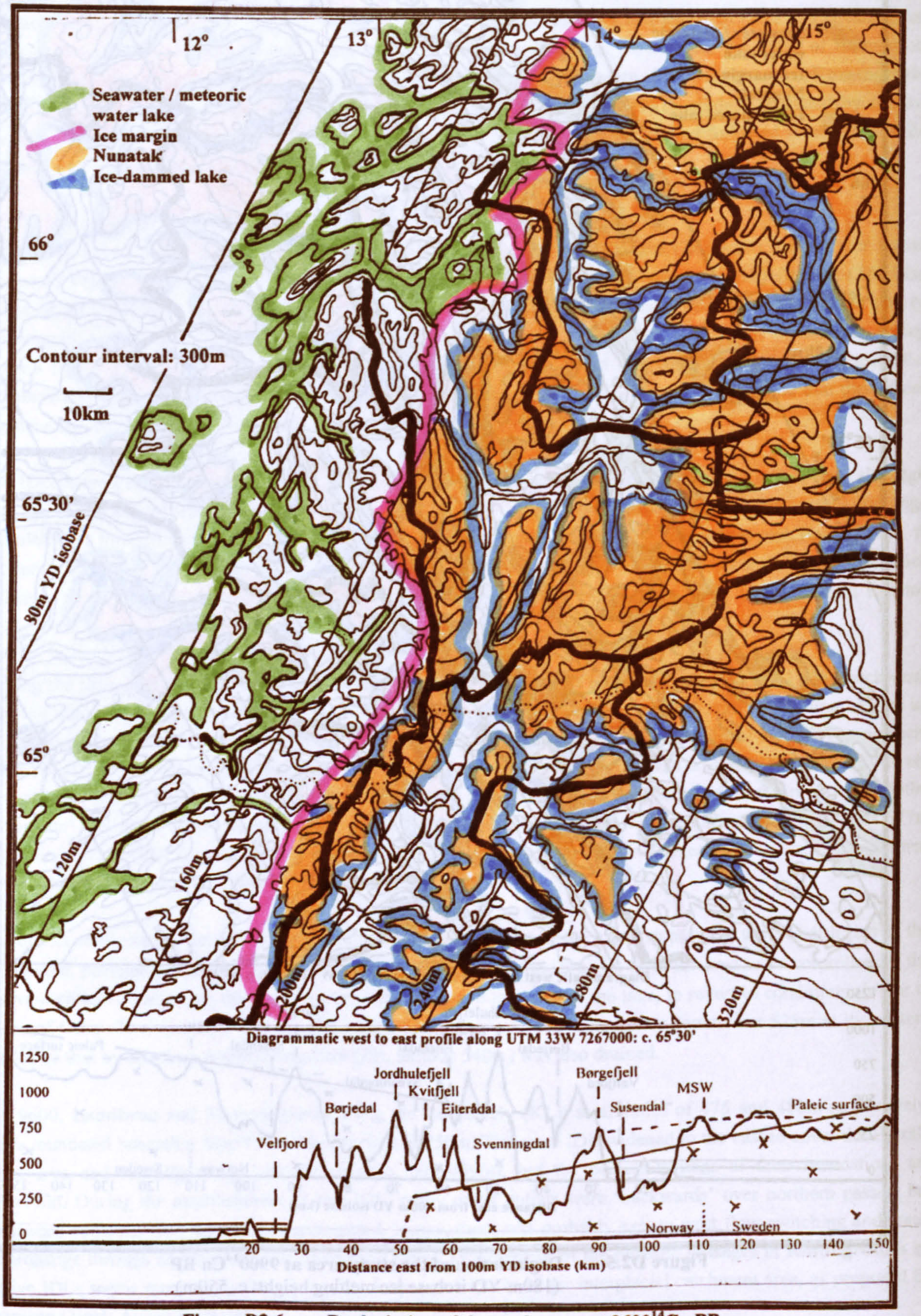

Figure D2.6 **Deglaciation of the study area at 9600^{14}Ca BP**
(180m YD isobase ice melting height: c. 350m)

The deglaciation of zone KL is more complex and the assignment of caves to the glacial situations previously defined is less relevant. These difficulties arise, firstly, because the MSW makes a major westward incursion here into Norway; secondly, because deglaciation was much more controlled by the lowering of the icesheet surface, with a receding ice margin hardly being recognisable; and thirdly, because a potentially huge IDL formed across the whole zone, which initially covered minor passes that became relevant later. Possible variations in the size of this IDL are indicated in Figures D2.6–D2.8. The problem is compounded because the zone contains **Korallgrottan**, the study area cave that is the longest by far and that is also the second deepest. Its assignment is therefore significant in characterising the mean dimensions of caves in each glacial situation. The 'major local ridge' for most of the caves in KL is taken to be the higher ground along the Norway / Sweden border that runs roughly north to south, rather then the high mountains that run west to east along the MSW to the north. Accordingly, all the Norwegian caves along the Rennselelv in KL are assigned GS=K, because they lie west of and below the pass (at 540m) to the Bjurälv area in Sweden, whose caves are all assigned GS=L. The caves near **Korallgrottan** are variously assigned GS=L or T, depending on their altitude. **Korallgrottan** itself is assigned GS=L, because the major length of this cave and probably all its relict phreatic passages are below the level of the lowest local pass, despite its highest active entrance being above this level.

D2.7 Deglaciation at 9300^{14}Ca BP: Figure D2.7

Moraines dated to c. 9300 (Bergstrøm, 1995) give the last reliable indication of the icesheet recession in the study area. All the fjords were by now ice-free, and the inland ice margin had crossed several mountain ranges to enter the Northern, Vefsn and Namsen catchment areas. The sea melted the glacier in the Vefsn valley upwards from its lower, northern, end to cover the **Nedre Laksfors Rising** and **Møllebekkgrottene** (Z5) and **Farewell Cave** (Z6), although it seems that **Øyåskjeleren** (Z4), **Øyfjellgrotta** and the caves associated with **Geitklauvgrotta** (Z5) were, by this time, uplifted too high isostatically to be reached by the sea (section 8.8.3). South of Korgen (ZA), **Remnant Cave** along the Røssåga and the huge arch of **Fjellbrygga** in Bryggfjelldal were probably just reached by the sea prior to their uplift above sea level. Deglaciation marine limits were reached at 131m in Svenningdal at 9150 and at 133m in Vefsndal at 9080 (Grønlie, 1975).

The only valley glaciers that remained near the 180m YD isobase were below 200m in altitude. The IDLs in the NW corner of the Eastern catchment area lowered below the levels of the MSW passes to occupy dead-ice positions above the present large surface lakes, with probably a slow eastward englacial drainage towards the Baltic in the east. Outlets to the north were no longer possible when the ice lake above Stor Blåsjön and the Rennselelv (KL) lowered to a 260m isobase level of 600m, so that flow was consistently westward through **Korallgrottan** and some of this meltwater then passed via **Marmorgrotta** and **Landbrua**. If, as seems likely, lake Limingen melted at this time, then several cols along the MSW to its west enabled strong overflows to the deglaciated Namsen valley. The highest part of **Korallgrottan** began to emerge above water level, but most other local caves remained submerged.

D2.8 Deglaciation at 9000^{14}Ca BP: Figure D2.8

By 9000, the ice-melting height reduced to the then sea level at Svenningdal, as the deglaciation marine limits had already been reached above Trofors and nearly as far as Hattfjelldal (Appendix D2.7). What was left of the ice margin crossed the Main Scandinavian Watershed and the diminishing and lowering Swedish eastward-flowing IDLs in the north retreated farther eastwards, eventually to flow away to the Baltic. The lake Limingen IDL lowered to a level of 400m, draining **Landbrua** and **Marmorgrotta** of deep phreatic water. However, when the Stor Blåsjön end of the IDL lowered below the level of the border passes at 540m and 530m, it became an eastward-flowing IDL, reversing the direction of the phreatic water flow through **Korallgrottan**. Because of its higher isobase at 280m, **Korallgrottan** did not drain until c. 8900, to receive its present allogenic inputs. Thus, **Korallgrottan** experienced deep reversing flows for up to 300a, a westerly flow for about 400a and a falling easterly-flowing submersion for about 100a. After 9300, the direction of phreatic flow remained consistently westward through both **Marmorgrotta** and **Landbrua**, which is also the present stream direction, because the Rennselelv flows westward before finally reversing direction at Røyrvik, to flow east into Sweden via lake Limingen.

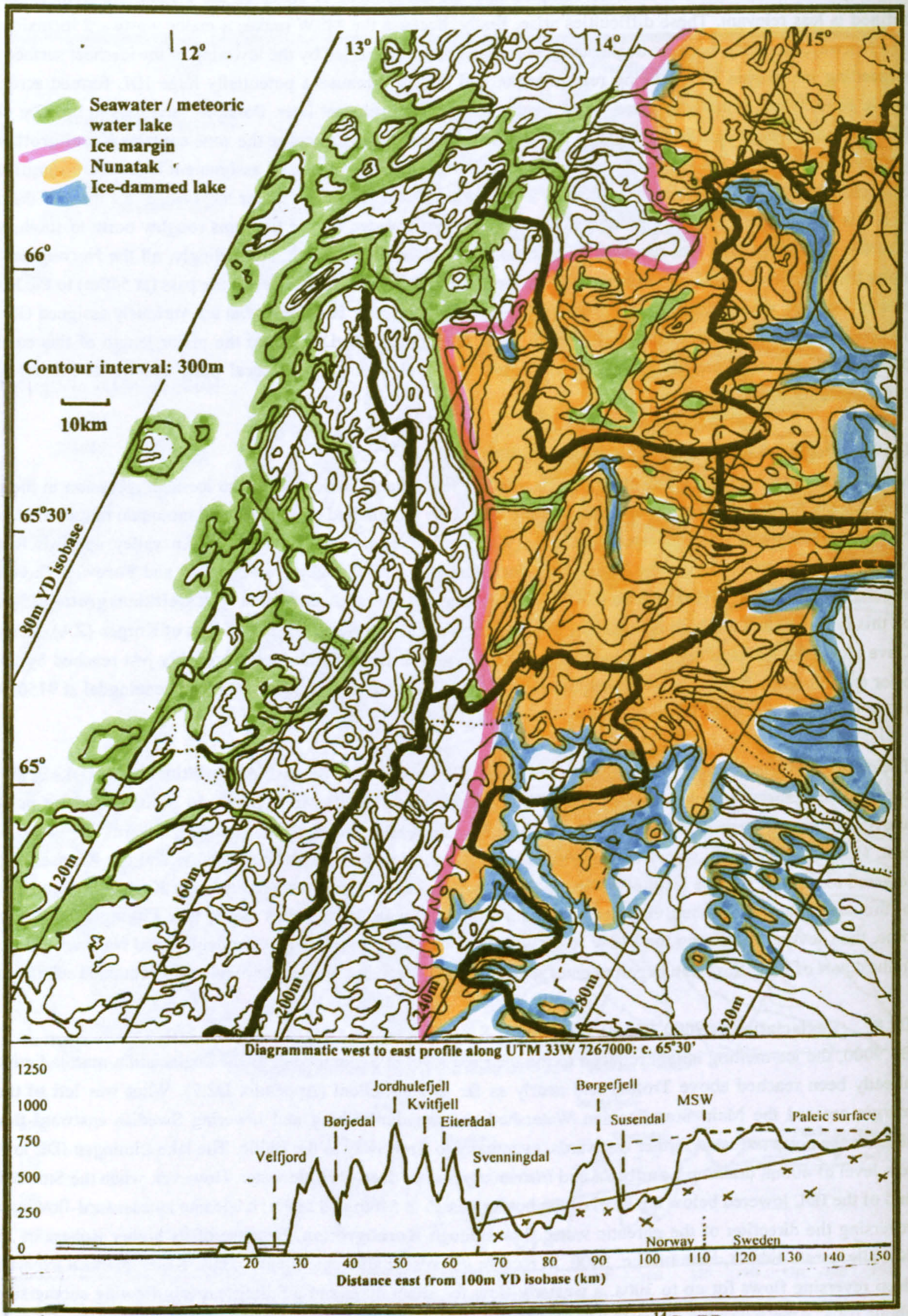

Figure D2.7 **Deglaciation of the study area at 9300^{14}Ca BP**
(180m YD isobase ice melting height: c. 200m)

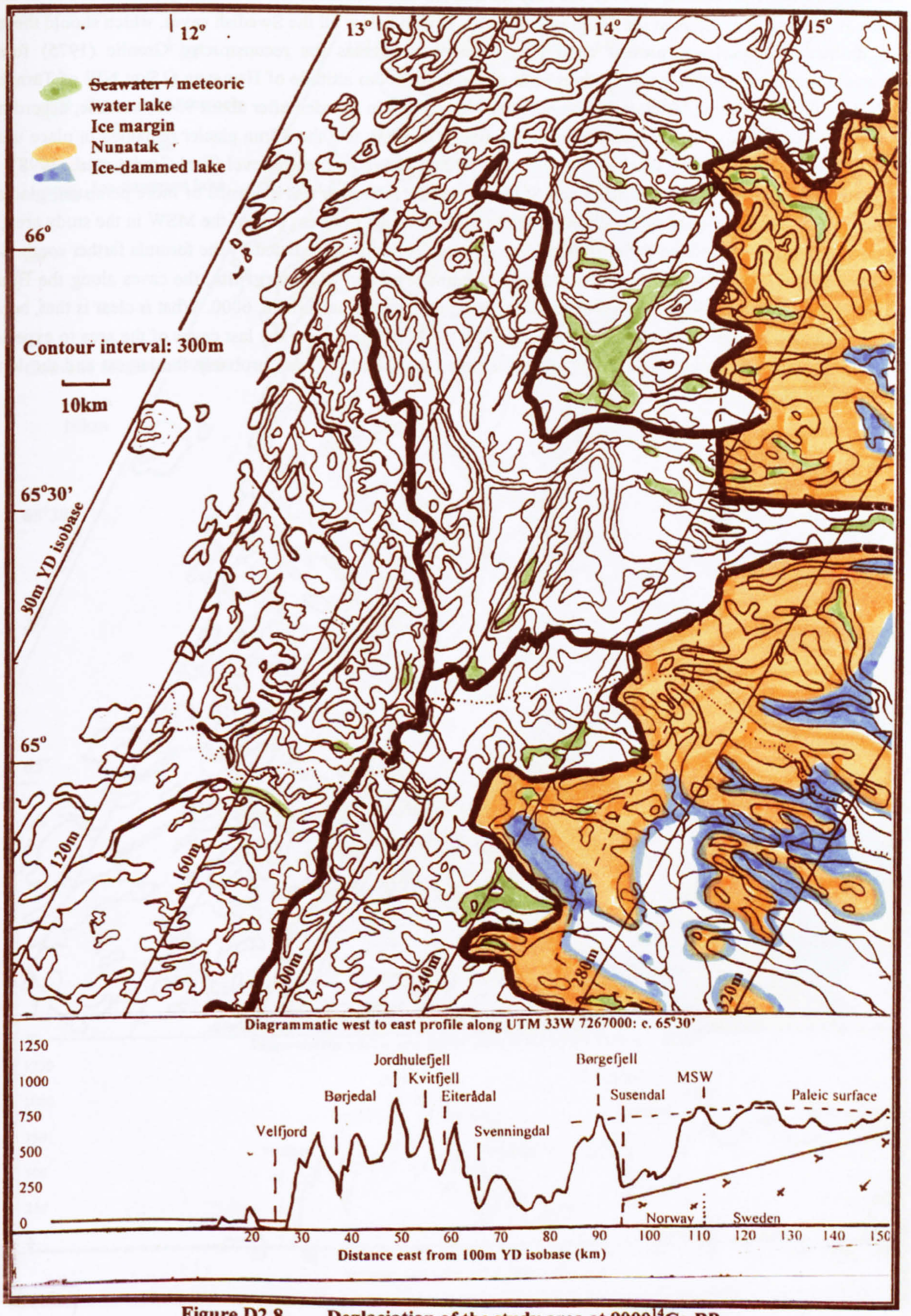

Figure D2.8 **Deglaciation of the study area at 9000^{14}Ca BP**
(East of the Main Scandinavian Watershed only)
(180m YD isobase ice melting height: c. 0m)

D2.9 Deglaciation at and after 8700^{14}Ca BP: Figure D2.9

Following the same procedure, by 8700 the only ice and ice-dammed lakes left in the study area would be at the SE corner, at an altitude of 300m at the 280m isobase. This is well below all the Swedish caves, which should therefore have drained to experience present conditions. However, whereas the reconstructed Grønlie (1975) formula indicates that the ice-melting height should have reached the 460m altitude of Hemavan (15km NW of Tärnaby at the 240m isobase) at about 9200, it can probably not be applied in Sweden after about 9300, because, according to Earl-Gulet *et al.* (1998), this area only became ice-free at c. 8000, and the Tärna glacier remained in place until c. 6000, when the local tree line reached a maximum of 200m above its present level (Earl-Goulet *et al.*, 1998), as it did in Eiterådal (Z4) at 8000 (Lauritzen and St.Pierre, 1982). Although this evidence of more persistent glaciation should not influence the times of the draining of the caves near the northern part of the MSW in the study area, it is suggestive that glaciers and ice-dammed lakes lasted much longer than predicted by the formula farther south. Thus, the timings of the flooding and eventual draining of **Landbrua** and **Marmorgrotta**, the caves along the Bjurälv, and the **Korallgrottan** system, are less clear. They may not have drained until c. 6000. What *is* clear is that, because of their locations at high YD isobases in the range 250 to 280m, these were the last caves of the area to experience the melting pulse and submersion below an ice-dammed lake, and this was probably the largest and the longest lasting IDL in the study area.

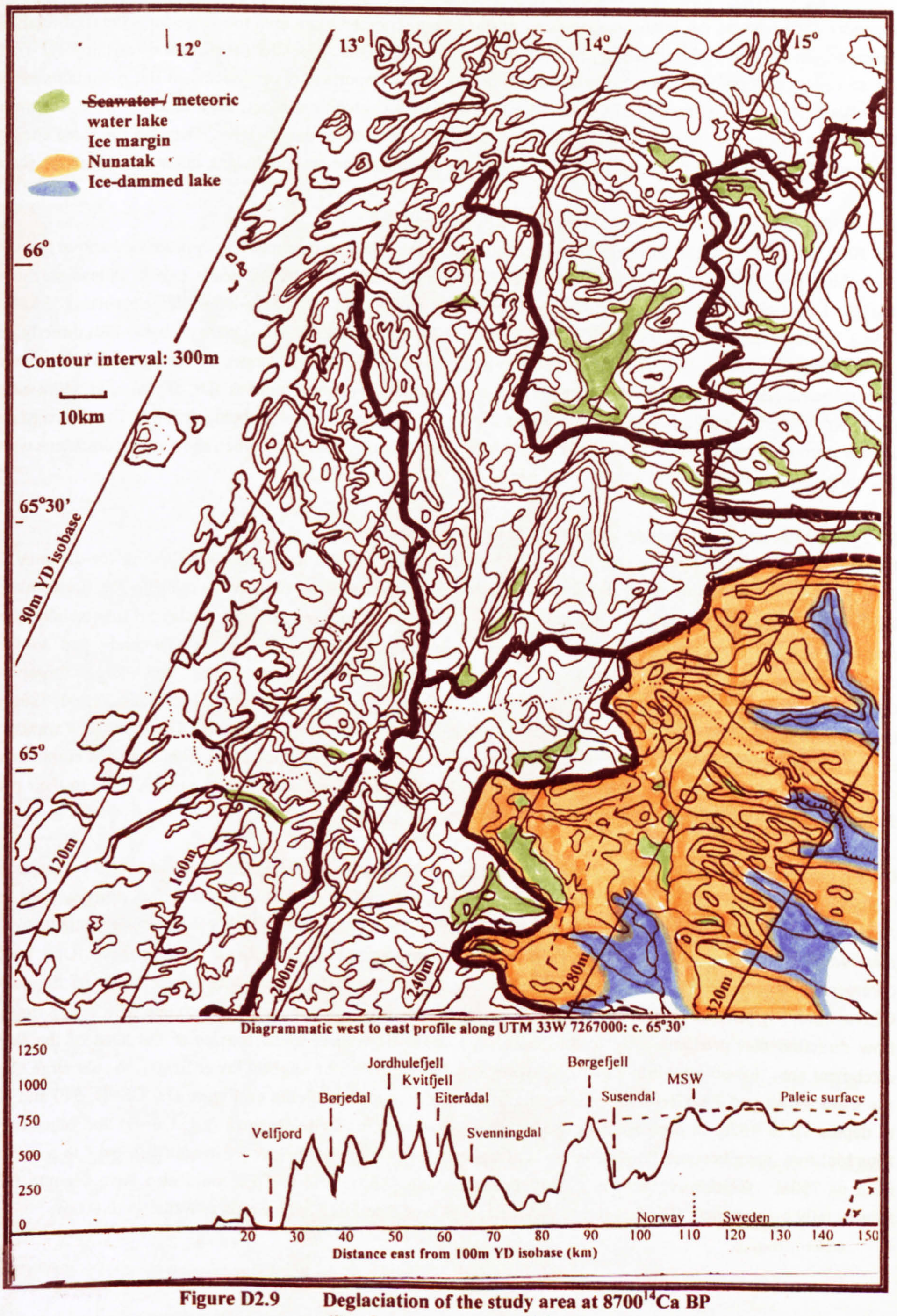

Figure D2.9 **Deglaciation of the study area at 8700^{14}Ca BP (Southeastern corner only)**
(280m YD isobase ice melting height: c. 300m)

APPENDIX D3 DEGLACIATION OF THE TOSENFJORD–FIPLINGDAL AREA

Appendix D2 reviewed the inland deglaciation of the whole study area, an area too large for a detailed analysis of the various hydrological conditions applying to individual caves. This Appendix focuses on a key part near Tosbotn (the so-called geographical centre of Norway) that has many important cave systems in the mountains between Tosenfjord (Z2) and Fiplingdal (Z7) of the Western and Vefsn catchment areas. Figures D3.1–D3.9 illustrate the Weichselian marine and inland deglaciation of this area and show major pass heights. They use the same constructs as Figures D2.1–D2.9 and the same 180m YD isobase for the upper ice-melting height, but at four times the scale.

D3.1 Deglaciation at Tosbotn at 11000^{14}Ca BP: Figure D3.1

At 11000, only a few nunataks along the eastern divide of the Western catchment area protruded above the 1000m ice-melting height. The only extensive (nunatak) ice-dammed lake was at the heads of the valleys surrounding Blåfjell, Langfjell and Langskardnåsen, which probably submerged the 861m-long **Blåfjellgrotta** (Z5; altitude 795m). Some of the caves on the south side of Kvitfjell (Z4; altitudes 809–900m) were probably also directly below a deep, narrow, nunatak IDL. Two shattered 7m-long caves on the eastern slopes of Jordhulefjell (Z4, given the Lappish name Jienemeguovdele in Figure D3) became covered by a small nunatak IDL at GS=U at 940m altitude. These only experienced static phreatic conditions during this deglaciation before being drained. The shattered nature of their entrances indicates that they suffered ice-wedging in winter, probably when they were coincident with the IDL surface (sections 8.4.4 and 8.9.4).

D3.2 Deglaciation at Tosbotn at 10700^{14}Ca BP: Figure D3.2

The ice-melting height lowered by 100m to c. 900m within c. 300a and backward-flowing ice-dammed lakes developed along the major ridge between Kvanlitinden in the south to Grundvasstinden in the north, although Jordhulefjell remained separate as a nunatak. Some of the IDLs in this area probably coalesced subglacially via Nye channels that followed the valleys downward, to inundate the upper parts of the Gåsvaselv and Jordbruelv catchments in high pressure subglacial reservoirs (SGRs). IDLs flooded the very large through-cave **Gåsvasstindhola** (Z4; GS=T; altitude 778m; Photo 8.1), the caves west of Jordhulefjell (Z4; GS=T; 860–730m) and **Elgfjellhola** (Z4, on the plateau east of Jordhulefjell; GS=L; 600m) at high pressures. The caves at Vargskar (Z5, east of Blåfjell; GS=T or L; 800–500m) probably received a speleogenetic 'kick start', although their common small size and predominant vadose character, with high present flow rates, indicates that most developed to their present dimensions during the Holocene (section 9.2.4).

During the falls of the ice-dammed lakes from 1000m to 900m, their surface levels were controlled by passes along the ridge at heights of (to the nearest 10m) 950, 910, 910, 910, 900, 940, 930 and 930m. Underlined heights in this Appendix D3 indicate that there is a significant gorge on the coastal side of the ridge, strongly suggestive of a *jökulhlaup* at the time of the change in lake level. Thus, strong reverse flows through these IDLs probably commenced around 10850 at a height of 950m. As all but the last of these passes are south of the caves at Gåsvasstind, Elgfjell and west of Jordhulefjell, if all these caves were submerged beneath one SGR at this time, their flow direction was predominantly to the south. The water from each of the passes at the head of the Western catchment area flowed west into a growing westward-flowing IDL, at a slightly lower height, to submerge **Cave of the Cold Wind** and **Toerfjellhola** (Z3, south of the peak named Tverrfjellet on Figure D3; GS=K; 640 and 485m) to depths up to 465m in high pressure SGRs. At about this time, **Sirijordgrotta** (Z4; GS=H) and other caves in Eiterådal may have become flooded in an SGR beneath a nunatak IDL below Visttinden (1236m), to a maximum head of 700m. **Geitklauvgrotta** and **Møllebekkgrottene** (Z5; GS=H and E) could also have become flooded subglacially by a nunatak IDL that formed on the east side of Eiteråfjell, with heads of water up to 800m.

PAGE/PAGES EXCLUDED UNDER INSTRUCTION FROM UNIVERSITY

D3.3 Deglaciation at Tosbotn at 10400^{14}Ca BP: Figure D3.3

After another 300a, the ice-melting height fell another 100m to c. 800m. The large eastern IDLs retreated down the sides of the steep ridges but widened, so that their combined subglacial reservoir may have reached what appear to be 'jaws' created by northward- and southward-pointing ridges on each side of the Gåsvaselv (shown by a dashed blue line in Figure D3.3). In this case, **Jegerhullet**, **Etasjegrotta**, **Invasjonsgrotta**, **Anastomosegrotta** and **Bjørkåsgrotta** (Z4, in the Jordbruelv valley; GS=L) were flooded, probably in mainly static conditions at this depth. Such an ice-dammed lake and reservoir was about 100km^2 in extent and 500m deep on its eastern side, but still with a general reverse flow towards the passes along the 'lengthening' western mountain ridge. *All* the previously mentioned caves east of this ridge remained submerged, *except* for the caves on Kvitfjell, and the higher ones west of Jordhulefjell, which, being higher than 800m, were drained by this time to revert to Holocene conditions.

During the falls in the eastern lake levels from 900–800m (Photo D3.1) their outlets were controlled by passes at heights of 830(S), 840(S), 810(S), 830(S), 890(S), 821(S), 830(S), 840(N) and 825(N)m, S and N indicating whether the outlets caused water to flow through the caves at Elgfjell towards the south or towards the north. The second to seventh of these passes all directed water into the falling and expanding westward-flowing IDL, which continued to cover **Cave of the Cold Wind** and **Toerfjellhola** (Z3).

Photo D3.1 **Nedre Jordbruvatn and Tverrfjell, from Jordhulefjell (Jienemeguovdele)**
View to the NW from the Jordhulefjell limestone outcrop. Horizontal snow patches (arrowed) possibly indicate some terrace levels of the deglacial ice-dammed lake that formed between the Tverrfjell (Toerfjell) ridge and the Jordhulefjell ridge. The prominent col south of Tverrfjell heads the valley leading west to Toerfjellhola.

The results of two of the jökulhlaup captures have been observed by this author. The valleys west of the passes at 821m (near Durmålstind) and at 830m (above **Toerfjellhola**) contain deep canyons and talus slopes where the valley sides consist of large areas of jumbled rocks several metres in size. The effects of such a jökulhlaup can be explained by considering that when a 100km^2 lake suddenly fell 10m as the remaining ice collapsed at the next lower pass-point, some 1km^3 of water, weighing 1000 million tonnes, flowed out before the eastern lake stabilised again. This water flowed into the western IDL with catastrophic effect, depositing rocks torn from the pass-point at the head of the valley, which could potentially fill the IDL and block any underlying cave entrances.

Simultaneously, the IDL overflowed westwards on to the surface of the continuing icesheet, with flow concentrated along the edges of exposed ridges at each side of the valley. Thus, blocks of rock were also wrenched from the upper valley sides and carried along the ice at high speed with low friction, until they were deposited at ridge crests where the water velocity reduced. Some of these rocks could tumble farther down the hillside when the ice later melted. This process could therefore account for the dry canyons and the large blockfields high on valley sides west of Durmålstind (Photos D3.2 and D3.3) and below **Toerfjellhola** (Photos D3.4 and D3.5). If this is the case, their location constrains the maximum width of the western IDL at the time of the jökulhlaup. However, the constraint is not tight enough to determine whether **Cave of the Cold Wind** or **Toerfjellhola** lay directly below the surface of the IDL or just below its SGR. The observed blockfields could be *autochthonous*, created by local permafrost or seismic activity, or *allochthonous* and deposited by glacier movement or by a jökulhlaup as described. A more detailed and lithological study is needed to confirm the jökulhlaup process in the examples given. An alternative explanation for large autochthonous blockfields could be the 'blowing up' of bedrock by deglacial earthquakes, as described by Mörner *et al.* (2000; section 6.3.1).

Photo D3.2 Durmålstind dry canyon (Z3)
View towards the ridge to the east

Photo D3.3 Durmålstind canyon blockfield
Blockfield at down-valley shoulder

Photo D3.4 Dry canyon beside Toerfjellhola plateau
Overengbakk canyon. Toerfjellhola is situated beneath the limestone bench. Tosenfjord in the distance.

Photo D3.5 Toerfjellhola resurgence
Blockfield above the resurgence at lower end of the Overengbakk canyon

If the formula given by Rudoy (2002; Appendix D4.5) also applies in the study area, then the above eastern IDL example would have $Q_{max}=7.5x10^3m^3s^{-1}$, and the continuing flow persisted for at least 36 hours. It is doubtful that some of this water passed at high velocity through either **Cave of the Cold Wind** or **Toerfjellhola** to cause significant enlargement by mechanical abrasion, because their SGR was unlikely to have a large lower outlet at this stage. Dawson *et al.* (2002) suggested that tectonic deformation accompanied the jökulhlaup drainage of IDLs in Scotland, and this also probably occurred in the study area, together with the formation of inception fractures.

The caves on Elgfjell experienced high flow regimes beneath the collapsing eastern IDL, especially those near the lake surface. However, those submerged caves along the Jordbruelv (**Jegerhullet** to **Bjørkåsgrotta**), which currently have flows eastwards towards Svenningdal, are likely to have experienced relatively slow movements of water (to the west) during the time that the large ice-dammed lake overflowed backwards, because of their depth below the lake surface. Another important factor during this period is that there were four switches of the direction of flow of the water that passed through the caves of Elgfjell, as two pass-points lie to the north. Whereas southward flow is most common, flow to the north was observed by north-pointing scallops in **Elgfjellhola, Paradox Cave and Pustehola** (Z4) during the 2000 field trip.

D3.4 Deglaciation at Tosbotn at 10200^{14}Ca BP: Figure D3.4

The deglaciation of the adjacent Velfjord area was briefly discussed in Appendices D2.3 and D2.4. The next fall of 100m in the ice-melting height took c. 200a to reach the 700m altitude. The eastward-retreating ice margin entered the area in Figure D3.4, so that the fjords of Visten, Storbørja and Langfjord terminated at tidewater glaciers. Small ice margin IDLs had temporary existences on eastern slopes, but on coastal western slopes (sections 8.1.5 and 8.4.3) the ice at the margin melted directly as *slope flow* (Appendix D4.2). The caves in Tettingsdal (Z3; GS=L, H and E) became submerged beneath an IDL east of Rakfjell, before being drained when the ice margin went past.

The large eastern ice-dammed lake narrowed in its upper valleys, and melted farther east into the 'jaws' on each side of the Gåsvaselv. However, other IDLs in the immediate vicinity grew larger, and coalesced to form an interconnected system of glacial lakes extending for c. 70km from south to north along the east side of the mountains, with a mean width of c. 3km, giving a total surface area of some 200km^2. Freshwater, meteoric, lakes at present positions were left behind in the mountains above 700m altitude. **Gåsvasstindhola** (Z4) and all the caves on the ridge west of Jordhulefjell were drained by now, but all the caves on and below Elgfjell remained submerged under the backward-flowing regime. The **Cave of the Cold Wind** and **Toerfjellhola** (Z3) were still submerged below the large westward-flowing ice-dammed lake that now surrounded the north end of the Tosenfjord glacier, and received a proportion of their flows from water that had already passed through caves on Elgfjell!

The pass-points available to drain the long south-to-north backward-flowing IDL during this period are at heights of 740 and 730m south of Elgfjell and at 700, 720, 782, 730, 750 and 710m north of Elgfjell. However, because of the orientations of the ridges around Elgfjell, the flow through the caves there remained consistently to the south during this period. Similarly, when, on four occasions, the outlets were many kilometres to the north of Elgfjell, the flows through the caves of the lower Jordbruelv became increasingly aligned down-valley. The only pass in this group observed by this author is the lowest, at 700m. It lies at the head of the Jordbruvatn lakes, below Grundvasstinden, and has a narrow gorge at the top, with a broad scree slope along the base of the side valley leading down into Godvassdal, providing evidence of a jökulhlaup that could have discharged some 2000 million tonnes of water, if the level change in this instance was 10m. In contrast to the valleys below Durmålstind and Tverrfjell, there is no blockfield on the east side of Godvassdal, because the Tosbotn IDL was now wide enough to absorb the energy of the jökulhlaup and reduce the speed of the overflow. This was the last jökulhlaup and the last pass to be used as a western outlet from the large ice-dammed lake trapped within the ring of mountains at the head of the Jordbruelv and the Gåsvaselv, as all the western pass heights were now above the level of the water surface.

Over a period of c. 800^{14}Ca, from 11000 to 10200, the level of the eastern ice-dammed lake fell abruptly on some 25 occasions, of which 15 created significant jökulhlaups that are recognisable from surface gorges. The possible terrace levels of some of these IDLs are indicated by horizontal lines of snow, seen when looking west across the Jordbruvatna lakes (Photo D3.1). The total level change was c. 300m, so that the total volume of rapidly-discharged water was of the order of 35km^3. Because 15 of the 25 passes discharged water towards the Tosenfjord glacier, the volume of the western IDL at the head of Tosenfjord is crudely estimated as at least 21km^3. With an ice-melting height of 700m at 10200, the lake occupied an area of c. 30km^2, which is in agreement with the area available within the local topography (Figure D3.4).

D3.5 Deglaciation at Tosbotn at 10000^{14}Ca BP: Figure D3.5

With the lowering of the ice-melting height to c. 600m at 10000, the size and level of the previously large ice-dammed lake east of Elgfjell gradually decreased as the water retreated down the sides of the valleys, with eastward flows towards the ice and northward flows along ice contact spillways. Summer flows became part of the hydrology of the large glacier occupying Svenningdal, via englacial conduits in the upper 200m above the plastic behaviour limit (section 8.1.8). All the caves along the Jordbruelv remained submerged, as did the many caves on Elgfjell that have altitudes just below 600m, including **Elgfjellhola** (Z4). Underground flow was commonly aligned with present stream flow directions. On the other side of the mountain, **Cave of the Cold Wind** was slowly drained by this time, but **Toerfjellhola** (Z3) remained submerged below the western ice-dammed lake at the head of the Tosenfjord glacier that was about to melt, as the sea and ice margin advanced towards its *side* via two low passes at Tosen at altitudes of 100 and 116m.

To the north, **Sirijordgrotta** (Z4) became increasingly inundated by an eastward-flowing IDL on the western side of the Eiterådal glacier. Later deglacial flows were to the north, opposing the direction of the present stream in **Sirijordgrotta**, according with reports of reversed flow from scallop directions and the dip of sediments (Valen *et al.*, 1997). **Geitklauvgrotta** and **Møllebekkgrottene** (Z5) remained flooded by almost static water in subglacial reservoirs. To the east, **Kvannlihola** and the many caves in Fiplingdal (Z7; GS=L; altitudes 700–400m) were submerged by subglacial reservoirs below a long and narrow nunatak IDL that started to form.

D3.6 Deglaciation at Tosbotn at 9800^{14}Ca BP: Figure D3.6

At the YD 170m isobase at Tosenfjord, the advancing sea flooded the two passes at Tosen to an altitude of c. 160m to reach the side of the Tosenfjord glacier, which had a surface at c. 480m and a base at -100m to -400m. The ice slowly melted over about the next 100a, creating a dead-ice lake in the middle of the glacier that expanded to north and south. Because the glacier remained frozen for 20km to the south (Figure D2.4), where its base deepened to -550m, the melting-front reached the 10km-distant northern end first. This end of the glacier was already supporting the large ice-dammed lake, so that when it finally collapsed at 9890±230 (from the moraine dates given by Andersen *et al.*, 1982), the pent-up water in the IDL surged forward as a superflood. All the caves lying above the deglaciation marine limit, including **Toerfjellhola** (Z3), were thus suddenly drained. The superflood water flowed west via the two low passes to Ursfjord. Some passed via **Neptune's Cave** (Z2) and other nearby caves and temporarily replaced their internal sea water with glacial meltwater, some of which had come from **Toerfjellhola**. Although it is possible that the demise of the Tosenfjord glacier was instead provoked by the jökulhlaup caused by the collapse of the 700m ice dam (Appendix D3.4), the Grønlie formula gives a date that is too early by c. 300a. On the other hand, the relentless approach of the warming sea water made the catastrophic collapse of the glacier inevitable.

All the western fjord glaciers had now melted and the sea inundated the coastal valleys to depths of ≤150m. During this interval, the ice margin rapidly crossed the deglaciated mountain range to the western side of what, by now, were valley glaciers in Svenningdal, lower Vefsndal and Eiterådal. The large but shrinking dead-ice lakes became ice margin IDLs, trapped between these valley glaciers and the ridge spurs, with a melting height down to c. 500m by 9800. Most of the caves on Elgfjell were now drained, after which they experienced a very large deglacial earthquake (section 8.1.10). The caves along the Jordbruelv remained submerged, but their flow rates (in present down-valley directions) increased as the ice continued to melt, and as the surfaces of the remnant ice-dammed lakes lowered towards the caves' entrances. Spring meltwater flowed north to the sea via ice contact spillways along the glacier edges. Similarly, the caves along the western sides of the Eiterådal, lower Vefsndal and Fiplingdal glaciers remained submerged.

D3.7 Deglaciation at Tosbotn after 9800^{14}Ca BP: Figures D3.7–D3.9

The pattern of commonly-shrinking IDLs behind receding valley glaciers continued until deglaciation was complete in the whole Tosenfjord–Fiplingdal area. The upper height of the inland valley glacier system reduced to c. 400m at 9700, to c. 300m at 9500 and to c. 200m at 9300. The outlet valleys of Svenningdal and upper Vefsndal remained occupied with long glaciers that merged at Trofors and continued, initially, to Vefsnfjord. All the caves along the Jordbruelv (Z4) below **Jegerhullet** (altitude 381m) remained flooded at 9700, with overflowing waters that probably created, or deepened, the dry valley beyond **Etasjegrotta**, the gorge below the Jordbruelv waterfall, and the Jordbru dry valley that bypasses the **Cliff Caves / Invasjonsgrotta / Vatnhullet** system (Figure B1.9). These caves were then progressively drained, the last one being **Bjørkåsgrotta** (altitude 284m) at about 9450. The large deglacial earthquake that created the 1m horizontal movement at **Cliff Cave** (section 6.3.3; Table D1.1: item 29; Photo D1.23) occurred a few years before the IDL lowered below its level at 9300 (section 8.1.10 and Appendix D5.5).

Several IDLs followed the retreating Eiterådal glacier northwards, flooding the southern end of the valley, and probably submerging the whole valley at the side of the Vefsndal glacier before 9500. Thus, **Sirijordgrotta** (Z4), with an altitude range from 275–197m, remained totally submerged by a strong northward flow until then, as did **Geitklauvgrotta** and the three **Møllebekkgrottene** (Z5, near Laksfors) beneath a narrow, northward-flowing IDL along the western side of the glacier in lower Vefsndal. **Kvannlihola** (Z7) continued to be submerged beneath a northward-flowing IDL (i.e. flowing in the opposite direction to the present cave stream) that occupied the whole width of Fiplingdal at 9700, but then soon drained as the Fiplingdal glacier retreated north towards upper Vefsndal.

At about 9500, the ice margin rapidly moved eastwards again, across the next range of deglaciated mountains. **Sirijordgrotta** and other local caves were suddenly drained at 9300, when the sea melted the end of the Vefsnfjord tidewater glacier adjacent to the junction with lower Eiterådal, but were at too high an altitude to be invaded by the sea. The sea continued to melt the glacier southwards, up lower Vefsndal, and encroached inland via Laksfors. The only glaciers then remaining were those in Svenningdal, and in upper and middle Vefsndal. Small dead-ice lakes may have remained up-valley of these glaciers, before becoming drained, probably catastrophically.

The low-lying caves at Møllebekk were all invaded by the sea soon after 9300. **Geitklauvgrotta** and its resurgence cave, **Lilleelvgrotta**, remained flooded by a northward-flowing ice-dammed lake until about the same time, when they were drained, but remained just above sea level. The final dead-ice lakes disappeared at 9080 (Grønlie, 1975), when the sea reached its deglaciation marine limits in Svenningdal and Vefsndal, by which time all caves above the contemporary sea level reverted to flow conditions similar to those at present.

APPENDIX D4 BREAKTHROUGH AND PASSAGE ENLARGEMENT UNDER EACH FLOW REGIME

Section 8.4 discussed the 13 liquid flow regimes applicable at each stage of the glacial cycle and sections 8.5.1–8.5.5 derived the likely constraints on the achievement of breakthrough and of phreatic passage enlargement at the maximum rate. This Appendix considers the opportunities for these first two cave development phases to occur under each flow regime, primarily using as examples the caves of Toerfjell (Z3) and of the Jordhulefjell / Elgfjell / Jordbruelv valley system (Z4), whose deglacial sequences were discussed in Appendix D3 and Figures D3.1–D3.9.

D4.1 Subglacial lake

Subglacial lakes occur under warm-based icesheets (section 8.4.2). They are exemplified by Lake Vostok, Antarctica, where Siegert *et al.*, (2001; Appendix A3.3) estimated that water circulation has a speed of 0.03cms^{-1}, driven by convection and by melting and freezing mechanisms.

Breakthrough

From Figure 8.8, a velocity of 0.03cms^{-1} (logV=-1.5) would only permit a 10m-long planar fracture with an aperture of 30cm and zero dissolved calcite at its entrance (which is probably impossible, as discussed below) to exhibit post-breakthrough behaviour and enlarge at the maximum rate, at logHR ~ -9 (m^{-1}). Extrapolation beyond the range of Figure 8.10 shows that with an initial aperture of 1cm, such a fracture would require ~10^6 years for breakthrough. Thus, any karstic inception fractures that were completely submerged below an SGL experienced little hydraulic flow and, except in trivial and exceptional cases, breakthroughs could not occur within glacial timescales. The possibility that meltwater could pass from the lake by *subglacial recharge* via the fracture system into a small lp-SGR is precluded because such fractures were well-below the plastic behaviour limit of the icesheet (section 8.1.8).

Enlargement

With no dissolved calcite in the inflow, post-breakthrough cylindrical tubes with lengths and initial apertures of 1m and 1cm, 10m and 10cm, 100m and 1m or 1km and 10m could enlarge at maximum rates at a flow velocity of 0.03cms^{-1} (Figure 8.8). From the various observations reported in section 3.2.3, the water in SGLs was relatively pure, with a low concentration of CO_2. The maximum dissolution rate would be c. 0.3mma^{-1} (section 8.5.3 and Figure 8.9), so that if these conditions lasted for 10ka, the diameters of such tubes could theoretically enlarge by 6m.

However, the estimated 0.03cms^{-1} water circulation speed represents a *maximum* flow velocity within any underlying conduit, because this would present a greater resistance to flow, and might not be aligned parallel to the external flow direction. Another impediment to karst conduit dissolution in this situation is that the meltwater at the base of the SGL would also be in contact with the limestone bedrock that contained the karst conduit, and would therefore enter any such conduit already relatively saturated with dissolved calcite. The discharging water would also add to the calcite concentration in this almost closed system, perhaps eventually creating an SGL that was completely saturated at 10mgL^{-1}, at the prevailing low temperature and low P_{CO2}. Indeed, Priscu *et al.* (1999) predicted that the concentration of Ca^{2+} in Lake Vostok is as high as 2.3mgL^{-1} (giving c. 6mgL^{-1} for $CaCO_3$), although there are no reports that the underlying bedrock contains carbonate. Siegert *et al.* (2001) also reported Ca^{2+} concentrations in the range 0.1–0.3meqL^{-1} (i.e. 2–6ppm=2–6mgL^{-1} Ca^{2+}, equivalent to 5–15mgL^{-1} $CaCO_3$) for subglacial environments, including Lake Vostok.

From the above data, it must be expected that karst conduits below SGLs had input waters with saturation ratios approaching 100%, i.e. much greater than the 60% limit for maximum dissolution rate in these conditions (section 8.5.2), so that dissolution reverted to slow, higher-order, kinetics with little passage enlargement. Slow-moving laminar flow in an SGL also allowed fine-grained sedimentation on all surfaces of any submerged caves, which would inhibit subsequent dissolution and which might also include calcitic clays that could precipitate from the poorly aggressive solution. Such clay occurs in the roof of **Luktindgrotta** (Z6), for example, and Lawson (1995, p26) suggested that fine-grained deposits in caves at Assynt in Scotland consist of glacial "rock flour" washed into the caves via fissures and deposited in still-water conditions.

Another, more uncertain, argument can be made against the likelihood of slow dissolution of karst conduits beneath SGLs. The most prevalent country rock in the study area is mica schist. It seems very likely that the tectonic events that are postulated to create inception fractures in marbles of the study area (Chapter 6) also created them within the mica schists (and other crystalline rocks). A component mineral of schists and these other rocks is quartz, and silica is more soluble than calcite in *pure* water (that contains no CO_2). Thus, the potential dissolution of schist below subglacial lakes is also worthy of consideration. No references are known that quantify the *kinetics* of the dissolution of silica to the extent that has been achieved for calcite, but long and large phreatically-formed caves in quartzites are well-known in other parts of the world (e.g. Wray, 1997). These are thought to have developed over very long timescales in stable conditions at low dissolution rates. If karst caves in the study area also developed when submerged over rather long timescales, then it could be assumed that caves and conduits would also develop from tectonic fractures synchronously in the local schists, with phreatic passages in mica schist that both connect to, and are completely separate from, the limestone caves. However, there is a complete absence of such conduits in the schists. Except along the contact between limestone and other country rocks, no passages divert away from the limestone, and no separate but phreatically-formed caves are known in other rocks. This absence of conduits in schists provides supporting evidence that the karst caves did not enlarge beneath SGLs.

A second uncertain idea to consider is that, if the caves enlarged from tectonic fractures at very high pressures below SGLs, there should be many more 'autogenic' openings into the cave passages, rather than the single relatively large entrances that are more commonly found at the extremities of the systems. These entrances suggest that Nye channels operated in sympathy with valley topography, providing focused flow into 'upstream' entrances at flow rates much higher than available under convective circulation, in a different glacial regime.

It is therefore concluded from the above reasoning that karst cave passages in the study area (and in all the Caledonides) did not enlarge significantly under subglacial lakes. Indeed, the following sections, as summarised in section 8.6.2, explain phreatic passage enlargement without the need for any dissolution below SGLs. Breakthrough and enlargement whilst submerged by films of water at the base of warm-based ice streams are even less likely, because a typical ice velocity of $225ma^{-1}$ (Appendix A3.5) equates to a potential water velocity of only $7x10^{-5}cms^{-1}$, which is three orders of magnitude slower than predicted for water flow in an SGL.

D4.2 Slope flow

The possibility of slope flow inundating fractures and caves in the Western catchment area at coastal western slopes was discussed in section 8.4.3. This would be a high-energy but short-lived flow regime. An extreme example of a 5km-long west-draining valley could have sustained powerful surface flows for c. 70a as the ice margin retreated eastwards at $70ma^{-1}$. However, the effects of earthquakes were muffled at the low altitudes near the coast where IDLs do not form (section 8.1.10), so that fracture systems were smaller and less frequent there. The almost complete absence of caves in these situations confirms that the slope flow remained on the surface, and was unable to enlarge any pre-or post-breakthrough fractures into explorable cave systems within the limited time available.

D4.3 Nunatak flow

Nunatak IDLs were almost static (section 8.4.4). The physical conditions applying at a near-static IDL have some similarities to those of a subglacial lake (Appendix D4.1), although, in contrast, nunatak IDLs were situated at the *highest* points of the landscape and had a maximum duration of only c. $200^{14}Ca$ (= c. 280 cal. a: section 8.5.3). Internal circulation was likely to be stratified, especially when ice formed at the surface in winter. Summer flows were driven by convection (mainly powered by solar heating of the upper layers), by winds blowing across the lake surface, by small fluvial inputs, and by melting and freezing mechanisms. It is possible to envisage mean circulatory water speeds that ranged from the $0.03cms^{-1}$ estimated for SGLs in winter to, perhaps, $10cms^{-1}$ in summer, with a possible annual mean of $5cms^{-1}$. In the majority of cases, any underlying karst fractures and conduits were parallel to the ridge and the IDL (section 8.4.8), and could, therefore, have aligned with any circulating flows. The water in an IDL equilibrated up to the prevailing atmospheric P_{CO2} within a few hours of melting. Atmospheric P_{CO2} remained at 0.020% during most of the Weichselian, and only reached 0.026% at the Younger Dryas, the period of importance here (Petit *et al.*, 1999, p431). The calcite concentration in the water of a nunatak IDL was also kept very low by dilution, as more low-carbonate-content glacier ice melted as the lake deepened, but water at 0°C that equilibrated

up to the YD atmospheric CO_2 concentration still became saturated at only c. 11mgL^{-1} of $CaCO_3$ (Palmer, 1991, Fig.7). Any sedimentation into fractures was extremely fine, and of low intensity, as, with small catchment areas, there was little eroded material to deposit.

Breakthrough

A mean velocity of 5cms^{-1} would permit planar fractures with lengths ≤50m and an aperture of 1cm to exhibit post-breakthrough behaviour and enlarge at the maximum rate, at a hydraulic ratio of 10^{-5}m^{-1} (Figure 8.8). Any 50m-long fracture with an aperture of 0.1cm and HR of 10^{-5}m would require 3300a to reach breakthrough (Figure 8.10), which was not available, even considering an order of magnitude reduction caused by the low temperature compared with the standard (Palmer, 1991) conditions. Thus, probably few karstic inception fractures that were submerged below a nunatak IDL were significantly advanced towards breakthrough before the IDL descended below their level. The possibility that meltwater could be sucked via the fracture system into an lp-SGR is not considered because the PBL was initially near the surface of the icesheet (section 8.4.4).

Enlargement

If a mean flow velocity of 5cms^{-1} could occur in *conduits* below a nunatak IDL from circulating currents, then any tubes and fissures with combined dimensions below the logV_{min} cms^{-1}=0.7 region in Figure 8.8 could enlarge at maximum rates. Taking the wall retreat rate of 0.35mma^{-1} estimated in section 8.5.3 for a glacial lake equilibrated to atmospheric CO_2, fractures and passages within the allowed range could widen by c. 20cm under a nunatak IDL in its maximum duration of c. 280 cal. a, a small amount in the context of explorable cave passages. Hence, it is concluded that as well as not promoting dissolutional breakthrough, nunatak IDLs did not persist long enough to allow any narrow tectonic breakthrough fractures to enlarge into explorable cave passages, although they could have contributed to the enlargement of existing passages. The significant rarity of recorded caves in glacial situation U (section 5.5.5) supports the conclusion that caves do not form beneath nunatak IDLs, even over several glacial cycles. The two known cave fragments at GS=U east of the summit of Jordhulefjell (Z4) probably formed during a previous deglaciation at GS=T, before subsequent glacial erosion changed the local landscape.

D4.4 Reverse flow

Reverse flow only occurred within a backward-flowing IDL (section 8.4.8). The applicable hydraulic parameters for a fracture or cave submerged beneath such an IDL are difficult to determine from topographic information. However, deductions about cave flow rates can be made from the sizes of the scallops, and perhaps from the sizes of sediment particles. The northward-facing scallops in **Elgfjellhola**, **Paradox Cave** and **Pustehola** (Z4) are roughly 20–25cm long. These indicate high-stage flow velocities up to c. 20cms^{-1} (section 3.1.7). Sediment collected from a ledge near the scallops in **Paradox Cave** consists of brown silt containing larger individual schist particles with diameters of c. 1mm. From a modified Hjulstrøm diagram (Andersen and Borns, 1997, p129), it is seen that the schist particles of 1mm size are *transported* at velocities above 20cms^{-1}, and *deposited* below 20cms^{-1}. The silt could have been deposited at around 0.2cms^{-1}, or slower, in perhaps a subglacial flow regime. Such silts are not eroded below a velocity of 20cms^{-1}. Thus, a flow velocity of 20cms^{-1} through these caves seems reasonable, and is taken as representative for post-breakthrough conduits of similar lengths situated below a backward-flowing IDL.

Breakthrough

From Figure 8.8, the range of planar fractures from 2m length and 0.01cm aperture, via 240m (the length of **Elgfjellhola**) and 1.2cm, to 2km and 10cm would be beyond breakthrough at a velocity of 20cms^{-1}. Thus, initially-narrower fractures with these *final* dimensions achieved breakthrough if given sufficient time, and tectonically-produced fractures with these geometries immediately widened at maximum rates.

The Darcy-Weisbach equation for turbulent flow is used to deduce applicable hydraulic parameters (Lauritzen *et al.*, 1985): $Q^2/A^2=2dgi/f$, where Q is the discharge, A is the cross-sectional area of the conduit, d is its diameter, g is the gravitational constant, i is the hydraulic gradient, and f is a dimensionless friction factor. Rearranging yields: $i=fQ^2/2dgA^2=fV^2/2dg$, where V is the mean flow velocity. For **Elgfjellhola**, V=0.2ms^{-1} (above), the mean A=20m^2, d=5m, g=9.81ms^{-2}. Hence, $i=4x10^{-4}f$.

The friction factor depends on the roughness of the cave walls, tortuosity and other obstacles to the flow. Lauritzen *et al.* (1985) found that in the submerged tube with mean cross-section c. $20m^2$ at the **Glomvatn Underground Outlet** in northern Norway, f varied from a constant 0.116 at discharges above $14m^3s^{-1}$ ($V=0.7ms^{-1}$), up to c. 2.5 for discharges down to $2m^3s^{-1}$ ($V=0.1ms^{-1}$). The mean annual runoff is $2.5m^3s^{-1}$, giving a mean flow velocity of $12.5cms^{-1}$. The flow rate through **Elgfjellhola** under the backward-flowing $IDL=VA=0.2x20m^3s^{-1}=4m^3s^{-1}$. By making the assumption that the hydraulic characteristics of **Elgfjellhola** and the tube studied by Lauritzen *et al.* (1985, Fig. 9) are similar, because they have similar cross-sections and are both mainly simple single conduits, the relevant friction factor for **Elgfjellhola** is taken to be c. 1.0, from their graph. Thus, the hydraulic gradient applicable to **Elgfjellhola** under a backward-flowing $IDL=4x10^{-4}xf=4x10^{-4}$. This value can be checked against Figure 8.8, because if the 240m-long **Elgfjellhola** achieved breakthrough at an aperture of 1.2cm, then it did so at a hydraulic ratio of $10^{-5.8}m^{-1}=1.6x10^{-6}m^{-1}$. Hence, the HG was $LxHR=240x1.6x10^{-6}=3.84x10^{-4}$, a similar result. The effective head of water at **Elgfjellhola** in this flow regime $=240x4\ x10^{-4}=$ c. 0.1m.

From the discussion in Appendix D3.3, the only opportunities for water to flow north via **Elgfjellhola** were when its IDL discharged water via cols at altitudes of 840 and 825m. The surface of the IDL was then some 240 and 225m above the cave, and some 500m above the valley bottom. As no other information has been obtained to correlate scallop sizes with depth below the surface of an IDL, the variation of effective head with depth is unknown, although artificial reservoirs are known to exhibit warmer-water surface overflow, interflow at thermoclines, and underflow of cold, dense, water along their bases. A value of 0.1m is taken to be *indicative* of the effective head that applies at all depths within a backward-flowing IDL. For fractures with lengths of 10–1000m, the applicable hydraulic ratios lie in the range 10^{-3}–$10^{-7}m^{-1}$. Although the effective head at Elgfjell has been derived from a consideration of phreatic flows during an *enlargement* phase at the end of the YD, a similar head must have applied during a previous *gestation* phase, prior to breakthrough, which might have been at a similar time or during the Saalian deglaciation or during a Weichselian interstadial.

The caves of Elgfjell were submerged beneath a backward-flowing IDL from c. 10850 (at the earliest, with flow over a col at 940m altitude) until c. 10200 (when the IDL became eastward-flowing), a maximum duration of some $650^{14}Ca$ (Appendices D3.2–D3.4) or 910 cal. a (section 8.5.3). From Figure 8.10, **Elgfjellhola** could only have reached breakthrough (at an aperture of 1.2cm) in 910 cal. a at a hydraulic ratio of $10^{-5.8}m^{-1}$ if its initial aperture was larger than c. 0.3cm. Fractures with initial apertures of 0.1cm could only achieve breakthrough in this timescale at a hydraulic ratio of $10^{-4.6}m^{-1}$. They would have to be less than 20m long under the same effective head of 0.1m.

From the above points, a major conclusion is that the inception–gestation phase of breakthrough from laminar to turbulent conditions under the effect of fourth-order dissolutional kinetics is unlikely to have completed for 20m-long karst fractures less than 0.1cm in aperture under a *uniquely* backward-flowing ice-dammed lake in the timescale available during a single deglaciation. Fractures of c. 0.3cm aperture ≤240m long could reach breakthrough in the time available, but this would leave little time for subsequent enlargement during the contemporary series of IDLs. It follows that the many caves that exist in this situation, including all the caves on Elgfjell, result from the subsequent enlargement of fractures that achieved *tectonic breakthrough* during seismic activity at the start of the deglaciation (even though apertures that are significant fractions of a centimetre are required to bypass the inception–gestation phase in conduits measuring over 20m in length), or else they reached chemical or tectonic breakthrough during a previous deglaciation. Because the Elgfjell IDL soon became a *wide* backward-flowing IDL (Figures D3.2–D3.5), there was little opportunity for its karst fractures to achieve breakthrough as part of low pressure SGR flow (section 8.4.5 and Appendix D4.8).

Enlargement

Inverting the estimation of the **Elgfjellhola** breakthrough aperture width, Figure 8.8 shows that all cylindrical tubes with a radius ≥0.4cm and a flow velocity $\geq 20cms^{-1}$ enlarge at maximum rates for all path lengths up to 250m. This therefore applied to many caves in the study area that were submerged beneath a backward-flowing IDL, including all those on Elgfjell, and continued to apply in a succeeding, faster, englacial flow regime. The actual dissolution rate in these conditions could be higher than the $0.35mma^{-1}$ estimated in section 8.5.3, because of enhanced mechanical erosion, and wall retreat rates up to $1.0mma^{-1}$ are considered. Thus, if the IDL at Elgfjell remained

backward- or eastward-flowing for 1190 cal. a (i.e. until 10000, when the caves drained), conduit and passage radii could have enlarged by 0.4–1.2m, giving *minimum* passage diameters of 0.8–2.4m. These are at the lower end of the range of explored phreatic passages on Elgfjell. As well as the dissolution of passage walls, pre-existing speleothems could also be corroded, especially stalactites, as the water would remain more aggressive at roof levels.

D4.5 Jökulhlaup flow

Many flowing IDLs experienced catastrophic jökulhlaups, which perhaps lasted for several hours whilst ice-dammed lake levels suddenly fell at least several metres (Appendices D3.3, D3.4 and section 8.4). Glacier-dammed lakes and "glacial superfloods" were studied by Rudoy (2002) in the mountains of southern Siberia, and various papers about these processes in northern America were reviewed by Fisher *et al.* (2002). The characteristic relief forms of water-forced hollows, niches, "drillpots" (jettegryter in Norway), outburst gorges with box-like profiles, dry canyons, and dry, possibly stepped, waterfalls are formed by *evorsion*, the destruction of rock caused by the rotation of water that falls sub vertically. Erratic, but *angular*, boulders can be transported high on to the slope of the watersheds. Rudoy (2002) suggested that maximum jökulhlaup discharge, $Q_{max}=0.0075xV^{0.667}m^3s^{-1}$, where Vm^3 is the IDL volume, and gave examples of velocities up to $32.5ms^{-1}$. Walder and Costa (1996) gave mean relationships of $Q_{max}=0.0046xV^{0.66}m^3s^{-1}$ for tunnel-drainages from 26 lakes and $Q_{max}=0.11xV^{0.44}m^3s^{-1}$ for non-tunnel collapses.

Breakthrough

Because of their short duration, it seems certain that jökulhlaups could have played no significant role in the breakthrough of inception fractures, unless they initiated seismic movements.

Enlargement

Each of the many jökulhlaups that occurred dramatically raised the head within an IDL, but as they each only persisted for several hours, the extra immediate dissolutional widening was insignificant. However, the mechanical erosion of existing passages in line with jökulhlaup flow must have been considerable. Large blocks of limestone, and contained clastic impurities, were rapidly transported along cave passages and either evacuated from the cave, or deposited at blockages. Subsequently, the limestone deposits were probably dissolved away at the contemporary maximum rate in some of the continuing IDL flow regimes, whilst the cave walls also regained a more smooth appearance. Thus, indirectly, jökulhlaup flows contributed to wall retreat rates, despite their short durations.

D4.6 Ice contact spillway flow

Overflow via ice contact spillways could occur from all IDLs at later stages of deglaciation (section 8.4). The applicable flow velocities at submerged fractures and conduits are difficult to determine, but may approximate to the $20cms^{-1}$ estimated for reverse flow (Appendix D4.4). This flow regime was also intermittent, only operating when englacial flows were restricted by freezing or were overwhelmed by high melting rates or high precipitation.

Breakthrough

Because of its intermittent behaviour, the contribution of ice contact spillway flow to the breakthrough of inception fractures was less than that of reverse flow, which itself did not last long enough to cause breakthrough of fractures with apertures below about 0.1cm (Appendix D4.4).

Enlargement

Appendix D4.4 showed that a flow velocity of $20cms^{-1}$ was sufficient to enable most post-breakthrough conduits to enlarge at the maximum rate applicable to the temperature and P_{CO2}. The next few sections show that enlargement also occurred at maximum rates in most other forward-flowing IDL flow regimes. Hence, it is not necessary to estimate the separate timescales over which ice contact spillway flows operated, if the total time that a cave was submerged by a forward-flowing IDL is taken into account.

D4.7 Englacial flow

Flow in englacial conduits above the plastic behaviour limit (PBL) occurred in westward- and eastward-flowing IDLs and in ice margin IDLs (sections 8.4.5, 8.4.9 and 8.4.10) to depths <200m below the icesheet surface. Using a typical icesheet lowering rate of c. $0.5m^{14}Ca^{-1}$ (section 8.1.4: Figure 8.2b), caves and fracture systems could

therefore remain submerged in this condition for a maximum of c. 400^{14}Ca or c. 560 cal. a (section 8.5.3). Caves and fractures >200m below the surface of a wide IDL previously experienced *circulatory* flow (Appendix D4.9). The regime at **Kvithola** (northern Norway; Lauritzen, 1986; section 3.3.2) is assumed to be representative of englacial flow, where water from a cave system completely submerged by an active IDL flowed fairly directly into Röthlisberger channels on the opposite side of the lake and then into outlets at the lower glacier surface. This contrasts with the view of Lauritzen (1986), whose Fig. 5 assumed that the flow from **Kvithola** was via Nye channels into a large high pressure subglacial reservoir below the PBL. From its 8cm-long scallops, **Kvithola** had a 1m^{3}s^{-1} high-stage flow rate, at a water velocity of c. 50cms^{-1}, making it unlikely that an SGR could accept such a high flow rate without causing the IDL to overflow the icesheet surface, which would reduce the velocity of the cave stream. The larger scallop size also makes it less likely that **Kvithola** was part of a meltwater SGW (section D4.10).

The maximum head for englacial flow is c. 200m, because the outlet can only occur above the PBL. However, the effective head at **Kvithola** was c. 10m (below). As the ice surface lowered, the PBL also lowered in altitude, so that the total head of water driving englacial flow through conduit or fracture systems and the icesheet remained roughly constant at a maximum of c. 200m, but more likely at an average near 10m, if **Kvithola** is typical. Thus, each individual cave hydraulic ratio (HR) also remained roughly constant, until the conduits and fractures emerged above the IDL and the phreatic flow was cut off. However, the flow velocity and effective head of water for englacial flow was extremely variable between caves, because they each depended on local glacier hydrology, and **Kvithola** may, in practice, not be typical for either its 10m head or its 50cms^{-1} flow velocity.

Breakthrough

From Figure 8.8, planar fractures from 5m length and 0.01cm aperture to 5km length and 10cm aperture would be beyond breakthrough at a flow velocity of 50cms^{-1}. A 130m-long planar fracture (the length of the **Kvithola** conduit) would coincide with breakthrough at HR= 6x10^{-4}m^{-1} at an aperture width of c. 0.25cm. Hence, **Kvithola** can be assumed to have experienced tectonic breakthrough to this aperture size, or alternatively, a smaller inception fracture with this *breakthrough* dimension could have reached breakthrough in this flow regime, given sufficient time. The effective head at breakthrough=HRxL^2= c. 10m, and this likely continued to drive the enlargement phase.

From Figure 8.8, the 240m-long **Elgfjellhola** would have had a HR of 1.7x10^{-4}m^{-1}, a flow velocity of 60cms^{-1} and an aperture of 0.4cm at breakthrough below a head of 10m, or a HR of 0.9x10^{-4}m^{-1}, a head of 5m and an aperture of 0.5cm if the velocity was 50cms^{-1}. The caves of Elgfjell were submerged in an englacial flow regime from c. 10200 until c. 10000, a maximum duration of some 200^{14}Ca (Appendix D3.5) or c. 280 cal. a (section 8.5.3). From Figure 8.10, the 240m-long **Elgfjellhola** could have reached breakthrough (at an aperture of 0.4cm) in 280 cal. a at a hydraulic ratio of 1.7x10^{-4}m^{-1} if its initial aperture was larger than c. 0.06cm. At a hydraulic ratio of 0.9x10^{-4}m^{-1}, an initial aperture of 0.08cm would be required to achieve breakthrough in this timescale. These are relatively small tectonic openings, showing how effective the englacial flow regime, with its large effective head, was in promoting chemical inception at those fractures not created large enough for immediate tectonic breakthrough.

Enlargement

From Figure 8.8, all 1km-long cylindrical conduits with a radius of 0.6cm or more enlarged at maximum rates when the flow velocity was 50cms^{-1}. This therefore applied to most phreatic caves in the study area. Extra mechanical erosion seems even more likely to raise the wall retreat rate to ~1mma^{-1} than in the lower velocity reverse flow case that was considered in Appendix D4.4. For caves submerged in this flow regime for the maximum time of 560 cal. a, the maximum diameter enlargement was 560x2x1mm = ~1.1m.

D4.8 Low pressure subglacial reservoir flow

This special flow regime probably occurred above the PBL of all *narrow* flowing IDLs that had fractures small enough to prevent the filling of the lp-SGR (section 8.4.5 and Figure 8.7). The head was ≤200m above the 'open' outlet, but the maximum duration was constrained by the 'fracture straddling' time when the fracture straddled the ice wall between the IDL's hp-SGR and the fracture-fed lp-SGR, without a continuous bypassing Nye channel above it, nor an enlarged parallel karst conduit. The duration of an lp-SGR can be estimated from the shorter of the time it took the ice wall to advance along the length of the fracture and the time it took the base of the hp-SGR to

descend through the vertical range of the fracture. From Figures D3.2–D3.5, the western extremity of the Tverrfjell IDL advanced some 4km in some $850^{14}Ca$, i.e. ~$5m^{14}Ca^{-1}$. This gives a first estimate of lp-SGR duration for a 1000m-long fracture of c. $200^{14}Ca$. Assuming that the bases of the SGRs lowered *at least* at the typical c. $0.5m^{14}Ca^{-1}$ rate of the ice-melting height (section 8.1.4), then the second estimate also gives a maximum duration of about $200^{14}Ca$ or 280 cal. a (section 8.5.3) for a steeply-inclined system with a vertical range of 100m.

Breakthrough

In this case, the breakthrough can be calculated more directly from the hydraulic parameters. Thus, a 1000m-long planar fracture under a maximum head of 200m has a hydraulic ratio of $2x10^{-4}m^{-1}$. From Figure 8.10, an initial 0.1cm aperture would achieve breakthrough in <40 cal. a, which is within the maximum time available. However, although the hydraulic ratios were higher for fractures with shorter path-lengths, reducing the time needed for breakthrough, the time taken for the ice wall to pass the fracture was also shorter. For example, a 100m-long fracture with 0.01cm aperture and a maximum HR of $0.02m^{-1}$ would take <100 cal. a to achieve breakthrough, but the ice wall would pass in only c. 28 cal. a, preventing breakthrough. However, 10m-long fractures with 0.01cm apertures would be at breakthrough instantaneously, despite the ice wall passing in only three years.

Enlargement

After breakthrough, the fracture would enlarge in turbulent flow at the maximum wall rate of $0.3mma^{-1}$ (section 8.5.3), but only whilst the large head was sustained above an outlet into the lp-SGR that remained unfilled. Thus, although a 1000m-long fracture might still have 240 cal. a before the ice wall passed (potentially giving a widening of 2x0.3x240mm = c. 15cm), it is assumed here that the lp-SGR would soon fill up after breakthrough, to become part of the hp-SGR at the base of the IDL, when the other flow regimes apply. Hence, the contribution that flow into a previous lp-SGR could make to the enlargement of post-breakthrough conduits is regarded as insignificant.

D4.9 Circulatory flow

The deeper parts of wide IDLs and hp-SGRs may have had slow, circulatory, flow regimes below the more direct flows towards western and ice contact spillways or into englacial channels above the PBL (Appendix D4.7). Flow rates through caves probably varied considerably with depth and locality. Maximum flow rates were perhaps somewhat greater than those of the stratified flows of nunatak IDLs (Appendix D4.3). A typical flow velocity of $10cms^{-1}$ is assumed, i.e. much more than would apply from just the enlargement of the SGRs by melting. Minimum flow velocities were $<<1cms^{-1}$, from the evidence of very fine sand deposited in **Invasjonsgrotta** (Z4; Appendix D5.5). From Figures D3.3–D3.6, this condition could have persisted for some $600^{14}Ca$ or 840 cal. a (section 8.5.3) at the base of the Jordbruelv IDL that had an initial water depth of 500m, before the PBL lowered below the base of the SGR, and any caves or fractures at the lowest levels became more directly in line with *englacial* flow.

Breakthrough

From Figure 8.8, a velocity of $10cms^{-1}$ at breakthrough required planar fractures to have maximum lengths of 10, 100 or 1000m for final aperture widths of 0.1, 1.0 or 10cm at hydraulic ratios of 10^{-2}, 10^{-5}, or $10^{-8}m^{-1}$. The applicable hydraulic gradients and hydraulic ratios are intermediate between the nunatak flow and the reverse flow cases. From Figure 8.10, only fractures with initial apertures as small as 0.2cm that are <100m long could achieve breakthrough within the maximum 840 cal. a available, at a hydraulic ratio of $10^{-5}m^{-1}$. A fissure 1000m long at HR=$10^{-8}m^{-1}$ could only have reached breakthrough if its initial aperture was about 3cm wide. At a flow velocity of $<1cms^{-1}$, all the above lengths would need to be reduced a factor greater than 10.

Enlargement

Figure 8.8 shows that cylindrical conduits with radius ≥1cm enlarge at maximum rates at a flow velocity of $10cms^{-1}$, for path lengths ≤300m. Thus, many caves in the study area perhaps enlarged at maximum contemporary rates even whilst being submerged deep beneath wide IDLs. The actual dissolution rate in these conditions may be near the $0.35mma^{-1}$ estimated in section 8.5.3. Thus, if the Jordbruelv IDL retained a mean circulatory flow regime of $10cms^{-1}$ for 840 cal. a, most of the pre-existing underlying passages could have enlarged their diameters by 840x2x0.35mm = c. 0.6m during this phase, as could most post-breakthrough conduits. However, for circulatory flow velocities of $1cms^{-1}$, only conduits with a radius of 1cm that were < 30m long could enlarge at maximum rates.

D4.10 Meltwater subglacial waterway

Meltwater SGWs flowed from IDLs that eventually became drained IDLs above the deglaciation marine limit (sections 8.4.5 and 8.4.6). In both cases of gradual and catastrophic draining, phreatic flow in any underlying cave commonly lasted until the level of the IDL and any ap-SGR fell below the level of the cave, when the cave was also drained. Figure 8.7f illustrates the case where the SGW flowed beneath a short tidewater glacier. The meltwater SGW flow regime may be compared to the present spring melt, but it was more powerful and it lasted initially all summer. Thus, endokarst caves and conduits that lay beneath the remnant Nye tunnel channel and that were above the deglaciation marine limit could continue to exhibit phreatic flows, dependent on their elevation, morphology and the seasonally-varying recharge. The large flows persisted until all the ice had melted, during which time the caves were either drained, to remain as relict phreatic passages, or else they reverted to mainly vadose stream passages.

For the dissolution of limestone, this regime only differs from that of the variable interglacial summer flows (Appendix D4.13) by the high flow rate, the lower water temperature (now slightly above 0°C), and by the continuing low P_{CO2}, prior to the re-establishment of vegetation. Thus, all three cave development phases could occur in this regime, even whilst cave entrances were still situated below glaciers.

The peak flow velocities in these situations probably reached the highest of all the flow regimes (except for jökulhlaup flow). According to Boulton *et al.* (1996, p407), simulated rates of glacially-driven flow are two orders of magnitude greater than modern flow rates. This can be related to an icesheet lowering rate up to $0.7m^{14}Ca^{-1}$ (Figure 8.2b), which (ignoring ablation) is equivalent to an annual calendar year precipitation of 0.45m. This must be added to a Preboreal precipitation rate that was greater than at present (section 2.4.1) and that lost little in evapotranspiration, because it fell directly on to the melting icesheet, before the growth of vegetation.

It is not unusual to find scallop lengths as short as 4cm in relict phreatic passages at valley floor locations, as in **Bulandsdalgrotta** (Z2; Photo D4.1). These indicate a high-stage flow velocity around $100cms^{-1}$, which is assumed to be representative of a meltwater SGW. For SGWs below stagnant glaciers, the ice melted at the fastest possible rate, at least $0.7m^{14}Ca^{-1}$. Because this ice had a maximum thickness of 200m, the maximum duration of this flow regime at any one cave was likely some $300^{14}Ca$ or 420 cal. a. [It would be a useful exercise to study if small scallops are only found at lower cave locations and glacial situations where CL=F or where GS=C, D, E, G or H, i.e. where deglacial flows were most severe].

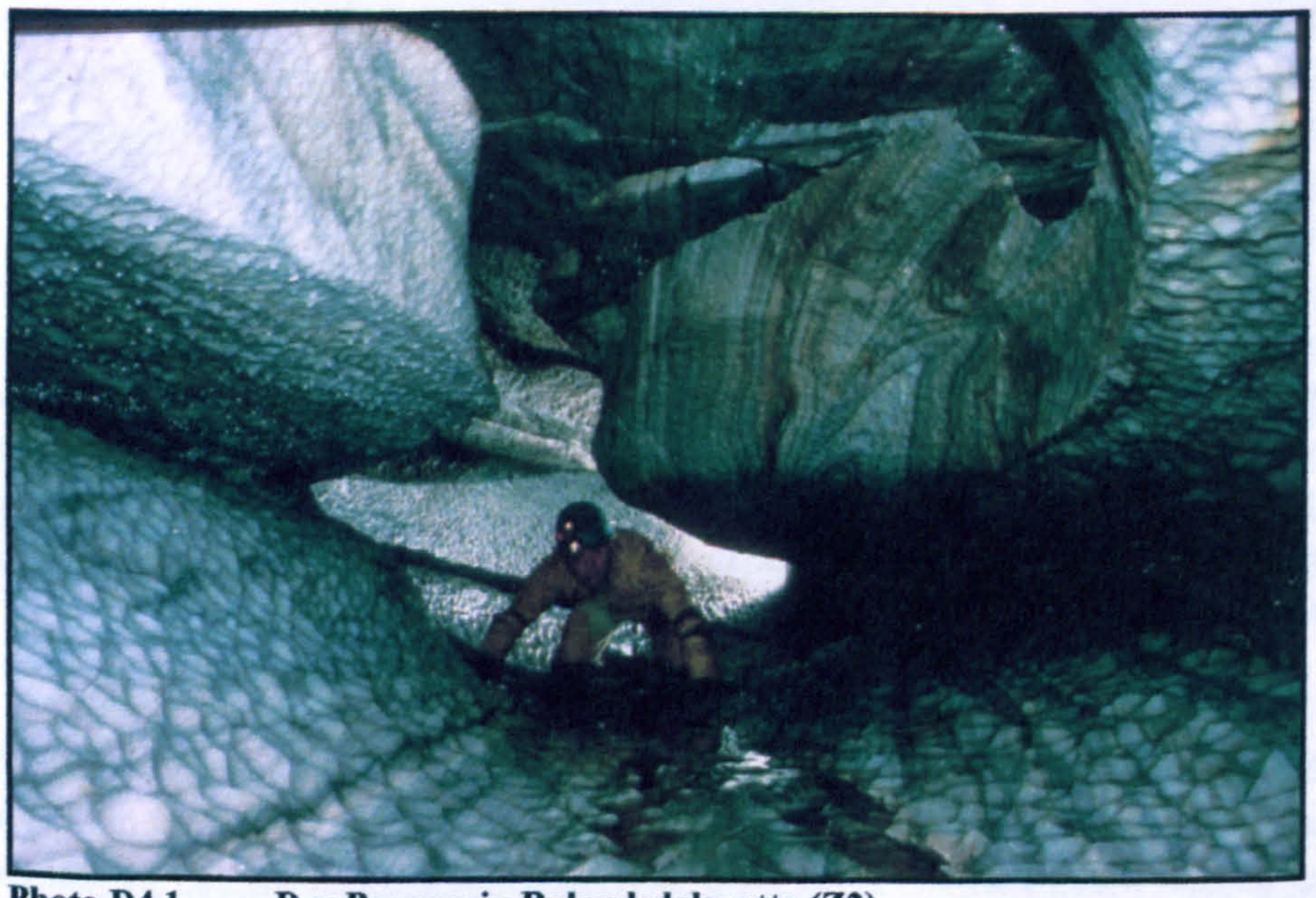

Photo D4.1 Dry Passage in Bulandsdalgrotta (Z2)
Formed in vertical stripe karst (with minor folding). Scallop size ~4cm. Photo by M. Smith.

Breakthrough

A velocity of $100cms^{-1}$ coincides with breakthrough for 10m-long planar fractures with apertures of 0.01cm at $HR=1m^{-1}$ to fractures 1000m long with apertures of 1cm at $HR=10^{-5}m^{-1}$ (Figure 8.8). The flow rates were very high,

but the hydraulic heads probably reduced to being little more than the vertical ranges of the fracture system, because the effective heads in the above two examples are 100m and 10m. From Figure 8.10, a 1000m-long fracture would achieve breakthrough within 420 cal. a at HR=$10^{-5}m^{-1}$ from an initial aperture of 0.2cm.

If the fracture was totally submerged below an ap-SGR, rather than below a hp-SGR, this could reduce the hydraulic parameters and increase breakthrough times. Alternatively, for any glaciers that melted at their lower ends above the contemporary sea level, if the lower end of the fracture was beyond the end of the SGR, this would increase the head and reduce breakthrough times. Otherwise, the hydraulic conditions in the karst could have been comparable to those which persisted during the 10000^{14}Ca of the Holocene. In this case, because the breakthrough times of fractures at low temperatures and low P_{CO2} levels are comparable to those at present ambient conditions (Appendix D4.13), the maximum 300^{14}Ca contribution of this regime to fracture breakthrough should not be significant.

Enlargement

For conduits submerged by flows at 100cms^{-1}, wall retreat rates of 1mma^{-1} can be assumed more safely, by also considering mechanical erosion. Thus, the diameter enlargement during the maximum 420 cal. a of this flow regime is 420x2x1mm=c. 0.8m. Enlargement below a meltwater SGW could explain the existence of the relict hybrid (phreatic / littoral) **Football Pitch Cave B** (Z1; section 8.4.3) and also **Neptune's Cave** (Z2; Appendix D5.3).

D4.11 Brackish subglacial waterway

Brackish SGWs commonly continued beyond meltwater SGWs and also occurred below drained IDLs, at active or stagnant short tidewater glaciers below the deglaciation marine limit (sections 8.4.5 and 8.4.6; Figure 8.7f). At this elevation, vadose flow was not possible early in the Holocene. The low hydraulic gradient is difficult to determine. The speed of flow could vary from 100cms^{-1} (near the contemporary sea level, being the maximum velocity of the inflowing meltwater SGW, Appendix D4.10) to practically zero (where tidal effects became paramount). A stagnant tidewater glacier was <200m thick above its valley floor at the onset of an SGW. Because of melting by the sea, this ice melted faster than the previous high rate of 0.7m^{14}Ca^{-1} (Figure 8.2b), i.e. in <300^{14}Ca.

Breakthrough

If the inflowing meltwater had a sufficient head to maintain a high velocity near sea level (perhaps creating an upwelling beyond the end of the tidewater glacier), breakthrough conditions at fractures at the deglaciation marine limit could approximate to those up-valley, beneath the meltwater SGW (Appendix D4.10), and the two regimes could be considered together. Fractures with entrances closer to the end of the tidewater glacier experienced dissolution in water of higher salinity, probably restricting further the achievement of chemical breakthrough (Appendix D4.12).

Enlargement

By comparison with Appendix D4.10, maximum wall retreat rates could perhaps be reached in conduits near the deglaciation marine limit. Flow velocities towards the end of the tidewater glacier may have remained as high, and can be assumed to have stayed above, say, 20cms^{-1}, even in tidal situations. Without considering salinity effects, by comparison with reverse flow (Appendix D4.4), a maximum dissolution rate (including mechanical erosion) could then have been sustained at most conduits beneath the waterway. Hence, diameter enlargement in the <420 cal. a available could have reached <420x2x1mm=<0.8m. However, from Appendix D4.12, marine salinity in the early Holocene appears to have prevented dissolution, so that conduits at low altitudes close to the end of the tidewater glacier probably did not enlarge at all.

Assuming that SGWs are always formed when the thickness of the tidewater glacier reduces to <200m, then the lower the altitude of the upper input to the fracture system, the shorter the time that inception fractures can experience breakthrough conditions as part of an *englacial* hydraulic flow path before becoming part of a subglacial waterway, or before the collapse of the tidewater glacier. This, together with the probable lack of conduit enlargement at low altitudes in marine conditions, provides an additional explanation for the comparative rarity of dissolutional karst systems both at the coastal strandflat, and below about 40m altitude (section 8.1.10).

D4.12 Marine inundation

The submarine conditions applicable at the onset of glaciation and during deglaciation and isostatic uplift were discussed in section 8.4.7. Referring to Calcite Compensation Depth (CCD; Appendix A2.1), Trudgill (1985, pp127–155) pointed out that, although oceanic surface sea water is supersaturated with respect to calcite, and commonly will not dissolve limestone, the chemistry of inter-tidal waters can vary considerably, especially if organic matter is present with restricted circulation. Both carbonate precipitation and dissolution can then occur, the latter even if the water is apparently saturated. At night, CO_2 levels rise and pH falls, due to respiration of marine organisms in the absence of photosynthesis. Additionally, grazing and boring molluscs and other organisms directly remove coastal limestone and also weaken the surface further for wave erosion (Photo D4.2). Tucker and Wright (1990, p33) stated that the supersaturation of sea water is limited to low latitudes: it is undersaturated in mid and high latitudes. Thus, dissolution of $CaCO_3$ can occur in temperate shallow seas. The likely enhanced dissolution in sea water diluted by glacial meltwater (which in winter could reach temperatures below 0°C) does not appear to be discussed in the literature. Singurindy *et al.* (2004) conducted laboratory experiments to examine calcite dissolution and precipitation in various NaCl and artificial seawater solutions, but at 23°C. However, EL Sjöberg (1978, p66) reported that the maximum rate of calcite dissolution at the CCD at 2°C is $2mgcm^{-2}a^{-1}$, equal to a wall retreat rate of $<0.01mma^{-1}$.

Photo D4.2 Mollusc borings
Roof of Football Pitch Cave D (Z1) at altitude of c. 25m. Pencil for scale.

The applicable chemistry during the formation of sea ice is complex. Papadimitriou *et al.* (2003) cited expectations of calcite precipitation during natural sea ice formation and suggested supersaturation or precipitation with CO_2 degassing, from their own experimental evidence.

Breakthrough and enlargement

Photographic evidence from **Neptune's Cave** (Z2), where barnacle shells are still attached to the walls and roof of a passage that was inundated by the sea for $550^{14}Ca$ after the barnacles died at the end of the Younger Dryas (Appendix D5.3), does not reveal any 'plinths' beneath the bases of the barnacles. Such plinths, and corrosion of the barnacle shells themselves, might be expected if there was strong dissolution in sea water, and their absence demonstrates that **Neptune's Cave** was enlarged prior to its marine inundation. Thus, it is deduced that, apart from the enlargement of entrances discussed in sections 8.8.2 and 8.8.3, submersion of study area caves below sea level during deglaciation has little effect, in the time available before uplift, on their speleogenetic enlargement. This argument may also be extended to submersion below sea level during glaciation. Although these submersion periods are probably longer than those for deglaciation, as discussed in section 8.1.3, they are not longer by orders of magnitude. Thus, in the absence of other evidence, it is concluded that marine inundation during glaciation also contributes little to karstic dissolution.

A special case is **Langfjordgrotta** (Z2), which has a resurgence entrance only 10m above fjord level that leads to a sump fed from the lake Fjelldalsvatn (altitude 43m), some 1400m to the southeast. Most of this (mainly unexplored) system was below sea level for much of the Holocene. However, the flow of fresh water from the lake after it emerged above sea level at c. 6400^{14}Ca BP (Appendix D5.3) was sufficiently strong to restrict marine incursion. Hence, the conduit probably enlarged at a high wall retreat rate to a diameter of several metres. A similar process likely accounts for **Olafs Kilden** (Z1; section 8.4.3). The chemical breakthrough of even short inception fractures during the periods of total marine inundation also seems very unlikely, especially because, after the tidewater glacier melted completely, marine inundation commonly reduced the hydraulic gradients and flow velocities to low values.

D4.13 Interglacial flow

Interglacial conditions were briefly discussed in section 8.4.11. Phreatic, closed system, dissolution rates for the Scandinavian Caledonide metalimestones under meteoric environments during the Holocene and previous interglacials are assumed to equal more closely those of the standard Palmer and Dreybrodt conditions of 10°C and 1% or 5% P_{CO2}. The approximation is closest for lower-altitude fracture, conduit and cave systems below the tree-line (which was also some 200m higher during the 1ka Boreal period: section 2.4.2). These have high vegetational P_{CO2} levels and organic acid concentrations. It may also remain fairly similar at higher altitudes above the tree-line, where a reduced mean annual temperature tends to counteract the reduction in calcite saturation concentration caused by a groundwater P_{CO2} that decreases to atmospheric levels.

Breakthrough

During interglacials, water seeps through the fracture network, driven by the local hydraulic gradient, whilst most of the flow is still along the surface. It is therefore assumed that allogenic stream sinks maintain constant heads for pre-breakthrough flows, for all considered apertures. Breakthrough times for the standard Palmer conditions of 10°C and 1% P_{CO2} are shown in Figure 8.10, from which a fracture with an initial aperture of 0.001cm required a hydraulic ratio of c. 0.1m^{-1} to reach breakthrough in the 10000^{14}Ca available during the Holocene. This could be realised by, for example, vertical fractures (HG=1) that lie close to valley walls and are <10m long. (In these calculations, the difference with the 11560 cal. a duration of the Holocene, Stuiver *et al.*, 1998, is not significant). Fractures with initial apertures of 0.01cm require hydraulic ratios of at least 10^{-3}m^{-1} to reach breakthrough within the Holocene. This could apply to fracture systems with vertical ranges of 40m that have path lengths <200m, such as a system in vertical stripe karst with orthogonal fracture sets with an allogenic sink into a 40m vertical fracture leading via a 160m horizontal fracture to an exit point. The same fractures with vertical ranges of 10m require path lengths shorter than 100m. Fractures with initial apertures as large as 0.1cm require a hydraulic ratio of only 5x10^{-6}m^{-1} to reach breakthrough in the same time. This could be achieved with fractures <1000m long with a vertical range as small as 5m. Thus, it is theoretically possible that most caves of the study area enlarged during the Weichselian deglaciation from 0.1cm-aperture fractures that achieved breakthrough during the Eemian interglacial, if these fractures were not eroded from the surface during glaciation.

Phreatic enlargement

The enlarged cave systems drained as they emerged above the levels of the lowering ice-dammed lakes, providing opportunities for rejuvenation as the water surface lowered to sea level or to the level of an inland lake. Phreatic enlargement was then only possible along the sumps of the active streamways of combination caves, and in the newly-forming mainly vadose caves. For the great majority of the relatively short active caves of the study area, which predominantly have allogenic catchments from non-carbonate rocks, both karst recharge and discharge remain highly *unsaturated* and *aggressive* despite autogenic recharge by percolation waters from overlying snow during the spring melt (Appendix A2.5). Hence, as in the glacial environments, it is assumed that dissolution occurs at maximum rates. During deglaciation, it is likely that flow was maintained at maximum rates when the air temperature was above freezing, perhaps for eight months of the year (as now). Holocene spring melts may reach similar flow rates sporadically, but are commonly only sustained for about one month per year. Indeed, some sumps dry out completely in winter, whereas others freeze partially. Hence, on an annual basis, Holocene wall retreat rates can commonly be expected to be a fraction of the 1mma^{-1} maximum rate that was calculated by Palmer (1991), and that was deduced for dissolution in various deglacial flow regimes.

From Appendix D2, most caves in the study area experienced interglacial conditions from 9000^{14}Ca BP at the latest, so that those active sumps that were not subject to changing water courses (probably the great majority) have remained in fairly constant hydrological conditions for at least 10000 calendar years. Estimates of the diameters of sump passages in the study area are difficult to check directly, because very few have been explored by divers. From cave surveys, the widths of sumps in mainly vadose caves lie almost invariably in the range 1–2m, with two thirds being c. 2m. Only **Dåaranjueniehola** (Z3) has an apparent sump width of 3m and it carries sustained high velocity flows from snow fields in summer months (although from a catchment area of only 0.5km^2). Assuming that the width of a sump shown on a cave survey commonly approximates to the width or diameter of a square or circular tube, it is concluded that the annual Holocene wall retreat rates for sumps within MV caves lie in the range 0.05–0.10mma^{-1}. This overlaps the 'one month in twelve' scenario at which dissolution occurs at the maximum 1mma^{-1} rate. Sustained flow or powerful mechanical erosion can increase the rate to 0.15mma^{-1}. Any sumps with widths less than 1m had probably not achieved breakthrough before the start of the Holocene.

Most of the sump widths in combination caves lie in the range 2–6m, with frequencies of the sump widths noted on cave surveys being: <2m (13); 2m (20); 3m (11); 4m (6); 5m (8); 6m (3). Outside this range, the main sump in **Landbrua** (KL) is 12m wide and the survey of **Stor Grubblandsgrotta** (KU) shows the width of the "sump lake" to be 24m (Appendix B1.13). However, these sumps may have roof heights of only 4m and 2m, giving equivalent diameters of roughly 7m. (Because phreatic passages tend to maintain their cross-sectional areas as their shapes change, it is reasonable to take the diameter of an equivalent cylindrical tube when considering dissolution rates).

Many of the 33 recorded sumps in combination caves with widths of 2m and less (some being less than 1m) may have enlarged to this size within the Holocene, so that they probably display the same characteristics as those of the MV caves. Subtracting 2m from the widths of the other combination cave sumps leaves a range of 1–5m for the enlargement of *pre-existing* lowest level phreatic passages from extra 'erosional' Holocene effects, from deglacial enlargement under IDLs, and possibly from enlargement that predated the Weichselian deglaciation. Section 8.6.2 shows that deglacial enlargement was likely to account for width increases in the range 1–2m. Hence, sumps up to a total width of 4m can be explained by the additions of deglacial and 'chemical' Holocene enlargements alone. Sumps with a width of 5m can gain the extra metre by a more sustained flow and high velocity Holocene erosion, from near-average catchment areas (as applies to all eight examples above). The sumps with widths (or equivalent widths) of 6m and 7m are all in caves in valley floor locations that are supplied by flows from catchment areas that are at least twice the mean study area size. For example, **Landbrua** (KL) and **Stor Grubblandsgrotta** (KU) have catchments of 42 and 19km^2. Thus, these caves have probably sustained high velocity erosional flows from spring melts for much more than just one month of the year. For pre-existing passages of 2m initial diameter to enlarge to 7m within the Holocene, a wall retreat rate of 0.25mm a^{-1} is required. As this is still well-within the theoretical maximum, it is not necessary, and probably not prudent, to consider any enlargement prior to the Weichselian deglaciation. Hence, it is estimated that the annual Holocene wall retreat rate for sumps within combination caves is also 0.05–0.10mma^{-1} for the general case, which can be increased to 0.15mma^{-1} by more powerful and more sustained mechanical erosion for caves with near-average catchment areas. Sustained, very high-power, spring melt from large catchment areas into valley floor caves can increase the rate to 0.20mma^{-1}, and exceptionally, to 0.25mma^{-1}. Because the highest magnitude seismic shocks that created inception fractures occurred at the time of maximum uplift (near the YD to Holocene transition) and followed the ice margin recession (section 8.1.10), it seems very likely that tectonic breakthrough and the start of new phreatic enlargement in mainly vadose caves and in combination caves occurred together at the same deglaciation event in each locality.

APPENDIX D5 APPLICATION OF THE TDMO MODEL

The models derived in Chapters 6–9 are used in this Appendix to outline the development histories of five cave systems that lie west and east of the ridge that separates the Western and Vefsn catchment areas. Reference should be made especially to the deglaciation sequences presented in Appendix D3 (Figures D3.1–D3.9), the flow regimes discussed in section 8.4, the breakthrough and enlargement possibilities discussed in sections 8.6–8.9, and the timings of cave development considered in Chapter 9. Each system and its local landscape are commonly discussed by working backwards in time. Thus, active vadose elements are considered first, followed by any possible relict vadose elements, and phreatic passages are treated upwards in turn, from active to relict. The deglacial IDL that first enlarged the highest relict phreatic passage then constrains the time when deglacial seismicity produced the tectonic fractures that led to the oldest existing passages. In this Appendix, dates refer to ^{14}Ca BP, unless stated otherwise.

D5.1 Cave of the Cold Wind (Z3; GS=K; Appendix B1.3: Figure B1.4)

Cave of the Cold Wind consists primarily of a single phreatic passage from the entrance (high on the side of the Overengbakk valley above **Toerfjellhola**) to a pair of avens up to 10m in height. The active vadose parts of the cave are small, immature, flow routes for misfit streams that only make brief appearances before resurging below the entrance. The water enters the cave at one of the tall avens that have acquired widths of c. 10m. However, in addition to these active vadose elements and fractures below the entrance that almost certainly derive from the Holocene, there are two small relict vadose inlet passages that join and lead to the end of the main passage from Ice Hall. These may derive from the Eemian interglacial, although, because of their proximity to two streams that cross the phreatic passage, they could be abandoned Holocene passages.

A pre-Eemian origin for the cave is also hinted at by the possibility of two enlarged entrance chambers in sequence. Thus, both the present entrance chamber and the inner Ice Hall (which is also close to the side of the valley) possess widened parallel walls of the type that signify enlargement when coincident with the surface of an ice-dammed lake (section 8.9.4). Ice Hall could therefore have enlarged near an entrance during the Saalian deglaciation, before the connection was made to the present entrance during the Weichselian deglaciation. However, it seems more likely that both chambers enlarged as the same (Weichselian) Tverrfjell IDL lowered past them, after the phreatic passage in the cave formed beneath the same IDL. The cave was submerged by this westward-flowing IDL to a maximum depth of 210m from 10700–10200 when the cave drained, an interval of 500^{14}Ca or 900 cal. a (Stuiver *et al.*, 1998, Figs. A7 and A8). Because the cave was probably in line with englacial conduits above the PBL for nearly all this time, dissolution was at a presumed rate of 1mma^{-1} (Appendix D4.7), so that the passage diameter widened by c. 1.8m. Although sections and cross-sections have not been published for this cave, the plan passage widths are commonly less than 2m, suggesting that total enlargement during the Weichselian deglaciation was likely.

If an englacial flow of 50cms^{-1} passed through the 160m-path length of the earlier cave fracture system, apertures of 0.3cm would have been at breakthrough immediately (Figure 8.8). From these arguments, it is likely that **Cave of the Cold Wind** originated from tectonic fractures that were produced early in the Weichselian deglaciation, with phreatic enlargement beneath the large Tverrfjell ice-dammed lake. However, some prior conditioning during the Saalian deglaciation is also a possibility.

D5.2 Toerfjellhola (Z3; GS=K; Appendix B1.3: Figure B1.3)

The powerful summer main stream in **Toerfjellhola** (Photo B1.2) appears to be an *overfit*, because the vadose entrenchments and waterfall recessions along the length of its streamway have dimensions that can be accounted for by normal Holocene erosion (sections 8.7.2 and 8.7.3). A Holocene headward capture process into an originally-phreatic conduit at White Water Passage progressively abandoned entrances and shafts situated SW of the present sink entrance. The keyhole cross-sections of the small active tributary that enters beyond here also show significant Holocene vadose entrenchments below phreatic roof sections, which continue down the main stream passage to the sump. None of the cross-sections in Figure B1.3 have a 'double vadose' profile, suggesting that the present streamway did not function as an active vadose passage in any interglacial prior to the Holocene.

Most of the cave comprises a complex series of relict phreatic passages. Among these, Second Roof Series (Figure B1.3: cross-sections 7, 8, and 9) and East–West Passage (cross-sections 17 and 18) have small, 1m-scale, relict vadose entrenchments at altitudes from 450–425m that indicate short-lived vadose flows. Because of their elevations, these are unlikely to be caused by present Holocene floods, although they could have acted as early Holocene flood overflow routes before the main streamway was enlarged to its present size. It is also just possible that they were carved as the Tverrfjell IDL lowered past them during the superflood that collapsed the Tosenfjord glacier at 9890±230 (Appendix D3.6), because the IDL was at an altitude of 450m at this 170m YD isobase at that time (section 8.1.4: Figure 8.2a). In either case, they confirm that all the relict phreatic passage elements were in existence prior to the start of the Holocene interglacial flow regime. Other relict vadose features include the wide sloping floors of Union Passage and Lower Union Passage (with clay-covered water-worn blocks) and possibly Sloping Chimney and The Ramp. The wide passages are quite distinct from the small relict keyhole passages mentioned above, and could have acted as inputs of the main stream during previous interglacials. The 10m Pitch below the Lower Entrance may have been enlarged as a vadose waterfall shaft in the earliest part of the history of the cave passages that remain at present.

Section 9.7 concluded that the truncated phreatic passages developed as half loops under ice-dammed lakes, and not as complete phreatic loops that were later truncated by valley deepening. During the Weichselian deglaciation, the westward-flowing Tverrfjell IDL submerged the cave to a maximum depth of 465m that reduced to 65m from 10700 until 9890, when the IDL collapsed dramatically. This duration was 810^{14}Ca or c. 1600 cal. a (Siemers *et al.*, 1998, Figs. 7A and 7B). If the passages only enlarged in englacial flow when above a PBL that was 200m below the IDL surface (Appendix D4.7), this only lasted from 10100 (section 8.1.4: Figure 8.2a) until 9890 for the lowest passage at 385m altitude. This duration was c. 450 cal. a. For higher passages with outlets at 425m, this condition lasted for an extra c. 200 cal. a. Thus, at a maximum dissolution rate of 1mma^{-1}, the diameter enlargements varied from 0.9–1.3m in these timescales. These are insufficient to account for the sizes of several passages below the Lower Entrance. Hence, passages enlarged in a circulatory flow regime whilst submerged by more than 200m (Appendix D4.9) and / or enlargement started under a deglacial IDL prior to the Weichselian. Cross-sections 11, 12 and 13 appear to have 'double phreatic' profiles, hinting at enlargements of Trunk Passage at two different times, and there is probable enlargement upwards of relict phreatic elements from The Hall via Trunk Passage to Union Passage.

A possible scenario for the cave's history is that deglacial seismicity at the end of the glaciation before the Elsterian created short fractures near the Lower Entrance that enlarged beneath an IDL into a short phreatic loop, with water emerging via conduits since removed above the Lower Entrance. At the same time, a separate phreatic loop formed down and up the deep shafts near the Main Entrance. During the following interglacial, the Overengbakk enlarged the 10m Pitch under vadose conditions, with a later capture via an aven to the north. The water left the cave via the highest relict phreatic passages at resurgences in the bed of the Overengbakk valley. The conduits near the Main Entrance remained relict. The process repeated at the Elsterian deglaciation, with the creation of a deeper loop via Union Passage and a longer loop from the Main Entrance to JoKe Exit. During the subsequent Holstein interglacial, the Overengbakk was captured farther upstream, and lowered and widened the floor of Union Passage (cross-section 15), but the upper end of the cave remained relict. The Saalian deglaciation created the loop from the Lower Union Passage and Trunk Passage to a phreatic outlet slightly farther down the Overengbakk valley. At the same time, a much longer phreatic conduit connected the upper end of the cave via the Second and Third Roof Series into the Trunk Passage. Another capture of the Overengbakk brought allogenic water into Lower Union Passage during the Eemian interglacial, with Trunk Passage remaining as a sump. The Main Entrance to **Toerfjellhola** still did not capture an allogenic stream, and so most of the cave remained relict. The final Weichselian deglacial IDL created a phreatic conduit along the roof of the present stream passage that led to Trunk Passage, which enlarged again. After draining, the entrances below Main Entrance progressively captured a tributary to the Overengbakk, which entrenched the stream passage along its entire length during the Holocene, and deepened and widened a conduit at the lowest part of the cave to create The Hall.

The path length of the fracture system that connected the upper end of the cave to Trunk Passage was some 200m long. If it was created with an aperture of 0.4cm and it experienced englacial flow at 50cms^{-1}, then it would immediately be at breakthrough and enlarge at the maximum rate (Figure 8.8), which seems feasible. The other,

earlier, fractures were shorter and therefore even more likely to enlarge at maximum rates from the outset. Thus, tectonic breakthrough at each stage of the development of **Toerfjellhola** could have been achieved early in the deglaciations considered above, and it is not necessary to postulate earlier glacial cycles to complete any chemical inception. From this analysis, **Toerfjellhola**, which appears to have developed over four glacial cycles, may contain the oldest surviving cave passages in the study area.

D5.3 Neptune's Cave (Z2; GS=E; Appendix B1.2: Figure B1.2)

Neptune's Cave was chosen for study because it contains unusual internal deposits, which the author arranged to be dated (Table A5.1), and because it is situated near the coast at only 126m altitude, where there was competition for deglaciation by flooding beneath an IDL or by recession of the ice margin and marine inundation.

The active vadose elements of the cave that occupy its lowest level are small, immature and consistent with development within the Holocene. Relict vadose elements include headward erosion of the shaft entrances and entrenchments of the floors of Bone Passage and Scallop Hall. These likely developed as the surface of an IDL lowered through the cave. A previous entrance above Scallop Hall is now blocked. The relict phreatic elements comprise a major loop that connects two shaft entrances via Bone Passage and Cockle Way and include smaller subsidiary connecting loops at lower levels. Thus, the phreatic passages increase in cross-section upwards, although this may arise from the relict vadose enlargements. Unconsolidated sediments in the cave show no stratigraphy as they contain assemblies of marine shells and organic sediments, which are assumed to have entered the cave during a major bog-burst flood event in the Holocene (see below). They therefore do not provide information about earlier phases of the cave's development. The sparse population of dated barnacles attached to the roof and walls of the passage Barnacle Street lived in the cave when it was submerged below sea level at the start of the Holocene. The shells are not corroded (Appendix D4.12), proving that the phreatic passages were already fully-formed at this time.

A strict application of the reconstructed Grønlie formula (Figures 8.2a and b) would expose Grønlifjell (1.3km south of **Neptune's Cave**) as a nunatak above the icesheet at 545m altitude at its YD isobase of 145m at c. 10200, apparently the earliest time that the cave could have been submerged beneath a (nunatak) IDL. However, Figures D2.3 and D2.4 show that the ice margin passed **Neptune's Cave** at c. 10210, when the cave was inundated by the sea, giving little opportunity for phreatic dissolutional enlargement below a local IDL. This problem is resolved by the consideration that the ice melted much faster nearer the coast than predicted by the formula (section 8.1.4). The proposed extrapolation in Figure 8.2a indicates that **Neptune's Cave** could have been submerged by the IDL at c. 10700, when the encroaching sea was about 10km to the west. The IDL likely became connected by Nye channels above a warm base to a meltwater subglacial waterway that eventually reached the sea (Figure 8.7f). Flow through such SGWs could reach 100cms^{-1} (Appendix D4.10), although scallop sizes are not recorded in **Neptune's Cave**. The period from 10700–10200 could equal 1000 cal. a (Stuiver *et al.*, 1998, Figs. A7 and A8), giving a diameter enlargement up to 2m (assuming dissolution at 1mma^{-1}). This is sufficient to account for the size of most phreatic passages in the cave.

The lengths of the inception fractures are <100m. At a flow speed of 100cms^{-1}, even 0.1cm apertures would be at breakthrough (Figure 8.8), so that **Neptune's Cave** probably formed totally during the Weichselian deglaciation. A similar development sequence could also apply to the adjacent and more complex **Svartdalgrotta** (Figure B1.1).

After **Neptune's Cave** was submerged below sea level at 10210, the approximate sea level curve (Figure 8.1b) shows that the sea level fell from an altitude of c. 150m to 105m (where the barnacles lived) at later than 9500. However, the radiocarbon date for the barnacles of 9900±110 (Table A5.1) indicates the date of their demise, well before they became elevated above sea level. A probable explanation is that the barnacles died when the Tosenfjord glacier collapsed (dated at 9890±230) and fresh glacial meltwater flowed through the cave (Appendix D3.6). The unconsolidated mollusc shells recovered from Bone Passage died at 9610±100 (Table A5.1). These were likely washed onto a beach above the cave by a storm, and left undisturbed on the forest floor until brought into the cave by a major flood at 1780±70 ^{14}Ca BP, the age of the organic material in the unconsolidated matrix. The mollusc shell age confirms that the main entrance to the cave at 120m was still below sea level at 9610, i.e. after the demise of the barnacles. This proposed Holocene history of **Neptune's Cave** will be amplified in a separate paper.

D5.4 Elgfjellhola (Z4; GS=L; Appendix B1.4: Figure B1.7)

The narrow 1–2m entrenchment in the floor of the passage leading to the waterfall shaft in **Elgfjellhola**, the 3.5m of depth of the shaft (Photo D1.11) and the c. 10m retreat of its north wall are all compatible with vadose development entirely within the Holocene (sections 8.7.2 and 8.7.3). This also confirms the prior existence of the relict phreatic parts of the cave, which are presently being bypassed at the entrance by the 'mainly vadose' inlet passage and below the Waterfall Chamber by a lower active conduit. Thus, the TDMO model applies even to **Elgfjellhola** with its relatively simple morphology. The fault gouge that protrudes 50mm at the sharp neotectonic movement of 11cm recorded in the face of a scallop 2m before the waterfall (Table D1.1, item 18, Photo D1.12) may result from extrusion or may indicate minor dissolution since this (assumed) seismic event, which therefore probably occurred after or soon before the cave was drained. (Section 8.1.10 and Appendix D5.5 deduce the former timing). The protruding fault gouge wafers observed north of the cave (Table D1.1, items 18 and 22) may indicate extrusion at a second (Holocene) tectonic event, or surface lowering by meteoric dissolution (section 6.3.3).

The Weichselian deglaciation sequence for the Tosenfjord / Fiplingdal area (Appendix D3) indicates that the site of **Elgfjellhola** was inundated by an IDL that became backward-flowing with a reverse flow velocity of c. 20cms^{-1} (Appendix D4.4) at an altitude of 950m at about 10850. From the reconstruction in Figure D3.4, the roof of the high pressure SGR below the IDL may have collapsed at about 10200, the time of the transition to eastward-flowing, to create the very wide and deep Jordbruelv IDL with a surface altitude of 700m. Until this time, the water flowed mainly south at Elgfjell, with occasional jökulhlaups and flow switches to the north. Thereafter, flow was consistently south as part of ice contact spillway flow and / or englacial flow at velocities from 20–50 cms^{-1} (Appendices D4.6 and D4.7) until 10000, when the IDL lowered to 600m and started to drain the cave. The whole 240m length of the passage (before the vadose shaft existed) was therefore subjected to turbulent phreatic flows for c. 850^{14}Ca or 1400 cal. a (Stuiver *et al.,* 1998, Figs. A7 and A8). During this time each wall probably retreated by 1.4m, at the maximum rate of 1mma^{-1} (section 8.5.2). Because the width and height of the passage vary up to 4–5m, it is unlikely that this phreatic enlargement phase occurred entirely within the Weichselian deglaciation, and a total enlargement during both the Saalian and Weichselian deglaciations is more likely. The (presumed) vertical inception fracture could have been created by early Saalian deglacial seismicity, but in this case it must have reached a minimum aperture of 1.2cm along its 240m length, to achieve tectonic breakthrough at a flow velocity of 20cms^{-1} (Appendix D4.4) prior to Saalian deglacial enlargement. More likely, a seismic event at the end of the Elsterian created the inception fracture with an initial aperture of c. 0.3cm, which then enlarged chemically to achieve breakthrough beneath an active Elsterian deglacial IDL, if that also submerged the **Elgfjellhola** fracture for c. 1400 cal. a at a hydraulic ratio of $10^{-5.8}$m^{-1} (Figure 8.10).

Elgfjellhola commonly possesses a double phreatic profile. This is unlikely to have arisen from the two opposing flow directions through the cave when beneath the Weichselian backward-flowing IDL (Appendix D3.3). If the *upper* profile originally dated from the Saalian deglaciation, then vadose entrenchment during the Eemian interglacial was possible. There is no sign of a double vadose profile now, although an early vadose phase could have been completely removed by dissolution of the lower phreatic profile during the Weichselian deglaciation. However, it is more likely that the cave remained relict during the Eemian, with a sediment fill occupying the Saalian phreatic passage that also accounted for the *lower* profile. The Weichselian enlargement was then partly paragenetic above this fill, forming the final upper profile, until the fill was washed out of the cave during deglacial outflows at a later stage. Remnants of such a gravel fill are stuck to the walls of the upper part of the lower phreatic profile, upstream of the waterfall. The calcitic mud acting as glue likely dates from the Eemian interglacial.

An issue to address is that any flow in the 'forward' (southern) direction would be expected to 'overwrite' the reverse flow scallops reported in **Elgfjellhola** and two other local caves (Appendix D3.3), especially if the walls retreated by 0.3m from 10200 to 10000, a period of 280 cal. a. Hence, perhaps the wall retreat rate under the backward-flowing Elgfjell IDL was somewhat greater than 1mma^{-1}, being supplemented by the high erosional flow rates from the many jökulhlaups that occurred (Appendix D4.5). The succeeding forward-flowing IDL may then have remained essentially static, perhaps above a thermocline, at the 'warmer' western end of the lake, whilst icemelt sank to its base and into a Nye channel at its eastern end.

D5.5 Etasjegrotta–Rockbridge system (Z4; GS=L; Appendix B1.4: Figures B1.8 and B1.9)

Etasjegrotta is discussed in section 9.2 as the ultimate example of a cave in vertical stripe karst that illustrates the TDMO model. The dimensions of the active vadose elements along its lower levels are all compatible with enlargement within the Holocene from its below-average catchment area of 3km^2. These include the 5m headward erosion at Twin Falls, the small size of the streamway between there and the phreas leading to the Surveyors Sump, and the minor captures occurring near and under the Entrance Chamber. A careful study of the survey section (Figure B1.8) also reveals several relict vadose features that include floor-lowering in Whichway Chamber, headward erosion below Ice Ledge Aven and steps in the floors of passages near the Explorers Sump, at Fall Aven and at the chamber above Eastwater Chamber. These may all represent vadose entrenchment as the Weichselian deglacial IDL slowly lowered through the cave (section 8.4.12), partly supplemented by the action of Holocene spring melt floods. At the resurgence end of the hydrological system (Figure B1.9), the only significant vadose passage is the steeply-inclined inlet to **Invasjonsgrotta**. This emerges at the roof of a relict phreatic passage, where the stream enters as a waterfall that has previously caused the drilling of two clean-washed potholes containing stones in the floor of the chamber Oddstue, at the base of which the stream is presently cutting a vadose channel that must eventually drain into Whybro Passage beneath. Again, these vadose developments probably occurred within the Holocene. Thus, there are no relict vadose passages indicative of Eemian entrenchment within the whole system.

The next question to address is the size of Whybro Passage, the sump :d passage that has been dived upstream for 340m northwards from the **Main Rising** and **Vatnhullet** towards the Surveyors Sump in **Etasjegrotta** (which is 160m farther north) and also towards the series of lakes formed by the . ɔrdbruelv in the gorge leading to the Jordbru (Rockbridge) dry valley. The cross-section of much of this passage i larger than that of the inclined entrance to **Vatnhullet** that is some 10m wide by 3m high and larger than the ɪ ɪssage at the **Main Rising** (6mx2m). Their relative positions show that the **Main Rising** (285m altitude) has captu ed the flow from a previous Vauclusian exit at **Vatnhullet** (300m altitude). From the discussion about phreatic inte glacial enlargement (Appendix D4.13), it is likely that the **Main Rising**, which discharges all the flow from the 30km^2 catchment area of the upper Jordbruelv, achieved this capture soon after the Weichselian deglaciation, via an inception fracture 120m long, and enlarged to its present size during the Holocene. The face of the rising is a *steephead*, which has cut back some 15m from the main valley at the end of the Rockbridge, an amount that is also compatible with the period of the Holocene.

The caves along the Jordbruelv valley were submerged beneath the backward- then forward-flowing IDL or its SGR from c. 10850–9450, a maximum time of c. 1400^{14}Ca (Appendix D3). This equates to 2200 cal. a (Stuiver *et al.*, 1998, Figs. A7–A9). If dissolution was at a maximum rate of 1mma^{-1} for all this time (unlikely), passages could have enlarged to diameters of c. 4.4m, giving cross-sections of c. 15m^2. Although sections 8.6.2 and 8.6.3 concluded that most relict caves and passages enlarged to their present size beneath an IDL, this cross-section is too small to account for the size of the **Vatnhullet** relict Vauclusian entrance, which must therefore have existed as a smaller conduit prior to the Weichselian deglaciation. The next earlier opportunity for this passage to have enlarged was the Eemian interglacial, assuming that deglaciation during Weichselian interstadials did not reach down to this altitude. From Appendix D4.13, the interglacial wall retreat rate of the **Vatnhullet** entrance was likely to be 0.25mma^{-1}, giving a possible width enlargement of 5m if Eemian interglacial flow was sustained for 10000 cal. a. It is therefore concluded that the outlet at **Vatnhullet** existed as a post-breakthrough conduit at the start of the Eemian, and it reached its present size by dissolution during the Eemian interglacial (as a Vauclusian rising) and during the Weichselian deglaciation. Whybro Passage probably enlarged via connections from the Jordbruelv lakes during the Eemian interglacial, the Weichselian deglaciation and the Holocene, and the **Main Rising** enlarged during the Holocene only. The present 300m altitude of the **Vatnhullet** entrance probably also indicates the minimum elevation of the floor of the adjacent Rockbridge area during the Eemian, because otherwise the flow at the initially-small Vauclusian rising would have been captured into lower fractures by the hydraulic gradient during the Eemian itself. This reasonably represents a lowering of the Jordbruelv valley by c. 12m during the Weichselian glaciation and by 3m during Holocene entrenchment.

The next passage to consider is the higher-level c. 2m-diameter relict phreatic passage at an altitude of 300m that comprises **Beehive Cave**, the inner part of **Cliff Cave** and Sand Passage in **Invasjonsgrotta** (Figure B1.9). Much of this is almost completely filled with stratified sandy sediments. These have been partly washed away by the

invading Holocene stream in **Invasjonsgrotta** to create the chamber Oddstue, where the 1.33m-high vertical northern exposure of the sand bank reveals cross-cut bedding that was sketched and sampled during the 2000 field trip (Photo D5.1). The sequence above bedrock in front of the sand bank comprises 20cm of large slabs below 40cm of angular and rounded cobbles and gravels. The southern part of the passage passes dried-out gour pools and has fine brown silt on the roof and 15cm-long scallops on the wall that point south to a silt choke.

The stratified sediments consist of mainly dry light-grey micaceous sand, with centimetre-scale laminations. They effervesce in dilute HCl, indicating the presence of calcite. There are no rocks, organics or other materials visible to the naked eye within the sand, which is fairly consistent in texture throughout the whole deposit, except for several darker layers. The lowest 18cm is layered fairly horizontally, the next 94cm commonly dips at c. 30°W, and the top 21cm consists of sub-horizontal, wavy, layers. The uppermost 2cm comprises a damp orange layer. Loss on Ignition (LoI) tests and grain size tests were undertaken at the University of Huddersfield on nine samples from the Oddstue sand bank, and on one sample (#64) of scrapings from the roof (Table D5.1).

Photo D5.1 Sand bank in Invasjonsgrotta, Z4
Sand bank at southern end of Sand Passage at entrance to Oddstue, Invasjonsgrotta (Figure B1.9). Water flow was from Sand Passage (which continues above top of sand bank) towards the camera. The dipping layers below wavy sub-horizontal laminations at the top are suggestive of seismic liquefaction of previously-horizontal laminations whilst still submerged beneath an ice-dammed lake, followed by continuing deposition and final vadose flow. The sand deposits in Oddstue were later removed by a different (vadose) stream in the Holocene.

Apart from sample #64, the LoI tests show that the sands contain little organic material, as expected for deposition beneath an ice-dammed lake, although there is some correspondence between LoI (%) and the darkness and colour of the samples. From photographs taken at c. 40X magnification, the angular nature of the sand grains and small size of the darker (presumably organic) strands suggests that these deposits have been transported by ice. The grain size tests were undertaken using a Malvern Instruments Ltd. Mastersizer 2000 Version 5.21 machine and all samples gave an approximately log-normal distribution of particle size v. volume (%). Minimum sizes were in the range 0.4–43μm (silts), modal values were in the range 0.06mm (very fine sand) to 0.22mm (fine sand) and maximum sizes were of medium sands, except for samples #31 and #167 (coarse sand) and #64 (very coarse sand).

Sand and silt particles with the observed sizes are deposited at speeds below $5cms^{-1}$ and eroded at speeds above $20cms^{-1}$ (Andersen and Borns, 1997, Fig. 3-31B). The sedimentation probably occurred annually, perhaps over a period of ~133a, from the layering. There is no indication of any progressive trend in the flow velocity during this time. Because there is no paragenetic enlargement above the sediments and because these are calcitic, the contemporary chemical environment in Sand Passage was probably not dissolutional. At a presumed path length of 200m and a passage radius of 100cm, Figure 8.8 shows that the dissolution could have been at a maximum rate at a flow velocity of $>0.05cms^{-1}$, suggesting that the flow rate was, in fact, much less than this. The wavy, disturbed nature of the top 21cm of the sediment, its change of colour at the top and the 40cm space below the roof (through which it is possible to crawl) indicates a later washing-out by water flowing at $>20cms^{-1}$ for a short time.

Table D5.1 Samples from sand bank in Invasjonsgrotta

Sample No.	Height (cm)	LoI %	Grain size			Appearance *in situ*	Photographic appearance under microscope at c. 40X magnification
			Min. (μm)	Mode (mm)	Max. (mm)		
64 *	roof	32.89	3	0.22	1.4	Dark gritty scrapings from roof	Buff matrix with much larger brown angular and curved grains
31 *	131	1.20	0.4	0.09	0.7	As #206, from orange wavy layer	Yellow angular grains with dark brown curved elongated strands
118	124	0.32	0.5	0.07	0.3	As #206, from dark wavy layer	Yellow–brown angular grains with some white angular grains and dark brown curved and elongated strands
167	105	0.14	14	0.20	1.0	As #206	Similar to #118, with larger grains and more pink colour
206	92	0.26	5	0.10	0.5	Dry grey very fine sand with mica	Similar to #118, but more pink
22	78	1.18	0.4	0.06	0.5	As #206, from darker layer	Similar to #31
52	65	0.13				As #206	Buff matrix with black elongated specks
165	52	0.18	43	0.15	0.4	As #206	Similar to #167
37	30	0.17	6	0.12	0.4	As #206	Similar to #31
216	15	0.33	0.4	0.07	0.4	As #206	Similar to #52

* Grain size test after 5 seconds ultrasonic. Others after 10 seconds sonic. All distributions are approximately lognormal. Laminations between 112 and 18cm height dip at c. 30°W.

The above observations can be explained by considering that the original **Beehive Cave–Cliff Cave–Invasjonsgrotta** conduit enlarged towards its present size during the Saalian deglaciation. After the plastic behaviour limit (PBL) of the Saalian ice sheet lowered below Sand Passage, the cobbles on the floor of Oddstue were transported there by powerful englacial flows (Appendix D4.7). Enlargement then continued during the Eemian interglacial (by dissolution in unsaturated waters flowing at 25cms^{-1}, from the size of the scallops south of Oddstue), synchronously with the enlargement of the lower Whybro Passage conduit, when the bottom of the Rockbridge gorge was a little above the upper conduit level of 300m. The water flowed out via a resurgence pool north of **Vatnhullet**. **Invasjonsgrotta** was covered by ice for most of the Weichselian glaciation, when its resurgence entrance was almost blocked by debris, and the thin layer of brown silt was deposited from a subglacial lake whilst under warm-based conditions (section 8.4.2). When the large Jordbruelv IDL formed during the Weichselian deglaciation, the whole system initially experienced circulatory flow at <<10 cms^{-1} (Appendix D4.9) and probably at <0.05cms^{-1} (above). After the IDL and the ice sheet lowered so that the PBL of the ice was below the level of the cave passages, most of the system experienced englacial flow, at a summer flow velocity of c. 50cms^{-1} (Appendix D4.7). However, the summer flow velocity through Sand Passage remained <0.05cms^{-1}, because its outlet remained almost sealed, and the fine sand was deposited in chemically-saturated conditions. Powerful, aggressive, englacial flow through the open **Cliff Cave** part of the system at ~50cms^{-1} is demonstrated by the scalloping and gravel deposits (Photo D1.23). Any sand originally deposited in Whybro Passage was flushed out during this powerful flow regime, and that passage was subsequently kept clear because it remained active throughout the Holocene. The hydraulic gradient steepened and the speed of flow at Oddstue increased after the level of the IDL lowered to the level of Sand Passage, so that the top layers of sand were removed or disturbed into wavy layers as the cave drained in vadose conditions.

The marginal valley development model for vertical limestone (Osborne, 1999, Fig.16) would explain these features by assuming that a blockage at the southern end of **Invasjonsgrotta** caused the excavation of the Jordbru gorge, which in turn was abandoned by the creation of Whybro Passage along the same vertical inception fracture. However, such an explanation could only apply here during excessively prolonged interglacial conditions, and would ignore the effect of glacial erosion and sedimentation beneath an ice-dammed lake.

The dip of 30°W of most of the sediment in **Invasjonsgrotta** can be explained by seismic liquefaction and slumping during the same earthquake that caused the c. 1m opening in the floor of **Cliff Cave** (section 6.3.3) and caused the other local tectonic movements (Photos Frontispiece 1and D1.22–D1.25), which are all within a few hundred metres of each other (Figure B1.9; Table D1.1, items 28–32). Indeed, the timing of this earthquake is probably represented by the sharp transition from dipping to horizontal beds near the top of the sand bank, after which the horizontal beds continued to be deposited for perhaps 30 years without further seismic disturbance, until the IDL surface.lowered below the level of Sand Passage at 9500 (Appendix D3.7). This supports the conclusion in section 8.1.10 that the IDL remained above the level of these passages for some time after the earthquake.

Because of its strength, it seems likely that the earthquake observed at **Cliff Cave** and **Invasjonsgrotta** is the same one that caused the movements in **Elgfjellhola, Paradox Cave** and on the surface of Elgfjell (section 6.3.3 and Appendix D5.4), which are 5km north. If this is the case, it occurred nearly 500^{14}Ca after the Elgfjell caves were drained at 10000 (Appendix D3.6), and the protruding fault gouge wafers seen in **Elgfjellhola** (Appendix D5.4) were formed by extrusion rather than by dissolution of adjacent wall rock.

Returning to the upstream end of the system, the **Etasjegrotta** tributary to the Whybro Passage phreas is commonly clean-washed, with no recorded sediments of fine sand comparable with those in **Invasjonsgrotta**. However, such deposits would have been expelled during Holocene floods (Appendix B2.2). From the survey section (Figure B1.8), the 40m depth of the Surveyors Sump below the entrance equates to the altitude of the **Main Rising** at 285m. Hence, all the rising phreatic limbs in **Etasjegrotta** are above the 300m altitude of Sand Passage in **Invasjonsgrotta**, hinting that the higher levels of **Etasjegrotta** also developed during the Saalian deglaciation. A more likely alternative is that all the relict phreatic loop passages in **Etasjegrotta** developed beneath the large Jordbruelv IDL during the Weichselian deglaciation after the local PBL descended below the level of the cave, with englacial flows into glacial conduits of sufficient velocity to permit rapid enlargement. After the upper parts of **Etasjegrotta** drained, its lower parts, including the present flooded connection to Whybro Passage, then enlarged during the Holocene, especially during floods. The dead-end fissures above the Surveyors Sump illustrate the effects of aggressive flood-water injections (section 3.1.16). The restricted nature of the underwater passage at both the Surveyors Sump and at the end of Whybro passage may indicate that this enlargement started later in the Holocene.

The inception fractures of the upper **Etasjegrotta** phreatic loops have path-lengths less than 200m long, so that at flow velocities of 50cms^{-1} their aperture widths at breakthrough were less than 4mm (Figure 8.8). Such apertures may have been created directly from tectonic activity, and the complex nature of **Etasjegrotta**, with ~20 tiers of passages, implies that it did achieve breakthrough very quickly (section 3.1.16). To enlarge the phreatic passages in **Etasjegrotta** to their common heights of <2m would take <1000 cal. a at a maximum rate of 1mma^{-1}, a time interval that is less than the duration of the Jordbruelv IDL of c. 2200 cal. a (above). It is therefore not necessary to postulate that the relict and vadose parts of **Etasjegrotta** existed as conduits prior to the Weichselian deglaciation. Indeed, if the relict passages had also enlarged during the Saalian deglaciation, they could be much larger.

The **Etasjegrotta** fractures, including those that connect to the caves at the Rockbridge, were probably created during Saalian deglacial seismicity. This total path length is c. 700m and the head to the **Vatnhullet** entrance is c. 25m, providing a hydraulic ratio of 5x10^{-5}m^{-1}. From Figure 8.10, a 1mm aperture would take <200a to achieve breakthrough in these interglacial conditions. Thus, chemical inception could have occurred either in the Eemian or early in the Holocene, still leaving time for Holocene enlargement to present passage sizes between the lower part of **Etasjegrotta** and Whybro Passage in **Vatnhullet**.

Because the present depth of the gorge below the Jordbruelv waterfall is some 35–40m beneath the gentler slope of the hillside, and as it was deduced that the gorge deepened by c. 15m during the last glacial cycle, it follows that the gorge has probably only existed for two complete cycles. This provides supporting evidence that the deeper passages of the immediate area probably postdate the Elsterian glaciation, because before that the depth of the valley was too shallow to provide sufficient hydraulic gradient to drive chemical inception and interglacial enlargement.

APPENDIX D6 OTHER CALEDONIDE TERRANES

This Appendix explores the extent to which the models derived in Chapters 5–9 apply to karsts within the other glaciated terranes of the Caledonides. The method used is to construct a cave database for most of these regions from the best available information, to the same format as used for central Scandinavia, but with a restricted set of parameters identified for each cave. These data are then compared with those of the main study area, and summarised in sections 10.1–10.5.

D6.1 The Scandinavian Caledonides

For convenience, the Scandinavian Caledonides are divided into three parts.

D6.1.1 Northern Scandinavia

That part of Scandinavia north of the Helgeland Nappe Complex is known to contain a large number of karst caves, mainly in the Norwegian county of Nordland and the Swedish county of Norrbottenslan. Several of these are much longer and / or deeper than any in central Scandinavia. To analyse the varying tectonic structures, the geomorphology, the glacial history, and the scattered references to caves for this large region would be a task greater in magnitude than that for the main study area. Instead, one, hopefully representative, karstic valley will be considered, together with a few of the longest and deepest systems. It is assumed that, in general, the range of external settings of the caves is comparable to that of central Scandinavia.

The karst valley chosen for review is Gråtådal in Beiarn, some 70km north of Ranafjord, a place with which the author is familiar. A Gråtådal cave database was constructed from St.Pierre (1966) and later references (Appendix C6). It includes the few caves in the adjacent valleys of Beiardal and Tollådal. The local Beiarn Nappe occupies an uncertain tectonic structural position in the Uppermost Allochthon, probably within the RNC. The caves commonly lie in very long, linear, N–S aligned, outcrops of amphibolite grade metalimestones that occur along the valley floors and their lower, commonly western, slopes. The foliation is steeply angled (commonly dipping to the west, i.e. into the west side of the valley), or vertical. Low angle karst is absent (Table D6.1). The outcrop width varies up to some 700m, so that, although cave trends are commonly strike-aligned, passages also exploit orthogonal joint systems. The setting is therefore similar to that of some of the western zones of the HNC, except that the western edge of the prime metalimestone outcrop is along a thrust internal to the Beiarn Nappe, and the mountains to the west are permanently glaciated. Some 7km of passages in 42 caves are reported in this area, which is characterised by large, almost 'over fit', underground streams, which are sporadically too powerful to permit complete exploration. Key parameters for each cave type and hydrological class are listed in Tables D6.2 and D6.3.

By comparing with Table 5.5, the caves in Gråtådal have mean dimensions considerably greater than those in central Scandinavia for most cave types, although types e and h do not occur, perhaps because of the relatively small sample size. The overall mean length and vertical range are twice as great, and mean cross-section some four times as great. These differences mean that the set of caves in Gråtådal would *not* fit comfortably within the zones of the main study area. However, the deepest cave, the **Rønålihullet** system at 140m, is still within the one-eighth relationship proposed for the main study area, as it lies in a valley some 1100m deep that extends from the Gråtåtind peak (1354m) to a floor at 180m. The valley wall also slopes down above the cave, reducing its maximum subsurface cave distance to c. 30m.

There are roughly equal numbers of caves in each of the three hydrological classes, and MV caves replace combination caves as the most numerous class, in comparison with central Scandinavia (Table 5.25). The MV proportion of total cave length is 20%, compared with 9% in the main study area. Of the three classes, the relict caves are the most similar to those in central Scandinavia. Although they have about twice the mean length and cross-section, the mean vertical range is less, and they only have slightly more entrances per cave (c.f. Table B2.1). On the other hand, the combination caves have twice the mean length, vertical range, and cave streams per cave, more entrances per cave, five times the mean cross-section but only have about half the mean number of sumps. The mainly vadose caves follow similar trends, although they have four times the mean length but a similar number of cave streams per cave.

Table D6.1 Gråtådal (northern Norway) Karst Types

Karst Type	V	A	L	C	X	ALL
Count	11	30			1	42
% of caves	26	72			2	100
Total cave length (m)	4497	2815			50	7362
% of total cave length	61	38			1	100
Mean cave length (m)	409	94			50	175
Mean cave VR (m)	32.1	10.9			3.0	16.3
Mean cave XS (m^2)	14.5	13.4			2.0	13.4

Table D6.2 Gråtådal (northern Norway) Cave Types

Cave Type	No. of caves	% of caves	Total cave length (m)	% of total cave length	Mean cave length (m)	Mean cave VR (m)	Mean cave XS (m^2)	Mean cave volume (m^3)
S	6	14	26	0.3	4	4.3	46.2	219
a	13	31	162	2	12	3.2	5.6	150
b	8	19	1404	19	176	15.3	12.1	1334
c	4	10	237	3	59	4.0	2.3	120
d	5	12	2102	29	420	25.6	7.3	4258
e								
f	1	2	390	5	390	13.0	2.0	780
g	4	10	2990	41	748	71.5	5.8	5685
h								
Hy								
I								
J								
M								
R								
T	1	2	51	0.7	51	51	45	2295
ALL	42	100	7362	100	175	16.3	13.4	1465

Table D6.3 Gråtådal (northern Norway) Cave Class comparisons

INTERNAL CAVE ATTRIBUTE	RELICT CAVES	COMBINATION CAVES	MV CAVES	ALL CAVES	UNITS
Count	13	14	15	42	No.
% of caves	31	33	36	100	%
Total cave length	963	4925	1474	7362	m
% of total cave length	13	67	20	100	%
Mean cave length	74	352	98	175	m
Mean cave VR	4.7	33.6	10.2	16.3	m
Mean cave XS	6.3	24.9	8.8	13.4	m^2
Mean cave Volume	168	3372	808	1465	m^3
Average of SE	0.00	0.71	0.80	0.52	No. per cave
Average of RE	0.00	0.29	0.73	0.36	No. per cave
Average of DE	1.62	1.07	0.67	1.10	No. per cave
Average of all entrances	1.62	2.07	2.20	1.98	No. per cave
Average of CS	0.00	2.21	1.00	1.10	No. per cave
Average of SP	0.00	0.43	0.20	0.21	No. per cave

The explanation for the greater mean vertical range in Gråtådal is that, according to four pieces of evidence, this area was subjected to greater seismic and aseismic tectonic movements at the end of each glaciation than most parts of the main study area. Firstly, the valley is much deeper than any valley with karst outcrops in the study area. Secondly, the seismic shocks accompanying the isostatic rebound immediately after deglaciation probably re-activated the internal thrust at the western edge of the limestone outcrop (which displays sharp slope changes along the skyline, diagnostic of differential uplift), magnifying the production of tectonic fractures. Thirdly, the existence of the 51m- and 22m-deep shafts of **Penkekjelen** (in Beiardal) and the shaft called La Fenêtre into **Øvre**

Svartvannsgrotta could be explained by differential uplift (St. Pierre, 1966, p25). Fourthly, the nearby postglacial 10m-deep, 4m-wide, *sackung trenches* on the ridge between Beiardal and Gråtådal (e.g. Olesen, *et al.*, 1995; Olesen, *et al.*, 2004, Fig. 6) demonstrate seismic or aseismic movements in the vicinity.

The reason for the much greater passage sizes in Gråtådal, especially in the active caves, lies in their recharge from permanent glaciers around the summit of Gråtåtind. In the main study area, it was assumed that the spring melt throughout the Holocene provided a maximum discharge for about one month per year. In valleys below glaciers, high discharge rates are maintained when the air temperature at the glacier remains above freezing. In the case of Gråtådal, this is for about 6–8 months per year. Thus, Holocene vadose floor lowering rates and (probably) phreatic wall retreat rates are higher by factors in Gråtådal compared with regions without permanent glaciers.

Relict vadose passages were established as a probable diagnostic for Eemian vadose entrenchment in Chapter 8, and a total of seven caves with such passages are recorded in the Gråtådal cave database. Most of these passages are of a 'normal' size, i.e. up to about 6m high and 1m wide, and are therefore assumed to indicate purely vadose development in the Eemian. Three of these occur in caves that are relict, creating three relict vadose caves, in contrast to the main study area that has none. These passages may have become choked during the Weichselian glaciation, so that they did not enlarge further in paragenetic deglacial conditions, or else they developed and became abandoned wholly within the Holocene. Just one internal relict vadose passage in a combination cave (the **Heståga system**) has a large size (10m high by 2m wide), but the present stream passage is relatively small, suggesting that in this case, it does represent a capture during the Holocene.

The deglaciation marine limit in this area reached into Beiardal, beyond its junction with Gråtådal, to an altitude approaching 140m. However, the floor of Gråtådal rises steeply above the confluence to about 180m, so that none of its caves were inundated by the sea. This is in agreement with a finding from cave surveys, that none of the cave entrances appears to have been enlarged by marine action, to the criteria established for the main study area. The enlarged entrances to **Unnamed Cave** and the adjacent **Smiths Cavern**, with parallel walls, and large, fallen blocks, were probably enlarged by ice wedging as an ice-dammed lake lowered past their level. In contrast to the main study area, many narrow bands of Beiarn Nappe marbles (RNC equivalents) pass beneath the Svartisen ice cap, south of Gråtådal. Their future study might confirm some of the glacio-hydrogeological relationships deduced in this thesis.

The deepest system in northern Europe is **Rågge Javre Raige** (RJR). It is contained in angled to vertical stripe karst (ASK to VSK) of the Fauske Nappe. This underlies the Beiarn Nappe tectonically, in the lower part of the Uppermost Allochthon, but has a *medium* metamorphic grade (Roberts *et al.*, 2002). The system has an upper entrance at an altitude of 580m, just 100m from the edge of the sloping wall of Hellemofjord (Løvlie *et al.*, 1995; Lauritzen *et al.*, 1991; Figures D6.1 and D6.2). Despite its vertical range of >580m (including its submarine resurgence), the commonly steeply-sloping shafts and passages in the cave remain within 173m of the fjord wall, indicating the role of tectonic inception in the cave's development. Local peaks rise to c. 1200m above the fjord that has a maximum depth of 455m, so that the system remains within the limit of the one-eighth relationship, if the fjord depth is included in the calculation. Sub-horizontal relict 'half-loop' (section 9.7) phreatic passages at altitudes that include 3m, 47m?, 80m, 127m, 535m and 560m pass from the predominantly vadose main shaft system towards the surface, some providing lower entrances to the fjord wall. Without undertaking a detailed study, it appears that the system has developed downwards in conjunction with the deepening of the fjord during successive glaciations, with each of the phreatic passages indicating the approximate level of the lowest submarine resurgence during each deglaciation. Thus, the present rising below fjord level is an outlet that developed during the Holocene, the Fjordgrotta entrance at 3m was the lowest outlet at the end of the Weichselian, a possible passage at 47m led to an early Eemian outlet, the passage at 80m was likely the Holstein outlet, and the passage at 127m the likely Cromerian outlet. Outlets between 127m and 535m, at intervals that decrease from c. 45m to c. 25m, probably await discovery.

From the above discussion, the cave has followed ever-deeper inception fractures created by successive deglacial seismic shocks at the end of each major glaciation, in the manner described by the TDMO model (section 9.2.4). A crude estimate for the first inception and enlargement of present passages indicates an age of 1.2Ma for the highest passages in the system, if sub-horizontal outlets, at a mean interval of 35m, represent some 16 major glacial cycles

(at 41ka intervals prior to the Mid Pleistocene Revolution, and at 100ka intervals thereafter). Even older passages may have existed above the present cave, before these were removed by the lowering of the plateau surface. Additionally, the present relict sub-horizontal passages probably extended farther north, before being shortened by the widening of the fjord. About ten deep, parallel, relict, inclined shafts in the centre of the cave also provide clues to the glacial history, as they may indicate progressive captures during successive interglacials, supplementing information about the inferred missing outlet levels. The shafts are some 3–12m wide, and would therefore have taken some 3–12ka to grow to their full extents (at 1mma^{-1}). Some of these times may equate roughly to an interglacial period. Others may indicate captures *within* an interglacial period.

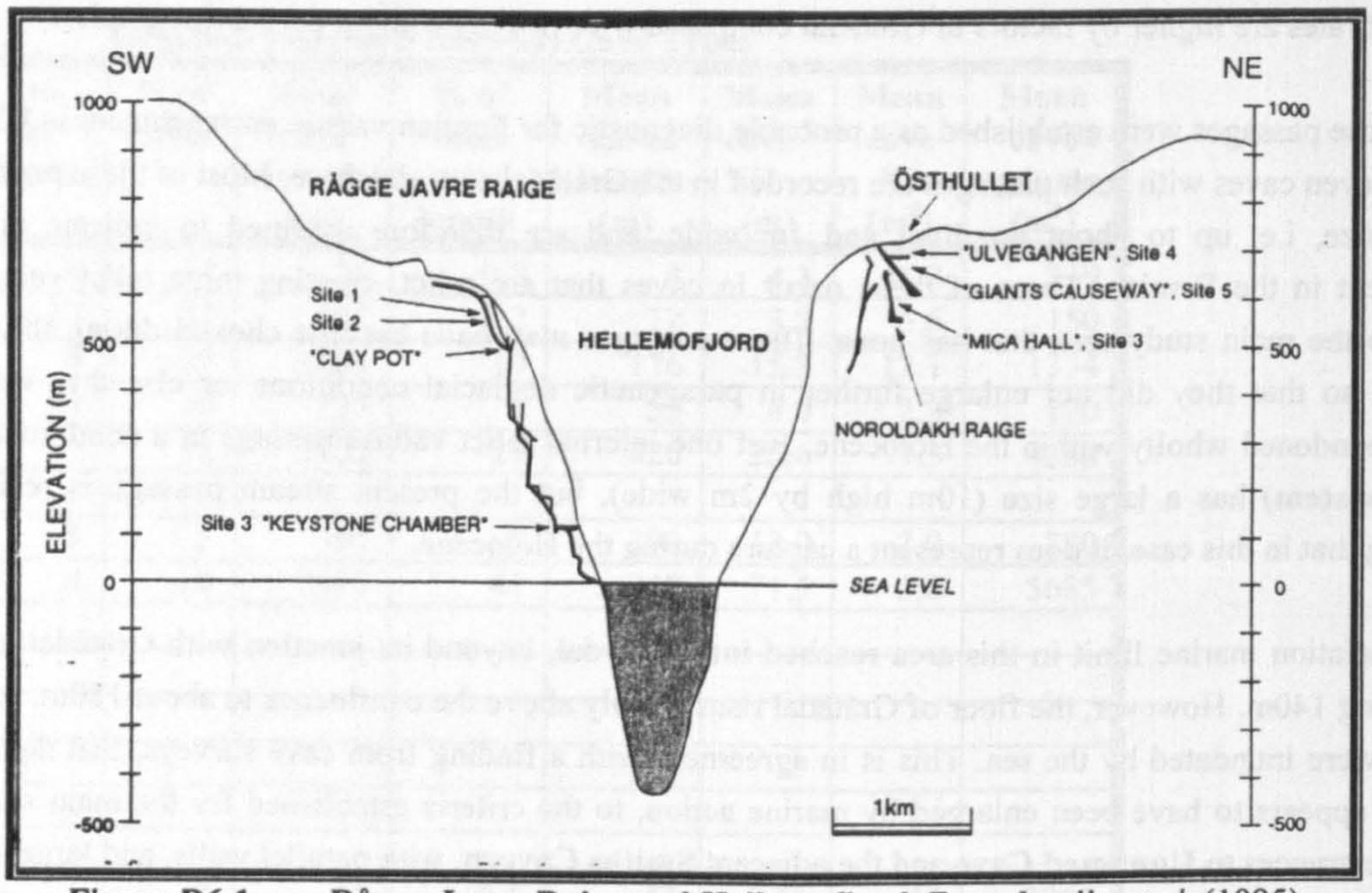

Figure D6.1 Rågge Javre-Raige and Hellemofjord. From Løvlie *et al.* (1995)

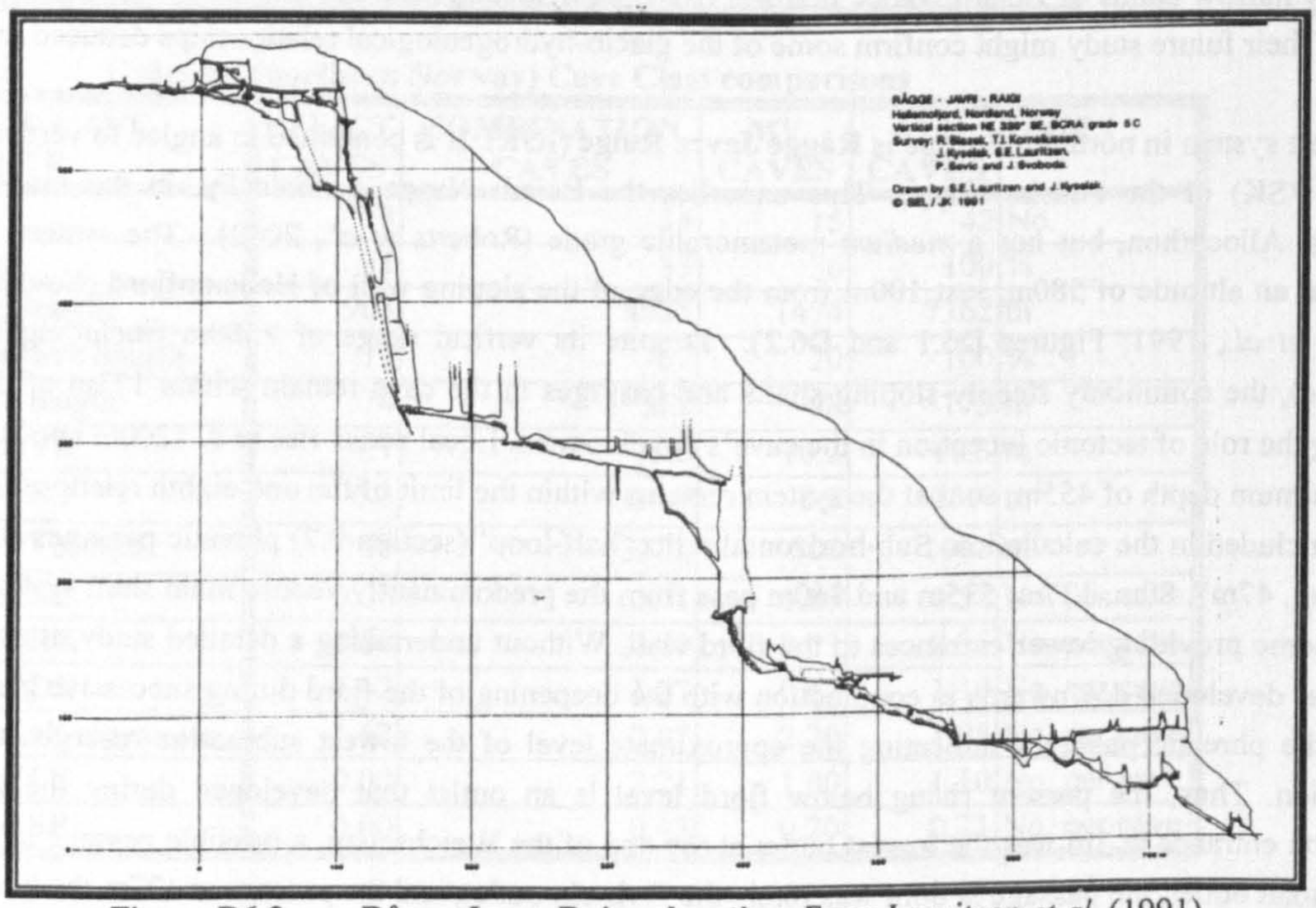

Figure D6.2 Rågge Javre-Raige elevation. From Lauritzen *et al.* (1991)

A fuller treatment of the development of the cave would need to consider the rates of fjord lowering and widening. The evolution must be more complex than the above simplified picture: making the crude assumption that the orthogonal fjord wall retreat distance between interglacials equals the difference in elevation of the two phreatic outlets, by about the third previous glacial, the known passages would be further from the surface than allowed by the one-eighth relationship. Hence, the unknown continuations of the horizontal levels probably lead to more shaft

(at 41ka intervals prior to the Mid Pleistocene Revolution, and at 100ka intervals thereafter). Even older passages may have existed above the present cave, before these were removed by the lowering of the plateau surface. Additionally, the present relict sub-horizontal passages probably extended farther north, before being shortened by the widening of the fjord. About ten deep, parallel, relict, inclined shafts in the centre of the cave also provide clues to the glacial history, as they may indicate progressive captures during successive interglacials, supplementing information about the inferred missing outlet levels. The shafts are some 3–12m wide, and would therefore have taken some 3–12ka to grow to their full extents (at $1mma^{-1}$). Some of these times may equate roughly to an interglacial period. Others may indicate captures *within* an interglacial period.

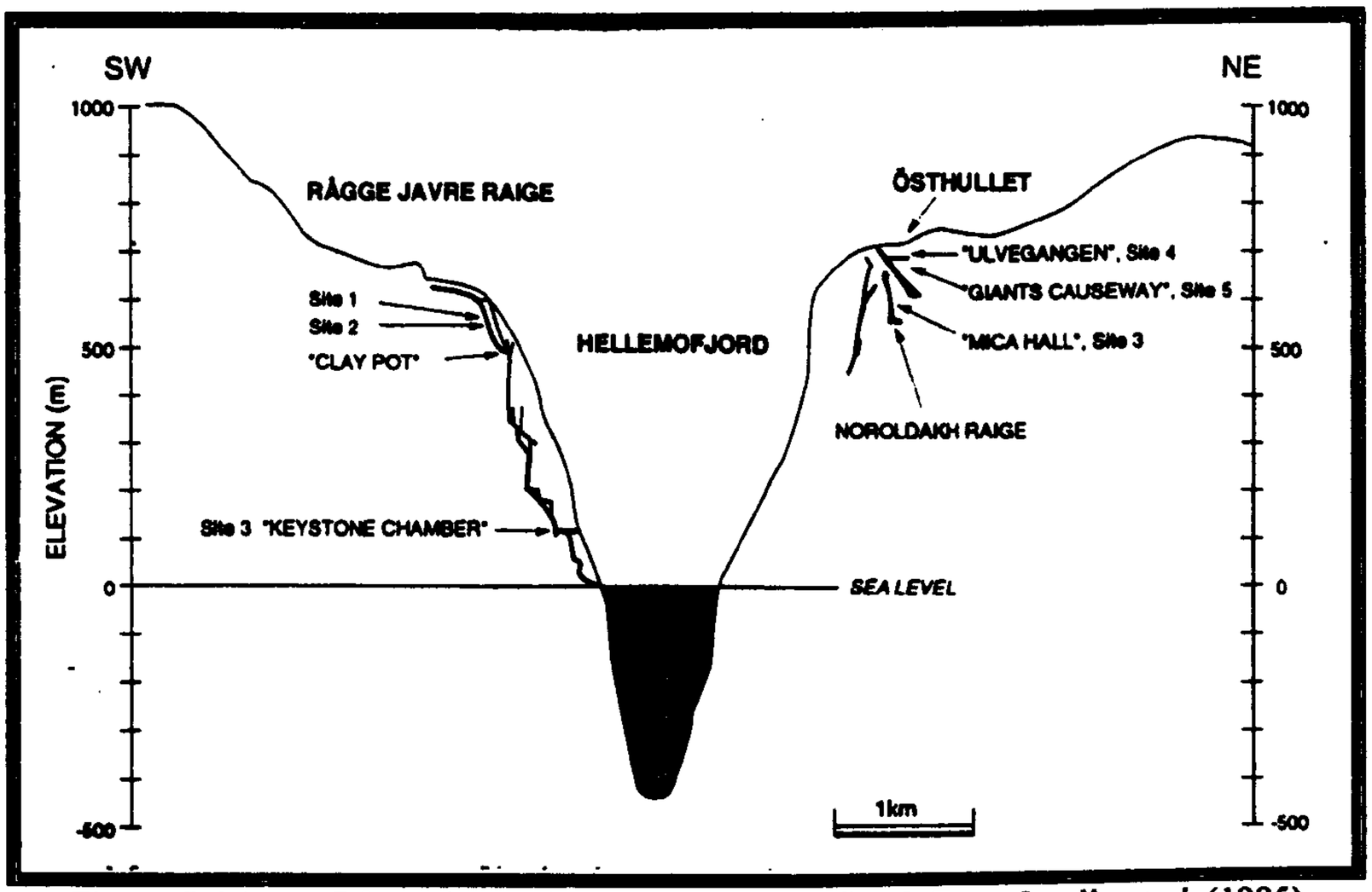

Figure D6.1 Rågge Javre-Raige and Hellemofjord. From Løvlie *et al.* (1995)

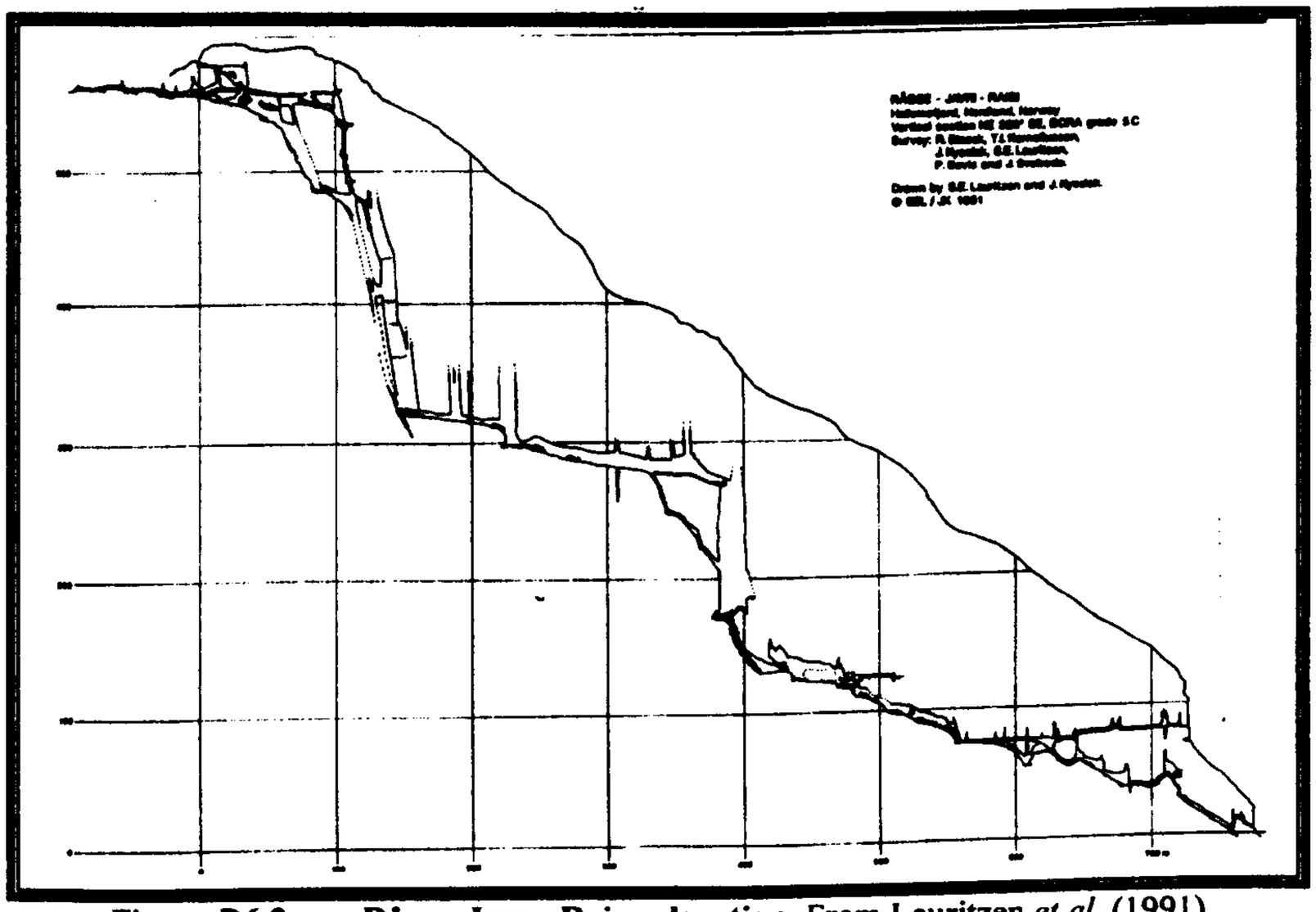

Figure D6.2 Rågge Javre-Raige elevation. From Lauritzen *et al.* (1991)

A fuller treatment of the development of the cave would need to consider the rates of fjord lowering and widening. The evolution must be more complex than the above simplified picture: making the crude assumption that the orthogonal fjord wall retreat distance between interglacials equals the difference in elevation of the two phreatic outlets, by about the third previous glacial, the known passages would be further from the surface than allowed by the one-eighth relationship. Hence, the unknown continuations of the horizontal levels probably lead to more shaft

systems closer to the fjord wall, which were formed within their contemporary one-eighth relationship. The explored passages were later directed towards the bases of these shafts (again, in accordance with the TDMO model) during the many deglacial periods when the cave was submerged beneath a Hellemofjord ice-dammed lake. Løvlie *et al.* (1995) reported sediments dated from 10900–10200^{14}Ca BP at an elevation of 560m. These were presumably deposited during the time of the last IDL, after any pre-existing deposits had been flushed out. There are no reports of sand deposits in the lower parts of the cave, which could have been inundated with sea water up to the level of the YD isobase at 140m (Sørensen *et al.*, 1987). This suggests that deglacial outflows through the cave remained sufficiently strong to withstand inflowing tidal water. Direct exploration of the 'missing' relict passages via the many unclimbed shafts could enable RJR to become the best example in the world of a karst cave that has its development directly related to the glacial evolution of its local topography, over a very long timescale. An analysis of the presence or absence of relict vadose passages at the higher levels could also verify the suggestion in section 8.7.4 that vadose entrenchment was less important during interglacials prior to the Holocene.

The next deepest system is **Tjoarvekrajgge**, in Sørfold. This is also the longest cave in Scandinavia, with a present survey length of nearly 17km. The cave has formed in an E–W limb of south-dipping low angle karst, also in the Fauske Nappe. Several entrances at altitudes around 600m lead via down-dip phreatic passages (some with active vadose trenches) towards an active vadose series with many sumps and unexplored sections, giving it a total vertical range of 502m. A looping series of strike-tending larger phreatic passages (with minimum dimensions of 1m high by 3m wide) connect the inlet series together, to create a system of great size and complexity. As represented on an unpublished survey, the cave morphology comprises an inclined rectilinear maze with N–S and E–W passage elements, supplemented by a meandering mainly vadose streamway at its lowest (southerly) level. All the upper passages are coated with a very fine slippery clay deposit on all surfaces, as observed during a visit made by the author in June 2000. The coating probably occurred when the cave was submerged beneath a warm-based subglacial lake at a glacial maximum but was not washed out again during deglaciation, perhaps suggesting that a deglacial IDL in the adjacent Bonnå valley remained static as it lowered past the upper levels of the cave, but leaving open the question of how the cave passages enlarged to their present sizes. The depth of Bonnådal is some 600m, but as the cave reaches a maximum depth of some 300m below the surface, it is clear that it does not fit within the constraints of the one-eighth relationship that applies to caves in VSK and ASK. Considerable study would be required to unravel the evolution of **Tjoarvekrajgge** within the context of the evolution of its local geomorphology.

The second longest cave is the **Okshola / Kristihola** system, near Fauske. It has also formed in a low angle karst of the Fauske Nappe, with a near-horizontal foliation. This system has a surveyed length of 11km and a vertical range of 185m, and resurges near the sea at an altitude of only 2m. Two very large entrances (30m x 30m and 15m x 15m) at altitudes of about 160m lead into a predominantly-phreatic maze series of passage near **Okshola**, and, directly from **Kristihola**, into a huge streamway that varies in size from 15m high x 5m wide to 30m high x 10m wide. Above the lower part of the 1km-long streamway and its six sumps is a descending rectilinear series of well-decorated (despite the distance to the surface above) phreatic passages with diameters up to c. 15m that maintain an elevation of some 50m above the floor of the adjacent stream. From the survey, the end of the cave appears to pass 200m below a 220m-high ridge. However, the nearest peaks are only at c. 800m, and as far away as 6km to the NE. Thus, this system also does not follow the one-eighth relationship, although draughting openings at possible higher-level relict resurgences, and the probable capture of the interglacial stream from the **Kristihola** entrance to a point just before the **Okshola** entrance, indicate that it may follow the TDMO model. Because of the size of most of its large phreatic galleries, this cave must have a long and complex history of development, spanning several complete glacial cycles. The vadose streamway seems very unlikely to have developed to its enormous size only during the Holocene, despite the large present recharge. Thus, each of the phreatic and vadose elements of the cave probably represent enlargement under successive deglacial and then interglacial regimes, although paragenetic modification of the streamway is not obvious from the survey cross-sections.

Another major system in northern Norway comprises the two adjacent caves **Greftkjelen** and **Greftsprekka** at Sørfjord, which are parts of the same system that are unconnected physically. The system has some 7km of passages and a VR of 315m, from entrances at 350m and 340m altitudes down to the incompletely-explored main streamway at 35m. The resurgence is at about 25m. It has formed in a complexly-folded, N–S aligned, stripe karst with an

apparently high metamorphic grade in the Beiarn Nappe (RNC). The deep **Greftkjelen** entrance shaft trends north in marble with a vertical foliation, but the continuing passage swings to the SW, across an anticline. The northward trend is resumed at the next syncline (Holbye, 1983a,b,c; Ford and Williams, 1989, Fig. 2.12, p40). The explored cave is dominated by vadose development at *higher* levels, with large, abandoned, vadose galleries overlying smaller, and more recent, meandering streamways. Phreatic development only seems *dominant* below about 120m altitude, where a relict passage reaches to within about 200m of the resurgence, at an altitude of 63m. Thus, **Greftkjelen** does *not* exhibit the upside-down morphology of higher-level phreatic passages overlying a single vadose channel. Because **Greftkjelen** reverses direction, and both caves have deep internal shafts, passages exist that are 300–400m from the surface at the dry valley between the entrances, or at the ridge to its west. Local peaks presently only reach to about 600m, and Sørfjord is only 207m deep, so that the depths of inception fractures in this system cannot be constrained by the one-eighth relationship that applies in central Scandinavia. A partial explanation was provided by Holbye (1983a), who described joints up to 130m deep that have formed at the crests of the anticlinal folds.

A complex, multi cycle, theory of cave development was proposed by Holbye (1983c; section 3.3.3), reinforced by the dating of stalagmites from elevations of c. 100m and c. 225m at c. 190000 and c. 178800a BP (Holbye and Lauritzen, 1983). An interesting feature of **Greftkjelen** is the presence of sand banks in and below the Low Level Gallery, at a maximum altitude of c. 110m, and at a distance of some 500m from the present resurgence. According to Sørensen *et al.* (1987), the YD isobase at Sørfjord is at 100m altitude and the sea invaded at c. 10000^{14}Ca BP. Therefore, the sea initially reached an altitude of 100m and there is likely to be a blocked lower entrance to the cave, into which the sea had easy access at the start of one or more interglacial, after the main deglacial flushing had ceased. The sand deposition at the highest level *may* have been at the start of the Eemian, rather than the start of the Holocene, when the deglacial marine limit was at a higher altitude (section 8.1.2). However, this seems unlikely, as all pre-Weichselian unconsolidated sediments were probably washed out during the final deglaciation. Thus, the difference between 110m and 100m probably represents tidal range, storm effects and mapping errors, allowing the sand banks to be of early Holocene age. The observation about phreatic development below about 120m may mean that large, pre-existing, vadose shafts and passages sent deglacial meltwaters down to this level, to create a short meltwater subglacial waterway. This would have been at a late stage of each deglaciation, but before marine incursion breached the Sørfjord tidewater glacier. Previous to this, the cave was submerged well-above 120m altitude by the local ice-dammed lake, but perhaps in fairly static water.

D6.1.2 Central Scandinavia

This is the main study area of this thesis. Refer to Chapters 4–9.

D6.1.3 Southern Scandinavia

The southern Scandinavia area comprises the whole of Norway and Sweden that lie within the Caledonide nappes south of the main study area. The widely-scattered metacarbonate outcrops fall into four groups: the Køli Nappes of the Upper Allochthon, which lie in a belt from Molde on the northern coast of southern Norway to Snåsavatn, some 15km south of the main study area; the Lower Allochthon (Norway), which variously crops out in the centre of southern Norway, particularly at Dummdalen in the Jotunheimen mountain range; the Seve Nappes of the Upper Allochthon in Sweden; and the Lower Allochthon (Sweden). The two Swedish groups lie adjacent to each other, near the villages of Åre and Ånge, west of Östersund. Karst caves have not been reported in the Seve Nappes in southern Norway, nor in the Middle Allochthon anywhere in southern Scandinavia. Caves in primarily sedimentary limestones, which occur at Oslo, Drammen and Skrimfjell in southern Norway, at Scania in southern Sweden and on the Swedish island of Gotland, have not been considered. Neither have caves that are sporadically described in the SSF magazine *Grottan* as lying within the Precambrian metacarbonates of the Baltic Shield.

The caves of southern Scandinavia are among the most poorly documented of all the Caledonide terranes, as caving reports commonly only give rough lengths, and few other details. Cave surveys are still awaited for many caves, or are inaccessible. The author has visited some of the caves in Dummdalen. A database of 47 caves (Appendix C7) is summarised in Tables D6.4–D6.7. Within this database, some gross estimates of altitudes, vertical ranges and cave

cross-sections are included. Because of this and the small sample size, the data quality is less than in the tables for the other Caledonide areas.

Table D6.4 Southern Scandinavian Karst Types

Karst Type	V	A	L	C	X	ALL
Count		17	22		8	47
% of caves		36	47		17	100
Total cave length (m)		2117	2035		86	4238
% of total cave length		50	48		2	100
Mean cave length (m)		125	93		11	90
Mean cave VR (m)		13.9	7.5		3.6	9.1
Mean cave XS (m^2)		5.6	2.7		1.4	3.5

Table D6.5 Southern Scandinavian Cave Types

Cave Type	No. of caves	% of caves	Total cave length (m)	% of total cave length	Mean cave length (m)	Mean cave VR (m)	Mean cave XS (m^2)	Mean cave volume (m^3)
S	4	9	30	1	8	6.5	2.3	19
a	10	21	95	2	10	2.8	3.2	37
b	11	23	404	9	37	4.9	2.3	116
c	4	9	178	4	45	3.0	1.8	87
d	7	15	1267	30	181	11.4	5.5	1641
e	3	6	239	5	80	15.7	1.3	199
f								
g	5	11	1742	41	348	31.2	8.4	3480
h	1	2	210	5	210	20.0	4.0	840
Hy	1	2	43	1	43	3.0	2.0	86
I								
J								
M								
R	1	2	30	1	30	4.0	2.0	60
T								
ALL	47	100	4238	100	90	9.1	3.5	692

Table D6.6 Southern Scandinavian Cave Class comparisons

INTERNAL CAVE ATTRIBUTE	RELICT CAVES	COMBINATION CAVES	MV CAVES	ALL CAVES	UNITS
Count	11	16	20	47	No.
% of caves	23	34	43	100	%
Total cave length	117	3454	667	4238	m
% of total cave length	3	81	16	100	%
Mean cave length	11	216	33	90	m
Mean cave VR	5.7	17.6	4.3	9.1	m
Mean cave XS	2.0	5.9	2.5	3.5	m^2
Mean cave Volume	18	1902	96	692	m^3
Average of SE	0.00	0.50	0.65	0.45	No. per cave
Average of RE	0.00	0.31	0.25	0.21	No. per cave
Average of DE	1.27	1.94	0.50	1.17	No. per cave
Average of all entrances	1.27	2.75	1.40	1.83	No. per cave
Average of CS	0.00	1.38	1.00	0.89	No. per cave
Average of SP	0.00	1.13	0.35	0.53	No. per cave

None of the caves occur in vertical stripe karst. In central Scandinavia, VSK occurs primarily in the Uppermost Allochthon, which is absent in southern Scandinavia. The caves in southern Sweden are probably all in low angle karst. However, because of the scarcity of cave surveys, few conclusions can be reached about internal cave morphology. The total length of passage in the 47 adequately-documented caves is only some 4200m. To this can be

added perhaps 1600m from a further 27 inadequately-reported caves. The longest caves have lengths c. 400–500m: **Gaulstadgrotta** (Ogndal) and **Trollkyrkegrotta** (near Molde), both probably in the Køli Nappes; **Kvarnbäckslabyrinten** (including Övre and Nedre caves) in the Seve Nappes; and **Øvre Elvegrotta** (Dummdalen) in the Lower Allochthon. Both **Kvarnbäckslabyrinten** and **Øvre Elvegrotta** have a vertical range of some 46m. All caves lie at altitudes well above marine limits.

Table D6.7 Southern Scandinavian Caves and Tectonostratigraphy

Alloch-thon	Nappes	No. of caves	% of caves	Total cave length (m)	% of total cave length	Mean cave length (m)	Mean cave VR (m)	Mean cave XS (m^2)	Mean cave volume (m^3)
Upper	Køli (Norway)	13	28	1853	44	143	11.8	3.9	1145
Upper	Seve (Sweden)	5	11	423	10	85	10.8	1.8	89
Lower	(Norway)	15	32	1420	33	95	11.8	5.4	1074
Lower	(Sweden)	14	30	542	13	39	3.3	1.8	79
ALL		47	100	4238	100	90	9.1	3.5	692

The mean length of the caves is some 90m, varying from 143m in the Køli Nappes to 39m in the Lower Allochthon in Sweden (Table D6.7). If the lengths of some 29 extra, inadequately reported, caves are included, the mean lengths of caves in each of the four groups all reduce, giving a total mean of 79m. Neither value is very different from the mean length for the main study area (85m). Similarly, the mean cave cross-section ($3.5m^2$), the mean cave volume ($607m^3$, adjusted for the over-representation of length) and the mean cave vertical range (9.1m) are also comparable (c.f. Table 5.5). However, the caves in the Lower Allochthon in Sweden are significantly smaller in most dimensions compared with those in the other three groups. The reason can be deduced from the extents of local relief differences at each major site in the Køli, Seve, Lower (Norway) and Lower (Sweden) groups, which are roughly 900m, 1000m, 1200m and 300m, respectively. Hence, whereas all the caves lie well inside the one-eighth relationship for their subsurface cave distance, there is a very strong suggestion that the *mean* depth of a group of caves is also determined by the local relief, perhaps equalling roughly 1% of the depth of the local valley. The data also hint that the relief difference also determines the mean *length* of the local caves.

The approximate distribution of the caves amongst the relict, combination and mainly vadose hydrological classes is shown in Table D6.6 (which should be treated with caution). As in central Scandinavia, the dimensions of the combination caves are significantly greater than those of the other two classes. The mean cross-section of the caves in the Lower Allochthon (Norway) is also much higher than the overall mean. These caves predominantly lie in Dummdalen in the mountains of southern Norway, and they are almost all combination or mainly vadose *active* caves. Although not fed directly from glaciers, the area has a high winter snowfall, so that the large stream that flows through some of the caves persists throughout the summer and autumn, giving a large vadose entrenchment throughout the Holocene. The proportions and rankings of entrance types, cave streams and sump pools are also fairly similar to those of the main study area (Table B2.1).

D6.2 The Laurentian Caledonides

The main area of interest in northern America is the northern Appalachian part of the Caledonides, along the western side of the New England states of Vermont, Massachusetts and Connecticut.

D6.2.1 New England carbonate geology

The structural geology of New England is more complex than that of central Scandinavia, because the area comprises a collage of some ten Caledonide terranes that have over-thrust older, Grenville-age, rocks of the Canadian Shield that crop out in New York state and in Canada. The thrust slices culminate in the Taconic Allochthons along the western extremity (Keppie, 1985). Some of these terranes and basement inliers contain karstic metacarbonates. These are commonly highly dismembered into lenses and merokarsts, with low angles of dip, rather than into long N–S aligned stripe karsts. Faulting, jointing and thrusting at a local scale also dominate. Individual metacarbonate blocks were sporadically transported across more competent rocks, and unconformities between rock types are sharply delineated. For example, it is sporadically possible to insert a hand between the upper surface of a metalimestone and an overlying phyllite. Metamorphism varies from high to low grade, in a S–N direction, and

intrusions are common at higher grades. The ages of the metacarbonates vary from Precambrian to Middle Ordovician. Some (short) caves are recorded in Winooski and Dunham "Dolomites" (Quick, 1994), although it is not known whether these refer to dolomitic limestones or to pure dolomite. Surface relief is rather subdued, with shallow valleys extending from altitudes below c. 200m up to vegetated ridges and peaks above 1000m.

D6.2.2 New England glacial history

The glacial history of the area is rather similar to that of central Scandinavia (sections 2.3 and 2.4). The Wisconsin glaciation also appears to have had less magnitude than the previous Illinolan and Kansan glaciations (Andersen and Borns, 1997, p40). [For example, Schroeder and Ford (1983) discussed three phases of varved sequences in Castleguard Cave, Canada, which they interpreted as depositions under full glacial conditions. As the youngest of these dated to 140ka, they suggested that the cave was not inundated during the Wisconsin]. At the LGM, the icesheet presumably extended over many areas of warm-based glaciation with subglacial lakes. According to Dyke *et al.* (2002) and Marshall *et al.* (2002), icesheet thickness increased from zero off the coast at Boston, via 1500–2500m across the Caledonides, to >3000m above Hudson Bay.

Wisconsin deglaciation was probably complete in New England by c. 13000^{14}Ca BP (Andersen and Borns, 1994) and the impact of YD cooling was much attenuated inland (Cwynar and Spear, 2001). The author is unaware of any detailed models of deglaciation that equate to the work of Grønlie (1975), but assumes that similar processes applied. The top-down melting of ice from mountain ridges to create IDLs, and a warming-front from the Atlantic that moved, in this case, from SE–NW, were confirmed by Stone and Borns (1986, Fig. 1) and by LaRocque *et al.* (2003). The Holocene uplift for the area varies from c. 60m in the south to c. 180m in the north (Andersen and Borns, 1997, p18). Rubin *et al.* (2002) discussed possible evidence of raised sea levels (including elevated sea caves, sea stacks and boulder beaches) on Mount Desert Island, Maine. The Atlantic coast contains many non-carbonate sea caves at and above the present sea level. However, they all have entrances that are only a few metres high. The complete absence of littoral caves with *very tall* entrances (Rubin, pers. comm., 2002) may indicate that the sea froze here before there was significant isostatic depression at the onset of the Wisconsin glaciation. In this case, there was no *glaciation* marine limit equivalent to the one suggested for north central Norway (section 8.1.3). However, as the karst areas are c. 180km from the coast at elevations >200m, probably none of the caves were inundated by the sea during either glaciation or deglaciation events, and the construction of isobase maps is less relevant to an understanding of cave development. The well-documented existence of many 'tectonic fissure' or 'fracture' caves and of many 'talus' caves in a variety of metamorphic rock types provides evidence that this area also experienced many severe seismic shocks following rapid deglaciation and uplift. The seismicity in *northern* New England was probably greater than that in the main study area, because, being nearer to the centre of the icesheet (in a position more comparable to eastern Sweden) the thickness of ice removed was even greater. However, the majority of the karst caves are located in the southern part of New England.

D6.2.3 New England karst caves

A brief study of the karst caves was undertaken by extracting information from Quick (1994) and from the *NE Caver* magazine into a North American Caledonides cave database (Appendix C8). The database is incomplete, because location and altitude information is commonly suppressed in northern America (to protect the interests of property owners). However, the recording of karst type, cave type, cave class, main dimensions, entrances and hydrology was achieved, mainly by a study of the well-presented cave surveys and descriptions. It is anticipated that these data are representative of the present state of knowledge. The completeness of exploration may, on one view, be higher than in the main study area, because groups of active cave explorers live locally. On the other hand, many karst outcrops and potential cave entrances are covered by extensive vegetation and glacial till. The author made brief field trips to the area in November 1996 and June 2002, visiting five of the 153 listed caves. Tables D6.8–D6.10 list some key parameters for the karst caves of the North American Caledonides.

The cave surveys for the area do not have the same 'feel' as those in the Helgeland Nappe Complex of central Scandinavia. The reason is apparent from Table D6.8, which shows that 52% of the caves occur in low angle karst (commonly monoclinal, with dip $\leq 30^{\circ}$). Some 12% are in angled karst ($\leq 80^{\circ}$), and *none* occur in vertical stripe karst. It is not easy to deduce the karst type for 37% of the caves, but many of these (shorter) caves in unknown karst types

are probably also in low angle karst. As a consequence, cave surveys are commonly less linear than in the main study area, and it is more difficult, and less relevant, to assign the caves to the *cave type* structure chosen for central Scandinavia. For example, only one cave is given cave type e (vertically tiered linear passages, Table D6.9), and, with the strong faulting and jointing, some caves fall into "fissure network" patterns (Palmer, 1991).

Table D6.8 New England Karst Types

Karst Type	V	A	L	C	X	ALL
Count		18	79		56	153
% of caves		11.8	51.6		36.6	100
Total cave length (m)		1370	6332		1385	9087
% of total cave length		15.2	69.7		15.2	100
Mean cave length (m)		76	80		25	59
Mean cave VR (m)		9.7	11.2		6.4	9.3
Mean cave XS (m^2)		1.6	3.0		3.1	2.9

Table D6.9 New England Cave Types

Cave Type	No. of caves	% of caves	Total cave length (m)	% of total cave length	Mean cave length (m)	Mean cave VR (m)	Mean cave XS (m^2)	Mean cave volume (m^3)
S	8	5.2	196	2.2	25	14.0	4.5	118
a	56	36.6	842	9.3	15	4.0	2.6	60
b	33	21.6	1121	12.3	34	5.6	2.5	109
c	17	11.1	1172	12.9	69	4.6	2.3	148
d	13	8.5	851	9.4	65	12.5	3.1	251
e	1	0.7	42	0.5	42	3.0	1.0	42
f	14	9.2	1893	20.8	135	18.9	3.4	510
g	3	2.0	578	6.4	193	39.0	4.3	781
h	4	2.6	2277	25.1	569	58.0	5.3	2993
Hy								
I	4	2.6	115	1.3	29	10.0	3.6	160
J								
M								
R								
T								
ALL	153	100.0	9087	100.0	59	9.3	2.9	234

Table D6.10 New England Cave Class comparisons

INTERNAL CAVE ATTRIBUTE	RELICT CAVES	COMBINATION CAVES	MV CAVES	ALL CAVES	UNITS
Count	81	52	20	153	No.
% of caves	53	34	13	100	%
Total cave length	1998	6189	900	9087	m
% of total cave length	22	68	10	100	%
Mean cave length	25	117	45	59	m
Mean cave VR	5.3	14.8	10.7	9.3	m
Mean cave XS	2.6	3.1	3.4	2.9	m^2
Mean cave Volume	75	473	237	234	m^3
Average of SE	0.00	0.38	0.80	0.24	No. per cave
Average of RE	0.00	0.21	0.20	0.10	No. per cave
Average of DE	1.16	0.68	1.00	0.97	No. per cave
Average of all entrances	1.16	1.27	2.00	1.31	No. per cave
Average of CS	0.00	1.23	1.15	0.58	No. per cave
Average of SP	0.00	0.47	0.15	0.18	No. per cave

With a mean length of only 59m, the caves are commonly shorter than those in the main study area: the longest (**Aeolus Bat Cave**, VT) is only 900m long. The mean cave cross-section ($2.9m^2$) and volume ($234m^3$) are

correspondingly smaller. Mean cave dimensions tend to increase with cave type (Table D6.9) and only four caves are assigned the most complex cave type, h. However, at 9.3m, the *mean* vertical range is remarkably similar, and deeper caves also occur in karsts with lower dip angles. The deepest (**Purgatory System**, VT) has a VR of 82m and a maximum subsurface cave distance of c. 40m. The passage with the greatest distance to the surface (68m) is in a deep sump in **Morris Cave** (VT). This is situated in a glaciated valley whose floor is at c. 210m, between peaks above 1000m. Thus, the known distance of its deepest passage from the surface is well-within the one-eighth relationship that was proposed for the creation of inception fractures in central Scandinavia (section 6.5.2).

The caves also commonly contain large amounts of breakdown on chamber floors away from entrance areas, and anecdotal reports indicate that there are *not any* chambers with smooth floors, also suggesting that caves were subjected to large seismic shocks. The author's 2002 visit to **Nickwackett Cave** and **Chaffee Mountain No. 2 Cave** (VT) revealed evidence of recent tectonic movements along joints, visible inside the caves, and commonly parallel to passage directions. [Isostatic rebound only triggers earthquakes at some postglacial faults in eastern Canada if they are in pre-stressed regions (Olesen, 1988)]. Cave passages sporadically occur at junctions of two marble lithologies, as at **Eldons French Cave** (MA) and at **Morris Cave**.

From Table D6.10, over half the caves are relict, a third are combination caves, and 13% are mainly vadose. This represents a much larger proportion of relict caves and a much smaller proportion of combination and MV caves than in central Scandinavia, suggesting that Holocene vadose development was less important than deglacial phreatic development in New England. However, although combination caves commonly have the largest dimensions, the small sample of MV caves commonly has larger mean dimensions than the short and extremely epigean relict caves, whose mean VR is only 5.3m and which may not contain many examples of longer multi cycle caves. Entrance occurrences decrease in combination caves in the order DE to SE to RE, as in central Scandinavia, but with smaller mean frequencies. Both combination and MV caves have slightly more cave streams per cave, but far fewer sump pools. Whereas relict and combination caves have mean cross-sections 16% and 31% smaller than in central Scandinavia (Table 5.25), the relatively few MV caves are 62% larger. The reason for the greater development of the active vadose parts of caves is probably that interglacial conditions started at c. 13000^{14}Ca BP, thus lasting longer than in central Scandinavia. They may also have larger catchment areas and shorter periods of winter freezing (not studied). However, there are no glaciers to provide sustained meltwater recharge in summer.

As expected from their elevations above probable marine limits (Appendix D6.2.2), the caves do not contain entrances that were obviously enlarged by marine action. This evidence provides more support to the hypothesis that caves in Norway with enlarged, tapering, entrances *were* enlarged by marine action. Only the entrance to **Skinner Hollow Cave** (VT) and the two entrances at the resurgence of **Horse Farm Road Cave** (VT) appear to be enlarged by IDL ice wedging, indicating their existence prior to final deglaciation. However, many entrances in northern America are vertical shafts into lower passages, or are themselves steep, shattered, passages. Although an analysis of variation with altitude has not been attempted, it seems likely that carbonate outcrops, cave occurrences and cave dimensions are primarily independent of altitude. The absence of reports of entrances situated very near peaks or ridge summits suggests that, as in the main study area, few caves exist in the 'uppermost' glacial situation (i.e. one that was only submerged by a static nunatak ice-dammed lake during deglaciation). However, as the metalimestone outcrops commonly dip at rather low angles, their vertical distribution may not be as random as in central Scandinavia, and an absence of very high altitude caves could arise from a corresponding lack of limestone at such elevations.

A study of the cave surveys found only six relict vadose passages in the whole area, which is even less proportionately than in central Scandinavia. As none appear to lie above subsequently-formed phreatic passages, they provide no evidence that any combination caves started their enlargement prior to the final glacial cycle. Only one occurs in a relict cave (**Bat's Den Cave**, MA), and so relict caves were predominantly formed phreatically, and therefore before the final deglaciation. There is no reported dating of speleothems to give any non-geomorphological indication of passage age, and significant speleothems are rare. The only indication of possible multi-cycle cave development may be the diameter of some passages. The entrance passage size of **Aeolus Bat Cave** (VT, 8m wide by 6m high above a floor of shattered limestone) does seem larger than most in this respect. However, northern

America has apparently experienced several deglaciation / reglaciation phases since the Laurentide LGM, as discussed in section 2.3.3. Thus, the caves were probably flooded under several deglacial IDLs for longer periods of time than occurred in Scandinavia, providing the opportunity for prolonged dissolution to produce larger diameter passages. Anecdotal reports indicate that some caves contain five or six cycles of rhythmic deposition of clay sediments and larger material. It is possible to speculate that these deposits were laid down during the N–S flow-switching that occurred as the Great Lakes region alternately melted and froze between the LGM and the Holocene (e.g. Clark *et al.*, 2001). This author's observation of two sizes of scallops in **Nickwackett Cave** (c. 10 and 30cm), giving approximate flow-rates of 40 and 13cms^{-1} (both southwards) are similar to the flow rates deduced for englacial flow and reverse flow beneath ice-dammed lakes in central Scandinavia (Appendices D4.7 and D4.4).

D6.2.4 Caves in the Adirondack Mountains of New York State

Although significant caves also occur in the metalimestone outcrops of the Canadian Shield, these have been not been included in the New England Cave Database, as they lie outside the Caledonide terranes. However, visits in 1996 and 2002 to six of the marble caves in the Adirondack Mountains, which are situated in 1–1.3Ba Grenville-age crystalline marbles with very large grain sizes, support a conclusion that marble caves in the Canadian Shield also fit within the conceptual Caledonide models described in this thesis. For example, **Crane Mountain Cave** contains many large dykes and sills, presumably of amphibolite (as does **Browns Cave**), and one of these forms the roof of the downstream sump. Although the cave is primarily in a low angle karst, with a dip of c. 30°NE, the first two waterfalls occur where the rock is folded complexly. A vertical fracture at the entrance shows tectonic movement, apparently with broken calcite, and at the base of the second waterfall is a fault with slickensides 15cm long, weathered to black. The commercial **"Natural Stone Bridge and Caves"** consists of a large stream captured by a large, complex, phreatic series of sumps beside a normally-dry limestone gorge. This has small rockmills in its floor, indicating formation during deglacial outflows. **Rusty Stove Cave** has an obvious tectonic movement along a fracture on the left side of its entrance. The cave itself has formed along a dyke wall, which is breached at an inner chamber. The nearby **Burroughs Cave** has two moved joints orthogonal to the entrance passage that are c. 10m apart. It contains the large Breakdown Chamber, formed by upward stoping of collapsed blocks, with no dissolution evident above its lowest level. The karst cave with the greatest vertical range is **Crane Mountain Cave** (c. 30m), and these caves also fit within the one-eighth relationship for depth of exploited fractures. The local presence of large numbers of talus and fissure caves also supports the concept of fracture generation by postglacial seismicity.

D6.2.5 Newfoundland

The island of Newfoundland forms a tectonic structural link between the northern Appalachians and the British Caledonides (van Staal *et al.*, 1998, p213), comprising an assemblage of some six terranes with similarities to those of Britain and Ireland. However, the Dalradian Supergroup of the British Isles, with its metamorphic carbonate outcrops, appears to narrow considerably in Newfoundland, either within the Notre Dame Subzone or in its outlying Fleur de Lys Supergroup. These subzones do not appear to contain significant metacarbonates, and no karst caves are reported there. The scattered outcrops of the Taconic Allochthons on the west of the island mainly consist of igneous and plutonic rocks. The Humber Zone on the St. Lawrence promontory contains large outcrops of sedimentary carbonates of Cambrian and Ordovician age, similar to the Durness Group limestones of northern Scotland (RA Gayer, University of Cardiff, pers. comm., 1998). Higham (2001) reported a 780m-long karst cave in this limestone, together with other exokarst features. He also noted the existence of many sea caves from all over the island, with entrances up to 15m high, but not elevated above sea level.

D6.3 The Caledonides of the British Isles

The Caledonide terranes of the British Isles comprise the Dalradian Supergroup in Scotland, Ireland and the isles of Shetland, which all contain metacarbonate outcrops.

D6.3.1 Scottish Dalradian Supergroup carbonate geology

The places of interest in Scotland are in the Grampian Caledonides, which lie between the Great Glen Fault and the Highland Boundary Fault (Stephenson and Gould, 1995). The whole area stretches from the Isle of Islay and the Mull of Kintyre at the Atlantic coast, via the Grampian Highlands mountain range, to the North Sea coast between the Moray Firth and Aberdeen. With an area of some 25,000km^2, it is over half the size of the main study area in

central Scandinavia. The scenery is among the most dramatic in Britain, and includes Ben Nevis (1322m), which is near both the coast and the Great Glen Fault, and the central Cairngorm massif, which rises to 1289m.

The Grampian Caledonides are commonly described stratigraphically as the Scottish Dalradian Supergroup (e.g. Gibbons and Harris, 1994). The Supergroup consists of the Grampian, Appin, Argyll and Southern Highland Groups, in a sequence that very roughly 'youngs' from NW–SE. Metacarbonate outcrops occur mainly in the Argyll and Appin Groups, but karst caves have only been recorded in the Tayvallich Subgroup of the Argyll, and in the Blair Atholl and Ballachulish Subgroups of the Appin. The Ballachulish Subgroup itself contains stratigraphically separate formations that are described as the Appin Limestone Formation (λ_A) and the Ballachulish Limestone Formation (λ_B), in both of which significant caves are located.

The ages of the original Dalradian sediments were thought to vary from the Grampian Group of Grenville age (1100Ma), via the Appin Group at c. 750Ma, to the Late Proterozoic age (670–570Ma) of the Argyll and Southern Highland Groups (e.g. Stephenson and Gould, 1995). The Appin and Argyll Groups are separated by a major unconformity (marked by the 670Ma Port Askaig tillite), which may correlate to the Varanger Ice Age observed in northern Norway. However, Thomas *et al.* (2004) compared $^{87}Sr/^{86}Sr$ data from Dalradian metalimestones with available data of Neoproterozoic seawater $^{87}Sr/^{86}Sr$ ratios. They concluded that the limestone diagenesis was wholly within a marine environment and that the whole Dalradian Supergroup was younger than previously reported, with all Grampian, Appin and Argyll deposition occurring probably from 700–600Ma.

The Groups were later subjected to subduction, folding and metamorphism during the Grampian (Caledonide) Orogeny, from the Cambrian to the Early Devonian. Metamorphic grade follows the stratigraphy, from upper amphibolite facies in Grampian Group rocks, down to greenschist facies in Southern Highland Group rocks. The metacarbonates commonly form stripe karst outcrops that look very similar to those in central Scandinavia when seen on maps, in the field, and in the hand. In particular, the metalimestones of the Appin Group (Blair Atholl and λ_A Subgroups) are similar to those of the Helgeland Nappe Complex of north central Norway, as they display attractive light-coloured foliations in stream passages and commonly contain intrusive dykes and sills that form underground waterfalls. The Appin Group (λ_B Subgroup) metalimestones are commonly black, with discontinuous white veins, in which intrusions have not been noted by the author.

The Dalradian Supergroup abuts the rocks of the Moine Succession that lie north of the Great Glen Fault and that have a broadly similar age range (Johnstone and Mykura, 1989). The only carbonates in the Moine Succession are small slivers of marbles contained in inliers of the much older Lewisian Complex, in which no caves are reported. Both the Moine and Dalradian sequences were overthrust across Cambrian sedimentary rocks. These include the karstic Durness Group sedimentary limestone, which is beyond the scope of this study.

D6.3.2 Scottish glacial history

The glacial history of the area followed the pattern of central Scandinavia (sections 2.3 and 2.4), but, being situated to the south in a more oceanic setting with smaller ice caps, the glaciations were less intense, more responsive to climate change, more difficult to interpret, and not necessarily synchronised with Scandinavian events. According to Stephenson and Gould (1995, p183), only an Anglian (480ka) and a Wolstonian (Saalian equivalent) glaciation are known to be represented in the Grampian Highlands prior to the stadials of the Devensian (Weichselian equivalent) glaciation. The main Late Devensian glaciation (the Dimlington Stadial) was thought to have lasted from 26–13 ^{14}Cka BP, reaching a maximum at 18 ^{14}Cka BP, when most of the area was covered by ice. McCabe *et al.* (1998) showed that there was widespread deglaciation of the British icesheet at coastal zones from 16.7–14.7 ^{14}Cka BP, followed by ice advance from 14.7–14.0 ^{14}Cka BP, when a maximum was reached that coincided with Heinrich event 1 and was nearly as extensive as the previous maximum. Rapid deglaciation occurred after 13.7 ^{14}Cka BP when the icesheet disappeared, except in the western mountains (the Windermere Interstadial). A major re-advance occurred at the Loch Lomond (YD) Stadial from 11–10 ^{14}Cka BP.

Icesheet thicknesses were less than in Scandinavia, and the coast of NE Scotland was incompletely covered by ice, even during glacial maxima (Stephenson and Gould, 1995, p181). Ballantyne *et al.* (1998) showed, in a

comprehensive study, that a single high-level weathering limit on 71 mountains in NW Scotland is a periglacial trimline, cut along the flank of former nunataks by the last Devensian (warm-based) ice sheet at its maximum. Erratics ≤140m above this were emplaced by a much earlier and thicker ice sheet [Wolstonian or Anglian?]. The ice-shed during the Devensian was situated above Rannoch Moor (SE of Ben Nevis), where the ice reached an elevation of some 1000m, but it reduced to sea level at the northern coast of the Grampian Highlands. Hence, the higher peaks probably remained above the icesheets as nunataks. Glacial erosion was mainly concentrated in the valleys, creating a radial pattern of lochs, glacial troughs and bedrock erosional forms in the western Grampians (e.g. Thorpe, 1987), and reduced from W–E (Glasser, 1995; Appendix A3.5). At the Loch Lomond re-advance, the smaller ice cap reached 700m altitude at Rannoch Moor (Payne and Sugden, 1990; Ballantyne, 1997, Fig. 4).

The icesheet retreated into valley glaciers during deglaciation, and the effects of IDLs and / or jökulhlaups can be recognised (e.g. at the Parallel Roads of Glen Roy: Dawson *et al.*, 2002, and in the Cairngorm Mountains: Brazier *et al.*, 1998). Isostatic depression by glaciation allowed the sea to inundate the coast up to 40m altitude prior to their subsequent elevation. However, as the lowest karst cave altitude is 75m, none could have been modified by marine action. As expected, none show the enlarged, rocky, tapering, entrances observed in many caves in north central Norway that lie below the deglaciation marine limit, providing more support to the hypothesis that such caves in Norway were, indeed, enlarged by marine action. Only **Uamh na Duilean Briste** (Bealach; λ_A) and **Heifer's Outwash Cave** (Glen Stockdale; λ_B) (both in Argyllshire) appear to have slightly enlarged entrances with parallel walls, indicative of enlargement by ice wedging and dissolution at the surface of ice-dammed lakes (section 8.9.4).

Davenport *et al.* (1989), Ringrose *et al.* (1991) and Stephenson and Gould (1995, p202) discussed Scottish seismicity, which they attributed to the reactivation of old faults during deglaciation and later. The Great Glen Fault Zone, the west coast of the area and Comrie near the Highland Boundary Fault are some of the most seismically active parts of Great Britain, with earthquakes recorded up to 5.2 magnitude. Several 'tectonic fissure' or 'fracture' caves in a variety of metamorphic rock types supports the evidence that this area also experienced seismic shocks and tectonic movements following rapid deglaciation and uplift at the start of both the Windermere Interstadial and the Holocene. Thus, the cave inception processes are probably similar to those in central Scandinavia.

D6.3.3 Scottish Dalradian Supergroup karst caves

Information was extracted from four regional cave guidebooks and from various issues of the *Grampian Speleological Group Bulletin* to create a Scottish Dalradian Supergroup cave database (Appendix C9). Karst type, cave type, cave class, main dimensions, entrances and hydrology were recorded from the comprehensive cave surveys and descriptions. It is anticipated that these data are a complete representation of the present state of knowledge. The completeness of exploration is, in some areas, higher than in the main study area, because of the activity of Scottish cave explorers. The Scottish Highlands were extensively deforested for sheep grazing in recent centuries, making the task of finding cave entrances commonly easier than in central Scandinavia. This has resulted in some karst outcrops being exhaustively searched and reported, whereas others have (so far) apparently been ignored. However, reforestation by the introduction of plantations is now sporadically obscuring entrances, including those that are already known. The author has made brief field trips to the area, and has visited 21 of the 152 listed caves. Tables D6.11–D6.14 list some key parameters for the karst caves of the Scottish Caledonides. The cave surveys for the area commonly have the same 'feel' as those in the Helgeland Nappe Complex of central Scandinavia. The reason is apparent from Table D6.11, which shows that the majority of the caves occur in angled or vertical stripe karst, and *none* are known to occur in low angle karst. Although the foliation angles are unknown in 41% of cases, the outcrops are narrow, and are unlikely to have low dip angles. As a consequence, cave surveys are commonly quite linear, as in the main study area.

With a mean length of only 28m, the caves are much shorter than those in the main study area: the two longest, **Poll Seomar** (Chamber Pot, in Coire Mulrooney; λ_B), and **Uamh nan Claig-ionn** (in Bealach; λ_B) (both in Argyllshire) are only 340m and 280m long. The mean cave cross-section (2.1m^2) and volume (84m^3) are correspondingly smaller. Mean cave dimensions tend to increase with cave type (Table D6.12), but commonly remain smaller for every cave type than the means in central Scandinavia (Table 5.5). Only **Poll Seomar** is assigned the most complex cave type, h. The mean vertical range of 5.9m is only about two thirds that of the main study area. The two deepest

caves are **Uamh nan Claig-ionn** and **Poll Seomar** at 48m and 40m, with similar maximum distances to the surface. The first of these is situated near Salachan Glen, whose floor is some 375m below adjacent peaks. The second lies in Glen Creran, which has peaks to its east almost at 1000m. Thus, the subsurface cave distances of the deepest passages are within the one-eighth 'limit' for the creation of inception fractures in central Scandinavia (section 6.5.2), although the depth of Sump 2 in **Uamh nan Claig-ionn** approaches it.

Table D6.11 Scottish Dalradian Supergroup Karst Types

Karst Type	V	A	L	C	X	ALL
Count	17	72			63	152
% of caves	11	47			41	100
Total cave length (m)	646	2624			955	4225
% of total cave length	15	62			23	100
Mean cave length (m)	38	36			15	28
Mean cave VR (m)	6.7	7.2			4.2	5.9
Mean cave XS (m^2)	1.8	2.3			1.9	2.1

Table D6.12 Scottish Dalradian Supergroup Cave Types

Cave Type	No. of caves	% of caves	Total cave length (m)	% of total cave length	Mean cave length (m)	Mean cave VR (m)	Mean cave XS (m^2)	Mean cave volume (m^3)
S	28	18	299	7	11	6.7	2.3	24
a	51	34	626	15	12	3.2	1.9	31
b	34	22	870	21	26	4.8	2.0	58
c	13	9	595	14	46	5.4	2.4	191
d	12	8	465	11	39	5.8	1.7	75
e	6	4	447	11	75	15.8	3.2	226
f	1	1	38	1	38	10.0	2.5	95
g	6	4	545	13	91	16.2	2.8	393
h	1	1	340	8	340	40.0	4.0	1360
Hy								
I								
J								
M								
R								
T								
ALL	152	100	4225	100	28	5.9	2.1	84

Table D6.13 Scottish Dalradian Supergroup Cave Class comparisons

INTERNAL CAVE ATTRIBUTE	RELICT CAVES	COMBINATION CAVES	MV CAVES	ALL CAVES	UNITS
Count	42	55	55	152	No.
% of caves	28	36	36	100	%
Total cave length	745	2736	744	4225	m
% of total cave length	18	64	18	100	%
Mean cave length	18	50	14	28	m
Mean cave VR	5.9	8.9	2.9	5.9	m
Mean cave XS	1.9	2.8	1.6	2.1	m^2
Mean cave Volume	44	175	25	84	m^3
Average of SE	0.00	0.55	0.49	0.37	No. per cave
Average of RE	0.00	0.22	0.44	0.24	No. per cave
Average of DE	1.21	0.71	0.29	0.70	No. per cave
Average of all entrances	1.21	1.48	1.22	1.31	No. per cave
Average of CS	0.00	1.25	1.04	0.83	No. per cave
Average of SP	0.00	0.47	0.25	0.26	No. per cave

The caves contain few significant chambers, apart from shaft bases at waterfalls, and none exceed c. 4m in any dimension. Internal chambers that do occur have breakdown on their floors, suggesting that they were subjected to seismic shocks. The author's 1999 visit to **Uamh Steall na Burich** (in Glenamuchrach, Argyllshire; λ_A) showed a small neotectonic movement along a horizontal joint, visible at the west wall of the entrance passage. During visits to **Poll Seomar** (whose chamber and upper passages formed by dissolution at a wide inclined fracture zone), **Uamh Coire Sheileach** (Coire Mulrooney; λ_B) and **Draught Caledonian** (Glen Duror, Argyllshire; λ_A) in 2004, many tectonic movements of up to 15cm were observed along sub-horizontal (e.g. Photo D6.1) and near-vertical fractures, with several passage elements aligned along two orthogonal fracture sets not directly related to the foliation.

Using the hydrological cave classification (Table D6.13), just less than one third of the caves are relict, just over a third are combination caves, and just over a third are mainly vadose. This distribution is quite similar to that in central Scandinavia. Furthermore, all the mean dimensions of combination caves are much greater than those of relict and mainly vadose caves, and the rank order for all mean dimensions is always combination: relict: mainly vadose, as it is in the main study area.

Photo D6.1 Tectonic movement in Poll Seomar
Movement of ~10cm after the formation of the passage in angled stripe karst. Both photos by Ivan Young.

Photo D6.2 Speleothems in Poll Seomar
The small sizes and the fragility of the stalagmites and stalactites suggests formation during the Holocene.

When comparing the mean cross-sections of caves in each of the hydrological classes (Table D6.13) with those of the caves in central Scandinavia (Table 5.25), it is found that they are all smaller. Combination caves are reduced from 4.8 to 2.8m^2 (42%), relict caves from 3.1 to 1.9m^2 (39%), and mainly vadose caves from 2.1 to 1.6m^2 (24%). A reduction in the timescale for phreatic enlargement is easy to understand. Because the smaller ice cap melted faster than would be expected from an application of the same reconstructed Grønlie formula (section 8.1.4), the IDLs that inundated inception fractures in Scotland were probably more short-lived than in central Scandinavia, despite coastal sites being deglaciated three times in the Late Devensian (Appendix D6.3.2). However, the vadose phase should have lasted for a similar duration in the Holocene in both countries, suggesting that Scottish caves experience less erosion during a shorter spring melt than occurs in the main study area. As in central Scandinavia, entrance occurrences of combination caves decrease in the same order from DE to SE to RE, but all hydrological classes have about 0.2 less DE per cave, probably because of the shorter mean lengths. Both combination and mainly vadose caves have similar numbers of cave streams per cave, but fewer sump pools (which is anomalous).

Several cave entrances lie in each of the 100m altitude ranges from 100–700m. Thus, it seems likely that carbonate outcrops, cave occurrences and cave dimensions are primarily independent of altitude. However, there are no recorded karst caves lower than 75m, despite several metalimestone outcrops extending down to sea level at the coast. The reason is assumed to be the same as discussed in section 8.1.10, i.e. that deglacial earthquakes were

muffled and reduced in magnitude when the sea encroached towards the deglaciation marine limit. The highest cave, **Cave of the High Ground** (Inverness-shire; λ_B), at an altitude of 895m, is below the level of a col to its south, suggesting that no caves exist in the 'uppermost' glacial situation (i.e. one that is above the level of the highest local col, and therefore only supporting static nunatak ice-dammed lakes during deglaciation).

A study of the cave surveys found no relict (fully) vadose passages in the whole area, meaning that the relict caves were predominantly formed phreatically and therefore before the completion of the final deglaciation. However, there are relict keyhole-shaped passages in the two combination caves **Poll Seomar** and **Draught Caledonian**, indicating vadose entrenchment before other passages formed at lower levels. Although these could represent early pathways in the Holocene, it is also possible that the vadose flows originated in the Ipswichian (Eemian) Interglacial, after prior phreatic enlargement during the Wolstonian (Saalian) deglaciation. There is no reported dating of speleothems to give any non-geomorphological indication of passage age, and stalagmitic flowstones are rare. The upper levels in **Poll Seomar** contain stalagmite bosses (Photo D6.2), but their sizes are too small to indicate growth over a longer timescale than just the Holocene. The small passage diameters of nearly all the caves in the Grampian Caledonides also argue against multi-cycle cave development.

The sediments in **Poll Seomar** and **Draught Caledonian**, which vary in size up to cobbles, are worthy of study, but they were probably deposited at late stages of the Devensian. For example, a sequence on the lower wall of the lower streamway in **Poll Seomar** has 10cm of gravels overlain by 5cm of clay that, in turn, is overlain by 10cm of gravels. The lower gravels could have been deposited during the deglaciation that preceded the Windermere Interstadial at 13.7^{14}Cka BP (Appendix D6.3.2), with the clay settling out during warm-based periods of the Younger Dryas re-glaciation. The upper gravels could then have been deposited during the YD deglaciation at the start of the Holocene. The present small stream is eroding these deposits.

Table D6.14 Scottish Dalradian Caves and Supergroup Stratigraphy

Group	Subgroup	No. of caves	% of caves	Total cave length (m)	% of total cave length	Mean cave length (m)	Mean cave VR (m)	Mean cave XS (m^2)	Mean cave volume (m^3)
Argyll	Tayvallich	33	22	481	11	15	4.6	2.2	35
Appin	Blair Atholl	40	26	658	16	16	3.4	1.3	25
Appin	Ballachulish - λ_A	29	19	982	23	34	7.8	2.5	105
Appin	Ballachulish - λ_B	50	33	2100	50	42	7.6	2.6	152
ALL		152	100	4225	100	28	5.9	2.1	84

λ_A Ballachulish Subgroup, Appin Limestone Formation
λ_B Ballachulish Subgroup, Ballachulish Limestone Formation

Table D6.14 shows the distribution of caves across the Scottish Dalradian Supergroup metalimestones. Although roughly similar numbers of caves are recorded in each of the four main limestone formations, they clearly fall into two groups. The caves in the Tayvallich and Blair Atholl Subgroup limestones have mean dimensions that are much less than those in the Ballachulish Subgroup (λ_A and λ_B) limestones, which contain all caves longer than 100m. The reason for this is not immediately obvious. The lengths and widths of outcrop types seem to range over similar values. If the one-eighth relationship applies, then caves up to 50m depth might be expected over much of the whole area. However, the Ballachulish Subgroup (λ_A and λ_B) outcrops all lie fairly close to the glaciation spreading centre at Rannoch Moor, where the icesheets were the thickest, and the deglacial seismic shocks were the strongest. The Tayvallich and Blair Atholl Subgroups are widely scattered across the Grampian Caledonides, and thus include caves in places where the ice thickness reduced towards the coasts (Appendix D6.3.2), the out-lying land remained exposed at relatively high elevations, the one-eighth relationship may be too generous in describing the maximum depth of fractures created there during deglaciation, and IDLs survived for less time.

D6.3.4 Ireland

The Dalradian Supergroup continues from Scotland into the Irish Caledonides in the NW part of Ireland, north of the very karstic Irish Carboniferous sedimentary limestones. The thrust boundaries and individual outcrops commonly run from SW–NE in the three separate areas of North Mayo, Donegal / Tyrone / Londonderry, and Antrim (with younging to the SE), and from W–E in the displaced and more complexly-folded terrane of Connemara (Wilson, 1972). The total area measures some 6000km^2. Metacarbonate outcrops, with a stripe karst appearance, occur within the Argyll Group in all four areas, and within the Appin Group in all areas except Antrim, as correlated with the Scottish rocks by Gibbons and Harris (1994). Only some 12 karst caves, with a total length of only 418m, are recorded to date. Few caves have been surveyed adequately, and only two caves are more than 30m long. The caves have only been found within the Argyll Group (Easdale Subgroup) in Connemara, and in the Appin Group (Blair Atholl Subgroup) in Connemara and Donegal. Faulkner (2000d) provided a more complete description of the caves and metacarbonate outcrops.

Ireland was probably covered by a mobile icesheet at the LGM, whose centre moved south during its growth, and north during its decay. Ballantyne *et al.* (1998) showed the maximum edge of this icesheet near the coast of Donegal and Connemara, with approximate thicknesses of 300m at Gweebarra Bay, 500m at Donegal Bay, and 700m at the Ox Mountains and Connemara. The western mountains may have acted as glaciation initiation centres. Ireland was also overrun by Scottish ice, forming a single British icesheet (McCabe *et al.*, 1998; McCabe and Clark, 2003) with three episodes of Devensian deglaciation (Appendix D6.3.2). Knight (1999) reported tectonic activity in NW Ireland during glacial unloading that led to metre-scale fault re-activation.

The longest cave explored to date is **Pollnapaste**. This is contained within the Falcarragh Limestone Formation of the Blair Atholl Subgroup, near Gweebarra Bay, Donegal (Parkes *et al.*, 1999). It is a combination cave with a relatively large sink entrance, 15m above sea level. The cave has formed in marble that, in places, is tightly folded and intruded by large dykes, within an overall vertical stripe karst setting. It has a length of c. 220m and a vertical range of c. 25m (including a steep inlet passage that rises above the entrance). The hills that overlook the Gweebarra valley from the south rise to about 300m, so that they were probably completely covered by ice at the LGM. Thus, the **Pollnapaste** inception fractures fall within the one-eighth relationship that governs the maximum depth of fractures caused by deglacial seismicity in central Scandinavia.

The entrance to **Pollnapaste** is intriguing, because, from this author's personal observation, it appears to have suffered marine enlargement. However, the thickness of Pleistocene icesheets over Ireland and local relative sea levels are still matters of dispute between 'thin ice' models based on the glacio-isostatic adjustment of the British Isles and observations of apparent Irish raised sea levels. Thus, according to Lambeck and Purcell (2001), there is a common absence of raised shorelines along the west coast of Ireland and their Fig. 2 shows that isostatic depression at Gweebarra Bay was exceeded by even lower eustatic sea levels at all times since the LGM, denying an opportunity for the sea to invade the **Pollnapaste** entrance. On the other hand, McCabe (1997, Fig. 2) reported sea level indicators from 19–13k^{14}Ca BP that are some 80–40m higher in eastern Ireland than predicted by an earlier version of the glacio-isostasy model. McCabe and Clark (2003) reported a sea level raised to 30m in Donegal at the deglaciation of LGM1 at 17k^{14}Ca BP and an ice sheet re-advance from 15–14k^{14}Ca BP [coincident with LGM2 in Scandinavia?], giving a sea level at +7m at one site. Thus, it seems likely that at least the first of these events caused some enlargement of the **Pollnapaste** entrance.

Another answer to the puzzle may be provided by Bowen *et al.* (2002). By using the new ^{36}Cl technique for dating the first exposure of glaciated rock surfaces to cosmic radiation, they suggested that the 'LGM' was *not* the largest Devensian icesheet in the British Isles. Instead, a combined British and Irish icesheet was in contact with the Scandinavian icesheet at about 40ka, and this icesheet fluctuated several times until the LGM at c. 22ka, apparently in association with Heinrich events. The 'Earlier Devensian Glaciation' apparently reached a maximum size at Heinrich 4, when the icesheet extended to the edge of the Irish continental shelf. After the deglaciation of the LGM, the icesheet surged forward to cover more than half of Ireland again during the Heinrich 1 event, although the Younger Dryas stadial does not appear to have created ice caps in Ireland.

The above scenario provides opportunities for the creation of tectonic inception fractures during glacial unloading at each fluctuation, and for subsequent phreatic enlargement beneath ice-dammed lakes. Thus, the phreatic passages in **Pollnapaste** could have enlarged beneath successive Devensian IDLs formed behind tidewater glaciers in Gweebarra Bay. If the 'Earlier Devensian Glaciation(s)' were larger than the so-called LGM, their ice thicknesses and isostatic depressions would be greater than modelled by Lambeck and Purcell (2001), allowing the sea to invade to higher levels along the west coast. The raised shorelines produced were probably eroded by the LGM glaciation, although McCabe *et al.* (1986) reported the existence of glaciomarine sequences ≤80m above sea level along the north coast of County Mayo, 60km south of **Pollnapaste**. Hence, the **Pollnapaste** entrance could have been enlarged by the sea during the un-modelled onset or decay of one or more of the 'Earlier Devensian Glaciations', but after the prior enlargement of phreatic passages. The lower, vadose, passages enlarged during the various interstadials, and especially during the Holocene. The absence of relict vadose passages in **Pollnapaste** suggests that enlargement does not pre-date the previous interglacial. The existing cave passages probably represent a single cycle of development, and comply morphologically with the TDMO model. This sequence contrasts sharply with that proposed by Parkes *et al.* (1999), who concluded that the cave developed mainly during the Holocene, when the upper phreatic passages enlarged until they were drained by the breaching of a metadolerite dyke inside the cave.

The second longest cave is **Kelly's Cave**, County Galway, in the Connemara Marble Formation, also in the Blair Atholl Subgroup (Faulkner, 2000d). This is a 70m-long, 11m-deep, relict cave, at an altitude of 310m, with rectilinear passages that run parallel to a low cliff. It has formed phreatically in marble with a foliation dip of c. 20° into the cliff, below a mica schist roof. The adjacent ridge rises to about 600m. The cave therefore fits the model of development below a deglacial lake, which perhaps existed above the line of loughs that lie south of the Maumturk Mountains. Table D6.15 summarises the attributes of the 12 recorded caves. None have been assigned to the mainly vadose class, perhaps because of the author's lack of familiarity with some of them. Despite the small sample size and the sparse written record, the approximated mean cave dimensions are commonly of the same order as those in the Scottish Caledonides.

Table D6.15 Irish Dalradian Supergroup Cave Class comparisons

INTERNAL CAVE ATTRIBUTE	RELICT CAVES	COMBINATION CAVES	MV CAVES	ALL CAVES	UNITS
Count	8	4		12	No.
% of caves	67	33		100	%
Total cave length	142	276		418	m
% of total cave length	34	66		100	%
Mean cave length	18	69		35	m
Mean cave VR	5.6	12.5		7.9	m
Mean cave XS	2.8	5.1		3.6	m^2
Mean cave Volume	70	314		151	m^3
Average of SE	0.00	0.75		0.25	No. per cave
Average of RE	0.00	0.50		0.17	No. per cave
Average of DE	1.13	0.00		0.75	No. per cave
Average of all entrances	1.13	1.25		1.17	No. per cave
Average of CS	0.00	1.50		0.50	No. per cave
Average of SP	0.00	1.00		0.33	No. per cave

D6.3.5 Shetland

The rocks of the Dalradian Supergroup also continue northward from Scotland, to the islands of Shetland, where they crop out east of the Walls Boundary Fault that is probably a continuation of the Great Glen Fault, in a total area of some 900km^2 (Mykura, 1976). Here, the Appin, Argyll and Southern Highland Groups are aligned N–S, forming ridges and glaciated valleys, with younging to the east. The Grampian Group is not represented (Gibbons and Harris, 1994). Metalimestone outcrops, ≤22km in length and ≤1km in width, occur primarily in the Tayvallich, Easdale and Islay Subgroups of the Appin Group. Where exposed at the surface, they commonly have a vertical stripe karst appearance, reminiscent of the HNC in Norway (Photo D6.3). In particular, the scenery at the western coastal outcrops is similar to that of the coastal limestone islands in Z1 of the main study area. None of the metacarbonates

has been identified as dolomite. However, there is a complete lack of a written record of karst activity in Shetland, despite the long and easily accessible marble outcrops, without forest cover, and despite the visits of cave explorers to sea caves, peat caves and copper mines in the 1960s. Small metacarbonate outcrops also occur west of the Walls Boundary Fault.

The paucity of both exokarst and endokarst development was confirmed during geological mapping (Flinn, pers. comm., 1997) and by the author during a one-week field trip to Shetland in August 1999, when c. 20km of limestone outcrops at some 20 sites were visited (Faulkner, 2000b). The Ordnance Survey maps for the area do not show any sinks or risings coincident with limestone outcrops, and only small seeps were found. Much of the limestone is covered by blanket peat that is 2m thick. There are very few dolines, and the largest are only 2m deep. Tiny streams that sink into these dolines seem to flow only along conduits in the peat. Where streams run across limestone outcrops, they do not go underground, but cut gorges up to 3m deep in the manner described by Osborne (1999, Fig. 13). The largest 'karst conduit' seen on Shetland is fist-sized.

Photo D6.3 Stripe karst in Shetland
Quartz crystals in a metalimestone block, Kergord Valley. Hammer for scale.

D6.4 The Arctic Caledonides

The Arctic Caledonide areas, which are presently permafrosted to varying depths, have not been visited by the author, and neither has he fully studied their glacial, isostatic uplift, and seismic histories. There are relatively few references to karst features. Smith (1972) measured a present surface denudation rate of only 2mmka^{-1} (Table A2.5) in sedimentary limestones in a broadly comparable climate at Somerset Island, Canada.

D6.4.1 Central East Greenland

The Greenland Caledonides are represented in three separate terranes that formed on the western side of Iapetus (Barker and Gayer, 1985), which are discussed from south to north. The area from 70–76°N comprises an Upper Riphean limestone–dolomite series overlain by Vendian (latest Proterozoic) age (Varanger) tillites that were themselves overlain by Early Cambrian to Mid Ordovician shelf carbonates (limestones and dolomites). These rocks were deformed, sporadically metamorphosed up to amphibolite facies, and thrust westwards in N–S aligned nappes over the Greenland Archean basement and its early Proterozoic and Grenville age cover sequences during the East Greenland / Ny Friesland (Caledonide) Orogeny, in the Early Silurian,. The basement rocks were also incorporated, to form the so called "crystalline region". Later in the Silurian, the rocks cooled and were then covered by Devonian sandstones and a succession of younger sediments, including Carboniferous and Cretaceous. The facies equivalence of Vendian dolostones from this terrane with dolostones from the Argyll Group, Islay Subgroup, on the isle of Islay, Scotland, was described by Fairchild (1989). Both formations lie above Varanger / Port Askaig tillites. The area from 76–80°N consists primarily of basement gneisses.

D6.4.2 North East Greenland

The area from 80°N to Danmark Fjord has a tectonic history similar to that of Central East Greenland, but the Varanger tillites do not occur, and there was no deposition during the Cambrian (Smith *et al.*, 1999). Ordovician–Silurian carbonates were deposited in the (western) foreland, prior to the East Greenland / Ny Friesland Orogeny, which only produced lower-grade metamorphism in this area. Folds commonly have gently-dipping eastern limbs and steep or overturned western limbs, with dislocations in carbonates. The Devonian 'red beds' are also absent.

This is the only terrane in the Greenland Caledonides in which karst caves are reported. These all occur near Lac Centrum, Kronprins Christians Land (Davies and Krinsley, 1960; Loubiere, 1987). A French expedition in 1983 covered an area of 1000km^2 of deglaciated massive Silurian (with some Ordovician) *sedimentary* carbonates, revisiting caves near Grottedalen, some 30km north of the lake, and finding a new cave, **Grotte des Quatre**, 8km to its south. Permafrost reaches a depth of 200m in this area, although 70 days were recorded with temperatures from 0–15°C. However, snow persisted on north-facing slopes and above 700m altitude. Relative humidity is only 20% and the precipitation is only 200mma^{-1}.

Twelve caves are located in a 450m-deep side valley to Grottedalen, at altitudes of 500–520m, 610–630m and 700m, i.e. they share the same three sub-horizontal limestone beds. These beds may lie above impermeable Silurian dolomites. The caves all appear to have developed phreatically, with some breakdown. According to Davies and Krinsley (1960), the passage diameters range from 5–12m, and lengths from 10–60m. The caves above 600m altitude are terminated by fills of ice and frozen orange / yellow and red silts, which in one cave are capped by a 10cm-thick flowstone. Caves below 600m are partly filled with glacial moraine, causing Davies and Krinsley to suggest that the latest ice advance down the valley was below this altitude. **Grotte des Quatre** lies at an altitude of c. 450m, and has formed in limestone with an almost vertical dip (but unknown metamorphic grade). The diameter of the main entrance is about 9m. This reduces in size to a passage to two small entrances, with a side passage to a fourth entrance. The total length is c. 70m and vertical range c. 14m (Loubiere, 1987, Fig. 3). The main entrance has clearly formed at a tectonic movement between near-vertical strata (*ibid.*, Photo 5). Dating of reworked stalagmite fragments using the ESR method apparently indicated an age around 1.0–1.4Ma. Additionally, microscopic fungus in one stalagmite acts as a climatic marker to suggest an early Pleistocene age, when the warmer local climate may have supported open boreal forest, and prevented the formation of ice caps, as evidenced from other research in northern Greenland. In the main study area, the tapering main entrance would be interpreted as being enlarged by marine activity, probably by a rising sea level at the onset of glaciation. In this case, its present altitude of 450m is partly indicative of the extent of erosional unloading during the Pleistocene.

Smith *et al.* (1999) reported the existence of *palaeoendokarsts* in Riphean-age stromatolitic, sub-horizontal, dolostones at three places around Lac Centrum, as exposed in valley sides. Phreatic conduits at shallow depths (up to c. 12m) below an unconformity surface range in size up to 5m high by 15m across. In one place, the conduits are connected by vadose channels to the upper surface, suggestive of an epikarst. At another, wide and steep vadose channels have truncated from above, to reach below the phreatic conduits, indicating a fall in base-level subsequent to the phreatic enlargement (and, incidentally, complying with the TDMO model of Chapter 9). All these conduits and channels are infilled by Vendian sandstones. The lower part of the unconformable lithology above comprises dolomitic sandstones of Ordovician age, either directly, or above the same formation of Vendian sandstones. The authors considered that soon after their formation in meteoric conditions (with no hydrothermal influence), the conduits and channels were infilled without causing collapse, and survived subsequent Caledonide tectonism.

D6.4.3 Northern Greenland Fold Belt

In northern Greenland, a fold belt trends E–W along the north coast into Ellesmere Island (Canada). It is very different to the East Greenland belts, and the main deformation post-dated the Caledonide Orogeny, taking place in the Devonian to Early Carboniferous. The Precambrian and Lower Palaeozoic rocks, folded and metamorphosed in the north, are unconformably overlain by Carboniferous deposits, but in central and south Peary Land, unfolded shelf deposits occur, overlain by Cambrian to Silurian carbonates. Major thrusting, crystalline basement, and granitic intrusions are absent in this belt.

D6.4.4 Spitsbergen

The semi-glacial archipelago of Svalbard lies at latitudes 76–80°N. The largest island is Spitsbergen. Although it is generally considered that the whole area is Caledonide (belonging to the eastern side of the former Iapetus Ocean), this is only definite for the eastern terrane that comprises Ny Friesland and Nordaustlandet. This has affinities with Central East Greenland (Harland, 1985). The central terrane probably also formed during the Caledonide Orogeny, outboard of North East Greenland, but the western terrane belongs to the northern Greenland fold belt, so that the whole island probably only came together completely during the Carboniferous (Barker and Gayer, 1985). Commonly, Precambrian metamorphic Hecla Hoeck lithologies, including marbles (with grades up to sillimanite facies), are overlain by Palaeozoic sediments that include limestones and dolostones (some with affinities to the Durness Group limestone of Scotland) in all terranes, as in East Greenland (but unlike in most of the other studied Caledonide areas). It appears from the large sizes of the sedimentary and metamorphic limestone outcrops that dip angles are small, creating low angle karst rather than stripe karst (section 5.3.1). The existence of both short karst caves and endokarstic drainage in some metamorphic limestones is well known (e.g. Corbel, 1957; Lauritzen, 1998), although, because of their remoteness, knowledge of all the karst outcrops has remained sparse.

Despite the ameliorating effect of the Gulf Stream, the exposed parts of Spitsbergen presently experience continuous permafrost to variable depths down to 450m. Precipitation is limited to about 400mma^{-1}, and surface runoff at sea level is limited to the four summer months when the atmosphere is above freezing. A consequence is that none of the explored dissolutional caves are active: they consist of relict passages with lengths up to 17m in cave **C5**, on the karst island of Blomstrandsøya in Kongsfjorden. Phreatic cross-sections vary up to 6m^2, but caves are blocked by permafrozen sediments and plugs of ice. The relict caves on Blomstrandsøya commonly, but not universally, occur below 100m altitude, and **C5**, at least, appears to have been enlarged by marine action. Strandflats here reach altitudes of 300m. Raised beaches also occur in Ny Friesland (R. Gayer, pers. comm., 1998). Many sea caves have also formed along the exposed limestone cliffs of Blomstrandsøya near the present sea level, at which freshwater springs sporadically emerge. This led Lauritzen (1998) to propose a hybrid speleogenesis, with mixing corrosion at a sub- or supra-permafrost groundwater / seawater halocline supplementing wave and ice action.

Lauritzen (1998) mentioned reports of palaeokarsts of various ages in Spitsbergen, including fills of Devonian Old Red Sandstone in cliff caves on Blomstrandsøya. Their proximity to the present surface suggests that there has been little glacial erosion of the metalimestones on this island, previous glaciations presumably only just removing the Palaeozoic strata above the Precambrian. Thus, caves that contain Devonian sediments may have prior origins. Alternatively, they were injected with this surface material during Quaternary glaciations.

A characteristic in Spitsbergen that is unique in the Caledonides is the process of *hydrothermal karstification*. This is evidenced by the guidance of passages along hydrothermal calcite veins, and by the presence of calcite spar around the walls of tubular dissolution cavities, both at Blomstrandsøya and at Hornsund in the south of Spitsbergen (Lauritzen, 1998). This thermal activity continues to the present, as numerous hot springs occur along the west coast, from several types of aquifer (including karstic), as a result of young volcanism associated with the spreading of the Atlantic sea floor. Apart from small summer springs from superficial layers above the permafrost, the thermoglacial karst springs arise from glacial recharge into deep, sub-permafrost, conduits with flows that can vary up to 70m^3s^{-1}. They have an exotic water chemistry that includes H_2S, brine and organics, at temperatures up to 27°C. There is no record that the morphology of any of these karstic springs has been studied by diving.

D6.4.5 Bjørnøya

The small island of Bjørnøya, which lies between Spitsbergen and Norway, has low angle karst sedimentary limestone outcrops of both pre-Caledonide age (at the southern tip) and post-Devonian age, but there are no reports of caves there (Corbel, 1957, p61). According to the tectonic reconstruction of Smith (2000), Bjørnøya remained part of the North East Greenland terrane of Laurentia until the Eocene, whereas Svalbard had amalgamated its separate terranes north of Greenland by the end of the Caledonide Orogeny. Svalbard and Bjørnøya subsequently moved together to their present positions under the influence of Atlantic spreading and the evolution of various Greenland Sea fracture zones.